Robert E. Riding
Stanley M. Awramik
Editors

Microbial Sediments

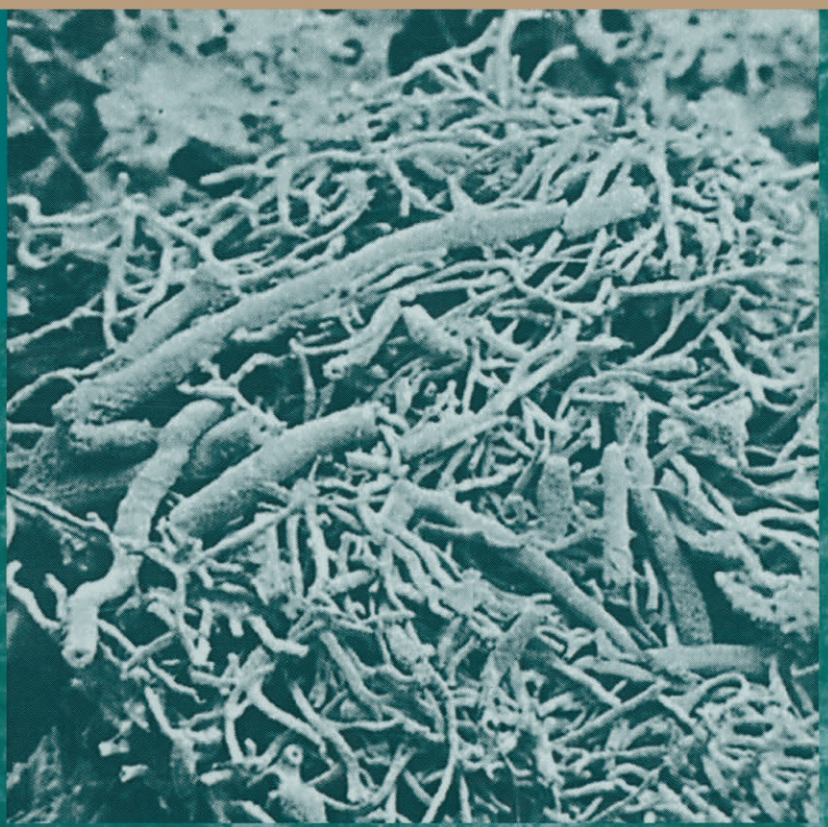

Springer

Springer-Verlag Berlin Heidelberg GmbH

Robert E. Riding and Stanley M. Awramik (Eds.)

Microbial Sediments

With 152 Figures in 387 Parts and 13 Tables

Springer

Dr. Robert E. Riding
Cardiff University, Department of Earth Sciences
Cardiff CF10 3YE, Wales, United Kingdom
Email: riding@cardiff.ac.uk

Dr. Stanley M. Awramik
University of California, Department of Geological Sciences
Santa Barbara, CA 93106, USA
Email: awramik@magic.geol.uscb.edu

ISBN 978-3-642-08275-7

Library of Congress Cataloging-in-Publication Data

Microbial sediments / Robert Riding ; Stanley M. Awramik eds.
p.cm.
Includes bibliographical references and index.
ISBN 978-3-642-08275-7 ISBN 978-3-662-04036-2 (eBook)
DOI 10.1007/978-3-662-04036-2

1. Microbial aggregation. 2. Sedimentation and deposition. 3. Diagenesis. 4. Geomicrobiology.
5. Marine microbiology. I. Riding, Robert. II. Awramik, S.M.
QR73.6.M53 2000
551.3'03–dc21
99-052961

Originally published by Springer-Verlag Berlin Heidelberg New York in 2000
Softcover reprint of the hardcover 1st edition 2000

Cover Design: E. Kirchner, D-69121 Heidelberg (Photograph by Robert Riding: *Girvanella problematica*, calcified cyanobacterium. Mid-Ordovician, Tarim, China)
Typesetting: FotoSatz Pfeifer GmbH, D-82166 Gräfelfing
Printed on acid-free paper – SPIN: 10551671 32/3136 – 5 4 3 2 1 0

Preface

Microbes are the most abundant and widespread organisms in sediments. Like all creatures, their activities are intently focused on making a living. The position of many microbes at or near the base of the food chain entails close interactions with the inorganic environment. Some microbes adhere to sedimentary surfaces in environments where they can carry out photosynthesis. For many others, sediment grains and surfaces provide not only stability, protection and suitable conditions, but also direct proximity to detrital particles that they oxidize and reduce in order to obtain nutrients and energy. To do this, they produce acids and other compounds that attack these minerals, dissolving and altering them. At the same time, microbial processes can create chemical environments that favour mineral precipitation. Mobile sediment and moving water encourage microbes to produce adhesive polysaccharide secretions for anchorage and protection. These stabilize grains and also provide sites for mineral nucleation. In these diverse ways, benthic microbes significantly modify, localize, contribute to, and create, sediment. Planktonic microbes in the water columns of lakes and seas contribute additional products that accumulate in the sediments below.

Microbes are microscopic organisms. Many of them are bacteria, but they also include small algae and fungi, and protozoans. In this book we have not applied strict definitions or attempted to be exhaustively comprehensive within such a diverse field. We have, however, endeavoured to convey the breadth of the subject, the range of organisms, processes and products involved, and the scale of these activities in space and time. Microbes have been leaving significant evidence of their presence and activities in sediments – in the form of fossils, fabrics and chemical signatures – from the Archaean onwards. This is the central theme of this book.

It would have been quite impossible for us alone to have produced this book. We are deeply indebted to many colleagues and friends who generously and without hesitation gave time and expert knowledge to the task of reviewing one or more of the contributions that make up this volume: Thomas F. Anderson, Julian Andrews, Janine Bertrand-Sarfati, David J. Bottjer, Roger Buick, Gilbert F. Camoin, S. Christopher Caran, Henry S. Chafetz, Matthew Collins, Paul Copper, Eileen J. Cox, Adrian Cramp, Paul R. Dando, Robert V. Demicco, Karl Föllmi, Christian Gaillard, Gisela Gerdes, Stjepko Golubic, Kathleen Grey, Li Guo, Michael K. Hein, Hans J. Hofmann, John Hudson, Brian Jones, Alan Kendall, Kurt O. Konhauser, Wolfgang E. Krumbein, Paul A. LaRock, José M. Martín Martín, Martina Merz-Preiß, Conrad Neumann, Fritz Neuweiler, Karsten Pedersen, Martyn Pedley, Allan Pentecost, Robert Raiswell, Pamela Reid, Lisa Robbins, Jean-Marie Rouchy, John F. Stolz, G. Stoops, Nigel Trewin, Eric P. Verrecchia, Heather Viles, Malcolm Walter, Frances Westall, Barbara Winsborough, V. Paul Wright.

Our unstinting gratitude goes to the publishing team headed by Wolfgang Engel – particularly Birgit Martin, Theodora Krammer, Victoria Pietsch, Wendy Ran, Joachim W. Schmidt and Andrea Weber-Knapp – whose professionalism conjured this book from our manuscript.

Finally, we thank the authors themselves. Books such as this ultimately achieve a life of their own. They grow into spirited offspring, recognizable, to be sure, but in possession of some unique features that, although certainly not unwelcome, were no more anticipated than they were planned. So we are very grateful to our contributors who, probably realizing much more clearly than we did how the final outcome would be different from the aim, nonetheless willingly joined us in this venture.

To all, our sincere thanks.

Robert Riding, Cardiff
Stanley M. Awramik, Santa Barbara

Contents

Structure of Microbial Mats and Biofilms

John F. Stolz

Department of Biological Sciences, Duquesne University, Pittsburgh, Pennsylvania 15282, USA

Abstract. The application of new technologies, such as confocal scanning laser microscopy and molecular probes, to the study of biofilms and microbial mats has dramatically changed our view of these systems. In particular, the old idea that biofilms are simply microbes suspended in a homogeneous and diffusion limited matrix has been shattered by the realization that this matrix is actually very hydrated and honeycombed with channels. The microbial species which form the microcolonies have been shown to express genes which are not expressed when the organisms are free-swimming. Thus, many models of microbial dynamics based on planktonic studies (e.g., growth, gene exchange, biocide resistance) do not necessarily apply to biofilms. Recent studies of microbial mats have also uncovered some startling phenomenon. For instance, active sulfate reduction has been measured in the oxic zone. The impact of diurnal fluctuations in the environment cannot be underestimated, as species have been shown to migrate within the mat and use totally different metabolic pathways in response to light and oxygen. This review will highlight some of the insights into the biological structure of biofilms and microbial mats, and how the structure is affected by the physical and chemical environment, species composition, and species interactions. The chapter begins with a comparison of microbial mats and biofilms and ends with some suggestions for future studies.

1 Introduction

To begin the discussion on the structure of microbial mats and biofilms, it is important to establish the similarities as well as the differences between the two. In the broadest sense, they are microbial communities, predominately populated by prokaryotes, that colonize surfaces. Implicit in this definition is the understanding that there is intimate interaction between the microbes, the colonized surface, and the surrounding environment. Thus, the physical and chemical environment, species composition, and species interaction are all involved in determining structure.

Microbial mats have been called algal mats, cyanobacterial mats, and potential stromatolites because of the predominance of cyanobacterial species and in acknowledgement of their role in the formation of laminated sedimentary structures (Krumbein 1983, 1994). These sedimentary structures, called stromatolites, are the result of the trapping, binding, and precipitation of sediment by the extracellular polymeric matrix (EPS) produced by the organisms (Krumbein 1994). The discoveries of fungal stromatolites and mats dominated by anoxyphototropic bacteria (e.g., thermal spring mats), chemoautotrophic bacteria (e.g., *Beggiotoa* mats), and diatoms (Winsborough, this Vol.) have resulted in a broadening of the definition to include these possibilities (Krumbein 1983). Microbial mats are further characterized by steep chemical gradients, the abundance of phototrophic microorganisms, and stratification of the microbial populations into distinct layers (Stolz 1990, 1991). In many cases, these complex communities may fulfill the definition of an ecosystem, in that all necessary trophic levels (e.g., primary producers, consumers, decomposers) are present (Stolz et al. 1989). Microbial mats have been studied as model ecosystems as well as analogues to ancient microbial communities (Awramik 1984). Several edited volumes summarizing this work have been published (Walter 1976; Schopf 1983; Cohen et al. 1984; Cohen and Rosenberg 1989; Schopf and Klein 1992; Stal and Caumette 1994; Krumbein et al. 1994).

Biofilms were described in Marshall (1984, 1992) as a collection of microorganisms and their extracellular products bound to a solid surface (Neu 1994). Thus, unlike microbial mats, biofilms form on solid substrates such as rocks, glass, plastic (e.g., catheters), steel (e.g., pipes) and wood. The bacterial colonization of surfaces is dependent on the formation of EPS (Marshall et al. 1971; Costerton et al. 1978, 1981). The EPS can trap inorganic and abiotic components (Characklis and Marshall 1990; Decho, this Vol.), as well as immobilize water (Krumbein 1994). In this respect, they are similar to microbial mats. Biofilms may also be involved in the formation of mineral precipitates, such as the ferromanganous tubercles of water pipes. The species composition, however, may vary greatly, from a single species to complex communities comprised of many species. Microbial mats, therefore, may be considered complex biofilms. Although the pioneering work of Zobell was done over 50 years ago (Zobell 1943), interest in biofilms has recently seen a resurgence with the application of confocal scanning laser microscopy and molecular biological techniques to their study. This interest has resulted in the publication of several books and edited volumes (Marshall 1976, 1984; Characklis

R. E. Riding and S. M. Awramik (Eds.)
Microbial Sediments

and Wilderer 1989; Characklis and Marshall 1990; Melo et al. 1992; Geesey et al. 1993; Lappin-Scott and Costerton 1995), review articles (Costerton et al. 1987, 1994, 1995; Costerton 1995), and most recently, a special two-volume edition of the *Journal of Industrial Microbiology* (Cooney and Laskin 1995). Images of various types of biofilms are available on a compact disc released by the American Society for Microbiology (ASM 1996).

2 Physical and Chemical Characteristics

The environment of a biofilm or microbial mat is determined by physical and chemical characteristics. Physical factors include light, temperature, water content, and flow rate. Pressure and density, also physical factors, are more significant in planktonic systems. Chemical factors include pH, alkalinity, oxidation/reduction potential (E_h), salinity, the concentration of oxygen and other chemical species (e.g., H_2S, NO_3^-, FeIII), and organic composition (e.g., dissolved organic carbon). The interplay between the physical and chemical factors create gradients and microenvironments which promote the growth and proliferation of certain species. This is particularly true in biofilms and microbial mats, where gradients may be steep and fluctuate.

Light has two important properties, quantity and quality. Phototrophic prokaryotes are major species in stratified microbial mats and their occurrence and distribution are determined by both the intensity (i.e., light quantity) and the available wavelengths of light (i.e., light quality). Although the typical surface illumination on a bright sunny day is about 1000 – 2000 μEinsteins, the optimum light intensity for cyanobacteria in the mats of Mellum Island is between 15 and 150 $\mu E/m^2$ (Stal et al. 1985). The optimum light intensity is even less, between 5 and 10 $\mu E/m^2$, for the purple phototrophic bacteria (Stal et al. 1985). Thus, these organisms are not found on the surface in direct sunlight. The selective penetration of specific portions of the electromagnetic spectrum into either water or sediment can establish zones of light quality. The common notion is that the majority of light between 400 and 700 nm is absorbed by 1 meter of water, with only blue-green light penetrating to any significant depth (Parsons et al. 1988). However, studies of intertidal mats have shown that, in sediments covered by scant surface water, it is actually the infrared radiation that penetrates furthest (Jorgensen 1989). Populations of different types of phototrophic organisms are found at different depths in microbial mats, and pigments which are visible to the human eye reveal this laminated structure. Detailed spectrophotometric analysis has confirmed these observations as well as established the layered distribution of chlorophylls, bacteriochlorophylls and accessory pigments (Stal et al. 1985; Pierson et al. 1987; Stolz 1990, 1991).

The influence of temperature on biofilms is a direct consequence of the need living systems have for liquid water. As long as liquid water is present, life processes can occur. The most striking example of this principle is the microbial life associated with thermal vents. The extreme thermophiles that are found in this habitat persist in the super-heated waters and have optimal growth temperatures in excess of 100 °C (Koenig and Stetter 1989). Microbes which survive in permafrost represent the other extreme (Gilichinsky et al. 1992). Thermal gradients associated with thermal spring outflows result in microbial communities with different species composition (Ward et al. 1989, 1994).

The availability and flow of water are also important. Growing microbial mats need to be submerged. However, they may be aerially exposed periodically and subject to desiccation. Intertidal mats, like those found at Great Sippewissett Salt Marsh, Cape Cod, are tidally inundated. In this case, the matric potential of the mat can effect the retainment of water. Mat building organisms such as *Microcoleus chthonoplastes* produce copious quantities of sheath material which retain water. In fact, periodic desiccation may induce sheath formation (Krumbein et al. 1991).

The effect the movement of water has is dependent on scale. At the microscale, the rate of flow of water over a surface can determine whether a site can be colonized, the shape of the ensuing structure, and the persistence of the structure (Costerton et al. 1995). At the macroscale, the gross morphology of stromatolites is determined by wave and current action (Riding 1994).

The chemical environment is as much a product of abiotic factors (e.g., diffusion, solubility) as it is of the activity of organisms. Oxygen concentration is effected abiotically by diffusion and biotically by oxygen generation (e.g., oxygenic photosynthesis) and respiration. Pockets of anoxia can exist almost anywhere where the diffusion of oxygen is inhibited or the rates of respiration are high. Chemical species other than oxygen that are of great importance are the alternative terminal electron acceptors nitrate, ferric iron, tetravalent manganese, and sulfate (and sulfur species other than sulfide). These compounds fuel the anoxic oxidation of organic carbon and establish the canonical stratified zones of reduction (e.g., the zone where nitrate reduction is the predominant process). The conversion of carbon dioxide to methane via methanogenesis may also be considerable in mats and biofilms (Cohen et al. 1994; Costerton et al. 1995). Further contributing to anoxia is the production of hydrogen sulfide by sulfate reducing bacteria. Microbial activity and growth can be controlled by the availability of organic carbon (e.g., dissolved organic carbon). The presence of autotrophic species is essential to the continued development of microbial mats. Cyanobacteria are the most common pioneering species in microbial communities (Stal et al.

1985; Stolz 1990). Biofilms devoid of such species are dependent on a source of exogenous carbon (Costerton et al. 1995).

As much as the physical and chemical factors influence the abundance and distribution of microbial species, they are both in turn influenced by microbial activity. The natural attenuation of light is enhanced by the light absorption of photopigments, as the different layers of microbial populations act as filters (Jorgensen 1989). Respiration not only affects oxygen concentration, but pH (as a function of CO_2 and organic acid production) as well. The many interactions between the abiotic and biotic components result in dynamic systems which can exhibit both spatial and temporal heterogeneity and provide a wide variety of environments supporting a rich diversity of species.

3 Species Composition and Interactions

Species composition and species interactions may be considered the biotic factors which are involved in determining structure. From the ecologist's point of view, the most important aspect of species composition is the presence or absence of representatives from the three basic functional groups, the primary producers (i.e., autotrophs), the consumers, and the decomposers. A biofilm without primary producers is dependent on an exogenous source of organic matter. Single species biofilms are particularly dependent on their environment to provide not only a source of oxygen and nutrients but also to transport waste products. Microbial mats, with their rich diversity of organisms, are sites of complex elemental transformations. For example, sulfur is actively cycled within a mat community (Visscher et al. 1992). As for the structures themselves, the construction of biofilms and laminated microbial mats is dependent on the presence of organisms capable of producing EPS. The deposition of laminated sediments did not occur in the stratified mats at Laguna Figueroa when *Microcoleus chthonoplastes* was absent from the mat community, although other species of cyanobacteria were present (Stolz 1990). In addition, there is evidence that species composition (e.g., the presence of green algae and diatoms) influences the microstructure of stromatolites (Riding 1994; Winsborough, this Vol.).

The structure of complex microbial communities is not only influenced by the individual species present, but also by the interaction of these species with each other. These interactions begin at the initial stages of colonization and continue throughout the development of the community (James et al. 1995). Interspecies metabolite transfer, predation, antibiotic production, competition for nutrients, and physical exclusion are just a few examples. The metabolic capability of a microbial consortium can be greater than that of the individual components (James et al. 1995). The degradation of certain xenobiotic compounds is only possible with a consortium (Wolfaardt et al. 1994). Furthermore, the close proximity of the microcolonies facilitates the interspecies transfer of nutrients and ions (Thiele et al. 1988). Species composition and species interaction do have an impact on the structure of microbial communities; however, many questions remain. Their importance relative to the physical and chemical factors is not fully understood. The question of what effect, if any, does genetic transfer between species have on the development and persistence of biofilms and mats (i.e., how common is it) is only now starting to be addressed.

4 Biological Structure

4.1 Microbial Mats

Microbial mats come in a variety of morphologies as determined by the dominant species of cyanobacterium and environmental factors. A classic example is the different mat types of the sabhka at Abu Dhabi, the Persian Gulf (Golubic 1992). Different mat types can be found in the intertidal zone, as the tidal conditions provide different environments of deposition. Six different mat types have been identified. The gelatinous laminated biscuits, formed by *Phormidium hendersonii*, are found in waters below the mean high tide level. The mamillate mat, built by *Entophysalis major*, resides in the lower intertidal zone. The low flat laminated mats, which occupy tidal pool bottoms and channels, are comprised of *Lyngbya aestuarii* and *Microcoleus chthonoplastes*. This mat appears very similar in composition to the *Microcoleus* mats from Laguna Figueroa, Great Sippewissett Salt Marsh, and Solar Lake. The high pinnacle mat covers the mounds between the pools and is composed primarily of *L. aestuarii* and an undermat of *Schizothrix splendida*. The convoluted mat and the folded mat are in the upper region of the intertidal zone and experience prolonged periods of dessication. These mats are leathery in texture and contain pockets of trapped gas bubbles. The predominate cyanobacteria in these mats are *M. chthonoplastes* and *S. spendida* (Golubic 1992).

Microbial mats are typically laminated and although the composition and gross morphology may be different, they share several features. The organisms exposed to direct sunlight at the surface are highly pigmented, either with carotenoids or other light attenuating substances (e.g., scytonemine). Beneath the surface layer, is a layer composed of cyanobacteria, in which most of the oxygenic photosynthesis takes place. Beneath this layer, a transition to anoxia occurs. Microelectrode profiling has shown that the oxygen peak is in the cya-

nobacterial layer, reaching at times supersaturation, and that the transition to anoxic conditions can be quite rapid, extending less than a few hundreds of microns in depth (Stal et al. 1985; Revsbech and Jorgensen 1986; DeWit et al. 1989). Where iron and sulfur are abundant, the sediment is often blackened by the presence of iron sulfides, and a population of anoxygenic phototrophs is found. When these sediments are allowed to oxidize, the presence of pigment can be discerned. There may also be more than one layer of anoxygenic phototrophs as well as a complement of colorless sulfur bacteria (Stolz 1990, 1991).

A striking feature of microbial mats is the sharp zonation of pigmentation. The distribution of the different species of phototrophic bacteria is determined by light, oxygen, and sulfide. The sandy mats of the Great Sippewissett Salt Marsh have five discernible layers (Nicholson et al. 1987). This layering reflects both pigment and microbial species composition (Pierson et al. 1987). The different layers may be compacted over a few millimeters, like in *Microcoleus* mats, or may extend many centimeters in depth (Stolz 1990; Stal et al. 1985; Nicholson et al. 1987). The flat laminate mat at Laguna Figueroa, dominated by the cyanobacterium *Microcoleus chthonoplastes*, has four readily discernable layers (Fig. 1a), a surface carotenoid rich layer (Fig. 1a, L-O), a green (chlorophyll a, phycocyanin, phycoerythrin) cyanobacterial layer (Fig. 1a, L-G), a pinkish layer comprised of anoxyphototrophic bacteria (Fig. 1a, L-P), and a salmon-colored bacteriochlorophyll b-enriched layer (Fig. 1a, L-S) (Stolz 1990). This last, pencil-thin layer, which is populated by various species of colonial purple sulfur bacteria (e.g., *Thiocapsa pfennigii*), has also been found in the *Microcoleus* mats of the Great Sippewissett Salt Marsh.

Despite these distinct layers, there is heterogeneity within the layers. Like biofilms, the functional biologi-

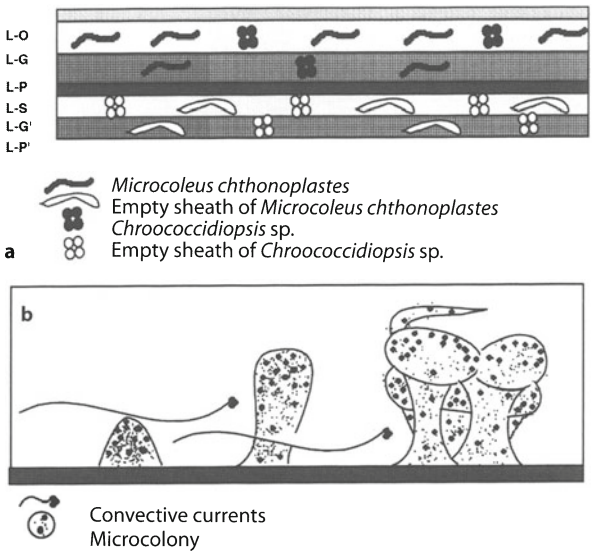

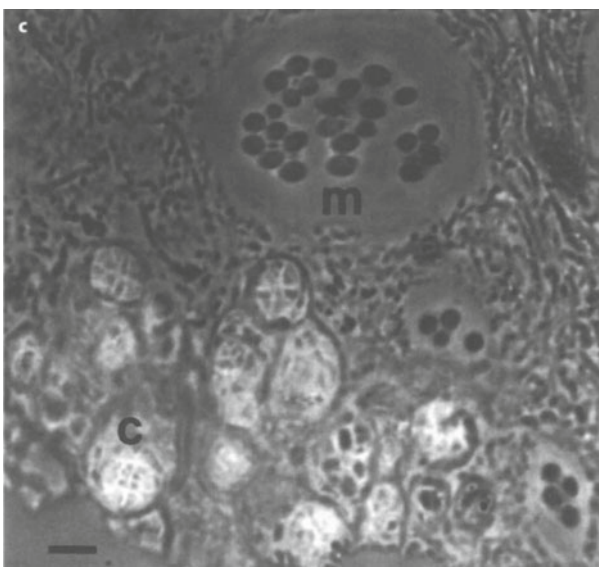

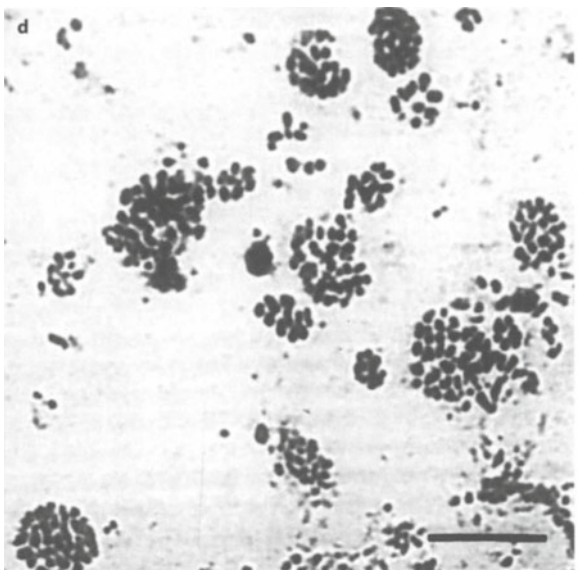

Fig. 1a–d. Idealized models and representative micrographs of the structure of microbial mats and biofilms. **a** Structure of the *Microcoleus* laminated mat from Laguna Figuroa, Baja California, Mexico. The large black filaments represent bundles of living *Microcoleus chthonoplastes*. The black tetrads represent microcolonies of the cyanobacterium *Chroococcidiopsis* sp. The white filaments and coccoids represent the empty sheaths of these same organisms. *L-O* Surface orange layer; *L-G* green layer; *L-P* pink layer; *L-S* salmon layer; *L-G'* previous years green layer; *L-P'* previous years pink layer. Redrawn from Stolz (1990). **b** Structure of a single species biofilm. The shape of these biofilms range from simple conical structures (*far left*) or elaborate mushroom-shaped structures (*far right*). The flow of convective fluid (*arrows*) occurs between and below the biofilms. Redrawn from Costerton et al. (1995), with permission. **c** Cross section through the green layer (*L-G*) of the laminated mat from Laguna Figueroa prepared for transmission electron microscopy (Stolz 1990). Note the microcolonies of *Chroococcidiopsis* sp. (*c*) and the bundles of *M. chthonoplastes* (*m*) filaments surrounded by a common sheath. Other filamentous bacteria and trapped ditritus are sandwiched in the interstices. **d** Image (inversed contrast) of mixed species natural biofilm showing individual microcolonies interspersed by water channels. (Costerton et al. 1994, with permission) *Scale bars* in **c, d** = 10 μm

cal unit of a population is the microcolony. These microcolonies may be filaments of *M. chthonoplastes* bundled by a common sheath or clusters of *Chroococcidiopsis* sp. (Fig. 1c). Even though certain species may be confined to a certain layer, other species may be present and active throughout the mat (Visscher et al. 1992).

Several discoveries have enlightened our view of microbial mats. The first is that the effect of diurnal fluctuation cannot be underestimated. The fact that photosynthesis is light dependent is obvious. However, other biological processes have been shown to have diurnal patterns (e.g., nitrogen fixation, methanogenesis). Populations of microbes have been shown to move in response to light and chemical gradients. Barbara and Mitchell (1996) have recently shown that highly motile mat microbes use their motility to form 30–40-μm thick laminations. Contrary to what is known about chemotaxis in enteric bacteria, apparently these bacteria increase their tumbling rate to remain in the layer (Barbara and Mitchell 1996). In benthic mat systems, a filamentous microbe, *Thioploca* sp., has been described which appears to couple the oxidation of hydrogen sulfide to the reduction of nitrate (Shulz et al. 1996). After accumulating nitrate in vesicles, it must migrate down into the sulfide-rich zone to complete the process. Bacteria with diverse metabolic capabilities may change their physiology depending on the time of day. *Thiocapsa roseopersicina* is capable of photoautotrophic growth under anoxic conditions and chemolithotrophic growth in the presence of oxygen (de Wit and Van Germeden 1987). Lastly, studies of sulfate reduction in microbial mats have shown that there is appreciable activity even in the presence of oxygen (Canfield and Des Marais 1991; Visscher et al. 1992). These discoveries underscore the notion that microbial mats are dynamic systems. Furthermore, their species richness, although well appreciated, has not been fully quantified. The simplistic description of mat types based on the predominant species of cyanobacteria is informative but incomplete. Appreciation of the contributions by algae and diatoms (Riding 1994) as well as anoxyphototrophic bacteria (Nicholson et al. 1987; Stolz 1990, 1991) and heterotrophic bacteria (Devereux et al. 1992; Visscher et al. 1992) is only now being realized.

4.2 Biofilms

The first in-depth views of biofilms were provided by transmission electron microscopy, and as a result gave the false impression of a uniform structure composed of microorganisms embedded in a homogeneous matrix that was diffusion limited (Costerton et al. 1978). The dehydration step dramatically altered the intricate substructure of the EPS. Recent advancements in biofilm imaging, which include the use of the confocal scanning laser microscope and fluorescent probes, have revolutionized this view (Costerton et al. 1995). The new paradigm describes the biofilm as a mass of microcolonies embedded in an EPS which is honeycombed with water channels (Fig. 1b). Viewed from above, a single species biofilm may take on the appearance of a labyrinth, with the individual microcolonies forming the walls (Costerton et al. 1995). The image of a mixed culture biofilm from an optical section taken by a confocal scanning laser microscope shows a patchwork of individual microcolonies, each of varying size and composition, held together by EPS and separated by channels of less dense hydrous matrix (Fig. 1d, Costerton and Lappin-Scott 1995).

The discovery of water channels and convective flow within them has several ramifications. These water channels deliver bulk fluid around, over, and beneath the microcolonies facilitating nutrient delivery and waste removal. Thus, diffusion limitation is encountered at the surface of the microcolonies, not at the surface of the biofilm. Lewandowski and coworkers have shown dissolved oxygen at all levels of the water channels (Lewandowski et al. 1993). Nevertheless, anaerobic patches do form but are confined within the microcolonies (DeBeer et al. 1994). These channels may also effect the transport of bacteria to the surface and the degree of biofilm erosion and sloughing. The microcolonies themselves may be simple mounds or complex mushroom shapes (Costerton et al. 1995). Costerton (1995) asserts that the location, size, and shape of the biofilm microcolonies are determined by non-random species-specific factors. He postulates that the shape is in response to growth regulation through quorum-sensing and complex cell-cell interaction. Physical factors (e.g., flow), however, can also strongly influence the morphology of the biofilm (Korber et al. 1995). Furthermore, Wimpenny and Colastanti (1997) have recently suggested that biofilm structure is determined by substrate concentration. It is obvious that this is one area of biofilm research that needs further investigation.

Species composition ranges from simple, single species to complex, multiple species biofilms. The essential distinction is that the species are phenotypically different from their planktonic relatives (Costerton 1995). Certain genes involving attachment are only expressed when the cells come in contact with a surface. In an eloquent set of experiments, Davies and co-workers (1993) showed that genes involved in alginate synthesis in *Pseudomonas aeruginosa* were turned on within 5 min. of the cells attaching to a surface. In fact, there are a number of genes that are involved in biofilm formation that are not expressed when the cells are living planktonically (Costerton et al. 1995). Thus, some fundamental assumptions about bacteria which were made based on studies of planktonic species (i.e., liquid culture)

may not necessarily be true for biofilms. One example is antibiotic resistance (Stewart et al. 1996).

In multispecies biofilms, there is a patchwork of microcolonies of individual species embedded in EPS. Each microcolony is delineated by its own polysaccharide sheath. As the biofilm develops, microcolonies of several different species may come together forming functional consortia (Costerton and Lappin-Scott 1995). Thus the degradation of certain compounds which are recalcitrant to degradation by a single species may be facilitated by these consortia (James et al. 1995).

5 Future Directions

The recent advances in our understanding of microbial mats and biofilms has challenged many of the present concepts in microbial ecology which were based on the study of planktonic systems. The application of new technologies in their study has already resulted in new paradigms. It seems clear from the work done on biofilms that these processes cannot be modeled using a planktonic system (e.g., liquid culture). Thus basic fundamental questions (e.g., species composition and structural morphology, interspecies nutrient and genetic element transfer, antibiotic and metal resistance) need to be reevaluated. The development of the microstat (Caldwell et al. 1992) holds great promise, as it is now possible to create steady-state chemical gradients and monitor the colonization, formation, and activities of the biofilm on a surface over time. Confocal scanning laser microscopy provides a window to examine these systems live and at high resolution. Microelectrodes will continue to be used to provide high resolution profiles of temperature, pH, and oxygen (Revsbech 1994). The further development of fiber-optic electrodes (Kuehl et al. 1994) and specific species chemical electrodes (Revsbech 1994) will expand these capabilities. Identification and enumeration of microbial species will be assisted by DNA amplification techniques (e.g., polymerase chain reaction) and genetic-based probes (Muyzer et al. 1993; Devereux et al. 1992). Gene probes can also be used to monitor the activities at the genetic level (e.g., gene expression). To this end, the design of these probes has been aided by advances in DNA technologies. These new technologies have resulted in a rapidly expanding gene sequence data base including ribosomal sequences (e.g., 16s rRNA, 23s RNA). Lastly, access to this information is being greatly facilitated by the World Wide Web, as it provides easy access to web pages (e.g., Center for Biofilm Engineering, Montana State University) and data bases (e.g., Genbank, Swissprot.).

These methods may greatly enhance our studies of the role microorganisms play in sediment composition (e.g., mineral formation), their contribution to the sedimentary fabric (e.g., microstructure), and their role in the lithification process. Indeed, the current Research Initiative on Bahamian Stromatolites (RIBS) is employing such an integrated approach (Reid et al. 1995; Visscher et al. 1998). The community structure of these modern marine stromatolites is being studied by SEM, TEM and confocal laser microscopy, as well as traditional light and fluorescence microscopy. Specific physiological groups, such as sulfate reducing bacteria, are being enumerated by culture (i.e., most probable number) and molecular methods (i.e., 16S rRNA), and their in situ activities monitored by microelectrode and radioisotope studies (Visscher et al. 1998). This work has shown a direct link between biological processes and the formation of micritic horizons.

References

American Society for Microbiology (1996) Diversity in the microbial world – biofilms. CD-ROM, ASM Washington DC

Awramik SM (1984) Ancient stromatolites and microbial mats. In: Cohen Y, Castenholz RW, Halvorson HO (eds) Microbial mats: stromatolites. Alan R Liss Inc, New York, pp 1–22

Barbara GM, Mitchell JG (1996) Formation of 30- to 40- micrometer-thick laminations by high-speed marine bacteria in microbial mats. Appl Environ Microbiol 62:3985–3990

Caldwell DE, Korber DR, Lawrence JR (1992) Confocal laser microscopy and digital image analysis in microbial ecology. In: Marshall KC (ed) Advances in Microbial Ecology Vol 12, Plenum Press, New York, pp 1–67

Canfield DE, Des Marais DJ (1991) Aerobic sulfate reduction in microbial mats. Science 241:1471–1473

Characklis WG, Wilderer PA (eds) (1989) Structure and function of biofilms. Wiley Interscience, New York

Characklis WG, Marshall KC (eds) (1990) Biofilms. Wiley Interscience, New York

Cohen Y, Helman, Y, Sigalevich, P (1994) Light-driven sulfate reduction and methane emission in hypersaline microbial mats. In: Stal LJ, Caumette P (eds) Microbial Mats: Structure, Development, and Environmental Significance. NATO ASI Series G35, Springer, Berlin Heidelberg New York, pp 421–427

Cohen Y, Castenholz RW, Halvorson HO (eds) (1984) Microbial Mats: Stromatolites. Alan R Liss Inc., New York

Cohen Y, Rosenberg E (eds) (1989) Microbial mats: physiological ecology of benthic microbial communities. American Society for Microbiology, Washington DC

Cooney JJ, Laskin AI (1995) Introduction to the first issue on biofilms. J Indust Microbiol Biotech 15:135

Costerton JW (1995). Overview of microbial biofilms. J Indust Microbiol Biotech 15:137–140

Costerton JW, Geesey GG, Cheng K-J (1978) How bacteria stick. Sci Am 238:86–95

Costerton JW, Irvin RT, Cheng K-J (1981) The bacterial glycocalyx in nature and disease. Annu Rev Microbiol 35:299–324

Costerton JW, Cheng K-J, Geesey GG, Ladd TI, Nickel JC, Dasgupta M, Marrie TJ (1987) Bacterial biofilms in nature and disease. Annu Rev Microbiol 41:435–464

Costerton JW, Lappin-Scott HM (1995) Introduction to biofilms. In Lappin-Scott HM, Costerton JW (eds) Microbial biofilms. Cambridge University Press, Cambridge, pp 1–11

Costerton JW, Lewandowski Z, de Beer D, Caldwell, DE, James GA (1994) Biofilms, the customized niche. J Bacteriol 176:2137–2142

Costerton JW, Lewandowski Z, Caldwell DE, Korber DR, Lappin-Scott HM (1995). Microbial biofilms. Ann Revs Microbiol 49:711–745

Davies DG, Chakrabarty AM, Geesey GG (1993) Exopolysaccharide production in biofilms: substratum activation of alginate gene

expression by *Pseudomonas aeruginosa*. Appl Environ Microbiol 59:1181–1186
DeBeer D, Stoodley P, Roe, FL, Lewandowski Z (1994) Effects of biofilm structures on oxygen distribution and mass transport. Biotech Bioeng 43:1131–1138
DeWit R, Van Gemerden H (1987) Chemolithotrophic growth of the purple sulfur bacterium *Thiocapsa roseopersicina*. FEMS Mircrobiol Ecol 45:117–126
DeWit R, Jonkers HM, Van den Ende FP, Van Gemerden H (1989) In situ fluctuations of oxygen and sulfide in marine microbial sediment ecosystems. Neth J Sea Res 23:271–281
Devereux R, Kane MD, Winfrey J, Stahl DA (1992) 16 s rRNA hybridization of probes to describe natural communities of sulfate reducing bacteria. Syst Appl Microbiol 15:601–609
Geesey GG, Lewandowski Z, Fleming H-C (eds) (1993) Biofouling and biocorrosion in industrial water systems. Lewis Publishers, New York
Gilichinsky DA, Vorobyova EA, Erokhina LG, Fyodorov-Davydov DG, Chaikovskaya NR (1992) Long term preservation of microbial ecosystems in permafrost. Adv Space Res 12:255–263
Golubic S (1992) Microbial mats of Abu Dhabi. In: Margulis L, Olendzenski L (eds) Environmental evolution, MIT Press, Cambridge, MA, pp 103–130
James GA, Beaudette L, Costerton JW (1995) Interspecies bacterial interactions in biofilms. J Ind Microbiol Biotech 15:257–262
Jorgensen BB (1989) Light penetration, absorption, and action spectra in cyanobacterial mats. In: Cohen Y, Rosenberg E (eds) Microbial mats: physiological ecology of benthic microbial communities. American Society for Microbiology, Washington DC, pp 123–137
Koenig H, Stetter KO (1989) Extremely thermophilic S^0-metabolizers. In Staley JT, Bryant MP, Pfennig N, Holt JG (eds) Bergey's manual of systematic bacteriology. Williams and Wilkins, Baltimore, pp 2236
Korber DR, Lawrence JR, Lappin-Scott HM, Costerton JW (1995) Growth of microorganisms on surfaces. In: Lappin-Scott HM, Costerton JW (eds) Microbial Biofilms, Cambridge University Press, Cambridge, pp 15–44
Krumbein WE, Carius RT, Stal LJ (1991) On the interaction of two mat forming cyanobacteria *Microcoleus chthonoplastes* and *Oscillatoria limosa* and laboratory experiments on bundle formation and de novo genesis of microbial mats. Kieler Meeresforsch 8:145–151
Krumbein WE, Paterson DM, Stal LJ (eds) (1994) Biostabilization of Sediments. Bibliotheks und Informationssystem der Carl von Ossietzky Universitat, Oldenburg, 529 pp
Krumbein WE (1983) Stromatolites – challenge of a term in space and time. Precambrian Res 20:493–531
Krumbein WE (1994) The year of the slime. In: Krumbein WE, Paterson D, Stal LJ (eds) Biostabilization of sediments. Bibliotheks und Informationssystem der Carl von Ossietzky Universitat, Oldenburg, pp 1–7
Kuehl M, Lassen C, Jorgensen BB (1994) Optical properties of microbial mats: light measurements with fiber-optic microprobes. In: Stal LJ, Caumette P (eds) Microbial mats: structure, development, and environmental significance. NATO ASI Series G35, Springer, Berlin Heidelberg New York, pp 149–166
Lewandowski Z, Altobelli SA, Fukushima E (1993) NMR and microelectrode studies on the hydrodynamics and kinetics in biofilms. Biotech Prog 9:40–45
Lappin-Scott HM, Costerton JW (eds) (1995) Microbial biofilms. Cambridge University Press, Cambridge
Marshall KC (1976) Interfaces in microbial ecology. Harvard University Press, Cambridge, Mass
Marshall K (1984) Microbial adhesion and aggregation. Springer, Berlin Heidelberg New York
Marshall KC (1992) Biofilms: an overview of bacterial adhesion, activity, and control at surfaces. ASM News 58:202–207
Marshall KC, Stout R, Mitchell R (1971) Mechanisms of the initial events in sorption of marine bacteria to solid surfaces. J Gen Microbiol 68:337–348
Melo LF, Bott TR, Fletcher M, Capdeville B (1992) Biofilms – science and technology. Kluwer Academic Publishers, Dordrecht
Muyzer G, DeWaal EC, Uitterlinden AG (1993) Profiling of complex microbial populations by denaturing gradient gel electrophoresis analysis of polymerase chain reaction-amplified genes coding for 16 s rRNA. Appl Environ Microbiol 57:695–700
Neu TR (1994) Biofilms and microbial mats. In: Krumbein, WE, Paterson DM, Stal LJ (eds) Biostabilization of sediments. Bibliotheks und Informationssystem der Carl von Ossietzky Universitat, Oldenburg, pp 9–15
Nicholson JAM, Stolz JF, Pierson BK (1987) Structure of a microbial mat at Great Sippewissett Marsh, Cape Cod, Massachusetts. FEMS Microbiol Ecol 45:343–364
Parsons TR, Takahashi M, Hargrave B (1988) Biological oceanographic processes, 3rd edn. Pergamon Press, New York
Pierson BK, Oesterle A, Murphy G (1987) Pigments, light penetration, and photosynthetic activity in the multi-layered microbial mats of Great Sippewissett Salt Marsh, Massachusetts. FEMS Microbiol Ecol 45:365–376
Reid RP, Macintyre IG, Brown KM, Steneck RS, Miller T (1995) Modern marine stromatolites in the Exuma Cays, Bahamas: uncommonly common. Facies 33: 1–8
Revsbech NP, Jorgensen BB (1986) Microelectrodes: their use in microbial ecology. Adv Microbial Ecol 9:293–352
Revsbech NP (1994) Analysis of microbial mats by use of electrochemical microsensors: recent advances. In: Stal LJ, Caumette P (eds) (1994) Microbial mats: structure, development, and environmental significance. NATO ASI Series G35, Springer, Berlin Heidelberg New York, pp 135–148
Riding RR (1994) Stromatolite survival and change: The significance of Shark Bay and Lee Stocking Island subtidal columns. In: Krumbein WE, Paterson DM, Stal LJ (eds) Biostabilization of sediments. Bibliotheks und Informationssystem der Carl von Ossietzky Universitat, Oldenburg, pp 183–202
Schopf JW (ed) (1983) Earth's earliest biosphere, its origin and evolution. Princeton University Press, Princeton
Schopf JW, Klein C (eds) (1992) The proterozoic biosphere, a multidisciplinary study. Cambridge University Press, New York
Shulz HN, Jorgensen BB, Fossing HA, Ramsing NB (1996) Community structure of filamentous, sheath-building sulfur bacteria, *Thioploca* spp off the coast of Chile. Appl Environ Microbiol 62:1855–1862
Stal LJ, van Gemerden H, Krumbein WE (1985) Structure and development of a benthic microbial mat. FEMS Microbiol Ecol 31:111–125
Stal LJ, Caumette P (eds) (1994) Microbial mats: structure, development, and environmental significance. NATO ASI Series G35, Springer, Berlin Heidelberg New York
Stewart PS, Hamilton MA, Goldstein B, Schneider BT (1996) Modeling biocide action against biofilms. Biotech Bioeng 49:445–455
Stolz JF, Botkin DB, Dastoor MN (1989) The integral biosphere. In: Rambler MB, Margulis L, Fester R (eds) Global ecology: towards a science of the biosphere. Academic Press, San Diego, pp 31–50
Stolz JF (1990) Distribution of phototrophic microbes in the flat laminated microbial mat at Laguna Figueroa, Baja California, Mexico. BioSystems 23:345–357
Stolz JF (1991) The ecology of phototrophic bacteria. In: Stolz JF (ed) Structure of phototrophic prokaryotes. CRC Press, Boca Raton, pp 105–123
Thiele JH, Zeikus JG (1988) Control of interspecies electron flow during anaerobic digestion: role of floc formation in syntrophic methanogenesis. Appl Environ Microbiol 54:10–19
Visscher PT, Prins RA, Van Germerden H (1992) Rates of sulfate reduction and thiosulfate consumption in a marine microbial mat. FEMS Microbiol Ecol 86:283–294
Visscher PT, Reid RP, Bebout BM, Hoeft SE, Macintyre IG, Thompson J Jr. (1998) Formation of lithified micritic laminae in modern marine stromatolites (Bahamas): the role of sulfur cycling. American Mineralogist 83: 1482–1491
Walter MR (ed) (1976) Stromatolites. Elsevier/North-Holland Publishing Co., Amsterdam
Ward DM, Weller R, Shiea J, Castenholz RW, Cohen Y (1989) Hot spring microbial mats: anoxygenic and oxygenic mats of possible evolutionary significance. In: Cohen Y, Rosenberg E (eds) Microbial mats: physiological ecology of benthic microbial communities. American Society for Microbiology, Washington DC, pp 3–15

Ward DM, Ferris MJ, Nold SC, Bateson MM, Kopczynski ED, Ruff-Roberts AL (1994) Species diversity in hot springs microbial mats as revealed by both molecular and enrichment culture approaches – relationship between biodiversity and community structure. In: Stal LJ, Caumette P (eds) Microbial mats: structure, development, and environmental significance. NATO ASI Series G35, Springer, Berlin Heidelberg New York, pp 33–44

Wimpenny JWT, Colastanti R (1997) A unifying hypothesis for the structure of microbial biofilms based on cellular automaton models. FEMS Microbiol Ecol 22:1–16

Wolfaardt GM, Lawrence JR, Roberts RD, Caldwell DE (1994) The role of interactions, sessile growth, and nutrient amendments on the degradative efficiency of a microbial consortium. Can J Microbiol 40:331–340

Zobell CE (1943) The effect of solid surfaces upon bacterial activity. J Bac 46:39–56

Exopolymer Microdomains as a Structuring Agent for Heterogeneity Within Microbial Biofilms

Alan W. Decho

Department of Environmental Health Sciences, School of Public Health, University of South Carolina, Columbia, SC 29208, USA

Abstract. It is now well-recognized that the majority, and often most active fractions, of microbial cells in many natural systems occur as surface-associated biofilms. In sedimentary environments, biofilm formation represents an important functional adaptation for microbial life. At the level of an individual sediment particle, the biofilm community represents a cacophony of cellular and extracellular processes enclosed within an amorphous biofilm. Recent studies using new analytical approaches now suggest that the seemingly amorphous biofilm instead may be a highly structured system, one in which microbial cells actively manipulate their extracellular polymers and overall microenvironment to accomplish specific tasks. At microspatial scales (nanometers to micrometers), biofilm polymers are important in sequestering of nutrients, localization of extracellular enzymes, and providing a protective and stabilizing microenvironment for cells. Examination of the three-dimensional nature of microbial biofilm communities and activities through the use of nuclear magnetic resonance (NMR) spectroscopy, confocal laser microscopy (CLM), atomic-force microscopy (AFM) and other techniques are beginning to provide quantitative evidence for microscale partitioning within biofilms. In light of these new data, the biofilm is explored here as an important structural matrix to partition microbial extracellular activities and effectively promote heterogeneity over very small (i.e., molecular) spatial scales. Structuring and partitioning may occur through the formation of "exopolymer-mediated microdomains." These are regions of a biofilm matrix where specific types of exopolymers are concentrated and impart unique physical/chemical properties to the biofilm. Accumulating evidence, derived from isotope sorption studies, electron microscopy, and CLM supports this idea. The presence of exopolymer microdomains may provide microorganisms with a structuring mechanism to spatially segregate extracellular activities over small spatial scales.

1 Introduction

The biofilm is a common feature of microorganisms in nature and consists of cells surrounded by a matrix of extracellular polymeric molecules or "exopolymers." It is now recognized that the majority, and often most active fractions, of microbial cells living under a wide range of conditions occur within biofilms. These are found as aquatic microbial communities on particle surfaces and suspended aggregates, dental caries on teeth, fouling on medical devices and infections, and microbially mediated metal corrosion. It is now thought that microbial cells in these very diverse systems utilize similar biofilm mechanisms (Costerton et al. 1995). The biofilm may represent a distinct growth phase of bacteria, differing fundamentally from planktonic forms from the same species.

In aquatic sediments, microbial biofilms are a ubiquitous and biogeochemically important feature (see Decho 1990 for review). They commonly occur on the surfaces of sediment and detrital particles and rapidly form on virtually any new surface placed in sediments. The exopolymer matrix of the biofilm secures the attachment of cells to the surface of a sediment particle. The collective actions of exopolymer secretions acts as a cohesive "glue" to bind sediment particles together. The macroscale effects of excessive biofilm mucilage secretion and cohesion have been observed in diatomaceous microbial mats. Here thick exopolymer secretion occurs and greatly reduces the suspension of underlying sediment material during periods of high currents or wave action (Dade et al. 1990; Underwood and Paterson 1993).

Exopolymers have potentially important roles in the structuring and maintenance of activities within microbial mat systems. In these systems, sharp geochemical gradients develop over very small (micrometer) spatial scales and originate from the concentrated activities of specific microbial groups within mat layers (Jørgensen and Des Marais 1990). The diffusion-slowing properties of exopolymers stabilize and even sharpen geochemical gradients, and may constitute an important adaptive feature for microbial groups within mats. The secretion of exopolymers by microbial cells in sediment systems is perhaps as old as life itself. The earliest remnants of life on earth, present as stromatolite fossils, were formed by cyanobacterial cells enclosed within an exopolymer biofilm. The biofilm-forming organisms involved in stromatolite formation were the dominant life form for over 85% of the history of life on earth (Grotzinger 1990).

The importance of the biofilm to sediment bacteria (and any other bacterial cells) lies in its ability to form an external "microbial microenvironment." The biofilm matrix allows microbial activities to operate more efficiently and remain robust under adverse conditions. The stabilizing properties of exopolymers serve many functions which enhance the ability of cells to survive and metabolize under the frequently fluctuat-

R. E. Riding and S. M. Awramik (Eds.)
Microbial Sediments

ing physical/chemical conditions which characterize natural sediment systems.

2 Emerging View of Microbial Biofilms

Our understanding of biofilm processes has significantly changed during recent years, owing to the applications of new techniques to biofilm research. The important pioneering works by J.W. Costerton and G.G. Geesey (Costerton et al. 1978, 1994, 1995), and more recently, D.E. Caldwell, J.R. Lawrence and colleagues (Caldwell et al. 1992; Korber et al. 1993; Lawrence et al. 1991, 1994; Lewandowski et al. 1993; Wolfaardt et al. 1994a,b), have posited the idea that the biofilm matrix is a highly structured and heterogeneous microenvironment, which cells can potentially manipulate over both spatial and temporal scales.

When observed using conventional light or electron microscopy techniques the exopolymer matrix of a biofilm, at first glance, may appear as an amorphous matrix composed primarily of polysaccharidic macromolecules. Polymeric molecules are copiously secreted around cells which appear to be randomly distributed within the matrix. Recent investigations using confocal laser microscopy (CLM) have examined in situ biofilms and have revealed a very different view regarding the arrangement of microbial cells within biofilms (Figs. 1, 2). CLM allows the investigator to "optically section" an intact biofilm at vertical intervals approximating 0.2 μm (Caldwell et al. 1992). Careful statistical examination of spatial patterns of bacterial cells within biofilms have shown that cells are arranged, not randomly, but often in aggregated (i.e., clumped) distributions within the exopolymer matrix (Korber et al. 1993). The areas of high cell concentrations and high microbial activities are often adjacent to sparsely populated areas, having much exopolymer and relatively few cells. A very interesting and highly relevant observation from this study was that microbial cells can be motile within an exopolymer matrix and adjust their position relative to each other within the biofilm. It was previously thought that once cells were anchored within the biofilm, their positions were relatively fixed. The ability to move within the exopolymer matrix provides microbial cells with the ability to optimize nutrient gathering and also avoid toxic compounds which have been sequestered within certain parts of the biofilm. An overall result of movement will be the ability of cells to optimize their locations within a biofilm.

A second important function of the biofilm matrix is in mediating the extracellular processing of organic matter by microbial cells. Most bacteria are osmotrophs, obtaining nutrients from the dissolved phase. Many exopolymers may act as a "sorptive sponge" to sequester dissolved organic molecules (DOM), especially large organic molecules. Exopolymers are chemically diverse and may contain a range of functional groups which can potentially sequester ions and molecules. These include carboxyl, hydroxyl and amine groups and *O*-acetyl, *O*-methyl and pyruvate ketal groups (Geesey and Jang 1989). These groups may act to chelate and concentrate DOM and possibly even colloids from the overlying water or sediment porewater. Extracellular enzymes, which are localized within the matrix, then hydrolyze large DOM to smaller oligomeric or monomeric forms (i.e., amino acids, peptides, sugars, etc.), which can be directly taken up by cells. Movement of molecules through the exopolymer matrix should occur largely via diffusion processes. In general, smaller molecules can diffuse through a biofilm more rapidly than larger molecules, probably due to greater charge densities and generally stronger sorption (Christensen and Characklis 1990). The binding

Fig. 1. The emerging view of a biofilm, constructed from observa-

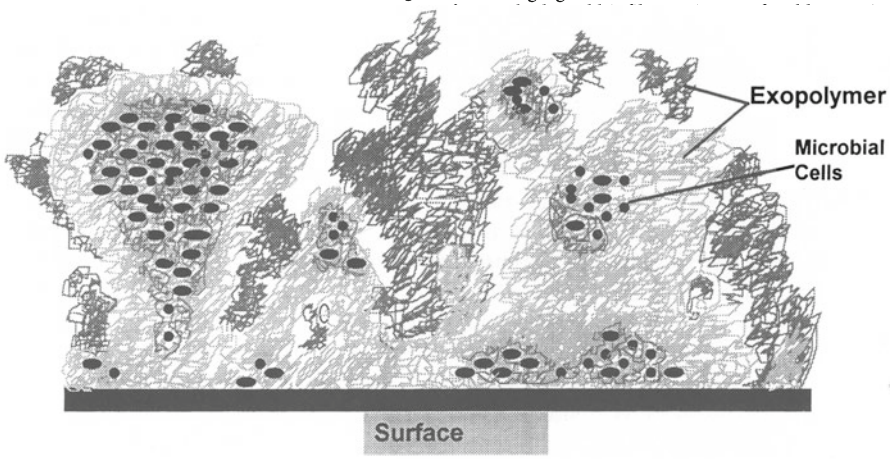

oscopy see ace is chan- he ma- en- ocesses n. Mi- ed, not gious nt of enced ors. eatly . The biofilm bility to ents from water phases

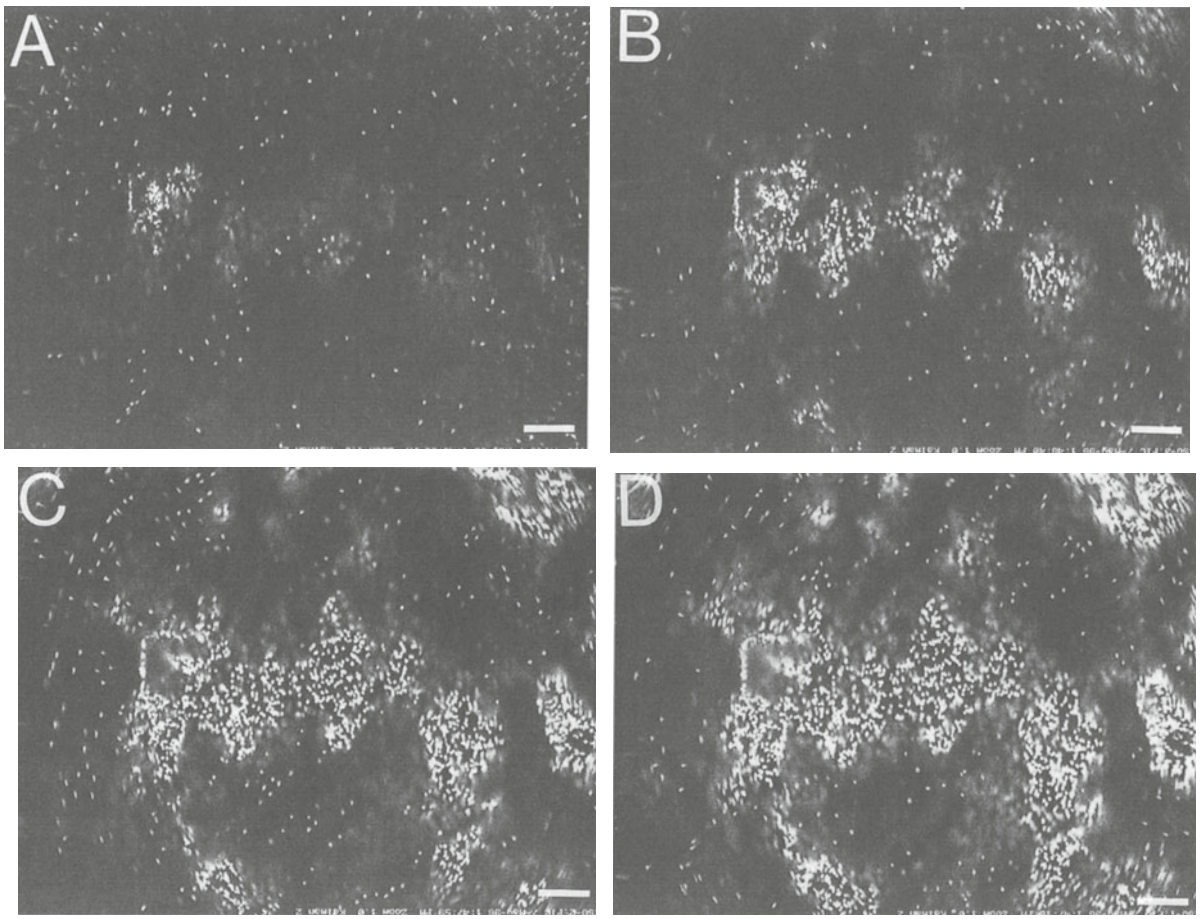

Fig. 2A–D. Confocal laser micrographs showing aggregated distribution and three-dimensional heterogeneity of cells within a biofilm. The biofilm was produced by the marine bacterium *Alteromonas atlantica*, in the presence of 50 mg/l Cr(III). Each micrograph represents a horizontal "optical section" taken at different focal depths within the same biofilm. **A** Biofilm surface to 1.5 μm; **B** 1.5–3.0 μm depth; **C** 3.0–4.5 μm; **D** 4.5–6.0 μm depth. Note how the distribution of cells becomes more aggregated with depth in the biofilm. Bacteria cells were stained with SYTO-16 (Molecular Probes Inc.) fluorescent stain (excitation = 488 nm; emission = 530 nm). *Scale* bars = 10 μm

and diffusion of monomers through a biofilm matrix is often quite variable and depends on the type of biofilm matrix (Siegrist and Gujer 1985; Lawrence et al. 1994). Diffusion of ions such as chlorine and copper (Cu^{2+}) has also been examined (Chen et al. 1993; Chen and Stewart 1996). Experimental evidence has indicated that biofilm polymers appear to facilitate diffusion of smaller molecules and ions. The most rapid diffusion coefficients often approach those of water. Therefore, the binding of larger DOM and the diffusion-slowing effects on smaller molecules by exopolymers facilitates more efficient processing of dissolved organic matter than adjacent areas. Recent studies have further suggested that the presence of cells within the biofilm matrix may affect ion penetration rates (Chen and Stewart 1996). Also, convective processes, enhanced by microchannels in biofilms, may additionally increase the efficiency of mass transfer through a biofilm (Costerton et al. 1994). Nuclear magnetic resonance (NMR) studies have demonstrated that physical channels permeate polymers (Lewandowski et al. 1993). Studies using CLM examining motile and nonmotile strains of a single bacterium, *Pseudomonas fluorescens*, showed that biofilms containing motile strains had abundant channels permeating the biofilm (Korber et al. 1993). It was suggested that these channels may facilitate diffusive exchange to deeper areas of the biofilm, which would be otherwise diffusion-limited (Siegrist and Gujer 1985; Lawrence et al. 1994).

The sediment biofilm also acts as a protective buffering microenvironment for cells. The extracellular environment in proximity to most free-living microbial cells is characterized by frequent fluctuations in environmental parameters such as osmotic conditions (i.e., salinity), micrometer-scale pH changes (due to high activities of microorganisms), and nutrient fluxes. These fluctuations have the potential to stress both microbial cells and the activities of their extracellular enzymes.

Biofilms buffer bacteria against the fluctuating and less than ideal conditions typical of natural systems (Sutherland 1980). The physical/chemical properties of exopolymers may act as a protective matrix from which cells may conduct physiological activities under more stabilized conditions than their free-living counterparts (Costerton et al. 1987). Enlightening evidence from the study of sediment biofilms in riverine systems, by Lock and colleagues, have indicated that bulk microbial cellular activities within biofilms remain stabilized even when significant nutrient fluctuations occurred in the overlying waters (Freeman and Lock 1995). This was probably due to concentration and storage of organic matter by biofilm exopolymers. The overall effect of the biofilm should result in generally higher and more constant microbial activities over time when compared with free-living cells in the overlying water. Currently, it is not understood how the potential protective and stabilizing effects of sediment biofilms affect activities of extracellular enzymes. Extracellular enzymatic hydrolysis of larger DOM to smaller forms is an important ecological process in the transformation of organic matter (Hoppe 1991). Extracellular enzymes associated with biofilms may remain active (i.e., protected from denaturation) for longer periods than enzymes released into the surrounding porewater. The exopolymer matrix may provide a more suitable ionic environment for enzymes.

Exopolymers also chelate potentially toxic compounds thereby reducing toxic exposure of cells. Metals, for example, are both a natural component and anthropogenic contaminant in sediments. Metals interact with sediment exopolymers in several potentially important ways. First, metal-exopolymer interactions may directly affect sediment stability. The physical properties of exopolymers (loose-slime vs gel) are strongly influenced by the types (and concentrations) of metals and other ions present (Parker et al. 1996). Alkali earth elements (e.g., Ca^{2+} and Mg^{2+}) form bidentate complexes, which generally form bridges between two adjacent polysaccharide molecules in an exopolymer matrix and contribute to their gel structure. These cations are competitively displaced, however, by transition metal ions, which often bind more tightly to the exopolymer matrix (Geesey and Jang 1989). Sorption of transition metals to exopolymers may result in the formation of more stable multidentate complexes. In these types of complexes, a metal cation forms a bridge with several (e.g., three or more) anionic ligands on adjacent exopolymer molecules (Decho 1994). Multidentate complexes generally show greater stability than bidentate complexes, formed with Ca and Mg (Geesey and Jang 1989). The overall effect of this will be to "shrink" the exopolymer matrix (Parker et al. 1996; Geesey and Jang 1989; Geesey et al. 1992) and possibly make the exopolymer more cohesive. Metal binding by exopolymers acts as a first line of defense to reduce concentrations of toxic transition metals reaching microbial cells.

A second important exopolymer-mediated activity, however, may involve the interactions of metals with extracellular enzymes. Exopolymers, in addition to being sites for binding and concentration of toxic metal ions, are also sites for the localization and concentration of extracellular enzymes (Sutherland 1980). Localization of these important organic molecules with potentially toxic metals in the same polymer matrix represents an apparent functional dilemma to the biofilm. The binding of metals often inactivates enzymes, either by blocking essential functional groups on the enzyme, displacing an essential metal ion already present in the enzyme, or modifying the active conformation of the enzyme (Babich et al. 1985). Given the large number of cellular and extracellular processes which simultaneously occur within a biofilm, the activities of one process may potentially interfere with the activities of other processes. For example, extracellular enzyme activities may be adversely affected by the sequestration of toxic metals. Currently, it is not known if extracellular enzymes are able to remain functional even when high concentrations of metals are present in the exopolymer matrix, or if enzymes may be excluded from metal-rich regions of the biofilm. This would require the exopolymer matrix to physically or chemically partition extracellular activities at molecular scales within the biofilm. This represents an important and exciting area of investigation in understanding how the exopolymer matrix may mediate microbial extracellular processes, especially in the presence of contaminants.

3 The Idea of Exopolymer "Microdomains"

The idea that the exopolymer matrix is not homogeneous throughout, but rather exists as a series of "microdomains" or microregions (Fig. 2) having different physical/chemical properties at the molecular scale, is derived from research on the structure of gels. A gel is formed by a three-dimensional network (i.e., polymer) and a solvent (i.e., water). The water prevents collapse of the network and entraps the solvent (Tam and Verdugo 1981; Verdugo 1984).

The physical/chemical basis for exopolymer microdomains is derived from information on polysaccharide gels. Chemists studying gel formation and stability have long understood that molecular heterogeneity exists within a gel, even when the gel is composed of a single type of polysaccharide. Polysaccharide conformations within a gel consist of "highly-ordered" and "highly-disordered" regions, having very different physical/chemical properties at a molecular scale (Rees et al. 1982). Studies using nuclear magnetic resonance (NMR) and circular dichroism (CD) have shown that

the more highly ordered regions tend to be hydrophobic while less-ordered regions are more hydrophilic. This has led polysaccharide chemists to view the gel as a collection of physical/chemical "microdomains." The unique physicochemical properties of a gel therefore result from the sum of its component microdomains.

3.1 Physical/Chemical Basis for Microdomains in Exopolymers

Exopolymers in natural sediment biofilms often consist of a range of different types of exopolymer molecules acting in concert. Compositional analyses of exopolymers derived from laboratory cultures demonstrate that even a single strain of bacterium may secrete several types of polymeric molecules, each having different physical/chemical properties. Cells may directly control the physical state of the biofilm by different types of polymer molecules which are secreted by them. Cells may indirectly control the biofilm matrix after secretion via extracellular enzymes. The physical (i.e., gel vs solution) state of exopolymers may be modified by extracellular enzymes localized within the exopolymer matrix (Alsop 1983). The bacterium *Leuconostoc mesenteroides* secretes a homogeneous exopolymer, dextran, composed of glucose monomers linked by either $\beta 1-4$ or $\alpha 1-3$ linkages. The bacterium will secrete copious amounts of this polymer in batch culture at 22 °C. At slightly higher temperatures, however, the polymer is rapidly degraded by extracellular enzymes. This represents an enzymatically mediated decomposition of polymers by the same microbial cells which secrete the polymer. Atomic-force microscopy (AFM) has been used to examine the molecular structure of bacterial biofilms (Blackford and Jericho 1991; Bremer et al. 1992). The studies are beginning to reveal how the molecular structure of exopolymers may impart physical stability to the biofilm.

3.2 Hydrophobic Microdomains

In sediment biofilms, hydrophobic microdomains will be important in the association of hydrophobic molecules, such as pesticides, with biofilms (Wolfaardt et al. 1994b) and in the trophic availability of these molecules. Hydrophobic microdomains occur largely due to differences in the nature and densities of cation bridges between adjacent polysaccharide molecules. Because areas of concentrated bridging often lead to a reduction in hydration, polysaccharide chemists have termed these areas "hydrophobic microdomains." The formation of exopolymer microdomains may result from the inherent physical/chemical properties of the exopolymers themselves (Neu 1996). Polyionic gels made of ampiphilic polymers (i.e., having both polar and nonpolar groups) can contain large hydrophobic domains. This occurs through the shielding effects of Ca^{2+} cations in natural polyelectrolyte gels, and stabilizes gel networks and promotes their condensation (Verdugo 1984). Exopolymers isolated from bacteria are known to contain a range of ampiphilic polymers (see Neu 1996 for review).

3.3 Enzyme Microdomains

In order for microbial cells to derive a net gain of C or N from a biofilm to act as a nutrient sequestering microenvironment, extracellular enzymes (and their hydrolysis products) must remain relatively close to cells so that diffusive transfer to cells of hydrolysis products can operate efficiently. Localization of extracellular enzymes close to microbial cells, within confined exopolymer-mediated microdomains, is a potentially useful strategy. Many enzymes require a relatively stable ionic and pH environment to function efficiently (Hoppe 1991). The exopolymer microenvironment can provide a stable domain for extracellular enzymes to function efficiently outside of the cell. Localization within exopolymers may prolong the activities of enzymes and prevent their denaturation.

3.4 Metal-Extracellular Enzyme Interactions

Initial work suggests that the abundances of hydrophobic microdomains increase as exopolymers bind higher concentrations of metals. Metal binding to polysaccharides often occurs through hydrolysis reactions, resulting in the release of water (Geesey and Jang 1989). Metal binding may also change the physical state of exopolymers by condensing their tertiary structure. In contrast, many enzymes require highly hydrated environments in order to function (Hoppe 1991). Therefore, during efficient biofilm functioning, toxic metal-sequestering exopolymers may be localized in separate domains that are further from cells, while enzymes may be found in domains in proximity to cells. This would be possible if different types of exopolymer molecules were used to localize extracellular enzymes, while other exopolymer molecules (e.g., carboxyl-rich) were used to preferentially bind metals. Such a mechanism would allow extracellular enzymes to function in the presence of high metals, while keeping toxic metals away from active cellular domains.

Certain extracellular processes, such as binding of toxic metals to exopolymers, may potentially interfere with other processes, such as extracellular enzyme activities. One possible way around this is to partition these activities between different parts of the biofilm. Extracellular enzyme activities may be concentrated

close to cells while toxic metal binding may be concentrated by other ligands away from these areas. Preliminary evidence for such partitioning is beginning to emerge from electron microscopy observations, coupled with energy-dispersive spectroscopy (EDS) of metal-exposed biofilms (Decho, unpublished). These studies suggest that concentrations of bound metals by the exopolymer matrix differ depending on their relative locations to cells. Areas closest to cells have generally lower concentrations of metals than areas further away from cells.

Sorption experiments examining the binding of DOMs to specific types of polymeric molecules (i.e., alginate, dextran, etc.) indicate that the compositional properties of the exopolymer strongly influences the binding of organic molecules to the matrix (Decho, unpublished). Secretions of a specific type of polymer within a confined area of the biofilm can result in the sorptive concentration of specific types of molecules within those areas (i.e., microdomains) of the biofilm matrix. Thus, hydrophobic compounds may bind and accumulate within an otherwise hydrophilic matrix. Studies of bacterial strains derived from sewage-treatment flocculation systems show that it is possible for cells to manipulate the types and relative quantities of each type of exopolymer molecule. The relative proportions of each type of polymeric molecule will collectively influence the physical/chemical properties of the biofilm matrix. This implies that regions of the biofilm may accomplish certain functional tasks, such as protection against metals, sequestering of nutrients and localization of extracellular enzymes.

4 Conclusion

The sediment environment contains areas of high microbial activity, much of which occurs within biofilm microenvironments on particulate surface coatings. Within a biofilm, there can be considerable heterogeneity in extracellular activities, many of which occur simultaneously and are mediated by exopolymers. The presence of specific exopolymer microdomains is postulated here and has far reaching implications. Microdomains allow different tasks (e.g., extracellular activities) to be efficiently conducted in close proximity to each other, while minimizing antagonistic interferences from other activities. An example of two such antagonistic activities in biofilms which may occur in proximity is metal sequestration and organic matter hydrolysis by extracellular enzymes. High concentrations of metals could potentially inactivate extracellular enzymes within a biofilm. The microbial biofilm appears to be composed of different exopolymers able to form separate microdomains. Exopolymer microdomains have the potential to segregate extracellular activities at molecular scales and to facilitate more efficient functioning of biofilm activities.

References

Alsop RM (1983) Industrial production of dextrans. Prog Indust Microbiol 18:1–44

Babich H, Devanas MA, Stotzky G (1985) The mediation of mutagenicity and clastogenicity of heavy metals by physicochemical factors. Environ Res 37:253

Blackford BL, Jericho MH (1991) Scanning tunneling microscope imaging of hoops from the cell sheath of the bacteria *Methanospirillum hungatei* and atomic force microscopy imaging of complete sheaths. J Vac Sci Technol B9:1242–1247

Bremer PJ, Geesey GG, Drake B (1992) Atomic force microscopy examination of the topography of a hydrated bacterial biofilm on a copper surface. Curr Microbiol 24:223–230

Caldwell DE, Korber DR, Lawrence JR (1992) Imaging of bacterial cells by fluorescence exclusion using scanning confocal laser microscopy. J Microbiol Methods 15:249–261

Chen D and Stewart PS (1996) Chlorine penetration into artificial biofilm is limited by a reaction-diffusion interaction. Environ Sci Technol 30:2078–2083

Chen D, Lewandowski Z, Roe F, Surapaneni P (1993) Diffusivity of Cu^{2+} in calcium alginate gel beads. Biotechnol BioEngineer 41:755–760

Christensen BE, Characklis WG (1990) Physical and chemical Properties of biofilms. In: Characklis WG, Marshall KC (eds) Biofilms. John Wiley and Sons, New York, pp 93–130

Costerton JW, Geesey GG, Cheng KJ (1978) How bacteria stick. Sci Am 238:86–95

Costerton JW, Lewandowski Z, Caldwell DE, Korber DR, Lappin-Scott HM (1995) Microbial biofilms. Annu Rev Microbiol 49:711–745

Dade WB et al. (1990) Effects of bacterial exopolymer adhesion on the entrainment of sand. Geomicrobiol J 8:1–16

Decho AW (1990) Microbial exopolymer secretions in ocean environments: their role(s) in food webs and marine processes. Oceanogr Mar Biol Annu Rev 28:73–153

Decho AW (1994) Molecular-scale events influencing the macroscale cohesiveness of exopolymers. In: Krumbein WE, Paterson DM, Stal LJ (eds) Biostabilization of sediments. Bis/Verlag, Oldenburg, Germany, pp 135–148

Freeman C, Lock MA (1995) The biofilm polysaccharide matrix: a buffer against changing organic substrate supply? Limnol Oceanogr 40:273–278

Geesey GG, Jang L (1989) Interactions between metal ions and capsular polymers. In: Beveridge TJ, Doyle RJ (eds) Metal ions and bacteria. John Wiley and Sons, NewYork, pp 325–358

Geesey GG, Bremer PJ, Smith JJ, Muegge M, Jang LK (1992) Two-phase model for describing the interactions between copper ions and exopolymers from *Alteromonas atlantica*. Can J Microbiol 38:785–793

Grotzinger JP (1990) Geochemical model for Proterozoic stromatolite decline. Am J Sci 290-A:80–103

Hoppe HG (1991) Microbial extracellular enzyme activity: a new key parameter in aquatic ecology. In: Chrost RJ (ed) Microbial enzymes in aquatic environments. Springer, Berlin Heidelberg NewYork, pp 60–95

Jørgensen BB, Des Marais DJ (1990) The diffusive boundary layer of sediments: oxygen microgradients over a microbial mat. Limnol Oceanogr 35:1343–1355

Korber DR, Lawrence JR, Hendry MJ, Caldwell DE (1993) Analysis of spatial variability within Mot+ and Mot– *Pseudomonas fluorescens* biofilms using representative elements. Biofouling 7:339–358

Lawrence JR, Korber DR, Hoyle BD, Costerton JW, Caldwell DE (1991) Optical sectioning of microbial biofilms. J Bacteriol 173:6558–6567

Lawrence JR, Wolfaardt GM, Korber DR (1994) Determination of diffusion coefficients in biofilms using confocal laser microscopy. Appl Environ Microbiol 60:1166–1173

Lewandowski Z, Altobelli SA, Fukushima E (1993) NMR and microelectrode studies of hydrodynamics and kinetics in biofilms. Biotech Prog 9:40 – 45

Neu TR (1996) Significance of bacterial surface-active compounds in interaction of bacteria with interfaces. Microbiol Rev 60:151 – 166

Parker DL, Schram BR, Plude JL, Moore RE (1996) Effect of metal cations on the viscosity of a pectin-like capsular polysaccharide from the cyanobacterium *Microcystis flos-aquae* C3 – 40. Appl Environ Microbiol 62:1208 – 1213

Rees DA, Morris ER, Thom D, Madden JK (1982) Shapes and interactions of carbohydrate chains. In: Aspinall GO (ed) The polysaccharides. Academic Press, New York, pp 196 – 291

Siegrist H, Gujer W (1985) Mass transfer mechanisms in a heterotrophic biofilm. Water Res 19:1369 – 1378

Sutherland IW (1980) Polysaccharides in the adhesion of marine and freshwater bacteria. In: Derkeley RCW et al. (eds), Microbial adhesion to surfaces. Ellis-Horwood, London, pp 228 – 329

Tam PY, Verdugo P (1981) Control of mucus hydration as a Donnan equilibrium process. Nature 292:340 – 342

Underwood JC, Paterson DM (1993) Seasonal changes in diatom biomass, sediment stability and biogenic stabilization in the Severn estuary. J Mar Biol Assoc UK 73:871 – 887

Verdugo P (1984) Hydration kinetics of exocytosed mucins in cultured secretory cells of the rabbit trachea: a new model. Ciba Foundation London 109:212 – 234

Wolfaardt GM, Lawrence JR, Robarts RD, Caldwell DE (1994a) Multicellular organization in a degradative biofilm community. Appl Environ Microbiol 60:434 – 446

Wolfaardt GM, Lawrence JR, Headley JV, Robarts RD, Caldwell DE (1994b) Microbial exopolymers provide a mechanism for bioaccumulation of contaminants. Microb Ecol 27:279 – 291

On Stromatolite Lamination

Lee Seong-Joo[1], Kathleen M. Browne[2], Stjepko Golubic[3]

[1] Department of Earth System Sciences, Yonsei University, Seoul 120-749, Korea
[2] Department of Geological and Marine Sciences, Rider University, Lawrenceville, NJ 08648-3099, USA
[3] Department of Biology, Boston University, 5 Cummington Street, Boston, MA 02215, USA

Abstract. Causes of lamination, the most salient property of stromatolitic structures, are examined in terms of sedimentary kinetics and stasis using case histories of modern stromatolite-building biota from the Bahama Carbonate Platform, Great Sippewissett Salt Marsh of New England, and Hamelin Pool, Shark Bay, Australia. The findings are compared with fossil evidence preserved in silicified Mesoproterozoic stromatolites of the Gaoyuzhuang Formation, northern China. Multitrichomous cyanobacteria and their responses to sedimentation characterize the conditions of fluctuating sedimentation rates, whereas coccoid cyanobacteria colonize and stabilize sediments during periods of sedimentary stasis.

1 Introduction

Today, the definition of the term "stromatolites" is generally accepted as: laminated organo-sedimentary structures produced by trapping and binding and/or precipitating of mineral matter resulting from metabolic activities of microorganisms (see Awramik et al. 1976). This definition is consistent with the original definition of the term as introduced by Kalkowsky (1908), which included the genesis of these structures, implying microbial origins. The definition excludes similar laminated sediments and rocks that result from rhythmic deposition in the absence of microorganisms as organizing elements. For practical reasons, it also excludes similar formations recognizable as skeletons of particular encrusting metaphytes and metazoans, such as laminated calcareous rhodophytes (e.g., rhodolites), bryozoans, worms, corals and others. The term, so defined, requires some evidence of microbial participation in stromatolite formation, thus posing considerable difficulties for interpretation of ancient examples where such evidence may have been diagenetically obliterated. The same limitation applies to the sedimentary component originally involved in stromatolite formation.

In view of objective limitations to the study of fossil stromatolites, an understanding of stromatolite genesis has been sought through the quest for modern analogues where the stromatolite-building microbiota could be studied in action. Extrapolations from modern comparative studies to ancient conditions, however, have other limitations. They are often hampered by the complexity of modern ecosystems dominated by diversified communities of eukaryotic micro- and macroorganisms. Eukaryotic organisms have, in the course of the Phanerozoic, either replaced or incorporated the ancient prokaryotic microbes that once constructed stromatolites, leaving stromatolites to form only in restricted environments. In addition, selective preservation has left an uneven field for modern-to-fossil comparisons.

The current contribution presents several case histories, including modern and ancient settings, that illustrate the complexities in stromatolite formation in conjunction with changing sedimentary conditions.

2 Causes of Stromatolite Lamination

To understand the genesis of a stromatolite, it is important to understand the genesis of its most salient feature, the laminated internal structure. Lamination always records some kind of past temporal oscillations either in microbial activities or in sedimentation. The distinction between laminae depends on the degree of any kind of discontinuity in the process of their formation. Thus, a model envisioning continuous microbial growth under constant sedimentation would produce no lamination.

Microbial processes in live and growing stromatolites are largely confined to the top 1–10 mm thick layer at the sediment-water interface, where the highest rates of microbial growth and metabolic activities take place. As sediment accumulates, both the sediment-water interface and the microbial action move upward. Therefore, a fossil stromatolite is viewed as the cumulative sedimentary record of microbial mat activities over time (Hofmann 1969). These considerations place a growing stromatolitic structure in its synsedimentary context. In this context each stromatolite lamina represents a time-profile in the development of a stromatolite, marking past positions of the sediment-water interface, i.e., the "synoptic profile," whereas the height of an ancient stromatolite documents the progress of the stromatolite building process (Hofmann 1969).

A variety of laminated internal fabrics have been described in ancient and modern stromatolites (e.g.,

R.E. Riding and S.M. Awramik (Eds.)
Microbial Sediments

Monty 1976, 1979). Several causes of lamination have also been documented for modern stromatolites and microbial mats. Lamination in relatively slowly accreting structures may record seasonal changes, or the frequency of storms that periodically deposit sediment over microbial mats, while minor, more frequent turbulence may incorporate sediment layers in intertidal mats (Golubic 1973; Park 1976). Fast accreting structures may form laminae daily, following either solar or lunar cycling. Such observations offer different interpretational models for ancient stromatolites (Golubic 1991).

A model of stromatolitic lamination following solar cycling, independent of changes in sedimentation rates, is represented by *Phormidium hendersonii* (Monty 1965, 1979; Gebelein 1969; Golubic and Focke 1978), where lamination is produced by the organism's phototactic response. The orientation of its trichomes changes from predominantly upright during the day to prostrate during the night. This behavior persists on the structure's steep slopes, where few sediment particles are trapped, as well as on top of the domes, where the laminae are loaded with sediment.

A different model of stromatolitic lamination is represented by the genera *Schizothrix* and *Microcoleus*. These multitrichomous cyanobacteria change their growth and movement orientation in response to burial by sediment. Their trichomes are predominantly horizontal when forming prostrate mats on the sediment surface, irrespective of light conditions. The trichomes become vertically oriented when assuming escape position following burial and return to a horizontal orientation as soon as they reach the sediment surface. Unlike in the first model, the resulting lamination depends on variation in sediment supply.

In a third model, extended sedimentation pauses allow for profound changes in species composition of the mat community. The resulting laminae may be similar to the previously described ones, although each lamina may be formed by a different microbial assemblage. The following sections describe several case histories in which stromatolitic lamination records biological and environmental changes associated with changes in rates of sedimentation (including extended sedimentary pauses).

3 Subtidal Stromatolites and Stromatolitic Reefs of the Bahamas

Subtidal stromatolites in the tidal channel between Lee Stocking Island and Adderly Cay (Dill et al. 1986), like many others spread between Exuma (Reid et al. 1995) and Eleuthera Islands (Dravis 1983) of the Bahamas, form steep-sloped, up to 2 m high, often coalescing bioherms. In the course of their development, these structures are covered by a spectrum of marine benthic communities ranging from simple prokaryotic, cyanobacterial mats to diverse eukaryotic, micro/macro-algal communities which support numerous invertebrates and fish (see Riding et al. 1991). The accretion of these bioherms and the formation of laminated stromatolitic fabric within them is accomplished by microbial sediment trapping and binding, and carbonate precipitation (Fig. 1a). This process occurs mainly within a prokaryotic mat dominated by the filamentous, multitrichomous cyanobacterium *Schizothrix gebeleinii* Golubic et Browne in conjunction with sedimentary kinetics of tidally shifting, ooid/peloidal sand shoals; a complex eukaryotic community develops during extended sedimentary stasis (Golubic and Browne 1996).

The bioherms of Lee Stocking Island occur in a 4–10 m deep tidal channel which connects the shallow waters of the Bahama Carbonate Platform with the surrounding deep waters of the Exuma Sound. Swift semidiurnal tidal currents entrain sediment above the sea floor and cause migration of up to 2 m high sand dunes past the stromatolitic bioherms, periodically burying and unburying them. Under the impact of tidal currents, sediments are suspended and transported along the sea floor; however, the amount of sediment in suspension as well as the average grain size diminishes rapidly in the water column above 50 cm. As the dunes migrate, the level of transported loose sediment oscillates in relation to the firmly embedded stromatolitic structures. Accordingly, different amounts of sediment reach the organisms colonizing the bioherm tops over time, exposing them to cyclic changes in sedimentary conditions. The crests of large dunes bury the bioherms while the dune troughs leave them exposed high above the sediment/water interface, depriving them of sediment supply. This cycling, modified by topographic and hydrographic irregularities, is on the order of months to several years. The structures grow during a critical period preceding and following burial, when sediment particles are trapped and bound by the *Schizothrix* mat. During that time, the sediment oscillation is on the order of days to weeks, governed by smaller ripples superimposed on the dune surfaces and by minor, local current irregularities. The sedimentary record of these oscillations has been monitored by carborundum marking, followed by microscopic analysis of the in situ relations between microorganisms and sediment (Browne 1993).

Species composition of the communities colonizing the bioherms appears to be controlled by the rates of sediment supply, since few organisms are able to overcome burial in sand. High sediment flux favors colonization and establishment of a *Schizothrix gebeleinii* mat on these bioherms. When the sediment grains adhere to the sticky surface of the *Schizothrix* mat and cover it,

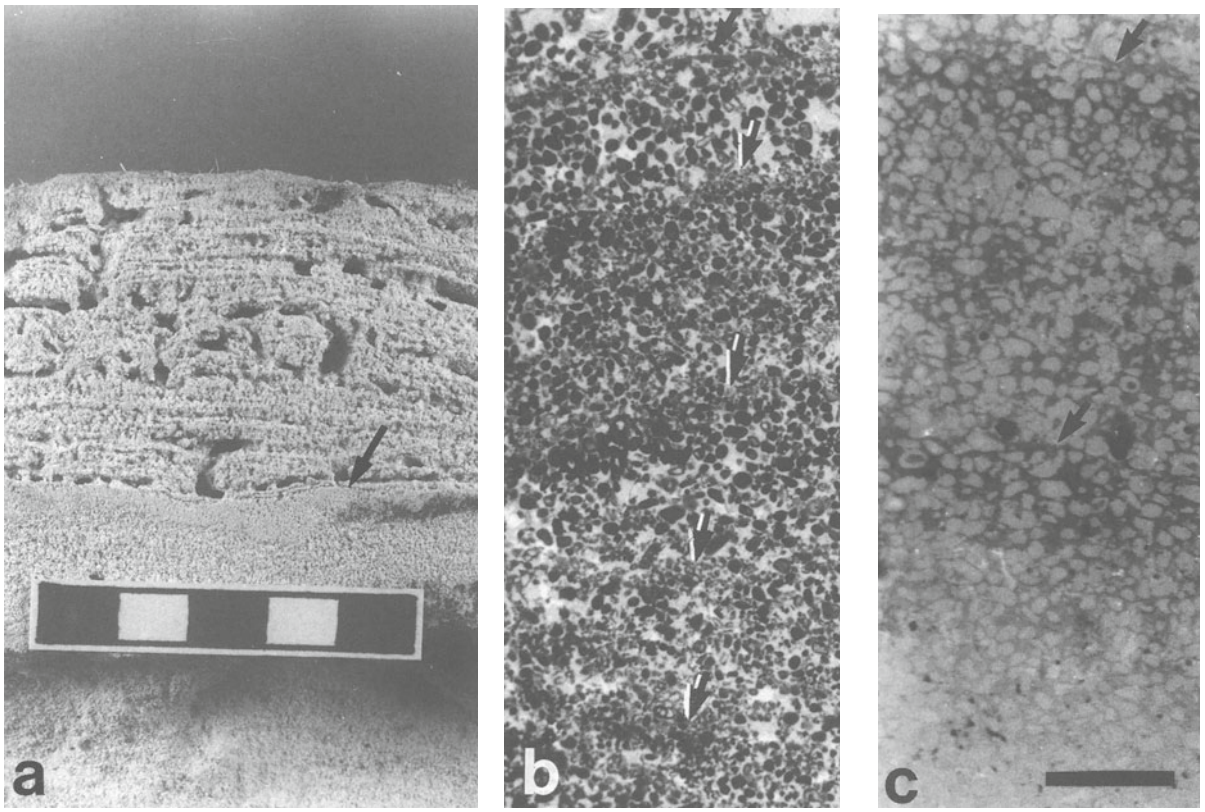

Fig. 1a–c. Millimeter-scale lamination in stromatolites of Lee Stocking Island, Bahamas. **a** Profile of lithified laminated fabric seen in vertical section through the bioherm. Stromatolite growth began on a contact with a lithified *Thalassinoides* chamber (*arrow*). Scale in centimeters. **b** Layering of ooid grains in a lithified stromatolite. *Arrows* indicate the positions of thin cement crusts. Petrographic thin section, transmitted light. Scale in **b** is 2 mm. **c** Vertical section through a resin-embedded mat of *Schizothrix gebeleinii*, showing entrapped grains and thin cement crust topping darker organic rich laminae (*arrows*). Incident light; *scale* 1 mm

the trichomes of the organism respond by gliding upward and around overlying sediment particles, effectively binding the grains. The mat contributes to sediment retention and thus to vertical accretion of the bioherm (Fig. 1b). Other settlers, unable to escape burial by the rapidly accumulating sediment, are excluded. The sheaths the *Schizothrix* trichomes leave behind as they move upward in response to sedimentation constitute a fibrous reinforcement to the mat and the incorporated sediment. During the accretionary period, the sediment is supplied in tidal pulses, so that up to 1 mm of newly added sediment may become incorporated into the *Schizothrix* mat within 10 days (measured above a marked time line). Fine sand- and silt-sized sediment, normally swept away by the tidal currents, accumulates within this mat. The size of sediment particles also varies with the strength of the current. As tidal currents slow and slacken, sediment flux as well as the particle size in suspension decreases, and for about 30 minut no sediment is supplied to stromatolite tops. Sediment supply rates vary from one tidal pulse to another due to microtopographic irregularities of the dune surface.

Lowering of the sedimentation rates permits an accumulation of *Schizothrix* trichomes on the top of the mat where they produce a dense layer of predominantly prostrate interwoven filaments (Fig. 1c, arrows). These filaments contain up to seven trichomes within a sheath and are distinguishable from those formed during upward migration of the organism, which typically contain only one trichome. Within these layers of increased *Schizothrix* biomass, delicate micritic cement crusts form parallel to the mat surface by precipitation of carbonate (primarily aragonite). The location of these cements within the living mat (Figs. 1b,c, 2a, arrow), their micritic nature and their laminar distribution indicate that the *Schizothrix gebeleinii* mat not only traps and binds sediment particles but also plays some role in the early cementation process (Fig. 2b,c). The alternation of organic-rich laminae with embedded cement horizons and sediment-rich/cement-poor laminae added during sediment accretion periods comprise the fine lamination of the mat which eventually forms the stromatolite fabric preserved in the lithified bioherms.

As long as the bioherm tops are close to the dune crest and the sediment flux is recurring frequently,

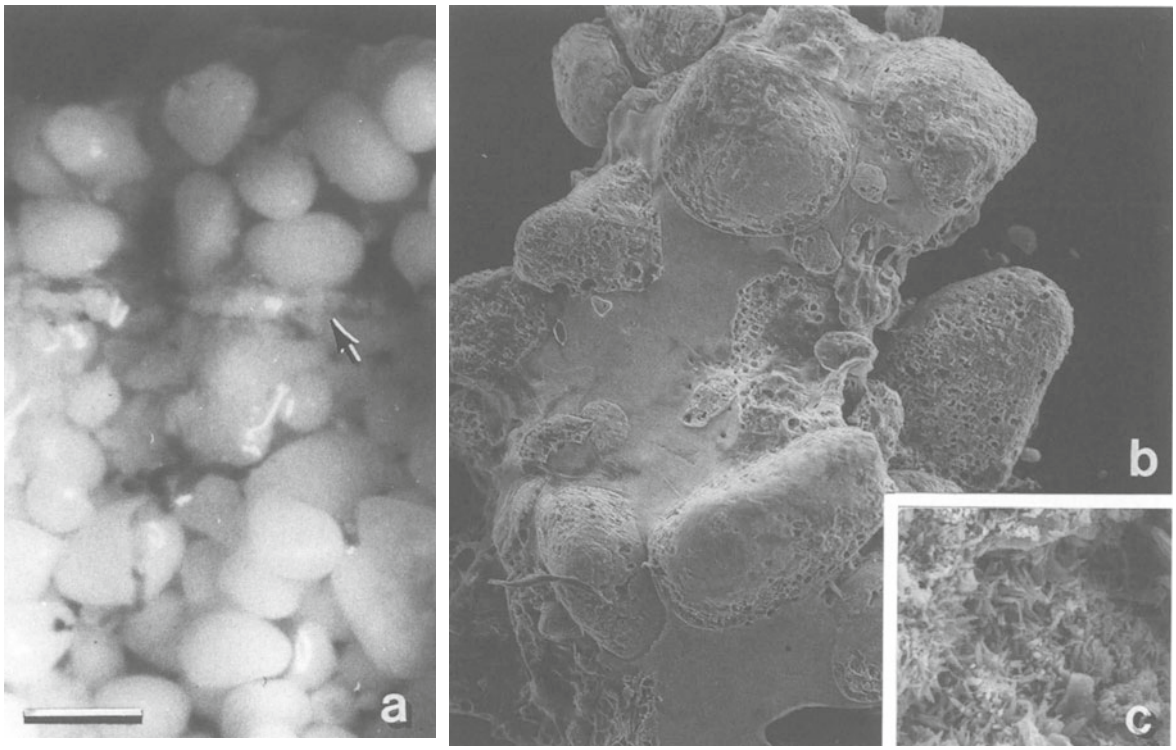

Fig. 2a–c. Cement crusts forming in live *Schizothrix* mats of Lee Stocking Island subtidal stromatolites. **a** Vertical section through wet mat sample. Note the horizontal spreading of a 60 μm thick cement crust (*arrow*) within the mat. Grains beneath the crust are connected by meniscus cement; incident light micrograph. **b** Top view of the microcrystalline cement crust tightly binding entrapped ooid grains (SEM). **c** Detail of the cement crust showing densely packed, submicron size aragonite crystals (confirmed by microprobe analysis); SEM. *Scale bars:* 200 μm for **a**, 120 μm for **b**, 4.5 μm for **c**

Schizothrix gebeleinii dominates, and few additional organisms (mostly diatoms) have an opportunity to colonize the mat. However, during the times of prolonged sedimentary stasis, when the tops of the bioherms are well above the sediment-water interface, the stromatolitic structures cease growth and harden. With decreased sediment stress, a more diverse benthic community (see Riding et al. 1991) develops through several successional stages. *Schizothrix* is first joined by other filamentous and coccoid cyanobacteria, a series of benthic diatom colonizers, and protozoa (mostly benthic foraminifera). With increased diversity, *Schizothrix* is suppressed and finally replaced by other, mostly eukaryotic, competitors. Settlements by various micro- and macroalgae, including encrusting chlorophytes and rhodophytes, constitute the next stage which, in turn, is followed by the macroscopic growth of brown algae (*Sargassum* spp.) and a variety of benthic invertebrates, including bryozoans, serpulid worms, hydroids and corals. The lithified surfaces may become colonized and bioeroded by microbial endoliths, boring sponges, worms and mollusks. These developments gradually render the bioherms indistinguishable from any hardground typically overgrown by the marine benthic communities of the region.

When *Schizothrix* inoculates bioherm surfaces, it forms small hemispherical domes as it spreads radially. Under conditions of high (albeit variable) sediment input rates, these colonies grow into a series of centimeter-scale, frequently coalescing, internally finely laminated protuberances located on the tops of larger meter-scale bioherms. Equivalent small stromatolitic domes consisting of alternating cement laminae and poorly cemented sediment laminae are encountered throughout the interior of lithified bioherms regularly dispersed between compact, nonlaminated and cavernous regions (see Fig. 1a). Nonlaminated internal parts within the bioherms may represent sediment trapped in the pockets between surface protuberances and may originate from events associated with sedimentary stasis or with the burial of these structures beneath sand dunes.

Burials beneath dunes also represent events of accretional stasis, possibly contributing to bioherm degradation. Burial results in death of the surface communities and in decay of accumulated organic matter. Newly exhumed stromatolites that were buried for extended periods often appear cavernous, possibly due to dispersal of loose sand following degradation of the organic binding. Secondary carbonate dissolution and

reprecipitation during burial may form interstitial cements, thus contributing to hardening of the structure. When uncovered, the emerging bioherm surfaces are subject to renewed colonization by the *Schizothrix* mat, opening another "window of opportunity" that favors stromatolite growth.

Is the *Schizothrix*-mat alone responsible for the formation of Bahamian bioherms? Probably not. Nonlaminated portions of the bioherm structures still require satisfactory explanation. Participation of unidentified chlorophytes in the growth of these bioherms has been proposed (Riding et al. 1991), but the mechanism of their action has not been documented and the resulting sedimentary structures not identified. In principle, many organisms, eukaryotic as well as prokaryotic, are able to stabilize and trap sediments and form stromatolites (Golubic 1976). For example, benthic diatoms which excrete extracellular substances and form attachment structures also trap and bind sediment particles (Duke and Reimann 1977; Awramik and Riding 1988; Riding et al. 1991; Hein et al. 1993; Riding 1994) or serve as templates for laminar arrangements of carbonate precipitates (Winsborough and Golubic 1987). Macroalgae, including those overgrowing Bahamian bioherms such as *Batophora* and *Acetabularia*, may entrap sediment by current baffling, a process known also to occur in higher plants (Evenari et al. 1985). However, the growth of these organisms on the bioherms under study coincides with the periods of low sediment supply, whereas the mat community of *Schizothrix gebeleinii* with few other cyanobacteria and diatoms grows when sediment supply is abundant.

4 Biogeochemically Stratified Microbial Mats: Great Sippewissett Salt Marsh

In contrast to the purely carbonate setting of the Bahamas, the Great Sippewissett Salt Marsh of Cape Cod, Massachusetts, represents a typical siliciclastic coastal setting. A broad, flat intertidal zone extends along the coast, protected by barrier beaches and drained by meandering tidal creeks. Large areas within this zone are covered by quartz sand at different stages of stabilization by microbial mats. These areas are rimmed by concentric zones of halophytic vegetation and salt marsh grasses (Gibson et al. 1984; Nicholson et al. 1987; Pierson et al. 1987).

The sedimentary kinetics of these siliciclastic sand flats depends on variable tidal and storm sediment transport. Brief sedimentary stasis events occur in active channels between tides. However, as sediment transport is shifted laterally, parts of the sand flat become increasingly deprived of sediment. In the course of extended sedimentary stases, the microbial mats diversify biologically and geochemically. Ultimately, the mat becomes overgrown and replaced by a salt marsh community.

During periods of high sediment flux, trapping and binding of sand particles are carried out by the filamentous, sheathed, multitrichomous, cyanobacterium *Microcoleus chthonoplastes*. Shortly following burial, the vertically oriented trichomes of this organism form an upward moving, profuse blue-green band, gradually accumulating at the surface, where the trichomes spread horizontally. There the organism forms bundles with a large number of trichomes within a common sheath. Like the members of the genus *Schizothrix*, the trichomes of *Microcoleus* continuously produce sheaths which they leave behind in the sediment as they move.

The sediment surface is also colonized by the large, sheathed filamentous cyanobacterium *Lyngbya aestuarii*. Although *Lyngbya* trichomes are also fast gliders, most of the inocula of this taxon are picked up by tides from isolated intertidal pools, where this organism grows optimally, and deposited on top of the mat, usually over a thin layer of sand.

At high sedimentation rates, neither of these microorganisms succeeds in establishing a mat at the sediment-water interface. At the onset of a sedimentary pause, however, both taxa participate in forming a mat. The properties and environmental requirements of the two dominant cyanobacteria are slightly different. In response to intensive solar radiation, *Lyngbya aestuarii* excretes a brown, light- and UV-protective extracellular pigment, scytonemin, into its sheaths (Garcia-Pichel and Castenholz 1991). *Microcoleus chthonoplastes* does not have that capacity but is more tolerant of lowered oxygen tensions (see D'Amelio et al. 1989). These inherent differences promote growth in a stratified arrangement optimal for both organisms, with *Lyngbya* occupying the top stratum underlaid by *Microcoleus*.

The first consequence of the sedimentary stasis is, therefore, cyanobacterial growth and accumulation of organic matter at the sediment-water interface. Colonization by heterotrophic bacteria soon follows. While oxygen is produced in the upper portion of the mat, bacterial degradation of the accumulated organic matter depletes the oxygen in the lower portion. Other settlers on this increasingly stable surface include diatoms, euglenoids, coccoid cyanobacteria (*Aphanocapsa, Chroococcus, Entophysalis*), and other filamentous cyanobacteria (*Schizothrix, Oscillatoria, Spirulina*). The considerable primary production of such microbial mats (Gerdes et al. 1985) offers subsistence to numerous heterotrophs, including bacteria, mastigophores, ciliates, and nematodes.

Rapid bacterial oxygen depletion creates a steep chemical gradient and a chemically stratified mat which attracts a broad spectrum of microorganisms with different environmental requirements. The conse-

quence is a biologically stratified microbial mat (see Potts 1980; Friedman and Krumbein 1985; Cohen and Rosenberg 1989) where changes in nutrient concentrations, redox potential, pH, and the associated metal solubilities occur, compacted within a few millimeters across the sediment-water interface. Competition in light utilization by microbial phototrophs results in strong shifts in spectral composition of available light (Pierson et al. 1987; Pierson and Olson 1987). Because the stratified settlers make different metabolic contributions to their immediate surroundings, a biogeochemically differentiated system develops with several efficient nutrient recycling schemes (Van Gemerden 1993). Among different metabolic types, conspicuous are sulfate-reducing bacteria, which carry most of the anaerobic respiration. Hydrogen sulfide released by these organisms is, in part, trapped by ferrous iron causing black coloration of the mud. Iron solubility changes as it switches between ferrous and ferric oxidation states and may be redistributed within the mat. Phototrophic purple sulfur bacteria (e.g., *Thiocapsa roseopersicina*) use H_2S as electron donor, releasing sulfate in the process (Van Gemerden and De Wit 1989). These bacteria commonly comprise a purple-pink stratum beneath the layers of cyanobacteria. Other possible anaerobic photosynthesizers of this community include *Chloroflexus*-like, motile filamentous bacteria which are abundant in the lower levels of the mat. Anoxic strata of the mat also contain spirochetes, methanogens and a variety of fermenting bacteria. The interface between the anoxic and oxygenated layers of the mat supports chemolithotrophy by colorless sulfur bacteria of the genera *Beggiatoa* and *Thioploca* (Larkin and Strohl 1983). These gliding microorganisms adjust their position and orientation according to the chemical gradient. They use the oxidation of hydrogen sulfide for their metabolic energy generation (Jørgensen and Revsbech 1993).

The development of such a highly differentiated, chemically and biologically stratified ecosystem requires some time to become established, even considering the high microbial reproduction rates. Thus, an extended sedimentary pause is required for its full development. If interrupted by the resumption of sediment flux, the process reverts to the simplicity of the sedimentary kinetic condition characterized by pioneer colonization and gliding motility of *Microcoleus chthonoplastes* and *Lyngbya aestuarii*. Less motile components of the vertically differentiated mat remain buried by the sediment and deteriorate. The decomposition of buried mats is initially anaerobic but it is completed aerobically, as atmospheric oxygen penetrates these coarse sediments during tidal drainage. Ultimately, most of the organic product of the buried Sippewissett mat is recycled, leaving little record of its past existence and complexity. Under different conditions, however, preservation of the accumulated organic matter or of associated insoluble minerals (e.g., pyrite) may mark such horizons in the fossil record as distinct laminae.

Prolonged sedimentary stasis, caused by lateral shift of sediment-transporting tidal channels, invites a succession of colonizing plants which changes the microbial mat into a salt marsh. At first, a stable, vertically stratified microbial mat becomes overgrown by the heterocystous cyanobacterium *Calothrix scopulorum*. Mat stabilization also enables seeding and germination of halophytic phanerogamic plants to occur. *Salicornia europaea* and *Limonium nashii* are among the first settlers in the establishment of a typical salt marsh, which becomes increasingly dominated by the grass *Spartina patens*, while *S. alterniflora* rims the remaining tidal pools. Parallel with these developments is an increased rate of incorporation of organic matter into the sediment, primarily by plant roots, resulting in peat accumulation and ground elevation. The consequence is a deepening of tidal pools which remain isolated and scattered in the marsh. Salt-tolerant bushes and trees follow as the salt marsh gradually gives way to development of a terrestrial coastal ecosystem.

5 Coccoid Cyanobacterial Mats: Shark Bay, Western Australia

The intertidal stromatolitic structures of the hypersaline Hamelin Pool, Shark Bay, Australia (Logan 1961), are covered by mamillate mats of the coccoid cyanobacterium *Entophysalis major* (Golubic 1985), forming a coherent belt in the lower intertidal range. Within the range of water supply optimal for this taxon, the *Entophysalis*-dominated microbial community overgrows domal stromatolites of various shapes, vast flat surfaces in protected embayments, as well as transitional terrain, where wave action carves out stromatolites from a platform of stabilized sediment (Golubic 1991). Stratiform *Entophysalis* mats also occur across similar tidal ranges along the protected coasts of the Arabian Gulf (Golubic 1992). Similar stromatolites and mats dominated by coccoid cyanobacteria have been reported in submersed stromatolites of Hamelin Pool (Golubic 1985), hypersaline lagoons of Baja California (Horodyski and Vonder Haar 1975) the salt pans of Peru (Montoya and Golubic 1991), and the Great Salt Lake (Haley 1976). The common feature in all these occurrences is an extremely slow sedimentation and accretion rate (see Playford and Cockbain 1976). These observations identify the mats dominated by coccoid cyanobacteria as microbial communities which become established under conditions of extended sedimentary stasis. It appears that the elevated salinity favors the persistence of coccoid cyanobacteria and prevents encroachment of algae and higher vegetation.

Hamelin Pool stromatolites are often internally indurated while externally coated by a soft, unlithified *Entophysalis* mat. At the peak of the summer season, however, when evaporation causes increased hypersalinity and supersaturation with respect to calcium carbonate of interstitial waters, a series of precipitation events were observed within the mat, producing submillimeter-scale laminae. Massive carbonate precipitation occurs in parts of the mamillate mat, destroying it in the process (Golubic 1983). This rapid lithification of the structure is followed by colonization of the hard surfaces by an epilithic-endolithic microbial community: the lithified stromatolite becomes subject to microbial bioerosion. Following seasonal lowering of salinity, the *Entophysalis* overgrows lithified horizons, starting another cycle of its development.

The internal texture of Hamelin Pool stromatolites, as evidenced by longitudinal sections, shows mostly coarse laminae frequently interrupted by cavities of different size, rather than the fine lamination characteristic of most Precambrian stromatolites (see Playford and Cockbain 1976, Fig. 10). Such horizons could be explained as sequences of episodic, discontinuous, accretionary events, caused by massive carbonate precipitation, modified by later diagenetic alterations within these slow-growing stromatolitic structures.

6
Evidence of Sedimentary Kinetics and Stasis in an Ancient Stromatolitic Setting

Cherty stromatolites of the 1.4–1.5 Ga-old Gaoyuzhuang Formation of northern China harbor well-preserved, coccoid and filamentous microfossils within a finely laminated fabric (Seong-Joo and Golubic 1998, 1999). The original mineralogy is replaced by silica; however, the assemblages of resident microfossils occur in growth position, so that their spacing reveals the relative amount of sediment originally surrounding them (Fig. 3). Pseudomorphs of carbonate minerals preserved in silica, and grain distribution of siliceous deposits as observed in cross-polarized light, identify traces of the original sedimentary fabric. Each microfossil assemblage correlates with a different synsedimentary context, and their orientation and mode of growth identifies contrasting paleoenvironments of sedimentary stasis vs sedimentary kinetics.

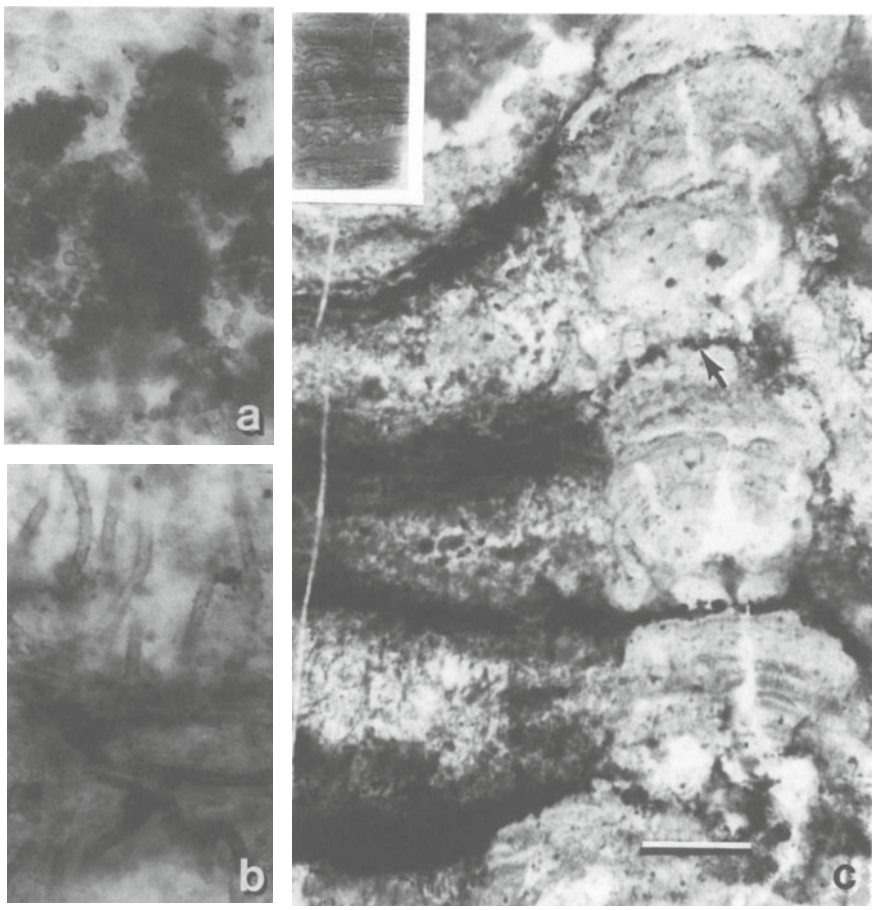

Fig. 3a–c. Lamination in cherty stromatolites from Gaoyuzhuang Formation, northern China. **a** Organic-rich layer composed of coccoid cyanobacteria. **b** Organic-rich layer composed of filamentous cyanobacteria showing a change from horizontal to vertical orientation. **c** Sequence of stromatolite laminae with multitrichomous cyanobacteria forming dark laminae of prostrate mats alternating with light laminae with upright filament orientation (*left*), which are interrupted by a series of upward radiating crystal fans capped by coccoid cyanobacterial coatings (*right*). *Inset* Thin section perpendicular to the bedding plane, showing an overview of laminae and crystal fans within the stromatolite. *Scale bars:* 75 μm for **a,b;** 500 μm for **c;** 15 mm for the *inset* in **c**

Wavy horizons composed of coccoid microfossils (Fig. 3a) alternate with filament dominated laminae (Fig. 3b). Coccoid microfossils regularly coat clear areas in the section and top the upward radiating chalcedonic fans, forming well-defined organic rims (Fig. 3c, right). The repeated, upward radiating, finely striated chalcedonic fans are best interpreted as pseudomorphs after originally aragonitic precipitates. Such precipitates, when formed rapidly in small hypersaline pools, created instant hard substrates which were subsequently colonized by coccoids (Fig. 3c, arrow). By analogy with modern occurrences, specifically following the Shark Bay model, establishment of coccoid horizons requires time, thus indicating periods of sedimentary pauses of considerable duration.

Organic-rich laminae within these stromatolites are predominantly composed of horizontal, densely interwoven filament webs, mostly preserved as empty sheaths (Fig. 3b, below). These mats could have accumulated organic biomass during low rates of sedimentation and brief sedimentary pauses. Periodically along the section, the filaments change their orientation from prostrate to upright, forming an organic-poor (i.e., sediment-rich) lamina (Fig. 3b, above). This loose web of predominantly upright cyanobacterial filaments shows avoidance and bypassing of grains embedded in the mat. While the prostrate mats contain bundled sheaths within common envelopes, the upright sheaths are predominantly single. The microfabrics of these sediment-rich layers contain upward diverging crystal fans, botryoidal grains, and finely laminated travertine-like coatings (Grotzinger and Reed 1983).

The pattern observed (Fig. 3c, left) is strikingly similar to that of modern multitrichomous cyanobacteria in their response to burial by sediment, suggesting a similar variation in sedimentation rate on this ancient site. This pattern differs from that of the noctidiurnal phototactic responses of *Phormidium hendersonii*-type, in which sediment accumulation correlates with horizontal rather than vertical filament orientation (Monty 1979). The *Phormidium hendersonii* model, which operates on the basis of a "solar clock" and marks nocti-diurnal lamination in stromatolites, has been invoked to interpret ancient laminated structures (e.g., Knoll and Golubic 1992). This model was also applied in interpretation of the alternating filament orientation in Gaoyuzhuang stromatolites (Zhang Zhongying 1986). The observations reported here show that the alternative model of behavioral response by multitrichomous cyanobacteria to sedimentation is more consistent with the synsedimentary context of these stromatolites (Seong-Joo and Golubic 1998).

Horizons of mat-building coccoid microfossils are common in cherty stromatolites throughout the Mesoproterozoic (Hofmann 1976; Oehler 1978; Horodyski and Donaldson 1980; Zhang Yun 1981; Sergeev et al. 1995), often interspersed with horizons with abundant filamentous fossils. It is possible that many of these reported occurrences formed under conditions similar to those described here, representing changing paleomicroenvironments with different sedimentary regimes. Thus, fine stromatolitic lamination in ancient stromatolites may have recorded alternating episodes of sedimentary kinetics and stasis.

Acknowledgements. We thank the staff of the Caribbean Marine Research Center (CMRC), Lee Stocking Island, and K. Vogel, University of Frankfurt/M and his research team for support during field work in the Bahamas, and Dr. Zhang Yun for field work on ancient stromatolites. This study is funded in part by the German Research Foundation – DFG-Vo.90/14, Hanse Institute for Advanced Studies, Delmenhorst, Germany, NOAA grant CMRC 94–24, and the Australian Museum of Natural History.

References

Awramik SM, Margulis L, Barghoorn ES (1976) Evolutionary processes in the formation of stromatolites. In: Walter MR (ed) Stromatolites: developments in sedimentology, vol 20. Elsevier, Amsterdam, pp 149–162

Awramik SM, Riding R (1988) Role of algal eukaryotes in subtidal columnar stromatolite formation. Proc Natl Acad Sci USA 85:1327–1329

Browne KM (1993) Lamination in Recent bahamian subtidal stromatolites: origin and lithification. PhD Diss, University of Miami, Miami, FL, 296 pp

Cohen Y, Rosenberg E (eds) (1989) Microbial mats, physiological ecology of benthic microbial communities. American Society for Microbiology, Washington, DC

D'Amelio, ED, Cohen Y, Des Marais DJ (1989) Comparative functional ultrastructure of two hypersaline submerged cyanobacterial mats: Guerrero Negro, Baja California Sur, Mexico, and Solar Lake, Sinai, Egypt. In: Cohen Y, Rosenberg E (eds) Microbial mats. American Society for Microbiology, Washington, DC, pp 97–113

Dill RF, Shinn EA, Jones AT, Kelly K, Steinen RP (1986) Giant subtidal stromatolites forming in normal salinity waters. Nature 324:55–58

Dravis J (1983) Hardened subtidal stromatolites, Bahamas. Science 219:385–386

Duke EL, Reimann BEF (1977) The ultrastructure of the diatom cell. In: Werner D (ed.) The biology of diatoms. University of California Press, Berkeley, p.65–109

Evenari M, Gutterman Y, Gavish E (1985) Botanical studies on coastal salinas and sabkhas of the Sinai. In: Friedman GM, Krumbein WE (eds) Hypersaline ecosystems. Springer, Berlin Heidelberg New York, pp 145–182

Friedman GM, Krumbein WE (eds) (1985) Hypersaline ecosystems, the Gavish Sabkha. Ecological studies 53. Springer, Berlin Heidelberg New York, pp 1–484

Garcia-Pichel F, Castenholz RW (1991) Characterization and biological implications of scytonemin, a cyanobacterial sheath pigment. J Phycol 27:395–409

Gebelein CD (1969) Distribution, morphology and accretion rate of Recent subtidal algal stromatolites, Bermuda. J Sed Petrol 39: 49–69

Gerdes G, Krumbein WE, Holtkamp E (1985) Salinity and water activity related zonation of microbial communities and potential stromatolites of the Gavish Sabkha. In: Friedman GM, Krumbein WE (eds) Hypersaline ecosystems. Springer, Berlin Heidelberg New York, pp 238–266

Gibson J, Leadbetter ER, Jannasch HW (1984) Great Sippewissett Marsh: a summary of projects carried out by students in the Microbial Ecology Course of the Marine Biological Laboratory, Woods Hole, during summers 1972–1981. In: Cohen Y, Casten-

holz RW, Halvorson HO (eds) Microbial mats: stromatolites, Alan R. Liss, New York, pp 95–100
Golubic S (1973) The relationship between blue-green algae and carbonate deposits. In: Carr NG, Whitton BA (eds) The biology of blue-green algae. Blackwell Scientific Publications, Oxford, pp 434–472
Golubic S (1976) Organisms that build stromatolites. In: Walter MR (ed) Stromatolites, developments in sedimentology, vol 20. Elsevier, Amsterdam, pp 113–126
Golubic S (1983) Stromatolites, fossil and recent: a case history. In: Westbroek P, Jong EW (eds) Biomineralization and biological metal accumulation. D Reidel, Dordrecht, pp 313–326
Golubic S (1985) Microbial mats and modern stromatolites in Shark Bay, Western Australia. In: Caldwell DE, Brierley JA, Brierley CL (eds) Planetary ecology. Van Nostrand Reinhold, New York, pp 3–16
Golubic S (1991) Modern stromatolites – a review. In: Riding R (ed) Calcareous algae and stromatolites. Springer, Berlin Heidelberg New York, pp 541–561
Golubic S (1992) Microbial mats of Abu Dhabi. In: Margulis L, Olendzenski L (eds) Environmental evolution: effects of the origin and evolution of life on planet earth. MIT Press, Cambridge, MA, pp 103–130
Golubic S, Focke JW (1978) *Phormidium hendersonii* Howe: identity and significance of a modern stromatolite building microorganism. J Sed Petrol 48:751–764
Golubic S, Browne KM (1996) *Schizothrix gebeleinii* sp. nov. builds subtidal stromatolites, Lee Stocking Islands, Bahamas. Arch Hydrobiol Suppl/ Algol Stud 83:273–290
Grotzinger JP, Reed JF (1983) Evidence for primary aragonite precipitation, lower Proterozoic (1.9 Ga) Rocknest dolomite, Wopmay orogen, northwest Canada. Geology 11:710–713
Haley RB (1976) Textural variation within Great Salt Lake algal mounds. In: Walter MR (ed) Stromatolites, developments in sedimentology, voll 20. Elsevier, Amsterdam, pp 435–445
Hein MK, Winsborough BM, Davis JS, Golubic S (1993) Extracellular structures produced by marine species of *Mastogloia*. Diatom Res 8:1–16
Hofmann HJ (1969) Attributes of stromatolites. Geological Survey of Canada, Pap 69–39, 58 pp
Hofmann HJ (1976) Precambrian microflora, Belcher Islands, Canada: significance and systematics. J Paleontol 50:1040–1073
Horodyski RJ, Vonder Haar SP (1975) Recent calcareous stromatolites from Laguna Mormona (Baja California) Mexico. J Sed Petrol 45:894–906
Horodyski RJ, Donaldson, A (1980) Microfossils from the middle Proterozoic Dismal Lakes Group, Arctic Canada. Precambrian Res 11:125–159
Jørgensen BB, Revsbech NP (1993) Colorless sulfur bacteria, *Beggiatoa* spp. and *Thiovulum* spp. in O_2 and H_2S microgradients. Appl Environ Microbiol 45:1261–1270
Kalkowsky E (1908) Oolith and Stromatolith im norddeutschen Buntsandstein. Z Dtsch Geol Gesellsch 60:68–125
Knoll AH, Golubic S (1992) Modern and ancient cyanobacteria. In: Schidlowski M, Golubic S, Kimberley MM, McKirdy DM, Trudinger PA (eds) Early organic evolution: implications for mineral and energy resources. Springer, Berlin Heidelberg New York, pp 450–462
Larkin JM, Strohl WR (1983) *Beggiatoa, Thiothrix,* and *Thioploca*. Annu Rev Microbiol 37:341–367
Logan BW (1961) Cryptozoan and associate stromatolites from the Recent of Shark Bay, Western Australia. J Geol 69:517–533
Monty CLV (1965) Recent algal stromatolites in the windward lagoon, Andros Island, Bahamas. Bull Ann Soc Géol Belg 88B:269–276
Monty CLV (1976) The origin and development of cryptalgal fabrics. In: Walter MR (ed) Stromatolites. developments in sedimentology, vol 20. Elsevier, Amsterdam, pp 193–249
Monty CLV (1979) Scientific Reports of the Belgian expedition on the Australian Great Barrier Reefs. 1967. Sedimentology 2. Monospecific stromatolites from the Great Barrier Reef tract and their paleontological significance. Ann Soc Géol Belg 101:163–171
Montoya TH, Golubic S (1991) Morphological variability in natural populations of mat-forming cyanobacteria in the salinas of Huacho, Lima, Peru. Arch Hydrobiol Suppl./Algol Stud 64:423–441
Nicholson JAM, Stolz JF, Pierson BK (1987) Structure of a microbial mat at Great Sippewissett Marsh, Cape Cod, Massachusetts. FEMS Microbiol Ecol 45:343–364
Oehler DZ (1978) Microflorta of the middle Proterozoic Balbirini Dolomite (McArthur Group) of Australia. Alcheringa 2:269–309
Park R (1976) A note on the significance of lamination in stromatolites. Sedimentology 23:379–393
Pierson BK, Oesterle A, Murphy GL (1987) Pigments, light penetration, and photosynthetic activity on the multi-layered microbial mats of Great Sippewissett Salt Marsh, Massachusetts. FEMS Microbiol. Ecol 45:365–376
Pierson BK, Olson JM (1987) Evolution of photosynthesis in anoxygenic photosynthetic prokaryotes. In: Cohen Y, Rosenberg, E (eds) Microbial mats. American Society for Microbiology, Washington, DC, pp 402–427
Playford PE, Cockbain AE (1976) Modern algal stromatolites at Hamelin Pool, a hypersaline barred basin in Shark Bay, Western Australia. In: Walter MR (ed) Stromatolites. Developments in sedimentology, vol 20. Elsevier, Amsterdam, pp 389–411
Potts M (1980) Blue-green algae (Cyanophyta) in marine coastal environments of the Sinai Peninsula; distribution, zonation, stratification and taxonomic diversity. Phycologia 19:60–73
Reid RP, Macintyre IG, Browne KM, Steneck RS, Miller T (1995) Modern marine stromatolites in the Exuma Cays, Bahamas: uncommonly common. Facies 33:1–18
Riding R (1994) Stromatolite survival and change: the significance of Shark Bay and Lee Stocking Island subtidal columns. In: Krumbein WE, Pateerson DM, Stal LJ (eds) Biostabilization of sediments. Bibliotheks und Informationssystem der Universitt, Oldenburg-Verlag, Odenburg, pp 183–202
Riding R, Awramik SM, Winsborough BM, Griffin KM, Dill RF (1991) Bahamian giant stromatolites: microbial composition of surface mats. Geol Mag 128:227–234
Seong-Joo L, Golubic S (1998) Multi-trichomous cyanobacterial microfossils from the Mesoproterozoic Gaoyuzhuang Formation, China: paleoecological and taxonomic implications. Lethaia 31:169-184
Seong-Joo L, Golubic S (1999) Microfossil populations in the context of synsedimentary micrite deposition and acicular carbonate precipitation: Mesoproterozoic Gaoyuzhuang Formation, China. Precambrian Res 96:183-208
Sergeev VN, Knoll AH, Grotzinger JP (1995) Paleobiology of the Mesoproterozoic Billyakh Group, Anabar Uplift, Northern Siberia. J Paleontol 69:1–37
Van Gemerden H (1993) Microbial mats: a joint venture. Mar Geol 113:3–25
Van Gemerden H, de Wit R (1989) Phototrophic and chemotrophic growth of the purple sulfur bacterium *Thiocapsa roseopersicina*. In: Cohen Y, Rosenberg E (eds) Microbial mats. Am Society for Microbiol., Washington, DC, pp 313–319
Winsborough B, Golubic S (1987) Stromatolitic structures of inland waters built by diatoms. J Phycol 23:195–201
Zhang Yun (1981) Proterozoic stromatolite microfloras of the Gaoyuzhuang Formation (early Sinian: Riphean) Hebei, China. J Paleontol 55:485–506
Zhang Zhongying (1986) Solar cyclicity in the Precambrian microfossil record. Palaeontology 29:101–111

Bacterial Calcification

Heike v. Knorre, Wolfgang E. Krumbein

University of Oldenburg, ICBM, AG Geomicrobiology, P.O. Box 2503, D-26111 Oldenburg, Germany

Abstract. Most heterotrophic bacteria are able to induce $CaCO_3$ precipitation in laboratory experiments. Carbonate precipitation by bacteria is apparently a by-product of physiological activities that increase carbonate alkalinity, rather than a result of a specific mechanism. Bacteria can function as nucleation sites and they become embedded in growing carbonate particles, but similar particles can also form in the absence of bacteria. The shape of particles larger than 10 μm is the same whether they were formed abiotically or induced by bacteria.

1 Introduction

Formation of $CaCO_3$ particles in microbial mats and other environments might, at least in part, be due to heterotrophic bacteria, as suggested, e.g., by Drew (1914), Krumbein et al. (1977), Chafetz andBuczynski (1992), and Castanier et al. (this Vol.).

Calcium carbonate often precipitates in laboratory experiments using different types of bacteria isolated from freshwater, marine and hypersaline environments and kept under a variety of culture conditions (e.g., Bavendamm 1932; Castanier 1987; Krumbein 1973; McCallum and Guhathakurta 1970; Ferrer et al. 1988). Throughout this century, possible mechanisms of bacterial calcification have been a matter of controversy. Some authors have suggested the existence of specific $CaCO_3$ precipitating bacteria (Drew 1914; Molisch 1925; Castanier 1987); others doubted whether $CaCO_3$ precipitation is more than an unwanted by-product of bacterial metabolism under special environmental conditions (Bavendamm 1932; Boquet et al. 1973). Some have emphasized the importance of changes in alkalinity due to bacterial metabolism (Nadson 1928; Krumbein 1979a). According to others, bacterial membranes, acting as sites of nucleation or Ca^{2+} enrichment in bacterial colonies, play a major role (Morita 1980; Danielli and Edington 1983). Rivadeneyra et al. (1985, 1994) showed that environmental factors such as salinity and composition of the medium greatly influence the products of bacterial calcification, e.g., in liquid media aragonite forms, and in solid media high magnesian calcite forms (see also Buczynski and Chafetz 1991). Thus, different types of bacteria as well as abiotic factors seem to contribute in a variety of ways to $CaCO_3$ precipitation in a wide range of different environments.

In order to study bacterial calcification in the laboratory, heterotrophic bacteria were isolated from microbial mats in which carbonate particles formed. We wanted to determine the mechanism by which the isolated bacteria might induce $CaCO_3$ precipitation, and whether particles formed by bacterial calcification differ from those formed abiotically.

2 Methods

$CaCO_3$ precipitation tests were performed in solid and liquid media containing artificial sea water (400 mM NaCl, 28 mM $MgSO_4$, 18 mM $MgCl_2$, 6.7 mM KCl, 15 mM $CaCl_2$), 9.4 mM NH_4Cl, 0.05 mM $FeSO_4$, and 0.16 mM K_2HPO_4, to which different carbon sources were added: sodium acetate, citrate, glutamate, glucose, glycolate, peptone, yeast extract (each 5–30 mM or 1–5 g/l) (Fig. 1). In some experiments the concentration of $CaCl_2$ was varied. The pH was adjusted to 7.5; after autoclaving it was between 6.3 and 6.8 and was not readjusted afterwards because it rose during the growth of bacteria to above 7.5. Cultures were incubated aerobically at room temperature or 27 °C. Sterile controls were run in all experiments.

The concentration of calcium in liquid media was measured by atomic absorption spectroscopy (AAS). The concentration of acetate in liquid cultures was determined titrimetrically. Bacterial numbers in liquid cultures were determined by counting under the microscope.

2.1 Scanning Electron Microscopy

$CaCO_3$ particles from liquid culture were fixed in glutaraldehyde, desalted, dehydrated in a series of ethanols, critical point dried, sputtered with gold, and studied in a Cambridge scanning electron microscopy (SEM) and a Hitachi S-450 SEM (Figs. 2, 3). The carbonate particles shown in Fig. 3a were air dried.

R.E. Riding and S.M. Awramik (Eds.)
Microbial Sediments

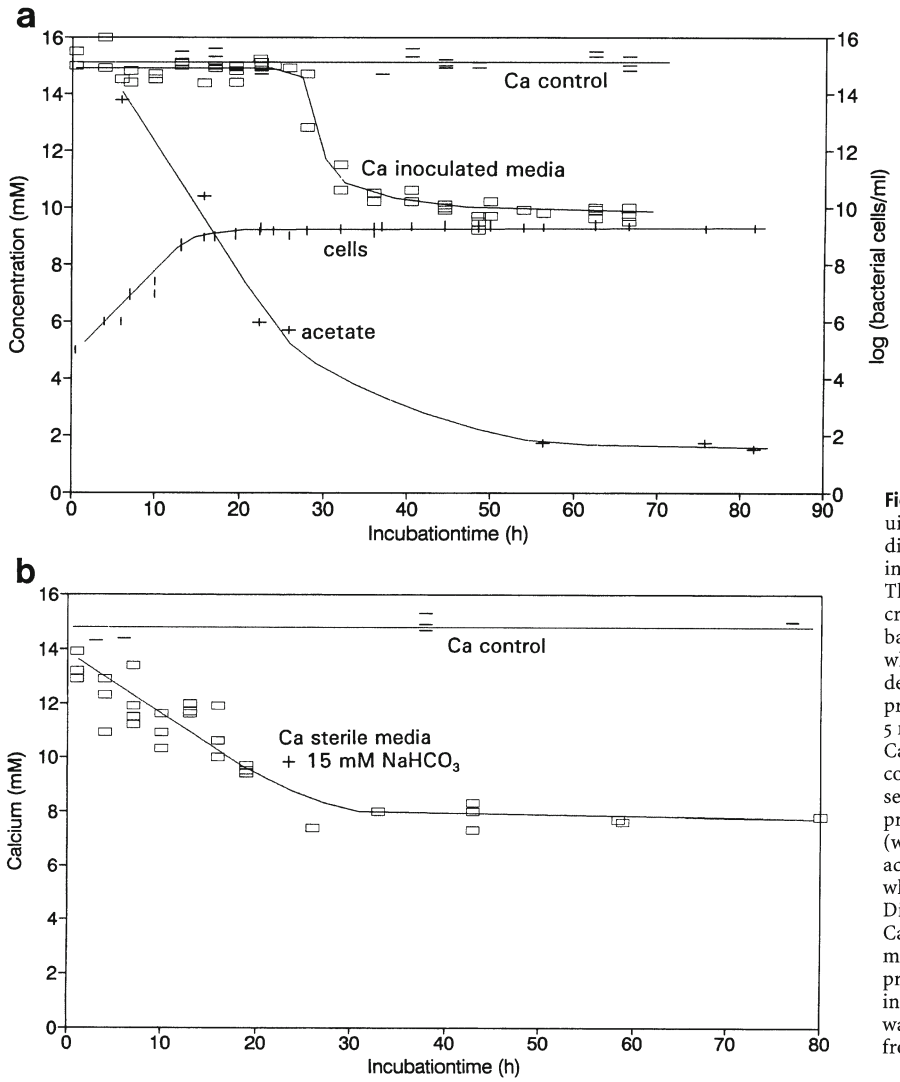

Fig. 1.a $CaCO_3$ precipitation in liquid culture containing 15 mM sodium acetate as a carbon source inoculated with bacteria at t = 0. The concentration of acetate decreased with increasing number of bacterial cells. $CaCO_3$ precipitated when more than 8 mM acetate was degraded. After 10–15 h carbonate precipitation stopped. About 5 mM $CaCO_3$ precipitated. No $CaCO_3$ precipitated in the sterile controls (graph shows data from several experiments). **b** $CaCO_3$ precipitation in sterile media (without bacteria, phosphate, and acetate or other carbon source), to which $NaHCO_3$ was added at t = 0. Directly after addition of $NaHCO_3$, $CaCO_3$ precipitated for approximately 24 h. About 6 mM $CaCO_3$ precipitated, but none precipitated in the controls, to which no HCO_3^- was added (graph shows data from several experiments)

2.2 Transmission Electron Microscopy

Carbonate particles from liquid culture were fixed in glutaraldehyde, embedded in a drop of 2% agar, decalcified in 4% EDTA, desalted, dehydrated in a series of ethanol, and embedded in EPON. Ultrathin-sections of these samples were stained with uranyl acetate and lead citrate, and studied by transmission electron microscopy (TEM) in a Zeiss EM 109 transmission electron microscope.

For further details of methods see Riege (1994).

▷

Fig. 2.a Bacterial calcification on solid medium; *b* bacterial colony, *c* $CaCO_3$ particles in agar, *arrow* large $CaCO_3$ particles on a bacterial colony; *scale bar* = 0.5 mm. **b** Spherical and irregularly shaped $CaCO_3$ particles (*c*) in the red anoxic layer of a microbial mat in a laboratory model; *f* filamentous sulfur bacteria; *scale bar* = 25 µm. **c** $CaCO_3$ particles formed after several weeks of hot sunny weather in microbial mats on Norderney, southern North Sea; *w* wheat grain-shaped $CaCO_3$ particles on sheaths of the cyanobacterium *Oscillatoria* sp., *r* small rod-shaped particles on a sheath of the cyanobacterium *Microcoleus chthonoplastes*, *s* larger spherical $CaCO_3$ particle; *scale bar* = 25 µm. **d** $CaCO_3$ particles, mainly shaped as dumbbells, formed in liquid bacterial cultures. Length of particles = 20–200 µm. **e** $CaCO_3$ particles formed in sterile liquid media (without bacteria, phosphate, and organic substances), but to which 15 mM $NaHCO_3$ was added; *s* spherical; *w* wheat grain-shaped, *d* dumbbell-shaped particle; *scale bar* in larger micrograph = 250 µm, *scale bar* in inserts = 25 µm. **f** $CaCO_3$ particles formed in liquid culture; *r* rod-shaped, *w* wheat grain-shaped, *s* spherical $CaCO_3$ particles; *scale bar* = 20 µm. **g** Partly dissolved $CaCO_3$ particle (*c*) from an agar plate, covered by extracellular polymeric substances (EPS) (*e*); *h* hole in the EPS cover left by CO_2 bubbles due to addition of HCl to the sample. Interference contrast; *scale bar* = 20 µm. **h** EPS covered $CaCO_3$ particles (liquid culture). *ew* EPS covering of wheat grain-shaped $CaCO_3$ particles, *b* bacteria, *e* fragile EPS structures not covering $CaCO_3$ particles. $CaCO_3$ was dissolved under the microscope by a drop of diluted HCl. Toluidine blue staining; *scale bar* = 20 µm. **i** EPS structures (*e*) in liquid culture. No $CaCO_3$ particles formed because yeast extract was used as the carbon source instead of an organic acid (see Sect. 3.1). Same scale as in **h**

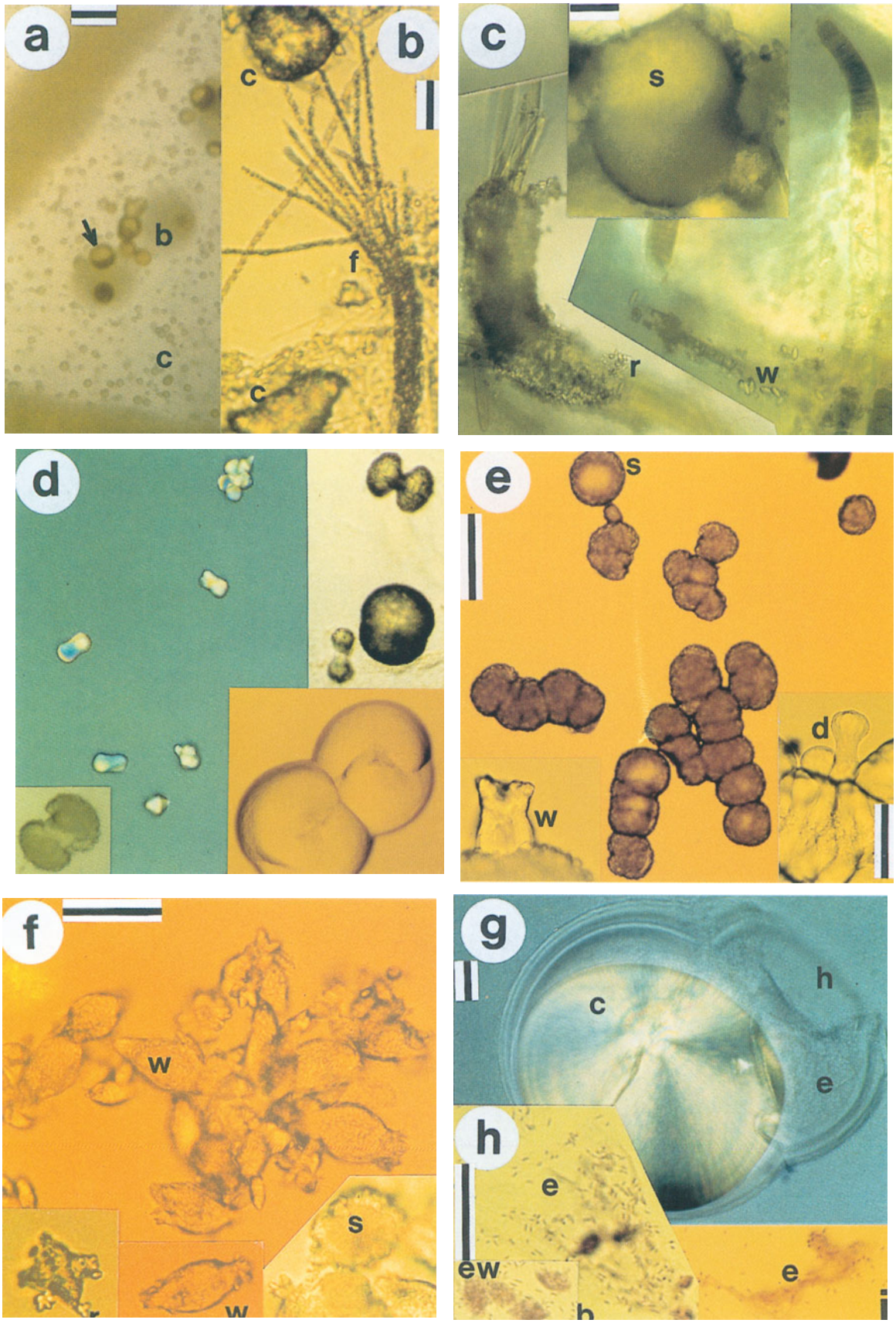
a
b
c
b
c
f
c
c
s
r
w
d
e
s
w
d
f
w
s
w
g
c
h
e
h
e
ew
e
b
i

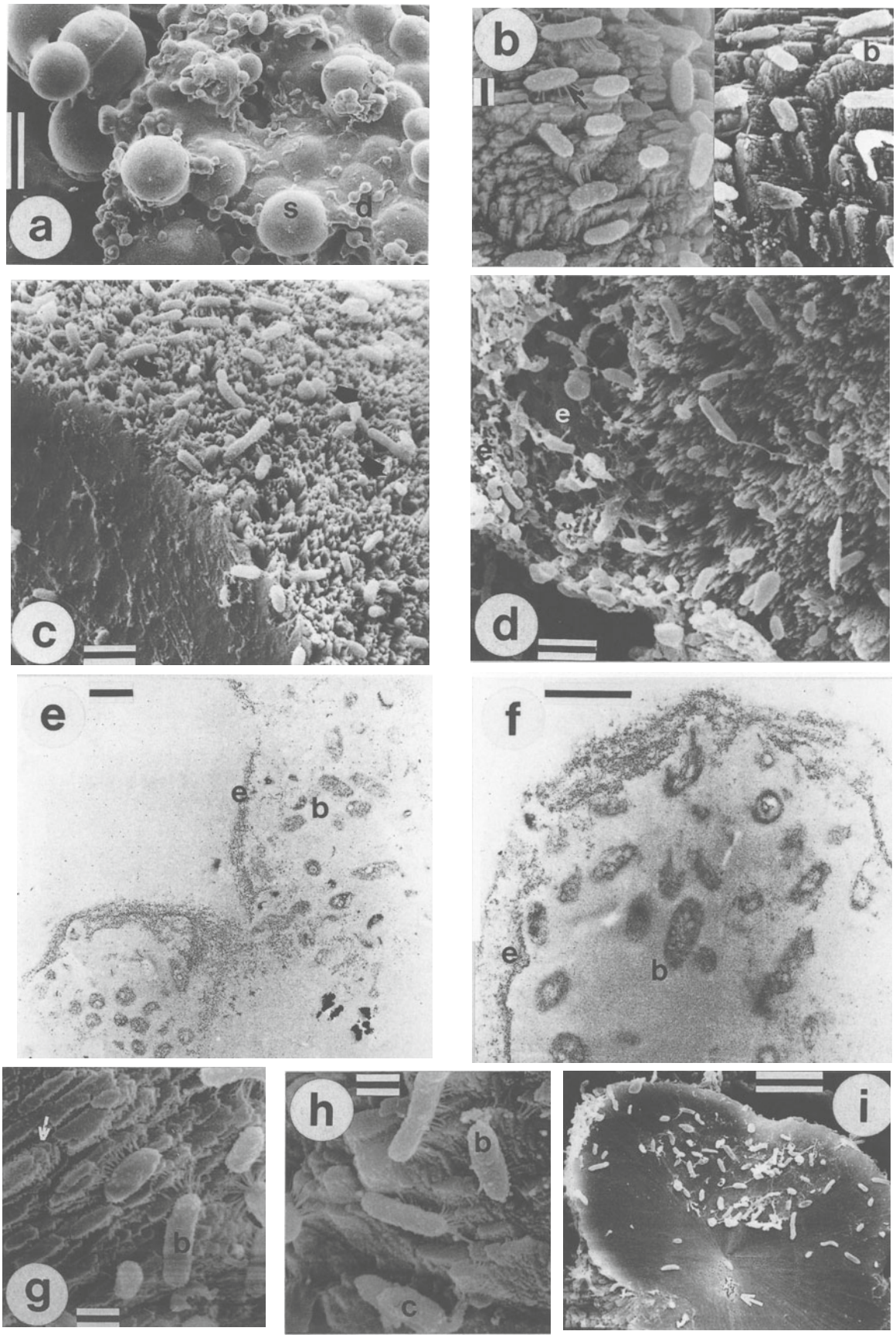
a
s
d
b
b
b
c
d
e
e
e
b
f
e
b
g
b
h
b
c
i

3 Results and Discussion

3.1 Carbonate Precipitation by Heterotrophic Bacteria: What Role Do the Bacteria Play in the Process?

Heterotrophic bacteria were isolated from microbial mats of the Janubio saltern, Lanzarote, Spain (see Gerdes et al., this Vol.), the islands of Mellum and Norderney, southern North Sea, Germany, and from a laboratory model in the ICBM Marine Station in Wilhelmshaven. The North Sea mats were initially chosen as a control in which no $CaCO_3$ precipitates, but, as we found during the experiments, carbonate particles formed even in them (Fig. 2c). The various isolates were tested to see whether they were able to precipitate $CaCO_3$ in sea water media containing different carbon sources.

Out of 128 isolates only two did not induce $CaCO_3$ precipitation on agar plates in an artificial sea water medium containing 3.5 g $CaCl_2 \times 2H_2O$, 15 mM sodium acetate, and 1 g yeast extract/l. Carbonate particles formed on agar plates are shown in Fig. 2a. Apparently, carbonate precipitation depended more on culture conditions than on the specific abilities of certain bacteria. Carbonate particles formed only:

1. a high cell densities (10^8–10^9 bacteria/ml in liquid culture, in colonies larger than 4 mm in diameter on agar plates, and if more than 5% of the surface of an agar plate was covered by colonies)
2. at a pH above 7.9 in liquid culture and 8.7 in agar plates (the media were almost unbuffered)
3. if free organic acids or amino acids were used as carbon source
4. if there was free gas exchange with the atmosphere, so that CO_2 could degas

3.2 Change in Carbonate Alkalinity

These observations are consistent with the following mechanism for $CaCO_3$ precipitation in sea water media containing sodium acetate as the sole carbon source in liquid culture (Fig. 1a; Riege et al. 1991). At the beginning of the experiment the medium has a pH above 6.0. So most of the acetate in the medium exists as negatively charged acetate ions and less than 2% as acetic acid. Products of aerobic degradation of acetate ions are:

$$CH_3COO^- + 2O_2 \rightarrow 2CO_2 + OH^- + H_2O$$

CO_2 buffers the pH by forming bicarbonate ions:

$$2CO_2 + OH^- \rightarrow CO^{2}\uparrow + HCO_3^-$$

Surplus CO_2 escapes to the atmosphere, the pH increases and carbonate ions form. The medium becomes supersaturated so that $CaCO_3$ precipitates:

$$2HCO_3^- + Ca^{2+} \rightarrow CaCO_3\downarrow + CO_2\uparrow + H_2O$$

With 15 mM acetate as the carbon source, the pH increased to values between 8.0 and 8.2. The medium was 10- to 20-fold supersaturated. After $CaCO_3$ precipitation, the medium was about 20-fold supersaturated.

If $CaCO_3$ precipitates in bacterial culture according to this mechanism, it should also be possible to induce carbonate precipitation in sterile media to which bicarbonate is added instead of acetate. This experiment should fail if bacteria were needed either as nucleation sites or to accumulate calcium ions or carbonate ions.

To sterile sea water media without a carbon source 15 mM $NaHCO_3$ was added. After 24 h in the incubator, the amount of $CaCO_3$ that precipitated was almost the same as in inoculated media with 15 mM Na-acetate as the sole carbon source, after a maximum cell density of about 10^9 bacteria/ml was reached (compare Fig. 1b and Fig. 1a). At the beginning of the experiment the medium was about 70-fold supersaturated (pH 8.5) and after carbonate precipitation 20-fold (pH 8.2).

In tests in which less than 10 mM acetate was used in inoculated media, or less than 10 mM $NaHCO_3$ in sterile media, no carbonate particles formed in either case. Apparently the medium was not supersaturated enough to induce carbonate precipitation under our experimental conditions.

It seems clear that, in our test systems, bacteria induced carbonate precipitation by the production of CO_2 and OH^-; the other steps in this process were purely chemical.

Many results of carbonate precipitation experiments with aerobic bacteria described in the literature can be explained by this mechanism. For example, McCallum and Guhathakurta (1970) used millimolar amounts of acetate as the carbon source, and Danielli and Edington (1983) used malate, succinate, and lactate.

Other bacterial processes that can lead to alkalization

◁

Fig. 3.a Air dried sample from an agar plate (SEM). **b–d, g-i** Critical point dried samples from liquid culture (SEM). **e,f** Samples from liquid culture (TEM). **a** $CaCO_3$ crust from a bacterial colony on agar plate; *s* spherical, *d* dumbbell-shaped $CaCO_3$ particle; *scale bar* = 100 µm. **b** Bacteria fixed by EPS threads onto a $CaCO_3$ particle (*arrow*). Many bacteria (*b*) position themselves according to the crystal structure of the particle; *scale bar* = 1 µm. **c** On a $CaCO_3$ particle consisting of needle-shaped crystals, some bacteria positioned parallel to the needles seem to be stuck between them (*arrows*); *scale bar* = 3 µm. **d** $CaCO_3$ particle partly covered by EPS (*e*). In the other samples the EPS covering was lost during SEM preparation; *scale bar* = 3 µm. **e,f** Ultrathin-sections of decalcified $CaCO_3$ particles; *e* EPS covering the particles, *b* bacteria embedded in the particles; *scale bars* = 1 µm. **g,h** bacteria (*b*) fixed to a $CaCO_3$ particle, *Arrow* in **g** and *c* in **h** are possible calcified bacterium; *scale bars* = 1 µm. **i** The inclusion (*arrow*) did not disturb the radial crystal structure of this particle; *scale bar* = 10 µm

of the medium, as reviewed in Krumbein (1979b), are denitrification, sulfate reduction, and production of ammonia by degradation of proteins, as well as production of trimethylamine (TMA) if trimethylamine oxide (TMAO) was used as the electron acceptor (Morita 1980). These processes may induce $CaCO_3$ precipitation only if:

1. Surplus CO_2 is removed from the system, e.g., by degassing or by autotrophic organisms.
2. Ca^{2+}-ions and nucleation sites are available.
3. A high supersaturation can be reached so that $CaCO_3$-particles form.

These conditions were given in the experiments mentioned above, as can be seen from the respective literature. In order to reach high supersaturation, often millimolar amounts of carbonate must be formed. An increasing pH, without production of high amounts of inorganic carbon, usually does not lead to carbonate precipitation.

3.3 Do $CaCO_3$ Particles Formed by Bacterial Induction Differ from $CaCo_3$ Particles Formed Abiotically?

Chemical processes similar to those in our laboratory experiments also occur in natural environments where $CaCO_3$ precipitates and where heterotrophic bacteria that might induce carbonate precipitation are present. Accordingly, we looked for qualities of $CaCO_3$ particles that indicate whether the particles formed under purely chemical conditions or whether bacteria contributed to their formation.

3.3.1 The Shape of $CaCO_3$ Particles Is Independent of the Bacterial Contribution to Carbonate Precipitation

In inoculated media with acetate as a carbon source, carbonate particles formed that were shaped like rods, wheat grains, dumbbells, and spheres (e.g., Fig. 2a, d, f, and Fig. 3a). Maximum diameters were 200 µm. Similar particles formed in sterile media to which $NaHCO_3$ was added (Fig. 2e). Rod-shaped particles were not found in sterile media. In microbial mats and enrichment cultures, spherical, dumbbell, wheat grain and rod-shaped $CaCO_3$ particles also occurred (Fig. 2b,c). They were similar in size to the particles in the carbonate precipitation tests.

Thus, neither the shape of the carbonate particles nor their mineralogy (see Introduction) provide any clue as to whether bacteria have contributed to their formation, with the possible exception of very small particles.

3.3.2 Bacteria as Nucleation Sites

Rod-shaped carbonate particles several microns in length were only found in inoculated media. Greenfield (1963) and Krumbein et al. (1977) observed bacteria embedded in carbonate particles of similar size and shape that formed in similar laboratory experiments. In the results of Krumbein (1973, Fig. 20), bacteria are shown with $CaCO_3$ precipitated on their surface (also see Krumbein et al. 1977). In these cases bacteria apparently acted as nucleation sites. In inoculated media with large cell densities (10^9 bacteria/ml), it is very probable that some of them function as nucleation sites for the formation of carbonate particles, irrespective of the mechanism of carbonate precipitation. Although in bacterial culture, $CaCO_3$ precipitated at a lower supersaturation than in sterile media containing $NaHCO_3$, in the experiments described here bacteria were obviously not necessary as nucleation sites. Otherwise no $CaCO_3$ particles would have formed in the sterile media to which $NaHCO_3$ was added. Obviously there were sufficient alternative nucleation sites, such as dust particles or scratches on the walls of the glass vessels.

Although bacteria can, and in experiments do, function as nucleation sites, in many natural environments, e.g., microbial mats or sediments, they are most likely not needed for this purpose, since there are enough other particles on which $CaCO_3$ crystals could easily grow. Some bacteria are very poor nucleation sites, as reported by Pentecost and Terry (1988) for bacteria isolated from limestone caves. In such calcareous environments, it may be advantageous for bacteria if $CaCO_3$ does not precipitate on their surface, otherwise they would die, as shown by Krumbein et al. (1977).

3.3.3 Bacteria and Extracellular Polymeric Substances Covering $CaCO_3$ Particles

In carbonate precipitation tests containing bacteria, we found bacteria attached to the surfaces of carbonate particles by extracellular polymeric substances (EPS; Fig. 3b). Often the bacteria arranged themselves according to crystal structures (e.g., Fig. 3b). On particles built by needle-shaped crystals, some bacteria lay parallel to the needles (Fig. 3c). Although bacteria covered some particles densely, they did not prevent crystal growth. Figure 3e,f shows ultrathin-sections of carbonate particles in which bacteria are embedded. In Fig. 3c some bacteria are partially embedded in the particles (see arrows).

One of the bacteria in Fig. 3g, h seems to be calcified. The radial crystal structure in Fig. 3i was not disturbed by the inclusion (marked with an arrow). Most likely, bacteria that were incorporated into growing crystals did not disturb crystal growth either.

In addition to thin strands of EPS, by which bacteria fixed themselves to carbonate particles, the bacteria produced larger amounts of EPS that covered the particles. This EPS covering is visible in interference contrast if the $CaCO_3$ is etched away by HCl (Fig. 2g). It can

be stained by toluidine blue. In Fig. 2h other EPS structures are visible apart from bacteria and EPS coverings of carbonate particles. These structures seem to be thinner than the EPS coverings of the $CaCO_3$ particles and were also formed in liquid culture without carbonate precipitation (Fig. 2i). The EPS covering of carbonate particles is visible in TEM (Fig. 3e, f), and sometimes also in SEM preparations (Fig. 3d), but neither under the light microscope nor in TEM were multilayered particles found. Apparently the growing particles did not integrate this EPS covering into their crystal structure in our experiments. The role of these EPS structures in $CaCO_3$ precipitation is not clear.

Carbonate particles in natural environments are often covered by EPS, which might be produced by carbonate-precipitating bacteria, but could also be produced by other organisms. The carbonate particles could also be formed by purely physico-chemical processes and nonetheless still be covered by EPS (Davies et al. 1978).

4 Conclusions

From data in the literature and our own experiments the following conclusions may be drawn:

1. Heterotrophic bacteria apparently do not precipitate carbonate particles by a specific mechanism. An increase in carbonate alkalinity is sufficient to explain $CaCO_3$ precipitation both in our own experiments and in most of those described in the literature. Increased carbonate alkalinity, if induced by bacteria, is usually a by-product of physiological activities.
2. Bacteria can function as nucleation sites, but in our carbonate precipitation experiments they were obviously not needed for this purpose. The same is most likely true for many environments where carbonate particles form.
3. The morphology of particles larger than 10 μm and their mineralogy give no hints as to whether bacteria have contributed to carbonate precipitation. Even the presence of EPS should be regarded with caution. Only embedded bacteria, and to a lesser extent the presence of particles that are shaped like the bacteria in question and which are only slightly larger than them, prove that bacteria were present when the carbonate particles formed. Whether the bacteria just happened to be there or whether they actually induced the carbonate precipitation cannot be deduced from the qualities of the particles but only from the physico-chemical conditions in the environment where the particles formed.

Although bacterial calcification is apparently only a by-product of bacterial metabolic activity and also largely depends on abiotic conditions, without bacteria no $CaCO_3$ would precipitate in some environments where carbonate particles form. Bacteria and other microorganisms change the abiotic parameters of their environment considerably. One of the results of these changes may be the precipitation of $CaCO_3$.

References

Bavendamm W (1932) Die mikrobiologische Kalkfällung in der tropischen See. Arch Mikrobiol 3:205–276

Boquet E, Boronat A, Ramos-Cormenzana A (1973) Production of calcite (calcium carbonate) crystals by soil bacteria is a general phenomenon. Nature 246:527–528

Buczynski C, Chafetz HS (1991) Habit of bacterially induced precipitates of calcium carbonate and the influence of medium viscosity on mineralogy. J Sediment Petrol 61:226–233

Castanier S (1987) Microbiogeologie: Processus et Modalites de la Carbonatogenese Bacterienne. Thesis, University of Nantes, Nantes, pp 535

Chafetz HS, Buczynski C (1992) Bacterially induced lithification of microbial mats. Palaios 7:277–293

Danielli HMC, Edington MA (1983) Bacterial calcification in limestone caves. Geomicrobiol J 3:1–16

Davies PJ, Bubela B, Ferguson J (1978) The formation of ooids. Sedimentology 25:703–730

Drew GH (1914) On the precipitation of calcium carbonate in the sea by marine bacteria. Carnegie Publication No. 182, Washington, pp 7–45

Ferrer MR, Quevedo-Sarmiento J, Bejar V, Delgado R, Ramos-Cormenzana A, Rivadeneyra MA (1988) Calcium carbonate formation by *Deleya halophila*: effect of salt concentration and incubation temperature. Geomicrobiol J 6:49–57

Greenfield LJ (1963) Metabolism and concentration of calcium and magnesium and precipitation of calcium carbonate by a marine bacterium. Ann NY Acad Sci 109:23–45

Krumbein WE (1973) Mikrobiologische Untersuchungen zur Fällung von Kalziumkarbonat aus Meerwasser. In: Jahresbericht 1973, Biologische Anstalt Helgoland, Heide, Boysen and Co, pp 50–54

Krumbein WE (1979a) Photolithotrophic and chemoorganotrophic activity of bacteria and algae as related to beachrock formation and degradation (Gulf of Aqaba, Sinai). Geomicrobiol J 1:139–203

Krumbein WE (1979b) Calcification by bacteria and algae. In: Trudinger PA, Swaine DJ (eds) Biogeochemical cycling of mineral-forming elements. Elsevier, Amsterdam, pp 47–68

Krumbein WE, Cohen Y, Shilo M (1977) Solar Lake (Sinai). 4. Stromatolitic cyanobacterial mats. Limnol Oceanogr 22:635–656

McCallum MF, Guhathakurta K (1970) The precipitation of calcium carbonate from seawater by bacteria isolated from Bahama bank sediments. J Appl Bacteriol 33:649–655

Molisch H (1925) Über Kalkbakterien und andere kalkfällende Pilze. ZBL Bakteriol Parasitenkunde, Infektionskrankheiten, Hygiene II, Abt 65:130–139

Morita R (1980) Calcite precipitation by marine bacteria. Geomicrobiol J 2:63–82

Nadson GA (1928) Beitrag zur Kenntnis der bakteriogenen Kalkablagerungen. Arch Hydrobiol 19:154–164

Pentecost A, Terry C (1988) Inability to demonstrate calcite precipitation by bacterial isolates from travertine. Geomicrobiol J 6:185–194

Riege H (1994) Untersuchungen zur Carbonatfällung in Mikrobenmatten. Thesis, University of Oldenburg, Oldenburg, 219 pp

Riege H, Gerdes G, Krumbein WE (1991) Contribution of heterotrophic bacteria to the formation of $CaCO_3$-aggregates in hypersaline microbial mats. Kieler Meeresforsch, Sonderh 8:168–172

Rivadeneyra MA, Ramos-Cormenzana A, Garcia-Cervigon A (1985) Etude de l'influence du rapport Mg/Ca sur la formation de carbonate par des bactéries telluriques. Can J Microbiol 31:229–231

Rivadeneyra MA, Delgado R, del Moral A, Ferrer MR, Ramos-Cormenzana A (1994) Precipitation of calcium carbonate by *Vibrio* spp. from an inland saltern. FEMS Microbiol Ecol 13:197–204

Bacterial Roles in the Precipitation of Carbonate Minerals

Sabine Castanier, Gaële Le Métayer-Levrel, Jean-Pierre Perthuisot

Laboratoire de Biogéologie et Microbiogéologie, Université de Nantes, 2 rue de la Houssinière, F-44072 Nantes Cedex 03, France

Abstract. Bacterial carbonate formation includes autotrophic pathways that induce local CO_2 depletion of the medium and heterotrophic pathways that can lead to active or passive precipitation. In active precipitation, solid carbonate is localised by ionic exchange through the cell membrane. In passive precipitation, processes such as ammonification, dissimilatory nitrate reduction, degradation of urea or uric acid, and sulphate reduction lead to carbonate and bicarbonate production and a pH increase, processes which induce solid carbonate precipitation. In heterotrophic bacterial communities, pathways of carbonate precipitation always appear to be responses to enrichment by organic matter, and the precise nutritional conditions play a major role in the relationships between bacteria and the developing crystals. Heterotrophic bacterial precipitation, evaluated by laboratory experiments, appears to be the most probable process in the formation of apparently abiotic limestones. Bacterial carbonate formation has applications for stonework preservation and restoration.

1 Introduction

In nature, carbonate precipitation may theoretically occur as a result of several processes. Abiotic chemical precipitation from saturated solutions can occur due to evaporation, reduction in CO_2 pressure, and temperature increase. Biogenic products include minerals produced by animals and plants (shells, skeletons, tests, etc.), precipitates influenced by photosynthesis, fungal carbonates (Callot et al. 1985; Verrecchia and Loisy 1997), and bacterial carbonates.

Abiotic processes, and also photosynthesis, are limited by either carbonate-bicarbonate ion concentrations or by the ionic strength of solutions. Furthermore, in eukaryotes photosynthesis may result in mineral production but is balanced by respiration, with the result that only cyanobacteria and other photosynthetic bacteria play a geological role through this process. Thus, apart from stromatolites, photosynthetic processes hardly account for extensive azoic limestone deposition or early diagenetic carbonate cement formation. On the other hand, skeletons and tests produced by animals and algae result in extensive biogenic limestones.

A bacterial contribution to limestone formation has been suspected for years (Drew 1910a,b; Berkeley 1919; Kellerman 1915; Lipmann 1924; Mollish 1924; Nadson 1928; Krumbein 1968, 1974, 1978) but remained controversial until recent experiments in geomicrobiological laboratories investigated the metabolic pathways involved and evaluated bacterial carbonate productivity (Krumbein 1979; Castanier 1987; Le Métayer-Levrel 1996; Castanier et al. 1997; see also Riege and Krumbein, this Vol.).

2 Metabolic Pathways of Bacterial Carbonate Formation

2.1 Autotrophic Pathways

Three principal kinds of bacteria are involved in autotrophic production. All obtain carbon from gaseous or dissolved CO_2, the origin of which is complex (atmosphere, eukaryotic and prokaryotic respiration, and fermentation; Fig. 1).

Non-methylotrophic methanogenesis is carried out by methanogenic archaebacteria, which use CO_2 and H_2 in strict anaerobiosis to give CH_4 (Marty 1983). These bacteria live at deep within the sediment, and the CO_2 and H_2 that they use are products of the activity of fermentative bacteria and anaerobic cellulolytic bacteria such as *Clostridium*.

Methylotrophic methanogenic bacteria are very different in that they use organic matter rather than CO_2 and H_2 to realise methane production.

Anoxygenogenic photosynthesis is carried out by sulphurous or non-sulphurous, purple and green photosynthetic bacteria. They do not produce oxygen and live in anaerobiosis (or, in some species, microaerophily) using infrared light as the energy source (735–755 nm for green bacteria; 800–1000 nm for purple bacteria). Sulphur bacteria use H_2S as an electron donor. These bacteria naturally live in anaerobic waters and microbial mats and may also be found in gypsum deposits (Pfennig and Trüper 1989).

Oxygenogenic photosynthesis is performed by cyanobacteria, which use visible light as a source of energy (680–685 nm). This type of photosynthesis leads to oxygen production.

R.E. Riding and S.M. Awramik (Eds.)
Microbial Sediments

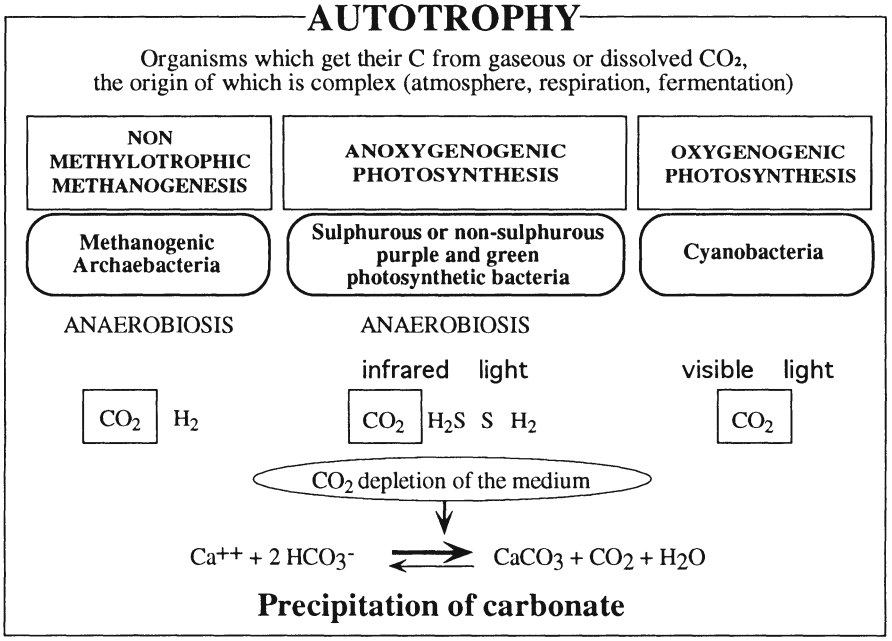

Fig. 1. Bacterial calcium carbonate production in autotrophy

All three pathways described above involve the use of CO_2 as a carbon source in the production of organic matter. Thus, these pathways induce CO_2 depletion either of the medium or of the immediate environment of the bacteria. When calcium ions are present in the medium, such depletion favours calcium carbonate precipitation.

2.2 Heterotrophic Pathways

In heterotrophy, two bacterial carbonate precipitation-enhancing processes may occur, often concurrently.

2.2.1 Active Precipitation

Active precipitation or active carbonatogenesis (Castanier 1987; Castanier et al. 1997) is independent of the other previously mentioned metabolic pathways. The carbonate particles are produced by ionic exchanges through the cell membrane by activation of calcium and/or magnesium ionic pumps or channels, probably coupled with carbonate ion production. Numerous bacterial groups are able to operate such processes.

2.2.2 Passive Precipitation

Passive precipitation or passive carbonatogenesis operates by producing carbonate and bicarbonate ions and inducing various chemical modifications in the medium that lead to the precipitation of calcium carbonate. Two metabolic cycles can be involved : the nitrogen cycle and the sulphur cycle.

In the nitrogen cycle, passive bacterial precipitation follows three different pathways : (1) ammonification of amino acids (in aerobiosis, in the presence of organic matter and calcium), (2) dissimilatory reduction of nitrate (in anaerobiosis or microaerophily, in the presence of organic matter, calcium and nitrate), (3) degradation of urea or uric acid (in aerobiosis, in the presence of organic matter, calcium, and urea or uric acid). Both urea and uric acid result from eukaryotic activity, notably that of vertebrates. These three pathways induce production of carbonate and bicarbonate ions and, as a metabolic end-product, ammonia, which induces a pH increase (Fig. 2). When the H^+ concentration decreases, the carbonate-bicarbonate equilibria are shifted towards the production of CO_3^- ions. If calcium ions are present, calcium carbonate precipitation occurs. If Ca^{2+} (and/or divalent cations) are lacking in the medium, carbonate and bicarbonate ions accumulate, and the pH increase and bacterial activity may favour zeolite formation. This happens in some soda lakes, e.g., in Kenya (Castanier et al. 1993).

To date, from our experiments (Pontoizeau et al. 1996) in highly magnesian media, none of the nitrogen cycle pathways has led to bacterial precipitation of rhombohedric, anhydrous, high magnesian carbonates (dolomite or magnesite). Only hydrated and hydroxylated compounds (Mg-carbonates and Mg-phosphates) were obtained.

In the sulphur cycle, bacteria use a single metabolic pathway: the dissimilatory reduction of sulphate (Fig. 3). The environment must be anoxic and rich in

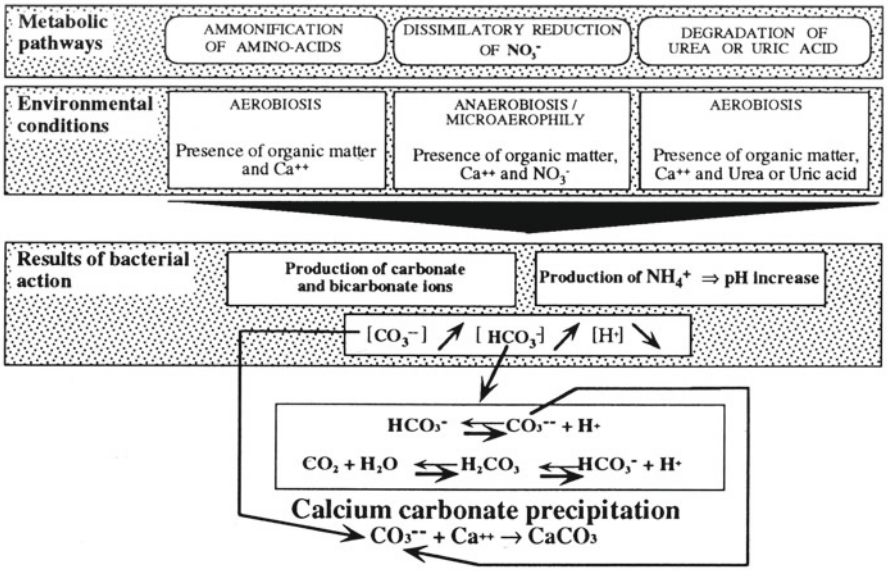

Fig. 2. Passive bacterial precipitation of calcium carbonate in the nitrogen cycle

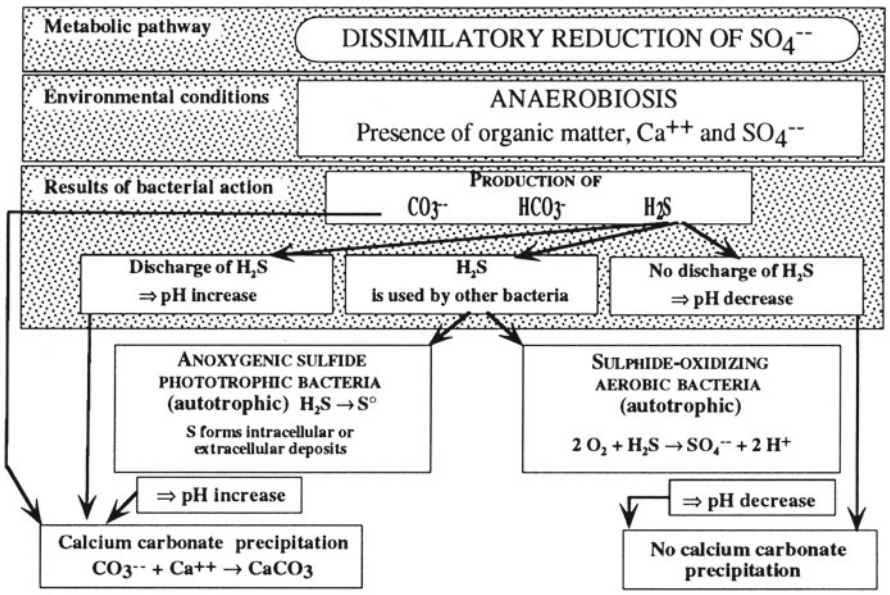

Fig. 3. Passive bacterial precipitation of calcium carbonate in the sulphur cycle

organic matter, calcium and sulphate. Using this pathway, the bacteria produce carbonate, bicarbonate ions and hydrogen sulphide. The precipitation of Ca-carbonates depends on the behaviour of the hydrogen sulphide. There are three possibilities.

Firstly, the hydrogen sulphide degasses, for example when the water depth is sufficiently shallow and when there is no impermeable barrier. This induces a pH increase and, if calcium ions are present, Ca-carbonate precipitation.

Secondly, hydrogen sulphide is used by other bacteria. If the bacteria involved are anoxygenogenic sulphide-phototrophic bacteria which live in autotrophy and anaerobiosis, the hydrogen sulphide is oxidised to sulphur, which forms intra-cellular or extra-cellular deposits around the cell wall. Hydrogen sulphide uptake induces a pH increase, favouring calcium carbonate precipitation. If the bacteria involved are autotrophic sulphide-oxidising aerobic bacteria, they form sulphate ions. Together with hydrogen ions from water this gives sulphuric acid, a decrease in pH and no Ca-carbonate appears.

Thirdly, the hydrogen sulphide is not used and is not discharged. This occurs, for example, when the water depth is high or when there is an impermeable layer (e.g., a microbial mat) present. In this case, the pH decreases and Ca- carbonates cannot precipitate.

Recent experiments on bacterial activation of the

sulphur cycle in an anaerobic hood led to the precipitation of magnesite and dolomite (Pontoizeau et al. 1997). In these experiments, H_2S could not escape from the jars containing bacteria and the nutritional medium. Thus, it seems that (moderately) low pH favours the integration of Mg ions into the carbonate rhombohedric network.

3 Experimental Data on Heterotrophic Bacterial Productivity

All heterotrophic metabolic pathways were tested in the laboratory. For example, a number of experiments were carried out with *Bacillus cereus*, which is a heterotrophic bacterium able to carry out ammonification of amino acids and dissimilatory nitrate reduction. In the experiment presented in Fig. 4, the medium initially contains 4 g organic matter per litre (Castanier 1984; Le Métayer-Levrel 1996). After a phase of latency, there is an exponential increase in bacterial growth together with the accumulation in the medium of metabolic end-products: carbonate, bicarbonate and ammonia ions. The ammonia produced induces a pH increase which favours carbonate precipitation. This phase ends in a steady state when most of the initial organic matter is consumed. Particulate carbonate precipitation occurs during the exponential phase and ends more or less after the beginning of the steady state. Active precipitation appears to start first. It is followed by passive precipitation which induces further growth of the initially produced particles.

Quantitatively, the production of calcium carbonate depends essentially upon the strain (or bacterial population) used, the environmental conditions (temperature, salinity, etc.), the quality and quantity of available nutrients, and time. In the above mentioned experiment (Fig. 4), with a nutritive input of 4 g/l of organic matter, 2.4 g of solid carbonate (calcite) were obtained per litre per day (Le Métayer-Levrel 1996). We define the "carbonatogenic yield" (or calcium carbonate yield) as the ratio of the weight of organic matter input to the weight of calcium carbonate produced. In the case presented here this value is 0.6. At the time of writing, we maintain 75 carbonatogenic strains belonging to different species collected in various natural environments. Most of them display carbonatogenic yields around 0.5, sometimes more; the lowest yield measured is 0.2.

4 Geological Implications

Presently, from the nutrient-poor, open ocean environment towards nearshore and lagoonal environments,

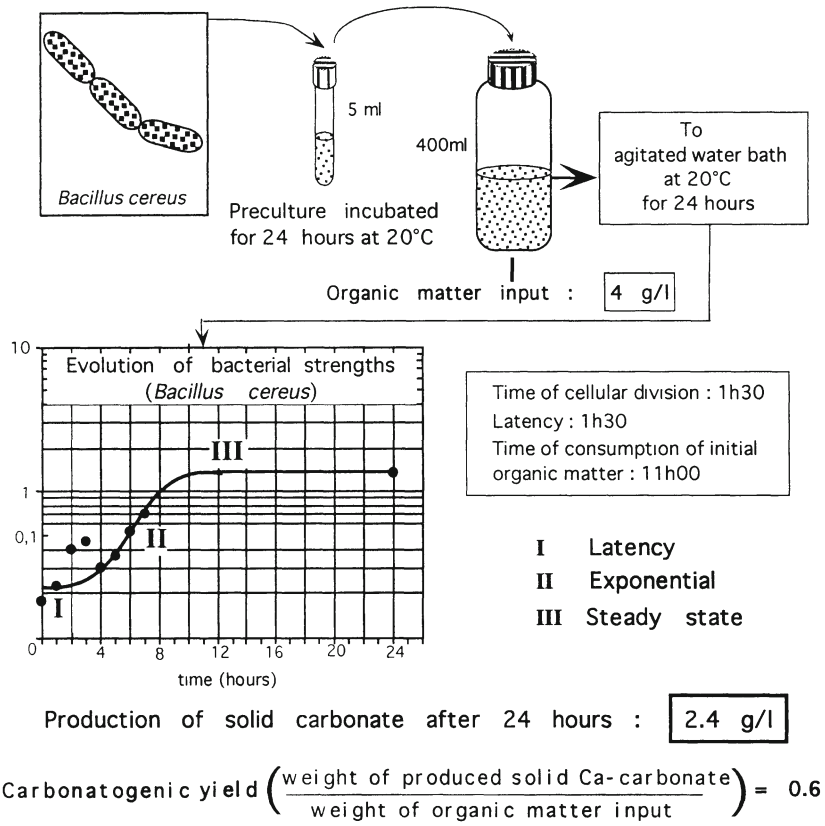

Fig. 4. Laboratory experiment using the heterotrophic bacterium *Bacillus cereus*

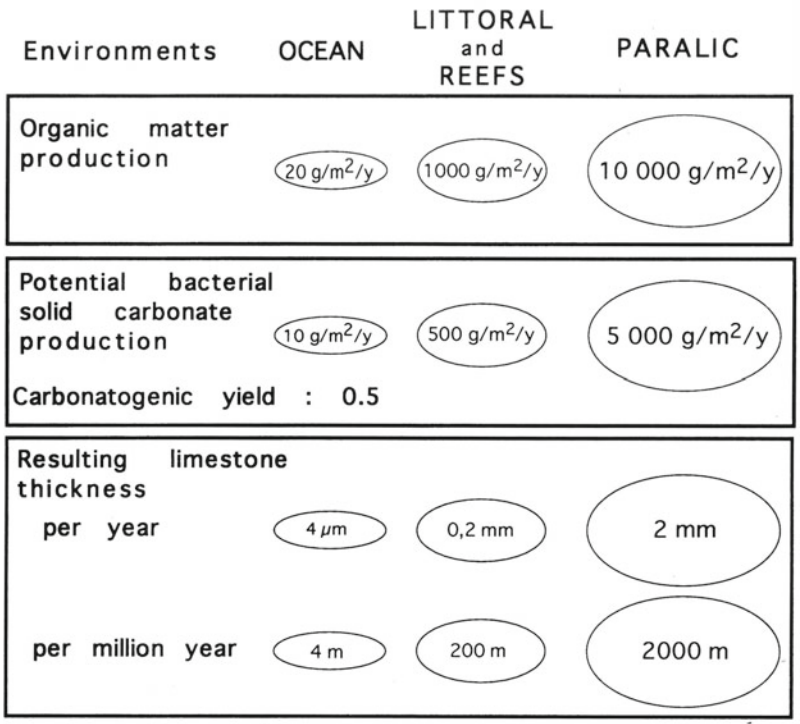

Fig. 5. The potential deposition rates of limestones through aerobic heterotrophic bacterial processes

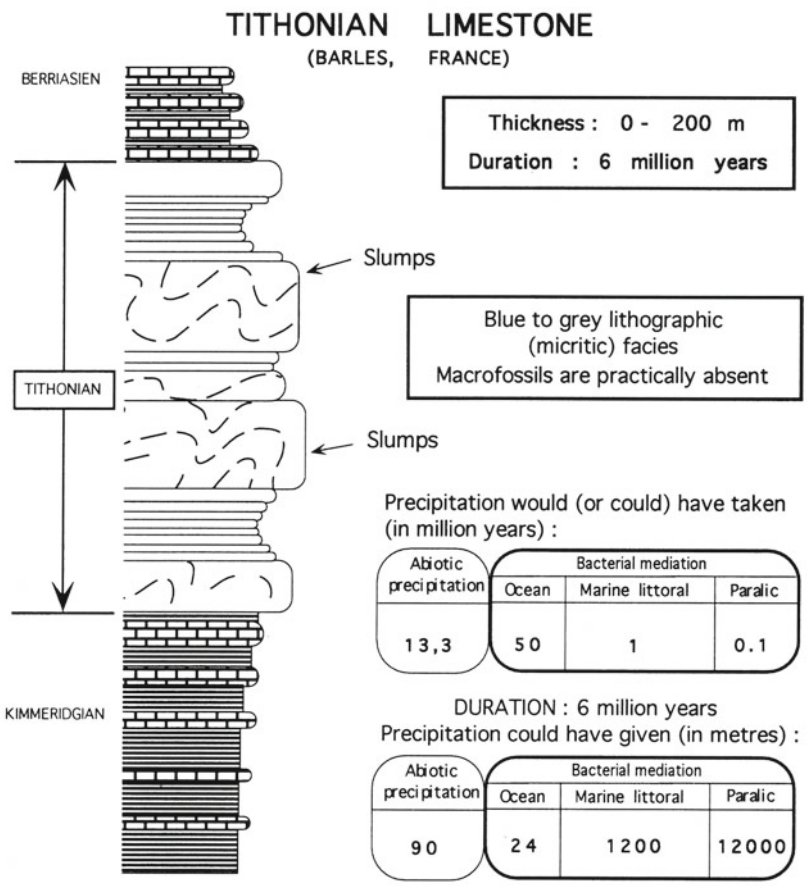

Fig. 6. Abiotic precipitation versus heterotrophic bacterial mediation in the formation of Tithonian limestone

organic matter sedimentation varies between 20 and 10,000 g/m^2 per year (Basson et al. 1977; Allen et al. 1979). Under such conditions, and assuming a calcium carbonate yield of 0.5 and a calcite density of 2.5, bacterial carbonatogenesis is able to produce in 1 year a $CaCO_3$ layer 4 µm – 2 mm in thickness. Bacterial carbonatogenesis thus could form a limestone layer 4 – 2000 m thick in 1 million years (Fig. 5).

With the present day composition of sea water, and assuming a mean oceanic evaporation rate of 150 mm/year, such a physical process would produce a $CaCO_3$ layer 15 µm thick, i.e., 15 m in 1 million years.

Such considerations can be applied to real examples from the geological record. We chose the Tithonian formation of the Western Alps as an example (Fig. 6). This is a micritic, azoic shelf limestone in which macrofossils or macroscopic shells debris are practically absent. The thickness is between a few metres and 200 metres or more. These variations are due to slumping, which also suggests a certain fluidity and instability of the initial sediment. The duration of the Tithonian is approximately 6 million years.

In that space of time, if conditions were similar to present day ones, abiotic precipitation could have formed only 90 m of limestone, whereas heterotrophic bacterial mediation could have produced a limestone layer ranging from 24 m thick in oceanic environments to 12,000 m thick in paralic environments. On the other hand, the deposition of 200 m limestone would have required 13.3 million years through abiotic precipitation, while it would have required from 50 Ma to as little as 0.1 Ma, depending upon the kind of environment, through heterotrophic bacterial carbonatogenesis. This assumes that the initial organic matter were-mainly produced by autotrophic microorganisms, which could also have contributed to carbonate precipitation. We should note, however, that such processes are necessarily limited by the amounts of carbonate

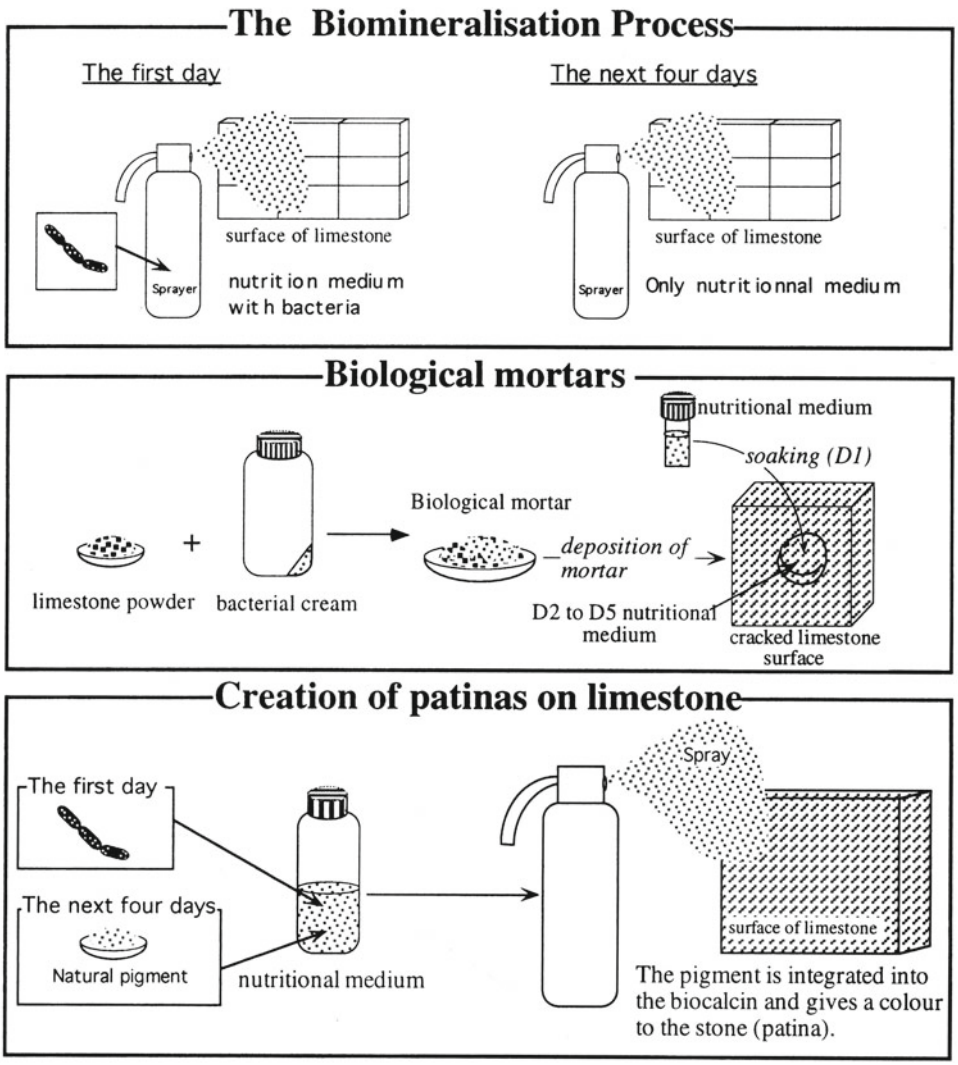

Fig. 7. Applications of bacterial carbonatogenesis to protection and restoration of stonework. (Optimisation of French patent number 89 03517 (Adolphe, Loubière, Paradas, Soleilhavoup, 1989; property of CALCITE S.A. and French patent number 95 05861; Castanier, Levrel, Loubière, 1995)

and bicarbonate ions present in the medium so that the carbonate production they account for hardly exceeds that of abiotic ones. However, abiotic evaporative carbonate deposition is unlikely and also presently barely observed.

5 Protection and Rejuvenation of Stone Surfaces

The capacity of bacteria for carbonate production may be used for biotechnological purposes, notably the protection and restoration of limestone monuments and statuary (Fig. 7; Orial et al. 1993). In this context, the so-called process of biomineralisation involves spraying a suitable bacterial suspension culture over the surface to be protected. Subsequently, the deposited culture is fed every 1 or 2 days with a suitable medium in order for the bacteria to form a carbonate coating, "biocalcin". Industrial and financial constraints normally restrict the number of feeding applications to five. The nutritional medium is designed to stimulate bacterial active and passive production of carbonate. Following laboratory simulation on miniature walls, the first full-scale experiment was made at Thouars (Deux Sévres) on the tower of St Médard Church. The final set of measurements (June 1994) confirmed the good quality and resistance of the biocalcin. Three years after treatment, the external aspect of the tower had not changed. Surficial biomineralisation by bacterial carbonate precipitation also appears to provide good protection of limestone statuary (Le Métayer et al. 1996, 1997).

During the application phase of the biomineralisation process, it is also possible to create surficial patinas on limestones by adding natural pigments to the nutritional medium. The pigments are incorporated into the biocalcin and thus impart a lasting colouring to the stone.

Another application of bacterial carbonatogenesis is based on the concept of biological mortars or cements. These are obtained from a mixture of bacteria, finely ground limestone and nutritional medium in variable proportions. The mortars can be used to paste small fragments back onto statues or to fill in small cavities in limestone surfaces. It is also possible to include pigments in the mixture to obtain coloured biological mortars. This new concept may be very useful in limestone monument restoration.

These applications aim to recreate naturally produced material that is as similar as possible to the limestone substrate, following the same metabolic pathways from which the latter was created in nature.

6 Discussion and Conclusions

The environmental conditions of heterotrophic, bacterial metabolic pathways are diverse (aerobiosis, anaerobiosis, microaerophily). However, carbonate precipitation always appears to be the response of heterotrophic bacterial communities to enrichment of the environment by organic matter.

Observations and experiments show that nutritional conditions play a major role in the relationships between crystals and bacteria (Perthuisot et al. 1997). In eutrophic conditions, bacterial activity is very high at the beginning. Early solid products as well as biomineral aggregates are probably amorphous (Castanier et al. 1988). They scarcely follow crystalline structures, which are initially overridden by biological processes, but may form later on by recrystallisation. By contrast, in oligotrophic conditions, bacterial production rates are low, so that the crystallographic rules soon overcome the initial biological disorder and the biological structures rapidly disappear in the large crystals. Thus, observations of recently formed or unmodified carbonate bacterial grains could provide information on their original nutritional microenvironment. In most cases, however, the primary bacterial origin of carbonate material leaves no trace.

The yield of heterotrophic bacterial carbonatogenesis and the scale of solid carbonate production by heterotrophic bacteria are potentially much higher than autotrophic carbonatogenesis or chemical sedimentation in most environments. Furthermore, bacterial heterotrophic carbonatogenesis is not restricted to particular taxonomic groups of bacteria nor to specific environments, so that it probably has been a ubiquitous phenomenon since Precambrian times; it merely requires organic matter enrichment. Thus, heterotrophic bacterial carbonatogenesis much more plausibly accounts for apparently abiotic limestone deposition, and for carbonate cementation, than any other single process. As far as biodetrital particles are concerned, it can be observed that carbonate shells and tests of organisms result from the activity of their mitochondria (or chloroplasts). Other organelles may be involved such as Golgi apparatus (Hemleben et al. 1986; de Vrind-de Jong and de Vrind 1997). Since these cellular organelles are nowadays considered by a number of biologists as endosymbiotic bacteria (Margulis and Sagan 1986), the great majority of limestones and dolostones, apart from those of purely evaporitic and autotrophic origin, can be considered as products of heterotrophic bacterial activity.

References

Allen GP, Laurier D, Thouvenin J (1979) Etude sédimentologique du Delta de la Mahakam. Compagnie Française des Pétroles, Paris (Notes et Mémoires, vol 15)

Basson PW, Burchard JE, Hardy JT, Price ARG (1977) Biotopes of the Western Arabian Gulf. Marine life and environments of Saudi Arabia. ARAMCO, Dhahran

Berkeley C (1919) A study of marine bacteria. Straits of Georgia B.C. Proc Trans R Soc Can (Ottawa Sect) 5(13):15 – 43

Callot G, Guyon A, Mousain D (1985) Inter-relations entre aiguilles de calcite et hyphes mycéliens. Agronomie 5:209 – 216

Castanier S (1984) Étude de l'évolution quantitative et qualitative des populations bactérienne précipitant le carbonate dans différents cas artificiels de confinement réalisés à partir d'eau et de sédiment lagunaires méditerranéens. Thesis, Aix-Marseille II University

Castanier S (1987) Microbiogéologie: processus et modalités de la carbonatogenèse bactérienne. Thesis, Nantes University

Castanier S, Maurin A, Perthuisot JP (1988) Les Cugnites: carbonates amorphes de Ca et Mg, précurseurs possibles de la dolomite. C R Acad Sci 306 II:1231 – 1235

Castanier S, Bernet-Rollande MC, Maurin A, Perthuisot JP (1993) Effects of microbial activity on the hydrochemistry and sedimentology of Lake Logipi, Kenya. Hydrobiologia 267:99 – 112

Castanier S, Le Métayer-Levrel G, Perthuisot JP (1997) La carbonatogenèse bactérienne. In: Causse F, Gasse F (eds) Hydrologie et géochimie isotopique. ORSTOM, Paris, pp 197 – 218

Drew GH (1910a) The action of some denitrifying bacteria in tropical and temperate seas, and the bacterial precipitation of calcium carbonate in the sea. J Mar Biol Assoc IX:142 – 155

Drew GH (1910b) On the precipitation of calcium carbonate in the sea by marine bacteria, and on the action of denitrifying bacteria in tropical and temperate seas. J Mar Biol Assoc IX:479 – 523

Hemleben C, Anderson OR, Berthold WU, Spindler M (1986) Calcification and chamber formation in foraminifera – a brief review. In: Leadbeater BSC, Riding R (eds) Biomineralization in lower plants and animals. Systematics Assoc 30:237 – 249

Kellerman KF (1915) Relation of bacteria to deposition of calcium carbonate. Geol Soc Am Bull 26:58

Krumbein WE (1968) Geomicrobiology and geochemistry of lime crusts in Israel. In: Muller G, Friedman GM (eds) Recent developments in carbonate sedimentology in Central Europe. Springer, Berlin Heidelberg New York, pp 134 – 147

Krumbein WE (1974) On the precipitation of aragonite on the surface of marine bacteria. Naturwissenschaften 61:167 – 177

Krumbein WE (1978) Algal mats and their lithification. In: Krumbein WE (ed) Environnemental biogeochemistry and geomicrobiology. The aquatic environnement, vol 1. Ann Arbor Science, Ann Arbor. pp 209 – 225

Krumbein WE (1979) Calcification by bacteria and algae. In: Trudinger PA, Swaine DJ (eds) Biogeochemical cycling of mineral-forming elements. Elsevier, Amsterdam, pp 47 – 68

Le Métayer-Levrel G (1996) Microbiogéologie du carbonate de calcium. Applications industrielles. Implications géologiques. Thesis, Nantes University

Le Métayer-Levrel G, Castanier C, Perthuisot JP (1997) From carbonatogenesis concepts to bacterial regeneration of limestones (microbial lifting) In: Microbial mediation in carbonate diagenesis. ASF Paris 26:41 – 42

Lipmann CB (1924) Further studies on marine bacteria with special reference to the Drew hypothesis on $CaCO_3$ precipitation in the sea. Carnegie Inst, Washington, Publ 391(26):231 – 248.

Margulis L, Sagan D (1986) Microcosmos. Four billion years of evolution from our microbial ancestors. Summit Books, Simon and Schuster, New York

Marty D (1983) Cellulolyse et méthanogenèse dans les sédiments marins. Thesis, Aix-Marseille I University

Mollish H (1924) Über kalkbacterien und ausere kalkfallende pilze. Zentralbl Bakteriol II 65:130 – 139

Nadson GA (1928) Beitrag zur Kenntis der baketriogen Kalkabla gerungen. Arch Hydrol 19:154 – 164

Orial G, Castanier S, Le Métayer G, Loubière JF (1993) The biomineralization: a new process to protect calcareous stone applied to historic monuments. Biodeterioration Cult Property 2:98 – 116

Perthuisot JP, Castanier S, Le Métayer-Levrel G, Loubière JF (1997) From bacteria to crystals in karstic waters. The role of nutritional conditions. In: Microbial mediation in carbonate diagenesis ASF Paris 26:55 – 56

Pfennig N, Trüper HG (1989) Anoxygenic phototrophic bacteria. In: Staley JT, Bryant MP, Pfennig N, Holt JG (eds) Bergey's manual of systematic bacteriology, III. Williams and Wilkins, Baltimore, pp 1635 – 1709

Pontoizeau P, Castanier S, Perthuisot JP (1996) Production bactérienne de struvite ($MgNH_4PO_4$, $6H_2O$) au cours d'expériences visant à produire des carbonates hypermagnésiens. C R Acad Sci Paris 323(IIa):21 – 128

Pontoizeau P, Castanier S, Perthuisot JP (1997) First bacterial production of magnesite $MgCO_3$ in anaerobic strictly controlled conditions. In: Microbial mediation in carbonate diagenesis. ASF Paris 26:57 – 58

Verrecchia EP, Loisy C (1997) Carbonate precipitation by fungi in terrestrial sediments and soils. In: Microbial mediation in carbonate diagenesis. ASF Paris 26:73 – 74

de Vrind-de Jong EW, de Vrind JPM (1997) Algal deposition of carbonates and silica. In: Banfiel JF, Nealson KH (eds) Geomicrobiology: interactions between microbes and minerals: 267 – 307. Rev Mineral 35, Mineralogical Society of America, Washington

Bacterially Induced Microscale and Nanoscale Carbonate Precipitates

Robert L. Folk[1], Henry S. Chafetz[2]

[1] Department of Geological Sciences, University of Texas at Austin, Austin, Texas, 78712, USA
[2] Department of Geosciences, University of Houston, Houston, Texas, 77204-5503, USA

Abstract. Bacteria are able to form carbonate rocks and minerals at all scales, from deposits many meters thick, to distinctive shrubs, to minute crystal forms. They are particularly common in peloids, stromatolites, and hot-water travertines. The peculiar crystal morphologies they produce can be duplicated in the laboratory. Nanobacteria are much smaller forms, spheroids 0.03–0.1 μm in diameter. A quantitative census of nanobacterial bodies in limestones from Holocene to Proterozoic, and in micrite vs ooids vs sparry calcite show that the abundance is enormously variable. In a 4 μm^2 area, most samples studied contain between one and 16 bacterial bodies; the median value is about four. Bacteria are significant producers of carbonate deposits.

1 Introduction

Many investigators have suggested that bacteria have been responsible for the precipitation of calcium carbonate in a wide variety of natural settings (Drew 1911, 1913; Dalrymple 1965; Monty 1965; Horodyski et al. 1977; Chafetz and Folk 1984; Chafetz 1986, 1994; Sun and Wright 1989; Buczynski and Chafetz 1991, 1993; Chafetz and Buczynski 1992; Soudry and Weissbrod 1995). In conjunction with these interpretations, it has been well-established, as a result of numerous laboratory experiments conducted under controlled conditions, that a whole host of bacteria are capable of inducing the precipitation of calcium carbonate (Kellerman and Smith 1914; Gerundo and Schwartz 1949; Lalou 1957; Oppenheimer 1961; Greenfield 1963; McCallum and Guhathakurta 1970; Deelman 1975; Krumbein and Cohen 1977; Krumbein 1979). The bacterially induced precipitates comprise a wide variety of mega-, macro- and micro-deposits. On a megascale, bacterially induced precipitates of calcium carbonate range from being the dominant component in thick sequences of travertine deposited from hot spring waters, such as those in the vicinity of Bagni di Tivoli-Tivoli-Guidonia, Italy, and Terrace Mountain, Mammoth Hot Springs, Yellowstone National Park (Chafetz and Folk 1984), to the cap rock of salt domes (Kreitler and Dutton 1983) and large mounds on the sea floor associated with hydrocarbon seeps (Roberts et al. 1993). Macroscale deposits include bacterial shrubs (Chafetz and Folk 1984), which are restricted to harsh hot spring deposits and which comprise bacterial stromatolites, bacterial pisoids, etc. (Folk and Chafetz 1983; Chafetz and Meredith 1983). Between the macroscale and microscale deposits are silt- to sand-sized equidimensional grains, commonly referred to as peloids, which have been reported from modern and ancient reef deposits (Chafetz 1986), deep water carbonate mud mounds (Monty 1995; Pratt 1995) stromatolites and thrombolites, as well as comprising a significant constituent in travertine accumulations (Chafetz and Folk 1984). Truly microscale features range from the commonly described dumbbells, as well as spheres, hemispheres, discs, tetragonal disphenoids, tetragonal dipyramids, etc. (Monaghan and Lytle 1956; Boquet et al. 1973; Krumbein 1979; Morita 1980; Novitsky 1981; Buczynski and Chafetz 1991; 1993; Chafetz 1994), to the nanoscale remains of nanobacteria themselves (Folk 1993b, 1994).

2 Peloids and Peloid-Like Allochems

At the lower size range of the macroscale and upper size range of the microscale are silt- to very fine sand-sized aggregates of micrite-sized crystals. These bacterially induced precipitates commonly occur as peloids in modern and ancient marine reef deposits, pellets in carbonate mud mounds, clotted and pelleted fabrics in stromatolites, and grains in hot water travertine accumulations.

2.1 Shallow Marine Reefs

Peloids have been described from numerous shallow marine reef deposits, both modern and ancient (Land 1971; Land and Moore 1980; Lighty 1985; Macintyre 1985; Sun and Wright 1989; Mock and Palmer 1991; Leinfelder et al. 1993; Neuweiler 1993; Reitner 1993); for more detailed descriptions devoted exclusively to peloids and their origin(s) see Macintyre (1985) and Chafetz (1986). Peloids, which can account for over 50% of the

▷

Fig. 1.A Scanning electron micrograph of a marine peloid with a well-developed rim of euhedral, high-magnesian calcite crystals. Holocene, Florida reef tract; *scale* 10 mm

R.E. Riding and S.M. Awramik (Eds.)
Microbial Sediments

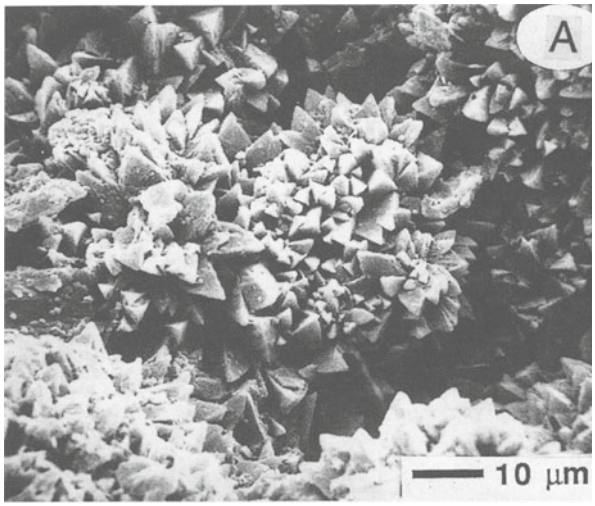

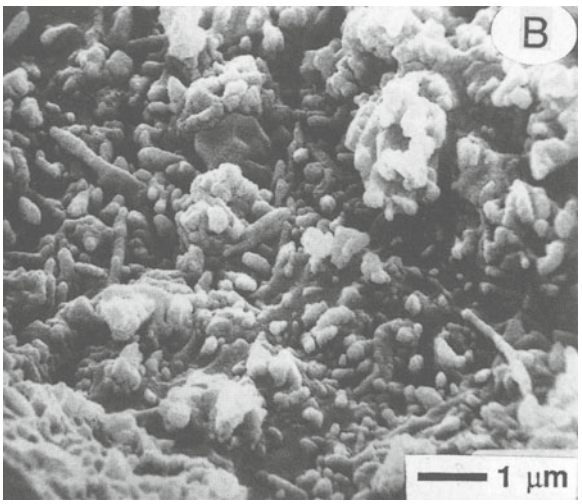

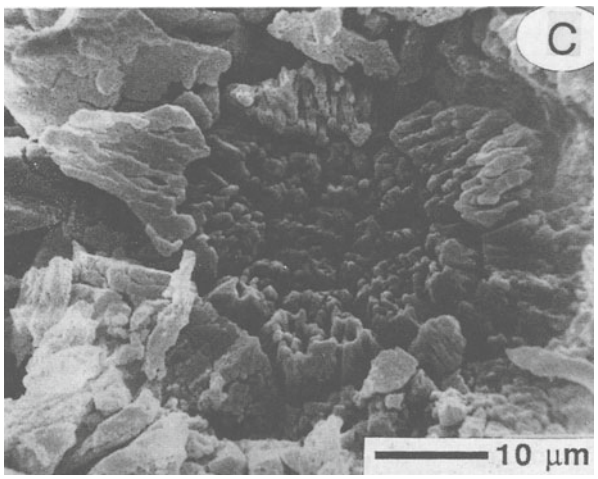

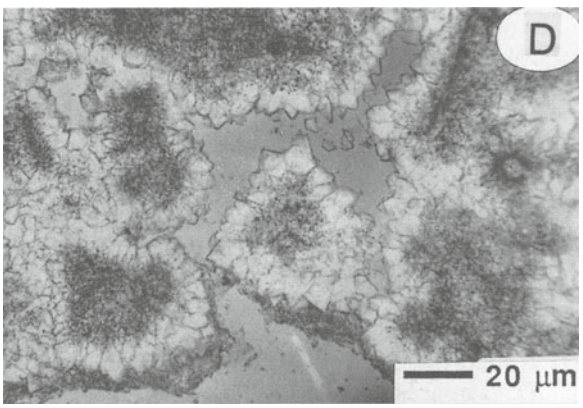

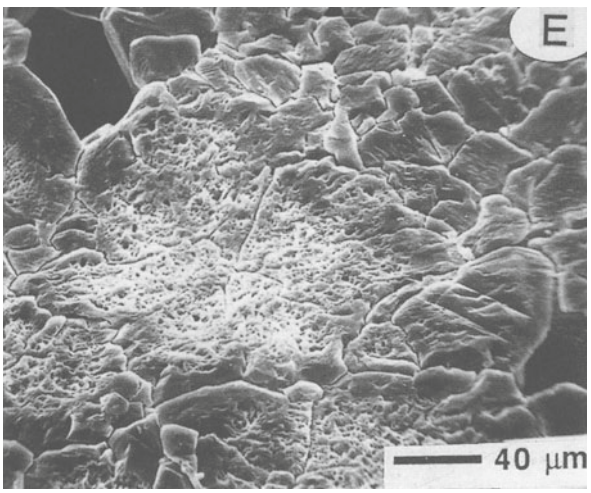

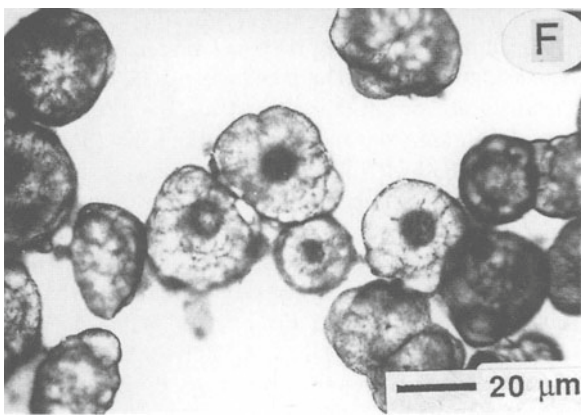

B Scanning electron micrograph of the central region of an acid-etched peloid with numerous bacterial fossils among etched calcite crystals. Holocene, Bonaire, Netherlands Antilles; *scale* 1 μm. **C** Scanning electron micrograph showing numerous micropores at the center of an acid-etched peloid. The micropores are only present in the central area of the peloid and represent the former sites of bacteria. Observe that no microporosity or bacterial fossils exist in the corona of well-developed, euhedral, high-magnesian calcite crystals surrounding the core of the peloid. Holocene, Florida; *scale* 5 μm. **D** Thin-section photomicrograph of a group of grains with clumps of bacteria (cloudy areas) at their centers. The calcite comprising the cores of these grains are bacterially induced precipitates. The bacterial centers are surrounded by clear, abiotically precipitated spar. Pleistocene travertine, Tivoli, Italy; *scale* 20 μm. **E** Scanning electron micrograph of acid-etched silt- to sand-sized grains which display microporosity at their centers. The microporosity corresponds to the former sites of bacteria similar to the cloudy areas shown in **D.** Observe that no microporosity or bacterial fossils exist in the spar which surrounds the microporous areas. Holocene, Mammoth Hot Springs, Yellowstone National Park, Wyoming; *scale* 40 μm. **F** Thin-section photomicrograph of bacterially induced precipitates grown under controlled laboratory conditions (see Buczynski and Chafetz 1991) in a fluid medium. They are composed of clumps of bacteria at their centers (cloudy areas) surrounded by radiating arrays of aragonite crystals; *scale* 20 μm

reef fabric (Reid 1987; Sun and Wright 1989; Mock and Palmer 1991), occur as laminated crusts and as cavity-fill precipitates, both between and within skeletal material. The occurrence of peloids within isolated to semi-isolated cavities in skeletal material strongly supports an in situ origin, especially within cavities in which detrital matter, such as bioclastic debris, is absent (Sun and Wright 1989). Data supplied by Leinfelder et al. (1993) and Neuweiler (1993) also strongly support in situ growth of peloids.

The peloids generally range from 10 to 60 μ in diameter and have cloudy centers, commonly 20 – 40 μm across, and clear exterior rims. In modern reefs, the rims commonly are composed of clear, dentate, high-magnesian calcite crystals which are considerably coarser than the material comprising the cores (Macintyre 1985, Fig. 1B; Chafetz 1986, Fig. 1A). It is the cores of the peloids that are interpreted as bacterially induced precipitates. The cores are most commonly composed of submicron- to micron-sized anhedral calcite grains and, in samples from modern reefs, display a light brown color indicative of organic remains (Macintyre 1977; Lighty 1985). In UV-light, the bright fluorescence of ancient peloids, in which no recognizable organic material is evident, indicates the occult remains of organic matter (Sun and Wright 1989) within these peloids. Land and Goreau (1970) invoked "presumably" biotic fractionation to account for the enrichment of $\delta^{13}C$ and $\delta^{18}O$ values found in modern peloids. Scanning electron microscopy (SEM) analyses of acid-etched, cloudy, peloid interiors display clots of bacterial fossils in examples from modern reefs from Jamaica, Belize, and Florida (Chafetz 1986, Fig. 2A – F; Fig. 1B) and from micropores within the calcite crystals of peloids from ancient reef deposits (Sun and Wright 1989; Mock and Palmer 1991, Fig. 4 A; Fig. 1C); the micropores are the result of the decay of the bacterial fossils (i.e., bacterial molds). Krumbein et al. (1977, p. 645) reported "that bacteria were destroyed within 96 h by the crystallites surrounding them....The bacterial cell in the interior [of the crystals] is first deflated and later completely destroyed." Reitner (1993, p. 24) examined modern peloids from the Great Barrier Reef and found that Chafetz's (1986) "conclusions are very close to my recent observations"; however, he came to a somewhat different conclusion. Reitner (1993, p. 24) did not observe any bacteria and thus concluded that the cores formed within "clumpy basophilic (acidic) organic mucilages (mucoproteins)." The deflation and concomitant destruction of bacteria described by Krumbein et al. (1977), and commonly observed as microporosity, probably accounts for the absence of bacterial bodies in the peloids examined by Reitner (1993). However, it is possible that the peloids examined by Reitner (1993) had a somewhat different origin. Nevertheless, there is no doubt that the acid-etched cores of the peloids examined by Chafetz (1986) from Jamaica, Belize, and Florida were composed of a mass of bacterial fossils whereas the surrounding clear, dentate, high-magnesian calcite crystals were free of bacterial fossils and micropores. Thus, it is our contention that the micron-sized calcite precipitates comprising the cores of the peloids are bacterially induced precipitates and that after envelopment of the clump of bacteria by the precipitate, abiotic marine cement, in the form of clear spar, precipitated around the exterior of the peloid.

2.2 Deep Water Carbonate Mud Mounds

A number of recent studies of deep water carbonate mud mounds have determined that the micrite and peloids (i.e., clotted fabric), which are important constituents of these mounds, are produced in situ by bacterial activity (Monty 1995, Pratt 1995; Garcia-Mondejar and Fernandez-Mendiola 1995), i.e., similarly to the conclusion regarding peloids in shallow water reefs. Evidence in support of an in situ origin includes: (1) abundance of micrite within the mounds and its paucity in the underlying and laterally adjacent strata, (2) differences in the mineralogy and constituents comprising the mounds as compared to the adjacent strata, and (3) lack of indications of transportation of sediment comprising the mounds. Interpretation of a bacterially induced origin for the micrite and peloids is supported by: (1) the in situ origin of this material, (2) formation in water depths below the photic zone, (3) common association of micritic constituents and the microbes capable of inducing micrite precipitation, (4) similarity with peloids from shallow water reefs, grains in travertine, clotted fabrics in thrombolites, etc. (Monty 1995), as well as (5) the absence of other plausible origins.

2.3 Stromatolites

Peloids, spherulites, micritic pellets, etc., from modern and ancient stromatolites have been described by many geologists (e.g., Monty 1965; Aitkin 1967; Krumbein and Cohen 1974; Kennard and James 1986). Buczynski and Chafetz (1991, 1993) have demonstrated that bacteria are capable of inducing the precipitation of aragonite and calcite grains, which are essentially identical to the peloids, spherulites, micritic pellets, etc., that lithify stromatolites. Additionally, under controlled laboratory conditions, Chafetz and Buczynski (1992) have demonstrated that bacteria preferentially induce the precipitation of calcium carbonate around dead cyanobacterial threads, as compared to live cyanobacterial threads, and thus form lithified stromato-

lites essentially identical to those from natural settings. The precipitates which lithify the cyanobacterial mats into stromatolites form around colonies of bacteria, similar to the process by which peloids in reefs originate.

2.4 Hot Water Travertines

Spherical to elliptical silt-sized aggregates found in harsh (H_2S-rich) hot spring travertine deposits commonly range from 10 to 60 μm in diameter. These grains have cloudy centers and clear rims (Fig. 1D); the cloudy center is generally composed of a single crystal of calcite which petrographically appears to contain an abundance of inclusions. The core is commonly surrounded by a clear polyhedral rim of inclusion-free calcite (Chafetz and Folk 1984, Fig. 22A). SEM examination shows that the cloudy nature of the cores is due to an abundance of either bacterial fossils, rarely preserved, or to an abundance of micropores, i.e., holes representing the former sites of the bacteria (Fig. 1E). The bacterial fossils and the microporosity are absent from the clear spar immediately surrounding the 10–60 μm diameter cores of these grains; hence, the clear appearance of the surrounding spar. These silt-sized grains form horizontally oriented laminae which alternate with the thicker shrub layers common in the shallow lake- and/or pond-fill hot water travertine accumulations, e.g., Bagni di Tivoli-Tivoli-Guidonia, Italy, and Terrace Mountain, Mammoth Hot Springs, Yellowstone National Park, Wyoming, USA. These grains are interpreted to represent bacterially induced precipitates which form during the winter season whereas the shrubs represent the growing season (Chafetz and Folk 1984).

2.5 Laboratory Analogues of Natural Peloids

It has been demonstrated under controlled laboratory conditions that bacterial colonies can induce precipitation of aggregates of calcium carbonate similar in essentially all aspects to the peloids, pellets, etc., described above (Buczynski and Chafetz 1991, 1993; Chafetz 1994). Each of the laboratory grown aggregates is commonly 4–10 μm long and composed of a monomineralic myriad of submicron- to micron-sized crystals, predominantly either all aragonite or all calcite. The aragonite crystals almost always have a needle-like morphology whereas the calcite most commonly resembles a flattened rhombohedron. These aggregates precipitate around clumps of bacteria. The laboratory produced aggregates, or bundles, most commonly resemble rods, hemispheres, or spheres, and also less commonly form a variety of other shapes, such as rhombohedra, tetragonal dispheroids, tetragonal dipyramids, discs, and brushes (Buczynski and Chafetz 1991). The rods with additional precipitation at their ends evolve into the common dumbbell shape, produced in many laboratory experiments as well as recognized in nature (Chafetz et al. 1991). Additional precipitation produces spherical forms with clumps of bacteria at their centers (Fig. 1F). The submicron- to micron-sized aggregates with bacterial clumps at the center are laboratory analogues of the fine-grained cores of the silt-sized peloids common in modern reefs, pellets in carbonate modern mounds, clotted and pelleted constituents in stromatolites, and silt- and sand-sized grains in hot water travertine deposits.

It is our thesis that all these peloids and silt- and sand-sized grains are essentially the same type of allochem formed in different environmental settings and are all bacterially induced precipitates which have precipitated around colonies of bacteria. The bacteria act as a *catalyst* to induce precipitation of submicron- to micron-sized crystals, or coarser single crystals as in harsh travertine deposits, of $CaCO_3$ that form the cores of these allochems. The initial organic-rich (cloudy) precipitates are then commonly overgrown by abiotic (clear) cement crystals.

3 Nanobacteria and Nanoscale Precipitates

Nanobacteria are dwarf forms, about one-tenth the diameter of normal bacteria, and were first discovered mineralized in the hot spring deposit of Viterbo, Lazio, Italy (Folk 1990, 1992, 1994). This led to their subsequent recognition in more normal limestones (Folk 1993b), ooids (Folk et al. 1996) and dolomites (Folk 1993a; Vasconcelos and McKenzie 1994; Vasconcelos et al. 1995). Further work showed their abundance in sulfide, silica (Folk et al. 1995) and even clay minerals (Folk et al. 1994; Folk and Lynch 1997). Previously, such tiny spheroids in the 0.03–0.2 μm range had not been clearly visible in most SEM examinations, or, if noticed, had been regarded as artifacts of gold coating, laboratory treatment or SEM artifacts.

Standard microbiological technique is to pass a bacteria-rich suspension through a 0.2 μm filter, under the assumption that all bacteria will be caught; the <0.2 μm fraction is regarded as free of bacteria. Thus, forms smaller than about 0.3 μm are very infrequently studied, even by microbiologists. Other common terms used for these forms are "ultramicrobacteria" and "bacterial spores," under the assumption that they are dormant and enduring stress (see references in Folk 1993b). However, we propose instead that they are very geochemically active and form perhaps the preponderant biomass on earth; they are not simply stressed forms of normal bacteria but may be a class of organ-

isms in their own right. Use of the term "nanobacteria" emphasizes this proposed difference; the word was first published by Morita (1988, p. 438). Inasmuch as these forms are in the nanometer range (0.03–0.2 μm, or 30–200 nm) the word is precisely appropriate. Viruses are typically 10–20 nm, and it is possible that some of the smaller spheroids are really viruses that have lost their tails and polyhedral shapes through fossilization; no fossilized viruses have yet been described.

F. Westall (personal communication, 1997) believes that "amorphous" organic matter, mucus, or organic polymers may form tiny balls as well. This is an interesting idea, but for carbonates we hold our ground, as we do not see evidence of sheets rolling up into uniformly sized balls.

Here, we examine the quantitative occurrence of nanobacteria in various limestone components, and extend their occurrence back through geologic time from the Holocene (Fig. 2A) to the Precambrian (Fig. 3D). A method is introduced for making quantitative population counts.

All specimens were treated in a standard way, etching in 1% HCl for 1 min. In most rocks, nanobacteria are only revealed by etching (a strong argument against the idea of contamination or coating artifacts). It is of the utmost importance that gold-coating be done for only 30 s; on our Denton gold coater, excess gold coating leads to formation of nanobacteria-resembling spheres of gold if coating is done for 60 s or more (Folk and Lynch 1997). Other machines may have different optimal times for gold coating; the reader must experiment. It is also vital to adjust the SEM for maximum performance – shortest possible working distance, highest voltage (30 kV), broad and dim spot size (setting of 9 on our JEOL-JSM-T330 A) and very careful stigmation and focus. And, one needs faith and optimism: "If I hadn't believed in them I never would have seen them."

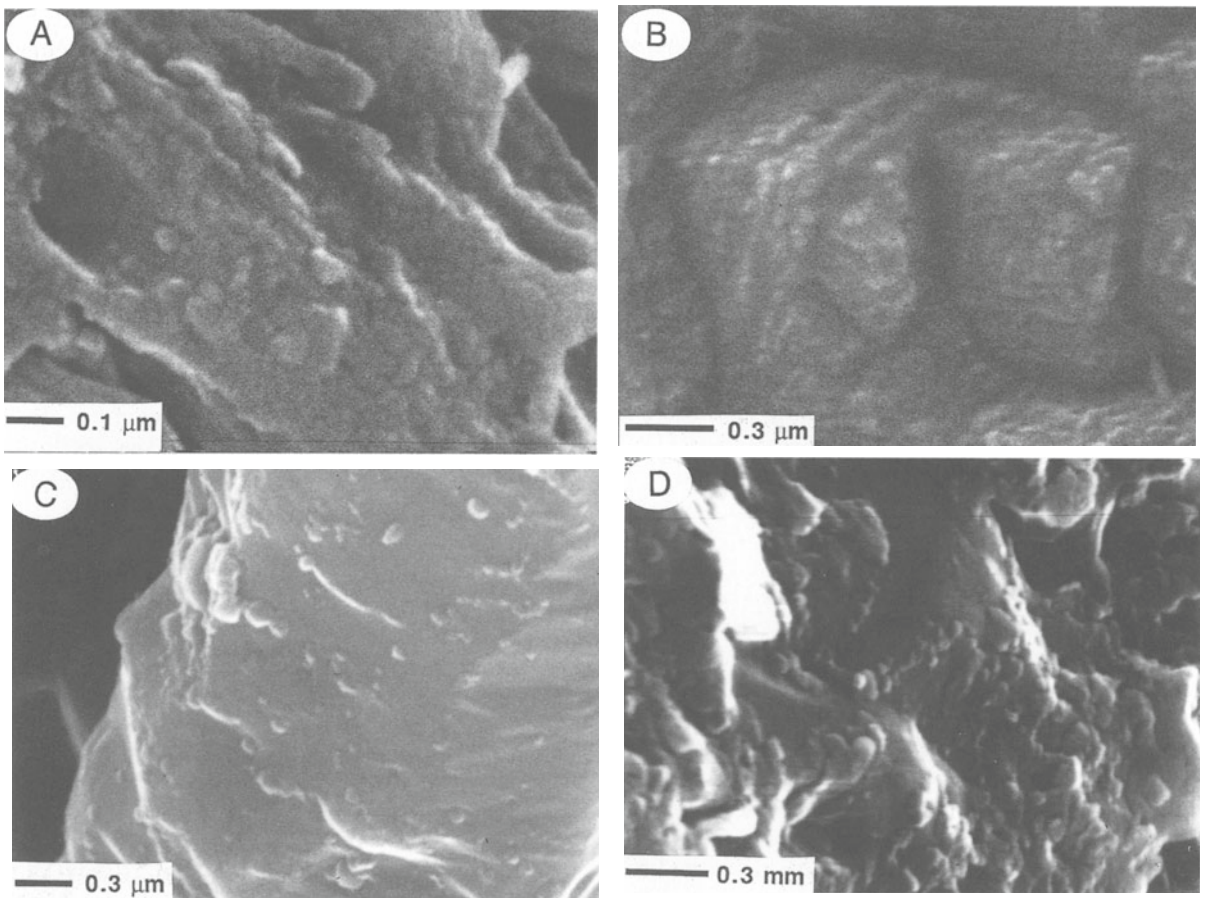

Fig. 2.A Modern pelleted aragonite-needle mud, Andros Island, Bahamas (University of Texas, sample DUI). At 100,000× the main needle is apparently made up entirely of closely packed, 25 nm spheroids, probably nanobacteria. **B** Pleistocene beachrock, Bahamas, (sample FYF, J. Lang collection). This crystal of sparry calcite cement appears to be completely formed of rows of closely packed 30–60 nm nanobacteria. **C** Cretaceous Fort Terrett (Fredericksburg) Limestone (oosparite bar), Pecos County, Texas (Collection C. Kerans). One radial calcite crystal in the oolite cortex (the center is to the lower left, off the screen). Typical field of nanobacteria, a few occurring in chains (*arrow*). **D** Jurassic Solnhofen Limestone, Marburg Quarry, Bavaria, Germany (Collection P. Braithwaite and E. Flugel, sample GKS). In this micrite, localized rich patches of 60 nm nanobacteria are interspersed with deserted areas

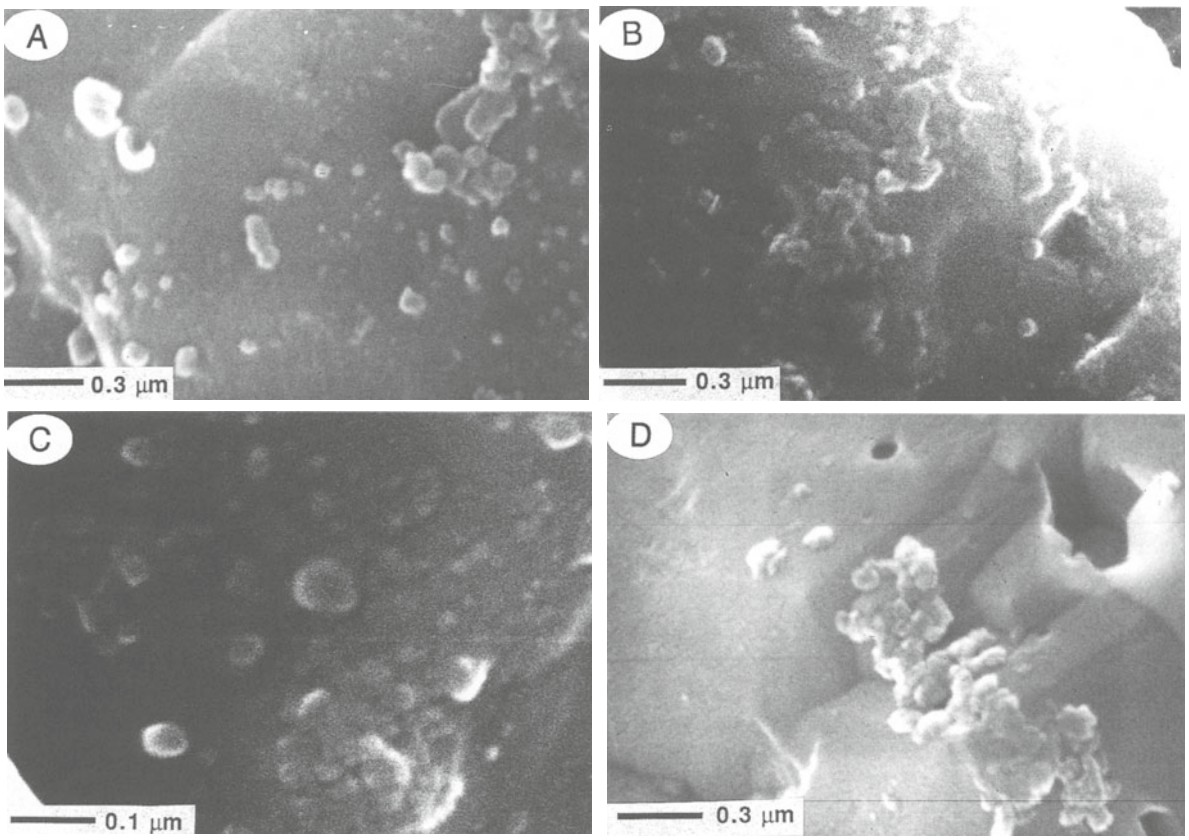

Fig. 3.A Ordovician Stonehenge (Beekmantown) Limestone, Centre County, Pennsylvania, (sample 802G, R. Folk's Ph.D. dissertation). This micrite shows an unusually wide range of sizes for nanobacteria, 20–100 nm. Some occur in chains (*center*). **B** Ordovician Cool Creek Limestone, Murray County, Oklahoma (sample CZH). Part of the radial cortex of an oolite, showing clumps of nanobacteria and deserted areas. **C** Proterozoic Bitter Springs limestone, Ellery Creek, Northern Territory, Australia (sample EGX). At 20,000× only a few bodies are visible; at 50,000× or higher, huge numbers are revealed. Size range is unusually large, 25–250 nm in this sample of microsparite. **D** Lower Proterozoic Rocknest dolomite, replacement after ray-crystal aragonite botryoids (Grotzinger and Read 1983; sample HDS), Northwest Territory, Canada. This dolomite was etched 10 min in 10% HCl. Most areas are barren, but this is a colony of 60 mm nanobacteria

Like most living organisms that gather and reproduce where food is most abundant, the distribution of nanobacteria in minerals is very patchy – large deserted areas contrast with areas where they are abundant, like human populations in the desert vs cities. Thus, it is difficult to make a truly valid census of their abundance. An attempt has been made using the following protocol:

1. Choose at random an area of the rock and examine at 1000× to select a relatively smooth, flat surface to insure the absence of "cliffs" or pore spaces. 1000× is too small a magnification to see nanobacteria, so this is an honest way to choose a field for counting.
2. With field of view now fixed, rack up the power to 20,000× and use the small EXP screen for best resolution. Higher power may be necessary to distinguish nanobacteria from mineral inclusions, but we always back down to 20,000× for the census. At this magnification, bodies as small as 0.03-0.05 μm (30–50 nm) are easily visible, and the EXP screen gives a census area of approximately 4 μm^2.
3. Because of the very wide range in abundance, it is not practical to make an exact count. We have divided the frequencies of nanobacteria-per-4 mm^2 area into log intervals of 0, 1–3, 4–10, 11–31, 32–100, and 101–310 nanobacteria per field, and tabulate at least 20 different fields chosen at random.

If the distribution of bodies in the carbonate areas were random, like raindrops on a pavement, we would expect a Poisson distribution of frequencies in which $\sigma = \sqrt{\bar{x}}$. Thus, for example, if the mean count were 10 bodies per counting cell, then 68% of the cells would contain between 7 and 13 bodies ($\bar{x} \pm \sigma$) or $\bar{x} \pm \sqrt{\bar{x}}$.

In fact, the distributions in the carbonates are radically different from Poisson; they tend to be very clustered (Neymann contagious distributions), with some completely empty areas contrasting with counting cells that have hundreds of nanobacteria in them (Figs. 2D, 3B,D). This distribution is also characteristic of living bacterial populations.

Figures 2 and 3 show the results, going from youngest to oldest ages, and Table 1 gives the census data. Some generalizations can be drawn from this initial attempt at a quantitative survey. It is very easy to prepare samples to reveal the bodies. Their appearance and abundance is very similar from Lower Proterozoic to Holocene, with spherical to slightly ellipsoidal or bean shapes; and sizes are typically in the range from 30 to 60 nm (0.03–0.06 μm). Because distributions tend to be so clustered, it is difficult to handle the data statistically. But most samples have similar slopes when plotted on log cumulative graph paper, so that about two-thirds of all areas counted contain between 1 and 10 bodies per 4 mm^2 area. This amounts to a value of the order of 100 billion (10^{11}) bodies per cubic millimeter.

However, some samples, e.g., sample FYF of Bahaman beachrock, have an enormous range, with 25% of the areas counted containing no bodies and 15% of the areas containing over 300 bodies. In some rocks it is evident that, as magnification is increased, huge swarms of very small nanobacteria, in the 25–40 nm range, are resolved, but we have counted only those bodies visible at 20,000× in order to keep some reasonable standard.

It is much easier to find nanobacteria than remnants of "normal" size bacteria or other microfossils. In fact, in all the rocks censused for nanobacteria we have never found one fossilized normal size bacterial body (over 0.3 μm). This implies that the total biomass contained in nanobacteria is far greater even than the biomass found in normal microbial organisms or, because of tough cell walls, nanobacteria are more easily preserved. Those who hunt for the earliest forms of life in the Precambrian should focus down on nanobacteria, as they are probably the most primitive forms. Perhaps they are even responsible for the oxidation of iron on Mars.

Dark-colored limestones (Fig. 3A–C) tend to be richer in nanobacteria than light ones (Fig. 2C), but there are many notable exceptions. The rock with highest occurrences is a white Bahaman beachrock, sample FYF (Fig. 2B). Off-white Solnhofen lithographic limestone (Fig. 2D) is also very rich, with a median value of about 15 bodies per counting area. In contrast, the body-count is very low in a dark Mississippian limestone. However, this low count occurs in distal, clear, coarse spar mosaic that is the final fill in a larger pore space (and, thus, is to be expected). Most dark micritic or oolitic specimens have median counts of 5–20 nanobacteria per unit area.

As to fabric, most spar areas have low body counts, with medians of 0–3 nanobacteria per area, while oolites and micrite have higher counts, medians typically being 3–15. But again, sample FYF, the Bahaman beachrock, is a notable exception because even the spar is very rich, with a median of 10–30 bodies and maximum of more than 300. In fact some spar crystals examined at 50,000× appear to be made entirely of closely packed bodies – this would give a count of several thousand per area (Fig. 2B). But nearby spar crystals have very few bodies, and there is no obvious fabric-related explanation for the variance.

A few notes on individual rocks are revealing. Modern pelleted aragonite-needle mud from Andros Island, Bahamas (UT sample DUI, Fig. 2A) shows essentially no bodies at 20,000×, but when examined at 100,000× it appears to be made entirely of densely packed, 10–30 nm balls. If these are indeed nanobacteria, then the body count would be in the thousands. Proterozoic Bitter Springs Limestone (Fig. 3C) also shows enormous numbers of bodies at 50,000×.

In Tiezzi's Waulsortian bioherm rock from the Mississippian of Montana, the cloudy, bladed initial cement on bryozoans has a median of around three bodies per area, while the equant clear spar in the center of the pores has a median count near zero. Tiezzi and Folk (1984) proposed that the cloudy cement was a bacterial precipitate, but at that time we knew nothing of the existence of nanobacteria. However, the drop in body count in the Mississippian bioherm cement is not nearly as dramatic as that shown by Pedone and Folk (1996) in brine-shrimp egg sediments from Salt Lake, Utah, where aragonite cement is crammed with nanobacteria near the decaying egg, but has only sparse occurrences distally.

Dolomites are not the subject of this chapter, but a Lower Proterozoic sample (Grotzinger and Read 1983) was the oldest rock studied (Fig. 3D). Dolomites have to be etched longer, e.g., 10 min in 10% HCl, but when etched, this sample shows colonies of nanobacteria just like those in the younger rocks.

4 Conclusion

We have presented evidence that nanobacteria occur in rocks of all ages but in greatly variable quantity. Some critics have claimed that these small bodies are just blips from excess gold-coating; this is wrong, because in many carbonates the tiny nanobodies are only seen upon etching, and gold-coat produces neither distinct colonies (Fig. 3D) nor scattered bodies on largely bare surfaces (Fig. 2C; see Folk and Lynch 1997 for a full discussion of the problem). Others have suggested for years that "minerals naturally dissolve into spheroids;" our Figs. 2 C, 3 A,D show single crystals with colonies or scattered bodies. If crystallographically directed solutions were the cause, one should see balls over the entire surface. In summary, the bacteria did it!

Acknowledgements. We gratefully acknowledge Cori Lambert for help with communications processing; Joe Jaworski for making plates; and Frances Westall for incisive comments.

Table 1. Census of number of nanobacteria visible in a 4 mm^2 area at 20,000×

Sample no.	Age	Locality	Munsell color	Fabric		Median	0	1–3	4–10	11–31	32–100	101–310	310–1000
DUI	Modern	Andros I, Bahamas	N8	Aragonite	Needle mud		none visible at 20.000x; thousands visible at 100.000x						
FYF	Pleistocene	Bahamas	N9	Beach rock	Spar cement	16	[a]25	0	15	20	15	10	15
FHp-2	Pleistocene	Florida	N9	Coquina	Spar cement	5	15	20	[a]35	20	10	–	–
DQA	Cretaceous	Cedar Park Ls, Travis County, TX	N8	Oosparite	Micrite ooids	3.5	10	30	[a]35	15	10	–	–
					Spar cement	0	[a]80	0	10	5	5	–	–
		Ft. Terrett Ls, Pecos County, TX	N8	Oosparite	Oolite cortex	4	10	30	[a]40	20	–	–	–
				Spar cement		0.5	[a]65	25	10	–	–	–	–
GKS	Jurassic	Solnhofen Ls, Germany	N8	Micrite		16	0	5	15	[a]60	20	–	–
Tiezzi	Mississippian	Waulsortian reef, Gallatin County, Montana	N4.5	Biolithite	Cloudy bladed spar	3	13	[a]35	29	20	3	–	–
					Equant clear spar	0.5	62	24	10	4	–	–	–
802G	L. Ordovician	Stonehenge Ls, Centre County, Pennsylvania	N4	Intrasparite	Micrite	13	0	0	35	[a]50	15	–	–
					Spar cement	11	5	15	20	[a]45	15	–	–
CZH	L. Ordovician	Cool Creek Ls, Murray County, Oklahoma	N4.5	Oosparite	Oolite cortex	18	0	0	20	[a]50	15	–	–
					Micrite nucleus	20	0	0	10	[a]70	20	–	–
EGX	Proterozoic	Bitter Springs Ls, N. Terr. Australia	N4.5	Microsparite	[b]	7	5	0	[a]55	25	15	–	–
HDS	Archean	Rocknest Ls, NW. Terr. Canada	N9	Dolomite	Aragonite ray crystals	1.5	30	[a]50	5	10	5	–	–

Rough medians estimated from a cumulative logarithmic graph. Samples are housed in Folk collection at University of Texas.
I, island; Ls, limestone.
[a] Modal counts.
[b] Thousands visible at 50,000×.

References

Aitken JD (1967) Classification and environmental significance of cryptalgal limestones and dolomites, with illustrations from the Cambrian and Ordovician of southwestern Alberta. J Sedimentary Petrol 37:1163–1178

Boquet E, Boronat A, Ramos-Cormenzana A (1973) Production of calcite (calcium carbonate) crystals by soil bacteria is a general phenomenon. Nature 246:527–529

Buczynski C, Chafetz HS (1991) Habit of bacterially induced precipitates of calcium carbonate and the influence of medium viscosity on mineralogy. J Sedimentary Petrol 61:226–233

Buczynski C, Chafetz HS (1993) Habit of bacterially induced precipitates of calcium carbonate: examples from laboratory experiments and recent sediments. In: Rezak R, Lavoie D (eds) Carbonate microfabrics. Springer, Berlin Heidelberg New York, pp 105–116

Chafetz HS (1986) Marine peloids: a product of bacterially induced precipitation of calcite. J Sedimentary Petrol 56:812–817

Chafetz HS (1994) Bacterially induced precipitates of calcium carbonate and lithification of microbial mats. In: Krumbein WE, Paterson DM, Stal LJ (eds) Biostabilization of sediments. Oldenburg Press, Oldenburg, p 526

Chafetz HS, Buczynski C (1992) Bacterially induced lithification of microbial mats. Palaios 7:277–293

Chafetz HS, Folk RL (1984) Travertines: Depositional morphology and the bacterially constructed constituents. J Sedimentary Petrol 54:289–316

Chafetz HS, Meredith JC (1983) Recent travertine pisoliths (pisoids) from southeastern Idaho, USA. In: Peryt TM (ed) Coated grains. Springer, Berlin Heidelberg New York, pp 450–455

Chafetz HS, Rush PF, Utech NM (1991) Microenvironmental controls on mineralogy and habit of $CaCO_3$ precipitates: an example from an active travertine system. Sedimentology 38:107–126

Dalrymple DW (1965) Calcium carbonate deposition associated with blue-green algal mats, Baffin Bay, Texas. Univ Texas Inst Mar Sci 10:187–200

Deelman JC (1975) Two mechanisms of microbial carbonate precipitation. Naturwissenschaften 62:484–485

Drew GH (1911) The action of some denitrifying bacteria in tropical and temperate seas, and the bacterial precipitation of calcium carbonate in the sea. J Mar Biol Assoc UK 9:142–155

Drew GH (1913) On the precipitation of calcium carbonate in the sea by marine bacteria, and on the action of denitrifying bacteria in tropical and temperate seas. J Mar Biol Assoc UK 9:479–524

Folk RL (1990) Bacteria and carbonate precipitation in Sulfurous Hot Springs, Viterbo, Lazio, Italy, (abs.). 13th Int Sedimentological Congr, Nottingham, p 172

Folk RL (1992) Bacteria and nanobacteria revealed in hardgrounds, calcite cements, native sulfur, sulfide minerals and (yes) travertines (Abstr). Cincinnati, Ohio, Oct 26–29, 1992, Geological Society America, Abstracts with Programs 18:A-104

Folk RL (1993a) Dolomite and dwarf bacteria (nanobacteria) (Abstr). Geological Society America, Abstracts with Programs 19:A-397

Folk RL (1993b) SEM imagining of bacteria and nanobacteria in carbonate sediments and rocks. J Sedimentary Petrol 63: 990–999

Folk RL (1994) Interaction between bacteria, nanobacteria and mineral precipitation in hot springs of Central Italy. Geogr Phys Quat 48:233–246

Folk RL, Chafetz HS (1983) Pisoliths (pisoids) in quaternary travertines of Tivoli, Italy. In: Peryt TM (ed) Coated Grains. Springer, Berlin Heidelberg New York, pp 474–487

Folk RL, Lynch FL (1997) The possible role of nanobacteria (dwarf bacteria) in clay mineral diagenesis and the importance of careful sample preparation in high magnification SEM study. J Sedimentary Res:67

Folk RL, Lynch FL, Major RP (1996) The role of nanobacteria (dwarf bacteria) in the formation of ooids and hardgrounds, Joulters Cays, Bahamas. Geological Society of America, Abstracts with Programs, 22:A-275

Folk RL, Lynch FL, Rasbury ET (1994) Evidence for bacterial precipitation of clay minerals upon sand grains. In: soils, and in the subsurface (Abstr): Geological Society America, Abstracts with Programs 20:A-308

Folk RL, Noble PJ, Gelato G, McLean RJC (1995) Precipitation of opal – CT lepispheres, chalcedony and chert nodules by nanobacteria (dwarf bacteria) (Abstr). New Orleans, Louisiana, Nov. 6-9, 1995, Geological Society America, Abstracts with Programs 21:A-305

Garcia-Mondejar J, Fernandez-Mendiola PA (1995) Albian carbonate mounds: Comparative study in the context of sea-level variations (Soba, northern Spain) In: Monty CLV, Bosence DWJ, Bridges PH, Pratt BR (eds) Carbonate mud-mounds: their origin and evolution. Blackwell Science, Oxford, International Association of Sedimentologists, Special Publication 23:359–384

Gerundo M, Schwartz GL (1949) The role of denitrifying bacteria in the genesis of formations found in the Carlsbad Cavern. Texas J Sci 1:58–61

Greenfield LJ (196) Metabolism and concentration of calcium and magnesium and precipitation of calcium carbonate by a marine bacterium. Ann NY Acad Sci 109:23–45

Grotzinger JP, Read JF (1983) Evidence for primary aragonite precipitation, Lower Proterozoic (1.9 Ga) Rocknest Dolomite, Wopmay Orogen, NW. Canada. Geology 11:710–713

Horodyski RJ, Bloeser B, Vonder Haar S (1977) Laminated algal mats from a coastal lagoon, Laguna Mormona, Baja California, Mexico. J Sedimentary Petrol 47:680–696

Kellerman KF, Smith NR (1914) Bacterial precipitation of calcium carbonate. J Wash Acad Sci 4:400–402

Kennard JM, James NP (1986) Thrombolites and stromatolites: two distinct types of microbial structures. Palaios 1:492–503

Kreitler CW, Dutton S.P (1983) Origin and diagenesis of cap rock, Gyp Hill and Oakwood Salt Domes, Texas. Report of Investigations no 131, Bureau of Economic Geology, Univ Texas, Austin, Texas, p 58p

Krumbein WE (1979) Photolithotropic and chemoorganotrophic activity of bacteria and algae as related to beachrock formation and degradation (Gulf of Aquaba, Sinai). Geomicrobiol J 1: 139–203

Krumbein WE, Cohen Y (1974) Biogene, klastische und evaporitische Sedimentation in einem mesothermen monomiktischen ufernahen See (Golf von Aqaba). Geol Rundsch 63:1035–1065

Krumbein WE, Cohen Y (1977) Primary production, mat formation and lithification: contributions of oxygenic and facultative anoxygenic cyanobacteria. In: Flugel E (ed) Fossil algae, recent results and developments. Springer, Berlin Heidelberg New York, pp 37–56

Krumbein WE, Cohen Y, Shilo M (1977) Solar Lake (sinai), IV. Stromatolitic cyanobacterial mats. Limnol Oceanogr 22:635–656

Lalou C (1957) Studies on bacterial precipitation of carbonates in sea water. J Sedimentary Petrol 27:190–195

Land LS (1971) Submarine lithification of Jamaican reefs. In: Brikker OP (ed) Carbonate cements. Johns Hopkins Univ, Baltimore, Maryland, Stud Geol 19:59–62

Land LS, Goreau TF (1970) Submarine lithification of Jamaican reefs. J Sedimentary Petrol 40:457–462

Land LS, Moore CH (1980) Lithification, micritization and syndepositional diagenesis of biolithites on the Jamaican Island slope. J Sedimentary Petrol 50:357–370

Leinfelder RR, Nose M, Schmid DU, Werner W (1993) Microbial crusts of the Late Jurassic: composition, palaeoecological significance and importance in reef construction. Facies 29:195–230

Lighty, R.G (1985) Preservation of internal reef porosity and diagenetic sealing of submerged early Holocene barrier reef, southeast Florida shelf. In: Schneidermann N, Harris PM (eds) Carbonate cements. Society of Economic Paleontologists and Mineralogists, Tulsa, Oklahoma, Special Publication 36:123–151

Macintyre IG (1977) Distribution of submarinecements in a modern Caribbean fringing reef, Galeta Point, Panama. J Sedimentary Petrol 47:503–516

Macintyre IG (1985) Submarine cements – the peloidal question. In: Schneidermann N, Harris PM (eds) Carbonate cements. Society of Economic Paleontologists and Mineralogists, Tulsa, Oklahoma, Special Publication 36:109–116

McCallum MF, Guhathakurta K (1970) The precipitation of calcium carbonate from seawater by bacteria isolated from Bahama Bank sediments. J Appl Bacteriol 33:649–655

Mock SE, Palmer TJ (1991) Preservation of siliceous sponges in the Jurassic of southern England and northern France. J Geol Soc Lond 148:681–689
Monaghan H, Lytle ML (1956) The origin of calcareous ooliths. J Sedimentary Petrol 26:111–118
Monty CLV (1965) Geological and environmental significance of Cyanophyta. Unpubl. PhD Dissertation, Princeton University, Princeton, New Jersey
Monty CLV (1995) The rise and nature of carbonate mud-mounds: an introductory actualistic approach. In: Monty CLV, Bosence DWJ, Bridges PH, Pratt BR (eds) Carbonate mud-mounds: their origin and evolution. Blackwell Science, Oxford, International Association of Sedimentologists, Special Publication 23:11–48
Monty CLV, Bosence DWJ, Bridges PH, Pratt BR (1995) Carbonate Mud-Mounds: their origin and evolution, Blackwell Science, Oxford, International Association of Sedimentologists
Morita RY (1980) Calcite precipitation by marine bacteria. Geomicrobiol J 2:63–82
Morita RY (1988) Bioavailability of energy and its relationship to growth and starvation survival in nature: Can J Microbiol 34: 436–446
Novitsky JA (1981) Calcium carbonate precipitation by marine bacteria. Geomicrobiol J 2:375–388
Neuweiler F (1993) Development of Albian microbialites and microbialite reefs at marginal platform areas of the Vasco-Cantabrian Basin (Soba Reef Area, Cantabria, N. Spain). Facies 29:231–250
Oppenheimer CH (1961) Note on the formation of spherical aragonite bodies in the presence of bacteria from the Bahama Bank. Geochim Cosmochim Acta 23:295–296
Pedone VA, Folk RL (1996) Formation of aragonite cement by nanobacteria in the Great Salt Lake, Utah. Geology 24:763–765
Pratt BR (1995) The origin, biota and evolution of deep-water mud-mounds. In: Monty CLV, Bosence DWJ, Bridges PH, Pratt BR (eds) Carbonate mud-mounds: their origin and evolution. Blackwell Science, Oxford, International Association of Sedimentologists, Special Publication 23:49–123
Reid RP (1987) Nonskeletal peloidal precipitates in Upper Triassic reefs, Yukon Territory (Canada). J Sedimentary Petrol 57: 893–900
Reitner J (1993) Modern cryptic microbialite/metazoan facies from Lizard Island (Great Barrier Reef, Australia): formation and concepts. Facies 29:3–40
Roberts HH, Aharon P, Walsh MM (1993) Cold-seep carbonates of the Louisiana contiental slope-to-basin floor. In: Rezak R, Lavoie D (eds) Carbonate microfabrics. Springer, Berlin Heidelberg New York, pp 95–104
Soudry D, Weissbrod T (1995) Morphogenesis and facies relationships of thrombolites and siliciclastic stromatolites in a Cambrian tidal sequence (Elat area, southern Israel). Palaeogeogr Palaeoclimatol Palaeoecol 114:339–355
Sun SQ, Wright VP (1989) Peloidal fabrics in Upper Jurassic reefal limestones, Weald Basin, southern England. Sedimentary Geol 65:165–181
Tiezzi A, Folk RL (1984) Vacuole-rich cements in Mississippian stromatactis and quaternary travertines: the bacterial connection. Society Economic Paleontologists and Mineralogists Mid-year Meeting, San Jose, California, Abstract, p 82
Vasconcelos C, McKenzie JA (1994) The microbial dolomite model: Anaerobe-induced dolomite precipitation and early diagenesis in a modern shallow-water lagoon (Lagoa Vermelho, Brazil) (Abstr). Geological Society America Annual Meeting, Seattle, A-5089
Vasconcelos C, McKenzie JA, Bernasconi S, Grujic D, Tien AJ (1995) Microbial mediation as a possible mechanism for natural dolomite formation at low temperatures. Nature 377:220–222

Calcification in Cyanobacteria

Martina Merz-Preiß

Institut für Geologie und Paläontologie, Philipps-Universität, Hans Meerwein Strasse, D-35032 Marburg, Germany

Abstract. Calcification in cyanobacteria depends on water chemistry as well as on physiological and morphological factors such as photosynthetic bicarbonate uptake and the existence of a suitable sheath. Physicochemical precipitation under high levels of supersaturation leads to the dense encrustation of the filaments, forming a solid micrite tube, while photosynthetic bicarbonate uptake in less supersaturated waters can lead to micrite precipitation within the sheath. Both forms of calcification are restricted to species which prefer oligotrophic, phosphate-poor environments. In this way, various environmental factors such as the saturation state of the water with respect to calcium carbonate minerals and the concentration of dissolved CO_2 and phosphate may be reflected in the occurrence of fossil calcifying cyanobacteria.

1 Introduction

Cyanobacteria are phototrophic prokaryotes, sharing many characteristics with heterotrophic bacteria. In most ecological aspects, however, they are similar to eukaryotic algae and their photosynthetic apparatus resembles that of plants. Photosynthesis generally uses CO_2, or, under low CO_2 concentrations, HCO_3^-, which is intracellularly transformed into CO_2. Many cyanobacteria are facultatively able to grow heterotrophically (Smith 1982).

Both unicellular cyanobacteria as well as genera in which the cells are arranged in rows, called trichomes, are found. Unicellular and multicellular forms can be surrounded by a mucilagenous sheath of well-defined shape. One or more trichomes embedded in a sheath is termed a filament. The existence of a sheath is a taxonomic criterion, although the formation of sheath material is also influenced by environmental conditions. A sheath is readily visible without staining. It can be embedded in a capsule (Bertocchi et al. 1990) of undefined shape. Both sheath and capsule consist of highly hydrated organic macromolecules (Stanier and Cohen-Bazire 1977). Sheath and capsule, together with a diffuse slime surrounding some cyanobacterial colonies, form the cell envelope. The mucilagenous material of the cell envelope probably has a protective function, buffering the cells against hazards or rapid environmental changes. Light-absorbing pigments encased in the sheath protect the cells from high light irradiance (Scherer et al. 1988; Garcia-Pichel and Castenholz 1991). Although rarely observed, the distinction between different layers within the cell envelope would be helpful when describing calcification in cyanobacteria.

Cyanobacteria live as plankton or benthos, submerged or subaerial, epi- and endolithic, in freshwater, sea water and hypersaline environments including a wide range of extreme conditions. They prefer alkaline waters and are not found where the pH is lower than 4 (Brock 1973).

The classification of modern cyanobacteria is difficult and controversial, and ambiguities arise depending on whether the botanical or bacteriological code is used (Castenholz 1992). Genetic classification of calcifying cyanobacteria might soon be available, but will not allow determination in the field. This chapter uses species determinations based on morphological characteristics given by the authors cited. These species may prove to be genetically heterogeneous.

The occurrence of cyanobacteria dates possibly from the Archean (Schopf 1992, 1996), a view which is disputed by some because of RNA analyses (Giovannoni et al. 1988, 1996). Silicified microfossils resemble modern filamentous cyanobacteria, sometimes with many details of cell differentiation. Cyanobacterial photosynthesis probably made a major contribution to the rise of atmospheric oxygen in the Precambrian. The fossil record of calcifying cyanobacteria is incomplete. Calcifying forms are rare in the Precambrian (Riding 1991, 1994; Knoll et al. 1993), a fact which is difficult to reconcile with current ideas of cyanobacterial evolution and the Precambrian environment. Micritic tubes, interpreted as representing calcified filamentous cyanobacteria, frequently occur from the Precambrian/Cambrian boundary until the Cretaceous in normal marine waters, apparently varying in abundance during this timespan (Riding 1992). After the Cretaceous they nearly exclusively occur in non-marine environments. For paleoenvironmental interpretations it is important to know the environmental and biological factors which influence calcification of modern cyanobacteria. These factors should be reflected by the occurrence of fossil calcified cyanobacteria.

R.E. Riding and S.M. Awramik (Eds.)
Microbial Sediments

2 Calcification in Modern Cyanobacteria

Calcifying cyanobacteria occur in a variety of present-day environments, especially in freshwater. Calcareous tufa deposits and oncoids contain abundant carbonate-encrusted cyanobacterial filaments (e.g., Pia 1933 and references therein; Golubic 1973; Pentecost 1978; Obenlüneschloß 1991; Winsborough et al. 1994). Cyanobacteria can produce considerable amounts of freshwater micritic mud (Gleason and Spackman 1974; Merz 1992). They also calcify in hypersaline environments and in a variety of waters with unusual composition (Horodyski and VonderHaar 1975; Golubic 1983; Kempe and Kazmierczak 1990a; Rasmussen et al. 1993; Defarge et al. 1994). Calcification often seems to be favored by local freshwater influx into restricted environments (Kempe et al. 1991; Rasmussen et al. 1993; Moore and Burne 1994; Wharton 1994). This could be due to increased carbonate (calcite or aragonite) saturation upon mixing of the two waters.

Golubic and Campbell (1981) described calcification of *Rivularia* from a marine setting. The appearance of whitings in freshwater and sea water has been attributed to photosynthetically induced precipitation around picoplanktonic cyanobacteria cells (Thompson and Ferris 1990; Robbins and Blackwelder 1992). Generally, however, calcifying cyanobacteria are rare in modern marine waters. Calcified cyanobacteria can also be found in subaerial environments, such as desert crusts and caves (Krumbein and Giele 1979; Cox et al. 1989; Jones and Kahle 1986).

Calcification in cyanobacteria is extracellular, closely associated with the organic macromolecules of the cell envelope (Pentecost and Riding 1986; Riding 1991; Merz and Zankl 1993b). Calcification depends on supersaturation of the ambient water with respect to carbonate, but it also depends on physiological prerequisites. This is shown by the fact that calcification is restricted to certain species, some of which even show species-specific crystal shapes (Gleason and Spackman 1974; Krumbein and Giele 1979; Obenlüneschloss 1991; Merz 1992). In different environments, calcification is under differing degrees of physicochemical versus biological influence. The mineralogy of the precipitated carbonate corresponds to the chemistry of the ambient water.

Calcification typical of coccoid cyanobacteria seems to be carbonate precipitation in the diffuse slime between the cells, just roughly following the outline of the colony. In filamentous cyanobacteria calcification leads to formation of a tube surrounding the trichome or filament. The crystals nucleate on the sheath surface and either grow radially outward or into the sheath towards the filament (Pentecost and Riding 1986; Obenlüneschloss 1991). Special preparation is necessary to decide whether material of the cell envelope is involved in the further growth of the crystals. This form of calcification seems to be a passive consequence of high degrees of supersaturation with respect to carbonate in the ambient water. The crystals can also nucleate within the cell envelope, completely embedded in organic material. This leads to impregnation of the sheath or capsule with carbonate (Riding 1977). It appears that sheath impregnation preferentially occurs when photosynthesis is the driving force for precipitation.

There must be a biological predisposition for calcification, as even in highly supersaturated environments not all cyanobacteria calcify. The physicochemical and physiological factors leading to calcification, as well as the environmental changes which might influence them, are discussed below.

3 Importance of the Cell Envelope

The cell envelope is very important for calcification. It can serve as a diffusion-limiting space in which high degrees of supersaturation might build up (Borowitzka 1989; Merz 1992). It localizes and possibly facilitates crystal nucleation, the step which requires the most energy, but it also seems to inhibit and direct crystal growth. All the well-known calcifying species secrete sheath material when grown under natural conditions, while species lacking a sheath do not calcify. Polysaccharides are a major component of the sheath. They can absorb high amounts of divalent metal ions (e.g., Decho 1990), raising concentrations far above those found in the ambient water. The polysaccharides have their highest binding capacity at a pH of around 8 (Decho 1990), which is a common value for cyanobacterial environments. Calcium adsorption followed by subsequent adsorption of CO_3^{2-} ions facilitates epitaxial crystal nucleation.

The sheath might also be responsible for the characteristic crystal forms which can be found in some species (Merz 1992). It might influence crystal growth either by its composition or by slowing the diffusion of ions. The amount and composition of the cell envelope material varies among species and depends on environmental conditions, such as availability of water, nutrient supply, and metal ion concentrations (Pentecost 1985; Bender et al. 1994; Sudo et al. 1995). Different species and genera seem to have different capacities for calcium adsorption (Weckesser et al. 1988). Composition might change depending on the available carbon and phosphorus sources (Bertocchi et al. 1990). Various environmental stress factors such as high light irradiance can increase the amount of excreted macromolecules (Merz and Zankl 1993a). Thus, there are numerous possibilities for environmental factors to influence the suitability of the cell envelope as a nucleation site.

From the above, it would seem that all cyanobacteria photosynthesizing in a carbonate-rich environment and enclosed by a sheath should calcify. This, however, is not the case. Calcified and uncalcified cyanobacteria species occur together and calcifying species can restrict calcification to limited zones within the sheath (Krumbein and Giele 1979; Obenlüneschloss 1991; Merz 1992; Winsborough et al 1994; Defarge et al. 1994). There are probably differences between the species regarding the suitability of their cell envelope for carbonate nucleation. High calcium binding capacities, however, can also be found in non-calcifying species such as *Microcoleus lyngbaceus* (Somers and Brown 1978). Aspartic acid, which is often enriched in organic material associated with carbonate precipitation (Mitterer 1989), can also be found in the sheath of both calcifying and non-calcifying cyanobacteria (*Chlorogloeopsis:* Schrader et al. 1982; *Phormidium:* Mikheyskaya et al. 1977; *Fischerella:* Pritzer et al. 1989). Unfortunately, there are no comparative analyses of the cell envelopes of calcifying and non-calcifying species or of potentially calcifying species under different environmental conditions. Therefore, it cannot be decided which are the essential differences in cell envelope composition.

There are also mechanisms to actively inhibit calcification. *Scytonema* filaments growing in cyanobacterial mats in the Everglades produce a bilayered sheath. The inner layer is denser, more structured, and has a clearly defined diameter, while the outer sheath layer (or capsule, following Bertocchi et al. 1990) is less dense and seems not to be as clearly confined. It is always only the outer part which is impregnated by carbonate crystals (Merz 1992). The inner part always remains uncalcified, although the hydroxyl ions, released as a consequence of photosynthetic uptake of HCO_3^- ions, obviously have to pass through it before inducing precipitation. The lack of calcification in the inner sheath is a consequence of a considerably lower pH, and thus lower saturation with respect to calcite. The lower pH is due to a pH gradient which builds up in the diffusion-limited space of the dense inner sheath, between the relatively low intracellular pH (around 7) and the alkaline ambient water (Merz et al. 1995).

There are obviously compositional differences between the two layers which also might influence calcification. Some organic macromolecules have been shown to facilitate crystal nucleation when firmly attached to a solid substrate. In solution, however, or possibly in a highly hydrated cell envelope, the same molecules can be absorbed onto a growing crystal surface and inhibit its growth (Wheeler and Sikes 1984; Addadi and Weiner 1985; Westbroek et al. 1994; Decho 1990).

4 Environmental Controlling Factors

4.1 Importance of Supersaturation

The major physicochemical factor controlling calcification is the saturation state of the water with respect to calcium carbonate minerals. As calcification in cyanobacteria is extracellular, the ambient water has to be supersaturated with respect to carbonate.

Physicochemical precipitation, due to supersaturation outside the cell envelope, forms solid, preservable tubes of coalescing carbonate crystals (Figs. 1a,b, 2). Tufa depositing environments are typical for physicochemical calcification. In these, precipitation is due to equilibration of the CO_2 concentration in the water with the CO_2 concentration in the ambient air, leading to a rapid rise of pH. When carbonate is pre-

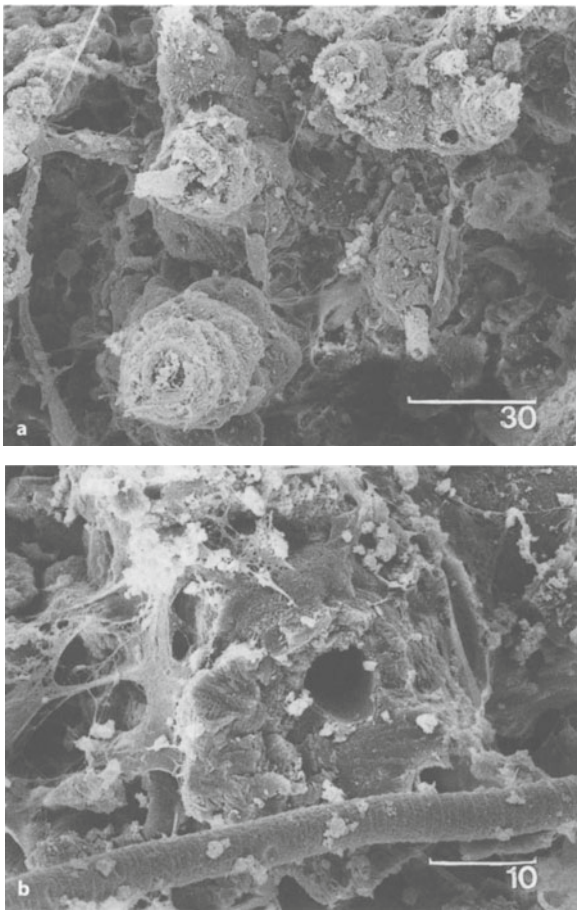

Fig. 1a. Surface of a tufa sample from a stream near Bad Urach, Schwäbische Alb, SW Germany. The sample is critical point dried, so that the filaments are well preserved. **a** The calcite tubes encrusting the filaments are sufficiently solid to protrude vertically from the surface. **b** After decomposition of the organic material a solid tube remains., and the broken tube tip exposes the coalescing calcite crystals. *Scale* in microns

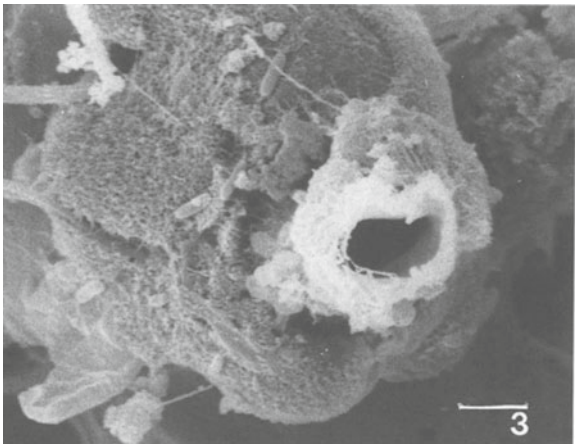

Fig. 2. Detail of cyanobacterium in tufa deposits from a stream near Bad Urach, Schwäbische Alb, SW Germany, showing encrustation of the sheath by calcite. The trichome is lacking in this sample. The sheath, however, is well preserved due to critical point drying, and it can be seen that precipitation is external to the sheath as compared to the impregnated sheath in Fig. 3. Precipitation in these tufa deposits is due to CO_2 evasion and the resulting high degrees of supersaturation of the water with respect to calcium carbonate minerals (saturation index = 0.8 and above; Merz-Preiß and Riding 1995). *Scale* in microns

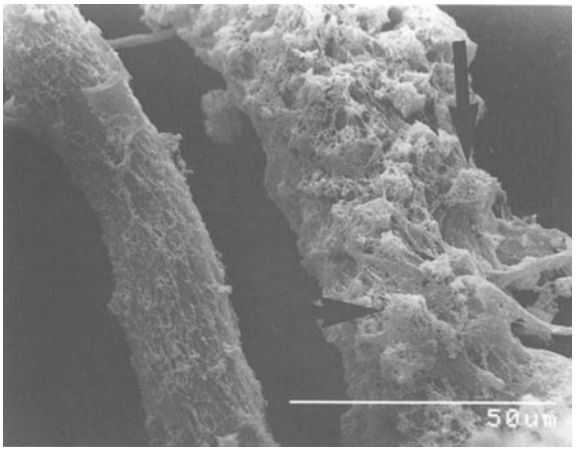

Fig. 3. A calcified filament of *Scytonema (right)* from the Everglades, Florida, critical point dried to minimize shrinking of the organic material, and an uncalcified filament (*left*). In the filament on the *right*, calcite crystals precipitated within the outer sheath layer due to photosynthetic bicarbonate uptake are clearly visible under a cover of dried sheath material (*arrows*) The crystals are completely embedded in the sheath and decay to form micritic mud upon death of the cyanobacteria. The smooth surface of the inner sheath and the thin cover of dried outer sheath material are visible in the uncalcified filament on the *left*

cipitated around the cyanobacterial cell envelopes, the ambient water shows supersaturations with respect to calcite around a saturation index (SI) = 0.8 and above ($SI_{calcite} = \log (Ca^{2+})(CO_3^{2-})/K_{calcite}$) (Kempe and Kazmierczak 1990b; Merz-Preiß and Riding 1995). The influence of photosynthesis on precipitation is minimal. Pentecost (1978) estimated that only 1–2% of the carbonate in tufa is precipitated by photosynthetic activity of cyanobacteria.

Carbonate impregnation of the sheath (Fig. 3) seems to occur when supersaturation is raised within the sheath. This can be due to active HCO_3^- uptake for photosynthesis, followed by excretion of hydroxyl ions into the cell envelope (Merz 1992). Carbonate is precipitated within rather than around the sheath. This form of calcification can start when the overlying water is only slightly supersaturated (SI = 0.2–0.3; Merz-Preiß, unpublished). In the shallow freshwater areas of the Everglades, Florida, cyanobacterial photosynthesis based on HCO_3^- accounts for nearly all the precipitated carbonate and results in a ratio of photosynthetically assimilated carbon to carbonate carbon of about 1:1. In the Everglades samples, the crystals are covered by organic material and consequently the tubes disintegrate upon decomposition of the cyanobacteria to form a micritic mud (Gleason and Spackman 1974; Merz 1992). Bicarbonate uptake for photosynthesis can be activated by the cells. This depends on the extracellular concentrations of inorganic carbon and the demand for carbon to fulfill maximum rates of photosynthesis. In tufa environments, sheath impregnation appears to be rare, probably because the supersaturation of the water with CO_2 and water agitation allow the cyanobacteria to photosynthesize using CO_2 only.

An increasing photosynthetic influence on calcification is reflected by an increase in the heavy carbon isotope (Pentecost and Spiro 1990; Merz 1992; Andrews et al. 1997). When enough inorganic carbon is available, the lighter ^{12}C is preferentially assimilated in photosynthesis and the heavier ^{13}C concentrates extracellularly. This leads to the precipitation of ^{13}C-enriched carbonate. In this way, the stable isotope composition of carbonate precipitated by cyanobacteria provides a clue to the degree of biological influence on precipitation.

4.2 Phosphate

Cyanobacteria are generally known as bloom organisms that thrive in eutrophic water bodies. It is therefore interesting to note that most genera with calcifying species occur in oligotrophic water. A negative effect of phosphate on calcareous periphyton in the Everglades has been described by Vymazal et al. (1994 and references therein) and Vymazal and Richardson (1995). Other authors ascribe cessation of oncolite growth and disappearance of calcifying cyanobacteria to pollution (Golubic 1973; Golubic and Fischer 1975; Kann 1985). The negative effect of pollution is probably due to the increase in phosphate concentration, since nitrogen does not have a negative effect on calcifying cyanobacteria and algae (Delgado and Lapointe 1994; Vymazal et

al. 1994). Observations in cultures of potentially calcifying cyanobacteria also indicate sensitivity to increased concentrations of phosphate. Phosphate concentrations of several millimole, commonly used in culture media for cyanobacteria (Schlösser 1982; Werner 1982), lead to a decrease in photosynthesis and death of the organisms, whereas they are successfully cultivated in media containing 10 µmol phosphate (Merz and Zankl 1993a).

Calcifying eukaryotic algae are also sensitive to phosphate. Concentrations around 8 µmol/l phosphate inhibit growth of charophytes (Forsberg 1965; Krause 1981). In green algae, phosphate enrichment enhances productivity of non-calcifying species more than that of calcifying algae and may even inhibit calcification in the latter (Delgado and Lapointe 1994). In coccolithophores, which calcify intracellularly, calcification is enhanced by phosphorus limitation (Paasche and Brubak 1994). Other carbonate producers might also be affected, as it is known that in nutrient-rich waters calcifying organisms are generally outcompeted by non-calcifying organisms (Westbroek et al. 1994). Thus, phosphate sensitivity seems closely related to the specific physiologic characteristics of calcifying cyanobacteria, algae and possibly other organisms. Physiologic prerequisites necessary for calcification appear to impede growth in nutrient-rich productive environments. The sensitivity to phosphate of calcifying cyanobacteria and algae might provide a clue to the question why many cyanobacteria and algae do not calcify, despite possible benefits from calcification. The physiologic characters that allow cyanobacteria and algae to thrive under high phosphate concentrations might negatively influence calcification.

These observations may have interesting implications for understanding the relationship between sea water phosphate concentration changes and calcification during the course of Earth's history.

5 Beneficial Effects of Calcification

Cyanobacterial calcification is not a mere side effect of photosynthesis in carbonate-rich waters. Calcification is restricted to certain species (although there are problems in defining cyanobacteria species), and there are species which produce sheath material and probably use bicarbonate but do not calcify. Some cyanobacteria simultaneously produce uncalcified as well as calcified cell envelope material (Obenlüneschloss 1991; Merz 1992). This suggests that active calcification has a beneficial effect for the organism and there are indeed several possible positive consequences of carbonate precipitation.

A 1:1 ratio of photosynthesis to calcification reduces alkalization and depletion of dissolved molecular CO_2 around the cells (McConnaughey 1994). Thus, precipitation might serve as an effective buffer against a pH rise in alkaline environments. pH buffering, as a beneficial effect of carbonate precipitation, has also been proposed for calcifying algae (coccolithophores: Paasche 1964; Sikes et al. 1980; charophytes: Raven et al. 1986).

Another effect of precipitation could be protection of the bicarbonate pump, which is possibly inhibited by carbonate ions (Lucas 1983). By neutralizing the carbonate ions in calcium carbonate, the function of the bicarbonate pump is ensured even under high pH conditions.

As cyanobacteria are low-light organisms, which nevertheless frequently inhabit environments of extreme light radiation, a light-shading function of the calcified sheath has been proposed for modern, and also for fossil, cyanobacteria (Van Liere and Walsby 1982; Rowland and Gangloff 1988). This idea, however, is not supported by laboratory experiments with high UV-B illumination, which show that the formation of non-calcifying rather than calcifying sheath material is enhanced under light stress (Merz and Zankl 1993a). Illumination with additional UV-A also did not increase calcification in laboratory cultures. But, even if calcification does not serve to physically shade the filaments it still could be a consequence of light protection, because an energy consuming carbon metabolism generally protects against the damaging effects of high light irradiance (Krause 1988). When more light energy, especially visible light and UV-A, than can be consumed in photosynthesis excites the photosystems, the photosystems may be irreversibly damaged. This process is called photoinhibition. Bicarbonate uptake is energized by photosystem II, the photosystem which is also more susceptible to photoinhibition. By using potentially damaging energy to increase the intracellular carbon pool, the energy is neutralized and the high intracellular carbon concentration allows higher rates of photosynthesis. The consumption of excessive light energy to protect the cells might thus be as important a function of the bicarbonate pump as the enhanced growth potential.

6 Calcification of Dead Cyanobacterial Material

Precipitation connected with dead cyanobacteria has been described by several authors (Winland and Matthews 1974; Kobluk and Risk 1977; Braithwaite et al. 1989; Chafetz and Buczynski 1992). It is probably due to carbonate precipitation by heterotrophic bacteria living on and from the organic material of the sheath. The bacteria produce characteristically dumbbell-shaped crystals (Chafetz and Buczynski 1992; Defarge et al. 1994; Szulc and Smith 1994), which seem distinguish-

able from crystals precipitated around living cyanobacteria. A reason for preferential bacterial calcification on dead rather than living cyanobacterial filaments (Chafetz and Buczynski 1992) can be found in the production of antimicrobial substances, which is widespread among cyanobacterial species (Cannell et al. 1988; Kellam et al. 1989). Only after death of the cyanobacteria, when production has ceased, can heterotrophic bacteria decompose the sheaths and undergo calcification.

7 Conclusions

Some filamentous cyanobacterial species calcify when growing in oligotrophic, carbonate-rich water. Calcification is dependent on the existence of a cell envelope, composed of organic macromolecules. High supersaturation with respect to calcite in the ambient water leads to encrustation of the filaments with calcite due to physicochemical processes. In only slightly supersaturated environments, a localized increase in saturation due to active photosynthetic bicarbonate uptake may lead to impregnation of the sheath.

Active uptake of bicarbonate as well as the composition of the cell envelope are influenced by environmental factors including CO_2 concentration, population density and nutrient supply. In the fossil record the occurrence of calcified cyanobacteria may reflect the saturation state of the water with respect to calcium carbonate minerals as well as other environmental factors which influenced their physiology.

References

Addadi L, Weiner S (1985) Interactions between acidic proteins and crystals: stereochemical requirements in biomineralization. Proc Natl Acad Sci USA 82:4110–4114

Andrews JA, Riding R, Dennis PF (1997) The stable isotope record of environmental and climatic signals in modern microbial carbonates from Europe. Palaeogeogr Palaeoclimatol Palaeoecol 129:171–189

Bender J, Rodriguez-Eaton S, Ekanemesang UM, Phillips P (1994) Characterization of metal-binding bioflocculants produced by the cyanobacterial component of mixed microbial mats. Appl Environ Microbiol 60:2311–2315

Berger S, Kaever MJ (1992) Dasycadales – an illustrated monograph of a fascinating algal order. Thieme, Stuttgart

Bertocchi C, Navarini L, Cesàro A, Anastasio M (1990) Polysaccharides from cyanobacteria. Carbohydr Polymers 12:127–153

Borowitzka MA (1989) Carbonate calcification in algae – initiation and control. In: Mann S, Webb J, Williams RJP (eds) Biomineralization. VCH Verlag, Weinheim, pp 63–94

Braithwaite CJR, Casanova J, Frevert T, Whitton BA (1989) Recent stromatolites in landlocked pools on Aldabra, Western Indian Ocean. Palaeogeogr Palaeoclimatol Palaeoecol 69:145–165

Brock TD (1973) Lower pH limit for the existence of blue-green algae: evolutionary and ecological implications. Science 179:480–483

Cannell RJP, Owsisnks AM, Walker JM (1988) Results of a large-scale screening programme to detect antibacterial activity from fresh-water algae. Br Phycol J 23:41–44

Castenholz RW (1992) Species usage, concept, and evolution in the cyanobacteria (blue-green algae). J Phycol 28:737–745

Chafetz HS, Buczynski C (1992) Bacterially induced lithification of microbial mats. Palaios 7:277–293

Cox G, James JM, Leggett KEA, Osborne RAL (1989) Cyanobacterially deposited speleothems: subaerial stromatolites. Geomicrobiol J 7:245–252

Decho AW (1990) Microbial exopolymer secretions in ocean environments: their role(s) in food webs and marine processes. Oceanogr Mar Biol Annu Rev 28:73–153

Défarge C, Trichet J, Couté A (1994) On the appearance of cyanobacterial calcification in modern stromatolites. Sed Geol 94:11–19

Delgado O, Lapointe BE (1994) Nutrient-limited productivity of calcareous versus fleshy macroalgae in a eutrophic, carbonate-rich tropical marine environment. Coral Reefs 13:151–159

Forsberg C (1965) Nutritional studies of *Chara* in axenic cultures. Physiol Plant 18:275–290

Garcia-Pichel F, Castenholz RW (1991) Characterization and biological implications of scytonemin, a cyanobacterial sheath pigment. J Phycol 27:395–409

Giovannoni SJ, Turner S, Olsen GJ, Barns S, Lane DJ, Pace NR (1988): Evolutionary relationships among cyanobacteria and green chloroplasts. J Bacteriol 170:3584–3592

Giovannoni SJ, Rappé MS, Gordon D, Urbach E, Suzuki M, Field KG (1996) Ribosomal RNA and the evolution of bacterial diversity. In: Roberts McL, Sharp P, Anderson G, Collins M (eds) Evolution of microbial life. 54th Symposium of the Society for General micobiology, Univ. of Warwick, March 1996, pp 63–85

Gleason PJ, Spackman WJr (1974) Calcareous periphyton and water chemistry in the Everglades. In: Gleason PJ (ed) Environments in South Florida, present and past. Miami Geological Society, pp 146–181

Golubic S (1973) The relationship between blue-green algae and carbonate deposits. In: Carr NG, Whitton BA (eds) The biology of blue-green algae. Blackwell, Oxford, pp 434–472

Golubic S (1983) Stromatolites, fossil and recent: a case history. In: Westbroek P, de Jong EW (eds) Biomineralization and biological metal accumulation. Reidel, Dordrecht, pp 313–326

Golubic S, Fischer AG (1975) Ecology of calcareous nodules forming in Little Connestoga Creek near Lancaster, Pennsylvania. Verh Int Ver Limnol 19:2315–2323

Golubic S, Campbell SE (1981) Biogenically formed aragonite concretions in marine *Rivularia*. In: Monty C (ed) Phanerozoic stromatolites: case histories. Springer, Berlin Heidelberg New York, pp 209–229

Horodyski RJ, VonderHaar SP (1975) Recent calcareous stromatolites from Laguna Mormona (Baja California), Mexico. J Sed Petrol 45:894–906

Jones B, Kahle CF (1986) Dendritic crystals formed by calcification of algal filaments in a vadose environment. J Sed Petrol 56:217–222

Kann E (1985) Benthische Cyanophyten-Gemeinschaften in Bächen und Seen. Arch Hydrobiol (Suppl) 71:307–310

Kellam SJ, Walker JM (1989) Antibacterial activity from marine microalgae in laboratory culture. Br Phycol J 24:191–194

Kempe S, Kazmierczak J (1990a) Chemistry and stromatolites of the sea-linked Satonda Crater lake, Indonesia: a recent model for the Precambrian sea? Chem Geol 81:299–310

Kempe S, Kazmierczak J (1990b) Calcium carbonate supersaturation and the formation of in situ calcified stromatolites. In: Ittekot V, Kempe S, Michaelis W, Spitzy A (eds) Facets of modern biogeochemistry. Springer, Berlin Heidelberg New York, pp 255–278

Kempe S, Kazmierczak J, Landmann G, Konuk T, Reimer A, Lipp A (1991) Largest known microbialites discovered in Lake Van, Turkey. Nature 349:605–608

Knoll AH, Fairchild IJ, Swett K (1993) Calcified microbes in Neoproterozoic carbonates: Implications for our understanding of the Proterozoic/Cambrian transition. Palaios 8:512–525

Kobluk DR, Risk MJ (1977) Calcification of exposed filaments of endolithic algae, micritic envelope formation and sediment production. J Sed Petrol 47:517–528

Krause W (1981) Characeen als Bioindikatoren für den Gewässerzustand. Limnologica 13:399–418

Krause GH (1988) Photoinhibition of photosynthesis: An evaluation of damaging and protective mechanisms. Physiol Plant 74:566–574

Krumbein, WE, Giele C (1979) Calcification in a coccoid cyanobacterium associated with the formation of desert stromatolites. Sedimentology 26: 593–604

Lucas WJ (1983) Photosynthetic assimilation of exogenous HCO_3^- by aquatic plants. Annu Rev Plant Physiol 34:71–104

McConnaughey TA (1994) Calcification, photosynthesis, and global carbon cycles. In: Doumenge F, Allemand D, Toulemont A (eds) Past and present biomineralization processes, Bull Inst Oceanogr 13:37–60

Merz MUE (1992) The biology of carbonate precipitation by cyanobacteria. Facies 26:81–102

Merz MUE, Zankl H (1993a) The influence of culture conditions on growth and sheath development of calcifying cyanobacteria. Facies 29:75–80

Merz MUE, Zankl H (1993b) The influence of the sheath on carbonate precipitation by cyanobacteria. Boll Soc Paleont Ital (Spec Vol) 1:325–331

Merz MUE, Schlue W-R, Zankl H (1995) pH-measurements in the sheath of calcifying filamentous cyanobacteria. Bull Inst Oceanogr 14:281–289

Merz-Preiß MUE, Riding R (1995) Supersaturation in Recent freshwater tufa streams: calibration of marine environmentally controlled $CaCO_3$ precipitation in the past? 10th Bathurst Meeting of Carbonate Sedimentologists, Royal Holloway, London, 2–5 July, Abstracts, pp 38, 44

Mikheyskaya LV, Ovodova RG, Ovodov YuS (1977) Isolation and characterization of lipopolysaccharides from cell walls of blue-green algae of the genus *Phormidium*. J Bacteriol 130:1–3

Mitterer RM (1989) Composition and association of organic matter with calcium carbonate and the origin of calcification. In: Crick RE (ed), Origin, evolution, and modern aspects of biomineralization in plants and animals. Plenum Press, New York, pp 309–323

Moore LS, Burne RV (1994) The modern thrombolites of Lake Clifton, Western Australia. In: Bertrand-Sarfati J, Monty C (eds) Phanerozoic stromatolites II. Kluwer, Dordrecht, pp 3–29

Obenlüneschloss J (1991) Biologie und Ökologie von drei rezenten Süßwasser-Rivularien (Cyanobakterien). Übertragbarkeit artspezifischer Verkalkungsstrukturen auf fossile Formen. Göttinger Arb Geol Paläont 50:86

Paasche E (1964) A tracer study of the inorganic carbon uptake during coccolith formation and photosynthesis in the coccolithophorid *Coccolithus huxleyi*. Plant Physiol (Suppl) III:1–82

Paasche E, Brubak S (1994) Enhanced calcification in the coccolithophorid *Emiliania huxleyi* (Haptophyceae) under phosphorus limitation. Phycologia 33:324–330

Pentecost A (1978) Blue-green algae and freshwater carbonate deposits. Proc R Soc Lond B 200:43–61

Pentecost A (1985) Investigation of variation in heterocyst numbers, sheath development and false-branching in natural populations of Scytonemaceae (Cyanobacteria). Arch Hydrobiol 102:343–353

Pentecost A, Riding R (1986) Calcification in cyanobacteria. In: Leadbeater SC, Riding R (eds) Biomineralization in lower plants and animals. The Systematic Association, Special Vol 30, Clarendon Press, Oxford, pp 73–90

Pentecost A, Spiro B (1990) Stable carbon and oxygen isotope composition of calcites associated with modern freshwater cyanobacteria and algae. Geomicrobiol J 8:17–26

Pia J (1933) Die rezenten Kalkgesteine. Z Kristall Mineral Petrogr Abt B, Mineralog Petrogr Mitt, Ergänzungsband, Leipzig

Pritzer M, Weckesser J, Jürgens UJ (1989) Sheath and outer membrane components from the cyanobacterium *Fischerella* sp. PCC 7414. Arch Microbiol 153:7–11

Raven JA, Smith FA, Walter NA (1986) Biomineralization in the Charophyceae sensu lato. In: Leadbeater SC, Riding R (eds) Biomineralization in lower plants and animals. The Systematic Association, Special Vol 30, Clarendon Press, Oxford, pp 125–139

Rasmussen KA Macintyre IG, Prufert L (1993) Modern stromatolite reefs fringing a brackish coastline, Chetumal Bay, Belize. Geology 21:199–202

Riding R 1977: Calcified Plectonema (blue-green algae), a recent example of Girvanella from Aldabra Atoll. Palaeontology 20:33–46

Riding R (1991) Calcified cyanobacteria. In: Riding R (ed) Calcareous algae and stromatolites. Springer, Berlin Heidelberg New York pp 55–87

Riding R (1992) Temporal variation in cacification in marine cyanobacteria. J Geol Soc Lond 149:979–989

Riding R (1994) Evolution of algal and cyanobacterial calcification. In: Bengtson S (ed) Early evolution on Earth Nobel Symposium No 84, Columbia UP, New York, pp 426–438

Robbins LL, Blackwelder PL (1992) Biochemical and ultrastructural evidence for the origin of whitings: a biologically induced calcium carbonate precipitation mechanism. Geology 20 464–468

Rowland SM, Gangloff RA (1988) Structure and paleoecology of Lower Cambrian reefs. Palaios 3, Reefs Issue 111135

Scherer S, Chen TW, Böger P (1988) A new UV-A/B protecting pigment in the terrestrial cyanobacterium *Nostoc commune*. Plant Physiol 88:1055–1057

Schlösser UG (1982) Sammlung von Algenkulturen. Ber Dtsche Bot Ges 95:181–276

Schopf JW (1992) Paleobiology of the Archean. In: Schopf JW, Klein C (eds) The Proterozoic biosphere, a multidisciplinary study. Cambridge University Press, Cambridge, pp 25–39

Schopf JW (1996) Are the oldest known fossils cyanobacteria? In: Roberts D McL (ed) Evolution of microbial life. 54th Symposium of the Society of General Microbiology. Cambridge Univ Press, Cambridge, pp 23–61

Schrader M, Drews G, Golecki JR, Weckesser J (1982) Isolation and characterization of the sheath from the cyanobacterium *Chlorogloeopsis* PCC 6912. J Gen Microbiol 128:267–272

Sikes CS, Roer RD, Wilbur KM (1980) Photosynthesis and coccolith formation: inorganic carbon sources and the net inorganic reaction of deposition. Limnol Oceanogr 25:248–261

Smith AJ (1982) Modes of cyanobacterial carbon metabolism. In: Carr NG, Whitton BA (eds) The biology of cyanobacteria. Blackwell, Oxford. Bot Monogr 19:47–85

Somers GF, Brown M (1978) The affinity of blue-green algae for calcium ions. Estuaries 1:17–28

Stanier RY, Cohen-Bazire G (1977) Phototrophic prokaryotes: the cyanobacteria. Annu Rev Microbiol 31:225–274

Sudo H, Burgess JG, Takemasa H, Nakamura N, Matsunaga T (1995) Sulfated exopolysaccharide production by the halophilic cyanobacterium *Aphanocapsa halophytica*. Curr Microbiol 30:19–222

Szulc J, Smyk B (1994) Bacterially controlled calcification of freshwater *Schizothrix*-stromatolites: an example from the Pienny Mts, Poland. In: Bertrand-Sarfati J, Monty C (eds) Phanerozoic stromatolites II. Kluwer, Dordrecht, pp 31–51

Thompson JB, Ferris FG (1990) Cyanobacterial precipitation of gypsum, calcite, and magnesite from natural alkaline lake water. Geology 18:995–998

Van Liere L, Walsby AE (1982) Interactions of cyanobacteria with light. In: Carr NG, Whitton BA (eds) The biology of cyanobacteria. Blackwell, Oxford. Bot Monogr 19:9–45

Vymazal J, Craft CB, Richardson CJ (1994) Periphyton response to nitrogen and phosphorus additions in Florida Everglades. Algol Stud 73:75–97

Vymazal J, Richardson CJ (1995) Species composition, biomass, and nutrient content of periphyton in the Florida Everglades. J Phycol 31: 43–354

Werner D (1982) Biologische Versuchsobjekte. Fischer, Stuttgart

Wheeler AP, Sikes S (1984) Regulation of carbonate calcification by organic matrix. Am Zool 24:933–944

Wharton RA Jr (1994) Stromatolitic mats in antarctic lakes. In: Bertrand-Sarfati J, Monty C (eds) Phanerozoic stromatolites II. Kluwer, Dordrecht, pp 53–70

Weckesser J, Hofmann K, Jürgens UJ, Whitton BA, Raffelsberger B (1988) Isolation and chemical analysis of the sheaths of the filamentous cyanobacteria *Calothrix parietina* and *C scopulorum*. J Gen Microbiol 134:629–634

Westbroek P, Buddemeier B, Coleman M, Kok DJ, Fautin D, Stal L (1994) Strategies for the study of climate forcing by calcification. In: Doumenge F, Allemand D, Toulemont A (eds) Past and present biomineralization processes. Bull Inst Oceanogr 13:37–60

Winland HD, Matthews PK (1974) Origin and significance of grapestones, Bahama Islands. J Sed Petrol 44:921–927

Winsborough BM, Seeler J-S, Golubic S, Folk RL, Maguire B Jr(1994) Recent fresh-water lacustrine stromatolitic mats and oncoids from Northeastern Mexico. In: Bertrand-Sarfati J, Monty C (eds) Phanerozoic stromatolites II. Kluwer, Dordrecht, pp 71–100

Cyanobacteria: Architects of Sedimentary Structures

Stjepko Golubic[1], Lee Seong-Joo[2], Kathleen M. Browne[3]

[1] Department of Biology, Boston University, Boston, MA 02215, USA
[2] Department of Earth System Sciences, Yonsei University, Seoul 120-749, Korea
[3] Department of Geological and Marine Sciences, Rider University, Lawrenceville, NJ 08648-3099, USA

Abstract. Cyanobacteria, the oldest oxygenic phototrophs on the planet, once made the most significant impact on sediments and left an impressive fossil record of organo-sedimentary structures. Today, cyanobacteria dominate extreme environments where they participate in sediment production, construction and destruction, and leave characteristic, often species-specific, traces of their activities. Microbial ecosystems at the sediment-water interface are built and supported by cyanobacteria as the principal primary producers. Cyanobacterial photosynthesis promotes carbonate precipitation, delivering new sediment particles. Cyanobacterial growth, movement and behavioral responses often guide the depositional process and shape the resulting sedimentary structures. Conversely, cyanobacterial colonization and growth is also guided by changes in depositional environment. Cyanobacterial primary production at the sediment-water interface, coupled with rapid bacterial oxidation of this organic product, maintains steep redox gradients, creating additional metabolic niches. The consequent changes in mineral solubility promote biogeochemical cycling of elements and may lead to recrystallization and rearrangement of minerals. Destruction and alteration of sediments may be caused by cyanobacterial activities indirectly, or be carried out directly by euendolithic cyanobacteria which actively penetrate carbonate substrates. Evidence of both sediment-constructing and -destructing cyanobacterial behavior is found in carbonate deposits of the Mesoproterozoic age. As pioneer settlers on marine, freshwater and terrestrial sedimentary deposits, modern cyanobacteria prepare the ground for successive invasion and expansion of eukaryotic flora and fauna. In the historical context, and on a geological time scale, analogous sequences of events illustrate the evolutionary progression of life's complexity, as cyanobacterially supported microbial ecosystems of marine and terrestrial environments gave way to eukaryote-dominated ones.

1 Introduction

The important historic role that life and living systems played in the formation of Earth's lithosphere, hydrosphere and atmosphere is now generally acknowledged (e.g., Bengtson 1994). This recognition is reflected in the ways that environmental scientific disciplines are organized, and in the terminology they use. Terms such as biogeochemical cycling of elements, biosedimentation, and bioerosion express, in fact, the importance and vigor of biocatalyzed reactions and their efficiency in altering environmental chemistry. Many such biogeochemical interactions take place at the sediment-water interface, so that they affect sediments directly. Other biocatalyzed interactions take place in the water column above the sediment or elsewhere. The record of these events may also end up buried in sediments representing allochthonous sedimentary elements. Cyanobacterial activities constitute a significant, historically most important component of these interactions.

Cyanobacteria, the oldest oxygenic photosynthesizers and the principal primary producers of organic matter on the early Earth, were directly responsible for the change of Earth's environments from reduced to oxidized. The endosymbiotic incorporation of cyanobacteria into eukaryotic cellular organization triggered evolutionary diversification of algae and plants (Mereschkowsky 1905; Margulis 1993). Such insights, confirmed by modern molecular phylogeny (Woese 1987; Giovannoni et al. 1988; Bhattacharya and Medlin 1995; Nelissen et al. 1995; Palenik and Swift 1996), place cyanobacteria at center-stage of biological and geological attention.

At present, cyanobacteria dominate in extreme environments, such as thermal springs (Castenholz 1984; Jørgensen and Nelson 1988; Ward et al. 1992), hypersaline basins (Horodyski et al. 1977; Golubic 1992a,b), and environments disturbed by human activities (Sorkhoh et al. 1992; Golubic 1994; Kühl et al. 1996; Pearl 1996; Heiskanen and Olli 1996). In all these environments, cyanobacteria are the main participants in sedimentary processes, and the sediments carry a clear mark of cyanobacterial activities. Extreme environments are, therefore, the favored models for interpretation of the role of cyanobacteria in ancient aquatic and terrestrial ecosystems.

In this chapter, we discuss the roles of cyanobacteria in sediment production, construction and destruction. Their role as organisms participating in sediment production includes not only the input of organic product into the sediment, but also the input of minerals precipitated through mediation of these organisms. Biogenic sediment construction is defined here as sediment frame-building by organisms, which organize sediment particles, or guide precipitation through their growth, movement and behavioral responses. (In this sense, precipitation of cements that bind sediment particles can be viewed as sediment produced as well as

R. E. Riding and S. M. Awramik (Eds.)
Microbial Sediments

constructed.) Biogenic sediment destruction encompasses degradation of organic sedimentary components as well as displacement of mineral matter by organisms through chemical (corrosion) and mechanical (abrasion) means.

2 Cyanobacteria and Sediment Production

Cyanobacterial contribution to sediments was historically most important prior to the evolution of eukaryotic algae and plants. As photoautotrophic primary producers, cyanobacteria enrich the sediments with organic matter, while depleting their environment of atmospheric and hydrospheric carbon dioxide and bicarbonate. Burial of their photosynthetic product in the sediments must have had, over geological time, significant climatic consequences. A concurrent increase of oxygen content of the atmosphere and an increased carbonate deposition are thought to be the most significant by-products of historic burial events of organic carbon (e.g., Holland 1984; Berner 1989; Kaufman and Knoll 1995). Cyanobacterial organic contribution to Holocene lake sediments is well documented by the presence of their specific pigments preserved in the sediment, enabling paleolimnological timing of past eutrophication events in these water bodies (Züllig 1961; Livingstone 1984). The present discussion focuses on the relationship between cyanobacteria and the mineral, specifically carbonate, component of sediments.

An immediate consequence of photosynthetic carbon removal from aquatic systems is the rise of the environmental pH, triggering precipitation of calcium carbonate in carbonate-saturated waters. Carbonate precipitation associated with photosynthetic activity of cyanobacteria has been documented in freshwater lakes and marshes (Schröder and Schneider 1983; Merz 1992; Merz and Zankl 1993), and the mechanism of this process is discussed by Merz (this Vol.).

The extent to which the origin of the resulting carbonate sediment particles can be recognized depends on the degree of cellular control over the carbonate nucleation process and on the specificity of crystal templating by organic matrices. The intracellular precipitation and templating of carbonate crystals, such as in the production of coccoliths, have not been observed in cyanobacteria. However, considerable control over crystal shaping and growth was found in precipitates associated with cyanobacterial extracellular polysaccharide envelopes and sheaths (Pentecost and Riding 1986; Pentecost 1991; Merz et al. 1995). Calcification is a property expressed specifically by some cyanobacterial taxa while other cyanobacteria remain uncalcified even when exposed to waters of the same level of carbonate saturation. *Scytonema julianum* filaments on periodically wetted limestone cliffs, for example, are consistently covered by calcite crystals, while co-occurring *S. myochrous* remains free of calcification (Golubic 1991). The resulting carbonate precipitates often exhibit genus- and species-specific differences in crystal morphology. The crystals formed within the sheaths of *Scytonema* sp. in the Everglades marshes, Florida, USA, were found to be consistently different from those formed in the sheaths of the nearby growing *Schizothrix* sp. (Merz 1992; Merz and Zankl 1993). Similarly, precipitates of calcite on the sheaths of *Scytonema julianum* are clearly distinguishable from those formed on co-occurring *Geitleria calcarea* (Geitler 1960; Couté 1982). Specific forms of carbonate precipitates were also reported for *Nostoc parmelioides* (Freytet and Verrecchia 1993). Calcitic grains formed in different species of *Rivularia* in the littoral zone of Austrian lakes, e.g. *R. haematites, R. periodica* and *R. varians* were morphologically discrete (Obenlüneschloss 1991). Similar species-specific distinction in formation of aragonitic precipitates has been documented for co-occurring marine intertidal *R. polyotis* and *R. mesenterica* (Golubic and Campbell 1981). The specificity of other morphologically characteristic mineral deposits is less clear. For example, aragonite precipitates of characteristic dumbbell morphology were found to precipitate from hot springs associated with cyanobacteria (Farmer and Des Marais 1994). However, quite similar aragonite crystals were found associated with cultured heterotrophic bacteria isolated from marine mats (Buczynski and Chafetz 1991). The extent to which such precipitates are induced or modified by cyanobacterial presence is not known. The observations (Fig. 1) that: (1) new crystal nucleation is initiated on particular locations (points) on top of existing crystals, and (2) the process is repeated at a wide range of sizes argue against templating by any particular microorganism or its organic product. The growth of these aragonite needles appears rather consistent with the patterns characteristic of an abiotic process. The possibility remains, however, that microbial metabolic activities contributed to supersaturation and a nonspecific triggering of carbonate precipitation.

Following death and disintegration of carbonate-encrusted cyanobacterial colonies, the specifically different carbonate precipitates, e.g., *Rivularia* grains (Fig. 2), may disperse and contribute to the fine carbonate sediment fraction, where their particular origins can be traced. Such contribution of benthic cyanobacteria to the sediments of oligotrophic alpine lakes has been identified and quantified (Schröder 1982). The contribution of planktic cyanobacteria consists of precipitates triggered by their photosynthetic activity in the water column, from where they settle, forming fine carbonate mud (marl, Seekreide). Calcite precipitation associated with picoplanktic cyanobacteria has been

Fig. 1. Dumbbell-shaped precipitates of radiating aragonitic needles associated with cyanobacteria *Synechococcus lividus* and *Spirulina* sp. in Mammoth thermal springs, Yellowstone National Park. Crystallization starts with precipitation of bundles of parallel or slightly diverging needles. Precipitation continues at both pointed ends of the primary needles resulting in radiating bundles. Further crystal growth completes two adjacent hemispherical cushions of radiating needles. Note that this process is repeated at a wide range of dimensions suggesting a process unrelated to the size of co-occurring microorganisms. The *arrow* marks a rare co-precipitating euhedral calcite crystal. SEM; *scale bar* = 50 μm

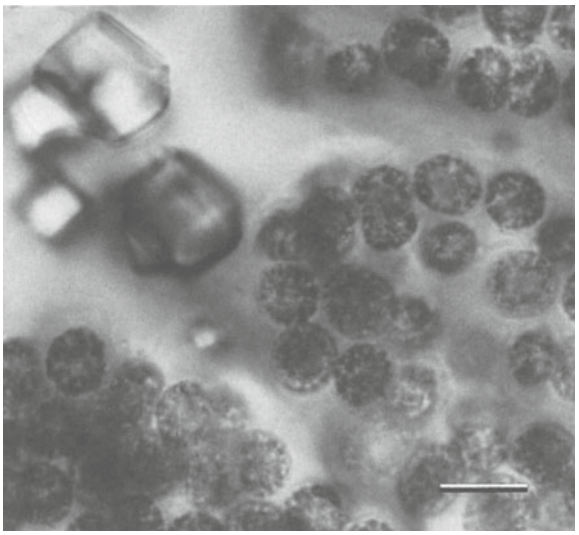

Fig. 3. Rhombohedral calcite crystals precipitated within loose extracellular polysaccharide of floating colonies of *Microcystis flos-aquae* in a eutrophic pond near Kiel, northern Germany. Following the collapse of the plankton bloom, these crystals sink and contribute to the lake sediment. Transmitted light micrograph; *scale bar* = 10 μm

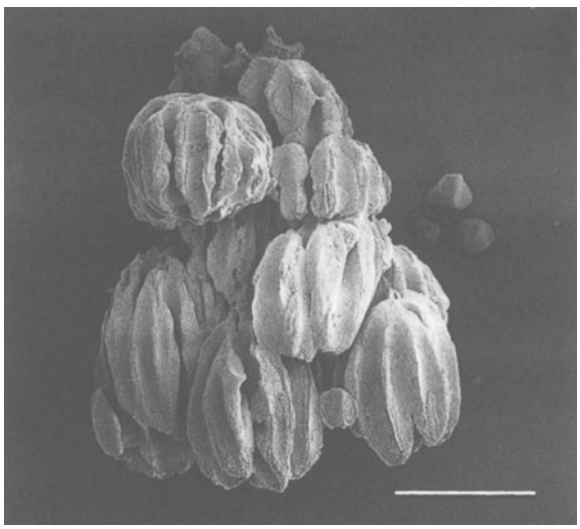

Fig. 2. A carbonate grain formed within colonies of benthic freshwater cyanobacterium *Rivularia haematites*, preserving characteristic oriented filament "imprints." Such grains contribute to the fine marl sediment upon disintegration of *Rivularia* colonies. Plitvice lakes, Croatia. SEM; *scale bar* = 100 μm

documented in the Green Lake, New York, USA (Schulze-Lam et al. 1992; Yates and Robbins 1995). Calcite precipitation also occurs within colonies of larger planktic cyanobacteria, such as the bloom-forming *Microcystis flos-aquae* (Fig. 3) and *Aphanothece clathrata* (L. Krienitz, personal communication, 1997). Episodic, massive, calcium carbonate precipitation in the water column, associated with sudden changes in pH during periods of intensive photosynthetic activity, may explain the phenomenon of whitings often observed in lakes and lagoonal waters (Robbins and Blackwelder 1992).

In the modern ocean, carbonate precipitation occurs mostly in eukaryotes such as red and green algae, coccolithophorids, foraminifera, anthozoans, mollusks and other invertebrates under tight, cellular and enzymatic control. Consequently, the majority of carbonate particles accumulating in modern marine sediments are skeletal bioclasts with highly specific and easily recognizable biological patterns. The contribution of cyanobacterial carbonate precipitates to modern marine sediments is relatively small. It has been postulated, however, that cyanobacterial contribution to carbonate precipitation must have been substantially higher in a Precambrian ocean, prior to the evolution of numerous eukaryotic organisms that now deplete their environment of calcium carbonate biocatalytically (reviewed by Riding 1993). Accordingly, an ancient ocean, deprived of enzymatically controlled skeletogenesis and with a lesser load of dissolved organics, must have been much closer to a state of spontaneous carbonate precipitation than its modern counterpart. Ancient oceans may have, therefore, responded more readily to photosynthetically induced pH changes, in a fashion more similar to that observed in freshwater today. It is conceivable that cyanobacterial photosynthesis contrib-

uted at that time substantially to carbonate sediment production, both in the form of carbonate mud and in the form of rhythmic, benthic carbonate precipitates observed in the sediments of the time (e.g., Grotzinger 1990). The mechanism of the construction of such stromatolitic sedimentary features and the possible role of ancient cyanobacteria in that process remain unclear.

3 Cyanobacteria and Sediment Construction

The role of cyanobacteria in stabilizing loose sediments has been recognized in the context of the study of microbial mats and stromatolites (e.g., Walter 1976). The gliding motility of filamentous cyanobacteria in conjunction with copious excretion of extracellular polysaccharide sheath material enables these organisms to spread rapidly over newly deposited sediments. Cyanobacteria regularly abandon their sheaths as they move, leaving them behind as an organic textural support for the sediment they have passed through. Several biologically and environmentally relevant consequences can be derived from the ability of cyanobacteria to thrive on loose sediment deposits and escape burial. These include: sediment support and prevention of sediment erosion, sediment accretion and buildup of organosedimentary structures, biogeochemical differentiation of microenvironments at the sediment-water interface, and successional replacement by other biota. These developments depend largely on sedimentation rates and may take place in sequence or in combination.

Cyanobacterial coatings on sediment surfaces protect the underlying sediments from erosion. This effect was quantified in plume experiments in which the current velocity needed to disrupt the biosedimentary structure was determined and compared with that applied to loose sediment. (Neumann et al. 1970; Madsen et al. 1993; Paterson 1994; Yallop et al. 1994). In peritidal ranges, where sediments are exposed to high environmental energies of tidal currents and wave scouring, coating by cyanobacterial mats prevents or delays erosion, thereby extending their own residence on the habitat as well as enabling colonization by others.

Motile, sheathed cyanobacteria of the multi-trichomous genera *Microcoleus, Schizothrix* and *Hydrocoleum* and the uni-trichomous genera *Lyngbya* and *Phormidium* form coherent mats of intertwined filaments. They are the most common pioneers in colonizing and stabilizing loose sediments (Fig. 4). Once stabilized, the sediment layers may be further fortified by coarser, non-motile and slower growing cyanobacteria of the genera *Scytonema, Calothrix, Dichothrix* and *Gardnerula*. Falsely branched filaments of these taxa grow inserted in the mat perpendicular to the mat's surface. Under hypersaline conditions, stabilized mats

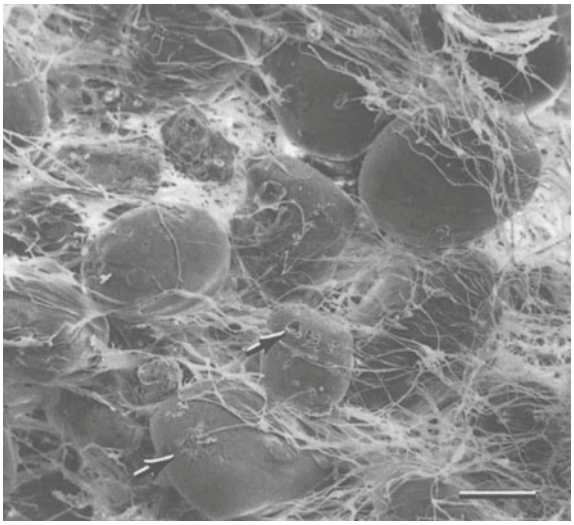

Fig. 4. Intertwined filaments of *Schizothrix gebeleinii* bind ooid grains in the process of stromatolite construction. The structure is later fortified by cementation. Note that the carbonate grains are damaged by endolithic cyanobacteria (*arrows*). Lee Stocking Island, Exuma Sound, Bahamas. SEM; *scale bar* = 100 μm

are often coated by coccoid cyanobacteria of the genus *Entophysalis*. Sediment stabilization and protection by microbial mats is a frequent phenomenon in a variety of marine, freshwater and terrestrial habitats. Under conditions of moderate temperatures and normal salinities, cyanobacteria are often joined and later replaced by eukaryotes.

Microbial mats stabilize sediments of different chemical composition, grain-size and geological origins. Clastic quartz sands are stabilized by *Microcoleus chthonoplastes* and *Lyngbya aestuarii* on sand flats along both coasts of North America (Horodyski 1977; Pierson et al. 1987; Stolz 1990). These species are global in distribution, although geographically, ecologically and genetically distinct races do exist (Karsten 1996). *M. chthonoplastes* persists in highly hypersaline conditions and has been applied since Roman times to stabilize fine argillaceous mud in salt pans of commercial marine salt works (Schneider and Herrmann 1980). Depending on the salinity range, these dominant taxa are joined by dozens of subdominant cyanobacteria and a number of other phototrophic and heterotrophic microorganisms (D'Amelio et al. 1989). Once stabilized, these sand flats are colonized by *Calothrix crustacea* and *C. scopulorum*, starting a succession toward development of a coastal salt marsh ecosystem (Seong-Joo et al., this Vol.).

Fine carbonate mud along the northwest coast of Andros Island of the Bahama carbonate platform is stabilized by a smooth, leathery, peach-colored mat comprised of a fine, filamentous *Schizothrix* species. The mat-covered areas form erosion-resistant horizons which are further fortified by the *Scytonema*-like *Ca-*

lothrix pilosa and punctuated by colonies of darkly pigmented, stalked pleurocapsalean cyanobacteria. Similar settings are known to have existed since Precambrian times, including comparable pleurocapsalean fossil *Polybessurus* (Green et al. 1987). Wherever these horizons collapse, the underlying sediment is rapidly removed, leaving undercut margins of the remaining top level. Stabilized mats of Andros coasts support the establishment of *Avicennia* mangrove stands.

A variety of mats, dominated by different cyanobacteria, characterize ecological niches on arid tropical coasts (e.g., Friedman and Krumbein 1985; Golubic 1992a,b). They exemplify consolidation of a range of combined sediments. Depending on local geography, geology and climate, these sediments are composed of terrigenous clasts, marine carbonate clasts and precipitates of carbonates, sulfates and halites. Differential sedimentation rates within these mats are responsible for the formation of sabkha-type coastal plains (Kinsman and Park 1976; Golubic 1992a). Similar developments form broad rims around playa lakes of inland evaporitic basins, which also harbor a variety of stromatolitic structures (e.g., Winsborough et al. 1994).

In terrestrial environments, cyanobacteria are common inhabitants of soils under different climatic conditions, including deserts. The multi-trichomous cyanobacterium *Microcoleus vaginatus* plays the main role in stabilization and accretion of loose soil particles, forming erosion-resistant "desert crusts" which become later fortified by *Scytonema tenellum* and by slower growing lichens (Campbell 1979; Garcia-Pichel and Belnep 1996). These subaerial cyanobacteria are responsible for the expansion of desert soils over bare sandstone rocks in Utah, USA, preparing the ground for colonization by grasses, bushes and, finally, pine forest (Campbell 1979). Similarly drought-resistant are epilithic cyanobacteria that coat sporadically wetted rock surfaces in the mountains (Jaag 1945; Golubic 1967a,b). It has, therefore, been postulated that cyanobacteria highly resistant to desiccation and UV-radiation must have colonized the continents during Proterozoic times, supporting fully functional, microbial soil ecosystems, possibly over a billion years before the evolution of higher land plants (Campbell 1979). The ability of modern cyanobacteria to protect themselves from UV-radiation (Garcia-Pichel and Castenholz 1991, 1994) and the existence of mature Proterozoic paleosols (Kimberley and Holland 1992) support this conclusion.

In addition to stabilizing and protecting sediments, cyanobacterial mats promote sediment accretion by selectively incorporating sediment particles which would otherwise be swept away by currents and winds. This is evident from differential sand-size distribution around mats (Awramik and Riding 1988). Precipitation of minerals promoted within cyanobacterial mats not only adds mineral to the deposit, but also lithifies the sediment. Such preferential incorporation of mineral matter within cyanobacterial thalli may result in the construction of elevated organo-sedimentary structures, such as domes and cones. Differences in size, growth patterns and behavioral responses among various participating cyanobacterial taxa may then be reflected in the external shaping and/or internal textures of the resulting organo-sedimentary structures. Radially spreading cyanobacteria may initiate structures that are circular in base projection and domal in profile. The internal textural patterns may be concentric, reflecting pulses in accretional process, or radial, reflecting the direction of microbial spreading. Concentric pulses in cyanobacterial growth are often marked by differentiation and zonal distribution of false branching, heterocysts and/or precipitated mineral grains. Carbonate precipitates within mats may conform either with the radial growth of the filaments (e.g., *Rivularia polyotis*) or with the zones of filament differentiation (e.g., *R. mesenterica*) (Golubic and Campbell 1981). In other cases, carbonate precipitation conforms with organic layers formed by laminar (tangential) arrangement of entire populations of motile cyanobacterial filaments (e.g., *Schizothrix gebeleinii*, Golubic and Browne 1996; Seong-Joo et al., this Vol.).

Alternation in tangential and radial orientation of modern gliding cyanobacteria results from two different behavioral patterns. The mat-building cyanobacteria *Microcoleus chthonoplastes* and *Schizothrix gebeleinii* change their orientation in response to sedimentation rates, alternately coating sediment surface and escaping burial. *Phormidium hendersonii* filaments which construct profiled domes alternate their orientation in response to day/night changes in solar luminosity. These different behaviors responding to different environmental stimuli, however, may result in similar rhythmic distribution patterns of both the cyanobacterial sheaths left in the sediment and the incorporated mineral grains (Seong-Joo et al. 1998, 1999 and this Vol.).

A different type of highly profiled growth of organo-sedimentary structures is exemplified by the formation of upright pointed cones and pinnacles. The Mesoproterozoic fossil record documents widely distributed cone-shaped stromatolites called *Conophyton*, ranging in size from a few centimeters to several meters and covering extensive areas of presumed shallow water paleoenvironments (Walter et al. 1992). These structures declined toward the end of the Proterozoic, leaving many questions as to their origin unanswered, which stimulated the quest for modern counterparts. Centimeter-sized, conical stromatolitic structures, rigidified by silica deposition and built by the cyanobacterium *Phormidium truncatum* var. *thermale* and *Chloroflexus aurantiacus*, an anoxygenic photosynthetic filamen-

tous bacterium, were compared with ancient conophytons (Walter et al. 1976). Pointed clumping of *Lyngbya aestuarii* in tidal lagoons of the American Pacific coast has been explained by the collapse of upright-radiating free filaments during tidal drainage (Horodyski 1977). Other pinnacles form more permanent structures and involve participation of *Schizothrix splendida* in support of *Lyngbya aestuarii* (Golubic 1992a). These formations invited explanations involving either chemotactic (oxygen-supply by drainage, Golubic 1992a) or phototactic responses (Awramik and Vanyo 1986).

Organo-sedimentary structures such as domes and cones may also be initiated by microbial metabolic activities. Photosynthetically produced oxygen bubbles may become entrapped beneath and between layers of interwoven cyanobacterial filaments and exert buoyancy. Following a day of intensive photosynthetic activity, large patches of some benthic cyanobacterial mats actually become dislodged from the bottom and float on the water surface, drifting in the wind. The networks of other cyanobacterial mats, however, exhibit elastic properties so that only localized areas project vertically upward as cones, pinnacles and towers held by gas bubbles. For example, thin bright-red veneers on coral reefs of Tahiti, formed by rapidly moving trichomes of *Hydrocoleum coccineum*, aggregate at the end of each day, while oxygen bubbles stretch the fabric into long upright towers (S. Golubic, and L., Mao Che, unpublished). When the process is accompanied by rapid mineral precipitation, as in some thermal springs, the resulting morphologies may become rigid and easily preservable. In Mammoth Springs, Yellowstone, for example, hollow towers several centimeters high form by *Spirulina*-dominated mats and become hardened by aragonite precipitation. Similarly profiled mats have been observed in other thermal springs, hypersaline pools and Antarctic lakes (Castenholz 1994). Whether any of these modern examples of upright conical mat growth could serve as models to explain Proterozoic *Conophyton* structures remains to be explored.

Cyanobacterial growth at the sediment-water interface provides the basis for the development of a chemically and biologically stratified microbial community (see contributions in Cohen et al. 1984; Friedman and Krumbein 1985; Cohen and Rosenberg 1989; Stal and Caumette 1994). In various extreme environments where microbial mats predominate, cyanobacteria are the main primary producers of organic matter, which is degraded most efficiently by bacterial aerobic respirers. The activities of these two functionally opposing groups differentiate the sediment-water interface into an oxidized trophogenic and a reduced tropholytic layer, compacted within a few millimeters in thickness. The oxygen-depleted layer supports various anaerobic respirers, including sulfate reducers, which, in turn, support sulfide oxidizing anoxygenic photosynthesizers in the illuminated parts of this layer. Growth and activities of fermenters and methanogens characterize the deeper parts of the anoxic layer. A sharp redox gradient spanning across mat layers is exploited by chemolithotrophic microorganisms that derive their metabolic energies by oxidizing reduced metabolic products such as methane, ammonia, sulfides and ferrous iron in the presence of molecular oxygen. Metabolically complementary groups in structurally and functionally stratified microbial mats establish and maintain efficient nutrient recycling schemes, creating microenvironments with different mineral solubilities and thus affecting mineral composition and preservability of such structures. All these activities, however, depend on cyanobacteria as frame-builders and primary suppliers of metabolic energy to the ecosystem. Prior to the evolution of higher plants and animals, similar microbial mats may have dominated sediment-water interfaces globally. This setting was severely disrupted and largely oxidized following the evolution of animals, causing sediment bioturbation, an evolutionary event for which the metaphor "agricultural revolution" (Seilacher and Pflüger 1994) was appropriately coined.

Deposition of travertines and calcareous tufa illustrates combined microbial biomineralization and sediment construction that may be relevant to our understanding of ancient marine systems (Monty 1973). In these systems, carbonate deposition often takes place in rapids and waterfalls rather than in sedimentary basins, because rapids are the preferred settling sites for organisms which serve as frame-builders of these sedimentary structures (see Pedley, this Vol.). Shifts in cyanobacterial dominance in these depositional systems can be observed along a gradient of declining temperature, showing an optimal range between 74 and 35 °C (Ward et al. 1992). At lower temperatures, cyanobacteria are gradually replaced by eukaryotes, including micro-algae, mosses and higher plants, but cyanobacteria continue to dominate under the stress of desiccation or water impact (Golubic 1967a; Golubic et al. 1993).

One of the characteristic properties of most modern organo-sedimentary structures is their porosity. Porosity of various size orders originates from spaces originally occupied by microorganisms, from those bridged over by microbial growth and water movement, and from those formed or expanded by metabolic gases. Carbonate precipitates around cyanobacterial filaments and lines the spaces incorporated into the rock (Fig. 5a). Imprints of microorganisms left in the carbonate deposit often conform closely with their shape and size, permitting an identification (Golubic and Fischer 1975; Golubic et al. 1993; Dragastan et al. 1996). An important environmental consequence of porosity within the sediment is that a relatively small amount of mineral matter is engaged in the construction of voluminous deposits which may dam riverbeds, form lakes

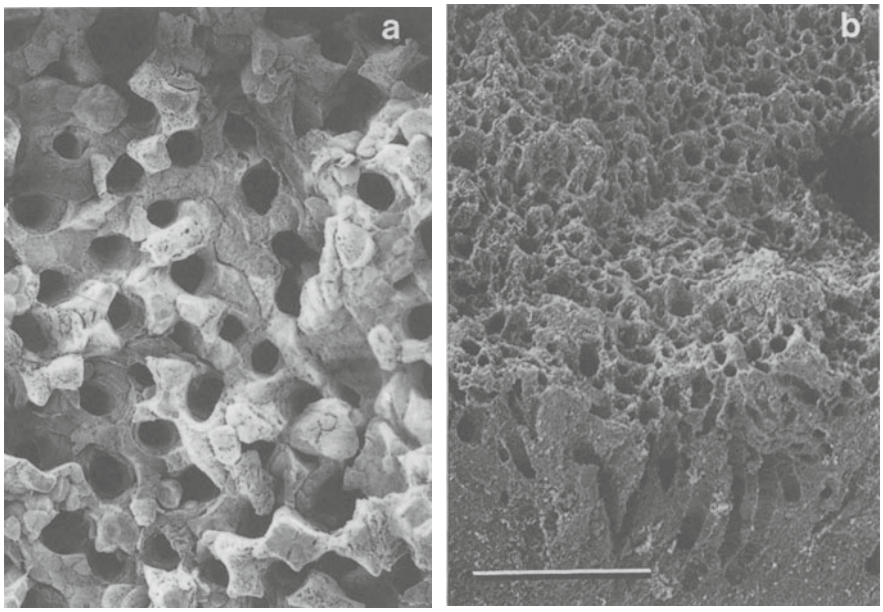

Fig. 5a,b. Constructive and destructive activities of cyanobacteria leave similar patterns in the sediments. **a** Carbonate precipitated around filaments of *Rivularia haematites*. **b** Dense field of perforations left in the intertidal ranges of coastal limestone at Marseille, France by endolithic cyanobacteria *Solentia paulo-cellulare* and *Hyella balani* removing up to 50% of the rock surface. SEM; *scale bar* = 100 μm

and waterfalls, and alter entire landscapes (Golubic 1969). This property contrasts with the dense, crystalline nature of mostly inorganic precipitates such as speleothems, calcretes and geyserites. Inorganic processes rarely produce highly porous sediments, and when they do (e.g., when associated with volcanic degassing), neither the mineral arrangement nor the pore distribution follows distribution patterns dictated by organismal requirements, growth and behavior. It follows then that growth (accretion), orientation and primary porosity contain important clues for determination of the biogenic versus abiogenic origins of ancient sedimentary structures. Such considerations may help separate, for example, marine stromatolites from the rhythmic cementation events described by Grotzinger and Knoll (1995).

4 Cyanobacteria and Sediment Destruction – Bioerosion

The involvement of cyanobacteria in destruction of sedimentary particles has been dramatized by the discovery of microbial micritization of Bahamian ooidal sand grains, which offered an explanation and paleoenvironmental interpretation for micrite envelopes frequently observed in fossil calcarenite rocks (Bathurst 1966). This type of grain obliteration occurs in shallow warm seas and advances through alternate carbonate precipitation within evacuated boreholes, followed by renewed microboring. Subsequent research has demonstrated that similar grain obliteration can result from chemical dissolution in cold, carbonate undersaturated waters (Alexandersson 1972) and that grain envelopes may be constructive (Kobluk and Risk 1977), i.e., a fine-grain carbonate precipitate. In addition, microboring of carbonate grains can be carried out in the deep ocean by non-phototrophic microorganisms (Hook et al. 1984). Nevertheless, most pervasive, carbonate grain micritization does take place in shallow tropical seas, where it is carried out almost exclusively by cyanobacteria (Lukas and Golubic 1983; Al-Thukair and Golubic 1991a,b, 1996; Al-Thukair et al. 1994). Thus, cyanobacteria have a significant impact on carbon cycling (Tudhope and Risk 1985).

Perpetual moving and churning of sediments distributes disadvantages and advantages equitably. Euendolithic, i.e., microboring (Golubic et al. 1981), cyanobacteria are among the few organisms able to exploit the advantages, while coping with the disadvantages of life in the shifting sand grains. The inhabitants of moving sand grains have to endure burial and extended light deprivation. However, by penetrating and spreading in the grain's interior, they also escape competition and surface abrasion. The selective pressure imposed by these conditions is probably responsible for the low diversity of the community of endolithic cyanobacteria in shifting grains, consisting of a few taxa belonging to genera *Hyella, Solentia, Cyanosaccus*, and *Plectonema*.

The endolithic microflora changes with stabilization of the sediment, approaching a species composition that is prevalent in larger, stable substrates such as invertebrate skeletons and solid limestone rocks. In the subtidal ranges, the dominance shifts from cyanobacteria to euendolithic chlorophytes and rhodophytes, specifically *Ostreobium queketii* and conchocelis stages

of bangialean rhodophytes (Laborel and Le Campion-Alsumard 1979; Le Campion-Alsumard et al. 1995; Radtke et al. 1996a,b). Cyanobacteria remain dominant and increase in biomass and diversity within the emergent intertidal and supratidal ranges of carbonate coasts. Dense populations of intertidal cyanobacterial endoliths perforate the rock, removing up to 50% of the carbonate substrate (Fig. 5b). Microbial boring leaves numerous perforations in carbonate rocks, a pattern which is superficially similar and difficult to distinguish from carbonate precipitate around cyanobacterial filaments (compare Fig. 5a,b).

In the emergent tidal ranges, cyanobacteria support dense populations of an array of grazing echinoderms, polyplacophores and gastropods (Radtke et al. 1996b). The phototrophic mode of life limits cyanobacterial activity to the top millimeter beneath the rock surface, where sufficient light penetrates. However, in conjunction with the activity of their invertebrate grazers, cyanobacterial rock penetration becomes a progressive, ecologically and geologically significant force (Schneider 1976; Torunski 1979). Invertebrate grazing of endoliths removes the carbonate substrate layer by layer, crushing the rock along the lines of microbial perforations. The removed rock fragments, sized by microboring densities and by the rasping organs of invertebrate grazers, pass through intestinal tracts packed in fecal pellets. These fragments disperse later and can be recognized as a specific contribution to fine-grain sediments. Following the removal of a substrate layer, the light penetrates deeper into the rock, permitting further advance of microboring cyanobacteria and their grazers (Schneider and Torunski 1983).

Some of the carbonate removed by partially endolithic cyanobacteria in lakes, such as *Schizothrix perforans* and *S. lacustris*, re-precipitates in thallus portions above the rock surface, from where it contributes to the fine-grain sediment fraction (Schröder 1982; Schröder and Schneider 1983). Similar observations were also reported from marine environments (Kobluk and Risk 1977).

Cyanobacterial microboring is the oldest known form of bioerosion. Fossil populations of *Eohyella campbellii* were found preserved in boring position, penetrating lithified horizons in 1,600 My-old Proterozoic stromatolites of Dahongyu Formation, northern China (Zhang Yun and Golubic 1987). By the end of the Proterozoic, endolithic cyanobacterial assemblages in ooids were quite similar in species composition to endoliths in modern ooid grains (Campbell 1982; Knoll et al. 1986).

5 Cyanobacteria, Sediments and Microbial Fossil Record

Microbial mats at the sediment-water interfaces of shallow aquatic and emergent environments belong to the oldest functioning ecosystems on Earth (Awramik 1984). Yet, the study of fossils in ancient mats is limited to a few fortuitously preserved, mostly silicified deposits. Most coccoid and filamentous microbial fossils described from ancient sediments were attributed to cyanobacteria based on morphological similarity with modern taxa (Schopf 1968, 1996). However, comparisons among modern microorganisms show that simple coccoid and filamentous morphologies occur among microorganisms with different metabolic properties and of different phylogenetic affinities, apparently as a consequence of convergent evolution (e.g., Schlegel 1976, Fig. 66). A number of such non-cyanobacterial taxa occur in modern microbial mat communities (Jørgensen 1988; Ward et al. 1992; Van den Ende and Van Gemerden 1994), which makes identification of fossil cyanobacteria tenuous, so that an increasing number of fossil descriptions are placed in the *incertae sedis* category (e.g., Knoll et al. 1991; Sergeev et al. 1995).

The study of modern interactions between cyanobacteria and sediments offers valuable models and criteria for recognition of cyanobacteria in ancient organo-sedimentary structures. The thermodynamic laws of energy preservation require today, as they did in the past, a pyramidal trophic structure in which the primary producers of an ecosystem constitute the base. It follows then that cyanobacteria must have been the most numerous members of ancient microbial assemblages (Golubic 1980). Considering, in addition, the high preservation potential of their modern counterparts, including particularly their exopolymer products (e.g., Golubic and Barghoorn 1977), ancient cyanobacteria remain the most likely candidates for microbial fossils of similar morphology.

The study of populations of microbial fossils in their synsedimentary context provides additional information and clues as to the requirements and responses of ancient microorganisms. Phototrophic and phototactic responses of ancient cyanobacteria are reflected in the distribution and orientation of cyanobacterial filaments and sheaths embedded in the sediment. Filaments and sheaths provided constructive frameworks to sedimentary structures that ranged from the microscopic scale of stromatolitic laminae to the construction of massive bioherms and reefs that rival those built later by calcareous sponges and corals.

Acknowledgements. This research was in part supported by Resources for the Future foundation, by NOAA grant CMRC 94–24, by the German Research Foundation (DFG-Vo.90/14), Australian Museum of Natural History and the National Geographic Society (4945–92).

References

Al-Thukair AA, Golubic S (1991a) New endolithic cyanobacteria from the Arabian Gulf, I: *Hyella immanis* sp. nov. J Phycol 27:766–780

Al-Thukair AA, Golubic S (1991b) Five new Hyella species from the Arabian Gulf. In: Hickel B, Anagnostidis K, Komarek J (eds) Cyanophyta/Cyanobacteria – morphology, taxonomy, ecology. Algol Stud 64:167–197

Al-Thukair AA, Golubic S (1996) Characterization of *Hyella caespitosa* var. *arbuscula* var. nov. (Cyanophyta, Cyanobacteria) from shoaling ooid sand grains, Arabian Gulf. Nova Hedwigia, Beiheft 112:81–89

Al-Thukair AA, Golubic S, Rosen G (1994) New euendolithic cyanobacteria from the Bahama Bank and the Arabian Gulf: *Hyella racemus* sp. nov. J Phycol 30:764–769

Alexandersson T (1972) Micritization of carbonate particles: Processes of precipitation and dissolution in modern shallow-marine sediments. Bull Geol Inst Univ Uppsala NS 3:201–236

Awramik SM (1984) Ancient stromatolites and microbial mats. In: Cohen Y, Castenlolz RW, Halvorson HO (eds) Microbial mats: stromatolites. Alan R. Liss, New York, pp 1–22

Awramik SM, Riding R (1988) Role of algal eucaryotes in subtidal columnar stromatolite formation. Proc Natl Acad Sci USA 85:1327–1329

Awramik SM, Vanyo JP (1986) Heliotropism in modern stromatolites. Science 231:279–1281

Bathurst RGC (1966) Boring algae, micrite envelopes and lithification of molluskan biosparites. Liverpool Manchester Geol J 5: 15–32

Bengtson S (ed) (1994) Early life on Earth. Columbia University Press, New York (Nobel Symposium 84)

Berner RA (1989) Biogeochemical cycles of carbon and sulfur and their effect on atmospheric oxygen over Phanerozoic time. Palaeogeogr Palaeoclimatol Palaeoecol 75:97–122

Bhattacharya D, Medlin L (1995) The phylogeny of plastids: a review based on comparisons of small-subunit ribosomal RNA coding regions. J Phycol 31:489–498

Buczynski C, Chafetz HS (1991) Habit of bacterially induced precipitates of calcium carbonate and the influence of medium viscosity on mineralogy. J Sediment Petrol 61:226–233

Campbell SE (1979) Soil stabilization by a prokaryotic desert crust: implications for Precambrian land biota. Origins Life 9:335–349

Campbell SE (1982) Precambrian endoliths discovered. Nature (Lond) 299:429–431

Castenholz RW (1984) Composition of hot-spring microbial mats: a summary. In: Cohen Y, Castenholz RW, Halvorso HO (eds) Microbial mats: Stromatolites. Alan R Liss, New York, pp 101–119

Castenholz RW (1994) Microbial mat research: the recent past and new perspectives. In: Stal LJ, Caumette P (eds) Microbial mats: structure, development and environmental significance. Springer, Berlin Heidelberg New York, pp 3–18

Cohen Y, Castenholz RW, Halvorson HO (1984) Microbial mats: Stromatolites. Alan R. Liss, New York

Cohen Y, Rosenberg E (eds) (1989) Microbial mats: physiological ecology of benthic microbial communities. Am Soc Microbiol, Washington

Couté A (1982) Ultrastructure d'une cyanophycée aerienne calcifiée cavernicole: *Geitleria calcarea* Friedmann (Hormogonophycidae, Stigonematales, Stigonemataceae). Hydrobiol 97:255–274

D'Amelio ED, Cohen Y, Des Marais DJ (1989) Comparative functional ultrastructure of two hypersaline submerged cyanobacterial mats: Guerrero Negro, Baja California Sur, Mexico, and Solar Lake, Sinai, Egypt. In: Cohen Y, Rosenberg E (eds) Microbial mats: physiological ecology of benthic microbial communities. Am Soc Microbiol, Washington, pp 97–113

Dragastan O, Golubic S, Richter DK (1996) *Rivularia haematites:* A case of the Recent versus fossil morphology. Taxonomic considerations. Rev Española Micropaleontol 28:43–73

Farmer JD, Des Marais DJ (1994) Biological versus inorganic processes in stromatolite morphogenesis: Observations from mineralizing sedimentary systems. In: Stal LJ, Caumette P (eds) Microbial mats: structure, development and environmental significance. Springer, Berlin Heidelberg New York, pp 61–68

Freytet P, Verrecchia E (1993) Complex calcitic crystallizations in *Nostoc parmelioides* Kütz. (freshwater cyanobacterium): Rhombs around trichomes inside *Nostoc* colonies and epiphytic bacterial microstromatolites. Geomicrobiol J 11:77–84

Friedman GM, Krumbein WE (eds) (1985) Hypersaline ecosystems, the Gavish Sabkha. Ecological studies 53. Springer, Berlin Heidelberg New York

Garcia-Pichel F, Belnep J (1996) Microenvironments and microscale productivity of cyanobacterial desert crusts. J Phycol 32:774–782

Garcia-Pichel F, Castenholz RW (1991) Characterization and biological implications of scytonemin, a cyanobacterial sheath pigment. J Phycol 27:395–409

Garcia-Pichel F, Castenholz RW (1994) On the significance of solar ultraviolet radiation for the ecology of microbial mats. In: Stal LJ, Caumette P (eds) Microbial mats: structure, development and environmental significance. Springer, Berlin Heidelberg New York, pp 77–84

Geitler L (1960) Schizophyceen. In: Zimmermann W, Ozenda P (eds) Encyclopedia of plant anatomy 4. Gebrüder Borntraeger, Berlin, pp 1–131

Giovannoni SJ, Turner S, Olsen GJ, Barns S, Lane DJ, Pace NR (1988) Evolutionary relationships among cyanobacteria and green chloroplasts. J Bacteriol 170:3584–3592

Golubic S (1967a) Algenvegetation der Felsen, eine ökologische Algenstudie im dinarischen Karstgebiet Binnengewässer 23. Schweizerbar, Stuttgart, pp 1–183

Golubic S (1967b) Die Algenvegetation an Sandsteinfelsen Ost-Venezuelas (Cumana). Int Rev Ges Hydrobiol 52:693–699

Golubic S (1969) Cyclic and noncyclic mechanisms in the formation of travertine. Verh Int Verein Limnol 17:956–961 [Internationale Vereinigung für theoretische und angewandte Limnologie, Verhandlungen]

Golubic S (1980) Early photosynthetic microorganisms and environmental evolution. In: Holmquist R (ed) Life sciences and space research 8, Pergamon Press, Oxford, pp 101–107

Golubic S (1991) Modern stromatolites – a review. In: Riding R (ed) Calcareous algae and stromatolites. Springer, Berlin Heidelberg New York, pp 541–561

Golubic S (1992a) Microbial mats of Abu Dhabi. In: Margulis L, Olendzenski L (eds) Environmental evolution, effects of the origin and evolution of life on planet earth. MIT Press, Cambridge, pp 131–147

Golubic S (1992b) Stromatolites of Shark Bay. In: Margulis L, Olendzenski L (eds) Environmental evolution, effects of the origin and evolution of life on planet earth. MIT Press, Cambridge, pp 103–130

Golubic S (1994) The continuing importance of cyanobacteria. In: Bengtson S (ed) Early life on earth. Columbia University Press, New York, pp 334–340 (Nobel Symposium 84)

Golubic S, Barghoorn ES (1977) Interpretation of microbial fossils with special reference to the Precambrian. In: Flügel E (ed) Fossil algae. Springer, Berlin Heidelberg New York, pp 1–14

Golubic S, Browne KM (1996) *Schizothrix gebeleinii* sp. nov. builds subtidal stromatolites, Lee Stocking Island, Bahamas. Algol Stud 83:273–290

Golubic S, Campbell SE (1981) Biogenically formed aragonite concretions in marine *Rivularia*. In: Monty CLV (ed) Phanerozoic stromatolites. Springer, Berlin Heidelberg New York, pp 209–229

Golubic S, Fischer AG (1975) Ecology of calcareous nodules forming in Little Connestoga Creek near Lancaster, Pennsylvania. Verh Int Verein Limnol 19:2315–2323. [Internationale Vereinigung für theoretische und angewandte Limnologie, Verhandlungen]

Golubic S, Friedmann I, Schneider J (1981) The lithobiontic ecological niche, with special reference to microorganisms. J Sediment Petrol 51:475–478

Golubic S, Violante C, Ferreri V, D'Argenio B. (1993) Algal control and early diagenesis in Quaternary travertine formation (Rocchetta a Volturno, central Apennines). In: Baratolo F, De Castro P, Parente M (eds) Studies on fossil benthic algae. Boll Soc Paleontol Ital (Spec Vol 1):231–247

Green JW, Knoll AH, Golubic S, Swett K (1987) Paleobiology of distinctive benthic microfossils from the Upper Proterozoic Lime-

stone-Dolomite "Series", central East Greenland. Am J Bot 74:928–940
Grotzinger JP (1990) Geochemical model for Proterozoic stromatolite decline. Am J Sci 290 A:80–103
Grotzinger JP, Knoll AH (1995) Anomalous carbonate precipitates: Is the Precambrian the key to the Permian. Palaios 10:578–596
Heiskanen A-S, Olli K (1996) Sedimentation and buoyancy of *Aphanizomenon* cf. *flos-aquae* (Nostocales, Cyanophyta) in a nutrient-replete and nutrient-depleted coastal area of the Baltic Sea. Phycologia 35:94–101
Holland HD (1984) The chemical evolution of the atmosphere and oceans. Princeton University Press, Princeton
Hook JE, Golubic S, Milliman JD (1984) Micritic cement in microborings is not necessarily a shallow-water indicator. J Sediment Petrol 54:425–431
Horodyski RJ (1977) *Lyngbya* mats at Laguna Mormona, Baja California, Mexico: Comparison with Proterozoic stromatolites. J Sediment Petrol 47:1305–1320
Horodyski RJ, Bloeser B, Vonder Haar S (1977) Laminated algal mats from a coastal lagoon, Laguna Mormona, Baja California, Mexico. J Sediment Petrol 47:680–696
Jaag O (1945) Untersuchungen über die Vegetation und Biologie der Algen des nackten Gesteins in den Alpen, im Jura und im schweizerischen Mittelland. Beitr Kryptogamenflora Schweiz 9:1–560
Jørgensen BB (1988) Ecology of the sulphur cycle: oxidative pathways in sediments. In: Cole JA, Ferguson SJ (eds) The nitrogen and sulphur cycle. Cambridge University Press, Cambridge, pp 31–63
Jørgensen BB, Nelson DC (1988) Bacterial zonation, photosynthesis and spectral light distribution in hot spring microbial mats of Iceland. Microbial Ecol 16:133–147
Karsten U (1996) Growth and organic osmolytes of geographically different isolates of *Microcoleus chthonoplastes* (Cyanobacteria) from benthic microbial mats: Response to salinity change. J Phycol 32:501–506
Kaufman AJ, Knoll AH (1995) Neoproterozoic variations in the C-isotopic composition of seawater: stratigraphic and biogeochemical implications. Precambrian Res 73:27–49
Kimberley MM, Holland HD (1992) Introduction to Precambrian weathering and paleosols. In: Schidlowski M, Golubic S, Kimberley MM, McKirdy DM, Trudinger PA (eds) Early organic evolution: Implications for mineral and energy resources. Springer, Berlin Heidelberg New York, pp 9–15
Kinsman DJJ, Park RK (1976) Algal belt and coastal sabkha evolution, Trucial Coast, Persian Gulf. In: Walter MR (ed) Stromatolites: developments in sedimentology 20. Elsevier, Amsterdam, pp 421–433
Knoll AH, Golubic S, Green J, Swett K (1986) Organically preserved microbial endoliths from the Late Proterozoic of East Greenland. Nature (Lond) 321:856–857
Knoll AH, Swett K, Mark J (1991) Paleobiology of a Neoproterozoic tidal flat/lagoonal complex: The Draken conglomerate formation, Spitsbergen. J Paleontol 65:531–570
Kobluk DR, Risk MJ (1977) Micritization and carbonate-grain binding by endolithic algae. Am Assoc Petrol Geol Bull 61:1069–1082
Kühl M, Glud RN, Ploug H, Ramsing NB (1996) Microenvironmental control of photosynthesis and photosynthesis-coupled respiration in an epilithic cyanobacterial biofilm. J Phycol 32:799–812
Laborel J, Le Campion-Alsumard T (1979) Infestation massive du squelette de coraux vivants par des rhodophycées de type Conchocelis. C R Acad Sci 288 (Serie D):1575–1577
Le Campion-Alsumard T, Golubic S, Hutchings P (1995) Microbial endoliths in skeletons of live and dead corals: *Porites lobata* (Moorea, French Polynesia). Mar Ecol Prog Ser 117:149–157
Livingstone D (1984) The preservation of algal remains in recent lake sediments. In: Haworeth EY, Lund JWG (eds) Lake sediments and environmental history. University of Minnesota Press, Minneapolis, pp 191–202
Lukas KJ, Golubic S (1983) New endolithic cyanophytes from the North Atlantic Ocean: II. *Hyella gigas*, sp. nov. J Phycol 19:129–136
Madsen KN, Nilsson P, Sundback K (1993) The influence of benthic microalgae on the stability of a subtidal sediment. J Exp Mar Biol Ecol 170:159–177
Margulis L (1993) Symbiosis in cell evolution: Microbial communities in the Archaean and Proterozoic Eons, 2nd edn. WH Freeman, New York
Mereschkowsky C (1905) Über Natur und Ursprung der Chromatophoren im Pflanzenreiche. Bot Zentralbl 25:593–604
Merz MUE (1992) The biology of carbonate precipitation in cyanobacteria. Facies 26:81–102
Merz MUE, Zankl H (1993) The influence of the sheath on carbonate precipitation by cyanobacteria. In: Barattolo F, De Castro P, Parente M (eds) Studies on fossil benthic algae. Boll Soc Paleontol Ital (Spec) 1:325–331
Merz MUE, Schlue WR, Zankl H (1995) PH-measurements in the sheath of calcifying filamentous cyanobacteria. Bull Inst Oceanogr (Monaco) (Spec Issue) 14:281–289
Monty CLV (1973) Precambrian background and Phanerozoic history of stromatolite communities, an overview. Ann Soc Geol Belg Bull 96:585–624
Nelissen B, van de Peer Y, Wilmotte A, De Wachteer R (1995) An early origin of plastids within the cyanobacterial divergence is suggested by evolutionary trees based on complete 16 S rRNA sequences. Mol Biol Evol 12:1166–1173
Neumann AC, Gebelein CD, Scoffin TP (1970) The composition, structure and erodability of subtidal mats, Abaco, Bahamas. J Sediment Petrol 40:274–297
Obenlüneschloss J (1991) Biologie und Ökologie von drei rezenten Süsswasser-Rivularien (Cyanobakterien) – Übertragbarkeit artspezifischer Verkalkungsstrukturen auf fossile Formen. Göttinger Arb Geol Paläontologie 50:1–86
Palenik B, Swift H (1996) Cyanobacterial evolution and prochlorophyte diversity as seen in DNA-dependent RNA polymerize sequences. J Phycol 32:638–646
Paterson DM (1994) Microbiological mediation of sediment structure and behavior. In: Stal LJ, Caumette P (eds) Microbial mats: structure, development and environmental significance. Ecological studies 35. Springer, Berlin Heidelberg New York, pp 97–109
Pearl HW (1996) A comparison of cyanobacterial bloom dynamics in freshwater, estuarine and marine environments. Phycologia 35:25–35
Pentecost A (1991) Calcification processes in algae and cyanobacteria. In: Riding R (ed) Calcareous algae and stromatolites. Springer, Berlin Heidelberg New York, pp 3–20
Pentecost A, Riding R (1986) Calcification in cyanobacteria. In: Leadbeater BSC, Riding R (eds) Biomineralization in lower plants and animals. Syst Assoc Spec 30:73–90
Pierson BK, Oesterle A, Murphy GL (1987) Pigments, light penetration, and photosynthetic activity on the multi-layered microbial mats of Great Sippewissett Salt Marsh, Massachusetts. FEMS Microbiol Ecol 45:365–376
Radtke G, Le Campion-Alsumard T, Golubic S (1996a) Microbial assemblages of the bioerosional "notch" along tropical limestone coasts. Algol Stud 83:469–482
Radtke G, Le Campion-Alsumard T, Golubic S (1996b) Microbial assemblages involved in tropical coastal bioerosion: an Atlantic-Pacific comparison. Proc 8th Int Coral Reef Sym 2:1825-1830
Riding R (1993) Phanerozoic patterns of marine $CaCO_3$ precipitation. Naturwissenschaften 80:513–516
Robbins LL, Blackwelder PL (1992) Biochemical and ultrastructural evidence for the origin of whitings: A biologically induced calcium carbonate precipitation mechanism. Geology 20: 464–468
Schlegel HG (1976) Allgemeine Mikrobiologie, 4th edn. Georg Thieme Verlag, Stuttgart
Schneider J (1976) Biological and inorganic factors in the destruction of limestone coasts. Contrib Sedimentol 6:1–112
Schneider J, Herrmann AG (1980) Saltworks – natural laboratories for microbiological and geochemical investigations during the evaporation of seawater. In: Coogan AH, Hauber L (eds) Fifth Symposium on Salt. Northern Ohio Geological Society, pp 371–381
Schneider J, Torunski H (1983) Biokarst on limestone coasts, morphogenesis and sediment production. P.S.Z.N.I. Mar Ecol 4:45–63
Schopf JW (1968) Microflora of the Bitter Springs Formation, Late Precambrian, Central Australia. J Paleontol 42: 651–588

Schopf JW (1996) Cyanobacteria: Pioneers of the early Earth. Nove Hedwigia, Beiheft 112:13–32
Schröder JG (1982) Biogene benthische Entkalkung als Beitrag zur Genese limnischer Sedimente. Beispiel: Attersee (Salzkammergut; Oberösterreich). PhD Diss, University of Göttingen, 179 pp
Schröder HG, Schneider J (1983) Bilanzierung der biogenen Karbonatproduktion eines oligotrophen Sees (Attersee, Salzkammergut, – Österreich). Arch Hydrobiol 97:356–372
Schultze-Lam S, Harauz G, Beveridge TJ (1992) Participation of a cyanobacterial S layer in fine-grain mineral formation. J Bacteriol 174:7971–7981
Seilacher A, Pflüger F (1994) From biomats to benthic agriculture: A biohistoric revolution. In: Krumbein WE, Paterson DM, Stal LJ (eds) Biostabilization of sediment. University of Oldenburg, Oldenburg, pp 97–105
Seong-Joo L, Golubic S (1998) Multi-trichomous cyanobacterial microfossils from the Mesoproterozoic Gaoyuzhuang Formation, China: paleoecological and taxonomic implications. Lethaia 31:169-184
Seong-Joo L, Golubic S (1999) Microfossil populations in the context of synsedimentary micrite deposition and acicular carbonate precipitation: Mesoproterozoic Gaoyuzhuang Formation, China. Precambrian Res 96:183-208
Sergeev VN, Knoll AH, Grotzinger JP (1995) Paleobiology of the Mesoproterozoic Billyakh Group, Anabar Uplift, northern Siberia. Paleontol Soc Mem 39:1–37
Sorkhoh N, Al-Hasan R, Radwan S, Höpner T (1992) Self-cleaning of the Gulf. Nature (Lond) 359:109
Stal LJ, Caumette P (eds) (1994) Microbial mats: structure, development and environmental significance. (Ecol Sci 35), Springer-Verlag, Berlin Heidelberg
Stolz JF (1990) Distribution of phototrophic microbes in the flat laminated microbial mats at Laguna Figueroa, Baja California, Mexico. BioSystems 23:345–357
Torunski H (1979) Biological erosion and its significance for the morphogenesis of limestone coasts and for nearshore sedimentation. Senckenbergiana Maritima 11:193–265
Tudhope AW, Risk MJ (1985) Rate of dissolution of carbonate sediments by microboring organisms, Davies Reef, Australia. J Sediment Petrol 55:440–447
van den Ende FP, van Gemerden H (1994) Relationship between functional groups of organisms in microbial mats. In: Stal LJ, Caumette P (eds) Microbial mats: structure, development and environmental significance. Ecological studies 35. Springer, Berlin Heidelberg New York, pp 339–352
Walter MR (ed) (1976) Stromatolites: Developments in sedimentology 20. Elsevier, Amsterdam
Walter MR, Bauld J, Brock TD (1976) Microbiology and morphogenesis of columnar stromatolites (*Conophyton, Vacerrilla*) from hot springs in Yellowstone National Park. In: Walter MR (ed) Stromatolites: developments in sedimentology 20. Elsevier, Amsterdam, pp 273–310
Walter MR, Grotzinger JP, Schopf JW (1992) Proterozoic stromatolites. In: Schopf JW, Klein C (eds) The Proterozoic biosphere. Cambridge University Press, Cambridge, pp 253–260
Ward DM, Bauld J, Castenholz RW, Pierson BK (1992) Modern phototrophic microbial mats: anoxygenic, intermittently oxygenic/anoxygenic, thermal, eukaryotic, and terrestrial. In: Schopf JW, Klein C (eds) The Proterozoic biosphere. Cambridge University Press, Cambridge, pp 309–324
Winsborough BM, Seeler J-S, Golubic S, Folk RL, Maguire B Jr (1994) Recent fresh-water lacustrine stromatolites, stromatolitic mats and oncoids from northeastern Mexico. In: Bertrand-Sarfati J, Monty CLV (eds) Phanerozoic stromatolites II. Kluwer Academic Publishers, Amsterdam, pp 71–100
Woese CR (1987) Bacterial evolution. Microbiol Rev 51:221–271
Yallop ML, De Winder B, Paterson DM, Stal LJ (1994) Comparative structure, primary production and biogenic stabilization of cohesive and non-cohesive marine sediments inhabited by microphytobenthos. Estuar Coastal Shelf Sci 39:565–582
Yates KK, Robbins LL (1995) Experimental evidence for a $CaCO_3$ precipitation mechanism for marine *Synechocystis*. Bull Inst Oceanogr (Monaco), Special Issue 14:51–59
Zhang Y, Golubic S (1987) Endolithic microfossils (Cyanophyta) from early Proterozoic stromatolites, Hebei, China. Acta Micropaleontol Sin 4:1–12
Züllig H (1961) Die Bestimmung von Myxoxanthophyll in Bohrprofilen zum Nachweis vergangener Blaualgenenfaltungen. Verh Int Verein Limnol 14:263–270 [Internationale Vereinigung für theoretische und angewandte Limnologie, Verhandlungen]

Fungi and Sediments

Eric P. Verrecchia

U.M.R. 5561 C.N.R.S., Biogéosciences, Centre des Sciences de la Terre, Université de Bourgogne, 6 Bd Gabriel, F-21000 Dijon, France

Abstract. Fungi are saprophytic organisms that can form lichens in symbiosis with an alga. Along with lichens, they excrete large quantities of organic acids, contributing to rock dissolution and neoformation of crystals, mainly oxalates and carbonates. Fungi contribute to the accumulation of manganese and iron as desert varnish and play a major role in the calcium cycle inside calcretes and carbonate soils in arid zones. Fungi constitute an important part of calcified filaments found in calcretes. They are covered with calcium oxalate crystals, which can transform into calcite during early diagenesis. They can also precipitate needle-fiber calcite, a common form of $CaCO_3$ found in soils and calcretes. Although their role has been neglected in sedimentary petrology, fungi are used in the ore industry for leaching metal and in land reclamation for dune fixation and recovering pollutants.

1 Introduction

Fungi are eukaryotic and organotrophic microorganisms. They are distinguished from algae by their lack of chlorophyll. During their growth, fungi form slender filaments, called hyphae (singular hypha), which may or may not be septate. Hyphae grow in intertwined branches called mycelium (plural mycelia). Mycelium can form a mat on a mineral substrate. Slime molds, sugar fungi, and *Fungi imperfecti* are the most common groups observed in the geological record. Fungi live in association with an alga to form lichen (Fig. 1a, b): this symbiotic relationship allows the fungi to obtain nutrients from organic matter produced by the alga photosynthesis and the alga is protected from excessive drying and erosion. Lichens constitute an important biogenic factor in rock weathering because they can excrete large quantities of organic acids.

Despite the recognition of mineralization by fungi more than a century ago (Braconnot 1825; Hamlet and Plowright 1877; Tilden 1897), there were few studies on their potential role in sedimentology, particularly in sediment deposition and early diagenesis. However, many studies were done on their role in the turnover and cycling of soil organic matter, weathering, neoformation and stabilization of soil minerals (e.g., Robert and Berthelin 1986) and aggregates (Clough and Sutton 1978). But these studies were limited to pedological processes in present day soils. Only a few experiments were performed to characterize the potential role of fungi in rock weathering (Krumbein 1972). These very resistant microorganisms can be found in the most extreme environments on Earth (Friedmann 1982; Staley et al. 1982), emphasizing their importance in the geological record during late Proterozoic and early Phanerozoic eras. In this chapter, a short synthesis on biomineralization by fungi and their role in sediment production and weathering will be presented.

2 Biomineralization in Fungi

2.1 Biochemical Characteristics of Fungi

The main characteristics of fungi are: (1) a hypha possessing a wall or membrane which is initially made of pectin and then later incorporates cellulose and/or excretes polysaccharides, (2) a capacity of absorption and excretion of substances through all parts of the hyphal wall, (3) a need for Ca^{2+} (Jackson and Heath 1993) and the possibility of Ca^{2+} storage in the thallus, preferentially in or on the membranes, (4) the capacity to excrete large quantities of organic acids, in particular oxalic acid, which is "the first oxidation product resulting from the aerobic breakdown of carbohydrate found to accumulate in fungus culture" (Foster 1949), and (5) the production of humic-like substances, known as fungal melanins, which are intra- and extracellular dark-colored polymers (Schnitzer and Chan 1986; Robert and Chenu 1992). Melanin-type pigments have been found associated with calcite crystals in travertines (Fig. 1c) and may play a role in the formation of desert varnish (Staley et al. 1992). Although the role of polysaccharides on crystal growth is well documented for cyanobacteria and bacteria, there are only a few studies of their influence on biocrystallization in fungi cultures (Callot et al. 1985a). However, fungal polysaccharides and melanin are very active in water stabilization of clay particles and mineral aggregates in surficial crusts and soils (Robert and Chenu 1992) and they play a major role in dune fixation (Clough and Sutton 1978).

R.E. Riding and S.M. Awramik (Eds.)
Microbial Sediments

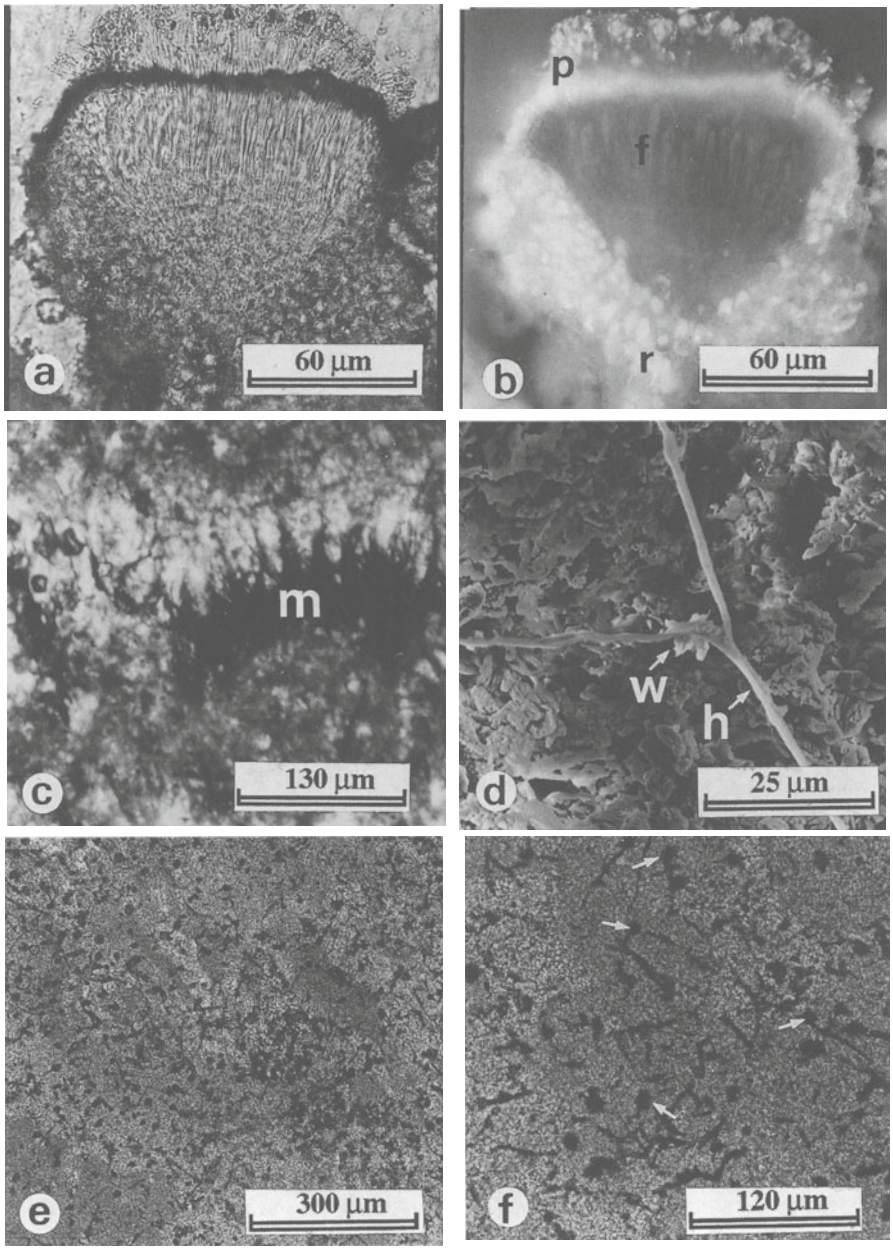

Fig. 1.a Lichen colonizing a carbonate rock surface (Senonian chalk from Galilee, Israel): the dark top is the algal layer. Fungal hyphae appear as a succession of parallel light filaments; plane polarized light (PPL). **b** As in (**a**) but in fluorescent light, emphasizing the fluorescent photosynthetic layer (bright orange, *p*) and the dull fungal hyphae (*f*). The rounded bright bottom cells (*r*) are the root-like connection to the substrate. **c** Fungal colony rich in melanin (*m*) inside a moss and *Scytonema* travertine (Saint Géry, Tarn, France): calcite and oxalate crystals form in this microbial mat, PPL. **d** Fungal filaments from a calcrete (Nazareth, Galilee, Israel): a cluster of whewellite (*w*, calcium oxalate dihydrate) adheres to the dichotomous filament (*h*). The background is composed of calcite; scanning electron microscope (SEM) view. **e** Present-day fungal microborings in a Cretaceous marine limestone: the borings are straight, thin and short; PPL. **f** Detail of fungal microborings in calcite having the shape of a straight line ending in a bulbous cavity (*arrows*): this particular shape is related to conodia and/or sporangia (fruiting bodies); PPL

2.2 An Example of Mineral Accumulation by Fungi: Desert Varnish

Stone varnish, in arid and semiarid environments, is a black to brown or orange coating found on rocks. It is a few micrometers to millimeters in thickness and is rich in manganese and iron oxides and in clay minerals (Krumbein and Jens 1981; Staley et al. 1992). Dragovich (1993) noted that the mineralogy and chemical composition of desert varnish is unrelated to its rock substrate, the main source of Mn and Fe being rainfall or dust. The predominant microorganisms observed on desert varnish are microcolonial fungi (MCF), *Lichenothelia* genus (Staley et al. 1992; Adams et al. 1992; Grote and Krumbein 1992; Dragovich 1993). As for Mn and Fe, the organic carbon needed for their growth must be supplied by windblown dust.

MCF play a major role in the accumulation of Mn and Fe. Manganese oxide precipitation by fungi has been demonstrated in soils by Golden et al. (1992). In desert varnish, Grote and Krumbein (1992) showed that the efficiency of Mn(IV)-precipitating fungi is related to the presence of iron and high concentrations of NaCl, conditions common in the desert. In addition, MCF are known to be well adapted to dry and hot con-

ditions. Staley et al. (1992) noted that MCF can survive 70–80 °C for periods of 21 days and some strains from Arizona can endure a temperature of 100 °C for 2 days. Therefore, if the rock substrate can resist the "microbial solution front" (Krumbein and Jens 1981), fungi can form mineral coatings on desert rocks because of their ability to endure high stress conditions and to accumulate Mn and Fe (Drake et al. 1993).

2.3 Significance of Calcium-Bearing Biominerals Associated with Fungi

Calcium, necessary for hypha growth, can be accumulated as Ca-oxalate and Ca-carbonate, which are minerals commonly found in sediments where fungi are numerous. The crystallization of Ca-oxalates in higher plants is considered to be a detoxification reaction against calcium and/or metabolic oxalic acid (Arnott and Pautard 1970; Franceschi and Horner 1980). Whitney (1989) suggested that the precipitation of Ca-oxalates allows the removal of Ca from excessively Ca-rich environments. Ca is disruptive to enzymatic activity, therefore its inhibition in the form of stable minerals ensures maximum enzymatic efficiency. This enzymatic activity is critical because enzymes degrade organic substances into simple molecules that can be assimilated through the hypha wall. Whitney (1989) observed that high levels of Ca^{2+} can inhibit fungal growth. Nevertheless, fungi are numerous in terrestrial carbonates and calcic soils. Their capacity to precipitate Ca-oxalates (Fig. 1d) is probably sufficient to detoxify Ca in vadose environments where solutions are only periodically supersaturated in Ca. However, a well aerated environment with a relatively high pH and an abundance of sugars favors excretion of large quantities of oxalic acid. This acid can react with the calcitic host rock to yield Ca-oxalates crystals. In this case, fungi provide one component of the molecule and crystals are the result of a chemical reaction occurring in the pore solution (Verrecchia 1990).

Certain fungi mineralize their mycelial strands with calcite instead of Ca-oxalates. This precipitation has two main forms: needles (needle-fiber calcite, NFC) or micrite encrusting the sheath. Precipitation of $CaCO_3$ seems to be related to either the external mucilagenous sheath (micrite) or to internal hypha (needles), where pH and Ca levels are high (Callot et al. 1985a; Klappa 1979b, Kahle 1977). Another possibility is the transformation by an oxidative reaction of Ca-oxalate into calcium carbonate (Cromack et al. 1977; Verrecchia et al. 1990).

3 Relationship Between Fungi and Sediments

3.1 Dissolution and Precipitation

Experiments on metamorphic rock weathering by fungi and lichens demonstrated the role of organic acids (2-ketoglutonic, citric, and oxalic acids) excreted during microorganism activity (e.g., Webley et al. 1963; Weed et al. 1969; Silverman and Munoz 1970; Ascaso et al. 1976; Galvan et al. 1981; Jones et al. 1981; Cooks and Otto 1990). The dissolution of calcite along the hypha during mycelia growth produces features such as pyramids and spiky calcite (Robert and Berthelin 1986; Jones and Pemberton 1987).

In addition to soils and sediments (Fig. 1e,f), fungi are active agents of biocorrosion and dark film deposition on stone buildings (Jeanson 1973; Del Monte et al. 1987; Krumbein et al. 1989). They act mechanically and chemically, causing desquamation, pits and the spongy appearance of walls. Their role in the organo-mineral coatings on stone walls and rock paintings has been clearly identified (Edwards et al. 1992; Torre et al. 1993; Russ et al. 1994). In addition, their capacity to remove metals from primary rocks can be used as a tool in the metallurgy industry: fungi can be used to leach copper or zinc from ore (Wenberg et al. 1971; Dave and Natarajan 1981) in a carbon and nitrogen-enriched medium, where neutral to slightly acidic conditions constitute the best environment. Fungi are also present in marine environments, where they dissolve crystals of carbonate rocks or bivalve shells (Gatrall and Golubic 1970; Friedman et al. 1971). In addition, fungi were reported as symbionts of corals, but a disturbance in the host-parasite equilibrium may result in increased fungal dissolution of coral aragonite leading to bioerosion of reefs (Le Campion-Alsumard et al. 1995).

Excretion by the hypha of large quantities of organic acids, and particularly oxalic acid, leads to reprecipitation of Ca-minerals in limestones or environments abundant in calcium carbonate. The reaction of oxalic acid with Ca^{2+} or $CaCO_3$ yields Ca-oxalates (whewellite or weddellite, Fig. 2a), minerals found in lichens (Wadsten and Moberg 1985), discomycetes (Horner et al. 1983), ectomycorhizes (Cromack et al. 1979; Lapeyrie et al. 1984) and Saprolegnales mycelia associated with decaying moss in travertines (Freytet and Verrecchia 1995, Fig. 2b,c). But Ca-oxalates are not the only minerals produced. Depending on the chemical composition of the substrate on which the organic acids can react, the weathering action of fungi or lichens leads to precipitation of various kinds of minerals (Table 1).

Another precipitate of fungi is calcium carbonate. In dry environments, pore solutions can be supersaturated in calcite favoring rapid $CaCO_3$ precipitation (e.g.,

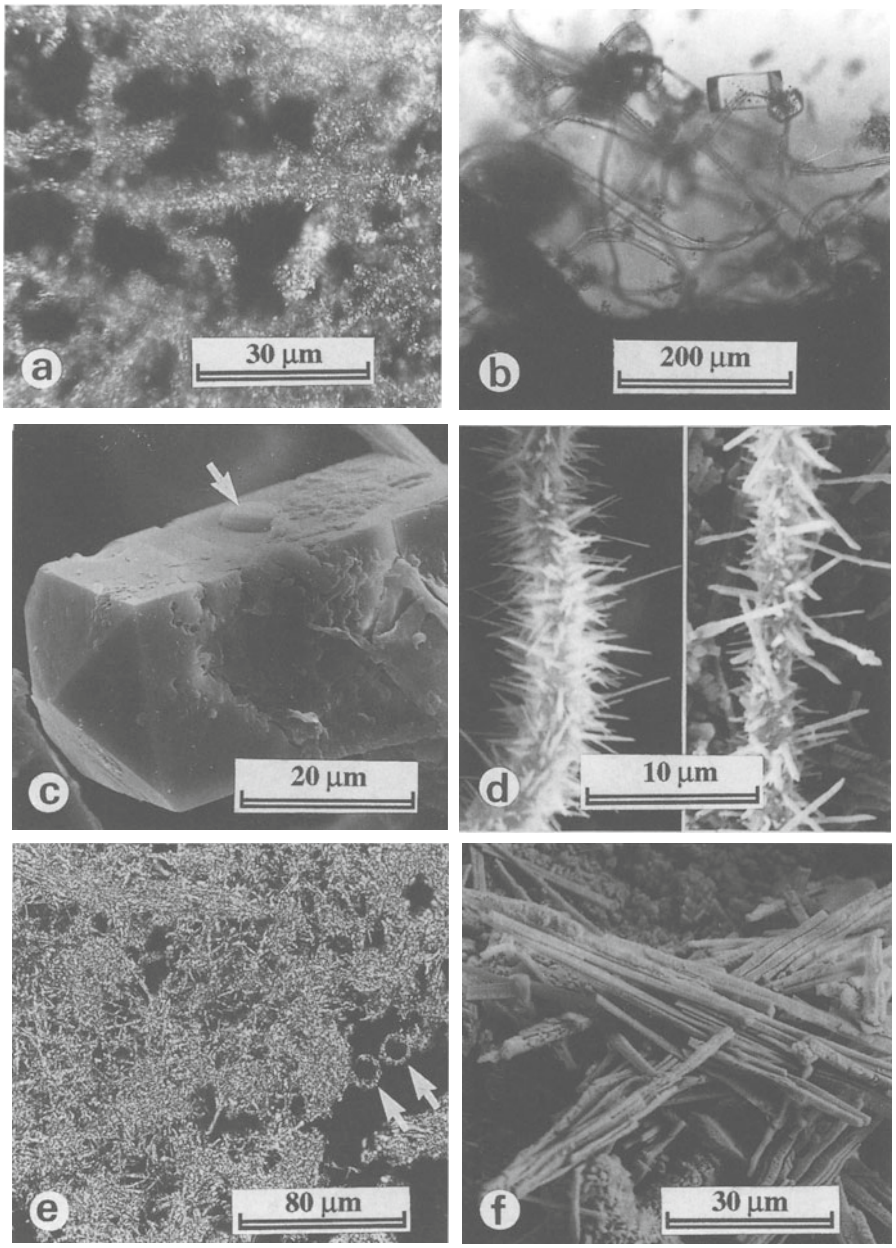

Fig. 2.a Fungal filaments covered by oxalate crystals in a calcrete (Galilee, Israel); cross-polarized light (XPL). **b** Prismatic tetragonal bipyramidal crystal of calcium oxalate associated with a fungal mat in a moss travertine (stream, southwestern France). **c** Same kind of crystal as in (**b**) observed with SEM; *arrow* shows a diatom. **d** Fungal filaments in calcrete covered by two different shapes of oxalate crystals (*left*, raphidic; *right*, styloidic); SEM photo. **e** Needle-fiber calcite (NFC) in calcrete (XPL). NFC can fill in large pores without hardening the sediment. The two *arrows* show sections of mineralized filaments. **f** Bundles of NFC resulting from calcification of fungal strands. After decaying of organic matter, the needles are released in the medium; SEM view

micrite), whereas humid environments with high levels of organic matter would favor host rock dissolution without notable reprecipitation. For example, Callot et al. (1985b) observed experimentally that in wet environments needles are flexible and often curved. This particular facies is confirmed in natural environments, such as Holocene glacial gravels cemented by carbonate-rich solutions (Strong et al. 1992) or Pennsylvanian hydromorphic paleosols (Goldstein 1988). In dry environments, hyphae are fragile and the needles are easily broken. Callot et al. (1985b) noted that the mineralized strands burst and release NFC from its organic coating.

3.2 Fungi, Oxalates, and Carbonates in Calcretes

Calcretes are terrestrial carbonate deposits related to interactions between sedimentary, pedogenic and microbiological processes occurring during early diagenesis. Calcified filaments (Fig. 2a) are widely reported in the literature on calcretes. Although some of these calcified filaments are obviously root hairs (e.g., Coniglio and Harrison 1983, Fig. 5A) or algae (Kahle 1977), most of them have the size and shape of fungal filaments. Another argument that can be used to attribute filaments to fungal hyphae is their association with oxalates (Ver-

Table 1. Examples of different minerals associated with fungi and lichens[a]

Mineral	Formula	Example of organisms	Example of occurrence
1. Calcite	$CaCO_3$	*Myxomycetes* *Hyphomycetes* *Fungi mperfecti*	Stalactite Quaternary eolianites and calcretes
2. Hydrocerussite	$Pb_3(CO_3)_2(OH)_2$	*Sterocaulon vesuvianum*	Mycobiont of lichen in ruins of a lead-smelting mill
3. Dahllite	$Ca_5(PO_4,CO_3)_3(OH)$	*Candida albicans*	Synthetic medium
4. Goethite	α FeO(OH)	*Parmelia conspersa, P. tiliacea*	Lichen on metamorphic rocks
5. Todorokite	$(Mn, Ca, Mg)Mn_3O_7.H_2O$	*Penicillium, Mucor, Rhizopus*	Cave deposits and waters
6. Ferrihydrite	$Fe_5HO_8.H_2O$ or $5Fe_2O_3.9H_2O$	*Stereocaulon vulcani* *Pertusaria corallina*	Lichen on recent lava flow Lichen action on augite and olivine of basalt
7. Ca-oxalate	$CaC_2O_4.xH_2O$ (x unknown)	*Verrucaria* sp.	Quaternary calcretes
8. Whewellite	$CaC_2O_4.H_2O$	*Fungal hyphae*	Nari limecrust; litter layer under spruce and fir
9. Weddellite	$CaC_2O_4.nH_2O$ ($2<n<2.5$)	*Hysterangium crassum*	Upper 10 cm of soil under Douglas fir
10. Glushinskite	$MgC_2O_4.2H_2O$	*Lecanora atra*	Lichen/rock interface on serpentinite
11. Birnessite	$(Na,Ca,K)Mn_7O_{14}.3H_2O$	*Cladosporium sp., Alternaria* sp.	Siderite boulder and Typic Natraqualf soil
12. Fe-oxalate	$Fe_2(3C_2O_4)$	*Caloplaca callopisma*	Lichen on Fe-rich crystalline limestone
13. Mn-oxalate	$MnC_2O_4.2H_2O$	*Pertusaria corallina*	Lichen on Mn ore
14. Cu-oxalate	$CuC_2O_4.nH_2O$ ($n\approx0.1$)	*Acarospora sp., Lecidea* sp.	Lichen on copper bearing rocks
15. Montmorillonite ($R = Na^+, K^+, Ca^{2+}, Mg^{2+}$) and/or Halloysite	$R_{0.33}Al_2Si_4O_{10}(OH)_2.nH_2O$ $Al_2Si_2O_5(OH)_4.2H_2O$	*Parmelia, Rhizocarpon, Lasallia* *Penicillium* sp., *Mucor* sp., *Rhizopus*	Action of lichens on rocks Cave deposits and waters
16. Micas	Biotite ⇒ Vermiculite	*Basidiomycetes*	Experimental

[a] Only a few references are given for each mineral: 1. Went (1969), Kahle (1977), Calvet (1982), Verrecchia et al. (1990); 2. Jones et al. (1982); 3. Ennever and Summers (1975); 4. Galvan et al. (1981); 5. Cunningham et al. (1995); 6. Jackson and Keller (1970), Jones et al. (1981); 7. Klappa (1979); 8. Verrecchia et al. (1993), Graustein et al. (1977); 9. Graustein et al. (1977), Cromack et al. (1979); 10. Wilson et al. (1980); 11. Golden et al. (1992); 12. Ascaso et al. (1982); 13. Wilson and Jones (1984); 14. Purvis (1984); 15. Ascaso et al. (1976), Cunningham et al. (1995); 16. Weed et al. (1969)

recchia et al. 1993). Unfortunately, Ca-oxalates were not always properly detected by some authors (e.g., Klappa 1979b; Phillips et al. 1987; Jones 1988). In some studies, the identification of minerals was made only on the basis of crystal shapes and/or the energy dispersive spectrometry (EDS) of Ca. Oxalates have shapes that can easily be confused with calcite and the use of Ca detection by EDS is insufficient to attribute calcium to calcite because other calcium-bearing minerals exist.

The Ca-oxalate cycle in calcretes and its role in early diagenesis of these terrestrial limestones are complex. During the fungi's life, the hydrolysis of oxalo-acetate produces oxalic acid, which is released in free form into the medium through the hyphal wall. The availability of Ca^{2+} in the calcrete environment leads to weddellite precipitation and, as observed by Whitney (1989), the crystals stretch and sometimes disrupt the outer wall of hypha during their growth (Fig. 2d). The uptake of calcium for weddellite formation releases carbonate anions into the pore solution, which can contribute to secondary precipitation of calcite outside the pore (Verrecchia and Dumont 1996). The metastable weddellite can easily transform into whewellite (by water loss, Frey-Wyssling 1981; Verrecchia et al. 1993), which in turn can be transformed into calcite after oxidation by bacteria. Therefore, the presence of fungi in the porosity allows a redistribution of calcium carbonate through a calcium oxalate step. After calcium carbonate dissolution by the organic acids, calcite is reprecipitated either in the matrix (contributing to its further cementation) or in the pore as calcified filaments after oxidation of oxalates following the fungi's death (Fig. 3). In addition, certain fungi are also able to directly precipitate calcite as needle-fibers (NFC).

NFC (Fig. 2e, f) is a common feature of carbonate soils and calcretes (see synthesis of NFC in Verrecchia and Verrecchia 1994). The ability of fungi to precipitate NFC has been demonstrated by Callot et al. (1985b). Briefly,

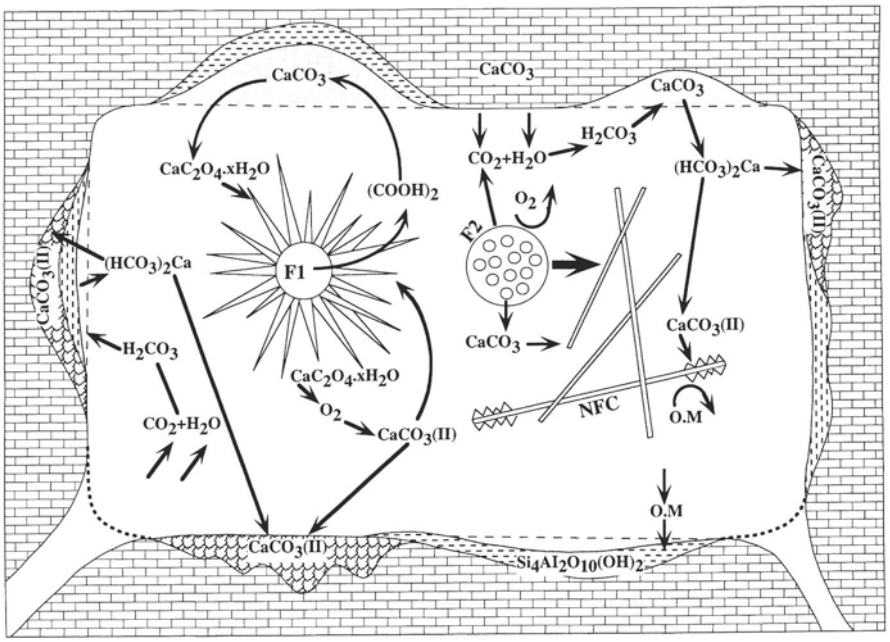

Fig. 3. The role of fungi calcium cycle: example ficial limestones (from chia and Dumont 1996) *F1* Fungal filament prec ing Ca-oxalates; *F2* fung ment precipitating need calcite (NFC); *O.M.* orga matter; *(II)* secondary p tation; *gray areas* dissol of host rock

there are three types of NFC: long and smooth monocrystalline (MA), long and serrated-edged monocrystalline (MB), and polycrystalline (P) crystals. Fungi form the long and smooth MA rods. The serrated-edged needles result from reprecipitation of calcite on MA rods after release of the needles from the hypha. In conclusion, fungi transform the carbonate rocks (Fig. 3), concomitantly increasing their porosity, strength, and calcite content. They seem to play a major role in the diagenesis of surficial carbonate in calcretes through complex reactions involving organic acid excretion, calcium oxalate precipitation, and calcium carbonate biocrystallization.

4 Conclusion

It is obvious that there is still much work to be done on fungi and their interaction with sediments. They have an important part in sedimentary petrology, mostly concerning terrestrial deposits. Fungi played a role in mineral cycling as early as the Paleozoic (Solomon and Walkden 1985; Wright 1986) and they are a prominent factor in early diagenesis of carbonate rocks from terrestrial environments, including the driest conditions. Although they are neglected in petrology, fungi have many uses in applied geology: they are good paleoecological markers (Briot et al. 1983) and their contribution to rock varnish formation makes dating possible. They can be used for leaching of metals in the mining industry, thus providing a process that is more ecological than a purely chemical one; they act as an efficient polysaccharidic network in dune fixation and they also have great potential for use in concentrating pollutants.

Acknowledgements. P. Freytet (University of Paris) kindly provided additional information on the topic. G. Stoops and B. Jones made helpful comments. This chapter is a contribution to the theme "Biogéochimie et diagenèse des carbonates", Unité Mixte de Recherche 5561 of the Centre National de la Recherche Scientifique (University of Burgundy, Dijon, France).

References

Adams JB, Palmer F, Staley JT (1992) Rock weathering in deserts: mobilization and concentration of ferric iron by microorganisms. Geomicrobiol J 10:99–114

Arnott HJ, Pautard FGE (1970) Calcification in plants. In: Schraer H (ed) Biological calcification: cellular and molecular aspects. North-Holland Publishing Company, Amsterdam, pp 375–446

Ascaso C, Galvan J, Ortega C (1976) The pedogenic action of *Parmelia conspersa*, *Rhizocarpon geographicum* and *Umbilicaria pustulata*. Lichenologist 8:151–171

Ascaso C, Galvan J, Rodrigiez-Pascual C (1982) The weathering of calcareous rocks by lichens. Pedobiologia 24:219–229

Braconnot H (1825) De la présence de l'oxalate de chaux dans le règne minéral: existence du même sel en quantité énorme dans les plantes de la famille des lichens, et moyen avantageux d'en extraire de l'acide oxalique. Ann Chim Phys 28:318–322

Briot P, Laroche-Collet S, Locquin M (1983) Rôle de champignons dans la genèse de certaines croûtes carbonatées. L'exemple des calcretes de l'Australie occidentale et du calcrete uranifère de Yeelirrie. 108e Congrès National des Sociétés Savantes, Sciences, 1, 2:153–165

Callot G, Mousain D, Plassard C (1985a) Concentrations de carbonate de calcium sur les parois des hyphes mycéliens. Agronomie 5:143–150

Callot G, Guyon A, Mousain D (1985b) Inter-relations entre aiguilles de calcite et hyphes mycéliens. Agronomie 5:209–216

Calvet F (1982) Constructive micrite envelope developed in vadose continental environment in Pleistocene eolianites of Mallorca. Acta Geol Hispanica 3:169–178

Clough KS, Sutton JC (1978) Direct observation of fungal aggregates in sand dune soil. Can J Microbiol 24:333–335

Cooks J, Otto E (1990) The weathering effects of the lichen *Lecida*

aff. Sarcogynoides (Koerb.) on Magaliesberg quartzite. Earth Surf Proc Landf 15:491–500
Coniglio M, Harrison RS (1983) Holocene and Pleistocene caliche from Big Pine Key, Florida. Bull Can Petrol Geol 31:3–13
Cromack Jr K, Sollins P, Graustein WC, Speidel K, Todd AW, Spycher G, Li CY, Todd RL (1979) Calcium oxalate accumulation and soil weathering in mats of the hypogeous fungus *Hystangium crassum*. Soil Biol Biochem 11:463–468
Cromack K Jr, Sollins P, Todd RL, Fogel R, Todd AW, Fender WM, Crossley ME, Crossley DA Jr (1977) The role of oxalic acid and bicarbonate in calcium cycling by fungi and bacteria: some possible implications for soil animals. Ecol Bull 25:246–252
Cunningham KI, Northup DE, Pollastro RM, Wright WG, LaRock EJ (1995) Bacteria, fungi and biokarst in Lechuguilla Cave, Carlsbad Caverns National Park, New Mexico. Environ Geol 25:2–8
Dave SR, Natarajan KA (1981) Leaching of copper and zinc from oxidised ores by fungi. Hydrometallurgy 7:235–242
Del Monte M, Sabbioni C, Zappia G (1987) The origin of calcium oxalates on historical buildings, monuments and natural outcrops. Sci Total Environ 67:17–39
Dragovich D (1993) Distribution and chemical composition of microcolonial fungi and rock coatings from arid Australia. Physical Geogr 14:323–341
Drake NA, Heydeman MT, White KH (1993) Distribution and formation of rock varnish in southern Tunisia. Earth Surf Landf 18:31–41
Edwards HGM, Farwell DW, Jenkins R, Seaward MRD (1992) Vibrational Raman spectroscopic studies of calcium oxalate monohydrate and dihydrate in lichen encrustations on Renaissance frescoes. J Raman Spectrosc 23:185–189
Ennever J, Summers FE (1975) Calcification by *Candida albicans*. J Bacteriol 122:1391–1393
Foster J.W. (1949) Chemical activities of fungi. Academic Press, New York
Franceschi VR, Horner HT (1980) Calcium oxalate crystals in plants. Bot Rev 46:361–427
Frey-Wyssling A (1981) Crystallography of the two hydrates of crystalline calcium oxalate in plants. Am J Bot 68:130–141
Freytet P, Verrecchia EP (1995) Discovery of Ca-oxalate crystals associated with fungi in moss travertines (Bryoherms, freshwater heterogenous stromatolites). Geomicrobiol J 13:117–127
Friedman GM, Gebelein CD, Sanders JE (1971) Micritic envelopes of carbonate grains are not exclusively of photosynthetic algal origin. Sedimentology 16:89–96
Friedmann EI (1982) Endolithic microorganisms in the Antarctic cold desert. Science 215:1045–1053
Galvan J, Rodriguez C, Ascaso C (1981) The pedogenic action oj lichens in metamorphic rocks. Pedobiologia 21:60–73
Gatrall M, Golubic S (1970) Comparative study on some Jurassic and Recent endolithic fungi using scanning electron microscope. In: Crimes TP, Harper TC (eds) Trace fossils. Seel House Press, Liverpool, pp 167–178
Golden DC, Zuberer DA, Dixon JB (1992) Manganese oxides produced by fungal oxidation of manganese from siderite and rhodochrosite. In: Skinner HCW, Fitzpatrick RW (eds) Biomineralization processes, iron, manganese. Catena Suppl 21:161–168
Goldstein RH (1988) Paleosols of Late Pennsylvanian cyclic strata, New Mexico. Sedimentology 35:777–803
Graustein WC, Cromack Jr K, Sollins P (1977) Calcium oxalate: occurrence in soils and effect on nutrient and geochemical cycles. Science 198:1252–1254
Grote G, Krumbein WE (1992) Microbial precipitation of manganese by bacteria and fungi from desert rock and rock varnish. Geomicrobiol J 10:49–57
Hamlet WM, Plowright CB (1877) On the occurrence of oxalic acid in fungi. Chem News 36:93–94
Horner HT, Tiffany LH, Cody AM (1983) Formation of calcium oxalate crystals associated with apothecia of the discomycete, *Dasyscypha capitata*. Mycologia 75:423–435
Jackson SL, Heath IB (1993) Roles of calcium ions in hyphal tip growth. Microbiol Rev 57:367–382
Jackson TA, Keller WD (1970) A comparative study of the role of lichens and "inorganic" processes in the chemical weathering of Recent hawaiian lava flows. Am J Sci 269:446–466
Jeanson C (1973) Altération du marbre d'un chapiteau de la basilique Saint Marc de Venise – Etude au microscope à balayage et à la microsonde. In: Third Int Petrol Symp Petrolio e Ambiante, Roma, pp 209–220
Jones B (1988) The influence of plants and micro-organisms on diagenesis in caliche: example from the Pleistocene Ironshore Formation on Cayman Brac, British West Indies. Bull Can Petrol Geol 36:191–201
Jones B, Pemberton SG (1987) Experimental formation of spiky calcite through organically mediated dissolution. J Sedim Petrol 57:687–694
Jones D, Wilson MJ, McHardy WJ (1981) Lichen weathering of rock-forming minerals: application of scanning electron microscopy and microprobe analysis. J Microsc 124:95–104
Jones D, Wilson MJ, Laundon JR (1982) Observations on the location and form of lead in *Stereocaulon vesuvianum*. Lichenologist 14:281–286
Kahle CF (1977) Origin of subaerial Holocene calcareous crusts: role of algae, fungi and sparmicritisation. Sedimentology 24:413–435
Klappa CF (1979a) Lichen stromatolites: criterion for subaerial exposure and a mechanism for the formation of laminar calcrete (caliche). J Sedim Petrol 49:387–400
Klappa CF (1979b) Calcified filaments in Quaternary calcretes: organo-mineral interactions in the subaerial vadose environment. J Sedim Petrol 49:955–968
Krumbein WE (1972) Rôle des microorganismes dans la genèse, la diagenèse et la dégradation des roches en place. Rev Ecol Biol Sol 9:283–319
Krumbein WE, Petersen K, Schellnhuber H-J (1989) On the geomicrobiology of yellow, orange, red, brown and black films and crusts developing on several different types of stone and objects of art. In: Proc Int Symp La pellicole da ossalati: origine e significato nella conservazione delle opere d'arte, Centro CNR Gino Bozza, Milano, pp 337–380
Krumbein WE, Jens K (1981) Biogenic rock varnishes of the Negev Desert (Israel), an ecological study of iron and managnese transformation by cyanobacteria and fungi. Oecologia 50:25–38
Lapeyrie F, Perrin M, Pepin R, Bruchet G (1984) Formation de weddellite extracellulaire en culture in vitro par *Paxillus involutus*; signification de cette production pour la symbiose ectomycorhizienne. Can J Bot 62:1116–1121
Le Campion-Alsumard T, Golubic S, Priess K (1995) Fungi in corals: symbiosis or disease? Interaction betwwen polyps and fungi causes pearl-like skeleton biomineralization. Mar Ecol Prog Ser 117:137–147
Phillips SE, Milnes AR, Foster RC (1987) Calcified filaments: an example of biological influences in the formation of calcrete in South Australia. Aust J Soil Sci 25:405–428
Purvis OW (1984) The occurrence of copper oxalate in lichens growing on copper sulphide-bearing rocks in Scandinavia. Lichenologist 17:111–116
Robert M, Berthelin J (1986) Role of biological and biochemical factors in soil mineral weathering. In: Huang PM, Schnitzer M (eds) Interactions of soil minerals with natural organics and microbes. Soil Sci Soc Am Spec Publ 17:453–495
Robert M, Chenu C (1992) Interactions between soil minerals and microorganisms. In: Stotzky G, Bollag J-M (eds) Soil biochemistry 7. Marcel Dekker, New York, pp 307–404
Russ J, Palma RL, Booker JL (1994) Whewellite rock crusts in the Lower Pecos region of Texas. Texas J Sci 46:165–172
Silverman MP, Munoz E (1970) Fungal attack on rock: solubilization and altered infrared spectra. Science 169:985–987
Schnitzer M, Chan YK (1986) Structural characteristics of a fungal melanin and a soil humic acid. Soil Sci Soc Am J 50:67–71
Solomon ST, Walkden GM (1985) The application of cathodoluminescence to interpreting the diagenesis of an ancient profile. Sedimentology 32:877–896
Staley JT, Palmer FE, Adams JB (1982) Microcolonial fungi: common inhabitants on desert rocks? Science 215:1093–1095
Staley JT, Adams JB, Palmer FE (1992) Desert varnish: a biological perspective. In: Stotzky G, Bollag J-M (eds) Soil biochemistry 7. Marcel Dekker, New York, pp 173–195
Strong GE, Giles JRA, Wright VP (1992) A Holocene calcrete from

North Yorkshire, England: implications for interpreting paleoclimates using calcretes. Sedimentology 39:333–347
Tilden JE (1897) Some new species of Minnesota algae which live in a calcareous or siliceous matrix. Bot. Gaz 23:95–104
Torre de la MA, Gomez-Alarcon G, Vizcaino C, Garcia MT (1993) Biochemical mechanisms of stone alteration carried out by filamentous fungi living in monuments. Biogeochemistry 19:129–147
Verrecchia EP (1990) Lithodiagenetic implications of the calcium oxalate-carbonate cycle in semi-arid calcretes, Nazareth, Israel. Geomicrobiol J 8:89–101
Verrecchia EP, Dumont J-L, Rolko KE (1990) Do fungi building limestones exist in semi-arid regions? Naturwissenschaften 77:584–586
Verrecchia EP, Dumont J-L, Verrecchia KE (1993) Role of calcium oxalate biomineralization by fungi in the formation of calcretes: a case study from Nazareth, Israel. J Sedim Petrol 63:1000–1006
Verrecchia EP, Verrecchia KE (1994) Needle-fiber calcite: a critical review and a proposed classification. J Sedim Res A64:650–664
Verrecchia EP, Dumont J-L (1996) A biogeochemical model for chalk alteration by fungi in semiarid environments. Biogeochemistry 35: 447–470
Wadsten T, Moberg R (1985) Calcium oxalate hydrates on the surface of lichens. Lichenologist 17:239–245
Webley DM, Henderson MEK, Taylor JF (1963) The microbiology of rocks and weathering building stones. J Soil Sci 14:102–112
Weed SB, Davey CB, Cook MG (1969) Weathering of mica by fungi. Soil Sci Soc Am Proc 33:702–706
Wenberg GM, Erbisch FH, Volin ME (1971) Leaching of copper by fungi. Soc Min Eng Transact AIME 250:207–212
Went FW (1969) Fungi associated with stalactite growth. Science 166:385–386
Whitney KD (1989) Systems of biomineralization in the Fungi. In: Crick RE (ed)Origin, evolution and modern aspects of biomineralization in plants and animals. Plenum Press, New York, pp 433–441
Wilson MJ, Jones D (1984) The occurrence and significance of manganese oxalate in *Pertusaria corallina* (Lichenes). Pedobiologia 26:373–379
Wilson MJ, Jones D, Russell JD (1980) Glushinskite, a naturally occurring magnesium oxalate. Min Mag 43:837–840
Wright VP (1986) The role of fungal biomineralization in the formation of Early Carboniferous soil fabric. Sedimentology 33: 831–838

Diatoms and Benthic Microbial Carbonates

Barbara M. Winsborough

Winsborough Consulting, 5701 Bull Creek Road, Austin, TX 78756, USA

Abstract. Benthic diatoms date from the Early Jurassic and since that time have probably been associated with stromatolites, travertines, and related microbial carbonates in much the same manner as they are today. Diatoms and the extracellular mucilage they produce are important in the stromatolite building process by trapping and binding grains and in the diagenesis of the sediments. Mucilage is produced and deposited on the substrate during migration by motile diatoms and comprises the stalks, tubes, filaments, and envelopes of sessile species. In marine stromatolite and associated habitats, diatoms coat ooids and larger grains and other hardgrounds, as well as the filaments of cyanobacteria and algae. In freshwater carbonate settings diatoms are also a significant component of most microbial communities. To determine the quality of diatom preservation in fossil freshwater microbial carbonates, material from extensive Quaternary travertine deposits in Mexico and Italy was analyzed. Samples were selected to represent as many travertine depositional facies as possible. Results show that diatoms are preserved within all the fossil travertine facies examined.

1 Introduction

Compared to the Paleozoic record of eukaryotic algae (Riding 1990) diatoms are relative newcomers. The oldest specimens known are from the Early Jurassic, with diverse assemblages of nearshore, benthic marine diatoms present by the Early Cretaceous (Harwood and Nikolaev 1995). Diatomite deposits of the Late Cretaceous indicate that the group became a major planktic element of the oceanic realm. The ancestors of the oldest-known nonmarine diatoms (Late Paleocene and Early Eocene) may be related to genera from the Lower Cretaceous nearshore assemblages that migrated from marine to freshwater environments during the Late Cretaceous. There is evidence of subsequent marine to freshwater migrations of other diatom groups through the Cenozoic (Harwood and Nikolaev 1995). Although some species of diatoms associated with fossil stromatolites and related benthic microbial carbonate deposits may be extinct, modern marine and freshwater microbial carbonates are colonized by diatoms living in the same ecological niche, with the same functional behavior. One of the most prominent characteristics of these diatoms is the production of extracellular mucilage.

This review examines the processes of diatom-sediment interactions in marine stromatolites and freshwater travertines (sensu Pentecost and Viles 1994; Pentecost 1996, see also Pedley, this Vol.) and explores the role of diatoms and their extracellular mucilage in sediment biogenesis and stability. Diatom extracellular polymeric substances are discussed as they relate to mechanisms of substrate attachment and sediment stabilization. Diatoms were extracted from a variety of carbonate facies associated with freshwater travertines to determine their preservation in ancient deposits.

2 Discussion of Diatom-Sediment Interactions

2.1 Mechanics of diatom-sediment interactions

Neumann et al. (1970) were among the first to describe the role of marine algae in sediment stabilization as the trapping and binding of sand grains into a rigid network by green and red algae and the binding of the grains together by benthic diatoms, increasing mat stability and resistance to erosion. Because of their ability to baffle, trap, and bind coarse sediments, algae, including diatoms, play an important role in the formation of the best known and most impressive modern examples of subtidal stromatolites, those found at Shark Bay Australia (Awramik and Riding 1988) and near Lee Stocking Island in the Bahamas (Riding et al. 1991; Riding 1994). A diverse community of benthic diatoms is associated with the Shark Bay stromatolites (John 1990, 1991), and an even larger number of species has been identified from the Bahaman stromatolites (Hein et al. 1993). Approximately 420 species of diatoms have been recovered from ooid sand grains, macroalgae, and other microhabitats associated with the stromatolites and other microbial carbonates near Lee Stocking Island (Hein and Winsborough, in prep.).

Awramik and Riding (1988) noted that stromatolite diatom behavior is analogous to cyanobacteria in that they are upwardly motile, produce copious gel, and bind sediment. Ecologically, the radiating, branched growth of stalked diatoms and the green algae *Oocardium* and *Gongrosira* (Pentecost 1982, 1988) are similar strategies to accommodate continuous sediment accumulation.

R.E. Riding and S.M. Awramik (Eds.)
Microbial Sediments

Included within extracellular mucilages associated with microbial mats and biofilms are the products of bacteria, cyanobacteria, diatoms and several other classes of algae. Boney (1981) elegantly referred to mucilage as the ubiquitous algal attribute, but it is the extracellular mucilage produced by most benthic diatoms that is of particular interest here. These mucilages are ecologically important in the binding and stabilization of intertidal sediments (Vos et al. 1988; Paterson and Black, this Vol.) much like *Schizothrix calcicola* binds particles (Monty 1967). Vos et al. (1988) demonstrated that biological stabilization of sediment depends on the density and mucilage secretion of two distinct groups of benthic diatoms. These authors describe a cohesive effect on sand grains that results from the organic coating of mucilage secreted by attached diatoms, and a network effect produced by tough, elastic mucus threads left behind when large numbers of motile diatoms migrate to the sediment surface. They conclude that the network effect is much more significant in increasing sediment stability by increasing the critical erosion velocity. Paterson (1990) examined the influence of sediment water content on the binding capacity of mucopolysaccharides produced by diatoms and found that as natural dewatering occurs during compaction, and the mucilage dries, the binding becomes stronger and more effective, altering the packing of sediment particles and erosional characteristics of the sediment.

2.2 Nature of Mucilage

Some benthic diatoms are motile, gliding up through the sediments for efficient light capture at a rate of up to 25/ms (Cohn and Disparti 1994). This movement, related to their rhythmic, diurnal, vertical migrations, is associated with diatom secretion of extracellular polymeric substances (EPS), called mucilages, composed primarily of polysaccharides (Edgar and Picket-Heaps 1984; Daniel et al. 1987; Hoagland et al. 1993). Diatom movement is coupled to mucilage secretion and substrate adhesion along the raphe or slit in the cell wall. Cohn and Weitzell (1996), investigating the ecological roles of motility in diatoms, demonstrated that species differ in the adherent strength of their mucilage depending on environmental conditions. The nonmotile benthic diatoms are sessile (attached to a substrate) and produce mucilage in the form of stalks, films, apical pads, fibrils, envelopes, or tubes that adhere to the substrate. Diatom mucilage sometimes accumulates in copious quantities forming laminae up to 3 cm thick on stromatolites and travertines in shallow streams (Winsborough and Golubic 1987). Pentecost (1990) also observed that diatoms usually produce a seasonal growth on top of the perennial cyanobacterial/chlorophyte flora on travertines.

EPS, not only from diatoms, but from bacteria, cyanobacteria, and eukaryotic algae, are essentially microfibrillar and polysaccharide in composition (Decho 1990). Cryo-scanning electron microscopy (SEM; preparation includes freeze-drying to preserve the microorganization of samples) studies of EPS in lacustrine stromatolites show that EPS is organized into three-dimensional organic networks that can form the framework of stromatolites and other deposits of benthic microbial communities (Défarge et al. 1996). Evidence at the molecular scale of the complex nature of microbial biofilms is provided by Decho (this Vol.). SEM studies of the morphology of EPS-rich biofilms and microbial mats from a diatomaceous sandy mud reveal a structure of varying thickness and texture consisting of amorphous material, fibrils, hemispherical masses or aggregates of bacteria and various minerals (Westall and Rincé 1994). On lacustrine stromatolites, a gelatinous mat with a less granular texture was illustrated and described by Braithwaite and Zedef (1996) as a smooth, laminated, diatom-dominated, microbial mat with surface-parallel layers of mucilage interbedded with hydromagnesite.

Travertine deposition generally is associated with spring water having low phosphate concentrations. Hoagland et al. (1993) report that the nitrate to phosphate ratio (N:P) of the culture medium appears to affect synthesis of EPS by diatoms, green algae and cyanobacteria, with increases in EPS production stimulated in a high N:P ratio (low phosphorous concentrations). However, according to Emeis et al. (1987, p. 607), "phytoplankton confronted with low nitrate concentrations tend to excrete mucus as a waste product because protein synthesis is reduced in the absence of a metabolizable nitrogen source." EPS creates a nutritional "microenvironment" around the diatom cell, providing organic-rich sites for the growth of other microbes, in addition to trapping fine sediment (Emeis et al. 1987, Fig. 11; Guo and Riding 1994). This mucilage is suggested to be an ideal site for bacterial biomineralization (Chafetz and Folk 1984; Chafetz and Buczynski 1992). The EPS biofilm functions in turn as a scavenger of both inorganic (phosphate and iron) and organic nutrients such as amino acids and macromolecules like proteins important to the development and maintenance of a bacterial colony (Westall and Rincé 1994). Other attributes of mucilage include water retention capacity as a protection against desiccation, the transmission of photosynthetically active radiation (usable light) throughout its extent, and spore release and attachment (Boney 1981). Bathurst (1967) suggested that, in addition to the characteristics of sediment binding, subtidal microbial mats produced by cyanobacteria, diatoms, and their mucilage in the Bahamas must occupy an essential position in the local food chain as the main source of food for all animals that browse on the sand floor. He observed also that although the mat is not evi-

dent after it is buried, the effect of the mat on sediment stability has geological significance in the interpretation of depositional environments. The physical, chemical, and biological aspects of the microbial mat and biofilm structure are discussed by Stolz (this Vol.).

Both micrite and sparry calcite nucleate on stalks and other EPS (Wallner 1935; Golubic 1967, 1976; Winsborough and Seeler 1986; Winsborough and Golubic 1987; Emeis et al. 1987; Winsborough et al. 1994, 1996; Chafetz et al. 1994), and in some instances diatoms themselves provide a nucleation site for developing crystals (Guo and Riding 1994). Direct precipitation of calcite under the influence of diatom mucilage is illustrated in Fig. 1a – e. In their study of the Plitvice traver-

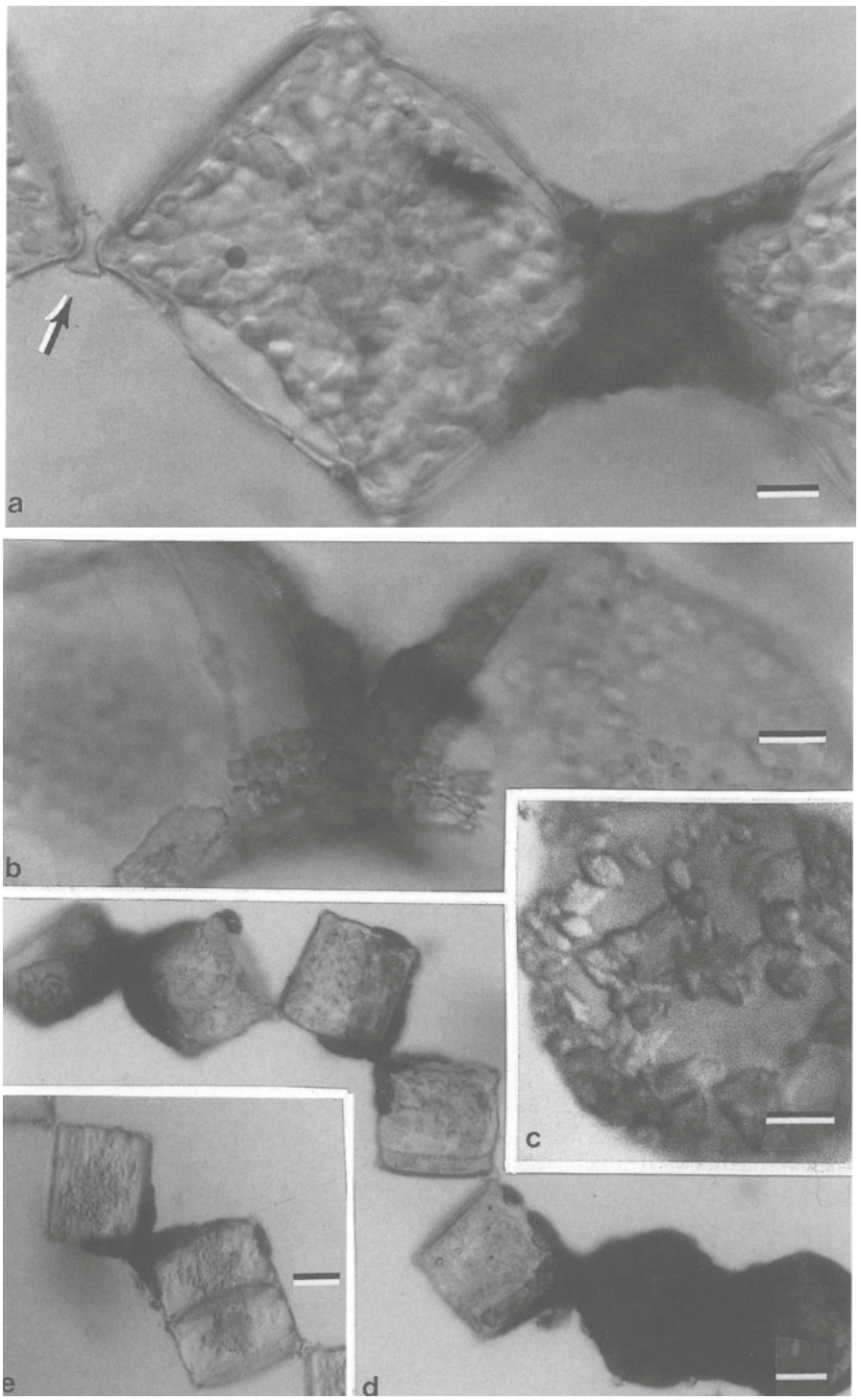

Fig. 1a – e. Zig-zag chains of the cylindrical diatom *Pleurosira laevis* (Ehrenberg) Compère growing on an actively forming stream travertine in Bull Creek, Austin, Texas. Photosynthesizing, discoid plastids are visible within the cells. **a** Precipitation of sparry calcite begins on the mucilage pad connecting the diatoms. *Arrow* points to an uncalcified pad. **b** Calcification progresses over the diatom faces and is proceeding to cover the sides of the diatoms in the form of thin, transparent sheets of sparry calcite. **c** Diatom face with interlocking crystals of sparry calcite. **d** Progressive calcification within single filament due to variable age of individual diatoms. **e** Calcifying diatom undergoing cell division. *Scale bars:* **a – c** = 10 μm, **d,e** = 20 μm

tines, Kempe and Emeis (1985, 1986) and Emeis et al. (1987) suggest that the formation of mucilage by diatoms and other microbes is one of the prerequisites for carbonate precipitation in freshwater environments. Défarge et al. (1996) describe a process of in situ precipitation called organomineralization in which the organic walls of EPS act as a matrix for calcification, initiating and supporting mineral growth. They suggest that crystal nucleation probably is initiated at acidic sites of the polysaccharide framework of the sediments, with the network alveoli that enclose the precipitates functioning as confining spaces favoring supersaturation within, then precipitation from, their inner solutions.

EPS becomes entrapped in carbonate deposits along with other organic components and after dehydration and degradation remains present over geologic time. Kerogen, the condensed, insoluble residue present in ancient sediments that arises from diagenetic transformation of deposited biomolecules, may serve as an ancient biosynthetic record of the original biomolecules (Hines and Burlingame 1984). Organic residues, possibly "proto-kerogens," consisting of EPS and the other insoluble remains of the microbial mats, have been extracted from ancient travertines and provide reliable radiocarbon ages for travertine deposition and stable isotopic information identifying the source and nature of the residue (Neely 1995; Neely et al. 1995; Caran et al. 1995, 1996; Winsborough et al. 1996). The diatoms, pollen, phytoliths, and occasional algal and bryophyte remains extracted with the EPS add paleoecological context.

In some stromatolite and travertine settings bacterial activity has been implicated in the dissolution of diatoms during mat diagenesis (Winsborough et al. 1994; Szulc and Smyk 1994). Szulc and Smyk (1994) demonstrated that, although the diatoms in cyanobacterial/diatom stromatolites associated with a mountain spring are completely dissolved within a year after deposition, the diatoms play a crucial role in the mineralization of the microbial mat. As they describe it, bacterial activities cause diatom mucilage (rich in amino acids, carbohydrates, proteins, lipids and mono- and polysaccharides) containing trapped and precipitated carbonates to undergo complex processes of penecontemporaneous dissolution of the siliceous frustules, followed by prevailing reprecipitation of carbonates. They suggest that this mucilage is important in the progressive neomorphism of carbonate microfacies.

3 Diatom Preservation in Travertines- A Case Study

Habitats associated with the production of freshwater travertine often support a microbial community that includes a diverse assemblage of diatoms (Wallner 1935; Hustedt 1938; Golubic 1967, 1976; Stockner 1968; Braithwaite 1979; Round 1981; Eggleston and Dean 1976; Winsborough and Seeler 1986; Kemp and Emeis 1985, 1986; Emeis et al. 1987; Winsborough and Golubic 1987; Davis et al. 1989; Pentecost and Tortora 1989; Plenkovic et al. 1989; Love and Chafetz 1990; Pedley 1990, 1994; Pentecost 1990, 1995; Winsborough 1990; Chafetz et al. 1991, 1994; Plenkovic 1993; Guo and Riding 1994; Moore and Burne 1994; Braithwaite and Zedef 1996). However, literature detailing the taxonomy and paleoecology of the diatom assemblages preserved in ancient freshwater stromatolites and travertines is scant (Neely et al. 1990, 1995; Caran et al. 1996; Winsborough et al. 1996). According to Pedley (1994) "fossilized diatoms are virtually unknown within tufa deposits away from the living biofilm...". This situation is remarkable in that "diatoms are the most abundant and best preserved algal remains in oceanic and freshwater sediments..." (Round 1981, p. 502).

To investigate the matter of diatom preservation in ancient travertines, extensive deposits of Pleistocene to Holocene travertines on the order of several kilometers in length located at Rocchetta a Volturno near Isernia, Italy (D'Argenio and Ferreri 1987; Brancaccio et al. 1988), Tehuacan (Woodbury and Neely 1972; Winsborough et al. 1996), and San Marcos Necoxtla in Puebla, Mexico (Caran et al. 1996), and Hierve el Agua in Oaxaca, Mexico (Neely et al. 1990) were sampled to obtain material from a variety of geochemical and depositional facies. Hierve El Agua provides an unusual chemical composition (high CO_2, although nonthermal) and a large variety of active facies (Neely et al. 1990). This site represents continuous travertine deposition since at least the Pleistocene and is currently active.

3.1 Results: Diatom Preservation in Fossil Travertines

Eighteen samples were analyzed from eight facies (cascade, stream, stromatolite, moss, plant stems, bioclastic sands, bubbles, and pisoids) found in the ancient travertines of Tehuacan, Hierve el Agua, San Marcos Necoxtla, and Rochetta a Volturno. Results show that diatoms are not only living in the biofilm of a variety of active travertine facies but are also well-preserved in ancient travertines. Approximately 130 species and varieties of diatoms were identified from the ancient travertines, with a core set of species found in the deposits at Tehuacan, San Marcos Necoxtla, and Volturno. The most abundant diatoms are (in order of abundance) *Achnanthes microcephala* Kützing (also called *Achnanthidium microcephalum* Kützing), *Navicula (Luticola) mutica* Kützing, *Denticula elegans* Kützing, *Amphora veneta* Kützing, *Cocconeis placentula* Ehrenberg, *Nitzschia amphibia* Grunow, *Hantzschia amphioxys* (Ehrenberg)

Grunow, *Gomphonema parvulum* (Kützing) Kützing, and *Amphora pediculus* (Kützing) Grunow. At Hierve el Agua, *Achnanthes microcephala* was replaced by *Achnanthes gibberula* Grunow, a very similar species that occupies the same ecological niche.

The number of species in any one sample (exept Hierve el Agua) varied from 13 species attached to lithified calcite bubbles at San Marcos Necoxtla to 61 species in a laminated cascade travertine from Tehuacan. A snail-rich bioclastic lacustrine sand from San Marcos Necoxtla was also relatively diverse. It contained diatoms found attached to plants and species associated with sand and mud in addition to the taxa attached directly to travertine, as is typical of the cascade facies. The cascade facies, formed by the action of water flowing down a wall or over a slope, is volumetrically the most important travertine morphology at all the sites. Cascade features associated with rapid degassing and a swift current, such as calcified bubbles, pisoids and steep cascades, contained fewer species than those facies formed under slightly less vigorous degassing or slower current regimes such as a laminated stream travertine, but all were quite diatomaceous. Waterfall mosses, regardless of location, were low in diversity, probably resulting from the more restrictive subaerial conditions and accelerated carbonate accretion. Another moderately low diatom diversity facies was a tufa (highly porous travertine, sensu Pedley 1990) deposit from San Marcos Necoxtla, precipitated around the stems of *Chara* and vascular plants.

The diatoms at Hierve el Agua are different from those at the other sites. The 18 modern samples analyzed include pisoids, stromatolites, cascade deposits, coated grains, calcified cyanobacteria, *Chara*, sedges and plant stems, calcite bubbles, crusts and rafts, and carbonate sand. Diatoms were present in every facies examined, including calcite bubbles and carbonate rafts, each of which contained five species. Precipitation is extremely rapid because the highly carbonated water degasses spontaneously and vigorously and increases pH. Pisoids, containing five to ten diatom taxa, accumulate in small terraces and pools on the gentle cascade slope. The dominant diatoms at Hierve el Agua are *Achnanthes gibberula, Amphora coffeaeformis* (Agardh) Kützing, *Cymbella norvegica* Grunow, *Denticula elegans* and *Nitzschia tropica* Hustedt. Of these species, only *Denticula elegans* is a common element of the ancient travertines described above (except the ancient deposits at Hierve el Agua). *A. coffeaeformis* is more characteristic of brackish than freshwater habitats, and the other common species often are found in water with a slightly elevated salinity.

3.2 Discussion of Case Study Results

The travertine diatom assemblages in this study consist of alkaliphilous, freshwater, epilithic diatoms found typically in temperate, carbonate-rich, spring-fed, sometimes seasonally flowing, alkaline springs, streams, and ponds with bare rock, or older travertine surfaces. *Achnanthes microcephala*, the most common species, requires abundant oxygen and develops best in clean running water (Ehrlich 1995). Many of the travertine diatoms, including *Achnanthes*, are well-adapted to colonize fresh travertine because they produce mucilage exudates in the form of stalks or pads that aid in firm attachment to the substrate (Korte and Blinn 1983; Rosowski et al. 1986; Blenkinsopp and Lock 1994). *Navicula, Denticula* and *Nitzschia* are motile and leave a mucilage trail. *Denticula elegans* adapts to damp or shallow standing water habitats by producing a large, firm, mucilaginous envelope that retains moisture. Of the species found commonly in the travertines studied, all but *Denticula elegans, Amphora veneta, Cocconeis placentula* and *Amphora pediculus* are also found in soils and subaerial habitats (Round 1981).

A mature, multilayered mat consists of adnate species such as *Cocconeis placentula* or short-stalked *Achnanthes microcephala* on the lower layer. Species of *Gomphonema* and *Cymbella* are found at the ends of long, branched, vertically oriented stalks; rosette-forming species such as *Fragilaria* spp, *Staurosira construens* and *Staurosirella* spp. fill in the upper layer. Differences in the proportions of common taxa in the different samples are to be expected because of variations in microhabitat, seasonal succession, mat maturity, and grazing pressures. Stockner (1968) found that in a thermal stream associated with travertine-depositing springs, succession was rather rapid, often with complete shifts in dominance within 2 weeks. The duration and time of year when the rainy season occurs at a travertine site clearly will affect local species composition because each diatom species has its own characteristic growing season.

4 Conclusions

These observations make clear that diatoms are an important component of both fine-grained and coarse-grained microbial carbonates. Marine stromatolites are constructed of relatively large grain size carbonates and support the development of a complex multilayered microbial community that includes macroalgae and their diatom epiphytes. The result is the presence of different microhabitats and a large variety in the kinds of diatom species present. Diatom species diversity is lower in freshwater carbonate facies associated

with the deposition of travertine, probably because the microbial mat is generally thinner and less complex.

It was already known that diatoms are plentiful on active travertines, but this study shows that benthic diatoms are present in a variety of fossil travertines at least as old as the Plio-Pleistocene. These results and travertine diatom literature in general suggest that diatoms associated with travertine are species typical of well-aerated, mineral-rich environments and are those species adaptable to short-term, high amplitude changes in local flow regime, water chemistry and precipitation rates. There are a combination of sessile species that use mucilage for attachment to firm carbonate surfaces and motile taxa that leave a mucilage trail as they migrate through unconsolidated sediment. *Achnanthes microcephala* is without doubt the most common and characteristic diatom species of ancient travertine mat communities. Further studies will demonstrate whether it is possible to distinguish ancient travertines with unusual water chemistry based on their diatom composition.

A biofilm or microbial mat containing diatoms and the extracellular polysaccharide substances secreted by them is intimately associated with all the carbonate precipitates, even rapidly growing facies such as coated bubbles and calcite rafts. This biofilm plays a central role in the precipitation, trapping, and binding of carbonate crystals, and its presence in ancient carbonates provides insights into possible diagenetic pathways. EPS and the other recalcitrant cell components of microbial mats are preserved in ancient travertines for at least several thousand years and probably for much longer. This EPS-sediment interaction has important sedimentological implications because of the role of EPS in carbonate precipitation, early diagenesis, and sediment binding and stabilization.

Acknowledgements. The author would like to acknowledge the help of Bruno D'argenio, Crescenzo Violante and Steve Golubic in collecting the Italian travertine material and that of James Neely and Chris Caran for field assistance in Mexico. Mexican field investigations were conducted with permission from the Instituto Nacional de Antropologia e Historia de Mexico, and funded by the H.J. Heinz III Charitable Fund Grant Program for Latin American Archaeology and a Robert Mellon Foundation Faculty Research grant to James Neely. Suggestions by David Harwood and other reviewers improved the manuscript.

References

Awramik SM, Riding R (1988) Role of algal eukaryotes in subtidal columnar stromatolite formation. Proc Natl Acad Sci USA 85:1327–1329

Bathurst RG (1967) Subtidal gelatinous mat, sand stabilizer and food, Great Bahama Bank. J Geol 75:736–738

Blenkinsopp SA, Lock MA (1994) The impact of storm-flow on river biofilm architecture. J Phycol 30:807–818

Boney AD (1981) Mucilage: the ubiquitous algal attribute. Br Phycol J 16:115–132

Braithwaite CJ (1979) Crystal textures of Recent fluvial pisolites and laminated crystalline crusts in Dyfed, South Wales. J Sediment Petrol 49:181–194

Braithwaite CJ, Zedef V (1996) Hydromagnesite stromatolites and sediments in an alkaline lake, Salda Golu, Turkey. J Sediment Res 66:991–1002

Brancaccio L, D'Argenio B, Ferreri V, Stanzione D, Taddeucci A, Voltaggio M (1988) I travertini di Rocchetta a Volturno (molise) datazioni con ^{230}Th e modello deposizionale. Mem Soc Geol It:1–11

Caran SC, Winsborough BM, Neely JA, Valastro S Jr (1995) Radiocarbon age of carbonate sediments (travertine, pedoconcretions, and biogenic carbonates): a new method based on organic residues, employing stable-isotope control of carbon sources. Current Res Pleistocene 12:75–77

Caran SC, Neely JA, Winsborough BM, Sorensen F, Valastro S Jr (1996) A late paleoindian/early archaic water well in Mexico – possible oldest water-management feature in the new world. Geoarchaeology 11:1–35

Chafetz HS, Folk RL (1984) Travertines: depositional morphology and the bacterially constructed constituents. J Sedimentary Petrol 54:289–316

Chafetz HS, Buczynski C (1992) Bacterially induced lithification of microbial mats. Palaios 7:277–293

Chafetz HS, Rush PF, Utech M (1991) Microenvironmental controls on mineralogy and habit of $CaCo_3$ precipitates: an example from an active travertine stream. Sedimentology 38:107–126

Chafetz HS, Srdoc D, Horvatincic N (1994) Early diagenesis of Plitvice lakes waterfall and barrier travertine deposits. Géogr Phys Quat 48:247–255

Chafetz HS, Lawrence JR (1994) Stable Isotopic Variability Within Modern Travertines. Geogr Phys Quat 48:257–273

Cohn SA, Disparti NC (1994) Environmental factors influencing diatom cell motility. J Phycol 30:818–828

Cohn SA, Weitzell Jr RE (1996) Ecological considerations of diatom cell motility. I. Characterization of motility and adhesion in four diatom species. J Phycol 32:928–939

Daniel GF, Chamberlain AHL, Jones EBG (1987) Cytochemical and electron microscopical observations on the adhesive materials of marine fouling diatoms. Br Phycol J 22:101–118

D'argenio B, Ferreri V (1987) A brief outline of sedimentary models for Pleistocene travertine accumulation in southern Italy. Rend Soc Geol It 9:167–170

Davis JS, Rands DG, Hein MK (1989) Biota of the tufa deposit of Falling Springs, Illinois. U.S.A. Trans Am Microsc Soc 108:403–409

Decho AW (1990) Microbial exopolymer secretions in ocean environments: their role(s) in food webs and marine processes. Oceanog. Mar Biol Annu Rev 28:73–153

Défarge C, Trichet J, Jaunet A, Robert M, Tribble J, Sansone FJ (1996) Texture of microbial sediments revealed by cryo-scanning electron microscopy. J Sediment Petrol 66:935–947

Edgar LA, Picket-Heaps JD (1984) Diatom locomotion. Progr Phycol Res 3:47–88

Eggleston JR, Dean WE (1976) Freshwater stromatolitic bioherms in Green Lake, New York. In: Walter MR (ed) Stromatolites. Developments in Sedimentology 20. Elsevier, Amsterdam, pp 479–488

Ehrlich A (1995) Atlas of the inland-water diatom flora of Israel. Geol Soc of Israel, Israel Academy of Sciences and Humanities, Jerusalem

Emeis KC, Richnow HH, Kempe S (1987) Travertine formation in Plitvice National Park, Yugoslavia: chemical versus biological control. Sedimentology 34:595–609

Golubic S (1967) Algenvegetation der Felsen. Binnengewasser 23. Schweizerbart, Stuttgart

Golubic S (1976) Organisms that build stromatolites. In:Walter MR (ed) Stromatolites. Developments in sedimentology 20. Elsevier, Amsterdam, pp 113–126

Guo L, Riding R (1994) Origin and diagenesis of Quaternary travertine shrub fabrics, Rapolano Terme, central Italy. Sedimentology 41:499–520

Harwood DM, Nikolaev VA (1995) Cretaceous Diatoms: Morphology, taxonomy, biostratigraphy, In: Blome CD et al. (convenors) Siliceous microfossils. Paleontol Soc Short Courses Paleontol 8:81–106

Hein MK, Winsborough BM, Davis JS, Golubic S (1993) Extracellular structures produced by marine species of *Mastogloia*. Diatom Res 8:73–88
Hein MK, Winsborough BM Diatoms of the Bahamas. Bibliotheca Diatomologica (in preparation)
Heinzelmann C, Baumgartner B, Rehse C (1991) Algal films stabilize the river bed. German Res 2:12–14
Hines HB, Burlingame AL (1984) Chemical degradations of residual organic matter from laminated cyanobacterial mats from Solar Lake, Israel. In: Cohen Y, Castenholz RW, Halvorson HO (eds) Microbial mats: stromatolites. Alan R Liss, New York, pp 391–410
Hoagland KD, Rosowski JR, Gretz MR, Roemer SC (1993) Diatom extracellular polymeric substances: function, fine structure, chemistry and physiology. J. Phycol 29:537–566
Hustedt F (1938) Systematische und Ökologische Untersuchungen uber die Diatomeen-Flora von Java, bali und Sumatra. Arch Hydrobiol (Suppl Band) XV:715–718
John J (1990) The diatom flora of the microbial communities associated with stromatolites at Shark Bay, Indian Ocean, West Coast of Australia. In: Ricard M (ed) Ouvrage dédié à la Mémoire du Professeur Henry Germain (1903–1989). O Koeltz, Koenigstein, pp 97–110
John J (1991) *Parlibellus panduriformis* sp. nov. (Bacillariophyta) from Shark Bay, Western Australia. Phycologia 30:556–562
Kempe S, Emeis K (1985) Carbonate chemistry and the formation of Plitvice Lakes. In: Degans ET, Kempe S, Herrera R (eds) Transport of carbon and minerals in major world rivers, pt 3. Mitt Geol-Paläont Inst Univ Hamburg (SCOPE/UNEP Sonderbd) 58:351–383
Kempe S, Emeis K (1986) Travertine formation in the Plitvice National Park. Proc 10th Int Speleol Congr Barcelona, pp 55–59
Korte VL, Blinn DW (1983) Diatom colonization on artificial substrata in pool and riffle zones studied by light and scanning electron microscopy. J Phycol 19:332–341
Love KM, Chafetz HS (1990) Diagenesis of laminated travertine crusts, Arbuckle Mountains, Oklahoma. J Sediment Petrol 58:441–445
Monty CL (1967) Distribution and structure of Recent stromatolitic algal mats, Eastern Andros Island, Bahamas. Ann Soc Géol Belg 90:55–100
Moore LS, Burne RV (1994) The modern thrombolites of Lake Clifton, Western Australia. In: Bertrand-Sarfati J, Monty C (eds) Phanerozoic stromatolites II. Kluwer Academic Publishers, Boston, pp 3–29
Neely JA (1990). Paleoecologia y Desarrollo Cultural de Hierve el Agua: Re-estudio de un Sitio Prehispanico en Oaxaca, Mexico. Consejo de Arqueologia Boletin 1989, no 1, Mexico, D.F., Instituto Nacional de Antropologia, pp 97–102
Neely JA (1995) Paleoecologia, Desarrollo Cultural, y los Usos de Aguas en el Valle de Tehuacán, Puebla, Mexico. Un Reportaje al Consejo de Arqueologia del Instituto Nacional de Antropologia e Historia de Mexico. Mexico, D.F.
Neely JA, Caran SC, Winsborough BM (1990) Irrigated agriculture at Hierve el Agua, Oaxaca, Mexico: In: Marcus J (ed) Debating Oaxaca archaeology. Anthropological Papers Museum of Anthropology, University of Michigan No 84, Ann Arbor, pp 115–189
Neely JA, Caran SC, Winsborough BM, Sorensen FR, Valastro S Jr (1995) An early Holocene hand-dug water well in the Tehuacan Valley of Puebla, Mexico. Curr Res Pleistocene 12:38–40
Neumann AC, Gebelein CD, Scoffin TP (1970) The composition, structure and erodability of subtidal mats. Abaco, Bahamas. J Sediment Petrol 40:274–297
Oreshkina TV, Radionova EP (1990) The transition of Pacific Ocean diatom complexes at the Middle-Late Miocene Boundary and the palaeoceanographic implications. In: Simola H (ed) Proceedings of the 10th International Diatom Symposium, Joensuu, Finland, Aug 28-Sept 2, 1988, Koeltz Scientific Books, Koenigstein, pp 205–212
Paterson DM (1990) The influence of epipelic diatoms on the erodability of an artificial sediment. In: Simola H (ed) Proceedings of the tenth international diatom symposium, Joensuu, Finland. 1988, Koeltz Scientific Books, Koenigstein, pp 345–355
Pedley, HM (1990) Classification and environmental models of cool freshwater tufas. Sediment Geol 68:143–154
Pedley HM (1994) Prokaryote-microphyte biofilms and tufas: a sedimentological perspective. Kaupia. Darmstadter Beitr Naturges 4:45–60
Pentecost A (1982) A quantitative study of calcareous Tintenstriche algae from the Malham district, northern England. Br Phycol J 17:443–456
Pentecost A (1988) Observations on growth rates and calcium carbonate deposition in the green alga *Gongrosira*. New Phytol 110:249–253
Pentecost A (1990) The algal flora of travertine: an overview. In: Herman JS, Hubbard DA (eds) Travaertine-Marl: stream deposits in Virginia. Commonwealth of Virginia Dept. of Mines, Minerals and Energy, Division of Mineral Resources, Charlottesille, Virginia, pp 117–127
Pentecost A (1995) Geochemistry of carbon dioxide in six travertine-depositing waters of Italy. J Hydrol 167:263–278
Pentecost A (1996) The Quaternary travertine deposits of Europe and Asia Minor. Quat Sci Rev 14:1005–1028
Pentecost A, Tortora P (1989) Bagni di Tivoli, Lazio: A modern travertine-depositing site and its associated microorganisms. Boll Soc Geol It 108:315–324
Pentecost A, Viles H (1994) A review and reassessment of travertine classification. Geogr Phys Quat 48:305–314
Plenkovic A (1993) Periphyton settlements and their interaction with travertine formation in lotic biotopes in Plitvice Lakes. PhD Diss, University of Zagreb, Zagreb, Croatia, 199 pp
Plenkovic A, Marcenko E, Srdoc D (1989) Periphyton growth on glass slides in aquatic ecosystem of Plitvice Lakes National Park. Periodicum Biol 91:88–89
Porter H (1861) The geology of Peterborough and its vicinity. T Chadwell, Peterborough, pp 24–28
Riding R (1990) Calcareous algae and stromatolites, Springer, Berlin Heidelberg New York
Riding R (1994) Stromatolite survival and change: the significance of Shark Bay and Lee Stocking Island subtidal columns. In: Krumbein WE, Paterson DM, Stal LJ (eds) Biostabilization of sediments, Bibliotheks und Informationssystem der Universitat, Oldenburg, pp 183–202
Riding R, Awramik SM, Winsborough BM, Griffin KM, Dill RF (1991) Bahaman giant stromatolites: microbial composition of surface mats. Geol Mag 128:227–234
Rosowski JR, Hoagland KD, Aloi JE (1986) Structural morphology of diatom-dominated stream biofilm communities under the impact of soil erosion. In: Evans LV, Hoagland KD (eds) Algal biofouling. Elsevier, Amsterdam, pp 247–299
Round FE (1981) The ecology of the algae. Cambridge University Press, London
Round FE, Sims PA (1981) The distribution of diatom genera in marine and freshwater environments and some evolutionary considerations. Ross R (ed) Proceedings of the 6th Diatom Symposium, Budapest 1–5 Sept 1980, Otto Koeltz, Koenigstein, pp 301–320
Stockner JG (1968) The ecology of a diatom community in a thermal stream. Br Phycol Bull 3:501–514
Szulc J, Smyk B (1994) Bacterially controlled calcification of freshwater Schizothrix- stromatolites: an example from the Pieniny Mts, southern Poland. In: Bertrand-Sarfati J, Monty C (eds) Phanerozoic Stromatolites II, Kluwer Academic Publishers, Boston, pp 31–51
Vos PC, de Boer PL, Misdorp R (1988) Sediment stabilization by benthic diatoms in intertidal sandy shoals. In: de Boer PL et al. (eds) Tide-influenced sedimentary environments and facies, D Reidel, Dordrecht, pp 511–526
Wallner J (1935) Diatomeen als Kalkbildner. Hedwigia 75:137–141
Westall F, Rincé Y (1994) Biofilms, microbial mats and microbe-particle interactions: electron microscope observations from diatomaceous sediments. Sedimentology 41:147–162
Winsborough BM (1990) Some ecological aspects of modern freshwater stromatolites in lakes and streams of the Cuatro Ciénegas Basin, Coahuila, Mexico. Dissertation, The University of Texas at Austin
Winsborough BM, Seeler J-S (1986) The relationship of diatom epiflora to the growth of limnic stromatoites and microbial mats. Proc 8th international diatom symposium 1984, Koeltz Scientific Books, Koenigstein, pp 395–407

Winsborough BM, Golubic S (1987) The role of diatoms in stromatolite growth: two examples from modern freshwater settings. J Phycol 23:195–201

Winsborough BM, Seeler J-S, Golubic S, Folk RL, Maguire BM (1994) Recent fresh-water lacustrine stromatolites, stromatolitic mats and oncoids from Northeastern Mexico. In: Bertrand-Sarfati J, Monty C (eds) Phanerozoic stromatolites II. Kluwer Academic Publishers, Boston, pp 71–100

Winsborough BM, Caran SC, Neely JA, Valastro S Jr (1996) Calcified microbial mats date prehistoric canals-radiocarbon assay of organic extracts from travertine. Geoarchaeology 11:37–50

Woodbury RB, Neely JA (1972) Water Control Systems of the Tehuacán Valley. In: MacNeish RS (ed) Chronology and irrigation. the prehistory of the Tehuacán Valley. TX.University of Texas Press, Austin, for the RS Peabody Foundation, 4:81–153

Carbon Isotopes and Microbial Sediments

Manfred Schidlowski

Max-Planck-Institut für Chemie (Otto-Hahn-Institut), Abt. Biogeochemie, Postfach 3060, D-55020 Mainz, Germany

Abstract. Microbial sediments of the biolaminated type, generated by the matting behavior of preferentially prokaryotic microbenthos, commonly carry the isotopic signatures of both the primary microbial biomass and of the carbonate of the surrounding sediment matrix. This is true for present-day stromatolites as well as for their fossil counterparts, which can preserve these signatures with a minor diagenetic overprint for billions of years. While the isotopic composition of the organic (kerogenous) carbon fraction may reflect the intrinsic fractionations of the microbial primary producers as well as several other parameters (productivity, temperature, salinity), the $\delta^{13}C$ and $\delta^{18}O$ labels, specifically of sub-Recent laminated stromatolitic carbonates, have encoded a wealth of palaeohydrological and palaeotemperature information which makes them important stores of palaeoclimatological data. Altogether, the stromatolitic carbon isotope record constitutes an exuberant archive of biogeochemical and palaeoenvironmental evolution that still awaits further evaluation.

1 Introduction

With their habitats usually situated at the immediate interface between the solid Earth (lithosphere) and the overlying fluid phases (hydrosphere and atmosphere), microbial ecosystems are particularly prone to transcribe their carbon isotope characteristics into newly formed sediments. While for higher life forms sediments principally serve as burial grounds, microbes have their proper domains in sedimentary and soil environments, completing their entire life cycle in intimate contact with mineral debris and the surrounding aqueous medium. Given, however, the ubiquity and abundance of allochthonous organic material at most places of sediment formation, the specific carbon isotope signatures of microbial ecosystems can only be obtained from typical sites of microbial sedimentation, such as lagoons and sabkhas, that suffer a minimum influx of organic matter from extraneous sources. In particular, the pristine carbon isotope characteristics of microbial mats and derivative sediments may be gleaned from artificial microbial ponds, where the microorganisms have been cultured under controlled conditions. The following overview examines the isotopic biogeochemistry of carbon from typical microbial sediments formed in both natural and experimental pond environments.

2 Microbially Mediated Carbon Isotope Fractionations: General Background

Biological carbon fixation is primarily the assimilation of carbon dioxide (CO_2) and bicarbonate ion (HCO_3^-) by autotrophic microorganisms and green plants. By a limited number of biochemical pathways (Table 1), all cellular components of autotrophs are synthesized from these simple inorganic carbon molecules. Like all primary producers of the present biosphere, microorganisms in general and benthic (mat-forming) cyanobacteria in particular are usually enriched in the light carbon isotope (^{12}C) as compared to the $^{13}C/^{12}C$ ratio of their feeder pool of inorganic carbon. This derives from the fact that all common pathways of autotrophic carbon fixation discriminate against heavy carbon (^{13}C) or, alternatively, favor the preferential uptake and metabolization of light carbon (^{12}C). This bias in favor of ^{12}C is principally due to kinetic isotope effects inherent in: (1) the diffusional transport of the feeder species (CO_2 or HCO_3^-) to the photosynthetically active sites within the cell or tissue, and (2) the first enzymatic carboxylation reaction of the assimilatory pathway that fixes CO_2 in the COOH (carboxyl) group of an organic acid (Park and Epstein 1960; Vogel 1980; O'Leary 1981; see also Fig. 1). While fractionations in the initial diffusion step are generally small (with the value for CO_2 diffusion in air of $-4.4‰$ representing an upper maximum), the ensuing enzymatic carboxylation reaction(s) may entail isotope discriminations of up to 30‰ and more depending on the carboxylating enzyme and the influence of environmental parameters such as pCO_2, pH, temperature, metal ion availability, and other variables that are known to influence enzymatic reactions (see, for example, Estep et al. 1978 a, b; Winkler et al. 1982; Roeske and O'Leary 1984). In this way, ^{12}C comes to be preferentially accumulated in all forms of biogenic matter as compared to the surficial pool of inorganic (oxidized) carbon represented by the terrestrial $CO_2 - HCO_3^- - CO_3^{2-}$ system.

The difference between the isotopic composition of cells and feeder substrate,

$$\Delta = \delta^{13}C_{cells} - \delta^{13}C_{substrate}$$

R.E. Riding and S.M. Awramik (Eds.)
Microbial Sediments

Table 1. Principal pathways of biological carbon fixation that are potentially relevant for the formation of microbial sediments

(1)	CO_2+ribulose-1,5-bisphosphate → phosphoglycerate Operated by: Green plants [those relying on (1) exclusively are termed *C3 plants], *eukaryotic algae, *cyanobacteria, *purple photosynthetic sulfur bacteria (Chromatiaceae), *purple nonsulfur bacteria (Rhodospirillaceae), chemoautotrophic bacteria
(2)	CO_2/HCO_3^- + phosphoenolpyruvate/pyruvate → oxaloacetate Operated by: Green plants [*C4 and *CAM species combine this reaction with (1)], anaerobic and facultatively aerobic bacteria
(3)	CO_2+CO_2 → acetyl coenzyme A/acetate Operated by: *Green photosynthetic bacteria (Chlorobiaceae) [primary CO_2 fixation via succinyl coenzyme A and α-ketoglutarate], anaerobic bacteria (*Acetobacterium woodii, Clostridium acidiurici*), *methanogenic bacteria [primary CO_2 fixation probably via C1 acceptors][a]
(4)	CO_2+acetyl coenzyme A → pyruvate/phosphoenolypruvate Operated by: *Green photosynthetic bacteria (Chlorobiaceae) [combined with (3) and (2)], *Clostridium kluyveri*, autotrophic sulfate reducing bacteria, *methanogenic bacteria[a]
(5)	CH_4 → formaldehyde (HCHO) HCHO+ribulose monophosphate → hexulose monophosphate Operated by: *Type I methanotrophic bacteria
(6)	CH_4 → formaldehyde (HCHO) HCHO+glycine → serine Operated by: *Type II methanotrophic bacteria

(1) – (4) are CO_2-fixing carboxylation reactions utilized in common autotrophic pathways. Note that reduction of CO_2 primarily gives rise to C3 compounds (with 3-carbon skeletons such as phosphoglycerate or pyruvate), C4 compounds (oxaloacetate), and C2 compounds (acetate, acetyl coenzyme A), while carbon assimilation in methanotrophic pathways (5) and (6) proceeds via a preceding oxidative transformation of CH_4 to formaldehyde (HCHO).
Groups of organisms for which carbon isotope fractionations are known are marked by an asterisk (for ranges of these fractionations, see Fig. 2).
[a] Details of the assimilatory pathway of methanogens are as yet poorly known, but the presence of both α-ketoglutarate and pyruvate synthases suggests the involvement of reactions (3) and (4).

is a convenient measure of the magnitude of ^{13}C discrimination based on the conventional δ-notation. This latter gives the per mill deviation of the $^{13}C/^{12}C$ ratio of a sample (sa) relative to that of a standard (st), i.e., $\delta^{13}C = [(^{13}C/^{12}C)sa/(^{13}C/^{12}C)st - 1] \times 1000$. The standard commonly used is Peedee belemnite (PDB) with $^{12}C/^{13}C = 88.99$.

Data on carbon isotope fractionations are available for several major groups of microorganisms, and notably cyanobacteria as the principal microbial mat builders (see O'Leary 1981; Schidlowski et al. 1983 and references therein). From a quantitative point of view, the most important isotope-selecting process carried out by the microbial world is the reductive pentose phosphate cycle or Calvin cycle, which is utilized by the bulk of photosynthetic and chemosynthetic bacteria as well as by eukaryotic algae (including colony-forming micro-algae). It is known that the Calvin cycle generally channels the bulk of the carbon transfer from the inorganic to the living world, with its principal CO_2-fixing carboxylation reaction catalyzed by the enzyme ribulose-1,5-bisphosphate (RuBP) carboxylase. Since the carboxylation product emerging from this reaction is a compound with a 3-carbon skeleton (phosphoglycerate), the corresponding assimilatory pathway has been termed C3 photosynthesis. Like the terrestrial biosphere as a whole, most microbial ecosystems and their fossil manifestations typically show the isotopic signature of C3 (or Calvin cycle) photosynthesis characterized by the sizable fractionations of the RuBP carboxylase reaction (mostly between −20 and −30‰).

Depending, however, on which of the isotope-discriminating steps (Fig. 1) and/or potentially carbon-fixing enzymatic reactions become dominant or rate-controlling in the specific instance, the isotopic composition of microbial autotrophs may vary over a considerable range. The carbon isotope characteristics of some major groups of photoautotrophic and chemo-

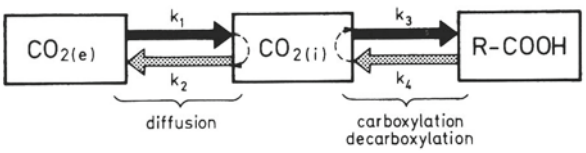

Fig. 1. The principal isotope-discriminating steps in the primary metabolism of CO_2-fixing (autotrophic) plants and microorganisms (*black* assimilatory reactions; *stippled* dissimilatory and other reverse processes; $k_1 - k_4$ are corresponding rate constants). $CO_{2(e)}$ and $CO_{2(i)}$ stand for environmental and internal (leaf- or tissue-hosted) CO_2, respectively, and *R-COOH* represents the product of the first CO_2-fixing enzymatic carboxylation reaction. In concert, these processes lead to a preferential enrichment of light carbon (^{12}C) in the synthesized biomass of the *right-hand box*. The largest single fractionation effect is commonly associated with the enzymatic carboxylation step

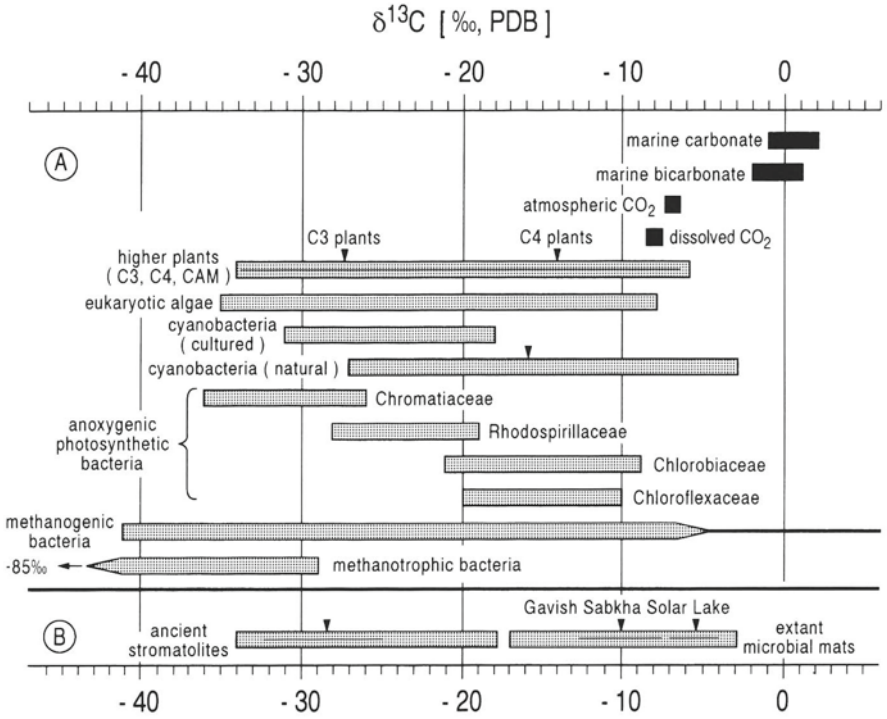

Fig. 2.A Carbon isotope spreads of major groups of higher plants and autotrophic microorganisms (*black arrows* indicate approximate means) as compared to the principal forms of inorganic carbon in terrestrial near-surface environments (adapted from Schidlowski et al. 1994). Note that cyanobacteria and selected groups of other photosynthetic bacteria serve as prime producers of isotopically heavy (^{13}C-enriched) biomass in the microbial world, while C4 species assume this role in higher plants. On the other hand, the isotopically lightest (^{13}C-depleted) biogenic matter encountered in the terrestrial biosphere has been furnished by methanotrophic bacteria (spread shown according to Freeman et al. 1990 and Summons et al. 1994). **B** Principal isotope spread of organic carbon (kerogen) from fossil laminated microbial ecosystems or stromatolites (*left*) and their contemporary counterparts in the form of benthic microbial mats (*right*). The *bar* inserted in the stromatolite band gives the mean and standard deviation (−28.5 ± 3.6‰) for 22 Precambrian stromatolites, reported by Eichmann and Schidlowski (1975), while respective *bars* in the spread of modern mats show the same for the biomass of two classical hypersaline microbial habitats (−10.0 ± 2.6‰ for Gavish Sabkha, −5.4 ± 1.1‰ for Solar Lake)

Figure 2 gives a graphic synopsis of these variations, showing the observed $\delta^{13}C$ spreads in relation to the terrestrial feeder pools of atmospheric CO_2 and marine HCO_3^-. Since the isotopic composition of atmospheric CO_2 ($\delta^{13}C = -7‰$) constitutes the base line for fractionations in the natural environment, data obtained from culture experiments relying on other carbon sources have been normalized to atmospheric CO_2.

2.1 Algae

Eukaryotic micro-algae, as potential contributors to microbial sediments, are known to operate C3 (or Calvin cycle) photosynthesis. $\delta^{13}C$ values of marine and freshwater algae are reported to range from −12 to −35‰ (e.g., Seckbach and Kaplan 1973; Smith and Epstein 1971; Wong and Sackett 1975). Algae also form the bulk of marine phytoplankton which, either directly or via consumption, will ultimately impart their isotopic composition to the total plankton population. Accordingly, the principal isotopic range of marine plankton (−18 to −31‰, Sackett et al. 1965) is likely to hold, with fair approximation, for the bulk of marine algae. Since the positive part of the spectrum shown in Fig. 2 ($\delta^{13}C > -20‰$) is not consistent with fractionations commonly obtained in Calvin cycle photosynthesis, a diffusion-limited CO_2 supply in the aquatic environment (O'Leary 1981) has been invoked for the suppression of the normal magnitudes of C3 fractionation.

2.2 Cyanobacteria

These microbial prokaryotes also carry out the C3 pathway, their naturally occurring mat communities commonly yielding $\delta^{13}C$ values between −8 and −21‰, with an average around −16‰ (Behrens and Frishman 1971; Calder and Parker 1973; Smith and Epstein 1971). Fractionations reported for cultured taxa were sometimes in excess of those observed in the natural environment (Pardue et al. 1976), with maximum values approaching −31‰ (normalized to atmospheric CO_2 with $\delta^{13}C = -7‰$ as carbon source). It is worth noting that the isotopically heaviest biomass (−3.5‰) hitherto encountered in the Earth's biosphere has been furnished by benthic cyanobacterial communities from two hypersaline environments (Solar Lake and Gavish Sabkha), both representing near-coastal brine pools on the shore of the Sinai Peninsula (Schidlowski et al. 1985; see also Sect. 3, below).

2.3 Photosynthetic Bacteria

Purple photosynthetic sulfur bacteria (Chromatiaceae) that presumably carry out the Calvin cycle have furnished fractionations consistent with isotope discriminations in the RuBP carboxylase reaction (see Fig. 2). $\delta^{13}C$ values of autotrophically grown cultures of *Chromatium* sp. were found to range between −30 and −36‰ (Wong et al. 1975), while single values reported by Sirevåg et al. (1977) and Quandt et al. (1977) for this purple sulfur bacterium were −29.5 and −26.6‰, respectively (normalized to atmospheric CO_2). Corresponding figures obtained for purple nonsulfur bacteria (Rhodospirillaceae) and specifically *Rhodospirillum rubrum* were −27.5‰ (Sirevåg et al. 1977) and −19.4‰ (Quandt et al. 1977), also suggesting an involvement of the RuBP carboxylase reaction. On the other hand, green photosynthetic bacteria (Chlorobiaceae) that operate the reductive carboxylic acid cycle or reverse Krebs cycle (a pathway unique to photosynthetic prokaryotes relying on ferredoxin-linked carboxylations that fix CO_2 as α-ketoglutarate and acetyl coenzyme A) have yielded consistently lower fractionations (Fig. 2). Sirevåg et al. (1977) and Barghoorn et al. (1977) have reported values of −19.2 and −20.8‰ for *Chlorobium thiosulfatophilum*, while Quandt et al. (1977) give a range of −9.5 to −12.2‰ for various species of this bacterium (all values recalculated for atmospheric CO_2 as carbon source). Hence, discrimination against ^{13}C appears to be decidedly less effective in this pathway than in the Calvin cycle, with the intrinsic fractionation of neither of the primary carbon-fixing reactions probably exceeding the maximum recorded in the assimilatory pathway as a whole (about −14‰ which would translate into −21‰ in the natural environment where atmospheric CO_2 as feeder substrate is close to −7‰). The isotopic composition of autotrophically grown flexibacteria (Chloroflexaceae) falls approximately into the same range (Fig. 2).

2.4 Methanogenic Bacteria

Isotope data for methanogens were primarily obtained from experimental work with *Methanogenium thermoautotrophicum*, a strictly anaerobic chemoautotrophic species growing on CO_2 and H_2 as the only carbon and energy sources. Normalized to atmospheric CO_2 ($\delta^{13}C = -7$‰) as the feeder substance, the fractionations reported by Fuchs et al. (1979) would give a range between −41 and +6‰ for the bulk biomass synthesized (it should be noted that the heavy values were obtained in the late stages of a batch process when most of the CO_2 source had already been converted to biomass and CH_4, the latter with an extreme preference for ^{12}C). On the other hand, growth experiments performed by Belyaev et al. (1983) on continuous cultures of *Methanobacterium* sp. gassed with carbon dioxide of constant isotopic composition at relatively high flow rates have yielded a much narrower fractionation range (−24 to −18‰) between feeder CO_2 and harvested cells. These latter fractionations coincide with the mainstream of respective values observed by Fuchs et al. (1979), and we may reasonably assume that ^{13}C /^{12}C differences of this magnitude (which translate into a range −25 to −31‰ for the cell material when normalized to atmospheric CO_2 as the feeder substrate) should be characteristic for the bulk of methanogenic biomass generated in natural habitats.

2.5 Methanotrophic Bacteria

Type I methanotrophs (*Methylococcus capsulatus* and *Methylomonas methanica*) utilizing the ribulose monophosphate cycle (see Table 1) and grown in cultures on pure CH_4 have yielded negative ^{13}C fractionations between 16 and some 30‰ in the synthesized biomass (Summons et al. 1994), with an additional shift of −10 to −14‰ displayed by selected metabolites, notably of the lipid fraction. In general, methanotrophic bacteria have furnished the isotopically lightest (most ^{12}C-enriched) biomass ever encountered in the terrestrial biosphere, with maximum fractionations up to about −80‰ in specific biomarker-type lipids of methanotrophic pedigree (Freeman et al. 1990). We may, therefore, reasonably assume that some "superlight" kerogen fractions, as primarily noted in Precambrian sediments (Schoell and Wellmer 1981; Schidlowski et al. 1983; Hayes et al. 1983), were derived from microbial ecosystems dominated by methanotrophic bacteria.

3 Isotopic Biochemistry of Carbon in Modern Microbial Mats

Paradoxically, early investigations of the carbon isotope chemistry of contemporary microbial ecosystems were encouraged by previous work on their fossil precursors, specifically the geologically oldest stromatolite occurrences from selected Archaean terrains (Hoering 1967). As was to be expected, laminated microbial communities from present-day habitats were found to display the same bias in favor of the light carbon isotope that is typical of autotrophic carbon fixation in general, albeit, surprisingly, with a markedly reduced magnitude. In fact, within the broad spectrum of negative $\delta^{13}C_{org}$ values that characterize the present biosphere, the isotopically heaviest biomass hitherto encountered was furnished by benthic microbial communities (Fig. 2b).

A pioneering study by Behrens and Frishman (1971) on cyanobacterial mats from Baffin Bay, Texas, yielded $^{13}C_{org}$ values around −16‰ [PDB] for the bulk organic matter of these microbial communities. Subsequent investigations by Calder and Parker (1973), Seckbach and Kaplan (1973), Barghoorn et al. (1977) and Estep (1984) performed on the benthic microbial ecosystems from various marine, freshwater and hot spring environments furnished values of −5 to −21‰, with a clustering of data points between −8 and −12‰. Values obtained for cultured cyanobacterial mats (Calder and Parker 1973; Pardue et al. 1976) were typically in excess of those from natural environments, with maximum fractionations observed in cultures grown at elevated pCO_2 (>0.5%) and low cell densities. Altogether, naturally occurring benthic microbial communities proved to be distinctly enriched in heavy carbon compared to average terrestrial biomass (Fig. 2).

A major revival and proliferation of relevant investigations commenced during the mid-1980s, with the focus on Solar Lake and Gavish Sabkha as two classical microbial habitats on the eastern shore of the Sinai Peninsula (Aizenshtat et al. 1984; Schidlowski et al. 1984, 1985). These studies decidedly confirmed the conspicuous slant towards ^{13}C enrichment in extant benthic microbial communities, with the Solar Lake ecosystem furnishing the isotopically heaviest biomass as yet encountered in the terrestrial biosphere. Solar Lake mats yielded an average $\delta^{13}C_{org}$ of -5.4 ± 1.1‰ [PDB] and a maximum positive single value of −3.5‰ (Schidlowski et al. 1985; see also graphic summary in Fig. 2b). Pooled with the results of similar work by DesMarais et al. (1989) on the microbial community of the Guerrero Negro salt pond of Baja California (Mexico), a formidable database had accumulated, prompting the quest for possible reasons for the remarkable degree of ^{13}C-enrichment in the microbial biomass of these and related hypersaline habitats. This quest seemed the more acute since it had been firmly established by many investigators (e.g., Schopf et al. 1973; Eichmann and Schidlowski 1975; Schidlowski et al. 1975) that the great majority of $\delta^{13}C_{org}$ values for fossil (and specifically Precambrian) stromatolites fell into the common spread of biogenic carbon between −20 and −30‰ (see Fig. 2b).

At the heart of the problems posed by the glaring mismatch between the isotope spreads of organic carbon from ancient and modern microbial ecosystems is the fact that the quantitatively predominant cyanobacterial population of these benthic communities is known to sequester carbon by the C3 pathway (Fuchs and Stupperich 1981; O'Leary 1981), characterized by the sizable isotope fractionations inherent in the RuBP carboxylase reaction of the Calvin cycle [Table 1, reaction (1)]. For instance, among the mat-building photosynthetic prokaryotes thriving in the Sinai habitats, coccoid and filamentous cyanobacteria clearly figure as the prevalent primary producers, with just minor admixtures of other prokaryotic and eukaryotic elements (see Krumbein and Cohen 1977; Cohen et al. 1980; Friedman and Krumbein 1985), and the same actually holds for all other benthic microbial ecosystems hitherto investigated. With these facts established, the crucial question is why the sizable fractionations of the RuBP carboxylase reaction are not manifest in the average isotopic composition of the microbial biomass from these habitats. To explain this apparent paradox, brief reference to Fig. 1 will be helpful.

As can be inferred from Fig. 1, the total magnitude of the fractionation effect inherent in photosynthetic carbon fixation is a composite of the fractionations that occur at two cardinal steps in the primary metabolism of autotrophs: (1) the diffusion of external CO_2 to the carboxylation sites of the photosynthetic apparatus, and (2) the first enzymatic reaction incorporating CO_2 into the carboxyl (COOH) group of an organic acid. Since assimilation rates commonly exceed by several times those of potential reverse (dissimilatory) reactions (such as decarboxylation in photorespiration), the gross isotopic composition of the organism is principally determined by these two processes. Further metabolic processing of the primary carboxylation product gives rise only to limited internal isotopic imbalance among individual metabolites without affecting the isotopic composition of the organism as a whole.

As set out in the previous section, the kinetic isotope effect imposed on the initial diffusion step is very small (with a maximum of −4.4‰), while fractionations in the subsequent carboxylation step are large when RuBP carboxylase serves as the main carboxylating enzyme, with values between −28‰ and −39‰ obtained from in vitro experiments with the pure enzyme isolated from selected eukaryotic (diatoms) and prokaryotic microorganisms (Estep et al. 1978a,b). Since the fractionations actually observed result from an interplay of the diffusional and enzymatic processes, we may envision two limiting scenarios: given an affluence of feeder carbon at the photosynthetically active sites, the intrinsic fractionation of the carboxylating enzyme should be fully expressed in the newly generated biomass, whereas, with the preceding diffusion step as the rate-limiting process, the small fractionations inherent in the diffusional transport of CO_2 should be imparted to the organic substance. With these constraints in mind, we may reasonably infer that the extreme enrichment of ^{13}C in the microbial carpets lining the sediment-water interface, notably in sabkha-type (lagoonal) habitats, must be due to a diffusion-limited assimilatory pathway in which retarded CO_2 logistics are responsible for a largely indiscriminate assimilation of all feeder carbon reaching the photosynthetic centres with a minimum of isotopic fractionation (Schidlowski et al. 1984, 1985). Consequently, the sizable fractionations of the

RuBP carboxylation reaction are bound to remain cryptic in a diffusion-limited pathway as they do in the compartmentalized biochemistry of C4 plants. In fact, the approximate coincidence of the isotope spreads of microbial photoautotrophs from aquatic environments with those of C4 plants (see. Fig. 2) argues persuasively for a straightforward analogy between the respective assimilatory pathways, involving, in both cases, a transduction of CO_2 to the photosynthetically active sites with little fractionation relative to the feeder substrate and a subsequent quantitative processing in the Calvin cycle under quasi-closed conditions.

While the work on the Sinai mats had established the crucial role of a diffusion- or supply-limited pathway for the generation of isotopically superheavy organic carbon, there remained a number of residual questions as to the specific factors responsible for making the initial diffusion step the bottleneck in the carbon uptake by aquatic photoautotrophs. Given a $\delta^{13}C$ value of −7‰ for atmospheric CO_2 as the ultimate feeder substrate, observed $^{13}C_{org}$ ranges in the mats were decidedly consonant with the highly reduced or even minuscule fractionations to be expected in diffusional carbon transport. It should be noted that the maximum kinetic isotope effect of −4.4‰ assigned to the diffusion step is the value for CO_2 diffusion in air. This gaseous effect is commonly modulated in the natural environment by dissolution, hydration and liquid transport of CO_2, all bringing down actual fractionations well below this maximum. Since liquid diffusion is considerably slower than the gaseous variant, the concomitant isotope effect is markedly reduced (between −3.2 and −1.6‰; see Vogel 1980) or may even approach unity within a few tenths of a per mill (O'Leary 1981). It is noteworthy that the minor fractionations associated with liquid diffusion of CO_2 had already been noted in aquatic plants such as sea grasses (Benedict et al. 1980). With the ^{13}C value of atmospheric CO_2 (−7‰) as reference, the exceptional mean of −5.4 ± 1.1‰ obtained for the Solar Lake mats might even indicate a reversal in the direction of the fractionation, but a large-scale involvement of isotopically heavy bicarbonate ion in the carbon logistics of the local ecosystem seems a more plausible alternative since cyanobacteria specifically have been shown to activate HCO_3^- ions as a carbon source (Badger 1987). In any case, there is little doubt that in the diffusion-limited assimilatory pathway of aquatic microorganisms carbon may be pushed into the role of a limiting nutrient, with a CO_2 shortage enforcing an isotopically indiscriminate metabolization of available carbon supplies.

With the generation of extremely heavy biomass thus ostensibly contingent on the assumption of a diffusion-limited assimilatory pathway, we had tentatively ascribed the CO_2 limitation of the microbial autotrophs from sabkha-type habitats to dramatically decreasing CO_2 solubilities in response to increasing salinity and temperature, which are bound to make CO_2 a rare commodity in heliothermal brines (Schidlowski et al. 1984, 1985). Given the inverse relationship between ionic strength and the quantity of dissolved CO_2 in hypersaline solutions, a plausible case could be made that salinity served as the principal steering variable for the synthesis of isotopically heavy biomass. However, the results of related work by Des Marais et al. (1989) on a brine habitat from the coast of Baja California displaying a crude salinity gradient seemed to caution against this explanation. For conclusive answers to these questions, a hypersaline habitat with a well-defined salinity gradient was obviously needed. This would allow quantitative correlation of changes in the isotopic composition of the benthic microbial mat with corresponding changes in salinity, temperature and other relevant environmental background parameters.

For this kind of investigation, the commercially utilized hypersaline, heliothermal or "solar" ponds (Tabor 1981; Kirkland et al. 1983), operated by Solmat Systems, Ltd., at the northern shore of the Dead Sea (Israel), seemed to be the ideal test grounds. These ponds permit monitoring, at fairly high resolution patterns, of the growth and isotopic composition of a standing cyanobacterial mat community as a function of narrowly constrained gradients of environmental (salinity, temperature, pH, luminosity) and biological (community composition, population density, productivity) parameters, thereby offering the prospect of identifying those variable(s) ultimately responsible for the generation of isotopically heavy biomass. Relevant investigations carried out on newly established (juvenile) cyanobacterial mats from such experimental ponds (Dor et al. 1992; Schidlowski et al. 1992, 1994) were indeed successful in this respect, furnishing conclusive evidence that salinity is not the principal factor controlling the synthesis of heavy biomass. Hence, the CO_2 limitation ultimately responsible for ^{13}C enrichment in the benthic mat must be enforced by other agents.

The experimental ponds utilized in this work were made up of concentrated Dead Sea brines, with artificial stratification induced by dilution with fresh water. This procedure resulted in the buildup of an inversely stratified water column (Fig. 3). The principal compartments of such ponds are: (1) an upper convective layer of highly diluted Dead Sea water ("epilimnion") of low salinity, with temperatures reflecting those of the surroundings (including seasonal variations), (2) a nonconvective transition zone comprising a sharp halocline and an *inverted* thermocline, and (3) a nonconvective and basically anoxic bottom layer ("hypolimnion") of highly concentrated brine (≤ 400 g/l) with temperatures approaching 60 °C at the pond bottom. A peculiar feature of nonconvective stratified water bod-

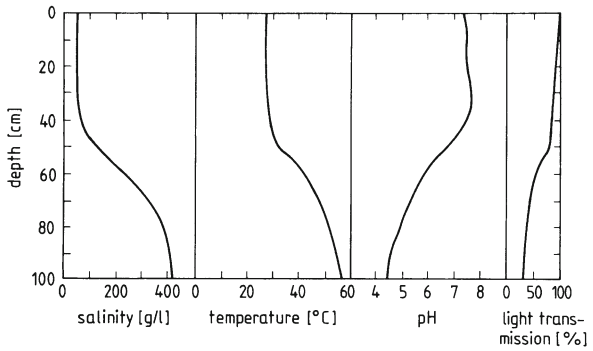

Fig. 3. Depth functions of the principal environmental background parameters in an experimental Dead Sea pond that affect microbial mat development along the pond profile. Variables shown reflect the physical environment of the microbial community whose biogeochemical characteristics are presented in Fig. 4. Attention is called to the sharp halocline and inverse thermocline that separate the upper littoral (epilimnic) compartment with exuberant mat development from the basal hypolimnic bottom stratum in which microbial activity is gravely impaired by extreme temperatures and salinities

ies of such kind is their inverse temperature gradient (i.e., the increase in temperature with depth) due to the harvesting by the hypolimnic brine compartment of formidable amounts of heliothermal energy.

Figure 4 gives a graphic summary of the response patterns of a number of biogeochemical key parameters (including $\delta^{13}C_{org}$) in a juvenile microbial mat lining the floor of a newly established pond that had been subjected to the environmental gradients shown in Fig. 3. The microbial carpet was basically made up of various strains of a single cyanobacterial species (*Aphanothece halophytica*) with a minor (but more diverse) diatom component, particularly in the littoral pond segment above the combined halo- and thermoclines. The visible lush-green mat appeared to gradually peter out upon entering the increasingly inhospitable gradient zone at a depth of 40–60 cm and the underlying hypolimnic stratum of high temperature and salinity. The visual evidence for this was excellently mirrored by the results of organic carbon and chlorophyll-a assays conducted along the depth profile (see Fig. 4a,b).

As can be inferred from the isotope traverses measured for organic carbon and carbonate carbon over the depth profile (Fig. 4c), $\delta^{13}C_{org}$ is clearly correlated with the depth functions of a number of productivity-related biological parameters, such as the C_{org} and chlorophyll-a content of the local mat sample, and with recorded cell densities. A corresponding trend for $\delta^{13}C_{carb}$ is largely blurred but emerges, albeit in dampened form, in an enlargement of the $\delta^{13}C_{carb}$ depth function (Fig. 4d). All biogeochemical parameters show a *prima facie* dependence on the changing temperature-salinity regimes over the pond profile (Fig. 3), which was obvious already from visual examination of the mat. As a whole, the distribution functions of the bio-

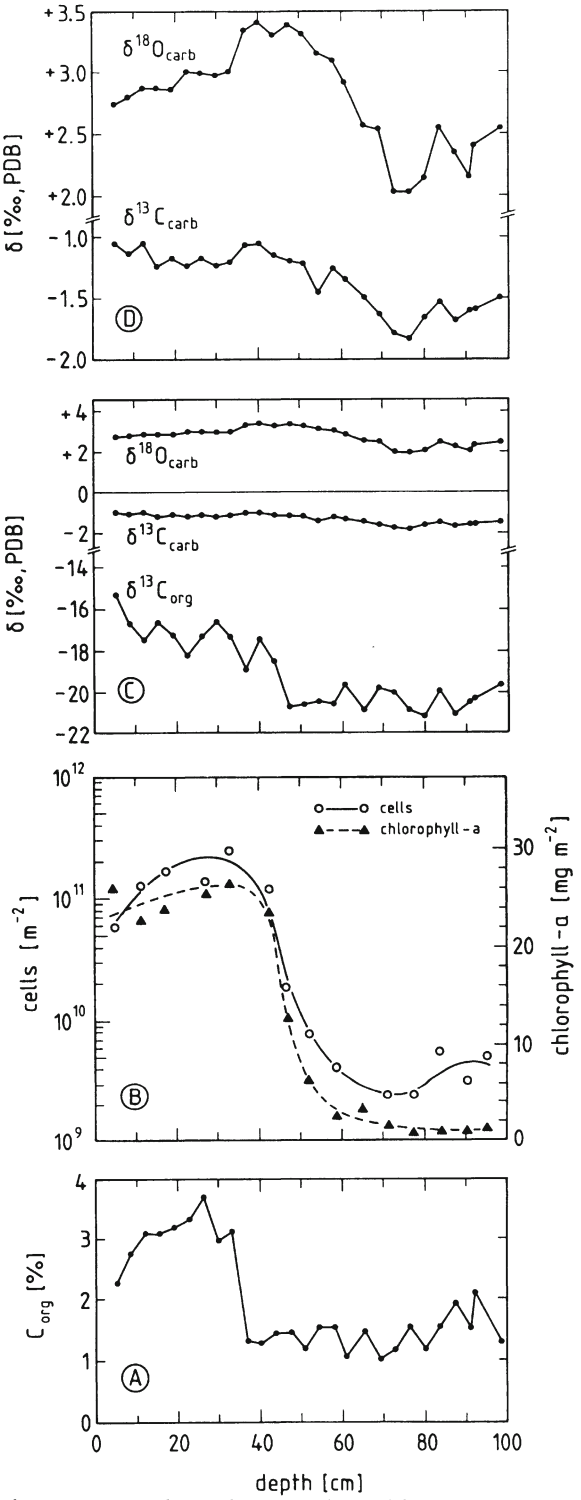

Fig. 4A–D. Biogeochemical traverse obtained for a juvenile microbial mat grown on the slope of a Dead Sea experimental pond characterized by the environmental background parameters shown in Fig. 3. **A** Organic carbon content of local mat sample and associated sediment. **B** Results of cell counts and content of chlorophyll-a. **C** Isotopic composition of organic carbon, carbonate carbon and carbonate-bound oxygen over the depth profile. **D** Enlargement of $\delta^{13}C_{carb}$ and $\delta^{18}O_{carb}$ functions from **C** to visualize small-scale trends of the respective isotope curves

geochemical parameters displayed in Fig. 4 match the visually perceptible changes of the microbial ecosystem over the pond profile with a remarkable degree of resemblance. Measured values were highest in the littoral zone of optimum mat development, then plummeted in the transition zone in correspondence with the conspicuous attenuation of the microbial carpet, and stabilized at low levels in the hypolimnic compartment where harsh environmental conditions evidently curb the proliferation of photoautotrophic microbenthos.

In combination with the environmental gradients of Fig. 3, the above index functions of microbial mat development along the pond profile give a clear indication of the factor promoting the synthesis of isotopically superheavy biomass. As demonstrated in Fig. 4c, the $\delta^{13}C_{org}$ values of the benthic mat show a general decrease from −15‰ at the pond margin to a minimum approaching −22‰ close to the center in the hypolimnic stratum. Though beset with second-order oscillations, the overall decline of the $\delta^{13}C_{org}$ depth function reflects corresponding trends in the productivity-related parameters (Fig. 4a,b), including their pronounced plummeting in the transition zone between the pond's upper and lower compartments. Evidently, the microbial biomass becomes progressively depleted in heavy carbon as the mat thins out and disappears with increasing depth which, in turn, corresponds with increasing temperature and salinity of the water body. These observations constitute conclusive proof that ionic strength cannot serve as the principal controlling variable for the production of ^{13}C-enriched microbial biomass in these and related brine habitats, since $\delta^{13}C_{org}$ values actually *decrease* with increasing salinity (see Figs. 3, 4c). While evidently contributing to the severe CO_2 depletion typical of heliothermal brine environments, decreased CO_2 solubility in hypersaline waters obviously cannot be invoked as a first-order control on the generation of isotopically heavy biomass.

By contrast, the comparative data set of Fig. 4 shows that high values of $\delta^{13}C_{org}$ are demonstrably coupled with maxima in biomass density (or mat development) as reflected by the C_{org} content of the local mat segment, cell counts and chlorophyll-a assays, of which the last two represent productivity-related parameters. Conversely, low $\delta^{13}C_{org}$ values, as encountered in the transition zone and the underlying hypolimnion, go along with minima in these productivity index functions. With these correlations at hand, there is little doubt that productivity is actually the main driving factor inducing photoautotrophic microbenthos to engage in the production of ^{13}C-enriched biomass. While an auxiliary function of high rates of productivity in the synthesis of heavy organic matter had already been inferred before (O'Leary 1981; Schidlowski et al. 1984), first results of relevant work from the Dead Sea experimental ponds (Schidlowski et al. 1988, 1989) clearly reflected the key role of productivity, which had also emerged in the work by DesMarais et al. (1989) in a natural microbial habitat. By analogy, we may assume that high rates of primary productivity were also responsible for the heavy microbial biomass reported from Antarctic freshwater environments (Wand and Mühle 1990; Böttger et al. 1993).

Altogether, the database assembled in Fig. 4 fully justifies the conclusion that the excessive CO_2 demand of the microbial mat in the pond's littoral segment caused by high rates of productivity could be satisfied only by an isotopically indiscriminate assimilation of CO_2 from the local inorganic carbon pool. In eutrophicated environments such as sabkhas, thriving microbial communities will utilize heavy carbon in particular, since excessive availability of phosphorus can push carbon into the exceptional role of a limiting nutrient. Under such conditions, any large-scale discrimination against ^{13}C apparently becomes a luxury for the microbial community, with the constraints of a diffusion-limited CO_2 supply consequently leading to a suppression of the intrinsic fractionations of the RuBP carboxylase reaction as the principal isotope-discriminating process in the primary metabolism of the resident cyanobacterial community. Summing up, the generation of ^{13}C-enriched microbial biomass can be explained as a habitat-specific metabolic response by microbial autotrophs to an acute shortage of inorganic feeder carbon in eutrophicated environments favoring high rates of primary productivity. It should be noted that microbial mats dominated by photoautotrophic prokaryotes have been shown to figure among the most productive ecosystems, with maximum performances of 8–12 g C_{org}/m^2 per day in the case of the Solar Lake community (see Krumbein and Cohen 1977; Cohen et al. 1980).

4 Isotopic Biogeochemistry of Carbon in Fossil Microbial Mats

As mentioned above, the quest for the biogenicity of the oldest laminated sedimentary structures of suspected microbial origin triggered the initial inquiries into the isotopic biochemistry of carbon in both ancient and Recent biolaminites, with investigations of the fossil forms considerably predating those of their modern counterparts. In fossil stromatolites, the residual organic substance of the original mat is preserved in the form of "kerogen", a chemically inert (acid-insoluble), polycondensed aggregate of aromatic and aliphatic hydrocarbons which represents the end-product of the diagenetic alteration of primary biogenic matter in sediments (Durand 1980) and commonly encodes the isotope label of the organic precursor substances with little change (Hayes et al. 1983; Schidlowski et al. 1983). With the bulk of stromatolites made up of carbonates,

this usually offers an opportunity to determine $^{13}C/^{12}C$ fractionations between coexisting carbonate and organic carbon and to subsequently utilize the diagnostic potential of this particular parameter.

Having been regarded for many years as the oldest and most reliable morphological evidence of life on Earth, Precambrian (and specifically Archaean) stromatolites were bound to be singled out as prime targets for carbon isotope studies. After preliminary studies by Hoering (1967) and Schopf et al. (1971) had called attention to the subject of isotopic fractionation between C_{org} and C_{carb} in geologically old stromatolites, Schidlowski et al. (1975), and notably Eichmann and Schidlowski (1975), subsequently generated a formidable database, which was further augmented by Hayes et al. (1983) and Schidlowski et al. (1983). As a result of these efforts, we know that isotopic fractionations between the kerogenous constituents and carbonate in ancient stromatolites scatter over roughly the same range of $\delta^{13}C$ values as they do in the average sediment (with a difference of 25–30‰), displaying perhaps a slight slant towards maximum values in the Archaean segment of the record that may be indicative of a methanotrophic component within the respective kerogens. For instance, a fair proportion of the kerogen values obtained for Macgregor's (1940) classical stromatolite occurrence from the Bulawayan Group (about 2.7 Ga) of Zimbabwe goes well below the −30‰ limit that commonly terminates the bulk of $\delta^{13}C_{org}$ values furnished by the living world, whereas the $\delta^{13}C_{carb}$ values of the host limestone are closely tethered to the zero per mill line (see Schopf et al. 1971; Eichmann and Schidlowski 1975). While the isotope data hitherto available for the kerogen constituents of most other Archaean stromatolites fall into the broader spread of the Bulawayan province (see Hayes et al. 1983; Walter 1983), selected stromatolite occurrences and their respective host sequences (such as those from the South African Insuzi Group and the Canadian Yellowknife Supergroup) contain distinctly heavier kerogens, with $\delta^{13}C_{org}$ values between −16 and −9‰ approaching those commonly encountered in modern microbial ecosystems. As a whole, however, the residual organic matter from the oldest microbial ecosystems comes fairly close to the average for the terrestrial biosphere as is attested, inter alia, by the mean of −28.5 ± 3.6‰ obtained for 22 Precambrian stromatolite samples (see Fig. 2b) that were included in the survey of Eichmann and Schidlowski (1975). Incidentally, these and related findings had prompted early conclusions that the overall fractionation factor governing biological fixation of inorganic carbon had been virtually constant over >3 Ga of geological history.

Apart from the well-documented isotope inventories of the geologically oldest microbial ecosystems, references to the carbon isotope geochemistry of fossil microbial benthos from Proterozoic and Phanerozoic formations are casual and scarce (for exceptions see Schidlowski et al. 1975; Banerjee et al. 1986; Andrews 1986; Sathyanarayan et al. 1987; Höhn 1989; Wright 1993). If part of a stromatolite or isotope stratigraphic study, the focus of carbon isotope work is commonly on the carbonate matrix of the biolaminated structures rather than their kerogen fraction because of the diagnostic potential of the carbonate values for facies analysis [generally, $\delta^{13}C_{carb}$ values close to zero per mill characterize marine carbonates, while averages slanted towards negative and positive values are indicative of freshwater and stagnant (evaporitic/lagoonal) environments, respectively]. Rare data for kerogen occasionally reported were found to mostly fall into the mainstream of sedimentary organic matter, between −20 and −30‰ (e.g., Höhn, 1989). A noteworthy example of a stromatolite province characterized by heavy kerogen constituents are the phosphate-bearing stromatolites of the Proterozoic Aravalli Supergroup of Peninsular India, with a $\delta^{13}C_{org}$ mean of −15.1 ± 2.9‰ (Banerjee et al. 1986). Incidentally, the Aravalli province seems to host one of the few stromatolite communities whose kerogen fraction conforms in isotopic composition with the organic matter commonly encountered in Recent microbial bioherms (see Sect. 3).

In contrast to the general paucity of isotope data for the currently known Phanerozoic stromatolite record, several carbon isotope surveys of geologically young (Tertiary and Quaternary) stromatolite-bearing sequences have been lately conducted that were specifically conceived with the aim of obtaining comprehensive sets of palaeoenvironmental and palaeoclimatological information. Examples are the investigations by Zamarreño et al. (1997) and Arenas et al. (1993, 1997) on non-marine stromatolite-bearing sequences from the Paleocene/Eocene and Miocene, respectively, of the Ebro Basin (Spain), as well as related work by Travé (1992) on the terminal Eocene from the same area. Particularly noteworthy are high-resolution carbon and oxygen isotope studies of sections of lacustrine stromatolites of Late Holocene (in part sub-Recent) age from several African tropical lakes (Casanova and Hillaire-Marcel 1992, 1993). This latter work decidedly served to prove the utility of Quaternary laminated microbialites as palaeoclimatological and palaeohydrological archives, with $^{13}C/^{12}C$ and $^{18}O/^{16}O$ of the carbonate laminae reflecting some basic hydrological parameters of the aquatic habitat of the original microbial mats. Specifically, the $\delta^{13}C_{carb}$ values broadly preserve the isotopic signature of dissolved inorganic carbon (DIC) in the primary aquatic medium with its inherent diagnostic potential, while the $\delta^{18}O_{carb}$ label of the carbonate-bound oxygen provides information on the temperature and residence time of the original water body. The results obtained in these and related investigations (e.g., Andrews et al. 1993, 1997) point to the con-

siderable potential of laminated microbial ecosystems as recorders of palaeoclimatological information notably for the most recent geological past.

5 Problems of the Stromatolitic Carbon Isotope Record

An intriguing question posed by the $\delta^{13}C_{org}$ record of stromatolitic bioherms through geologic time is the conspicuous mismatch between the carbon isotope spreads of modern and ancient microbial ecosystems (see Fig. 2b). While the ^{13}C-enriched organic carbon typical of contemporary benthic communities has its counterpart in some fossil stromatolite occurrences (such as those from the mid-Proterozoic phosphorite-bearing Aravalli Province of India), the great bulk of the kerogenous materials from fossil (specifically Precambrian) microbialites falls into the range of "normal" organic carbon (between −20 and −30‰) or even below. Since a whole generation of early stromatolite students had been stunned by this discrepancy, a brief discussion of this problem might be in order.

As pointed out above (Sect. 3), the generation of isotopically heavy microbial biomass currently proceeds in hypersaline lagoonal or sabkha-type habitats where it is apparently dictated by a set of forcing variables that permit high rates of primary productivity at the expense of an extraordinary drain on the local feeder pool of DIC. Given the habitual eutrophication of such coast-marginal brine pools with regard to otherwise critical nutrients (notably phosphorus), the excessive rates of primary productivity sustained by the resident microbial communities tend to push carbon into the role of a rare commodity, with the resulting CO_2 limitation enforcing a large-scale utilization of the isotopically heavy species from the local DIC pool. Since heterotrophic grazers are largely barred from these pools by high salinities, sabkha-type habitats have come to figure as prime sanctuaries for extant microbial communities, with the bulk of well-developed benthic microbial ecosystems of the present world consequently showing the isotopic signature of the severe CO_2 limitation prevailing in their aquatic environment.

Against such a neobiological background, an assessment of the mismatch between the $\delta^{13}C_{org}$ ranges of ancient (notably Precambrian) and contemporary stromatolites is considerably facilitated. Having fair proof that the ^{13}C-enrichment in modern microbial mats is not intrinsic to the assimilatory pathway of the microbial photoautotrophs, but rather results from the CO_2 depletion that characterizes their hypersaline host habitats in the present world, a good case can be made that the increased $\delta^{13}C_{org}$ values represent the environmental signature of the ecological sanctuaries into which benthic cyanobacterial ecosystems had to retreat after heterotrophic Metazoa had burst upon the scene at the close of the Precambrian (see Glaessner 1983). Hence, the buildup of ^{13}C-enriched biomass by extant microbial ecosystems could be primarily a response to the severe degree of CO_2 depletion in their hypersaline aquatic environments. There is little doubt that an elimination of the diffusion barrier responsible for a retarded CO_2 supply (by either a decrease in CO_2 demand, or an increase in ambient CO_2 pressure) would automatically reinstate the first enzymatic carboxylation reaction of the photosynthetic pathway as the dominant isotope-discriminating step, with a corresponding increase in carbon isotope fractionation. A convincing validation of this interpretation is furnished by culture experiments in which cyanobacteria (Calder and Parker 1973; Pardue et al. 1976) as well as green algae (Vogel 1980) were grown under partial pressures of CO_2 that were markedly increased as compared to present atmospheric levels ($pCO_2 \approx 0.03\%$). In both cases, the $\delta^{13}C_{org}$ values of the microbial biomass were found to cover a range fully compatible with average fractionations in the C3 pathway.

Hence, if the principal biotopes conducive to an optimum proliferation of microbial ecosystems in the present world were not sabkha-tpye hypersaline wetlands, in which high degrees of primary productivity commonly correspond with retarded CO_2 logistics, the actual carbon isotope fractionations in such ecosystems might well approach the normal range of the RuBP carboxylase reaction. A reduced performance or even absence of a diffusion barrier as rate-limiting agent in the assimilatory pathway of microbial autotrophs would be readily conceivable during the early history of the Earth when, in the absence of grazing stress imposed by metazoan invaders, the emplacement of microbial ecosystems could take place in the normal marine realm instead of being relegated to hypersaline niches. Alternatively, diffusion limitation of CO_2 supply might have been overwhelmed by higher partial pressures of carbon dioxide in the Precambrian atmosphere, as proposed by Mizutani and Wada (1982). In principle, both the above processes (or their combination) could account for the disparity in the observed isotope spreads of organic carbon between Precambrian stromatolites and their modern analogs.

References

Aizenshtat Z, Lipiner G, Cohen Y (1984) Biogeochemistry of carbon and sulfur cycle in the microbial mats of the Solar Lake (Sinai). In: Cohen Y, Castenholz RW, Halvorson HO (eds) Microbial mats: stromatolites (MBL Lectures in Biology 3). A R Liss, New York, pp 281–312

Andrews, JE (1986) Microfacies and geochemistry of middle Jurassic algal limestones from Scotland. Sedimentology 33:499–320

Andrews JE, Riding R, Dennis PF (1993) Stable isotopic composition of Recent freshwater cyanobacterial carbonates from the British Isles: local and regional environmental controls. Sedimentology 40:303–314

Andrews JE, Riding R, Dennis PF (1997) The stable isotope record of environmental and climatic signals in modern terrestrial microbial carbonates from Europe. Palaeogeogr Palaeoclimatol Palaeoecol 129:171–189

Arenas C, Pardo G, Casanova J (1993) Bacterial stromatolites in lacustrine Miocene deposits of the Ebro Basin (Aragón, Spain). In: Barattolo F, de Castro P, Parente M (eds) Studies on fossil benthic algae. Boll Soc Paleont Ital Spec Vol 1. Mucchi Editore, Modena, pp 9–22

Arenas C, Casanova J, Pardo G (1997) Stable isotope characterization of the Miocene lacustrine systems of Los Monegros (Ebro Basin, Spain): palaeogeographic and palaeoclimatic implications. Palaeogeogr Palaeoclimatol Palaeoecol 128:133–155

Badger MR (1987) The CO_2-concentrating mechanism in aquatic phototrophs. Biochem Plants 10:219–274

Banerjee DM, Schidlowski M, Arneth JD (1986) Genesis of upper Proterozoic-Cambrian phosphorite deposits of India: isotopic inferences from carbonate fluorapatite, carbonate and organic carbon. Precambrian Res 33:239–253

Barghoorn ES, Knoll AH, Dembicki H, Meinschein WG (1977) Variation in stable carbon isotopes in organic matter from the Gunflint iron formation. Geochim Cosmochim Acta 41:425–430

Behrens EW, Frishman SA (1971) Stable carbon isotopes in blue-green algae mats. J Geol 79:94–100

Belyaev SS, Wolkin R, Kenealy WR, De Niro MJ, Epstein S, Zeikus JG (1983) Methanogenic bacteria from the Bondyuzhskoe oil field: general characterization and analysis of stable carbon isotopic fractionation. Appl Environ Microbiol 45:691–697

Benedict CR, Wong WWL, Wong JHH (1980) Fractionation of the stable isotopes of inorganic carbon by seagrasses. Plant Physiol 65:512–517

Böttger T, Schidlowski M, Wand U (1993) Stable carbon isotope fractionation in lower plants from the Schirmacher and Untersee oases (Central Dronning Maud Land, East Antarctica). Isotopenpraxis Env Health Stud 29:21–25

Calder JA, Parker PL (1973) Geochemical implications of induced changes in ^{13}C fractionation by blue-green algae. Geochim Cosmochim Acta 37:133–140

Casanova J, Hillaire-Marcel C (1992) Late Holocene hydrological history of Lake Tanganyika, East Africa, from isotopic data on fossil stromatolites. Palaeogeogr Palaeoclimatol Palaeocecol 91:35–48

Casanova J, Hillaire-Marcel C (1993) Carbon and oxygen isotopes in African lacustrine stromatolites: palaeohydrological interpretation. In: Swart PK, Lohmann KC, McKenzie J, Savin S (eds) Climate change in continental isotopic records (Geophys Monogr 78). American Geophysical Union, Washington, DC, pp 123–133

Cohen Y, Aizenshtat Z, Stoler A, Jørgensen BB (1980) The microbial geochemistry of Solar Lake, Sinai. In: Ralph JB, Trudinger PA, Walter MR (eds) Biogeochemistry of ancient and modern environments. Springer, Berlin Heidelberg New York, pp 167–172

Des Marais DJ, Cohen Y, Nguyen H, Cheatham M, Cheatham T, Munoz E (1989) Carbon isotopic trends in the hypersaline ponds and microbial mats at Guerrero Negro, Baja California Sur, Mexico: implications for Precambrian stromatolites. In: Cohen Y, Rosenberg E (eds) Microbial mats: physiological ecology of benthic microbial communities. Am Soc Microbiol, Washington, pp 191–203

Dor I, Carl N, Schidlowski M (1992) Experimental hypersaline ponds as model environments for stromatolite formation 1. Microbenthos composition and biomass accumulation. In: Schidlowski M, Golubic S, Kimberley MM, McKirdy DM, Trudinger PA (eds) Early organic evolution: implications for mineral and energy resources. Springer, Berlin Heidelberg New York, pp 483–493

Durand B (ed) (1980) Kerogen – insoluble organic matter from sedimentary rocks. Editions Technip, Paris, 519 pp

Ehrlich A, Dor I (1985) Photosynthetic microorganisms of the Gavish Sabkha. In: Friedman GM, Krumbein WE (eds) Hypersaline ecosystems: the Gavish sabkha. Ecological studies 53. Springer, Berlin Heidelberg New York, pp 381–401

Eichmann R, Schidlowski M (1975) Isotopic fractionation between coexisting organic carbon – carbonate pairs in Precambrian sediments. Geochim Cosmochim Acta 39:585–595

Estep MF (1984) Carbon and hydrogen isotopic compositions of algae and bacteria from hydrothermal environments, Yellowstone National Park. Geochim Cosmochim Acta 48:591–599

Estep MF, Tabita FR, Van Baalen C (1978a) Purification of ribulose-1.5-bisphosphate carboxylase and carbon isotope fractionation by whole cells and carboxylase from *Cylindrotheca* sp. (Bacillariophyceae). J Phycol 14:183–188

Estep MF, Tabita FR, Parker PL, Van Baalen C (1978b) Carbon isotope fractionation by ribulose-1.5-bisphosphate carboxylase from various organisms. Plant Physiol 61:680–687

Freeman KH, Hayes JM, Trendel JM, Albrecht P (1990) Evidence from isotope measurements for diverse origins of sedimentary hydrocarbons. Nature 343:254–256

Friedman GM, Krumbein WE (eds) (1985) Hypersaline ecosystems: the Gavish sabkha. Ecological studies 53. Springer, Berlin Heidelberg New York, X + 484 pp

Fuchs G, Thauer R, Ziegler H, Stichler W (1979) Carbon isotope fractionation by *Methanobacterium thermoautotrophicum*. Arch Microbiol 120:135–139

Fuchs G, Stupperich E (1981) Wege der autotrophen CO_2-Fixierung in Bakterien. Forum Mikrobiol 4:198–201

Glaessner M (1984) The dawn of animal life. Cambridge University Press, Cambridge, XI + 244 pp

Hayes JM, Kaplan IR, Wedeking KW (1983) Precambrian organic geochemistry: preservation of the record. In: Schopf JW (ed) Earth's earliest biosphere: its origin and evolution. Princeton University Press, Princeton, pp 93–134

Hoering TC (1967) The organic geochemistry of Precambrian rocks. In: Abelson PH (ed) Researches in geochemistry. Wiley, New York, pp 89–111

Höhn A (1989) Stable isotopes of lacustrine stromatolites from the Permo-Carboniferous Saar- Nahe Basin (SW-Germany): preliminary results. In: Kennard JM, Burne RV (eds) Stromatolite Newsletter 14. Bureau of Mineral Resources, Geology and Geophysics, Canberra, Australia, pp 36–39

Kirkland DW, Bradbury JP, Dean WE (1983) The heliothermic lake – a direct method of collecting and storing solar energy. Arch Hydrobiol Suppl 65 (1):1–60

Krumbein WE, Cohen Y (1977) Primary production, mat formation and lithification chances of oxygenic and facultative anoxygenic cyanophytes (cyanobacteria). In: Flügel E (ed) Fossil algae. Springer, Berlin Heidelberg New York, pp 37–56

Macgregor AM (1940) A Precambrian algal limestone in southern Rhodesia. Trans Geol Soc S Afr 43:9–15

Mizutani H, Wada E (1982) Effect of high atmospheric CO_2 concentration on $\delta^{13}C$ of algae. Origins Life 12:377–390

O'Leary MH (1981) Carbon isotope fractionation in plants. Phytochemistry 20:553–567

Pardue JW, Scalan RS, Van Baalen C, Parker PL (1976) Maximum carbon isotope fractionation in photosynthesis by blue-green algae and a green alga. Geochim Cosmochim Acta 40:309–312

Park R, Epstein S (1960) Carbon isotope fractionation during photosynthesis. Geochim Cosmochim Acta 21:110–126

Quandt L, Gottschalk G, Ziegler H, Stichler W (1977) Isotope discrimination by photosynthetic bacteria. FEMS Microbiol Lett 1:125–128

Roeske CA, O'Leary MH (1984) Carbon isotope effects on the enzyme-catalyzed carboxylation of ribulose bisphosphate. Biochemistry 23:6275–6284

Sackett WM, Eckelmann WR, Bender ML, Bé AWH (1965) Temperature dependence of carbon isotope composition in marine plankton and sediments. Science 148:235–237

Sathyanarayan S, Arneth JD, Schidlowski M (1987) Stable isotope geochemistry of sedimentary carbonates from the Proterozoic Kaladgi, Badami and Bhima Groups, Karnataka, India. Precambrian Res 37:147–156

Schidlowski M, Eichmann, R, Junge CE (1975) Precambrian sedimentary carbonates: carbon and oxygen isotope geochemistry and implications for the terrestrial oxygen budget. Precambrian Res 2:1–69

Schidlowski M, Gorzawski H, Dor I (1988) Experimental solar ponds 2. Isotopic composition of microbial biomass as a function of productivity rates and salinity. Terra Cognita 8:229

Schidlowski M, Gorzawski H, Dor I (1989) Isotopically heavy bio-

mass from microbial mats: predictor variables from experimental hypersaline ponds. Abstr 28th Int Geol Congr Wash 3:45–46
Schidlowski M, Gorzawski H, Dor I (1992) Experimental hypersaline ponds as model environments for stromatolite formation 2. Isotopic biogeochemistry. In: Schidlowski M, Golubic S, Kimberley MM, McKirdy DM, Trudinger PA (eds) Early organic evolution: Implications for mineral and energy resources. Springer, Berlin Heidelberg New York, pp 494–508
Schidlowski M, Gorzawski H, Dor I (1994) Carbon isotope variations in a solar pond microbial mat: role of environmental gradients as steering variables. Geochim Cosmochim Acta 58:2289–2298
Schidlowski M, Hayes JM, Kaplan IR (1983) Isotopic inferences of ancient biochemistries: carbon, sulfur, hydrogen and nitrogen. In: Schopf JW (ed) Earth's earliest biosphere: its origin and evolution. Princeton University Press, Princeton, pp 149–186
Schidlowski M, Matzigkeit U, Krumbein WE (1984) Superheavy organic carbon from hypersaline microbial mats: assimilatory pathway and geochemical implications. Naturwissenschaften 71:303–308
Schidlowski M, Matzigkeit U, Mook WG, Krumbein WE (1985) Carbon isotope geochemistry and ^{14}C ages of microbial mats from the Gavish Sabkha and the Solar Lake. In: Friedman GM, Krumbein WE (eds) Hypersaline ecosystems: the Gavish sabkha. Ecological studies 53. Springer, Berlin Heidelberg New York, pp 381–401
Schoell M, Wellmer FW (1981) Anomalous ^{13}C depletion in Early Precambrian graphites from Superior Province, Canada. Nature 290:696–699
Schopf JW, Oehler DZ, Horodyski RJ, Kvenvolden KA (1971) Biogenicity and significance of the oldest known stromatolites. J Paleontol 45:477–485
Seckbach J, Kaplan IR (1973) Growth pattern and ^{13}C /^{12}C isotope fractionation of *Cyanidium caldarium* and hot spring algal mats. Chem Geol 12:161–169
Sirevåg R, Buchanan BB, Berry JA, Troughton JH (1977) Mechanisms of CO_2 fixation in bacterial photosynthesis studied by the carbon isotope fractionation technique. Arch Microbiol 112:35–38
Smith BN, Epstein S (1971) Two categories of ^{13}C /^{12}C ratios for higher plants. Plant Physiol 47:380–384
Summons RE, Jahnke LL, Roksandic Z (1994) Carbon isotope fractionation in lipids from methanotrophic bacteria: relevance for interpretation of the geochemical record of biomarkers. Geochim Cosmochim Acta 58:2853–2863
Tabor H (1981) Solar ponds. Solar Energy 27:181–194
Travé A (1992) Sedimentologia, petrologia i geoquímica (elements traca i isòtopes) dels estromatòlits de la conca Eocene sudpirinenca. PhD Thesis, Univ de Barcelona, 386 pp
Vogel JC (1980) Fractionation of the carbon isotopes during photosynthesis. Sitzungsber Heidelb Akad Wiss, Math-Nat Kl 1980(3): 111–135
Wand U, Mühle K (1990) Extremely ^{13}C-enriched biomass in a freshwater environment: examples from Antarctic lakes. Geodät Geophys Veröff (Berlin), Reihe 1,16:361–366
Walter MR (1983) Archean stromatolites: evidence of the Earth's earliest benthos. In: Schopf JW (ed) Earth's earliest biosphere: its origin and evolution. Princeton University Press, Princeton, pp 187–213
Winkler FJ, Kexel H, Kranz C, Schmidt HL (1982) Parameters affecting the $^{13}CO_2/^{12}CO_2$ isotope discrimination of the ribulose-1.5-bisphosphate carboxylase reaction. In: Schmidt HL, Förstel H, Heinzinger K (eds), Stable isotopes. Anal Chem Symp Ser 11. Elsevier, Amsterdam, pp 83–89
Wong WW, Sackett WM, Benedict CR (1975) Isotope fractionation in photosynthetic bacteria during carbon dioxide assimilation. Plant Physiol 55:475–479
Wong WW, Sackett WM (1978) Fractionation of stable carbon isotopes by marine phytoplankton. Geochim Cosmochim Acta 42:1809–1815
Wright DT (1993) Carbon isotope geochemistry of Cambrian stromatolites, NW Scotland. In: Barattolo F, De Castro P, Parente M (eds) Studies on fossil benthic algae. Boll Soc Paleont Ital, Spec Vol 1. Mucchi Editore, Modena, pp 415–420
Zamarreño L, Anadon P, Utrilla R (1997) Sedimentology and isotopic composition of upper Paleocene to Eocene non-marine stromatolites, eastern Ebro Basin, NE Spain. Sedimentology 44:159–166

Sulphur Isotopes and Microbial Sulphur Cycling in Sediments

S.H. Bottrell, R. Raiswell

Dept. of Earth Sciences, Leeds University, Leeds LS2 9JT

Abstract. The relative abundances of the main isotopes of sulphur (^{32}S, ^{34}S) in sediments are influenced only by kinetic fractionations, which principally occur during the the formation of H_2S by microbial sulphate reduction. The isotopic composition of the H_2S being produced at any instant varies with rates of oxidation recycling of sulphate (which determine the maximum fractionation) and rates of sulphate supply relative to rates of sulphate reduction (which determine the isotopic composition of the sulphate being reduced).The isotopic composition of seawater sulphate fluctuates over geological time, consistent with variations in the amounts of sulphate removed to form pyrite by microbial sulphate reduction. Analogous variations are seen in the composition of marine pyrite through time. By contrast variations in the isotopic composition of sulphate oxygen are affected by sulphate reduction and also by sulphid oxidation (since oxygen can be supplied both from atmospheric O_2 or water). Future research is likely to focus increasingly on the role of oxidation processes in modifying sulphur isotope and sulphate oxygen isotope signatures.

1 Introduction

Sulphur in the primordial crust was monotypic. It existed exclusively as sulphide and had an homogeneous isotopic composition inherited from cosmogenic processes. By contrast present-day sulphur exhibits a diversity of oxidation states (−2 to +6) each with a distinctive range of isotopic compositions. This increase in the number of oxidation states and divergence in isotopic composition is directly attributable to the appearance of atmospheric oxygen, which created surficial oxidising conditions and displaced reducing conditions to shallow burial depths. The resulting range of redox potentials stabilises all the main redox states of sulphur and enables transformations between redox states to occur where different redox environments are in close proximity. A variety of microbial processes occur in these redox gradients, catalyse these redox transformations and extract energy from them (e.g., Froelich et al. 1979).

The gross details of the interactions between the oxygen and sulphur cycles are reasonably well-understood (Garrels and Lerman 1984; Berner and Canfield 1989). Oxygen and organic matter are formed during photosynthesis and any organic matter which escapes immediate oxidation through burial in sediments is accompanied by the addition of an equivalent amount of oxygen to the atmosphere. Retention of a steady state in atmospheric oxygen requires that this oxygen be consumed, principally by oxidising: (1) sulphide sulphur to sulphate sulphur, (2) ferrous iron to ferric iron, and (3) organic matter to CO_2. The nature of the sulphur oxidation pathways and the role of sulphur species with intermediate oxidation states are poorly understood, particularly with respect to their influence on sulphur isotope behaviour. This review will seek to show how recent studies by Jørgensen (1990), Canfield and Thamdrup (1994), Canfield and Teske (1996), Habicht and Canfield (1997) and Habicht et al. (1998) influence the interpretation of sulphur isotope data and to establish a foundation for the application of sulphate oxygen isotope studies to the hitherto neglected oxidative part of the sulphur cycle.

2 Sulphur Isotope Systematics

Natural sulphur is composed of four isotopes with mass numbers 32, 33, 34 and 36, and respective abundances of 95.00%, 0.75%, 4.22% and 0.02%. Variations in the isotopic composition of a sample are expressed as per mill values (‰) relative to Canyon Diablo Troilite (CDT for which $^{34}S/^{32}S = 1/22.22$),

$$\delta^{34}S = 1000\,[(^{34}S/^{32}S)_{sample} - (^{34}S/^{32}S)_{CDT}]/(^{34}S/^{32}S)_{CDT}$$

Marked variations in the relative proportions of these two isotopes can occur as a result of fractionation due to isotopic exchange or unidirectional reaction processes. For example, a mixture of $H_2{}^{34}S$ and $^{32}SO_4{}^{2-}$

$$H_2{}^{34}S + {}^{32}SO_4{}^{2-} \rightarrow H_2{}^{32}S + {}^{34}SO_4{}^{2-}$$

can exchange isotopes to produce an equilibrium distribution given by:

$$K = \frac{\{^{34}SO_4{}^{2-}\}\{H_2{}^{32}S\}}{\{^{32}SO_4{}^{2-}\}\{H_2{}^{34}S\}} = 1.075 \text{ at } 25°C$$

However, equilibrium is not necessarily achieved, for example unless temperatures are sufficiently elevated to overcome the energy barriers to exchange, as is the case for the above sulphide-sulphate exchange (where

R.E. Riding and S.M. Awramik (Eds.)
Microbial Sediments

there is no evidence of isotopic exchange below 100° C). It is an important simplification of sulphur isotope behaviour in sedimentary processes that fractionation effects are mainly attributable to unidirectional kinetic processes.

Isotope fractionation during unidirectional processes arises because the ^{32}S- and the ^{34}S-bearing molecules react at different rates. One of the most important fractionations of sulphur isotopes arises from microbial sulphate reduction (Goldhaber and Kaplan 1974; Froelich et al. 1979; Machel, this Vol.). Under anoxic conditions sulphate reducing bacteria utilise organic matter to produce H_2S and alkalinity

$$2\,CH_2O + SO_4^{2-} \rightarrow H_2S + 2\,HCO_3^-$$

The sulphate produced reacts with iron minerals (mainly oxides) to produce iron monosulphides (FeS) which then react with more H_2S (Rickard and Luther 1997) or elemental sulphur or polysulphides (Rickard 1975) to produce pyrite (FeS_2). Pyrite is the main reduced sulphur-bearing mineral in rocks and can occur in a variety of crystallographic forms (Canfield and Raiswell 1991).

During sulphate reduction the $^{32}SO_4^{2-}$ is reduced faster than the $^{34}SO_4^{2-}$, so that the first H_2S produced is depleted in ^{34}S relative to the original isotope composition of the sulphate. The extent of this depletion is termed the fractionation factor ($\alpha_{A\text{-}B} = R_A/R_B$, where R is the ratio $^{34}S/^{32}S$ in either A or B, often expressed as $\Delta_{A\text{-}B} = \delta^{34}S_A - \delta^{34}S_B$‰). The removal of a relatively ^{34}S-depleted fraction from the original sulphate must obviously cause the residual sulphate to become ^{34}S-enriched. Any further H_2S produced is still depleted in ^{34}S to the same extent relative to the residual SO_4^{2-} but, since the residual SO_4^2 is now ^{34}S-enriched, the later formed H_2S is also ^{34}S-enriched relative to that initially produced. Thus as reaction proceeds the H_2S produced at any time becomes more ^{34}S-enriched in parallel with the composition of the residual SO_4^{2-}. The aggregate composition of the H_2S produced will also become progressively enriched in ^{34}S but at a much slower rate, because the overall composition is the average of the most ^{34}S-depleted batch formed initially with all the subsequent, more ^{34}S-enriched batches.

In a closed system, where there are no additions or losses of SO_4^{2-} or H_2S, the resulting isotopic changes can be mathematically modelled by the Rayleigh distillation equations:

$$R_o/R_t = F^{(1-1/\alpha)} \quad (1)$$

$$P_t/R_o = \frac{1 - F^{1/\alpha}}{1 - F} \quad (2)$$

where R_o and R_t are the $^{34}S/^{32}S$ ratios in the initial SO_4^{2-} and residual SO_4^{2-} respectively, F is the fraction of SO_4^{2-} remaining, and P_t is the $^{34}S/^{32}S$ ratio in the accumulating product. Figure 1 shows plots of R_t and P_t for reduction of a batch of seawater sulphate (+20‰) with a fractionation of 50‰. Complete reduction produces H_2S with a mean composition identical to that of the initial SO_4^{2-}.

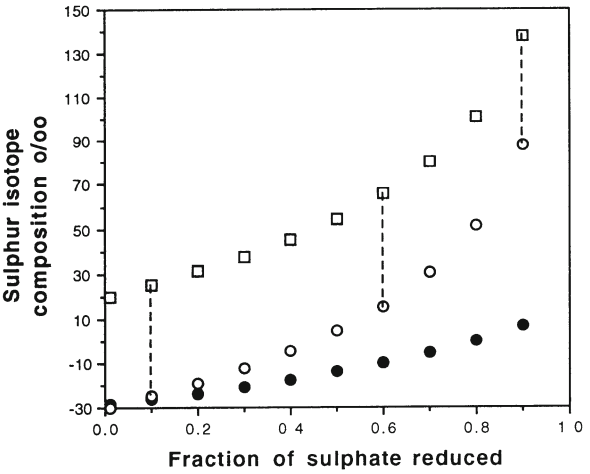

Fig. 1. Rayleigh fractionation during closed system reduction of seawater SO_4^{2-} at +20‰ with a fractionation of 50‰. *Open squares* show the composition of the residual SO_4^{2-}, *open circles* the H_2S being produced at any moment and *filled circles* the accumulating H_2S. *Lines* between the SO_4^{2-} and instantaneous H_2S represent equal fractionations of 50‰

The Rayleigh equations are of only qualitative use in sedimentary systems for two reasons. Firstly, the Rayleigh models apply only to reduction of a single batch of SO_4^{2-} *in a closed system*, thus Eq. (1) can only be used where there are no additions or losses of SO_4^{2-} or H_2S. In fact natural systems are only rarely closed (with respect to either SO_4^{2-} or H_2S) and more typically exhibit behaviour which is intermediate between closed and open (in an open system SO_4^{2-} is replaced at the same rate as removal occurs, and H_2S is removed as fast as it is formed). Intermediate behaviour arises where the rates of replacement of SO_4^{2-}, or removal of H_2S, are less than their respective rates of removal and addition by reaction. The isotopic behaviour of intermediate systems is complex because the rates of replacement of SO_4^{2-} and removal of H_2S may be unrelated (thus a system could be almost open for SO_4^{2-} but almost closed for H_2S). Moreover the different isotopic forms of SO_4^{2-} and H_2S may also differ in their rates of supply and removal by diffusional transport (Chanton 1985). Thus the ^{32}S and ^{34}S dissolved sulphate and sulphide species may each exhibit different degrees of open or closed system behaviour depending on their rates of addition or removal by reaction and transport. Finally many sediments may begin sulphate reduction in open (or almost open) systems, which progressively become more closed with burial. During this progression different masses of pyrite may be formed which will differ in isotopic composition from each other (and will not them-

selves be isotopically homogeneous, if sulphate is being depleted). For example, open system reduction of seawater sulphate (+20‰) with a fractionation of 50‰ will produce sulphide at −30‰. However open system reduction could produce 1, 10 or 100 mg of sulphide, each of which could be followed by closed system reduction of 1 cm^3 of seawater producing nearly 1 mg of sulphur with a mean isotopic composition of +20‰. These three different mixes of open and closed system products would produce bulk pyrite phases with compositions of −5, −25.5 and −27.1‰ respectively. Thus, one of the main difficulties in using the Rayleigh equations is that we never really know the amounts and compositions of the open, partially closed and closed system products which are present. Zaback et al. (1993) have described a novel approach which avoids some of these difficulties by focusing on the relative rates of sulphate transport and sulphide precipitation.

Unfortunately, however, there is also a second major source of difficulty arising from uncertainty over the value of the fractionation factor during sulphate reduction. Laboratory experiments on pure cultures show fractionations of approximately −4 to −46‰ depending on the experimental conditions (Kaplan and Rittenberg 1964) and the rate of reduction (the largest fractionation factors occur at the slowest rates of reduction). A comparable range in fractionations (approximately −16 to −42‰), and a similar variation with rate, have also been found in experiments with natural populations (Habicht and Canfield 1997). There is considerable variation in the fractionation factor at any given rate of reduction, although Habicht and Canfield (1997) show that high rates (above 10 μmol cm^{-3} day^{-1}) give uniformly low fractionations of −20‰. Habicht and Canfield (1997) also suggest that fractionations are mainly controlled by, and may very more consistently with, specific rates of reduction (mass/cell/unit-time) rather than absolute rates (mass/volume/time). Fractionation seems to be independent of sulphate concentrations from 29 to 1.4 mM, which spans the range in marine porewaters in which sulphate reduction is quantitatively significant.

Laboratory experiments do not however seem to replicate the fractionations found in sediments, where the H_2S formed from seawater SO_4^{2-} (at +20‰) is very commonly more depleted in ^{34}S (by 45−70‰). An important insight in this respect (Canfield and Thamdrup 1994) is that the magnitude of the fractionation observed in sediments is related to the degree of sulphide re-oxidation, with the larger fractionations (up to 58‰ in their study) occurring in sediments with higher degrees of re-oxidation. Canfield and Thamdrup (1994) attribute this to isotopic effects arising from the microbial disproportionation of elemental sulphur (formed during oxidation), a process which can further deplete H_2S in ^{34}S by about 8‰. Studies of pure and enrichment cultures of sulphur disproportionating bacteria (Canfield et al. 1998) provide further support for this conclusion, and similar fractionations have also been found in pure and enrichment culture experiments involving the reduction and disproportionation of thiosulphate and sulphite (Habicht et al. 1998).

The largest fractionations observed would require several cycles of oxidation and disproportionation and the over-riding consideration may be the progress of sulphide and sulphate toward isotopic equilibrium (a fractionation of about 70‰), as a result of isotopic exchange occurring during the redox cycling of sulphur. Under abiotic conditions and at porewater pH, the rate of equilibrium is extremely slow because suitable species of intermediate oxidation state (which are required for isotopic exchange to occur) have exceedingly low concentrations. However, cyclic bacterial reduction and reoxidation will form sulphur species of intermediate oxidation state (some of which may be intracellular) which may catalyse sulphur isotopic exchange, a process suggested by Chambers and Trudinger (1979). Indeed, modelling of isotopic effects associated with bacterial sulphate reduction and reoxidation in a closed system at a redox boundary show that an equilibrium distribution of isotopes between sulphate and sulphide can be attained (Belyy 1990). Thus, the magnitude of the fractionation observed will be related to the relative rates of sulphur cycling and sulphide removal; the greater the extent of sulphur cycling in a given environment, the greater the degree of equilibration achieved before sulphide is fixed, and thus the larger the fractionation observed. An extreme case would be one in which sulphur underwent cyclic oxidation-reduction but sulphide was not removed from the porewaters, which should produce large, near-equilibrium fractionations. This is virtually impossible in sediments, since iron is generally available to fix sulphide, but sulphidic groundwaters in carbonate aquifers provide a comparable natural situation. Bottrell et al. (1991) investigated sulphate reduction in the Bahamas and found large fractionations of 47−57‰, while near-equilibrium fractionations have been found in the Floridan aquifer (54−65‰; Rye et al. 1981) and the Lincolnshire Limestone, England (60‰; Bottrell et al., submitted). These studies indicate that redox cycling of sulphur does promote isotopic equilibrium and thus the variable fractionation factors observed in sediments could result from the competition between rates of recycling (or re-oxidation) and fixing of sulphide.

If sulphur cycling does promote isotopic exchange toward equilibrium it should also be true that different fractionations should be observed within the same sediment if there is a change in the extent of oxidative recycling with depth. Upper sediment layers which are accessible to the diffusive penetration of oxygen, or which are bioturbated, or which contain iron and manganese oxides should allow cycling to occur and should exhibit

relatively large fractionations. Conversely, at greater depths oxidation of H_2S may be impossible and smaller fractionations should result. Unfortunately, the determination of fractionation factors from isotopic measurements of sulphide and sulphate compositions in marine sediments is complex (see Goldhaber and Kaplan 1980; Chanton et al. 1987). The simplest approach is to plot the logarithmic form of the Rayleigh Eq. (1) as

$$\text{Log } R_t = \text{Log } C_t(1-1/\alpha)+[\log R_o-(1-1/\alpha)\log C_o] \quad (3)$$

where C_t and C_o are the concentrations of sulphate at time t and at the start of reduction. A graph of log R_t against log C_t has a slope of $(1-1/\alpha)$. Goldhaber and Kaplan (1974, 1980) have shown that some sediments do indeed show changes in slope which are consistent with a decrease in the fractionation factor with depth, as expected if oxidation were no longer possible. However Jørgensen (1979) and Goldhaber and Kaplan (1974) have pointed out that changes in slope may also arise for other reasons. Use of the Rayleigh equation assumes a closed system, which is often incorrect because significant amounts of sulphate can be added to sediments by diffusion and bioturbation. In these circumstances changes in slope on Rayleigh plots can arise when there is a change towards more open system behaviour with depth, for example due to a decrease in sedimentation rate, an increase in the rate of sulphate reduction and a decrease in the diffusion coefficient. Decreases in sedimentation rate and increases in the rate of sulphate reduction with depth would only occur with non-steady state conditions, but a decrease in the diffusion coefficient would occur even under steady state conditions, if there were a decrease in porosity with depth.

Numerical modelling approaches (see Chanton et al. 1987) could be used to establish the magnitudes of the depth changes in sedimentation rates, sulphate reduction rates, and porosity which are required to induce significant slope changes in Rayleigh plots. Unfortunately, there is relatively little data of sufficient detail even to assess whether slope changes in Rayleigh plots generally occur at depths which are consistent with changes in the potential for sulphide oxidation. Goldhaber and Kaplan (1974, 1980) and Jørgensen (1979) show Rayleigh plots with changes in slope for core 50G of the Santa Barbara Basin ($\alpha = 1.042$ for depths <15 cm, and 1.025 at >15 cm), Core 49 off the Baja coast ($\alpha = 1.034$ depths <40 cm and 1.019 at >40 cm), and the Kiel Bay core 2092 ($\alpha = 1.045$ depths <10 cm and 1.016 at >10 cm). These slope changes occur at depths below which the absence of bioturbation might prevent large fractionations being established through redox cycling of sulphur. However, in other cases breaks in slope are absent (Joides site 27) or occur at depths which are too large for bioturbation influences (core 38G, Santa Barbara Basin). These data suggest that Rayleigh plots could still provide a valuable perspective on the influence of sulphide oxidation on depth changes in fractionation factors, provided sites were carefully selected for their steady state characteristics and measurements were also made of variables that might control the depth range of sulphide oxidation (for example, the presence of iron and manganese oxides.

3 The Sulphate Sulphur Reservoir

The previous section has established the importance of the fractionation which accompanies sulphate reduction in producing H_2S, which is initially very ^{34}S-depleted but which can also vary over an exceedingly wide range (from about +50‰ to −50‰). The implications of these observations are not only seen within individual sediments, but are also apparent on a global scale from a consideration of the main features of the sulphur cycle (Fig. 2; after Garrels and Lerman 1984). At present the main reservoirs of sulphur are gypsum evaporites and pyrite sulphur in shales, and both reservoirs are about five times larger than the amount of sulphur present as dissolved sulphate in the oceans. No other sulphur reservoirs are quantitatively significant compared to those of pyrite and gypsum. Figure 2 also shows the mean isotopic compositions of each reservoir. The isotopic composition of gypsum (and other sulphate minerals) crystallising from evaporating seawater are only affected by a very small fractionation (+1.65 +/− 0.12‰; Thode and Monster 1965), so that there is little isotopic effect on seawater SO_4^{2-} unless large amounts of gypsum are precipitated. Weathering and dissolution of sulphate minerals occurs without any fractionation and thus the operation of the oxidi-

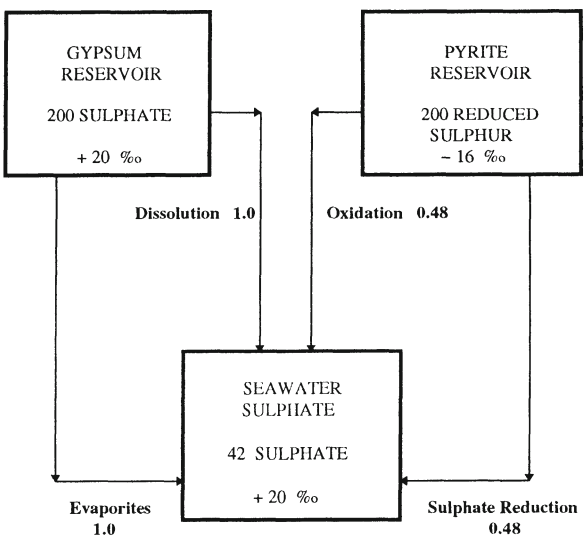

Fig. 2. The present-day global sulphur cycle. Masses are shown in units of 10^{18} mol, fluxes in units of 10^{18} mol/year. (Garrels and Lerman 1984)

sed part of the sulphur cycle in Fig. 2 only modifies the isotopic composition of seawater SO_4^{2-} significantly under exceptional circumstances.

By contrast, the reduced part of the sulphur cycle exerts an extremely powerful influence on the isotopic composition of seawater SO_4^{2-}. The process of microbial sulphate reduction requires anaerobic conditions, which are common in continental margin sediments (e.g., Berner 1982) where oxygen is often consumed over the top few millimetres or centimetres of the sediment. Below this depth sulphate reduction is the most important microbial process (sulphate reduction also occurs in deep-sea sediments although at a much slower rate; Canfield 1991). The continued metabolic activity of the microbial sulphate reducers requires that SO_4^{2-} is continuously replenished from overlying seawater by diffusion and bioturbation. A typical, fine-grained, marine continental margin sediment has a porosity of about 85%, but contains only enough seawater SO_4^{2-} to form about 0.2% pyrite sulphur. Since sediments often contain several per cent pyrite sulphur, it is clear that pore volumes can be replenished many times and are acting as an open system. Now, recall that sulphate reduction preferentially favours $^{32}SO_4^{2-}$ over $^{34}SO_4^{2-}$ and, in an open system the SO_4^{2-} can be replenished in the same proportions as it is reduced. In these circumstances pyrite will always be enriched in ^{32}S relative to seawater SO_4^{2-} (on average by 55 ± 2.5‰, see Fig. 4 below). The overall result of sulphate reduction is therefore to fix ^{32}S in sedimentary pyrite and hence drive seawater SO_4^{2-} towards relatively ^{34}S-enriched compositions.

The final part of the sulphur cycle (Fig. 2) simply shows the effects of uplift and weathering, which expose pyritic shales to oxidation with the dissolved SO_4^{2-} product being returned to the oceans via rivers. Pyrite weathering and oxidation usually occur with little or no fractionation so that overall sulphate reduction exerts the main influence on the isotopic composition of seawater SO_4^{2-}.

These arguments suggest that there should be variations in the sulphur isotope composition of seawater SO_4^{2-} through geological time, with periods dominated by the formation of pyritic shales being correlated with periods when seawater sulphate was ^{34}S-enriched (and vice versa). Claypool et al. (1980) have analysed the sulphur isotope composition of sulphate evaporites of different geological ages (Fig.3) whose isotope compositions essentially reflect that of the contemporaneous seawater (see above). The data do indeed show fluctuations through geological time, with the excursions to more positive values generally being associated with periods when black shales were deposited (e.g., Cambro-Ordovician 600–450 Ma, Upper Devonian-Mississippian 330–370 Ma, Jurassic and Cretaceous 70–180 Ma). However, the potential of this record is limited by the irregular distribution of data and by errors in age determinations

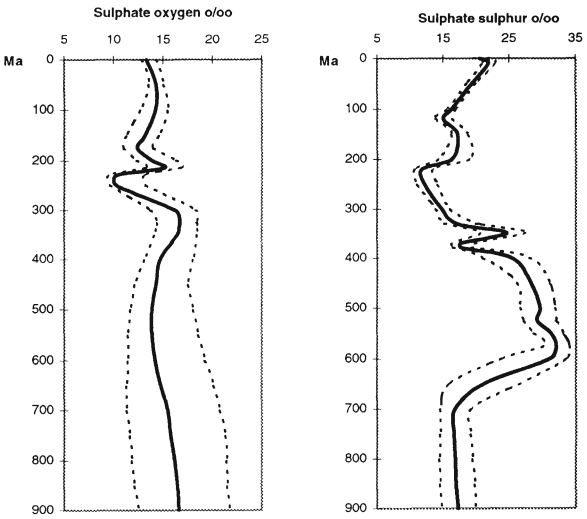

Fig. 3. Variations in the isotopic composition of seawater SO_4^{2-} through geological time for sulphate oxygen ($\delta^{18}O$) and sulphate sulphur ($\delta^{34}S$). (After Claypool et al. 1980)

(Strauss 1997). Improved resolution of this curve is an important priority (Strauss 1993), but it is clear that microbial sulphate reduction in sediments exerts an important influence on seawater composition and the global sulphur cycle (see Goldhaber and Kaplan 1974, Garrels and Lerman 1984, Berner and Raiswell 1983).

4 The Pyrite Sulphur Reservoir

Data for the $\delta^{34}S$ compositions of sedimentary sulphides have recently been compiled by Canfield and Teske (1996) from the present to 1.6 Ga (Fig. 4). They interpret these data in relation to variations in the isotopic composition of seawater SO_4^{2-} through time (see earlier). The upper two trends in Fig. 4 define an envelope (width 5‰) around the mean isotopic composition of seawater, and the lowest trend is the mean curve displaced by −55‰. The most ^{34}S-depleted sulphides crudely follow the lowest trend (indicating typical depletions of 55‰ with respect to seawater SO_4^{2-}) through the Phanerozoic. Through this time period the fractionation of 55‰ indicates the existence of an oxidative sulphur cycle, as required to increase fractionations from those values typically found during experimental sulphate reduction (see earlier). The same pattern persists through to 0.67 Ga, and possibly back to 0.86 Ga. However, before 0.86 Ga there are no isotopic values which yield fractionations >45‰ with respect to seawater SO_4^{2-}. In fact only seven data points give fractionations >35‰. Canfield and Teske (1996) conclude that the data demonstrate a fundamental change in the processes controlling the isotopic composition of sedimentary sulphides before the period 0.67–1.05 Ga. This, they believe, represents the period over which an

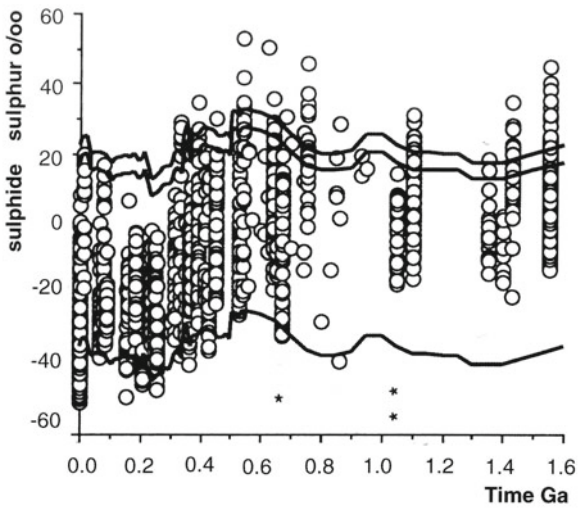

Fig. 4. Isotopic composition of sedimentary sulphides over the past 1.6 Ga (after Canfield and Teske 1996). The *upper band* of width 5‰ represents the isotopic composition of seawater SO_4^{2-} (see Fig. 3), and the *lower line* is the same curve displaced by 55‰. The *single asterisk* marks the time at which the pyrite isotope record shows the first unequivocal evidence for the operation of an oxidative cycle, and the *double asterisk* shows the first appearance of an oxidative cycle in the coupled carbonate carbon and sulphate record. (According to Strauss 1993)

oxidative sulphur cycle was initiated, due to the accumulation of oxygen in the atmosphere at levels 5–18% of present-day values.

5 The Organic and Elemental Sulphur Reservoirs

Organically bound sulphur comprises a wide range of different sulphur compounds. However, most measurements have been made on the bulk phase organic matter (usually termed kerogen) and the organic matter extractable in solvents such as dichloromethane (termed bitumen). Elemental sulphur (S^o) data are often considered together with data from organic sulphur, since there is a strong probability that the two are genetically related.

Sulphur assimilated by living organisms essentially reflects the isotopic composition of the source, hence in marine organisms assimilated organic sulphur has a composition close to that of seawater SO_4^{2-}. Organic S in marine sediments is, however, always depleted in ^{34}S relative to seawater SO_4^{2-}, which clearly points to reaction with the ^{34}S-depleted products of sulphate reduction. The reactive species are generally believed to be H_2S or its oxidation products (usually S^o or polysulphides). Anderson and Pratt (1995) have compiled an isotopic data base to explore the relationships between kerogen S and accompanying pyritic and elemental sulphur. To this data base we have added a further 20 samples from Dean (1994) and have corrected all data to a constant +20‰ isotopic composition of seawater.

Figure 5 shows the resulting relationship between bitumen and kerogen S which give a regression line

$$\text{Bitumen S} = 0.95\ (\text{Kerogen } \delta^{34}S) + 4.3 \qquad (4)$$

with a correlation coefficient of 0.87. The intercept (4.3 ± 0.9‰) is reasonably consistent with the observation of Orr (1985) that the sulphur isotope ratios of oils are no more than 2‰ ^{34}S-enriched than the sulphur in their source kerogens. However, these gross relationships almost certainly conceal large variations between individual compounds, or groups of compounds. Dean (1994) has separated the bitumens studied by Raiswell et al. (1993) into asphaltene and maltene fractions based on their solubility in n-pentane. Asphaltenes (insoluble in n-pentane) represent fragments of kerogen and may be intermediates on the path from kerogen to hydrocarbons. The asphaltenes were always ^{34}S-depleted by up to 8.5‰ relative to the maltenes, and kerogens were generally ^{34}S-enriched by up to 8.6‰ compared to asphaltenes.

Figure 5 shows the relationship between kerogen S and pyrite S which gives a regression line

$$\text{Kerogen } \delta^{34}S = 0.74\ (\text{Pyrite } \delta^{34}S) + 9.7 \qquad (5)$$

with a correlation coefficient of 0.89 (see also Anderson and Pratt 1995).

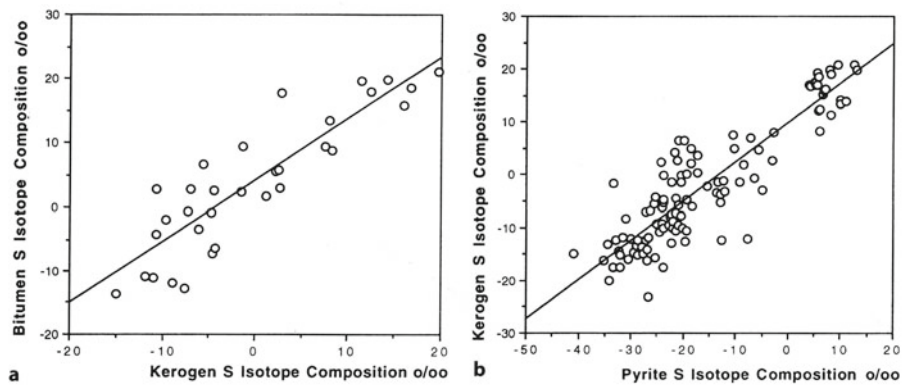

Fig. 5. Relationships bet
the sulphur isotope con
tion ($\delta^{34}S$) of bitumen a
ogen (*left*), and kerogei
pyrite (*right*)

Anderson and Pratt (1995) use isotope mass balance models to deduce the contributions from different sulphur sources to organic S. They noted that the slope of the regression line in Eq. (5) is less than 1, indicating the presence of at least one sulphur source with a constant sulphur isotope composition (denoted by subscript b) which is ^{34}S-enriched compared to pyrite S. This sulphur is assumed to be assimilated sulphur with an isotopic composition the same as seawater SO_4^{2-} (20‰). The remaining sulphur is assumed to be derived from the same source as the co-existing pyrite (subscript p) plus an unknown source (subscript h). A mass balance equation can be written

$$X_p+X_b+X_h = 1 \quad (6)$$

where X is the mole fraction of each sulphur component. The isotopic composition of kerogen S is then given by

$$\delta^* = \delta_p X_p + \delta_b X_b + \delta_h X_h \quad (7)$$

and substituting Eq. (7) into Eq. (6) gives

$$\delta^* = \delta_p(1-X_b-X_h) + \delta_b X_b + \delta_h X_h \quad (8)$$

which can be modified to

$$\delta^* = \delta_p(1-X_b) + \delta_b X_b + \Delta_{h-p} X_h \quad (9)$$

where Δ_{h-p} represents the fractionation between component h and component p.

The slope of the regression line in Fig. 5 produces an estimate for $(1-X_b)$ of 0.74 indicating an unexpectedly large value of approximately 26% for assimilated S in kerogen.

The intercept ($\delta_b X_b + \Delta_{h-p} X_h$) only produces limited constraints on component h, and Anderson and Pratt (1995) explore the possibilities that this component could be late diagenetic H_2S, early diagenetic polysulphides and early diagenetic sulfoxyanions. We can advance this argument a stage further based on Peru Margin data (Mossman et al. 1991; Raiswell and Canfield 1996) which strongly suggest that there can be little late diagenetic addition of sulphide to kerogen. The Peru Margin is unusual in possessing an extensive thickness (50–70 m) of dissolved sulphide-bearing porewaters which, combined with a slow sedimentation rate, give several million years of sediment exposure to dissolved sulphide. Most S is incorporated into organic matter at shallow burial depths, probably before sulphide accumulates in the porewater but, despite prolonged exposure to dissolved sulphide, the sulphur isotope evidence of Mossman et al. (1991) suggest that there is little or no subsequent incorporation of S into the organic matter. Furthermore, Raiswell and Canfield (1996) have been able to show that sulphidation of silicate iron can account for the removal of all the dissolved sulphide to form pyrite. Thus component h cannot be late diagenetic dissolved sulphide in the Peru Margin sediments.

The isotopic data of Mossman et al. (1991) for S present in kerogen, pyrite and in the elemental state can be used to perform a multiple regression to examine the dependence of kerogen S on the other two isotopic pools of sulphur in the Peru Margin sediments

$$\text{Kerogen } \delta^{34}S = 0.58(\text{Elemental } \delta^{34}S) + 0.14(\text{Pyrite } \delta^{34}S) + 0.47 \quad (10)$$

with a correlation coefficient of 0.94 (significant at the 0.1% level). Analogy with Eq. (5) suggests that using elemental S for component h provides a satisfactory explanation of the observed variations in the sulphur isotope data (also the favoured source of Anderson and Pratt 1995). Equation (10) is an extremely interesting result in suggesting that the isotopic composition of kerogen S indicates a greater contribution from S^0 than from the sulphide used to form pyrite.

The same approach can be used for the full data set compiled here. The Peru Margin represents an extremely favourable environment for the incorporation of late diagenetic dissolved sulphide into kerogen, yet no such incorporation is observed. It seems reasonable to suggest that contributions from late diagenetic sulphide can generally be ignored and that variations in the isotopic composition of kerogen S can be adequately explained by reference to the variations in pyritic and elemental S. Multiple regression ($r = 0.86$) for the full data set gives

$$\text{Kerogen } \delta^{34}S = 0.43(\text{Elemental } \delta^{34}S) + 0.30(\text{Pyrite } \delta^{34}S) + 4.77 \quad (11)$$

Thus, the kerogen sulphur is derived from the same sulphur sources as elemental S ($43 \pm 15\%$), pyrite S ($30 \pm 17\%$) and assimilated S ($27 \pm 22\%$). The intercept data are in close agreement with a 27% contribution from assimilated sulphur at approximately 20‰. These regression data again point to a significant role for sulphur of intermediate oxidation states, although caution is required because the dependent variables are themselves fairly well-correlated ($r = 0.80$ for S^0 with pyrite S, see also Anderson and Pratt 1995), so the regression cannot be thoroughly tested.

6 The Isotopic Composition of Oxygen in Sulphate

Oxygen is comprised of stable isotopes with masses 16 (99.763%), 17 (0.0375%) and 18 (0.1995%). Variations are expressed as $\delta^{18}O$ values and defined similarly to $\delta^{34}S$, but the reporting standard is usually V-SMOW. The isotopic composition of oxygen in SO_4^{2-} is affected by oxidation and reduction processes in the global sulphur cycle and may be used in conjunction with sulphur isotope studies to clarify oxidation and reduction mechanisms and pathways.

During bacterial sulphate reduction the residual SO_4^{2-} generally becomes enriched in ^{18}O in a similar

fashion to the enrichments observed in ^{34}S. Indeed, there may be a microbial preference for the lighter oxygen isotope during sulphate reduction. Isotopic enrichment factors ($\varepsilon^{34}S$ and $\varepsilon^{18}O$) can be defined for each isotope as $10^3/\ln\alpha$ to give the ‰ enrichments associated with sulphate reduction, and the ratios of these enrichment factors ($\varepsilon^{34}S/\varepsilon^{18}O$) determined experimentally (e.g., Mizutani and Rafter 1973) are generally between ~2.5 and ~4.5 (though with some smaller values). However, Fritz et al. (1989) pointed out that, during bacterial sulphate reduction, the oxygen isotopic composition of the SO_4^{2-} moves toward equilibrium with the oxygen in the environmental water and in most natural systems this results in enrichment of ^{18}O in the SO_4^{2-}. In their experiments, where SO_4^{2-} was initially more enriched in ^{18}O than it would be at equilibrium with water, the SO_4^{2-} became less ^{18}O-enriched as reduction proceeded, again moving toward equilibrium with the water. This demonstrates that bacterial reduction is promoting exchange of oxygen isotopes between SO_4^{2-} and water and explains why a range of enrichment factors is observed. Dissolved SO_4^{2-} is believed to interact with sulphate bound to microbially produced enzymes. These enzymes contain oxygen derived from water and exchange occurs when SO_4^{2-} is resolvated from the enzyme complex without undergoing reduction (Fritz et al. 1989; Toran and Harris 1989). In the absence of bacterial reduction (which promotes isotopic exchange), SO_4^{2-} and water only exchange oxygen isotopes extremely slowly under most environmental conditions. Lloyd (1968) showed that such an exchange was temperature and pH dependent; the rate of exchange increasing with lower pH and higher temperatures.

During oxidation of sulphide to SO_4^{2-} the oxygen molecules in the SO_4^{2-} may be derived from two sources; atmospheric O_2 (which has a composition of +23‰) and environmental water (which has a variable isotopic composition but which is generally 0‰ for seawater or ^{18}O-depleted for meteoric waters). The oxygen isotopic composition of SO_4^{2-} will thus carry a record of its environment of formation during the oxidative part of the sulphur cycle. The oxygen isotopic composition of the SO_4^{2-} is described by

$$\delta^{18}O = F_A.(\delta_A + \varepsilon_A) + (1-F_A).(\delta_W + \varepsilon_W) \qquad (12)$$

where F_A is the fraction of oxygen incorporated from atmospheric O_2, δ_A and δ_W are the isotopic compositions of atmospheric and water oxygen respectively, and ε_A and ε_W are the isotopic enrichment factors associated with incorporation from these sources. Lloyd (1967, 1968) reports essentially no isotopic fractionation associated with incorporation of oxygen from water into SO_4^{2-} ($\varepsilon_W = 0$), but a depletion in ^{18}O of 8.7‰ in the oxygen incorporated from O_2 ($\varepsilon_A = -8.7$). Most importantly, the oxygen isotopic composition can distinguish between sulphates formed under aerobic conditions by direct reaction with O_2 (where F_A is large, up to 0.875) and those formed anaerobically with Fe^{3+} as the oxidising agent (where all the oxygen is incorporated from water and F_A~0; Taylor et al. 1984; Van Everingden and Krouse 1985).

The SO_4^{2-} in seawater has an isotopic composition of ~+9.5‰ and is not in isotopic equilibrium with water despite a residence time vastly longer than even the slowest estimates of exchange half-lives (Lloyd 1968). This implies that the isotopic composition of seawater SO_4^{2-} is controlled by some dynamic process. Lloyd (1967) used experimental simulations to show that reoxidation of sulphide formed by sulphate reduction in marine sediments [with $F_A = 0.32$ in Eq. (12)] would generate SO_4^{2-} of the appropriate composition. This process must operate far more rapidly than isotopic reequilibration between SO_4^{2-} and water. Thus sulphate reduction consumes organic carbon in sediments using SO_4^{2-} as an electron acceptor, but the electrons are shunted back to O_2 when this is used to reoxidise sulphide. Clearly, microbial sulphate reduction in marine sediments plays a critical role in determining the oxidation state of the Earth's surface. An alternative mechanism influencing the $\delta^{18}O$ of marine sulphate, which may act in concert with the above, is thermal isotopic equilibration between SO_4^{2-} and water during hydrothermal circulation at mid-ocean ridges. It is difficult to assess the relative contributions of these processes.

The oxygen isotopic composition of seawater SO_4^{2-} has varied through time, around a value of ~9.5‰ (Fig. 3) but, since the effects of sulphate reduction are less important than for sulphur isotopes, the magnitude of the variation is smaller. Evaporite sulphate minerals are enriched in ^{18}O relative to dissolved SO_4^{2-} (by ~2‰; Lloyd 1968), so evaporite formation also affects seawater composition. Sulphate in sediment porewaters which have undergone sulphate reduction also become enriched in ^{18}O as a result, as shown by the compositions of diagenetic barites formed by barium mobilisation into the base of the sulphate reduction zone (Rafter and Mizutani 1967; Sakai 1971).

7 Conclusions

The main features of the global sulphur cycle are well-understood and, on a gross scale, the isotopic compositions of the pyrite and gypsum reservoirs can be used to track important changes in the composition of the oceans and the atmosphere over geological time. Unfortunately the unambiguous interpretation of sulphur isotope data has proved much more difficult on a microscale, where progress has been hindered by two problems. The first arises from difficulties in quantifying the different contributions from sulphides formed under open, partially closed and closed system condi-

tions. These may be resolved with the fine-scale analytical resolution of laser ablation and compound-specific organic S measurements. The second problem arises from the variable fractionation factors which apparently occur during the formation of sedimentary sulphides. Here there has been significant recent progress, and there is a real opportunity to quantify the environmental controls on fractionation factors. Partially oxidised sulphur species appear to play a critical role, and attention will need to be focused on the kinetics and mechanisms of their formation and destruction.

References

Anderson TF, Pratt LM (1995) Isotopic evidence for the origin of organic sulfur and elemental sulfur in marine sediments. In: Vairavamurthy MA, Schoonen MAA (eds) Geochemical transformations of sedimentary sulfur. Am Chem Soc Symp Ser 612:378–396

Belyy VM (1990) Sulphur isotope redistribution at a moving redox boundary. Geochem Int 27:31–50

Berner RA (1982) Burial of organic carbon and pyrite sulfur in the modern ocean; its geochemical and environmental significance. Am J Sci 289:451–473

Berner RA, Canfield DE (1989) A new model for atmospheric oxygen over Phanerozoic time. Am J Sci 289:333–361

Berner RA, Raiswell R (1983) Burial of organic carbon and pyrite sulfur over Phanerozoic time: a new theory. Geochim Cosmochim Acta 47:855–862

Bottrell SH, Moncaster SJ, Tellam JH, Lloyd JW, Fisher QJ, Newton RJ (submitted) Controls on bacterial sulphate reduction in a dual porosity aquifer: the Lincolnshire Limestone aquifer, England. Chem Geol

Canfield DE (1991) Sulfate reduction in deep-sea sediments. Am J Sci 291:177–188

Canfield DE, Raiswell R (1991) Pyrite formation and fossil preservation. In: Allison PA, Briggs DEG (eds) Taphonomy: releasing the data locked in the fossil record. Plenum Press, New York, pp 337–387

Canfield DE, Thamdrup B (1994) Production of ^{34}S-depleted sulfide during bacterial disproportionation of elemental sulfur. Science 266:1973–1975

Canfield DE, Teske A (1996) Late Proterozoic rise in atmospheric oxygen from phylogenetic and stable isotope results. Nature 382:127–132

Canfield DE, Thamdrup B, Fleischer F (1998) Isotope fractionation and sulfur metabolism by pure and enrichment cultures of elemental sulfur-disproportionating bacteria. Lmnol Oceanogr 43:253–264

Chambers LA, Trudinger PA (1979) Microbiological fractionation of stable sulphur isotopes. Geomicrobiol J 1:249–292

Chanton JP (1985) Sulfur mass balance and isotopic fractionation in an anoxic marine sediment. Thesis, University of North Carolina, Chapel Hill

Chanton JP, Martens CS, Goldhaber MB (1987) Biogeochemical cycling in an organic-rich coastal marine basin.7. Sulfur mass balance, oxygen uptake and sulfide retention. Geochim Cosmochim Acta 51:1187–1199

Claypool GE, Holser WT, Kaplan IR, Zak I (1980) The age curves of sulfur and oxygen isotopes in marine sulfate and their mutual interpretation. Chem Geol 28:199–260

Dean S (1994) A study of the organic and inorganic geochemistry of sulphur in shales. Thesis, Leeds University, Leeds

Fritz P, Barshamal GM, Drimmie RJ, Ibsen J, Qureshi RM (1989) Oxygen isotope exchange between sulphate and water during bacterial reduction of sulphate. Chem Geol 79:99–105

Froelich PN, Klinkhammer GP, Bender ML, Luedtke NA, Heath GR, Cullen D, Duaphin P, Hammond D, Hartman B, Maynard V (1979) Early oxidation of organic matter in pelagic sediments of the eastern equatorial Atlantic: suboxic diagenesis. Geochim Cosmochim Acta 43:1075–1090

Garrels RM, Lerman A (1984) Coupling of the sedimentary sulfur and carbon cycles-an improved model. Am J Sci 284:989–1007

Goldhaber MB, Kaplan IR (1974) The sulfur cycle. In: Goldberg ED (ed) The sea 5:569–655

Goldhaber MB, Kaplan IR (1980) Mechanisms of sulfur incorporation and isotope fractionation during early diagenesis in sediments of the Gulf of California. Mar Chem 9:95–143

Habicht KS, Canfield DE (1997) Sulfur isotope fractionation during bacterial sulfate reduction in organic-rich sediments. Geochim Cosmochim Acta 61:5351–5361

Habicht KS, Canfield DE, Rethmeier J (1998) Sulfur isotope fractionation during bacterial reduction and disproportionation of thiosulfate and sulfite. Geochim Cosmochim Acta 62:2585–2595

Jørgensen BB (1979) A theoretical model of the stable sulfur isotope distribution in marine sediments. Geochim Cosmochim Acta 43:363–374

Kaplan IR, Rittenberg SS (1964) Microbiological fractionation of sulfur isotopes. J Gen Microbiol 34:195–212

Lloyd RM (1967) Oxygen-18 composition of oceanic sulfate. Science 156:1228–1231

Lloyd RM (1968) Oxygen isotope behaviour in the sulfate-water system. J Geophys Res 73:6099–6110

Mizutani Y, Rafter TA (1973) Isotopic behaviour of oxygen in the bacterial reduction of sulphate. Geochem J 6:183–191

Mossmann J, Aplin AC, Curtis CD, Coleman ML (1991) Geochemistry of inorganic and organic sulphur in organic-rich sediments from the Peru Margin. Geochim Cosmochim Acta 55:3581–3595

Orr WL (1985) Kerogen/ashaltene/sulfur relationships in sulfur-rich Monterey oils. Org Geochem 10:499–516

Rafter TA, Mizutani Y (1967) Oxygen isotopic composition of sulphates and the relationship to their environment and to their $\delta^{34}S$ values. NZ J Sci 10:816–840

Raiswell R, Bottrell, SH, Al-Biatty HJ, Tan M Md (1993) The influence of bottom water oxygenation and reactive iron content on sulfur incorporation into bitumens from Jurassic marine shales. Am J Sci 293:569–596

Raiswell R, Canfield DE (1996) The kinetics of reaction between silicate iron and dissolved sulfide in Peru Margin sediments. Geochim Cosmochim Acta 60:2777–2787

Rickard DT (1975) Kinetics and mechanisms of pyrite formation at low temperatures. Am J Sci 275:636–651

Rickard DT, Luther GW III (1997) Kinetics of pyrite formation by the H_2S oxidation of iron (II) monosulfide in aqueous solutions between 25° C and 125° C: the mechanism. Geochim Cosmochim Acta 61:135–147

Rye RO, Back W, Hanshaw BB, Rightmire CT, Pearson FJ (1981) The origin and isotopic composition of dissolved sulfide in groundwater from carbonate aquifers in Florida and Texas. Geochim Cosmochim Acta 45:1941–1950

Sakai H (1971) Sulfur and oxygen istopic study of barite concretions from the banks in the Japan sea off northeast Honshu, Japan. Geochem J 5:79–93

Strauss H (1993) The sulfur isotope record of Precambrian sulfates: new data and a critical evaluation of the existing record. Precambrian Res 63:225–246

Strauss H (1997) The isotopic composition of sedimentary sulfur through time. Palaeogeog Palaeoclimatol Palaeoecol 132:97–118

Taylor BE, Wheeler MC, Nordstrom DK (1984) Isotope composition of sulphate in acid mine drainage as a measure of bacterial oxidation. Nature 308:538–541

Thode HG, Monster J (1965) Sulfur isotope geochemistry of petroleum evaporites in ancient seas. Am Assoc Petrol Geol Mem 4:367–377

Toran L, Harris RF (1989) Interpretation of sulfur and oxygen isotopes in biological and abiological sulfide oxidation. Geochim Cosmochim Acta 53:2341–2348

Van Everingden RO, Krouse HR (1985) Isotope composition of sulphates generated by bacterial and abiological oxidation. Nature 315:395–396

Zaback DA, Pratt LM, Hayes JM (1993) Transport and reduction of sulfate and immobilisation of sulfide in marine black shales. Geology 21:141–144

Products and Depth Limits of Microbial Activity in Petroliferous Subsurface Settings

Hans G. Machel[1], Julia Foght[2]

[1] Department of Earth and Atmospheric Sciences, University of Alberta, Edmonton, T6G 2E3, Canada
[2] Department of Biological Sciences, University of Alberta, Edmonton, T6G 2E3, Canada

Abstract. Most microbes live in near-surface or shallow subsurface diagenetic settings where temperatures and pressures are relatively low and nutrients are abundant. With increasing depth, temperature and pressure increase and nutrients become scarce, which leads to a general decrease in the rates of metabolic activity and eventually to the death of all microbes. The major objective of this chapter is to characterize microbial activity and products in petroliferous subsurface settings, with an attempt to place absolute depth limits on the geologically significant groups of microbes.

Four groups of microbes are known to be geologically significant in petroliferous subsurface settings, i.e., the aerobic respiratory bacteria, and three anaerobic groups that commonly live in consortia/communities: fermentative, sulfate-reducing, and methanogenic bacteria. These microbes form a number of economically important products and by-products in subsurface settings, including napthenic crude oils and tar in the form of tar sand deposits (aerobic biodegraders), H_2S, metal sulfides and elemental sulfur (sulfate-reducing bacteria), and dry methane gas (methanogens). The role of fermentative microbes is mainly in the partial breakdown of organic molecules that then serve as nutrients for the sulfate reducers and the methanogens. In all cases, carbonate cements with distinctive isotopic compositions may be formed as by-products. In addition, nanobacteria might be important in clay mineral diagenesis in buried sandstones.

Various types of these microbes can be used for microbially enhanced recovery of oil. Ultramicrobacteria constitute a special class, as they are injected in a dormant state and then resuscitated in situ to form biobarriers.

With increasing subsurface depth, temperature appears to be the principal factor limiting microbial metabolism (and life), besides the availability of suitable nutrients. The activity of all four groups of bacteria is commonly limited by a maximum subsurface depth of about 2000 m, except for rare cases where aerobic biodegradation or sulfate reduction may occur as deep as about 3000 m. Sulfate-reducing bacteria appear to be able to tolerate the highest temperatures (up to at least 110 °C) and, consequently, they appear to be vegetative at the relative greatest depths. However, sulfate reducers are usually limited to about the same depths (less than 2000 – 2200 m) as aerobic biodegraders whose waste products they may use as nutrients. The lower limit of the biosphere probably is marked by other types of bacteria at much greater depths.

1 Introduction

The subsurface biosphere may constitute as much as 50% of Earth's biomass (Fisk et al. 1998). Diverse communities of microbes, particularly bacteria, produce a large number of solids and gases in diagenetic environments, i.e., geologic environments in the upper 6000 – 7000 m of the Earth's crust. These products include, but are not restricted to, carbonates, metal oxides and sulfides, sulfur, methane, and H_2S. They are found mainly in near-surface and shallow subsurface diagenetic settings, which is a reflection of the fact that most microbes live in these settings, where temperatures and pressures are relatively low and nutrients are abundant (e.g., Ehrlich 1996).

With increasing subsurface (or burial) depth, the environmental conditions change in several ways: temperature, pressure, and water salinity increase, the redox-potential decreases, pore spaces decrease, and organic nutrients decrease in abundance except where petroleum is generated, migrates, or is pooled (e.g., Hanor 1983; Domenico and Schwartz 1990). These changes are generally detrimental to microbes in that they lead to an overall decrease in metabolic activity, reproduction rate and population density, then to cessation of microbial activity, and eventually to the death of all microbes (e.g., Atlas 1983; Ehrlich 1996; Fredrickson and Onstott 1996). Of all the factors that limit microbial life with increasing subsurface depth, temperature generally appears to be the most important. This is indicated by laboratory and field evidence. Firstly, with increasing temperature the metabolic rates of most microbes go through a maximum and then decrease, provided all other factors (such as water chemistry and nutrients) are held constant, until the microbes cease to metabolize and are then killed by thermal stress (Ehrlich 1996). Secondly, microbes may survive in geologic settings that differ only in temperature but otherwise are similar in water salinity, redox potential, availability of organic nutrients, and an oxidant such as sulfate. For example, sulfate-reducing bacteria will proliferate at depths of less than 2000 m with temperatures of < 70 °C, but not at a depth of ca. 4500 m with a temperature of about 120 – 130 °C, which is high enough to kill nearly all known bacteria, including sulfate-reducers (e.g., Stetter et al. 1993).

Two questions arise. Firstly, what are the "geologically significant" microbial products in deep subsurface environments that constitute the environmental limits of microbial life, particularly in petroliferous (containing kerogen, oil, gas, or bitumen) settings that

R. E. Riding and S. M. Awramik (Eds.)
Microbial Sediments

commonly are of economic significance? Secondly, at which depth does microbial metabolism cease to be a geologic agent or, in other words, where is the depth limit of the biosphere?

The major objective of this chapter is to answer the first question and to present the salient supporting data, especially from field studies. "Geologically significant" microbial products are here defined as "economically viable solid and gaseous products," i.e., products that are volumetrically abundant enough and can be retrieved (through drilling or mining) to be exploited and marketed at a profit. This definition implicitly places an emphasis on petroliferous (as defined above) subsurface settings, i.e., oil and gas fields and associated source rocks, because organic compounds are essential to most types of microbes. Hence, this chapter will concentrate on petroliferous subsurface settings, with the objective of providing a critical analysis helpful in the exploration for and development of hydrocarbon reservoirs. To this end, geologically significant *by-products* are here defined as "detectable accessories to economic viability," such as increased porosity through mineral dissolution, or textural and geochemical characteristics that help in the exploration for and development of the resources in question. These products and by-products may provide textural and/or geochemical evidence for a microbial origin. An example would be framboidal pyrite with $\delta^{34}S$ values of about −30‰ CDT in a petroleum source rock, where the combination of fabric, facies association, and geochemical composition leave no doubt as to the bacterial origin of the pyrite.

Occurrences of the above products and by-products are evidence only for *past* microbial activity. In order to prove *present* microbial activity (also called vegetative = alive, metabolizing and reproducing), one traditionally has had to find and culture the in situ microbes, which requires retrieval of microbial communities from the study site and their culture in the lab. This approach, however, is time consuming and difficult on a routine basis in petroleum geological studies (e.g., Fredrickson and Onstott 1996), and it is limited to culturable organisms. Moreover, the recently developed novel genetic methods that can infer microbial presence without culture (e.g., Cayol et al. 1995; Voordouw et al. 1996) are not common practice. Even if viable microbial communities are retrieved from a subsurface setting, i.e., in a drill core sample, the very presence of microbes that can be cultured in the lab does not necessarily mean that these microbes are active at the in situ conditions from which they were retrieved. Examples of this phenomenon would be the retrieval of sulfate-reducing bacteria from a sweet (negligible H_2S) oil reservoir in the East Paris Basin (L'Haridon et al. 1995) or from thirteen petroliferous formations in the USA (Azadpour et al. 1996). Although sulfate-reducing bacteria were isolated from all, and could be cultured from several, of these locations, in situ microbial H_2S production did not appear to take place in any of these locations. Hence, only the combined evidence of finding the microbes in the rock material along with their metabolic products and by-products is convincing evidence for active microbial activity at the subsurface site under investigation.

In the present context, particularly from an economic point of view, it is of prime importance to find and characterize the microbial products and by-products, and to deduce why the microbes may not be active at the in situ conditions. It is of secondary importance to characterize the metabolic pathways of the involved microbes, which is important for a number of other reasons, but beyond the scope of this chapter (see Zehender 1988, and Ehrlich 1996, for comprehensive treatments of this subject).

Nevertheless, geological and geochemical data help to define the maximum depths of the various microbial communities that are geologically significant (as defined above). As discussed below, virtually all microbial products are so scarce at depths below about 2000–3000 m and at temperatures greater than about 70–80 °C that they are geologically and economically insignificant. This, however, does not preclude the presence of life below such depths and above such temperatures. Some microbes are known to live at temperatures as high as 113 °C in deep sea volcanic vents, a limit that may increase as research progresses (e.g., Kerr 1997; Fisk et al. 1998). Indeed, some researchers speculate that microbial life might be possible up to about 140 °C (e.g., Fredrickson and Onstott 1996). The recovery of ultra-fine grained magnetite suspected to be of microbial origin from a depth of 6.7 km (Gold 1992) suggests that the biosphere may extend to at least that depth and commensurate temperatures.

2 Definitions of Subsurface Settings and Depth Limits

Subsurface (burial) settings are commonly divided into "shallow," "intermediate," and "deep," although these terms are ill defined. At one extreme, sediments buried to depths of more than 10 m are referred to as "deep" in soil science and microbiological studies (Frederickson et al. 1989), whereas depths in excess of about 3000 m are referred to as "deep" in diagenetic studies and petroleum geology (e.g., Machel 1990; Hunt 1996). Lovley and Chapelle (1995) made an excellent argument that, in microbiological and hydrogeochemical studies, the term "deep subsurface" should be defined hydrogeologically. Accordingly, they suggested using the term "deep subsurface" to be independent of total depth but restricted to intermediate and regional flow systems (as

defined by Tóth 1963), where water levels, rates of recharge, and water composition do not respond to individual precipitation events. However, in the present context this definition is too broad.

In this chapter, which is concerned with the absolute depth limits of microbes and their products in subsurface settings, "shallow" is defined as settings that contain oxygenated, surface-derived groundwater that has experienced little or no water-rock interaction whereby the maximum penetration depth of dissolved oxygen is commonly around 600–1000 m (Andreev et al. 1968; Krouse 1983). In addition, 300–600 m is the interval where pressure solution (stylolitization) commonly commences in carbonate rocks, with pronounced development of stylolites at depths below about 600 m, the depth at which stylolites form even in chalks (e.g., Machel 1990; Lind 1993). Combining these arguments, the boundary between "shallow" and "intermediate" subsurface/burial settings is here defined to be located at depths of approximately 600–1000 m. Hence, as a generalization, sediments and rocks that have a predominantly oxidized mineralogy (e.g., iron and manganese oxides) and where interbedded carbonates have no or only poorly developed stylolites are defined to have undergone only shallow burial diagenesis. Implicit in this distinction between shallow and intermediate subsurface settings is that the shallow settings are governed by local groundwater flow systems that may respond to individual events of precipitation and certainly respond to variations due to the seasons and latitude, whereas deeper settings are located within intermediate or regional groundwater flow systems, just as in Lovley and Chapelle's (1995) definition.

The lower limit of "intermediate" subsurface settings, and thereby the upper limit of "deep" subsurface settings, is here defined relative to the top of the (liquid) oil window. This depth offers another natural defining limit and has indeed been used to define the boundary between "diagenesis" and "catagenesis" in petroleum geology (e.g., Bustin et al. 1985; Hunt 1996). In mineral diagenesis this boundary is useful because the introduction of oil commonly arrests precipitation and dissolution. Unfortunately, the depth of the top of the oil window varies widely, depending on kerogen type, geothermal history, and surface temperature. Hunt (1996, p. 128) stated that the top of *most* oil windows is at a temperature of about 60 °C, but the considerable number of case studies and geothermal modeling exercises that he discussed document a range of about 50–130 °C. Accordingly, the depth of the top of the oil window ranges from about 1500 m (kerogen I: Monterey Formation, California) to 3400 m (kerogen III: Lower Miocene in the South Padre Island COAST No. 1 well, Texas), with a distribution maximum between about 2000 and 3000 m. Hence, this depth interval is here taken as the top of "deep" subsurface settings.

The above zonation of shallow, intermediate and deep burial diagenetic settings is sufficient in the present context and applicable to sedimentary basins in general. A more comprehensive discussion of diagenetic settings, which also includes hydrocarbon-contaminated plumes above leaking petroleum traps, can be found in Machel (1999).

3 Major Groups of Microbes, Products, Depth Limits

The types of microbes and the solid and gaseous products of their metabolism in intermediate and deep subsurface settings are likely to be similar to those found in near-surface and shallow subsurface settings (Pederson 1993). In fact, nearly all microbes from near-surface settings have been found in at least shallow to intermediate subsurface settings (Lovley and Chapelle 1995, their Table 1), which includes more than 9000 strains of microbes (mostly bacteria, some fungi and yeast) (e.g., Fredrickson and Onstott 1996). The major expected differences between shallow and deeper settings are that in the intermediate to deep subsurface only meso- and thermophilic microbes are vegetative, although their metabolic and reproduction rates are generally much lower than in cooler and shallower settings.

The major groups of microbes in diagenetic settings are commonly classified according to their type of metabolism in decreasing order of energy gain and/or increasing distance from the sediment-water interface or meteoric recharge area (e.g., Claypool and Kaplan 1974; Lovley and Chapelle 1994): aerobic respiratory bacteria – denitrifying bacteria – Mn(IV)-reducing bacteria – Fe(III)-reducing bacteria – sulfate-reducing bacteria – methanogenic bacteria. (Note: Lovley and Chapelle (1995) discussed a number of reasons to suggest that the above sequence of microbial zones is not solely a reflection of decreasing energy gain but also, or largely, the result of competition and nutrient supply.) In addition, fermentative bacteria, as a group, overlap the above groups in their energy gain. In petroliferous subsurface settings, four of these groups are geologically significant and, therefore, are the focus of this chapter: aerobic respiratory bacteria, fermentative bacteria, sulfate-reducing bacteria, and methanogenic bacteria. The other groups are not important because oxygen and nitrate inputs from groundwaters are low to negligible in most intermediate to deep subsurface settings, and nitrate, Mn(IV), as well as Fe(III) are limited by the indigenous mineralogy.

Although these groups of microbes are discussed in separate sections below, it is important to realize that these groups do not live as "monocultures" largely or completely isolated from other microbes (as much of the older literature appears to suggest). Rather, it has become increasingly clear in recent years that microbes

live in subsurface *consortia* (communities) that commonly contain several groups with competing and complementary metabolic requirements (e.g., Bernard et al. 1992; Mueller and Nielsen 1996). We will allude to some of the interactions of microbial groups where necessary, but will discuss the groups separately for the sake of characterizing their geologically significant products.

Lastly, other microbes can be economically important in subsurface settings through artificial, controlled uses. The most promising examples are the control of radioactive spills and nuclear disposal sites with certain microbes (e.g., Lovley and Phillips 1992; Pederson 1996) and, in petroliferous settings, the use of "ultramicrobacteria" (UMB) in enhanced oil recovery (e.g., Cusack et al. 1992; Cunningham et al. 1997). The latter are briefly discussed here.

4 Aerobic Biodegradation of Crude Oil

Aerobic biodegrading bacteria are well known from a multitude of petroleum geochemical studies (e.g., Atlas 1984; Peters and Moldowan 1993). The term "biodegradation" is here used synonymously with aerobic biodegradation, as is common practice in petroleum geochemistry (e.g., Hunt 1996). Anaerobic biodegradation includes compositional changes in oil through fermentative, sulfate-reducing, and methanogenic bacteria, which are covered under separate headings below.

A wide variety of microbes can utilize hydrocarbons as a sole source of carbon and energy in their metabolism, and almost all of these are obligately aerobic, i.e., they require molecular O_2 (as opposed to facultative aerobes that *can* use molecular O_2 but do not require it). More than 30 genera and far more than 100 species of various bacteria, fungi, and yeast metabolize hydrocarbons that include gaseous, liquid, and solid paraffins, napthenes, aromatics, and sulfur heterocyclic compounds (e.g., Westlake 1983; Atlas 1984; Connan 1984; Peters and Moldowan 1993). Most biodegrading microbes are bacteria that belong to the Pseudomonadaceae, Comamonadaceae, and Actinomycetaceae.

4.1 Main Products

Aerobic biodegraders generate a series of compositional and isotopic modifications of crude oil. In general, hydrocarbons are oxidized in a series of enzyme-catalyzed steps to their oxidized derivatives, i.e., to alcohols, fatty acids, ketones, phenols, etc., which then are further oxidized to CO_2. This is exemplified by the following net mass balance reactions, whereby ethane (an alkane/paraffin) is first oxidized to acetic acid (Eq. 1) and then to carbon dioxide (Eq. 2):

$$C_2H_6 + O_2 \rightarrow C_2H_4O_2 + H_2 \quad (1)$$

$$C_2H_4O_2 + 2O_2 \rightarrow 2CO_2 + 2H_2O \quad (2)$$

Importantly, aerobic bacteria often perform only the reaction in Eq. (1), or one of its analogues, but not the reaction in Eq. (2), or only partially. Hence, partially oxidized, "intermediate" organic compounds, such as acetic acid/acetate (or other organic acids, alcohols, etc.), are left in the system. As discussed further below, these intermediates are essential organic nutrients for many anaerobic microbes. A simplified list of changes in gross properties due to aerobic biodegradation is provided in Table 1 (more detailed lists and supporting chromatograms can be found in Connan 1984). Gas and gasoline-range compounds, initially largely alkanes, later also aromatics and eventually napthenes and other compounds, are preferentially removed. The residual oils generally become more viscous and greater in density (lower API gravity), richer in sulfur, nitrogen, and asphaltenes (Connan 1984).

Changes on a molecular level usually happen in a sequential way, which has led to the establishment of scales of increasing biodegradation, i.e., degradation "levels" or "ranks" (e.g., Volkman et al. 1983; Connan 1984; Hunt 1996). Table 2 is a list of such degradation levels with the accompanying molecular changes. Changes during levels 1–5 sequentially affect the relatively easily biodegradable compounds and can be monitored with simple gas chromatography. During more advanced levels of biodegradation even the much more stable biomarker molecules are sequentially altered and removed, and new biomarkers are formed (such as certain norhopanes), which can only be determined with advanced techniques such as GC-MS. Hence, biodegradation is also important in biomarker studies. Under favorable circumstances, certain biomarker molecules, such as methylhopanes, can be assigned to specific source microbes and/or paleoenvironments, which is of obvious use in oil-source rock correlations. Excellent treatments of these topics are provided by Moldowan et al. (1992) and Peters and Moldowan (1993).

Table 1. Aerobic biodegradation effects on gross properties of petroleum (modified from Connan 1984)

Decreases in:
1. Wet gas (C_2–C_6), in some cases also C_1
2. Gasoline–kerosene range (C_6–C_{15})
3. API gravity
4. n-paraffins (alkanes), aromatics
5. Gas/oil ratio
6. Pour point
Increases in:
1. Asphaltenes and NSO compounds
2. Sulfur and nitrogen contents
3. Vanadium and nickel contents
4. Viscosity
5. $\delta^{13}C$ of whole oil and alkanes

Table 2. Changes in molecular properties with increasing level of aerobic biodegradation (compiled from Volkman et al. 1983; Connan 1984; Hunt 1996)

Level	Organic geochemical characteristics	Description
0	Paraffinic crude oil	Not biodegraded
1	C_1 to C_{15} n-alkanes depleted	Minor
2	90% of C_1 to C_{35} n-alkanes removed	Light
3	Alkylcyclohexanes and alkylbenzenes removed Isoalkanes (including isoprenoids) reduced	Moderate
4	Isoprenoids and methylnaphthalenes removed Aromatics depleted in order of increasing molecular weight and alkyl substitution	Moderate
5	C_{14} - C_{16} bicyclic alkanes removed	Extensive
6	Smaller steranes removed, larger steranes altered 25-norhopanes formed	Heavy
7	All steranes removed 25-norhopanes more abundant	Heavy
8	Hopanes altered	Very heavy
9	Hopanes removed Disteranes altered	Severe
10	Disteranes and tricyclic terpanes removed Aromatic steroids altered	Extreme

A potentially significant reaction by-product of aerobic biodegradation is the formation of secondary porosity in carbonates and clastics. CO_2 formed as the oxidation product of aerobic biodegradation can and often does form secondary porosity via the formation of carbonic acid and subsequent dissolution of carbonates (mainly calcite) (e.g., McMahon et al. 1992; Kelly et al. 1997). On the other hand, the carbonate equilibria can also be driven towards precipitation (depending mainly on solution pH, which would tend to increase if organic acids are consumed, as well as on other fluid parameters; Canfield and Raiswell 1991a), and the CO_2 ends up in carbonate cements or concretions. Such carbonate usually has very low, negative $\delta^{13}C$ values, around - 25‰ PDB, similar to the source organics (e.g., Irwin et al. 1977). If released into a relatively bicarbonate-rich pore water (commonly marine with $\delta^{13}C$ values close to 0‰ PDB), mixing of the two dissolved carbonate populations results in a gradation of $\delta^{13}C$ values between the two end members. A case in point is the study of carbonate cements from various heavy oil/tar sand deposits by Dimitrakopoulos and Muehlenbachs (1987), who analyzed calcite cements from Brazil, Zaire, and Malagasy that formed as a by-product of aerobic biodegradation with $\delta^{13}C$ values ranging from -9.1 to -20.6‰ PDB. Similarly, Gould and Smith (1978) reported a range of $\delta^{13}C$ values of about +5 to -29‰ PDB for carbonate cements from a biodegraded oil field in Australia.

4.2 Geologic and Economic Significance

The major economic significance of aerobic biodegradation depends on its extent. At low to moderate levels of biodegradation, highly valuable, high-API gravity paraffinic crudes are degraded to less valuable, medium- to heavy-gravity napthenic crude oils (Philippi 1977). At higher levels of biodegradation oil is transformed to heavy oil, asphalt, and tar, which often form a special class of unconventional resources as "tar sands" (e.g., Brooks et al. 1988).

Significant secondary porosity is generated in some settings as a result of carbonic acid formation. However, it is not clear how important this process is on a basin-wide or worldwide scale, i.e., whether significant additional accommodation space for oil or gas are commonly generated in this way.

A negative aspect is that many aerobic bacteria, such as many pseudomonads, tend to form "biofilms" in secondary oil recovery schemes using water injection (e.g., Carlson et al. 1961; Cusack et al. 1987). Such biofilms consist of a combination of microbes, exopolysaccharide slime (that the microbes produce and that sticks to the mineral grains), and trapped particulates. Injection of vegetative bacteria tends to produce biofilms very close to the injection site, thereby forming a "skin plug" up to a few inches thick that is an obvious nuisance because it decreases injection and production efficiency (e.g., Cusack et al. 1992). Special clean-up strategies are required to remove such plugs, i.e., injection of strong oxidants and acids (e.g., Cusack et al. 1987, 1992).

4.3 Depth and Temperature Limits

Considering that the vast majority of oil biodegradation occurs aerobically, biodegradation is usually restricted to oxygenated near-surface and shallow subsurface settings, i.e., usually to depths of less than about 600 - 1000 m in continental settings. For example, in an extensive stable isotope study of natural gases from the Western Canada Sedimentary Basin, Krouse (1983) found abundant evidence for oxidation of methane, ethane and propane at depths of less than 1000 m, which delineates the penetration depth of dissolved oxygen in this basin, and Andreev et al. (1968) cited 600 m as an average penetration depth of dissolved oxygen. Generally, local groundwater flow systems with vigorous flow carry meteoric groundwaters with low total dissolved solids and oxygen concentrations around 2 - 8 ppm (e.g., Bockmeulen et al. 1983; Domenico and Schwartz 1990) into contact with the microbes and oil. The fastest and most severe aerobic biodegra-

dation commonly occurs in near-surface and shallow subsurface settings at temperatures around 20–60 °C (Connan 1984).

Biodegradation also occurs at greater depths and temperatures, albeit much less commonly, at much lower rates, and generally to a much more limited extent. In continental areas as well as off-shore, biodegradation at greater depths and temperatures is possible in flow systems with great permeability and rapid flow (where oxygen is transported to greater depths before being used up in microbial or inorganic redox reactions), if there is enough hydraulic head from an adjacent land mass to push meteoric water down and out into the off-shore strata. A good example of the latter is the Troll Field off the coast of Norway that contains biodegraded oil at depths of around 1530–1560 m. Biodegradation at the Troll Field appears to have occurred at little less than the present depths while the field was overlain by the North Sea, whereby oxygen was supplied by a meteoric groundwater flow system that originated at the adjacent Norwegian land mass (Horstad and Larter 1997).

The absolute depth limits of aerobic biodegradation have been established, directly or indirectly, in a number of studies. Philippi (1977), in his landmark paper on the origin of naphthenic crude oils through aerobic biodegradation, found a sharply defined temperature of 66 °C in several petroliferous basins as an upper temperature limit for aerobic biodegradation, which is barely higher than the average temperature of 60 °C for the top of the oil window (Hunt 1996). Using 10 °C as an annual mean surface temperature and 25–30 °C/km as average geothermal gradients, Philippi's findings limit aerobic biodegradation to the shallow and intermediate subsurface, with maximum depths of about 1700–2000 m. Connan (1984), summarizing all salient data on aerobic biodegradation then available, cited 88 °C as the maximum temperature for aerobic biodegradation, which would imply maximum depths of about 2700–3000 m. Coincidentally, the greatest depth from which biodegraded oils have been reported so far is 3048 m in the Bolivar field of Venezuela, but this appears to be a case where biodegradation occurred at much shallower depths with subsequent burial of the reservoir(s) (Bockmeulen et al. 1983). It is safe to conclude that, as a generalization, cases of aerobic biodegradation below depths of about 2000 m and above temperatures of about 65 °C are very rare. Hence, the temperature limit established by Philippi (1977) and the corresponding depth limits can be taken as approximate limits to aerobic biodegradation worldwide.

5 Fermentative Bacteria

Fermentative bacteria grow anaerobically using organic carbon compounds without requiring an external electron acceptor such as molecular oxygen, nitrate, Mn(IV), sulfate, etc. (Madigan et al. 1997). That is, fermentative bacteria decompose diverse organic "source" compounds and release simpler organic end products (often also CO_2 and H_2). The organic source compounds used by fermentative microbes commonly are partially oxidized products of aerobic bacterial metabolism. In turn, many fermentation products are carbon and energy sources for other anaerobic bacteria, including other fermentors, sulfate-reducers, and methanogens. For this reason, fermentative bacteria are assumed to be important members of subsurface consortia (Bernard et al. 1992), forming a metabolic link between aerobic and anaerobic bacteria, as shown schematically in Fig. 1.

While the products of aerobic biodegradation may or may not be used directly by the sulfate-reducing bacteria and methanogens, the simple end products of fermentation typically are substrates for these bacteria. For example, incomplete aerobic biodegradation of long chain alkanes produces fatty acids that in turn can be fermented to key products such as lactate, acetate, H_2, and CO_2, suitable substrates for sulfate reduction and methane production. Furthermore, some sulfate-reducing bacteria can also function as fermentative bacteria under certain conditions (e.g., Widdel and Hansen 1992; Krumholz et al. 1997). For example, Rosnes et al. (1991) identified a sulfate reducer from North Sea oil field waters that fermented pyruvate in the absence of sulfate. The products of such fermentation are typically simple compounds like acetate and CO_2. Whichever microbes act as fermentors, the main prod-

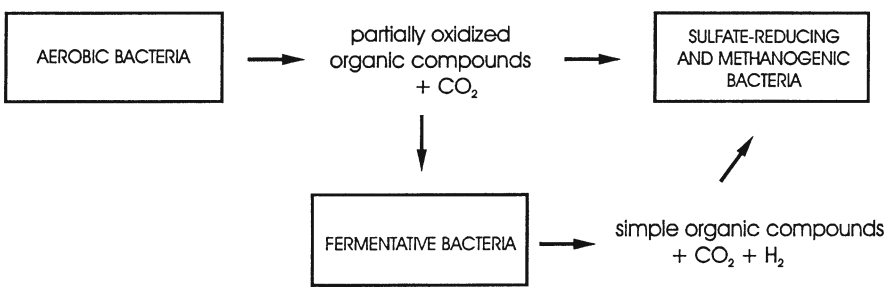

Fig. 1. Schematic diagram of fermentative microbes forming metabolic links

ucts of fermentation usually are *transient* and do not accumulate as geologically significant products.

The depth and temperature limits of fermentative microbes are difficult to ascertain. Thermophilic fermentative bacteria have rarely been isolated from oil fields, possibly because of the historical emphasis on finding sulfate reducers and methanogens. Recently, however, microbiological analyses of oil fields at depths of up to 2100 m and ambient temperatures of 68 – 92 °C have revealed the presence of thermophilic anaerobes capable of fermenting carbohydrates (Cayol et al. 1995; Ravot et al. 1995). The significance of these anaerobes in those oil wells is not clear, however, because the fermentable substrates used by these bacteria (glucose, lactose, etc.) are rare or essentially absent in oil fields. Fermentative bacteria may be more common and significant in water-flooded oil fields (e.g., Voordouw et al. 1996) where organic carbon is introduced with the injection waters (Mueller and Nielsen 1996).

6 Sulfate-Reducing Bacteria

Most sulfate-reducing bacteria are dissimilatory (H_2S-excreting) and form a heterogeneous assemblage of microbes that consists of many genera *Desulfo-x* (e.g., Postgate 1984). They commonly thrive in aquatic settings that range from the surface to several thousand meters of depth, in terrestrial surface to intermediate and deep subsurface environments (Machel 1989, and references therein). In the present context, a particularly important constraint is that sulfate-reducing bacteria commonly thrive within or near the aerobic/anaerobic transition zone between paraffinic crude oil and oxygenated groundwater (e.g., Sassen 1980; Sassen et al. 1988). In this type of setting, aerobic bacteria partially oxidize the crude oil and the anaerobic sulfate-reducing bacteria utilize metabolic products of the aerobes for their own growth (e.g., Jobson et al. 1979). Another spatial constraint, i.e., that to sandstone-shale interfaces, is discussed further below.

There are at least four sources of carbon for sulfate-reducing bacteria: (1) organic residues/products from aerobic biodegradation, as most sulfate reducers cannot thrive on petroleum without aerobic bacteria concomitantly providing nutrients in the form of oxidized derivatives of petroleum compounds, such as organic acids and alcohols (e.g., Bailey et al. 1973; Jobson et al. 1979; Westlake 1983; Lovley and Chapelle 1995); (2) organic residues from fermenting bacteria, which attack organic compounds to generate smaller organic molecules, including organic acids or alcohols, that are then used by the sulfate reducers as nutrients (Mueller and Nielsen 1996); (3) saturated hydrocarbons and alkylbenzenes in petroleum, which can be used by *some* sulfate reducers directly (Aeckersberg et al. 1991; Rueter et al. 1994; L'Haridon et al. 1995); (4) CO_2, which can be used by some sulfate reducers as the sole carbon source (Widdel and Hansen 1992). The relative importance of these metabolic pathways in subsurface environments is not known. Furthermore, the above carbon sources may also serve as energy sources for the sulfate-reducing bacteria, although many sulfate reducers may use H_2 as an energy source (Widdel and Hansen 1992), thereby competing with methanogens (see below).

There are several other requirements for bacterial generation of H_2S. The most important aspects to note are (e.g., Cochrane et al. 1983; Westlake 1983; Postgate 1984; Cypionka et al. 1985; Nazina et al. 1985; Stetter et al. 1987; Reis et al. 1992; Ehrlich 1996):

1. All sulfate-reducing bacteria are strictly anaerobic and require an Eh of less than −100 mV for growth, either in the bulk environment or in reducing microenvironments that may be present within an otherwise more oxidizing milieu; sulfate-reducing bacteria can survive for limited times at significantly higher Eh, yet they do not form H_2S under these conditions.
2. Most sulfate-reducing bacteria thrive at temperatures between 0 and 45 °C, although some are known to metabolize at higher temperatures (see Sect. 6.3, "Depth and Temperature Limits").
3. Sulfate-reducing bacteria poison their environments with their own "waste product," i.e., H_2S: *Desulfovibrio sp.* is inhibited in its metabolism (but not yet killed) at 16 mM H_2S (547 mg/l) in cultured media (this concentration should be taken as a very rough figure, considering that the experiments did not truthfully replicate natural conditions).

6.1 Main Products

All dissimilatory sulfate-reducing bacteria can reduce sulfate to hydrogen sulfide, as represented by the following schematic reaction:

$$2CH_2O + SO_4^{2-} \rightarrow 2HCO_3^- + H_2S + \text{solid bitumen} \quad (3)$$

whereby CH_2O is taken to represent a host of possible organic compounds that can be used as energy sources (including certain compounds of crude oil, organic acids, and methane); SO_4^{2-} represents dissolved sulfate that usually is derived from the dissolution of gypsum or anhydrite; and solid bitumen represents a number of sulfurized and polymerized compounds that may be formed in small quantities during bacterial sulfate reduction (Postgate 1984; Machel 1987, 1989, and references therein). Equation (3) obviously encompasses the metabolic pathways of Eq. (1) and Eq. (2) outlined in the previous section. Based on the available literature we suspect that only the associations of sulfate re-

ducers with aerobic and fermentative bacteria, i.e., the metabolic pathways of Eq. (1) and Eq. (2), are common and volumetrically important. Otherwise, virtually all subsurface settings, particularly all oil reservoirs with sulfate-rich formation waters (including most carbonate reservoirs that are associated with gypsum or anhydrite), would contain measurable quantities of H_2S. This obviously is not the case.

H_2S, the principal product of sulfate reduction, will first occur exclusively in aqueous solution (to some degree dissociated to HS^-, depending on pH). H_2S evolves as a gas phase as soon as its concentration exceeds that of its aqueous solubility. It is important to note, however, that the amounts of H_2S thus generated are limited. It is well known that sulfate-reducing bacteria poison their own environments with H_2S (e.g., Reis et al. 1992, and references therein). Hence, if the system is closed and/or the H_2S cannot escape as fast as it is generated, bacterial sulfate reduction will stop as soon as the inhibitory H_2S concentration is reached. Empirically, H_2S concentrations of more than about 5–10% (in the gas phase) require that the gas, if bacterial, was not generated in situ (such a gas was not formed where it is found, but the H_2S immigrated from a site of sulfate reduction where it escaped before reaching inhibitory or lethal concentration), or that the H_2S is thermogenic (Orr 1977; Machel 1987).

The fate of the other products of reaction shown in Eq. (1) is determined mainly by their aqueous concentrations and those of a few common ions, particularly Ca^{2+}, base metals, and H^+ (pH). If base metals are present, even at very low concentrations, metal sulfides MeS_x (pyrite, galena, sphalerite, and others) readily precipitate because of their extremely low aqueous solubilities (e.g., Berner 1980). In fact, the most commonly encountered solid evidence for bacterial sulfate reduction is bacteriogenic pyrite, which commonly occurs in the form of the well-known framboids or octahedral clusters (e.g., Canfield and Raiswell 1991b). It appears that both forms can grow simultaneously, whereby some subtle, poorly understood, fluid chemical and/or crystal growth parameters control morphology (e.g., Rickard et al. 1995). Also, bacteriogenic pyrite can occur as a replacement of, or as a cement/encrustation on, calcium carbonate shells, depending on whether the pore waters are undersaturated with respect to calcium carbonate or not (Raiswell 1997).

In addition, the sulfur isotopes of H_2S, the metal sulfides, and organic sulfur compounds formed by bacterial sulfate reduction are distinctive. Bacterial sulfate reduction imparts a large, negative, kinetic sulfur isotope fractionation (commonly between −15 and −65‰) relative to the source sulfate, which contrasts with much smaller fractionations (−20 to −15‰) via thermochemical sulfate reduction (Machel et al. 1995a and references therein). Hence, unless the system is partially or completely closed and Rayleigh fractionation occurs (Rees 1973), sulfides generated by bacterial sulfate reduction are highly depleted in ^{32}S relative to the source sulfate, which typically results in highly negative $\delta^{34}S$-values (e.g., McKibben and Eldridge 1989; Riciputi et al. 1996; Raiswell 1997). Thereby, the largest negative fractionations result from redox cycling of sulfur (between sulfate and sulfide) near oxic-anoxic interfaces, smaller fractionations result within anoxic settings where redox cycling is inhibited (Canfield and Thamdrup 1994; Bottrell and Raiswell, this Vol.). Furthermore, sulfur isotope ratios can also be used to typify a number of the organic compounds that are being formed or altered during bacterial sulfate reduction.

Table 3. Summary of sulfur isotope variations that result from maturation (THERMAL), bacterial sulfate reduction (BSR), and thermochemical sulfate reduction (TSR) in the NSO compounds of kerogen, crude oil, and solid bitumens

Kerogen (immature)	Depleted approximately −15‰ (relative to SO_4^{2-})
Kerogen (mature)	Unchanged relative to immature kerogen
Crude (immature)	Depleted approximately −15‰ (relative to SO_4^{2-})
Crude (mature)	Enriched < +2‰ (relative to kerogen)
$Crude_{BSR}$	Enriched or depleted (relative to kerogen and crude)
Solid $bitumen_{BSR}$	Enriched or depleted (relative to kerogen and crude
Solid $bitumen_{THERMAL}$	Slightly depleted (relative to kerogen and crude)
Solid $bitumen_{TSR}$	Strongly enriched (relative to kerogen and crude)

Adapted from Machel et al. (1995a). Subscripts refer to the process responsible for the changes listed.

Tables 3 and 4 present a summary of these isotopic characteristics. Given that most of the isotope signatures are relative, changes imparted by bacterial sulfate reduction are contrasted with those generated by thermochemical sulfate reduction and/or thermal maturation (Tables 3, 4).

The bicarbonate evolved during the reaction of Eq. (3) commonly precipitates as $CaCO_3$, utilizing the Ca^{2+} liberated during the dissolution of calcium sulfate. Such carbonates are isotopically distinct, in that they commonly have negative $\delta^{13}C$ values that range between that of the reduced organic matter and that of marine calcite (e.g., Machel 1989; Machel et al. 1995a).

6.2 Geologic and Economic Significance

H_2S, carbonates, bitumen, metal sulfides, and elemental sulfur resulting from bacterial sulfate reduction and partial reoxidation of sulfide are generally formed in near-surface and shallow subsurface environments,

Table 4. Distinguishing criteria of solid bitumens formed by thermal maturation and/or bacterial sulfate reduction (BSR) compared to bitumen formed by thermochemical sulfate reduction (TSR) Table is adapted from Machel et al. (1995a); see also Bottrell and Raiswell (this Vol.)

	Formed by maturation or BSR	Formed by TSR
Solubility	**Often soluble**	**Partly to largely insoluble**
δ^{34} S ke/cr-bit (relative to SO_4^{2-})	~15‰	−15–0‰
H/C	Relatively high	Relatively low
S%	4–10	10–28
δ^{34} S vs S%		Positive correlation
Asphaltenes %	Relatively low	Up to 65%
S^0	Absent	Present
δ^{13} C vs depth of sat, NSO, asph	Increasing	Decreasing?

ke, kerogen; *cr*, crude oil; *bit*, bitumen; *sat*, saturates; *asph*, asphaltenes.
Solubility designates solubility in standard organic solvents, such as CS_2.

particularly in petroliferous salt dome cap rocks where minable quantities of sulfides and sulfur may be formed (e.g., Pawlowski et al. 1979; Price and Kyle 1983; several papers in Wessel and Wimberly 1992). Meteoric water is the vehicle to transport oxygen and/or microbes into contact with subsurface hydrocarbon pools via aquifers, faults, and fractures (Milner et al. 1977), where it facilitates aerobic biodegradation and concomitant or subsequent bacterial sulfate reduction along/below the oil-water interface of relatively shallow oil reservoirs (Ashirov 1962). The main cause of H_2S oxidation to S^0 in shallow sulfur deposits probably is inorganic oxidation via oxygenated groundwater, although sulfide is also microbially oxidized to sulfur by the colorless and colored sulfur bacteria (e.g., Machel 1992; Madigan 1997). Where bitumen is absent, and the carbon isotope ratios of precipitated carbonates are lower than those of oil, methane is indicated as the main reactant hydrocarbon, as, for example, in the limestone buttes of west Texas (Kirkland and Evans 1976).

H_2S in *some* sour gas reservoirs is partially or largely due to bacterial sulfate reduction (e.g., Krouse 1977; Cody and Hutcheon 1994; Hutcheon et al. 1994). However, sour gas in intermediate and deep subsurface settings is virtually always formed by thermochemical sulfate reduction (e.g., Orr 1977; Machel 1987; Machel et al. 1995a). In either case, sour gas is a valuable resource for sulfuric acid and elemental sulfur production.

Bacterial sulfate reduction can also have economically detrimental effects. One possibility is the partial occlusion of porosity in aquifers and reservoir rocks via carbonate cementation. Another possibility is the souring of sweet oil reservoirs. It is not uncommon that sulfate-reducing bacteria are introduced into oil reservoirs during water injection, which leads to a number of problems. Firstly, sulfate-reducing bacteria are known to plug reservoir rocks (e.g., Carlson et al. 1961), even to significantly greater depths than aerobic bacteria (Shaw et al. 1985), which tends to decrease injection and production efficiency. Secondly, the microbes can turn a sweet crude into a sour crude over a period of weeks to months (e.g., Iverson and Olson 1984; Cochrane et al. 1988). This is highly undesirable, as it leads to corrosion and breakage of production equipment, including storage tanks, pipelines, and pumps, as well as to other problems, such as plugging of production equipment with colloidal FeS and calcite, or failure of oil production in polymer-flooding operations (Iverson and Olson 1984). Souring of sweet crude via bacterial sulfate reduction could occur even if no sulfate reducers are introduced. Cases are known where thermophilic sulfate-reducing bacteria appear to be present yet dormant in relatively deeply buried oil reservoirs (1670 m depth, in situ temperatures of about 65–70 °C: (L'Haridon et al. 1995). Such microbes could be triggered into action involuntarily via injection of surface waters during enhanced recovery.

Besides the spatial relationship of bacterial sulfate reduction to the oxic-anoxic transition zone (see above), there is another spatial relationship of possible significance. Pore sizes in well compacted, carbonaceous shales are often too small to permit bacterial growth, even though all other conditions are favorable for microbial activity (McMahon et al. 1992). Based on this finding, Krumholz et al. (1997) suggested that sulfate reduction may be confined to, or particularly rapid at, a band within a sandstone near the sandstone-shale interface, where the pore spaces are large enough and the organic nutrients are provided via diffusion from the shale. Hence, geologic effects, such as bacteriogenic pyrite, should be restricted to that band, if the pyrite formed after significant shale compaction. Conversely, if bacteriogenic pyrite occurs throughout a shale, bacterial sulfate reduction must have taken place before and/or during compaction.

6.3 Depth and Temperature Limits

The depth limit of bacterial sulfate reduction in subsurface environments is somewhat controversial because of a discrepancy between: (a) the maximum temperatures to which these bacteria are known to survive, and (b) data from sedimentary basins in which hyperthermophilic sulfate reducers have been retrieved from drill core samples. In the latter case, it is not always clear whether the sulfate reducers found are indigenous

or the result of contamination, and whether they are dormant or vegetative at the relatively great depths and temperatures from which they were retrieved.

Machel (1987, 1989) contended that bacterial sulfate reduction is generally limited to settings with maximum temperatures of about 60–80 °C, the empirically determined temperature range above which almost all sulfate-reducing bacteria cease to metabolize. Since that time, a number of studies have reported higher temperatures at which sulfate-reducing microbes can be vegetative, particularly from submarine hydrothermal vents, but also from some oil fields. Hyperthermophilic sulfate-reducing bacteria from marine hydrothermal vents can live at temperatures as high as at least 102 °C (e.g., Jørgensen et al. 1992; Elsgaard et al. 1994), and the suggestion has been made that "microbial rather than thermochemical sulfate reduction could be a possible source of H_2S in sulfide deposits with formation temperatures at about 100 °C" (Elsgaard et al. 1994, p. 3335). Furthermore, sulfate reducers have been retrieved from oil reservoirs in Alaska with temperatures of up to 110 °C and depths of about 3000 m (Stetter et al. 1993). These reservoirs have a history of in situ H_2S production, and enrichment cultures grew and formed H_2S at temperatures of up to 102 °C in the lab. However, these sulfate reducers do not appear to be indigenous but probably are introduced into the reservoirs with the injected sea water that is used to enhance recovery (Stetter et al. 1993). Nevertheless, this study shows that bacterial sulfate reduction is possible (a artificial) at temperatures of up to about 102 ° depths of about 3000 m. The greatest depth from w sulfate-reducing bacteria have been reported is 32 in a Russian oil field, albeit with a considerably l temperature of 84 °C (Rosanova and Khudya 1974). Furthermore, it is possible that sulfate redı survive in the form of endospores at even gr depths and temperatures, as suggested by the findi endospores that were produced by thermophilic fate-reducing bacteria from some North Sea oil waters. These endospores are extremely tempera resistant, surviving heating to temperatures of 1 for at least 20 min (Rosnes et al. 1991). Hence, it is p able that sulfate-reducers survive in the form of (vegetative) endospores at depths considerably gr than the parent vegetative microbes can tolerate. (ously, a viable sulfate-reducing microflora could b suscitated by uplift and cooling of such a subsu setting, or via injection of relatively cool water.

Although these studies show that some hyper... mophilic sulfate-reducing bacteria are vegetative at temperatures of up to about 110 °C and depths of more than 3000 m, it is clear that bacterial sulfate reduction does not normally occur at such temperatures and depths. Otherwise, no sweet oil reservoirs could occur, especially in basins that contain abundant carbonate reservoirs with associated calcium sulfate. On the contrary, there are many examples of carbonate reservoirs in, for example, the Western Canada Sedimentary Basin or the Jurassic Basin of the United States Gulf Coast that contain sweet crude oils at depths of 1000–3000 m. Hence, the temperatures and depths at which bacterial sulfate reduction commonly occurs in subsurface settings cannot be deduced from isolated reports of hyperthermophilic sulfate-reducers but must be determined from basin-wide studies of H_2S occurrences.

In his summary of gas composition and isotope data from three sedimentary basins (Alberta Basin, US Gulf Coast Basin, Wild River Basin), Krouse (1977) provided the best assessment of the depth limits of bacterial sulfate reduction in petroliferous basins so far:

1. Gases with less than about 5% H_2S, commonly taken as a loose upper limit for bacterial sour gases, occur at temperatures of less than about 80 °C.
2. In Devonian reservoirs of the Alberta Basin, $\delta^{34}S$ of dissolved sulfate in the formation waters (the residual from sulfate reduction) is higher than $\delta^{34}S$ of the associated H_2S in reservoirs with temperatures less than about 65 °C, as expected from bacterial sulfate reduction.
3. Isotope data from all three basins show that bacterial sulfate reduction is commonly restricted to subsurface settings of less than about 2000–2200 m and commensurate temperatures of 60–80 °C (Fig. 2).

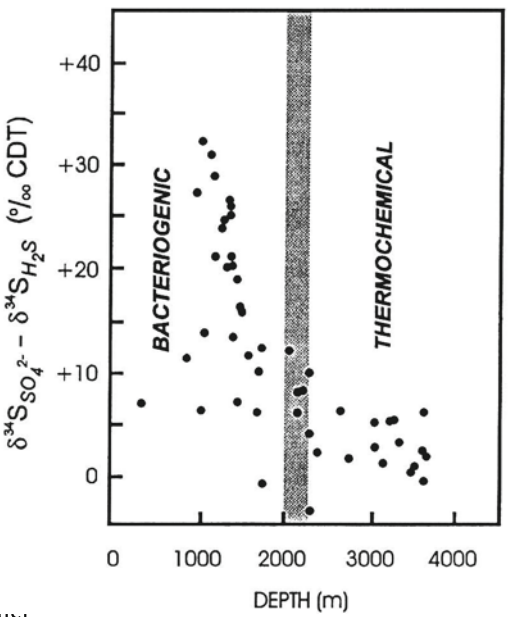

Fig. 2. The difference in sulfur isotope composition between sulfate dissolved in formation waters and hydrogen sulfide versus depth from three sedimentary basins. High isotope difference values at depths less than about 2000 m indicate in situ bacterial sulfate reduction, the effect of which diminished with increasing depth. At depths below about 2200 m, bacterial sulfate reduction appears to be volumetrically insignificant and all H_2S is thermogenic. (After Krouse 1977)

In addition, recent data from the Nisku sweet oil reservoirs in the Alberta Basin show that these reservoirs are not biodegraded at depths of 3070 – 3220 m and in situ temperatures of 102 – 108 °C, neither by aerobic bacteria nor by sulfate-reducers, even though there are abundant organic nutrients and calcium sulfate (Machel et al. 1995b; Manzano 1995; Manzano et al. 1997; Machel and Foght, unpublished data), and even though these reservoirs are at temperatures that some hyperthermophilic sulfate reducers can tolerate. Quite obviously, a depth of about 3000 m and temperature of about 100 °C are too deep/high for bacterial sulfate reduction under "normal" circumstances.

Hence, despite the recent reports of hyperthermophilic sulfate-reducing bacteria, the conclusion that bacterial sulfate reduction is generally limited to settings with maximum temperatures of about 60 – 80 °C and, therefore, to depths of less than about 2000 – 2200 m (Machel 1987, 1989; Machel et al. 1995a) is still valid. The available data also suggest that temperature is not the main limiting factor of bacterial sulfate reduction in most subsurface settings. With few exceptions, bacterial sulfate reduction appears to be limited by the fact that hyperthermophilic strains of sulfate-reducing bacteria are absent from most subsurface settings and/or by the paucity of suitable nutrients. As mentioned above, many sulfate-reducing bacteria need partially oxidized organic compounds as nutrients, which are usually provided by aerobic bacteria. Hence, the depth to which sulfate reducers are geologically significant is limited by the depth to which aerobic biodegraders or their metabolic products are significant.

7 Methanogenic Bacteria

Similar to microbial sulfate reduction, methanogenic microbial activity is a nearly ubiquitous process in near-surface, shallow subsurface, and in intermediate subsurface settings (e.g., Ehrlich 1996). There are many types of methanogenic bacteria, all of which are strict anaerobes, with various metabolic pathways that use organic compounds (e.g., formate, alcohols, fatty acids) from sedimentary organic mater, kerogen, oil, or natural gas as a carbon source. There also are many lithoautotrophic methanogens that do not use organic compounds as a carbon source but form methane from abiogenic hydrogen and carbon dioxide (Stevens and McKinley 1995).

7.1 Main Products

Two particularly common modes of microbial methane production are the reduction of CO_2 (Madigan et al. 1997) and the dissociation of acetate to methane and carbon dioxide (e.g., Lovley and Chapelle 1995):

$$CO_2 + 4H_2 \rightarrow CH_4 + 2H_2O \quad (4)$$

$$C_2H_4O_2 \rightarrow CH_4 + CO_2 \quad (5)$$

Natural gases from methanogenic bacteria typically are "dry", i.e., the hydrocarbon fraction of such gases consists almost exclusively of methane (as opposed to thermogenic gases, which invariably contain significant amounts of ethane, propane, and longer-chain alkanes; e.g., Hunt 1996). Stable isotope values of microbial methane are very low (commonly $\delta^{13}C \leq -40$‰ PDB, in extreme cases as low as −110‰ PDB, and $\delta D \pm -250$ to −150‰ SMOW; Schoell, 1983, 1988).

Microbial methanogenesis has been shown to generate carbonate (most commonly calcite) cements as by-products, directly or indirectly. "Direct" cementation occurs where the CO_2 generated in the reaction of Eq. (5) is hydrolyzed to carbonate and precipitated as calcium carbonate. "Indirect" cementation occurs where the methane is oxidized to CO_2 that is then precipitated as carbonate cement. The former is possible in any setting where methanogenesis occurs, including intermediate subsurface settings to depths of some 2000 m, whereas the latter is possible only in oxygenated settings, i.e., in near-surface to shallow subsurface settings. Under favorable circumstances, the source of the carbonate can be deduced using carbon isotope values because the methane and carbon dioxide are isotopically distinct: methane and CO_2 resulting from its oxidation have very low, negative $\delta^{13}C$ values, whereas CO_2 that originates along with methane according to Eq. (5) has high, positive $\delta^{13}C$ values of up to about +15‰ PDB (e.g., Irwin et al. 1977). Carbonate cements from the Alberta tar sand deposits are examples of "direct" carbonate cements, with $\delta^{13}C$ values of up to +14.3‰ PDB (Dimitrakopoulos and Muehlenbachs 1987). Examples of "indirect" carbonate cements occur in a number of submarine "pockmarks", i.e., craters that originated from the escape of large methane pockets near the ocean floor. In the North Sea pockmarks investigated by Hovland et al. (1987), for example, carbonate cements formed via the oxidation of predominantly biogenic methane to bicarbonate, which then precipitated as carbonate cements with $\delta^{13}C$ values as low as about −56‰ PDB.

7.2 Geologic and Economic Significance

Microbial methane is of paramount economic significance, albeit largely in surface to shallow subsurface settings. Worldwide, a significant amount of conventional dry natural gas is bacteriogenic (e.g., Schoell 1983, 1988; Davydova-Charakhch'yan et al. 1992; Hunt 1996), but much larger amounts appear to be fixed as clathrates in near-surface arctic and oceanic settings. It has been estimated that the amounts of methane in

clathrates exceed those in commercial natural gas reservoirs (biogenic plus thermogenic combined) by at least two orders of magnitude (e.g., Kvenvolden and Barnard 1984). This resource may become important in the future. In intermediate and deep subsurface settings, however, natural gas reservoirs contain almost exclusively thermogenic methane (e.g., Hunt 1996).

The authigenic carbonates formed as "direct" or "indirect" by-products of bacterial methanogenesis are usually volumetrically unimportant. They do, however, provide important isotopic evidence for the involved diagenetic processes.

7.3 Depth and Temperature Limits

Based on isotopic evidence, Schoell (1983) was the first to cite about 2000 m as the approximate depth limit for the occurrence of bacteriogenic methane in commercial quantities and, by implication, for the occurrence of methanogenic metabolism. This depth limit was established and later confirmed on the basis of data from several basins around the world: natural gases commonly become "wet" (increasing amounts of C^{2+}) and isotopically heavier between about 1600 and 2000 m, where vertical mixing of gases is minimal or prohibited, i.e., where thermogenic gases from greater depths do not diffuse upward into biogenic reservoirs (Hunt 1996). Figure 3 is a graphic representation of one of these data sets.

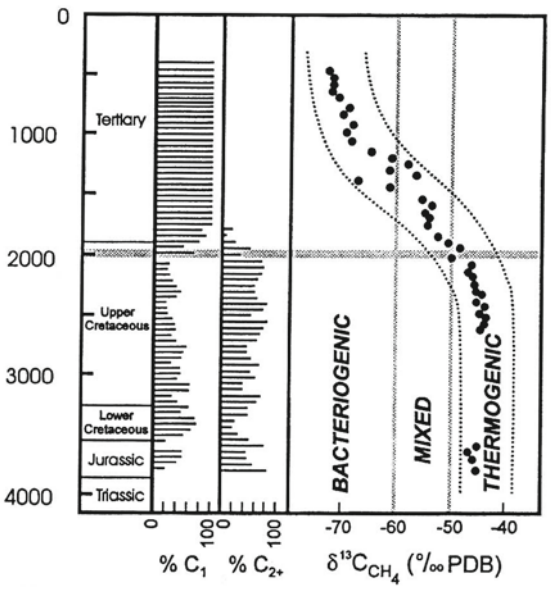

Fig. 3. Change in $\delta^{13}C$ and the percentages of CH_4 (C_1) and C_{2+} in head space gas from well 33/6–1 in the North Sea. The gases generated above about 2000 m are dry and biogenic, with very low methane $\delta^{13}C$ values of about –70‰ PDB. Gases generated below about 2000 m are wet and thermogenic, with much higher methane $\delta^{13}C$ values of about –40‰ PDB. The transition shown by the $\delta^{13}C$ values between about 1000–2000 m indicates upward escape of thermogenic gas and mixing with the biogenic gas. (After Schoell 1984)

The depth interval of about 1600–2000 m coincides with the depth (and commensurate temperature) limits for aerobic biodegraders established by Philippi (1977), but is considerably shallower than that for sulfate-reducing bacteria. This is shown not only by the distribution of the respective microbial products and by-products, including the isotopic data, but also from direct counts of microbes. Reports of thermophilic methanogenic bacteria from deep aquifers are quite rare compared to sulfate-reducing bacteria (e.g., Olson et al. 1981). Apparently, as a generalization, sulfate-reducers are more heat-tolerant than methanogens and can be expected at greater depths. In addition to temperature, another limiting factor for methanogens appears to be the abundance of sulfate. Plummer et al. (1990) noted that intermediate subsurface settings with significant gypsum or anhydrite, and, therefore, with high dissolved sulfate contents, lack significant microbial methane production, probably because of competition with sulfate-reducing bacteria for H_2 (Mueller and Nielsen 1996).

Lastly, it is interesting to note that living lithoautotrophic methanogenic bacteria have been recovered from basalt aquifers at depths of up to about 1350 m (Stevens and McKinley 1995). This finding suggests that at least some methanogens may be able to live independently of an organic carbon source at even greater depths.

8 Nanobacteria

Another group of very small microbes, yet one order of magnitude smaller in average diameter (0.05–0.2 μm), of possible geologic and economic significance are the so-called nanobacteria. Folk and Lynch (1997) recently raised the possibility that nanobacteria may be actively involved in the precipitation and transformation/recrystallization of clay minerals (mainly chlorite and illite/smectite) in buried petroliferous sandstones. These authors showed scanning electron microscopy (SEM) evidence suggestive of past and/or present nanobacterial activity from sandstones buried to depths of 2232–4421 m. At present it is speculative, however, if the suspected nanobacteria are vegetative or not, what their geologic significance is, and what their depth and temperature limits are.

9 Microbially Enhanced Oil Recovery (MEOR)

Microbially enhanced oil recovery (MEOR) is controlled uses of microbes in subsurface settings with considerable economic benefit. MEOR can be subdivided into two principal groups of procedures: (1) making oil flow that otherwise would not move, and (2) redirecting the flow of oil.

The first group entails the liquification or solubilization of viscous oil and the reduction of interfacial tension to release oil from reservoir surfaces. The involved processes are complex and include the stimulation of oil recovery as a result of increased gas pressure, production of solvents and/or acid by microbes; an increase in the viscous forces or a decrease in the interfacial tension between the oil and associated brine; solubilization of microbially produced gas in oil resulting in precipitation of asphaltenes and formation of a better flowing oil; or an improvement of the microscopic oil displacement efficiency and the volumetric sweep efficiency (e.g., McInernay and Westlake 1990).

Redirecting the flow of oil can be accomplished with ultramicrobacteria (UMB), which are non-vegetative, dormant bacteria with sizes of only $\pm$ 0.3 µm, compared to 1–4 µm for vegetative bacteria (e.g., Novitsky and Morita 1976; Kjelleberg 1993). UMB form by starvation of vegetative non-spore-forming bacteria. In their vegetative state, the bacteria metabolize and reproduce normally, including the formation of exopolysaccharide slime. Once shrunk to UMB, metabolism and reproduction are halted and the bacteria assume complete dormancy. UMB occur in nature but can also be produced quite easily in the lab from a large variety of microbes. UMB survive for many years without nourishment and can be resuscitated rapidly via the supply of suitable nutrients (e.g., Kjelleberg 1993; Cunningham et al. 1997).

These properties can be used in petroleum development. If injected into a reservoir in their vegetative state, the bacteria are essentially immobilized by their relatively large sizes and the formation of biofilms (as discussed above for aerobic and sulfate-reducing bacteria). As UMB, however, the microbes can be injected and swept relatively far into almost any reservoir rock with a permeability of > 110 md (e.g., Cusack et al. 1992; Cunningham et al. 1997). A common application of this phenomenon in petroleum development is to generate a "biobarrier" in the subsurface in order to prevent injection water from escaping through thief zones, which are undesired parts of the reservoir into which injection water escapes (injection water is supposed to push the oil toward the production wells). First UMB are injected into a reservoir where they are swept into the area to be plugged. Then nutrients are supplied, and the microbes are thereby resuscitated, upon which they form profuse exopolysaccharide slime and multiply, thus completely plugging up the formation to form a biobarrier, which then redirects subsequent injection water toward the production well(s). Such biobarriers can be constructed with a very large variety of aerobic and anaerobic microbes (nearly all that can be starved to UMB). Furthermore, the microbes can be controlled to construct relatively "tight" or relatively "loose" biobarriers. The reader is referred to Cunningham et al. (1997) for an excellent recent summary of applications of UMB in petroleum development, as well as in other fields, such as contaminant hydrogeology.

The use of microbes in oil recovery can also be detrimental. Examples include corrosion of drilling or production equipment, reservoir souring, and loss of injectivity (e.g., McInernay and Westlake 1990).

10 Sources of Microbes in Subsurface Settings

Except in those cases where microbes have been involuntarily or deliberately introduced to hydrocarbon reservoirs, the natural sources of the microbes living in intermediate and deep subsurface settings continue to be a topic of hot debate (e.g., Lovley and Chapelle 1995). Some authors suggest that life may have originated and evolved in deep subsurface settings (e.g., Gold 1992). Regardless of whether that turns out to be true, most microbes found in intermediate and deep subsurface settings today appear to be relic communities of those (much more diverse) communities that inhabited the source and/or reservoir sediments and rocks at the time of their deposition (e.g., Fredrickson and Onstott 1996). At least some microbes appear to be imported into their present habitats via groundwater flow systems, as, for example, the lithoautotrophic microbes found in basalts (Stevens and McKinley 1995). In cases where an intermediate to deep subsurface setting has been hydrologically isolated from the surface for geologically significant periods of time, i.e., particularly in regional groundwater systems, it is probable that the microbes presently found are biologically evolved derivatives of a relic community. This aspect should be considered in settings where petroliferous sedimentary units have been hydrologically isolated from surface recharge since the Mesozoic or Paleozoic, as for example in the deep subsurface parts of the Western Canada Sedimentary Basin (e.g., Bachu 1995).

11 Conclusions

Four groups of microbes are known to be geologically significant in petroliferous subsurface settings: the aerobic respiratory bacteria and three anaerobic groups, i.e., fermentative, sulfate-reducing, and methanogenic bacteria. These microbes form a number of economically important products and by-products in subsurface settings, including napthenic crude oils and tar in the form of tar sand deposits (aerobic biodegraders), H_2S, metal sulfides, and elemental sulfur (sulfate-reducing bacteria), and dry methane gas (methanogens). The role of fermenting microbes is mainly in the partial breakdown of organic molecules that then serve as nutrients for the sulfate-reducers and the methanogens.

In all cases, carbonate cements with distinctive isotopic compositions may be formed as by-products. In addition, nanobacteria might be important in clay mineral diagenesis in buried sandstones.

Various types of microbes from the above groups can be used for microbially enhanced recovery of oil. Ultramicrobacteria constitute a special class, as they are injected in a dormant state and then resuscitated in situ to form biobarriers.

With increasing subsurface depth, temperature appears to be the principal factor limiting microbial life, besides the availability of suitable nutrients. However, other factors that vary with the type of bacteria may also be important. This critical summary of available data of the products and by-products of microbial activity (including isotopic evidence) in petroliferous subsurface settings indicates that, as a rule of thumb, geologically significant microbial consortia are restricted to shallow and intermediate depths of less than about 2000–2200 m. In rare cases microbial consortia may be vegetative in petroliferous subsurface settings to depths of about 3000 m. These assessments are supported by microbiological studies on the basis of microbial counts and laboratory culturing (e.g., Bernard et al. 1992).

Most microbes found in intermediate and deep subsurface settings today appear to be relict communities of the communities that inhabited the source and/or reservoir sediments and rocks at the time of their deposition. At least some microbes appear to be imported into their present habitats via groundwater flow systems. The lower limit of the biosphere probably is marked at much greater depths and quite possibly by bacteria other than the four groups discussed above.

Acknowledgements. Numerous colleagues have made significant contributions to our understanding of microbes in petroliferous subsurface settings. Special thanks go to Phil Fedorak, Roy Krouse, and Roger Sassen. The review by Robert Raiswell was very helpful. The editorial patience of Robert Riding was exceptional and is much appreciated. Funding was provided by the Natural Science and Engineering Research Council of Canada (NSERC) and the Alexander von Humboldt Foundation.

References

Aeckersberg F, Bak F, Widdel F (1991) Anaerobic oxidation of saturated hydrocarbons to CO_2 by a new type of sulfate-reducing bacterium. Arch Microbiol 156:5–14

Andreev PF, Bogomolov AI, Dobryanskii AF, Kartsev AA (1968) Transformation of petroleum in nature. Pergamon Press, Oxford

Ashirov KB (1962) Life activity of formational microflora as an index of geologic environment and processes obtaining in petroliferous formations. In: Kuznetsov SI (ed) Geologic activity of microorganisms. Trans Inst Microbiol IX:84–91

Atlas RM (ed) (1984) Petroleum microbiology. MacMillan, New York

Azadpour A, Brown LR, Vadie AA (1996) Examination of thirteen petroliferous formations for hydrocarbon-utilizing sulfate-reducing microorganisms. J Industrial Microbiol 16:263–266

Bachu S (1995) Synthesis and model of formation water flow, Alberta Basin, Canada. Am Assoc Petrol Geol Bull 79:1159–1178

Bailey NJL, Jobson AM, Rogers MA (1973) Bacterial degradation of crude oil: comparison of field and experimental data. Chem Geol 11:203–221

Berner RA (1980) Early diagenesis. Princeton University Press, New Jersey

Bernard FP, Connan J, Magot M (1992) Indigenous microorganisms in connate water of many oil fields: a new tool in exploration and production techniques. SPE Pap No 24811:467–476

Bockmeulen H, Barker C, Dickey PA (1983) Geology and geochemistry of crude oils, Bolivar Coastal Fields, Venezuela. Am Assoc Petrol Geol Bull 67:242–270

Brooks PW, Fowler MG, Macqueen RW (1988) Biological marker and conventional organic geochemistry of oil sands/heavy oils, Western Canada Basin. Organic Geochem 12:519–538

Bustin RM, Barnes MA, Barnes WC (1985) Diagenesis 10. Quantification and modeling of organic diagenesis. Geosci Can 12:4–21

Canfield DE, Raiswell R (1991a) Carbonate precipitation and dissolution – its relevance to fossil preservation. In: Allison PA, Briggs DEG (eds), Taphonomy: releasing the data locked in the fossil record. Topics in Geobiology 9. Plenum Press, New York, pp 411–453

Canfield DE, Raiswell R (1991b) Pyrite formation and fossil preservation. In: Allison PA and Briggs DEG (eds), Taphonomy: Releasing the data locked in the fossil record. Topics in geobiology 9. Plenum Press, New York, pp 337–387

Canfield DE, Thamdrup B (1994) Production of ^{34}S-depleted sulfide during bacterial disproportionation of elemental sulfur. Science 266:1973–1975

Carlson V, Bennett EO, Rowe JA Jr (1961) Microbial flora in a number of oil-field water-injection systems. Soc Petrol Eng J 1:71–80

Cayol J-L, Ollivier B, Patel BKC, Ravot G, Magot M, Ageron E, Grimont PAD, Garcia J-L (1995) Description of *Thermoanaerobacter brockii* subsp. *lactiethylicus* subsp. nov, isolated from a deep subsurface French oil well, a proposal to reclassify *Thermoanaerobacter finii* as *Thermoanaerobacteri brockii* subsp. *finii* comb. nov, and an amended description of *Thermoanaerobacter brokkii*. Int J Syst Bacteriol 45:783–789

Claypool GE, Kaplan IR (1974) The origin and distribution of methane in marine sediments. In: Kaplan IR (ed) Natural gases in marine sediments. Mar Sci 3:99–139

Cody JD, Hutcheon I (1994) Regional water and gas geochemistry of the Mannville Group and associated horizons, southern Alberta. Bull Can Petrol Geol 42:449–464

Connan J (1984) Biodegradation of crude oils in reservoirs. In: Brooks J, Welte D (eds) Advances in petroleum geochemistry, vol 1. Academic Press, London, pp 299–335

Cochrane WJ, Jones PS, Sanders PF, Holt DM, Mosley MJ (1988) Studies on the thermophilic sulfate-reducing bacteria from a souring North Sea oil field. SPE Pap 18368:301–316

Cunningham A, Warwood B, Sturman P, Horrigan K, James G, Costerson WJ, Hiebert R (1997) Biofilm processes in porous media – practical applications. In: Amy PS, Haldeman DL (eds) The microbiology of the terrestrial deep subsurface. CRC Lewis Publishers, Boca Raton, pp 325–344

Cusack F, Brown DR, Costerson JW, Clementz DM (1987) Field and laboratory studies of microbial/fines plugging of water injection wells: Mechanism, diagnosis and removal. J Petrol Sci Eng 1:39–50

Cusack F, Singh S, McCarthy C, Grieco, J, DeRocco M, Nguyen D, Lappin-Scott H, Costerson WJ (1992) Enhanced oil recovery – three-dimensional sandpack simulation of ultramicrobacteria resuscitation in reservoir formation. J Gen Microbiol 138: 647–655

Cypionka H, Widdel F, Pfennig N (1985), Survival of sulfate-reducing bacteria after oxygen stress, and growth in sulfate-free oxygen-sulfide gradients. FEMS Microbiol Ecol 31:39–45

Davydova-Charakhch'yan IA, Kuznetsova V.G, Mityushina LL, Belyaev SS (1992) Methane-forming bacilli from oil fields of Tataria and western Siberia. Microbiology 61:202–207

Dimitrakopoulos R, Muehlenbachs K (1987) Biodegradation of petroleum as a source of ^{13}C –enriched carbon dioxide in the formation of carbonate cement. Chem Geol 65:283–291

Domenico PA, Schwartz FW (1990) Physical and chemical hydrogeology. John Wiley and Sons, New York
Ehrlich HL (1996) Geomicrobiology, 3rd edn. Marcel Dekker, New York
Elsgaard L, Isaksen MF, Jørgensen BB (1994), Microbial sulfate reduction in deep-sea sediments at the Guayamas Basin hydrothermal vent area: influence of temperature and substrates. Geochim Cosmochim Acta 58:3335 – 3343
Fisk MR, Giovanni SJ, Thorseth, IH (1998) Alteration of volcanic glass: textural evidence of microbial activity. Science 281: 978 – 980
Folk RL, Lynch FL (1997) The possible role of nanobacteria (dwarf bacteria) in clay mineral diagenesis and the importance of careful sample preparation in high-magnification SEM studies. J Sediment Res 67:583 – 589
Fredrickson JK, Onstott TC (1996) Microbes deep inside the Earth. Scientific American October, pp 68 – 73
Fredrickson JK, Garland TR, Hicks RJ, Thomas JM, Li SW, McFadden SM (1989) Lithotrophic and heterotrophic bacteria in deep subsurface sediments and their relation to sediment properties. Geomicrobiol J 7:53 – 66
Gold T (1992) The deep, hot biosphere. Proc Natl Acad Sci USA 89:6045 – 6049
Gould KW, Smith JW (1978) Isotopic evidence for microbiological role in genesis of crude oil from Barrow Island, Western Australia. Am Assoc Petrol Geol Bull 62:455 – 462
Hanor JS (1983) Fifty years of development of thought on the origin and evolution of subsurface sedimentary brines. In: Boardman, SJ (ed) Revolution in the earth sciences: Advances in the past half-century. Kendall/Hunt, Dubuque, pp 99 – 111
Horstad I, Larter SR (1997) Petroleum migration, alteration, and remigration within Troll Field, Norwegian North Sea. Am Assoc Petrol Geol Bull 81:222 – 248
Hovland M, Talbot MR, Qvale H, Olaussen S, Aasberg L (1987) Methane-related carbonate cements in pockmarks of the North Sea. J Sediment Petrol 57:881 – 892
Hunt JM (1996) Petroleum geochemistry and geology. Second Edition. WH Freeman and Company, New York
Hutcheon I, Cody J, McLellan S, Abercrombie H (1994) Controls on the distribution of non-hydrocarbon gases in the Western Canada Sedimentary Basin. In: Ross GM (ed) Alberta Transects Workshop, Lithoprobe Report no 37, Lithoprobe Secretariat, University of British Columbia, pp 199 – 224
Irwin H, Curtis C, Coleman ML (1977) Isotopic evidence for source of diagenetic carbonates formed during burial of organic-rich sediments. Nature 269:209 – 213
Iverson WP, Olson GJ (1984) Problems related to sulfate-reducing bacteria in the petroleum industry. In: Atlas RM (ed) Petroleum microbiology. McMillan Publishing, New York, pp 619 – 641
Jobson AM, Cook FD, Westlake DWS (1979) Interaction of aerobic and anaerobic bacteria in petroleum biodegradation. Chem Geol 24:355 – 365
Jørgensen BB, Isaksen MF, Jannasch HW (1992) Bacterial sulfate reduction above 100°C in deep sea hydrothermal vent sediments. Science 258:1756 – 1757
Kelly WR, Herman JS, Mills AL (1997) The geochemical effects of benzene, toluene, and xylene (BTX) biodegradation. Appl Geochem 12:291 – 303
Kerr RA (1997) Life goes to extremes in the deep earth – and elsewhere? Science 276:703 – 704
Kirkland DW, Evans R (1976) Origin of limestone buttes, gypsum plain, Culberson County, Texas. Am Assoc Petrol Geol Bull 60:2005 – 2018
Kjelleberg S (1993) Starvation in bacteria. Plenum Press, New York
Krouse HR (1977) Sulfur isotope studies and their role in petroleum exploration. J Geochem Explor 7:189 – 211
Krouse HR (1983) Stable isotope research in support of more effective utilization of gas fields in Alberta. Alberta – Canada Energy Resource Research Fund Agreement U – 30, 100 pp
Krumholz LR, McKinley JP, Ulrich GA, Suflita JM (1997) Confined subsurface microbial communities in Cretaceous rock. Nature 386:64 – 66
Kvenvolden KA, Barnard LA (1984) Hydrates of natural gas in continental margins. Am Assoc Petrol Geol Mem 34:631 – 640
L'Haridon S, Reysenbach AL, Glénat P, Prieur D, Jeanthon C (1995) Hot subterranean biosphere in a continental oil reservoir. Nature 377:223 – 224
Lindt IL. (1993) Stylolites in chalk from Leg 130, Ontong Java Plateau. In: Berger WH, Kroenke JW, Mayer LA (eds) Proceedings of the Ocean Drilling Program, Scientific Results, 130:445 – 451
Lovley DR, Chapelle FH (1995) Deep subsurface microbial processes. Rev Geophys 33:365 – 381
Lovley DR, Phillips EJP (1992) Bioremediation of uranium contamination with enzymatic uranium reduction. Environ Sci Technol 26:2228 – 2234
Machel HG (1987) Some aspects of diagenetic sulphate – hydrocarbon redox – reactions. In: Marshall JD (ed) Diagenesis of sedimentary sequences. Geological Society Special Publication, No 36, pp 15 – 28
Machel HG (1989) Relationships between sulphate reduction and oxidation of organic compounds to carbonate diagenesis, hydrocarbon accumulations, salt domes, and metal sulphide deposits. Carbonates Evaporites 4:137 – 151
Machel HG (1990) Burial diagenesis, porosity and permeability development in carbonates. In: Bloy GR, Hadley MG (eds) The development of porosity in carbonate reservoirs. Canadian Society Petroleum Geologists Short Course Notes:2-1 – 2-18
Machel HG (1992) Low-temperature and high-temperature origins of elemental sulfur in diagenetic environments. In: Wessel GR, Wimberly BH (eds) Native sulfur – developments in geology and exploration. Society for Mining, Metallurgy and Exploration, Littleton, Colorado, pp 3 – 22
Machel HG (1999) Effects of groundwater flow on mineral diagenesis, with emphasis on carbonate aquifers. Hydrogeology Journal: 7: 94 – 107
Machel HG, Krouse HR, Sassen R (1995a) Products and distinguishing criteria of bacterial and thermochemical sulfate reduction. Appl Geochem 10:373 – 389
Machel HG, Krouse HR, Riciputi LR, Cole DR (1995b) Devonian Nisku sour gas play, Canada: A unique natural laboratory for study of thermochemical sulfate reduction. In: Vairavamurthy MA, Schoonen MAA (eds) Geochemical transformations of sedimentary sulfur. ACS Symposium Series, No 612, pp 439 – 454
Madigan MT, Martinko JM, Parker J (1997) Brock biology of microorganisms. 8th edn. Prentice Hall, Upper Saddle River, NJ
Manzano BK (1995) Organic geochemistry of oil and sour gas reservoirs in the Upper Devonian Nisku Formation, Brazeau River Area, Central Alberta. Unpub. MSc Thesis, Univ of Alberta, 101 pp
Manzano BK, Fowler MG, Machel HG (1997) The influence of thermochemical sulfate reduction on hydrocarbon composition in Nisku reservoirs, Brazeau River area, Alberta, Canada. Organic Geochemistry 27: 507 – 521
McInerney MJ, Westlake DWS (1990) Microbial enhanced oil recoovery. In: Ehrlich HHL, Brierley CL (eds) Microbial mineral recovery. MGraw-Hill, New York, pp 409 – 445
McKibben MA, Eldridge CS (1989) Sulfur isotope variations among minerals and aqueous species in the Salton Sea geothermal system: a SHRIMP ion microprobe and conventional study of active ore genesis in a sediment-hosted environment. Am J Sci 289:661 – 707
McMahon PB, Chapelle FH, Falls WFF, Bradley PM (1992) The role of microbial processes in linking sandstone diagenesis with organic-rich clays. J Sediment Petrol 62:1 – 10
Milner CWD, Rogers MA, Evans MA (1977) Petroleum transformation in reservoirs. J Geochem Explor 7:101 – 153
Moldowan JM, Albrecht P, Philp RP (eds) (1992) Biological markers in sediments and petroleum. Prentice Hall, Englewood Cliffs
Mueller RF, Nielsen, P.H (1996) Characterization of thermophilic consortia from two souring oil reservoirs. Appl Environ Microbiol 62:3083 – 3087
Nazina TN, Rozanova EP, Knzetsov SI (1985) Microbial oil transformation Processes accompanied by methane and hydrogen sulfide formation. Geomicrobiol J 4:103 – 130
Novitsky JA, Morita RY (1976) Morphological characterization of small cells resulting from nutrient starvation of a psychrophilic marine vibiro. Appl Environ Microbiol 32:617 – 622
Olson GJ, Dockins WS, McFeters GA, Iverson WP (1981) Sulfate-reducing bacteria from deep aquifers in Montana. Geomicrobiol J 2:327 – 339

Orr WL (1977) Geologic and geochemical controls on the distribution of hydrogen sulfide in natural gas. In: Campos R, Goni J (eds) Advances in organic geochemistry. Enadisma, Madrid, pp 571–597

Pawlowski S, Pawlowska K, Kubica B (1979) Geology and genesis of the Polish sulfur deposits. Econ Geol 74:475–483

Pedersen K (1993) The deep subterranean biosphere. Earth Sci Rev 34:243–260

Pedersen K (1996) Investigations of subterranean bacteria in deep crystalline bedrock and their importance for the disposal of nuclear waste. Can J Microbiol 42:382–391

Peters KE, Moldowan JM (1993) The biomarker guide: interpreting molecular fossils in petroleum and ancient sediments. Prentice Hall, Englewood Cliffs

Philippi GT (1977) On the depth, time, and mechanism of origin of the heavy to medium- gravity naphthenic crude oils. Geochim Cosmochim Acta 41:33–52

Plummer LN, Busby JF, Lee RW, Hanshaw BB (1990) Geochemical modeling of the Madison aquifer in parts of Montana, Wyoming, and South Dakota. Water Resour Res 26:1981–2014

Postgate JR (1984) The sulfate-reducing bacteria., 2nd edn. Cambridge University Press, Cambridge

Price PE, Kyle JR (1983) Metallic sulfide deposits in Gulf Coast salt dome cap rocks. Trans Gulf Coast Assoc Geol Soc 33:189–193

Raiswell R (1997) A geochemical framework for the application of stable sulphur isotopes to fossil pyritization. J Geol Soc Lond 154:343–356

Ravot G, Magot M, Fardeau M-L, Patel BKC, Prensier G, Egan A, Garcia J-L, Ollivier B (1995) *Thermotoga elfii*, sp. nov, an novel thermophilic bacterium from an African oil-producing well. Int J Syst Bacteriol 45:308–314

Rees CE (1973) A steady-state model for sulfur isotope fractionation in bacterial reduction. Geochim Cosmochim Acta 37:1141–1162

Reis MAM, Almeida JS, Lemos PC, Carrondo MJT (1992) Effect of hydrogen sulfide on growth of sulfate reducing bacteria. Biotechnol Bioeng 40:593–600

Riciputi LR, Cole DR, Machel HG (1996) Sulfide formation in reservoir carbonates of the Devonian Nisku Formation, Alberta, Canada. Geochim Cosmochim Acta 60:325–336

Rickard D, Schoonen MAA, Luther III GW (1995) Chemistry of iron sulfides in sedimentary environments. In: Vairavamurthy MA, Schoonen MAA (eds) Geochemical Transformations of sedimentary sulfur. ACS Symp Ser 612:168–193

Rosanova EP, Khudyakova AI (1974) A new non spore-forming thermophilic sulfate-reducing organism, *Desulfovibrio thermophilus*, nov. sp. Microbiology 43:908–912

Rosnes JT, Torsvik T, Lien T (1991) Spore-forming thermophilic sulfate-reducing bacteria isolated from North Sea oil field waters. Appl Environ Microbiol 57:2302–2307

Rueter P, Rabus R, Wilkes H, Aeckersberg F, Rainey FA, Jannasch HW, Widdel F (1994) Anaerobic oxidation of hydrocarbons in crude oil by new types of sulphate-reducing bacteria. Nature 372:455–458

Sassen R (1980) Biodegradation of crude oil and Mineral deposition in a shallow Gulf Coast salt dome. Organic Geochem 2:153–166

Sassen R, Chinn EW, McCabe C (1988) Recent hydrocarbon alteration, sulfate reduction and formation of elemental sulfur and metal sulfides in salt dome cap rock. Chem Geol 74:57–66

Schoell M (1983) Genetic characterization of natural gases. Am Assoc Petrol Geol Bull 67:2225–2238

Schoell M (1984) Recent advances in petroleum geochemistry. Organic Geochem 6:645–663

Schoell M (1988) Multiple origins of methane in the earth. Chem Geol 71:1–10

Shaw JC, Bramhill B, Wardlaw NC, Costerson JW (1985) Bacterial fouling in a model core system. Appl Environ Microbiol 49:693–701

Stetter KO, Lauerer G, Thomm M, Meuner A (1987) Isolation of extremely thermophilic sulfate reducers: evidence for a novel branch of archaebacteria. Science 236:822–824

Stetter KO, Fiala G, Huber G, Huber R, Segerer A (1990) Hyperthermophilic microorganisms. FEMS Microbiol Rev 75:117–124

Stetter KO, Huber R, Blöchl E, Kurr M, Eden RD, Fielder M, Cash H, Vance I (1993) Hyperthermophilic archaea are thriving in deep North Sea and Alaskan oil reservoirs. Nature 365:743–745

Stevens TO, McKinley JP (1995) Lithoautotrophic microbial ecosystems in deep basalt aquifers. Science 270:450–454

Tóth J (1963) A theoretical analysis of groundwater flow in small drainage basins. J Geophys Res 68:4795–4812

Volkman JK, Alexander R, Kagi RI, Woodhouse GW (1983) Demethylated hopanes in crude oils and their applications in petroleum geochemistry. Geochim Cosmochim Acta 47:785–794

Voordouw G, Armstrong SM, Reimer MF, Fouts B, Telang AJ, Shen Y, Gevertz D (1996) Characterization of 16 S rRNA genes from oil field microbial communities indicates the presence of a variety of sulfate-reducing, fermentative, and sulfide-oxidizing bacteria. Appl Environ Microbiol 62:1623–1629

Wessel GR, Wimberly BH (eds) (1992) Native sulfur – developments in geology and exploration. Society for Mining, Metallurgy and Exploration

Westlake DWS (1983) Microbial activities and changes in the chemical and physical properties of oil. In: Donaldson EC, Clark JB (eds) Proceedings of International Conference on Microbial Enhancement of Oil Recovery, Afton, Oklahoma. US Department of Energy, pp 102–111

Widdel F, Hansen TA (1992) The dissimilatory sulfate- and sulfur-reducing bacteria. In: Balows A, Trüper HG, Dworkin M, Harder W, Schliefer KH (eds) The prokaryotes, I, 2nd edn. Springer, Berlin Heidelberg New York, pp 583–624

Zehender AJB (ed) (1988) Biology of anaerobic microorganisms. John Wiley and Sons, New York

Microbe-Metal Interactions in Sediments

F. G. Ferris

Department of Geology, University of Toronto, 22 Russell Street, Toronto, Ontario, M5S 3B1 Canada

Abstract. Microbial contributions to the solid phase partitioning of metals in sediments span a continuum of sorption and precipitation reactions. Passive involvement of microorganisms in these processes relates to the behavior of individual microbial cells as sorbents of dissolved metals and heterogeneous nucleation templates for authigenic mineral deposition. Active microbial intervention is also possible with metal precipitation being induced in response to metabolic production of reactive inorganic ligands such as sulfide, or through enzyme mediated changes in metal redox state. The deposition of authigenic iron-aluminum-silicates and metallic gold on microbial surfaces comprise unique examples of passive microbe-metal interactions, while the reductive precipitation of uranium is representative of metabolic metal precipitation by microorganisms.

1 Introduction

Sediments constitute an important sink for the solid phase immobilization and accumulation of metals. The extent to which this occurs depends not only on the provenance and depositional history of particulate materials deposited in sediments, but also on diagenetic processes that modify sediment mineralogy and chemistry (Stumm and Morgan 1996). Variations in the forms of metals that accumulate in sediments evolve principally in response to differential partitioning among the various inorganic solids and organic materials comprising the sedimentary matrix. These include detrital minerals and chemical precipitates formed directly within the sedimentary environment as well as insoluble humic materials, biological debris, and living organisms (Tessier et al. 1996).

Within sediments, sorption and precipitation reactions are the main protagonists in the solid phase partitioning of metals (Tessier et al. 1996; Stumm and Morgan 1996). Sorption reactions tend to predominate over precipitation when metals are undersaturated with respect to their least soluble compounds. The opposite is generally true when porewater concentrations of dissolved metals exceed equilibrium constraints on mineral solubility. Both types of reactions tend to be sensitive to pH and/or redox potential, while their overall progress is commonly sustained at least in part, if not entirely, by microorganisms indigenous to sedimentary environments (Buffle 1990; Stumm and Morgan 1996).

Microbiological contributions to metal sorption and precipitation reactions are remarkably diverse. In the absence of metabolic activity, passive interactions may occur in which microbial cells (living or dead) behave as solid phase sorbents of dissolved metals, and heterogeneous nucleation templates for authigenic mineral deposition (Beveridge 1989; McLean et al. 1996). On the other hand, metabolic activities of some microorganisms bring about metal precipitation indirectly through production of reactive inorganic ligands, e.g., sulfide, phosphate, dissolved inorganic carbon, or directly through enzyme mediated changes in redox state, e.g., oxidation of reduced iron and manganese (Bachofen 1994).

The scope of microbe-metal interactions in sediments is vast and impinges on the subject matter of other chapters in this volume. For this reason, much of the following discussion is focused on some of the more fundamental geochemical relationships between microorganisms and metals in sediments. This forms a bridge to a brief consideration of the impact of dissimilatory iron-reducing bacteria on metal cycling in sediments and their role in the reductive precipitation of uranium, metallic gold deposition by microorganisms, and formation of polymetallic iron-aluminum silicates on microbial cell surfaces.

2 Sources of Metals in Recent Sediments

The most immediate source of metals available for incorporation into sediments is the overlying water column. Concentrations of metals in aquatic systems are often highly variable, depending largely on the environmental and geochemical history of the water in transit. More specifically, dissolved metal concentrations are strongly influenced by chemical weathering reactions involving water-rock interactions, and geographic differences in hydrology and lithology (Stumm and Morgan 1996).

A significant portion of the total metal load in aquatic systems is associated with particulate materials, often to the extent of exceeding the dissolved fraction in solution. These metal-laden particulates include

R. E. Riding and S. M. Awramik (Eds.)
Microbial Sediments

various detrital minerals, inorganic precipitates produced directly within the water column, humic compounds, and biological debris (Sigg 1994). Removal of particulates from the water column by sedimentation plays a particularly important role in the physical transport of metals to bottom sediments (Stumm and Morgan 1996). At the same time, steep concentration gradients that commonly develop across the sediment-water interface sustain an additional downward movement of dissolved metals into sediments (Tessier et al. 1994). Thus, with ongoing sedimentation and diffusion, microorganisms in sediments are exposed to a combination of both dissolved and particulate metals.

3 Microbial Cell Structure and Metal Ions

Cell walls isolated from microbial cells grown on laboratory media typically contain measurable quantities of metal ions. The presence of these bound metals attest not only to the chemical reactivity of structural polymers in the walls of microorganisms, but also infer an important role for metals in the maintenance of cell shape and integrity (Bachofen 1994). Salt-bridging by magnesium ions, for example, helps stabilize the alignment of secondary polymers, like teichoic or teichuronic acids which are threaded through the peptidoglycan wall matrix of gram-positive bacteria such as *Bacillus subtilis*. Similarly, gram-negative bacteria such as *Pseudomonas aeruginosa* or *Escherichia coli* depend on magnesium or calcium ions to conserve the structural integrity of their outer membranes (Beveridge 1989).

Extracellular capsules and sheaths produced by many microorganisms can extend large distances away from the cell wall (Fig. 1). Their production is controlled not only by nutrient availability (e.g., carbon and nitrogen abundance), but also by the various dissolved metal ions to which the cell is exposed. For example, extracellular capsule production in *Chromobacterium violaceum* is stimulated by iron and calcium (Beveridge 1989). Moreover, the physical state of capsular polymers seems to be influenced by the type and quantity of metals that are incorporated. In the case of *Azotobacter chroococcum*, a condensed capsule is produced when the cells are grown with iron or molybdenum in the medium, whereas the capsule is more extensive and diffuse in the absence of the metals (Beveridge 1989). There is even some evidence that capsules provide microbial cells with a measure of protection from the toxic effects of heavy metals in contaminated environments (Al-Aoukaty et al. 1990).

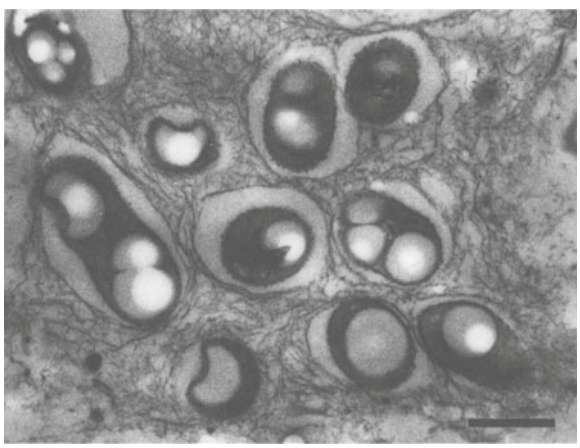

Fig. 1. Thin-section transmission electron micrograph of a bacterial microcolony surrounded by a fibrous matrix of extracellular capsular material (*bar* = 500 nm)

Of the various extracellular surface structures that are produced by microorganisms, proteinaceous S-layers depend critically on metal ions for their assembly on and adherence to the underlying wall. Those of *Aquaspirillum* spp. and *Sporosarcina ureae*, for example, require either calcium or magnesium for proper assembly (Beveridge 1989). Similarly, the external cell sheaths of *Methanospirillum hungatei* and *Methanothrix concilii* have been shown to preferentially accumulate metals from their growth media. In the case of *Methanothrix*, zinc and iron are taken up by the sheath, whereas that of *Methanosprillum* seems to prefer calcium and magnesium (Beveridge 1989).

4 Microbial Sorption of Metal Ions

The behavior of microbial cells as sorbents of metal ions is related to the presence of acidic functional groups (e.g., carboxyl and phosphoryl substituents) in the structural polymers of their cell walls and extracellular sheaths or capsules. Deprotonation of these various functional groups contributes directly to the solid phase reactivity of individual cells by providing discrete complexation sites for metal sorption. A general competitive sorption reaction for a metal ion (Me^{z+}) at a surface carboxyl binding site on a microbial cell (B-COOH) can be written as follows:

$$B\text{-}COOH + Me^{z+} \longleftrightarrow B\text{-}COOMe^{z-1} + H^{+}$$

The release of protons and sorption of metal ions is described by apparent (Ka) and conditional (KpH) sorption constants (Buffle 1990; Tessier et al. 1994):

$$KpH = Ka/\{H^{+}\} = \{B\text{-}COOMe^{z-1}\}/\{B\text{-}COOH\}\{Me^{z+}\}$$

where {} denotes activities of surface bound or dissolved species in solution. This equilibrium expression emphasizes that metal ion sorption by microorganisms is dependent not only on pH and dissolved metal ion concentrations, but also on the number of reactive chemical groups per cell (i.e., B-COOH+B-$COOMe^{z-1}$).

An additional assumption, which is not obvious from the equilibrium condition or easily extended to microbial cells, is that all reactive surface groups are structurally and chemically fully equivalent (Buffle 1990).

The total number of reactive groups contributing to microbial metal ion sorption is related to the architecture and macromolecular composition of the different enveloping layers around the cells. Considerable ultrastructural variation exists between different types of microorganisms and can even arise within a single species as growth conditions change (Beveridge 1989). Rather pronounced differences in metal-binding capacity therefore arise between dissimilar microorganisms. For example, isolated cell walls from gram-positive *Bacillus subtilis* bind more metal than cell envelopes from gram-negative *Escherichia coli.* Moreover, metal sorption can be mediated simultaneously by a number of different structural polymers (McLean et al. 1996). This makes it extremely difficult to apply equilibrium surface complexation models to microbial metal sorption, a difficulty that is common to most heterogeneous solids encountered in sedimentary environments (Stumm and Morgan 1996).

The pH dependence of metal ion sorption is an important intrinsic feature of the metal uptake by solid phase sorbents, including microorganisms (Ferris et al. 1989; Buffle 1990). For those metals that exist predominantly as cationic species in solution, sorption is enhanced significantly as pH increases and surface groups deprotonate. Conversely, metals or metalloids present as oxyanions sorb better at lower pH values as surface groups become protonated. These basic principles explain why natural microbial biofilms in acidic metal contaminated waters immobilize less metal than those exposed to more dilute metal concentrations under circumneutral pH conditions (Ferris et al. 1989). The chemical properties of the sorbing metals will also influence the extent of sorption. Often there is a strong positive correlation between the tendency of a metal to undergo hydrolysis in solution and its affinity for a solid phase sorbent (Buffle 1990). Thus, in natural systems different metals present at similar concentrations will be differentially sorbed.

Understanding the importance of microbial metal sorption in natural sediments is not an easy exercise as sedimentary organic material consists of a complex mixture of detrital biological debris in varying stages of decomposition and variable amounts of microbial biomass. Nevertheless, selective chemical extraction with strong oxidants (e.g., H_2O_2, NaOCl) indicates that sedimentary organic matter comprises a sink for 5–20% or more of the total trace metal load of terrigenous sediments (Sigg 1994). Moreover, the influence of organic matter on metal immobilization can be distinguished visually in organic-rich lake and marine sediments. Specifically, transmission electron microscopic studies of sediments from such environments show that the membranous cellular remains of microbial cells acquire a high degree of electron contrast through in situ sorption of metals (Ferris et al. 1987; Degens and Ittekkot 1982).

5 Microbial Precipitation of Metals

Microorganisms contribute to the precipitation of a wide variety of authigenic minerals including oxides, phosphates, carbonates, sulfides, and silicates (Ferris et al. 1987–1989, 1995; Konhauser et al. 1993, 1994a,b; Konhauser and Ferris 1996). The mechanisms of microbial mineral precipitation are diverse, but generally involve two distinct stages. These are nucleation and crystal growth (Stumm and Morgan 1996). Nucleation is the most critical stage for mineral precipitation and occurs either homogeneously or heterogeneously. In homogeneous reactions, mineral nuclei are formed by the random collision of ions in solution. Conversely, heterogeneous nucleation involves formation of crystal nuclei on the surfaces of foreign solids like microbial cells. Once a stable nucleus has formed, crystal growth can proceed spontaneously providing that the concentration of ions in solution continues to exceed the solubility product of the solid mineral phase (i.e., the solution must be oversaturated).

The free energy of crystal nucleation is constrained thermodynamically by the bulk free energy of the solution and the interfacial free energy of the corresponding solid phase (Stumm and Morgan 1996). The bulk free energy term is a function of the degree to which a solution is oversaturated, whereas the interfacial free energy depends on the interfacial surface tension of the solid phase and surface area of the nucleus. These thermodynamic relationships provide a useful working model to better understand microbial contributions to mineral precipitation.

Microbial metabolic activity will often trigger a change in solution chemistry that leads to oversaturation. This alone can induce mineral precipitation by lowering the bulk free energy term for both homogeneous and heterogeneous nucleation reactions (Stumm and Morgan 1996); however, chemically reactive sites on microbial cell surfaces that facilitate metal sorption at the nucleation sites will tend to reduce the interfacial surface tension of the solid phase and decrease the surface area of the nucleus that is in contact with the bulk solution. The expected result is a reduction in the overall interfacial free energy of the nucleus that is conducive towards heterogeneous nucleation and precipitation.

Changes in the amount of metals associated with solid phases, particularly authigenic precipitates, tend to bring about rather large changes in dissolved metal

concentrations in sediments (Tessier et al. 1994). These variations are fairly sensitive indicators of ongoing diagenetic reactions, many of which are directly mediated by microorganisms. Moreover, the apparent chemical evolution of interstitial waters in sediments generally parallels sharp vertical gradients in microbial activity and redox potential (Stumm and Morgan 1996). Near the sediment water interface, microorganisms rely on oxygen as an electron acceptor to derive energy from the oxidation of organic matter. Once the oxygen is depleted, microbial energy metabolism is sustained by other electron acceptors including nitrate, iron and manganese oxides, sulfate, and even organic matter in the case of methanogens (Bachofen 1994).

Of the various microorganisms active in anaerobic sediments, dissimilatory iron and manganese reducers are particularly notable as agents of diagenetic transformations involving metals (Lovley 1991; Nealson and Saffarini 1994). The hydrous iron and manganese oxides utilized by these microorganisms occur as discrete particles or as coatings on clay minerals, carbonates, and other particulate material (e.g., microbial cells) that may serve as heterogeneous nucleation sites for oxide deposition (Fortin et al. 1993). The status of iron and manganese oxides as a major sink for trace metals is well established, owing to sorption and co-precipitation reactions (Warren and Zimmerman 1994; Tessier et al. 1996; Herbert 1996); however, microbial reduction and dissolution of metal-laden iron and manganese oxides in anaerobic sediments will tend to release sorbed trace metals (Nealson and Saffarini, 1994). In turn, these metals may subsequently be precipitated in a zone of microbial sulfate reduction to produce an assemblage of sulfide and carbonate minerals (Ferris et al. 1987; Coleman et al. 1993).

The reduction of soluble uranium (VI) to insoluble uranium (IV) is an important reaction for the immobilization of dissolved uranium in sedimentary environments. Until recently, this reaction was thought to be mediated strictly by inorganic reactions involving chemical reduction of uranium by sulfide, hydrogen, or organic matter; however, a number of sulfate and iron reducing bacteria have been shown to use uranium (VI) as a terminal electron acceptor for anaerobic respiration (Lovley et al. 1991). The kinetics of uranium reduction by electron transport during anaerobic microbial respiration appear to be much faster than reduction by inorganic chemical processes under defined laboratory conditions and in aquatic sediments. Thus, immobilization of uranium by reductive microbial precipitation has been proposed to account for the deposition of uranium in such environments as marine sediments, roll-type deposits, and bleached reduction spots in iron oxide-rich red beds (Lovley 1991). Similar processes may account for the polymetallic uranium, copper, bismuth, cobalt, and nickel mineralization that has been reported to accumulate on the external surfaces of microbial cells in some peat bog and flood plain silts (Milodowski et al. 1990).

Spontaneous formation of colloidal metallic gold particles within the cytoplasm and walls of microbial cells exposed to solutions containing Au^{3+} is one of the most intriguing processes involving microorganisms and metals (Fig. 2a; Southam and Beveridge 1994). The mechanism(s) of the reaction(s) are not clear, although it probably encompasses a combination of sorption and reductive precipitation reactions. Active metabolic participation of the microorganisms is not needed, as gold precipitates are formed equally well by living or dead cells. The implication is that some organic constituent of microbial cells serves as a chemical reductant for Au^{3+} precipitation, probably in much the same way as some low molecular weight organic compounds promote the reductive dissolution of iron oxides (Stumm and Morgan 1996).

Studies on Alaskan gold placer deposits have revealed small cauliform aggregates of gold comprised of spherical bodies equivalent in shape and size to bacte-

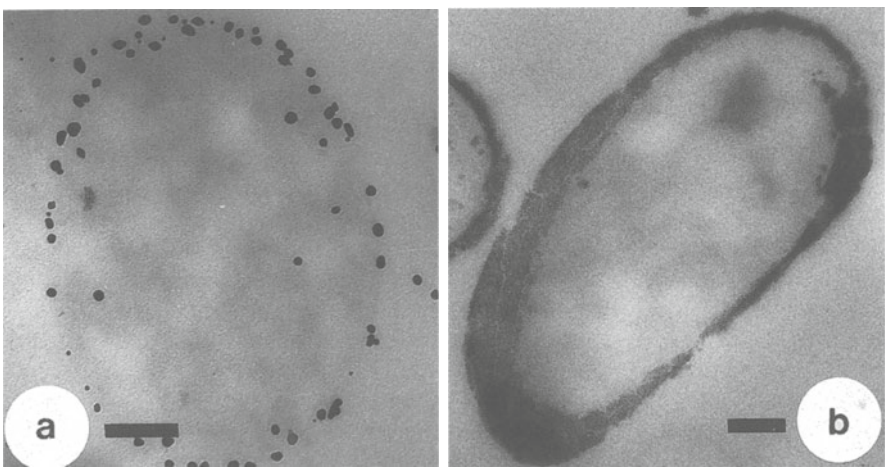

Fig. 2. Thin-section transmission electron micrographs of **a** electron dense gold particles that have developed in association with the cell wall of a bacterial cell exposed to dissolved Au^{3+}, and **b** iron-silica precipitates encrusting a bacterial cell in a hot spring sediment sample from Iceland (*bars* = 100 nm)

rial cells (Watterson 1991). Similar microbial textures occur in carbonaceous gold-bearing conglomerates of the Witwatersrand in South Africa (Hallbauer and van Warmelo 1974). In addition, isotopic analyses on carbonaceous gold ores and host rocks from the Abitibi belt in Canada have yielded δ^{13} C values that extend from −15 to −47 (Strauss 1986; Wilson and Rucklidge 1987), a range consistent with a biogenic origin for the carbon (Schidlowski 1987).

Diagenetic reactions involving fine-grained iron-aluminum silicate minerals are known to play an important role in the solid phase partitioning of metal ions in both freshwater and marine sedimentary systems. This is true of major dissolved species like sodium, potassium, calcium, and magnesium, as well as trace metals such as copper, zinc, and lead (Mackenzie and Kump 1995; Stumm and Morgan 1996). While these minerals are common products of weathering and may accumulate in sediments as detrital particulates, some appear to evolve in situ as authigenic precipitates on the surfaces of microbial cells (Ferris et al. 1987; Konhauser et al. 1994a;1994b). Microbially mediated iron smectite deposition (i.e., nontronite) near deep-sea hydrothermal vents has been found to produce delicate mineralized filaments that are similar in size and form to sheath forming bacteria (Köhler et al. 1994). Mineralization and preservation of microbial cells by iron-silica precipitates also occur in terrestrial hot spring sediments (Fig. 2b) (Ferris et al. 1986; Konhauser and Ferris 1996). In addition, the ability of microorganisms to serve as nucleation templates for the formation of siliceous minerals has been demonstrated in a number of laboratory studies (Ferris et al. 1988; Urrutia and Beveridge 1993, 1995), as has the enhanced retention capacity of the silicate precipitates for metals such as lead, cadmium, zinc, chromium, nickel and copper (Urrutia and Beveridge 1994).

6 Conclusion

The widespread occurrence of microorganisms in sediments contributes to the immobilization of metals through a continuum of sorption and authigenic mineral precipitation reactions. Because of their unique structure and macromolecular composition, microbial cells exhibit a high affinity for the chemical fixation of dissolved metal ions. Depending on the prevailing environmental conditions and activity of indigenous microbial populations, individual cells can facilitate the nucleation and growth of distinct mineral phases. These processes contribute collectively to the solid phase enrichment of metals in sediments, and are presumed to have been instrumental in the formation of some strata-bound ore deposits.

References

Al-Aoukaty A, Appanna VD, Huang J (1990) Aluminum, chromium and manganese detoxification mechanisms in *Pseudomonas syringae:* an X-ray flurorescence study. Microbios 70:12–22

Bachofen R (1994) Cell structure and metabolism and its relation with the environment. In: Buffle J, DeVitre RR (eds) Chemical and biological regulation of aquatic systems. Lewis Publishers, Boca Raton, p 231

Beveridge TJ (1989) Role of cellular design in bacterial metal accumulation and mineralization. Ann Rev Microbiol 43:147–171

Buffle J (1990) Complexation reactions in aquatic systems. Ellis Horwood, London

Coleman ML, Hedrick DB, Lovley DR, White DC, Pye K (1993) Reduction of Fe(III) in sediments by sulfate-reducing bacteria. Nature 361:436–438

Degens ET, Ittekkot V (1982) In situ metal-staining of biological membranes in sediments. Nature 298:262–264

Ferris FG, Beveridge TJ, Fyfe WS (1986) Iron-silica crystallite nucleation by bacteria in a geothermal sediment. Nature 320:609–611

Ferris FG, Fyfe WS, Beveridge TJ (1987) Bacterial as nucleation sites for authigenic minerals in a metal-contaminated lake sediment. Chem Geol 63:225–232

Ferris FG, Fyfe WS, Beveridge TJ (1988) Metallic ion binding by Bacillus subtilis: Implications for the fossilization of microorganisms. Geology 16:149–152

Ferris FG, Schultze S, Witten TC, Fyfe WS, Beveridge TJ (1989) Metal interactions with microbial biofilms in acidic and neutral pH environments. Appl Environ Microbiol 55:1249–1257

Ferris FG, Fratton CM, Gerits JP, Schultze-Lam S, Sherwood Lollar B (1995) Microbial precipitation of a strontium calcite phase at a groundwater discharge zone near Rock Creek, British Columbia, Canada. Geomicrobiol J 13:57–67

Fortin D, Leppard GG, Tessier A (1993) Characteristics of lacustrine diagenetic iron oxyhydroxides. Geochim Cosmochim Acta 57:4391–4404

Hallbauer DK, van Warmelo KT (1974) Fossilized plants in thucholite from Precambrian Rocks of the Witwatersrand, South Africa. Precambrian Res 1:199–212

Herbert RG (1996) Metal retention by iron oxide precipitation from acidic ground water in Dalarna, Sweden. Appl Geochem 11:229–235

Köhler B, Singer A, Stoffers P (1994) Biogenic nontronite from marine white smoker chimneys. Clays Clay Mineral 42:689–701

Konhauser KO, Ferris FG (1996) Diversity of iron and silica precipitation by microbial mats in hydrothermal waters, Iceland: implications for Precambrian iron formations. Geology 24:323–326

Konhauser KO, Fyfe WS, Ferris FG, Beveridge TJ (1993) Metal sorption and mineral precipitation by bacteria in two Amazonian river systems: Rio Solimoes and Rio Negro, Brazil. Geology 21:1103–1106

Konhauser KO, Schultze-Lam S, Ferris FG, Fyfe WS, Longstaffe FJ, Beveridge TJ (1994a) Mineral precipitation by epilithic biofilms in the speed river, Ontario, Canada. Appl Environ Microbiol 60:549–553

Konhauser KO, Fyfe WS, Schultze-Lam S, Ferris FG, Beveridge TJ (1994b) Iron phosphate precipitation by epilithic microbial biofilms in Arctic Canada. Can J Earth Sci 31:1320–1324

Lovley DR (1991) Dissimilatory Fe(III) and Mn(IV) reduction. Microbiol Rev 55:259–287

Mackenzie FT, Kump LR (1995) Reverse weathering, clay formation, and oceanic element cycles. Science 270:586–587

McLean RJC, Fortin D, Brown DA (1996) Microbial metal-binding mechanisms and their relation to nuclear waste disposal. Can J Microbiol. 42:392–400

Milodowski AE, West JM, Pearce JM, Hyslop EK, Basham IR, Hooker PJ (1990) Uranium-mineralized microorganisms associated with uraniferous hydrocarbons in southwest Scotland. Nature 347:465–467

Nealson KH, Saffarini D (1994) Iron and manganese in anaerobic respiration: Environmental significance, physiology, and regulation. Annu Rev Microbiol 48:311–343

Schidlowski M (1987) Application of stable carbon isotopes to early biochemical evolution on Earth. Annu Rev Earth Planet Sci 15:47–72

Sigg LR (1994) Regulation of trace elements in lakes: the role of sedimentation. In: Buffle J, DeVitre RR (eds) Chemical and biological regulation of aquatic systems. Lewis Publishers, Boca Raton, p 175

Southam G, Beveridge TJ (1994) The in vitro formation of placer gold by bacteria. Geochim Cosmochim Acta 58:4527–4530

Strauss H (1986) Carbon and sulfur isotopes in Precambrian sediments from the Canadian Shield. Geochim Cosmochim Acta 50:2653–2662

Stumm W, Morgan JJ (1996) Aquatic chemistry, 3rd edn. John Wiley, New York

Tessier A, Carignan R, Belzile N (1994) Processes occurring at the sediment-water interface: Emphasis on trace elements. In: Buffle J, DeVitre RR (eds) Chemical and biological regulation of aquatic systems. Lewis Publishers, Boca Raton, p 137

Tessier A, Fortin D, Belzile N, DeVitre RR, Leppard GG (1996) Metal sorption to diagenetic iron and manganese oxyhydroxides and associated organic matter: Narrowing the gap between field and laboratory measurements. Geochim Cosmochim Acta 60: 387–404

Urrutia MM, Beveridge TJ (1993) Mechanism of silicate binding to the bacterial cell wall in *Bacillus subtilis*. J Bact 175:1936–1945

Urrutia MM, Beveridge TJ (1994) Formation of fine-grained metal and silicate precipitates on a bacterial surface (*Bacillus subtilis*). Chem Geol 116:261–280

Urrutia MM, Beveridge TJ (1995) Formation of short-range ordered aluminosilicates in the presence of a bacterial surface (*Bacillus subtilis*) and organic ligands. Geoderma 65:149–165

Warren LA, Zimmerman AP (1994) Suspended particulate oxides and organic matter interactions in trace metal sorption reactions in a small urban river. Biogeochemistry 23:1–14

Watterson JR (1991) Preliminary evidence for the involvement of budding bacteria in the origin of Alaskan placer gold. Geology 20:315–318

Wilson GC, Rucklidge JC (1987) Geology, geochemistry, and economic significance of carbonaceous host rocks in gold deposits of theTimmins area. In Milne VG (ed) Geoscience research grant program summary of research 1986–1987, Ontario Geological Survey, Miscellaneous Paper 136, p 66

Microbial Phosphate Sediment

David Soudry

Geological Survey of Israel, 30 Malkhe Israel St., Jerusalem 95501, Israel

Abstract. Research on phosphorites from the fossil record and from present-day phosphogenic environments indicates that benthic microbial communities are pivotal in phosphate formation and that in many cases their activity is imprinted in the framework of these rocks. The microbiota involved in this activity include bacterial, fungal and cyanobacterial mat-forming microphytes bearing in their extracellular structures a large part of the phosphate phase of these sediment deposits. The textural state of the phosphate-fossilized microbial structures commonly points to rapid mineralization, under conditions of shallow burial and high concentrations of dissolved porewater phosphate. This is consistent with porewater profiles in sites of presently forming phosphate where apatite precipitation is constrained to the uppermost sediment layer, regulated by the redox interval of organic matter decomposition, porewater phosphate concentration, fluorine diffusion, and pH conditions. An essential and major step in phosphorite formation in bottom sediments is the recycling of the primary production biomass into a benthic biomass of secondary producers. Mat-forming microbial communities, proliferating through breakdown of primary producers in nutrient-rich marine environments, presumably intervene at different chronological levels of phosphorite formation: by recycling and storing the initially fixed planktonic phosphorus, by supplying in vivo and postmortem dissolved phosphate and capping the diffusive phosphorus flux out of the sediment, and by providing abundant substrates for apatite precipitation after death of the benthic microbiota. The Campanian Negev phosphorites exemplify some other microbial pathways also involved in phosphorite sedimentation, including the production of phosphate grains and their fixation by a meshwork of benthic microphytes to produce phosphorite rocks. Diagenetic and compactional processes mask these structures in the Negev phosphorites and their role as common frame-builders of these rocks.

1 Introduction

Benthic microbial activity commonly plays a central role in mineral-forming processes in marine sedimentary systems. Among the many pathways of this activity are production and breakdown of organic matter, release of inorganic compounds and metabolic products in the decay environment, shifting of chemical gradients in porewaters toward supersaturation, and providing sites for nucleation and growth of solid phases (Golubic 1976; Bauld 1981; Riding 1991). Other aspects of this activity concern mechanisms of sediment accretion and comprise fabrication of peloids (Chafetz 1986), transformation of skeletal grains via boring and micritization (Friedman et al. 1971), and fixation of sedimentary particles on bottom sediments to produce microbial buildups (Monty 1976). To date, this biosedimentary activity was mostly documented from carbonate sediments (Walter 1976 and references therein), and one of its most spectacular manifestations is probably the production of stromatolites (e.g., Awramik 1984). These biogenic constructions are generated by the interaction of mat-forming microorganisms with the physical and chemical environment (Krumbein 1983) and, as such, commonly constitute an excellent record of this activity through time and space.

Research on phosphorites both from the fossil and the Recent record during the two last decades demonstrates that benthic microbial activity is also important in promoting phosphate formation and that in many cases the imprint of this activity is embodied in the sediment patterns of these rocks. As a matter of fact, many of the microbial mechanisms involved in carbonate accretion in marine sediments are commonly also active in phosphate accumulation. This chapter briefly reviews the role of microbial activity in phosphate-forming processes and shows some of the pathways of this activity using the Negev phosphorites of southern Israel as an example.

2 Microorganisms and Apatite Formation

2.1 Sedimentary Record

The existence of fossil microorganisms within the phosphate fraction of phosphorites has long been reported. Cayeux (1936) was the first to mention the existence of apatite-fossilized bacteria within the phosphate grains of phosphorites. With increasing use of scanning electron microscopy (SEM), structures of this kind were observed in granular phosphorites of all ages and formational settings (see Krajewski et al. 1994 and references therein). These apatite-fossilized microrganisms commonly form a large part of the phosphate phase of these rocks, occurring in a variety of shapes that resemble bacterial structures, as observed in natu-

R. E. Riding and S. M. Awramik (Eds.)
Microbial Sediments

ral environments and laboratory cultures (e.g., Chafetz and Buczynski 1992). Rod-like bodies (Lamboy 1990), spindle-shaped forms (Bréhéret 1991), capsule-like cells (Lucas and Prévôt 1985), and solitary and colonial coccus-like forms (Zanin et al. 1987) are observed. Bacterial structures also make up the major part of the phosphate framework of Recent phosphorites on the East Australian (O'Brien et al. 1981), Western Indian (Rao and Nair 1988), and Peruvian (Lamboy 1990) shelves. At sites of presently forming phosphate (Froelich et al. 1988; Glenn and Arthur 1988), they typically occur as filamentous mats immediately capping the zone of apatite precipitation. These living mats closely associated with current phosphate formation consist of sulfur-oxidizing bacterial populations of the family Beggiatoaceae (mostly *Thioploca* spp.; Gallardo 1977), and tend to develop where the O_2-rich zone and the underlying H_2S-rich zone in the upper sediment layer nearly overlap. Bacterial mat laminations are also associated with zones of pristine phosphate in the Miocene Monterey Formation, California (Garrison et al. 1987) and phosphatized bacterial structures resembling *Beggiatoa* filaments have been observed in laminae of these deposits (Reimers et al. 1990).

Other kinds of microbial populations found to be associated with phosphate production are cyanobacterial and fungal mats. In the Negev phosphorites, a polygenic mat-forming assemblage composed of filamentous cyanobacteria together with fungal hyphae and bacteria is closely involved in phosphate accretion (Soudry and Champetier 1983; Soudry 1987). These cyanobacterial and fungal mats have been preserved as apatite-encrusted tubules that now make up a large part of the phosphate fraction in the Negev phosphorites. Fungal mats showing branching, and chlamydospore-like structures mineralized by phosphate were also reported from Eocene Moroccan phosphorites (Dahanayake and Krumbein 1985) and from the mid-Cretaceous Vocontian basin (SE France) concretional phosphorites (Bréhéret 1991). Tubular structures were also found to form many of the Cambrian phoscrete profiles of Australia (Southgate 1986) and part of the Upper Cretaceous phosphorites of Columbia (Zanin et al. 1987). Most of these microbial tubules are hollow, with phosphate mineralization commonly limited to the extracellular parts (sheaths and walls), and as a rule show little or no compression at all.

Other structures forming the phosphate framework of phosphorites are unicell envelopes of coccoid-dominated microbial mats (Soudry and Southgate 1989, Soudry 1992). Similar forms also compose phosphate cements in the Albian glauconitic limestone of the Western Carpathians (Krajewski 1984) and form omission-surface apatitic crusts within the Negev phosphate sequence (Soudry and Lewy 1990). These coccoid structures are commonly preserved as phosphate-encrusted capsule-like forms, closely recalling the structures obtained in the laboratory during microbial phosphate experiments (Lucas and Prévôt 1985; Krajewski et al. 1994). Spherical and rod-shaped bacterial communities are also often involved in the preservation of vertebrate and invertebrate soft parts in the fossil record (e.g., Martill 1988). These microorganisms occur as phosphatized replicas replacing the soft tissues, often with detail at the subcellular level.

Filamentous cyanobacterial mats, thought to be fed by P-rich endo-upwelling fluxes, were also found to be the origin of the present-day forming insular phosphorites in Tahitian atolls (Jehl 1996). As in the Negev phosphorites, these structures are fossilized as phosphatized sheaths forming part of the apatitic fraction of the deposits. In addition, filamentous cyanobacterial mats build phosphate stromatolites, widespread in the Precambrian of the Indian subcontinent (e.g., Banerjee 1971; Chauhan 1979) and also encountered elsewhere locally in Cambrian times (e.g., Southgate 1980). The phosphate matter in these buildups is usually restricted to the stromatolitic columns; however the mode of phosphate emplacement in these structures as well as its interdependence with the stromatolite-building communities is variable. It ranges from direct apatite precipitation on the cyanobacterial mat structures (Southgate 1980) to replacement of precursor carbonate previously precipitated within the stromatolitic framework (Chauhan 1979). Stromatolitic phosphorites also occur in the Mesozoic in various peri-Tethyan areas and at various stratigraphic intervals (see Föllmi 1989; Martin-Algarrra and Sanchez-Navas 1995 for some examples). However, in contrast to the Precambrian-Cambrian occurrences, the Mesozoic forms are tiny structures made up by mini-and micro-stromatolites, essentially occurring at stratigraphic breaks, mostly generated by bacterial communities, and formed by in situ apatite precipitation onto the organic mat structures. Stromatolitic phosphorites of Cenozoic age, closely resembling the Mesozoic structures, were recently also reported from the Eocene of central Negev in southern Israel (Soudry and Panczer 1994). To date, this is the sole occurrence of phosphatic stromatolites known from the Cenozoic.

2.2 Causal or Accidental Link?

The close connection between the phosphate phase and microbial organisms in phosphorites of all ages has raised the question of the significance of this link and its geological implications. There are two main issues: (1) the role of benthic microbiota in P concentration in sediments, and (2) their intrinsic role in apatite crystallization. Various studies have shown that microbial metabolism, either directly (via living microbiota; Carlton

and Wetzel 1988; Gächter et al. 1988) or indirectly (by catalyzing the Fe redox cycle; Mortimer 1971), affects phosphorus dynamics at the sediment-water interface and thereby may influence P concentations in porewaters. These studies demonstrated that P cycling across the sediment-water interface is redox-dependent. Phosphorus is sequestered in the oxidized microzone at the sediment surface and released in the burial environment following the onset of anoxic conditions. Gächter et al. (1988) demonstrated from laboratory experiments that, in addition to PO_4^{3-} release by Fe^{+3} reduction, bottom-dwelling living microrganisms, responding to variations in redox potential and nutrient concentrations, play a direct role in uptake and release of soluble phosphate. Bacterial cultures in these experiments almost depleted the soluble phosphate concentration when grown in aerated P-limited medium and released up to 25% of the stored P when the conditions became anoxic. Moreover, sterilization of oxic sediments was found to greatly reduce their phosphate retention capability. Under aerobic conditions and excess phosphate (Gächter et al. 1988), bacterial organisms store P in the form of polyphosphate as the final step of oxidative phosphorylation, whereas in anaerobic conditions, when O_2 is no longer available, the stored poly-P is used as a source of energy to synthesize an organic electron acceptor, resulting in P release to the aqueous medium. Interestingly, the microaerophilic growth conditions of the sulfur-oxidizing mat-forming bacteria capping apatite formation in present-day phosphogenic sites (Reimers et al. 1990) fit this model well, as they enable accelerated biological P pumping from the sediment-water interface. It is also well known that various microorganisms, including fungi, bacteria and cyanobacteria, are able to store P when it is available in excess (Trudinger 1978). In addition, it has been found (Lehman and Sandgren 1982) that with equal access to phosphorus, coccoid cyanobacteria may surpass coexisting eukaryotes in phosphate-uptake capability. Furthermore, modern *Beggiatoa* in the Santa Barbara basin (Reimers et al. 1990) show an organic C/P mole ratio of 68, significantly less than the planktonic Redfield ratio of 106 (Redfield et al. 1963). This low C/P ratio of the Beggiatoaceae was attributed to the accumulation of polyphosphate granules in their cell walls (Wiessner 1981). In this respect, Reimers et al. (1990) suggested an active microbial role in phosphatization and also linked formation of the Miocene Monterey phosphorites (Garrison et al. 1987) to the growth and postmortem degradation of massive microbial communities, resulting in abundant release of organic-bound phosphate to porewaters (see also Krajewski et al. 1994). An active role of microbial mats in P concentration was previously suggested for Negev phosphorites (Soudry and Champetier 1983), whereas in Australian phosphorites Soudry and Southgate (1990) speculated that the coccoidal mats now forming laminae of pristine phosphate are only the remnants of a much larger microbial community which was largely degraded. In this way, large quantities of phosphate could have been supplied to porewaters, enabling phosphatization of those remaining mat structures that escaped total degradation. Moreover, differential post-mortem degradation is a common feature of present-day microbial systems (Knoll 1985), resulting from differences in preservation potential or in decomposing conditions of the mat-forming microorganisms. In addition, mat-forming microorganisms may also behave as a physical barrier (Bubela 1980), reducing P escape to the overlying water column and contributing in this way to a further increase in porewater phosphate concentration.

The role of microorganisms in apatite crystallization is more ambiguous. The intimate connection between the phosphate matter and microbial remnants in many phosphorites would a priori suggest that apatite precipitation was triggered by these organic constituents. As mentioned above, extracellular microbial structures are the common support of the phosphate fraction in many phosphorites. Whether these structures behave as active or just passive templates for apatite crystallization is uncertain. Lucas and Prévôt's (1985) laboratory experiments, showing that apatite precipitation in sea water is possible only when bacteria are involved, would indicate that microbes are in some way instrumental in phosphate precipitation. In these experiments and others (Hirschler et al. 1990), bacterial growth was stimulated by RNA used as a phosphorus source, and phosphate was released to the medium through the enzymatic activity of the bacterial alkaline phosphatase. Hirschler et al. (1990) also showed that the synthesized apatite crystals were located on or near the bacterial cells and noted that similar mineral fabrics are produced even where bacteria are substituted for by enzymes. Where precipitated in the presence of bacteria, the apatitic phase mostly occurred as extracellular mineral encrustation, producing capsular and tubular phosphate-coated structures, very similar to those observed in fossil phosphorites. The quasi-exclusive support of the phosphate phase by extracellular parts of benthic microorganisms has led several workers to ask whether these bodies might act as preferential substrates for apatite nucleation (O'Brien et al. 1981; Southgate 1986; Soudry 1987). The ability of microorganisms to accumulate mineral precipitates on their walls is well known (e.g., Dexter-Dyer et al. 1984). This is generally explained (Beveridge and Fyfe 1985) by the high reactivity of organic compounds in sheaths and envelopes of microorganisms. Because of their anionic nature, these structures will tenaciously bind metal cations during early diagenesis, thus providing sites for mineral nucleation and growth. Nonetheless, it remains unclear whether microbial

structures are really preferred substrates for phosphate precipitation; in both Recent phosphogenic environments (Burnett 1977) and laboratory experiments (Krajewski et al. 1994), apatite was found to crystallize on any available substrate. In addition, experiments on fossilization of soft-tissues (Briggs and Kear 1993) show that phosphate precipitation indifferently occurs on muscle fibrils and on associated decomposer bacteria. Indeed, it is possible that the common support of phosphate matter by microbial structures in many fossil phosphorites is only apparent, and is merely linked to the preponderance of organic remnants within the phosphate-precipitating decay environment. Moreover, the acidic conditions (Nathan and Sass 1981) associated with apatite precipitation in natural environments (resulting from oxidation of upward-diffusing H_2S and/or CO_2 release from aerobic oxidation of organic matter) would also lead to dissolution of associated calcite components, leaving microbial remnants as sole substrates for apatite nucleation. Actually, it is highly probable that the intrinsic role of microbes in apatite crystallization is mainly in releasing dissolved phosphate from decaying organic matter, speeding geochemical reactions and shifting chemical gradients in porewaters, and providing confined microenvironments enhancing supersaturation of phosphate solutions. In this sense, vacated sheaths and envelopes of filamentous and coccoid microbiota would function as *biological microniches* in which high levels of dissolved phosphate could locally develop, enabling rapid mineralization of these forms.

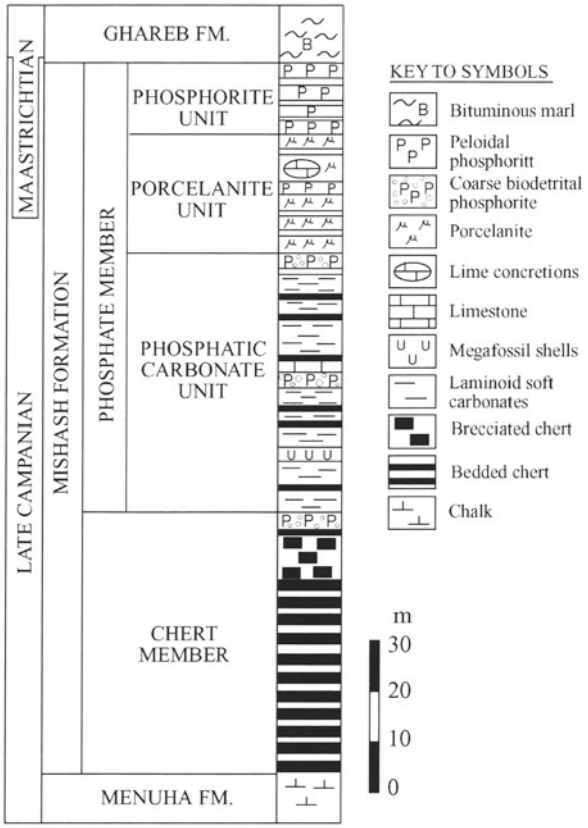

Fig. 1. C
Mishasl

3
Microbial Pathways in Phosphorite Accumulation: The Negev Phosphorites as an Example

3.1
Background

The Negev phosphorites are part of the Late Cretaceous-Eocene phosphogenic Tethyan belt, developed at the northeastern edges of the Arabo-Nubian paleocraton and now stretching all along the southern margins of the present-day Mediterranean Sea from Turkey to Morocco. The phosphorites are Late Campanian in age and occur together with cherts, porcelanites and organic-rich carbonates, forming a shallow marine rock-suite known in the Negev as the Mishash Formation (Fig. 1). This sequence has been intensively studied, and a great deal of information has accumulated on its paleogeography and stratigraphy, and on the geochemistry and petrogenesis of its sedimentary products (e.g., Kolodny 1980; Lewy 1990). The depositional conditions have been interpreted as reflecting environments controlled by the high productivity Mishash sea that flooded the Negev in the Campanian. The high productivity was due to an extensive upwelling regime that prevailed during the Late Cretaceous along the southeastern reaches of the Tethys, resulting in abundant accumulation of organic matter in the area. The Negev phosphorites mostly occur within the Phosphorite Unit (Fig. 1) in the uppermost part of the Mishash Formation. They are poorly lithified, fine- to medium-grained, with a common internal flat layering made up by repetitively alternating phosphate-rich and carbonate-rich laminae, and their apatitic fraction is mostly composed of sand-sized phosphate peloids ("pellets"). Various amounts of bone fragments are usually associated with the pelletal fraction of these rocks, and in most cases their intergranular fraction consists of micrite-sized calcite and/or finely crystalline apatite.

The sedimentary activity of microorganisms in the accumulation of the Negev phosphorites is expressed in two ways, *destructive* and *constructive*. These two aspects of microbial activity in the Negev phosphorites may co-occur within the same phosphate body; however, in most cases, they are superimposed both in time and in space.

3.2
Destructive Microbial Pathways

This activity mostly affects bone fragments forming part of the granular phosphate fraction of the phosphorites and is expressed as a centripetal infestation of these skeletal components by endolithic microphytes (Soudry 1979), producing destructive rims. The microbiota responsible for this boring activity are rather uncertain, as microborings are produced by various microorganisms (Friedman et al 1971) and distinction between them is usually rather problematic (see Bathurst 1976). It is possible that they are due to fungi. Similar microborings have been reported from human and animal skeletal fossil tissues (Garland 1989) and have been also attributed to fungi. In the Negev phosphorites, the microborings are of variable diameter (mainly 4–10 μm), and in advanced infestation they appear as a dense network of cross-cutting tunnels undermining the bony matter (Fig. 2A). The excavated tunnels are either empty or partly in-filled with fine-grained micritic phosphate, probably in situ microbially reprecipitated from the dissolved bony fraction. The end product of this bio-corrosion is conversion of bone fragments into phosphate peloids. This grain transformation observed in phosphorites is in all respects equivalent to the well-known micritization process occurring in carbonates and affecting calcareous bioclasts (Friedman et al 1971). In places, constructive-destructive microbial rims, similar to those described in carbonate sediments (Kobluk and Risk 1977), also develop inwardly and outside the biocorroded bone debris.

3.3
Constructive Microbial Pathways

This constructive activity is expressed in the generation of phosphate grains and in the buildup of phosphate rocks as well. The microbial structures involved include phosphate-encrusted remnants of various filamentous and coccoid microorganisms.

3.3.1
Microbial Fossils

The filamentous structures associated with the Negev phosphorites are commonly 5–10 μm wide with a variety of forms. These include curved and cylindrical structures with a dense phosphate coating (Fig. 2B), straight tubes with an aggregate-like phosphate coating, tubes with a needle-like phosphate coating, spiral structures, and tubes with serial constrictions (Soudry 1987). Branched forms are also observed in places. Most of the tubes are empty, display no variations in diameter, show few or no compressional features, and phosphate overgrowths, where abundant, are preferentially accreted on the outer parts of the structures. Energy dispersive (EDS) analysis shows in all cases no trace of carbonates in the coatings, suggesting direct phosphate precipitation on the extracellular structures, as is also indicated by the different phosphate textures of the coatings. These differences in coating textures have been tentatively explained by differences in composition and structure of the extracellular matter of the various microbes, implying some sort of biochemical control on phosphate crystallization (see Eliott 1985). The globular structures observed in the Negev phosphorites consist of closely packed and gently compressed capsule-shaped forms (Fig. 2C) that resemble extracellular envelopes of coccoid microbes. They are of various sizes, are commonly hollow, and make up recurrent pristine laminae of primary apatite within the phosphate Mishash sequence. Similar structures, though of larger size (Fig. 2D), have been also found to form the phosphate framework of Cambrian primary phosphorites of Australia (Soudry and Southgate 1989). These tubular and globular structures of the Negev phosphorites have both been interpreted as the fossilized remnants of a polygenic assemblage of mat-forming microorganisms of probable cyanobacterial and fungal affinities that colonized the Mishash sea floor during times of phosphate formation. Rod- and coccus-shaped phosphate bodies, presumably remains of decomposer bacterial populations, are commonly associated with the tubular and the globular structures.

3.3.2
Generation of Phosphate Grains

Many of the Negev phosphate grains look structureless when observed by optical microscopy. Nevertheless, some sort of internal arrangement is commonly discerned in these bodies when examined in thin-sections ground thinner than normal. In most cases this arrangement consists of a concentric, faint banding mimicking ooidal fabrics. Careful investigations show however that this concentric banding results from microbial accretion and that these ooid-like phosphate grains are in fact micro-oncolites (Soudry and Champetier 1983). The microorganisms involved in this accretionary growth are best revealed by SEM examination and consist of phosphate-coated tubules (Fig. 2E) that build the cortical layers. Other forms of microbial involvement also occur. Many of the seemingly structureless grains are shown to be formed by bunches of tangled and vertically stacked phosphate tubules, and packets of apatitic coccoid envelopes, or consist of microlaminated, stromatolite-like phosphate clasts (Soudry 1987). Comparative fabric analyses led to interpreting these granular phosphate components as fragmentary products of early, phosphatized mat-forming microorganisms that recurrently colonized the Mishash sea

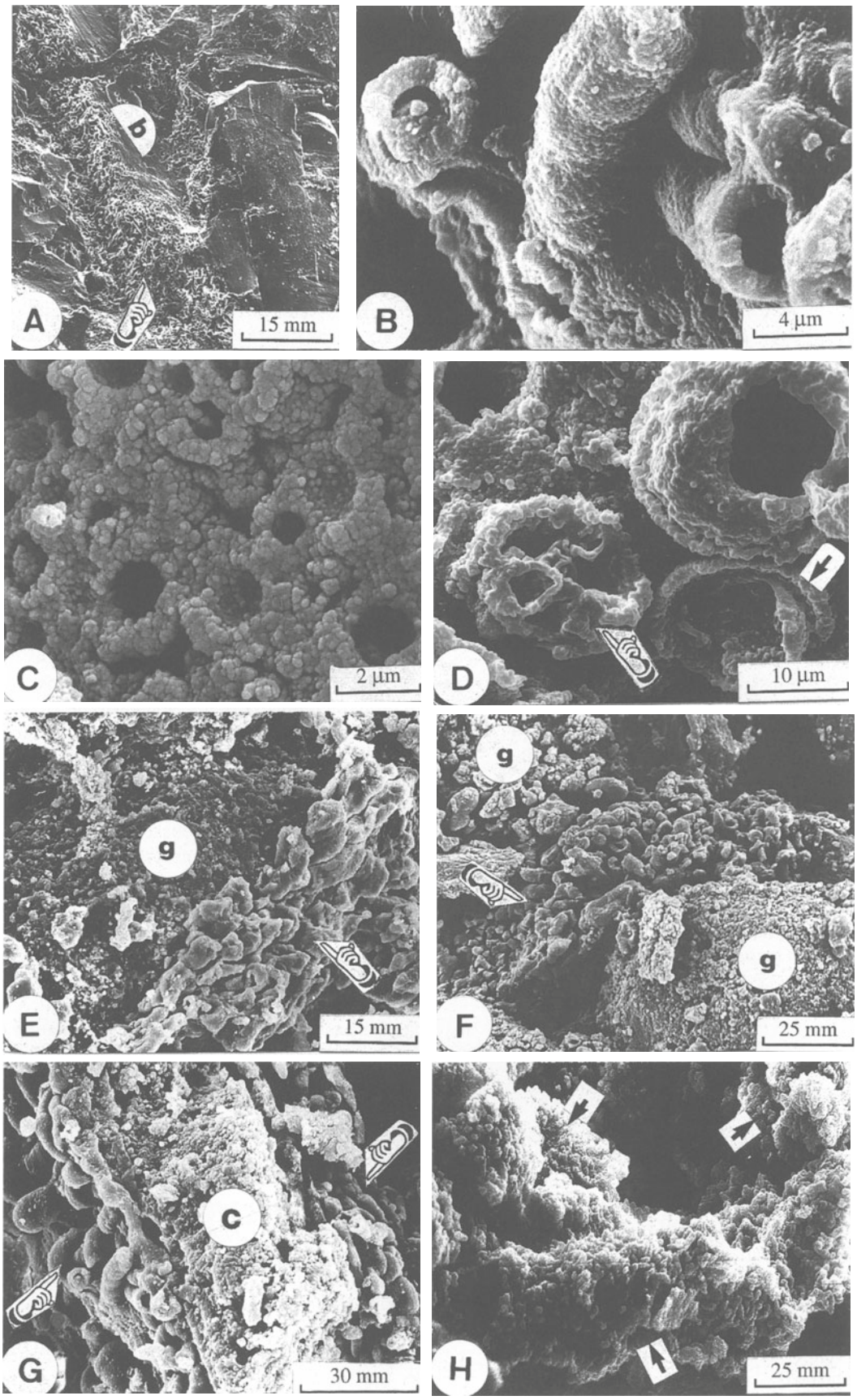
b
A
15 mm
B
4 µm
C
2 µm
D
10 µm
g
E
15 mm
g
g
F
25 mm
c
G
30 mm
H
25 mm

floor and were reduced to sand-sized debris during high energy episodes.

3.3.3
Buildup of Phosphorite Rocks

Many of the Negev phosphorite rocks, particularly those of high phosphate content, are characterized by an intergranular matrix which is also apatitic. In most cases, this matrix appears as a faint, vermiform, phosphate groundmass under light microscopy, but when observed by SEM turns out to be formed by a spectacular meshwork of interlaced apatitic tubules enveloping (Fig. 2E) and binding (Fig. 2F) the phosphate grains. SEM resolution is generally improved when the phosphorite samples are slightly etched. The arrangement of this microbial component making-up the intergranular binder of the phosphorites is not random. A micro-layering is often detected where phosphate overgrowths and compactional phenomena are not strong. The most common organization consists of alternating tubular and micritic phosphate layers (Fig. 2G), each a few to several decimicrons thick. Another kind of arrangement comprises vertically stacked layers of various phosphate-mineralized tubular populations, each layer characterized by a different diameter of the constituent microbial biota (Soudry 1987). Both kinds of organization are generally poorly preserved, switching off suddenly as a result of overgrowth and collapse masking or destroying the microbial ordering.

3.4
Mineralization and Diagenetic Fate of the Negev Microbial Fossils

Several lines of evidence allow some conclusions to be drawn as to the site and timing of phosphate mineralization of the microbial structures making up part of the Negev phosphorites. Their initially easily deformable consistency, the well-preserved cylindrical and spherical shapes of many of these filamentous and coccoid structures, as well as their recycling as clastic products via synsedimentary mat disintegration indicate rapid mineralization close to the sediment-water interface. This is further indicated by the development of phosphate micro-oncolites (Soudry and Champetier 1983) and also confirmed from Recent phosphate-forming environments where apatite precipitation is essentially limited to the top sediment layer (Glenn and Arthur 1988; Jarvis et al 1994) and occurs together with suboxic degradation of organic matter. Only here, very close to the sediment-water interface, are the conditions jointly required for apatite precipitation met, i.e., fluorine diffusion, carbonate alkalinity, and porewater phosphate concentration. This situation of living mat-forming microbiota in the topmost sediment, underlain by mineralized structures in near proximity, is fairly consistent with the model of microbial P pumping of Gächter et al. (1988) and the dysaerobic environmental conditions associated with current phosphate-forming settings (Reimers et al 1990). Rapid mineralization of these structures (probably through a metastable phosphate precursor, as direct apatite precipitation is kinetically a slow process; Van Cappelen and Berner 1991) will produce rigid forms on the sea floor, enabling their synsedimentary fragmentation to produce clastic phosphate grains. Low sediment accumulation rates, forced by gentle bottom-sweeping currents, will keep the microbial structures close to the sediment-water interface where apatite precipitation takes place, ensuring in this way their early mineralization and their subsequent disintegration. Many of the primary apatite layers in the Negev phosphorites in fact occur in association with sedimentary breaks (Soudry and Lewy 1990), and condensed sedimentation is moreover a characteristic of most phosphate sequences.

The microbial structures constituting the Negev phosphorites are commonly largely masked, and thus

◁

Fig. 2A–H. Scanning electron micrographs of some microbial phosphate fabrics in the Negev and other phosphorites. **A** Bone fragment (*b*) showing a centripetal rim of microphyte borings (*fingered*) encircling a non-corroded inner part. This microphyte infestation leads to in situ recycling of the dissolved bone matter as micritic phosphate, ultimately producing a phosphate peloid. **B** Some of the tubular microorganisms constituting part of the Negev phosphorites. These bodies support on their extracellular structures a large part of the phosphate fraction of these rocks and build phosphate grains and intergranular matrices of part of the phosphorites. Note the well-preserved cylindrical shapes of these forms denoting rapid mineralization under conditions of shallow burial depth. **C** Closely packed, capsule-like phosphate structures that constitute many of the pristine phosphate laminae in the Negev phosphorite sequence. These structures have been interpreted as the phosphatized remnants of former mat-forming coccoid prokaryotes. Part of the structures are empty, whereas others are in-filled by micritic phosphate leading to their gradual ghosting. **D** Phosphate-coated envelopes of coccoid unicells forming the framework of pristine phosphate layers in Cambrian Australian (Georgina Basin) phosphorites. Most of these structures are empty. Some show a single envelope (*upper right corner*), others (*arrow*) show encapsulated envelopes, or (*finger*) are divided into cell-like units by thin phosphate walls. **E** In situ coating of a Negev phosphate grain (*g*) by a meshwork of phosphate-coated remnants of filamentous microphytes (*fingered*). Phosphate micro-oncolites are produced by these accretionary processes. **F** Phosphate grains (*g*) bound by an intergranular phosphate matrix made up by a meshwork of phosphate-coated tubular microphytes (Negev phosphorites). Such matrices are particular to phosphorites with a high phosphate content and are mostly responsible for the high enrichment of these rocks. **G** One of the spatial arrangements of the intergranular phosphate binder in the Negev phosphorites. Sandwiched structures of phosphate-coated microphyte laminae (*fingered*) and cryptocrystalline phosphate laminae (*c*) between the phosphate grains. **H** A hollow microphyte (*lower arrow*) with a dense needle-like phosphate coating. Heavy coatings lead to the gradual obliteration of these structures and their conversion into a peloidal groundmass (*upper arrows*)

frequently ignored. Several factors contribute to the obliteration of these structures. Most important are phosphate overgrowths (Fig. 2H) that coat the filamentous and globular structures, resulting in severe deformation of these forms. Likewise, bacterial rods are converted into stubby forms through heavy mineral phosphate accretion. Where this process is intense, these structures are gradually masked by a fine-grained apatite coating and eventually converted into micritic phosphate groundmasses (Fig. 2H). Additional factors are collapse-compactive phenomena which break up the apatitic tubes sandwiched between the phosphate grains into tiny debris, and dissolution-reprecipitation processes which convert the microbial structures into aggregates of micritic phosphate (Soudry 1987). These phenomena together tend to wipe out the microbial imprint in Negev phosphorites and are in part responsible for the chaotic textures now displayed by many of these rocks.

4 Concluding Remarks

Formation of sedimentary phosphate requires two critical conditions: high rates of phosphorus supply to the sea floor, and high retention of this element within the uppermost sediment layers. Accelerated P transfer to the bottom sediments occurs in upwelling nutrient-rich waters, driven through intense primary production in the photic zone. Many fossil and Recent phosphorites are associated with upwelling-dominated environments. Shallow depth and/or establishment of an oxygen-minimum depositional setting will ensure that high quantities of particulate organic matter reach the sea floor. An efficient way for most of the regenerated phosphorus to be retained in bottom sediments (and thereby to prevent its reflux to the overlying water column), is for it to be recycled as a microbial biomass of benthic secondary producers. Massive microbial communities, proliferating through breakdown of the sedimented primary producers, hence will function as phosphorus traps, enabling increasing biological storage of this element in the uppermost bottom sediments. In vivo as well as mainly postmortem delivery of organically bound phosphate from the mat populations will lead to supersaturation and apatite precipitation onto the mat structures.

It has been suggested (Föllmi and Garrison 1991) that high postmortem P release derives from catastrophic burial of the microbial biomass by allochthonous sediment beds, provoking sudden decomposition of the mat populations. However, substantial amounts of porewater-dissolved phosphate may be also released just by self-burial and decomposition of the stratified microbial communities. Indeed, phosphatization of the easily decomposable microbial structures indicates rapid mineralization, which might suggest (Föllmi and Garrison 1991) sudden pulses of dissolved phosphate provoked by massive catastrophic burial. On the other hand, the preservational state of many of the mineralized structures (Soudry 1987) as well as porewater chemical profiles at sites where phosphate is presently forming (Glenn and Arthur 1988) both argue for minimal burial below the sediment-water interface during mineralization. Several studies (e.g., Glenn and Arthur 1988) have shown that phosphate precipitation in Recent phosphogenic settings is controlled by burial depth, regulated by the redox interval of organic matter decomposition. The somewhat conflicting requirements, of shallow burial depth on the one hand, and rapid supply of dissolved phosphate on the other, might be reconciled in conditions of episodic deposition. Prolonged residence-time of vacant microbial structures close to the sediment-water interface arising from non-deposition will converge upward-diffusing phosphate ions from decaying subjacent sediments toward this apatite-precipitating surficial level, leading to rapid mineralization of the microbial remnants and their preservation.

Thus, microbial activity seems to intervene at different chronological levels of phosphorite accumulation: by counteracting the diffusive phosphorus flux from bottom sediments to the overlying water column, by supplying in vivo and postmortem dissolved phosphate to the interstitial environment, and by providing substrates for apatite precipitation after death of the benthic microbiota. Other common sedimentary aspects of this activity are production of phosphate grains,and build-up of phosphorite rocks through fixation of phosphate grains by a synsedimentary meshwork of mat-forming microphytes. Massive microbial communities growing and reproducing through breakdown of sedimented primary producers, and in this way recycling most of the initially fixed phosphorus, appear to constitute a major and *essential* step in processes of phosphorite formation. In many cases, diagenetic and compactive phenomena mask the sedimentary impact of this activity and the role of microbial organisms as common frame-builders of phosphorites. Nevertheless, textural fingerprints left in many of these rocks still deliver a clear message as to the central role of benthic microbial communities in phosphorite formation through time.

Acknowledgements. I would like to express my thanks to Karl Föllmi and Robert Riding for carefully reviewing this paper.

References

Awramik SM (1984) Ancient stromatolites and microbial mats. In: Cohen Y, Castenholz R, Halvorson HO (eds) Microbial mats: stromatolites. BML Lectures in Biology 3. Alan R. Liss Inc, New York, pp 1–22

Banerjee DM (1971) Precambrian stromatolitic phosphorites of Udaipur, Rajasthan, India. Geol Soc Am Bull 82:2319–2330

Bathurst RGC (1976) Carbonate sediments and their diagenesis, 2nd edn. Developments in sedimentology 12. Elsevier, Amsterdam, p 658
Bauld J (1981) Geobiological role of cyanobacterial mats in sedimentary environments: production and preservation of organic matter. BMR J Aust Geol Geoph 6:307–317
Beveridge TJ, Fyfe WS (1985) Metal fixation by bacterial cell walls. Can J Earth Sci. 22:1893–1898
Bréhéret J-G (1991) Phosphatic concretions in black facies of the Aptian-Albian Marnes bleues Formation of the Vocontian basin (SE France), and at site DSDP 369: evidence of benthic microbial activity. Cretaceous Res 12:411–435
Briggs DEG, Kear AJ (1993) Fossilization of soft tissue in the laboratory. Science 259:1439–1442
Bubela B (1980) Some aspects of the interstitial water movements in stimulated sedimentary systems. BMR J Aust Geol Geoph 5: 257–263
Burnett WC (1977) Geochemistry and origin of phosphorite deposits from off Peru and Chile. Geol Soc Am Bull 88:813–823
Carlton RG, Wetzel RG (1988) Phosphorus flux from lake sediments: Effect epipelic algal oxygen production. Limnol Oceanogr 33:562–570
Cayeux L (1936) Existence de nombreuses bactéries dans les phosphates sédimentaires de tout âge. Conséquences . CR Acad Sci Paris 203:1198–1200
Chafetz HS (1986) Marine peloids: a product of bacterially induced precipitation of calcite. J Sedim Petrol 56:812–817
Chafetz HS, Buczynski C (1992) Bacterially induced lithification of microbial mats. Palaios 7:277–293
Chauhan DS (1979) Phosphorite bearing stromatolites of the Precambrian Aravalii phosphorite deposits of Udaipur region, their environmental significance and genesis of phosphorite. Precambrian Res 8:95–126
Dahanayahe K, Krumbein WE (1985) Ultrastructure of a microbial mat-generated phosphorite. Min Deposita 20:260–265
Dexter-Dyer B, Kretzschmar M, Krumbein WE (1984) Possible microbial pathways in the formation of Precambrian ore deposits. J Geol Soc Lond 141:251–262
Eliott JC (1985) Controlled crystallization. Nature 317:387–388
Föllmi KB (1989) Evolution of the Mid-Cretaceous Triad: platform carbonates, phosphatic sediments, and pelagic carbonates along the northern Tethys margin. Lecture Notes in Earth Science 23. Springer, Berlin Heidelberg New York, p 153
Föllmi KB, Garrison RE (1991) Phosphatic sediments, ordinary or extraordinary deposits? The example of the Miocene Monterey Formation (California). In: Muller DW, McKenzie JA, Weissert H (eds) Controversies in modern geology. Academic Press, London, pp 55–84
Friedman GM, Gebelein C, Sanders JE (1971) Micritic envelopes of carbonate grains are not exclusively of photosynthetic algal origin. Sedimentology 16:89–96
Froelich PN, Arthur M, Burnett WC, Deakin M, Hensley V, Jahnke R, Kaul L, Kim K, Roe K, Soutar A, Vatakanon, C (1988) Early diagenesis of organic matter in Peru continental margin sediments: phosphorite precipitation. Mar Geol 80:309–346
Gächter R, Meyer JS, Mares A (1988) Contribution of bacteria to release and fixation of phosphorus in lake sediments. Limnol Oceanogr 33:1542–1558
Gallardo VA (1977) Large benthic microbial communities in sulfide biota under Peru-Chile subsurface countercurrent. Nature 268:331–332
Garland AN (1989) Microscopical analysis of fossil bone. Appl Geochem 4:215–229
Garrison RE, Kastner M, Kolodny Y (1987) Phosphorites and phosphatic rocks in the Monterey Formation and related Miocene units, coastal California. In: Ingersoll RV, Ernst WG (eds) Cenozoic Basin development of coastal California. Prentice Hall, Englewood Cliffs, pp 349–38.
Glenn CR, Arthur MA (1988) Petrology and major element geochemistry of Peru margin phosphorites and associated diagenetic minerals: authigenesis in modern organic-rich sediments. Mar Geol 80:231–276
Golubic S (1976) Organisms that build stromatolites. In: Walter MR (ed) Stromatolites. Elsevier, Amsterdam, pp 113–126
Hirschler A, Lucas J, Hubert J-C (1990) Apatite genesis: a biologically induced or biologically controlled mineral formation process? Geomicrobiol J 7:47–57
Jarvis I, Burnett WC, Nathan Y, Almbaydin FSM, Attia AKM, Castro LN, Flicoteaux R, Hilmy ME, Husain V, Quatawnah AA, Serjani A, Zanin YN(1994) Phosphorite geochemistry: state-of-the-art and environmental concerns. Eclogae Geol Helv 87:643–700
Jehl C (1996) Les mattes cyanobactériennes (kopara) des atolls de Tuamotu: biochimie, productivité et signification écologique. Insertion dans un modèle de phosphatogenèse. Thèse, Doct Univ Française du Pacifique. Orstrom éditions, Paris
Knoll AH (1985) A paleobiological perspective on sabkhas. In: Friedman GM, Krumbein WE (eds) Hypersaline ecosystems: the Gavish Sabkha. Springe, Berlin Heidelberg New York, pp 407–425
Kobluk DR, Risk MJ (1977) Calcification of exposed filaments of endolithic algae, micrite envelope formation and sediment production. J Sedim Petrol 47:517–528
Kolodny Y (1980) Carbon isotopes and depositional environment of high productivity sedimentary sequence – the case of the Mishash Formation, Israel: Isr J Earth Sci 29:147–156
Krajewski KP (1984) Early diagenetic phosphate cements in the Albian condensed glauconitic limestone of the Tatra Mountains, western Carpathians. Sedimentology 31:443–470
Krajewski KP, Van Cappellen P, Trichet J, Kuhn O, Lucas J, Martin-Algarra A, Prévôt L, Tewari VC, Gaspar L, Knight RI, Lamboy M (1994) Biological processes and apatite formation in sedimentary environments. Eclogae Geol Helv 87:701–745
Krumbein WE (1983) Stromatolites – the challenge of a term in space and time. Precambrian Res 20:493–531
Lamboy M (1990) Microstructures of a phosphatized crust from the Peruvian continental margin: phosphatized bacteria and associated phenomena. Oceanol Acta 13:439–451
Lehman JT, Sandgren CD (1982) Phosphorus dynamics of the procaryotic nannoplankton in a Michigan lake. Limnol Oceanogr 27:828–838
Lewy Z (1990) Transgressions, regressions and relative sea level changes on the Cretaceous shelf of Israel and adjacent countries. A critical evaluation of Cretaceous global sea level correlations. Palaeoceanogr 5:619–637
Lucas J, Prévôt L (1985) The synthesis of apatite by bacterial activity: mechanism. Sci Géol Mém 77:83–92
Martill DM (1988) Preservation of fish in the Cretaceous of Brazil. Palaeontology 3:1–18
Martin-Algarra A, Sanchez-Navas A (1995) Phosphate stromatolites from condensed cephalopod limestones, Upper Jurassic, southern Spain. Sedimentology 42:893–919
Monty CLV (1976) The origin and development of cryptalgal fabrics. In: Walter MR (ed) Stromatolites. Elsevier, Amsterdam, pp 193–249
Mortimer DH (1971) Chemical exchanges between sediments and water in the Great Lakes – speculations on probable regulatory mechanisms. Limnol Oceanogr 16:387–404
Nathan Y, Sass E (1981) Stability relations of apatites and calcium carbonates. Chem Geol 34:103–111
O'Brien GW, Harris JR, Milnes AR, Veeh HH (1981) Bacterial origin of East Australian continental margin phosphorites. Nature 294:442–444
Rao VP, Nair RR (1988) Microbial origin of the phosphorites of the western continental shelf of India. Mar Geol 84:105–110
Redfield AC, Ketchum BH, Richards FA (1963) The influence of organisms on the composition of sea water. In: Hill MN (ed) The sea, vol 2. Wiley, New York, pp 26–77
Reimers CE, Kastner M, Garrison RE (1990) The role of bacterial mats in phosphate mineralization with particular reference to the Monterey Formation. In: Burnett WC, Riggs SR (eds) Phosphate deposits of the world, vol 3. Neogene to modern phosphorites. Cambridge University Press, Cambridge, pp 300–311
Riding R (1991) Calcified cyanobacteria. In: Riding R (ed) Calcareous algae and stromatolites. Springer, Berlin Heidelberg New York, pp 55–87
Soudry D (1979) Intervention de schizophytes dans la phosphomicritization des débris osseux. CR Acad Sci Paris 288 D:669–671
Soudry D (1987) Ultra-fine structures and genesis of the Campa-

nian Negev high-grade phosphorites (southern Israel). Sedimentology 34:641–660
Soudry D (1992) Primary bedded phosphorites in the Campanian Mishash Formation, Negev, southern Israel. Sedim Geol 80:77–88
Soudry D, Champetier Y (1983) Microbial processes in the Negev phosphorites (southern Israel). Sedimentology 330: 311–423
Soudry D, Southgate PN (1989) Ultrastructure of a Middle Cambrian primary nonpelletal phosphorite and its early transformation into phosphate vadoids. J Sediment Petrol 59:53–64
Soudry D, Lewy Z (1990) Omission-surface incipient phosphate crusts on early diagenetic calcareous concretions and their possible origin, Upper Campanian, southern Israel. Sedim Geol 66:151–163
Soudry D, Panczer G (1994) Stromatolitic phosphorites in the Eocene of the Negev (southern Israel). In: Bertrand-Sarfati J, Monty C (eds) Phanerozoic stromatolites II. Kluwer Academic Publishers, Dordrecht, pp 255–276
Southgate PN (1980) Cambrian stromatolitic phosphorites from the Georgina Basin, Australia. Nature 285:395–397
Southgate PN (1986) Cambrian phoscrete profiles, coated grains, and microbial processes in phosphogenesis: Georgina Basin, Australia. J Sedim Petrol 56:429–441
Trudinger PA (1978) Microbiological controls on phosphate accumulation. In: Cook PJ, Shergold JH (eds) Proterozoic-Cambrian Phosphorites. Canberra Publ Print Co, Canberra, pp 39–40
Van Cappellen P, Berner RA (1991) Fluorapatite crystal growth from modified seawater solutions. Geochim Cosmochim Acta 55:1219–1234
Walter MR [ed] (1976) Stromatolites. Developments in sedimentology 20. Elsevier, Amsterdam, p 790
Wiessner W (1981) The family Beggiatoaceae. In: Starr MP, Stolp H, Truper HG, Balows A, Schegel HG (eds), The prokaryotes. Springer, Berlin Heidelberg New York, pp 380–389
Zanin YuN, Gorlenko VM, Mirtov YuV, Krasil'nikova NA, Letov SV (1987) Bacteriomorphic formations in nodular and granular phosphorites. Geol Geofiz 28:43–49 (in Russian)

Microbes and Black Shales

Wolfgang Oschmann

Institut und Museum für Geologie und Paläontologie, Universität Tübingen, Sigwartstrasse 10, D-72076 Tübingen, Germany
New adress: Geologisch-Paläontologisches Institut, Universität Frankfurt, Senckenberganlage 32–34, 60054 Frankfurt am Main, Germany

Abstract. Black shales, in general, form under low oxic to anoxic conditions, where microbes have evolved a variety of metabolic pathways. Modern oxygen-depleted environments typically contain anaerobic heterotrophic bacteria, aerobic chemolithoautotrophic bacteria (which partly live in mutualistic relationship with certain metazoa) and anaerobic photoautotrophic bacteria. These bacteria mainly degrade but partly also form organic matter. Their metabolic pathways and their preservational potential in the fossil record are discussed here. In many cases only metabolic waste products, e.g. pyrite, and certain bacterial derived biomarkers are preserved. Relicts of microbials mats occur as rare exceptions.

1 Introduction

The organic carbon cycle is in general balanced. Rates of photosynthesis (biological reduction of inorganic carbon) and respiration (biological oxidation of organic carbon) are almost equal. Only a small amount of organic matter escapes re-oxidation and is transported from the site of primary production (land areas or ocean surface waters) to depositional centers, such as lakes or marine basins (e.g. Berger et al. 1989), where it is further degraded aerobically until either oxygen or the organic matter itself is consumed. Organic matter is normally the first to be exhausted but if the amount of organic matter is sufficiently large to consume all the oxygen, further degradation takes place within the sediment anaerobically. However, in most environments, the water column and the topmost part of the sediment is oxygenated and the amount of organic matter within the sediments is very low (less than 0.5%) and consists of barely degradable compounds such as lignin and humic material.

By contrast, black shales are characterized by a remarkable excess of organic matter. High organic inputs occur from areas of primary productivity with density stratification within the water column, which prevents mixing of surface and bottom waters, and allows rapid oxygen depletion or complete removal of oxygen in benthic environments (e.g. Demaison and Moore 1980; Oschmann 1988, 1990, 1994). The main contributors to organic matter are land plants with leaves, resins and highly resistant woody tissues (since early Devonian) and various groups of unicellular eukaryotic primary producers (mainly Chrysophyta, diatoms, and Dinophyta). These eukaryotes form organic (and frequently mineralized) cell walls, which are in part also very resistant. Degradation of high concentrations of organic matter causes rapid consumption of oxygen within the upper part of the sediment or even within the water column, and excess organic matter is then degraded anaerobically.

Microbes contribute to primary production to only a minor extent (e.g. Hartgers et al. 1994) but, together with fungi, they are the main degraders responsible for the remineralization of organic matter. Microbes are particularly successful aerobic and anaerobic degraders for the resistant compounds of land plants and unicellular eukaryotes (e.g. cellulose, xylan, sterols and lignin; Schlegel 1993). Unfortunately, their preservational potential is very low. The cellular membranes of bacteria are even less resistant and degrade much more readily (again with the help of bacteria) than those of eukaryotes and metazoans. Therefore, in most cases hardly any remains are preserved from this important group of organisms. Under certain circumstances, however, bacteria are preserved as filamentous mats, precipitates of metabolic waste products, and biomarker molecules (see other chapters). The probability of preservation of microbial relicts increases with the inhospitability of the depositional environment, because more highly evolved competitors are excluded, whereas certain bacteria are well-adapted to those harsh environments. This is particularly true for black shales which have been deposited under oxygen-deficient or even oxygen-free bottom waters, which inhibit or even exclude the permanent occurrence of eukaryotes and metazoans.

2 Metabolic Pathways and Adaptations of Bacteria in Modern Oxygen Depleted or Anoxic Environments

There are various life habits and metabolic pathways used by bacteria under anoxic conditions or in the weakly oxic conditions close to the redox boundary: (1) anaerobic heterotrophic bacteria are the ultimate degraders below the redox-boundary, (2) aerobic chemolithoautotrophic bacteria live slightly above the redox

R.E. Riding and S.M. Awramik (Eds.)
Microbial Sediments

boundary and use the reduced compounds of the anaerobic heterotrophs. In rare cases chemolithoautotrophy also occurs in anaerobic environments, (3) chemosymbiosis characterizes mutualistic relations of metazoans and endobiontic aerobic, chemolithoautotrophic bacteria, (4) in some environments anoxic photosynthesis may occur, indicating the position of the redox boundary within the photic zone (Figs. 1, 2).

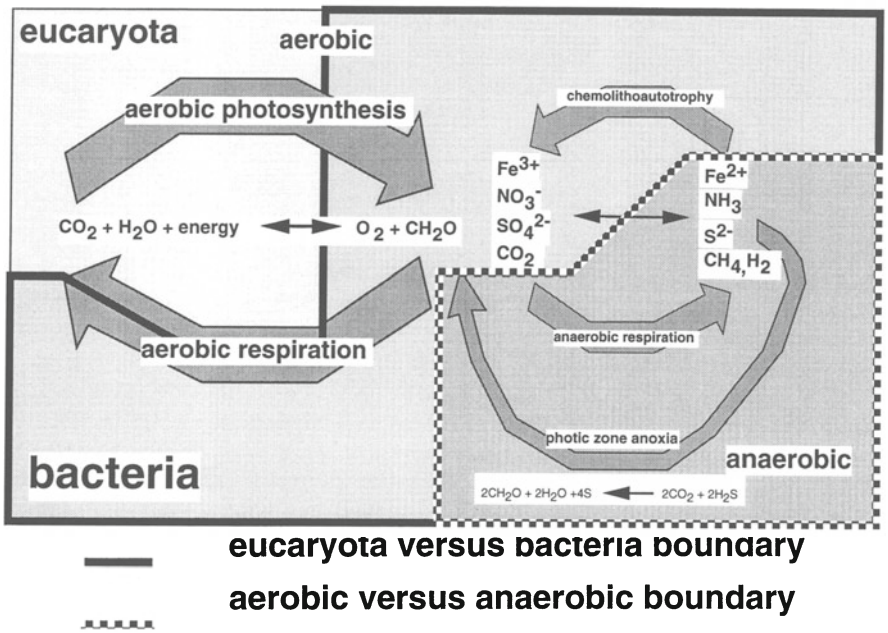

Fig. 1. Interlinked pathways of aerobic, anaerobic and chemolithoautotrophic primary producers and degraders

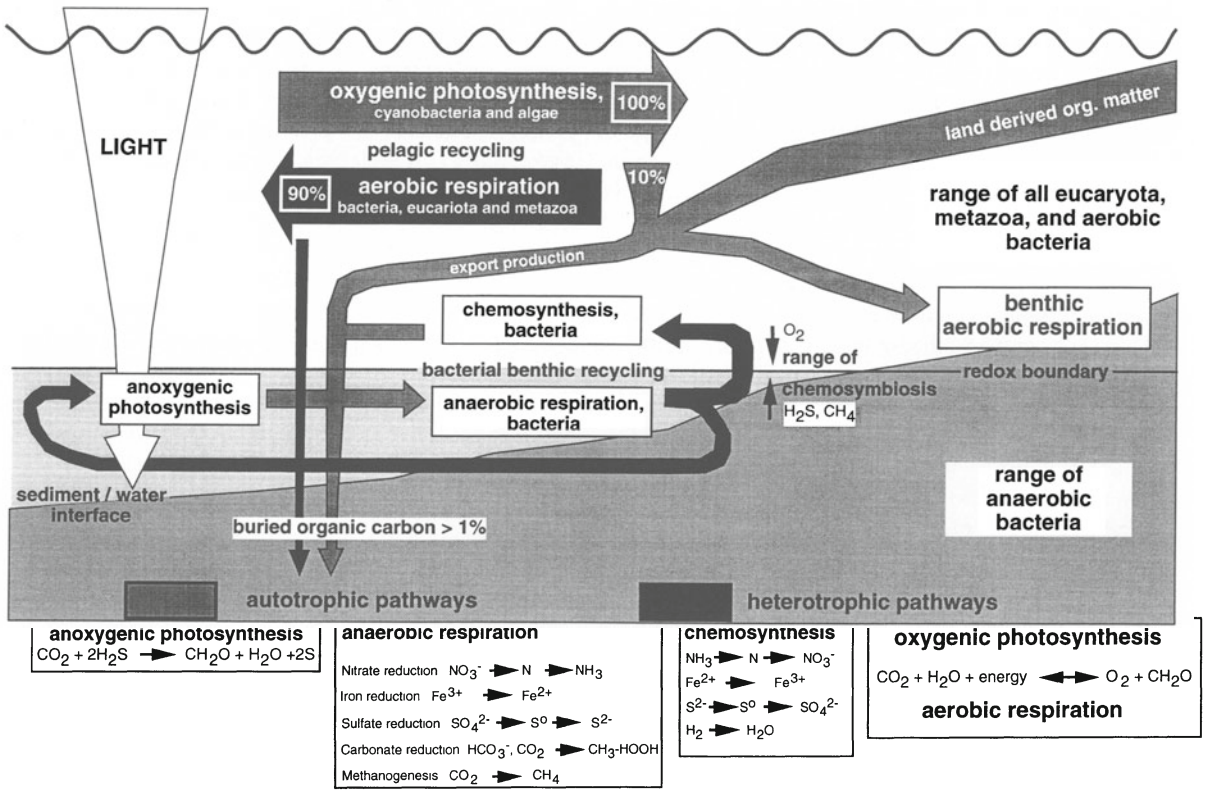

Fig. 2. The organic carbon cycle and the main related redox reactions

2.1 Anaerobic Heterotrophic Bacteria

A number of bacteria are adapted to live facultatively or as obligate anaerobes using the organic matter which is left from aerobic degradation as a carbon and hydrogen source. Respiration is achieved by reducing inorganic compounds such as nitrate (NO_3^-), sulfate (SO_4^{2-}), and bicarbonate (HCO_3^-), or CO_2. Other sources are highly oxidized metal ions, particularly Fe^{3+} and to a minor extent Mn^{4+}. All these bacteria represent end-member degraders of the respiratory part of the organic carbon cycle and depend on accumulations of organic matter and the availability of the inorganic compounds. The succession of the reactions is strictly controlled by the redox potential, starting with manganese reduction in oxygenated environments, followed by nitrate, iron, sulfate, and carbonate reduction. The start of each successive reaction depends on the decline or the absence of the precursor substance, however some overlap occurs (Fig. 2; e.g. Canfield et al. 1993; Schlegel 1993). The total amount of organic carbon decomposition by anaerobic heterotrophs may exceed 90%, depending on the circumstances (e.g. Canfield et al. 1993).

Nitrate reduction prevails in freshwater environments (ponds and lakes) and in soils, where NO_3^- is reduced either to N_2O, to N_2 or to NH_3. All products are gaseous and escape without forming any solid precipitates. Typical bacteria involved in nitrate reduction are *Pseudomonas denitrificans* and *Thiobacillus denitrificans*. They occur as cylindrical, vibroform, or spiriliform cells (Schlegel 1993) and in general are only of minor importance in black shale environments.

Bicarbonate (HCO_3^-) and CO_2 are reduced to methane (CH_4) in a large variety of terrestrial (soils and swamps), freshwater, and marine environments. The production of methane may reach remarkable levels, but again the end product is gaseous and cannot generally be preserved. The growth form of the bacteria involved (e.g. *Methanobacterium, Methanococcus*) varies from cylindrical to spherical (cocciform) and spiriliform. These bacteria contribute to the formation of methane or methane hydrate, which is trapped in plumes at a number of localities in near surface sediments of modern oceans (e.g. Lammers et al. 1995).

The reduction of iron (Fe^{3+} to Fe^{2+}) and, to a lesser extent, of other metals (e.g. manganese, Mn^{4+} to Mn^{2+}) produces soluble ions and occurs in marine and freshwater environments and in soils. Iron reduction is caused by a variety of bacteria and is particularly important in association with sulfate reduction. Both reactions provide the precursors for pyrite formation (see below, Figs. 2, 4). Iron reduction by the bacteria *Alteromonas, Desulfovibrio* and *Desulfobacter* (the latter two are generally known as sulfate reducers) partly forms very strongly ferromagnetic Fe(II, III)-oxides (magnetite) and is thus very important for generating magnetic signals in sediments (Loveley et al. 1993; Schlegel 1993).

In natural environments, sulfate reduction is mainly restricted to salt lakes, brackish waters and marine areas, where sulfate is relatively abundant. Sulfate reduction takes place in several steps, from sulfate (SO_4^{2-}) to sulfite (SO_3^{2-}), then thiosulfate ($S_2O_3^{2-}$) and sulfur (S^0), and finally to sulfide (S^{2-}). A variety of bacteria (e.g. *Desulfovibrio, Desulfobacter, Desulfomonas, Desulfotomaculum*) are involved, but many are responsible for only part of the reaction chain. Some taxa (e.g. *Desulfovibrio, Desulfobacter*) also adopt a facultative autotrophic growth mode (Schlegel 1993). These bacteria are heterogeneous and consist of a variety of different morphologies of Eubacteria and Archaebacteria. In most cases, they form mats or filament-like structures and, together with iron reducing bacteria, they are responsible for pyrite formation (see below). In many modern environments the biomass of this microbial community shows a marked seasonal variation, with high values during periods of phytoplankton production in spring and summer and low values in autumn and winter (Rajendran and Matsuda 1995; Holmer and Kristensen 1996). Most of them have cylindrical, vibroform, or spiriliform shapes (Schlegel 1993) and may occur within the sediment and in the water column in large numbers. Ramsing et al. (1996) estimate cell numbers of the order of 10^4–10^5/ml for marine sulfate reducers. Parkes et al. (1993) discuss the microbial activity of methanogenetic and sulfate reducing bacteria at depths of up to 80 m below the surface of Peru margin sediments. The bacterial concentration reached a maximum at 12 cm depth (4×10^9 cells/cm^3), but was still high at 80 m depth (3×10^8 cells/cm^3).

2.2 Chemolithoautotrophic Bacteria

There is a large group of gram-negative bacteria with an elongate cylindrical or vibroform outline (e.g. Schlegel 1993) which mainly use CO_2 as a carbon source, water as a hydrogen source, and reduced inorganic compounds such as NH_4^+, NO_2^-, S^{2-}, S, H_2, and Fe^{2+} for oxidation as a source of energy. Most members of this group are obligate aerobes. Some can exist facultatively as anaerobes and then partly switch to the heterotrophic metabolism described above. The preservational potential of these bacteria is very low, because they normally occur in (weakly) oxygenated environments and are rapidly decomposed after death. The most important chemolithoautotrophic pathways are as follows.

Nitrification is the oxidation of ammonia and nitrite by, e.g. *Nitrosomonas* and *Nitrobacter*, which occur mainly in soils but also in freshwater and marine environments.

Sulfur oxidation from H_2S to SO_4^{2-} and iron oxidation (Fe^{2+} to Fe^{3+}) are known from various environments such as soils and subaerial volcanic springs. Sulfur oxidation is particularly well-known from subaquatic hydrothermal vents in the ocean. There, these bacteria are the primary producers in an ecosystem completely independent of any photic energy source (see below).

Oxidation of hydrogen (H_2) or carbon monoxide (CO) mainly takes place in soils but also in marine and freshwater environments, forming acetic acid (CH_3COOH), nitrate and partly also methane and H_2S as metabolic products. The latter two are further oxidized by other chemolithoautotrophic bacteria.

2.3 Gliding Bacteria

A special group of aerobic chemolithoautotrophic bacteria are the gliding bacteria *Beggiatoa* and *Thioploca*, which have the unusual capability of active gliding movement. Their metabolism is chemolithoautotrophic via oxidizing reduced inorganic compounds. They mainly use H_2S as a source of energy which is oxidized either to S^0, $S_2O_3^{2-}$ or to SO_4^{2-}. Elemental sulfur commonly is stored in small liquid intracellular inclusions, which are also liberated by excretion (e.g. Schlegel 1993; Arntz et al. 1991; Fossing et al. 1995). Their natural habitat in highly productive freshwater, and particularly marine, environments is restricted to muddy surfaces (Arntz et al. 1991; Sweerts et al. 1990), cold seeps (e.g. Hovland 1992) and hydrothermal vent ecosystems (e.g. Van Dover 1995). There, they may form dense microbial mats, occurring at or immediately above the redox boundary, which is commonly situated at the sediment water interface. This position guarantees the contemporaneous supply of H_2S and O_2 (Schlegel 1993).

Thioploca has been found in the upwelling system off Peru from depths of 12 m to over 400 m, where it forms temporary microbial mats. The mats consist of thread-like bacteria which partly accumulate as thick and dense filaments (e.g. Arntz et al. 1991; Fossing et al. 1995). Oxygen values immediately above the mats are rather low (less than 0.4 ml/H_2O), but may permit coexistence of some eukaryotic and metazoan life, according to Arntz et al. (1991). Fossing et al. (1995) found no oxygen within the topmost sediment or even, in some cases, in the water column during in situ measurements. Therefore, these workers assume that *Thioploca* can adopt a very effective double strategy using not only O_2 but also NO_3^- for H_2S oxidation. NO_3^- is taken from the sea water above and stored in the interior of the cells in a liquid vacuole, whereas H_2S is abundant in deeper parts of the sediment and is accessed by bacterial threads which reach downward to guarantee the contemporary availability of H_2S and NO_3^- (which normally occur at different redox levels). Sulfur globules are the metabolic waste products and occur embedded in the cytoplasm. This strategy probably enables *Thioploca* to outcompete other chemolithoautotrophic bacteria and to form the bacterial mats well-known in modern oxygen-depleted environments.

2.4 Chemosymbiosis

The mutualistic relation of metazoans and endobiontic chemolithoautotrophic bacteria has been described as chemosymbiosis (e.g. Fisher 1990). The metazoans (mainly vestimentiferans, mollusks, polychaetes, and arthropods) provide protection to the endobiontic chemolithoautotrophs which live within the gills, muscular tissues or other organs. These bacteria produce glucose or starch which is shared with the metazoans. The hosts have commonly lost their feeding appendices and their digestive systems depend on obligatory bacterial symbiosis (e.g. the vestimentiferan worm *Riftia pachyptila* and the bivalve *Solemya*). The metabolic pathway of the metazoans operates via glycolysis and the citric acid cycle and requires O_2. The bacteria, in contrast, require H_2S and at least a minimum amount of oxygen to oxidize H_2S for their metabolic processes. Chemosymbiosis therefore can only take place in environments with a balanced juxtaposition of both gases at the redox boundary (Fig. 2).

H_2S is an extremely potent neurotoxin and causes cessation of pulmonary function. Chemosymbiontic metazoans which provide H_2S to the endobiontic bacteria need H_2S-binding and transporting pigments in order to prevent blocking of cytochrome c and oxygen-binding pigments in their blood. Some have a separate H_2S-carrying molecule (e.g. *Calyptogena magnifica*), in others large heme molecules (*Riftia pachyptila*) can bind both O_2 and H_2S contemporarily (Bryant 1991). The bacteria oxidize H_2S to sulfate or thiosulfate and prevent poisonous effects for metazoans.

Chemosymbiontic metazoans therefore have to manage the supply of chemical compounds from above and below the redox boundary simultaneously. The semi-endobenthic to epibenthic vent bivalve *Calyptogena* achieves this by extending its large foot into the H_2S regime deep in the substrate, whereas the remaining part of the body, or at least the upper part with the gills, rests in the O_2 regime. Roux et al. (1983), Hashimoto et al. (1989), and Schein et al. (1991) report changes of position relative to the sediment water interface for *Calyptogena*, depending on growth stage and vent activity.

Endobenthic bivalves (solemyids, thyasirids and lucinids) maintain this balance by burrowing deep and obtaining H_2S from the reduction zone within the sub-

strate and oxygen from the oxygenated water column. The tolerance of the gutless *Solemya reidi* extends to concentrations of up to 100 µmol H_2S. Detoxification of H_2S takes place in the bivalve mitochondria and produces thiosulfate, which is further oxidized by bacteria. Excess sulfide inhibits aerobic respiration and can be detoxified only temporarily, with the help of bacteria (Vetter et al. 1991). Burrows of solemyids and thyasirids reach down to many times their body size. Moving up and down their burrows (solemyids) or pumping water with their foot acting as a piston in a well (thyasirids) enables these bivalves to live in optimum conditions (e.g. Seilacher 1990; Savrda et al. 1991).

Besides H_2S, methane (CH_4) has also been discovered in hydrothermal vents and cold seeps and is used by methanotrophic gram-negative bacteria. These bacteria co-exist as symbionts in some benthic invertebrates together with sulfide oxidizing bacteria, e.g. in the mytilid bivalve *Bathymodiolus* (Cavanaugh et al. 1987; Van Dover 1995).

2.5 Anoxic Photosynthesis

The ability to maintain anoxic photosynthesis is known for a number of cyanobacteria and purple non-sulfur bacteria (facultatively), and particularly for purple and green sulfur bacteria (obligatory). The main difference in the metabolic pathway of purple sulfur bacteria (e.g. *Thiospirillum*) and green sulfur bacteria (e.g. *Pelodictyon*) as compared to oxic photosynthesis is that they use H_2S instead of H_2O as a hydrogen donor and therefore depend on free H_2S in the environment (e.g. Schlegel 1993). Modern purple sulfur and green sulfur bacteria occur in marine and freshwater environments. They form films or filaments on the substrate in shallow water environments and even occur as mid-water aggregates. Some groups are able to adopt a gliding mode of movement. Their photopigments are carotinoids with a maximum absorption capacity between 400 and 550 nm wavelength, which represents the blue end of the visible light spectrum (Schlegel 1993). Therefore, they can also occur at great depths, depending on the clarity of the water, e.g. down to 200 m depth in the Black Sea (Dickman and Artuz 1978). Purple sulfur and green sulfur bacteria store sulfur globules as metabolic by-products intracellularly or extracellularly attached to the cell membrane, as do *Beggiatoa* and *Thioploca*.

2.6 Microbial Mats

Microbial mats are laminated organo-sedimentary structures with a strong redox gradient from free oxygen to free H_2S (e.g. von Gemerden 1993). The most well-known and probably best studied examples are intertidal mudflat microbial mats, which represent a community of photosynthetic cyanobacteria as the main primary producers in the topmost layer. Slightly below, colourless sulfur bacteria exist under fluctuating oxygenated and anoxic conditions. During the daytime the cyanobacteria above provide oxygen, and during the night the H_2S level rises from below. Purple sulfur bacteria maintain an anoxic photosynthesis and sulfate reducers represent the lowermost part of the mat (von Gemerden 1993). The particular coexistence of primary producers (which provide organic matter) and of degraders (which remineralize the inorganic compounds) represents a kind of recycling system.

Similarly, in a number of modern oxygen-depleted environments, microbial mat-resembling recycling systems are developed. The chemolithoautotrophic gliding bacteria *Thioploca* use the metabolic products of anaerobic heterotrophic bacteria from below, and vice versa. Therefore, microbial communities are

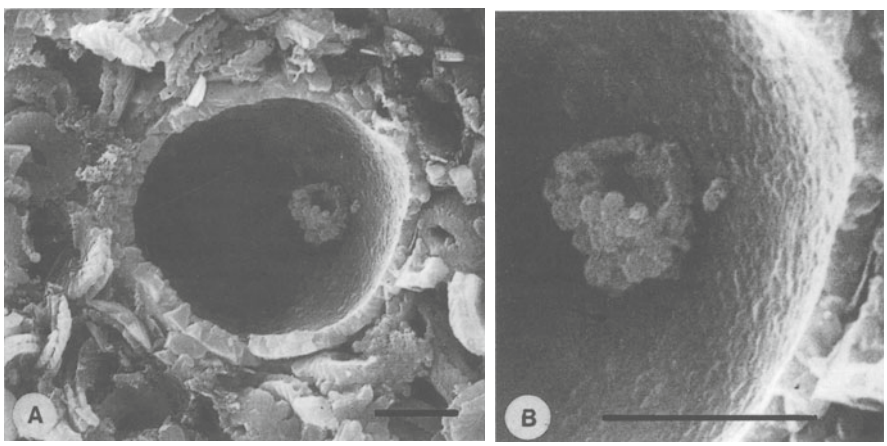

Fig. 3A,B. Mineralized remains resembling a bacterial aggregate attached to the inner surface of a calcisphere wall. The size of the assumed bacterial cells is approximately 0.5 µm. **B** Detail of **A**; Kimmeridge Clay, Yorkshire, England. **A** and **B** *scale* 5 µm

in many cases complex ecosystems consisting of chemolithoautotrophic bacteria and anaerobic heterotrophs co-existing close together, slightly above and slightly below the redox boundary (e.g. Rajendran and Matsuda 1995; Holmer and Kristensen 1996; Figs. 1, 2).

3 Microbes in Ancient Black Shales

The direct visual detection of bacteria in black shales is almost impossible, but there is some circumstantial evidence for the presence of some of the groups of bacteria discussed above, either during deposition or early diagenesis. A rare example of preserved mineralized

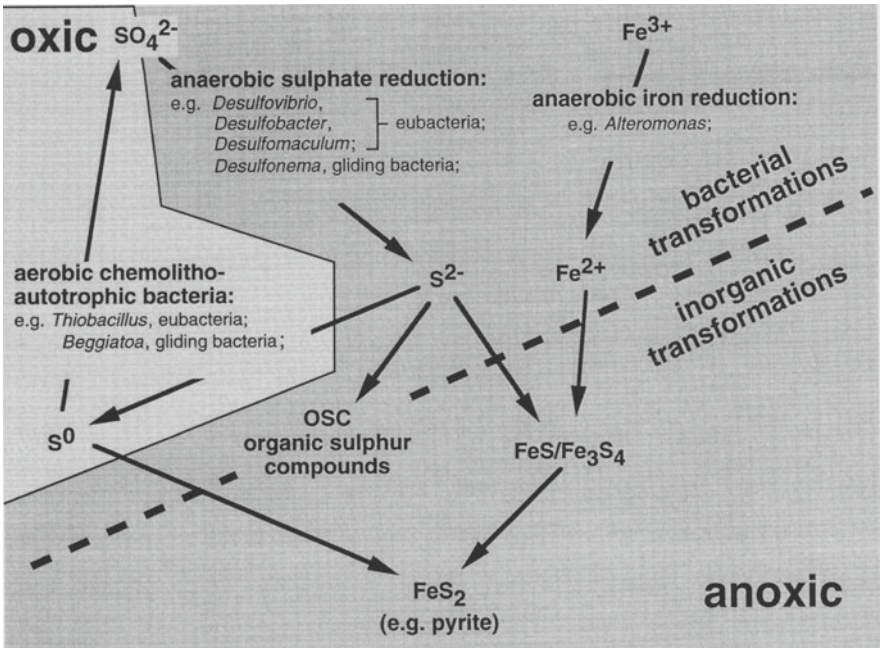

Fig. 4. The sulfur cycle in marine environments with the main bacterial and inorganic transformations

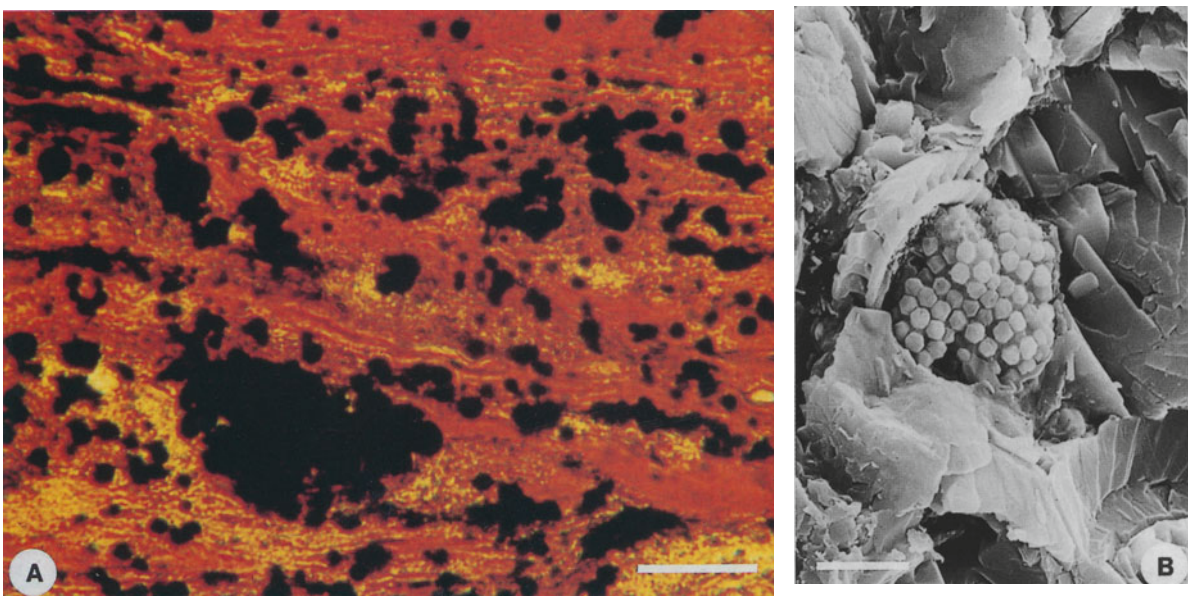

Fig. 5.A Very small globular pyritic aggregates (*black*) occur preferentially within layers rich in organic matter (*orange*). **B** Framboidal pyrite enclosed in corroded coccoliths. The framboid consists of pyritohedral microcrystals precipitated as a metabolic waste product of bacteria. **A** Thin-section, *scale* 20 µm; **B** SEM, *scale* 2 µm; Kimmeridge Clay, Yorkshire, England

remains which might be related to cellular aggregates of bacteria is given in Fig. 3. The size of the cocciform cells is 0.5 µm and they occur attached to the inner side of the wall of a calcisphere. Clear examples of mineralized bacterial remains have been reported from the Eocene Messel Formation, which represents a freshwater black shale environment (e.g. Schmitz and Ernst 1994; Richter 1994).

Another definite proof of fossil bacteria is biomarker molecules of the extended hopanoids. Geohopanoids are diagenetic alteration products of biohopanoids, a certain group of lipids, which occur as bacterial cell membrane constituents (Ourisson and Rohmer 1992). Detection of these molecules in most ancient black shales is possible using GC/MS analysis of the aliphatic fraction of organic matter. However, so far geohopanoids are not diagnostic for specific bacterial groups or metabolic pathways (Ourisson and Albrecht 1992).

3.1 Precipitation of Metal Sulfides

The activity of iron reducing bacteria, together with sulfate reducing bacteria, can be detected by their metabolic waste products, which form disseminated solid precipitates (Fig. 4). These are metal sulfides, mainly pyrite and precursor iron sulfides (e.g. FeS as mackinawite

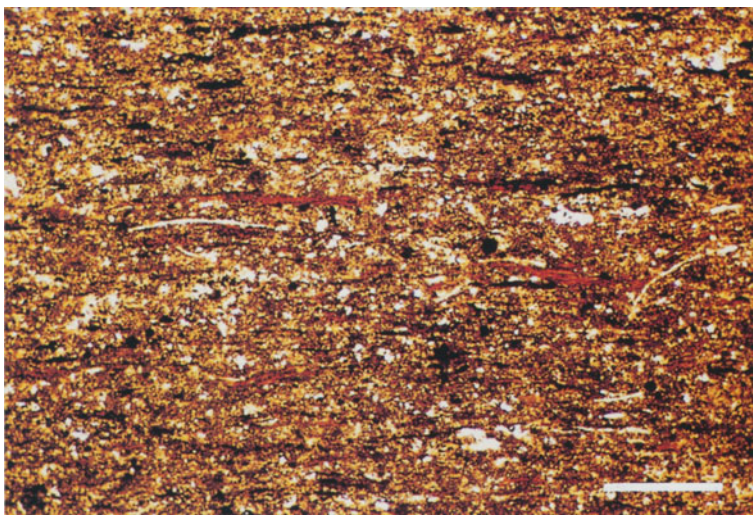

Fig. 6. Phytoplankton remains in black shales mainly consisting of disrupted particulate organic matter dispersed in rocks; *scale* 200 µm, TOC 4.5%, Kimmeridge Clay, Yorkshire, England

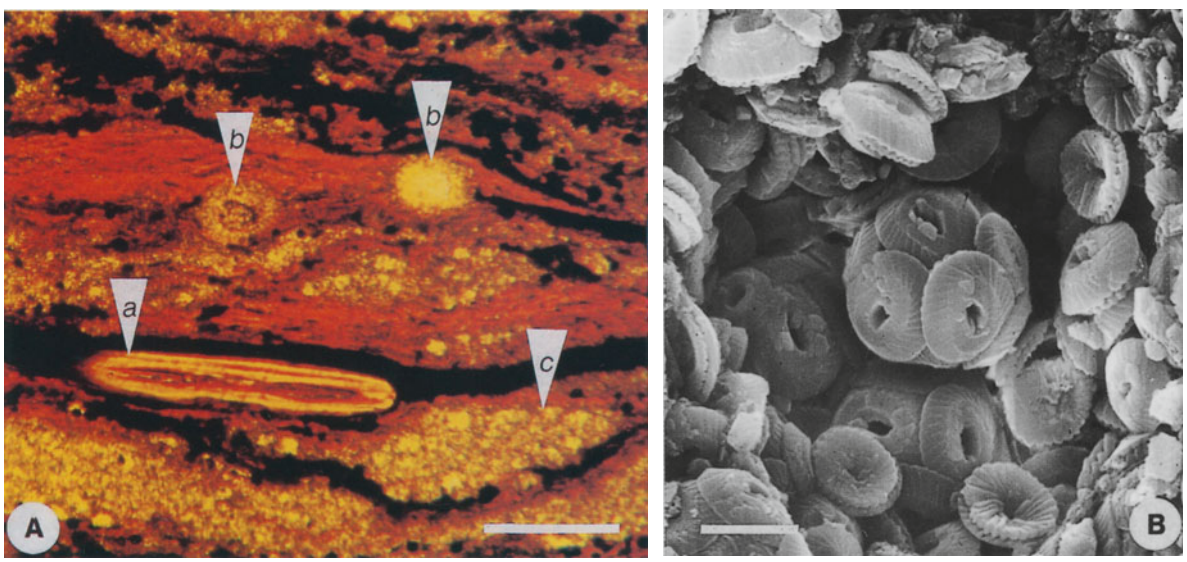

Fig. 7.A Organic matter in black shales mainly occurs as remains of disrupted and compacted tissues from land plants and eukaryotic primary producers, or occasionally as complete cells, e.g. of Tasmanales (*a*). Mineralized hard parts derive from calcispheres (*b*) and coccospheres (**B**). The latter are particularly common in pellets (*c*). **A** Thin-section, *scale* 40 µm, TOC 7.5%; **B** SEM, *scale* 5 µm; Kimmeridge Clay, Yorkshire, England

and pyrrhotite, and Fe_3S_4 as greigite). Sedimentary sulfide minerals occur at scales which range from microscopic aggregates and framboids to mesoscale fecal pellets, macroscale burrows and pyritized fossils, and even concretions and concretionary layers (e.g. Hudson 1982). In the present context, only synsedimentary and very early diagenetic processes which form microscopic sulfides are important.

Pyrite precipitation is a three-phase process in which organic carbon, iron and sulfate have to be available in sufficient quantities. In marine clastic sediments iron and sulfate occur in large concentrations but the amount of organic matter is limited in most environments. Precipitation of iron sulfides takes place immediately when Fe^{2+} and S^{2-} are produced and buffer proportions of free H_2S to low levels. Where sufficient organic matter occurs, different pathways of precipitation may take place. Either Fe^{2+} is transported to the place of sulfate reduction in the case of sufficient reactive iron, i.e. mainly hydroxide and hematite, or mobile sulfides diffuse to less reactive, particulate iron minerals, i.e. mainly silicates (e.g. Allison 1988; Canfield and Raiswell 1991; Canfield et al. 1992; Coleman et al. 1993). Normally Fe^{2+} is available prior to S^{2-} which is generated at a lower redox level. Therefore, Raiswell et al. (1993) postulate pyrite precipitation very close to the site of organic matter decomposition via sulfate reduction. Diffusion parameters limit the growth of the precipitates to a maximum size of approximately 50 µm. The very small framboidal and aggregated pyrite crystals which occur within organic-rich sediments may be explained in this way (Fig. 5).

Pyrite, however, might also form from the sulfur globules stored intra- and extracellularly by chemolithoautotrophic bacteria (e.g. *Thioploca*) or by purple and green sulfur bacteria. This sulfur might either disproportionate and react with iron sulfides, i.e. mackinawite and pyrrhotite (FeS) or greigite (Fe_3S_4), or it might be further reduced by heterotrophic anaerobic bacteria and precipitated with iron. These tiny sulfur droplets might in this way be converted to monosulfides and to pyritic framboids or aggregated pyrite, or might act as nuclei for precipitation (see Dickman and Artuz 1978). The main difference, however, between the chemolithoautotrophic bacteria, purple sulfur bacteria, and green sulfur bacteria, on the one hand, and anaerobic heterotrophs, on the other, is that the former are primary producers (and therefore might be associated with very high amounts of organic matter), whereas the latter consume organic matter. The minimum amount of organic carbon consumed (C-loss) can be estimated from the amount of newly formed metal sulfides (plus the organic sulfur compounds, see below), since 1 mol of S^{2-} forms from the degradation of 2 mol of organic carbon.

Raiswell and Berner (1985), Leventhal (1987), and Fisher and Hudson (1987) have produced plots of organic C vs sulfur and DOP (degree of pyritization) for modern and ancient sediments. These plots indicate iron-limited pyrite precipitation if the DOP is independent of the organic carbon content. Additionally, an euxinic sedimentary basin (with free H_2S in the bottom water) is probable if the C/S correlation in the plots (with C organic as *x*- and S as *y*-axis) shows a non-zero (positive) S intercept for a zero C intercept.

In addition, subsequent diagenetic reactions, which occur during or after compaction, can result in the replacement of other minerals (e.g. carbonates) by pyrite (Canfield and Raiswell 1991). These reactions and the occurrence of late diagenetic thermal sulfate reduction and pyrite precipitation, which occurs under p/t conditions of wet and dry gas generation (e.g. Machel et al. 1995), involve little or no microbial activity and are not important in the present context.

3.2 Formation of Organic Sulfur Compounds

The formation of organic sulfur compounds (OSC) indicates a high rate of sulfate reduction in an environment depleted in reactive iron (and similar cations). The sulfidic compounds then react with organic matter, particularly with double bonds of ketone and aldehyde functionalities and with certain aromatics (DeLeeuw et al. 1995). OSC within sediments therefore represent excellent biomarkers indicating the activity of sulfate reducing bacteria. For calculation of the organic carbon consumed (C-loss) during sulfate reduction, the sulfidic proportion of the OSC has to be added to the proportion of sulfide bound to metal cations (see precipitation of metal sulfides).

3.3 Fossil Chemosymbiosis

Chemosymbiosis is detectable in the fossil record from the close taxonomic relationship of modern and ancient chemosymbionts. This mainly refers to bivalves, which have the highest preservation potential of all metazoan groups that presumably hosted chemosymbionts. Well-known examples are solemyids, thyasirids and lucinids (e.g. Seilacher 1990; Oschmann 1994). In the Kimmeridge Clay many specimens of *Mesomiltha* (lucinid) have been covered with a faint, light yellow layer of sulfur-rich material which has been detected via EDAX analysis. No other fossils in this deposit showed a similar feature. This faint cover is probably composed of elemental sulfur or a sulfur-rich mineral, possibly alumite $KAl_3(SO_4)OH_6$ or jarosite $KFe_3(SO_4)OH_6$), representing diagenetically overprinted relicts of sulfur stored by the chemolithoautotrophic endosymbionts.

Chemolithoautotrophy and chemosymbiosis in cold

seeps and hydrothermal vents are commonly associated with early diagenetic carbonate precipitation (e.g. Beauchamp and Savard 1992; Gaillard et al. 1992; Kauffman et al. 1996). The main carbon source for precipitation is methane, which is oxidized by methanotrophic bacteria to CO_2 and HCO_3^-. Methane is formed from organic matter which is depleted in $\delta^{13}C$ (values range from −25 to −35‰). Bacterially driven methanogenesis and methanotrophy additionally reduce the isotopic ratio by remarkable vital effects (e.g. De Leeuw et al. 1995). The precipitated carbonates which form from the oxidized methane therefore might show $\delta^{13}C$ values in the range of −20 to −45‰ (e.g. Kauffman et al. 1996).

3.4
Anaerobic Photosynthesis in the Fossil Record

Anaerobic photosynthetic bacteria (purple sulfur bacteria and green sulfur bacteria) synthesize carotinoid photopigments, with very specific diaromatic structures (e.g. isorenieraten and clorobacten). These carotinoids are restricted to these groups of bacteria and are therefore diagnostic. Biomarker analysis of black shales commonly reveals the diagenetic alteration products of these carotinoids (e.g. arylisoprenoids), which can be detected using liquid/gas chromatography mass spectrometry (L/GC-MS) (e.g. Hartgers et al. 1994; Kenig et al. 1995; De Leeuw et al. 1995; Sinninghe Damste et al. 1995). The occurrence of these compounds is generally accepted to be indicative of water column stratification with photic zone anoxia.

3.5
Microbial Mats in Black Shales

The fine, particulate organic matter of black shales consists of remains of land plants and eukaryotic primary producers (e.g. Tissot and Welte 1978; Stach et al. 1982; Hartgers et al. 1994). In general these remains occur as unrecognizable, disrupted and compacted cuticles, spores and pollen (Fig. 6), and occasionally of complete unicellular eukaryotes (e.g. *Tasmanales*, Fig. 7). They are dispersed within the rock but are visible in thin-section and are characterized by yellow, orange, and reddish-brownish colors. In terms of coal petrology, they are described as alginites (e.g. Stach et al. 1982). Filamentary structures which might be related to bacterial activity occur rarely and there is no clearly defined optical evidence for a bacterial origin. Densely packed alginites of eukaryotic plankton remains and seasonal cycles of primary production might also produce laminated fabrics.

However, at certain levels within the Kimmeridge Clay "alginitic filaments" are probably of bacterial origin. These layers are very thin (1–5 μm) and easily overlooked, and the laminae in these filaments are very fine and laterally more persistent than in normal microlaminated alginites. The surfaces of the laminae are somewhat wrinkled (Figs. 8, 9). Commonly the filaments show structures resembling microscale gliding or slumping (Fig. 8), which is only possible among cohesive mat-like structures of benthic bacteria. Continuous sedimentation of land- or plankton-derived particulate organic matter cannot produce such structures. The benthic origin of the mats is proved by silty sedimentary particles, which are scattered within the filaments and have been deposited during benthic growth (Fig. 8). From the thin-section data it is not possible to identify the types of bacteria involved. However, the pathways discussed above suggest that anaerobic heterotrophs (mainly sulfate reducers) and aerobic chemolithoautotrophic gliding bacteria were involved. The amount of organic carbon is high (10–22%) and might partially result from autotrophic rather than from heterotrophic bacteria (which would have reduced the amount of organic carbon). Microscale pyritic aggregates, however, confirm the activity of sulfate reducers. Occasionally the bacterial mats are very well-laminated and do not contain internal silt particles (Fig. 9). These probably formed as mid-water mats (see Dickman and Artuz 1978) and were deposited later. Mid-water mats have also been postulated for the Grenzbitumenzone (mid-Triassic of Thessin, Swizerland) by Bernasconi (1994). In the Kimmeridge Clay they might either represent anaerobic heterotrophs (sulfate reducers) or anaerobic photoautotrophs (purple or green sulfur bacteria). The high concentrations of organic carbon and much lower proportions of microscale pyritic aggregates, compared to the sediments above and below, again favor a predominantly autotrophic formation.

4
Conclusions

Bacteria are the most important group of organisms in oxygen-controlled environments. They mainly degrade, but partly also form, organic matter. Despite their significance in modern environments, their preservation in black shales is rare and is mainly restricted to precipitated iron sulfides as the metabolic waste products of iron reducing and sulfate reducing anaerobic heterotrophic bacteria. Other detection methods have been developed through organic geochemistry. OSC prove the activity of sulfate reducing bacteria in environments depleted in reactive iron. The diagenetic alteration products of carotinoids (bacterial photo pigments, e.g. arylisoprenoids) are indicative of anoxic photosynthesis. Geohopanoids are relics of bacterial cell membrane constituents, but are not diagnostic of particular bacterial groups. Fossil examples of chemosymbiosis can be identified from certain groups of shelly metazoans (mainly bivalves), and by extremely light $\delta^{13}C$ values (−20 to −45‰) of early diagenetic carbonate precipitates. Chemolithoautotrophic bacteria

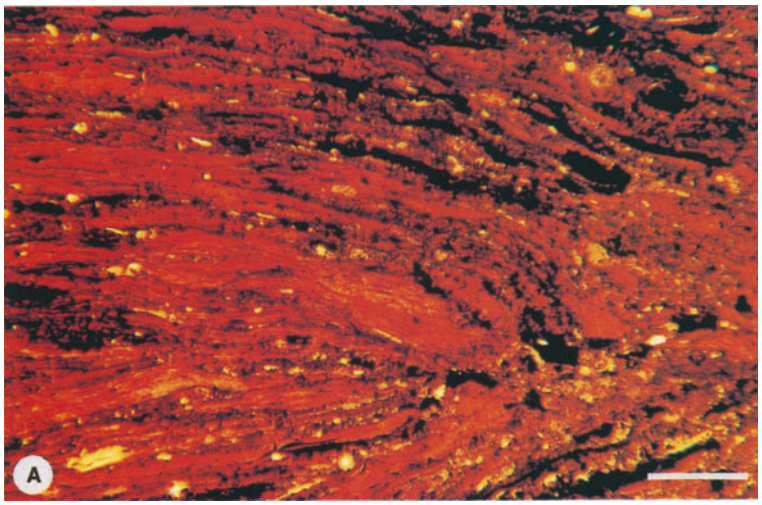

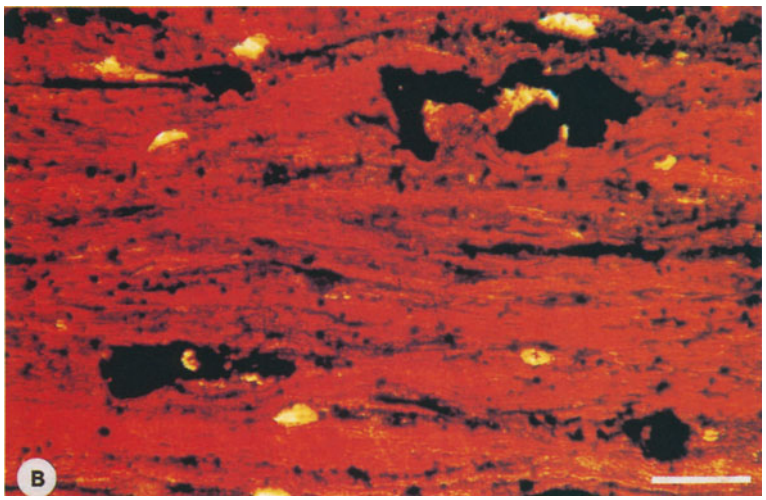

Fig. 8A,B. Filamentous mat-like structures of probable bacterial origin with dispersed, silt-size sedimentary particles which have been deposited during benthic growth of the mats. **A** Commonly the filaments show structures resembling microscale gliding of cohesive mat-like structures of benthic bacteria. **B** The laminae of the filaments are very fine (~1–2 µm) and laterally more persistent than compacted particulate organic of phytoplanktic origin. Thin-section; **A** *scale* 100 µm; **B** *scale* 40 µm; Kimmeridge Clay, Yorkshire, England, TOC 12%

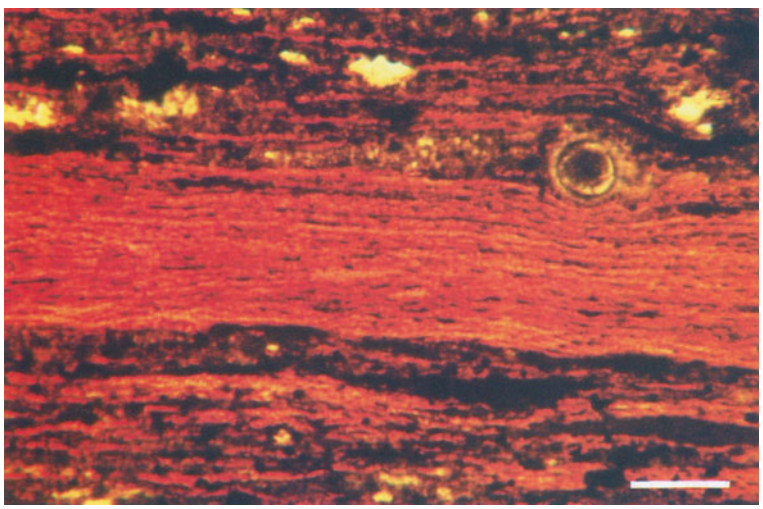

Fig. 9. Occasionally, the bacterial mats are very well-laminated (lamina thickness ~1–2 µm) and do not contain internal silt particles. They probably formed as mid-water mats, which were subsequently deposited. Thin-section, *scale* 40 µm, TOC 15% Kimmeridge Clay, Yorkshire, England

might be recognized by very high concentrations of organic matter, and in rare cases probably by remains of microbial mats in fossil black shales.

Acknowledgements. I am grateful to E. Gischler and C. Mundle (Tübingen) for reading and improving the manuscript and to A. and J. Röhl (Tübingen) for numerous stimulating discussions. J. P. Herbin (Institut Français du Pétrole, Rueil Malmaison) provided the Kimmeridge Clay samples of Yorkshire and the laboratory facilities at IFP in Rueil Malmaison. F. Kenig (Chicago) and L. Schwark (Köln) kindly introduced me to the fascinating world of biomarkers. The comments and improvements of style of two anonymous reviewers and of Robert Riding have been very helpful.

References

Allison PA (1988) Konservat-Lagerstätten: cause and classification. Paleobiology 14:331–344

Arntz WE, Tarazone J, Gallardo VA, Flores LA, Salzwedel H (1991) Benthos communities in oxygen deficient shelf and upper slope areas of Peruvian and Chilenian Pacific coast, and changes caused by El Niño. In: Tyson RV, Pearson TH (eds) Modern and ancient continental shelf anoxia. Geol Soc Spec Publ 58:131–154

Beauchamp B, Savard M (1992) Cretaceous chemosynthetic carbonate mounds in the Canadian Arctic. Palaios 7:434–450

Berger WH, Smetacek VS, Wefer G (eds) (1989) Productivity of the ocean; present and past. Wiley and Sons, Chichester

Bernasconi SM (1994) Geochemical and microbial controls on dolomite formation in anoxic environments. A case study from the middle Triassic (Ticino, Switzerland). Contributions to sedimentology 19. Schweizerbart, Stuttgart

Bryant C (ed) (1991) Metazoan life without oxygen. Chapman and Hall, London

Canfield DE, Raiswell R (1991) Pyrite formation and fossil preservation. In: Allison PA, Briggs DEG (eds) Taphonomy, vol 9. Plenum Press, New York, pp 338–387

Canfield DE, Raiswell R, Bottrell SH (1992) The reactivity of sedimentary iron minerals towards sulfide. Am J Sci 292:659–683

Canfield DE, Jorgensen BB, Fossing H, Glud RN, Gundersen JK, Ramsing NB, Thamdrup B, Hansen JW, Nielsen LP, Hall, POJ (1993) Pathways of organic carbon oxidation in three continental margin sediments. Mar Geol 113: 27–40

Cavanaugh CM, Levering PR, Maki JS, Mitchell R, Lidstrom MS (1987) Symbiosis of methylotrophic bacteria and deep-sea mussels. Nature 325:346–348

Coleman ML, Hedrick DB, Loveley DR, White DC, Pye K (1993) Reduction of Fe(III) in sediments by sulfate reducing bacteria. Nature 261:436–438

De Leeuw JW, Frewin NL, Van Bergen PF, Sinninghe Damsté JS, Collinson ME (1995) Organic carbon as a palaeoenvironmental indicator in the marine realm. In: Bosence DWJ, Allison PA (eds) Marine palaeoenvironmental analysis from fossils. Geol Soc Spec Publ 83:43–71

De Zwaan A, (1991) Molluscs. In: Bryant C (ed) Metazoan life without oxygen. Chapman and Hall, London, pp 186–217

Demaison GJ, Moore GT (1980) Anoxic environments and oil source bed genesis. AAPG Bull 64:1179–1209

Dickman M, Artuz I (1978) Mass mortality of photosynthetic bacteria as a mechanism for dark lamina formation in sediments of the Black Sea. Nature 275:191–195

Fisher CR (1990) Chemoautotrophic and methanotrophic symbiosis in marine invertebrates. Rev Aquat Sci 2:399–436

Fisher IS, Hudson JD (1987) Pyrite formation in Jurassic shales of contrasting biofacies. In: Fleet A, Brooks J (eds) Marine petroleum source rocks. Geol Soc Spec Pub 26:69–78

Fossing H, Gallardo VA, Jorgensen BB, Hüttel M, Nielsen LP, Schulz H, Canfield DE, Forster S, Glud RN, Gundersen JK, Küver J, Ramsing NB, Teske A, Thamdrup B, Ulloa O (1995) Concentration and transport of nitrate by the mat-forming sulfur bacterium *Thioploca*. Nature 374:713–715

Gaillard C, Rio M, Rolin Y (1992): Fossil chemosynthetic communities related to vents or seeps in sedimentary basins: the pseudobioherms of southeastern France compared to other world examples. Palaios 7:451–465

Hartgers A, Sinninghe Damsté JS, Requejo AG, Allan J, Hayes JM, de Leeuw JW (1994) Evidence for only minor contributions from bacteria to sedimentary organic carbon. Nature 369:224–226

Hashimoto J, Ohta S, Tanaka T, Hotta H, Matsuzawa S, Sakai H (1989) Deep-sea communities dominated by the giant clam *Calyptogena soyoae* along the slope foot of Hatsushima Island, Sagami Bay, central Japan. Palaeogeo Palaeoclimat Palaeoecol 71:179–192

Holmer M, Kristensen E (1996) Seasonality of sulfate reduction and pore water solutes in a marine fish farm sediment: The importance of temperature and sedimentary organic matter. Biogeochemistry 32:15–39

Hovland M (1992) Hydrocarbon seeps in northern marine waters – their occurrence and effects. Palaios 7:376–382

Hudson JD (1982) Pyrite in ammonite-bearing shales from the Jurassic of England and Germany. Sedimentology 29:639–667

Kenig F, Sinninghe Damsté JS, Frewin NL, Hayes JM, de Leeuw JW (1995) Molecular indicators for palaeoenvironmental change in a Messinian evaporitic sequence (Vena del Gesso, Italy). II. High-resolution variations in abundances and C contents of free and sulfur-bound carbon skeletons in a single marl bed. Organic Geochem 23:485–526

Kauffman EG, Arthur MA, Howe B, Scholle PA (1996) Widespread venting of methane-rich fluids in the Late Cretaceous (Campanian) submarine springs (Tepee Buttes), Western Interior seaway, USA. Geology 24:799–802

Lammers S, Suess E, Hovland M (1995) A large methane plume east of Bear Island (Barents Sea); implications for the marine methane cycle. Geol Rundsch 84:59–66

Leventhal JS (1987) Carbon and sulfur relationship in Devonian shales from the Appalachian Basin as indicator of environment of deposition. Am J Sci 287:33–49

Loveley DR, Roden EE, Phillips EJP, Woodward JC (1993) Encymatic iron and uranium reduction by sulfate-reducing bacteria. Mar Geol 113:41–53

Machel HG, Krouse HR, Sassen R (1995) Products and distinguishing criteria of bacterial and thermochemical sulfate reduction. Appl Geochem 10:373–389

Oschmann W (1988) Kimmeridge Clay sedimentation. A new cyclic model. Palaeogeo Palaeoclimat Palaeoecol 65:217–251

Oschmann W (1990) Environmental cycles in the late Jurassic northwestern European epeiric basin: interaction with atmospheric and hydrospheric circulations. In: Aigner T, Dott RH (eds) Sedimentary geology, vol 69. Elsevier, Amsterdam, pp 217–251

Oschmann W (1994) Adaptive pathways of benthic organisms in marine oxygen-controlled environments. N Jahrb Geol Paläont Abh 191:393–444

Ourisson and Albrecht (1992) Hopanoids. 1. Geohopanoids: the most abundant natural products on earth? Acc Chem Res 25:398–402

Ourisson and Rohmer (1992) Hopanoids. 2. Biohopanoids: a novel class of bacterial lipids. Acc Chem Res 25:403–408

Parkes RJ, Cragg BA, Getliff JM, Harvey SM, Fry JC, Lewis CA, Rowland SJ (1993) A quantitative study of microbial decomposition of biopolymers in recent sediments from Peru margin. Mar Geol 113:55–66.

Raiswell R, Berner RA (1985) Pyrite formation in euxinic and semi-euxinic sediments. Am J Sci 285:711–724

Rajendran N, Matsuda O (1995) Fatty acid analysis to determine the seasonal variation in microbial biomass and its community structure of coastal sediments. J Fac Appl Biol Scien Hiroshima Univ 34: 21–32

Ramsing NB, Fossing H, Ferdelman TG, Andersen F, Thamdrup B (1996) Distribution of bacterial populations in a stratified Fjord (Mariager Fjord, Denmark) quantified by in situ hybridization and related to chemical gradients in the water column. Appl Environ Microbiol 62:1391–1404

Richter G (1994) Bacteria and bacterial like structures from the oil-shale of Messel. Kaupia 4:21–28

Roux M, Rio M, Fatton E, Marien G, Pachiaudi C (1983) Taux de croissance des grands lamellibranches et reconstitution de l'activité hydrothermale à 21 °N (dorsale du Pacifique oriental) enregistrée par la coquille pendant 5 années. CR Acad Sci 297:495–500

Savrda CE, Bottjer DJ, Seilacher A (1991) Redox-related benthic events. In: Einsele G, Ricken W, Seilacher A (eds) Cycles and events in stratigraphy. Springer, Berlin Heidelber, New York, pp 524–541

Schein E, Roux M, Barbin V, Chiesi F, Renard M, Rio M (1991) Enregistrement des paramètres écologiques par la coquille des bivalves: approche pluridisciplinaire. Bull Soc Géol Fr 162:687–698

Schlegel HG (1993) General microbiology. Cambridge University Press, Cambridge

Schmitz M, Ernst K (1994) Microspheroidal objects within the Eocene Messel Formation (Messel Oilshale Pit/Germany). Kaupia 4: 13–19

Seilacher A (1990) Aberrations in bivalve evolution related to photo- and chemosymbiosis. Historical Biol 3:289–311

Sinninghe Damsté JS, Kenig F, Koopmans MP, Köster J, Schouten S, Hayes JM, de Leeuw JW (1995) Evidence for gammacerane as an indicator of water column stratification. Geochim Cosmochim Acta 59:1895–1900

Stach E, Mackowsky M-Th, Teichmüller M, Taylor GH, Chandra D, Teichmüller E (eds) (1982) Coal petrology. Borntraeger, Stuttgart

Sweerts JPRA, De Beer D, Nielsen LP, Verdouw H, Van den Heuvel JC, Cohen Y, Cappenberg TE (1990) Denitrification by sulfur oxidizing *Beggiatoa* spp. mats on freshwater sediments. Nature (Lond) 344:762–763

Tissot B, Welte DH (1978) Petroleum formation and occurrence. Springer, Berlin Heidelberg New York

Van Dover CL (1995) Ecology of Mid-Atlantic ridge hydrothermal vents. In: Parson LM, Walker CL, Dixon DR (eds) Hydrothermal vents and processes. Geol Soc Spec Publ 87:257–294

Von Gemerden H (1993) Microbial mats; a joint venture. Parkes RJ, Westbroek P, de Leeuw JW (eds) Marine geology, vol 113. Elsevier, Amsterdam, pp 3–25

Vetter RD, Powell MA, Somero GN (1991) Metazoan adaptations to hydrogen sulfide. In: Bryant C (ed) Metazoan life without oxygen. Chapman and Hall, London, pp 109–128

Organic and Biogeochemical Patterns in Cryptic Microbialites

Joachim Reitner[1], Volker Thiel[2], Heinrich Zankl[3], Walter Michaelis[2], Gert Wörheide[1], Pascale Gautret[4]

[1] Institut und Museum für Geologie und Paläontologie, Universität Göttingen, Goldschmidtstr. 3, D-37077 Göttingen, Germany
[2] Institut für Biogeochemie und Meereschemie, Universität Hamburg, Bundesstr. 55, D-20146 Hamburg, Germany
[3] Institut für Geologie, Universität Marburg, Lahnberge, D-35043 Marburg, Germany
[4] Institut de Paléontologie, Université de Paris, 11-Orsay Bat. 505, F-91405 Orsay Cedex, France

Abstract. Cryptic non-cyanobacterial microbialites from reef caves at Lizard Island (Great Barrier Reef, Australia) and the Salt River Canyon, St.Croix (US Virgin Islands) exhibit very distinctive organic patterns. The Lizard Island microbialites consist of various types of automicrite. The biofacies is mainly characterized by highly diverse biofilms, foraminifers, sponges, brachiopods, and bryozoans. Biomarker characteristics of various microbes and sponges (e.g. demosponge acids and mid-chain branched, monomethylalkanoic acids) support histological observations. The microbialite sequence exhibits a light-decreasing facies succession – in this particular case a transgressive sequence with an age of ~3500 years B.P. Macromolecular analyses of the automicrites reveal an excess of acidic macromolecules, which are a feature of calcifying systems. Microbialites from the Salt River Canyon consist of peloids and thin automicritic layers (calcified biofilms) and also exhibit a light-decreasing sequence. The peloids are automicrites that are formed in acidic mucilage in the presence of bacterial remains and mucus. Biomarkers indicate a significant input of terrestrial plant remains and autochthonous heterotrophic bacteria, particularly anoxygenic ones. Sponge and other metazoan biomarkers were not observed in microbialites of the Salt River Canyon. In neither case cyanobacteria were noted, neither in histological sections nor by using biochemical methods.

1 Introduction

Microbialites are organosedimentary deposits which are formed under the control of various benthic microbial biofilms, organic matter degrading microorganisms, benthic metazoan communities, free organic matter, and sediment trapping (e.g. Burne and Moore 1987; Reitner 1993; Reitner et al. 1995a,b; Reitner and Neuweiler 1995). Most microbialites so far investigated consist of carbonate minerals (Mg calcite, aragonite). Marine microbialites are common structures in cryptic niches of reef complexes and are commonly linked to continental-silica weathering influx (Reitner 1993). Comparable occurrences have been described by Marshall (1983, 1986) and Webb (1996) from the Great Barrier Reef, Macintyre (1977, 1978, 1984, 1985) and Zankl (1993) from the Caribbean, Brachert and Dullo (1991) from deep water in the Red Sea, and Montaggioni and Camoin (1993) from Tahiti.

This chapter describes and summarizes the automicrite types observed in sea caves at Lizard Island and St. Croix, using diverse biochemical, histochemical and organic geochemical approaches. The automicrite concept (e.g. formation via organic matrices) may help to explain the formation of significant amounts of microcrystalline calcite (micrite) and related products in so-called mud mounds, extinct fossil micritic reefs mostly associated with filter feeding, benthic, metazoan sponge communities.

2 Localities

Studies in the northern Great Barrier Reef were carried out at fringing reefs at Lizard Island, Queensland, and adjacent outer ribbon reefs. Two reef caves were selected for investigation: at the southeast corner of the island (South Island reef cave (LIZ), 6 – 9 m water depth), and at the northeast fringing reefs (Bommie Bay reef cave (BB) 10 m water depth). In the ribbon reefs, studies focused on Hicks Reef, Hilder Reef, and Ribbon Reef No. 10 in water depths between 5 and 35 m (Fig. 1a). Samples from St. Croix (US Virgin Islands) were collected from a cave of the Salt River Canyon in a water depth of approximately 25 m on the northern side of the island (Fig. 1b).

3 Methods

Immediately after collection, samples were fixed in a sodium cacodylate-buffered, 4% glutaraldehyde solution in sea water for 24 h, washed in filtered sea water, taken through ascending ethanol concentrations, and stored in 70% ethanol. Selected microbialite specimens were stained with Ca^{2+}-chelating fluorochromes (calcein, Na_2-calcein, achromycin-HCl, and chlorotetracycline-HCl) and alizarin complexion. The fluorochroming with Ca^{2+}-chelating complexes permits investigation of growth rates and loci of the calcification fronts (see Reitner 1993; Reitner et al. 1995). Additionally, the microbialites were stained with fluorochrome acridine orange to locate microbes, thiacine red to mark sponge tissues, and also with non-fluorochroming dyes such as pure basic fuchsin, methylene blue, and toluidine blue O. All specimens studied were embedded in araldite or Epon and cut with a hardpart microtome. Samples for

R.E. Riding and S.M. Awramik (Eds.)
Microbial Sediments

transmission electron microscopy (TEM) and scanning electron microscopy (SEM) were post-fixed with a 2% OsO_4 solution. For TEM the specimens were first decalcified with EDTA and then desilicified in 5% HF. Samples for SEM were not demineralized and were dried after dehydration with 100% ethanol with PELDRI II (Plano). Backscatter analyses, energy dispersive X-ray analysis (EDX) mapping and spot analyses were done on polished surfaces.

Biochemical analyses of the intraskeletal and crystalline matrices of the microbialites were carried out on air-dried and freeze-dried specimens. Molecular weights, charges, amino acids, and elementary sugar compositions were analyzed, together with hydrocarbons. After 6 N HCl hydrolysis (24 h in 110 °C, in free air sealed tubes) and phenyl-isothiocyanate (PITC) derivatization, proteinaceous substances were detected by reverse phase chromatography using a HPLC-Beckman system (Na-phosphate buffer with a nonlinear gradient of acetonitrile) and a 5 µm-C18 Nucleosil column. The carbohydrate components were hydrolyzed with 2 N TFA (4 h in 110 °C) and the proteins removed. Sugar analyses were performed by a HPAE (high performance anion exchange) DIONEX system using pulsed amperometric detection (PAD) of polar compounds dissolved in a pH 12 buffer (Reitner et al. 1995).

Comparative biomarker investigations were performed on subrecent microbialites. Prior to solvent extraction, the upper horizons were removed mechanically to a depth of ~1 cm. The samples were cleaned by washing with diluted HCl and acetone. Subsequently, the carbonate matrix of each sample was slowly removed by dropwise addition of 6 N HCl. The dried residues were saponified by stirring in 6% KOH/methanol, and further extracted with a dichloromethane/methanol mixture (3 : 1; v : v). Hydrocarbons and carboxylic acids were separated from the total organic extracts by silica gel column chromatography. Further analyses were carried out by gas chromatography (GC) and combined gas chromatography/mass spectrometry (GC-MS), as described by Hefter et al. (1993).

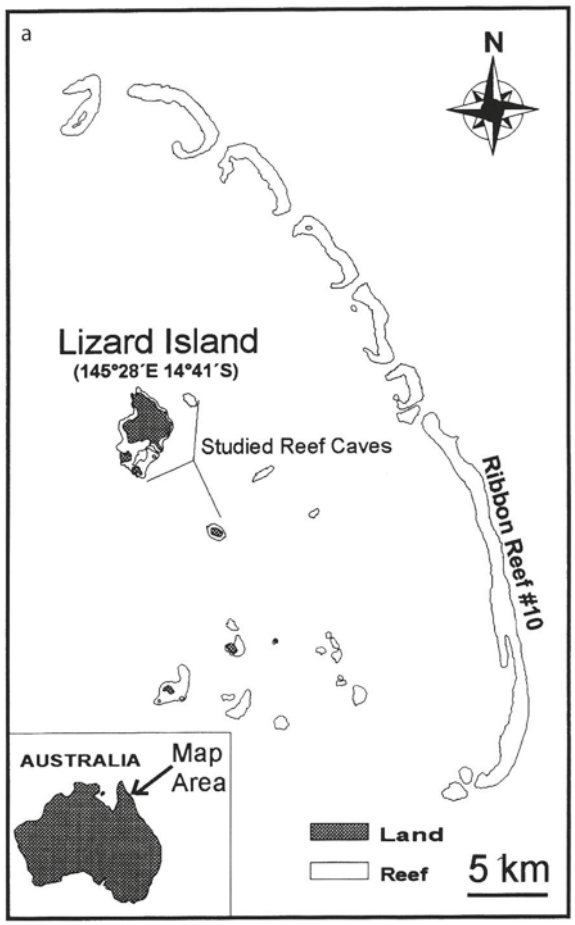

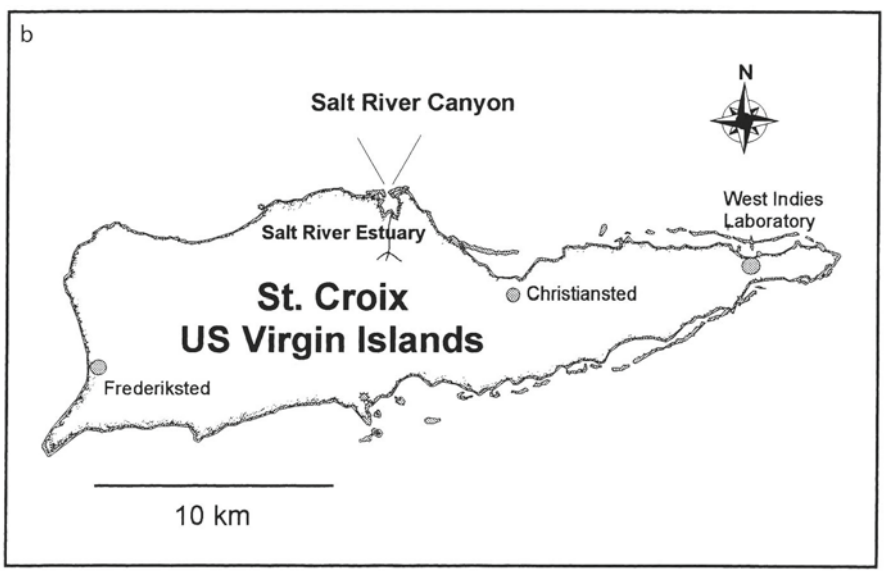

Fig. 1. Sample localities at **a** Lizard Island and **b** St. Croix

4
Lizard Island Biofilm/Metazoan Microbialites

Lizard Island is a small granitic island surrounded by narrow fringing reefs in the northern Great Barrier Reef, east of Cooktown. The reefs contain many small reef caves which all demonstrate the same facies patterns and ecological distribution of benthic organisms. In contrast to the reefs of the outer barrier, the reefs of Lizard Island have well developed thrombolitic microbialites.

4.1
Horizontal Reef Cave Zonation

In all the shallow water reef caves investigated (water depths 5–15 m, entire length 6–14 m), four main facies zones could be distinguished:

Zone 1: Actively growing corals, and light intensities between 600 and 2000 lx at noon time
Zone 2: Thick crusts of coralline red algae and reduced light conditions (5–100 lx)
Zone 3: Thrombolitic microbialites, abundant rapidly growing epifauna (e.g. thin sponges crusts), increased sedimentation rates, and thick biofilms, in more or less dark conditions (1–4 lx)
Zone 4: Hardground-type microbialites formed under reduced sedimentation rates, mainly comprising very slowly growing, coralline sponges, e.g. *Spirastrella (Acanthochaetetes) wellsi, Astrosclera willeyana, Stromatospongia micronesica*, associated with thecidean brachiopods, serpulids, bryozoans, hydrocorals, ahermatypic corals, various sessile foraminifers, many ferromanganese microbial crusts, and very thin biofilms, all formed under dark conditions (0–1 lx)

The microbialites investigated show two distinctive types: (1) Microbialites on upward facing surfaces are characterized by small (~1–3 cm), irregular thrombolitic pillars which are often orientated in the direction of the main water current and inclined towards the cave entrances. The upper surface is often dominated by baffling organisms such as branching hydrozoans, serpulids, bryozoans, foraminifers, and sponges. (2) Microbialites on downward facing surfaces are developed beneath protruding reef rocks and on cave ceilings. These surfaces are flat except for protruding organisms. Very little sediment is trapped by the biofilms. Normally these surfaces are dark gray or brown and are covered by either microbial biofilms or thin sponge crusts. This sediment protected niche is dominated by slow-growing organisms such as coralline sponges, boring sponges (*Aka, Clinoa*), brachiopods, crustose bryozoans, and serpulids.

4.2
Vertical Structure of the Microbialites

All observed microbialites exhibit a distinct vertical facies succession (Figs. 2a, 3), commencing with a coral-gal facies followed by a prominent crust of various coralline red algae alternating with zooxanthellate deeper water corals (e.g. *Leptoseris*). Both these basal biofacies correspond with zones 1 and 2 of the horizontal community succession in the cave. The coralline red algae facies is replaced by micritic carbonates which exhibit *an "Acanthochaetetes"* community dominated by calcified coralline sponges (*Spirastrella [Acanthochaetetes] wellsi, Astrosclera willeyana, Stromatospongia micronesica*, etc.), foraminifers (*Homotrema, Planorbulina, Carpenteria, Acervolina,* etc.), serpulids, and brachiopods. The micrites are strongly bored by sponges (*Cliona, Aka*) and lithophage bivalves forming small cavities.

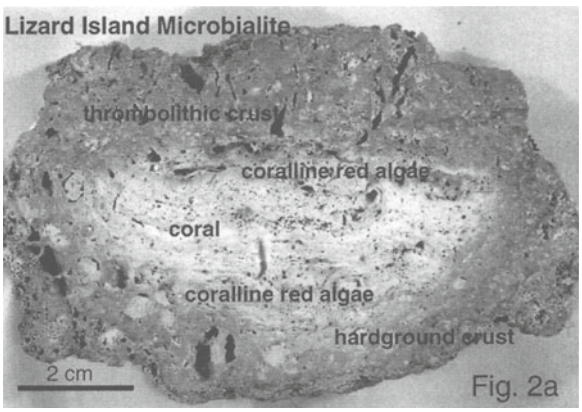

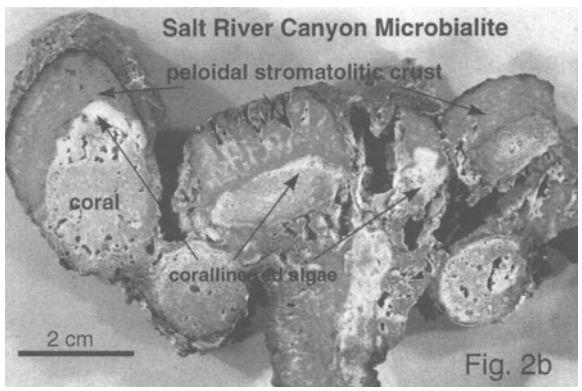

Fig. 2.a Vertical section of Lizard Island microbialite from Bommie Bay reef cave (zone 4, 15 m water depth). At the *top*, a thrombolitic crust is developed due to relatively high sedimentation rates. In the *lower portion*, the microbialite sequence is represented by a hardground crust constructed of Fe/Mn biofilms which cause strong electrochemical dissolution. This facies is developed on ceilings and is thus protected from sediment influx. **b** Vertical section of a St. Croix microbialite from Salt River Canyon, characterized by dark gray stromatolitic and thrombolitic microfabrics. The entire microbialite succession is comparable with Lizard Island microbialites except for the hardground facies present in Lizard Island

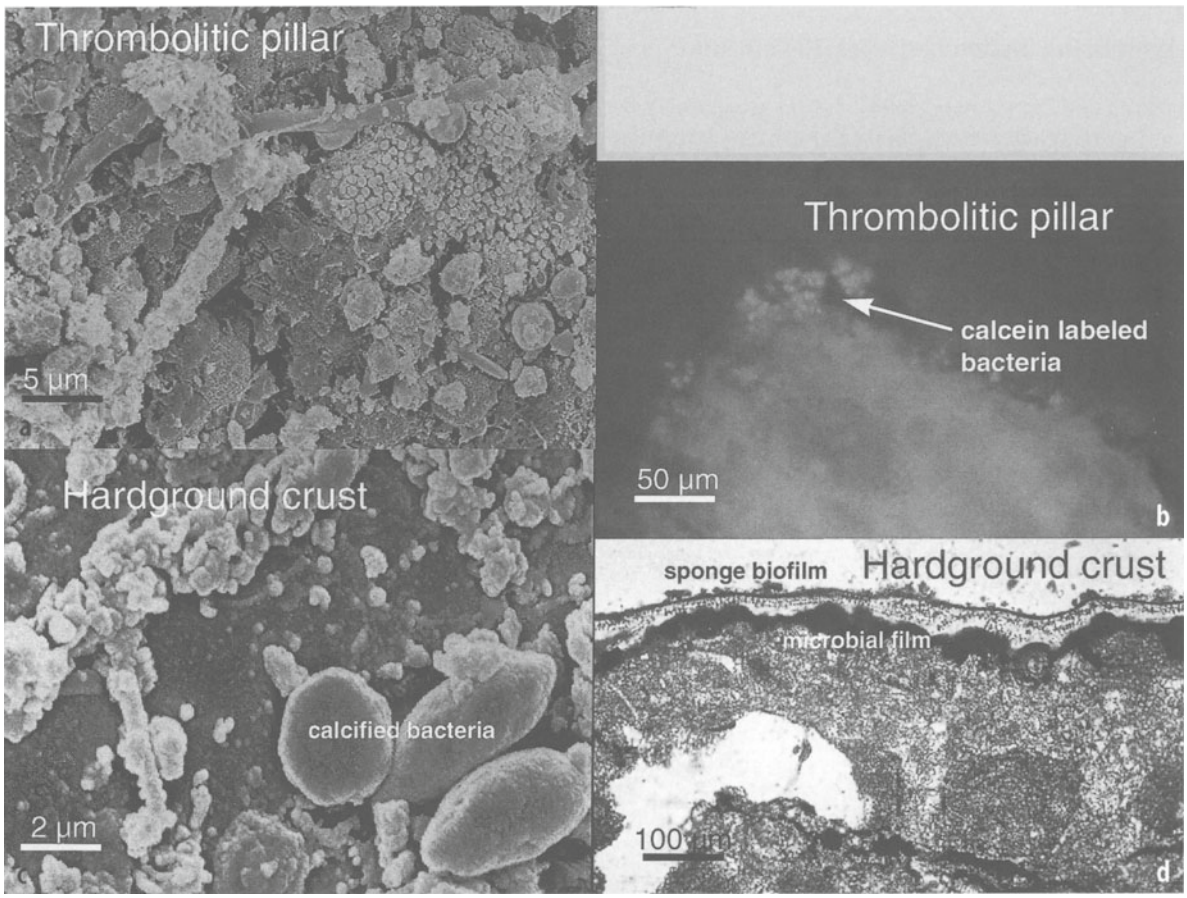

Fig. 3a–d. Biofilms on thrombolitic pillars and hardgrounds at Lizard Island. **a** On thrombolitic pillars the biofilms are relatively thick (50–150 µm) and the diversity of microorganisms is high. **b** Often a mixture of filamentous and coccoid bacteria is observed (no cyanobacteria!); both exhibit calcification. Calcifying microbes were stained with calcein a fluorochrome, which is used to detect calcification fronts. **c** The hardground crust biofilms are thinner (10–50 µm) than the biofilms in the pillars and are often associated with thin sponge or coralline sponges **d**. Rods of calcified bacteria are common

The vertical facies succession of the microbialites demonstrates a light-decreasing development during prograding reef growth, which means that the oldest portions are dominated by algae and corals and the youngest portions are characterized by light-independent organisms. The age of the crusts is ~3500 years (AMS^{14}C). Horizontal and vertical successions are more or less similar and prove a diachronic facies development caused by horizontal and vertical reef growth (Fig. 3).

4.3 Calcifying Soluble and Insoluble Matrices Within Microcavities and Pocket-Like Structures

None of the investigated microbialites shows clear horizontal laminae, as observed in true stromatolites. They are constructed of irregular pocket structures (IPS) or microcavities, less than 1 cm in size, which are delimited and surrounded by brownish Fe/Mn biofilms, short fibrous Mg calcite cements, or by truncation surfaces linked to changes in the textural character of the pocket filling caused by the boring activity of sponges. The IPS and microcavities exhibit different generations of growth and maturity grades, depending on the amount of organic matter. They are filled with organic mucus which traps and binds fine-grained detrital material. Histological investigation revealed significant amounts of acidic proteins and polysaccharides. All observed immature IPS exhibit similar staining behavior when stained with toluidine blue O, the intensity of staining depending upon the grade of mineralization. Young IPS with acidic organic mucilage and packstone fabrics are semidurable and exhibit a strong blue color. Under crossed nicols they exhibit few mineralization events. Completely mineralized portions do not stain. The newly formed micrite is honey brown. Fluorescent dyes were used to locate the calcification fronts. The specimens were injected with Ca^{2+}-chelates (tetracyclines, calcein) in vivo. Using these dyes, it was possible

to recognize the loci of calcification fronts in statu nascendi. The acidic proteins, glycoproteins, and proteoglycans have a strong affinity to bind and trap divalent cations, especially Ca^{2+}. They concentrate these ions and, within the basophilic mucilages (soluble matrices), seed nuclei of different Ca-salts grow. The fluorochromes chelate Ca^{2+} ions on the surfaces of the very small seed crystals or trap free Ca^{2+} ions. Tetracyclines were the most successful ones. The mineralizing process takes place via Ca^{2+}-binding macromolecules which are rich in acidic amino acids (Asp 19.2 mol%, Glu 12.8 mol%) (EDTA soluble matrices), and common insoluble matrices are mostly dislocated collagenous fibers (Hypro 4–6 mol%). This mineralization is a typical, irregular, matrix-mediated calcification process without any control by organisms. Carbonate alkalinity in the reef cave water is slightly increased (2.6 meq/l) in comparison with the ambient sea water (2.2 meq/l). Total alkalinity in decaying reef cave sponges is believed to be largely a result of heavy sulfate reduction (8 meq/l). Increased values (4–6 meq/l) were also measured in small, organic mucus-rich, closed cavities of the microbialites from zone 3. Stable isotope data clearly show mineralization close to the expected equilibrium of ambient seawater (Reitner 1993; Reitner et al. 1995a,b).

4.4 Biofilms and Microorganisms

Various biofilms are observed on the microbialite surfaces and the bioactivity is visible using fluorochromes in vivo and in fixed material (Fig. 4). Calcifying bacteria were detected with tetracyclines and non-calcifying ones with toluidine blue O, acridine orange and thiacine red. Fe/Mn mineralizing bacteria, which exhibit a strong fluorescence using calcein (UV), are very common. All the biofilms observed are a system of bacteria and fungi, sometimes with protozoans such as foraminifers. Algae are never observed within the dark environments. The basal films are thin, only 10–12 µm thick. The interfaces of the basal and liquid films have not yet been extensively studied. Many different, often stalked, microorganisms and fungal hyphae present on the surface films are combined with the interior surface

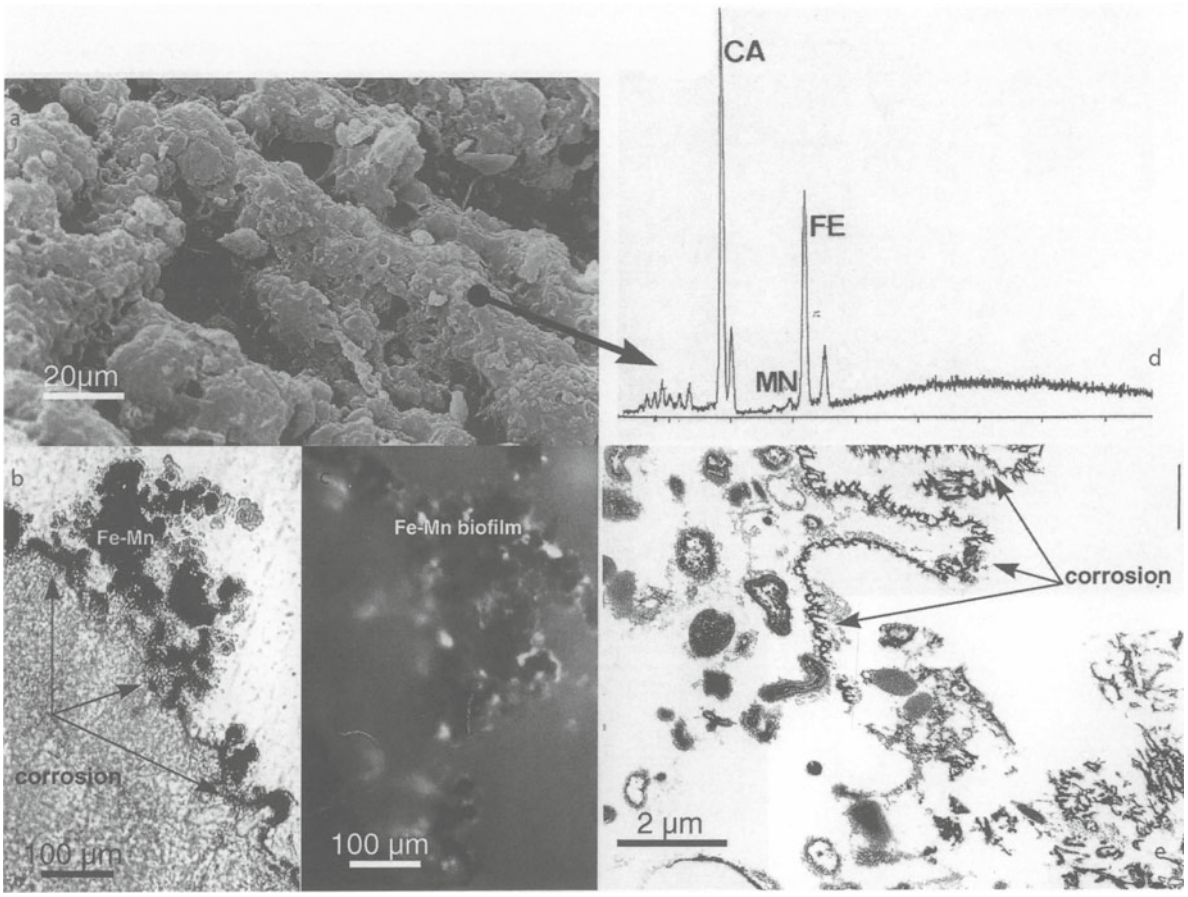

Fig. 4a–e. In zone 4, Fe/Mn biofilms are common which are important for subaquatic electrochemical corrosion. This corrosion process controls hardground formation. **a** The surface structure of Fe/Mn biofilms (SEM). **b** Fe/Mn biofilm showing the corrosion patterns. **c** The calcein stained living biofilm exhibits a strong fluorescence which indicates enrichment in Ca^{2+}. **d** EDX analysis showing dominance of Fe versus Mn. **e** TEM image of the boundary layer between the Fe/Mn biofilm and the calcified substrate

layer. Some of the microbes on the surface layer were primarily enriched in the overlying liquid phase. The surface films sometimes have small (1 µm) openings resembling sponge ostias. The biofilms exhibit strong EPS (exopolymer substances) networks which control the microbialite formation. Within the basal parts of some biofilms, special types of calcified bacteria and filamentous structures were observed. Normally they occur in rosette-like aggregates. Broken examples are hollow and the cavity is covered by an organic phragma which may be the remains of the murein sheet. Calcified filamentous structures are common and play a significant role in the microbialites of zone 3. The filaments are not related to cyanobacteria, and have diameters between 4 and 15 µm. No traces of thylakoid membranes were observed in TEM sections. The calcifying microbes observed do not play a significant role in microbialite formation but the activity of the biofilms may control the transport of calcifying organic substances to the microcavities underneath the biofilms via the EPS systems. The particle trapping ability of the basal parts *of* the biofilms is a likely explanation for the formation of the thrombolitic pillars of the microbialites in zone 3. The basal films can be mineralized, because the main microbial activity occurs there. Basal films are firm mucus layers with abundant EDTA insoluble substances, and decaying basal films have a strong ability to mineralize, as detected by Ca^{2+}-binding fluorochromes. All observed microbialites exhibit numerous brown to blackish brown films, are more or less horizontally oriented, and display a pseudo-stromatolitic structure. They are present on nearly all inner surfaces of microcavities and also on some areas of the upper surfaces of the microbialites. EDAX and X-ray diffraction (XRD) analyses have shown that light brown crusts are rich in Fe (goethite) and the darker ones have a significant amount of Mn (Mn oxides) (Fig. 5). They are also enriched in clay minerals. The surfaces of the Fe/Mn crusts are extremely irregular and sometimes form grape-like structures. High magnifications show lumpy aggregates of 2–5 µm spherical elements. Using calcein stained specimens, the surface of the lumpy aggregates fluoresces strongly under UV-light. This fluorescence indicates a strong metabolic activity under the presence of divalent cations, and the microbes are seen in TEM sections as well as under SEM. Videla (1989) de-

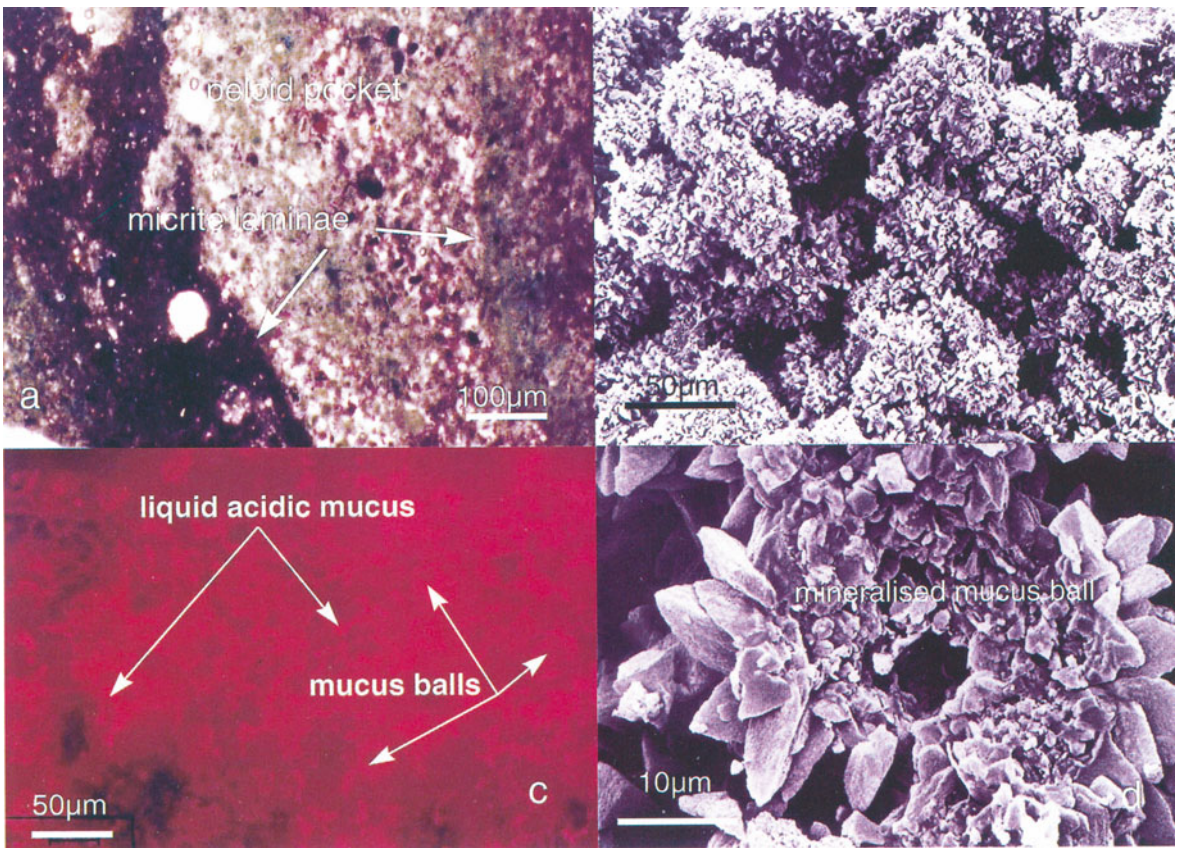

Fig. 5a–d. The Salt River Canyon microbialite is mainly formed by peloids which are a product of organomineralization. **a** Acidic organic mucus is enriched in small container-like pockets or pores. The containers are closed by micrite laminae. **b** SEM micrograph of peloids. **c** Peloids growing in liquid acidic organic mucus. Mucus balls are "swimming" in the liquid phase; autofluorescence (nm). **d** Detailed SEM micrograph of a mineralized mucus ball (peloid)

scribes the principal processes of microbiological corrosion, which explains the dissolution phenomena observed. Corrosion is an electrochemical process characteristic of all except noble metals, caused by the flow of electrons from one metal to another if an electrolyte is present. Dissolution (corrosion) occurs at the anode, and electrons are consumed at the cathode. An important cathodic reaction in aerated solutions close to pH 7 is oxygen reduction. The metal biofilms, the underlying calcium carbonate crusts, and the sea water are a natural electrochemical cell. The calcium carbonate crusts and the biofilms have anode and cathode functions, respectively. Videla (1989) observed colloidal, hydrated, iron oxide spheres as a corrosion product after settlement of marine *Vibrio* bacteria on steel. These goethite spherules are very similar to those in the brownish crusts and may also be interpreted as a corrosion product at the cathode. Calcium carbonate corrosion increases the alkalinity and may support calcification in closely related microcavities and thin underlying areas, despite their electrochemical dissolution. This may explain the extremely slow growth of the microbialite.

4.5
Role of Sponges and Sponge Tissue Diagenesis

The hardground-type microbialites are intensively bored by sponges, mainly by *Aka* cf. *coralliphaga*, which forms larger cavities from 1–10 mm in size. Different types of *Cliona* (e.g. *C.* cf. *viridis*) produce smaller cavities often arranged like rows of pearls. The boreholes are occupied by the boring sponges themselves, or by a secondary settlement of sponges, mainly poecilosclerids, hymedesmiid demosponges, and axinellids, but never by coralline sponges or Calcarea. In many cases the sponge tissues exhibit a different staining behavior from intensively red to brownish red when basic fuchsin is used. The boreholes are often separated by intensively stained organic phragmas that separate living from dead parts of the sponge. The phragmas are normally penetrated by the spicules of the sponge, which indicate that the dead portion is related to the sponge. The living cells of the sponge tissue exhibit normal fuchsin red staining, whereas the dead portions are stained dark brownish red. Under crossed nicols, these portions exhibit a strong birefringence of newly formed calcite crystals. The sponge tissue is degraded into an irregular lumpy structure. These lumps become mineralized in the same manner as observed during peloid formation. Using thiacine staining dyes such as methylene blue and toluidine blue O, the decayed organic matter is stained dirty blue and exhibits a strongly basophilic behavior. The calcifying soluble matrix is extremely enriched in sulfated organic matter (proteoglycans, glycoproteins) which concentrate Ca^{2+} ions. An important source for Ca^{2+} ions in this particular case are lysing cells of the sponges and bacteria. The decaying proteins support a further calcification process via ammonification (Berner 1968). The bacterial community in sponges was recently studied by Schumann-Kindel et al. (1997) and Reitner and Schumann-Kindel (1997). Determinations based on in situ hybridization have shown the presence of numerous sulfate-reducing bacteria (*Desulfobacter*-group) which increase alkalinity during early decay of the sponge tissue. Many sponge related automicrites bear pyrite clusters, indicating the role of anaerobic sulfate-reducing bacteria.

5
St. Croix Peloidal Microbialites of the Salt River Canyon

St. Croix is one of the US Virgin Islands and is geologically characterized by a metamorphic basement nucleus. St. Croix is larger than Lizard Island, small rivers form estuaries and canyons, and fringing reefs are better developed. Microbialitic crusts comparable with those from Lizard Island occur in caves in the fringing reefs (Zankl 1993).

The Salt River locations differ from those at Lizard Island in several respects. The water depth is 25 m in a low energy environment. The cave investigated had temporarily been closed and was reopened when a large block slid downslope. The history of the cave can be reconstructed from its sediments. In the first stage, coarse *Acropora cervicornis* coral rubble was piled up under an overhang, and the loosely packed pieces were coated by thick crusts of red algae and foraminifers under reduced light conditions. Light penetration and water turbulence were drastically reduced when the cave was subsequently closed, either by lateral framework growth or by a block barring the entrance. During this stage, rough laminated microbialites 2–3 cm thick grew on the upper side of the coral fragments, but apparently no benthic skeletal organisms grew on the crusts. After reopening of the cave, a benthic community of serpulids and bryozoans started to settle on the microbialite hardground. Finally, red algae recolonized, indicating improving light conditions. At present, this history of carbonate accretion is buried under fine reef sediment preventing erosion.

5.1
Microbialite Microfabrics

Within the crusts on the *Acropora cervicornis* debris there is a distinct boundary between the first encrusting benthic community of red algae and foraminifers and the subsequent micritic carbonate cap (Fig. 2b). Each cap is composed of closely spaced laminated pillars which grew vertically on the upper sides of the for-

algal-encrusted coral fragments. The pillars look like millimeter-sized erect stromatolites. The weakly developed lamination is only pronounced in some more densely lithified laminae. The sediment particles are coated by cryptocrystalline rims. Growth forms and sediment trapping indicate a calm environment within the caves, and fine sediment particles were only trapped on the upper surfaces of the crusts. The microbial mucus bound sediment particles and favored carbonate crystallization. Both processes are responsible for the stromatolitic growth observed under the restricted conditions of a closed reef cave. During microbialite growth, there was almost no skeletal encrustation, and mineralization recommenced once microbialite formation terminated. The microbialites consist of in situ formed peloids (peloidal automicrites) and thin automicritic horizontal laminae (Chafetz 1986; Reitner 1993; Reitner et al. 1995a, b; Reitner and Neuweiler 1995). The laminae form flat pockets in which the peloids grew. These laminae are the lithified basal layers of the biofilms. Acidic organic mucus is enriched within the flat pockets and exhibits a 20–50 µm grape-like structure. These mucus balls are "swimming" in a more liquid mucilage and demonstrate strong epifluorescence when stained with acridine orange, suggesting the presence of highly degraded microbial organic substances. The mucus matrix exhibits a strong tetracycline-induced fluorescence which is explained by high Ca^{2+} concentrations. In some cases, the mucus balls are composed of dead bacteria. Mineralization commences in the mucus balls, forming very small, anhedral Mg calcites (100 nm). Organic remains are often preserved in the core of the peloids. Short, fibrous, high-Mg calcite crystals grew on the micrite core, controlled by the Ca^{2+} enriched liquid mucilage. The pocket environment was probably anaerobic (see biomarker analyses). As a result of this process, peloidal stromatolites were created which are common in many Neoproterozoic and Phanerozoic microbialites. In addition to the authigenic carbonates, allochthonous material (terrestrial organic remains, clay minerals) derived from the Salt River is trapped on the surface of the biofilms. Metazoans are rare and sponges are never observed.

Illumination seems to be critical for the transition from algal- to microbial-dominated encrustation. Above a certain illumination threshold, crustose algae can outgrow the microbialites. Martindale (1992) found that the illumination limit for crustose coralline algae in semicryptic habitats in shallow water at Bellaires, Barbados, was reached at 25% of the near surface values. In the South Shore reefs of St. Croix, algae appear to tolerate lower levels of illumination, and replacement by microbial crusts occurs at 10% of maximum values measured at 5 m depth. Coralline algae may, therefore, push the limits for growth of microbial crusts further into cryptic habitats. In a core drilled into a Holocene high-energy reef at Tahiti, Montaggioni and Camoin (1993) found a sequence of coral framework encrusted by coralline algal communities that are overgrown by 5-cm-thick stromatolitic crusts of microbialites. The isotopic compositions of the microbialites measured by Montaggioni and Camoin (1993; $\delta^{18}O$, 0.0 to −1.0‰, and $\delta^{13}C$ 3.5 and 4.5‰), are in exactly the same ranges as those of the microbialites at St. Croix. These values indicate precipitation of $CaCO_3$ nearly in equilibrium with the ambient sea water (Reitner 1993). The biologic influence on the isotopic composition of the precipitated carbonates is weak and may be restricted to calcification processes directly controlled by microbes. Andrews et al (1993, 1997) have shown that freshwater cyanobacteria from various places in Europe mineralize close to the equilibrium of the ambient lake and river waters. They have suggested a weak isotopic fractionation by microenvironmental photosynthetic processes of the microorganisms. However, the amount of calcifying microorganisms within the studied marine microbialites is very low and the suggested stable isotope fractionation is negligible. The automicrites are a product of a very slow growing, nonenzymatic organomineralization which explains the heavy carbon isotope values (Reitner et al. 1995a). McConnaughey (1989) has shown that fast growing calcium carbonate minerals should have light $\delta^{13}C$ values (+1–+2). The enrichment of the heavy ones is a characteristic kinetic fractionation. Most of the biologically controlled carbonates are in disequilibrium due to enzymatic fractionation (e.g. via carbonic anhydrase), recognizable in the measured coralgal facies of the microbialite succession.

Riding et al. (1991) have described more or less stromatolitic crusts from *Porites* corals forming Upper Miocene (Messinian) reefs from southern Spain (Almeria). These Mg calcitic crusts exhibit a strong coincidence with the microfabrics observed within the Salt River Canyon. The *Porites* corals are overgrown by coralline algae and sessile foraminifers and roughly laminated peloidal crusts. Within the peloidal crusts sessile foraminifers are also present. Some of the crusts exhibit a digitate growth pattern. The large irregular and poorly sorted peloids described are comparable with those of the Salt River Canyon. Riding et al. (1991) have suggested that the observed bushy growth fabrics are linked with cyanobacteria and that they therefore have an important role during crust formation. Similar fabrics were observed within the Salt River Canyon crusts but without any cyanobacterial growth control. The spaces between the *Porites* corals are cryptic, light-depleted niches. An aphotic environment and light-depleting facies development of the Messinian peloidal microbialites, as seen in the Salt River Canyon situation, could also be possible.

6
Comparative Biomarker Investigations of Lizard Island and St. Croix Microbialites

Gas chromatograms of the total hydrocarbon and carboxylic acid fractions are shown in Fig. 6. Each peak represents an individual compound and peak areas are directly proportional to the concentrations of the respective components. Variations in the occurrence and the relative abundance of these compounds signify the roles of different sources of organic matter contributing to the respective facies types (Fig. 6).

6.1
Hydrocarbons

The hydrocarbon patterns of microbialites from both locations reveal smooth distributions of short-chain n-alkanes with chain lengths from 16 to 22 carbon atoms. Such patterns are generally attributed to autochthonous aquatic sources – usually marine algae. They are typically found in sediments in which a pronounced activity of heterotrophic bacteria is observed, e.g. in aphotic microbialites from Cebu Island (Reitner et al. 1996), or the deeper sections of phototrophic microbial mats (e.g. Dobson et al. 1988). In both samples studied, a strong imprint of heterotrophic organic matter decomposition is further indicated by the significant peak of an unresolved, complex hydrocarbon mixture (UCM; e.g. Grimalt et al. 1987; Sassen et al. 1994). A distinctive feature of the peloidal microbialite from St. Croix is the presence of a second n-alkane distribution in the high molecular weight range from C_{25} to C_{39}. The observed pattern obviously results from an interference of a smooth n-alkane series maximizing in n-C_{28} with a second suite of homologues showing a marked

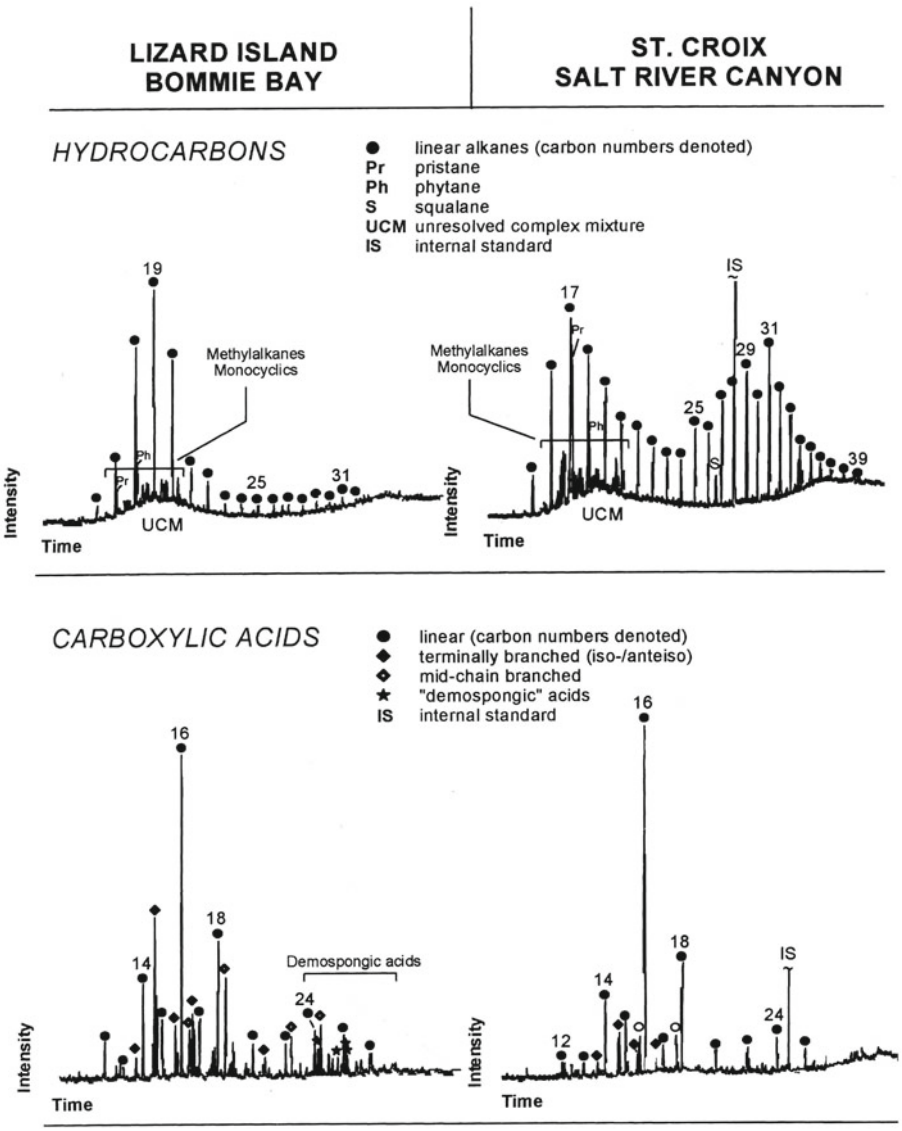

Fig. 6. Gas chromatograms of the total hydrocarbons (*top*) and the carboxylic acids (methyl ester derivatives; *bottom*) extracted from Lizard and St. Croix microbialites

preference of carbon odd-numbered homologues (n-C_{29}, n-C_{31}). Smooth distributions of long-chain n-alkanes have often been reported from anoxygenic bacteria (e.g. Han and Calvin 1969; Shiea et al. 1991). Long-chain n-alkanes with carbon odd-number preferences are generally believed to derive from terrigenous organic matter, since they occur as major constituents in the waxes of vascular plants (Eglinton and Hamilton 1967; Tissot and Welte 1984). Their occurrence in the St. Croix microbialites is indicative of incorporation of higher plant derived and, thus allochthonous, organic matter.

6.2 Carboxylic Acids

Linear alkanoic acids with 12–26 carbon atoms comprise 50 and 82% of the total carboxylic acid fractions in the Lizard and St. Croix microbialites, respectively. They are characterized by abundant, straight chain, even-numbered alkanoic acids, especially $C_{16:0}$ (palmitic acid) and $C_{18:0}$ (stearic acid). Unsaturated acids of this type are of minor quantitative importance and mainly consist of mono-unsaturated C_{16} and C_{18} homologues. All these compounds are generally attributed to marine autochthonous sources. Due to their ubiquitous occurrence in marine organisms (including bacteria, algae, and animals), it is, however, difficult to recognize their origins in the particular samples studied.

Significant amounts of terminally branched (iso- and anteiso-) alkanoic acids are present in both samples and comprise 23% (Lizard Island) and 13% (St. Croix) of the total carboxylic acid fractions. In both microbialites, i/ai-C_{15} and i/ai-C_{17} are found as the predominant homologues. These compounds are common constituents of various bacteria (e.g. Kaneda 1967; Edlund et al. 1985; Goossens et al. 1986), but appear to be absent from cyanobacterial lipids (e.g. Cohen and Vonshak 1991). According to their widespread distribution, they are frequently found in modern and fossil, marine and lacustrine sediments (Cranwell 1974; Tissot and Welte 1984) and in naturally grown bacterial mats (e.g. Zeng et al. 1992). Their presence as major compounds in the Lizard Island and St. Croix microbialites indicates a significant contribution of organic matter derived from their component anoxygenic bacteria.

A remarkable difference between the carboxylic acid patterns of the investigated microbialites is the occurrence of distinctive, long-chain, unsaturated homologues in the carbonate from the Lizard Island reef caves. Since the early studies by C. Litchfield and coworkers, several investigations have proven the presence of these acids in a variety of sponges, all of which are members of the Demospongiae (e.g. Litchfield et al. 1976; Lawson et al. 1988). Other groups of organisms apparently lack these characteristic compounds, which have thus been introduced as "demospongic acids" in the literature. Another unique feature of the Lizard microbialites is the abundant presence of mid-chain, branched monomethylalkanoic acids. These compounds account for 18% of the total carboxylic acid fraction. Careful investigation of their mass spectrometry properties led to the characterization of an intriguing variety of structural isomers (methyl groups at the w5–w9 positions) over a wide range of carbon chain lengths (C_{14}–C_{24}). Until now, such suites of mid-chain, branched alkanoic acids have been found exclusively in demosponges and can be attributed to the lipids of their specific bacterial symbionts (Thiel 1997). Both demospongic acids and mid-chain branched alkanoic acids represent specific chemofossils for sponges and their associated microorganisms. These biomarkers distinctively differentiate the Lizard Island microbialites from the St. Croix samples at the molecular level and strongly support the constructive role of a sponge-microbial biocommunity in the formation of this particular facies type.

7 Conclusions

1. Cryptic microbialites from Lizard Island reef caves exhibit a distinctive vertical facies succession from light-dominated environments (coralgal biofacies) to light-independent biota (coralline sponges). Microbialite growth started before ~3500 years B.P. It is possible to distinguish a thrombolitic top facies and hardground ceiling facies. The latter is characterized by abundant Fe/Mn biofilm layers which cause a very strong electrochemical dissolution. In addition to biofilm related microbes, bacteria-rich sponges play a central role in the formation of the microbialite carbonate. The Lizard Island microbialites are characterized by various types of automicrites such as aphanitic micrite, sponge related minipeloids, peloids in pores and lithified biofilms.
2. Biochemical characteristics of the Lizard Island microbialites show enrichment of acidic macromolecules (Asp- and Glu-rich proteins, glycoproteins, and polysaccharides) which control the initial calcification. Characteristic biomarkers are demosponge acids and mid-chain, branched monomethylalkanoic acids derived from symbiontic bacteria in sponges.
3. The rough, layered stromatolitic microbialites from the Salt River Canyon of St. Croix (US Virgin Islands) generally also exhibit an illumination dependent, light-decreasing facies development. The succession starts with corals, followed by coralline red algae, and finally microbialite. A change of light conditions is marked by red algal overgrowth. The microbialite is formed by thin, horizontal micritic laminae and numerous peloids which grow between the

laminae. Clay minerals and allochthonous debris are bound and fixed onto the laminae. The peloids are formed within a very acidic organic mucus which filled spaces between the laminae. Sometimes remains of bacterial sheets are visible. Metazoans are extremely rare (serpulids) and sponges are never observed.

4. A distinctive feature of the peloidal microbialite from St. Croix is the presence of a second n-alkane distribution in the high molecular weight range from C_{25} to C_{39}. Smooth distributions of long-chain n-alkanes are typical of anoxygenic bacteria. Long-chain n-alkanes with odd carbon-number preferences are generally believed to derive from terrigenous organic matter. Their occurrence in the St. Croix microbialite is indicative of incorporation of higher plant derived and, thus allochthonous, organic matter. This feature was not observed in Lizard Island microbialites. Characteristic sponge biomarkers such as demosponge acids and mid-chain, branched monomethylalkanoic acids were not observed in Salt River Canyon microbialites.
5. In samples studied from both locations, a strong imprint of heterotrophic organic matter decomposition is further indicated by a significant peak of an unresolved complex hydrocarbon mixture (UCM). Lizard Island and St. Croix microbialites indicate a significant contribution of organic matter derived from their component anoxygenic bacteria.

Acknowledgements. We thank the co-directors, Drs. L. Vail and A. Hogget, at Lizard Island Research Station, for extensive help and support. The investigations were permitted by the Great Barrier Reef Marine Park Authority (G92/041, G93/046, G93/133, G95/70, G94/098, G95/071, G96/025). The Deutsche Forschungsgemeinschaft is greatly acknowledged for financial support (Re 665/4-1/2/3, Re 665/8-1/2, Re 655/12-1 Leibniz Award - Evolution of Multicellular Systems and Organomineralisation EMSO, Mi 157/10-5, -6, Za 22/31-1/2). This chapter is a contribution to IGCP Project 380 "Biosedimentology of Microbial Buildups", and SFB 468 "Wechselwirkungen an geologischen Grenzflächen" No. 5.

References

Andrews JE, Riding R, Dennis PF (1993) Stable isotopic composition of Recent freshwater cyanobacterial carbonates from the British Isles: local and regional environmental controls. Sedimentology 40:303-314

Andrews JE, Riding R, Dennis PF (1997) The stable isotope record of environmental and climatic signals in modern terrestial microbial carbonates from Europe. Palaegeogr Palaeoclimatol Palaeoecol 129:171-189

Berner RA (1968) Calcium carbonate concretions formed by the decomposition of organic matter. Science 159:195-197

Burne RV, Moore LS (1987) Microbialites: organosedimentary deposits of benthic microbial communities. Palaios 2:241-254

Chafetz HS (1986) Marine peloids: a product of bacterially induced precipitation of calcite. J Sed Petrol 56:812-817

Cohen Z, Vonshak A (1991) Fatty acid composition of Spirulina and Spirulina-like cyanobacteria in relation to their chemotaxonomy. Phytochemistry 30:205-206

Cranwell PA (1974) Monocarboxylic acids in lake sediments: indicators, derived from terrestrial and aquatic biota, of palaeoenvironmental trophic levels. Chem Geol 14:1-14

Dobson G, Ward DM, Robinson N, Eglinton G (1988) Biogeochemistry of hot spring environments: extractable lipids of a cyanobacterial mat. Chem Geol 68:155-179

Edlund A, Nichols PD, Roffey R, White DC (1985) Extractable and lipopolysaccharide fatty acid and hydroxy acid profiles from *Desulfovibrio* species. J Lipid Res 26:982-988

Eglinton G, Hamilton RJ (1967) Leaf epicuticular waxes. Science 156:1322-1335

Goosens H, Rijpstra WIC, Düren RR, De Leeuw J-W, Schenck PA (1986) Bacterial contribution to sedimentary organic matter; a comparative study of lipid moieties in bacteria and recent sediments. Org Geochem 10:683-696

Grimalt JO, Torras E, Albaigés J (1987) Bacterial reworking of sedimentary lipids during sampling storage. Org Geochem 13:741-746

Han J, Calvin M (1969) Hydrocarbon distribution of algae and bacteria and microbiological activity in sediments. Proc Natl Acad Sci USA 64:436-443

Hefter J, Thiel V, Jenisch A, Galling U, Kempe S, Michaelis W (1993) Biomarker indications for microbial contribution to Recent and Late Jurassic carbonate deposits. Facies 29:93-106

Kaneda T (1967) Fatty acids in the genus *Bacillus*. Iso- and anteiso-fatty acids as characteristic constituents of lipids in 10 species. J Bacteriol 93:894-903

Lawson MP, Thompson JE, and Djerassi C (1988) Cell membrane localization of long chain C_{24}-C_{30} fatty acids in two marine demosponges. Lipids 23:741-749

Litchfield C, Greenberg, A J, Noto G, Morales RW (1976) Unusually high levels of C_{24}-C_{30} fatty acids in sponges of the class Demospongiae. Lipids 11:567-570

Macintyre IG (1977) Distribution of submarine cements in a modern Caribbean fringing reef, Galeta Point, Panama. J Sed Petrol 47:503-516

Macintyre IG (1978) Reply: Distribution of submarine cements in a modern Caribbean fringing reef, Galeta Point, Panama. J Sed Petrol 48:669-670

Macintyre IG (1984) Extensive submarine lithification in a cave in the Belize Barrier Reef Platform. J Sed Petrol 54:11-25

Macintyre IG (1985) Submarine Cements - the peoidal question. In: Schneidermann N, Harris PM (eds) Carbonate cements. SEPM Spec Publ 36:109-115

Marshall JF (1983) Submarine cementation in a high-energy platform reef: One Tree Reef, southern Great Barrier Reef. J Sed Petrol 53:1133-1149

Marshall JF (1986) Regional distribution of submarine cements within a epicontinental reef system: central Great Barrier Reef, Australia. In: Schroeder JH, Purser BH (eds) Reef diagenesis. Springer, Berlin Heidelberg New York, pp 8-26

Martindale W (1992) Calcified epibionts as palaeoecological tools: examples from the Recent and Pleistocene of Barbados. Coral Reefs 11:167-177

Montaggioni LF, Camoin GF (1993) Stromatolites associated with coralgal communities in Holocene high-energy reefs. Geology 21:149-152

McConnaughey T (1989) 13 C and 18 O isotopic disequilibrium in biological carbonates. II. In vitro simulation of kinetic effects. Geochim Cosmochim Acta 53:163-171

Reitner J (1993) Modern cryptic microbialite/metazoan facies from Lizard Island (Great Barrier Reef, Australia). Formation and Concepts. Facies 29:3-39

Reitner J, Neuweiler F (coord) (1995) Mud Mounds: a polygenetic spectrum of fine-grained carbonate buildups. Facies 32:1-70

Reitner J, Gautret P, Marin F, Neuweiler F (1995a) Automicrites in a modern marine microbialite. Formation model via organic matrices (Lizard Island, Great Barrier Reef, Australia). Bull Inst Océanogr Monaco No Spec 14 (2):237-263

Reitner J, Neuweiler F, Gautret P (1995b) Modern and fossil Automicrites: implications for mud mound genesis. In: Reitner J, Neuweiler F (coord) Mud mounds: a polygenetic spectrum of fine-grained carbonate buildups. Facies 32:4-17

Reitner J, Schumann-Kindel G (1997) Pyrite in mineralised sponge

tissue – product of sulfate reducing sponge-related bacteria? In: Neuweiler F, Reitner J, Monty C (eds) Biosedimentology of microbial buildups. IGCP Project No 380, Proceedings of 2nd Meeting. Facies 36:272 – 276

Riding R, Martin JM, Braga JC (1991) Coral-stromatolite reef framework, Upper Miocene, Almería, Spain. Sedimentology 38:799 – 818

Sassen R, MacDonald IR, Requejo AG, Guinasso NL Jr, Kennicutt MC II, Sweet ST, Brooks JM (1994) Organic geochemistry of sediments from chemosynthetic communities, Gulf of Mexico slope. Geo-Mar Lett 14:110 – 119

Shiea J, Brassel SC, Ward DM (1991) Comparative analysis of extractable lipids in hot spring microbial mats and their component photosynthetic bacteria. Org Geochem 17:309 – 319

Schumann-Kindel G, Bergbauer M, Manz W, Szewzyk U, Reitner J (1997) Aerobic and anaerobic microorganisms in modern sponges: a possible relationship to fossilisation processes. In: Neuweiler F, Reitner J, Monty C (eds) Biosedimentology of microbial buildups. IGCP Project No 380, Proceedings of 2nd Meeting. Facies 36:268 – 272

Thiel V (1997) Organische Verbindungen in Porifera und biogenen Carbonaten – Fazies, Chemotaxonomie und molekulare Fossilien. PhD Thesis, Univ Hamburg

Tissot BP, Welte DH (1984) Petroleum formation and occurrence. Springer, Berlin Heidelberg New York

Videla HA (1989) Metal dissolution/redox in biofilms. In: Characklis WG, Wilderer PA (eds) Structure and function of biofilms. Dahlem Konferenzen, John Wiley, Chichester, pp 301 – 320

Webb GE (1996) Was Phanerozoic history controlled by the distribution of non-enzymatically-secreted carbonates (microbial carbonate and biologically-induced cement)? Sedimentology 43:947 – 971

Wilderer PA, Characklis WG (1989) Structure and function of biofilms. In: Characklis WG, Wilderer PA (eds) Structure and function of biofilms. Dahlem Konferenzen, John Wiley, Chichester, pp 5 – 17,

Zankl H (1993) The origin of high-Mg calcite microbialites in cryptic habitates of Caribbean coral reefs – their dependence in light and turbulence. Facies 29:55 – 59

Zeng YB, Ward DM, Brassell SC, Eglinton G (1992) Biogeochemistry of hot spring environments 3. Apolar and polar lipids in the biologically active layers of a cyanobacterial mat. Chem Geol 95:347 – 360

Subaerial Microbial Mats and Their Effects on Soil and Rock

Anna A. Gorbushina[1], Wolfgang E. Krumbein[2]

[1] Institute of Biology, St Petersburg State University, Stary Peterhof, Russia
[2] Geomicrobiology, ICBM, Carl von Ossietzky Universität Oldenburg, P.O. Box 2503, D-26111 Oldenburg, Germany

Abstract. Microbial mats (or biofilms) under permanent water cover contain 95–98% biologically stabilised water at ambient temperature, while biofilms in atmospheric environments can be regarded as the maximum biomass maintaining metabolic potential in the presence of the minimum amount of water. Rock or other subaerial biofilms are made up primarily of poikilotroph micro-organisms which thrive on the lowest water activity possible. Biofilms on and in rocks are the main factors in rock decay and the production of patinas, films, varnishes, crusts and stromatolites growing on and in rocks. A poikilotroph microflora is instrumental in maintaining life in truly extreme conditions and over considerable periods of time. The importance of the activity of the rock-dwelling biota and biofilms can be explained in terms of the fractal dimension of the reactive surface of sediment and rock with water and atmosphere, respectively. The weight of the living (mainly microbial) biomass of the planet is recalculated to be 10^{21} g instead of 10^{17} g, by including estimates of deep sedimentary and deep rock microbial biospheres. Poikilotroph biofilms under subaerial conditions are involved in both rock-destroying and rock-forming processes.

1 Introduction

In this chapter we deal with microbial growth structures on and in rock surfaces. Microbial participation in the complex relationships of soils and rock surfaces involve subaquatic and subaerial biofilms and microbial mats. Microbial sediment very often represents something that is growing upward ("Aufwuchs"). On its way upward, the biofilm community often meets and embeds particles coming down or tumbling along the surface. Other particles are generated within the microbial system by biomineralisation processes. The same complexity is evident with erosion and weardown processes on air-exposed soil and rock surfaces. Erosion is usually regarded as the mechanical weardown of rock. Chemical attack and dissolution is often called corrosion. Microbial erosion or corrosion have not been defined in the literature. Krumbein and Dyer (1985), however, suggested terms such as biotransfer, biocorrosion and bioerosion, when biological processes are involved as a mediating, catalysing or direct force.

Useful terms in discussing the interaction of rock surfaces, microbes and the atmosphere are "constructive and destructive biokarst" (Viles 1984; Wang Fuxing 1993). Other terms in use for microbially mediated rock surface changes are biogenic rock varnish, crust, caliche, calcrete, desert stromatolite, microstromatolite, and lichen stromatolite, to name but a few (Klappa 1979; Krumbein and Giele 1979). Most calcareous surface structures, especially in Mediterranean-type environments for example, are microbially mediated carbonate accretions.

In contrast to subaquatic biofilms and microbialites, subaerial ones at first sight appear to be a rather marginal phenomenon. Generally it is assumed that 70% of the Earth is covered by water and 30% is land. Thus most (bio-) sedimentary rocks are expected to form under water-cover. However, simple physical and geomorphological assumptions and fractal equations justify the conclusion that the "reactive surface area" (RSA) for microbe/atmosphere and microbe/water interactions should be reconsidered. Intertidal sedimentary surfaces, as well as deep sea biofilms, are relatively smooth, fine-grained flat areas, whereas rock and soil on the scale of the microbial environment exhibit far greater relief. The RSA of the continents (rock, soil) as compared to the aquatic RSA (under standing and flowing water) of the globe may be about 10,000:1 (rock/soil exposed to atmosphere, as compared to sediment exposed to the hydrosphere/atmosphere). Thus, biofilms and microbial mats of the subaerial exposure type may be much more important for the exogenic cycle than subaquatic ones. They actually represent the highest RSA, or skin, of our planet. Microbial exchange of energy and gases across this "membrane" can be regarded in a parahistological sense (Wachendörfer et al. 1994), in the same way as the exchange of gases and dissolved minerals through membranes or tissues bordering an organism.

Hutton (1788) and Krumbein (1996) assumed that reactive surfaces and biogeomorphogenetic processes (Viles 1984) in the interplay of atmosphere, water, rock, energy (or sun) and mineral compounds have to be considered on the scale of microbes or, as Hutton placed it, on a scale of global physiology, which at his time was synonymous with physics. We have calculated the living biomass of the planet as being 10^{21} g. The macroscopically visible organisms (ordinary plants and animals) however, make up a maximum of 10^{17} g

R.E. Riding and S.M. Awramik (Eds.)
Microbial Sediments

(Lide 1993). The life history (physical, chemical, geometrical and physiological) of any interaction between rock and atmosphere thus, in a global sense, has to be measured and calculated at the scale of the "niche" of the microbe. This niche can be crowded with the awesome sum of 10^{11} individuals per 1 cm^3. On this basis, and even respecting the roughness factor of oceanic floors and waves, fractal physics tells us that the interactive space/time microbe-rock-atmosphere relationship is to be regarded as about 10,000 times more frequent than the interactive microbe-water-atmosphere relationship (Krumbein 1995). The subaerial or pore space biofilm on a global scale is thus expected to have a higher photosynthetic, chemosynthetic and respiratory potential than the subaquatic one. This, in turn, would include the potential of new approaches to the reservoirs and fluxes of, e.g., carbon, oxygen and water on a global scale. The latter have so far been regarded more or less as sedimentary processes rather than as geomorphological ones.

2 The Subaerial Environment, Microbiota Within, and Their Products

2.1 Living Rocks

Beachrock, carbonate or iron oxide cemented intertidal sand or gravel, forming dipping concrete-like plates on the shore, can form biologically and continue to show metabolic activities in erosional and depositional cycles in relation to the physical shift of the coastline (Krumbein 1979). Elsewhere rocks are also "alive and well" (Friedman 1993); a concept that is well-accepted in reefs but to a lesser extent in biofilm generated and regulated rock surfaces. The number of micro-organisms encountered on all rock surfaces of the world is so high that the photosynthetic, respiratory and biomineralisation – as well as biocorrosion – activity of a living biofilm covering and coating external and internal rock surfaces can be measured using classical and modern physiological and biochemical techniques (Sterflinger et al. 1994). In this approach, the rock is regarded as a complex symbiotic community, as in the case of a coral reef (in this case, e.g., a lichen). The microflora living within the rock reaches a depth of 20 cm, and globally the pore- and fissure-colonising biofilms penetrate as deep as the geothermal gradient allows (120 °C or up to 4000 m depth within oceanic sediment and continental rocks and rock crevices).

The microbiota of these rocks exhibit different metabolic activities according to exposure to the sun, water availability (water activity), nutrient availability, and energy sources reaching the biofilm, mainly from the atmosphere but also from within the rocks that they live in. The metabolic rates are: (1) fast in intertidal and tropical rain forest areas, (2) peculiarly expressive in Mediterranean and dry arid zones, (3) slower, but marked, in temperate and cold arid zones, and (4) quite slow in sedimentary deposits under a 3 km water cover and an overburden of 500 m or more of sediment. The slow-down of metabolic processes naturally also applies to deep rock crevices under a cover of several hundred meters of rock overburden in the continental crust. However, evidence from drill-holes, mines and contact zones of intrusive granites with the surrounding sedimentary rocks (hydrothermal activity) shows the same peaks of metabolic activities as, for example, in a "black smoker" ecosystem of the Pacific compared with a "normal" Pacific bottom sediment. The ecology of the present-day sediment surface microbiota is well-separated from the so-called deep biosphere, i.e. the microbial systems growing deep in deep sea sediments. The same term (deep biosphere) can also be applied to the microbiota encountered in deep terrestrial drill-holes, and fissures and cracks in rocks. It has been established, e.g. by a Swiss programme on atomic waste disposal, that for each individual granite massif of the Swiss Alps investigated, a separate characteristic microflora was encountered in the circulating deep ground water (NAGRA, internal reports). The similarity of microbial biodiversity detected hints at connected water pathways; such an open environment would render these granites insecure for atomic waste disposal.

2.2 Subaerial vs Subaquatic Biofilms and Microbial Mats

Subaerial biofilms differ considerably from subaquatic biofilms. Many types of microbial mats and stromatolite-generating systems have been described embracing cyanobacteria-dominated systems as well as fungi- or bryozoa-dominated ones. Even very similar structures may exhibit entirely different microbial diversity at the molecular level. Shark Bay stromatolites, for example, may actually have been built by a combination of fungi, bacteria and bryozoa which trapped shells and sediment particles while they were bio-eroded and bio-corroded by cyanobacteria (Krumbein and Villbrandt 1994; Scholz 1996; Scholz and Krumbein 1996). On the other hand, microbial mats formed by *Microcoleus chthonoplastes* may form in intertidal zones around the globe as well as in the utterly different dry environments of the Negev and Mojave deserts. Despite the apparent similiarities of the organisms involved, the survival strategies of the micro-organisms in subaerial biofilms seem to be entirely different from those of subaquatic ones.

2.3
Microbial Wear-Down and Buildup of Rock Surfaces

Microbially catalysed or mediated wear-down or build-up of rocks can be 10,000 times faster than physical or chemical wear-down and build-up. This acceleration is brought about because the micro-organisms largely enhance the mechanical (physical) destruction of rocks (Dornieden 1997) or produce aggressive acids and chelating compounds (Braams 1992). Both microbial erosion and decohesion, and microbial corrosion, were demonstrated by field measurements and laboratory experiments in environments where microbes establish themselves efficiently and thus contribute to the processes. A comparison of biodestruction in the field with subsequent laboratory measurements was made, for example, by Sterflinger (1995). Microbial rock decay has been called biodeterioration or biotransfer (Krumbein and Dyer 1984), and biokarst (Viles 1984; Wang Fuxing 1993; Gorbushina et al. 1996a), or has been described under the term biogeomorphogenesis (Krumbein 1993). Biosedimentary processes are thus efficiently matched and linked to biodeteriorative ones.

2.4
Establishment and Diversity of Rock Micro-organisms

Microbes establish themselves in subaerial conditions virtually everywhere, including the coldest and hottest, the driest and wettest, and the physically and chemically most adverse conditions measurable on this planet. There are, however, two exceptions worth mentioning: (1) desert rocks in areas that have received less than 100 mm rainfall in the past 10 years, and (2) the interior of massive halite blocks in mines and salt diapirs. However, the microbial biomass in deep sea sediments, and deep in the rocks and rock crevices of the continental crust as well as in sub-oceanic basalt masses is considerable. It will rarely be below 1000 micro-organisms per gram of rock or sediment (Karl 1995; Wolf and Krumbein 1996). Humboldt (1793) was the first to point out that practically all underground rock surfaces in contact with water are populated by minute organisms. The deep biosphere is the new term for that part of deep sea sediments which is no longer influenced by energy and nutrient exchange with the overlying water body. Various types of microbiota live deep in marine and other sediments, as well as deep in rocks. Subsurface sediment and rock environments may exhibit a high biodiversity vertically and laterally in relation to interstitial nutrient solutions and gas diffusing through these systems. Biofilms growing within the pore space of sediments and rocks may be exposed to an aqueous as well as to a gas phase depending on the conditions prevailing. They may be aerobic or anaerobic. All major groups of micro-organisms (Archaea, bacteria, actinomycetes, fungi) have been reported to exist in such deeply buried environments, which may represent "the last huge untapped and unexplored portion of the biosphere" (Baross and Deming, in Karl 1995, p. 206). The deepest sea floor sediments have characteristics which may make them comparable even to deep continental rock environments in terms of compaction, cementation and circulating liquids and gases. Actually, subaqeous and subaerial in the sediment and rock pore space may be applied as co-existing terms. Thus, it may be more appropriate to distinguish subaqeous, subaerial, and interstitial biofilms. All three types initially grow in small rock crevices, on the surface and in small depressions, as well as on grains in the interstitial pore space (e.g. Krumbein and Jens 1981). At surface conditions, however, those micro-organisms will gradually take over which are best suited to attach to interfaces and to survive the hazards of atmospheric exposure. Which, then, are the types of organisms contributing to the biodiversity of such rock and sediment environments exposed mainly to a gaseous environment with liquid water being scarce, or where water activity is low for other reasons (salt concentration, boiling point, etc.)? An answer may lie in the so-called poikilotroph type of micro-organism that we have identified on rocks.

3
The Poikilotroph Principle

Extreme environments sometimes are misinterpreted as extremely hot, cold, salty or dry in comparison with the physiology and ecology of humankind. The environments in which any organism (including micro-organisms) really has severe adaptational problems actually exhibit extreme changes of the conditions for life maintenance, rather than permanently extremely high or extremely low values. Such environments are characterised by sudden, or slow but long-lasting, oscillating, episodic or sporadic changes in temperature, water availability, salinity pH, redox potential, gas concentration, and so on. The micro-organisms in such environments must develop special life and also survival strategies. The response pattern of several groups of micro-organisms to desert or desert-like conditions on and in rocks is similar, despite large differences in their taxonomic position. Examples come from true deserts (Namib, Mojave, Sinai) or from pseudo-deserts such as sun-exposed building surfaces (Krumbein 1966). Less information exists on the microflora of dry salt mines, deep buried ore deposits under rock cover, and other remote places (Hofmann 1989). The micro-organisms thriving and persisting routinely in such conditions have been termed poikilotrophs (Gorbushina et al. 1996b). Rock-inhabiting micro-organisms can be classified into three groups based on survival strategy.

When a rock surface is excavated or exposed by weardown to the atmosphere, it is initially characterised by either oligotroph communities (i.e. growing and metabolising slowly but steadily at low concentrations of energy sources, nutrients and water) or by copiotroph/eutroph life forms (i.e. growing and metabolising fast at high energy source, nutrient and water levels, but being forced into survival and escape strategies such as spores and conidia when the conditions on and in the rock change). Which community occurs initially depends on the initial levels of energy sources, nutrients and water supply. Prolonged absence of nutrients and energy sources with periodic or episodic supply of organics from the atmosphere or elsewhere, however, are characteristic of the subaerial rock environment, especially in desert regions. Extreme dryness, or low water activity, only rarely or sporadically interrupted by short periods of rain or other supplies of water, also characterise the rock surface. However, reduced energy and nutrient supply, as well as extremely low water activity and extreme temperature changes, also characterises hypersaline and hydrothermal environments, as well as many building and material surfaces. Once such an environment is established, the poikilotroph strategy will ultimately become dominant on and in the subaerial surface.

The poikilotroph micro-organism is characterised by generally slow growth, and dense and usually irregular node-like packages of cells of irregular shape. Specialised propagative or survival cells and structures are rarely, if ever, formed. On the contrary, each individual cell and cell cluster is equipped and structured to survive as a whole. In addition, irradiation-resistant pigmentation (dark to black), and high water storage potential through thick cell walls and extracellular polymeric substances (EPS) are frequent. Photosynthetic representatives (e.g. *Chroococcidiopsis*) grow at low levels of light and water activity. Chemo-organotrophic representatives (e.g. *Geodermatophilus, Monodyctis, Trimmatostroma, Coniosporium*) grow slowly by budding or similar types of division. They exhibit typical small and leathery, or even stone-like, micro-colonies. The latter can develop into braid-like structures or intertwined strands resembling macrohyphae, and not unlike the slime embedded bundles of another representative of the phototrophic poikilotroph type: *Microcoleus* sp. from desert soil and rock. Long-term maintenance of each individual cell, formed in one place for periods of time that reach 50 years or more, is a typical feature.

Micro-organisms dwelling on and in rock need to be able to maintain all cell material produced as long as possible. They have to be capable of surviving long periods of dormancy until conditions are favourable for photosynthesis or chemosynthesis. In many rock surface and deep environments, sufficient energy sources (including light), together with nutrients and water, are only occasionally available simultaneously. Thus, optimal conditions for life processes are rarely guaranteed in such environments. Poikilotroph microbe cells have an optimal volume:surface ratio (e.g. spherical yeast-like growth in fungi instead of hyphae development, as described by Cooke and Whipps 1993). This reduces the net rate of evaporation. The poikilotrophic organism is also characterised by a resistant cell wall with photoprotective pigments, and is well equipped with special coatings and envelopes to survive desiccation. These are usually made up of polysaccharides, in addition to proteins, fatty acids, and some very important macromolecules such as melanins, carotenes, lignin and lignin-related substances such as sporopollenins. The poikilotroph microbe channels energy and nutrients into polysaccharide production for the maintenance and accumulation of the layers of EPS. It produces compounds such as trehalose, a nonreducing disaccharide which, coupled with the synthesis of lipids with an elevated level of non-saturation, keeps phospholipids in a liquid-crystal phase (Schrödinger 1944; Potts 1994). Spherical cells of these organisms also help form compact spherical colonies, enabling them to reduce evaporation rate and other environmental hazards. This holds true even for fungi, whose normal growth pattern is different from spherical cell clusters. Such "microcolonial fungi" were described in desert varnish by Staley et al. (1982). When discovered simultaneously as plant and animal pathogens and on rock surfaces (Gorbushina et al. 1993), they were termed black yeasts or yeast-like fungi. These budding microcolony-forming fungi are typical examples of poikilotroph micro-organisms. Some pleurocapsalean cyanobacteria, the actinomycete *Geodermatophilus*, and other related genera (Frankiaceae and coryneforms) also belong to the new metabolic class detected mainly in the rock-biofilm environment (Eppard et al. 1996).

A typical pattern of poikilotroph micro-organisms and biofilms is the production of extracellular compounds such as sugars, exopolymers and polymerised pigments (carotenoids, melanins). Further biomineralisation (microbially mediated and precipitated minerals) is represented by organic and inorganic mineral types ranging from oxalates through carbonates to sulphates and silicates. Multilayered and multicoloured microbially stabilised chemical gradients occur in very thin but often multilayered systems. The resulting rock stromatolite or patina is usually more finely laminated than a marine stromatolite. The diversity of biologically formed minerals is even greater subaerially than subaqueously. Although glauconite (as a biogenic subaqueous product) has not yet been found in subaerial conditions, minerals such as forsterite, weddellite, whewellite, gypsum, and a large variety of iron, manganese and copper oxalates, oxides and hydroxides occur. Even

clay minerals, hydrocerussite (lead hydroxycarbonate), glushinskite, and humboldtine have been reported (Jones and Wilson 1986). The subaerial biomineralisation products of biofilms on air-exposed rocks thus seem even more diverse than those in the context of subaqueous biofilms and stromatolites. Patinas, rock varnishes, internal and external crusts, and desert or subaerial stromatolites and microstromatolites may develop, and under special conditions even form a variety of silicates usually known only from magmatic differentiation (Krumbein and Jens 1981; Rivadeneyra et al. 1985, 1994; Gorbushina et al. 1996a; Sterflinger et al. 1996).

Subaerial biofilms and microbial mats on and in rocks are active in biogeomorphogenetic processes at reaction rates 100–10,000 times faster than physicochemical ones would achieve (Schwartzman and Volk 1990, 1991). They create constructive (growth, "Aufwuchs") and destructive (wear-down, corrosion, erosion) biokarst structures (Viles 1984; Wang Fuxing 1993; Gorbushina et al. 1996a). Bio-erosion rates of 10 cm/100 years have been extrapolated from laboratory experiments with black yeasts (Sterflinger 1995).

4 Subaquatic vs Subaerial Biofilms and Microbial Mats

We subdivide microbial growth at interfaces into: (1) subaqeous, (2) subaerial, and (3) interstitial. In our understanding of the literature, more substantially developed, and especially multilayered, biofilms entrapping allochthonous materials and/or producing minerals within them are to be considered as microbial mats. Most work so far has been done on subaqueous and subaerial biofilms, while interstitial biofilms have received less attention so far.

4.1 Terminology

The term microbial mat was introduced by Doemel and Brock (1974). In the beginning the three terms "algal mat", "bacterial mat" and "microbial mat" were used simultaneously and not always discriminatively. Ludwig and Theobald (1852) mentioned carpets of protists building stable films in the running water of a spa in Bad Nauheim. Ooids forming within these microbial carpets were washed out as the carpets decayed or as water flow increased, and collected downstream in depressions as an oolite. Paracelsus (about 1538, quoted in Krumbein 1996 and in Potts 1996) called the mineral and rock creating biofilm a "living mucilago cementing the rock particles with time".

One is tempted to ask which of the terms is most appropriate to describe the subaerial rock microbiota? Biological crust and biological solution front (Krumbein 1969), lichen stromatolite/laminar calcrete (Klappa 1979), desert stromatolite (Krumbein and Giele 1979; Krumbein 1983), and biogenic patina (Krumbein 1993) have been used. Today, biopatina, rock biofilm, and rock microbial mat are regarded as general terms encompassing all types of microbial communities settling on and in subaerial rocks. What types of micro-organisms are then typically found in subaerial and/or subaquatic microbialites? Will the biodiversity be different? Invariably one will find cosmopolitan cyanobacteria such as *Microcoleus chthonoplastes* (Hofmann-Bang in Flora Danica 1813; Abeliovich, personal communication) and *Nostoc* sp. (Paracelsus, 1538; Potts 1996). Indeed, all types of micro-organism, – Archaea, eubacteria, coryneform bacteria, fungi, including yeasts, cyanobacteria, algae, Protozoa, and Protoctista exist in both subaerial and subaquatic environments (Mitchell and Shewan 1968; Gorbushina et al. 1993; Eppard et al. 1996; Krumbein et al. 1996; Roelleke et al. 1996). Even the species are often the same in subaquatic and subaerial biofilms, e.g. *Microcoleus chthonoplastes* as a desert crust forming species, or *Spirulina subsalsa and Arthrospira platense*, which we found on exposed glass and rock surfaces, and halophilic Archaea found in mural paintings in churches (Roelleke et al. 1996).

The word biofilm has been defined numerous times, e.g. Characklis and Marshall (1990), Krumbein (1987a,b, 1994) and Neu (1994). The average subaquatic biofilm can be regarded as microbially stabilised water; it can consist of more than 99% water. Subaerial biofilms, in contrast, can be regarded as a maximum of cell mass surviving at minimal concentrations and supply of water. The microbial communities living on and in subaerially exposed rocks have rarely been treated within the context of biofilm or microbial mat literature. Descriptions coming close to the topic are biofilms in porous media, such as sand or soil (Cunningham et al. 1990; Rivadaneyra et al. 1985, 1994), and biofilms or microbial mats that create desert stromatolites (Krumbein and Giele 1979; Friedman and Ocampo-Friedman 1984; Krumbein and Villbrandt 1994). Krumbein and Jens (1981) have described microbial films and endolithic intertwined and interconnected communities as the creators of biopitting, biochipping and exfoliation, as well as of thin mineral skins or rock varnishes sometimes exhibiting stromatolitic patterns. These stromatolite-like structures can be mono- and multilayered and reach thicknesses comparable to aquatic sinters or stromatolites (0.2–50 cm). The biomineralisation products may be carbonates of calcium, iron and manganese, oxides of iron and manganese, calcium phosphates and oxalates, and even biogenic gypsum and vaterite (Garcia-Valles et al. 1996: Gorbushina et al. 1996a,b). Observations of biogenic oxalate skins and other biogenerated minerals, such as microbially precipitated and structured gypsum, forsterite,

and even opal, have also been reported (Gorbushina et al. 1996a). Thus, at a first glance all possible characteristics of subaqueous biofilms also seem to be valid for subaerial ones. They create rocks, chemical gradients and diffusion barriers. They enclose and maintain chemical and physical conditions against overall physico-chemical surface gradients. They further exhibit biomorphogenetic features comparable to the "Aufwuchs" community of subaquatic stromatolites. When, however, a subaerial biofilm is studied more closely in terms of time/space relationships, it may be considered as the exact opposite of a subaqueous biofilm.

4.2 Description of Subaerial Biofilm Communities and Their Activities

1. Subaqueous biofilms consist of more than 99% microbially stabilised water where the extracellular material (EPS) is the main water storage system for the biofilm (Paracelsus 1538; Haeckel 1877; Krumbein 1984; Neu 1994).
2. In contrast, subaerial biofilms on exposed rock, soil or sand dune systems may contain less than 0.5% water and can be regarded as an extremely drought resistant accumulation of cell material together with large masses of highly specialised EPS, maintaining life in the presence of a minimum of water. Subaerial biofilms live and survive using the poikilotrophy principle, sometimes for more than 50 years in the absence of sufficient water potential or activity to allow for physiological processes and cell division (Ehrenberg, 1838; Krumbein and Jens 1981; DeWinder 1990; Gorbushina et al 1993, 1996a; Potts 1994; Neu 1996). We observed a sample of episodically flooded cataract crust from the upper Nile (comparable to A. von Humboldt's Orinoco cataract crusts) that had lain untouched in the rock collection of a geomorphologist who collected the rock specimen in 1955. Cultivation in 1996 showed that the biofilm flora was still alive, and it remains alive in the rock environment now in our collection drawer. Contamination of this sample with typical poikilotroph cyanobacteria and actinomycetes of desert environments was practically excluded in the environmental conditions of the collection cases in Würzburg and Oldenburg.

These highly drought resistant accumulations of cells, with a high potential for meristematic tissue-like adaptations or with a remarkable capacity for vegetative cell survival, are the true poikilotroph biofilm communities of dry subaerial surfaces. They usually do not form spores, akinetes or other propagative structures. However, they protect their vegetative cells with thick cell walls containing several types of photoprotective and drought resistant compounds, and accumulate EPS layers when dryness is the typical environmental condition. By the excretion of surface active compounds that regulate the water exchange potential, poikilotroph micro-organisms are capable of decreasing their water demand to the absolute minimum and can retain water better than any other water dependent living system. As a consequence, subaerial biofilm communities cannot be detected by methods of respirometry gas exchange measurements or enzyme tests unless activated by prolonged periods of wetness in a generally dry environment. They do not metabolise under normal conditions, in order to save water for future survival. This may also hold true for "deep biosphere" biofilms in the hot deep rock environment and not only for surficial rock biofilms of the geomorphogenetic environment.

In order to identify these subaerial rock-dwelling communities, one has to use petrographic methods, scanning electron microscopy (SEM), or ESEM (environmental SEM). Some examples of such poikilotroph biofilm communities are depicted in Figs. 1–6. Another feature of these poikilotroph micro-organisms is retarded or accelerated cell division. This leads to nanobacteria and nanobacterial phases in a life cycle extending sometimes over several decades. The state of suspended life or metabolic activity (dormancy) can theoretically last as long as that of freeze-dried cells. The possibility exists to prove experimentally that subaerial biofilms can survive periods of up to 500,000 years. If our theory is correct, then biofilms under the hafting of flint tools differ from those on the directly air-exposed surfaces tools dated at 0.5 Ma that were discarded by an out-of-Africa community in Israel, and we could prove such survival times of poikilotroph bacteria and fungi (Gorbushina et al. 1996b).

4.3 Examples of Subaerial Biofilms

The most impressive and well documented, although probably not the dominant, type of subaerial biofilm is represented by lichens (Fig. 1). Lichens are widespread synergistic communities of heterotrophic and phototrophic micro-organisms. The typical subaerial lichenic biofilm (locally creating lichen stromatolites) is the epilithic and endolithic crustose lichen film that covers surfaces of rocks, trees, house roofs, caves, etc. It thrives and metabolises in all regions of the world and is only outcompeted by specialised fungal, actinomycetal and bacterial biofilms.

A second example of subaerial biofilm is the distinctive community of mainly poikilotroph algae and cyanobacteria first described by O. Jaag (e.g. Jaag 1945) and later elegantly elaborated by Golubic (1967) under the name of "Tintenstrichflora" (ink-streak flora). These very characteristic black streaks of microbial growth

on rock surfaces and buildings (Figs. 2–4) are dominated by drought resistant but water demanding cyanobacteria. They can create considerable carbonate deposits and terrestrial stromatolites on many surfaces, including buildings and monuments, and result in layers of carbonate and silica mineral veneers that seriously darken ancient murals such as Aboriginal art in Australia (Watchman 1996). Dark microbial growths may be composed of algae, cyanobacteria, fungi and lichens, or a mixture of these. A microscopic view of a cyanobacterial film is shown in Fig. 5.

A third example of subaerial biofilm, practically invisible to the naked eye, is the thin spider-web-like growth of fungi and actinomycetes that occurs on bare

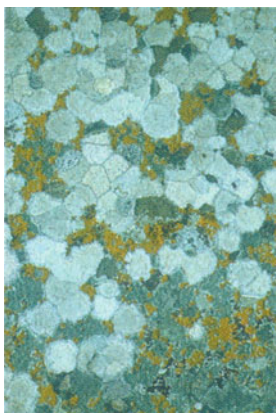

Fig. 1. Lichen biofilm. The rock surface is totally covered by a carpet of growth which, in the case of endolithic lichens, can extend more than 1 cm into the interior of the rock

Fig. 2. A tombstone in the Jewish Cemetery at Hannover. A green algal biofilm covers the *left side* of the stone except for those parts where toxic metal leachates from the copper plate are keeping the original rock surface clean of growth. On the *right side* the black appearance is created by a "Tintenstrich-Flora" (ink-streak) made up of cyanobacteria and melanin-producing fungi. Individual biofilms can easily be confused with dirt and soot

Fig. 3. The Roraima-Tepui ("Inselberg"), Venezuela. The surface of the plateau is covered by a black carpet of a cyanobacteria-dominated community. The steep walls carry also "ink-streak"-type biofilms, not yet studied in detail. This view stresses the considerable extent that subaerial rock biofilms can reach

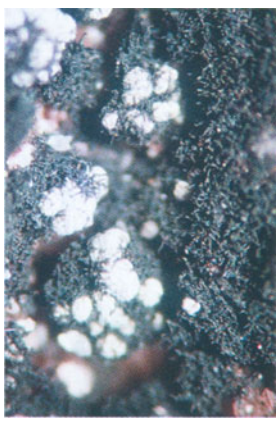

Fig. 4. Rose-coloured quartzitic rock of a Tepui ("Inselberg") in Venezuela (detail of Fig. 3), covered with a black biofilm or microbial mat of the cyanobacterium *Stigonema* sp. and forming a thick carpet with forsterite depositing lichens of the genus *Peltula*. The lichen deposit is reminiscent of microstromatolites or lichen stromatolites

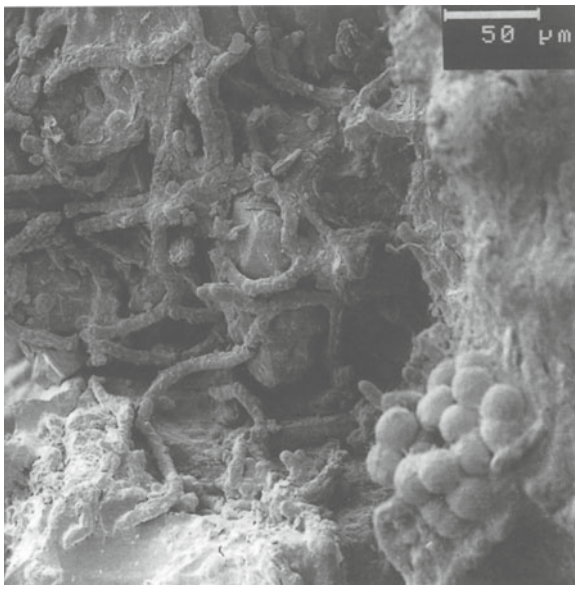

Fig. 5. SEM micrograph of the cyanobacterial biofilm/carpet shown in Fig. 4. Individual quartz grains are entangled and partially broken by *Stigonema*. EPS layers cover large parts of the rock. A colony of a pleurocapsalean cyanobacterium is partially detached by the preparation

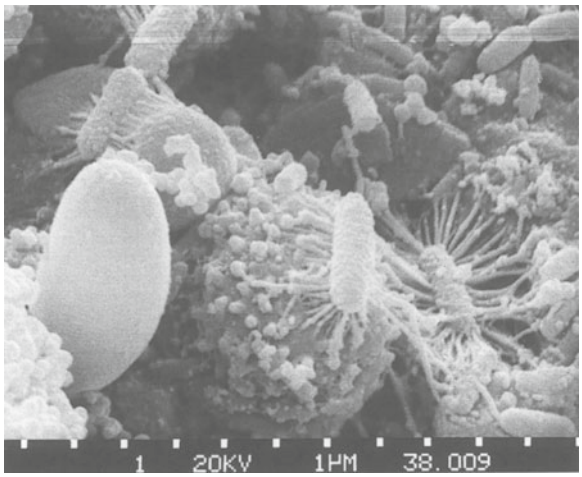

Fig. 6. Microbial growth on the surface of Keuper sandstone at Würzburg. A fungal spore awaits improved conditions. Chains of bacteria "walking" over the mineral surfaces leave behind slime threads. Minibacteria and nanobacteria exhibit as little surface area as possible to the harsh conditions. The smallest bacteria encountered in rock biofilms, but not cultivated and named, are smaller than 100 nm (*Scale bar* = 1 µm)

rock under harsh environmental conditions. These biofilms form networks that cover rock surfaces on a large scale, filling the deeper parts of karstic relief with black lines that have invisible and hard to detect extensions into the surrounding, apparently bare, rock surfaces. These fragile and frail extensions, often made up by nanobacteria-like actinomycetal structures, are difficult to trace even in SEM.

The fourth and final example of subaerial biofilm is where rock surfaces are covered by minute bacteria, which may have cell sizes in this harsh environment of less than 0.2 µm, and which are virtually out of the range of most current analytical techniques and skills. A bacterial biofilm from a Keuper sandstone in Würzburg (Fig. 6) gives an impression of these layers.

5 Rocks and Their Biofilms as a Living Entity

Rocks and rock surfaces can be regarded as living systems (Krumbein and Lapo 1996). Productive and destructive biokarst (including phenomena and processes such as biocorrosion, biodeterioration, bioerosion, biolamination, biomineralisation, bioencrustation, biogeomorphogenesis) are the results of exchanges or biotransfer processes of material and energy (including heat) between two heterogeneous open systems: the solid substrate and the atmosphere (more or less enriched with water or water vapour, also physically expressed as water potential and/or water activity). Both systems are defined by their physical (mass, volume, surface, pressure, porosity, permeability, water activity, etc.), chemical (composition, reactivity, stochiometry), and biological (poikilotrophic behaviour, physiological, biochemical, biophysical, genetic survival potential, and highly selective asymmetric processes across membranes, cell walls and EPS) properties. Their activities and life processes are characterised by innate and permanently or episodically/sporadically added or subtracted energies. The mutual interaction of all components and processes, including asymmetric biological membrane generated catalysis and control (Krumbein and Levit 1997), leads to a more-or-less complete turnover of the initial materials and organisms/membrane structures at the border zone between the two systems. The natural limit of the turnover activities is determined by the penetration depth of physical factors, chemical gradients, gases, solutions, and organisms (including their metabolic products and forces) into the rock material. The resulting productive or destructive biokarst may periodically come to a standstill when conditions between rock and atmosphere approach equilibrium (e.g. through the formation of patina, crust, stromatolite, etc.). Determination of the true Earth-internal interface of these important geomicrobiological processes still awaits experimental testing.

However, poikilotrophic microbial processes may be revived even if only one of the components or processes involved changes or is exposed to change. In directly subaerial microbial biofilms or mats, the main factor undergoing considerable but erratic change is the

availability and activity of water. In the deep rock and sediment biosphere, the activity-controlling factors may be energy and nutrient availability, and temperature and pressure.

Thus, subaerial biofilms and microbial mats are either biodestructive or bioconstructive systems in a natural interplay of biogeomorphogenetic processes. According to many authors (e.g. Kant, quoted by Krumbein 1993), the latter may even be important factors in the stabilisation of the Earth's climate and temperature. Biodestructive activities are rock solution and mechanical disintegration brought about by biofilms. There is experimental evidence for biologically controlled pitting, chipping, sanding, exfoliation, and even desquamation, i.e. the detachment of large blocks of the rock under attack (Sterflinger 1995; Gehrmann-Jannsen 1996). Equations and dynamic calculations of the catalysing effects of these biota on erosion speed and climate are documented by Schwartzman and Volk (1990, 1991). Bioconstructive activities lead to microstromatolite, desert stromatolite, lichen stromatolite (including opal and forsterite mineralisations), sinter, caliche, and crust formation, sometimes reaching 10 m or more in thickness. However, both activities are less dependent on rock/mineral composition and structure, or on the biodiversity of the biofilm or microbial mat. They depend solely on water and energy availability. Thus, rock biofilms or microbial mats are not only the best candidates to search for the origin of life on Earth, but also on Mars and other relatively dry but cool planets, or on planets where ice is the normal physical state of water, with the exception of where conditions make poikilotroph life possible (i.e. life faced with high extremes of temperature and water availability and activity).

The interactive zone between rock biota and atmosphere by far exceeds the physical dimension of the interaction between aquatic biofilms and hydrosphere. The general lack of information on subaerial biofilms may stem from the already mentioned assumption that 70% of the Earth's surface is covered by water and only 30% by rock. In reality, however, the reactive surface of rock and soil with the atmosphere is about 10,000 times larger than that of rock or sediment with the hydrosphere (Krumbein 1995).

It is to be expected that geoscientists and biologists will increasingly combine knowledge and techniques in order to fully analyse the fascinating topic of subaerial microbial films and mats. In the future, a major in-depth topic in biofilm research may be to consider whether biokarst and related biogeomorphogenetic processes are the ultimate bioregulative force which (within certain limits) maintains the stability of atmospheric composition, global temperature, weather and climate, and even the composition, thickness and mobility of the crust (perhaps including biologically induced and controlled plate tectonics). Thus, subaerial and subaquatic biofilms may represent the main driving force for the maintenance of life on Earth.

Acknowledgements. We acknowledge support from the DFG, Federal Ministry of Science and Technology, Volkswagen Foundation, EU, and INTAS, for research in the fields of subaerial biofilm and biokarst phenomena.

References

Braams J (1992) Ecological studies on the fungal microflora inhabiting historical sandstone monuments. PhD Thesis, Oldenburg
Characklis WG, Marshall KC (eds) (1990) Biofilms. Wiley, New York
Cloud PE (1942) Notes on stromatolites. Amer J Sci 240, 363–379
Cooke, RC, Whipps JM (1993) Ecophysiology of fungi. Blackwell Scientific Publications, Oxford
Cunningham AB, Bouwer EJ, Characklis WG (1990) Biofilms in porous media. In: Characklis WG, Marshall KC (eds) Biofilms. Wiley, New York, pp 697–732
DeWinder B (1990) Ecophysiological strategies of drought-tolerant phototrophic micro-organisms in dune soils. PhD Thesis, Amsterdam
Doemel WN, Brock TD (1974. Bacterial stromatolites. Origin of laminations. Science 184:1083–1085
Dornieden, Th (1997) Untersuchungen zu physikalischen (mechanischen) Auswirkungen von Pilzen auf Minerale. MSc Thesis, Oldenburg
Ehrenberg CG (1838) Über das im Jahre 1686 in Curland vom Himmel gefallene Meteorpapier und über dessen Zusammensetzung aus Conferven und Infusorien. Abh königl Akad Wiss Berlin, Physikal Klasse, 44–60
Eppard M, Krumbein WE, Koch C, Rhiel E, Staley J, Stackebrandt E (1996) Morphological, physiological and molecular biological investigations on new isolates similar to the genus *Geodermatophilus* (Actinomycetes). Arch Microbiol 166:12–22
Friedman EI (ed) (1993) Antarctic microbiology, Wiley, New York
Friedmann EI, Ocampo-Friedmann R (1984) Endolithic micro-organisms in extreme dry environments: analysis of a lithobiontic microbial habitat. In: Klug MJ, Reddy CA (eds) Microbial ecology. Current Perspectives ASM, Washington, pp 177–187
Garcia-Valles M, Vendrell-Saz M, Krumbein WE, Urzi C (1996) Biological pathways leading to the formation and transformation of oxalate rich layers on monument surfaces exposed to Mediterranean climate. In: Realini M, Toniolo L (eds) The oxalate films in the conservation of works of art. EDITEAM Castello d'Argile (BO), pp 319–334
Gehrmann-Jannsen, CK (1996) On the biopitting corrosion by epilithic and endolithic lichens on carbonate rocks – bio-physical and bio-chemical weathering aspects. PhD Thesis, Oldenburg
Golubic S (1967) Algenvegetation der Felsen, eine ökologische Algenstudie im dinarischen Karstgebiet. Binnengewässer 23, Schweizerbarth, Stuttgart
Gorbushina AA, Krumbein WE, Hamann C-H, Panina L, Soukharjevski S, Wollenzien U (1993) On the role of black fungi in colour change and biodeterioration of antique marbles. Geomicrobiol J 11:205–221
Gorbushina AA, Krumbein WE, Vlasov D (1996a) Biocarst cycles on monument surfaces. In: Pancella R (ed) Preservation and restoration of cultural heritage. Proceedings of the 1995 LPC Congress. EPFL, Lausanne, pp 319–332
Gorbushina AA, Krumbein WE, Rosenfeld A, Goren-Inbar N (1996b) On the microbiology of flint tools and silica skins. In: Int Union of Microbiological Societies (ed) 8th Int Congress of Bacteriology and Mycology Div of IUMS, Jerusalem, p 103
Haeckel E (1877) Bathybius und die Moneren. Kosmos 1:293–305
Hofmann, B (1989) Genese, Alteration und rezentes Fließsystem der Uranerzlagerstätte Krunkelbach (Menzenschwand, Südschwarzwald). PhD Thesis, Bern
Hofmann-Bang N (1813) *Conferva chthonoplastus*. In: Hornemann JWE (ed) Flora Danica. Schultz, Kopenhagen

Humboldt AV (1793) Florae Fribergensis specimen plantas cryptogamicas praesertim subterraneas exhibens. Rottmann, Berlin
Hutton J (1788) Theory of the Earth. Trans R Soc Edinb. Book version 1795 vol 1+2, Edinburgh
Jaag O (1945) Untersuchungen über die Vegetation und Biologie der Algen des nackten Gesteins in den Alpen, im Jura und im Schweizerischen Mittelland. Beitr Kryptogamenflora, Schweiz, 9:1–560
Jones D, Wilson MJ (1986) Biomineralization in crustose lichens. In: Leadbeater SC, Riding R (eds) Biomineralization in lower plants and animals. Clarendon Press, Oxford, pp 91–106
Karl DM (ed) (1995) The microbiology of deep-sea hydrothermal vents. CRC Press, Boca Raton
Klappa CF (1979) Lichen stromatolites. Criterion for subaerial exposure and a mechanism for the formation of laminar calcretes (caliche). J Sed Petrol 49:387–400
Krumbein WE (1966) Zur Frage der Gesteinsverwitterung (Ueber geochemische und mikrobiologische Bereiche der exogenen Dynamik) PhD Thesis, Wuerzburg
Krumbein WE (1969) Über den Einfluß der Mikroflora auf die exogene Dynamik (Verwitterung und Krustenbildung). Geol Rdsch 58:333–363
Krumbein WE (1979) Photolithotrophic and chemoorganotrophic activity of bacteria and algae as related to beachrock formation and degradation (Gulf of Aqaba, Sinai): Geomicrobiol J 1: 139–203
Krumbein WE (1983) Stromatolites – challenge of a term in space and time. Precambrian Res 20:493–531
Krumbein WE (1987a) Die Entdeckung inselbildender Mikroorganismen. In: Gerdes G, Krumbein WE, Reineck H-E, Kramer (eds) Mellum – Portrait einer Insel. Frankfurt am Main, pp 62–75
Krumbein WE (1987b) Das Farbstreifensandwatt: Bau, Struktur und Erdgeschichte von Mikrobenmatten. In: Gerdes G, Krumbein WE, Reineck H-E, Kramer (eds) Mellum – Portrait einer Insel. Frankfurt am Main, pp 170–187
Krumbein WE (1993) Microbial biogeomorphogenesis – an appraisal of Immanuel Kant. In: Guerrero R, Pedros-Alio C (eds) Trends in microbial ecology. Spanish Soc for Microbiology, Spain, pp 483–488
Krumbein WE (1994) The year of the slime – instead of an introduction. In: Krumbein WE, Paterson DM, Stal LJ (eds) Biostabilization of sediments. BIS, Oldenburg, pp 1–7
Krumbein WE (1995) A neglected carbon sink? Biodegradation of rocks. In: Allsopp D, Colwell RR, Hawksworth DL (eds) Microbial diversity and ecosystem function. UNEP/CAB International, Egham, UK, pp 113–123
Krumbein WE (1996) Geophysiology and parahistology of the interactions of organisms with the environment. Mar Ecol 17:1–21
Krumbein WE, Diakumaku E, Gehrmann C, Gorbushina AA, Grote G, Heyn C, Hilge C, Kuroczkin J, Petersen K, Rudolph C, Schostak V, Sterflinger K, Warscheid Th, Wolf B, Wollenzien U, Kyung Y (1996) Chemoorganotrophic micro-organisms as agents in the destruction of monuments and objects of art. Proceedings of the 8th International Congress on Deterioration and Conservation of Stone, Sept 30 – Oct 04, 1996, Berlin, Möller, Berlin, pp 631–636
Krumbein WE , Dyer BD (1985) This planet is alive. Weathering and biology – a multifaceted problem. In: Drever JI (ed) The chemistry of weathering, Reidel, Dordrecht, pp 143–160
Krumbein WE, Giele C (1979) Calcification in a coccoid cyanobacterium associated with the formation of desert stromatolites. Sedimentology 26:593–604
Krumbein WE, Jens K (1981) Biogenic rock varnishes of the Negev Desert (Israel) an ecological study of iron and manganese transformation by cyanobacteria and fungi: Oecologia 50:25–38
Krumbein WE, Lapo A (1996) Vernadsky's biosphere as a basis of geophysiology. pp.115–134 In: Bunyard P (ed) Gaia in action. Science of the living Earth. Floris, Edinburgh
Krumbein WE, Levit G (1997) Die Erde – ein Lebewesen (Earth – a living being). Einblicke (Forschungsmagazin der Carl von Ossietzky Universitaet, Oldenburg) 25:4 –7
Krumbein WE, Villbrandt M (1994) Biofilme und Mikrobenmatten extremer Lebensraeume. In: Hausmann K, Kremer BP (eds) Extremophile. VCH, Weinheim, pp 113–139
Lide DR (ed) (1993) CRC handbook of chemistry and physics, CRC Press, Boca Raton
Ludwig R, Theobald G (1852) Über die Mitwirkung der Pflanzen bei der Ablagerung des kohlensauren Kalkes. Pogg. Ann Phys Chem 87:91–107
Mitchell TG, Shewan JM (1968) Aspects of taxonomy with respect to biodeterioration. In: Walters AH, Elphick JJ (eds) Biodeterioration of materials. Elsevier, Amsterdam, pp 13–21
Neu Th (1994) Biofilms and microbial mats. In: Krumbein WE, Paterson DM, Stal LJ (eds) Biostabilization of sediments. BIS, Oldenburg, pp 9–16
Neu Th (1996) Significance of bacterial surface-active compounds in interaction of bacteria with interfaces. Microbiol. Rev 60:151–166
Potts M (1994) Desiccation tolerance in prokaryotes. Microbiol Reviews 58:755–805
Potts M (1996) Etymology of the genus name *Nostoc* (cyanobacteria). Int J Syst Bact 47:584–584
Rivadeneyra MA, Ramos-Cormenzana A, Garcia-Cervigon A (1985) Etude de l'influence du rapport Mg/Ca sur la formation de carbonate par les bactéries telluriques. Can J Microbiol 31:229–231
Rivadeneyra MA, Delgado R, delMoral A, Ferrer M, Ramos-Cormenzana A (1994) Carbonate precipitation by Bacillus sp. isolated from saline soils. Geomicrobiol J 11:175–184
Roelleke S, Muyzer G, Wawer C, Wanner G, Lubitz W (1996) Identification of bacteria in a biodegraded wall painting by denaturing gradient gel electrophoresis of PCR-amplified gene fragments coding for 16 S rRNA. Appl Environ Microbiol 62:2059–2065
Scholz J (1996) Eine Feldtheorie der Bryozoen, Mikrobenmatten und Sedimentoberflächen. Habilitationsschrift, Hamburg
Scholz J, Krumbein WE (1996) Microbial mats and biofilms associated with bryozoans. In: Gordon DP, Smith AM, Grant-Mackie JA (eds) Bryozoans in space and time. Proceedings of the 10th Int Bryozoology Conference, Wellington, New Zealand. National Institute of Water and Atmosphere Research Ltd, Wellington, NZ, pp 283–298
Schrödinger E (1944) What is life? Cambridge Univ Press, Cambridge
Schwartzman DW, Volk T (1990) Biotic enhancement of weathering and the habitability of earth. Nature 340:457–460
Schwartzman DW, Volk T (1991) When soil cooled the world. New Sci 51:33–36
Staley JT, Adams JB, Palmer FE (1992) Desert varnish: a biological perspective. In: Stotzky G, Bollag JM (eds) Soil biochemistry 7. Marcel Dekker, New York, pp 173–195
Sterflinger K (1995) Geomicrobiological investigations on the alteration of marble monuments by dematiaceous fungi (Sanctuary of Delos, Cyclades, Greece). PhD Thesis
Sterflinger K, Becker T, Krumbein WE, Warscheid T (1994) The respiration bell jar – a rapid non-destructive technique for the measurement of the activity of micro-organisms on and in objects of cultural value. Dtsch. Gesellschaft für zerstörungsfreie Prüfung, Berichte, 45:382–391
Sterflinger K, Blazquez F, Garcia-Vallès M, Krumbein WE, Vendrell-Saz M (1996) Patina, microstromatolites and black spots as related to biodeterioration processes of granite. In: Vicente MA., Delgado-Rodrigues J, Acevedo J (eds) Degradation and conservation of granitic rocks in monuments. Protection and Conservation of the European Cultural Heritage. Res Rep Nr 5, pp 391–397
Viles HA (1984) Biokarst. Review and prospect. Progr Physical Geogr 8:532–542
Wachendörfer V, Riege H, Krumbein WE (1994) Parahistological sediment in thin sections. In: Krumbein WE, Paterson DM, Stal LJ (eds) Biostabilization of sediments. BIS, Oldenburg, pp 257–277
Wang Fuxing (1993) Biokarst. Int Geol Corr Program 299. Geol Publ House, Beijing
Watchman AL (1996) Properties and dating of silica skins associated with rock art. PhD Thesis, Canberra
Wolf B, Krumbein WE (1996) Tiefenbesiedlung und Biodeterioration an Marmorkapitellen des Freundschaftstempels im Park von Sanssouci (Potsdam). Int Z Bauinstandsetzen 2:15–32

Microbial Sediments in Tropical Karst Terrains: A Model Based on the Cayman Islands

Brian Jones

Department of Earth and Atmospheric Sciences, University of Alberta, Edmonton, Alberta, T6G 2E3, Canada

Abstract. Microbes play an important role in the formation of karst landscapes by mediating a wide array of destructive and constructive processes. The destructive processes, which include substrate dissolution and boring, commonly lead to the formation of sparmicrite and the release of $CaCO_3$ into the system. Constructive processes, which include trapping and binding of detrital grains to a substrate, commonly lead to the formation of microstromatolites. The microbial processes operative in any given area are controlled by numerous factors that are related to the type of microbe and the microenvironment in which they live. The diversity of processes operative in a tropical karst terrain is related to the broad array of ecological niches that are available in such landscapes.

1 Introduction

Microbes are commonly the architects of the delicate and intricate structures that adorn a tropical karst landscape. These talented organisms mediate destructive and constructive processes that leave distinctive imprints on the karst landscape (e.g., see references in Sasowsky and Palmer 1994). In many parts of the karst, however, the influence of microbes is subtle because mineral dissolution or precipitation may result from microenvironmental modifications caused by the microbes. Such activity can only be inferred from the evi-

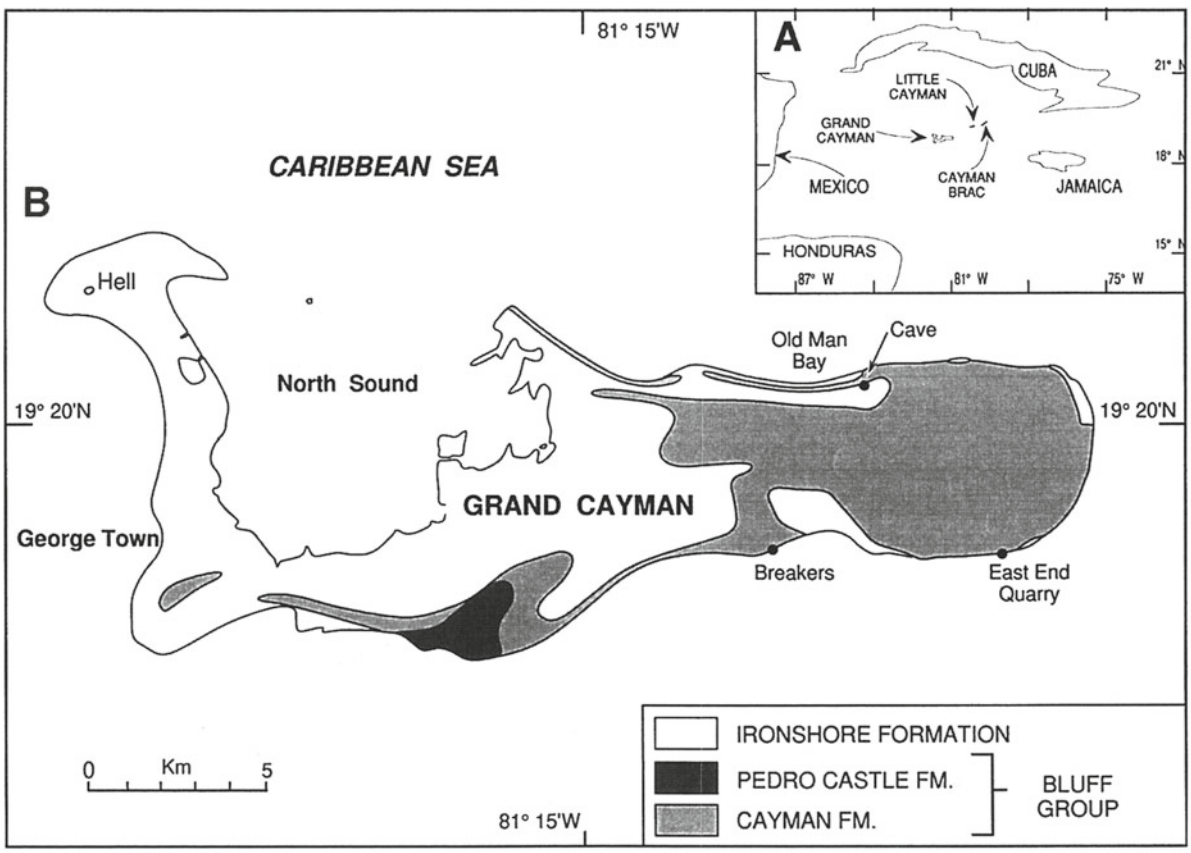

Fig. 1.A Location of Grand Cayman. **B** Map of Grand Cayman showing surface geology (Jones et al. 1994) and localities

R. E. Riding and S. M. Awramik (Eds.)
Microbial Sediments

dence found in the rocks. Using this approach, the scope of microbially mediated processes is illustrated by considering the tropical karst landscape on the Cayman Islands.

Each of the Cayman Islands is formed of a core of the Oligocene-Pliocene Bluff Group (Brac, Cayman, and Pedro Castle formations; Jones et al. 1994) that is flanked and unconformably overlain by limestones of the Late Pleistocene Ironshore Formation (Fig. 1). The Bluff Group has undergone repeated phases of karst generation (Jones and Smith 1988; Jones 1992a,b). The Cayman Formation (Miocene), which is widely exposed on these islands, is formed of white, dense, finely crystalline dolostone (Pleydell et al. 1990; Jones et al. 1984, 1994) and has poorly defined bedding but well-defined joint systems (Ng et al. 1992). This formation is characterized by phytokarst surfaces (Folk et al. 1973; Jones 1989) with honeycombed rock pinnacles, fissures, sinkholes and numerous caves (Jones and Smith 1988; Lips 1993). Karst on the soft limestones of the Ironshore Formation is more subdued than on the harder dolostones of the Bluff Group. The limestones of the Ironshore Formation are commonly capped by calcrete crusts (Jones 1988) and locally contain rhizoliths (Jones and Ng 1988).

2
Survey of Microbial Features by Location

2.1
Caves

2.1.1
Cave Interiors

Transverse sections across some modern and old stalactites from Grand Cayman (Jones and Motyka 1987) show that they are formed of a "soda-straw" that is surrounded by radiating, internally laminated columns (2–3 mm wide at their base, 3–6 mm at their top), and an outer spar calcite zone (Fig. 2A). Filamentous microbes and bacteria-like bodies are present in the core and spar calcite (Fig. 2B,C). The isodiametric calcified filaments (Fig. 2B), with a central tube 2–4 μm in diameter, are encrusted with "spike-like" calcite crystals, 2–4 μm long. These filaments trapped and bound grains to the substrate, added mass by virtue of their calcification, and provided micrite for binding to the substrate following breakage (Jones and Motyka 1987). These microbes may have triggered calcite precipitation by modifying the microenvironment. The bacteria-like bodies, 3–24 μm in diameter, which have selectively fixed Mn, Fe, and Al into their structures (Jones and Motyka 1987), are commonly arranged in shrub-like masses like the bacterial bushes described by Chafetz and Folk (1984).

2.1.2
Cave Pisoliths

Cave pisoliths (up to 8 cm long), found in terraced pools in Old Man Village Cave (Fig. 1B), have nuclei formed of bone (from birds and bats) fragments, calcite crystals, or terra rossa lithoclasts (Jones and MacDonald 1989). Their cortices are formed of thin (pseudo-) concentric laminae of micrite and dendritic and trigonal calcite crystals. Many cortical laminae contain calcified, isodiametric, irregularly branching filaments up to 20 μm in diameter. These filaments are most obvious on the outer pisoliths surfaces and in the porous laminae where there is little calcification. Associated with the filaments are (sub)spherical spores, 7–30 μm in diameter, that are commonly calcified.

Growth surfaces in the cortices are commonly covered by dense, interwoven mats or irregularly branching filamentous microbes that have been calcified to varying degrees. Poorly calcified filaments are visible whereas heavily calcified filaments, commonly only a few microns away, are barely discernible. Calcified spores also contribute to these laminae. There is no evidence of filamentous microbes trapping and binding detrital grains to the oncoid surfaces, or boring into the substrates.

2.1.3
Twilight Zone

Biofilms on cave walls in the twilight zone, highlighted by their green colour, are produced by a diverse array of microbes (Jones 1995) that have substantially modified the dolostones (Cayman Formation) that they cover. Although detrital particles are trapped and bound to the substrate, microstromatolites (see Jones and Kahle 1985) are not evident. Microbially mediated dissolution of calcite cements in the dolostones produced irregular etching, spiky calcite, and "blocky topographies". Locally, there is evidence of boring and micritization of the substrate (Jones 1995). Substrate destruction on this scale also released $CaCO_3$ into the system. Nevertheless, there is no evidence of new crystal growth and microbe calcification is limited.

2.2
Surface Substrates

2.2.1
Phytokarst

Surface exposures of the Bluff Group are characterized by honeycombed rock pinnacles, ridges, fissures, solution-widened joints, and sinkholes (e.g., Jones and Smith 1988; Jones 1989). These features are more subdued on the softer limestones of the Ironshore Forma-

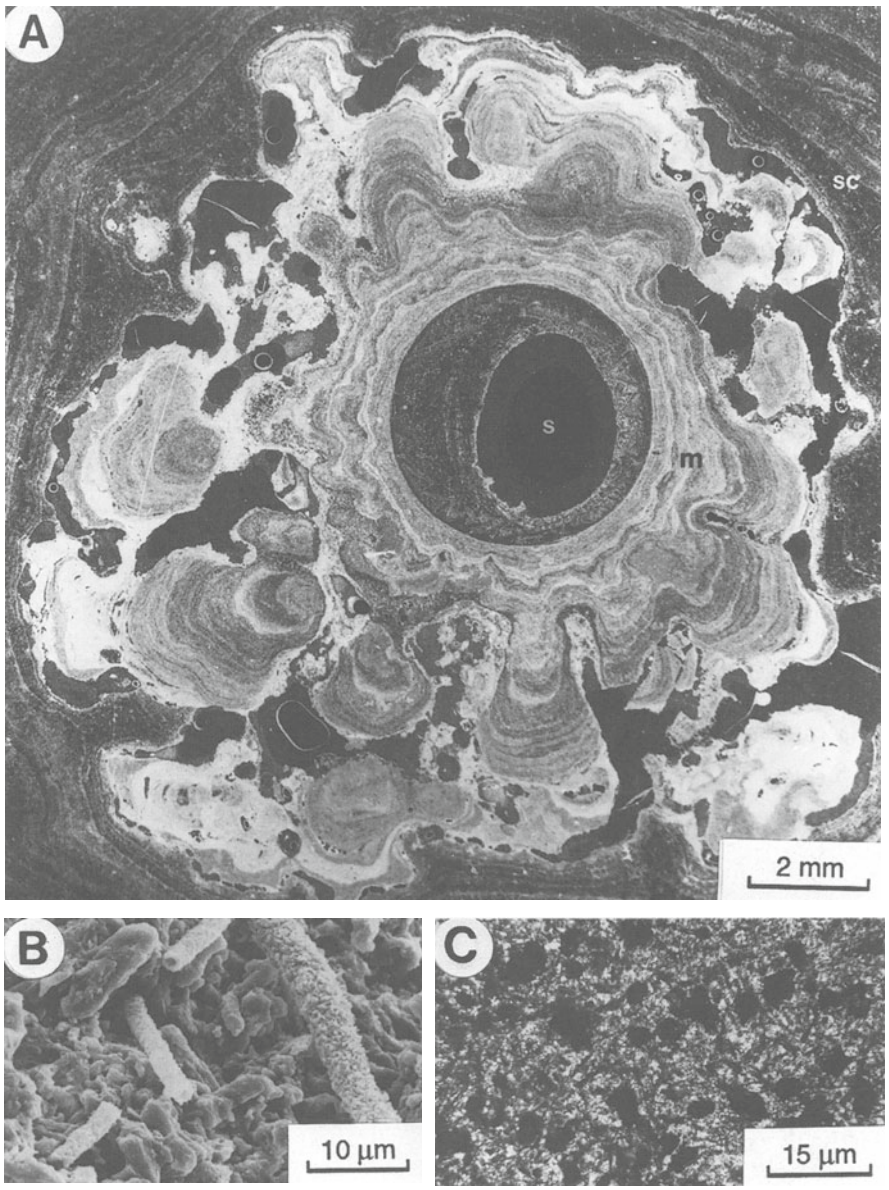

Fig. 2.A Negative black and white photograph of a cross-section through a stalactite from a cave near Old Man Village. Note "soda-straw" (*s*) surrounded by radiating columns of laminated micrite (*m*) and outer zone of spar calcite (*sc*). **B** Calcified filaments in the laminated columns shown in **A. C** Bacterial (?) bodies (*black*) in spar calcite in outer part of the stalactite

tion. Folk et al. (1973), using exposures of the Cayman Formation at Hell (Fig. 1), coined the term phytokarst for "...a landform produced by rock solution which boring plant filaments are the main agents of destruction." The black to grey phytokarst surfaces are characterized by endolithic and epilithic microbes.

The endolithic microbes produce borings, up to 10 µm in diameter and up to 200 µm deep, in the hard dolostone of the Cayman Formation and 6–10 µm in diameter and up to 350 µm long in the softer limestones of the Ironshore Formation. Although many borings are straight, others meander and branch at irregular intervals. Many borings contain the filamentous microbe responsible for their formation. The density of borings in the limestones of the Ironshore Formation is generally greater than that in the dolostones of the Cayman Formation. Epilithic microbes, which are common on the surfaces of the dolostones and limestones, include sporangia, spores, filamentous microbes, and mucus.

The microbes mediated dissolution of the underlying substrate. Thus, surfaces on the dolostones of the Cayman Formation are characterized by etched dolomite rhombs, dolomite rhombs pierced by holes up to 50 µm in diameter, and dolomite crystals with missing faces and/or cores. These features were attributed to microbially mediated dissolution (Jones 1989). Constructive processes are limited to minor amounts of microbial calcification.

2.3 Sinkholes

2.3.1 Terrestrial Oncoids

Terrestrial oncoids, up to 4.3 mm long, are found in some cavities in the Cayman Formation (Jones 1991). The diverse microbial flora on these coated grains, which includes filamentous microbes, spores, mucus(?), and bacteria, mediated oncoid formation through microbe calcification, trapping and binding detrital dolomite, calcite, and clays, and triggering calcite precipitation by modifying the microenvironment (Jones 1991). Microbial calcification added mass and stabilized the substrate. Calcification, however, progressively disguised the microbes until they eventually became buried. Detrital grains were washed into the cavities by vadose waters that flowed through and over the dolostone bedrock, calcite cements, and terra rossa. Oncoid development involved three stages (Jones 1991). In stage I a diverse microbial flora was established that trapped and bound detrital grains to the grain surface. There was, however, little microbial calcification. Stage II began with microbial calcification. As calcification progressed, the amount of trapping decreased. With stage III, calcification reached its maximum and most microbes were fully calcified and almost completely disguised.

2.3.2 Microstromatolites

Sinkholes (1.5–2 m deep, 1 m in diameter) in the Cayman Formation, near East End Quarry (Fig. 1B), are commonly filled with breccias that contain limestone and dolostone clasts (up to 80 × 35 × 25 mm) (Jones and Kahle 1985, 1986). Irregular interclast cavities are lined by a complex succession of cements that locally comprise, in a clast to pore direction, zones of: (1) black amorphous (high Mn content) material with bulbous projections, (2) spar calcite, (3) microstromatolites (Figs. 3, 4A), (4) spar calcite, and (5) sparmicrite (Figs. 3, 4B). Microbes controlled the formation of zones 1, 3 and 5.

The black, Mn-rich coatings of zone 1 may be crustose lichens (Jones and Kahle 1985). The laminated structures of zone 3 are treated as stromatolites because they contain sediment-binding microbes and are identical in appearance, except for size, to known cyanobacterial stromatolites. Micrite in the microstromatolites is bound by filaments that are up to 120 μm long and 3 μm in diameter. Where visible, the outer surfaces of the microstromatolites are green, covered with dense, interwoven mats of filaments, and have insect moults bound onto them by the filamentous microbes (Jones and Kahle 1985). The microbial flora in these microstromatolites: (1) trapped and bound micrite around the cavity walls, (2) made a direct contribution to the cements in the cavities via microbial calcification, and (3) may have caused calcite precipitation by modifying the microenvironment (Jones and Kahle 1985). These microstromatolites cemented the clasts together and reduced interclast porosity and permeability.

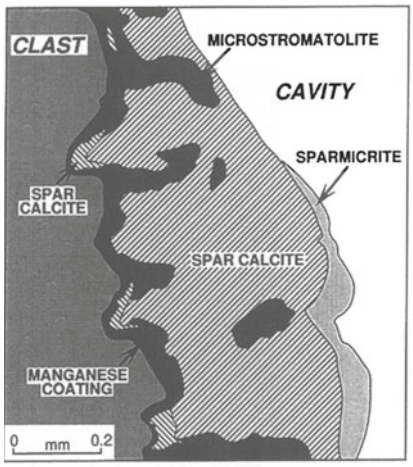

Fig. 3. Sketch (from thin section) showing the cement zones on the walls of interclast cavities in breccia from East End Quarry (Fig. 1B). Note location of microstromatolites relative to the sparmicrite

Zone 5, the most poreward zone (Fig. 3), is characterized by numerous filaments, up to 8 μm diameter, that extend into the micrite from the pore surface (Fig. 4B). The lack of evidence of microbial calcification indicates that this is not a constructive micrite envelope (see Kobluk and Risk 1977). Similarly, the lack of internal laminations like those in the microstromatolites indicates that this zone did not form by accretion. The irregular boundary between zones 4 and 5 was caused by borings penetrating the spar calcite. Collectively, the evidence indicates that the micrite formed by sparmicritization.

The micrite in zones 3 and 5 formed by different processes despite the fact that they are only 1–2 mm apart (Fig. 3). The micrite in zone 3 originated by the constructional activity mediated by filamentous microbes whereas the micrite in zone 5 originated by destructive processes caused by filamentous microbes boring into spar calcite. Although this example highlights the complexity of microbial activity, it does not explain the factors that controlled these processes.

2.3.3 Etching and Constructive Micrite Envelopes

A breccia, formed of white dolostone clasts cemented by two generations of brown calcite, crops out in East

on the crystal surfaces (Fig. 4G). The etch pits are like those found in weathered hypersthene, augite (Berner et al. 1980), feldspar (e.g., Berner 1978) and hornblende (Berner 1981) crystals. Although some features can be attributed to microbial activity, the relationship of other features to microbes is questionable. In many cases the location of etched surfaces beneath microbes or their associated mucus indicates a genetic linkage. Conversely, some etched surfaces no longer have microbes on their surfaces. Although such a situation argues against the microbes being responsible for the etching, it is possible that the microbes were once present but since removed.

2.4 Terra Rossa

Little work has been done on the microbes in the modern and ancient terra rossa that fills cavities and lies on the surface of the Cayman Formation. Spar calcite crystals in some lithified terra rossa's on Grand Cayman were nucleated around clusters of spores (Jones 1992c). These spores, 0.8–1.2 μm in diameter, had thin (0.1–0.15 μm) perforated walls that are commonly coated with anhedral calcite crystals, 0.05–0.10 mm long. Spar calcite, precipitated inside and around these spores, eventually formed crystals up to 0.5 mm long.

2.5 Rhizoliths

Rhizoliths are common in the friable limestones of the Ironshore Formation that are exposed near the airport on Cayman Brac (Jones and Ng 1988). The rhizolith walls include dense arrays of grain-coating calcite needle mats, isolated calcite rhombs, calcite rhomb chains, calcified filamentous microbes, and calcified spherical spores (?). Formation of the rhizoliths was attributed to precipitation of cements and calcification of microbes that lived around the plant root systems.

2.6 Calcrete Profiles

On Cayman Brac, trees and bushes of the dry evergreen bushland are rooted into the caliche that caps the Ironshore Formation (Jones 1988). Large roots penetrate to depths of at least 4 m. Intimately associated with the root borings are numerous microborings, up to 8 μm in diameter and 200 μm long, that were probably formed by filamentous microbes. Walls of the root borings are lined by uncalcified and calcified filamentous and coccoid microbes. The calcified filaments are up to 15 μm in diameter with walls up to 4 μm thick. The uncalcified coccoid microbes, 0.5–3.0 μm in diameter, form extensive mats with copious amounts of mucus.

3 Overview of Microbial Processes Operative in Karst Terrains

Microbes that colonized substrates in tropical karst terrains can mediate destructive or constructive processes (Fig. 5). In many cases, these diametrically opposed processes operate within microns of each other. Destructive processes include substrate dissolution that is commonly concentrated beneath filamentous microbes or their mucus. On calcitic substrates this can produce spiky calcite (Fig. 4D), "blocky topographies", or etch-pits (Fig. 5). On dolomite substrates this can produce hollow rhombs or rhombs pierced by small holes. Significant substrate destruction takes place when fila-

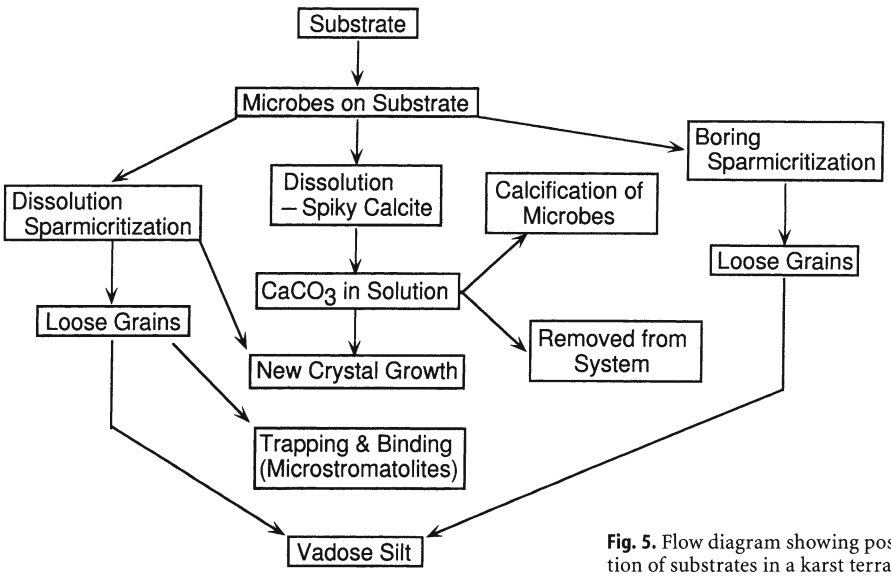

Fig. 5. Flow diagram showing possible results of microbial infestation of substrates in a karst terrain

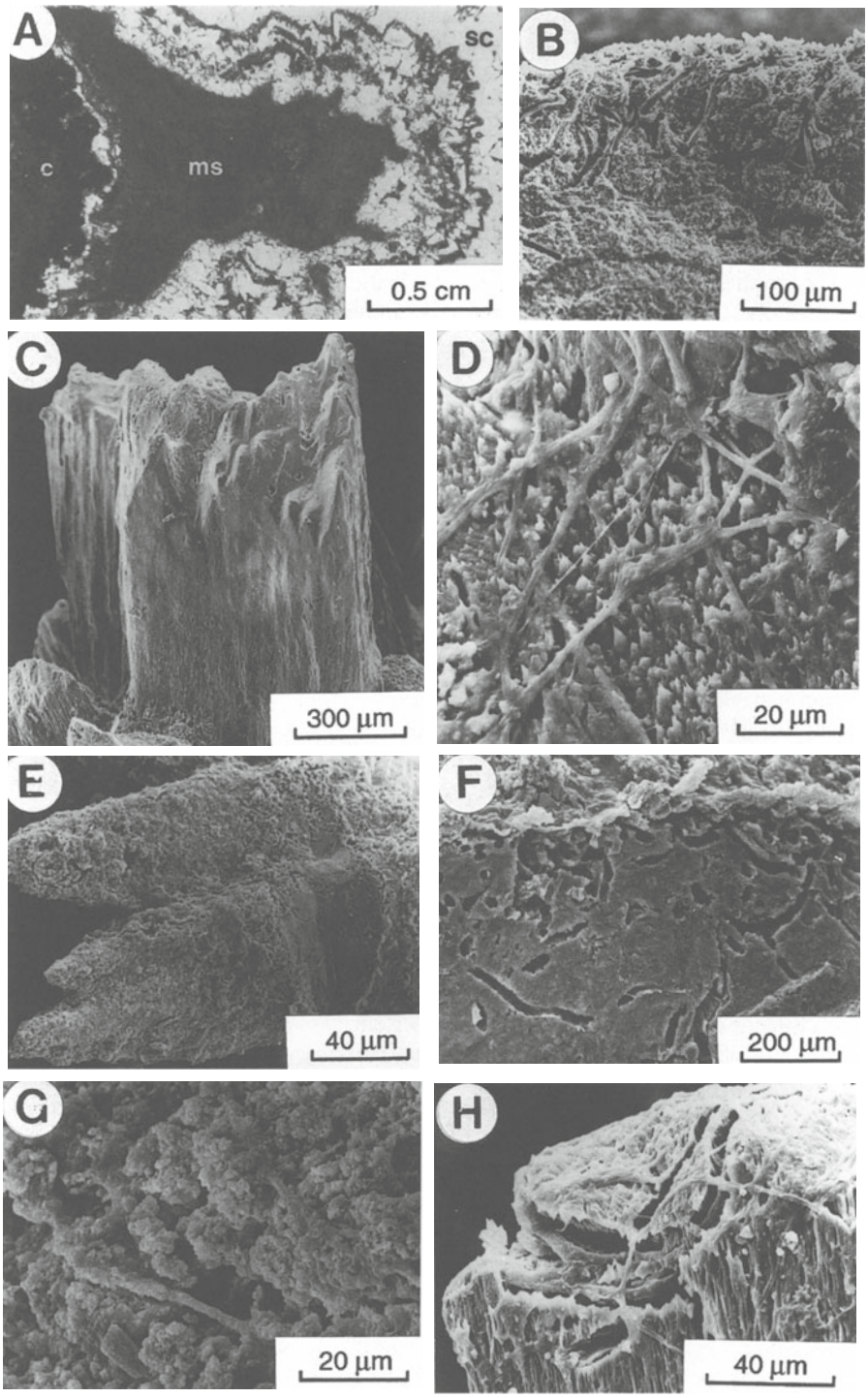

Fig. 4.A Microstromatolite on the surface of a clast in breccia, East End Quarry (Fig. 1B). **B** Sparmicrite (Fig. 3) on outer surface of spar calcite crystals that line intraclast cavities in breccia, East End Quarry. **C** Calcite crystal from a breccia, East End Quarry, that is encased in a constructive micrite envelope. **D** Enlarged view of surface of crystal in Fig. 3C showing filamentous microbes and mucus coating surface. Note spiky calcite beneath mucus. **E** Spar calcite crystals from breccia in East End Quarry. The surfaces are covered by a constructive micrite envelope. Note V-shaped notch. **F** Enlarged view of V-shaped notch in Fig. 3E showing microbial borings and micrite envelope on outer surface. **G** Enlarged view of crystal surface showing micrite envelope with scattered filamentous microbes. **H** Terminal region of calcite crystal showing etching of crystal surface and scattered filaments microbes

End Quarry (Fig. 1B) ~3 m below the breccia that contains the microstromatolites. The calcite crystals have been altered (Fig. 4C–H) by the endolithic, epilithic and chasmolithic microbes that are only rarely calcified (Jones 1987). Associated with the filaments are spherical and hemispherical bodies that may be fruiting bodies of fungi and/or bacteria. Their affinity is unknown because they are heavily calcified. Features evident in or on the calcite crystals are: (1) spiky calcite (Fig. 4D), (2) borings (Fig. 4F), (3) constructive micrite envelopes (Fig. 4C,G), (4) almond-shaped etch pits, (5) surfaces with a "blocky topography", and (6) etched surfaces (Fig. 4H). The constructive micrite envelopes (see Kobluk and Risk 1977) formed by calcification of filaments

mentous microbes bore into substrates (Fig. 4F). Many of these processes lead to sparmicritization and the dislodgment of small grains that can be transported by flowing waters (Fig. 5).

Microbe calcification contributes directly to substrate construction (Fig. 5). Some filaments remain intact whereas others will be broken down into small grains that can be moved by flowing water. Filamentous microbes commonly trap and bind detrital grains to substrates (Fig. 5). This process is critical to the formation of the microstromatolites and terrestrial oncoids.

4 Discussion

The karst terrain on Grand Cayman encompasses diverse ecological settings. Light conditions, for example, range from the dark interiors of caves, to the twilight zone of caves, to subdued light conditions on substrates beneath the tropical vegetation, to bright sunlight in open coastal areas. Similarly, the type and amount of moisture varies from the inland areas that are washed by rainwater to coastal areas that are washed by rainwater, sea spray and, during severe storms, marine waters. Many niches in the karst terrain are ideal for microbe growth and it is therefore not surprising that they play a critical role in the formation of the karst landscape.

Microbes mediate destructive and constructive processes through their ability to bore into substrates, dissolve substrates, trap and bind detrital particles to substrates, and calcify their filaments or spores. Not all processes are operative in all areas. Thus, some areas are dominated by destructive processes whereas other areas are dominated by constructive processes. Indeed, the net impact of microbes in any area is a balance between the constructive and destructive processes that they mediate.

The factors that control microbial processes is dictated by complex factors that are difficult to decipher. Boring into a substrate, for example, may take place because the microbes wish to escape physical stresses such as wave action (e.g., Ercegoviç 1934), grazing pressures, and/or obtain nutrients or moisture (Kobluk and Kahle 1978). Conversely, the absence of any of these factors may mean that the microbes do not need to adopt an endolithic life mode. This pattern is evident on Grand Cayman. In protected areas, such as in cave pools, on cave walls in the twilight zone and on the surfaces of terrestrial oncoids that grow in protected cavities, endolithic microbes are rare. Conversely, exposed substrates are characterized by endolithic microbes. Similarly, calcite cements in sinkhole-filling breccias have been substantially modified by endolithic microbes. Such patterns indicate that microbes which colonize substrates in protected settings preferentially adopt an epilithic life mode that leads to trapping and binding. Conversely, microbes that colonize exposed substrates are more likely to adopt an endolithic life mode that leads to substrate destruction.

Microscale destructive processes are commonly attributed to the boring activity of endolithic microbes. Of equal, or perhaps greater, importance is microbially mediated dissolution. The importance of mucus in this process has been demonstrated experimentally (Jones and Pemberton 1987a,b) and from natural examples (Jones 1987, 1989). Establishing the affects of mucus on substrates is difficult because its preservation potential is far lower than that for the parent microbes. The distribution of mucus in the karst terrain appears to be controlled by the composition of the microbial community rather than by location. Substrate dissolution mediated by mucus is, for example, equally as important in the protected setting of the walls in the twilight zones of caves (e.g., Jones 1995) as it is on the exposed surfaces of the phytokarst (e.g., Jones 1989). The role of mucus, however, is not restricted to mediating substrate dissolution. While that process is operative along the contact between the rock and the mucus, the upper surface of the mucus mat may be actively trapping and binding detrital particles. The constructive role of mucus is, for example, readily apparent in the microstromatolites (Jones and Kahle 1985), terrestrial oncoids (Jones 1991), and cave pisoliths from Grand Cayman (e.g., Jones and MacDonald 1989).

Some microbially mediated processes may be taxa-specific. The validity of this suggestion is difficult to ascertain because of the problems associated with microbe identification. Microbe preservation in karst terrains is selective and it is typically only the sheath that is preserved by calcification (e.g., Phillips et al. 1987; Jones 1991). In addition, collapsed or poorly preserved uncalcified microbes are found in some samples. Irrespective, the taxonomically critical features are typically missing and specific identifications are virtually impossible. There does, however, appear to be differences in the diversity of the microbial biota found in different niches of the karst terrain. For example, the diversity of the microbial biota in stalactites and cave pisoliths appears to be far lower than that found on the cave walls in the twilight zone. Caution must be exercised with such comparisons because it may be a reflection of preservational processes rather than the original biota. Elsewhere in the world, for example, diverse biotas of algae, cyanobacteria, fungi, and bacteria, live on cave walls (e.g., Høeg 1946), stalactites and stalagmites (e.g., Nagy 1965; Went 1969), and in water-filled depressions (e.g., Nagy 1965).

5 Conclusions

Microbes play an important role in the formation of karst terrain in tropical settings. These organisms control a variety of destructive and constructive processes that influence the architecture of the karst landscape. Not all processes are operative in all areas and it appears that the process operative in any area is controlled by a complex array of variables that are difficult to deduce. The fact that these variables operate on a microscale is demonstrated by the fact that diametrically opposed processes may affect the same substrate under similar environmental conditions.

Acknowledgements. This research project was funded by the Natural Sciences and Engineering Research Council of Canada (grant A6090). I am indebted to George Braybrook, who took most of the SEM photomicrographs used in this chapter.

References

Berner RA (1978) Rate control on mineral dissolution under earth surface conditions. Am J Sci 8:1235–1252

Berner RA, Sjöberg EL, Velbel MA, Krom MD (1980) Dissolution of pyroxenes and amphiboles during weathering. Science 207: 1205–1206

Berner RA (1981) Kinetics of weathering and diagenesis. In: Lasaga AC. Kirkpatrick RJ (eds) Kinetics of Geochemical Processes. Am Min Soc Rev Min 8:111–134

Chafetz HS, Folk RL (1984) Travertines: depositional morphology and the bacterially constructed constituents. J Sed Petrol 54: 289–316

Ercegoviç A (1934) Wellengang und Lithophytenzone on der Ostadriatischen Kuste. Acta Adriatica 1:1–20

Folk RL, Roberts HH, Moore CH (1973) Black phytokarst from Hell, Cayman Islands, British West Indies. Geol Soc Am Bull 84: 2351–2360

Høeg OA (1946) Cyanophyceae and bacteria in calcareous sediments in the interior of limestone caves in Nord-Rana, Norway. Nyatt Mag Naturvid 85:99–104

Jones B (1987) The alteration of sparry calcite crystals in a vadose setting, Grand Cayman Island. Can J Earth Sci 24:2292–2304

Jones B (1988) The influence of plants and micro-organisms on diagenesis in caliche: example from the Pleistocene Ironshore Formation on Cayman Brac, British West Indies. Bull Can Pet Geol 36:191–201

Jones B (1989) The role of microorganisms in phytokarst development on dolostones and limestones, Grand Cayman, British West Indies. Can J Earth Sci 26:2204–2213

Jones B (1991) Genesis of terrestrial oncoids, Cayman Islands, British West Indies. Can J Earth Sci 28:382–397

Jones B (1992a) Void-filling deposits in karst terrains of isolated oceanic islands: a case study from Tertiary carbonates of the Cayman Islands. Sediment 39:857–876

Jones B (1992b) Caymanite, a cavity-filling deposit in the Oligocene-Miocene Bluff Formation of the Cayman Islands. Can J Earth Sci 29:720–736

Jones B (1992c) Construction of calcite crystals around spores. J Sed Petrol 62:1054–1057

Jones B (1995) Processes associated with microbial biofilms in the twilight zone of caves: examples from the Cayman Islands. J Sed Res A65:552–560

Jones B, Kahle CF (1985) Lichen and algae: agents of biodiagenesis in karst breccia from Grand Cayman Island. Bull Can Pet Geol 33:446–461

Jones B, Kahle CF (1986) Dendritic calcite crystals formed by calcification of algal filaments in a vadose environment. J Sed Petrol 56:217–227

Jones B, MacDonald RW (1989) Micro-organisms and crystal fabrics in cave pisoliths from Grand Cayman, British West Indies. J Sed Petrol 59:387–396

Jones B, Motyka A (1987) Biogenic structures and micrite in stalactites from Grand Cayman Island, British West Indies. Can J Earth Sci 24:1402–1411

Jones B, Ng K-C (1988) The structure and diagenesis of rhizoliths from Cayman Brac, British West Indies. J Sed Petrol 58:457–467

Jones B, Pemberton SG (1987b) Experimental formation of spiky calcite through organically mediated dissolution. J Sed Petrol 57:687–694

Jones B, Pemberton SG (1987a) The role of fungi in the diagenetic alteration of spar calcite. Can J Earth Sci 24:903–914

Jones B, Smith DS (1988) Open and filled karst features on the Cayman Islands: implications for the recognition of paleokarst. Can J Earth Sci 25:1277–1291

Jones B, Hunter IG, Kyser K (1994) Revised stratigraphic nomenclature for Tertiary strata of the Cayman Islands, British West Indies. Carib J Sci 30:53–68

Jones B, Lockhart EB, Squair C (1984) Phreatic and vadose cements in the Tertiary Bluff Formation of Grand Cayman Island, British West Indies. Bull Can Petrol Geol 32:382–397

Kobluk DR, Kahle CF (1978) Geologic significance of boring and cavity-dwelling marine algae. Bull Can Petrol Geol 26:362–379

Kobluk DR, Risk MJ (1977) Calcification of exposed filaments of endolithic algae, micrite envelope formation, and sediment production. J Sed Petrol 47:7–528

Lips RFA (1993) Speleogenesis on Cayman Brac, Cayman Islands, British West Indies. Thesis, McMaster University, Hamilton

Nagy JP (1965) Preliminary notes on the algae of Crystal Cave, Kentucky. Speleology I, pp 479–490

Ng K-C, Jones B, Beswick R (1992) Hydrogeology of Grand Cayman, British West Indies: a karstic dolostone aquifer. J Hydrol 134:273–295

Phillips SE, Milnes AR, Foster RC (1987) Calcified filaments: an example of biological influence in the formation of calcrete in South Australia. Aust J Soil Res 25:405–428

Pleydell SM, Jones B, Longstaffe FJ, Baadsgaard H (1990) Dolomitization of the Oligocene-Miocene Bluff Formation on Grand Cayman, British West Indies. Can J Earth Sci 27: 1098–1110

Sasowsky ID, Palmer MV (eds) (1994) Breakthroughs in karst geomicrobiology and redox geochemistry. Karst Waters Inst Spec Publ 1, Karst Waters Institute Inc., USA, 111 p

Went FW (1969) Fungi associated with stalactite growth. Science 166:386–387

Ambient Temperature Freshwater Microbial Tufas

Martyn Pedley

Department of Geology (Leicester), and School of Geography, University of Hull, Hull HU6 7RX, UK

Abstract. Ambient temperature tufas are formed by a combination of physico-chemical and biological precipitation processes. The former dominate higher flow regimes, where escape of CO_2 directly into the atmosphere provides the stimulus for calcium carbonate precipitation. Deposition associated with microbiological processes (biofilms) appear to be most efficient at sheltered or even static water sites. Here, carbonate is precipitated in association with the biofilm as a by-product of microbial metabolic activity. The majority of biofilm associations include diatoms, cyanobacteria (filamentous and coccoid forms)and heterotrophic bacteria, forming prokaryote-microphyte biofilms. Carbonate precipitates, frequently a by-product of microbial metabolism, accumulate as surficial coatings on microbes and their extracellular polymeric substances (EPS), and sometimes within the EPS. Additionally, microdetrital carbonate can adhere to the sticky mucilaginous surfaces. Biomediated precipitates typically form clotted to thrombolitic micritic layers. Precipitation of calcite associated with purely physico-chemical processes produces coarser fringes of sparite.

1 Introduction

The term "tufa" will be used throughout this chapter to identify all ambient temperature freshwater carbonates in which macrophyte stands (mosses, lichens, aquatic and marginal higher plants, and trees) may comprise significant parts of the depositional frameworks.

A common belief is that tufa precipitation is entirely controlled by inorganic processes, such as degassing of CO_2 (e.g. Braithwaite 1979; Kempe and Emeis 1985; Ordoñez et al. 1986; Emeis et al. 1987; Lorah and Herman 1988). Many reports, however, demonstrate that growing surfaces are dominated by diatoms, bacteria and cyanobacteria (Love and Chafetz 1985; Pedley 1992, 1994). In contrast, thermal waters frequently are too inhospitable for higher vegetation generally and produce deposits (travertines) dominated by bacteria and cyanobacteria alone (see Chafetz and Folk 1984; Folk et al. 1985). Nevertheless, travertine fabrics can pass laterally into tufa fabrics with higher vegetation frameworks when waters approach ambient temperatures. Water chemistry (thermogene deposits; Pentecost and Viles 1994), however, may be distinctly different from ambient tufa systems (e.g. high sulphur content) and abnormally high strontium isotopic signatures may be passed on to the subsequent carbonate precipitates (Cipriani et al. 1977).

Studies from both botanical (Pentecost and Lord 1988; Irion and Muller 1968; Schneider et al. 1983) and geochemical viewpoints (Geurts 1976; Kempe and Emeis 1985) are common. A few have attempted working syntheses or classifications at either hand specimen or deposit scale (e.g. Buccino et al. 1978; Ordoñez and Garcia del Cura 1983; Pedley 1990; Pentecost 1993; Pentecost and Viles 1994; Violante et al. 1994; Pentecost 1995; Ford and Pedley 1996).

This chapter aims to draw together a range of observations and concepts leading to a clearer definition of the role of micro-organisms within tufas.

2 Physico-chemical vs Prokaryote-Microphyte Processes

Field observations (Kempe and Emeis 1985; Lorah and Herman 1988; Adolphe et al. 1989; Chafetz et al. 1994) demonstrate that both abiotic and biological precipitation occurs in active tufa settings These two complementary processes ensure that low-Mg calcite accumulates very rapidly. Generally abiotic calcite develops as coarse bladed fringes of rhomboidal crystals on all surfaces exposed to flow in sites proximal to groundwater resurgences enriched with calcium carbonate (see discussions in Pedley 1987, 1992). These spar fabrics develop rapidly, particularly if seed sites (detrital or biomediated micrite) are available. For example, fringe widths of up to 70 μm are recorded in tufa at Matlock Bath, Derbyshire, England (April to July) and such fringes rapidly entomb living leaves and stems of aquatic bryophytes (e.g. *Cratoneuron*) and liverworts. Initially, these non-luminescent calcite spar fringes do not appear to affect macrophyte survival (Pentecost 1998). However, photosynthesis becomes increasingly difficult under failing light and the older parts of the plants die back, but provide anchors for the growing shoots. Spar dominated deposits are best developed proximal to source or in areas where there is active agitation of the water body and degassing of CO_2.

In addition to spar there is a parallel development of biomediated micrite-grade cement. This is considered a true precipitate as it develops equally well in both

R.E. Riding and S.M. Awramik (Eds.)
Microbial Sediments

slow flowing and static water situations. It may alternate with spar layers or may totally dominate the deposit. Micritic fabrics range from fine particulate, through peloidal (70 to several hundred microns in diameter), to complex clotted or grummose textures (Pedley 1994). Potentially, micrite can develop on all exposed surfaces within tufa environments but it is less frequent or discontinuously developed in areas of fast flow (e.g. spar fringes). Scanning electron microscopy (SEM; Pedley 1994) and fluorescence light studies have revealed that the micrite precipitates are always associated with micro-organisms dominated by diatoms but sometimes associated with filamentous green algae, filamentous and coccoid cyanobacteria (esp. *Phormidium* and *Pleurocapsa*), and heterotrophic bacteria. Collectively, these comprise the prokaryote-microphyte biofilm community (Pedley 1992, 1994). The diatoms produce copious amounts of mucus (extracellular polymeric substances, EPS) used for adhesion to exposed surfaces (Fig. 1a,b). Significant amounts of EPS are also produced by the cyanobacteria and heterotrophs. The biofilm is composed of a dense association of individuals lying within and upon the communal EPS sheet which frequently is invested millimetres into the underlying tufa substrate.

A few prokaryote members of the biofilm (e.g. *Rivularia*) are obligatory precipitators of sparry calcium carbonate which is employed as colony support. Most others are non-obligatory precipitators; however, invariably there is an intimate association of micrite-grade precipitates on the microbes and within the EPS immediately around them (e.g. Winsborough and Golubic 1987).

The reason and precise mechanisms for carbonate bio-precipitation are uncertain but are discussed by Krumbein (1979) and Riding (1991). In cyanobacteria and heterotrophic bacteria the micrite precipitates appear to be an accidental by-product resulting from their metabolic processes. In essence, the biofilm community is a victim of its own success. Higher rates of metabolism lead to accelerated carbonate precipitation and burial.

Baker (1988) and Pedley (1992) suggested that gradients of decreasing CO_2 concentrations are developed in the immediate vicinity of biofilm surfaces. This is partly the result of CO_2 extraction during macrophyte photosynthesis (many biofilms develop directly on the submerged stems of semi-aquatic vegetation) and partly the result of diatom and cyanobacterial photosynthesis. In addition, a high organic nutrient supply generally is available for heterotrophic bacteria in active sites. This is supplemented by organic detritus from the autumn leaf fall.

Consequently, in areas with sluggish flow, local depletion of CO_2 by microbes may be the principal trigger for carbonate precipitation. The micritic precipitates appear to seed on to pre-existing nucleation sites such as peloids, embryonic crystals lining cyanobacterial sheaths and detrital particles. It is also clear from SEM studies (Lowe 1985; Winsborough and Golubic 1987; Love and Chafetz 1988; Pedley et al. 1996) that new precipitation sites may be initiated on the attachment pedicles of diatoms, on the outer surfaces of bacteria and possibly scattered within the communal EPS sheets. However, there is no clear evidence that the biofilm EPS act as "templates" for carbonate precipitation.

The micrite develops as fine microgranular aggregates intimately associated with living bacterial cell clumps (Fig. 1a) and commonly coats individual cocci. The multinucleate peloids subsequently appear to grow by further nucleation on to peripheral bacterial clumps and a macroscopic peloid results (Fig. 2a, b). Fluorescence microscopy reveals that cocci can remain alive within peloids even when heavily coated in precipitates. Significantly, macroscopic oncoids grow fastest on their most protected surfaces (i.e. down towards the

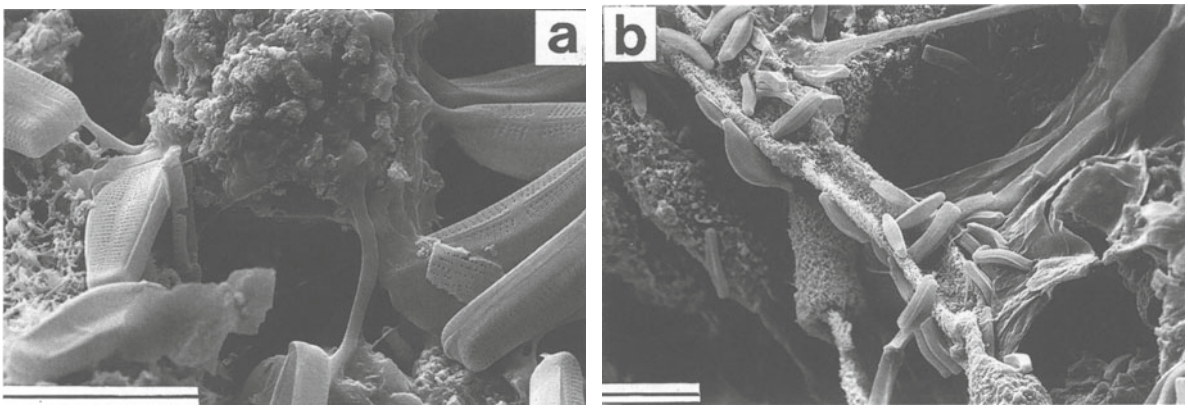

Fig. 1.a Biofilm association of micrite peloids and pennate diatoms (*Achnanthes* sp) attached by EPS stalks to substrate. River Lathkill, northern Derbyshire, England; *scale bar* = 10 μm. **b** Biofilm association of diatoms and filamentous cyanobacteria, the latter coated by biomediated micrite precipitates. River Lathkill, Derbyshire, England; *scale bar* = 20 μm

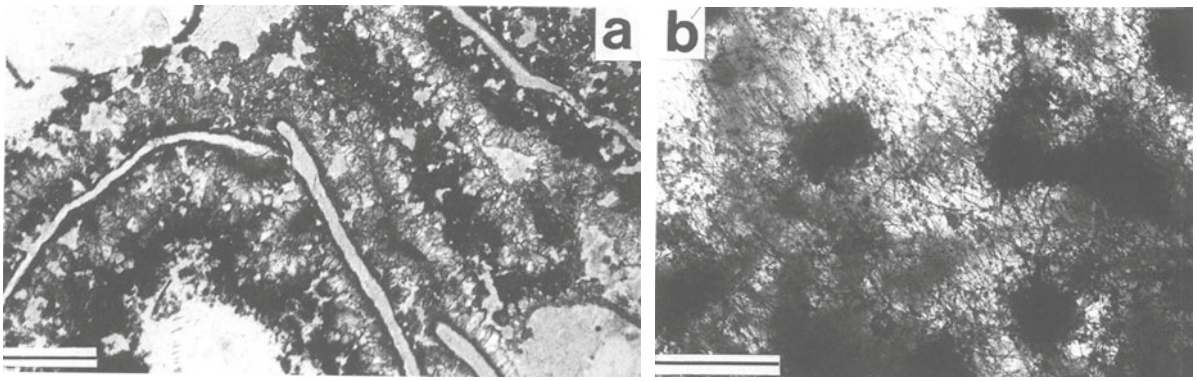

Fig. 2.a Typical development of freshwater isopachous fringe cements within a Holocene tufa. An initial thin, micritic isopachous fringe coats slot-like cavities, once leaves. (This is the fine "dust"line which is discontinuous and becomes peloidal towards the *extreme left*.) This is succeeded by a clear, coarse, sparry calcite fringe. A second, thick micrite fringe with a clotted texture coats the spar fringe. Caerwys quarry, North Wales; *scale bar* = 250 μm. **b** A biomediated fabric typical of static and sluggish flow situations. Multi-nucleate bacterial micrite pricipitates (fine clumps to large multinucleate peloids) suspended by green algal filaments (*Spirogyra*) within a 600-ml beaker experiment; *scale bar* = 25 mm

substrate, see Golubic and Fischer 1975). This suggests that the communal EPS may play a significant role in the colonial redistribution of nutrients and waste products.

Peloids grow fastest under near static conditions, 1 month being necessary to produce the prokaryote-microphyte biofilm mediated peloids shown in Fig. 2b, which were grown in a 600 ml glass beaker (see Pedley 1994). Peloids rapidly coat both macrophyte and microphyte surfaces with a thin micrite layer showing a characteristic clotted texture. Further growth gives rise to the characteristic thrombolitic micrite textures seen in freshwater stromatolites and oncoids (cyanoliths).

Thick thrombolitic micrite growth is rarely observed where there is frequent biofilm damage. Here, alternations between spar and micritic isopachous fringes occur (Fig. 2a), giving rise to thick polycyclic cement developments often with discontinuous micrite fringe development.

Figure 3 summarises precipitate styles and locations (based on active sites in Croatia, Spain, the UK, and USA). In flowing water tufa encrustation coats all semi-aquatic and fully aquatic macrophytes, and freeform oncoids (black areas in Fig. 3a). Commonly, tufa growth is eccentrically developed on the leeward side of objects (Fig. 3c). Fluvial stromatolites are likewise elongated parallel to flow. Additionally, thin surficial films of tufa develop where carbonate-rich waters cover moss hummocks and plants in paludal settings (Fig. 3b). Under static and relatively slow flow velocities micritic precipitates alone develop and give rise to poorly banded thrombolitic fabrics (Fig. 3d). In areas of more active flow biofilms (Fig. $3e_1$) may temporarily be replaced by inorganic spar fringes (Fig. $3e_2$). When tranquil conditions return biofilms reestablish and micrite precipitation resumes as in Fig. 3f, taken from a subaqueous plant leaf (*Elodea*) in a static water body. These concepts fit well with the observation that inorganic precipitation dominates at resurgence points (Merz and Zankl 1991), headwater regions, and winter precipitates.

3 Tufa: A Freshwater Reef

Individual parts of tufa complexes (e.g. barrages) are best considered as freshwater reefs (see Pedley 1992, 1994). The majority are mound-like in profile. However, tufa reefs are dominated by in situ vegetable frameworks provided by aquatic mosses, liverworts, marsh and marginal higher plants, etc. (Lang et al. 1992). Animals play no significant role in freshwater reef development, consequently the descriptive terms phytoherm or phytostrome has been adopted by some workers (e.g. D'Argenio et al. 1981; Pedley 1992; Golubic et al. 1993).

The reef frameworks are ephemeral, often with rapid die-back each autumn. This loss is compensated by the early development of sparry and micritic, low-Mg calcite cements up to centimetres in thickness. Phytoherms in active flow situations typically are dominated by sparry, physico-chemical precipitated fringe cements.

Within the shelter porosity there are colonisation opportunities for grazing gastropods, insect larvae, ostracods, and isopods. Detrital and micritic carbonates frequently enter the framework interstices. Any remaining cavities remain voids in Holocene phytoherms and phytostromes though clear spar in-fills, sometimes with associated speleothems with iron and manganese oxide coatings developing in older deposits. Dissolution within cavities may be bacterially induced (Golubic 1979) and later developments of speleothems further obscure many primary fabrics (Golubic et al. 1993). Chafetz et al. (1994) records considerable fungal activ-

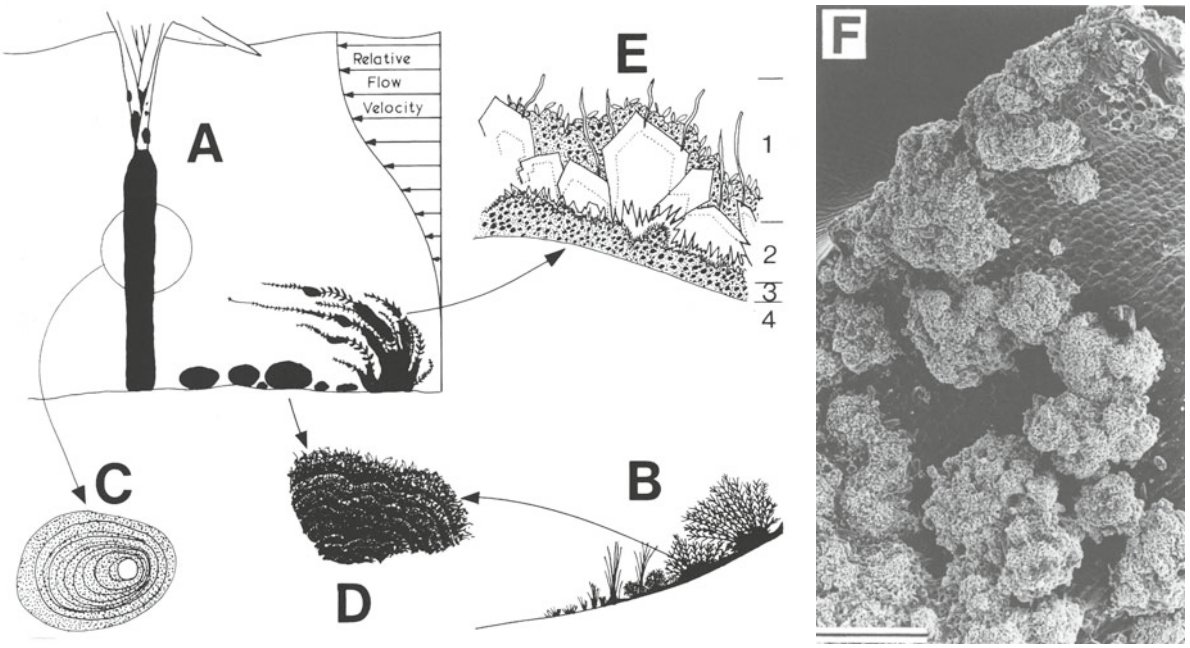

Fig. 3A–E. Summary diagram illustrating the types of precipitates common in tufa fabrics: **A** Sluggish flow situation with semi- and fully aquatic macrophytes being actively coated in precipitates (*black areas*). **B** Subaerial macrophyte growths on a poorly drained slope with accumulation of carbonate precipitate on all wetted surfaces (*black*). **C** Eccentric growth of fringe cements, frequently with greatest development of precipitates on the sheltered (leeward) side. **D** Oncoids as well as bryophyte bases subjected to static conditions are totally dominated by biofilm growth and repeated thrombolitic to powdery micrite precipitation; **E** Sites exposed to fluctuating flow suffer constant biofilm damage, recorded by switches from static to slow flow controlled microbially biomediated micritic fringes (*1, 3*) to high flow dominated, physico-chemical, sparry calcite fringes (*2*). The leaf surface is labelled *4*. **F** Typical clotted to peloidal, biomediated micrite precipitates on a leaf of *Elodea* from a pond site; *scale bar* = 200 μm

ity leading to extensive sparmicritisation within surficial gloomy cavities in waterfall sites at Plitvice, Croatia. The process is minor in fully subaqueous situations. Sparmicritisation appears, however, to be particularly common within cascade spray zones. Analogous fungal activity leading to sparmicritisation may commence at any time subsequent to deposition on damp tufa surfaces.

4
Examples of Contrasting Active Tufa Fabrics

In the following accounts three examples of active tufas from contrasting regimes serve to illustrate the common relationships between cement fabrics and microbial communities in: (1) natural flowing, (2) natural static water, and (3) anthropogenic leachate situations.

4.1
Ddol, Caerwys, North Wales

A Holocene paludal deposit here supports an active natural tufa regime associated with a small carbonate-rich stream originating in the Carboniferous Limestone scarp to the immediate northeast (see field description in Pedley 1987).

4.1.1
Framework and Microbial Community

Microbial biofilm communities are developed on all semi-aquatic vegetation (e.g. *Petasites*, grasses and fallen branches). In sheltered sites initial low-Mg, micritic carbonate encrustations are associated with diatoms, coccoid bacteria, cyanobacteria and occasional filamentous blue-green cyanobacteria (Fig. 4a). These thin coatings (10–50 μm) frequently bear irregular upper surfaces which are developed into thrombolitic textures comprised of micro-peloidal aggregates (see Figs. 1a, 2a, 3f), 30–80 μm in diameter.

In sites of aggressive water flow spar precipitation predominates. Here, the microbial biofilms are almost exclusively diatom frustules. The spar cements frequently bear holes, sometimes resulting from the poikilotopic development of spar crystals around cyanobacterial filaments (see Pedley 1987; Love and Chafetz 1988), but, as shown in Fig. 4b, the pock-marked spar surface may also result from spar growth around mucilaginous diatom anchorages (reported from elsewhere by Lowe 1985; Emeis et al. 1987; Winsborough and Golubic 1987; Chafetz et al. 1991; and Pedley et al. 1996).

Collectively (see Fig. 2a from the nearby Caerwys quarry site, Pedley 1987) the two cement types form

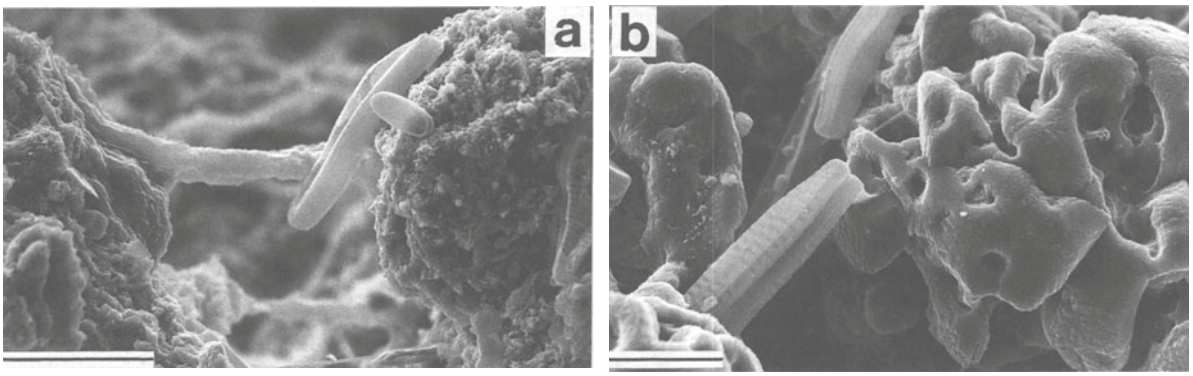

Fig. 4.a Peloid development associated with diatoms and coccoid bacteria at a sheltered site within the stream, Ddol Nature Reserve, near Caerwys, North Wales; *scale bar* = 20 μm. **b** Spar precipitates in an active flow situation at Ddol, showing the development of pits and depressions around former attachment points of diatoms EPS; *scale bar* = 10 μm

distinct isopachous fringes, commonly, first micrite then bladed spar. Thrombolitic (micro-peloidal) micrite fills much of the remaining void space. The majority of the barrage construction in the Caerwys quarry is composed of these associations, which contrast markedly with the friable lime mud-dominated pool deposits between the barrages.

4.2
Lagunas Lengua and Redondilla, Ruidera Natural Park, Spain

This example involves microbial dominated, skeletal stromatolitic tufas developed in static lake bodies within the Ruidera Pools Natural Park, about 75 km east of Albacete, central Spain (see Pedley et al. 1996). In this semi-arid region transverse barrages (internal fabrics identical to the Caerwys example) have developed in a gorge site forming barrage lakes (12–20 m deep). Thick lacustrine stromatolitic growths are developed around the vertical lake and spill-over margins.

The stromatolitic developments, accessible in Laguna Lengua and L. Redondilla when these pools virtually dried out (1991–1996), can be divided into three depth zones: an upper overhang which forms a flat topped bench upon which the marginal aquatic vegetation formerly stood; a middle zone dominated by laterally accreting mammilate growth forms; a lowest level, down to the lake floor lime mud sediments, dominated by short, vertically orientated, conical stromatolite colonies.

4.2.1
Framework and Microbial Community

The scanty primary framework of the mammilate growth forms is composed of delicate fronds of aquatic bryophytes (see *Didymodon, Barbula*) together with their extensive rhizoids. The microbial community developed upon the surfaces of this primary framework is almost totally dominated by diatoms, coccoid bacteria and cyanobacteria (*Chlorococcales*). Diatom "stalks" are commonly coated by abundant, discrete micritic grains which appear perforated by the stalks (Fig. 5a). Some of these micro-crystals grow to spar grade and may be shed to the lake floor immediately beneath the vertical stromatolite wall. Others, held in place by mucilaginous strands, become bound together by coccoid bacterial clump developments(Fig. 5b). Clumps of micro-peloid aggregates progressively develop into thrombolitic micrite sheets, showing macroscopic pustular surfaces to the stromatolites.

A weakly developed alternation of micrite-dispersed, granular spar fringes (diatom biomediation) and micro-peloidal fringes (coccoid bacterial dominated layers) gives rise to a banded fabric within the stromatolite heads. The conical stromatolite fabrics are identical to the mammilate developments except that the moss frameworks appear to be absent in these shady sites.

4.3
Anthropogenic Leechate Tufa

At Brook Bottom, 2 km south of Buxton, Derbyshire, England, an unusual, active tufa site is developed immediately downstream of an old waste tip containing calcium hydroxide ($Ca(OH)_2$), produced by lime burning earlier this century (Ford and Pedley 1996). Ambient temperature, meteoric water acting on the lime has formed a lime water solution which colours the entire stream milky white. The pH of this water is very high (approximately 12.0) in comparison to more typical values of 8.2 in active tufa sites of N. Derbyshire, and 7.2 in Laguna Lengua, Spain (Pedley et al. 1996). Small, weakly cemented micro-terraced dams, up to 1 m high, of calcite precipitates are developed along the water course, and finer, microgranular pool deposits are also forming. The dam morphologies are identical to ther-

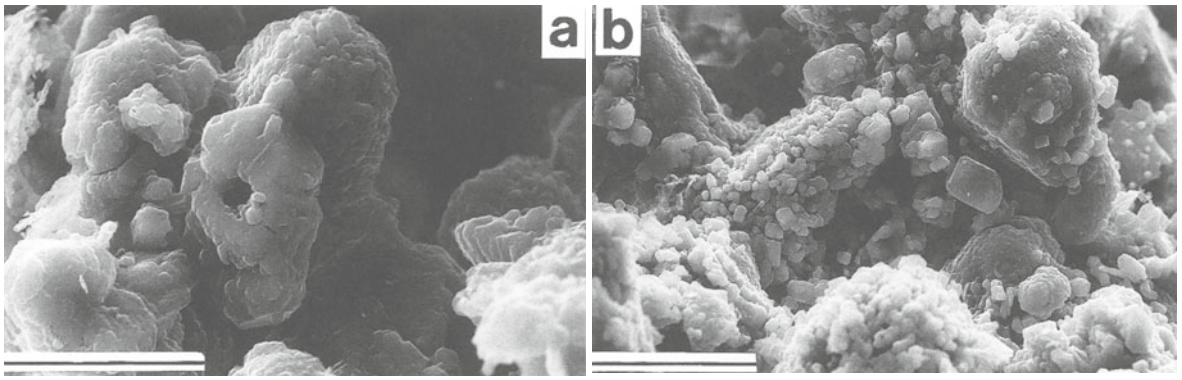

Fig. 5.a Holes in a calcite crystallite from marginal lake muds beneath a stromatolite overhang, typical of precipitates forming around diatom pedicles on the stromatolite surface. Laguna Lengua, Ruidera Pools Park, central Spain; *scale bar* = 5 μm. **b** Micrite association, binding larger calcite crystallites shown in **a**, formed by bacterial biomediation within outer living surfaces of laterally growing Laguna Lengua stromatolite; *scale bar* = 10 μm

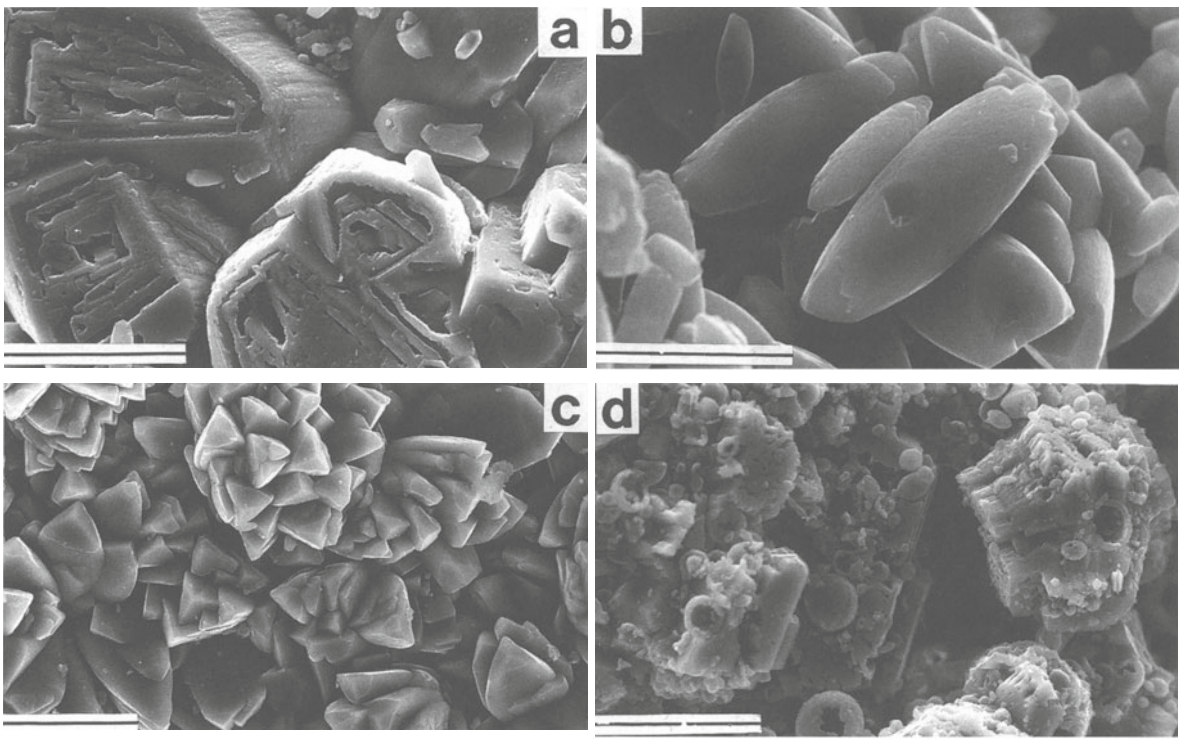

Fig. 6a–d. Typical calcite growth forms from physico-chemical precipitated tufa at Brook Bottom, Harpurhill, Buxton, England. **a** "Ruminant-tooth" calcite from the better cemented layers; *scale bar* = 10 μm. **b** "Rice-grain" calcite typical of softer layers; *scale bar* = 5 μm. **c** "Trigonal" spar from the better cemented layers;. *scale bar* = 10 μm. **d** "Bubble" micrite initially consisting of hollow spheres (common within pools). In this sample the bubbles have subsequently been incorporated into blocky "Swiss cheese" calcite cements (frequently with curved faces) within the harder layers; *scale bar* = 10 μm

mal travertine deposits with microgours and terracettes and have buried the upper part of the valley bottom in up to 1.6 m of carbonate precipitates.

4.3.1 Framework and Microbial Community

There is no effective framework within these deposits although marginal grasses do receive thick oncoidal coatings of up to 15 mm each growing season. The deposits are banded and this may be enhanced by surficial iron staining sometimes developed during the winter months.

An extensive search has revealed almost no microbial community. Rather, all the carbonate appears to be rapidly grown physico-chemical precipitate showing several bizarre crystal morphologies built on imperfect calcite lattices, allowing the development of curved crystal faces. Within the micro-dams the largest crystals (up to 15 μm wide), informally called "ruminant tooth" spar (Fig. 6a), show truncated faces normal to

the C-axis, barrel shaped curved sides and laminar to helical internal septae. "Rice grain" micrite (Fig. 6b) is extremely common, the crystals being 2–8 μm long with typical barrel shaped sides and imperfect rhombic terminations. Even the 8–12 μm-long rhombic spar (Fig. 6c) has an unusual trigonal habit with curved faces. Finally, "bubble" micrite is extensively developed as discrete, 2–6 μm diameter, hollow spherical grains within the pools and can be found incorporated into poikilotopic rhombohedral spar (also frequently with curved faces) to form "Swiss cheese" calcite (Fig. 6d). Banding within the micro-dams is achieved by an alternation of poorly cemented rice-grain and hollow bubble growth-forms with the better cemented ruminant tooth and Swiss cheese varieties. The pools are carpeted in loose bubble micrite.

5 Conclusions: Process and Product

Collectively, the foregoing examples illustrate that microbial biofilms are best established under tranquil to low velocity situations. Here, they mediate micrite-grade low-Mg calcite, usually in clotted or peloidal accumulations. Where flow conditions are variable and biofilm damage occurs the micrite fringes are succeeded by physico-chemical sparite fringes developed under aggressive flow conditions. Progressively, with establishment of the phytoherm fringe cement framework, internal flow velocities within the frameworks decrease and continuous microbial colonisation ensues. The latter manifests in the development of a final thick precipitate of thrombolitic micrite (e.g. Fig. 2a).

Where water is always static (e.g. Ruidera Pools) well defined spar fringe cements never develop on stromatolite surfaces. Although banded, the stromatolites are totally dominated by biofilm biomediated, thrombolitic, micrite- and microspar-sized crystals associated with diatom stalk holes.

Finally, in situations with exceptionally high physico-chemical precipitation rates (e.g. Brook Bottom), the microbial community is virtually absent. This is partly due to damage caused by stream flow but mainly is due to the chokingly rapid carbonate burial rates. Entirely inorganic sparry precipitates are dominant, especially bizarre crystalline calcite growth forms and a macro-morphology within the deposit resembling thermal travertine. The bubble micrite, on size grounds alone, could represent micrite coatings to coccoid bacteria, though no bacteria has so far been recognised within the spheres.

Acknowledgements. The content and style of this article have been greatly improved by suggestions from R. Riding, S. Golubic, H. Viles and two anonymous referees. All are warmly thanked for their suggestions.

References

Adolphe JP, Hourimeche A, Loubiere J, Soleilhavoup F (1989) Les formations carbonatees d'origine bacterienne: formations continentales d'Afrique Nord. Bull Soc Geol Fr 8:55–62

Anadon P, Zamarreno I (1981) Paleogene nonmarine algal deposits of the Ebro Basin, northeastern Spain. In: Monty CLV (ed) Phanerozoic stromatolites. Springer, Berlin Heidelberg New York. pp 140–154

Baker JH (1988) Epiphytic bacteria. In: Austin B (ed) Methods in aquatic bacteriology. John Wiley and Sons, pp 171–191

Braithwaite CJR (1979) Textures of recent fluvial pisoids and laminated crystalline crusts in Dyfed, south Wales. J Sediment Petrol 49:181–193

Buccino G, D'Argenio B, Ferreri V, Brancaccio L, Ferreri M, Panichi C, Stanzione D (1978) I travertini della bassa valle del Tanagro (Campania) Studio geomorfologia, sedimentologia e geochimico. Bol Soc Geol Ital 97:617–646

Cipriani N, Malesani P, and Vannucci S (1977) I travertini dell Italia centrale. Boll Serv Geol Ital 98:85–115

Chafetz HS, Folk RL (1984) Travertines: depositional morphology and bacterially constructed constituents. J Sediment Petrol 54:289–316

Chafetz HS, Rush PF, Utech NM (1991) Microenvironmental controls on mineralogy and habit of $CaCO_3$ precipitates: an example from an active travertine system. Sedimentology 38:107–126

Chafetz HS, Srdoc D Horvatincic N (1994.)Early diagenesis of Plitvice lakes waterfall and barrier travertine deposits. Geogr Phys Quat 48:247–256

D'Argenio B, Ferreri M, Ferreri V, Stanzone D (1981) Travertines of southern Italy. Texture, geochemistry and sedimentary model. Int Assoc Sedim Second Eur Meet Abstr, pp 43–36

Emeis KC, Richnow HH, Kempe S (1987) Travertine formation in Plitvice National Park, Yugoslavia: chemical versus biological control. Sedimentology 34:595–610

Folk RL, Chafetz HS, Tiezzi PA, (1985) Bizarre forms of depositional and diagenetic calcite in hot spring travertines, central Italy. In: Schneidermann N, Harris PM (eds) Carbonate cements. Soc Econ Pal Min Spec Publ 36 pp 349–369

Ford TD, Pedley HM (1996) A review of tufa and travertine deposits of the World. Earth Sci Revs 41:117–175

Geurts M-A (1976) Formation des travertines postglaciairs en Belgique In: Voigt T (ed) Colloque types Croutes et leur repartition regionales. Univ Louis Pasteur, Strassburg, pp 76–79

Golubic S (1979) Carbonate dissolution. In: Trudinger PM, Swaine DJ (eds) Biological cycling of mineral forming elements. Elsevier, Amsterdam, pp 107–129

Golubic S, Fischer AG (1975) Ecology of calcareous nodules forming in Little Connestoga Creek near Lancaster, Pennsylvania. Verh Int Verein Limnol 19:2315–2323

Golubic S, Violante C, Ferreri V, D'Argenio B (1993) Algal control and early diagenesis in Quaternary travertine formation (Rocchetta a Volturno, central Apennines. In: Baratolo F, DeCastro P, Parente M (eds) Studies on fossil benthic algae. Boll Soc Paleont It Spec 1:231–247

Irion G, Muller G (1968) Mineralogy, petrology and chemical composition of some calcareous tufa from the Scwäbische Alb, Germany. In: Muller G, Friedman GM (eds) Recent developments in carbonate sedimentology in central Europe, Springer, Berlin Heidelberg New York, pp 156–171

Kempe S, Emeis K (1985) Carbonate chemistry and the formation of Plitvice lakes. Mitt Geol-Paleont Inst Univ Hamburg 58:351–383

Krumbein WE (1979) Calcification of bacteria and algae. In: Trudinger P, Swain DJ (eds) Biogeochemical cycling of mineral forming elements. Elsevier, Amsterdam, pp 47–68

Krumbein WE (1987) Biolaminated deposits. Springer, Berlin Heidelberg New York, p 183

Lang T, Pascal A, Salomon T (1992) Caractérisation pétrographique de divers carbonates continentaux holocènes du Jura français (Arbois, Chalain, Dortan). Implications paléogeographiques. Z Geomorph NF 36:273–291

Love KM (1985) Petrology of Quaternary travertine deposits Arbuckle mountains, Oklahoma. Thesis, Houston University, p 240

Love KM, Chafetz HS (1988) Diagenesis of laminated travertine crusts, Arbuckle Mountains, Oklahoma. J Sediment Petrol 58:441–445

Mertz M, Zankl H (1991) The influence of sheath on carbonate precipitation by cyanobacteria. Spec Vol Boll Soc Paleont Ital 1:325–331

Ordoñez S, Garcia del Cura MA (1983) Recent and Tertiary fluvial carbonates in central Spain. In: Collinson JD, Lewin J (eds) Ancient and modern fluvial systems. Spec Publ Int Assoc Sediment 6:485–497

Ordoñez S, Gonzalez-Martin JA, Garcia del Cura MA (1986) Sedimentacion carbonatica actual y paraactual en las Lagunas de Ruidera. Rev Mat Proc Geol (Universidad Complutense, Madrid) 4:229–255

Pedley HM (1987) The Flandrian (Quaternary) Caerwys tufa, north Wales: an ancient barrage tufa deposit. Proc Yorks Geol Soc 46:141–152

Pedley HM (1990) Classification and environmental models of cool freshwater tufas. Sedim Geol 68:143–154

Pedley HM (1992) Freshwater (Phytoherm) reefs: the role of biofilms and their bearing on marine reef cementation. Sedim Geol 79:255–274

Pedley HM (1994) Prokaryote-microphyte biofilms and tufas: a sedimentological perspective. Kaupia. Darmstadter Beitr Naturges 4:45–60

Pedley HM, Ordonez S, Gonzalez-Martin JA, Garcia del Cura MA, Taylor D (1996) Climatically controlled fabrics in freshwater carbonates: a comparative study of barage tufas from Spain and Britain. Palaeogeogr Palaeoclimatol Palaeoecol 121:239–257

Riding R (1991) Classification of microbial carbonates. In: Riding R (ed) Calcareous algae and stromatolites. Springer, Berlin Heidelberg New York, pp 21–51

Pentecost A (1993) British travertines: a review. Proc Geol Assoc 104:23–39

Pentecost A, Lord T (1988) Postglacial tufas and travertines from the Craven district of Yorkshire. Cave Sci 15:15–17

Pentecost A, Viles H (1994) A review and reassessment of travertine classification. Geogr Phys Quat 48:305–314

Pentecost A (1995) The Quaternary travertine deposits of Europe and Asia Minor. Quaternary Science Reviews 14:1005–1028 classification. Geogr Phys Quat 48:305–314

Pentecost A (1998) The significance of calcite (travertine) formation by algae in a moss-dorunated travertine from Matlock Bath, England. Archy Hydrobiol 143:487–509

Schneider J, Schroeder HG Le Campion-Alsumard T (1983) Algal micro-reefs- coated grains from freshwater environments. In: Peryt TM (ed) Coated Grains. Springer, Berlin Heidelberg New York, pp 284–298

Violante C, Ferreri V, D'Argenio B, Golubic S (1994) Quaternary travertines at Rochetta a Volturno (Isernia, central Italy). Facies analysis and sedimentary model of an organogenic carbonate system. Pre-meeting fieldtrip guidebook, International Association of Sedimentologists ‚Ischia'94' 15th regional Meeting, Italy, p 23

Winsborough BM, Golubic S (1987) The role of diatoms in stromatolite growth: two examples from modern freshwater settings. J Phycol 23: 195–201

Microbial Precipitates Around Continental Hot Springs and Geysers

Robin W. Renaut[1], Brian Jones[2]

[1] Department of Geological Sciences, University of Saskatchewan, Saskatoon, Saskatchewan, S7N 5E2, Canada
[2] Department of Earth and Atmospheric Sciences, University of Alberta, Edmonton, Alberta, T6G 2E3, Canada

Abstract. Thermophilic microbes have long been implicated in the formation of travertine and siliceous sinter. Precipitation of $CaCO_3$ at thermal springs is induced mainly through degassing of CO_2. Cyanobacteria and other bacteria can play a role in calcite and aragonite nucleation in warm (20–40 °C) and mesothermal (40–75 °C) hot springs, and through photosynthesis and other biochemical processes may mediate some mineral precipitation. Many fabrics in warm-spring and mesothermal travertines preserve evidence of microbes. Travertine precipitated at hyperthermal (>75 °C) spring vents is mainly abiotic and commonly exhibits high-disequilibrium crystal morphologies. Silica precipitation in hyperthermal springs and geysers results mainly from rapid cooling and evaporation. Microbes, however, can play an important role by providing templates for silica nucleation and by controlling development of many sinter and geyserite fabrics.

1 Introduction

Microbial communities form brightly coloured mats around hot springs and geysers that are in stark contrast to the pale siliceous sinter or travertine that precipitates from the thermal waters. The possibility that microbes contribute to mineral precipitation at hot springs was first studied in detail by Weed (1889), who examined hot spring deposits at Yellowstone National Park, Wyoming. Walter's (1976; Walter et al. 1972, 1976) research on siliceous microbialites at Yellowstone rejuvenated interest because they resemble some Precambrian forms, including *Conophyton*. The seminal study by Chafetz and Folk (1984), however, stimulated much interest in spring deposits by showing that bacteria can play an important role in travertine formation.

Hot spring deposits commonly contain bizarre crystal textures (e.g., Folk et al. 1985; Jones and Renaut 1995, 1996a). The resemblance of some silicified hydrothermal microbes to microfossils in Archean chert has motivated taphonomic research (e.g., Oehler 1976; Ferris et al. 1988). Recently, there has been speculation that extraterrestrial fossils may resemble modern thermophiles (Bock and Goode 1996). Thermal spring deposits, therefore, may answer many questions related to microbial roles in mineral precipitation.

Using examples from Canada, Kenya, and New Zealand (Fig. 1), we review the main types of precipitates found around continental hot springs and geysers, and consider the role of microbes in their formation.

2 Continental Hot-Spring Deposits

Hot spring deposits can be divided into "travertine" ($CaCO_3$), and "siliceous sinter" (mainly opaline silica: $SiO_2.nH_2O$). We agree with Ford and Pedley (1996) that the term "sinter" should be limited to siliceous spring deposits. Fossil travertines are mainly formed of calcite, whereas most paleosinters are quartz formed by diagenetic transformation of hydrous silica (e.g. Trewin 1994; Walter et al. 1996). Although other minerals, such as Fe-Mn oxides, metal sulphides, zeolites and clays, are precipitated at some springs they are not considered here.

There is no formal definition of "warm" and "hot" springs in sedimentological usage. We use warm for springs with a vent water temperature of 20–40 °C; hot springs have water temperatures of >40 °C. Above ~40 °C aragonite is the dominant $CaCO_3$ polymorph precipitated from spring waters (Folk 1994). Hot springs with temperatures from 40–75 °C are referred to as "mesothermal", whereas those with temperatures of >75 °C are termed "hyperthermal". Hyperthermal springs are hotter than the maximum tolerance temperature of cyanobacteria.

Travertine or sinter is precipitated (1) at and around the spring vent, and (2) on the discharge apron, where thermal waters flow into the local drainage system. Generally, warm and mesothermal springs precipitate $CaCO_3$, whereas hyperthermal springs with neutral to alkali chloride waters precipitate amorphous silica. Where alkali chloride waters have a high HCO_3^- content, $CaCO_3$ and silica may precipitate from the same fluid (Jones et al. 1996). Hydrothermal alteration and sulphide precipitation dominate at springs with acid sulphate waters; only minor sinter precipitates because H^+ ions inhibit polymerization of dissolved silica. If the thermal waters remain undersaturated with respect to $CaCO_3$ and amorphous silica, travertine and sinter do not form even if microbes are abundant.

The morphology of spring deposits is broadly similar in travertine- and sinter-precipitating systems. Nevertheless, there are differences that are related to water temperature and (or) hydrodynamics. Precipitates

R.E. Riding and S.M. Awramik (Eds.)
Microbial Sediments

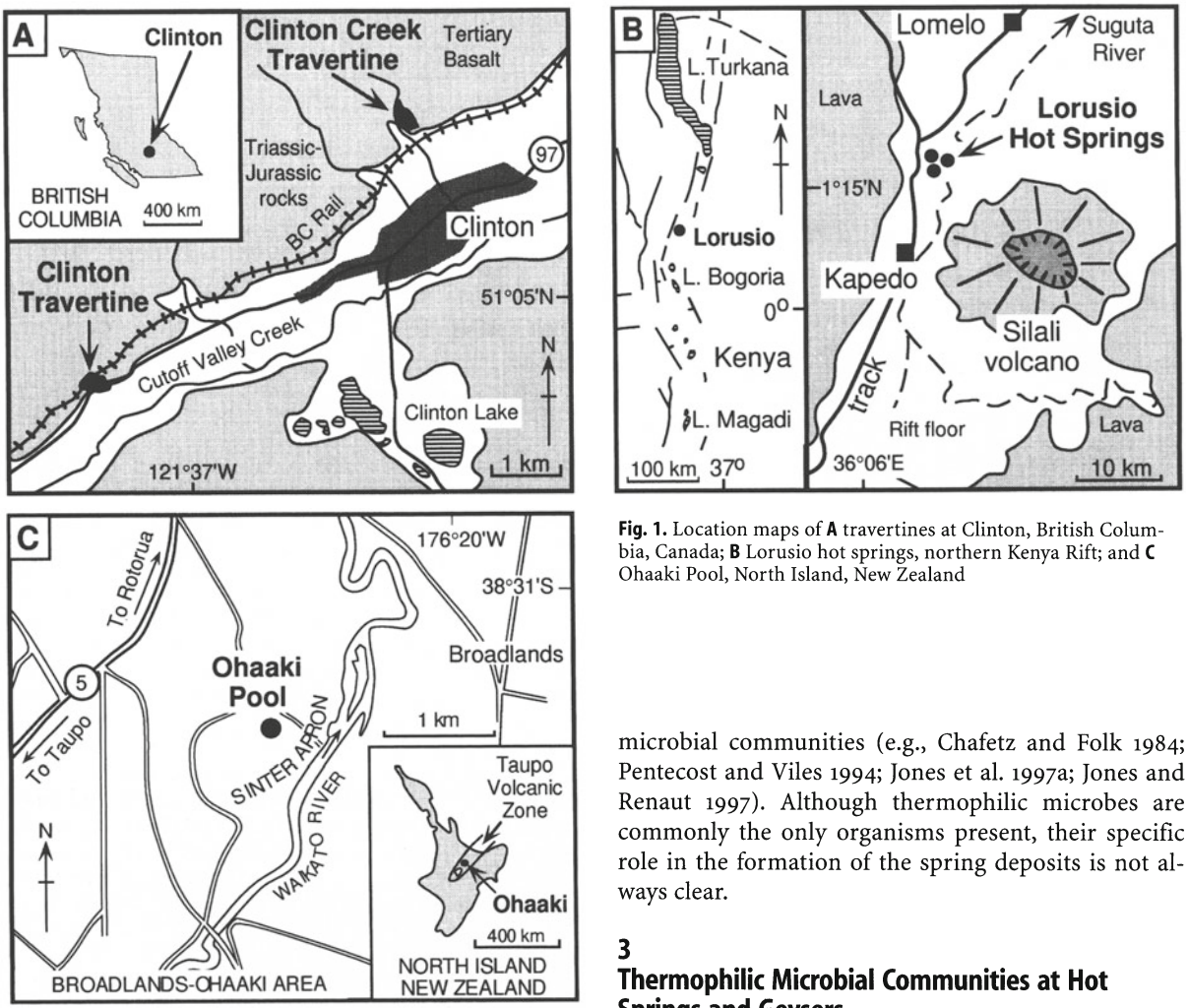

Fig. 1. Location maps of **A** travertines at Clinton, British Columbia, Canada; **B** Lorusio hot springs, northern Kenya Rift; and **C** Ohaaki Pool, North Island, New Zealand

from spray, for example, are more common in sinter because travertine rarely precipitates from boiling spring water. *Vent deposits* include mounds (cones, chimneys), pool-rim dams, fissure ridges, spicules, pisoids, and hydrothermal explosion breccias. Water flows across the discharge apron in unconfined sheets or shallow channels. *Discharge apron deposits* include rimstone pools and dams (terraces), sloping fan-shaped surfaces, coated grains, lily-pads, pond deposits and various outflow-channel flowstones (Chafetz and Folk 1984; Pentecost and Viles 1994). The boundary between vent deposits and discharge-apron deposits is commonly transitional. Travertine precipitated at sublacustrine thermal springs can form chimney-like structures. In contrast, sublacustrine hydrothermal silica is commonly gelatinous and rarely forms vent mounds.

Spring deposits exhibit fabrics and structures that reflect the temperature, hydrochemistry and dynamics of the spring waters and locally, the activity of benthic microbial communities (e.g., Chafetz and Folk 1984; Pentecost and Viles 1994; Jones et al. 1997a; Jones and Renaut 1997). Although thermophilic microbes are commonly the only organisms present, their specific role in the formation of the spring deposits is not always clear.

3 Thermophilic Microbial Communities at Hot Springs and Geysers

Hot-spring microbial mats are typically zoned downstream according to temperature (Brock 1978). In waters from ~ 75–100 °C, the organisms are nonphotosynthetic prokaryotes that include heterotrophic and chemolithotrophic bacteria, and archaea (Stetter 1996; Barns and Nierzwicki-Bauer 1997). Where visible, bacteria form streamers attached to rock surfaces. Cyanobacteria are present in waters <74 °C, commonly with photosynthetic bacteria such as *Chloroflexus*, and other bacteria. From ~74 to 65 °C, the dominant species at Yellowstone is *Synechococcus lividis*. In waters cooler than 65 °C, filamentous cyanobacteria appear (e.g., *Oscillatoria, Phormidium, Fischerella, Calothrix*), with eukaryotic algae (< 60 °C) and fungi. Diatoms are common where the temperature is < 40 °C. Most microbial mats develop vertical zonations that reflect chemical gradients which result from decomposition and other biological factors. Typically, photoautotrophs (mainly cyanobacteria) overlie heterotrophic prokaryotes at the base of a mat (Castenholz 1984; Ward et al. 1987).

4
Role of Microbes in Travertine Precipitation

4.1
Travertine Precipitation in Warm and Mesothermal Springs

Travertines precipitated from spring waters with temperatures of 20–75 °C have been described from Italy (e.g., Folk 1994; Guo and Riding 1994), the USA (e.g., Love and Chafetz 1990; Chafetz et al. 1991) and many other sites worldwide. Travertines precipitated at temperatures of < 40 °C are mainly calcite, whereas those precipitated at > 40 °C are typically aragonite (Folk 1994). Mesothermal travertines, therefore, are more prone to textural alteration during diagenesis. Rapid precipitation with accretion rates of several centimetres per year is common (Pentecost 1996).

Most carbonate precipitation at thermal springs is related to degassing of CO_2 when groundwaters rich in Ca^{2+} and HCO_3^- encounter the atmosphere. Evaporative concentration is locally significant. The role of microbes in travertine precipitation has been controversial. Pentecost (1996) showed that phototrophic and chemolithotrophic thermophilic microbes (e.g., *Synechococcus, Chloroflexus, Oscillatoria, Calothrix, Thermothrix*) can mediate precipitation by the reaction:

$$Ca(HCO_3)_2 = CaCO_3 + H_2O + CO_2$$

Other possible reactions involve denitrifying bacteria (e.g., *Pseudomonas*), ammonia producers, or the oxidation of S or H (Pentecost 1996). Many thermophilic bacteria and archaea utilise oxidised S-compounds as electron acceptors (e.g., *Desulfovibrio*). Sulphide is released as H_2S gas:

$$CaSO_4 + 2(CH_2O) = CaCO_3 + CO_2 + H_2O + H_2S$$

or may combine with reduced metallic ions to form sulphide minerals. Pentecost (1996, p. 104) estimated that up to 20% of the $CaCO_3$ precipitated at a hot spring may be attributable to biological activity.

The effects of microbes on travertine fabrics and structures are more obvious. Stromatolites and oncoids are common in terrace pools, ponds and on sloping surfaces, where $CaCO_3$ is precipitated upon and in microbial mats. Precipitation may be extracellular or replacive, and may affect unicells, filaments, sheaths, biofilms and extracellular polymeric substances (EPS). In some cases, the microbes are preserved; elsewhere, the evidence remains as fenestral or mouldic porosity (Fig. 2E).

One of the more remarkable microbial features are bacterial "shrubs" (Chafetz and Folk 1984). These aggregate structures, 1–3 cm in height and composed of $CaCO_3$ or Mn-Fe oxides (Fig. 2C,D), contain clumps, ~20 μm in diameter, of rod-shaped bacteria. They commonly form beds in terrace pools, especially in sulphurous springs. Chafetz and Folk (1984) suggested that $CaCO_3$ precipitates externally upon successive colonies of bacteria living on the substrate until laminated shrub-like structures are produced. Mediation by S-reducing and S-oxidising bacteria may be important in their growth. The term "shrub" has also been applied to other travertine structures, some of which may be partly abiotic crystal aggregates (e.g., Guo and Riding 1994). Other fabrics in travertines (e.g., some crystal rafts, vadose and phreatic cements) may have an dominantly abiotic origin.

Holocene Travertines at Clinton, British Columbia, Canada. Two travertine mounds are found near Clinton in Interior British Columbia (Fig. 1A). The Clinton Travertine is a fossil terrace-mound, 200 m wide and ~40 m high, that was precipitated from a warm spring which discharged on the lower valley-side slope of a paleomeltwater channel after deglaciation.

The Clinton Travertine formed as a series of terraces with local fan-shaped surfaces, similar to the larger examples at Mammoth, Yellowstone (Fig. 2A–C,E). The mound is entirely calcite. The interpretation as a warm spring deposit is based primarily on the travertine facies and fabrics. Cool water indicators (e.g., moss tufa; see Pedley, this Vol.) are sparse, although plant moulds are common near the mound margins. During travertine precipitation, a volcano (Meagher Mountain) was active < 50 km west of the spring.

The terrace pools are built by beds of micritic calcite (including skeletal crystals), honeycomb rock, crystal rafts, and stromatolites, preserved mainly as fenestral porosity (Fig. 2F). On sloping (< 10°) fan-shaped surfaces, beds of dendritic calcite crystals locally extend over many square metres. Rimstone dams bounding terrace pools (Fig. 2B) are composed of dendrites or palisade calcite, similar to "ray crystals" (see Chafetz and Folk 1984). Bacterial shrubs are rare, but bacterial clumps mineralised by Mn-oxides are found in the neighbouring Clinton Creek Travertine (Fig. 2D). Both calcite and aragonite precipitated at the latter terrace mound, due to temperature control or a variable Mg/Ca ratio in the spring waters.

4.2
Travertine Precipitation in Hyperthermal Springs

Hyperthermal travertines composed of calcite and (or) aragonite are present in Kenya, New Zealand and Japan. Strong degassing of CO_2 can yield high levels of supersaturation and rapid precipitation, resulting in high-disequilibrium crystal morphologies, including skeletal, platy and dendritic forms (Folk et al. 1985; Jones and Renaut, 1995, 1998; Renaut and Jones 1997). In boiling springs, high supersaturation is commonly attained when steam separates from the fluid, driving off CO_2 and resulting in an abrupt rise in pH. Precipitation is commonly pulsatory, particularly in intermittent and boiling springs, and growth by successive addition of subcrystals is common.

At temperatures of > 75 °C only nonphotosynthetic bacteria and archaea are likely to be present, but evidence for a significant microbial role in $CaCO_3$ precipitation is lacking. Filaments (1–4 μm diameter) and EPS locally cover crystal surfaces, but these form when cooler waters percolate through older crystal beds. Distal travertine facies can have the characteristics of cooler mesothermal travertines.

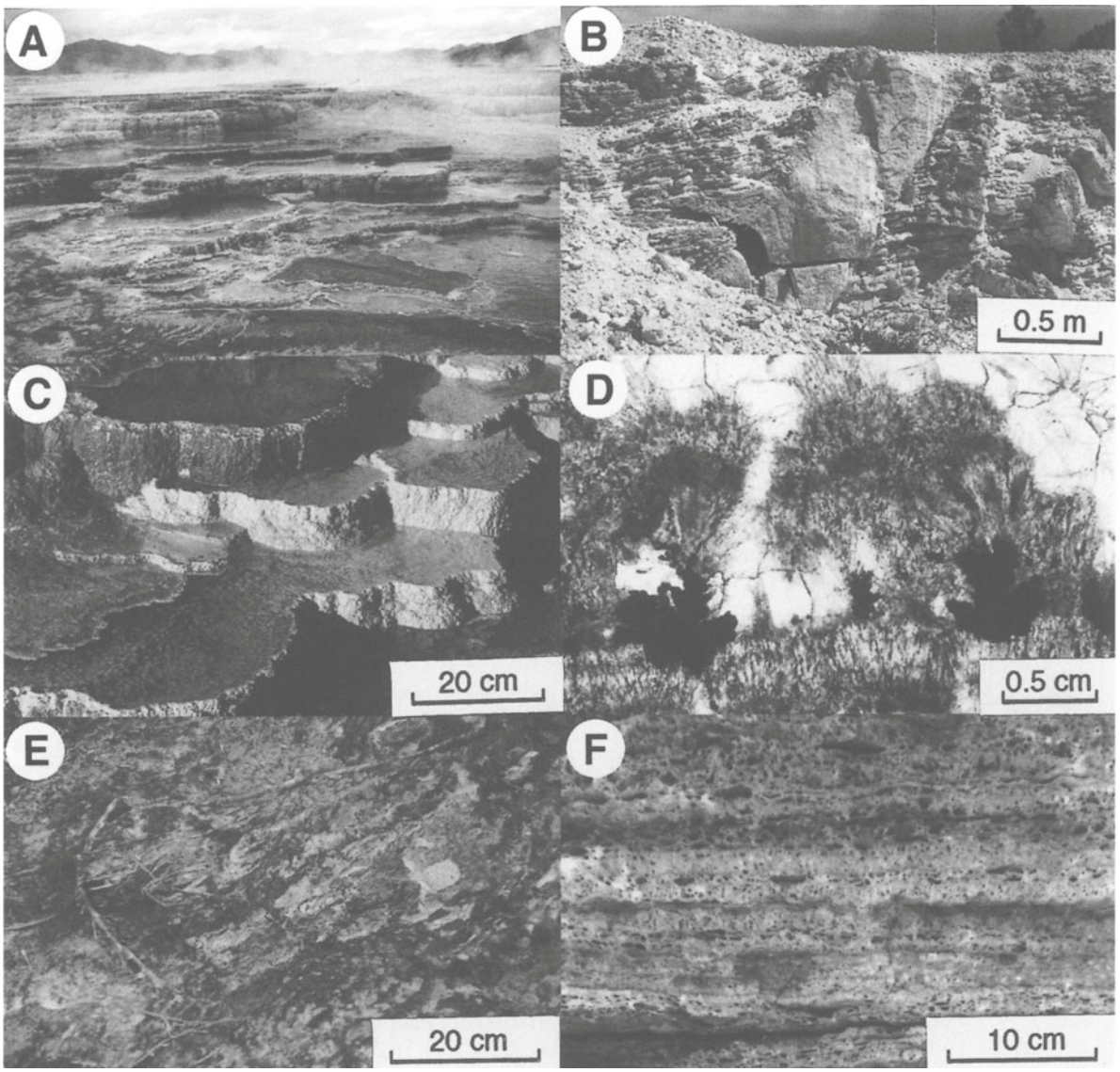

Fig. 2.A Large travertine terraces at Mammoth Hot Springs. **B** Section through rim of a terrace pool in the Clinton Travertine. **C** Terraces at Mammoth Hot Springs showing shallow pools behind rims. **D** Photomicrograph of small bacterial? Fe-Mn shrubs from a terrace pool in Clinton Creek Travertine. Shrubs are overlain by spherulitic fans of acicular aragonite that have partly inverted to calcite. **E** Microbial mat in outflow from Canary Spring, Mammoth, showing twigs being incorporated into travertine. **F** Clinton Travertine: stromatolitic layers with fenestrae and twig moulds that formed in a pool similar to that in **B**

Travertine Precipitation at Lorusio, Kenya Rift Valley. Hot springs at Lorusio in Kenya (Fig. 1B) discharge alkaline (pH 7.6), Na-HCO_3 waters (7.5 g/l TDS) at 82 °C from alluvial sediments. The largest spring pool, which lies at the edge of a low travertine mound, has a protruding ledge (Fig. 3A,B). Small „lily-pads" are forming in shallow (< 3 cm) outflow waters near the vent (< 4 m), where temperatures are 65 – 80 °C (Fig. 3C,D). Microbial mats are present where waters have cooled below 65 °C, but are not visible at most sites of active carbonate precipitation.

The ledges and lily-pads are composed of platy calcite crystals (Figs. 3E,G – I) up to 4 mm long, 4 mm wide, and 0.3 mm thick. Each platy crystal has its c-axis parallel to the shortest dimension. Aggregates of these crystals are arranged in complex branching structures (Fig. 3G) termed "pseudodendrites" (Jones and Renaut 1998). These structures have: (1) a straight to gently curved stem, (2) branches of variable length and orientation relative to the main plate, and (3) junctions between the branches and main plate that are planar or with shallow insets. Growth stages are marked by distinct discontinuities (Fig. 3E,F).

There is no visible evidence that microbes mediate the formation of the pseudodendrites in the Lorusio lily pads. This is also true for other dendritic, platy and skeletal crystals at other Kenyan hot springs (see Jones and Renaut 1995, 1996, 1998). In each case CO_2 degassing appears responsible for calcite precipitation. The microbes and biofilms found with the Lorusio lily-pads, for example, are located on crystal surfaces and are not interred inside the crystals (Fig. 3J).

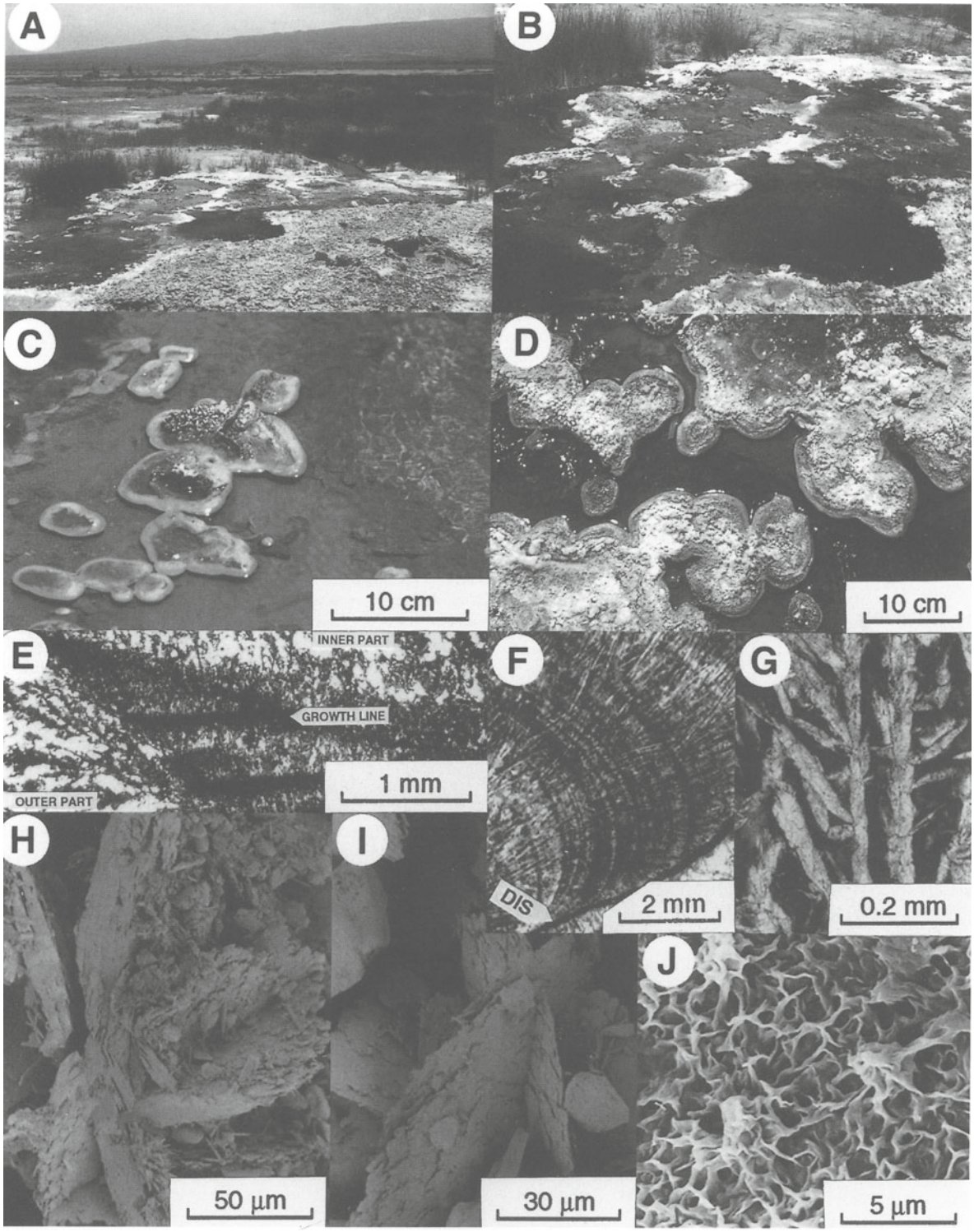

Fig. 3. Lorusio Hot Springs. **A** General view of spring LS-1 and travertine. **B** Travertine forming around main pool. **C** Lily-pads growing in shallow water next to the vent pool. **D** Close-up of lily-pads showing coalescence during growth. **E** Thin-section photomicrograph through rim of lily-pad showing growth lines and open framework of platy calcite crystals. **F** Thin-section photomicrograph through edge of a lily-pad showing a growth discontinuity. Radiating platy-calcite crystals form the edge of the lily-pad. **G** Thin-section photomicrograph showing platy calcite crystals with complex side-branches. Vertical cut through plates. **H, I** SEM photomicrographs of platy calcite crystals showing their complex interlocking morphology. **J** Reticulate coating (silicified EPS or clay?) that covers the surfaces of some platy calcite crystals

5 Role of Microbes in Sinter and Geyserite Precipitation

The finely laminated variety of sinter termed "geyserite" that is precipitated around the vents of geysers and boiling springs is commonly knobby, columnar or spicular (Fig. 4A–D). These attributes typify many stromatolites, thus a microbial role in sinter genesis has been discussed for more than a century (Weed 1889; Allen 1934). Boiling waters were formerly assumed to be sterile. Consequently high-temperature sinters were long considered abiotic in origin.

Silica solubility increases with increasing temperature, pressure and pH. Most silica precipitation at thermal springs has been attributed to the abrupt cooling of thermal fluids that have equilibrated with respect to quartz, chalcedony or volcanic glass at depth and then risen rapidly to the surface (White et al. 1956; Rimstidt and Cole 1983; Fournier 1985). Other processes that may induce silica polymerization include fluid loss upon boiling, evaporative concentration and changes in the pH of outflow waters. Silica polymerization is favoured at a neutral to slightly alkaline pH, but at high pH dissociation of silicic acid increases the amount of silica in solution (Fournier 1985). An abrupt decrease in pH might induce amorphous silica to precipitate from an alkaline thermal fluid that mixes with neutral cool lake- or groundwaters (Renaut and Owen 1988) or is microbially acidified (Pentecost 1996).

Waters discharging from most geysers and many hot springs are highly supersaturated with respect to amorphous silica. Thus, abiotic precipitation of sinter upon rapid cooling almost certainly takes place, following homogeneous or heterogeneous nucleation of amorphous silica (Fournier 1985). However, recent studies of sinter formation in Iceland (Konhauser and Ferris 1996; Schultze-Lam et al. 1995), New Zealand (Jones et al. 1997a,b, 1998), Kenya (Renaut et al. 1998), and Yellowstone (Cady and Farmer 1996) have shown that microbes can play an important role in the formation of many types of sinter and geyserite. Their role extends beyond controlling fabrics; in many cases, they serve as the initial sites of silica nucleation in hyperthermal springs and can become both encrusted and replaced (Cady and Farmer 1996; Jones et al. 1997a; Renaut et al. 1998). This process takes place through H-bonding between hydroxyl or carboxyl groups on microbial substrates and monosilicic or polysilicic acid in spring waters. Silica crystallites form then grow by subsequent hydrolysis and polymerization of the bound silicic acid (see Leo and Barghoorn 1976; Schultze-Lam et al. 1995). With time the weak hydroxyl and carboxyl bonds transform to stronger siloxane bonds. Spheroidal silica "beads" then precipitate upon the silicified microbial templates and agglomerate to form sinter.

Sinter precipitation at Ohaaki Pool, New Zealand. Ohaaki Pool (~850 m^2) is a former hot spring surrounded by ~10,000 m^2 of sinter. Before anthropogenic modifications related to geothermal power development, it discharged alkaline Na-HCO_3-Cl water at 95 °C (Browne and Lloyd 1987; Fig. 1C). The sinter around Ohaaki Pool incorporates an array of fabrics that are controlled by the filamentous and coccoid microbes that inhabited the area when the spring was active (Jones et al. 1998).

The pool rim is formed of columnar stromatolites, up to 2 cm in diameter, that radiate upward from a basal area on the pool wall (Jones et al. 1997a; Fig. 4C,D). The stromatolites are formed of amorphous silica that was precipitated on and around filamentous microbes. The proximal discharge apron, ~5 m wide, is formed of interlaminated calcite and sinter layers that contain few microbes. The sinter covering most of the discharge apron, however, exhibits several distinctive microbial fabrics. Stratiform stromatolites (Fig. 4G) are formed of alternating laminae of erect (<5 mm thick) and prostrate (<2 mm thick) filaments (Fig. 4G,H). These silicified mats contain *Calothrix* (Fig. 4E), *Phormidium*-like microbes, *Synechococcus*, and unidentified filamentous microbes. White coccoid microbial mats (Fig. 4I,J) are intercalated with the stratiform stromatolites. Some of their laminae appear devoid of microbes, whereas others contain densely packed coccoid microbes (*Synechococcus*? sp.) encased in amorphous silica. Beds of columnar "*Conophyton*" (Fig. 4F), 1–12 cm thick, are scattered across the discharge apron. The columns are formed around nonbranching filaments akin to *Phormidium*. Coccoid microbes are found in the columns and in sheets that connect the columns. The *Conophyton* are similar to those at Yellowstone (see Walter et al. 1976).

6 Discussion

Although we have progressed significantly since Weed's (1889) pioneering research, many questions that he posed still cannot be answered unequivocally. Microbes clearly contribute to many fabrics and facies in hot spring deposits (Figs. 2–4). It is less easy to determine if they play a *major* role in mineral precipitation, or were merely encased in essentially abiotic deposits because they are the only organisms that can survive

▷

Fig. 4.A Daisy Geyser, Yellowstone National Park. Sinter is actively precipitating on the discharge apron. **B** Geyserite mound at El Tatio, Chile, with silica oncoids (see Jones and Renaut 1997). **C-J** Sinters from Ohaaki Pool, New Zealand. **C** Stromatolitic rim around Ohaaki Pool. Note laminated sinter behind the rim. **D** Vertical cross section through columnar stromatolites that form around the rim of Ohaaki Pool. **E** Silicified filamentous microbes (*Calothrix*?) on the discharge apron. **F** Thin section photomicrograph through "*Conophyton*" that are found in isolated pockets on the discharge apron. **G** Thin section photomicrograph through stratiform stromatolites that form much of the discharge apron. **H** Thin section photomicrograph showing filaments changing from a prostrate to erect attitude. **I** White coccoid mat intercalated with stratiform stromatolites on the discharge apron. **J** Thin section photomicrograph showing stromatolitic banding in white coccoid mats

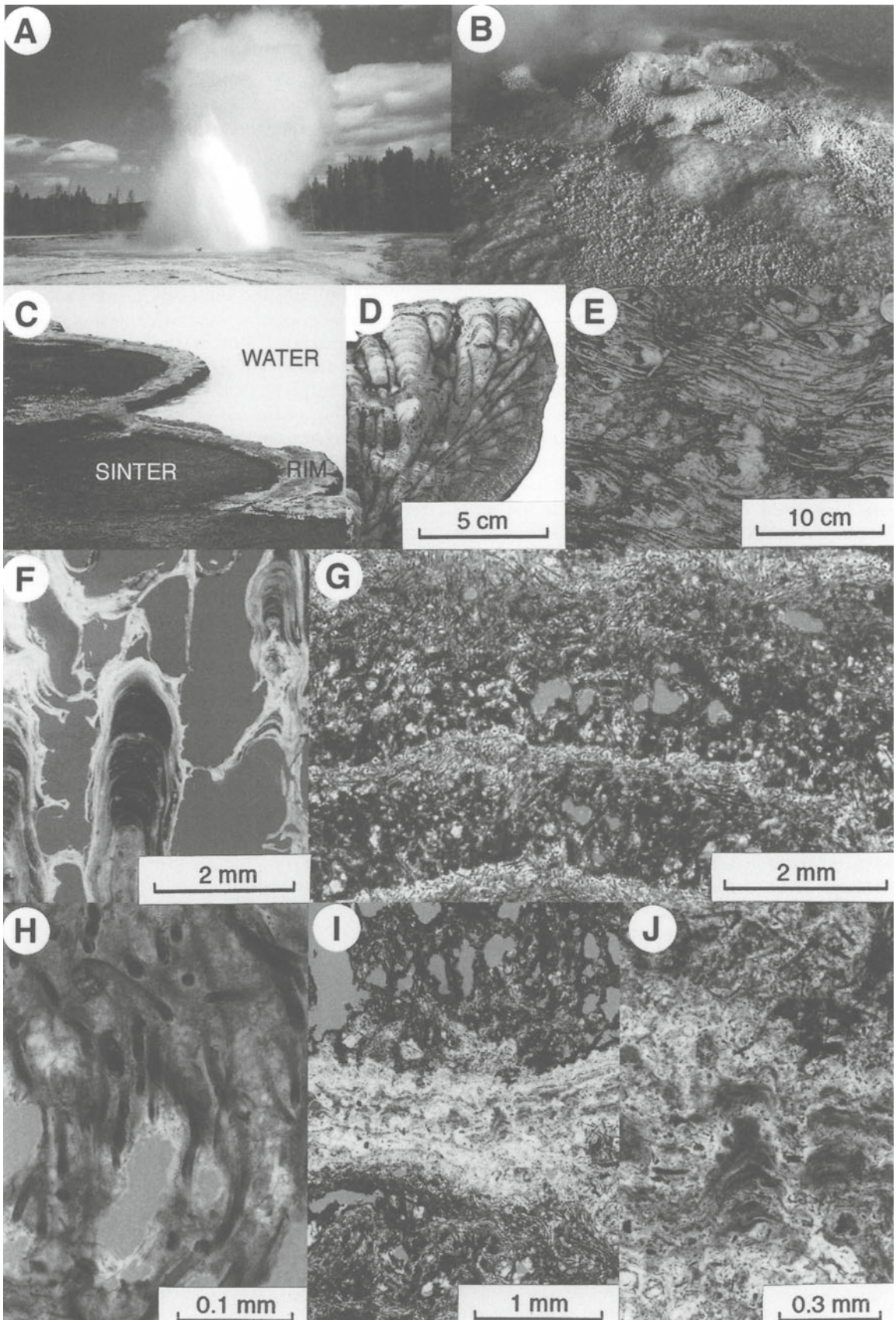
A
B
C
WATER
SINTER
RIM
D
5 cm
E
10 cm
F
2 mm
G
2 mm
H
0.1 mm
I
1 mm
J
0.3 mm

the harsh environment. Much of the recent evidence indicates that microbes and their extracellular secretions commonly mediate crystal nucleation at hot springs. Once stable nuclei have formed, crystal growth may continue in already supersaturated fluids. In such cases, which may apply to some sinters, it becomes semantic to argue whether the precipitate is "biotic" or "abiotic" (i.e., biotic nucleation vs abiotic precipitation). For sinter, mediation appears to be passive, in the sense that the physicochemical properties of the organic substrate induce nucleation.

There is a clearer case for arguing for biotic precipitation and active mediation when metabolic processes (e.g., photosynthetic removal of CO_2) not only induce nucleation, but *maintain* the level of mineral supersaturation needed for continued precipitation. This may be the case for some, but not all, travertines or parts of some travertine systems. The role of the microbes in mineral precipitation may become more important as their abundance and diversity increase with distance from the spring vent (Chafetz and Folk 1984). However, very high levels of supersaturation with respect to $CaCO_3$ or amorphous silica are common at hot springs. Sinter and calcite line many vent pools and shallow plumbing systems in boiling springs. Although anaerobic hyperthermophiles may live in such settings, it remains to be shown whether they influence mineral precipitation. Both for sinter and many travertines, microbes may mediate some mineral precipitation without being essential.

Despite these reservations, there is clear evidence that microbes play an important role in the formation many hydrothermal spring deposits. Bacterial clumps and shrubs and microbial mats have been recognised and described from many modern and ancient travertines world-wide. Although still controversial, nanobacteria have been recognised by scanning electron microscopy from carbonate- and silica-precipitating spring systems (Folk 1994; Folk and Chafetz, this Vol.), but their significance in mineral precipitation remains unclear. The role of hyperthermophilic archaea in mineral precipitation at continental hot springs is poorly known. Mineralised archaea would probably be difficult to distinguish from bacteria.

There are still many other problems in understanding the role of microbes in the formation of travertine and sinter. Many travertines exhibit exotic crystal morphologies, including skeletal crystals, dendrites and spherulites, that commonly result from rapid precipitation. Unusual crystal forms have commonly been attributed to microbial activity, but some of these crystals mimic the morphology of silicate minerals (e.g., feldspars) that crystallise from quenched magmas under conditions of high disequilibrium. It is important to discriminate those that are truly influenced by microbes from those that are abiotic precipitates forming under high disequilibrium (Jones and Renaut 1995), the influence of "foreign ions" (e.g., Fernández-Díaz et al. 1996), or other factors such as growth medium viscosity (Bucynski and Chafetz 1991). Do microbes and their exopolymers "poison" normal crystal growth or induce high disequilibrium, or are the unusual crystals simply reflecting complex crystal-growth patterns upon a biotic template?

7 Conclusions

In both carbonate and silica-precipitating spring systems, microbes control the development of many fabrics and structures. Most travertine precipitation results from degassing of CO_2 from fluids that are saturated with respect to $CaCO_3$ upon discharging at the surface. In warm and mesothermal springs cyanobacteria and other bacteria may mediate some carbonate precipitation. They can serve as sites for mineral nucleation, and through photosynthesis and other processes they may continue to mediate crystal growth. In hyperthermal springs only bacteria and archaea are present at the vent, but their role in carbonate precipitation remains to be demonstrated. Most hyperthermal travertines appear to be abiotic precipitates. In hyperthermal springs and geysers where sinter forms, microbes can act as templates for silica precipitation, mainly because of their active (hydroxyl and carboxyl) surfaces that act as magnets for silica in solution as mono- or polysilicic acid.

Acknowledgements. We thank Brian Pratt and two anonymous reviewers whose comments helped to improve the original manuscript.

References

Allen ET (1934) The agency of algae in the deposition of travertine and silica from thermal waters. Am J Sci 27:373–389

Barns S, Nierzwicki-Bauer, SA (1997) Microbial diversity in ocean, surface and subsurface environments. In: Banfield JF, Nealson KH (eds) Geomicrobiology: interactions between microbes and minerals. Min Soc Am Rev Mineral 35:35–79

Bock GR, Goode JA (eds) (1996) Evolution of hydrothermal ecosystems on Earth (and Mars?). Wiley, Chichester (Ciba Foundation Symposium no 202)

Brock TD (1978) Thermophilic microorganisms and life at high temperatures. Springer, Berlin Heidelberg New York

Browne PRL, Lloyd, EF (1987) Water dominated geothermal systems and associated mineralisation. NZ Geol Surv Rec 22:85–146

Buczynski C, Chafetz HS (1991) Habit of bacterially induced precipitates of calcium carbonate and the influence of medium viscosity on mineralogy. J Sed Petrol 61:226–233

Cady SL, Farmer JD (1996) Fossilization processes in siliceous thermal springs: trends in preservation along thermal gradients. In: Bock GR, Goode JA (eds) Evolution of hydrothermal ecosystems on Earth (and Mars?). Wiley, Chichester (Ciba Foundation Symposium no 202), pp 150–173

Castenholz RW (1984) Composition of hot spring microbial mats: a summary. In: Cohen Y, Castenholz RW, Halvorsen HO (eds) Microbial mats: stromatolites. Liss, New York, pp 107–109

Chafetz HS, Folk RL (1984) Travertines: depositional morphology and the bacterially constructed constituents. J Sed Petrol 54:289–316
Chafetz HS, Rush PF, Utech NM (1991) Microenvironmental controls on mineralogy and habit of $CaCO_3$ precipitates: an example from an active travertine system. Sedimentology 38:107–126
Fernández-Díaz L, Putnis A, Prieto M, Putnis CV (1996) The role of magnesium in the crystallization of calcite and aragonite in a porous medium. J Sed Res A66:482–491
Ferris FG, Fyfe WS, Beveridge TJ (1988) Metallic ion binding by *Bacillus subtilis:* implications for the fossilization of microorganisms. Geology 16:149–152
Folk RL (1994) Interaction between bacteria, nannobacteria, and mineral precipitation in hot springs in central Italy. Géog Phys Quat 48:233–246
Folk RL, Chafetz HS, Tiezzi PA (1985) Bizarre forms of depositional and diagenetic calcite in hot-spring travertines, central Italy. In: Schneidermann N, Harris PM (eds) Carbonate cements. Spec Publ Soc Econ Paleontol Mineral 36:349–369
Ford TD, Pedley HM (1996) A review of tufa and travertine deposits of the world. Earth Sci Rev 41:117–175
Fournier RO (1985) The behavior of silica in hydrothermal solutions. In: Berger BR, Bethke PM (eds) Geology and geochemistry of epithermal systems. Soc Econ Geol Rev Econ Geol 2:45–61
Guo L, Riding R (1994) Origin and diagenesis of Quaternary shrub fabrics, Rapolano Terme, Italy. Sedimentology 41:499–520
Jones B, Renaut RW (1995) Noncrystallographic calcite dendrites from hot-spring deposits at Lake Bogoria, Kenya. J Sed Res A65:154–169
Jones B, Renaut RW (1996) Skeletal crystals of calcite and trona from hot-spring deposits in Kenya and New Zealand. J Sed Res A66:265–274
Jones B, Renaut RW (1997) Formation of silica oncoids around geysers and hot springs at El Tatio, northern Chile. Sedimentology 44:287–384
Jones B, Renaut RW (1998) Origin of platy calcite crystals in hot-spring deposits in the Kenya Rift Valley. J Sed Res 68: 913–927
Jones B, Renaut RW, Rosen MR (1996) High-temperature (>90 °C) calcite precipitation at Waikite Hot Springs, North Island, New Zealand. J Geol Soc Lond 153:481–496
Jones B, Renaut RW, Rosen MR (1997a) Biogenicity of silica precipitation around geysers and hot-spring vents, North Island, New Zealand. J Sed Res A67:88–104
Jones B, Renaut RW, Rosen MR (1997b) Vertical zonation of biota in microstromatolites associated with hot springs, North Island, New Zealand. Palaios 12:220–236
Jones B, Renaut RW, Rosen MR (1998) Microbial biofacies in hot-spring sinters: a model based on Ohaaki Pool, North Island, New Zealand. J Sed Res 68:413–434
Konhauser KO, Ferris FG (1996) Diversity of iron and silica precipitation by microbial mats in hydrothermal waters, Iceland: implications for Precambrian iron formations. Geology 24:323–326
Leo RF, Barghoorn ES (1976) Silicification of wood. Bot Mus Leaflets Harvard Univ 25:1–47
Love KM, Chafetz HS (1990) Petrology of Quaternary travertine deposits, Arbuckle Mountains, Oklahoma. In: Herman JS, Hubbard DA (eds) Travertine – marl: stream deposits in Virginia. VA Div Min Resour Publ 101:65–78
Oehler JH (1976) Experimental studies in Precambrian paleontology: structural and chemical changes in blue-green algae during simulated ossilization in synthetic chert. Geol Soc Am Bull 68:117–129
Pentecost A (1996) High temperature ecosystems and their chemical interaction with their environment. In: Bock GR, Goode JA (eds) Evolution of hydrothermal ecosystems on Earth (and Mars?). Wiley, Chichester, (Ciba Foundation Symposium no 202), pp 99–111
Pentecost A, Viles H (1994) A review and reassessment of travertine classification. Géog Phys Quat 48:305–314
Renaut RW, Jones B (1997) Controls on aragonite and calcite precipitation in hot spring travertines at Chemurkeu, Lake Bogoria, Kenya. Can J Earth Sci 34:801–818
Renaut RW, Owen RB (1988) Opaline cherts associated with sublacustrine hydrothermal springs at Lake Bogoria, Kenya Rift Valley. Geology 16:699–702
Renaut RW, Jones B, Tiercelin J-J (1998) Rapid in situ silicification of microbes at Loburu hot springs, Lake Bogoria, Kenya Rift Valley. Sedimentology 45:1083–1103
Rimstidt JD, Cole RR (1983) Geothermal mineralization I: The mechanism of formation of the Beowawe, Nevada, siliceous sinter deposit. Am J Sci 283:861–875
Schultze-Lam S, Ferris FG, Konhauser KO, Wiese RG (1995) In situ silicification of an Icelandic hot spring microbial mat: implications for microfossil formation. Can J Earth Sci 32:2021–2026
Stetter KO (1996) Hyperthermophilic procaryotes. FEMS Microbiol Rev 18:149–158
Trewin N (1994) Depositional environment and preservation of biota in Lower Devonian hot-springs of Rhynie, Aberdeenshire, Scotland. Trans R Soc Edin Earth Sci 84:433–442
Walter MR (1976) Geyserites of Yellowstone National Park: an example of abiogenic ‚stromatolites'. In: Walter MR (ed) Stromatolites. Elsevier, Amsterdam, pp 87–112
Walter MR, Bauld J, Brock JD (1972) Siliceous algal and bacterial stromatolites in hot spring and geyser effluents of Yellowstone National Park. Science 178:402–405
Walter MR, Bauld J, Brock TD (1976) Microbiology and morphogenesis of columnar stromatolites (*Conophyton, Vacerrilla*) from hot springs in Yellowstone National Park. In: Walter MR (ed) Stromatolites. Elsevier, Amsterdam, pp 273–310
Walter MR, Desmarais D, Farmer JD, Hinman NW (1996) Lithofacies and biofacies of mid-Paleozoic thermal spring deposits in the Drummond Basin, Queensland, Australia. Palaios 11:497–518
Ward DM, Tayne TA, Anderson KL, Bateson MM (1987) Community structure and interactions among community members in hot-spring microbial mats. In: Fletcher M, Gray TRG, Jones JG (eds) Ecology of microbial communities 41:179–210
Weed WH (1889) Formation of travertine and siliceous sinter by the vegetation of hot springs. US Geol Surv, 9th Annu Rep, pp 613–676
White DE, Brannock WW, Murata KJ (1956) Silica in hot-spring waters. Geochim Cosmochim Acta 10:27–59

Evaporite Microbial Sediments

Gisela Gerdes[1], Wolfgang E. Krumbein[2], Nora Noffke[1]

[1] Carl von Ossietzky Universität Oldenburg, Marine Laboratory of the ICBM, Schleusenstraße 1, D-26382 Wilhelmshaven, Germany
[2] Geomicrobiology, Institute for Chemistry and Biology of the Marine Environment (ICBM), Carl von Ossietzky Universität Oldenburg, P.O. Box 2503, D-26111 Oldenburg, Germany

Abstract. Signatures of microbial life in shallow evaporite systems are discussed using examples from modern coastal hypersaline settings. Organisms contributing to microbial sediments are assigned to moderate halophiles (e.g. cyanobacteria, other phototrophic bacteria, diatoms, non-phototrophic eubacteria) and extremely halophilic taxa (e.g. green algae and halobacteria). Primary production creates the organic base upon which biogeochemical cycles are based that produce a variety of authigenic minerals found in deposits of hypersaline settings. Characteristic microbial sediments include stromatolitic laminae, biolaminoid facies and sedimentary augen structures. Communities dominated by stenotopic major taxa often contribute with less unambiguous laminated structures, e.g. flocculent organics, to the sedimentary record. Based on the criteria of brine depth and salinity, a biofacies classification of marine-derived microbial sediments is proposed.

1 Introduction

Evaporite microbial sediments are depositional records of microbial life in the presence of salt. These sediments occur in systems at different depths in which evaporites accumulate either within sediments, on the bottom of shallow bodies of brines, or due to pelagic crystal rains. Similarly, organics interlayered with evaporites either may originate from the pelagic rain of plankton blooms, or from benthic in situ formation of biomass.

Whereas in deeper evaporite basins benthic autotrophic processes may be due to colorless sulfur bacteria and ammonia oxidizers (Javor 1989), basin-margin evaporite systems are characterized worldwide by the abundance of photoautotrophic species. Mainly benthic cyanobacteria are producers of the organic substrate which supports the succession of numerous other microbes and metabolic pathways. Benthic cyanobacteria contribute to layered accretions of microbial biomass termed microbial mats. In the light of studies on modern hypersaline microbial mats, it is assumed that stromatolites were produced by similar diverse ecosystems.

Modern microbial systems of shallow surface brines provide ecologic models for the biomineralization capacity of analogous ancient systems, but nowadays do not have the extent shown by the evaporites of ancient epeiric seas. Under brine depths of a few meters or even less, evaporites in association with microbial mats have covered areas over hundreds of thousands of square kilometers (Decima et al. 1988). Such habitats concentrate organic matter that provides the base for biogeochemical cycles that have played a role in the formation of stratiform ore deposits (Brongersma-Sanders 1992). Sulfide-enriched microbial mats in contact with metal-enriched brines favor the accumulation of metal-sulfide complexes. When buried, the polymer-enriched mats act as permeability barriers that reduce brine migration and thus favor the contact of metal-bearing brines with organics produced and concentrated via microbial primary production. A well-known metalliferous deposit associated with significant amounts of organics is the Zechstein Kupferschiefer (Renfro 1974). Other metals associated with evaporite microbial sediments are gold (Dyer et al. 1994), lead, zinc and cobalt. A thorough discussion has been given by Javor (1989).

Microbial mats and related forms create and diversify the structural phenomena of evaporite sediments. The purpose of this chapter is to: (1) document characteristic depositional signatures of microbial life in shallow evaporite systems using examples from coastal hypersaline settings, and (2) introduce a biofacies classification that emphasizes the ecologic role of brine depth and salinity.

2 Heterogeneity of Coastal Evaporite Environments

Hypersaline settings favoring evaporite microbial sediments can be classified using the parameters listed in Table 1. The composition of athalassic (continental) brines is usually more variable than that of thalassic (marine-derived) saline waters. Various coastal evaporite settings take an intermediate position in as much as they receive water from both the sea and continental run-off. Microbial mats which thrive luxuriously in coastal evaporite settings are thus in contact with a great variety of dissolved ions from continental and marine sources.

The variation in environmental conditions in shallow evaporite settings is also a function of brine depth. This ranges from intrasedimentary brine tables (referred to as sabkhas) to several meters of surface brines (Table 1; Fig. 1).

R.E. Riding and S.M. Awramik (Eds.)
Microbial Sediments

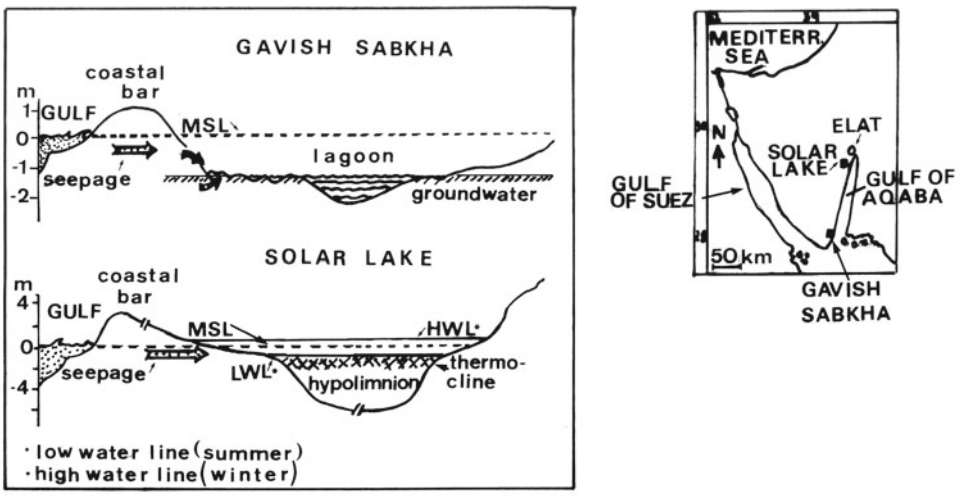

Fig. 1. Schematic cross-sections of the Gavish Sabkha (*top*) and Solar Lake (*bottom*), on the western shore of the Gulf of Aqaba, Sinai. Both are anchialine-type basin-marginal evaporite systems: depressions below sea-level closed by permeable bars, and constantly fed by seepage seawater. Both contain shallow littoral zones and deeper parts constantly filled with brine. Sabkha Gavish lagoon is 30–60 cm deep; Solar Lake basin is up to 6 m deep, and density-stratified during most of the year. (Modified after Gerdes and Krumbein 1987)

Table 1. Types of evaporite settings in which microbial sediments form

Continental vs marine evaporite settings (geographical terms)	
Continental	Focus of internal drainage, subterranean aquifers and/or streams, springs and surface run-off (Friedman 1980)
Marine	Fed by seawater (coastal settings often also by ephemeral streams and sheet floods from adjacent mountains)
Athalassic vs thalassic saline waters (brine composition)	
Athalassic:	Systems receive water from continental sources (see above)
Thalassic:	Systems fed by seawater
Shallow vs deep evaporite systems (bathymetric view)	
Intrasedimentary brines	Sabkhas (saline/dry mud flats)
Ephemeral surface brines	Ephemeral playas, salt pans
Perennial surface brines	
0.01–0.1 m	Shallow rims of lagoons
0.1–1 m	Peritidal lagoons, anchialine pools (e.g. Gavish Sabkha lagoon, 0.60 m)
1–10 m	Deeper anchialine pools (e.g., Solar Lake, Sinai, 6 m)
10–100 m	Playa lakes (e.g., Great Salt Lake, Utah, 10–12 m
>100 m	*Salt lakes (e.g., Dead Sea, 340 m); deep sea brines (Javor 1989)
Stratified vs non-stratified systems	
Stratified:	Most perennial surface brines more than a few meters deep
Non-stratified:	Shallow surface brines (water-mixing due to wind drift or imbalance between rates of evaporation and influx)
Plankton- vs benthos-dominated evaporite habitats	
Plankton dominance	Possible factors: greater basin depth, higher nutrient (phosphate) concentrations, competition (planktonic forms compete best for environmental resources), extreme salinity
Benthos dominance:	Possible factors: shallowness, ephemeral surface brines, benthic forms compete best under conditions of broader ranges of environmental factors (salinity and others)

2.1 Sabkhas

The Arabic word "sabkha" means a salt enriched flat (Kinsman 1969). Friedman et al. (1992) defined sabkhas as surfaces of deflation formed by the removal of dry, loose particles down to the top of the capillary water zone (For discussions of sabkha variation see Purser 1985 and Kendall 1992). In this chapter, the term sabkha refers to settings of subsurface groundwater. Because biofilms and mats are able to develop even at the lowest moisture levels, sedimentary surface layers wetted by capillary water are still ecologically important.

2.2 Shallow Surface Brines

Settings characterized by shallow surface brines are referred to as salinas, playas, hypersaline peritidal lagoons and "anchialine pools". Anchialine pools (Por 1985) are bodies of water within depressions below sea level closed by emergent reefs or porous bars and constantly fed by seepage seawater. Solar salt works are man-made anchialine pools controlled by dykes and flood gates. The Gavish Sabkha (Gulf of Aqaba) contains a natural anchialine pool (Fig. 1A). This area includes a variety of different facies (dry and moist saline flats, ephemeral and perennial surface brines, metahaline, moderate- and extremely-hypersaline water bodies). Such systems are traps of salts and nutrients which are concentrated to extraordinarily high values. They provide important models for understanding stromatolite diversification and biogeochemical cycles (Javor 1989; Cornée et al. 1992).

2.3. Stratified Surface Brines

Shallow surface brines are rarely density- or temperature-stratified since wind drift or the imbalance between rates of evaporation and influx cause short-term water mixing. On the other hand, perennial surface brines more than a few meters deep usually establish a stratification with denser brines at the bottom. Effects of stratification on the distribution of evaporites are considered by Kendall (1992). Solar Lake (Gulf of Aqaba) shows that stratification also has consequences for the composition of microbial communities. This marine-fed lake, up to 6 m deep, is density stratified during most of the year (Fig. 1B). The hypolimnion is anaerobic, hypersaline up to 180% TDS, and the temperature of the bottom brine can reach 65 °C. The complex, seasonally controlled hydrologic system of the lake causes mixing of the water body between July and September (Cohen et al. 1977). The shallow shelf of the lake is covered by microbial mats dominated mainly by eurytopic cyanobacteria (Fig. 2). In contrast, the anoxic hypolimnion reveals a clear dominance of soft flocculent fabrics composed of halophilic cyanobacteria (*Oscillatoria limnetica, Aphanothece halophytica*). Sulfur-dependent anoxy-photobacteria and anaerobic bacteria increase in number (Krumbein et al. 1977).

3 Major Groups Contributing to Microbial Sediments

At the level of primary production, hypersaline settings are dominantly characterized by few, but highly pro-

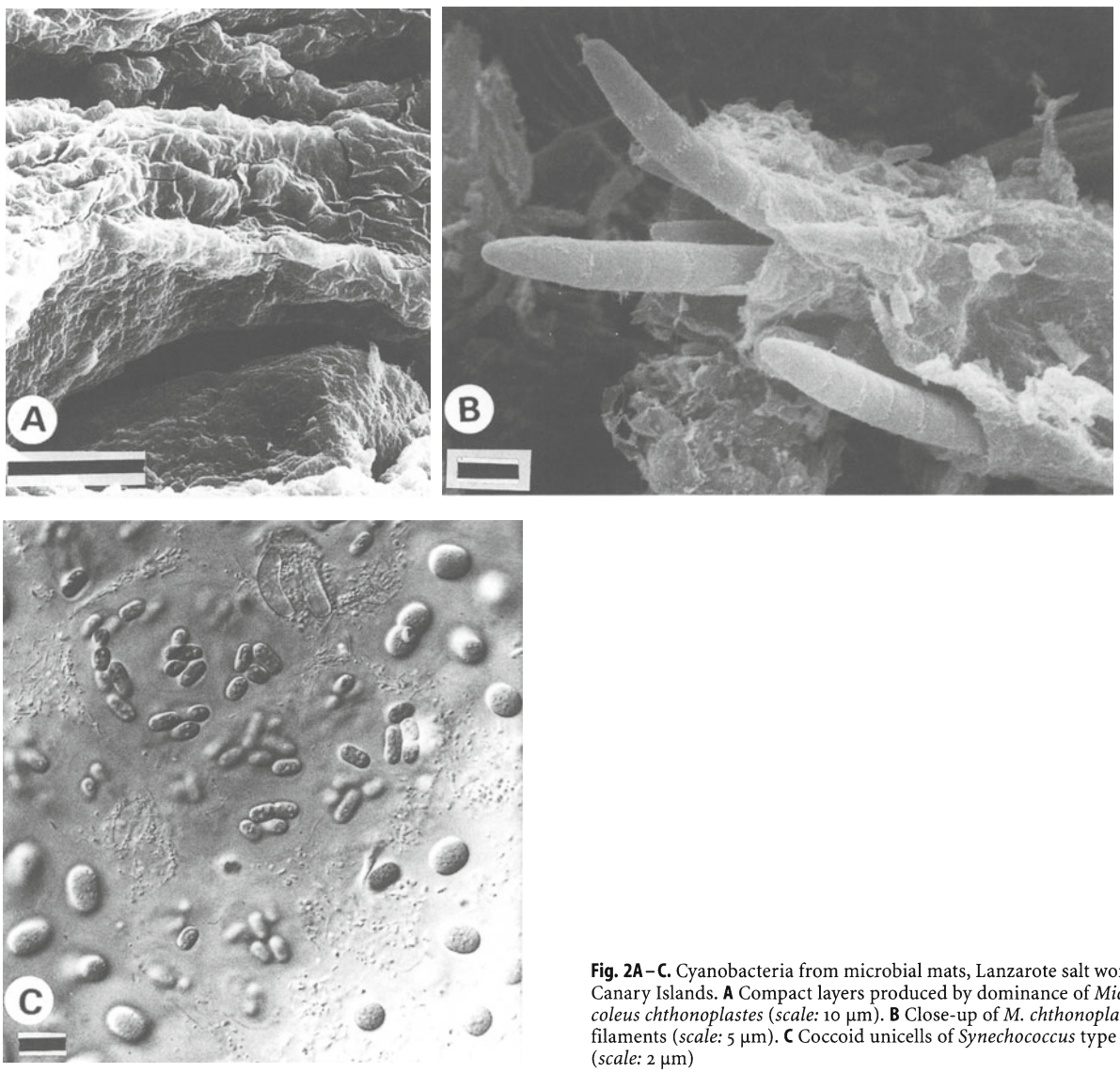

Fig. 2A–C. Cyanobacteria from microbial mats, Lanzarote salt works, Canary Islands. **A** Compact layers produced by dominance of *Microcoleus chthonoplastes* (*scale:* 10 μm). **B** Close-up of *M. chthonoplastes* filaments (*scale:* 5 μm). **C** Coccoid unicells of *Synechococcus* type (*scale:* 2 μm)

ductive, major groups. Among these are cyanobacteria, other phototrophic bacteria, diatoms and halophilic green algae.

Sabkhas and shallow brine bodies exhibit high levels of environmental variability. In such settings, microbial mats formed by benthic eurytopic cyanobacteria make the greatest contribution to sediments and sedimentary structures. Several of these systems exhibit regular recurrence of the species *Microcoleus chthonoplastes, Lyngbya* sp., *Entophysalis* sp. and *Synechococcus* sp. (Fig. 2). These mat-forming taxa are embedded in matrices of extracellular polymeric substances (EPS) which hold large amounts of water and thus serve as a protective mechanism against the osmotic stress that is particularly high in shallow surface brines. The EPS also buffers extreme temperatures and light intensity.

Distributional limits of mat-forming eurytopic cyanobacteria appear to correlate with a complex interaction of factors, rather than with a single factor such as salinity (Fig. 3). In the extremely shallow surface brines of the Gavish Sabkha, cyanobacteria-dominated microbial mats occur in almost all salinity ranges, beginning at the metahaline fringe (4–7%) and ending almost at the level of potash salts (>30%). In other hypersaline settings, perhaps only a few decimeters deeper, salinities just above the saturation value of gypsum (14–16%) limit the distribution of mats. Another aspect that probably controls mat-forming cyanobacteria is nutrient supply. Studies of solar salterns show that phosphate availability is a determinant of plankton dominance rather than benthic microbial mat development. Plankton dominance additionally has a shading effect on the benthic community development (Javor 1989).

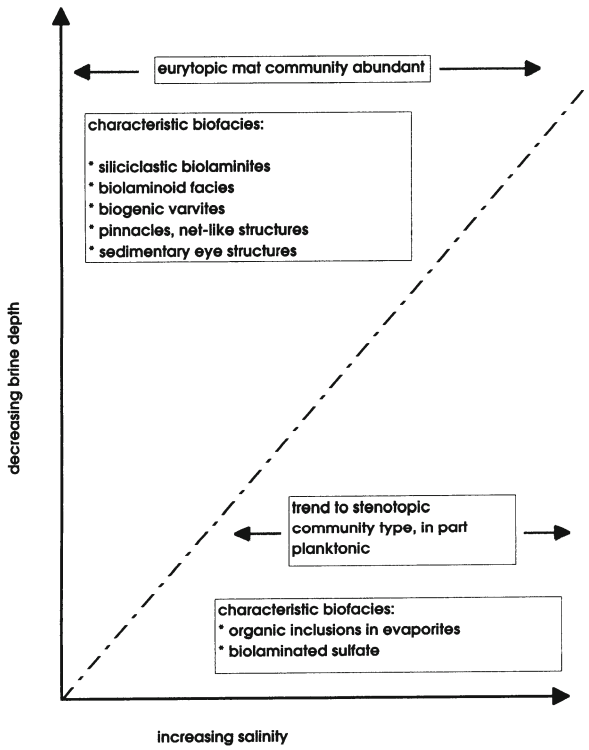

Fig. 3. Distribution model of major groups contributing to microbial sediments in evaporite settings, in relation to salinity and brine depth. Although both factors are not necessarily correlated, both control the local abundances of major microbial taxa and, thus, biofacies. Local decrease of brine depth usually correlates with broader environmental fluctuations that select for increased abundance of eurytopic major taxa that produce characteristic biogenic fabrics (summarized as biofacies characteristics). The shallower the setting, the less the eurytopic community type is limited by increasing salinity. Both increasing depth and extreme salinities select for increasing abundance of specialists (stenotopic taxa) only tolerating narrow ranges of environmental factors

Mats built by the eurytopic species mentioned above are not restricted to thalassic hypersaline environments. Javor (1989, Table 2.1) also reported their distribution in inland lakes and playas. As in the marine realm, true benthic microbial mats are restricted to lake margins. This may correlate with the plankton dominance in these lakes. In the Great Salt Lake, Utah, microbial mats made by filamentous cyanobacteria are restricted to shallow water areas. Javor (1989) refers to several alkaline hypersaline lakes that are nutrient enriched and plankton-dominated.

Increasingly uniform environmental conditions select for the distribution of specialized microbes (Fig. 3). Examples cultured from Solar Lake are *Oscillatoria limnetica*, *Phormidium* sp. and *Aphanothece halophytica* (Golubic 1980). These species can tolerate only narrower changes in salinity, thus, their distribution is restricted to zones where salinity fluctuations are minimal. In Solar Lake, this is mainly the hypolimnion (Fig. 1B). Mats produced by the halophiles are flocculent and differ considerably from the compact, rubber-like mats built by the eurytopic shallow-water community.

Purple sulfur bacteria (Chromatiaceae, Ectothiorhodaceae), and purple non-sulfur bacteria (Rhodospirillaceae) are well-documented in hypersaline microbial mats. Their enrichment obviously is favored by the gelatinous and fibrillar meshwork of cyanobacteria that acts as a light filter and oxygen protection shield. Extreme halophile phototrophic bacteria of the genus *Ectothiorhodospirillum* are also abundant in continental salt lakes. A detailed review is presented by Imhoff (1988; see also Javor 1989).

Planktonic eukaryotic green algae of the genus *Dunaliella* are abundant and widespread in inland lakes (e.g. the Great Salt Lake and the Dead Sea), in various solar salt ponds, and in the Gavish Sabkha lagoon. Most species are extremely halophilic, maintaining osmotic balance by the production of low molecular organic compounds such as glycerol.

Relatively large numbers of diatom species are abundant in hypersaline environments and contribute to

microbial mats, but never appear to dominate the benthic microbial biomass.

Almost ubiquitous in evaporite settings are halophilic archaebacteria and non-phototrophic eubacteria. Halobacteria possess specialized mechanisms to control Na^+Cl^- ion concentrations by the uptake of inorganic compounds such as KCl. This group is particularly abundant in extremely hypersaline brines where cyanobacteria-dominated microbial mats almost disappear. Various physiological groups of non-phototrophic eubacteria join in the evaporite microbial sediments. Their distribution in extremely hypersaline brines has been discussed by Javor (1989). It is assumed that Mg^{2+} intolerance may be an important factor limiting moderate halophile eubacteria in marine-derived strong brines. Moderate halophiles are relatively intolerant of Mg^{2+} and Cl^-, but relatively tolerant of K^+ and SO_4^{2-}. Halobacteria, on the other hand, show an opposite behavior with respect to Mg^{2+}, Cl^- and SO_4^{2-} (Javor 1989).

4 Depositional Records

Biogenic fabrics occurring in evaporite settings occupied by microbial mats are related to (1) species dominance, (2) biomineralization processes, (3) evaporite precipitation, and (4) stress deformation of mat-stabilized sediments.

4.1 Mat Facies Related to Species Dominance

Species diversity is defined as the degree to which different species in a given community are evenly distributed over the total number of individual organisms. In evaporite environments, a numerically even distribution of species does not occur or is rare. Numerical dominance of individual species is more common. The facies relevance of dominant morphotypes (filamentous or coccoid) is emphasized in the next section.

4.1.1 Stacks of L_h-/L_v-Laminae, Biolaminoids

Ensheathed filamentous cyanobacteria are very common in evaporite settings (Fig. 2). *Microcoleus chthonoplastes* is a cosmopolitan species found in various environments (discussions in Gerdes and Krumbein 1987). Multiple ensheathed filament bundles are typical of this species. The organisms are able to glide up and down in order to position themselves as close as possible to optimal light intensities. Mainly hormogonia, which differentiate from longer cell filaments, are motile. If the surface cover increases, or light conditions are reduced due to increasing water cover after intermittent exposure, hormogonia are able to respond phototactically and move upwards accumulating on or close to the new surface (Gerdes et al. 1991). Such repositioning establishes well-laminated internal structures (Fig. 4A). The buried organic matter, consisting of empty abandoned sheaths, immotile filaments and unicells, and EPS of other mat biota, provides significant cohesive strength.

Coccoid slime-ensheathed cyanobacteria with binary fission represent another very common type in evaporite systems. Examples are *Gloeothece* sp. and *Synechocystis* sp. These organisms increase their slime production in order to escape phototoxic conditions when they form the surface mats. Slime production is also stimulated by increase in salinity and temperature. Sediments composed of, or interwoven with, the polysaccharides are yogurt-like if brine is maintained, due to the dispersal and partial dissolution of the mucilage. All these conditions are particularly characteristic of shallow evaporite environments. Photosynthetically active populations of other species under the translucent mat benefit from the production of large quantities of gel since it is an ideal medium for the channeling of light.

In vertical section, *Microcoleus*-dominated mats appear as horizontally layered, bedding plane concordant laminae, which we call L_h-laminae. Since slime-supported coccoid mats are thicker than the flat and bedding-plane concordant L_h-laminae, we term them L_v-laminae (Fig. 4A,B). Under superficial surface brines, couplets of L_h- and L_v-laminae produce more or less regularly spaced biolaminated sequences. Guerrero and Mas (1989) postulated a physical sediment intercalation necessary to prevent the L_h- and L_v-laminae from mixing. In the shallow shelf of Solar Lake and in various solar salt works studied, such physical base is almost lacking due to the rarity of sedimentation events.

▷

Fig. 4A – E. Fabrics of evaporite microbial sediments. **A** X-ray of a vertical section showing various couplets of dark (L_h-) and light-gray (L_v-) laminae. L_h-laminae are made by winter populations of filamentous cyanobacteria (*M. chthonoplastes* dominant); L_v-laminae are made by summer populations of coccoid cyanobacteria (Solar Lake shallow shelf mats; *scale:* 2 cm). **B** Light microscopy of a stained thin-section showing a couplet of L_h-/L_v-laminae. *Top* L_h-lamina; *lower part* L_v-lamina (only laminoid). (Lanzarote salt works, *scale* 50 μm). **C** Thin section of calcareous ooze intermixed with coccoid cyanobacteria and EPS. *Arrow*, Pleurocapsalean nodules and faint sheaths of filamentous taxa (Gavish Sabkha, rim of lagoon; *scale:* 500 μm). **D** Thin-section showing the laminoid fabric due to dominance of coccoid cyanobacteria (compare *lower part* of **B**). *Arrow* In situ-formed carbonate particle. Gavish Sabkha lagoon (*scale:* 200 μm). **E** Macroscopic view of mat surface resembling "elephant skin texture" due to the formation of micropinnacles and net-like structures (Tunisia, shallow surface brines; *scale:* 3 cm)

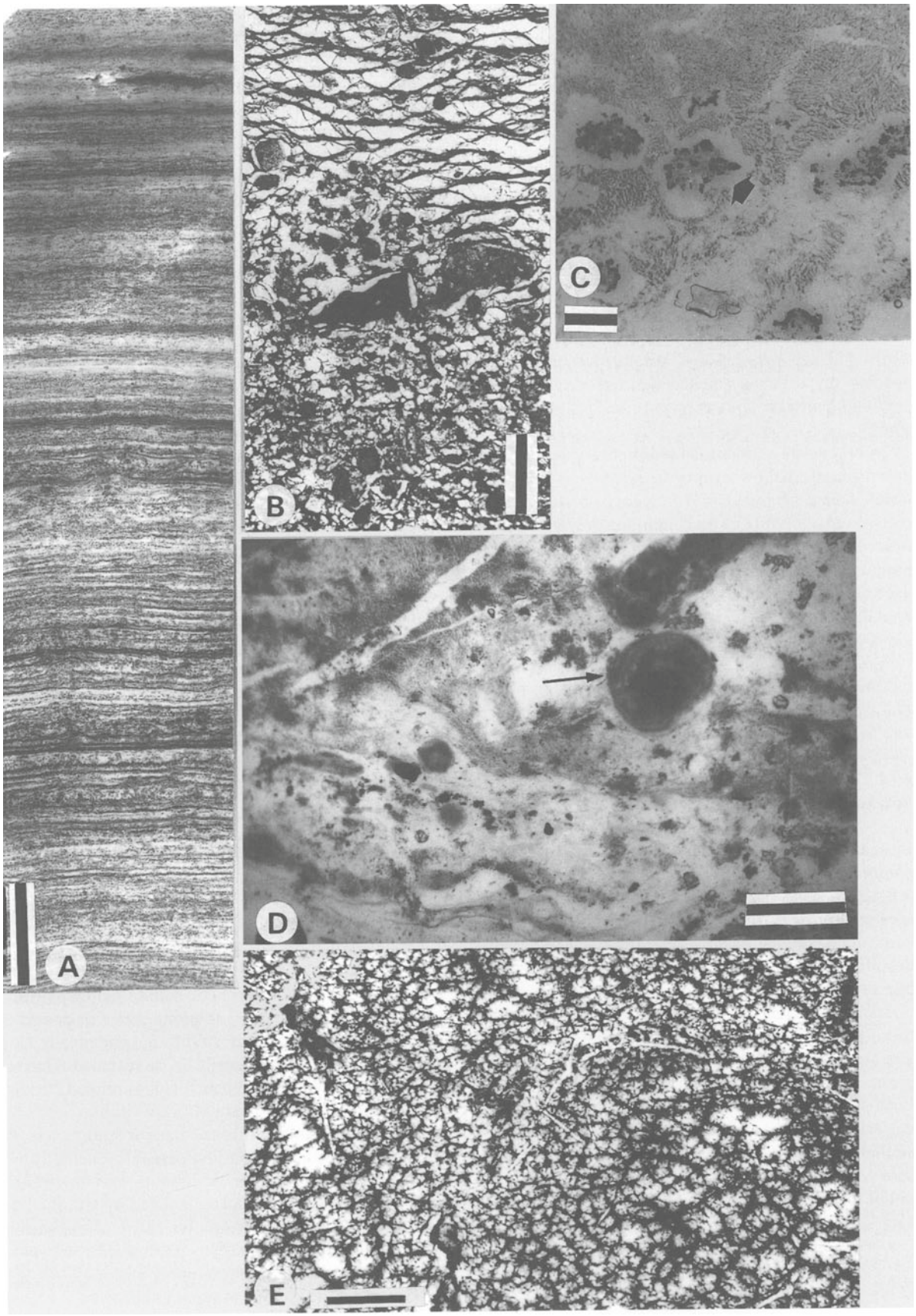
A
B
C
D
E

Nevertheless, *Microcoleus*-dominated and EPS-dominated couplets of laminae are clearly developed (Fig. 4A). This kind of lamination proceeds via mat-by-mat overgrowth. The microbes overgrow other surface mats in order to gain the most favorable positions within environmental gradients. The main triggering factor may be self-shading, although a chemocline shifting in day-night rhythm across the mat-water interface may also account for overgrowth phenomena. In salterns studied, the recurrence of lamina sets seems most likely to be a pattern of change in seasonal dominance between *Microcoleus*-dominated mats (associated with diatoms) in winter and coccoid cyanobacteria in summer (Gerdes et al. 1991). Dor and Paz (1989) described a similar seasonal dominance change between surface populations. We termed the regular spacing of vertically stacked laminae evolving from seasonal patterns "biogenic varvites" (Gerdes et al. 1991).

Another type of microbial sedimentary feature characteristic of shallow evaporite systems is "biolaminoid" fabric (Fig. 4C,D). The matrix material often consists of a mixture of mucilaginous polysaccharides, unicells and microcrystalline carbonates. Although filamentous taxa or their tubular relicts of empty sheaths are not infrequent, the unambiguous structure of horizontally continuous L_h-laminae is lacking. Only vague signs of lamination (laminoids) occur (Fig. 4D). This type of microbial sediment is dominantly characterized by unicellular cyanobacteria. The slime producers are mainly species of the genera *Gloeothece, Synechococcus* and *Synechocystis*.

4.1.2
Nodules, Pinnacles, Net-Like Surface Structures

In shallow surface brines of moderate hypersalinity, common coccoid cyanobacteria with multiple fission are pleurocapsaleans. Species of this group form colonies wherein each individual cell is encased by thick concentric lamellar sheaths. Pleurocapsalean colonies do not form flat and bedding-plane concordant mats but develop discontinuous, more or less concentric nodules (Fig. 4C). Sediment surfaces colonized by these populations exhibit a pustular structure. Other characteristic surface structures of microbial mats are pinnacles and net-like ornamental features (Fig. 4E). Both preferentially form under calm sheets of shallow surface brine. James G. Gehling (pers. comm.) found similar textures on fossil microbial mats of the Ediacara Member (South Australia) that resemble an "elephant skin".

4.2
Microbial Sediments in Evaporite Systems Associated with Carbonates

4.2.1
Basic Processes

Calcium carbonates are the dominant biogenic minerals precipitated in microbial mats of sabkhas and anchialine pools. Ca^{2+} enrichment is characteristic of hypersaline waters, but precipitation of carbonates in the water column above the microbial mats is rare (Javor 1989). However, various studies have provided clues that the microbial degradation of the in situ-formed organic matter and biogeochemical reactions lead to $CaCO_3$ precipitation (Fig. 5), thus governing the carbonate equilibrium in these mats (Krumbein et al. 1977; Cornée et al. 1992; Riege and Krumbein, this Vol.).

Several authors have stressed that bacterial sulfate reduction may be the main agent that also supports dolomite precipitation. However, although bacterial sulfate reduction is particularly active in microbial mats of hypersaline areas, precipitates more often consist of high Mg-calcite. Friedman et al. (1985) observed high Mg^{2+} enrichment of Solar Lake water and the organic material of the mats, but low dolomite contents in the carbonates. Instead, high Mg-calcite (up to 40% $MgCO_3$) was found. Conversely, gypsum and dolomite both occur where bacterial sulfate reduction is limited by extremely high salinities, as in salt pans or below the pycnocline of salt lakes (Friedman 1980). Hardie (1987) assumed that the increase in dissolved HCO_3^- due to metabolic activity is more important for dolomite formation than sulfate reduction.

Similarly, dolomite in ancient microbial deposits may be post-depositional, resulting from the high Mg^{2+} concentration in carbonates and organic matter. A bituminous character of many ancient dolostones may reflect the involvement of microbial communities (Fan et al. 1992).

Sulfate reduction is involved in a great variety of other secondary mineral formations (Ehrlich 1990). The presence of chemosynthetic sulfide-oxidizing bacteria (e.g. *Thiobacillus* sp.) suggests that it is possible that sulfur forms from the sulfide. Biochemically enriched elemental sulfur usually is ^{32}S-enriched relative to the associated sulfate. Ehrlich (1990) related ^{32}S enrichment in Messinian (Late Miocene) sulfur deposits of Sicily to processes within the narrow sulfur cycle of microbial sediments. Non-phototrophic chemolithotrophic sulfur bacteria in sediments and microbial mats of Australian saline lakes, isolated by Wood et al. (1991), contribute to the oxidative phase of the sulfur cycle in addition to oxidation by phototrophs or *Beggiatoa* sp. Such environments support a remarkably diverse range of physiological types of bacteria.

4.2.2
Mat Facies Associated with Carbonate Particles

In biolaminated buildups of hypersaline origin, in situ formation of non-skeletal carbonate particles is common (Friedman 1978; Krumbein 1979, Cornee et al. 1992; see also Riege and Krumbein, this Vol.). By analogy with structurally similar "augen" gneiss, the in situ formation of nonskeletal carbonate particles in microbial sediments is termed "sedimentary augen structure" (Fig. 5A,B; Dahanayake et al. 1985). Particle types precipitating in the microenvironment of microbial mats include oncoids, ooids and grapestone (Krumbein et al. 1977; Friedman et al. 1985). Folk (1973) mentioned peloid formation in microbial mats presumably by crystallization processes. Concentrically laminated phosphorite and iron particles are also interpreted to have formed in microbial mats (Soudry and Champetier 1983; Dahanayake and Krumbein 1985, 1986).

Coexistence of different morphotypes (ooids, oncoids, peloids and aggregate grains) in one and the same unit of microbial sediments reflects in situ formation (Gerdes et al. 1995). Within mat laminae, the particles characteristically are irregularly distributed. This points to the usually heterogeneous fabric of the microbiogenic matrix. If a small number of cells or cell colonies providing nucleation centers occur within large portions of viscous slime, this may give rise to separate carbonate particles (Fig. 4D). If groups of cells occur close together, this evidently favors the formation of grain aggregates (Fig. 5A). Particle growth causes the deformation of elastic tissues of filamentous mats (Fig. 5B).

4.3
Mat Facies Associated with Evaporites

In vertical sections of sabkha sequences, intrasedimentary gypsum crystals penetrate buried mats (Fig. 6A). Park (1977) stressed that evaporite minerals distort and even destroy lamination. In the Gavish Sabkha and several solar salt works studied, massive evaporite crusts develop at the sedimentary surface. The protective

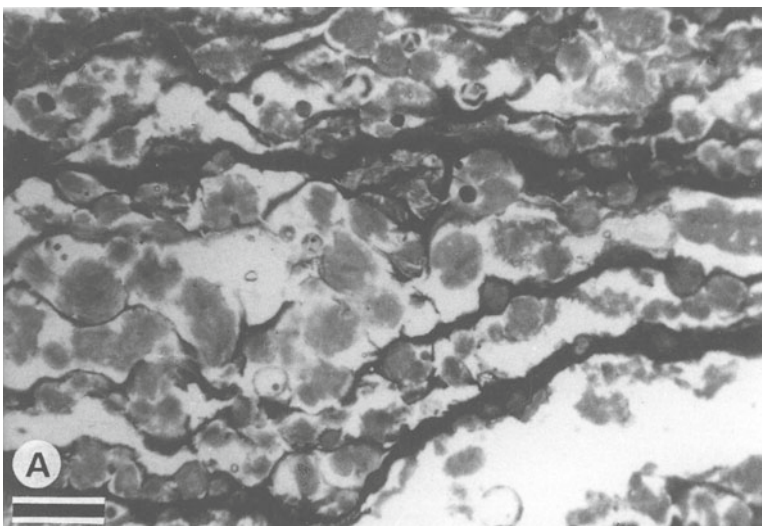

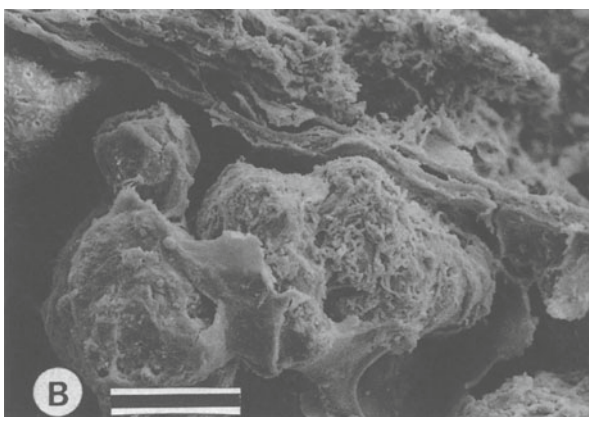

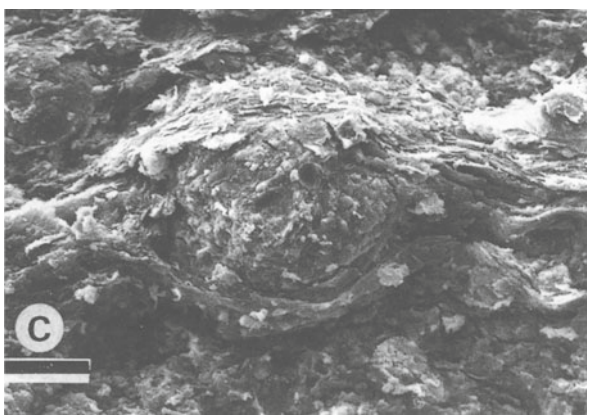

Fig. 5A–C. In situ carbonate precipitation in evaporite microbial sediments. **A** Granular appearance of mineral inclusions in a plastic gel of microbial origin and banded arrangement of the particles due to filamentous L_h-laminae create "sedimentary augen structures" (thin-section, Lanzarote salt works, Canary Islands; *scale:* 150 µm). **B** Close-up of carbonate particles in microbial mats (SEM photograph, *scale:* 100 µm). **C** Growing carbonate particle that has partially pushed apart the microbial laminae (SEM photograph, *scale:* 30 µm)

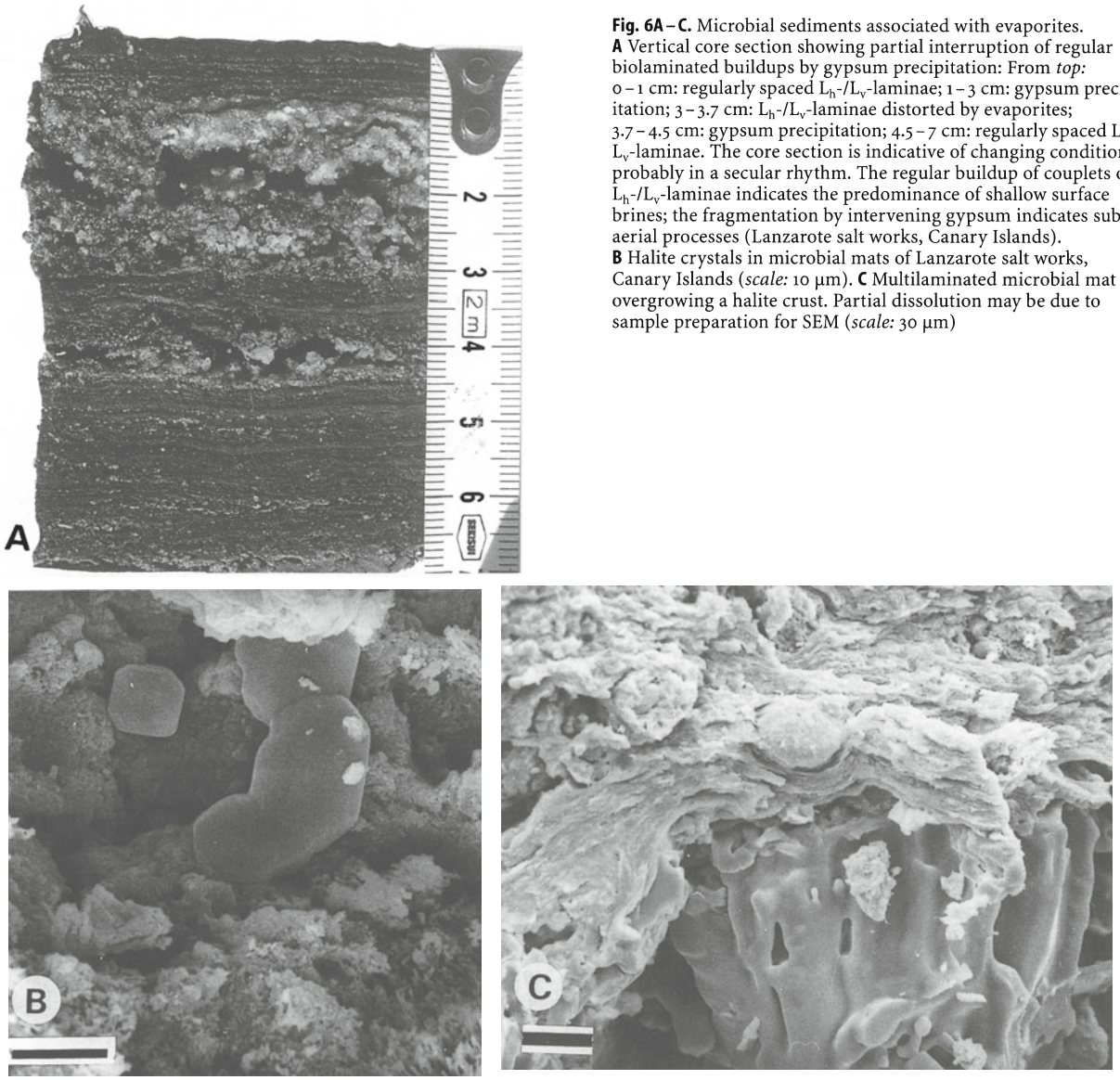

Fig. 6A–C. Microbial sediments associated with evaporites. **A** Vertical core section showing partial interruption of regular biolaminated buildups by gypsum precipitation: From *top:* 0–1 cm: regularly spaced L_h-/L_v-laminae; 1–3 cm: gypsum precipitation; 3–3.7 cm: L_h-/L_v-laminae distorted by evaporites; 3.7–4.5 cm: gypsum precipitation; 4.5–7 cm: regularly spaced L_h-/L_v-laminae. The core section is indicative of changing conditions, probably in a secular rhythm. The regular buildup of couplets of L_h-/L_v-laminae indicates the predominance of shallow surface brines; the fragmentation by intervening gypsum indicates subaerial processes (Lanzarote salt works, Canary Islands). **B** Halite crystals in microbial mats of Lanzarote salt works, Canary Islands (*scale:* 10 μm). **C** Multilaminated microbial mat overgrowing a halite crust. Partial dissolution may be due to sample preparation for SEM (*scale:* 30 μm)

crusts retain moisture and act as light-transferring systems. Since nutrients are also concentrated by evaporative pumping, the growth of prolific microbial mats is favored below and within the crusts. Massive gypsum often shows inclusions of vertically stratified microbial mats. Individual layers are yellow, orange, purple-red, and light and dark green, due to the distribution of different taxonomic and physiological groups (e.g. coccoid and filamentous cyanobacteria, phototrophic and chemoorganotrophic bacteria). In salt crusts, each single microbial layer usually is thicker than in similar sediment-supported microbial mats. This may be traced back to the ideal light channeling system of a salt crust (Gerdes et al. 1985).

Mats at or close to the bottom of stratified brines contribute to biolaminations in subaquatic gypsum (Fig. 3). In the Solar Lake hypolimnion, the filamentous cyanobacterium *Oscillatoria limnetica*, in association with coccoid cyanobacteria, anoxy-photobacteria and anaerobic bacteria, forms flocculent layers undergoing rapid anaerobic decay. Gypsum crystals form within and around these flocculent fabrics. Thin-section studies of the bottom sediments reveal a vertically laminated succession in which 5–10 mm thick layers composed of gypsum crystals alternate with thin organic laminae usually 100–500 m thick. The loose form of the flocculent mats provides hollow space filled with brine and fine-grained gypsum mush. The microbial assemblages are refractory and scattered within the gypsum mush.

Microbial inclusions and interlaminations in large gypsum crystals may reflect recrystallization of origi-

nally fine-grained gypsum mush during diagenesis. Krumbein cored Solar Lake sediments and found gypsum crystals more than 4 cm in size, with laminated mats embedded in them (Gavish et al. 1985). Microbial inclusions appear as thin laminae, often also showing faint, refractory and clotted microfabrics. Other origins of microbial mat layers within large gypsum crystals may be related to the replacement of carbonate sediments upon burial of former surface mats (Purser 1985).

In shallow brines, e.g. the Gavish Sabkha lagoon (Fig. 1A), salinities in the range of gypsum saturation (at about 14%) do not limit in situ production of biomass, and sulfate reduction proceeds as long as water is available. Thus, low gypsum contents are preserved in the sediment. Carbonate coatings around single sulfate particles commonly indicate solution and replacement of the sulfate by microbial activity. Only further salinity increase, decreasing water availability, or both, leads to the enrichment of gypsum in microbial sediments, since microbial productivity and sulfate reduction decrease (Fig. 6A).

In extremely hypersaline brines, large cell densities of halobacteria can change the precipitation behavior of halite (Krumbein 1985; Lopez-Cortes et al. 1994). Crystals contain more and larger fluid inclusions than crystals formed in sterile salt solutions (Norton and Grant 1988). Lopez-Cortes et al. (1994) found that the cells serve as templates for halite formation, resulting in a larger number of cubic crystals of smaller size than in sterile control experiments. They also observed that the proteinaceous compounds of the surface layers of the cells contribute to a modification of the halite crystal structure resulting in a dendritic shape. In Fig. 6B,C, some examples of halite crystals are shown in microbial mats.

4.4
Stress-Deformation Behavior of Biostabilized Sediments

In shallow evaporite settings, a variety of different physical processes (desiccation, crystal pressure and gas upheaval) affect the sedimentary surfaces and initiate deformation. Microbial mats embedded in the sediments act as a kind of soft tissue which effectively alters the effects of physical deformation (Reineck et al. 1990).

Drying, tearing of mats, and upcurling of mat margins may give rise to microbial chips (Fig. 7A). In shallow surface brines, subaqueous biofilms loosely attached to the substrate tend to scour and tear. Results are folds and tears, also known from ancient examples (Bernier et al. 1991).

Another reason for surface folding and doming is gas accumulating beneath surface mats. Hypersaline settings occupied by biofilms and microbial mats and enriched in reduced sulfur compounds are known for their high potential of gas production, mainly methane (Kiene et al. 1986). Gas accumulation elevates the cohesive biostabilized surface that retards the escape of gas into air or water, respectively (Fig. 7B). In ephemeral surface brines, such gas domes experience changes of flooding and exposure that in turn have a considerable influence on the microbiology and mineralogy of the area, inasmuch as wetting enables microbes to form new mats, and desiccation adds new gypsum crusts to the mats. Results are multilaminated domes resembling cabbage heads (Fig. 7C).

Taher et al. (1995) found selenitic gypsum mounds in a salina near Port Said, Egypt, produced by continu-

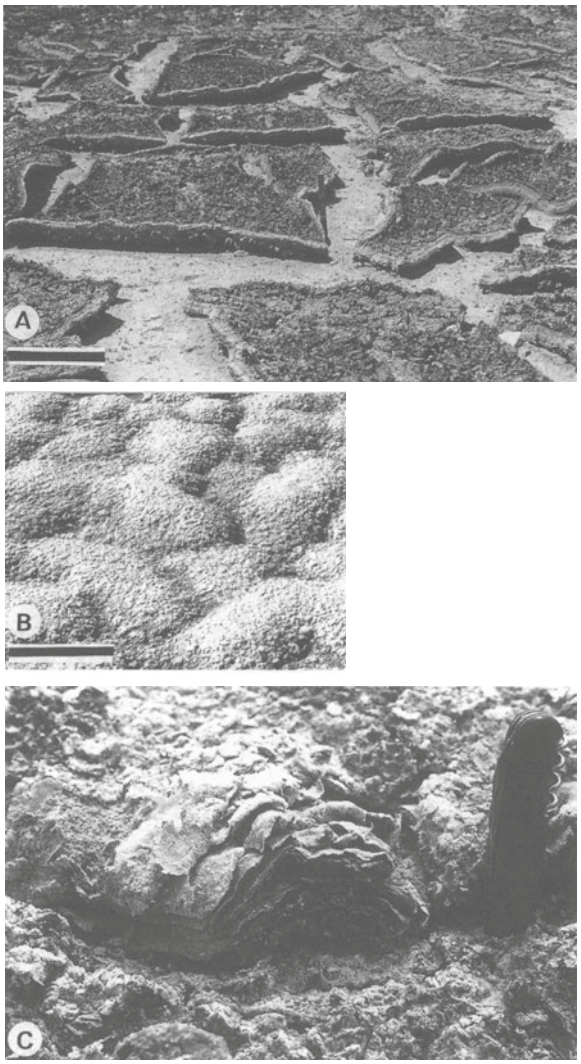

Fig. 7.A Desiccation cracks and upcurling of mat margins giving rise to chip formation (Lanzarote, Canary Islands, abandoned salt works, *scale:* 30 cm). **B** Gypsum-encrusted gas domes in microbial mats (*scale:* 20 cm). **C** Repeated exposure and gypsum encrustation of the gas domes, followed by re-establishment of surface brines and recolonization by microbial mats, create typical "cabbage heads" (length of knife = 9 cm; photographs courtesy of Professor H.E. Reineck)

ous gypsum laminae interlayered with microbial mats. The mounds were hard, massive, more or less circular, and up to about 35 cm in width. The topmost part of the domes was a thick layer (2 – 4 cm) of light brown, loosely packed coarse aggregates of tabular to block-like selenite crystals, more-or-less vertically orientated and highly twinned. The lower parts of the domes were more or less circular and formed of multi-layered porous masses of randomly orientated gypsum crystals. Comparable domes have been found in solar salt ponds (Reineck et al. 1990; Schreiber and Kinsman 1975) along the Red Sea coastal sabkhas of Egypt (Taher 1988), and in the Quaternary gypsum deposits of South Australia (Warren 1982).

Lateral expansion of surface crusts by the continual increment of evaporite minerals is particularly active at zones of weakness, causing buckling and folding of surface crusts (Assereto and Kendall 1977). The addition of crystals usually generates folds in consolidated crusts. Upfolding of the surface due to mineral encrustation is typical of subaerial conditions in arid climate. Another type of folding structure, termed enterolithic folds, develops from the conversion of gypsum mush above the mats to anhydrite. Additional anhydrite, derived from occasional storm flood water after evaporation, contributes to the expanding anhydrite zone (Hardie 1984; Shinn 1986).

5 Biofacies Classification of Marine-Derived Evaporite Microbial Sediments

Based on brine depth and salinity (Fig. 3), a classification of the biofacies types described in the foregoing section can be proposed. Although both factors are not necessarily correlated, both rule the local abundance of major microbial taxa and, thus, biofacies. Local decrease in brine depth usually correlates with broader environmental fluctuations which select for the increasing abundance of eurytopic major taxa that produce characteristic biogenic fabrics. The shallower the setting, the less the eurytopic community type is limited by increasing salinity. Both increasing depth and extreme salinities select for the increasing abundance of specialists (stenotopic taxa) tolerating only narrower ranges of environmental factors. The following first three sections summarize biofacies characteristics of eurytopic mat communities. The fourth is related to the dominance of stenotopic groups. Although using the Solar Lake example, these biofacies may contribute to deposits in brines of far greater depths.

5.1 Brine Table Below the Surface

In this case, biofacies characteristics are intrasedimentary biolaminites dominated by the L_h-lamina type, associated with gypsum. Deformation of the biofilm-stabilized surface is common, including cracks, doming and folding. Evaporative pumping is active, also providing moisture to the growth sites of microbial sediments. The mats are additions to clastic sediments (mud, sand; carbonate or non-carbonate) imported into the area by wind, episodic sheet floods or washover from the sea. Environmental settings are sabkhas.

5.2 Ephemeral Surface Brine

Biofacies characteristics include biolaminoid structures and initial biogenic varvites (Fig. 4). In metahaline conditions, cerithid gastropods meeting the growth areas of the biolaminoid facies leave shells behind. Biogenic varvites commonly occur at increasing salinities that exclude the gastropods. The biolaminites are frequently wrinkled due to net-like structures and pinnacles on the one hand (growth-related), and cracking, folding and doming on the other (related to physical stress; Fig. 7). The mat community shows increasing abundance of coccoid species. Sulfate crystals still occur. Coating of sulfate particles by carbonates indicates partial solution/reduction of the sulfate by microbes. Environmental settings are the rims and lower supratidal flats of playa lakes, salinas and peritidal lagoons. The hydrological regime is still variable, with moisture being supplied to the growth sites of microbial sediments by seepage and capillary action.

5.3 Perennial Surface Brine

Biofacies characteristics include regularly spaced biogenic varvites (Fig. 4A,B) and sedimentary augen structures. The biolaminites commonly are wrinkled due to pinnacle formation. Folding and doming is still common due to gas production in the subsurface sediments. The mat community is relatively the most diverse and productive of the depth zones compared. Due to high rates of sulfate reduction, there is almost no gypsum preserved. Carbonate minerals form in situ due to microbial conversion of organic matter, internal diffusion controls, microbial mineral solution by gypsum reduction, increase in dissolved HCO_3^-, and precipitation of secondary calcite (Fig. 5). Associated features may include burial by clastics brought in by occasional sheet floods. Environmental settings are shallow, permanently water-filled saline basins like the Gavish Sabkha lagoon, man-made salinas and the deeper Solar Lake shelf.

5.4 Stratified Basins Several Meters Deep (e.g., Solar Lake)

In the anoxic hypolimnion, soft flocculent fabrics of microbial mats occur, composed of halophilic filamen-

tous cyanobacteria (e.g. *Oscillatoria limnetica*) and unicelluar species (*Aphanothece halophytica*). Below the pycnocline, sulfur-dependent anoxy-photobacteria and anaerobic bacteria increase in number. The flocculent mats undergo rapid anaerobic decay. The bottom sediments are marked by faint interlamination of microbial mats in and between large gypsum crystals that precipitate subaquatically at the lake bottom.

6 Summary

1. The harsh conditions of evaporite environments exclude many groups of organisms, but those that thrive in hypersaline areas maintain high reproduction rates. Among these are cyanobacteria, other phototrophic bacteria, and halophilic green algae.
2. Primary production creates the organic material upon which biogeochemical cycles are based that produce a variety of authigenic minerals.
3. Evaporite settings vary from widely fluctuating to fairly uniform environmental conditions. Local decrease of brine depth usually correlates with broader environmental fluctuations, including salinity shifts. These conditions select for increasing abundance of eurytopic taxa, mainly benthic cyanobacteria.
4. Cyanobacteria initiate highly productive microbial mat ecosystems in which externally fluctuating conditions of the shallow evaporite environment are moderated due to the capacity of these organisms to produce water-retaining slime, to store energy by light-harvesting systems, to transform and transfer nutrients in biogeochemical cycles, and to establish vertically stratified benthic systems that withstand periods of dryness.
5. Increasing depth and extreme salinity both select for increased abundance of specialists (stenotopic taxa) tolerating only narrower ranges of environmental factors.
6. Communities dominated by benthic eurytopic cyanobacteria produce characteristic microbial sediments including stromatolitic laminae, biolaminoid facies, sedimentary augen structures, and pinnacle structures. Communities dominated by stenotopic major taxa often contribute less unambiguous structures, e.g. flocculent organics, to the sedimentary record.
7. In nutrient-enriched hypersaline basins, plankton dominance may outcompete benthic microbial mats, but also contribute to organic-rich strata.

References

Assereto RLAM, Kendall CGStC (1977) Nature, origin and classification of peritidal tepee structures and related breccias. Sedimentology 24:153–210

Bernier P, Gaillard C, Gall JC, Barale G, Bourseau JP, Buffetaut E, Wenz S (1991) Morphogenetic impact of microbial mats on surface structures of Kimmeridgian micritic limestones (Cerin, France). Sedimentology 38:127–136

Brongersma-Sanders M (1992) On the association of ore deposits with stromatolites. In: Schidlowski M et al. (eds) Early organic evolution: Implications for mineral and energy resources. Springer, Berlin Heidelberg New York, pp 478–482

Cohen Y, Krumbein WE, Goldberg M, Shilo M (1977) Solar Lake (Sinai). 1. Physical and chemical limnology. Limnol Oceanogr 22:597–608

Cornée A, Dickman M, Busson G (1992) Laminated cyanobacterial mats in sediments of solar salt works: some sedimentological implications. Sedimentology 39:599–612

Dahanayake K, Krumbein WE (1985) Ultrastructure of a microbial mat generated phosphorite. Miner Deposita 20:260–265

Dahanayake K, Krumbein WE (1986) Microbial structures in oolitic iron formations. Miner Deposita 21:85–94

Dahanayake K, Gerdes G, Krumbein WE (1985) Stromatolites, oncolites and oolites biogenically formed in situ. Naturwissenschaften 72:513–518

Decima A, McKenzie JA, Schreiber BC (1988) The origin of "evaporative" limestones: an example from the Messinian of Sicily (Italy). J Sed Petrol 58:256–272

Dor I, Paz N (1989) Temporal and spatial distribution of mat microalgae in the experimental Solar ponds, Dead Sea area, Israel. In: Cohen Y, Rosenberg E (eds) Microbial mats, physiological ecology of benthic microbial communities. ASM, Washington, DC, pp 114–122

Dyer BD, Krumbein WE, Mossman DJ (1994) Accumulation of gold in the sheath of *Plectonema terebrans* (filamentous marine cyanobacteria). Geomicrobiology J 12:91–98

Ehrlich HL (1990) Geomicrobiology. Dekker, New York

Fan P, Li J, Meng Q, Ju X, Li Z (1992) Biomarkers and other hydrocarbon in Upper Sinian stromatolitic dolostones from southwest China. In: Schidlowski M et al. (eds) Early organic evolution: Implications for mineral and energy resources. Springer, Berlin Heidelberg New York, pp 308–316

Folk RL (1973) Carbonate petrography in the post-Sorbian age. In: Ginsburg RN (ed) Evolving concepts in sedimentology. John Hopkins University, Baltimore, pp 118–158

Friedman GM (1978) "Solar Lake": a sea-marginal pond of the Red Sea (Gulf of Aqaba or Elat) in which algal mats generate carbonate particles and laminites. In: Krumbein WE (ed) Environmental biogeochemistry and geomicrobiology 1. The aquatic environment. Ann Arbor, pp 227–235

Friedman GM (1980) Dolomite is an evaporite mineral: Evidence from the rock record and from sea-marginal pond of the Red Sea. SEPM Spec Publ 28:69–80

Friedman GM, Sneh A, Owen RW (1985) The Ras Muhammad Pool: Implications for the Gavish Sabkha. In: Friedman GM, Krumbein WE (eds) Hypersaline ecosystems: the Gavish Sabkha. Ecological Studies 53. Springer, Berlin Heidelberg New York, pp 218–237

Friedman GM, Sanders JE, Kopaska-Merkel D (1992) Principles of sedimentary deposits. MacMillan, New York

Gavish E, Krumbein WE, Halevy J (1985) Geomorphology, mineralogy and groundwater geochemistry as factors of the hydrodynamic system of the Gavish Sabkha. In: Friedman GM, Krumbein WE (eds) Hypersaline ecosystems: the Gavish Sabkha. Ecological studies 53. Springer, Berlin Heidelberg New York, pp 186–217

Gerdes G, Krumbein WE (1987) Biolaminated deposits. In: Bhattacharya S, Friedman GM, Neugebauer HJ, Seilacher A (eds) Lecture Notes in Earth Sciences 9. Springer, Berlin Heidelberg New York

Gerdes G, Krumbein WE, Holtkamp EM (1985) Salinity and water activity related zonation of microbial communities and potential

stromatolites of the Gavish Sabkha. In: Friedman GM, Krumbein WE (eds) Hypersaline Ecosystems – The Gavish Sabkha. Ecological Studies 53. Springer, Berlin Heidelberg New York, pp 238 – 266
Gerdes G, Krumbein WE, Reineck HE (1991) Biolaminations – ecological versus depositional dynamics. In: Einsele G, Ricken W, Seilacher A (eds) Cycles and events in stratigraphy. Springer, Berlin Heidelberg New York, pp 592 – 607
Gerdes G, Dunajtschik-Piewak K, Riege H, Taher AG, Krumbein, WE., Reineck HE (1995) Structural diversity of biogenic carbonate particles in microbial mats. Sedimentology 41:1273 – 1294
Golubic S (1980) Halophily and halotolerance in cyanophytes. Origins Life 10:169 – 183
Guerrero R, Mas J (1989) Multilayered microbial communities in aquatic ecosystems: Growth and loss factors. In: Cohen Y, Rosenberg E (eds) Microbial mats, physiological ecology of benthic microbial communities. ASM, Washington, DC, pp 37 – 51
Hardie LA (1984) Evaporites: marine or non-marine? Am J Sci 284:193 – 240
Hardie LA (1987) Dolomitization: a critical view of some current views. J Sed Petrol 57:166 – 183
Imhoff JF (1988) Halophilic phototrophic bacteria. In: Rodriguez-Valera F (ed) Halophilic bacteria. CRC Press, Boca Raton, pp 85 – 108
Javor B (1989) Hypersaline environments. Springer, Berlin Heidelberg New York
Kendall AC (1992) Evaporites. In: Walker RG, James NP (eds) Facies models. Geol Assoc Can, pp 375 – 409
Kiene RP, Oremland RS, Catena A, Miller LG, Capone D (1986) Metabolism of reduced methylated sulfur compounds by anaerobic sediments and a pure culture of an estuarine methanogen. Appl Environ Microbiol 52:1037 – 1045
Kinsmann DJJ (1969) Modes of formation, sedimentary associations, and diagnostic features of shallow-water and supratidal evaporites. Am Assoc Petrol Geol Bull 53:830 – 840
Krumbein WE (1979) Calcification by bacteria and algae. In: Trudinger PA, Swaine DJ (eds) Biogeochemical cycling of mineral-forming elements. Elsevier, Amsterdam, pp 47 – 67
Krumbein WE (1985) Applied and economic aspects of sabkha systems – genesis of salt, ore and hydrocarbon deposits and biotechnology. In: Friedman GM, Krumbein WE (eds) Hypersaline ecosystems: the Gavish Sabkha. Ecological studies 53. Springer, Berlin Heidelberg New York, pp 426 – 436
Krumbein WE, Cohen Y, Shilo M (1977) Solar Lake (Sinai) 4. Stromatolitic cyanobacterial mats. Limnol Oceanogr 22:635 – 656
Lopez-Cortes A, Ochoa JL, Vazquez-Duhalt R. (1994) Participation of halobacteria in crystal formation and the crystallization rate of NaCl. Geomicrobiol J 12:69 – 80
Norton C, Grant WD (1988) Survival of halobacteria within fluid inclusions in salt crystals. J Gen Microbiol 134:1365 – 1373
Park RK (1977) The preservation potential of some recent stromatolites. Sedimentology 24:485 – 506
Por FD (1985) Anchialine pools – comparative hydrobiology. In: Friedman GM, Krumbein WE (eds) Hypersaline ecosystems: the Gavish Sabkha, Ecological studies 53. Springer, Berlin Heidelberg New York, pp 136 – 145
Purser BH (1985) Coastal evaporite systems. In: Friedman GM, Krumbein WE (eds) Hypersaline ecosystems: the Gavish Sabkha. Ecological studies 53. Springer, Berlin Heidelberg, New York, pp 72 – 102
Reineck HE, Gerdes G, Claes M., Dunajtschik-Piewak K, Riege H, Krumbein WE (1990) Microbial modification of sedimentary surface structures. In: Heling D, Rothe P, Förstner U, Stoffers P (eds) Sediments and environmental geochemistry. Springer, Berlin Heidelberg New York, pp 254 – 276
Renfro AR (1974) Genesis of evaporite-associated stratiform metalliferous deposits – a sabkha process. Econ Geol 69:33 – 45
Schreiber BC, Kinsman DJJ (1975) New observations on the Pleistocene evaporites of Montallegro, Sicily and a modern analog. J Sed Petrol 45:469 – 479
Shinn E (1986) Modern carbonate tidal flats: their diagnostic features. In: Hardie LA, Shinn EA (eds) Carbonate depositional environments modern and ancient, part 3. Tidal flats. Colorado School of Mines Quarterly 81:7 – 35
Soudry D, Champetier Y (1983) Microbial processes in the Negev phosphorites (southern Israel). Sedimentology 30:411 – 423
Taher AG (1988) Sedimentology and geochemistry of the coastal sabkha, Ras Shukheir, Gulf of Suez, Egypt. MSc Thesis, Cairo University, Egypt
Taher AG, Wahab Abd el, Philip G, Krumbein WE, Wali AM (1995) Evaporitic sedimentation and microbial mats in a salina system (Port Fouad, Egypt). Int J Salt Lake Res 4:117 – 131
Warren JK (1982) The hydrological setting, occurrence and significance of gypsum in late Quaternary salt lakes in south Australia. Sedimentology 29:609 – 637
Wood A, Burke Ch, Knott B (1991) Chemolithotrophic surfur bacteria in sediments, mats, and stromatolites of Western Australian saline lakes. Geomicrobiol J 9:41 – 49

Gypsum Microbial Sediments: Neogene and Modern Examples

J. M. Rouchy[1], C. Monty[2]

[1] CNRS-ESA 7073, Laboratoire de Géologie, Muséum National d'Histoire Naturelle, 43 rue Buffon, F-75005 Paris, France
[2] Laboratoire de Biosédimentologie, Université de Nantes, 2 rue de la Houssinière, F-44072 Nantes Cedex 03, France

Abstract. Neogene gypsum deposits provide good examples of microbially induced structures (planar laminites, columnar build-ups) whose study elucidates the intimate relations between microbial components and gypsum crystallization. This study closely links petrography and comparisons with modern settings. All the examples studied in both modern and ancient gypsum deposits show that the microbial features in gypsum result from periodically controlled phases of microbial mat development and gypsum precipitation. Although most of the traces of microbial communities proliferating in the evaporitic settings are poorly preserved or absent in the fossil record, the relations between microbial remains and gypsum seems to be controlled by three main processes: (1) interstitial precipitation of gypsum within microbial mats, (2) incorporation of organic material within crystals during gypsum precipitation, and (3) organic material deposited on the surface of gypsum crystals during interruption of crystal growth.

1 Introduction

Studies carried out in modern hypersaline settings over the last few decades have emphasized the importance of the microbial contribution to sedimentation. This contrasts with the scarcity of biological features usually recognized in ancient equivalents and suggests that the importance of this contribution has been considerably underestimated in the fossil record. This discrepancy results from the specific conditions which characterize hypersaline environments in terms of: (1) harsh physico-chemical constraints on life, and (2) alteration of the original sedimentary structures by intense diagenetic processes. The distribution, composition and ecology of the microbial communities in modern evaporitic settings are discussed by Gerdes et al. (this Vol.). The criteria usually employed to characterize microbially controlled features in ancient sediments are difficult to apply to evaporite sequences. Well-developed columnar or domal stromatolitic morphologies are scarce in evaporites, and laminated features which are widespread in calcium sulfate deposits (gypsum and anhydrite) are ambiguous. Lamination linked with biological activity may be similar to that resulting exclusively from physico-chemical processes, e.g. mineralogical changes due to periodic variations in brine concentration, and reworking by currents, waves or turbiditic processes.

When a microbial contribution is clearly established by unquestionable features, such as columnar or domal morphologies or microbial remains preserved in evaporitic minerals, another question arises concerning the contribution of these organisms to gypsum formation. Were these organisms passively incorporated in the calcium sulfate minerals during crystallization or did they contribute biochemically to their precipitation?

The relationships between microbial mats and gypsum formation have been investigated in many modern settings and in various Neogene gypsum formations which provide good examples for reconstructing the intimate relations between microbial components and gypsum crystallization. The following discussion is focused only on gypsum deposits that exhibit evidence of microbially induced features and it excludes ambiguous laminated structures.

2 Stromatolitic Occurrences in Ancient Gypsum Formations

2.1 Bioconstructed Features in Microcrystalline Gypsum

Examples of stromatolitic build-ups in gypsum have been reported in the Upper Miocene (Messinian) gypsum of the Polemi area, western Cyprus (Orszag-Sperber et al. 1980; Rouchy and Monty 1981; Rouchy 1982). Other occurrences are also known in the Messinian of Sicily and Crete (Hardie and Eugster 1971; Schreiber 1988; B. Delrieu, unpublished), Upper Miocene (Tortonian) of Bulgaria (Trashliev 1969), Middle Miocene (Badenian) of Poland and the Ukraine (Kasprzyk 1993; Peryt et al. 1994), Neogene of Egypt (Youssef 1988), and Paleogene of Bresse in France (Guillevin 1980).

2.1.1 Microbially Controlled Sedimentary Features

In the Messinian of Cyprus, stromatolitic features are present in a 3 m-thick uppermost gypsum bed of the Upper Evaporite Unit. This bed is dominantly composed of planar to undulating laminated gypsum com-

R. E. Riding and S. M. Awramik (Eds.)
Microbial Sediments

prising, at some levels, columnar to conical stromatolitic structures up to 10 cm high and 5 cm in diameter (Fig. 1A,B). The laminations in these structures are similar and grade laterally into each other, suggesting that they resulted from the same bio-sedimentary processes. The fossil content is mainly composed of brackish to freshwater organisms (*Melanopsis*, Limnocardiidae, *Cyprideis*; Orszag-Sperber et al. 1980). Synsedimentary erosion of columnar build-ups and laminites and their reworking in sands or conglomerates interbedded within the stromatolitic layers or filling the interdomal spaces (Fig.1C) demonstrates that precipitation of gypsum occurred early, alternating with episodes of microbial mat growth. Laminated gypsum also contains single or clustered large selenite crystals which either deform the lamination or are enveloped by

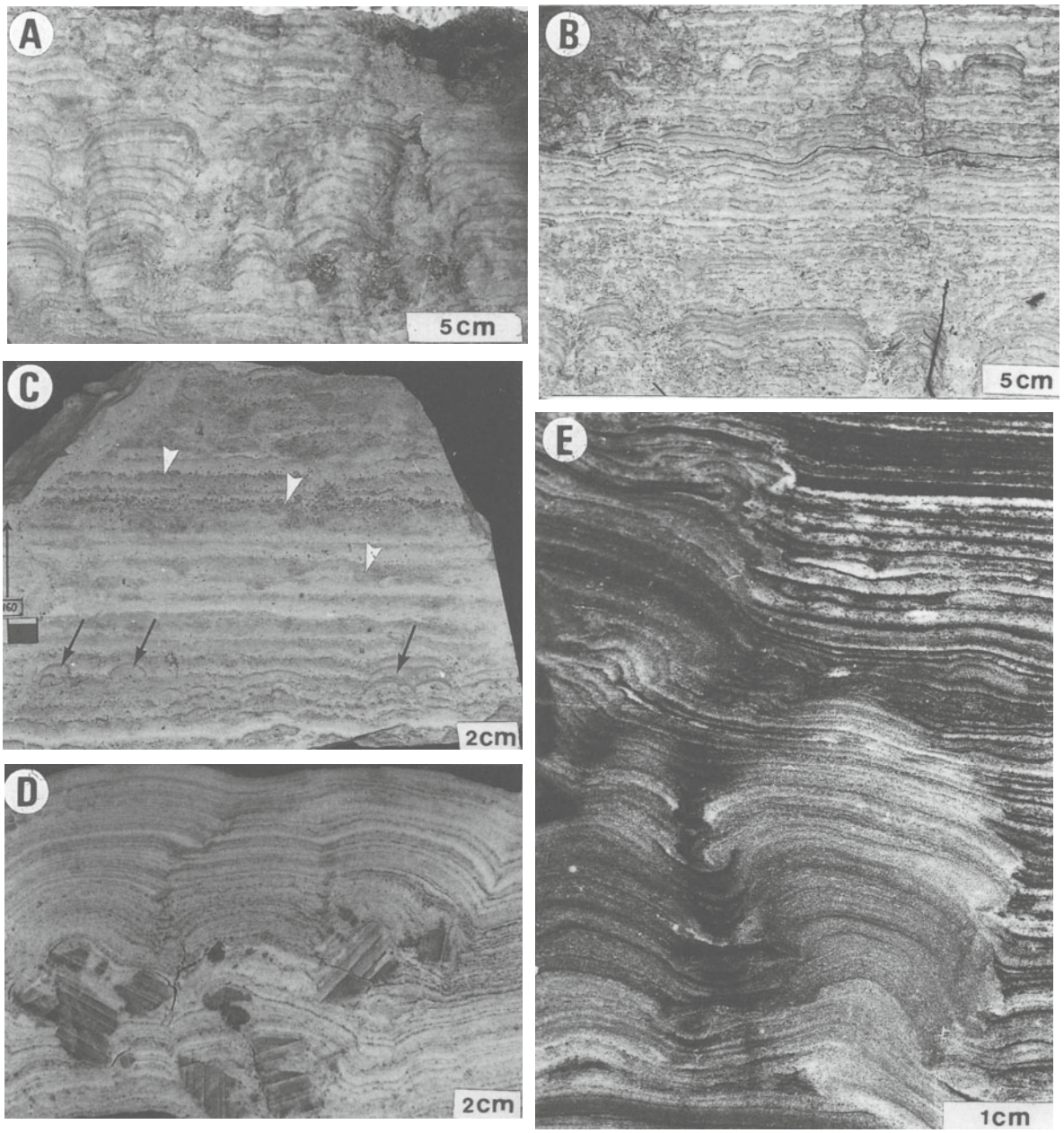

Fig. 1A–E. Biological structures in Miocene gypsum deposits. **A** Columnar stromatolites. Yiolou, Cyprus (Polemi basin). **B** Dome-shaped stromatolites and microbial-laminated gypsum. Yiolou, Cyprus (Polemi basin). **C** Laminated gypsum showing incipient dome-shaped structures (*black arrows*). The laminated gypsum is often eroded and reworked as sand layers intercalated within the laminites (*white arrows*); Yiolou, Cyprus (Polemi basin). **D** Undulating microbial-laminated gypsum deformed by the growth of large selenite gypsum crystals; Tsangaraki, Crete. **E** Biolaminated and columnar stromatolitic features in the Middle Miocene gypsum from the Suchowola borehole, Holy Cross Mountains, southern Poland. (Courtesy of A. Kasprzyk)

the microbial mats, indicating that their crystallization also occurred very early (Fig. 1D). True stromatolitic build-ups have also been described in the Badenian of southern Poland by Kasprzyk (1993), who distinguishes between biolaminites and stromatolites (Fig. 1E). The domal, columnar or branching morphologies of the stromatolites are basically formed by local thickening of the biolaminites.

The laminated gypsum is basically composed of triplets comprising a basal, millimeter-thick lamina composed of calcite and gypsum, a white homogeneous gypsum lamina 0.5 cm thick, and a millimeter-thick, uppermost brownish gypsum lamina. A second-order sub-millimetric lamination may be seen in the lower and middle laminae. The gypsum crystals exhibit various shapes including ameboid, globular or lozenge-shaped; reverse size-sorting, ranging from less than 20 μm in the basal lamina to several hundred microns in the uppermost brownish one, is also present (Fig. 2A). The basal lamina comprises large amounts of micrite with scattered gypsum crystals; the middle lamina is formed of small crystals with disseminated calcite grains, whereas the upper one corresponds to densely interlocked aggregates of larger crystals (Fig. 2A, B). The gypsum crystals enclose variable amounts of calcite grains indicating that they grew interstitially within microbial layers (Fig. 2B). The diagenetic growth of gypsum in the mats has so deformed or erased the microbial morphologies that their identification is obscured, except for some structures which have been compared with present-day calcified films built by tiny filaments of *Schizothrix* (Rouchy and Monty 1981).

2.1.2 Environment and Processes of Formation

Gypsum deposits are usually devoid of fossils capable of providing information about ambient conditions. An exception is the Messinian of Cyprus, where the fossil content and the isotopic composition of the gypsum both indicate that gypsum precipitated from brines derived from original brackish waters (Rouchy and Pierre 1979; Orszag-Sperber et al. 1980; Rouchy 1982), However, it is likely that similar deposits can also be formed in settings where only sea water is evaporated.

Each gypsum layer basically results from a single period of gypsum crystallization within a previously deposited microbial mat, while the second-order lamination is determined by sub-millimetric mostly calcitic films that determined the primary organic lamination. The thickness of the initial layer is noticeably expanded by the interstitial growth of gypsum crystals. This type of composite lamination results from two superimposed processes controlled by seasonal variations of salinity: (1) growth of finely laminated mats during periods of lower salinity, and (2) interstitial crystallization of gypsum when the trapped brines reached salinities high enough to inhibit the growth of most of the microbial communities and to precipitate gypsum. According to observations in modern settings, gypsum crystallization happens either subaqueously in the bottom sediments or by capillary evaporation during short periods of desiccation.

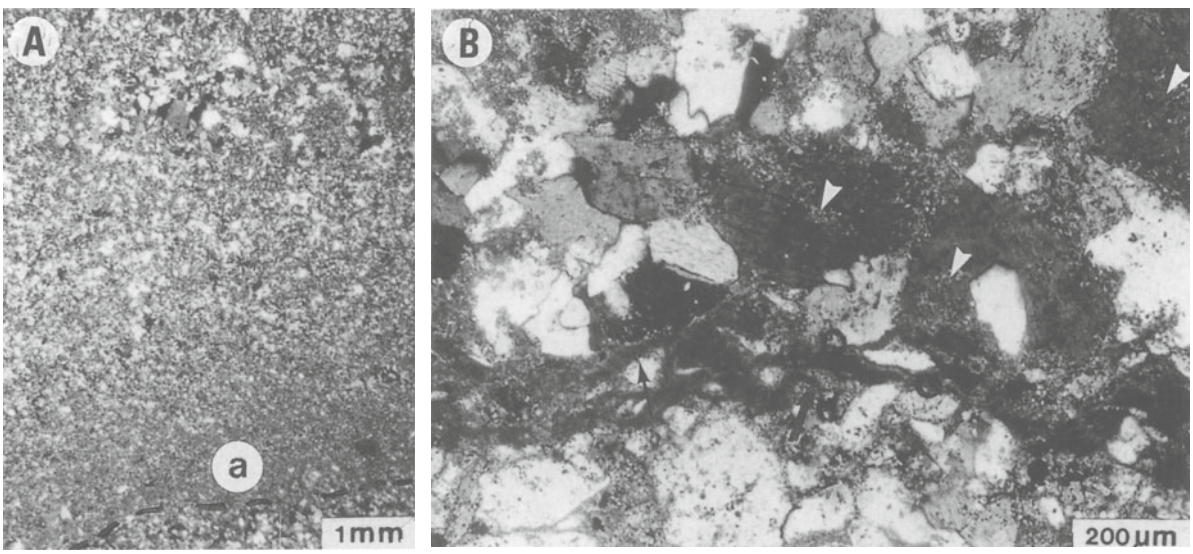

Fig. 2A,B. Messinian gypsum from Yiolou, Cyprus (Polemi basin). **A** Detail of the lamination showing the basal micritic laminae (*a*) and the upward increase in both the density and size of the gypsum crystals; photomicrograph. **B** Detail of the basal micritic lamina showing relics of filaments (*black arrows*) deformed by the interstitial growth of gypsum crystals. Note that the larger crystals enclose large amounts of micrite (*white arrows*); SEM

2.2
Microbial Laminites Within Large Selenite Crystals

2.2.1
Organic Features

This unusual gypsum facies is composed of vertically erect selenite crystals, from 1cm to about 1m high, arranged in continuous layers and showing internal lamination that horizontally cross-cuts adjacent crystals. Two main types are distinguished.

The first type, observed in the Messinian gypsum of Cyprus and Crete (Rouchy and Monty 1981), consists of centimetric vertically erect crystals (gypsum grass) displaying millimetric planar lamination (Fig. 3A). The laminae are composed of interwoven calcified filaments alternating with darker laminae containing few or no filaments. The gypsum crystals formed by subaqueous growth of crystals that nucleated on the substrate. Crystals and filaments exhibit different relationships (Fig. 3B): (1) filaments are deformed downward along crystal sides, indicating that crystals penetrated downward into a soft organic substrate, (2) filaments are enclosed within crystals, and (3) filaments rest upon horizontal discontinuities due to interruption of crystallization followed by new phases of syntaxial growth.

The second type has been reported from the Messinian of the northern Apennines, Sicily, Ionian islands, Algeria, Crete and Cyprus, as well as in the Middle Miocene of Sinai (Vai and Ricci-Lucchi 1977; Rouchy and Monty 1981; Rouchy 1982; Monty et al. 1987). It is com-

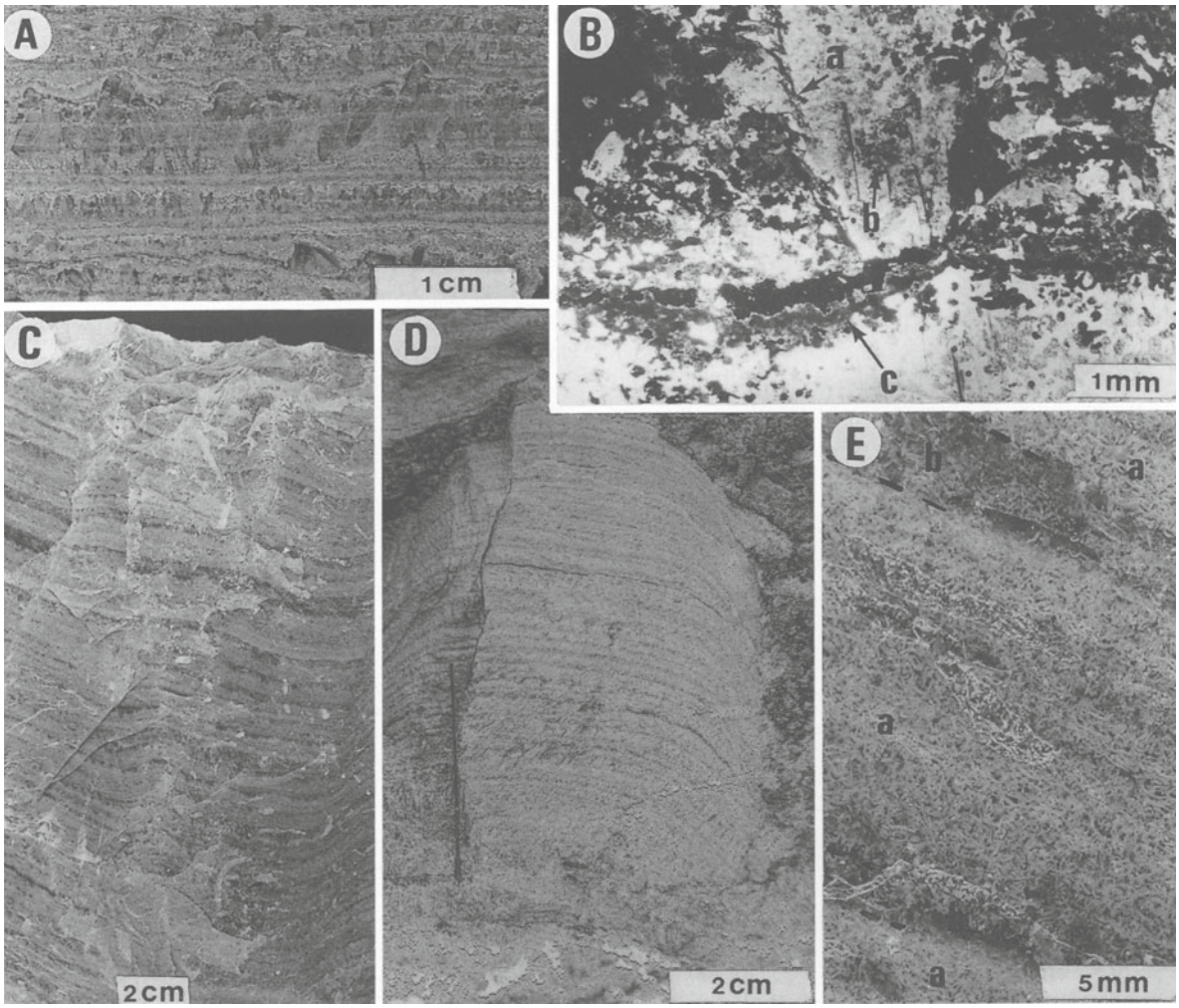

Fig. 3A–E. Microbial laminites within Miocene selenite gypsum. **A** Sample showing layers of centimeter-high, vertically erect gypsum crystals crossed by a planar lamination; Elhediou, Cyprus (Polemi basin). **B** Detail of **A:** (*a*) filaments deformed along the walls of the crystals, (*b*) filaments enclosed in the crystal, and (*c*) filaments resting on the top of the crystals. **C** Gypsum crystal showing on its (010) cleavage surface an internal lamination composed of regularly alternating clear and opaque layers; Kalavasos, Cyprus (Psematismenos basin). **D** Dome-shaped stromatolitic structure enclosed within a monocrystal of gypsum; Tsangaraki, Crete. **E** Detail of **C** showing that the white laminae are composed of a dense network of microbial filaments (*a*) while the darker interlayers contain fewer filaments (*b*)

posed of decimeter to meter-high, vertically erect selenite crystals which form continuous layers in the basal part of many Messinian evaporitic sequences (Fig. 3C).This gypsum is characterized by an internal lamination crossing more or less horizontally through adjacent crystals which do not display any crystalline discontinuities. The lamination is usually planar or undulose, but it can be deformed by the crystal growth (commonly on the plane 120) producing a crenulated pattern which can mimic stromatolitic fabrics. Typical domal stromatolitic morphologies occur in the Messinian of Crete in the form of decimetric-high domal structures, entirely enclosed within a single gypsum crystal (B. Delrieu, unpublished; Fig. 3D).

In both types, the lamination is formed by an alternation of dark-colored translucid layers (1–5mm in thickness) and light-colored opaque laminae (5mm to 1cm or more) which differ from each other by the density of microbial filaments floating in the gypsum matrix, giving this facies a "spaghetti-like" aspect (Vai and Ricci-Lucchi 1977). Opaque laminae are composed of a dense felt of filaments, while the dark translucent ones contain fewer filaments (Fig. 3E).

Filaments are 40 and 80 μm in diameter and >1 cm long; they differ in the two types by the nature of the filament filling. In the first type, this is composed of aggregates of small crystals of calcite, 1–3μm in size (Fig. 4A). In the second type, filaments generally appear as ghosts defined by minute grains of organic matter (amino acids) and rare calcite grains, disseminated within the gypsum crystals (Fig. 4B). In places, such laminated crystalline gypsum overlies (Cyprus) or grades laterally (Northern Apennines) into calcareous stromatolites composed of very similar filaments (Vai and Ricci-Lucchi 1977; Rouchy and Monty 1981).

The morphology of the filaments and the presence of true domal build-ups demonstrate that these organic remains correspond to cyanobacteria, and not to fecal pellets of the brine shrimp *Artemia* which are commonly observed in gypsum (Schreiber et al. 1976). The filaments exhibit inserted funnel-shaped units which are very reminiscent of those of *Scytonema* sheaths (Monty 1965), the large diameter of the filaments resulting from the clustering of elementary filaments into bundles (Monty 1965; Rouchy and Monty 1981).

2.2.2 Environment and Processes of Formation

In both varieties of gypsum, the microbial mats were built by a simple community of filamentous cyanobacteria dominated by a form similar to *Scytonema* (Rouchy and Monty 1981); they differ mainly in the manner in which the filaments are preserved and by the relationships between crystals and microbial mats.

The first type of gypsum, with calcified filaments, grew in shallow, restricted brackish ponds in which sea water entered periodically by percolation (Rouchy and Pierre 1979; Rouchy and Monty 1981). This setting is similar to the freshwater marshes of the Bahamas where *Scytonema* sheaths are rapidly calcified by bacterial breakdown of microbial mucopolysaccharides (Monty 1965, 1972; Monty and Hardie 1976). In contrast, the mats with uncalcified filaments developed in marine lagoons periodically affected by evaporitic processes.

In the first type, the inclusion of a felt of filaments within the crystals shows that these crystals grew, at least partly, by interstitial crystallization within an already formed microbial mat. However, there are microbial filaments which rest upon crystal discontinuities. This indicates that the gypsum crystallization which was initiated in the sediment continued subaqueously and was periodically interrupted by episodes of water dilution during which microbial filaments colonized the surfaces of the crystals before a new phase of synta-

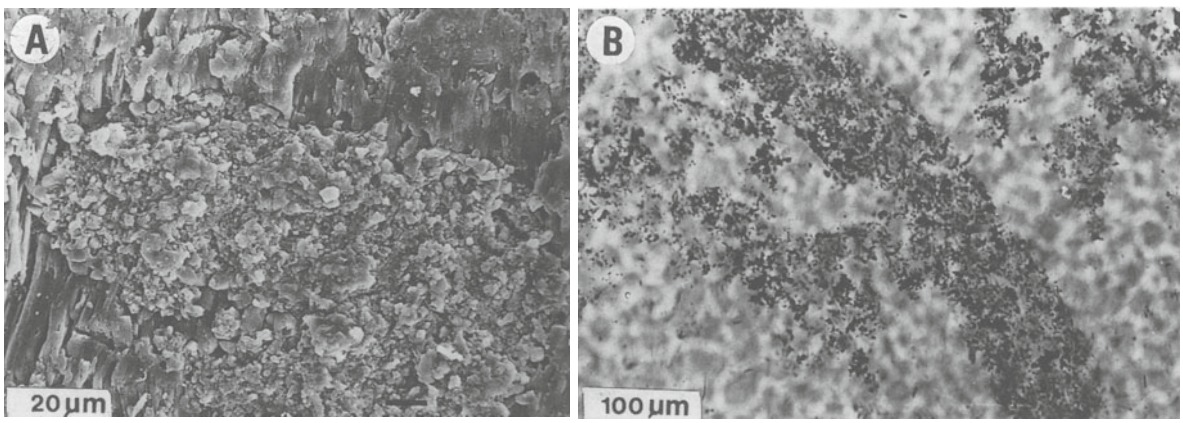

Fig. 4A,B. Details of filaments. **A** SEM view of a calcified filament of the first type of microbial laminites; Elhediou, Cyprus (Polemi basin). **B** Second type of microbial laminites, composed of uncalcified filaments. Most molds of filaments are made by minute grains of organic matter and scattered micritic carbonate; Kalavasos, Cyprus (Psematismenos Basin);. photomicrograph

xial growth. Such a process may be compared to the lamination induced by clastic grains deposited periodically on the surface of growing crystals, as described in some Recent gypsum from Australian lagoons (Warren 1985).

The second type does not result from repetitive processes of gypsum precipitation and microbial mat growth since the crystals do not show any discontinuities linked with the mats. The crystals grow interstitially within a layer of mats. As reported in the Apennine outcrops, the sharp lateral transition between gypsified laminites and calcareous stromatolites, both built by the same microbial filaments, suggests that crystallization was mainly governed by groundwater processes. The floating appearance of the filaments in the gypsum matrix resulted from expansion caused by the crystallization. The most frequent site of occurrence of this type of gypsum is the basal part of the gypsum units, where it locally overlies calcareous stromatolites. This indicates that this facies records the onset of gypsum precipitation following a period of preevaporitic metasaline conditions characterized by a luxuriant development of microbial mats. At higher salinities, microbial growth is inhibited and only scattered filaments appear disseminated in the overlying gypsum.

3 Modern Equivalents

Microbial mats are a dominant sedimentary component in many modern hypersaline settings, either in natural ponds or solar salt works, where they grow in brines reaching salinities of more than 150 g/l. They participate in the formation of a variety of laminated deposits composed of an alternation of gypsum and microbial layers. Most of these deposits are seasonally controlled, precipitating gypsum during the dry season when the brines are generated, whereas microbial mats grow during periods of brine dilution.

Such laminated deposits have been described at Ras Mohamad Pool, a small hypersaline pond located in the Sinai (Kushnir 1981; Friedman et al. 1985). Here, they are composed of layers of gypsum mush and finely laminated mats several millimeters to several centimeters in thickness. After sedimentation, early diagenetic transformation takes place below the floor of the pond and the former organic-gypsum laminated fabric is deformed or destroyed by the development of gypsum crystals growing interstitially from trapped saturated brines. These crystals tend to coalesce, forming layers or lenses separated from each other by thin and discontinuous calcitic laminae, which represent relics of the initial microbial mats. The resulting sediment is a coarsely laminated gypsum in which the interstitial growth of crystals within the organic material has noticeably increased the thickness of the laminae with respect to the initial microbial mat.

In the Laguna Mannar of Sri Lanka, gypsum precipitates within the upper centimeters of microbial mats composed of a mixture of *Schizothrix* and a red alga (*Porphyridium*) during the dry season (Gunatilaka 1975). Similar processes of microbial mat gypsification by early diagenetic crystallization of gypsum in the mats are common in solar salt works (Fig. 5A, B; Rouchy 1982; Dronkert 1985; Orti et al. 1986). In the more intensely gypsified mats, microbial remains are reduced to thin organic or calcified films, discontinuously disseminated in the basal part of the gypsum layers which sometimes display a reverse grain sorting (Fig. 5C). Thus, the formation of these gypsified microbial mats involves two different processes: the first corresponds to the alternation of gypsum precipitation and microbial mat colonization of the bottom, the second is controlled by early diagenetic processes occurring beneath the sediment surface.

In solar salt ponds near Almeria city, in southern Spain (Dronkert 1985), gypsum commonly crystallizes during periods of mat desiccation through capillary evaporation. The crystals grow preferentially in the top part of small stromatolitic domes characterized by more aerated conditions than the underlying zone where anoxic conditions are maintained longer. The formation of stromatolitic build-ups embedded in laminated gypsum in Poland (Fig. 1E) could be explained by such a process. In the Laguna Mormona (Baja California), some ponds are characterized by decimeter-high dome-shaped stromatolites whose upper parts are subaerially exposed during the dry season, causing intense gypsification (Pierre, personal communication; Fig.5D). Columnar stromatolitic features from the Messinian gypsum were probably formed by similar mechanisms.

Most of the organic structures formed in hypersaline environments are poorly preserved or destroyed, due to the interaction of processes such as the degradation of the organic matter or the destruction of the stromatolitic morphologies by the interstitial crystallization of gypsum. Krumbein and Cohen (1977) noted, for instance, that decay processes lead to the formation of pellet-like structures larger than microbial filament bunches. Accordingly, the microbial contribution is undoubtedly considerably underestimated in the fossil record and many gypsum/carbonate laminated deposits have probably been formed in close association with microbes, even if no typical biological structures can now be detected.

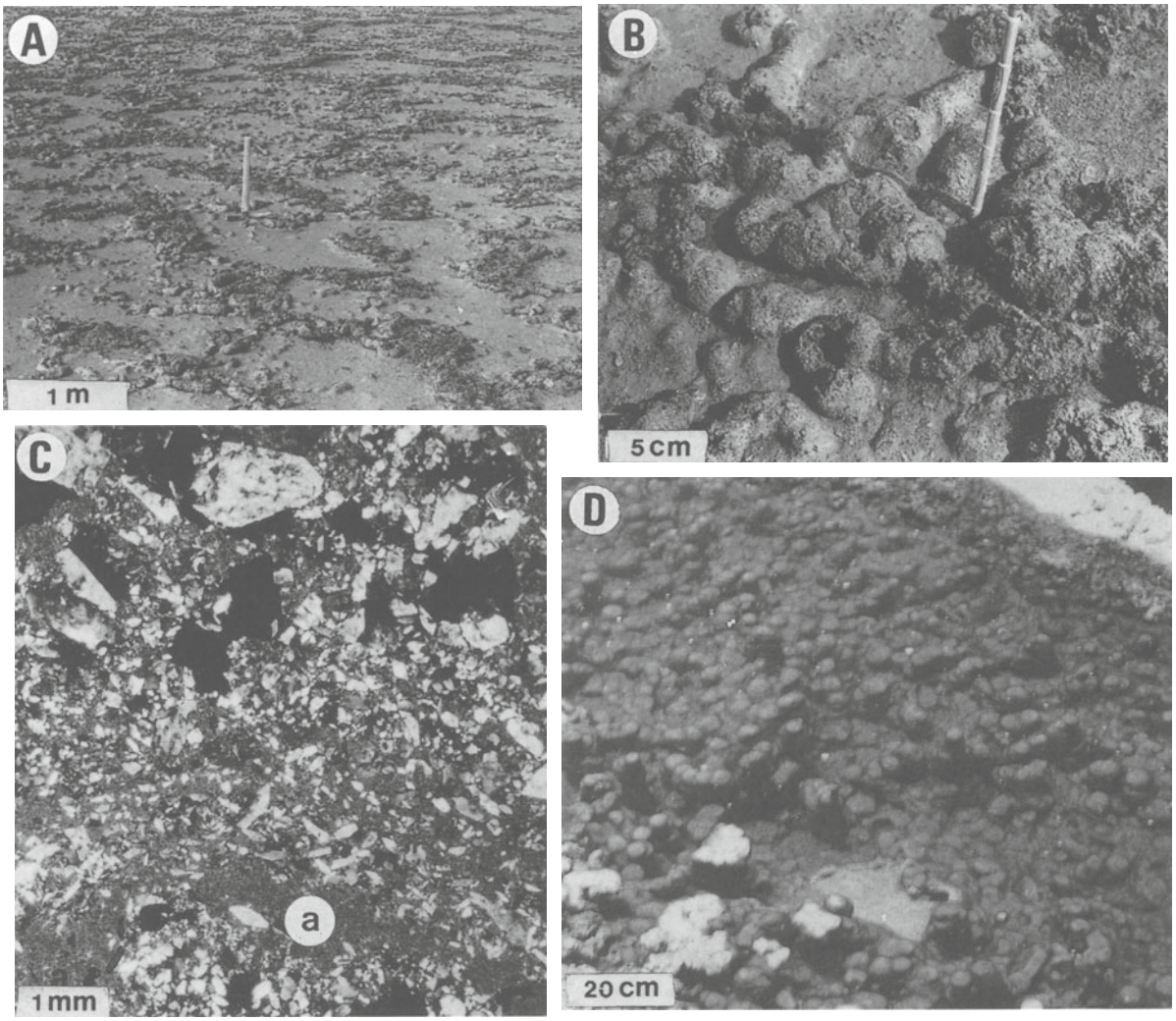

Fig. 5A–D. Modern examples. **A** Surface of a desiccated pond showing gypsified bulbous stromatolites. Abandoned salt works, near Alicante airport, SE Spain. **B** Close-up of **A. C** Detail of the lamination showing the basal micritic part (*a*) and the upward increase in both the density and size of gypsum crystals; same location; photomicrograph; crossed nicols. **D** Columnar gypsified stromatolites in hypersaline pond; Laguna Mormona, Baja California. (Courtesy of C. Pierre)

4 Conclusions

It is known that some prokaryotic organisms live in brines with salinity higher than 350‰ and have even been reported surviving in fluid inclusions trapped in halite crystals (Rotschild et al. 1994). Nevertheless, microorganisms living at such high concentrations do not contribute to the construction of well-developed microbial mats such as those described in Neogene examples. Mats are widespread at salinities lower than 150‰ (Cornée 1986; Orti-Cabo et al. 1986) and more rarely in the range 150–200‰ (Gerdes et al. 1985). In this concentration range, gypsum precipitates either subaqueously on the sediment surface or within the sediments from interstitial fluids, and thus microbial development and gypsum crystallization can occur concurrently. The luxuriant development of microbial communities in hypersaline environments occurs mainly because of their resistance to constraining physicochemical conditions which are lethal for most other organisms and which include abnormally elevated osmotic pressures, rapid changes in salinity and temperature, low content of dissolved oxygen, and periodic desiccation. In ancient deposits, growth of microbial mats is interpreted to have started during periods of dilution and to have continued until the onset of gypsum precipitation. The mats became rare or disappeared later in permanent evaporitic conditions, even if scattered microbial remains are still observed in the rest of the gypsum deposit.

Microbial assemblages are commonly observed in modern and ancient gypsum, but no direct relation be-

tween microbial activity and gypsum precipitation is implied. In contrast, microbial organisms are involved in processes of gypsum destruction by bacterial reduction of sulfates, which often prevent or limit the crystallization of gypsum in the upper reducing part of the sedimentary column. All the examples reported, in both modern and ancient gypsum deposits, show that microbial mat accretion and gypsum precipitation result from different processes. One of the biological processes able to enhance the precipitation of evaporitic minerals is osmoregulation, which can increase the concentration of interstitial brines and thus facilitate the gypsification of microbial mats (Perthuisot and Jauzein 1978; Castanier et al. 1995). So far as is known, the various types of microbial features described in gypsum deposits are due to the passive incorporation of microbial remains by mostly inorganic precipitation of gypsum. Thus, the term "gypsified microbial deposit" is preferred to "microbial gypsum," which implies that crystallization is more or less directly linked to microbial activity.

References

Castanier S, Perthuisot JP, Rouchy JM, Maurin A, Guelorget O (1992) Halite ooids in lake Asal, Djibouti: biocrystalline buildups. Géobios 25:811–821

Cornée A (1986) Etude préliminaire des bactéries des saumures et des sédiments des salins de Santa Pola (Espagne). Comparaison avec les marais salants de Salin-de-Giraud (Sud de la France). Rev Invest Geol Barcelona 38/39:109–122

Dronkert H (1985) Evaporite models and sedimentology of Messinian and Recent evaporites. Gua Pap Geol 24:283 pp

Friedman GM, Sneh A, Owen RW (1985) The Ras Muhammad Pool: Implications for the Gavish Sabkha. In: Friedman GM, Krumbein WE (ed) Hypersaline ecosystems. Springer, Berlin Heidelberg New-York, pp 218–237

Gerdes G, Spira Y, Dimentman C (1985) The fauna of the Gavish Sabkha and the Solar Lake – a comparative study. In: Friedman GM, Krumbein WE (eds) Hypersaline ecosystems. Springer, Berlin Heidelberg New-York, pp 322–345

Guillevin Y (1980) Eléments de pétrographie des évaporites oligocènes des bassins de Bresse et de Valence (Est de la France, vallée de la Saône et du Rhône). In: Dépôts évaporitiques, illustration et interprétation de quelques séquences. Technip, Paris, p 155

Gunatilaka A (1975) Some aspects of the biology and sedimentology of laminated algal mats from Mannar lagoon, Northwest Ceylon. Sediment Geol 14:275–300

Hardie LA, Eugster HP (1971) The depositional environment of marine evaporites: a case for shallow, clastic accumulation. Sedimentology 16:187–220

Kasprzyk A (1993) Stromatolitic facies in the Badenian (middle Miocene) gypsum deposits of southern Poland. N Jahrb Geol Abh 187:375–395

Krumbein WE, Cohen Y (1977) Primary production, mat formation and lithification: contribution of oxygenic and facultative anoxygenic Cyanobacteria. In: Flügel E (ed) Fossil algae. Recent results and developments. Springer, Berlin Heidelberg New York, pp 37–56

Kushnir J (1981) Formation and early diagenesis of varved evaporite sediments in a coastal hypersaline pool. J Sed Petrol 51: 1193–1204

Monty CLV (1965) Geological and environmental significance of Cyanophyta. Thesis, Princeton University, Princeton, NJ

Monty CLV (1972) Recent algal stromatolitic deposits, eastern Andros Island, Bahamas. Prelim Rep Geol Rundsch 61:742–783.

Monty CLV, Hardie LA (1976) The geological significance of the fresh-water blue-green algal calcareous marsh. In: Walter MR (ed) Stromatolites. Elsevier, Amsterdam, pp 193–259

Monty CLV, Rouchy JM, Maurin A, Bernet-Rollande MC, Perthuisot JP (1987) Reef-stromatolites-evaporites facies relationships from Middle Miocene examples of the Gulf of Suez and Red Sea. Springer, Berlin Heidelberg New York, pp 133–188

Orti-Cabo F, Pueyo-Mur JJ, Geisler-Cussey D, Dulau N (1986) Evaporitic sedimentation in the coastal salinas of Santa Pola (Alicante, Spain). Rev Invest Geol 38/39:169–220

Orszag-Sperber F, Rouchy JM, Bizon G, Bizon JJ, Cravatte J, Muller C (1980) La sédimentation messinienne dans le bassin de Polemi (Chypre). Géol Méd VII:91–102

Perthuisot JP, Jauzein A (1978) Le Khour el Aadid, lagune sursalée de l'Emirat de Qatar. Rev Géogr Phys Géol Dyn XX:347–358

Peryt TM, Poberezski AW, Jasionowski M, Petryczenko OI, Peryt D, Ryka W (1994) Facje gipsow badenskich Ponidzia i Naddniestrza. Przeglad Geol XLII:771–776

Rotschild LJ, Giver LJ, White MR, Mancinelli RL (1994) Metabolic activity of microorganisms in evaporites. J Phycol 30:431–438

Rouchy JM (1982) La genèse des évaporites messiniennes de Méditerranée. Mém Mus Nat Hist Nat Paris 50:267 pp

Rouchy JM, Pierre C (1979) Données sédimentologiques et isotopiques sur les gypses des séries évaporitiques d'Espagne méridionale et de Chypre. Rev Géogr Phys Géol Dyn 21:267–280

Rouchy JM, Monty CLV(1981) Stromatolites and cryptalgal laminites associated with Messinian gypsum of Cyprus. In: Monty CLV (ed) Phanerozoic stromatolites. Springer, Berlin Heidelberg New York, pp 155–178

Schreiber BC (1988) Subaqueous evaporite deposition. In: Schreiber BC (ed) Evaporites and hydrocarbons. Columbia Univ Press, New York, pp 182–255

Schreiber BC, Friedman GM, Decima A, Schreiber E (1976) Depositional environments of Upper Miocene (Messinian) evaporite deposits of three Sicilian basins. Sedimentology 23:729–760

Trashliev S (1969) Structure of the Tortonian gypsum rocks in Northwestern Bulgaria. Sediment Geol 3:291–316

Vai GB, Ricci-Lucchi F (1977) Algal crusts, autochtonous and clastic gypsum in a cannibalistic evaporite basin: a case history from the Messinian of Northern Apennines. Sedimentology 24: 211–244

Warren JK (1985) On the significance of evaporite lamination. In: Schreiber BC (ed) Proc Sixth Int Symp on Salt 1, pp 161–170

Youssef ESAA (1988) Sedimentological studies of Neogene evaporites in the northern Western desert, Egypt. Sediment Geol 59:261–273

Siliciclastic Intertidal Microbial Sediments

David M. Paterson, Kevin S. Black

Sediment Ecology Research Group, Gatty Marine Laboratory, University of St. Andrews, St. Andrews, Fife, KY16 8LB, Scotland

Abstract. Here, we briefly discuss the physical properties and biological nature of the surface region of intertidal sediments. Data to highlight the microspatial variability within sediments and emphasise the inherent linkage between physical properties and biological processes are presented. The nature of the intertidal depositional environment is discussed with reference to the conditions which sediment-inhabiting microbes must withstand. The horizontal and vertical distribution of microbial assemblages is considered against the penetration of light and oxygen into cohesive sediments. These data are supported by fine scale analysis of sediment properties using a novel freeze sampling and sectioning technique. The visualisation of sediment assemblage microstructure by low-temperature scanning electron microscopy is shown against the background of the extremely steep gradient of change found across the surface sediment layers. The biodiversity of microbial assemblages is considered in relation to recent developments in molecular techniques. The requirement for an integrated approach to the processes occurring at the sediment/water interface isemphasised.

1 Introduction

Siliciclastic intertidal sediment deposits support a wide variety of organisms largely represented by infaunal invertebrates and heterotrophic and autotrophic microbes (Admiraal 1984; Patterson 1989). The biomass of organisms can be high while assemblage diversity is generally low because of the specialised conditions and sharp gradients of change within periodically exposed sediments. Microbes, however, can flourish and are not merely passive components of the sediment ecosystem. The role of microbes in the physical structure, physicochemical conditioning and erosional potential of cohesive sediment is becoming increasingly recognised. The most well-known microbial sediments are stromatolites (Riding 1994) and the interpretation of these sedimentary features is important in terms of understanding the environmental conditions that pertained in the geological past and in the interpretation of the fossil record (Grotzinger and Rothman 1996). It is clear that microbes influence the sediment matrix, the distribution and transport of particles and the resistance of sediments to erosion in more subtle ways than through stromatolite development (Montague 1986; Underwood and Paterson 1993; Yallop et al. 1994; Paterson 1997). It is misleading to think of intertidal sediments in wholly physical or biological terms and it should be recognised that even sediment surfaces without obvious visual reminders of microbial biomass are active sites of biogeochemical transformation supporting significant microbial assemblages. Recent studies of such systems have begun to integrate biological and physical expertise (Paterson 1997), and the influence of microbial populations on the sediment surface properties are an excellent example of the close relationship between the physical and biological properties of sediments.

A broad definition of "microbial" is taken to include heterotrophic and autotrophic microbes whether eukaryotic (algae, fungi and protozoa) or prokaryotic (eubacteria and archaebacteria). There is no attempt to cover all aspects of sediment microbiology but only to introduce some of the recent areas of research activity. Many excellent sources exist for additional information on bacterial metabolism in sediments (Ehrlich 1990; Libes 1992), diatom ecology (Admiraal 1984) and sediment dynamics (Perillo 1995; Burt et al. 1997).

2 The Physical Environment

Broad intertidal sand and mudflats are found bordering many of the world's estuaries. These are formed as detrital particles from marine, fluvial and local erosion sources are deposited in areas of low current velocity. The characteristics and physical environment of intertidal sediment deposits contrast quite markedly with their terrestrial and shallow subtidal counterparts. Regular tidal emersion exposes the surficial sediment layers to wind and rain erosion, drying and compaction and extremes of temperature. However, a predominant characteristic of intertidal sediments is a shore-normal textural zonation produced by hydrodynamic forcing.

2.1 Horizontal Zonation

Horizontal zonation between a main (tidal) channel and the upper limit of tidal influence commonly consists of four identifiable sedimentary sub-environ-

R. E. Riding and S. M. Awramik (Eds.)
Microbial Sediments

ments: (1) saltmarsh, comprising vegetated fine silt and clay sediments, (2) higher mudflats, (3) sandy mud flats (mixed flats) which extend to approximately mid-tide level, and (4) lower sandflats, comprising wave-washed sands. Thus, an onshore fining of surface sediment with perhaps a zone of slightly coarser sediments around the mid-shore position is generally found (Evans 1965). Amos (1995) provides a useful intercomparison of the zonation patterns in a number of the world's major estuaries. Intertidal areas are also characterised by strong shore-normal gradients in subaerial exposure contingent upon site elevation and the tidal curve. In mid-latitude temperate estuaries, where semi-diurnal tides predominate (two inundations per 24 h), higher mudflat areas will be submerged for only a few hours and there is therefore great potential for modification by subaerial processes. Lower areas will be submerged for longer, and less influenced by exposure. Higher mudflat areas are also distinct because, during neap tides, sediments may be completely exposed for several consecutive days.

2.2
Compaction and Consolidation

The surface layers of sediments on tidal flats are regions of physical instability. The term "active layer" is used to denote sediments which are periodically resuspended, advected offshore, mixed and then settled again to the bed. The frequency of strong tidal currents (spring tides) and storms broadly controls the physical state of these sediment layers. Fine-grained sediments may display a variable porosity or degree of consolidation. It is not uncommon to find pools of comparatively fluid mud adjacent to much firmer muds at the surface of mudflats. A volume concentration of solid grains of about 10% is necessary before a matrix supported bed is formed (James et al. 1986), and hence the maximum porosity of soft, water-rich muds is around 90%. Typical porosity values for firmer muds are between 65 and 75%. The porosity of interface muds, unlike that of clean sands, is observed to change temporally. Self-weight consolidation following deposition of suspended floc aggregates under a tidal flow brings grains closer together, increasing the bulk density and decreasing the porosity. Even small changes in interface porosity can give rise to significant changes in sediment strength (Delo 1988), and this process is inherently linked to sediment stability. Temporal changes in interface porosity are the basis for tidal flat accretion over longer time scales (Hawley 1981). The process of self-weight consolidation is more dramatic following tidal recess, when deposited floc aggregates no longer have the support of the seawater. Consequently, they collapse more quickly and density (and erosion resistance) rises more rapidly (Black 1991). The physical properties of sediments vary on a microscale at the sediment/air interface (Fig. 1). Periodically exposed fine-grained sediments may thus acquire greater erosion resistance than fully submerged sediments. Amos et al. (1988) noted that tidal mudflat sediments in the Bay of Fundy were around 80 times stronger than comparable subtidal muds.

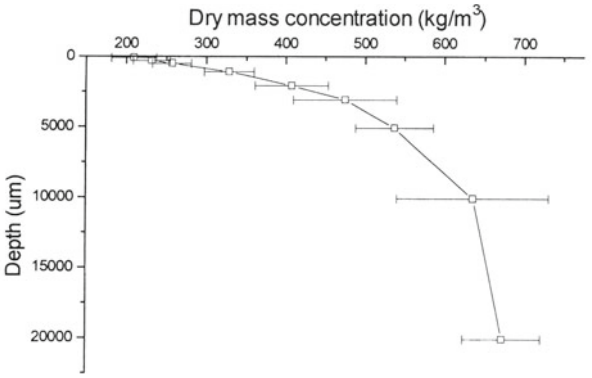

Fig. 1. Vertical microprofiles of the variation in dry mass concentration with depth from an intertidal cohesive sediment. Data were obtained by specialised freezing and sectioning techniques (Wiltshire et al. 1997) at a resolution of 200 μm ($n = 8$)

3
The Biological Environment

Intertidal rocky shores have been extensively studied because of "zonation," where visible bands of species (mainly macroalgae) appear in a predictable order progressing up the intertidal shore (Little and Kitching 1996). Zonation is thought to be caused by an interplay of biological and physical factors and indicates that physical and biological pressures are closely interlinked. Many of the conditions that cause zonation on intertidal rocky shore apply to intertidal depositional systems but with the added complexity of a soft-substratum which may itself be "zoned" by hydrodynamic sorting. A broad comparison of the conditions for life with respect to major environmental variables is given in Table 1.

3.1
Horizontal Zonation

Zonation on intertidal sediments has been noted for infauna but has been less studied for microbial assemblages. It seems likely that microbial zonation is probable and might be expressed in both assemblage structure and physiological activity, given the physicochemical gradients present between the lower and upper shore. Data indicate that microbial activity and biomass increase from the low water mark to the high water mark (Fig. 2; Paterson et al. 1990) This is likely to re-

Table 1. Summary comparison between major physico-chemical conditions after emersion during a daylight exposure period on solid and soft substrata

Variable	Hard substratum	Soft substratum
H_20	Rapid drying, therefore physiological adaptation by algae to tolerate desiccation, some surface moisture retained in crevices and by canopy development.	Evapotranspiration, followed by dehydration if conditions sufficiently severe. Microbes may produce EPS as a response to desiccating conditions.
Light	Irradiance exploited by epilithon and endolithon, high intensities of light can be damaging to phototrophs. Bleaching may occur.	Phototrophs must accumulate on or close to sediment surface, light attenuation extremely rapid. Avoidance of high intensities by migration beneath surface possible. Shallow oxic layer replaced by anaerobic conditions with associated bacteria.
Salinity	Salinity may vary in rock pools, particularly near at or above MHW.	Variation in salinity is driven by the marine or estuarine waters. Only on the high intertidal does rainfall or evapo-transpiration have a major effect on salinity levels.
Nutrients	Basis of food web is autochthonous production by algal primary production on sheltered shore. Allochthonous supply of organics dominates on exposed shores, usually exploited by filter feeders or surface scrapers.	Depositional systems are often considered to be detrital but carbon input may be equally distributed between water column processes, riverine and marine detrital sources and benthic productivity. The latter become more significant under turbid conditions. Nutrient generally considered to be readily available. More recent information suggest peak activity may well be nutrient-limited under conditions of rapid growth and high standing stock.
Breaking waves	High energy environment and particularly extreme on exposed shores, biota limited by wave force. Maximal effect in mid-tidal areas. Zones on exposed shore may be elevated by spray. Organisms adapted to tolerate or avoid wave crash.	Low energy environment but re-suspension of material by breaking wave-influential in short term dynamics. Episodic storm events may be extremely important in determining shore dynamics. Organisms must tolerate deposition and erosion.
Currents	Currents less influential than wave crash for intertidal forms. Deeper water forms may be limited by tidal currents.	Tidal current important in redistribution of sediments. Maximum transport occurs around the peaks of ebb and flood currents when suspended sediment load is maximal.

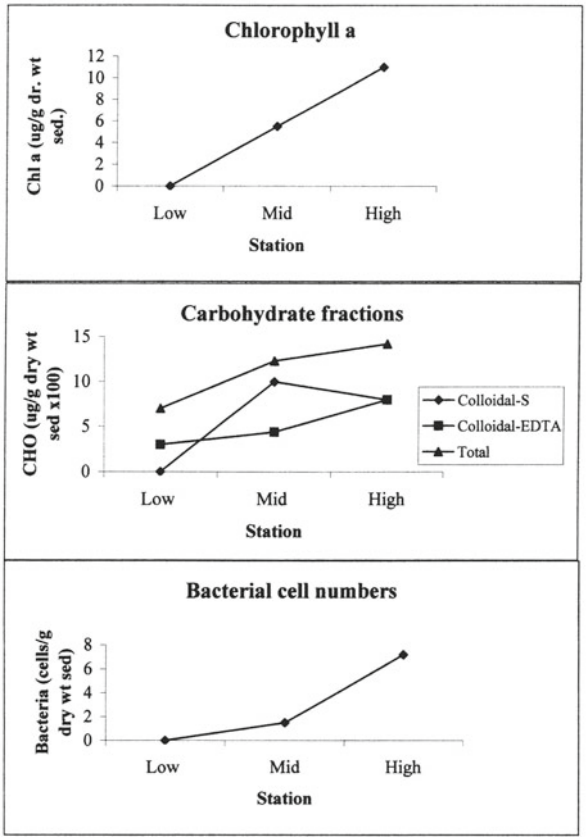

Fig. 2. Changes in the concentration of chlorophyll-a (autotrophic biomass), carbohydrate, and bacterial cell numbers measured along a shore-normal transect across an intertidal mudflat on the Severn Estuary. In general, there is an increase in these components from low to high shore positions

flect the less stable conditions around low water and the increasing exposure to light with tidal height. Cyanobacteria are often found in greater biomass towards the upper limit of the intertidal zone although trichomes can often be isolated by selective culturing of mid-intertidal sediments (Paterson, personal observation). On intertidal flats, the dominant autotrophs are pennate diatoms (Bacillariophyceae) and a few studies have suggested that zonation occurs (Carter 1933; Oppenheim 1988; Paterson and Underwood 1992).

3.2 Vertical Zonation

The interface region of microbial sediments is an area dominated by extreme gradients. The nature and metabolic linkages between closely associated populations and their remarkable adaptations to life within such gradients is becoming more evident (Van Germeden 1993). Gradients are established between sources and sinks through diffusive transport. Diffusion into cohesive beds is limited by the packing of the sediments and the consequent lack of void space. The diffusion of oxygen into sediments is limited and cohesive sediments become anaerobic within a short distance of the surface (Yallop et al. 1994). The oxic and anoxic zones support

a variety of bacteria each with particular abilities that help to define their niche within the system (Ehrlich 1990). The zones are not static but vary depending on many factors (Blackburn and Blackburn 1993) such as organic supply, in situ metabolism and light availability (Fig. 3). The depth profiles of oxygen obtained by micro-electrodes (Revsbech 1989) indicate the variable and transient nature of oxygen penetration. Some organisms may stay in position and cope with changes in the local physicochemical environment as the gradients alter. Others may move within the sediment to maximise their position in terms of resources such as light, nutrients or electron donors (Huettel et al. 1996; Stal 1996). Diatoms undergo a complex migration in which they arrive at the sediment surface when conditions are suitable for photosynthesis but depart from the surface as light fades or before the return of the tide (Round 1981; Hay et al. 1993). Many cyanobacteria can also position themselves in terms of available light, while the sulphur bacterium *Thioploca* spp. can migrate and actually extrude from the sediment to capture nitrate from overlying water (Huettel et al. 1996). The movement and activity of the microbes in turn influences the sources and sinks of elements within the bed. Thus it should be recognised that micro-organisms not only respond to changing gradients but are themselves responsible for inducing and changing gradients through their metabolic activity (oxygen production, respiration). In spatially compressed regions of rapid change, even limited locomotive abilities become significant. The rate of diatom locomotion through cohesive sediment has been calculated at around only 0.2 μm/s (Hay et al. 1993). This suggests that diatoms would rarely penetrate further than a few millimetres into the sediment, yet this is easily sufficient to reach the anoxic zone, acquire nutrients and be in complete darkness (Kuhl et al. 1994; Yallop et al. 1994).

4 Key Biological Processes

Identification of "key" biological processes in intertidal sediments is difficult given the complex natural biogeochemistry of sediment systems (Libes 1992). However, in terms of the illuminated surface layers, carbon fixation and the production of extracellular organic matter have a great impact on the ecology and physical dynamics of the system.

4.1 Primary Production

Primary production on the natural surface of intertidal flats should ideally be expressed in terms of carbon fixed during photosynthesis. This can be measured directly using radiolabelled carbon or by employing the stoichiometric relationship between carbon fixed and oxygen evolved. This relationship does not always ac-

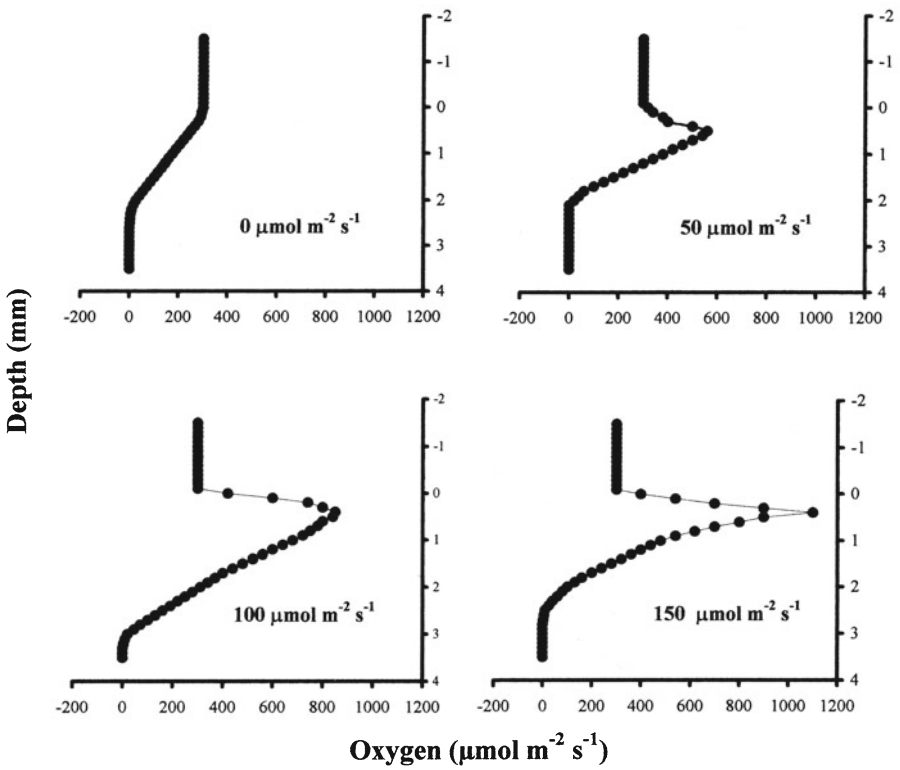

Fig. 3. Depth profiles of oxygen concentration within intertidal cohesive sediments inhabited by photosynthetic microbes. The profiles demonstrate the influence of light quantity (mol m^{-2} s^{-1}) and photosynthesis on oxygen within the sediments. When no light energy reaches the sediment surface, there is a steady decline in oxygen concentration. Where light is available, oxygen is produced in the surface layers of sediment resulting in a surface, or subsurface, peak in oxygen concentration depending on the microspatial distribution of the producers

curately reflect useful carbon fixation since alternative pathways exist which may not result in net gains in productivity (e.g. photorespiration). Until recently, most production measurements in sediments were based on modifications of the ^{14}C technique or the oxygen exchange method. These techniques have been superseded by oxygen micro-electrodes (Revsbech 1989). These can be applied in situ but are more generally used in laboratory studies, from which rates are later extrapolated to the field and linked to ambient conditions of biomass, light and tidal state. Such data (Fig. 3) can then be used to construct and later validate models to predict annual productivity from the surface of intertidal flats (Pinckney and Zingmark 1993). These models still have a number of limitations but represent a great improvement over calculations based on few and sporadic measurements. Problems still exist with the use of oxygen microsensors. Their use in the field is unusual but has been carried out by a number of groups. Many workers still obtain cores and then flood these to make measurements under constant conditions which are unlike the natural conditions. The flooding of a core can alter the migratory behaviour of the organisms leading to spurious results (Miles and Paterson, unpublished data). A recent and potentially exciting advance is the use of in situ fluorescence measurements based on the principle of pulse amplitude modulated (PAM) fluorescence. Pulses of low light and brief pulses of saturating light are used to investigate the activity of the photosynthetic reaction centres (Genty et al. 1989). This technology has a great deal to recommend it. It is non-invasive and provides a measure of the number of active photosynthetic sites, the molecular units responsible for photosynthesis, rather than the total chlorophyll. Recent studies have also shown that the system can be miniaturised to investigate the photosynthetic efficiency of single chloroplasts (Oxborough and Baker 1997) and can be applied to diatoms within biofilm layers (Oxborough, personal communication). These advances may mean that more accurate estimates of annual carbon budgets from intertidal areas will become available with more experimental evidence linking transient conditions to the photosynthetic efficiency of individual cells. This is of interest because of the ecological importance of the coastal systems and as a bench mark against which to estimate environmental change such as the global increase in CO_2 levels likely to affect primary productivity (Watson et al. 1996).

4.2 Extracellular Polymeric Substances

Organisms within sediments secrete complex organic material, often termed extracellular polymeric substances (EPS), composed of proteins, carbohydrates and lipids. EPS secretions perform a variety of functions within marine sediments systems including protection from abrasion and desiccation and sequestration of toxic compounds; they also act as a food source (Decho 1990). Interest in EPS has grown because of their influence on the physical properties of the sediment and the general adaptive significance of EPS (Decho 1994, and this Volume). Studies have shown that the erosion threshold and erosion rate of sediment may be modified by the presence of microbial assemblages (Grant and Gust 1987; Paterson 1994). Predictive relationships are unreliable because of the variable nature and patchiness of biological effects. Despite this, considerable work on the mediation of sediment transport by biological action and the measurement of EPS is underway (Underwood et al. 1995).

5 Biophysical Processes

5.1 The ETDC Cycle

The ETDC (erosion, transport, deposition, and consolidation) cycle describes the fundamental processes that govern the geomorphology of intertidal mudflats. These incorporate the biological properties of the system. Given the pervasive occurrence of microbes, it is not unfair to suggest that much previous work may have been inadvertently and unknowingly affected by microbial processes. Sheng (1983) pointed to the activity of bacteria as a confounding influence in his "abiotic" erosion experiments. For this reason it is important to understand the ecology of microbes and the influence that they can exert on sediments. Each stage of the ETDC cycle can be examined for biological modification. Most work has been done on the erosion process itself, dating from the innovative studies of Neumann et al. (1970), using an early in situ flume, and the laboratory studies of Holland et al. (1974). The conclusions of these early studies have been supported by further work and the focus now is on ways to predict biological effects (Grant and Gust 1987; Black 1997; Paterson 1997). The transport of material is dependent on the density and size of the eroded particles and subsequent flocculation. Therefore flocculation is a critical process and the deep sea phenomenon of marine snow is perhaps the most widely known example of biodeposition, although fecal pellet formation and pseudofecal production in shallow waters should also be included. The consolidation of sediments is affected by bioturbation (Grant and Daborn 1994) while the biogeochemistry may be influenced through gas production and bubble formation. Of most relevance to this chapter is the influence of benthic micro-organisms on sediment properties and strength.

A number of field and laboratory experiments have correlated various indices of microbial biomass (e.g. chlorophyll-a, ATP content, cell numbers) with erosion resistance (Montague et al. 1992). In some cases order of magnitude reductions in erosion have been reported for heavily colonised sediments (Paterson and Daborn 1991). More detailed experiments have examined the binding mechanism of the polysaccharide (Grant and Gust 1987; Dade et al. 1990; Krumbein et al. 1994). The importance of this phenomenon, particularly during summer months when biological processes are naturally more rapid, is being realised. However, it is important to remember that whilst the instantaneous state of the sediment may reflect the interplay of biological and physical processes, powerful winter storms cannot be resisted and will ultimately redistribute sediments. Yet, the occurrence of organic material in eroded flocs and remaining in the sediment may enhance the recovery of the system. There is evidence that organic material in the sediment enhances accretion rates (Underwood and Paterson 1993).

5.2
Sediment Matrix Microstructure

Water is an important structural element within microbial assemblages and hydrated sediments. Water may occur in two states, bound or free. Free water is available for reactions and evaporation but bound water is complexed within organic material or within clay mineral particles and requires energy to be released. Removal of the water and organic material is the normal practise where information on the nature of the primary particles is required (Whalley 1978), but is not appropriate where details of the natural matrix requires are required. Advances have been made in the use of low-temperature scanning electron microscopy (LTSEM; Paterson 1995; Défarge et al. 1997), parahistology (Wachendorfer et al. 1994) and confocal microscopy (de Beer et al. 1997), to visualise the "natural" structure of assemblages (Fig. 4). This work demonstrates the biogenic nature of the sediment, and it is informative to contrast the natural matrix with images of clay minerals, devoid of organics, produced for sedimentological studies (Whally 1978). Accurate visualisation of the surface shows the relative position of the micro-organism and the concentration of biomass. This helps to place the steep gradients found using microsensor technology in a clear conceptual framework and explain the high concentration of microbial metabolites and markers (e.g. carbohydrates and chlorophylls) found in the upper millimetres/microns of the sediment (Wiltshire et al. 1997). LTSEM shows the variability in the void space with depth (Paterson 1994, 1995) and at slightly higher resolution (1 mm) cat-scan tomography has identified surface "buoyant" zones that may be a result of intense microbial activity at the sediment/water interface of natural submerged sediments (Sutherland 1996).

6
Some Recent Developments

6.1
Community Analysis: Biodiversity

The reductionist approach to the understanding of microbial assemblages is to identify each contributory population and examine its metabolic capacities within the niche occupied. In microbial terms, this goal is far from being achieved and may be impossible. The requirement to culture cells is a major limitation since the vast majority of marine bacteria have never been cultured. Many groups of cells also operate in consortia and cannot be examined independently. This limitation applies to diversity analysis and to quantification based on most-probable number techniques. Direct counts may be preferable but give little information on assemblage diversity. Where cultures can be obtained problems in the interpretation of "species" may still arise. Until the advent of molecular techniques, cyanobacterial species were identified on the basis of their appearance (phenotype). However, 16 S rDNA analysis of "different" cyanobacteria, identified as belonging to genus *Merismopedia*, were found to be the same species although displaying significant phenotypic variability (Palinska et al. 1996). The answer may again lie on the ability to extract and amplify pieces of genetic directly from natural assemblages (polymerase chain reaction methods, PCR) to produce a "fingerprint" of diversity (Vandamme et al. 1996). Some components of the fingerprint may even be identified against existing sequence databases which are continually being extended. Eukaryotes are not exempt from difficulty. Many flagellate and ciliate protists inhabit the interstitial voids of sediments (Patterson 1989) but have become a rather specialised area of study, since they move rapidly and are difficult to identify although their ecological role may be significant. Diatoms are less motile and species are traditionally separated on the basis of the patterning on the surface of their silica cell wall. However, closely related species can appear very similar, even to the expert, and separation may require electron microscopy or a molecular approach (Medlin et al. 1991). It seems certain, given our present state of knowledge, that the biodiversity of microbial assemblages is vastly underestimated.

6.2
Remote Sensing

The Fifth European Action Programme on the Environment (Com (92) 23 final 27/3/92) identified growing

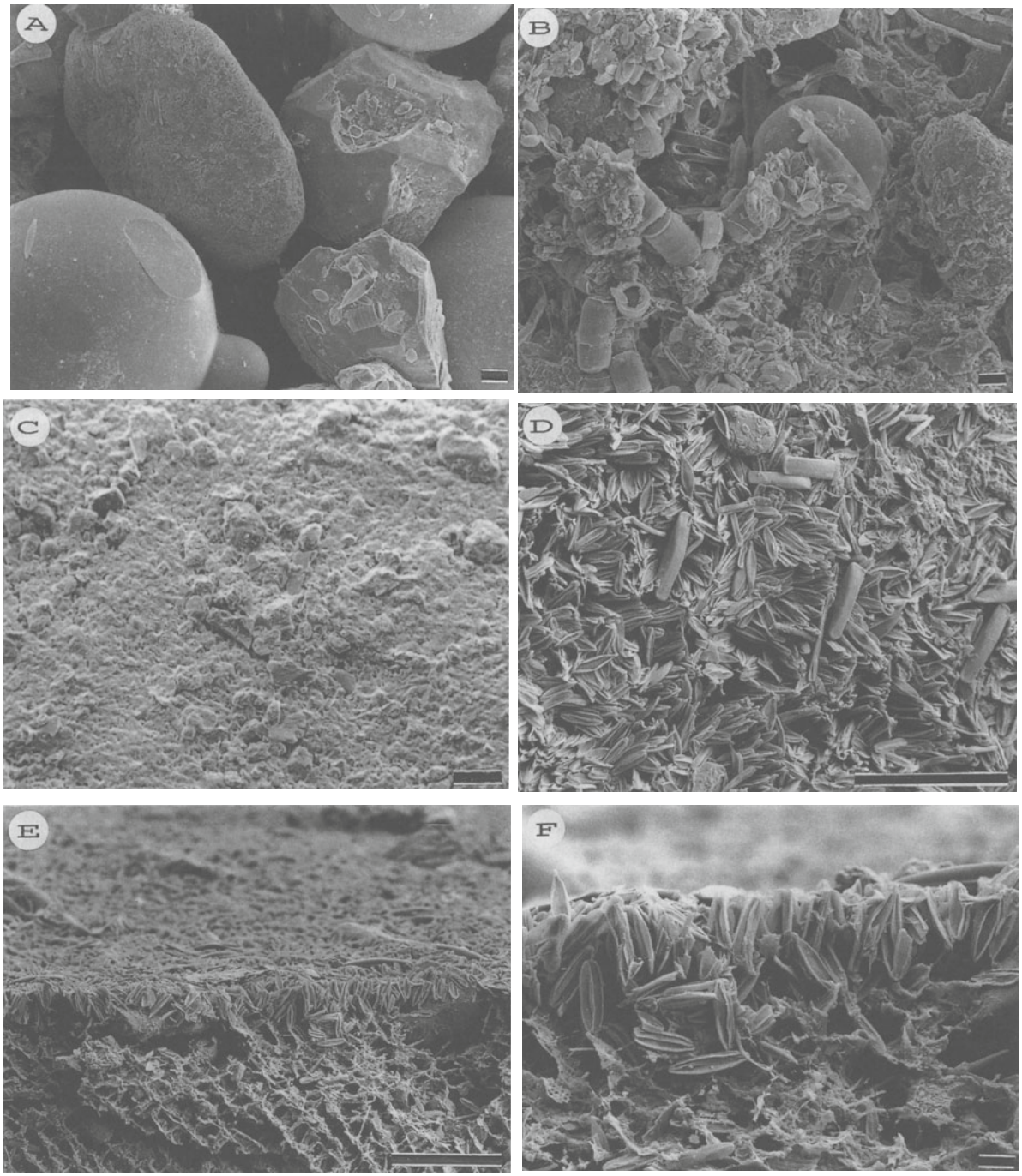

Fig. 4A – F. Low-temperature scanning electron micrographs of sediments. **A** Natural sediment mixed with marker beads (Ballontini balls) and then cleaned of organic material. The beads and natural particles are clear of most surface "contamination" and their outline is clearly visible (*scale bar* = 10 μm). **B** Similar material as that shown in **A**, but without treatment to remove organics. The beads are obscured by fine particles and organic material, no discrete grains can de seen (*scale bar* = 10 μm). **C** The surface of a natural sediment with no obvious biofilm (*scale bar* = 20 μm). **D** The surface of similar sediment with a surface assemblage of diatoms, mainly *Nitzschia spp.* (*Scale bar* = 100 μm). **E** Fracture-face across the surface of sample **D**. The diatoms form a dense layer above a card-house sediment structure (*scale bar* = 100 μm). **F** Detail of the highly compacted surface layer of diatom biomass (*scale bar* = 10 μm)

industrial and demographic threats to the 58,000 km of European coastline. The region around the coast is too extensive to monitor regularly by ground survey techniques but too environmentally and economically important to ignore. Remote discrimination of sediment type (mapping) of intertidal regions (Doerffer and Murphy 1989; Yates et al. 1993) has led to attempts to infer the distribution of biomass of a certain type. This includes analysis of the distribution of wading birds, determined from the nature of the feeding grounds. Further research has shown that the optical properties of the sediment vary with the microbial biofilm that inhabit the surface (Kuhl et al. 1994). This has been further developed (Paterson, unpublished data) to show that the spectral reflectance from the surface of natural sediments is influenced by the biomass, assemblage structure and microspatial distribution of phototrophs within the sediment matrix. These data suggest the intriguing possibility that links could be established between the spectral reflectance signal and microbial assemblages on surface sediments. This linkage could have fundamental importance for wide-scale monitoring of the ecology and possibly dynamics of intertidal systems. A note of caution is essential. The biomass in the surface layers of intertidal sediments is unlike a forest canopy, which remains stable on a temporal scale of weeks and months. Microbial assemblages undergo cyclic migration, are subject to grazing, influenced by episodic events, reproduce rapidly, and respond quickly to physicochemical changes. The result is a highly dynamic system with heterogeneous distributions of biomass in both space and time. Thus interpretation of the remote signal requires knowledge of the ecology of the organisms and local conditions before the data can be properly interpreted, but it has exciting potential.

7 Integrated Studies

Given that almost no surface sediments are devoid of life, it is surprising that the integration of physical and biological science in this field has taken so long. However, system responses can be extremely complex, as exemplified by the work of Daborn et al. (1993) in the Bay of Fundy. They found that the erodibility of the intertidal sediment is at least seasonally modified by microbial processes. Sediment stability was influenced by the production of EPS by algae (diatoms) living within the sediments. This enhanced the stability of the sediment but the diatom populations were normally limited by the grazing activity of the amphipod *Corophium volutator*. When the grazers were removed, either by experimental treatment or by flocks of feeding birds, the diatom biomass increased dramatically as did relative stability of the sediment. This may be a common scenario linking physical and biological properties but more integrated studies are required before this can be shown (Black and Paterson 1996). Several European programmes and national agencies are now encouraging interdisciplinary research to promote the holistic investigation of microbial sediments (NERC, UK LOIS programme, EC Environment and MAST programmes) and it is to be hoped that these initiatives will continue to increase our knowledge of the biophysics of depositional environments.

Acknowledgements. Several agencies supported work reported in this review, including the EC Environment Programme (PRO-MAT project, EV5V-CT94-0411) and the EC MAST Programme (INTRMUD project MAS-CT95-0022). Irvine Davidson completed the LTSEM photography. Some sediment samples were supplied by Dr Karen Wiltshire. Figures 2 and 4 arise from the Ph.D. studies of Ms. I. Taylor and are used with her kind permission. All sources and help are gratefully acknowledged including the contribution of two anonymous reviewers. This paper represents contribution No 219 from the NERC LOIS special topic award to the LISP (Littoral Investigation of Sediment Properties) group and NERC award GST/02/787.

References

Admiraal W (1984) The ecology of estuarine sediment-inhabiting diatoms. In: Round FE, Chapman DJ (eds) Progress in phycological research. 3. Biopress, UK

Amos CL (1995) Siliciclastic tidal flats In: Perillo GME (ed) Geomorphology and sedimentology of estuaries developments in sedimentology 53. Elsevier, Amsterdam

Amos CL van Waggoner NA, Daborn GR (1988) The influence of subaerial exposure on the bulk properties of fine-grained intertidal sediment from the Minas Basin Bay of Fundy. Estuar Coastal Shelf Sci 108:175-196

Black KS (1991) The erosion characteristics of cohesive estuarine sediments: some in situ experiments and observations. Thesis, University of Wales, Swansea, UK

Black KS (1997) Biophysical factors contributing to erosion resistance in natural cohesive sediments. In: Burt N, Parker R, Watts J (eds) Cohesive sediments. Wiley, Chichester, UK

Black KS, Paterson DM (1996) LISP-UK: An holistic approach to the interdisciplinary study of tidal flat sedimentation. Terra Nova 8(4):304-308

Blackburn, TH, Blackburn ND (1993) Rates of microbial processes in sediments. Philos Trans R Soc Lond 344:49-58

Burt N Parker R, Watts J (1997) Cohesive sediments. Wiley, London

Daborn GR, Amos CL, Berlinsky M, Christian H, Drapeau G, Faas RW, Grant J, Long B, Paterson DM, Perillo GME, Piccolo MC (1993) An ecological "cascade" effect: migratory birds affect stability of intertidal sediments. Limnol Oceanogr 38(1):225-231

Dade BW, Davis JD, Nichols PD, Nowell ARM, Thistle D, Trexler MB, White DC (1990) Effects of bacterial exopolymer adhesion on the entrainment of sand. Geomicrobiol J 8:1-16

Carter N (1933) A comparative study of the algal flora of two slat marshes. Part III. J Ecol 21:385-403

de Beer D, Stoodley P, Lewandowski Z (1997) Measurement of local diffusion coefficients in biofilms by microinjection and confocal microscopy. Biotech Bioeng 53(2):151-158

Decho AW (1990) Microbial exopolymer secretions in ocean environments: Their role(s) in food webs and marine processes. Oceanogr Mar Biol Annu Rev 28:73-153

Decho AW (1994) Exopolymers in microbial mats: assessing their adaptive roles In: Caumette P, Stal LJ (eds) Microbial mats. NATO ASI series, 35:97

Défarge C, Trichet J, Jaunet A, Robert M, Tribble J, Sansone, FJ (1996) Texture of microbial sediments revealed by cryo-scanning electron microscopy. J Sediment Res 66:935-947

Delo EA (1988) Estuarine muds manual. Rep SR 164, Hydraulics Research Ltd, Wallingford, UK

Doerffer R, Murphy D (1989) Factor analysis and classification of remotely sensed data for monitoring tidal flats. Helgol Meeres 43:275–293
Ehrlich HL (1990) Geomicrobiology. Marcel Dekker, New York
Evans G (1965) Intertidal flat sediments and their environment of deposition in the Wash. J Geol Soc Lond 121:209–245
Genty B Briantais JM, Baker NR (1989) The relationship between the quantum yield of photosynthetic electron transport and quenching of chlorophyll fluorescence. Biochim Biophys Acta 990:87–92
Grant J, Daborn G (1994) The effects of bioturbation on sediment transport on an intertidal flat. Neth J Sea Res 32(1):63–72
Grant J, Gust G (1987) Prediction of coastal sediment stability from photopigment content of mats of purple sulphur bacteria. Nature 330:244–246
Grotzinger JP, Rothman DH (1996) An abiotic model for stromatolite morphogenesis. Nature 383(3):423–425
Hawley N (1981) Mud consolidation during a short time interval. Geomar Lett 1:7–10
Hay SI, Maitland TC, Paterson DM (1993) The speed of diatom migration through natural and artificial substrata. Diatom Res 8:371–384
Holland AF, Zingmark RG, Dean JM (1974) Quantitative evidence concerning the stabilization of sediments by marine benthic diatoms. Mar Biol 27:191–196
Huettel M, Forster S, Kloser S, Fossing H (1996) Vertical migration in the sediment-dwelling sulfur bacteria *Thioploca* spp in overcoming diffusion limitations. App Environ Microbiol 62(6): 1863–1872
James AE, Williams DJA, Williams PR (1986) Small strain low shear rate rheometry of cohesive sediments In: Dronkers J, van Leussen W (eds) Physical processes in estuaries. Springer, Berlin Heidelberg New York
Krumbein WE, Paterson DM, Stal LJ (1994) Biostabilization of sediments. Carl von Ossietzky Universität Oldenburg
Kühl M, Lassen C, Jorgensen BB (1994) Optical measurements of microbial mats: Light measurements with fibre-optic microprobes. In: Stal LJ, Caiumette P (eds) Microbial mats. NATO ASI Series 35:149
Libes SM (1992) An introduction to marine biogeochemistry. Wiley and Sons, Chichester
Little C, Kitching J (1996) The biology of rocky shores. Oxford Univ, Oxford
Medlin LK, Elwood HJ, Stickel S, Sogin ML (1991) Morphological and genetic variation within the diatom *Skeletonema costatum* (Bacillariophyta): Evidence for a new species *Skeletonema pseudocostatum*. J Phycol 27:514–524
Montague CL (1986) Influence of biota on the erodibility of sediments. In: Mehta AJ (ed) Lecture notes on coastal and estuarine studies. 14:251
Montague CL, Parchure T, Paulic MJ (1992) The stability of sediments containing microbial communities: initial experiments with varying light intensity In: Mehta AJ (ed) Nearshore and estuarine cohesive sediment transport. Springer, Berlin Heidelberg New York
Neumann AC, Gebelein CD, Scoffin TP (1970) The composition structure and erodibility of subtidal mats. Abaco Bahamas J Sed Petrol 40:274–297
Oppenheim DR (1988) The distribution of epipelic diatoms along an intertidal shore in relation to principal physical gradients. Bot Marina 31:65–72
Oxborough K, Baker NR (1997) An instrument capable of imaging chlorophyll a fluorescence from intact leaves at very low irradiance and at the cellular and sub-cellular levels of organisation. Plant Cell Environ 20:1473–1483
Palinska KA, Liesack W, Rhiel E, Krumbein WE (1996) Phenotype variability of identical genotypes: the need for a combined approach in cyanobacterial taxonomy demonstrated on *Merismopedia*-like isolates. Arch Microbiol 166:224–233
Paterson DM (1994) Microbiological mediation of sediment structure and behaviour In: Caumette P, Stal LJ (eds) Microbial mats. NATO ASI Series 35:97
Paterson DM (1995) The biogenic structure of early sediment fabric visualised by low-temperature scanning electron microscopy. J Geol Soc 152:131–140
Paterson DM (1997) Biological mediation of sediment erodibility: Ecology and physical dynamics In: Burt N, Parker R, Watts J (eds) Cohesive sediments. Wiley, Chichester
Paterson DM, Daborn GR (1991) Sediment stabilisation by biological action: Significance for coastal engineering. In: Peregrine DH, Loveless JH (eds) Developments in coastal engineering. University of Bristol Press, UK
Paterson DM, Underwood GJC (1992) The mudflat ecosystem and epipelic diatoms.1991 Proc Bristol Nat Soc 50:74–82
Paterson DM, Crawford RM, Little C (1990) Subaerial exposure and changes in the stability of intertidal estuarine sediments. Estuar Coastal Shelf Sci 30:541–556
Patterson DJ (1989) The ecology of heterotrophic flagellates and ciliates living in marine sediments. Prog Protistol 3:185–277
Perillo GME (1995) Geomorphology and sedimentology of estuaries. Elsevier, Amsterdam
Pinkney J and Zingmark RG (1993 Modelling intertidal benthic microalgal production in estuaries. J Phycol 29:396–407
Revsbech NP(1989) An oxygen sensor with a guard cathode. Limnol Oceanogr 34:474–478
Riding R (1994) Stromatolite survival and change: the significance of Shark Bay and Lee Stocking Island subtidal columns In: Krumbein WE, Paterson DM, Stal LJ (eds) Biostabilisation of sediments. Carl von Ossietzky, Universität Oldenburg, pp 183–202
Round FE (1981) The ecology of the algae. Cambridge University Press, Cambridge
Round FE (1996) What characters define diatom genera species and infra-specific taxa? Diatom Res 11(1):203–218
Sheng YP (1983) Transport entrainment and deposition of cohesive sediments Mathematical modelling of 3-dimensional coastal currents and sediment dispersal. Technical Report CERC-83–2 Vicksburg Mississippi US Army WES
Stal LJ (1996) Physiological ecology of cyanobacteria in microbial mats and other communities New Phytol 131:1–32
Sutherland T (1996) Biostablization of estuarine subtidal sediments. Thesis, Dalhousie University, Nova Scotia, Canada
Underwood GJC, Paterson DM (1993) Recovery of intertidal benthic diatoms after biocide treatment and associated sediment dynamics. J Mar Bio Assoc UK 73:24–45
Underwood GJC, Paterson DM, Parkes RJ (1995) The measurement of microbial carbohydrate exoploymers from intertidal sediments. Limnol Oceanogr 40(7):1243–1253
Van Germeden H (1993) Microbial mats: A joint venture. Mar Geol 113:3–25
Vandamme P, Pot B, Gillis M D, Vos P, Kesters K, Swings J (1996) Polyphasic taxonomy a consensus approach to bacterial systematics. Microbiol Rev 60:407–438
Wachendorfer V, Riege H, Krumbein WE (1994) Parahistological sediment thin sections In: Caumette P, Stal LJ (eds) Microbial mats, vol 35. NATO ASI Series
Watson RT, Zinyowera MC, Moss RH, Dokken DJ (1996) Climate Change 1995 Impacts adaptations and mitigation of climate change. Scientific-Technical analyses. Cambridge University Press, Cambridge
Whalley WB (1978) Scanning electron microscopy in the study of sediments. Geol Abs Ltd, UK
Wiltshire KH, Blackburn J, Paterson DM (1997) The Cryo-lander: A new method for in situ sampling of unconsolidated sediments minimising the distortion of sediment fabric. J Sed Res 67(5):980–984
Yallop ML, de Winder B, Paterson DM, Stal LJ (1994) Comparative structure primary production and biogenic stabilization of cohesive and non-cohesive marine sediments inhabited by microphytobenthos. Estuar Coastal Shelf Sci 39:565–582
Yates MG, Jones AR, McGrorty S, Goss-Custard JD (1993) The use of satellite imagery to determine the distribution of intertidal surface sediments of the Wash England. Estuar Coastal Shelf Sci 36:333–344

Subaqueous Siliciclastic Stromatolites: A Case History from Late Miocene Beach Deposits in the Sorbas Basin of SE Spain

Juan C. Braga, José M. Martín

Departamento de Estratigrafia y Paleontologia, Universidad de Granada, Campus de Fuentenueva, 18002 Granada, Spain

Abstract. Agglutination of particles is a major process involved in microbial dome formation. Early lithification by biogenic precipitation or early cementation is also essential for dome accretion and preservation. Although it is possible for agglutinated grains to be siliciclastic, reports of siliciclastic microbial domes are scarce. Early lithification of microbial mats seems to have taken place only rarely in settings with terrigenous influx in marine environments. The few recorded examples of siliciclastic stromatolites and thrombolites occur, however, in a wide range of sedimentary environments, from coastal lakes to relatively deep subtidal settings, and from the Cambrian to the late Cenozoic.

We describe a new example of siliciclastic stromatolites in a Messinian (Late Miocene) post-evaporitic unit (the Sorbas Member) near Sorbas town in the Sorbas Basin of Almería, southern Spain. These stromatolites occur in beach deposits. Stromatolite domes formed at the transition from the lowermost beach shoreface to the shelf. They are made up of dense, peloidal, clotted and bushy micrite, interpreted as microbial precipitates, together with siliciclastic particles which constitute up to 40% of the rock volume. Within a single stromatolite bed there is variation in dome composition and morphology. Proximal domes contain sand-grade siliciclastics, distinct lamination and high synoptic relief with steep sides. Downslope, they grade into large, flattened, silty stromatolites with gentle sides, intercalating with silt lenses. Microbial mats developed at the bottom of the lowermost part of the beach, but were inhibited by stronger wave energy at shallower settings. Deeper waters on the shelf were probably too dark for mat growth and dome formation.

1 Introduction

Siliciclastic stromatolites and thrombolites were defined by Martín et al. (1993) as those containing more than 10% siliciclastic particles. Martín et al. (1993) subdivided these deposits into siliciclastic-carbonate and sandstone stromatolites and thrombolites, when the siliciclastic content is 10–50% and +50%, respectively.

Microbial carbonates can form by processes involving variable proportions of organically controlled precipitation of carbonate (biomineralization), trapping (agglutination) of particles, and cementation (Riding 1991). Nothing in these processes predetermines the nature of the trapped particles or prevents the agglutinated grains from being siliciclastic. In fact, small amounts of terrigenous grains, representing low percentages of the rock volume, commonly occur in Recent and fossil carbonate stromatolites (Logan 1961; Davis 1966). Terrigenous influx in sites of microbial growth, precipitation and/or early cementation would suffice to form siliciclastic microbial carbonates. However, such a situation seems to have been uncommon in the geological record, as trapped particles are carbonate in most known examples.

Prokaryotes and microalgae, the organisms promoting the accretion of microbial carbonates, form biofilms and microbial mats on terrigenous sediments and contribute to their stabilization in present-day subaqueous environments (e.g. Grant 1988, 1991; Paterson 1989; Meadows et al. 1994), but have low preservation potential (Cameron et al. 1985; Gerdes and Krumbein 1987).

Early lithification, necessary for the accretion and preservation of agglutinated microbial domes (Logan 1961; Park 1977), does not take place in most present-day mats and biofilms on terrigenous substrates (Schwarz et al. 1975). This was probably the usual situation in the past as well, since recorded examples of siliciclastic domes are scarce. Early precipitation of carbonate in microbial mats and biofilms only rarely occurred together with an influx of siliciclastic grains in marine environments.

The early lithification essential for microbial dome preservation can only take place in tropical and subtropical marine environments, where water temperature and carbonate saturation favor microbial calcification and early cementation. Terrigenous influx from rivers in humid tropical settings is nearly continuous, probably causing turbidity too high to allow significant microbial mat development. At the same time, continuous freshwater input is likely to reduce carbonate saturation, thus decreasing chances of early lithification. In contrast, in arid and semiarid tropical to subtropical areas, where river discharge is episodic, sporadic terrigenous supply may occur in the same settings in which mature microbial mats are able to develop and early lithification can take place. Such palaeoclimatic contexts would seem to have been the most appropriate ones for siliciclastic microbial dome formation, but our present knowledge of the palaeoenvironments in which examples from the fossil record developed is too limited to allow generalization.

R.E. Riding and S.M. Awramik (Eds.)
Microbial Sediments

2 Geological Record of Siliciclastic Microbial Domes

Despite the scarcity of their records, siliciclastic stromatolites and thrombolites have formed in an unexpected variety of palaeoenvironments, including lakes and relatively deep subtidal settings, from the Cambrian to Late Cenozoic. The oldest known examples occur in the Lower Cambrian from southern Israel (Soudry and Weissbrod 1995). Stromatolitic domes made up of 70% siliciclastic grains, cemented by calcite and dolomite spar, occur within cross-stratified sandstones. They have laminar and pseudocolumnar to columnar macrofabrics. These domes grew in a tidal sandflat cut by channels (Soudry and Weissbrod 1995).

Davis (1968) described laterally linked stromatolite domes made up of quartz sandstone with thin laminae of dolomite from the Lower Ordovician in Minnesota. The domes formed at the transition from a carbonate bank, with frequent carbonate stromatolites to quartz sandy sediments.

In Lower Carboniferous examples in delta deposits from the Algerian-Libyan border, described by Bertrand-Sarfati (1994), siliciclastic stromatolite domes occur in two distinct units which crop out for tens of kilometers. The lower unit formed in a delta-plain lake. The upper unit is made up of domes of diverse shape and size, surrounded by oolitic and bioclastic carbonates and shales. This latter unit formed in a quiet subaqeous setting in an intertidal lagoon. In both units the dominant stromatolite microfabric consists of thin micritic laminae with fenestrae and 10–50% fine-grained siliciclastics.

Harwood (1990) described sandstone stromatolites from nearshore equivalents of the Permian Capitan Reef in New Mexico. These stromatolites formed in shallow, quiet submarine settings at the transition from coastal siliciclastic to carbonate back-reef deposits.

The youngest record of fossil, shallow-marine, siliciclastic microbial domes is from the Upper Miocene (Messinian) in southern Spain (Martín et al. 1993; Braga et al. 1995). These domes developed on fan deltas at the northern margin of the Sorbas basin. Domes occur along transects from a shallow shelf down a palaeoslope to the basin. High-relief and steep-sided thrombolites and stromatolites grew at the shelf break, where they trapped poorly sorted coarse siliciclastics finer than grains in the surrounding conglomerates and sandstones. Domes on the slope and in the basin are gentle-sided stromatolites containing better-sorted sand-grade grains (Martín et al. 1993). Microfabrics are similar throughout the transect, consisting of dense, bushy or clotted micrite with fenestrae and varying amounts of siliciclastics, comprising up to 60% of the rock volume. Domes throughout these settings accreted by microbial calcification combined with agglutination of both terrigenous and carbonate grains (Braga et al. 1995). The associated biota points to nomal marine salinities during dome development (Martín et al. 1993).

Stromatolites covering boulders and pebble layers have also being described in upper Miocene coastal deposits from Cabrera in the Balearic Islands (Fornós and Pomar 1984).

We report here a new example of siliciclastic stromatolites from the Messinian in southern Spain. Although the stratigraphic context of these stromatolites is similar to the microbial domes mentioned above, which formed on fan deltas, their sedimentary setting is different, having formed in distal beach palaeoenvironments. These new examples therefore represent an additional sedimentary environment in which siliciclastic microbial carbonates are known to develop.

3 Stromatolites in Beach Deposits from the Sorbas Basin

3.1 Geological Setting

The siliciclastic stromatolites studied occur in beach deposits from the Sorbas Member in the Sorbas Basin, a small, intramontane Neogene basin within the Betic Cordillera (Fig. 1). In this area the Sorbas Member (Ruegg 1964) constitutes the transgressive systems tract of the Upper Messinian Depositional Sequence (Martín and Braga 1994, 1996; Fig. 2), which can be correlated with the TB 3.4 cycle of Haq et al. (1987). The palaeogeography of the Sorbas basin at the time of Sorbas Member deposition was a bay opening to the east (Dabrio and Polo 1995), with a well-developed beach system at its inner, westernmost, side (Roep et al. 1979) and fan deltas at the northern margin (Martín et al. 1993).

The beach deposits of the Sorbas Member have been studied in detail at the type locality ("Sorbas village") by Roep et al. (1979) and Dabrio et al. (1985). Most of the following description and interpretation of these beach sediments is based on these two papers. A typical section of the Sorbas Member is made up of three units that represent successive lowstand, transgressive, and highstand systems tracts of a fourth-order parasequence. Stromatolites occur only within the two upper units. Each of these units, with an average thickness of about 25 m, consists of the following lithological subunits, from bottom to top (Fig. 3):

1. Finely laminated clay to silt, with mud-cracks, bird and mammal footprints, rain-drop prints, and salt-crystal moulds, corresponding to lagoonal deposits.
2. Well-sorted sand to microconglomerates that interfinger with and prograde westwards over (1). These represent back-barrier, washover fan deposits.

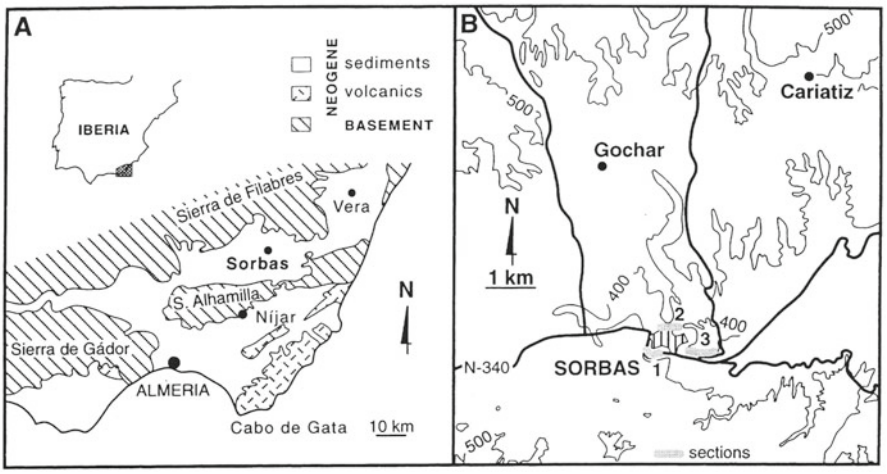

Fig. 1. A Regional setting of the marginal Mediterranean Sorbas Basin in Almería Province, SE Spain. **B** Locations of the sections studied near Sorbas

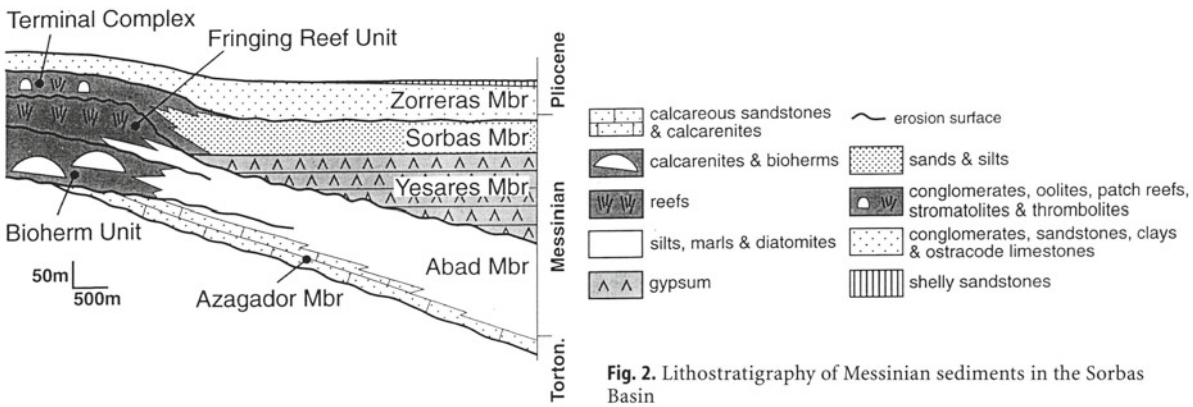

Fig. 2. Lithostratigraphy of Messinian sediments in the Sorbas Basin

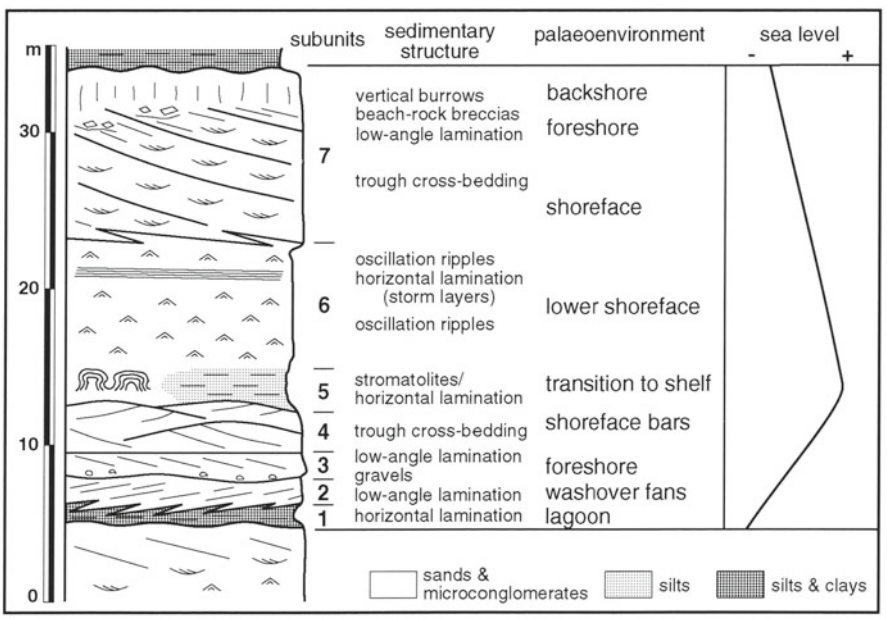

Fig. 3. Stratigraphy and facies of a unit in the beach deposits at Sorbas village (modified from Roep et al. 1979). Three such units constitute the Sorbas Member at this locality. Stromatolites in subunit 4 occur only in the two upper units

3. Well-sorted sand to microconglomerates, with well-developed, low-angle, parallel swash lamination dipping eastwards, representing foreshore beach deposits. An irregular erosional surface with abundant pebbles separates this from the underlying subunit.
4. Oolitic and siliciclastic sands and microconglomerates, exhibiting tabular cross-bedding, and representing shoreface bar deposits.
5. Micaceous silt and dark clay, locally containing planktonic foraminifers, deposited in a shelf environment below normal wave base (approximately 10 m in depth according to Roep et al. 1979).
6. Fine sand with abundant small wave ripples, deposited in a lower shoreface subenvironment, intercalated with thin beds of parallel, horizontally laminated sand corresponding to storm deposits.
7. Thick (3–5 m) sand banks with well-developed, eastward-dipping megacross bedding, each bank marking a different episode of beach progradation. Within each bank there is a lateral transition downslope from: (a) unlaminated fine sand with abundant vertical burrows (backshore deposits), to (b) eastward-dipping, parallel-laminated sand locally containing well-cemented, pebble-to-cobble sized, beach-rock conglomerate (foreshore deposits), to (c) trough cross-bedded sands representing the lowermost part of the beach system (shoreface deposits).

   The lower five subunits (1–5) correspond to the transgressive part of the unit and the uppermost two subunits (6–7) to the regressive part (Fig. 3). Micaceous silt and dark clay (subunit 5) constitutes the most distal facies and reached its most landward position during the maximum transgression phase of each unit.

3.2 The Stromatolite Beds

Two stromatolite beds are intercalated with sediments of the second and third beach units. They crop out in three different sections. The lower bed (belonging to the second unit) occurs in the section beside road N-340 (section 1, Fig. 1B), a few hundred meters east of the main entrance to Sorbas town, and in the section in the canyon walls immediately to north of Sorbas (section 2, Fig. 1B). The upper bed, which crops out at the junction of the N-340 with the road north to La Mela, on the eastern side of Sorbas town (section 3, Fig. 1B), occurs within the third unit. These two stromatolite beds show similar development and sedimentary settings.

3.2.1 The Lower Stromatolite Bed

In its two outcrops, the lower stromatolite bed overlies sand and conglomerate shoreface bars (subunit 4) from the transgressive part of the second unit, and is covered by wave-rippled sands, corresponding to the lowermost shoreface deposits (subunit 6) from the regressive part of the unit. It therefore occurs just at the transition from the transgressive to the regressive portions of the unit. The stromatolite bed grades laterally into micaceous silts from the shelf (subunit 5). The palaeoenvironmental setting of the stromatolite bed was therefore at the leading edge of the beach system, at the transition from the lowermost shoreface to the shelf.

Section 1 (Fig. 1B) was selected for detailed study of the lower stromatolite bed, which at this locality can be traced NW-SE laterally for about 200 m. The bed reaches a maximum thickness of 5 m at its northwestern-most proximal edge, where it consists of three distinct zones. The lowermost zone (0.5 m thick) contains small (up to 1 m in length), well-lithified, sandy stromatolite domes, with a synoptic relief of up to 15–20 cm. The intermediate zone (3 m thick) is characterized by large, flat, silty domes, up to 10 m long, with very diffuse lamination (Fig. 4A) and pockets of intercalated silt sediment. They locally exhibit a nodular structure which is diagenetic in origin. Small (2–3 m long) domes with digitated macrofabrics occur at the base of this zone. The uppermost zone (up to 1.5 m thick) consists once again of medium-sized (2–4 m long), well-lithified sandy stromatolites, with steep to vertical sides and synoptic relief up to 1 m (Fig. 4B).

The proximal, well-lithified, sandy stromatolites located at the bottom and top of the stromatolite bed laterally give way basinwards within a few tens of meters to large, flat, weakly lithified, silty stromatolites, through an intermediate zone of medium-sized (a few meters long) silty domes with digitate macrofabrics. These silty stromatolites flatten considerably just before disappearing. At the northwestern edge of the outcrop, the vertical zonation of the stromatolite bed, which is made up successively of proximal-distal-proximal stromatolites, can be interpreted as the result of the transgressive-regressive evolution of the unit in which it occurs.

3.2.2 The Upper Stromatolite Bed

In Section 3 (Fig. 1B), which is orientated W-E, the upper stromatolite bed can be followed laterally for about 500 m in a stratigraphic position very similar to that of the stromatolites in the underlying unit. The upper bed overlies oolitic sands and siliciclastic (quartz-rich) conglomerates with conspicuous tabular cross-bedding (subunit 4) and underlies wave-rippled sands (subunit 6) which locally contain abundant small bivalves. Laterally, the stromatolites pass basinwards (eastwards) to micaceous silts (subunit 5). In this outcrop the oolitic and microconglomerate bars from sub-

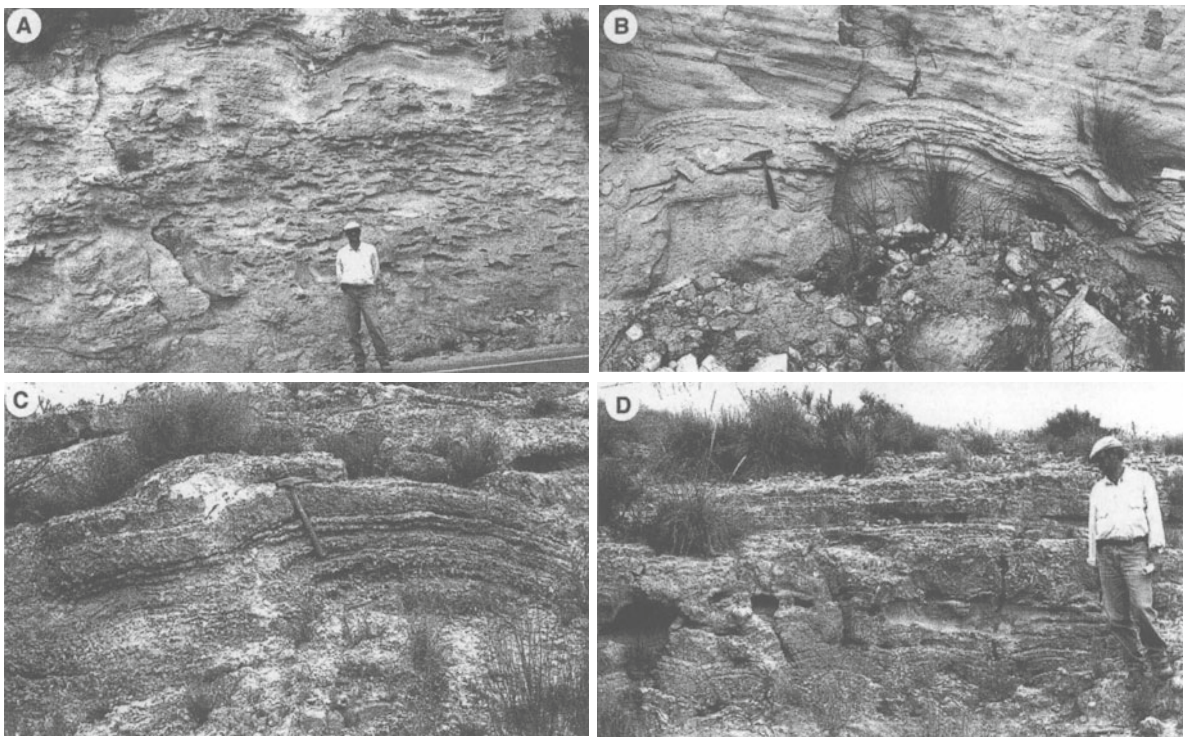

Fig. 4.A Middle-upper part of lower stromatolite bed showing a 10 m long, silty (distal) stromatolite dome, overlain (top 1.5 m of bed) by smaller (2–3 m long) but more conspicuous, sandy (proximal) domes (JMM is 1.75 m tall). **B** Uppermost part of lower stromatolite bed at its northwesternmost outcrop, showing 3 m long, sandy (proximal) dome covered by wave-rippled sands (hammer is 33 cm long). **C** Proximal, sandy stromatolites from westernmost outcrop of upper stromatolite bed (hammer is 33 cm long). **D** Upper stromatolite bed, some 100 m east of site of **C**, consisting of three distinct parts: lower part (20 cm) of small, sandy (proximal) domes; intermediate part (50 cm) of heavily weathered, silty (distal) domes, and upper part (30 cm) of sandy (proximal) domes

unit 4 unconformably directly overlie the top of the lagoonal deposits of subunit 1, and sediments corresponding to subunits 2 and 3 are missing. Coastal retreat associated with transgression in this unit took place very rapidly and was accompanied by significant erosion and lack of net sedimentation.

On the western side of the outcrop, the stromatolite bed is 3 m thick. It consists of flat, E-W elongated, sandy stromatolites 0.5–2 m long (Fig. 4C), which become longer (up to 4 m) and steeper-sided towards the top. Approximately 100 m basinwards, the bed thins considerably to 1 m and consists of three distinct parts: (1) a lowermost zone of small (10–20 cm long), well-lithified, sandy domes, (2) an intermediate zone (50–60 cm) of poorly lithified, very gentle-sided domes, and (3) an uppermost zone (30 cm thick) of well-lithified, finely laminated sandy domes (35 cm in length) (Fig. 4D). This zonation is on a smaller scale, but otherwise similar to that of the proximal end of the lower stromatolite bed.

Some 150 m basinwards, the stromatolite bed thins to 60 cm but still retains its internal zonation. Here the stromatolite domes are flat and gentle-sided, and silty in the middle zone. Some 400 meters east of the first site, the bed is 50 cm thick and lacks internal zonation. These distal stromatolites are silty, extremely flat and diffuse. Some 100 m further basinwards, they interlayer with silt before disappearing.

3.3 Internal Structure of the Stromatolites

Proximal stromatolites are distinct (Fig. 5A), with thin laminae (up to 1 mm thick) of dense (sometimes clotted) micrite (Fig. 5B) alternating with thicker laminae (up to 5 mm) of peloidal (peloids around 0.1 mm in size) to clotted (individual clots ranging in size from 0.1 to 0.6 mm) to bushy micrite, with abundant fenestrae 0.2–3 mm wide. Siliciclastic grains, which may have thin oolitic coatings, range from 0.1 to 0.4 mm in size. Locally they represent up to 40% of the rock, but usually constitute less than 10%, and are either concentrated in laminae and pockets or are dispersed throughout the domes. Locally, lamination is crude to diffuse, and patches of dense micrite occur between areas dominated by clotted to bushy micrite.

Distal stromatolites are usually very finely laminated (Fig. 5C). Thin (up to 1 mm), dense micrite laminae alternate with thicker (2–5 mm), silt-rich laminae, in which silt content normally ranges from 15 to 50%

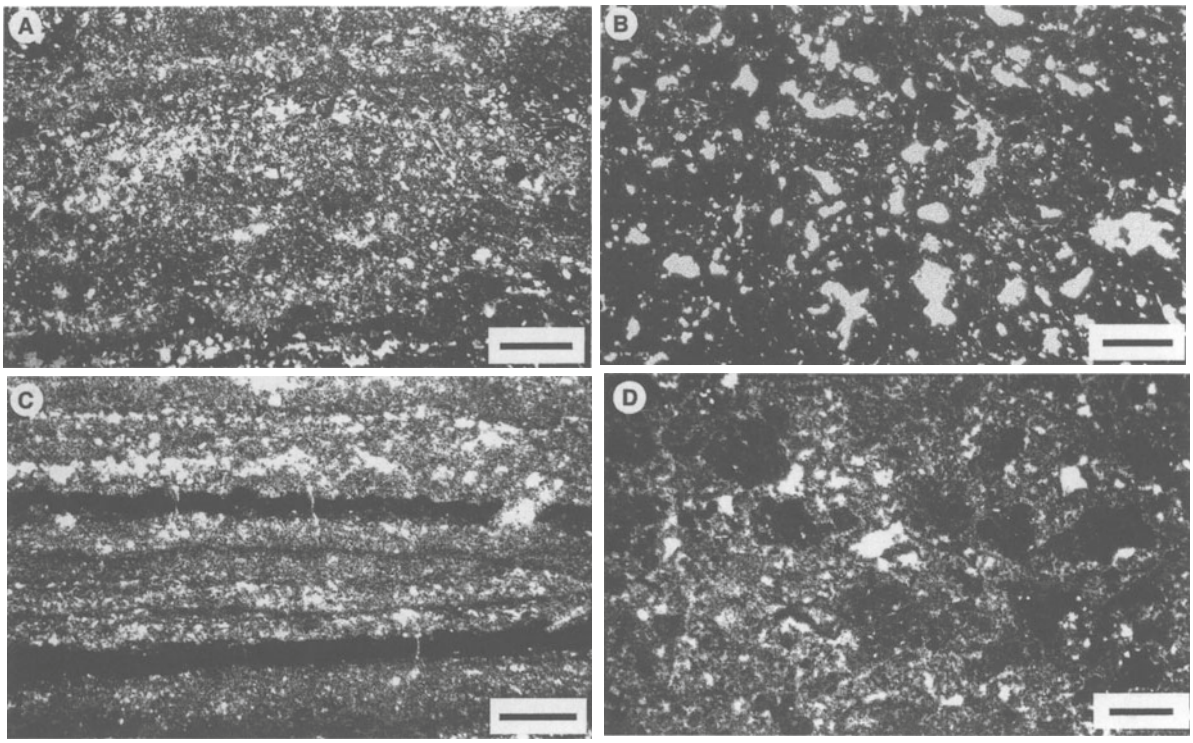

Fig. 5.A Dark, very thin micrite laminae alternating with thicker sediment (sand)-rich laminae in a proximal stromatolite. Bottom of lower stromatolite bed. Sample SBS-0; *scale bar* = 1 mm; crossed nicols. **B** Micrite-rich area consisting of crudely laminated, dense to bushy micrite with abundant fenestrae. Proximal stromatolite from middle part of upper stromatolite bed at its westernmost outcrop, shown in Fig. 4C. Sample SBS-21; *scale bar* = 1 mm. **C** Thin, dark micrite laminae alternating with thicker, sediment (silt)-rich laminae. Distal stromatolite from upper stromatolite bed. Sample SBS-28; *scale bar* = 1 mm; crossed nicols. **D** Microfabric of distal stromatolite, consisting of clotted to bushy micrite in a sediment (silt)-rich matrix. Most distal outcrop of lower stromatolite bed. Sample SBS-12; *scale bar* = 1 mm

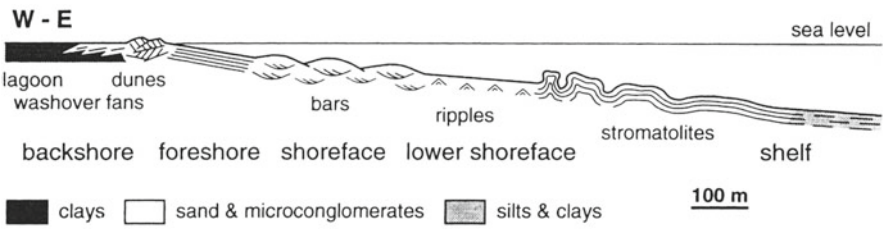

Fig. 6. Palaeoenvironmental setting schematically showing the lateral changes in shape of the stromatolites in the Sorbas Member at Sorbas town

but is found locally up to 65%. Small peloids (0.02 mm in size) and rods (up to 0.05 mm long), presumably respectively corresponding to transverse and longitudinal sections of calcified filaments, occur isolated or interconnected in the silty laminae, together with clotted micrite (clots about 0.2 mm in size) and small fenestrae (0.1–1 mm wide). Some very fine, sand-size siliciclastic grains locally occur scattered in the micrite. Less frequently these distal stromatolites exhibit crude lamination with predominantly bushy micrite (Fig. 5D) around stromatactis-like fenestrae that are 0.3–1.5 mm in size.

Except for very small filaments occurring in the distal stromatolites, the observed microfabrics are similar to those in the coeval siliciclastic domes associated with fan delta deposits at the northern margin of the basin (Braga et al. 1995).

A late, sparry, mosaic calcite cement in-fills fenestral voids and intergranular spaces in the siliciclastic-rich portions of proximal and distal stromatolites alike.

3.4 Model of Stromatolite Development

These siliciclastic stromatolites, as inferred from their associated sequences and sedimentary structures, developed within a beach environment in an area of relatively low energy at the transition from the lowermost shoreface to the shelf, at depths around 10 m (Fig. 6). Microbial carbonate precipitation together with trapping of siliciclastic grains were the two major processes involved in their formation, and synsedimentary lithification contributed to their preservation.

Two main factors seem to have controlled stromatolite development: water energy and light intensity. In

the lowermost part of the beach the energy was presumably low enough to allow microbial mats to colonize the bottom. In shallower locations, wave energy was stronger and prevented their growth. In the lowermost shoreface area, the water was still clear enough for mat development but just a few hundred meters along the gently descending slope to the shelf, suspended silt made conditions too unfavorable for mat growth.

Within a single stromatolite bed there are significant variations in stromatolite morphology, internal structure, degree of lithification, and the nature of the trapped sediment. The shallowest stromatolites are sandy and distinctly laminated, with steep sides and high synoptic relief. Downslope they grade into gentler-sided, but still sandy, stromatolites with digitate to crudely laminated macrofabrics. The deepest domes, those in the transition to the shelf, consist of large, flattened and slightly undulose, very finely laminated, silty stromatolites that are poorly lithified and intercalated with silt lenses (Fig. 6). Higher rates of sediment supply and episodic erosion by waves or currents favored the higher synoptic relief and the steeper sides of the shallowest stromatolites.

Stromatolite formation was especially significant in the western Mediterranean during the Upper Messinian, at the time of deposition of the Sorbas Member, which is the unit immediately overlying the Messinian evaporites. Microbial mats colonized a variety of different environments at this time, including ones that could initially be considered hostile to their development, such as fan deltas and the beach systems described here. In the Sorbas Basin, they coexisted with an impoverished but omnipresent normal marine biota and this situation seems to apply to the entire western Mediterranean. In this respect, the microbial associations can be considered as opportunistic biotas that rapidly colonized all the available environments immediately after the Messinian Salinity Crisis, promoting unusual development of microbial deposits (Martín and Braga 1994).

Acknowledgements. This work was supported by the DGICYT (Project PB93–1113) and the Junta de Andalucia (Grupo 4076). We thank Christine Laurin for correcting the English text.

References

Bertrand-Sarfati J (1994) Siliciclastic-carbonate stromatolite domes in the Early Carboniferous of the Ajjers Basin (eastern Sahara, Algeria). In: Bertrand-Sarfati, Monty CLP (eds) Phanerozoic Stromatolites II. Kluwer, Dordrecht, pp 395–419

Braga JC, Martín JM, Riding R (1995) Controls on microbial dome fabric development along a carbonate-siliclastic shelf-basin transect, Miocene, SE Spain. Palaios 10:347–361

Cameron B, Cameron D, Jones JR (1985) Modern algal mats in intertidal and supratidal quartz sands, northeastern Massachusetts, USA. In: Curran HA (ed) Biogenic structures: their use in interpreting depositional environments. SEPM Special Publication 35, pp 211–223

Dabrio CJ, Polo MD (1995) Oscilaciones eustáticas de alta frecuencia en el Neógeno superior de Sorbas (Almería, sureste de España). Geogaceta 18:75–78

Dabrio CJ, Martín JM, Megías, AG (1985) The tectosedimentary evolution of Mio-Pliocene reefs in the Province of Almería. In: Milà MD, Rosell J (eds) 6th European Regional Meeting of Sedimentologists, Excursion Guidebook, Lleida, Spain, pp 269–305

Davis RA Jr (1966) Willow River dolomite: Ordovician analogue of modern algal stromatolite environments. J Geol 74:908–923

Davis RA Jr (1968) Algal stromatolites composed of quartz sandstone. J Sediment Petrol 38:953–955

Fornós JJ, Pomar L (1984) A composite sequence of alluvial-fan coastal and sea-cliff deposits in the upper Miocene of the Cabrera Island (Balearics, Spain). Publ Geol Univ Autón Barcelona 20:85–95

Gerdes G, Krumbein WE (1987) Biolaminated deposits. Lecture Notes in Earth Sciences 9. Springer, Berlin Heidelberg New York, 183 pp

Grant CW (1991) Lateral and vertical distributions of textural features of filamentous bacterial (Beggiatoa) mats in Santa Barbara Basin, California. Bull Am Assoc Petrol Geol 75:585

Grant J (1988) Intertidal bedforms, sediment transport, and stabilization by benthic microalgae. In: de Boer PL et al. (eds) Tide-influenced sedimentary environments and facies. Riedel, Dordrecht, pp 499–510

Haq BU, Hardenbol J, Vail PR (1987) Chronology of fluctuating sea levels since the Triassic. Science 235:1156–1167

Harwood G (1990) 'Sandstone stromatolites'- An example of algal-trapping of sand grains from the Permian Yates Formation, New Mexico, USA. Sediments 1990. 13th International Sedimentological Congress, Nottingham, England, Abstracts of Posters, p 97

Logan BW (1961) Cryptozoon and associate stromatolites from the Recent, Shark Bay, Western Australia. J Geol 69:517–533.

Martín JM, Braga JC (1994) Messinian events in the Sorbas basin of southeastern Spain and their implications in the recent history of the Mediterranean. Sediment Geol 90:257–268.

Martín JM, Braga, JC (1996) Tectonic signals in the Messinian stratigraphy of the Sorbas basin (Almería, SE Spain). In: Friend PJ, Dabrio CJ (eds) Tertiary basins of Spain. The stratigraphic record of crustal kinematics. Cambridge University Press, Cambridge, pp 387–391

Martín JM, Braga JC, Riding R (1993) Siliciclastic stromatolites and thrombolites, late Miocene, S.E. Spain. J Sediment Petrol 63: 131–139

Meadows A, Meadows, PS, Muir Wood D, Murray JMH (1994) Microbiological effects on slope stability: an experimental analysis. Sedimentology 41:423–435

Park RA (1977) The preservation potential of some recent stromatolites. Sedimentology 24:485–506

Paterson DM (1989) Short-term changes in the erodability of intertidal cohesive sediments related to the migratory behaviour of epipelic diatoms. Limnol Oceanogr 34:223–234

Riding R (1991) Classification of Microbial Carbonates. In: Riding R (ed) Calcareous algae and cyanobacteria. Springer, Berlin Heidelberg New York, pp 21–51

Roep ThB, Beets DJ, Dronkert H, Pagnier H. (1979) A prograding coastal sequence of wave-built structures of Messinian age, Sorbas, Almería, Spain. Sediment Geol 22:135–163

Ruegg GJH (1964.) Geologische onderzoekingen in het bekken van Sorbas, S Spanje. Amsterdam Geological Institute, University of Amsterdam, Holland, 64 pp

Soudry D, Weissbrod T (1995) Morphogenesis and facies relationships of thrombolites and siliciclastic stromatolites in a Cambrian tidal sequence (Elat area, southern Israel). Palaeogeogr Palaeoclimatol Palaeoecol 114:339–355

Schwarz HE, Einsele G, Herm D (1975) Quartz-sandy, grazing-contoured stromatolites from coastal embayments of Mauritania, West Africa. Sedimentology 22:539–561

Shallow Marine Microbial Carbonate Deposits

Kathleen M. Browne[1], Stjepko Golubic[2], Lee Seong-Joo[3]

[1] Department of Geological and Marine Sciences, Rider University, Lawrenceville, NJ 08648-3099, USA
[2] Department of Biology, Boston University, Boston, MA 02215, USA
[3] Department of Earth System Sciences, Yonsei University, Seoul 120-749, Korea

Abstract. In normal marine, shallow, subtidal carbonate settings, microbial communities that stabilize sediment to some degree are invariably present and typically are composed of a large variety of organisms, including invertebrates that disrupt the community. These diverse communities do not commonly form mats with a distinctive fabric. Only in settings where some environmental condition favors the growth of a small number of species will a microbial mat develop and construct a biosedimentary deposit with a distinctive fabric. Subtidal conditions that will restrict diversity include chemical extremes and frequent sediment movement. In intertidal settings, desiccation-related factors keep diversity low, enabling microbes to flourish. Dramatic microbial community zonations can develop as a result of competitive exclusion and adaptation. Lithification of some mats results from complex biogeochemical processes and is poorly understood.

1 Introduction

A wide range of organisms live on the modern sea floor, ranging from unicellular prokaryotes to complex multicellular skeletal eukaryotes. Benthic communities will generally be very diverse in relatively clear normal marine subtidal settings that are oxygenated and well-mixed. Specific conditions and competitive interactions between organisms ultimately determine the community members present in a given setting. Many of these organisms influence or contribute to the sedimentary deposit produced in their environment. Microbial activity in marine sediments is ubiquitous and, just as in soils on land, marine microorganisms are an integral part of any eukaryote-dominated ecosystem, from pelagic plankton-generated systems, to benthic algal and sea grass beds, to coral reefs. As on land, the principal role in degradation of organic matter and recycling of nutrients is carried out by microorganisms. Where environmental conditions extend beyond the tolerance limits of most macro-organisms, in particular peritidal, hypersaline and high sediment stress settings, microbes dominate the community at all levels. Extremes in conditions such as temperature, salinity, pH, dissolved gases, atmospheric exposure and desiccation, as well as wave and current energy, limit the distribution of macro-organisms and their impact on sedimentation. In contrast, many micro-organisms, particularly cyanobacteria, diatoms and bacteria, exhibit high tolerance to these environmental conditions and can become the main biotic force that interacts with, and modifies the prevailing hydrodynamic, sedimentological and chemical processes. Microorganisms are the main factor influencing the accretion of sediment in these environmental settings, and the net result is the production of microbial deposits.

Specific ecological conditions that impact the microbial community may select microbes that are most tolerant of those conditions (e.g., see Gerdes and Krumbein 1994) allowing the specialists to increase in biomass and distribution and form more or less coherent organic coatings over the sea floor, or "microbial mats." These microorganisms may tolerate harsh environmental conditions and dominate the intertidal microbial mats, whereas growth under normal conditions is curtailed by consumption and competition (reviewed by Golubic 1991). Although the distribution of microbes in a particular setting is likely controlled by complex interacting environmental factors, specific factors may dominate a setting and cause a distribution that is unique compared to settings that are similar but where these specific factors may not be as important. In addition, although desiccation is a significant limiting factor in intertidal environments, other factors related to desiccation may control the distribution of species that can withstand long exposure times (e.g., depleted O_2 or reduced availability of nutrients).

The study of microbial mats as stratified microbial ecosystems has attracted considerable attention in microbial ecology (e.g., Cohen et al. 1984; Stal and Caumette 1994, Cohen and Rosenberg 1989). As we discuss in Chap. 3 (Seong-Joo, Browne, and Golubic), differentiation of a microbial mat into biologically and functionally different strata develops under conditions of sedimentary stasis ("biogenic" in Table 1) and should be distinguished from stratigraphic sediment lamination such as observed in stromatolites ("biogenic and sediment" in Table 1). Stratified communities are by no means unique to microbial mats (e.g., Guerrero and Mas 1989). Eutrophic conditions and increased organic production in these systems are the main driving forces for metabolic processes that sharpen the geochemical differences between the strata and increase the clines of

R.E. Riding and S.M. Awramik (Eds.)
Microbial Sediments

various environmental parameters, ultimately creating an oxic/anoxic interface. In the case of microbial mats, this interface is located near the sediment/water boundary with extremely sharp gradients concentrated within a few millimeters of depth. The biogeochemistry of microbial deposits is complex and involves the entire microbial community in an interactive fashion (see, e.g., Cohen et al. 1984; Stal and Caumette 1994, Cohen and Rosenberg 1989). An understanding of mat chemistry is critical in explaining many aspects of microbial deposits including biological and chemical stratification and zonation, productivity and decomposition, and destruction, preservation and lithification of microbial carbonate deposits.

The study of modern microbial deposits has also been useful for geologists in paleoenvironmental reconstructions using biosedimentary structures as environmental indicators, in attempting Precambrian biostratigraphy, and in understanding variations in microbial deposit types through geologic time. Precambrian sedimentary sequences are particularly fascinating for several reasons. Microbial deposits formed in a much wider range of environments including water depths in open marine settings that are now (and have been for most of Phanerozoic time) occupied by very diverse communities of skeletal and nonskeletal eukaryotes as well as prokaryotes. Not only did they occupy settings now dominated by eukaryotes but, with the aid of intensive penecontemporaneous lithification, they produced their own versions of large-scale reefal deposits. Precambrian stromatolites commonly contain finer-scale structures and much more elaborate macrostructures than younger stromatolites, possibly resulting from differences in the microbes involved and/or other factors including sediment grain size and lithification. Finally, Precambrian stromatolites may record evolutionary changes in the microbial communities that produced them, as suggested by distinct changes in morphology, branching patterns and microstructures (see Semikhatov et al. 1979).

Several authors have recently summarized information on various aspects of microbial mats and can provide readers with additional details (e.g., Demicco and Hardie 1994; Gerdes and Krumbein 1994; Stal 1994; Stal and Caumette 1994; van Gemerden 1993). This chapter presents a summary of the nature and distribution of different modern shallow marine microbial carbonate deposits and the apparent factors, thus far understood, that control this distribution.

2 Microbial Deposits

Microorganisms dominate throughout the entire trophic pyramid and the order or arrangement of the microbes in a given mat typically develops into a highly efficient community oriented toward maximal gains and minimal losses of C and N (Paerl et al. 1993). Microbial primary producers include cyanobacteria, phototrophic anoxygenic bacteria, chemolithotrophic bacteria and microscopic eukaryotic algae. Primary production is usually dominated by cyanobacteria and microalgae. These assemblages are consumed and degraded by micro-invertebrates, fungi and heterotrophic bacteria. Geochemical changes introduced by intensive bacterial degradation of the primary organic output produce fine-scale stratified microbial communities, which in turn significantly increase the diversity and complexity of these microbial systems. The interactions between microorganisms and their sedimentary environment define, in fact, a microbial ecosystem.

A deposit can be regarded as essentially microbial if it is substantially influenced and shaped by the activities of a microbial community. This pragmatic definition would exclude sedimentary bodies formed predominantly by hydrodynamic factors. Sedimentary bodies that are framed and shaped by macroscopic skeletal organisms, such as reef corals, and non-skeletal organisms, such as sea grasses, are similarly excluded by this definition. There are obvious difficulties in delineation and, consequently, recognition of microbial deposits because they are subjected to both environmental selection of particular microorganisms and direct modification by environmental forces.

The prevalent role of microorganisms in formation of many shallow marine carbonate deposits has been recognized and is commonly expressed in terminology that implies microbial origins. Terms such as stromatolites (Kalkowsky 1908), cryptalgal laminates (Aitken 1967), thrombolites (Aitken 1967), microbialites (Burne and Moore 1987), microbial mounds (James and Bourque 1992) and leiolites (Braga et al. 1995) all imply microbial origins. However, the nature and extent of the microbial processes involved in their formation are rarely identified and even more rarely quantified. Research on microbial contribution to sediments and microbial sediments has historically developed along three approaches: (1) analyses of sediment composition and textures, determining microbial presence and seeking clues and indicators of their activities; (2) analyses of geochemical changes within microenvironments at the sediment water interface caused by microbial actions, and (3) experimental approaches that analyze microbial processes having the potential to influence sediments under culture conditions. The linkage of these approaches has yet to be established and would require evaluating microbial metabolic potential in relation to actual microbial performance in actual sedimentary context, and relating microbial geochemical performance to sedimentary textures. As a consequence, there is a wide area of uncertainty within which opinions may vary.

Microbial deposits are expected to differ from sediments deposited in the same environment with little or no influence of microbes. Microbes in sediments, for example, are responsible for retention of finer grain size fractions in environments where waves and currents would otherwise wash those grains away (e.g., Black 1933; Neuman et al. 1970; Golubic and Focke 1978; Dravis 1983; Guerrero et al. 1994). In addition to trapping, binding and packing sedimentary particles, microorganisms are associated with (and presumably influence) mineral precipitation, thus contributing to sediment grain production (e.g., peloidal and clotted carbonate) and grain-binding by cementation (e.g., Friedman et al. 1973; Horodyski and Vonder Harr 1975; Monty and Hardie 1976; Golubic 1983; Rasmussen et al. 1993; Gerdes et al. 1994; Golubic and Browne 1996; Seong-Joo, Browne and Golubic, this Vol.). The construction of microbial mats commonly produces microenvironments where exchange between pore waters, and with overlying seawater, is restricted. In these microenvironments, mineral precipitation may be promoted by: (1) changes in the microenvironmental chemistry and hence saturation state caused by microbial metabolic processes (see below), (2) nucleation on surfaces of microorganisms or microbial products. Metabolic activities contribute to carbonate dissolution as well as promote carbonate precipitation.

Microbial activities affect the timing, rates and extent of early lithification of sedimentary structures, thus increasing the chances that the structures will be preserved. And early lithification may influence the external morphology (e.g., Golubic 1991) and the relief (e.g., Dill et al. 1986; Dravis 1983) that a microbial mat-generated bioherm can develop. A microbial deposit as a whole contains within it a stratigraphic record of some of the processes, and changes in processes, involved in the deposition of the biosediment. The preserved microbial sedimentary deposit is a result of environmental selection of particular microbes, the interaction between the microbes selected and environmental factors, and the microbial influences on pore water chemistry. If one set of environmental factors predominates in a given depositional setting, than the type of microbial deposit will likely remain uniform. If, on the other hand, environmental factors change or alternate, the nature of the microbial deposit produced is likely to be heterogeneous, or banded (e.g., see Monty 1976).

2.1 Biosedimentary Structures

The biosedimentary deposit produced in a particular setting can contain fabrics formed from the microbial mat, fenestrae and blisters produced by gas bubbles and decay of organics, desiccation and erosional features (mat crinkling, polygonal cracks, prism cracks, flat pebbles and rip-up clasts, flat pebble conglomerates), hydrodynamically deposited sediment (thin beds, isolated ripples and lenses), sediment agglutinated or baffled by the mat, evidence of bioturbation (open or sediment-filled burrows, homogenized zones) and calcareous precipitates (crusts and tufas; e.g., Demicco and Hardie 1994). The preservation of that fabric is dependent upon whether sediment is included and deposited in a unique pattern and/or the fabric is enhanced by mineral precipitation.

Table 1 lists the different mat types documented in shallow marine carbonate settings and, for each, briefly summarizes the dominant microbes, typical internal structures, locations where they have been found, and some of the references from which this information can be obtained. Many types are discussed and illustrated in the following sections. The proportions of dominant microbes and the ranges of all types of organisms found in each mat type can vary between locations. Mat fabrics are controlled by the dominant microbe(s) and result from how those microbes influence accumulation of organic and mineral matter (see Riding 1991). Millimeter-scale lamination can result from vertical zonation of microbes (e.g., biogenic laminated *Microcoleus chthonoplastes* mats, Canfield and Des Marais 1991, Fig.1), alternations of communities dominated by different microbes (e.g., *Scytonema* alternating with *Schizothrix*, Monty 1976, Figs. 4, 5, 20), alternations of the same microbe with each layer representing different growth rates and responses to external conditions (e.g., *Phormidium hendersonii* biscuits, Golubic and Focke 1978, Figs. 2–4; Monty 1976, Fig. 2), or alternations of organic and sediment layers (e.g., smooth *Schizothrix* mats, Hardie and Ginsburg 1977, Figs. 34–39; crinkly lamination from *Scytonema* mats in the inland algal marsh of Andros Island, Hardie and Ginsburg 1977, Fig. 43). Precipitated carbonate can enhance layering (Seong-Joo, Browne, and Golubic, this Vol., Fig. 1a) or can be the cause of layering as in the crudely developed layering in colloform-produced stromatolites (see below). Pinnacle, tufted and pin-cushion structures consist of upright-oriented, coarse filamentous microbes, sediment entrapped between the filaments and, in some cases, precipitated carbonate (Hardie and Ginsburg 1977, Figs. 43–50; Monty 1976, Figs. 6–8). Scalloped lamination produced by the reticulate mat forming *Lyngbya*-dominated community results from interconnected thin ridges of upright filaments (Logan 1974, Fig. 17a; Logan et al. 1974, Fig. 8d). Mats dominated by coccoid microbes commonly produce clotted fabrics, such as with *Entophysalis*-dominated mats (Monty 1976, Fig. 26; Logan et al. 1974, Fig. 25), although some fine scale layering can occur and is likely the product of a succession of desiccated mats alternating with cement layers (see below).

Table 1. Summary of mat types found in shallow marine carbonate environments

Mat type[b] (setting[c])	Dominant microbes	Internal structure	Location
Smooth[a] (S)	*Schizothrix gebeleinii*	BS lam; cement layers	EI
Flocculose[d] (S)	Prokaryotic and eukaryotic microbes, macro-algae, invertebrates	None recognized; possibly "leiolitic" fabric	See text
Colloform[a,d] (S)	Diatoms, coccoid and filamentous cyanobacteria	BS crude lam; crude cement layers	SB
Biscuits (S-LI)	*Phormidium hendersonii*	BG-BS lam	AD, AI, BE, FK, GB
Laminated[c] (S-LI)	*Microcoleus chthonoplastes*	BG lam	LM, GN, SL,CI
Gelatinous (S)	*Aphanothece* sp., diatoms	Homogenous	SB
Smooth[a] (LI)	*Schizothrix* spp., *Microcoleus chthonoplastes, Phormidium* spp.	BS lam; cement layers	SB, SG, EI; AI, CA, GE
High pinnacle (MI)	*Lyngbya aestuarii; Schizothrix splendida*	Surface pinnacles; oxidized sediment beneath	AD
Low flat (MI)	*Lyngbya aestuarii, Microcoleus chthonoplastes*	BG/BS lam	AD, FK
Pincushion (MI-UI)	*Scytonema* *Gardnerula corymbosa*	BS thin beds BS radiating filaments and trapped grains	AI, CA, CB SB, LSI[a]
Tufted (MI-UI)	Scytonematacean cyanobacteria	Undescribed	SB
Pustular[a] (MI-UI)	*Entophysalis major*	BS clotted: clusters of coccoid cells, cement	SB, AD, LM
Reticulate (UI/WL)	*Lyngbya aestuarii* *Microcoleus chthonoplastes*	BG/BS scalloped laminae lam and thin beds	SB, SG, LM
Film (UI)	*Hormoathonema luteobrunneum, H. violaceonigrum*	Destructive	SB
Blister/convoluted (UI)	Several I mat types minitopography causes cm-scale microbe zonation	Bubbled, convoluted	SB, AD

S, subtidal; I, intertidal; LI, lower intertidal; MI, mid-intertidal; UI, upper intertidal; WL, water-logged.
Structures: BG, biogenic only or predominantly; BS, biogenic and sediment; lam, laminated.
Locations: AI, Andros Island (see Demicco and Hardie 1994); AD, Abu Dhabi (Golubic 1991); BE, Florida/Bermuda (Golubic and Focke 1978); CA, Caicos (Wanless et al. 1988); CB, Chetumal Cay (Rasmussen et al. 1993); CI, Canary Islands (Gerdes et al. 1994); EI, Exuma Islands (Golubic and Browne 1996; Reid and Browne 1991); FB, Florida Bay (Ginsburg et al. 1954; Shinn 1968); FK, Florida Keys (Ginsburg and Lowenstam 1958); GB, Great Barrier Reef (Monty 1979); GE, Gladstone Embayment (Skyring and Bauld 1990); GN, Guerro Negro; LM, Laguna Mormona (Horodyski et al. 1977); LSI, Lee Stocking Island (unpubl.) SB, Shark Bay (Golubic 1985; Logan and Brown 1986; Playford and Cockbain 1976); SG, Spencer Gulf (Bauld 1984); SL, Solar Lake (Gerdes et al. 1985).
[a] $CaCO_3$ precipitation occurs.
[b] Mat type name may vary between authors.
[c] Setting may vary slightly between locations.
[d] Dominant microbes variable.

3 Controls and Distribution

3.1 Subtidal

3.1.1 "Normal Marine"

In normal marine subtidal environments, benthic communities are typically dominated by skeletal macro-organisms which can have a much greater influence on sedimentation than co-existing microbes. As a result, although microbes are typically abundant and can form noticeable accumulations, subtidal cohesive microbial mats with unique mat fabrics are very rare. Microbes can concentrate on hardground surfaces and sediment surfaces subjected to intermittent sediment transport and potentially impact sedimentation. But they must avoid predation (grazing) and compete for space with macro-algae and invertebrates. Many types of microbes, including diatoms, filamentous and coccoid cyanobacteria, bacteria, ciliated protozoa, foraminiferids, ostracods, and tiny invertebrates (micromollusks, nematodes, polychaete worms and arthropods) commonly colonize subtidal sediment surfaces and increase the stability of the sediment to some degree (Fig.1a; e.g., Newell et al. 1959; Purdy 1963; Bathurst 1967, 1975; Gebelein 1969; Neumann et al. 1970; Scoffin 1970; Frost 1974; Hardie and Garrett 1977; Watling 1988). In fact, some variety of this high diversity community is very common in shallow marine environments and is typically absent only in settings where high rates of bioturbation or sediment movement prevent the microbes

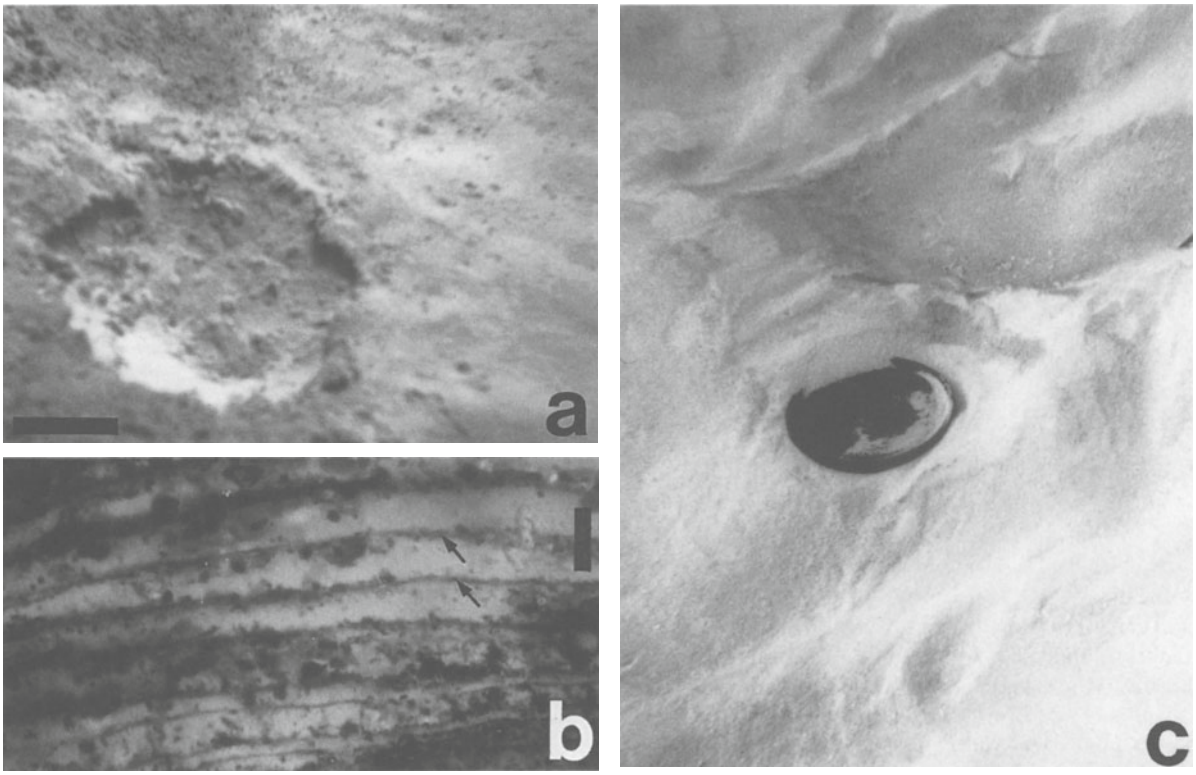

Fig. 1.a Subtidal flocculose mat loosely binding sediment nearby 20 m deep Perry Reef on east side of Lee Stocking Island, Bahamas. Sediment surface is disrupted revealing a loosely bound, surficial layer approximately 3 mm thick which overhangs along the edges of the depression. Lighter colored sediment on right side consists of looser sediment above the darker, organic-bound sediment shown on the left side; scale = 5 cm. **b** Photomicrograph of section through *Phormidium hendersonii* biscuit from Florida Keys showing 15–40 μm thick layers of prostrate filaments (*arrows*) alternating with layers up to 650 μm thick of vertically oriented filaments. Sediment concentrated on some parts of the thinner prostrate layers enhances the layering (see Golubic and Focke 1978). Sample fixed in 3% formaldehyde and stained with methyl blue; *scale* = 1 mm. **c** Subtidal ooid sand from Adderly Channel, Lee Stocking Island, Bahamas. *Lyngbya* filaments loosely stabilize the surface of rippled sediment above lens cap (6.2 cm wide) during slack tide but eroded from ripple crests

from densely colonizing sediment surfaces (Gebelein 1976). In sediment that undergoes rapid continuous movement or is subjected to intense bioturbation, many of these microbes can be present but they do not have sufficient time to concentrate into a mat before they are moved again and/or consumed (Gebelein 1969).

The diversity of most normal-marine subtidal microbial communities is typically high and because no one organism serves as the architect of the mat fabric, the degree of sediment stabilization is limited since some microbes and their metabolic products are less effective in stabilizing sediment than others (e.g., Meadows et al. 1994; Stal 1994; Yallop et al. 1994). For example, although bacteria (Meadows et al. 1994) and diatoms (e.g., Holland et al. 1974; Vos et al. 1990) and each organisms' secreted exopolysaccharides (EPS) have been shown to increase sediment stability, filamentous microbes (notably cyanobacteria, fungi) are generally more effective due to the intertwined fabric of the filaments (Meadows et al. 1994; Stal 1994; Yallop et al. 1994). In some cases, large amounts of EPS produced by diatoms appear to make it more difficult for mat organisms to produce an intertwined and/or cohesive fabric (Stal 1994; Yallop et al. 1994). In addition, although some diatom-secreted EPS can be highly persistent, EPS secreted to aid in locomotion was found to have only a short-term impact on sediment stability since it is highly soluble (see Decho 1990). The frequent presence of diatom-rich communities in some settings has led some workers to suggest that cyanobacteria alone cannot effectively trap and bind sandy sediment (e.g., Awramik and Riding 1988; Riding et al. 1991; Riding 1994). However, cyanobacterial mats from subtidal and intertidal stromatolites in the Bahamas appear to very effectively trap and bind fine sand (see below; Golubic and Browne 1996; Seong-Joo, Browne, and Golubic, this Vol.; Reid and Browne 1991) indicating that although diatoms and other eukaryotes may contribute to sediment accumulation in some microbial deposits, eukaryotes are not necessarily needed in the trapping and binding of fine-sand and finer sediment sizes. The additional help from diatoms may allow for coarser sizes to be trapped and bound (Awramik and Riding 1988).

Finally, the fauna that feed on the microbes (e.g., echinoderms, holothurians, gastropods, crustaceans, fish and polychaetes, Bathurst 1967; Neumann et al. 1970) disrupt mat continuity and limit microbe biomass and mat cohesion. Heterogeneity of the microbe components, excretion of their metabolic products and disruption of a mat typically result in loose, flocculose mats (Fig. 1a) with crudely developed fabrics which are typically not distinguishable from sediments deposited without the influence of a microbial community.

Localized *Phormidium hendersonii* colonies are one exception to the more typically heterogeneous microbial communities found in shallow, normal to near-normal marine environments (Ginsburg and Lowenstam 1958; Monty 1965, 1979; Golubic and Focke 1978; Golubic 1992a). Laminated, centimeter- to decimeter scale, low-relief, hemispherically shaped stromatolites and oncoids produced by this filamentous cyanobacteria can be found in lagoonal, back reef and reef settings from lower intertidal to 10m water depth, where they are not overgrown, diluted by other microbes or continuously disrupted by grazers (e.g., coral heads, coral rubble, around and between sea grass blades, stabilized sand; see Golubic and Focke 1978, Figs. 2–4). In both the shallow subtidal of Bermuda (Gebelein 1969) and the sand flats of Joulters ooid shoals (Gebelein 1976; Harris 1979), biscuits are most common within and on the deeper margins of grass beds. In Bermuda, the biscuits are found in areas experiencing sediment movement rates of 8–40 g/h per foot, suggesting that currents or sediment movement may impact the distribution by affecting either *P. hendersonii* or other organisms that might limit the growth of *P. hendersonii*. In many locations (e.g., Gebelein 1969), *Phormidium* "biscuits" are found immediately adjacent to loose, flocculose, diverse mats which more loosely bind muddy sands ("algal mats" in Gebelein 1969). *P. hendersonii* filaments in the biscuits create laminated internal layering and trap and bind sediment if it is deposited on the mat surface. Submillimeter-scale lamination is defined by alternating thin layers of horizontally oriented filaments positioned during the night time with thicker layers of vertically oriented filaments formed during the day time (Fig.1b; Monty 1976, Fig.2). Sediment can concentrate in the thinner layers but is not always present. The accretion of *Phormidium hendersonii* stromatolites and oncoids is a product of the microbe's response to diurnal changes in light (Gebelein 1977; Golubic and Focke 1978; Seong-Joo, Browne, and Golubic, this Vol.).

3.1.2 Sediment Movement

Excluding *Phormidium* deposits, subtidal microbial deposits that contain fabrics distinctive from non-microbial deposits more typically occur in settings where some environmental condition(s) limits or eliminates most of the macro-organisms that overgrow or disrupt the mat. In settings subjected to continuous or near-continuous current/wave energy, disturbance by sediment movement selects for motile and episammic organisms such as diatoms and cyanobacteria. Motile microbes can momentarily concentrate along a sediment surface during brief moments of current quiescence but their product is soon disrupted and eroded away when current velocities increase again. For example, decimeter-scale patches of *Lyngbya* can be found on the surface of ooid sand megaripples nearby subtidal stromatolites in the Exuma Islands, Bahamas, during slack tides (Fig. 1c). As tidal currents increase, the thin surficial mat is torn apart and eroded. Microbes in this environment therefore have a difficult time permanently colonizing an unstable sediment substrate and the extent, thickness and duration of mats are controlled by the rate and frequency of sediment movement. In the case of more cohesive subtidal mats attributed to *Schizothrix calcicola* (e.g., Gebelein 1969; Harris 1979), several layers of mat and domed accumulations can be found. Frequent mat disruption commonly results in the formation of sandy flat clasts that concentrate in ripple troughs and depressions producing flat pebble conglomerates (Gebelein 1969, Fig.6). Hardground substrates in these subtidal settings, including lithified submarine sediment, paleosols, bioclasts, and lithified reworked *Calianassa* burrows, can provide stable surfaces for colonization by a variety of micro-organisms that would otherwise not be able to produce mats. With a stabilized substrate, other environmental conditions influence the types of microbes that will survive and dominate. For example, on lithified stromatolites exposed in dune troughs in Adderly Channel, Bahamas (Dill et al. 1986; Riding et al. 1991; Golubic and Browne 1996), coatings of large numbers of diatoms and a variety of other eukaryotes and prokaryotes produce very loose, flocculose microbial mats (Riding et al. 1991; Fig. 2a,b). However, when the frequency of periodic burial and unburial and sediment movement across these substrates is high enough, these environmental stresses select for organisms that can adjust most rapidly to sediment accretion (Golubic and Browne 1996). *Schizothrix gebeleinii*, a filamentous cyanobacterium, is the most adaptable to this setting and can produce laminated, nearly monospecific, dense, fine sand-rich colonies (Fig. 2c) without a diatom presence and without the baffling influence of upright algae such as *Batophora*, found on the Eleuthera subtidal stromatolites (Dravis 1983). These mats also typically do not contain the unidentified, upright, stiff filamentous chlorophyte found in the diatom-rich, flocculose community on the Lee Stocking stromatolites (Riding et al. 1991) most common when the stromatolites sit in mega-ripple troughs. A laminated, stromatolitic fabric in the *Schi-*

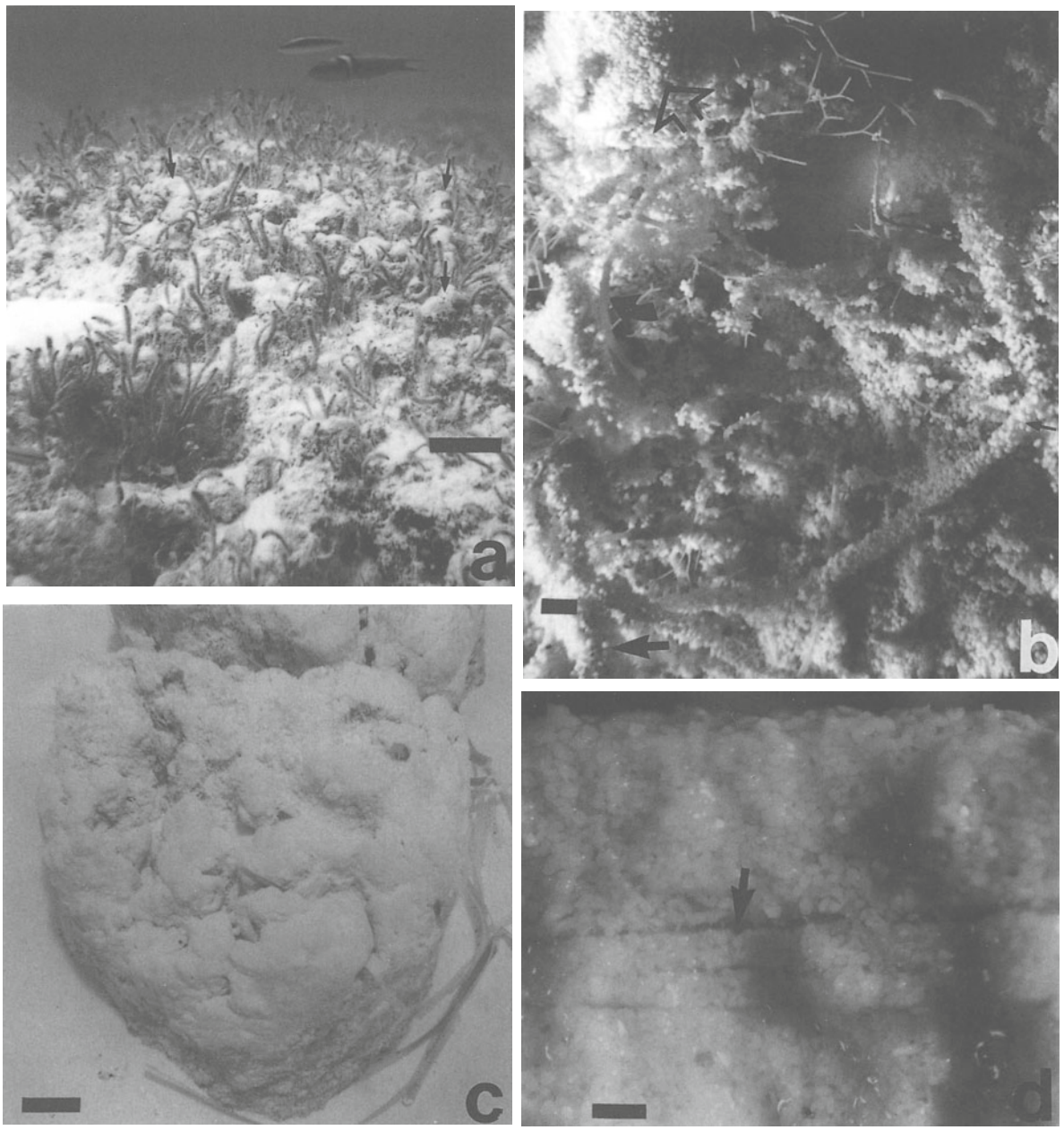

Fig. 2.a View of diverse microbial and macroscopic algal community on the top of a meter-tall subtidal stromatolite from Adderly Channel, Lee Stocking Island, Bahamas. Community includes abundant *Batophora*, the upright alga, small knobs of *schizothrix gebeleinii*-bound sediment (*arrows*) and sediment loosely bound by a eukaryote/prokaryote microbial community; scale = 5 cm. **b** Close view of sediment loosely bound by the eukaryote/prokaryote community in **a**. View includes: a portion of a *Schizothrix* knob in upper left corner (hollow arrow); branching calcareous red alga to the *right* of the knob; loosely agglutinated worm tubes (*small arrow*); stiff, thin upright alga (*curved arrow*), possibly the unidentified chlorophyte from Riding et al. (1991); sediment covered *Batophora (large arrow)*; sediment loosely bound by diatoms and cyanobacteria throughout; *scale* = 2 mm. **c** View of 30 cm-tall subtidal stromatolite covered with smooth, cohesive *Schizothrix gebeleinii* mat from Adderly Channel, Lee Stocking Island, Bahamas. Note absence of macroalgae and loosely bound sediment particularly on the *top* and *side* of the stromatolite facing the camera; scale = 5 cm. **d** Side view of *Schizothrix* mat showing lamination defined by alternating mm-scale sediment-rich layers with finer layers of sediment-poor, dense felts of filaments (*arrow*). These felts can contain small patches of precipitated aragonitic crusts (see Seong-Joo, Browne, and Golubic, this Vol.); *scale* = 1 mm

zothrix mats is produced as the microbes adjust to sediment addition (Seong-Joo, Browne, and Golubic, this Vol.). Lamination consists of couplets of sub-millimeter-thick, dense organic-rich, sediment-poor felt layers with embedded cement crusts and millimeter-thick, loosely cemented sediment-rich layers (Fig. 2d; Golubic and Browne 1996). Grazing pressure by nocturnal grazing gastropods (*Cerithium eberneum*) observed on

the stromatolite mats does not appear to be significant since they are few in number, were only found actively grazing during night hours and are found predominantly in the loose flocculose mats (unpublished observations by KM Browne). The laminated mat fabric is eventually preserved in the lithified bioherms as couplets of cement crusts and porous silt and fine sand layers. Early cementation enables the microbe-accumulated sediment to develop into bioherms with considerable relief (up to 2.5 m; Dravis 1983; Dill et al. 1986; Reid et al. 1995; Riding 1997). Riding et al. (1991) concluded that the stromatolites of this setting are likely constructed by eukaryote-dominated communities but the inclusion of both laminated and unlaminated portions within sectioned stromatolite examples indicates they are more likely net products of the *Schizothrix*-dominated community and prokaryotic/eukaryotic communities (see Golubic and Browne 1996; Seong-Joo, Browne, and Golubic, this Vol.). Sections of a stromatolite from Eleuthera Bank, Bahamas (Dravis 1983; provided by J. Dravis to KMB), also show laminated fabrics suggesting that laminated microbial mats may play some role in their formation (see Golubic and Browne 1996). The sandy, unlaminated portions of all the Bahamian stromatolites might be considered "leiolitic," based on the terminology of Braga et al. (1995), while laminated portions would be considered stromatolitic.

3.1.3 Salinity

High salinities in subtidal settings can also eliminate many macro-organisms allowing microbes to increase their biomass dramatically. For example, in Hamelin Pool and Gladstone Embayment, Shark Bay, Western Australia, high salinities enable subtidal microbial mats to flourish producing colloform mats (Table 1; Fig. 3a). The mats are typically dominated by a variety of coccoid and filamentous cyanobacteria and large numbers of a diverse community of EPS-secreting diatoms (e.g., 79 species of diatoms, an entophysalidacean coccoid cyanophyte, *Schizothrix* sp.; Davies 1970; Golubic 1985; John 1990; Logan et al. 1974). Gastropods do not occur and other grazing metazoa are rare. With a high microbial diversity, although certain organisms can dominate these mats, the influence of large numbers of other microbes limits the degree of mat cohesiveness and the development of a laminated fabric. In places where the filamentous cyanobacteria dominate, the mats are more cohesive; in places where they are less dominant, the mats are less cohesive and more easily eroded during storms (Bauld et al. 1979). Colloform mats can be vertically zoned, include silt and sand sized sediment, are typically crudely laminated and can contain patches of precipitated carbonate crusts. Lithified portions of the stromatolites beneath colloform mats contain crudely developed lamination defined by 1–3 mm thick, discontinuous aragonitic cement crusts and irregular laminoid fenestrae amongst porous sand and silt (Fig. 3a). In addition to impacting the types of microbes present, salinity can influence the rates of biochemical processes for different microbes. Pinckney et al. (1995) found that reduction of hypersaline conditions for *Scytonema*-dominated mats caused a significant increase in CO_2 and N_2 fixation rates while higher salinities did not inhibit productivity in *Microcoleus* mats although did suppress N_2 fixation.

3.2 Intertidal

The vertical stress gradient in intertidal zones affects the distribution of benthic marine organisms since many conditions that are normally constant or near-constant in continuously submerged settings become important variables (Raffaelli and Hawkins 1996). At increasing elevations above mean low water, desiccation risks increase, temperature and salinity ranges can increase, light intensity increases to detrimental levels for some organisms, and with an increase in desiccation, the opportunity for respiration, feeding and nutrient uptake decreases. Variations in drainage and water flow will also impact the dissolved oxygen content of the mat pore water. Species of cyanobacteria and bacteria can withstand a wide range of intertidal conditions but eukaryotic microbes, although present in small numbers in some intertidal deposits, appear to be primarily limited to the lower intertidal and deeper (e.g., see Monty 1976, Fig.33). Consequently, the diversity of the benthic community decreases landward. Different species occur along the gradient depending on their ability to deal with physical variables, such as desiccation related factors, and biological variables, such as competition and predation (Raffaelli and Hawkins 1996). Organisms less sensitive to desiccation and related factors can dominate a mat community in the higher intertidal where they escape predation and competition with microbes that are more sensitive and restricted to lower intertidal environments. The outcome of competition and adaptation to varying degrees of desiccation related factors is a zonal distribution of mat types. Wave and current energy and sediment movement can secondarily impact the species that dominate mats (Hoffman 1976; Logan et al. 1974).

Although mat zonations are found in peritidal settings adjacent to normal and near-normal marine waters, including Andros Island (e.g., Hardie and Garrett 1977), Caicos Platform (Wanless et al. 1988), Cape Sable (Gebelein 1977), and Florida Bay islands (Ginsburg et al. 1954), the intertidal gradients are particularly important in arid, protected lagoons and embayments where restricted circulation causes high water salini-

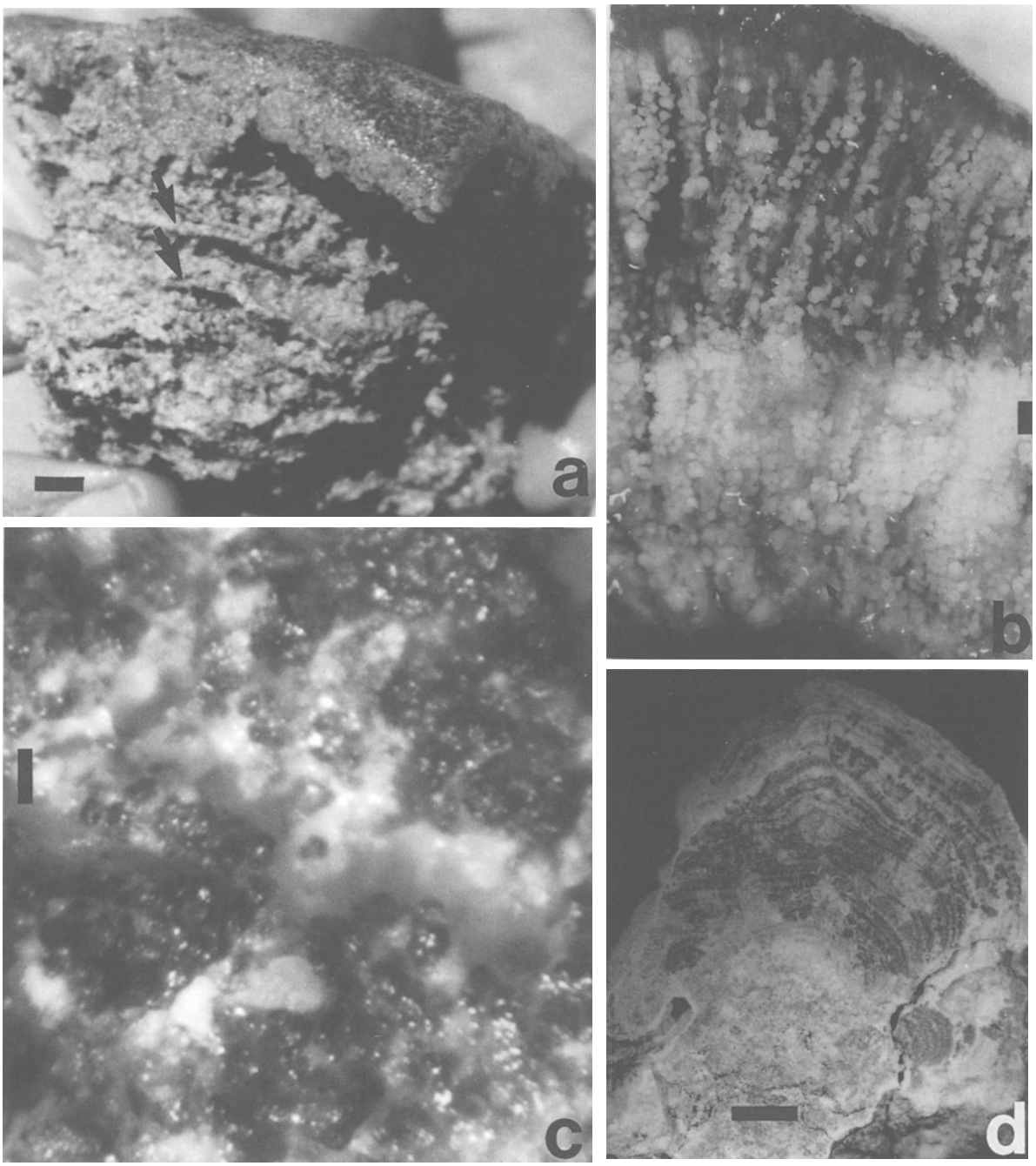

Fig. 3.a Section through subtidal stromatolite from Hamelin Pool, Shark Bay, Western Australia, covered with colloform mat. Semi-cohesive eukaryotic/prokaryotic surficial mat is approximately 2–3 mm thick and can contain small patches of precipitated crusts. Millimeter-thick, discontinuous cement crusts (*arrows*) can be seen in lithified portion below the surficial mat; scale = 5 mm. **b** Section through *Gardnerula* mat from intertidal stromatolite on Lee Stocking Island, Bahamas. *Upper section* contains live filaments and trapped sediment; *lower section* contains trapped, very weakly lithified sediment, dead filaments, calcified molds of filaments (*arrow*), and faint pattern of upright filaments left where filaments once were; *scale* = 500 μm. **c** Close view of intertidal *Entophysalis* pustular mat from Hamelin Pool, Shark Bay, Western Australia. Rough surface created by clusters of coccoid cells produces depressions (some of which, in this view, are cement encrusted) where current/wave transported sediment can be trapped; scale = 500 μm. **d** Section through lithified knob from intertidal *Entophysalis* stromatolites from Hamelin Pool. The more typical clotted internal structure produced by this mat type can be seen in the *lower part* of the section. Uncommon 100 μm-scale laminae and millimeter-scale bush-like structures occur in *upper part* of section; *scale* = 5 mm (7 mm long)

ties. Examples include Hamelin Pool and Gladstone Embayment, Western Australia (Golubic 1992b, Fig. 2), Khor al Bazam, Abu Dhabi, southwestern Persian Gulf (Kendall and Skipwith 1968, Fig. 5) and Spencer Gulf, south Australia (Bauld et al. 1980; Bauld 1981; see Gerdes and Krumbein 1994). Evaporation rates significantly exceed rainfall causing hypersaline conditions, the potential for frequent carbonate precipitation and elimination of most grazing and burrowing metazoans. Dramatic intertidal zonations in microbial communities at these localities are controlled primarily by the desiccation gradient which is influenced by frequency of tidal flooding, drainage and water table position (Logan et al. 1974). Several mat communities can be easily distinguished by color and texture and occur as distinct bands if the shoreline topography is smooth and in patches if it is irregular. More complex topography resulting from microbial growth and metabolic processes can result in water pooling and lateral microbial community zonation on a centimeter scale (e.g., Golubic 1992a). Strikingly similar zonations of microbial communities can be found in several intertidal locations spread over very large distances (Gebelein 1974) and in spite of differing climatic and intertidal conditions (Gerdes and Krumbein 1994). The latter observation has led to the conclusion that the presence of particular mat-forming microbes does not provide proof of a specific growth environment but certain mat types do appear to indicate some environmental conditions (see Gerdes and Krumbein 1994). For example, smooth mats indicate moderate energy conditions with mobile sediment while tufted, pinnacle and pustular mats indicate lower energy settings where sedimentation occurs at a lower rate (Gerdes and Krumbein 1994).

3.2.1 Salinity

Periodic abrupt fluctuations in certain environmental conditions can cause alternations in the dominant microbes that construct the deposit. On the seaward margins of the freshwater interior marshes on eastern Andros Island, *Scytonema*, a freshwater species, dominates mat surfaces during the dry season when water is nearly fresh, whereas *Schizothrix* concentrates beneath the mat surface finding moisture there (Monty 1976). When periodic saline water from storms and equinoctial high tides flood the area and the mats are temporarily soaked with saline water, *Schizothrix* rises to the surface. The salinity is subsequently gradually reduced from the addition of fresh groundwater and rainwater and *Scytonema* becomes the dominant microbe again. The microbial deposit produced in this environment would depend on the timing and duration of saline periods and could consist of a porous palisade or pin-cushion fabric from *Scytonema* alternating with laminated mats of *Schizothrix* (Monty 1976, Figs. 4, 5, 20).

3.2.2 Sediment Movement

Wave energy and sedimentation can secondarily impact the distribution of microbes in the intertidal and the microbial deposits they produce. With constant wave agitation, microbes that might withstand other environmental conditions may not be able to successfully colonize the sediment until a primary colonizing microbial assemblage, often dominated by *Microcoleus*, stabilizes the sediment (Golubic 1985). Once stabilized however, these surfaces are colonized by more specialized assemblages that can typically withstand smaller ranges in environmental conditions and form narrow belts in the intertidal zone like those found in Hamelin Pool. High sedimentation rates can inhibit mat formation since the microbes that might withstand the other environmental conditions would be continually adjusting to movement and/or burial and never have a chance to concentrate along an exposed surface. Variations in sediment influx can impact the dominant microbe and therefore affect the type of microbial deposit formed. For example, in addition to having different tolerances to exposure and/or schizohaline conditions, the smooth mat dominated by *Schizothrix* spp. and *Microcoleus chthonoplastes* from the lower intertidal of Shark Bay can apparently tolerate higher sedimentation rates than the *Entophysalis* pustular mat (Hoffman 1976). Variations in sedimetation rates can therefore result in alternations in these two mat types (Logan et al. 1974). *Schizothrix gracilis* dominates mats found in the intertidal backreef zone of fringing reefs in the Exuma Islands, Bahamas where sediment movement resulting from breaking waves is greatest (Reid and Browne 1991; Reid et al. 1995; Macintyre et al. 1996). The distribution of mats dominated by *Schizothrix* and *Scytonema* on the tidal flats on both coastal tidal flat complexes on the western side of Andros Island, Bahamas and southern sides of Caicos Islands may be impacted by a combination of sedimentation rates and salinity fluctuations (Hardie and Garrett 1977; Wanless et al. 1988). The plot of mat type distributions from Andros Island versus exposure index (EI) in Ginsburg et al. (1977) indicates that both mats occur in areas experiencing exposure indices from 60 to 100 and *Schizothrix*-dominated mats can also occur in areas experiencing lower exposure indices (down to at least 40). *Schizothrix*-dominated mats generally occur in higher elevation, higher exposure zones in the Andros tidal flat (levee crests and beach washovers, EI = 98 – 99.7; levee and beach ridge backslopes, EI = 95 – 98; channel banks, EI = 40 – 90; intertidal channel bars, EI up to 90; beach terraces,

EI = 85–95; mounds in embayment beach areas, EI up to 80; high algal marsh lineation troughs), most are submerged generally only during storms and exceptionally high tides, and can receive up to a millimeter or more of sediment during storm deposition (Hardie 1977). *Scytonema*-dominated mats occur at lower elevations in the channeled belt where they are frequently submerged in seawater and receive less sediment during storms (levee and beach ridge high algal marsh, EI = 85–95; levee and beach ridge low algal marsh, EI = 65–85; high algal marsh current lineation crests; upturned edges of desiccation polygons), and in the more landward supratidal fresh water marsh (EI = 0–100) (Hardie and Garrett 1977; Wanless et al. 1988). In the tidal flats of the Caicos Islands, however, lower-relief channel levees are dominated by *Scytonema* rather than *Schizothrix* since the orientation of the tidal flats relative to storm and predominant wind patterns prohibits frequent onshore storm deposition (Wanless et al. 1988). In this setting, *Schizothrix* mats can be found at elevations lower than *Scytonema* mats where more frequent sedimentation occurs (Wanless et al. 1989). In both tidal flat locations, motile *Schizothrix* filaments adjust to storm deposition more rapidly than non-motile *Scytonema* (Hardie and Garrett 1977; Wanless et al. 1989) and recolonize surfaces first even when *Scytonema* dominated the area prior to storm deposition. And, in the interior freshwater marshes of eastern Andros, *Schizothrix* dominates mat surfaces when they are covered with seawater for prolonged periods while *Scytonema* dominates the surface when the water is diluted from rainfall (Monty 1976; see above). These observations indicate that variations in sedimentation rates and salinity can impact the distribution of these two dominant microbes while exposure interval appears to be is less important.

For mats dominated by motile filamentous cyanobacteria, including the *Schizothrix* mats, the combination of sediment supply to the mat surface and sediment agglutination by the motile microbes can result in millimeter-scale, biosediment lamination (Fig. 2d), and can be enhanced by carbonate precipitation (e.g., see Seong-Joo, Browne, and Golubic, this Vol.; Table 1). For mats dominated by non-motile microbes, carbonate particles added to the mat can be accomplished via (1) current baffling by upright filaments, such as with *Scytonema* pincushion mats from Andros Island (Monty and Hardie 1976; see Demicco and Hardie 1994) and Caicos Platform (Wanless et al. 1988) and *Gardnerula* mats from Lee Stocking Island, Bahamas (Fig. 3b) (unpubl. observ. by K.M. Browne, S. Golubic and B. Winsborough) and Shark Bay (Golubic 1985); (2) increased roughness of the mat surface, such as with pustular *Entophysalis* mats from Shark Bay (Fig. 3c); (3) hydrodynamic deposition with little impact from the presence of the mat; and/or (4) carbonate precipitation, such as with *Scytonema* mats from both Andros Island and Chetumal Bay, Belize, *Gardnerula* mats from Lee Stocking Island, Bahamas, and *Entophysalis* pustular mats from Shark Bay (Fig. 3c,d) (Golubic 1983) and Laguna Mormona (Horodyski et al. 1977).

In addition to the rate at which sediment is added to the mat, grain size may affect the rate at which some microbes recolonize the sediment surface. For example, *Microcoleus lyngbyaceus* was found in laboratory experiments to rapidly recolonize a few millimeters of silt sized sediment but had a much more difficult time recolonizing sand-size sediment (Pentecost 1984). In non-carbonate tidal flats, sandy sediments are commonly very nutrient poor and are more typically colonized by cyanobacteria since they have minimal nutrient requirements (Krumbein et al. 1993). Diatom-rich mats are more common on finer silt and clay sediments however, the lack of cyanobacteria as a dominant component may also be related to grazing stress since diatoms can migrate vertically to the surface when the sediment is exposed to the atmosphere and downward when submerged to avoid predation (Krumbein et al. 1993). The grain size of sediment added during each sedimentation event may act as an environmental stress directly or indirectly and partly influence which microbes can tolerate the setting or whether any will (Pentecost 1984).

3.2.3 Grazing

Grazing invertebrates can significantly impact microbial communities in some settings while in others, their impact appears to be negligible. In the upper intertidal and supratidal flats of western Andros (>50% flooding frequency isograd), *Schizothrix* and *Scytonema* mats flourish and very few grazing gastropods are found in part due to high desiccation risks (Garrett 1970, 1977; Ginsburg et al. 1977). In contrast, in the adjacent mid-intertidal and deeper zones, *Schizothrix* colonizes the sediment surface but abundant gastropods often graze on the microbes and prevent the formation of a coherent mat. In tidal flat ponds, cerithids and infaunal polychaetes (*Marphysa*) disrupt mat formation as they graze on an incoherent mat dominated by cyanobacteria identified as *Anacystis aeruginosa, Schizothrix calcicola, Scytonema* sp., *Microcoleus lyngbyaceus* and *M. vaginatus* (Hardie and Garrett 1977). When cerithids are not present, *Schizothrix* can form a soft rubbery mat binding the surface together but is still disrupted by burrowing polychaetes and rising air bubbles. Gebelein (1977) found a similar relationship between gastropod density and mat presence in Cape Sable although the boundary between disrupted and undisrupted mats occurred at the 25% flooding frequency isograd, suggesting that the location of the boundary is depen-

dent upon the types of algae and invertebrates present (Garrett 1970). In the Gavish Sabkha, microbial mats do not occur in the metahaline zone where gastropods (*Pirenella conica*) are abundant (Gerdes et al. 1985; Gerdes and Krumbein 1987). However, when *P. conica* is present but not particularly abundant in higher salinity environments, their gut contents indicate a preference for coccoid cyanobacteria and diatoms as do most other primary consumers of the mats including turbularians, rotatorians, nematodes, ostracods, copepods, flies and mosquito larvae, and aquatic and terrestrial beetles. Presumably then, grazing invertebrates can coexist with microbial mats dominated by sheathed filamentous cyanobacteria if the former are not too abundant or the latter are not the only source of food.

3.2.4 Solar Radiation

Extremes in solar radiation, particularly ultraviolet, can be toxic to some mat species and can therefore also select for certain species or impact the order in which microbes occur in stratified microbial mats in settings stressed by other environmental conditions (e.g., Garcia-Pichel and Castenholz 1994; Jørgensen 1989). Photosynthetic rates for *Microcoleus lyngbyaceus*, for example, can decrease if exposed to light intensities greater than 5 klx and the microbes can move laterally away from the light source (Pentecost 1984). Mat cultures exposed to UV dosages show a marked decrease in photosynthetic rates not only at the mat surface but also throughout the major part of the euphotic zone in the mat (Garcia-Pichel and Castenholz 1994). Cyanobacteria in mats from Guerro Negro, Mexico migrate downward during the daytime to avoid even small doses of UV-A (Garcia-Pichel and Castenholz 1994). Rates of highest mat productivity have been documented 1 to 4 mm beneath the surface of some mats indicating that this subsurface environment is more favorable for productivity and that the surface felt of microbes may serve as a protective covering for the most productive microbes beneath them (e.g., Revsbech and Ward 1984). In many mats dominated by motile *Oscillatoria* species, trichomes clumped together on the mat surface provide self-shading for trichomes beneath the surface (Garcia-Pichel and Castenholz 1994). In Gavish Sabkha mats, *Microcoleus* is found beneath a surface layer of coccoid cyanobacteria (*Gloeothece, Synechococcus* and *Synechocystis*) and voluminous amounts of EPS where it is protected from high light intensities (as well as increases in salinity and temperature) but still receives sufficient light to be photosynthetically active (Castenholz 1984; Gerdes and Krumbein 1987). Some microbes, like *Entophysalis major*, can withstand excessive solar radiation by producing extracellular pigments, in this case the sheath pigment scytonemine, or intracellular sunscreens to protect the cells (Garcia-Pichel and Castenholz 1994; Golubic 1992a). In Solar Lake from the Gulf of Aqaba, Sinai Peninsula, filamentous cyanobacteria dominate the surface of the lake shelf mats during fall, winter and spring while unicellular cyanobacteria (*Synechococcus, Synechocystis*) and diatoms (*Nitzschia, Amphora,* and *Navicula*), which produce enormous amounts of EPS and carotenoid pigments, predominate as incident light increases and water level drops into the summer (Gerdes and Krumbein 1987; see Gerdes, Krumbein, and Noffke, this Vol., for descriptions of mat fabrics).

3.2.5 Dissolved Gases

Dissolved oxygen in mat pore waters or ponded waters can impact the vertical zonation in a mat or the dominant microbe in a community and therefore the mat architecture. *Microcoleus chthonoplastes* not only tolerates large salinity fluctuations but also tolerates or even prefers low O_2 concentrations and can dominate in settings that many other microbes can not tolerate well. For example, it can survive deeper within a mat than other cyanobacteria and can even function in the transition zone between oxygenated and anoxic zones of a mat (Golubic 1992a). *M. chthonoplastes* also dominates the mat surfaces in depressions of folded, convoluted mats forming in the intertidal of Abu Dhabi where the ponded water found in these depressions is often O_2-depleted (Park 1977 Fig. 3; Golubic 1991). *Schizothrix splendida* dominates fold tops where O_2 depletion is not a problem. The distinctive high pinnacle mats also from Abu Dhabi may result from greater growth of filamentous microbes upwards, primarily *Lyngbya aestuarii*, where O_2 is more available (Golubic 1992a; Fig. 4a,b). The layer beneath *Lyngbya aestuarii* is occupied by *Schizothrix splendida* which would presumably require less O_2 than *L. aestuarii.*

4 Lithification of Microbial Deposits

Mechanisms of mineralization of microbial deposits are poorly understood in part due to the complex biochemical system that drives precipitation (and dissolution) as well as both the isolated pore water micro-environments created by the mat fabrics and the minute scale at which biochemical reactions and mineral crystallization occur in these micro-environments. Recently, advancement of this field has been accomplished through *in situ* geochemical monitoring (e.g., Revsbech and Ward 1984; Paerl et al. 1989; Canfield and Des Marais 1991; Merz 1992; Visscher et al. 1992; Visscher et al. 1998), experimental (e.g., Krumbein 1979; Pentecost and Bauld 1981; Buczynski and Chafetz 1991;

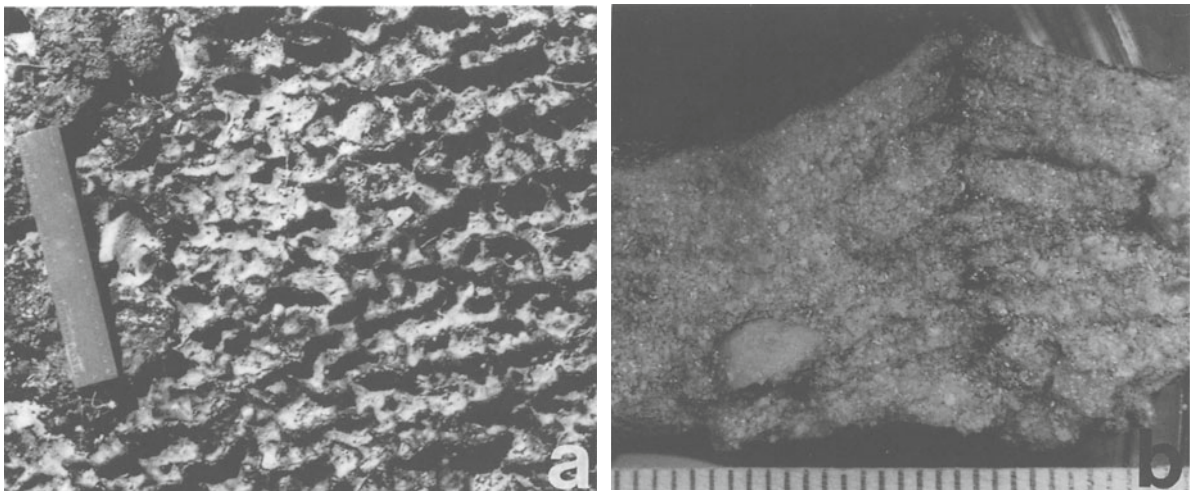

Fig. 4.a Intertidal reticulate mat from Hamelin Pool, Shark Bay, Western Australia. Ridges are composed of *Lyngbya* and depressions contain both *Lyngbya* and *Schizothrix*. Ruler is 15 cm long. **b** Section through reticulate mat showing sequence of super-imposed *Lyngbya*-dominated ridges and faint scalloped layering (sample fixed in 3% formaldehyde; mm scale)

Table 2. Equations for some organic processes occurring within microbial mats that can alter mat pore water pH, alkalinity and/or saturation state of $CaCO_3$

Process	Reaction	Consequence
Photosynthesis[a]	$106CO_2 + 16NO_3^- + HPO_4^{2-} + 122H_2O + 18H^+ +$ (trace elements, energy) $= C_{106}H_{263}O_{110}N_{16}P + 138O_2$	Rise in pH and $CaCO_3$ saturation state
Aerobic decay[a]	$C_{106}H_{263}O_{110}N_{16}P_1 + 138O_2 = 106CO_2 + 16NO_3^- + HPO_4^{2-} + 122H_2O + 18H^+$	Drop in pH and $CaCO_3$ saturation state
Deamination of amino acids[a]	(a) [Amino acid] = [N-free compounds]$+NH_3$ (b) NH_3 reacts: $NH_3 + H_2O + CO_2 = NH_4^+ + HCO_3^-$	Net rise in pH and alkalinity
Sulphate reduction[b]	(a) $1/53(CH_2O)_{106}(NH_3)_{16}H_3PO_4 + SO_4^{2-} = 2HCO_3^- + HS^- + 16/53NH_3 + 1/53H_3PO_4 + H^+$ (b) NH_3 reacts: $NH_3 + H_2O + CO_2 = NH_4^+ + HCO_3^-$	Initial drop in pH and rise in alkalinity Net rise in pH and alkalinity

[a]Drever (1988).
[b]Morse and Mackenzie (1990).

Chafetz and Buczynski 1992) and microstructural studies (e.g., Defarge et al. 1996; Folk 1993; Gerdes et al. 1994). However, each approach has its limitations in pinpointing the role of specific microbes and their metabolic activities. Geochemical monitoring is limited since even on a microelectrode scale, some chemical changes recorded are the products of net biological activity and documented changes must be correlated with actual precipitates. Experimental work has mostly addressed the potential of microbe activities to cause precipitation and now requires connection with actual performances in real mats. Although microstructural studies offer clues to the origin of carbonate particles, they are limited in that they can not document supporting chemical evidence that connects precipitates with biochemical changes that occur on the same scale as the carbonate crystals.

The principal biochemical processes that have been recognized to affect carbonate saturation state and therefore may cause carbonate precipitation include (Table 2): (1) environmental carbon depletion by autotrophs during photosynthesis (and possibly chemolithotrophy), (2) deamination of amino acid in the course of bacterial proteolysis, and (3) anaerobic bacterial dissimilatory sulfate reduction (and see Castanier, Le Métayer-Levrel, and Perthuisot, this Vol.; Riege and Krumbein, this Vol.). All result in an increase in pH and/or alkalinity which promote carbonate precipitation. In addition, there is indication that crystal nucleation and growth may occur under the guidance of an organic template (e.g., Gerdes et al. 1994; Defarge et al. 1996), similar to the carbonate skeletogenesis in plants and animals (see Lowenstam and Weiner 1989), although the architecture of the organic or mineral structures may not be as elaborate as observed in eukaryotic intracellular and extracellular calcification (reviewed by Golubic, Seong-Joo, and Browne, this Vol.). A recent *in situ* geochemical study of intertidal stromatolite mats dominated by *Schizothrix* (Visscher et al. 1998) has revealed that photosynthesis, sulfate reduction and anaerobic sulfide oxidation are responsible for carbonate precipitation within the millimeter-scale laminae

while aerobic respiration and aerobic sulfide oxidation cause carbonate dissolution. The results also indicate that photosynthesis coupled to sulfate reduction and sulfide oxidation is more important than photosynthesis coupled to aerobic respiration in the formation of lithfied micritic crusts in these mats.

To determine exactly how, when and where carbonate precipitation occurs, several questions must be addressed. (1) At what levels of solution supersaturation is a correlation between micro-organismal presence and carbonate precipitation expressed? (2) What are the causalities involved in the process? (3) Does the influence of microorganisms operate at the level of solution chemistry? (4) If so, which metabolic activities by which ecological guilds of microorganisms are involved (photosynthetic or chemolithotrophic incorporation of carbon dioxide or bicarbonate ion, sulfate reduction-deamination)? (5) Is the effect expressed through pH changes or Ca-ion flux? (6) Do the influences of microorganisms or organismal organic products operate at the level of crystal nucleation of the precipitates, and does this influence continue in guiding further crystal growth? (7) Does the relative importance of these influences change within the range of the conditions under which mineral fabrics form? (8) What are the characteristics of the resulting biomineral deposits in terms of: (a) distribution and competition for nucleation sites, developments after the initial nucleation, crystal growth, and diagenesis, (b) crystallographic properties, (c) chemical composition, including trace minerals and their distribution, and stable isotope composition relative to that in the source solution and (d) organic matter incorporation.

5 Summary

Microbial mats occur in locations where microbes can dominate the benthic community and are most common today in environmentally stressed settings where most macro-organisms and many micro-organisms are eliminated and therefore do not influence sedimentation. Specific environmental conditions influence which micro-organism(s) dominates the mat community and it is the dominant microbe(s) that controls the fabrics of the mat (Table 1). These fabrics are the product of microbial activities and interaction with the hydrodynamic setting. If too many microbes dominate a community or the metabolic products of the microbes (e.g., EPS) limit cohesiveness, distinctive fabrics generally do not result. While fabric-less flocculose mats are very common in marine subtidal settings, distinctive mat fabrics are uncommon and typically result from either water chemical stresses or high sediment movement stresses. Many mat types from peritidal settings occur in lateral zonations which visually illustrate the significant impact of intertidal gradients on microbe distribution. Vertical zonations of both primary producers and decomposers occur in every mat to some degree and the vertical distributions result from gradients in sunlight radiation and pore water chemistry as well as the amount and frequency of sediment addition. Carbonate precipitation occurs in only some mat types and in only certain settings. The complex processes that influence zonations, mat fabrics and morphologies and lithification or dissolution are difficult to document due to the size of the microbes and organic surfaces, the volume of pore waters involved and the magnitude of chemical reactions taking place. Remarkably, in spite of the large number of microbes present on this globe and the complexities involved in ecosystem processes, only a small number of microbes have been found to dominate most microbial mats and some help construct more than one mat type. As a result, only a small number of mat types have been documented from shallow marine carbonate settings.

Acknowledgements. Research conducted by the authors related to the contents of this paper was in part supported by: Resources for the Future Foundation, NOAA grant CMRC 94-24, German Research Foundation (DFG-Vo.90/14), Hanse Institute for Advanced Studies, Delmenhorst, Germany, Kanagawa Museum of Natural History and the Australian Museum of Natural History, and the National Geographic Society (4945-92).

References

Aitken JD (1967) Classification and environmental significance of cryptalgal limestones and dolomites with illustrations from the Cambrian and Ordovician of southwestern Alberta. J Sed Petrol 37:1163-1178

Awramik SM, Riding R (1988) Role of algal eukaryotes in subtidal columnar stromatolite formation. Proc Natl Acad Sci USA 85:1327-1329

Bathurst RGC (1967) Subtidal gelatinous mat, sand stabilizer and food, Great Bahama Bank. J Geol 75:736-738

Bathurst RGC (1975) Carbonate sediments and their diagenesis, Developments in Sedimentology 12. Elsevier, Amsterdam, 658 pp

Bauld J (1981) Geobiological role of cyanobacterial mats in sedimentary environments: production and preservation of organic matter. BMR J Austr Geol Geophys 6:307-317

Bauld J (1984) Microbial mats in marginal marine environments: Shark Bay, Western Australia, and Spencer Gulf, South Australia. In: Cohen Y, Castenholz RW, Halvorson HO (eds) Microbial mats: stromatolites. Alan R. Liss, New York, pp 39-58

Bauld J, Chambers LA, Skyring GW (1979) Primary productivity, sulfate reduction and sulfer isotope fractionation in algal mats and sediments of Hamelin Pool, Shark Bay, W. A. Aust J Freshwater Res 30:753-764

Bauld J, Burne RV, Chambers LA, Ferguson J, Skyring GW (1980) Sedimentological and geobiological studies of intertidal cyanobacterial mats in northeastern Spencer Gulf, South Australia. In: Trudinger PA, Walter MR, Ralph BJ (eds) Biogeochemistry of ancient and modern environments. Aust Acad Sci Canberra, pp 157-166

Black M (1933) The algal sediments of Andros Island, Bahamas. Philos Trans R Soc Ser B 222:165-192

Braga JC, Martin JM, Riding R (1995) Controls on microbial dome fabric development along a carbonate-siliciclastic shelf-basin transect, Miocene, S.E. Spain. Palaios 10:347-361

Buczynski C, Chafetz HS (1991) Habit of bacterially induced precip-

itates of calcium carbonate and the influence of medium viscosity on mineralogy. J Sed Petrol 61:226–233
Burne RV, Moore LS (1987) Microbialites: organosedimentary deposits of benthic microbial communities. Palaios 2:241–245
Canfield DE, Des Marais DJ (1991) Biogeochemical cycles of carbon, sulfur, and free oxygen in a microbial mat. Geochim Cosmochim Acta 57:3971–3984
Castenholz RW (1984) Composition of hot spring microbial mats: a summary. In Y Cohen, RW Castenholz, HO Halvorson (eds.) Microbial Mats: Stromatolites, Alan R. Liss, New York, pp 101–120
Chafetz HS, Buczynski C (1992) Bacterially induced lithified microbial mats. Palaios 7:277–293
Cohen Y, Rosenberg E (eds) (1989) Microbial mats: physiological ecology of benthic microbial communities. Am Soc Microbiol, Washington, DC, 490 pp
Cohen Y, Castenholz RW, Halvorson HO (1984) Microbial Mats: Stromatolites. Alan R. Liss, New York, 498 pp
Davies GR (1970) Algal-laminated sediments, Gladstone Embayment, Shark Bay, Western Australia. In: Logan BW, Davies GR, Read JF, Cebulski DE (eds) Carbonate sedimentation and environments, Shark Bay, Western Australia. Am Assoc Petrol Geol Mem 13:169–205
Decho AW (1990) Microbial exopolymer secretions in ocean environments: their role(s) in food webs and marine processes. Oceanogr Mar Biol Annu Rev 28:73–153
Defarge C, Trichet J, Maurin A, Robert M, Tribble J, Sansone FJ (1996) Texture of microbial sediments revealed by cryo-scanning electron microscopy. J Sed Petrol 66:935–947
Demicco RV, Hardie LA (1994) Sedimentary Structures and Early Diagenetic features of shallow marine carbonate deposits. SEPM Atlas Ser No 1, 265pp
Drever JI (1988) The geochemistry of natural waters, 2nd edn. Prentice Hall, Englewood Cliffs, 437 pp
Dill RF, Shinn EA, Jones AT, Kelly K, Steinen RP (1986) Giant subtidal stromatolites forming in normal salinity waters. Nature 324:55–58
Dravis JF (1983) Hardened subtidal stromatolites, Bahamas. Science 219:385–386
Folk RL (1993) SEM imaging and nanobacteria in carbonate sediments in rocks. J Sed Petrol 63:990–999
Friedman GM, Amiel AJ, Braun M, Miller DS (1973) Generation of carbonate particles and laminites in algal mats: example from sea-marginal hypersaline pool, Gulf of Aqaba, Red Sea. Am Assoc Petrol Geol Bull 57:541–557
Frost JG (1974) Subtidal algal stromatolites from the Florida backreef environment. J Sed Petrol 44:532–537
Garcia-Pichel F, Castenholz RW (1994) On the significance of solar ultraviolet radiation for the ecology of microbial mats. In: Stal. LJ, Caumette P (eds) Microbial mats: structure, development and environmental significance. NATO ASI Series, vol G35. Springer, Berlin Heidelberg New York, pp 76–84
Garrett P (1970) Phanerozoic stromatolites: noncompetitive ecological restriction by grazing and burrowing animals. Science 169:171–173
Garrett P (1977) Biological communities and their sedimentary record. In: Hardie LA (ed) Sedimentation on the modern carbonate tidal flats of northwest Andros Island, Bahamas. John Hopkins Univ Studies in Geol No 22, John Hopkins Univ Press, Baltimore, pp 124–158
Gebelein CD (1969) Distribution, morphology, and accretion rate of Recent subtidal algal stromatolites, Bermuda. J Sed Petrol 39:49–69
Gebelein CD (1974) Biologic control of stromatolite microstructure: implications for Precambrian time stratigraphy. Am J Sci 274:575–598
Gebelein CD (1976) Open marine subtidal and intertidal stromatolites (Florida, the Bahamas and Bermuda). In: Walter MR (ed) Stromatolites: developments in sedimentology 20. Elsevier, Amsterdam, pp 381–388
Gebelein CD (1977) Dynamics of recent carbonate sedimentation and ecology: Cape Sable, Florida. EJ Brill Publ, Leiden
Gerdes G, Dunajtschik-Piewak K, Riege H, Taher AG, Krumbein WE, Reinick H-H (1994) Structural diversity of biogenic carbonate particles in microbial mats. Sedimentology 41:1273–1294
Gerdes G, Krumbein WE (1987) Biolaminated deposits. In: Bhattacharji S, Friedman GM, Neugebauer HJ, Seilacher A (eds) Lecture Notes in Earth Sciences 9. Springer, Berlin Heidelberg New York
Gerdes G, Krumbein WE (1994) Peritidal potential stromatolites – a synopsis. In: Bertrand-Sarfati J, Monty CLV (eds) Phanerozoic Stromatolites II. Kluwer, Dordrecht, pp 101–129
Gerdes G, Spira J, Dimentam C (1985) The fauna of the Gavish Sabkha and the Solar Lake – a comparative study. In: Friedman GM, Krumbein WE (eds) The Gavish Sabkha. Springer, Berlin Heidelberg New York, pp 322–345
Ginsburg RN, Isham LB, Bein SJ, Kuperburg J (1954) Laminated algal sediments of South Florida and their recognition in the fossil record. Unpubl Final Rep to NSF Inst of Mar Sci, Univ Miami Publ. no 8034
Ginsburg RN, Lowenstam HA (1958) The influence of marine bottom communities on the depositional environment of sediments. J Geol 66:310–318
Ginsburg RN, Hardie LA, Bricker OP, Garrett P, Wanless HL (1977) Exposure index: a quantitative approach to defining position within the tidal zone. In LA Hardie (ed.) Sedimentation on the modern carbonate tidal flats of northwest Andros Island, Bahamas. John Hopkins Univ Studies in Geol No 22, John Hopkins Univ Press, Baltimore, pp 7–11
Golubic S (1983) Stromatolites, fossil and recent: a case history. In P Westbroek, EW de Jong (eds.) Biomineralization and biological metal accumulation. Reidel, Dordrecht, pp 313–326
Golubic S (1985) Microbial mats and modern stromatolites in Shark Bay, Western Australia. In: Caldwell DE, Brierley JA, Brierley CL (eds) Planetary ecology. van Nordstrand Reinhold, New York, pp 3–16
Golubic S (1991) Modern stromatolites – a review. In: Riding R (ed) Calcareous algae and stromatolites. Springer, Berlin Heidelberg New York, pp 541–561
Golubic S (1992a) Microbial mats of Abu Dhabi. In L Margulis, L Olenzenski (eds.) Environmental Evolution: Effects of the Origin of Life on Planet Earth. MIT Press, Cambridge, pp 131–147
Golubic S (1992b) Stromatolites of Shark Bay. In: Margulis L, Olendzenski L (eds) Environmental evolution, effects of the origin and evolution of life on planet earth. MIT Press, Cambridge, pp 103–130
Golubic S, Browne KM (1996) *Schizothrix gebeleinii* sp. nova builds subtidal stromatolites, Lee Stocking Island, Bahamas. Algol Stud 83:273–290
Golubic S, Focke JW (1978) *Phormidium hendersonii* howe: identity and significance of a modern stromatolite building microorganism. J Sed Petrol 48:751–764
Guerrero M-C, Tadeo A-B, de Wit R (1994) Environmental factors controlling the development of microbial mats in inland saline lakes; the granulometric composition of the sediment. In: Stal LJ, Caumette P (eds) Microbial mats. NATO ASI Ser, vol G35, Springer, Berlin Heidelberg New York, pp 85–90
Guerrero R, Mas J (1989) Multilayered microbial communities in aquatic ecosystems: growth and loss factors. In: Cohen Y, Rosenberg E (eds) Microbial mats: physiological ecology of benthic microbial communities. Am Soc Microbiol, Washington, DC, pp 37–51
Hardie LA (1977) Sedimentation on the modern carbonate tidal flats of northwest Andros Island, Bahamas, John Hopkins Univ Studies in Geology No 22. John Hopkins Univ Press, Baltimore, 202 pp
Hardie LA, Garrett P (1977) General environmental setting. In LA Hardie (ed.) Sedimentation on the modern carbonate tidal flats of northwest Andros Island, Bahamas. John Hopkins Univ Press, Baltimore, pp 12–49
Hardie LA, Ginsburg RN (1977) Layering: the origin and environmental significance of lamination and thin bedding. In: Hardie LA (ed) Sedimentation on the modern carbonate tidal flats of Northwest Andros Island, Bahamas. John Hopkins Univ Press, Baltimore, pp 50–123
Harris PM (1979) Facies Anatomy and Diagenesis of a Bahamian Ooid Shoal. Sedimenta VII, Comparative Sed Lab, Miami, 163 pp
Hoffman PE (1976) Stromatolite morphogenesis in Shark Bay, Western Australia. In: Walter MR (ed) Stromatolites: developments in sedimentology 20. Elsevier, Amsterdam, pp 261–272

Holland AF, Zingmark RG, Dean JM (1974) Quantitative evidence concerning the stabilization of sediments by marine benthic diatoms. Mar Biol 27:191–196
Horodyski RJ, Bloeser B, Vonder Haar S (1977) Laminated algal mats from a coastal lagoon, Laguna Mormona, Baja California, Mexico. J Sed Petrol 47:680–696
Horodyski RJ, Vonder Haar SP (1975) Recent calcareous stromatolites from Laguna Mormona (Baja California) Mexico. J Sed Petrol 45:894–906
James NP, Bourque P-A (1992) Reefs and mounds. In RG Walker, NP James (eds) Facies models response to sea level changes. Geol Assoc Can Reprint Ser, pp 323–345
John J (1990) The diatom flora of the microbial communities associated with stromatolites at Shark Bay, Indian Ocean, west coast of Australia. Ouvrage dédié à H Germain, Koeltz, pp 97–110
Jørgensen BB (1989) Light penetration, absorption, and action spectra in cyanobacterial mats. In: Cohen Y, Rosenberg E (eds) Microbial mats: physiological ecology of benthic microbial communities. Am Soc Microbiol, Washington, DC, pp 123–137
Kalkowsky E (1908) Oolith and stromatolith in norddeutschen Bundsandstein. Dtsch Geol Ges Z 60:112
Kendall CGStC, Skipwith PAd'E (1968) Recent algal mats of a Persian Gulf lagoon. J Sed Petrol 38:1040–1058
Krumbein WE (1979) Photolithotrophic and chemolithotrophic activity of bacteria and algae as related to beachrock formation and degradation (Gulf of Aqaba, Sinai). Geomicrobiol J 1:139–203
Krumbein WE, Paterson DM, Stal L-J, Wippermann T (1993) Microbially mediated processes in tide-influenced deposits and their importance in stabilization and diagenesis of sediments. In: Barthel K-G, Bohle-Carbonell M, Fragakis C, Weydert M (eds) Marine sciences and technologies, MAST days and Euromar market, vol 1, Commission European Communities, pp 242–259
Logan BW (1974) Inventory of diagenesis in Holocene-Recent carbonate sediments, Shark Bay, Western Australia. Am Assoc Petrol Geol Mem 22:195–249
Logan BW, Brown RG (1986) Field seminar handbook of Shark Bay and Macleod Basin, Western Australia. Univ W Aust, 236 pp
Logan BW, Hoffman P, Gebelein CD (1974) Algal mats, cryptalgal fabrics, and structures, Hamelin Pool, Western Australia. Am Assoc Petrol Geol Mem 22:140–194
Lowenstam HA, Weiner S (1989) On biomineralization. Oxford Univ Press, Oxford, 320 pp
Macintyre IG, Reid RP, Steneck RS (1996) Growth history of stromatolites in a Holocene fringing reef, Stocking Island, Bahamas. J Sed Res 66:231–242
Meadows A, Meadows PS, Wood DM, Murray JMH (1994) Microbiological effects on slope stability: an experimental analysis. Sedimentology 41:423–435
Merz MUE (1992) The biology of carbonate precipitation by cyanobacteria. Facies 26:81–102
Monty CLV (1965) Recent algal stromatolites in the windward lagoon, Andros Island, Bahamas. Ann Soc Geol Belge, T 88, 1964–1965, Bull no 6, pp B269–279
Monty CLV (1976) The origin and development of cryptalgal fabrics. In: Walter MR (ed) Stromatolites, developments in sedimentology 20. Elsevier, Amsterdam, pp 193–249
Monty CLV (1979) Monospecific stromatolites from the Great Barrier Reef Tract and their paleontological significance. Ann Soc Geol Belge 101:163–171
Monty CLV, Hardie LA (1976) The geological significance of the freshwater blue-green algal calcareous marsh. In: Walter MR (ed) Stromatolites, developments in sedimentology 20. Elsevier, Amsterdam, pp 447–477
Morse JW, Mackenzie FT (1990) Geochemistry of sedimentary carbonates. Elsevier, Amsterdam, 707 pp
Newell ND, Imbrie J, Purdy EG, Thurber DT (1959) Organism communities and bottom facies, Great Bahama Bank. Am Mus Nat Hist Bull 117:117–228
Neumann AC, Gebelein CD, Scoffin TP (1970) The composition, structure and erodibility of subtidal mats, Abaco, Bahamas. J Sed Petrol 40:274–297
Paerl HW, Bebout BM, Joye SB, Des Marais DJ (1993) Microscale characterization of dissolved organic matter production and uptake in marine microbial mat communities. Limnol Oceanogr 38:1150–1161
Paerl HW, Bebout BM, Prufert LE (1989) Naturally occurring patterns of oxygenic photosynthesis and N_2 fixation in a marine microbial mat: physiological and ecological ramifications. In: Cohen Y, Rosenberg E (eds) Microbial mats: physiological ecology of benthic microbial communities. Am Soc Microbiol, Washington, DC, pp 326–341
Park RK (1977) The preservation potential of some Recent stromatolites. Sedimentology 24:485–506
Pentecost A (1984) Effects of sedimentation and light intensity on mat-forming Oscillatoriaceae with particular reference to *Microcoleus lyngbyaceus* Gomont. J Gen Microbiol 130:983–990
Pentecost A, Bauld J (1988) Nucleation of calcite on the sheaths of cyanobacteria using a simple diffusion cell. Geomicrobiol J 6:129–135
Pickney J, Paerl HW, Bebout BM (1995) Salinity control of benthic microbial mat community production in a Bahamian hypersaline lagoon. J Exp Mar Bio Ecol 187:223-240
Playford PE, Cockbain AE (1976) Modern algal stromatolites at Hamelin Pool, a hypersaline barred basin in Shark Bay, Western Australia. In: Walter MR (ed) Stromatolites: developments in sedimentology 20. Elsevier, Amsterdam, pp 389–411
Purdy EG (1963) Recent carbonate facies of the Great Bahama Bank II. Sedimentary facies. J Geol 71:472–497
Raffaelli D, Hawkins S (1996) Intertidal Ecology. Chapman and Hall, New York, 356 pp
Rasmussen KA, Macintyre IG, Prufert L (1993) Modern stromatolite reefs fringing a brackish coastline, Chetumal Bay, Belize. Geol 21:199–202
Reid RP, Browne KM (1991) Intertidal stromatolites in a fringing reef complex, Bahamas. Geol 19:15–18
Reid RP, Macintyre IG, Browne KM, Steneck RS, Miller T (1995) Modern marine stromatolites in the Exuma Cays, Bahamas: uncommonly common. Facies 33:1–18
Revsbech NP, Ward DM (1984) Microprofiles of dissolved substances and photosynthesis in microbial mats measured with microelectrodes. In: Cohen Y, Castenholz RW, Halverson HO (eds) Microbial mats: stromatolites. Alan R. Liss, New York, pp 171–188
Riding R (1991) Classification of microbial carbonates. In R Riding (ed) Calcareous algae and stromatolites. Springer, Berlin Heidelberg New York, pp 21–51
Riding R (1994) Stromatolite survival and change: the significance of Shark Bay and Lee Stocking Island subtidal columns. In: Krumbein WE, Paterson DM, Stal L-J (eds) Biostabilization of sediments. Bibliotheks und Informationssystem der Universitdt Oldenburg-Verlag, Oldenburg, pp 183–202
Riding R (1997) Stromatolite decline: a brief reassessment. Facies 36:52–67
Riding R, Awramik SM, Winsborough BM, Griffin KM, Dill RF (1991) Bahamian giant stromatolites: microbial composition of surface mats. Geol Mag 128:227–234
Scoffin TP (1970) The trapping and binding of subtidal carbonate sediments by marine vegetation in Bimini Lagoon, Bahamas. J Sed Petrol 40:249–273
Semikhatov MA, Gebelein CD, Cloud P, Awramik SM, Benmore WC (1979) Stromatolite morphogenesis – progress and problems. Can J Earth Sci 16:992–1015
Shinn EA (1968) Practical significance of bird's-eye structures in carbonate rocks. J Sed Petrol 38:215–223
Skyring GW, Bauld J (1990) Microbial mats in Australian coastal environments. In KC Marshall (ed) Advances in microbial ecology, vol 11. Plenum Press, New York, pp 461–498
Stal LJ (1994) Microbial mats in coastal environments. In: Stal LJ, Caumette P (eds) Microbial mats. NATO ASI Ser, vol G35, Springer, Berlin Heidelberg New York, pp 21–32
Stal LJ, Caumette P (1994) Microbial mats: structure, development and environmental significance. NATO ASI Ser, vol G35, 463 pp
van Germerden H (1993) Microbial mats: a joint venture. Mar Geol 113:3–25
Visscher PT, Prins RA, van Gemerden H (1992) Rates of sulfate reduction and thiosulfate consumption in a marine microbial mat. FEMS Microbiol Ecol 86:283
Visscher, PT, Reid RP, Thompson JA Jr (1998) Formation of lithified

laminae in modern marine stromatolites (Bahamas): the role of sulfur cycling. Am Miner 83:14-82-1493
Vos PC, deBoer PL, Misdorp R (1990) Sediment stabilization by benthic diatoms in intertidal sandy shoals: qualitative and quantitative observations. In: deBoer PL et al. (eds) Tide-influenced sedimentary environments and facies. Reidel, Dordrecht, pp 511–526
Wanless HR, Tyrrell KM, Tedesco LP, Dravis JJ (1988) Tidal-flat sedimentation from Hurricane Kate, Caicos Platform, British West Indies, J Sed Petrol 58:724–738
Wanless HR, Dravis JJ, Tedesco LP, Rossinsky V (1989) Carbonate environments and sequences of Caicos Platform, IGC Fieldtrip Guidebook T374, 75 pp
Watling L (1988) Small-scale features of marine sediments and their importance to the study of deposit-feeding. Mar Ecol Prog Ser 47:135–144
Yallop ML, de Winder B, Paterson DM, Stal LJ (1994) Comparative structure, primary production and biogenic stabilisation of cohesive and non-cohesive marine sediments inhabited by microphytobenthos, Estuar Coast Shelf Sci 39:565–582

Microbial Whitings

Joel B. Thompson

Department of Marine Science, Eckerd College, 4200 54th Avenue South, St. Petersburg, Florida 33711, USA

Abstract. Two whitings case studies are reviewed for the role of bacteria in their formation. The first case study is from Fayetteville Green Lake in upstate New York. In this lake, *Synechococcus* plays a major role in the initiation of an annual whiting event. The whiting calcite precipitates principally in the microenvironment surrounding *Synechococcus* cells and is isotopically enriched in ^{13}C due to the fractionation of ^{12}C. *Synechococcus* possesses an S-layer that acts as a template for carbonate precipitation and the S-layer is shed from the cell surface once it is mineralized.

The second case study is from the Great Bahama Bank west of Andros Island, Bahamas. Here, the whitings are much more complex and are still unresolved to the satisfaction of most investigators. Present data suggest the role of an intricate biophysicochemical coupling between the microbial community, physical circulation on the Bank, and water chemistry. Further, detailed interdisciplinary studies are needed to fully resolve the marine whitings on the Great Bahama Bank.

1 Introduction

When fine grained carbonate precipitates in the open water column of lakes or seas, it gives the water a milky white appearance called whitings or whiting events (Bathurst 1975; Fig. 1). Whitings may result in large carbonate mud deposits over geological time in both marine and freshwater environments. The biotic versus abiotic origins of whitings have been vigorously debated over the last century (Drew 1914; Smith 1940; Cloud 1962; Wells and Illing 1964; Broecker and Takahashi 1966; Brunskill 1969; Morse et al. 1984; Shinn et al. 1989; Robbins and Blackwelder 1992; Thompson et al. 1997).

The two main explanations proposed for the origin of whitings has come full-circle over the past century. Early investigators (Drew 1914; Kellerman and Smith 1914; Black 1933; Greenfield 1963; McCallum and Guhathakurta 1970) related bacteria to whiting production. This early hypothesis of bacterial precipitation was followed by a hypothesis invoking inorganic precipitation mechanisms (Broecker and Takahashi 1966; Brunskill 1969; Morse et al. 1984; Milliman et al. 1993). More recent, detailed electron microscopy and stable carbon isotope studies showed that some whitings are caused by bacterial picoplankton activity (Thompson and Ferris 1990; Robbins and Blackwelder 1992; Robbins et al.

Fig. 1. Aerial photograph of whitings on the Great Bahama Bank west of Andros Island on September 19, 1995. The whitings range in size from a few tens of square meters to a few square kilometers

R. E. Riding and S. M. Awramik (Eds.)
Microbial Sediments

1997; Thompson et al. 1997). In this review I will deal with the possible microbial mechanisms for the origin of whiting sediment, as either freshwater marl or marine carbonate mud. The important question addressed here is, by what mechanisms are the carbonate minerals precipitated from the open water column of lakes and seas? Two whiting case studies are presented, a freshwater case study from Fayetteville Green Lake and a marine case study from the Great Bahama Bank.

2 Freshwater Case Study: The Annual Whiting Events in Fayetteville Green Lake

Fayetteville Green Lake (FGL) is located in upstate New York, near the city of Syracuse. We have studied this lake in great detail over the last decade (Thompson and Ferris 1990; Thompson et al. 1990, 1997). FGL makes an excellent case study owing to its strong oligotrophic nature and simple ecological system.

Due to low nutrient levels, FGL has a simple phytoplankton community dominated by small (~0.5 μm in diameter) cyanobacterial picoplankton of the genus *Synechococcus*. *Synechococcus* dominates due to a combination of diverse chemical and physical factors. First, it appears that environmental conditions in the lake favor picocyanobacteria over microalgae. Furthermore, *Synechococcus*' size and shape greatly enhance its ability to take up dilute nutrients and to utilize low light levels relative to larger microalgae (Stockner and Antia 1986).

2.1 History of Calcification Studies

Fayetteville Green Lake has a history of research dating back to the early 20th century (Davis, in Walcott 1914; Bradley 1963 1968; Brunskill 1969; Thompson and Ferris 1990; Thompson et al. 1990, 1997). Davis and Bradley recognized the presence, and possible involvement, of minute microbial cells in carbonate precipitation in FGL. For example, Davis (in Walcott 1914) refers to the formation of the microbialites in FGL:

"It is probable, from the color of the broken fragments, that the algae are responsible for the formation of the whole of these deposits, or for most of them. Further work on the identity of the blue-green alga [cyanobacteria] most abundant in the spongy calcareous covering ... shows that the organism is a cellular blue-green alga [cyanobacteria], and not a filamentous one like *Zonotrichia*. This cellular type develops irregular aggregations of rounded or oval very small cells, which apparently seldom arrange themselves in strings. The genus or species [i.e., *Synechococcus* ; Fig. 2] has not been identified."

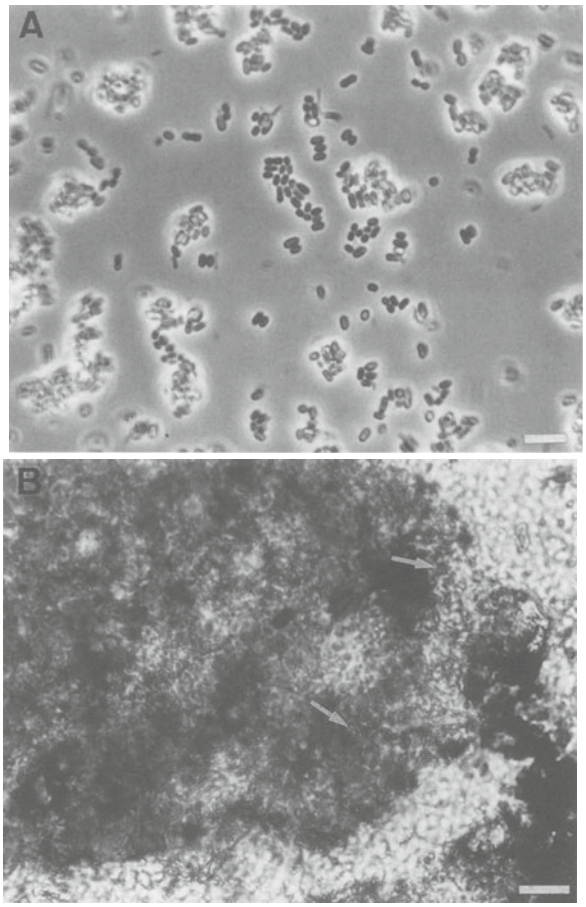

Fig. 2.A Phase contrast photomicrograph of *Synechococcus* sp. isolated from Fayetteville Green Lake (FGL). **B** Petrographic thin-section photomicrograph of a calcite grain from FGL showing the inclusion of numerous small bacterial cells within the overall micritic grain (*arrows*). These are the same small bacterial cells recognized by Bradley (1963). Note similar size to the *Synechococcus* cells in **A**; *bar scales* = 5 μm. (Thompson and Ferris 1990)

Bradley (1963) stated that "an estimated 20 percent of these calcite crystals [marl crystals from the bottom of FGL] are gray and contain about 2.2 percent of organic matter in the form of enormous numbers of minute black, spherical bacterial cells... The bacterial cells range in diameter from a little less than 0.4 to nearly 0.7 μm." Bradley (1963) also reported "The process by which the Green Lake bacteria are entombed still goes on, though we do not yet know exactly how they operate."

Unfortunately, Bradley retracted this work in 1968, due to a misunderstanding that led him to believe that his observations were the result of an artifact. Subsequently, Brunskill (1969) concluded that the whiting in FGL was the result of inorganic chemical reactions. He reported that "temperature is the direct causal factor in the initiation of calcite precipitation in Green Lake, with photosynthesis playing only a secondary, and probably a minor role."

Since then we have revived Bradley's earlier (1963) ideas by isolating and experimentally showing that *Synechococcus* is the cyanobacterium being entombed in the FGL sediments (Fig. 2). In addition, Schultze-Lam et al. (1992) illustrated the important participation of a protein surface array (S-layer) in fine-grain mineral formation by *Synechococcus*. The presence of an S-layer has helped to illustrate the process by which the *Synechococcus* cells are entombed and how they might survive the entombing process.

2.2 Annual Whiting Event

Whitings in freshwater lakes usually occur as annual events in late spring or early summer. This is true not only for FGL, but also for the Great Lakes (Strong and Eadie 1978; Vanderploeg et al. 1987) and certain lakes in Switzerland (Pulvermuller et al. 1995). In FGL the whiting begins in mid-to-late May and is easily noted by a dramatic change in water clarity and color. The normal deep blue-green water turns greenish-white and Secchi disk measurements drop by approximately 8–10 m over a short period (Thompson et al. 1997).

Transmission electron micrographs (TEM) have shown that the whiting material consists of many *Synechococcus* cells with associated calcite crystals (Fig. 3). The onset of the whiting event is correlated, temporally, with the exponential bloom of *Synechococcus* (Fig. 4). Direct epifluorescence microscopy cell counts showed a range of *Synechococcus* cell concentrations, from 6.5×10^3 cells/ml$^-$ in May to 1.5×10^5 cells/ml in September (Thompson et al. 1997). Peak concentrations of suspended calcite (~3.5–4.0 mg l^{-1}) were found between 4 and 8 m water depth from late May through June (Fig. 4; 8 m data not shown). This depth interval contains the highest *Synechococcus* cell abundance, and

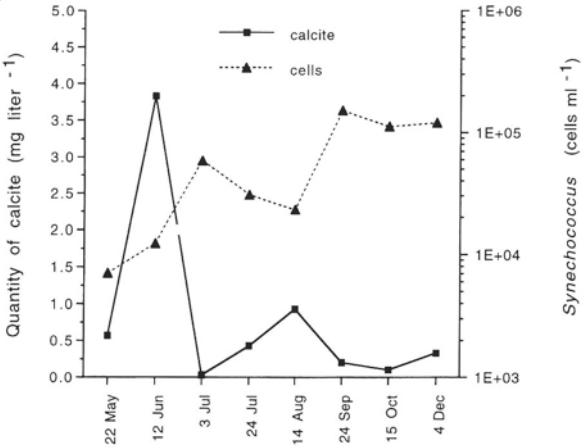

Fig. 4. Graph of calcite and *Synechococcus* cell abundance for 4 m water depth in Fayetteville Green Lake (FGL) from May to December 1989. Note that during the exponential *Synechococcus* bloom, ~4 mg/l of suspended calcite was present. (Thompson et al. 1997)

is located just below the seasonal thermocline (Thompson et al. 1997).

The milky color remains throughout the summer, although the quantity of suspended calcite varies due to complex biological and chemical factors (Thompson et al. 1997). At the onset of the fall turnover, the lake returns to its previous deep blue-green color that then lasts until the process is repeated the following May. TEM observations have shown that small quantities of gypsum ($CaSO_4.nH_2O$) precipitate on *Synechococcus* during the periods of cooler water temperatures (Fig. 5). It appears that the water temperature is too cold, and the cells too metabolically inactive, for much calcite precipitation to occur during the fall, winter, and early spring.

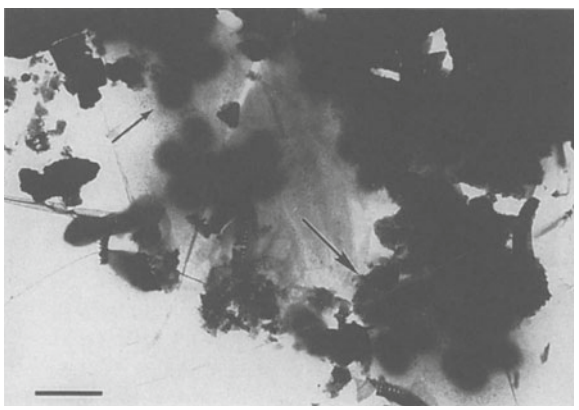

Fig. 3. Transmission electron micrograph (unstained wholemount) of whiting material (*Synechococcus* cells and associated calcite crystal; *arrows*) collected from 12 m depth in Fayetteville Green Lake (FGL). Note the varying degree of mineralization on *Synechococcus* cells; *bar scale* = 1 μm

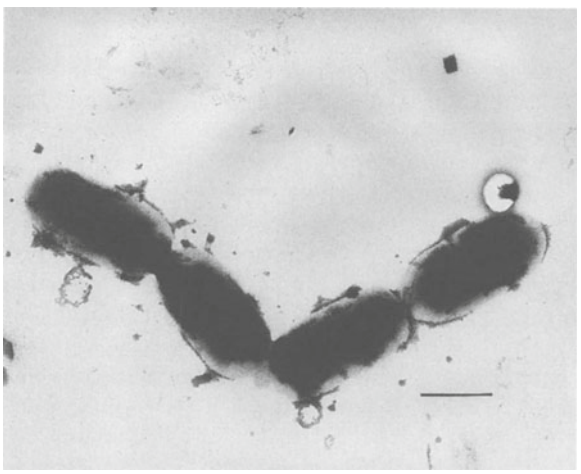

Fig. 5. Unstained transmission electron micrograph wholemount of four *Synechococcus* cells collected from the Fayetteville Green Lake (FGL) water column on May 1, 1989. Note gypsum forming on their surface array (S-layer) and that some crystals are being shed from the surface

Stable carbon isotope data provide additional evidence that the whitings are strongly biologically influenced. Suspended whiting material and bottom marl are highly enriched in ^{13}C compared to the dissolved inorganic carbon (DIC) in the lake (Thompson et al. 1997). Their ^{13}C values ranged between −1.5 and −2.5‰, while the ^{13}C values of the DIC ranged seasonally from −9.5‰ in January-March to −6.5‰ in July and August. This 3‰ seasonal variation in the $^{13}C_{DIC}$ values is mainly the result of ^{12}C fractionation by *Synechococcus* during organic biosynthesis. This biological fractionation is also shown by the −28‰ ^{13}C value for the organic fraction of the whiting material filtered from the lake. Therefore, a total ^{13}C enrichment of ~4‰ (−2.5 vs −6.5‰) occurs in the whiting calcite and marl sediment. This is because most of the calcite precipitates during the summer months when the DIC value of the water is about −6.5‰. Ecosystem simulations conducted with *Synechococcus* (at ~10^5 cells/ml) in filtered sterilized lake water showed a similar 4‰ ^{13}C enrichment, as did the natural ecosystem (Thompson et al. 1997).

tation is a by-product of *Synechococcus*' use of bicarbonate as its inorganic carbon source for photosynthesis. Our results show that in experimental cell batches, precipitation takes place only when incubated in the light, when the cells are actively photosynthesizing.

Detailed ultrastructural studies of the cell surface and of the initial events in mineral growth have revealed the presence of an S-layer (Figs. 6A and 7; Schultze-Lam et al. 1992). The peripheral location of the S-layer allows it to interact first with the soluble ions in the external milieu. This hexagonally symmetric paracrystalline surface array (or S-layer) acts as a template for carbonate mineralization on the outermost cell surface. It templates gypsum and calcite precipitation by providing discrete, regularly spaced nucleation sites for the crucial initial events in the mineral formation process (Schultze-Lam et al. 1992). Initially, calcium ions seem to bind to the S-layer, so that mineralization can occur. The abundance of Ca^{2+} and SO_4^{2-} in the lake water may make the formation of gypsum and calcite an inevitable consequence of *Synechococcus*' metabolism.

2.3 *Synechococcus* Precipitation Mechanism

Data suggest that *Synechococcus* has a unique micr
vironment (i.e., envelope of water) around each
(Fig. 6, Thompson et al. 1997). The microenviron
is chemically and physiologically different from
the surrounding bulk water and the cells' peripla
space. Precipitation initiates on the cell's surface i
unique envelope of water, due to its elevated pH
Ca^{2+} concentration (Fig. 6B). The pH is driven h
in this envelope due to a photosynthetic alkaliz
process (i.e., HCO_3^-/OH^- exchange across the
membrane) carried out by the cell. The initial precipi-

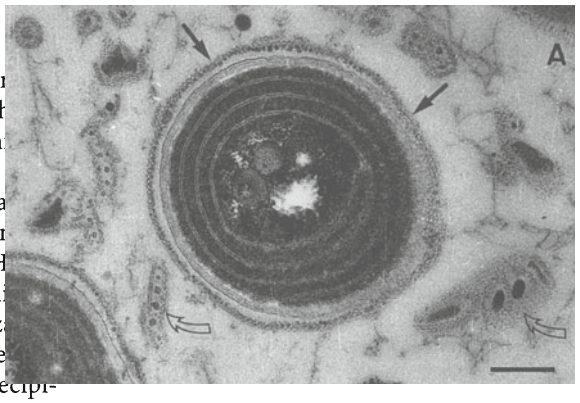

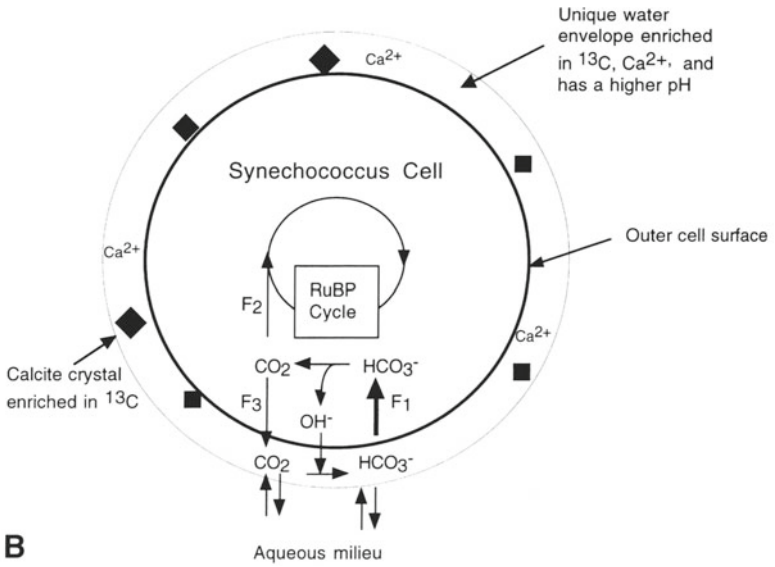

Fig. 6.A Transmission electron microg
a stained, thin-sectioned *Synechococ*
showing the surface array or S-layer (
arrows). Note also the S-layer materia
from the cell surface (*open arrows*); *b*
scale = 100 nm. **B** Schematic model of
croenvironment surrounding each *Sy*
coccus cell. Calcite precipitates in this
environment due to elevated pH and
higher [Ca^{2+}] via surface binding and
cium excretion from the cell. In addit
calcite being precipitated in this micr
ronment is enriched in ^{13}C due to the
tionation of ^{12}C by the cells. (From Tl
son et al. 1997)

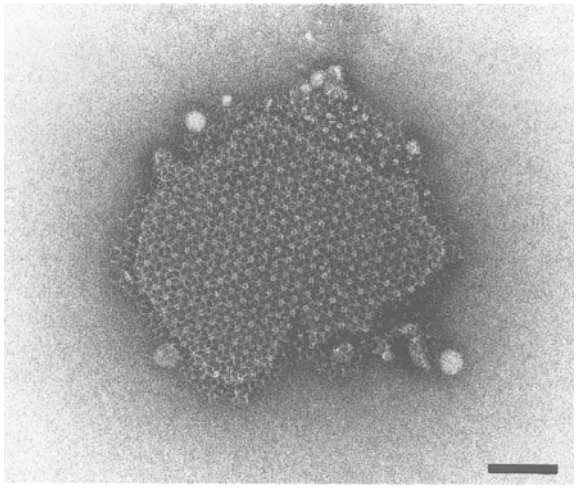

Fig. 7. Transmission electron micrograph of a negatively stained S-layer fragment showing the symmetrical structure of the hexagonal surface array; *bar scale* = 100 nm

Schultze-Lam et al. (1992) showed that the stages of S-layer mineralization are easily discernible as pore channels are filled and obscured by the growing minerals. Using computer imaging, they revealed the S-layer to have two separate pore systems (Fig. 8). Computer imaging also revealed that the initial binding events and mineral growth took place at sites that were evenly spaced (Schultze-Lam et al. 1992). Consequently, this regularly spaced mineralization pattern is due to the intrinsic symmetry of the S-layer itself.

Because the S-layer is the outermost surface layer that lies between the external milieu and the cell's gram-negative outer membrane, it may act as a protective barrier. S-layer material can be easily shed from the cell when it becomes highly mineralized. The S-layer in effect prevents the encrusting minerals from interfering with vital cell processes, such as growth and division, nutrient and waste transport, and photosynthesis (Schultze-Lam et al. 1992; Thompson et al. 1997). Therefore, it appears that the release of S-layer material is not an energetically wasteful activity but a necessary one for protection.

In summary, it is now easy to envision how whiting events can initiate and proceed in FGL. During late spring, water temperature, daylight, and photosynthesis increase and result in the *Synechococcus* bloom. As *Synechococcus* grows exponentially, it surrounds itself with an alkaline microenvironment (Fig. 6B). This microenvironment alters the mineralization process from gypsum to calcite based on the various pH and temperature conditions present at the time. Thus, each cell in the *Synechococcus* bloom (~10^5 cells/ml) acts as a small, biologically active, nucleation site for the growth and development of minerals.

3 Marine Case Study: Whitings on the Great Bahama Bank

The origin of the whitings on the Great Bahama Bank (GBB) has puzzled researchers for many generations, and still remains a paradox (Drew 1911; Kellerman and Smith 1914; Black 1933; Smith 1940; Cloud 1962; Broekker and Takahashi 1966; Morse et al. 1984; Shinn et al. 1989; Robbins and Blackwelder 1992; Boss and Neumann 1993). Marine whitings are known to occur in other locations, such as the Persian Gulf, Gulf of Carpentaria, Florida Bay, and Belize (Wells and Illing 1964; Boss and Neumann 1993; Robbins et al. 1996). A detailed review of the Bahamian whitings was conducted by Bathurst (1975). The main question, then and now, is what is the origin of most of the carbonate mud on the GBB, and elsewhere such as Florida Bay (Bathurst 1975)? The current thought is that ~25–50% of the bulk mud fraction is aragonite needles from decomposing calcareous green algae (codiaceans and dasycladaleans; Bathurst 1975; Milliman et al. 1993). The remaining 50–75% is the result of inorganic and/or bio-induced whitings (Shinn et al. 1989).

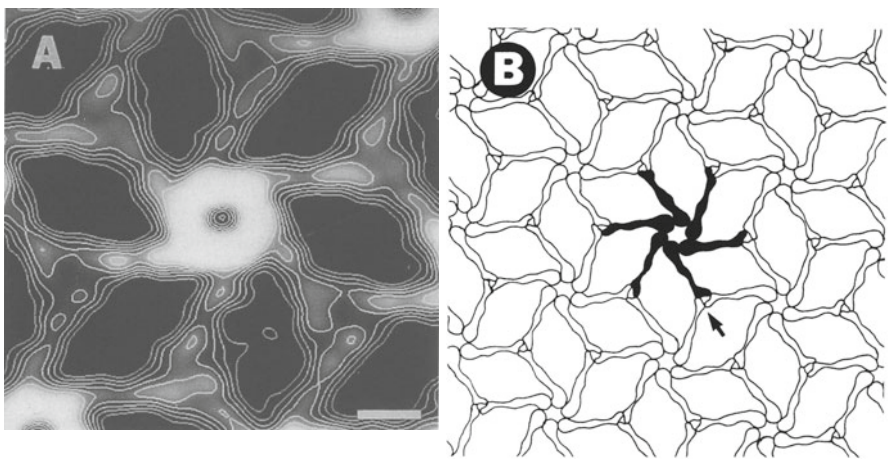

Fig. 8.A Contoured, computer processed image of an individual pinwheel from an S-layer fragment. Note the presence of the pore and subunit morphologies; *bar scale* = 5 nm.
B Two-dimensional model of the *Synechococcus* S-layer showing the general shape and arrangement of the protomer subunits that make up a hexamer, or single morphological unit, shown in *black*. This is the center of six-fold symmetry; *arrow* indicates a center of three-fold symmetry or Y linker. (Schultze-Lam et al. 1992)

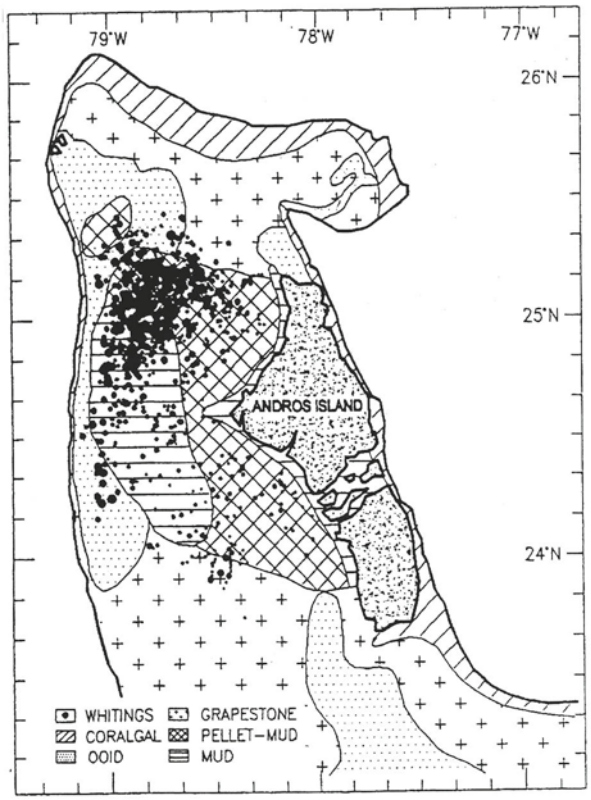

Fig. 9. General location map showing the whitings "bulls-eye" area located northwest of Andros Island in the Bahamas. Spatial distribution of whitings is shown by the *black dots* superimposed on a sediment facies map of the Great Bahama Bank. (Robbins et al. 1997)

Whitings on the GBB west of Andros Island (Fig. 9) are elongate features with both sharp and diffuse boundaries. Aerial observations show that the whitings are not randomly distributed, occurring predominantly on the north central part of the Bank. They are typically hundreds of meters wide and 1–2 km long; however their size and shape can vary extensively. Both sharp billowing and broad diffuse boundaries occur along the margins of the whitings (Fig. 1; Shinn et al. 1989). Regularly spaced, digitate features, several meters to tens of meters long, are also commonly observed.

Some whitings may be caused by resuspension of the bottom sediment by various phenomena (Boss and Neumann 1993); however, others are caused by bio-induced or inorganic precipitation of aragonite in suspension (Cloud 1962; Wells and Illing 1964; Shinn et al. 1989; Robbins and Blackwelder 1992). Therefore, the aragonite muds west of Andros Island hold a pivotal position in the debate over the origin of carbonate muds, both ancient and modern (Bathurst 1975; Morse and Mackenzie 1990).

3.1 Biological Evidence

Drew's pioneering research (1911, 1914) gathered the first evidence that argued for a bacterial origin of whitings. His preliminary experiments showed that carbonate was being precipitated by the metabolic activity of denitrifying bacteria and possibly other kinds of bacteria. He named the bacterium that he thought was predominantly responsible for the precipitation, *Bacterium calcis*. According to his conclusions in 1914:

"It can be stated with a fair degree of certainty that the very extensive chalky mud flats forming the Great Bahama Bank and those which are found in places in the neighborhood of the Florida Keys are now being precipitated by the action of the *Bacterium calcis* on the calcium salts present in solution in sea-water. From this the suggestion is obvious that the *Bacterium calcis*, or other bacteria having a similar action, may have been an important factor in the formation of various chalk strata."

Drew's work was supported by Kellerman and Smith (1914) and they reclassified his *B. calcis* as a pseudomonad, *Pseudomonas calcis* (Drew). Drew, and Kellerman and Smith, suggested three possible bacterial processes that may form calcium carbonate in seawater.

The first process produces ammonia by decomposing proteins in organic matter or by dissimilative nitrate reduction. The ammonia reacts with carbonate ions to produce ammonium carbonate. This ammonium carbonate in turn reacts with calcium sulfate in seawater to form calcium carbonate and ammonium sulfate according to the formula:

$$CaSO_4 + (NH_4)_2CO_3 = CaCO_3 + (NH_4)_2SO_4$$

The carbon dioxide necessary for this reaction may be produced by the bacterial catabolism of organic matter, or by bacterial fermentation (Drew 1914; Kellerman and Smith 1914).

The second process suggests that calcium carbonate may be precipitated from seawater laden with calcium bicarbonate by bacterial production of ammonia according to the formula:

$$Ca(HCO_3)_2 + 2NH_4OH = CaCO_3 + (NH_4)_2CO_3 + 2H_2O$$

Thirdly, they suggested that calcium carbonate may be precipitated through bacterial decomposition of calcium salts of organic acids such as calcium succinate, calcium acetate, or calcium malate. In this case, calcium is provided for the precipitation process by its liberation from the decomposing organic calcium salts.

In spite of this solid early work on bacterial precipitation, Lipman (1922) challenged Drew's findings. He found that added calcium salts usually had to be supplied for the process to be completed. Lipman also provided some chemical evidence and suggested that the

quantity of nitrifying bacteria was too low to cause the precipitation. Lipman (1924) found that all the bacteria he isolated and studied seemed to have the ability to precipitate calcium carbonate in various media, however they all failed when tested in seawater only. He noted that it "seems irresistible, therefore, that if lime precipitation from sea-water is accomplished by bacteria under natural conditions, proof therefore is wanting."

Subsequently, Bavendamm (1932) showed that aragonite crystals were being produced by the high rate of bacterial metabolism in the mangrove swamps on Andros Island. He demonstrated the presence of a rich bacterial flora and that some species can alter the chemistry of the seawater to cause calcium carbonate precipitation. Subsequent bacterial investigations that helped to clarify and support Drew's early works include Greenfield (1963) and McCallum and Guhathakurta (1970).

Besides the role of heterotrophic bacteria mentioned above, subsequent investigators (Cloud 1962; Wells and Illing 1964; Robbins and Blackwelder 1992; Robbins et al. 1996) have implicated a possible role for autotrophic phytoplankton in the formation of the marine whitings. Wells and Illing (1964) found a diatom bloom associated with a whiting event in the Persian Gulf. They suggested that a sharp population increase in phytoplankton could trigger whitings through the removal of carbon dioxide. Lastly, they noted that it is not known whether the diatoms were the only agents involved, as other smaller, less easily recognized, organisms were not examined. Robbins and Blackwelder (1992) proposed that the Bahamian whitings are partially the result of biological precipitation by picoplankton (similar to Thompson and Ferris 1990). More recently, Robbins et al. (1996) reported that their picoplankton cell counts were significantly higher inside whitings than in the surrounding clear waters. I can confirm similar unpublished picoplankton cell counts from a cruise, west of Andros, in August 1992. Enrichment cultures from whiting material collected on that cruise showed a very diverse and complex microbial community (Fig. 10; unpublished data). Many bacteria from the enrichment culture possess elaborate S-layers (Fig. 11). They are very similar to those found on *Synechococcus* from FGL and may also template carbonate mineralization.

3.2 Chemical Evidence

Black (1933) was first to conduct a chemical study of whitings on the GBB. His water chemistry transects showed that the mid-southern region of the Bank was hypersaline, up to 38.5‰, due to evaporation. He postulated that precipitation was being caused by the increasing salt concentration and the concurrent loss of carbon dioxide due to increasing water temperatures. He also noted that the precipitation was not continual, but quite varied temporally and spatially. Black suggested it varied with the availability of suitable nuclei.

Smith (1940) also extensively investigated the water chemistry and circulation where most of the whitings occur on the GBB (Fig. 9). He found that a salinity maximum occurred near the shore of Andros Island and noted that isoclines appeared to push outwards to form a high salinity wedge toward the northwest. The apex of this salinity wedge lies quite close to latitude 25°N. Smith noted that water coming onto the Bank from the Florida Channel could take several weeks to reach Andros Island. The winds shifted so regularly that water bodies, once on the Bank, could drift back and forth for

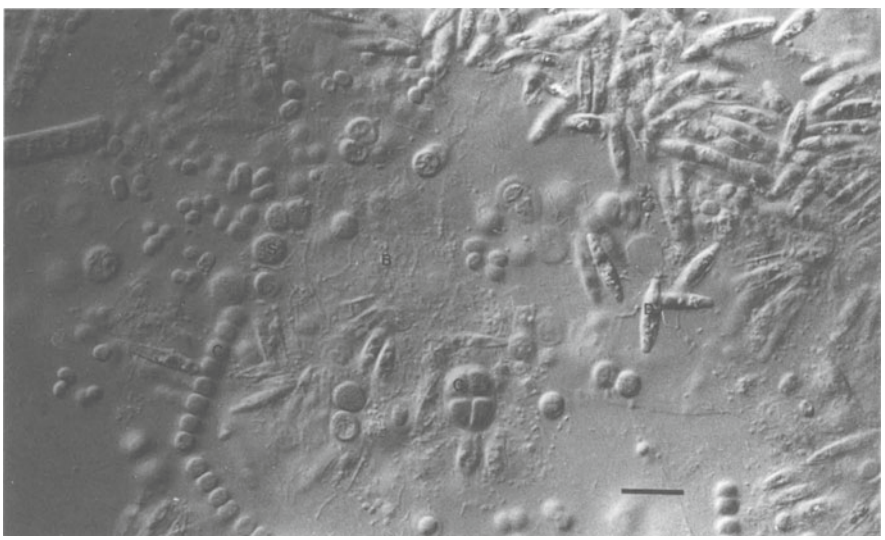

Fig. 10. Differential interference contrast (DIC) photomicrograph of an enrichment culture started from a water sample collected from a Bahamian whiting in August 1992. Note the complex microbial diversity in the sample; *bar scale* = 10 μm. The sample predominantly contains diatoms (*D*), cyanobacteria (*G, Gloeocapsa; C, Anabaena; S, Synechocystis*), and bacteria (*B*)

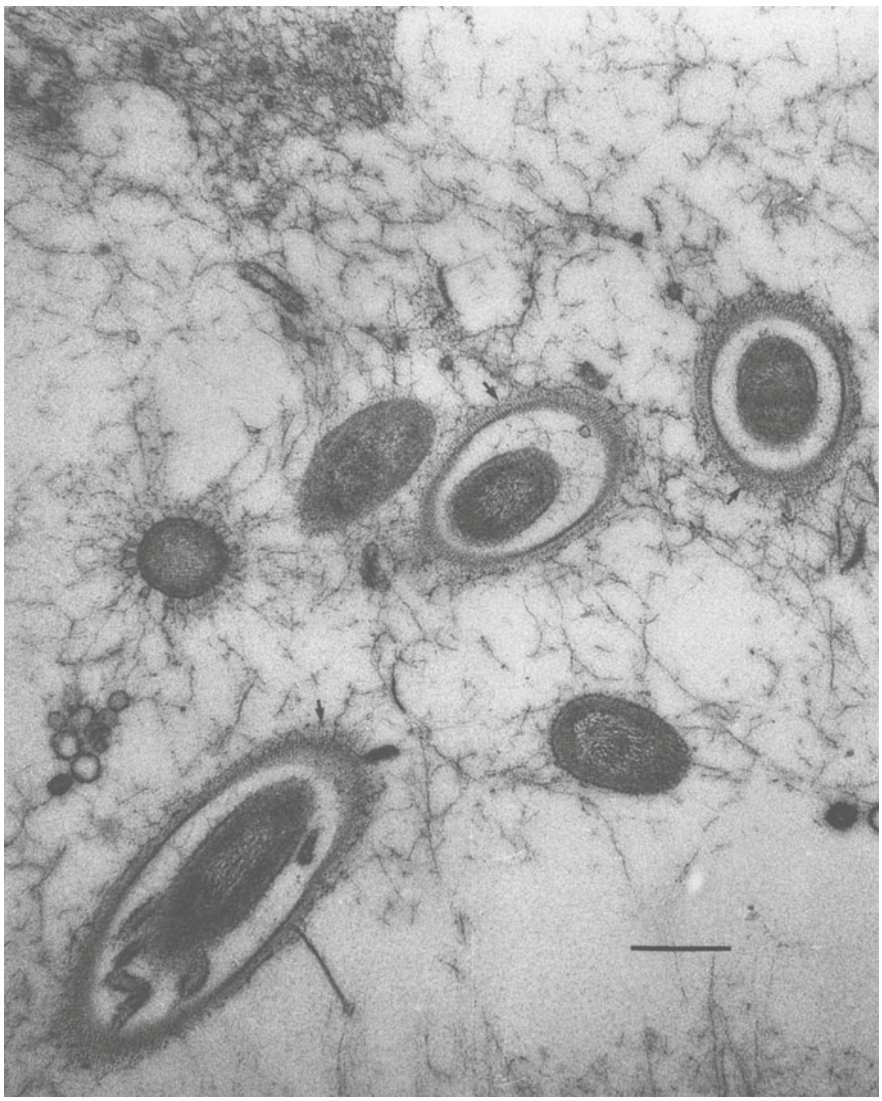

Fig. 11. Transmission electron micrograph of a stained thin-section of the enrichment culture from a Bahamian whiting (Fig. 10). Note the complex bacterial S-layers (*arrows*) on the surface of the bacteria; *bar scale* = 500 nm. Some bacteria seem to possess double S-layers, for added protection. These S-layers may template carbonate mineralization

months, thereby forming their high salinity through evaporation. He also found that there is a zone of very rapid salinity change close to the Bank edge during September and April. During these months, the main current was towards the west or northwest, carrying the high salinity waters out toward the open ocean. In December he observed drift in the opposite easterly direction, which carried low salinity ocean water toward Andros Island. Based on his observations he developed a physico-chemical mixing model for the region.

Smith (1940) found strong seasonal variation in the precipitation of calcium carbonate. His observations showed that the amount of precipitation during the summer was probably double that of the winter. He noted that the physical features of the area, together with the water chemistry and semi-stagnant water conditions, are all conducive to the deposition of calcium carbonate from the supersaturated ocean water that flows onto the Bank. Lastly, he noted that it is quite possible that some bacterial precipitation may occur in areas rich in organic matter, but believed this to be very small compared with that produced by physico-chemical precipitation.

Cloud (1962) built upon Smith's physico-chemical data set, as did Traganza (1967). Cloud's $^{18}O/^{16}O$ ratios suggested that carbonate precipitation occurs mainly during the warmer summer months. His field data and experimental results showed that the mineralogy of the precipitated calcium carbonate depends mainly on the degree of supersaturation, which depends on kinetic or biologic factors. Both Cloud and Traganza reopened the biologic question by concluding that the shallow hypersaline Bank waters yield aragonite sediments, implying precipitation during the warmer periods, when

the synergisms of evaporation, increased salinity, maximal temperature, and photosynthetic removal of CO_2 result in high supersaturation values.

Broecker and Takahashi (1966) documented the long residence time (~250 days) of water bodies on the Bank. They also noted that the rate of precipitation is proportional to the degree of supersaturation. However, they were unable to balance the CO_2 budget for the Bank. They found that about 50% more CO_2 was being lost from the Bank water than could be accounted for by their calculated precipitation rate. Consequently, they suggested that large quantities of CO_2 were being removed physically from the area as suspended organic matter. Broecker and Takahashi concluded that most of the whiting material had to be resuspended bottom sediment, based on radiocarbon dates and a lack of any change in the water chemistry.

Morse et al. (1984) found mixing of different water masses near the whitings. Their general results are in good agreement with Broecker and Takahashi (1966). Both studies measured pH, total alkalinity, and total carbon dioxide from inside whitings and in adjacent clear water and found no statistical difference between the two water masses. As a result, their findings are in disagreement with those favoring inorganic precipitation from a concentrated area. Additionally, Morse and He (1993) concluded from their nucleation studies that the GBB waters are not supersaturated enough for pseudo-homogeneous carbonate nucleation to occur on its own.

Shinn et al. (1989) analyzed suspended whiting material and bottom sediment using radiocarbon and carbon and oxygen isotope analyses. Based on their isotope data, whiting material and bottom sediments could not be statistically distinguished so they suggested a sediment resuspension mechanism. Sediment resuspension, however, does not answer the question of how the bottom sediment was originally derived. A possible explanation, if the sediments are precipitated from seawater, might be that the whitings are not precipitated in isotopic equilibrium with the surrounding seawater. Isotopic disequilibrium can result from bacterial fractionation processes, as shown in the FGL whiting by Thompson et al. (1997).

In summary, the chemical evidence to date suggests that these whitings cannot be some purely inorganic precipitation process. They must be the result of a sediment resuspension process or an unexplained biochemical process. Morse et al. (1984) and Morse and Mackenzie (1990) favor the idea that suspended carbonate particles act as nuclei for inorganic precipitation. Morse and Mackenzie (1990) suggest that a repetitive resuspension process could produce the whitings and a large portion of the sediment forming on the Bank.

3.3 Physical Evidence

As noted by Shinn et al. (1989) "chemists favor a sedimentologic origin [i.e., a sediment suspension mechanism] and sedimentologists a chemical [or biological] origin" for whitings. Sediment resuspension appears to play some kind of role in the whiting phenomenon. However, many studies (Cloud 1962; Wells and Illing 1964; Shinn et al. 1989) have highlighted the difficulties in accepting the idea that the whitings are produced by resuspended bottom sediments. These authors have noted that the whitings have been observed over coarse-grained bottom sediments and even over hardgrounds. They have also noted the paucity of bottom feeding fish to stir up the bottom. Also, in some cases clear water has been observed beneath whitings, which seems to exclude a resuspension mechanism.

Boss and Neumann (1993) proposed an alternative resuspension mechanism to the idea of fish stirring up the bottom. They hypothesized "that whitings are the observable manifestation of the bursting cycle of turbulent production at flow boundaries." Their postulation includes the idea that the visible, roiling nature of active whitings (Cloud 1962; Shinn et al. 1989) is the expression of the turbulent processes on the Bank top during tidal cycles. A hypothetical bursting cycle begins as organized boundary-layers flowing in alternating low and high velocity "streaks" and can be observed in transverse velocity profiles (Boss and Neumann 1993). Unfortunately, no such velocity profiles have been collected from the GBB. However, there is some visual evidence for this from Bahamian whitings, in terms of the frequent occurrence of subparallel, digitate structures with zones of varying turbidity (Shinn et al. 1989). However, alternatively, these features could be the result of Langmuir circulation cells on the Bank. Boss and Neumann (1993) concluded that these physical features of the whitings are similar to expected turbulent flow features and that physical processes have largely been ignored to date.

3.4 Remote Sensing of Whitings

So far only a few preliminary investigations (Tao 1994; McCarthy 1996; Robbins et al. 1997) have turned to observations from space to examine the temporal and spatial distributions of whitings on the GBB. First, Tao (1994) and Robbins et al. (1997) studied the whitings using 69 photographs taken by various space shuttle missions. They noted that the whitings occur year-round with peak occurrences in April and October. It should be noted that these peak whiting occurrences are temporally similar to Smith's (1940) observed rapid

salinity changes near the Bank edge and that they are centered on the 25° N latitude, the whiting "bulls-eye" area (Fig. 9).

Secondly, McCarthy (1996) used satellite images from the Advanced Very High Resolution Radiometer (AVHRR) on the NOAA-12 and -14 satellites. These images have a resolution of 1.1 km^2 at nadar. The high reflectance of whitings is easily distinguished from normal clear Bank water. However, many whitings are less than 1 km^2 in size. This results in the AVHRR data excluding many small (<1 km^2) whitings.

Given these limitations, McCarthy (1996) was still able to confirm Tao's (1994) seasonal pattern. Her data show that the spring (March and April) and fall (September) months have the most whitings. The fewest whitings occurred in the summer months, August, July, and June. McCarthy noted that this seasonal abundance in whitings may lend insight into their cause. It suggests that they are either chemical or biological due to seasonal changes. If they were strictly physical events related to tidal turbulence over the Bank, we would not expect a strong seasonal change in their frequency. We might, however, expect variation within monthly tidal cycles. Instead, the relative high abundance of whiting in the spring and fall, and low abundance in the summer, supports the hypothesis that the whitings are biologically precipitated by phytoplankton blooms (McCarthy 1996). McCarthy noted a similarity between the estimated phytoplankton cycle and the whiting cycle for the Bank (Fig. 12). However, a study of the actual phytoplankton cycles in the Bahamas is necessary to validate this association. Finally, future remote sensing studies (as better satellites become available) of phytoplankton distributions and possible physical mixing processes on or near the Bank will help resolve the various scales and complexities of whitings.

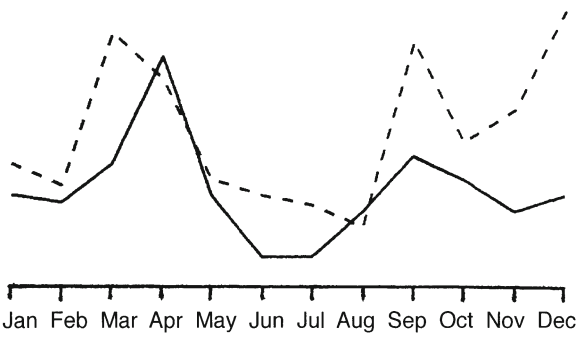

Fig. 12. Estimated phytoplankton cycle for the Great Bahama Bank, shown by the *solid line*. The *dotted line* represents the average number of whitings per month calculated from AVHRR satellite images. (McCarthy 1996)

3.5 Biophysicochemical Coupling

Clearly, as illustrated above, the marine whitings are much more complicated than the whitings in FGL. All the conflicting evidence to date for the GBB whitings suggests that intricate biophysicochemical coupling is involved in their formation. There is likely biophysical coupling between the various planktic organisms and the physical turbulent flow described by Boss and Neumann (1993), which give rise to the high cell counts in the whitings. Biophysical coupling would also result in strong bacterioplankton blooms of both autotrophic and heterotrophic bacteria. Both nano- and picoplankton have been reported to respond by increased production when turbulence-induced mixing or sediment resuspension occurs (Wainright 1987, Ducklow and Carlson 1992). Furthermore, heterotrophic microorganisms, collectively termed "the microbial loop," can become involved within minutes to hours and recycle the organic matter locally (Azam et al. 1983; Daly and Smith 1993). The resulting bacterioplankton blooms would, in turn, catalyze the biochemical coupling needed to bring about the whitings and account for the precipitation (possibly similar to the biochemical coupling between *Synechococcus* and water chemistry in FGL). As stated by Boss and Neumann (1993), a complete understanding of these marine whitings will require an integrated interdisciplinary effort dealing with the biological, physical, chemical, and sedimentological coupling that occurs on the Great Bahama Bank.

4 Conclusions and Future Research

In the case of FGL, evidence now appears clearly to point to *Synechococcus* as responsible for the occurrence of whitings. However, the question is still mainly unresolved in the Bahamian whitings. Most likely, they involve some form of complex biophysicochemical coupling between various forms of autotrophic and heterotrophic bacterioplankton. Biophysicochemical coupling would help explain the lack of a chemical difference between the whitings and clear water masses. Similar to *Synechococcus*, the apparent chemical shifts are on the microscale, which we presently cannot measure (Thompson et al. 1997). In addition, the bacterial pathways suggested by Drew (1914) would not require any measurable chemical change, because the CO_2 and Ca^{2+} are supplied by the breakdown of organic matter. Lastly, the enrichment of ^{13}C in the marine whiting carbonate and bottom sediment (Shinn et al. 1989) suggests a bacterial fractionation process, similar to that which occurs in the FGL whitings. In conclusion, I return to Drew (1914):

"As it now stands, the [current marine whiting] investigation[s] can at most be considered to offer a mere indication of the part played by bacterial growth in the metabolism of the sea. To obtain a real insight into the question, it would be necessary to make more extensive bacterial and chemical observations in tropical, temperate, and arctic waters, to study the bacteriology of other areas where calcium carbonate is being precipitated from the sea, and to make further investigations in the laboratory into the chemistry of the reactions that can be brought about by various species of marine bacteria."

References

Azam F, Fenchel T, Field JG, Gray JS, Meyer-Reil LA, Thingstad F (1983) The ecological role of water column microbes in the sea. Mar Ecol Prog Ser 10:257–263

Bathurst RGC (1975) Carbonate sediments and their diagenesis. Developments in sedimentology 12, Elsevier, Amsterdam

Black, M (1933) The precipitation of calcium carbonate on the Great Bahama Bank. Geol Mag 70:455–466

Boss SK, Neumann AC(1993) Physical versus chemical processes of "whiting" formation in the Bahamas. Carbonates Evaporites 8:135–148

Bradley WH (1963) Unmineralized fossil bacteria: Science 141: 919–921

Bradley WH (1968) Unmineralized fossil bacteria: a retraction. Science 160:437

Broecker WS, Takahashi T (1966) Calcium carbonate precipitation on the Bahama Banks. J Geophys Res 71:1575–1602

Brunskill GJ (1969) Fayetteville Green Lake, New York. II. Precipitation and sedimentation of calcite in a meromictic lake with laminated sediments. Limnol Oceanogr 14:830–847

Cloud PE Jr (1962) Environment of calcium carbonate deposition west of Andros Island, Bahamas. US Geol Surv Prof Pap 350

Daly KL, Smith WO Jr (1993) Physical-biological interactions influencing marine plankton production. Annu Rev Ecol Syst 24: 555–585

Davis CA (1914) In: Walcott CD (ed) Pre-Cambrian Algonkian algal flora. Smithsonian Misc Coll 64:77–157

Drew GH (1911) The action of some denitrifying bacteria in tropical and temperate seas and the bacterial precipitation of calcium carbonate in the sea. United Kingdom Mar Biol Assoc J 9:142–155

Drew GH (1914) On the precipitation of calcium carbonate in the sea by marine bacteria, and on the action of denitrifying bacteria in tropical and temperate seas. Carnegie Inst Wash Publ 182:9–45

Ducklow HW, Carlson CA (1992) Oceanic bacterial production. Adv Microb Ecol 12:113–181

Greenfield LJ (1963) Metabolism and concentration of calcium and magnesium and precipitation of calcium carbonate by a marine bacterium. NY Acad Sci Ann 109:23–45

Kellerman KF, Smith NR (1914) Bacterial precipitation of calcium carbonate. J Wash Acad Sci 4:400

Lipman CB (1922) Further studies on the Drew hypothesis of $CaCO_3$ precipitation in seawater, Year Book No 21, Carnegie Inst Washington

Lipman CB (1924) A critical and experimental study of Drew's bacterial hypothesis on calcium carbonate precipitation in the sea. Carnegie Inst Washington, Publ No 340, Pap from Tortugas Lab

McCallum MF, Guhathakurta K (1970) The precipitation of calcium carbonate from seawater by bacteria isolated from Bahama Bank sediments. J Appl Bact 33:649–655

McCarthy MC (1996) An evaluation of remote sensing data for the detection of marine whitings in the Bahamas. Senior Thesis. Ekkerd College, St Petersburg, FL

Milliman JD, Freile D, Steinen RP, Wilber RJ (1993) Great Bahama Bank aragonitic muds: mostly inorganically precipitated, mostly exported. J Sed Petrol 63:589–595

Morse JW, He S (1993) Influences of T, S and P_{CO2} on the pseudo-homogenous precipitation of $CaCO_3$ from seawater: implications for whiting formation. Mar Chem 41:291–297

Morse JW, Mackenzie FT (1990) Geochemistry of sedimentary carbonates. Elsevier, Amsterdam

Morse JW, Millero FJ, Thurmond V, Brown E, Ostlund HG (1984) The carbonate chemistry of Grand Bahama Bank waters: after 18 years another look. J Geophys Res 89:3604–3614

Pulvermuller AG, Kleiner J, Mauser W (1995) Calcite patchiness in Lake Constance as viewed by LANDSAT-TM. Aquat Sci 57: 338–349

Robbins LL, Blackwelder PL (1992) Biochemical and ultrastructural evidence for the origin of whitings: a biologically induced calcium carbonate precipitation mechanism. Geol 20:464–468

Robbins LL, Yates KK, Shinn EA, Blackwelder P (1996) Whitings on the Great Bahama Bank. Bahamas J Sci 4:2–7

Robbins LL, Tao Y, Evans CA (1997) Temporal and spatial distribution of whitings on Great Bahama Bank and a new lime mud budget. Geol 25:947–950

Schultze-Lam S, Harauz G, Beveridge TJ (1992) Participation of a cyanobacterial S-layer in fine-grain mineral formation. J Bacteriol 174:7971–7981

Shinn EA, Steinen RP, Lidz BH, Swart PK (1989) Perspectives: whitings, a sedimentologic dilemma. J Sed Petrol 59:147–161

Smith CL (1940) The Great Bahama Bank. I. General hydrographical and chemical features. II. Calcium carbonate precipitation. J Mar Resour, Sears Fdn, Mar Res 3:147–189

Stockner JG, Antia NJ (1986) Algal picoplankton from marine and freshwater ecosystems: a multidisciplinary perspective. Can J Fish Aquat Sci 43:2472–2503

Strong AE, Eadie BJ (1978) Satellite observations of calcium carbonate precipitation in the Great lakes. Limnol Oceanogr 23: 877–887

Tao Y (1994) Whitings on the Great Bahama Bank: distribution in space and time using space shuttle photographs. Masters Thesis, University of South Florida, Tampa, FL

Thompson JB, Ferris FG (1990) Cyanobacterial precipitation of gypsum, calcite, magnesite from natural alkaline lake water. Geol 18:995–998

Thompson JB, Ferris FG, Smith DA (1990) Geomicrobiology and sedimentology of the mixolimnion and chemocline in Fayetteville Green Lake, New York. Palaios 5:52–75

Thompson JB, Schultze-Lam S, Beveridge TJ, Des Marais DJ (1997) Whiting events: Biogenic origin due to the photosynthetic activity of cyanobacterial picoplankton. Limnol Oceanogr 42:133–141

Traganza ED (1967) Dynamics of the carbon dioxide system on the Great Bahama Bank. Bull Mar Sci 17:348–366

Vanderploeg HA, Eadie BJ, Liebig JR, Tarapchak SJ (1987) Contribution of calcite to the particle-size spectrum of Lake Michigan seston and its interactions with the plankton. Can J Fish Aquat Sci 44:1898–1914

Wainright SC (1987) Stimulation of heterotrophic microplankton production by resuspended marine sediments. Science 238:1710–1712

Wells AJ, Illing LV (1964) Present-day precipitation of calcium carbonate in the Persian Gulf. In: van Straaten, LM (ed.) Deltaic and shallow marine deposits. Developments in sedimentology 1. Elsevier, Amsterdam, pp 429–435

Cold Seep Carbonates in the Tertiary of Northwest Italy: Evidence of Bacterial Degradation of Methane

P. A. Clari, L. Martire

Dipartimento di Scienze della Terra, Università degli Studi di Torino, I-10123 Torino, Italy

Abstract. Microbial degradation of methane seeping to the sea floor can result in the precipitation of carbonates, characterized by strongly negative ^{13}C values. Masses of carbonate-rich sediments that crop out within the siliciclastic Oligo-Miocene succession of Monferrato, northwest Italy, are interpreted as ancient records of such a process. Two types of carbonate rock are recognized. The first is a fine-grained, marly limestone characterized by rich assemblages of chemosymbiotic lucinid clams. The second type is barren of fossils and consists of completely lithified mudstones and sandstones. These rocks are carbonate-rich only because of localized, early precipitation of cements in the pores of siliciclastic sediments. Other carbonates, both internal sediments and cements, fill cavities due to burrowing, dissolution of shells and fractures. Direct evidence of bacterial activity is provided by laminated sediment linings of cavities, peloidal textures, and dolomite spheroids with dumbbell-shaped hollow cores.

1 Introduction

In the last 10 years an increasing number of carbonates, precipitated around cold seeps of methane-rich fluids at the sea floor, has been recognized in the geological record. These unusual rocks, for which the term *chemoherms* has been introduced (Aharon 1994), originated in various geodynamic settings during a long span of time, ranging at least from Devonian to Recent, and display a wide range of textures and fossil content (e.g. Goedert and Squires 1990; Beauchamp and Savard 1992; von Bitter et al. 1992; Gaillard et al. 1992; Campbell and Bottjer 1995). Nevertheless, all reported examples have some particular, distinctive features in common which are the "trademarks" of their anomalous origin:

- The carbonate-rich rocks crop out as discrete masses of limited (up to some tens of meters) extent, embedded in siliciclastic carbonate-poor formations.
- The carbonate masses enclose abundant fossil remains of distinctive, chemotrophic biotic assemblages which are absent in the surrounding rocks. These assemblages are dominated by tube worms and large vesicomid or lucinid clams.
- The stable isotope composition of the carbonate minerals is characterized by strong depletion of ^{13}C. Values of $\delta^{13}C$ range from -25 to -40‰ PDB, but can be even lower. This extreme ^{13}C depletion is interpreted to be a result of the incorporation into the carbonates of isotopically light CO_2, deriving from bacterial degradation of methane, whose carbon isotopic composition is the lightest in nature ($\delta^{13}C$ from -35 to -50‰ PDB for thermogenic methane, and less than -60‰ PDB for biogenic methane; Claypool and Kaplan 1974). For details of chemical reactions and products linked to bacterial degradation of methane see Aharon (this Vol.).

The sedimentary and biotic characteristics of fossil chemoherms may change considerably from site to site, and even between different parts of a single chemoherm. Such great variability, as indicated by increasing evidence obtained from the study of present-day analogues, is a result of the combination of many factors such as: (1) grain size, mineral composition and porosity of the surrounding siliciclastic sediment, (2) composition of the seeping fluids (H_2S, CH_4, heavier hydrocarbons) and the rate of seepage, both of which, in turn, regulate (3) the type and rate of macro- and microbiological activity (e.g. Roberts and Aharon 1994; Sassen et al. 1994).

Chemoherms of Miocene age cropping out in Monferrato (northwestern Italy; Fig. 1a) represent one of the first described examples of ancient cold seep carbonates (Clari et al. 1988, 1994) and can be taken as a model of one of the most widespread types of occurrence of cold seep carbonates in the geologic record. More than thirty outcrops of coeval and quite similar "anomalous" carbonates have, in fact, been reported in the Northern Apennines and Sicily (Ricci Lucchi and Vai 1994; Terzi et al. 1994).

2 Geological Setting of Tertiary Chemoherms

The hilly region of Monferrato represents the western termination of the Apenninic chain and consists of a strongly deformed Oligo-Miocene sedimentary succession resting unconformably on deformed units of Mesozoic age (Piana and Polino 1995; Clari et al. 1995). Sediments in the western part of Monferrato, where the anomalous carbonate facies are found, consist mostly

R. E. Riding and S. M. Awramik (Eds.)
Microbial Sediments

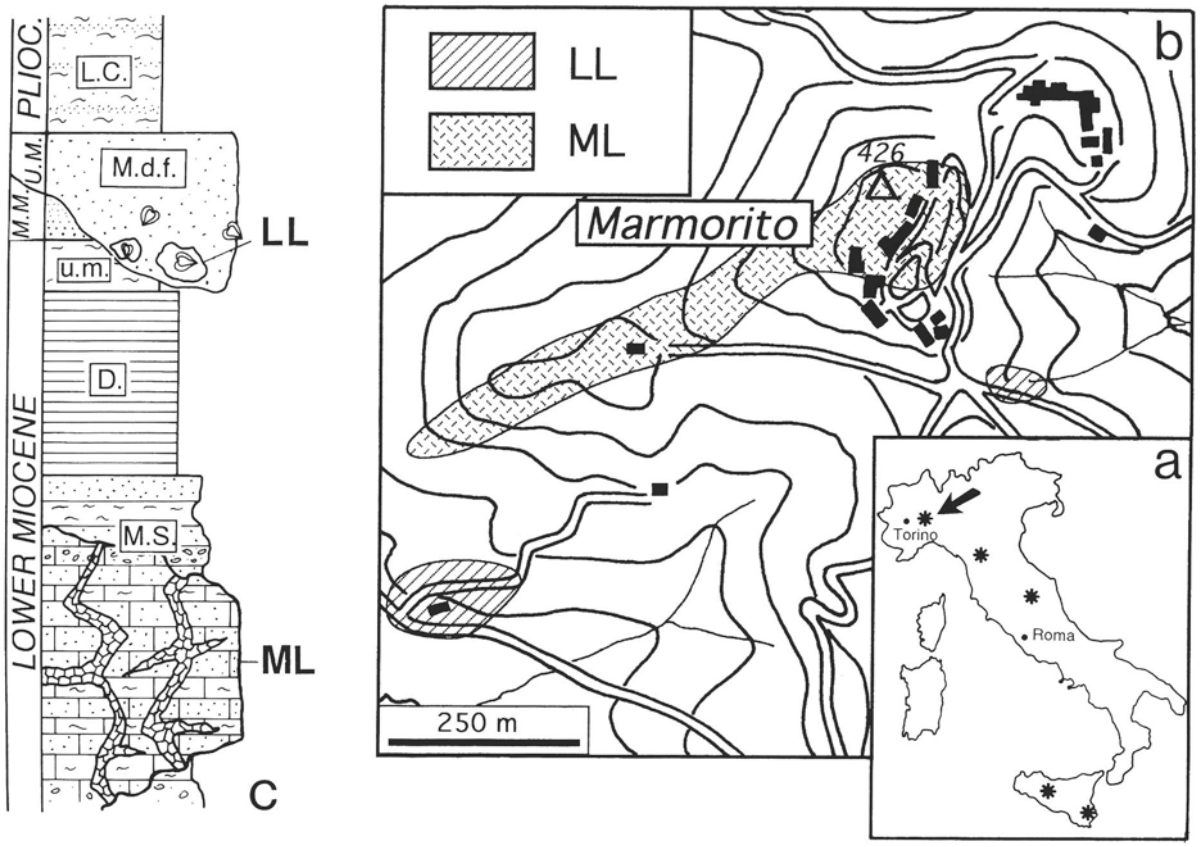

Fig. 1.a Schematic location of main fossil chemoherms in Italy. The *arrow* indicates the examples studied here. **b** Topographic sketch of the outcrops studied. *LL* Area of distribution of *Lucina* limestone blocks; *ML* area of distribution of Marmorito limestone. **c** Schematic lithostratigraphic succession in the area. *M.S* Marmorito sandstones; *D* diatomites; *u.m.* upper marl member; *M.d.f.* Messinian debris flow; *L.C.* Lugagnano clays; *LL Lucina* limestone; *ML* Marmorito limestone; *M.M.* Middle Miocene; *U.M.* Upper Miocene

of coarse- to fine-grained siliciclastic and locally diatomitic sediments deposited in a slope to inner shelf environment (Fig. 1c; Clari et al. 1988, 1995). This succession is truncated by a subaerial erosion surface due to the dramatic Messinian sea-level fall and is unconformably overlain by a shallowing-upward sequence of silty clays and sandstones of Pliocene age.

Near the small village of Marmorito, about 30 km east of Torino, two different types of anomalous carbonate-rich rocks occur (Fig. 1b). The first is a cream to light-brown colored marly limestone, with abundant fossil remains mostly of large clams of the genus *Lucina* (*Lucina* limestone, Clari et al. 1988; Fig. 2a). Occasionally, remains of other fossil groups, e.g. worms, are found (Fig. 2b). The second type consists of light to dark gray, tightly calcite- and dolomite-cemented mudstone and sandstone crossed by carbonate-filled veins. These rocks, barren of fossils, are known as Marmorito limestone (Clari et al. 1988).

The *Lucina* limestone shows an unusual fossil content and sedimentary features strikingly similar to the ones described from present-day cold-seep carbonates (for details, see Clari et al. 1994).

3 The *Lucina* Limestone: A Sedimentary By-Product of Fluid Venting at the Sea Floor

In the Marmorito area the original stratigraphic relationships of the *Lucina* limestone are completely lost, because this fossiliferous limestone occurs only as centimeter- to meter-sized blocks and clasts scattered in the fields or as part of debris flows of Messinian age (Fig. 1b,c). Single blocks display slightly different sedimentary and petrographic features, which can be interpreted as the result of a variety of sedimentary and diagenetic histories. However, two main carbonate fabrics may be recognized in all blocks: microcrystalline calcite (or dolomite) which forms the groundmass, and coarser-sized cements and internal sediments filling veins and cavities.

3.1 Groundmass

The "micritic" groundmass in which the *Lucina* remains are embedded consists of microcrystalline low-

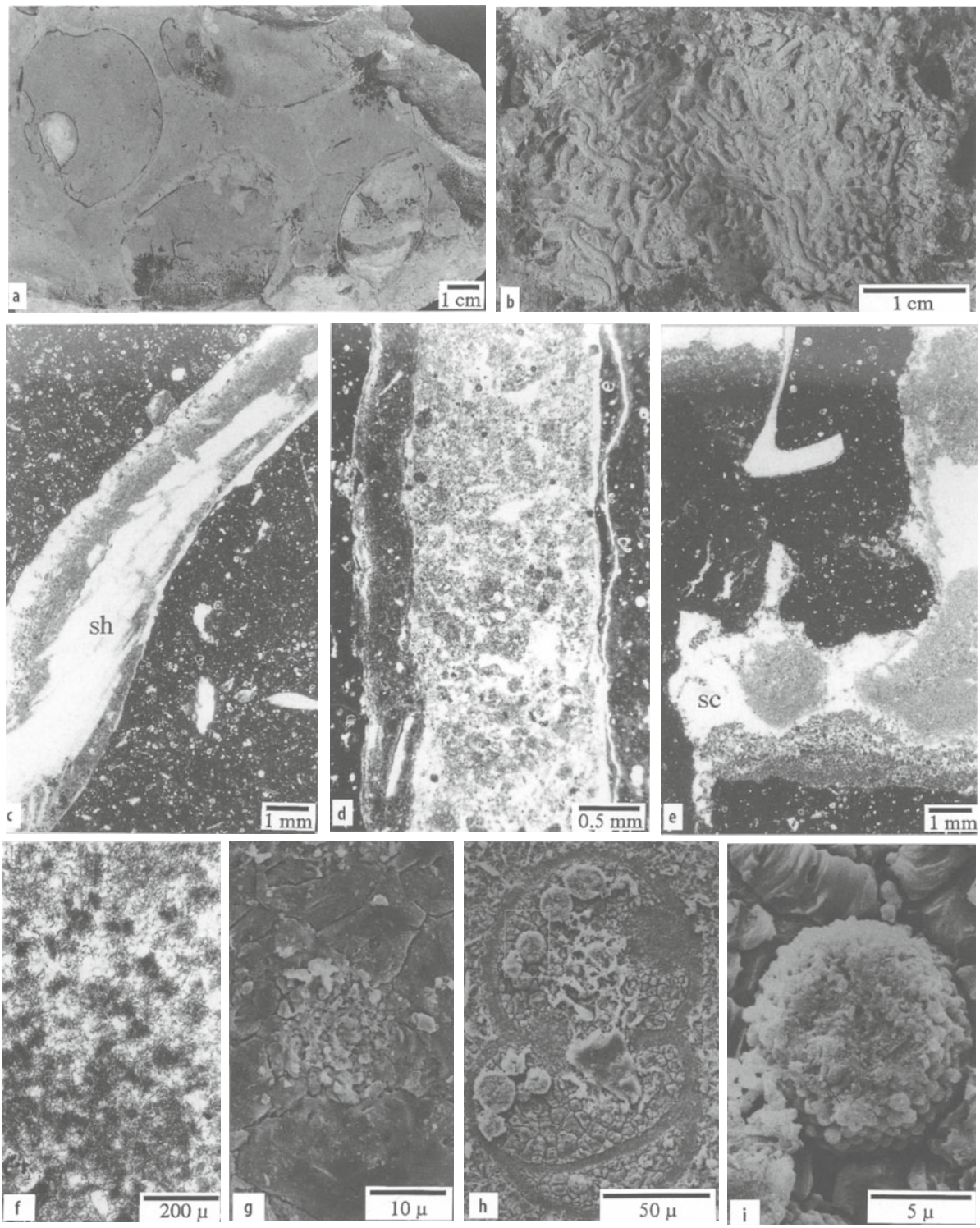

Fig. 2a–i. Macro- and microscopic features of *Lucina* limestone. **a** Cluster of lucinid clams in a microcrystalline marly limestone; sawed surface of a block. Note that shells are replaced by a lighter colored sediment. **b** Detail of a cluster of (serpulid?) worm tubes; broken surface. **c** Partially dissolved lucinid shell. The resulting moldic cavity is filled with peloidal and biomicritic sediment and sparry cement. Note abundant planktonic foraminifers in the fine-grained host sediment; *sh* remains of the shell. **d** Detail of a completely leached lucinid shell filled with two generations of sediment; the first biomicritic and the second peloidal. **e** Complex fill of a burrow with clear-cut margins. Several generations of internal sediment and a sparry calcite cement (*sc*) can be recognized. **f** Close-up of the peloidal internal sediment of **e. g** SEM image of a single peloid in **f**. Note the presence of clay flakes (light colored) and the large poikilotopic crystals of sparry calcite cement; etched polished surface. **h** SEM image of a planktonic foraminifer. Pyrite framboids, clay flakes and calcite cement fill the chambers. **i** SEM detail of a pyrite framboid; etched polished surface

Mg calcite filling the pores of a fine-grained siliciclastic host sediment. In thin-section the rock appears as a homogeneous, calcite-cemented, siliciclastic mudstone with sparse sand and silt-sized quartz and mica grains. In most cases a substantial biogenic fraction, consisting mainly of tests of planktonic foraminifers, is still recognizable (Fig. 2c). In other cases, microsparfilled voids suggest the presence of a similar, original biogenic fraction dissolved during an early diagenetic phase. Pyrite framboids and grains are locally present, both scattered in the "micritic" cement and in-filling cavities such as chambers of foraminifer tests (Fig. 2h,i). The former widespread presence of pyrite grains, now oxidized, is suggested by abundant rusty and reddish-colored grains and stains. Evidence of an early phase of dissolution of the skeletal fraction, in particular of lucinid shells, is ubiquitous (Figs. 2c,d).

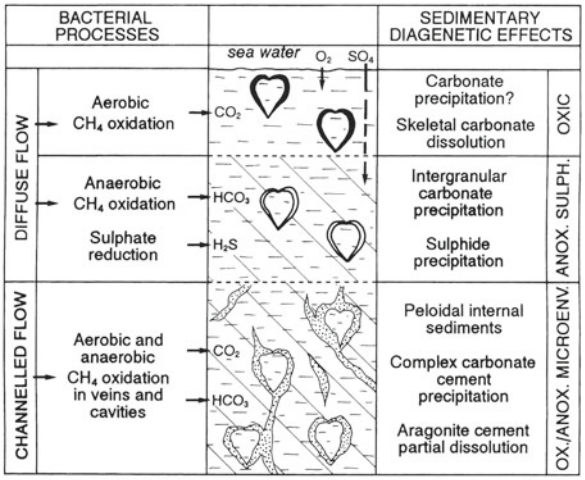

Fig. 3. Possible model of formation of the *Lucina* limestone. Microbial processes and sedimentary effects taking place within a vertical sediment column affected by seepage of methane-rich fluids are schematically represented

3.2 Cavity-Filling Carbonates

The micritic groundmass of the *Lucina* limestone is locally crossed by a network of subvertical fissures, burrows and moldic cavities left by the dissolution of *Lucina* shells. This network of cavities is partially or completely plugged by carbonate sediments and cements (Figs. 2c–e). Carbonate mineralogy of the cements is primarily calcitic, but in some samples relict morphologies and zoning suggest the former presence of dolomite and aragonite. Different generations of internal sediments, often separated by thin cement fringes, are recognizable (Fig. 2e). Most of the internal sediments display clotted, peloidal textures (Figs. 2e–g); locally, an intraclastic and bioclastic fraction may be present. SEM observation of the peloidal sediments reveals a locally abundant dolomitic fraction.

Micritic groundmass, internal sediments and cements always show strongly negative $\delta^{13}C$ values ranging from – 12.2 to – 35.5‰ PDB (Clari et al. 1988, 1994). A reconstruction of the genetic and diagenetic history of the *Lucina* limestone can be outlined as follows (Fig. 3):

1. A dense, specialized community, dominated by large infaunal lucinid clams, colonized an area of diffuse methane-rich fluid venting at the sea floor. Bivalves lived buried in the uppermost (oxic) layer of the sediment and were sustained by a chemosynthetic food chain supported by sulfide produced in the underlying sulfate-reducing zone by concurrent bacterial anaerobic oxidation of methane and sulfate reduction. In the oxic pore water of the sediments surrounding living clams, aerobic oxidation of the upward-migrating flux of methane produced large amounts of CO_2, which caused a decrease in pH and consequent dissolution of skeletal carbonate. This carbonate dissolution was locally enhanced by oxidation of sulfide diffusing upward from the sulfate-reduction zone.
2. The oxic/anoxic interface slowly migrated upward, keeping pace with continuing sedimentation, and the sediments enclosing dead and partially or completely leached lucinids shells passed through the sulfate-reducing zone. Here, CH_4 was anaerobically oxidized by bacteria, and pyrite and HCO_3^- were produced with a resulting large increase in alkalinity (Hovland et al. 1987; Beauchamp and Savard 1992). The precipitation of the finely crystalline, ^{13}C-depleted, authigenic carbonates forming the *Lucina* limestone groundmass took place.
3. The substantial precipitation of carbonate cement progressively blocked diffuse fluid flow. As a result, ascending methane-charged fluids were channeled through a network of cavities consisting of shell-dis-

▷

Fig. 4a–j. Macro- and microscopic features of the Marmorito limestone. **a** Outcrop view of dolomite-cemented sandstone. Cementation is particularly strong along irregular "pillars" nearly normal to bedding emphasized by differential weathering and lighter color. *Arrows* highlight bedding. **b** Detail of a large vein incompletely filled by multiple generations of limpid and turbid carbonate cements. **c** Microscopic aspect of the cemented sandstones of **a** and **b**. Euhedral, zoned dolomite crystals making up the cement are clearly recognizable in cathodoluminescence (**d, e**). **f** Cement rim around a mica grain in a pelitic bed. Note the microsparitic aspect of the groundmass.

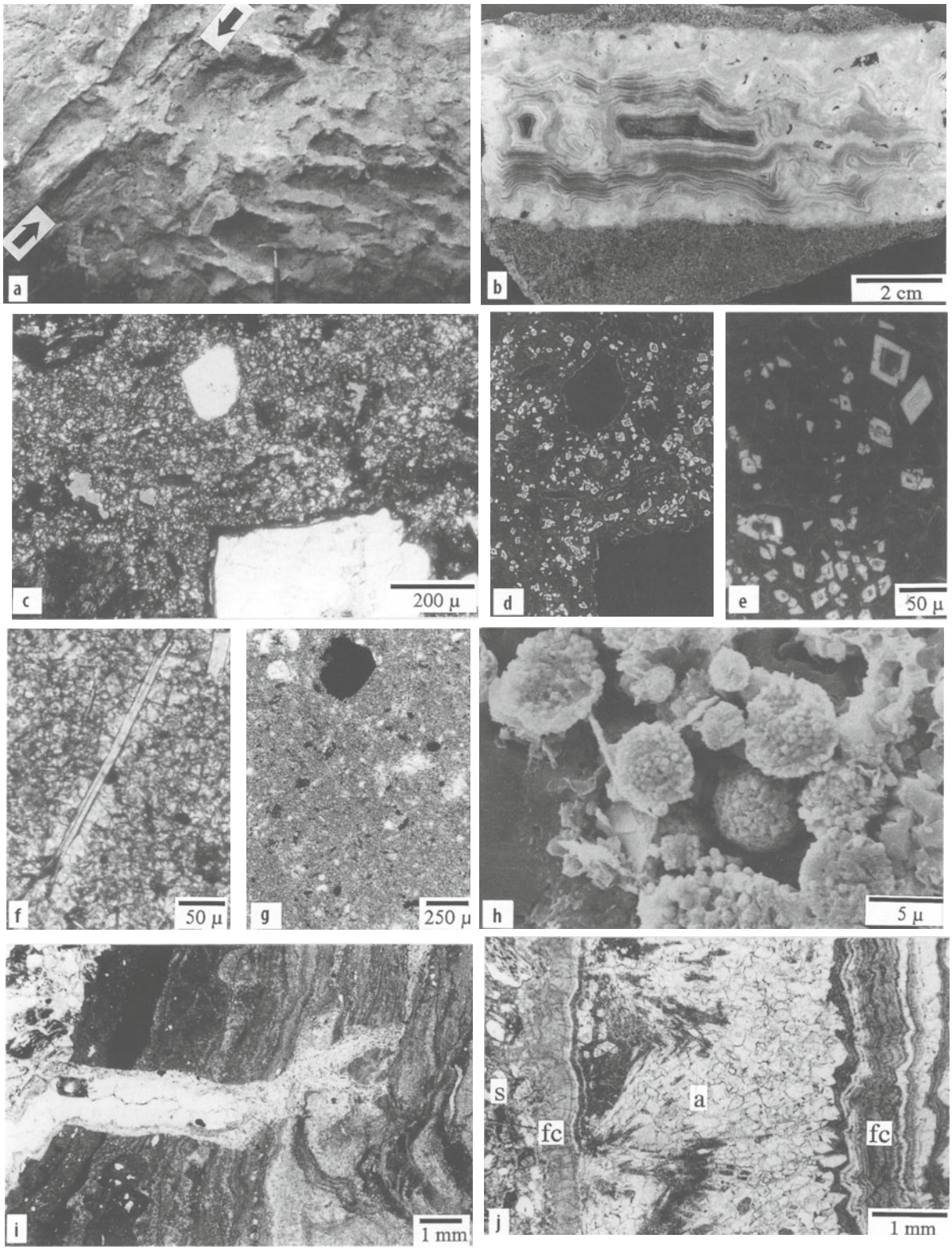

g Pyrite grains in a fine-grained, tightly cemented bed. Note the large, subhedral grain. **h** SEM image of pyrite framboids in the groundmass; etched polished surface. **i** An irregularly laminated sediment fill is cross-cut by a spar-filled second-generation vein. The host sandstone is visible in the *upper left*. **j** Detail of a vein filled by several generations of cements; *s* enclosing sediment; *fc* fibrous calcite; *a* aragonite. Note that the aragonite splays are partially dissolved and totally recrystallized. Opaque cores are due to fills of abrasive powder during thin-section preparation

solution voids, burrows and fractures. Sediment in-filling and carbonate cement precipitation progressively reduced and eventually also plugged this network of cavities.

4 The Marmorito Limestone: Evidence of Fluid Venting Below the Sea Floor?

The tightly cemented mudstones and sandstones crossed by carbonate-filled veins that form the Marmorito limestone differ from the *Lucina* limestone chiefly in the total absence of macroscopic fossil remains of the distinctive chemotrophic organisms so abundant in the *Lucina* limestone and the different, much clearer, stratigraphical framework. The Marmorito limestone masses are in place and may be easily recognized as carbonate-cemented portions of the local siliciclastic sequence (Figs. 1b, 4a). The resulting cemented masses have a lateral extent of some tens of meters and cover a stratigraphic thickness of several meters, up to a maximum of about 20 m.

The only "anomalous" outcrop features of these rocks are their extreme hardness, unknown in local coeval sediments, which commonly are only slightly cemented, and the presence of a complex network of carbonate-filled veins (Fig. 4b).

The extreme hardness results from the presence of a pervasive intergranular carbonate cement which seals all the pores of the siliciclastic host sediment (Figs. 4c–f). The abundance of cement and the loose packing of grains indicate that carbonate precipitation took place in still uncompacted siliciclastic muds and sands. Cathodoluminescence (CL) and SEM reveal that dolomite and, to a lesser extent, calcite make up this intergranular cement (Figs. 4d,e). Pyrite framboids and grains are abundant (Fig. 4g,h).

The complex network of fractures with sharp, straight, boundaries that cross the tightly cemented rocks is completely plugged by coarse-grained cements and cemented internal sediments. Several carbonate mineral phases and fabrics can be distinguished in the cements. Precipitation phases alternate with dissolution events and with the opening of new fractures (Fig. 4i). Each cement phase may display different mineralogies (aragonite, calcite, dolomite) and crystal morphology (radial fibrous, botryoidal, peloidal, sparry. Fig. 4i). Morphologies and growth stages are evidenced by inclusion-rich and inclusion-free bands (Figs. 4b,j). The CL zonation pattern consists of oscillatory, concentric alternations of dull brown to moderate yellow bands with only minor, bright yellow hairlines. Some cements, especially the aragonitic ones, have been totally leached, others are recrystallized, and some others still retain relics of the original composition and morphology (Fig. 4j).

Internal sediments are similar to the ones recognized in the *Lucina* limestone. Peloidal structures are common and fine-grained siliciclastic detritus is generally present.

Isotopic signatures of both intergranular and vein-filling carbonates are unequivocal evidence of a methane-related origin. Values of $\delta^{13}C$ of the pore-filling dolomitic cement of the indurated mudstones and sandstone range from −16 to −36‰ PDB. Coarse-grained cements and internal sediments filling the veins are generally even more ^{13}C-depleted ($\delta^{13}C$ from −20 to −40‰ PDB) and display values consistently lower that those measured in the encasing rocks.

Most of the sedimentary and petrographic features and the isotopic signatures of the Marmorito limestone match the ones found in the *Lucina* limestone and suggest a closely related origin. Precipitation of the pore-filling cement of the Marmorito limestone occurred at very shallow burial depths, near the sediment-water interface, as the content of carbonate cement (60–75%) is well within the range of initial porosity values for uncompacted mudstones and sandstones. The dolomitic nature of the cement is not surprising because dolomite cements are precipitated in many modern chemoherms near the sediment-water interface following bacterial hydrocarbon oxidation (e.g. Aharon and Sen Gupta 1994; Jørgensen 1989). Absence of fossil remains of seep-related organisms in the Marmorito limestone may reflect either original environmental conditions unfavorable to their settling or, more likely, precipitation of cement within buried sediments, well below the seawater interface. More difficult to envisage are the details of the sedimentary and diagenetic environments of the various events recorded in the network of veins crossing the Marmorito limestone (vein opening, precipitation of different carbonate mineralogical phases, dissolution, deposition of internal sediments). However, petrographic and isotopic evidence suggest that alternating precipitation and dissolution events, and precipitation of different carbonate phases and fabrics, likely reflect fluctuating rates of upward methane flow and of downward advection of seawater. This interplay regulated bacterial activity, which in turn produced chemical gradients conducive to the precipitation and dissolution of various mineralogical phases and fabrics of calcium and magnesium carbonates.

▷

Fig. 5a–l. Possible microscopic evidence of microbial activity. **a** Laminated sediment fill of a burrow. Note the different types of sediment, loose packing of grains, and laminae hanging from the cavity roof; *Lucina* limestone. **b** Type-1 peloidal texture of the internal sediments. **c** SEM image of two peloids surrounded by sparry calcite (*dark colored*). Clay flakes and tiny dolomite crystals are visible in the peloid.

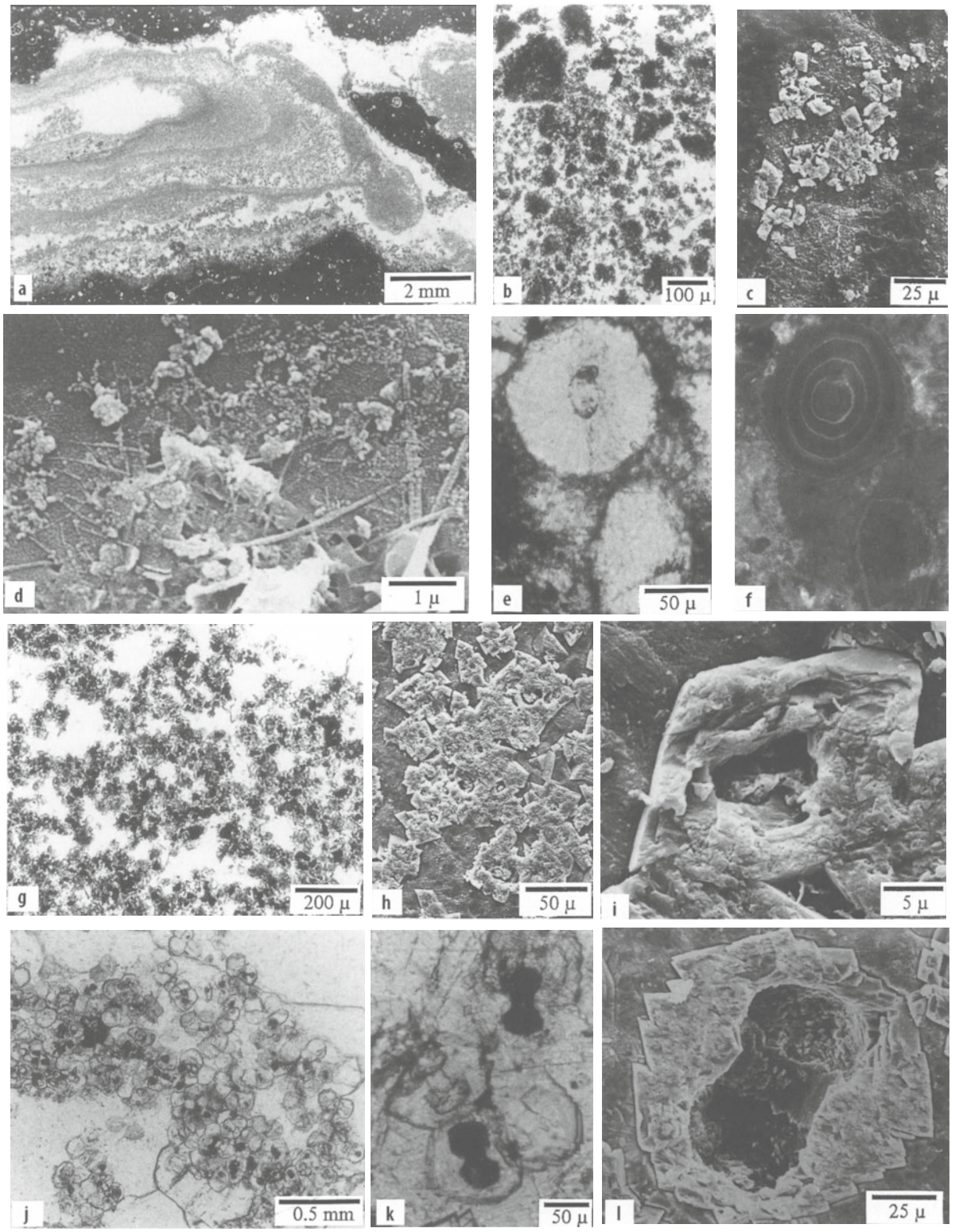

d Close-up of the periphery of a peloid showing clay flakes and elongated fibres, probably of palygorskite; etched polished surface, *Lucina* limestone. **e** Dolomite spherulites in a vein fill. Note the fibrous structure and (**f**) the concentric zoning in cathodoluminescence ; Marmorito limestone. **g** Type-2 peloidal texture. SEM images (**h, i**) highlight the hollow cores of dolomite crystals (etched polished surfaces) which appear opaque in **g** thin section; *Lucina* limestone. **j** Dolomite spherulites "floating" in coarse sparry calcite cement. Microscopic (**k**) and SEM (**l**) images show the dumbbell shape of the hollow cores. Note the last stage of euhedral, syntaxial, overgrowth of the dolomite spherulite, particularly evident in the SEM image; etched polished surface. Opaque cores are due to fills of abrasive powder during thin-section preparation; Marmorito limestone

5 Direct Evidence of Bacterial Activity

The responsibility of microbial activity for the substantial carbonate precipitation that produced both *Lucina* and Marmorito limestone is strongly suggested by the geological and geochemical features described above. Hence an attempt has been made to find direct evidence of the presumably diverse and thriving bacterial colonies.

The first and most obvious evidence supports the presence of sulfate-reducing bacteria. It is provided by the abundant pyrite fraction recognizable in the groundmass of both carbonates (Figs. 2h,i; 4g,h).

More unusual structures and fabrics, seldom described in marine siliciclastic rocks, are displayed by carbonate cements and internal sediments. The largest features are laminated sediment fills of millimeter to centimeter sized cavities due to burrowing or shell leaching in the *Lucina* limestone (Fig. 5a). The lamination is reflected by slight textural changes and by occasional interposition of thin cement layers between laminae. However, laminated sediments are not limited to the floors of the cavities but line them completely, giving rise to irregular concentric structures hanging from the roof. Laminae of internal sediments with loose packing of grains can stick to the walls of a cavity only if an organic film is present to bind them and to trigger precipitation of cement. Similar organo-sedimentary laminated sediments have been described in fossil chemoherms by Campbell et al. (1993), and also in lacustrine microbialites (Kempe et al. 1991) and Recent subaerial calcretes (Verrecchia et al. 1995).

Most of the internal sediments show a peloidal fabric. Two kinds of peloids may be distinguished, both of which show sizes of several tens of microns. The first type consists of microcrystalline aggregates (Fig. 5b). SEM observation of etched samples reveals the presence of tiny, euhedral dolomite crystals, detrital clay flakes, and interwoven palygorskite (?) fibers within the microcrystalline calcite matrix of the peloid (Figs. 5 c,d). The second type of peloid is actually represented by small, euhedral to subhedral dolomite crystals with hollow cores that, during preparation of the thin-section, are filled with abrasive powder and thus appear dark and opaque.(Fig. 5g–i).

In the Marmorito limestone dolomite is also present in the form of larger aggregates with a fibrous-raggiate structure. These spherulites, about 100–200 μm in diameter, show a dull brown color in CL, with concentric yellow hairlines marking the growth of the subspherical structure (Fig. 5e,f). Many of these spherulites have a distinctive hollow core characterized by a dumbbell shape (Fig. 5j,k). Dolomite spherulites and peloidal textures have been often related to microbial activity (e.g. Chafetz 1986; Gunatilaka 1989; Guo and Riding 1992a). Additional support in clotted textures is observed in the loose packing of peloids, enclosed by poikilotopic crystals of internally zoned, pore-filling sparry calcite (Fig. 5a,g,j).

Possible direct evidence of the former presence of bacteria is provided by the dumbbell-shaped hollow cores of dolomite spheroids. With the single exception of Fernandez-Diaz et al. (1996), who obtained spherical to dumbbell Mg-calcite aggregates inorganically, such shapes have been reported mostly in continental environments (travertine, calcretes, etc.) where the role of bacteria on carbonate precipitation is well documented (Buczynsky and Chafetz 1991; Guo and Riding 1992b; Folk 1993).

6 Concluding Remarks

Bacterial degradation of methane may result in very different products: (1) typical chemoherms, by now well known in the literature, characterized by rich and revealing fossil associations (e.g. *Lucina* limestone), (2) less distinctive, tightly cemented mudstones or sandstones (e.g. Marmorito limestone). These two types of carbonate-rich rocks may be interpreted as genetically linked, and possibly also contemporaneous, by-products of methane venting, which triggered settling and growth of chemotrophic and chemosymbiotic organisms on the sea floor and drove a variety of diagenetic mechanisms in the underlying sediment column. In addition to palaeobiological criteria, therefore, possible clues to methane venting are unusual diagenetic features: a much greater degree of lithification than the laterally equivalent sediments, and irregular, carbonate-filled non-tectonic veins are the most obvious of these. Carbon isotope analyses are needed to definitely confirm the methane-related, and hence microbially driven, origin.

The spectrum of sedimentary rocks with a fundamental imprint of microbial activity is extended by cases such as those reported here, which may easily be overlooked during routine fieldwork.

Acknowledgements. Suggestions by D. Bottjer and C. Gaillard are gratefully acknowledged. Many thanks to R. Riding for revision of the English text. Isotopic analyses and SEM observations were performed in the laboratories of the Dipartimento di Scienze della Terra of the University of Torino. The authors are indebted to G. Coppo and R. Cossio for technical assistance. CL and microscopic equipment were kindly provided by the Centro Studi Dinamica Catene Collisionali of the Italian CNR. Research was funded by Italian MURST, grants to P.A. Clari.

References

Aharon P (1994) Geology and biology of modern and ancient submarine hydrocarbon seeps and vents: an introduction. Geo-Mar Lett 14:69 – 73

Aharon P, Sen Gupta BK (1994) Bathymetric reconstructions of the Miocene-age "calcari a *Lucina* " (northern Apennines, Italy) from oxygen isotopes and benthic foraminifera. Geo-Mar Lett 14:219 – 230

Beauchamp B, Savard M (1992) Cretaceous chemosynthetic carbonate mounds in the Canadian Artic. Palaios 7:434 – 450

Bitter von PH, Scott SD, Schenk PE (1992) Chemosynthesis: an alternate hypothesis for Carboniferous biotas in Bryozoan/microbial mounds, Newfoundland, Canada. Palaios 7:466 – 484

Buczynsky C, Chafetz HS (1991) Habit of bacterially induced precipitates of calcium carbonate and the influence of medium viscosity on mineralogy. J Sediment Petrol 61:226 – 233

Campbell KA, Bottjer DJ (1995) Brachiopods and chemosymbiotic bivalves in Phanerozoic hydrotermal vent and cold seep environments. Geology 23:321 – 324

Campbell KA, Carlson C, Bottjer DJ (1993) Fossil cold seep limestones and associated chemosymbiotic macroinvertebrate faunas, Jurassic-Cretaceous In: Graham SA, Lowe DR (eds) Advances in the sedimentary geology of the Great Valley Group, Sacramento Valley, California. Pac Sec SEPM 73:37 – 50

Chafetz HS (1986) Marine peloids: a product of bacterially induced precipitation of calcite. J Sediment Petrol 56:812 – 817

Clari, Gagliardi C, Governa ME, Ricci B, Zuppi GM (1988) I Calcari di Marmorito: una testimonianza di processi diagenetici in presenza di metano. Boll Mus Regionale Sci Nat Torino 6:197 – 216

Clari P, Fornara L, Ricci B, Zuppi GM (1994) Methane-derived carbonates and chemosymbiotic communities of Piedmont (Miocene), northern Italy: an update. Geo-Mar Lett 14:201 – 209

Clari P, Dela Pierre F, Novaretti A, Timpanelli M (1995) Late Oligocene-Miocene sedimentary evolution at the critical Alps/Apennines junction: the Monferrato area, northwestern Italy. Terra Nova 7:144 – 152

Claypool GE, Kaplan IR (1974) The origin and distribution of methane in marine sediments. In: Kaplan IR (ed) Natural gases in marine sediments. Plenum Press, New York, pp 99 – 139

Fernandez-Diaz L, Putnis A, Prieto M, Putnis CV (1996) The role of magnesium in the crystallization of calcite and aragonite in a porous medium. J Sediment Res 66:482 – 491

Folk RL (1993) SEM imaging of bacteria and nannobacteria in carbonate sediments and rocks. J Sediment Petrol 63:990 – 999

Gaillard C, Rio M, Rolin Y, Roux M (1992) Fossil chemosynthetic communities related to vents or seeps in sedimentary basins: the pseudobioherms of southeastern France compared to other word examples. Palaios 7:451 – 465

Goedert JL, Squires RL (1990) Eocene deep-sea communities in localized limestones formed by subduction-related methane seeps, southwestern Washington. Geology 18:1182 – 1185

Gunatilaka A (1989) Spheroidal dolomites – origin by hydrocarbon seepage? Sedimentology 36:701 – 710

Hovland M, Talbot M, Qvale H, Olaussen S, Aasberg L (1987) Methane-related carbonate cements in pockmarks of the North Sea. J Sediment Petrol 57:881 – 892

Guo L, Riding R (1992a) Aragonite laminae in hot water travertine crusts, Rapolano Terme, Italy. Sedimentology 39:106 – 1079

Guo L, Riding R (1992b) Microbial micritic carbonates in uppermost Permian reefs, Sichuan Basin, southern China: some similarities with Recent travertines. Sedimentology 39:37 – 53

Jørgensen NO (1989) Holocene methane-derived, dolomite-cemented sandstone pillars from the Kattegat, Denmark. Mar Geol 88:71 – 81

Kempe S, Kazmierczak J, Landmann G, Konuk T, Reiner A, Lipp A (1991) Largest known microbialites discovered in Lake Van, Turkey. Nature 349:605 – 608

Piana F, Polino R (1995) Tertiary structural relationships between Alps and Apennines: the critical Torino Hill and Monferrato area, northwestern Italy. Terra Nova 7:138 – 14

Ricci Lucchi F, Vai GB (1994) A stratigraphic and tectonofacies framework of the "calcari a *Lucina* " in the Apennine Chain, Italy. Geo-Mar Lett 14:210 – 218

Roberts HH, Aharon P (1994) Hydrocarbon-derived carbonate buildups in the Gulf of Mexico continental slope: a review of submersible investigations. Geo-Mar Lett 14:135 – 148

Sassen R, Mac Donald IR, Requejo AG, Guinasso NL, Kennicutt MG II, Sweet SJ, Brooks JM (1994) Organic geochemistry of sediments from chemo-synthetic communities, Gulf of Mexico slope. Geo-Mar Lett 14:110 – 119

Terzi C, Aharon P, Ricci Lucchi F, Vai GB (1994) Petrography and stable isotope aspects of cold-vent activity imprinted on Miocene-age "calcari a *Lucina* " from Tuscan and Romagna Apennines, Italy. Geo-Mar Lett 14:177 – 184

Verrecchia EP, Freytet P, Verrecchia KE, Dumont JL (1995) Spherulites in calcrete laminar crusts: biogenic $CaCO_3$ precipitation as a major contributor to crust formation J Sediment Res A65:690 – 700

Microbial Processes and Products Fueled by Hydrocarbons at Submarine Seeps

Paul Aharon

Department of Geology and Geophysics, Louisiana State University, Baton Rouge, LA 70803, USA

Abstract. Two kinds of records preserve the imprints of microbial processes in submarine seep environments. One record tracks transient changes in pore fluid chemistry and is based on the fact that microbial activities leave indelible marks on the pore fluids, which serve as the transport media of microbial metabolic products. The other record, consisting of the geologic products of seeps such as massive carbonates and carbonate-cemented sandstones, is permanent and provides long-lasting archives which can be used to infer the geochemical and microbiological history of seeps. Both types of records encompassing pore fluids and sediments of extant seeps are reviewed here.

1 Introduction

Recent investigations have indicated that hydrocarbon-rich fluid emissions are widespread on the ocean sea floor (Fig. 1). These emissions (see Aharon 1994a for a summary and reference list) have been documented over the past decade from tectonically active convergent margins (e.g., northwest Pacific; Japan Trench; Barbados; Peru; Mediterranean) as well as passive continental margins (e.g., North Sea; Gulf of Mexico; Arctic Basin), typically at bathyal to abyssal depths but also in intertidal environments (e.g. the Danish coast, Schmaljohann et al. 1990; Dando et al. 1994a). The exits of the hydrocarbon-rich fluid emissions at cold, ambient sea floor temperatures are commonly termed "seeps" in order to distinguish them from the generally more vigorous and hot fluid emissions ("vents") occurring at mid-ocean ridge settings (Fig. 1). In addition to fluid temperature, they are also distinguished by the fact that cold seeps release hydrocarbon-rich fluids pressurized by sediment squeezing, gas production or hydrostatic head, whereas hot vents are driven by heat-induced convection. Submarine seeps are commonly patchy and their spatial continuity is limited to a radius not exceeding a few meters. Their presence on the sea floor is typically revealed by the luxuriant chemosynthetic

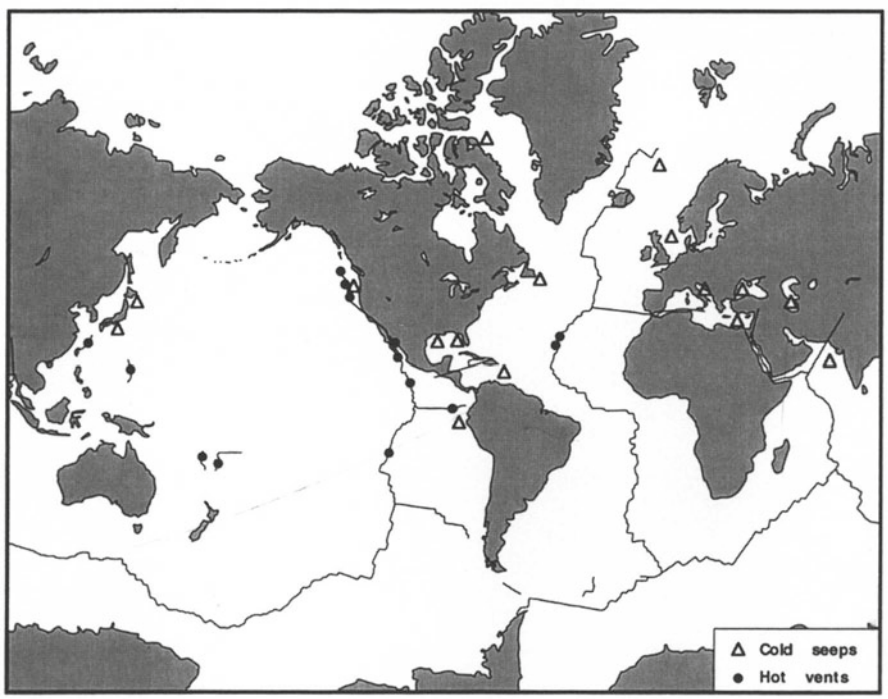

d distribution of carbon seeps and n the ocean floor. from Aharon 1994a)

R. E. Riding and S. M. Awramik (Eds.)
Microbial Sediments

fauna associated with massive carbonate deposits that stand in sharp contrast to the more desolate surroundings.

Seeps are highly unusual marine habitats where toxic compounds derived directly or indirectly from hydrocarbons are turned into life-nourishing elements and innocuous, long-lasting, geologic deposits. Although it is generally accepted that microbial activities are fundamental to the sustenance of seep habitats, few studies have attempted to evaluate the role played by bacteria in seeps, and to establish beyond anecdotal levels the significance of hydrocarbons in fueling microbial processes. Exceptional are the studies of Dando et al. (1994a) Gamo et al. (1992), Masuzawa et al. (1992), Paull et al. (1992), and Suess and Whiticar (1989), which investigated pore fluid chemistry alterations resulting from interaction between seeping methane and microbial communities from near-surface sediments in extant seeps from the Oregon subduction zone, Florida Escarpment, Sagami and Nankai Troughs, and the Danish shoreline.

The objectives of this review are to: (1) delineate the transient and permanent records of microbial processes in seeps; (2) determine the level of interaction between the diverse and highly specialized microbial communities, and (3) elucidate the links between microbially derived chemical reactions and geological products. The narrative that follows emphasizes the geochemical aspects of microbial processes in seeps, rather than the taxonomic aspects of seep bacteria and draws examples primarily from the northern Gulf of Mexico (Fig. 2). The geographic bias is predicated by the author' s hands-on experience with the Gulf of Mexico extant seeps and is justified because of the pervasiveness of hydrocarbon seeps, diversity of hydrocarbon types, and richness of chemosynthetic fauna hosted by these seeps (Roberts and Aharon 1994; Carney 1994; Aharon et al. 1997).

2 Biological and Geological Indicators of Microbial Activity

Observations from submersibles have led to the recognition that seeps occurring at bathyal to abyssal depths are essentially anoxic enclaves surrounded by oxygen-rich bottom waters. The transitional oxic to anoxic habitats, characteristic of seeps, support diversified microbial communities that are living: (1) free in the water column above seeps; (2) within the tissues of specialized benthic fauna which developed resistance to sulfide toxicity and with whom they have symbiotic relationships; (3) in mat-forming communities at the sediment-water interface, and (4) within the sediment.

Prominent among the chemolithotrophs are bacteria deriving their energy from oxidation of reduced sulfur compounds, these are the mat-forming, giant, filamentous *Beggiatoa* spp. blanketing the seeps (Fig. 3A; Sassen et al. 1993; Larkin et al. 1994) and endosymbiotic bacteria encapsuled in the tissues of vestimentiferan tube worms and clams (Fig. 3B; Southward et al. 1981). Other chemolithotrophs common in seeps derive their energy from oxidation of methane (aerobic methanotrophs) and occur either in symbiotic association with mussels (Fig. 3C; Childress et al. 1986; Fisher et al. 1987), with tube worms (Schmaljohann and Flügel 1987; Schmaljohann et al. 1990), or as free-living bacteria in the water column above the seeps (LaRock et al. 1994; Hyun et al. 1997).

In addition to chemosynthetic fauna, massive carbonates (Roberts and Aharon 1994; Clari and Martire, this Vol.) and carbonate-cemented sandstones (Jørgensen 1976; Dando et al. 1994b) associated with seeps (Figs. 3C,D) also serve as prominent indicators of microbial activity. This is because hydrocarbon-consuming bacteria produce unusually high levels of alkalinity

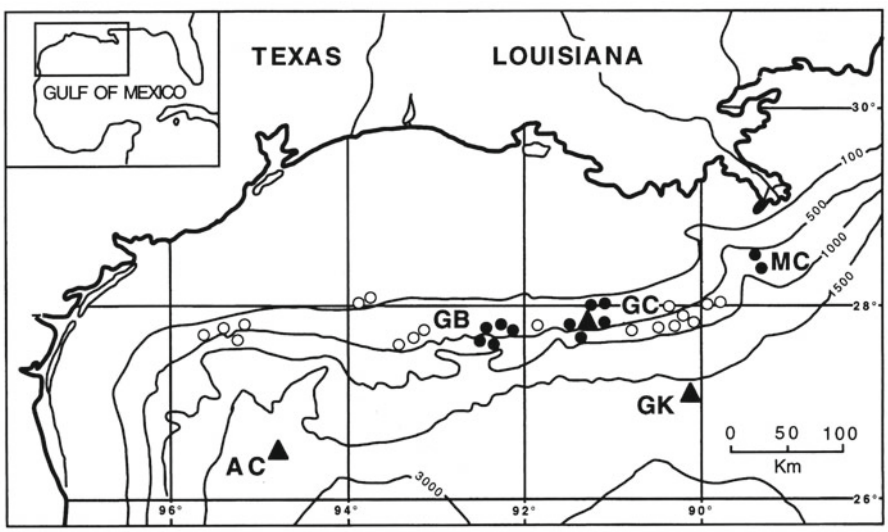

Fig. 2. Bathymetric map of the northern Gulf of Mexico showing distribution of extant hydrocarbon seeps. *Filled circles* indicate seep sites documented with Johnson-Sea-Link submersible; *filled triangles* show location of seeps investigated with DSV Alvin; *empty circles* represent known seeps that have not yet been explored. *Letters* indicate Mineral Management Service (MMS) lease blocks: *AC* Alaminos Canyon; *GB* Garden Banks; *GC* Green Canyon; *GK* Green Knoll; *MC* Mississippi Canyon

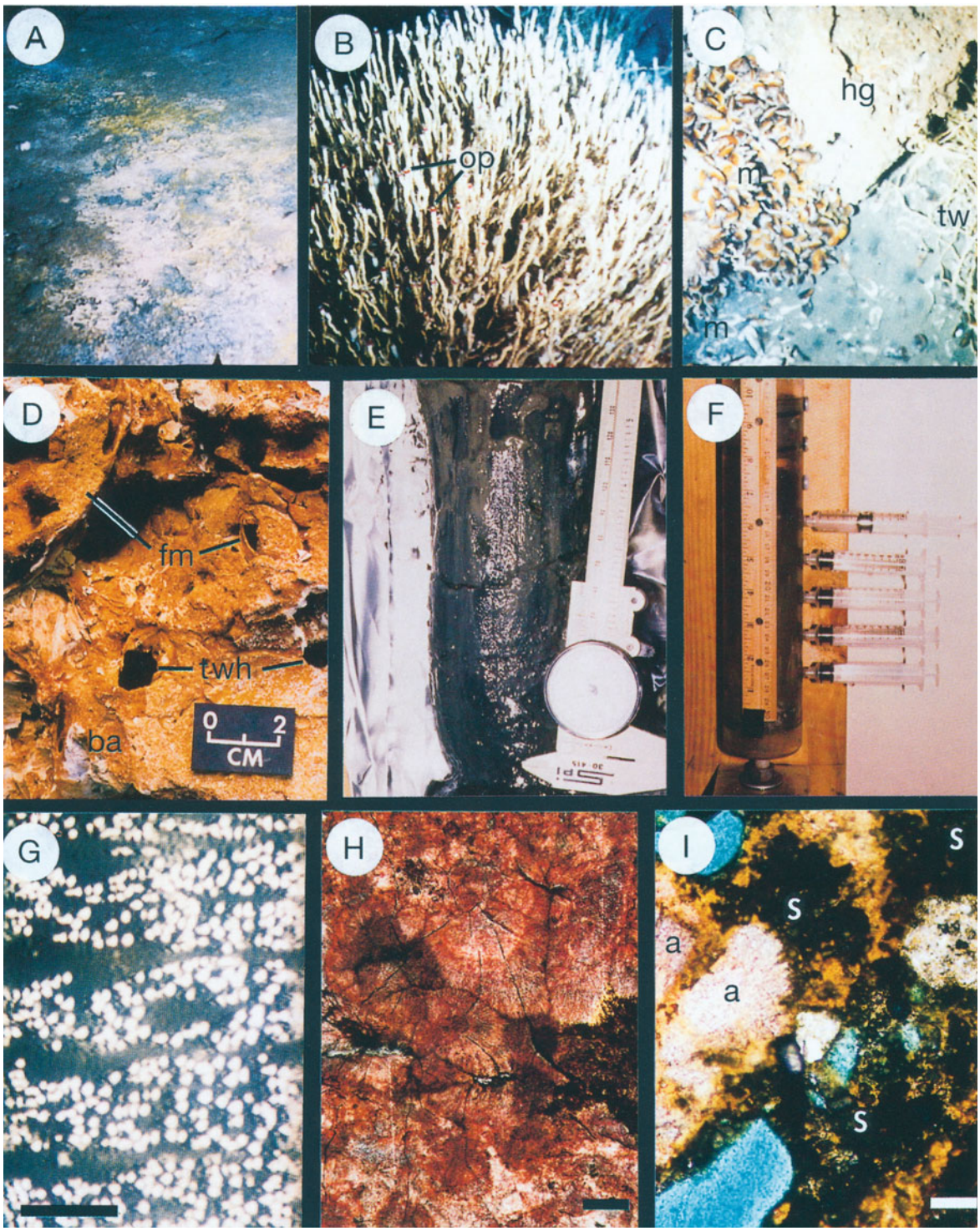

Fig. 3A–I. Sea floor and laboratory aspects of extant submarine seeps on the northern Gulf of Mexico slope and deep basin. Photographs of the chemosynthetic fauna associated with seeps at Bush Hill (GC-185) in 543 m water depth were taken in September 1995 with a camera mounted on the exterior of the Johnson-Sea-Link submersible. **A** *White* and *orange*-colored patches of *Beggiatoa* sp. mats blanketing seeps; field of view is about 2 m. **B** Cluster of vestimentiferan tube worms plumed with *deep-red* tissues (*op*) serving as conduits for transportation of H_2S and O_2 through the circulatory system (Jones 1981); field of view is about 1 m. **C** Carbonate hardground bounded by chevron fractures filled with densely packed methanotrophic mussels (*Bathymodiolus* sp.) on the *left*, and vestimentiferan tube worms on the *right*; field of view is about 1 m. **D** Massive carbonate buildup (chemoherm, Aharon 1994a) retrieved by DSV Alvin from Alaminos Canyon (see Fig. 2) at 2200 m depth. Note shelter porosity resulting from variable orientations of framework fossil methanotrophic mussel shells (*fm*) lithified by botryoidal aragonite splays (*ba*). Holes (*twh*) represent position of tube worms whose growth rates were matched by carbonate

and dissolved inorganic carbon (DIC) in the pore fluids which drive the carbonate system to supersaturation and consequently to carbonate deposition. Hydrocarbon seepage at any given locality has a geologically short life span, from a few to several hundred thousand years (Aharon et al. 1997). Once seepage is extinguished, the benthic chemosynthetic fauna which it supported vanishes as well. Therefore, the only vestige of the seep microbial processes that remains is the long-lasting carbonate buildups which contain a detailed record of seep history (Aharon et al. 1997).

3 Hydrocarbon Imprints in Seep Habitats

Recognition of the role of bacteria in seeps was preceded by the observation that hydrocarbon-derived carbon permeated all aspects of the seep habitats. The most compelling evidence of microbial utilization of hydrocarbons as energy and nutritional carbon sources, and of the pathway of carbon flow through the chemosynthetic seep fauna and carbonates, is provided by the distribution of carbon isotopes (Paull et al. 1984; Kennicutt et al. 1985; Kulm et al. 1986; Brooks et al. 1987; Hovland et al. 1987; Aharon 1994b). This is because the $^{13}C/^{12}C$ ratios in hydrocarbons, expressed in the customary $\delta^{13}C$ notation in permil relative to the PDB standard (Craig 1957), are significantly lower relative to other marine carbon sources and remain practically unchanged during carbon cycling. For example, crude oils from the northern Gulf of Mexico show a $\delta^{13}C$ range of −26‰ to −31‰ (Anderson et al. 1983; Kennicutt et al. 1992) whereas thermogenic and biogenically derived methane and higher molecular weight gases ($>C_1$) display a $\delta^{13}C$ range of −35 to −72‰ (Rice 1980). In contrast, particulate organic matter (POM) formed in the photic zone of the Gulf of Mexico ($\delta^{13}C$ = -20.6‰, Jasper and Gagosian 1989) and incorporated in the seep sediments is enriched in ^{13}C relative to hydrocarbons and is therefore distinguishable as a carbon source.

The $\delta^{13}C$ compositional ranges of biological and geological seep products in the northern Gulf of Mexico basin allow comparison with the isotope values of seeping hydrocarbons in liquid and/or gas forms

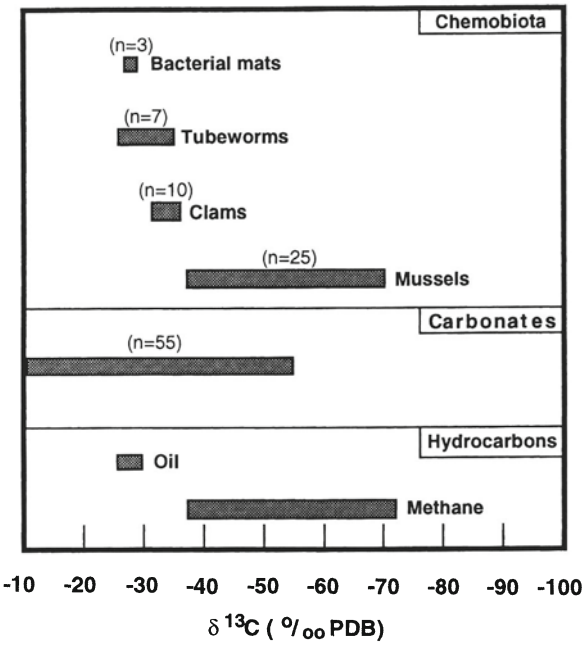

Fig. 4. Bar diagram showing $\delta^{13}C$ ranges in chemosynthetic biota and carbonates from the northern Gulf of Mexico seeps analyzed at the LSU laboratory; number of samples determined are shown in *parentheses*. For comparison, $\delta^{13}C$ distributions in hydrocarbon sources (oil and methane) are also shown. (Crude oil data from Anderson et al. 1983 and Kennicutt et al. 1992; methane data from Rice 1980)

(Fig. 4). Tube worms (*Lamellibrachia* sp. and *Escarpia* sp., $\delta^{13}C$ from −25.6 to −34.9‰, $n = 7$) and clams (*Calyptogena* sp. and *Lucina* sp., $\delta^{13}C$ from −31.2 to −35.8‰, $n = 10$) hosting aerobic sulfur-oxidizing bacteria and the chemolithotrophic sulfur bacteria *Beggiatoa* sp. ($\delta^{13}C$ from −26.6 to −27.9‰, $n = 3$) are clearly distinguishable as a group from the methanotrophic symbiont-hosting mussels (*Bathymodiolus* sp., $\delta^{13}C$ from −37.4 to −70.2‰, $n = 25$). The latter yields $\delta^{13}C$ values that overlap with those of methane, thus confirming the contribution of methane-derived carbon to the mussels (Childress et al. 1986; Fisher et al. 1987). The $\delta^{13}C$ values of the sulfur-based chemosynthetic group are consistent with the utilization of carbon derived from either crude oil fractions, the residual pool of heavily fractionated methane (Sassen and MacDonald 1997) and/or saturated, straight-chain, aliphatic

◁

accretion vertical rates. The radiocarbon age of the sample is 12.3 ± 0.2 Ka (Aharon et al. 1997). **E** *Dark-gray to black* seep sediment impregnated with microbially degraded crude oil and extruded from a core taken with Alvin's robot arm from an orange bacterial mat. **F** Modified "Jahnke" squeezer (Jahnke 1988) with mounted syringes on board the surface ship producing continuous pore fluid profiles from seep cores. **G** Native sulfur (S^o) globules occurring in *Beggiatoa* sp. cells external to the cytoplasmic membranes observed in reflected light with a laser confocal microscope (photomicrograph courtesy of J. Larkin); *scale bar* is 5 μm. **H** Photomicrograph of isopachous botryoidal aragonite splays stained by Alizarin-red in a lithified carbonate hardground from Bush Hill seeps (*plane view*). Dark centers of botryoids are filled with dead bacterial bodies (Roberts et al. 1992). The aragonite yields $\delta^{13}C = -26.5$‰ PDB, testifying to hydrocarbon-derived carbon recycled through microbial processes. Sample 89−12−1/b yields a ^{230}Th age of 1.4 ± 1.4 Ka (Aharon et al. 1997); *scale bar* is 200 μm. **I** Photomicrograph of co-existing botryoidal aragonite (*a*) and sulfide mineral phases (*s*) recording microbial sulfate reduction processes in seep pore fluids (cross-nichols). Enrichment of CO_3^{2-} resulting from CO_2 withdrawal by chemolithotrophs, and release of H_2S metabolic waste, led to precipitation of solid carbonate and sulfide (pyrite ?) phases; *scale bar* is 100 μm

fractions ($C_2 - C_5$ gases) derived from sublimating gas hydrates. Unlike the chemosynthetic fauna, the massive carbonates yield $\delta^{13}C$ values that are spread over a wide range of values (generally between −10 and −55‰) suggesting the availability of multiple sources of hydrocarbon-derived inorganic carbon dissolved in the pore fluids and mixed with DIC from the overlying seawater (Aharon 1994b).

4 Contribution of Microbial Processes to Alteration of Pore Fluid Chemistries in Seeps

Although it is widely claimed that seep anoxia is maintained by anaerobic microbial communities living below the sediment/water interface, no attempt has been made so far to identify and quantify these microbes either directly through culture assays or indirectly through radioisotope assays (e.g., Sand et al. 1975) or molecular probe sequences (Amann et al. 1995). However, it is safe to assume that significant alterations occurring in the chemistry of carbon, sulfur and nitrogen compounds dissolved in seep pore fluids relative to that of normal seawater reflect contributions from microbial processes. For the purpose of this review, only the pore fluids contained in the upper 40 cm of seep sediment are considered, as this represents the typical depth penetrated by cores using a submersible robot arm. Sediment cores from seep habitats in the northern Gulf of Mexico (Fig. 3E) can be easily distinguished from normal marine sediments at comparable depths on account of their dark gray to black color caused by ferrous sulfide deposits, the distinctive smell of hydrogen sulfide and aromatic hydrocarbons, and the presence of bacterially degraded crude oil and/or asphaltic constituents (primarily at oil seeps).

A number of devices are available to retrieve pore fluids from sediments. In my group, cored sediments are taken to the laboratory on the support surface ship immediately after the recovery of the submersible. Pore fluids released by core squeezing in a modified "Jahnke" device (Jahnke 1988) pass into plastic disposable syringes screwed into the core barrel at 3–4 cm intervals and provide continuous profiles along the core length (Fig. 3F). The fluids are filtered through a 0.20-μm membrane filter capping the syringe and are partitioned into 5-ml bottles sealed with rubber stoppers and aluminum vacuum caps for subsequent determinations of solutes and their isotope compositions (Graber and Aharon 1991; Aharon et al. 1992; Fu et al. 1996).

4.1 Anaerobic Sulfate Reduction

The most common microbial alteration observed in pore fluid chemistry of seep sediments is the marked impoverishment in sulfate accompanied by enrichment in reduced sulfur compounds, primarily as hydrogen sulfide (Suess and Whiticar 1989; Masuzawa et al. 1992; Dando et al. 1994a). The reversed sulfur chemistry in anoxic pore fluids relative to normal seawater is generally attributed to the anaerobic respiration of *Desulfovibrio* inhabiting the seep sediments and poised to take advantage of the supply of seawater-derived sulfate and reduced carbon forms serving as electron acceptor and donor, respectively. Metabolic wastes other than H_2S that are released into the pore fluids during anaerobic sulfate respiration include carbonate species and ammonia whose concentration and type depend on the nature of the reduced carbon substrates and on the buffering capacity of the environment. Chemical reactions depicting microbial sulfate reduction and its products using three types of reduced carbon substrates common in seeps are illustrated below.

1. Nitrogen-deficient POM:

$$2(CH_2O) + SO_4^{2-} = 2CO_2 + H_2S + 2OH^- \quad (1)$$

$$2CO_2 + 2OH^- = 2HCO_3^-$$

2. Nitrogen-rich POM:

$$2(CH_2O)(NH_3)_x + SO_4^{2-} = 2CO_2 + H_2S + 2xNH_3 + 2OH^-$$

$$2CO_2 + 2OH^- = 2HCO_3^- \quad (2)$$

$$2HCO_3^- + 2NH_3 = 2CO_3^{2-} + 2NH_4^+$$

3. Light aliphatic hydrocarbons (C_nH_{2n+2}):

$$CH_4 + SO_4^{2-} = CO_2 + H_2S + 2OH^- \quad (3)$$

$$CO_2 + 2OH^- = CO_3^{2-} + H_2O$$

The sulfate/sulfide relation observed in the pore fluids of the northern Gulf of Mexico seeps is linear (Fig. 5) and indicates that bacterial sulfate reduction is active within the seep sediments. The intensity of the bacterial sulfate reduction can be gauged from the observed rapid obliteration of the sulfate below the sediment/water interface (Fu and Aharon 1997), and the highly elevated levels of H_2S (up to 22 mM, Fig. 5) exceeding by factors of 67 and 4 the levels determined in the Sagami Trough (Masuzawa et al. 1992) and Florida Escarpment (Paull et al. 1992) seep habitats, respectively.

4.2 Methanogenesis

Methane-producing obligatory anaerobes (methanogens) are believed to be ubiquitous in the seep habitats, although no direct assays have been reported. Methanogens have a restricted range of carbon and energy sources (e.g., hydrogen, acetate) and frequently form consortia with other anaerobic bacteria that can supply them with required metabolites (Ehrlich 1990). The microbial consortium converts organic carbon substrates

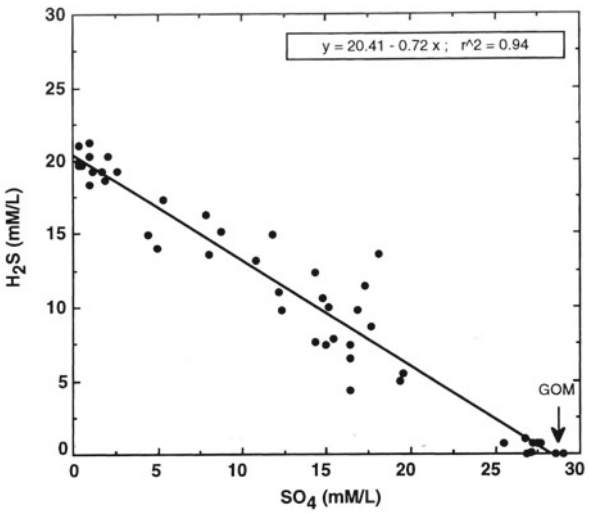

Fig. 5. Relationship between SO_4 and H_2S concentrations in pore fluids from the northern Gulf of Mexico seep sediments (Fu and Aharon, unpubl. data). *Arrow* indicates sulfate value in seep-free Gulf of Mexico waters. About 28% of H_2S generated by microbial sulfate reduction is removed into solid mineral sulfides deposited in sediments and native sulfur globules stored in chemolithotrophs

available in seeps (i.e., POM and/or crude oil fractions) into metabolites desirable to methanogens (e.g., acetate, carbon dioxide and molecular hydrogen) as follows:

$$3CH_2O + H_2O \rightarrow H_3COOH + CO_2 + 2H_2 \quad (4)$$

In anoxic sediments, methanogens are outcompeted by sulfate reducers in their quest for nutrients and therefore the methanogenic zone typically underlies the sediment layer exhibiting sulfate-reducing activity (Irwin et al. 1977; Ehrlich 1990). Methane formation by methanogens during anaerobic respiration in seeps is represented by the following exothermic chemical reactions (modified from Kaplan 1994):

1. Acetate fermentation

$$CH_3COOH \rightarrow CH_4 + CO_2 \quad (5)$$

2. CO_2 reduction

$$4H_2 + CO_2 = CH_4 + 2H_2O \quad (6)$$

Although the exact position of methane-forming bacteria in the seep sediment profiles has not yet been established, their effect on the alteration of pore fluid chemistries is well known. Methane is ubiquitous in pore fluids from all seep settings at levels varying from 4.0 and 6.7 μM in the deep seeps of the Nankai Trough and Oregon subduction zone, respectively (Gamo et al. 1992; Suess and Whiticar 1989) to 780 μM in the shallow seeps off the coast of Denmark (Dando et al. 1994a). In spite of its low solubility in water (3.5 ml/100 ml or 156.3 μM at STP, Ehrlich 1990), pressure buildup of methane in seep sediments is common and causes large gas bubbles to escape. Production of biogenic methane within the seep sediments, as opposed to transport from distant reservoirs, can be recognized by the large carbon isotope partitioning occurring between the CH_4 and CO_2 (on the order of 70‰, Kaplan 1994), the former showing anomalous depletions in the ^{13}C isotope typical of biogenically derived methane (−45 to −90‰) whereas the latter displays unusual ^{13}C enrichments.

4.3 Aerobic Microbial Oxidation of Sulfide and Methane

Sulfide-oxidizing bacteria (thiotrophs) and methane-oxidizing bacteria (methanotrophs), recycling reduced metabolic wastes generated by anaerobes within the sediment, are important constituents of the surficial seep habitat. A prominent group of sulfide oxidizers are the Beggiatocea, which live in mats at the seep/water interface (Fig. 3A). *Beggiatoa* derives energy to metabolize CO_2 from oxidation of H_2S, using O_2 as the terminal electron acceptor, and deposit S^o granules resulting from sulfide oxidation in the cells external to the cytoplasmic membrane (Fig. 3G; Larkin et al. 1994). These internal sulfur granules can serve as stored energy and be further oxidized when sulfide is limited (Ehrlich 1990; Larkin et al. 1994). Also common in seep habitats are the symbiotic sulfide-oxidizing bacteria living in epithelial cells of vestimentiferan tube worms (Fig. 3B), and in vesycomyid, thyasirid, solemyid and lucinid clams (Felbeck et al. 1981; Southward et al. 1981; Cavanaugh 1983; Fisher and Hand 1984). The reduced sulfur is a source of energy and reducing power for these symbiotic chemolithotrophs which generally fix CO_2 by the Calvin-Benson cycle and share some of the carbon they assimilate with their host (Ehrlich 1990).

In methane-rich seeps, only a small fraction of the methane is oxidized to CO_2 within the anoxic sediment without the benefit of O_2. The largest fraction of the methane, which is not trapped as a solid hydrate, escapes into the oxygen-rich water column overlying the seeps and is oxidized to CO_2 by aerobic methanotrophs living either as symbionts in the gill epithelial cells of mussels (*Bathymodiolus* sp., Fig. 3C) (Childress et al. 1986; Fisher et al. 1987; Cavanaugh et al. 1987) or as free-living aggregates (LaRock et al. 1994; Hyun et al. 1997). Studies have also indicated that methanothrophs assimilate up to 30% of their carbon in the form of CO_2 (Ehrlich 1990). The chemical reactions depicting microbial sulfide and methane oxidation pathways are as follows:

1. Sulfide oxidation

$$H_2S + 1/2O_2 = S^o + H_2O \quad (7)$$

2. Methane oxidation

$$CH_4 + 2O_2 = CO_2 + 2H_2O \quad (8)$$

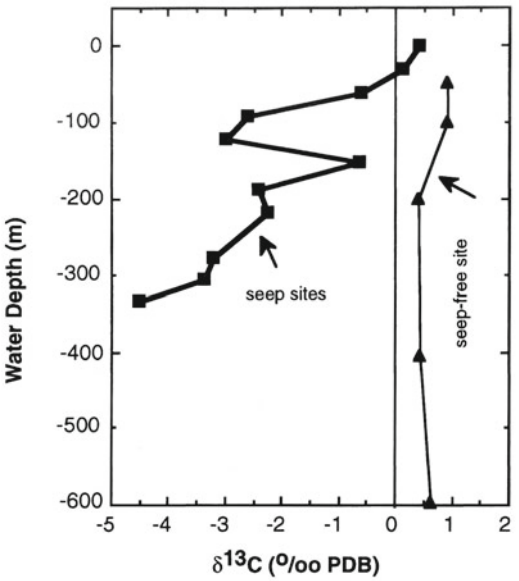

Fig. 6. Transient record of microbial processes imprinted on the water column overlying seeps. Contrasting $\delta^{13}C$ depth profiles above active seeps (*squares*) and control seep-free site (*triangles*) in the northern Gulf of Mexico (modified from Aharon et al. 1992). The negative $\delta^{13}C$ anomalies above seeps are attributed to methane oxidation by free-living methanotrophs (LaRock et al. 1994; Hyun et al. 1997)

Chemical alterations attributed to the thiotrophic and methanotrophic microbial activities in the surficial pore fluids and water column overlying the seeps consist of: (1) declining H_2S and CH_4 levels caused by microbial consumption via Eqs. (7) and (8), respectively; (2) declining CO_2 levels related to microbial metabolism, and (3) CO_2 enrichments caused by the respiration of the methanotrophs and leading to increased DIC levels, decreased pH and negative $\delta^{13}C$ shifts (Fig. 6).

5 Carbon Flow in Seeps

Prominent among the types of reduced carbon substrates in seeps are: (1) fresh organic matter of either planktic or chemosynthetic origin, (2) fossil organic matter of terrestrial or marine origin that has undergone bacterial degradation, and (3) fresh and/or biodegraded crude oil, and (4) gas hydrocarbons ($C_1 - C_5$) of thermogenic origin and/or methane (C_1) of biogenic origin. Fresh POM of planktic origin has a typical C/N weight ratio of 6.4 (Levorsen 1967), while chemosynthetically derived POM is slightly more enriched in nitrogen and has a C/N ratio of 4.8 (Paull et al. 1992). POMs of terrestrial or marine origin that have undergone microbial degradation are low in nitrogen (typical C/N ratios of 15–30, Paull et al. 1992) whereas kerogens derived from ancient sediments and crude oils are strongly depleted in nitrogen (C/N ratios of 243 and 213, respectively, Levorsen 1967). Therefore, in the simplest case, accumulation of NH_4^+ in the anoxic pore fluids provides a sensitive indicator for the type of carbon substrate oxidized by microbial sulfate reducers. For example, ammonia concentrations exceeding that of nitrogen dissolved in seawater and accompanied by sulfate deficiencies were measured in the seep pore fluids of the Oregon subduction zone (up to 1.5 mM, Suess and Whiticar 1989), Florida Escarpment (up to 4.5 mM, Chanton et al. 1991) and Sagami Trough (up to 1.8 mM, Masuzawa et al. 1992), indicating that a fraction of nitrogen-rich POM serves in these seeps as carbon substrate for the sulfate-reducing bacteria. On the other hand, anaerobic oxidation of hydrocarbons in crude oil by sulfate-reducing bacteria would produce an insignificant amount of ammonia because of excess carbon and impoverished nitrogen contents (Aharon and Fu, unpubl. data).

In more complex cases, an appraisal of carbonate species dissolved in the pore fluids and their $\delta^{13}C$ compositions is also required. Carbonate alkalinity (Alk_c) and DIC are two variables that describe well the dissolved carbonate species in pore fluids of seeps (Aharon et al. 1992).

$$Alk_c = HCO_3^- + 2CO_3^{2-} \quad (9)$$

$$DIC = HCO_3^- + CO_3^{2-} + CO_2aq \quad (10)$$

Carbonate alkalinity, expressed in units of meq (meq/l), is a measure of the concentration of the negatively charged carbonate ions that interact with H^+, whereas DIC is the sum of concentrations of all dissolved carbon species expressed in units of mM (mmol/l). Carbon forms derived from microbial oxidation processes, e.g., Eqs. (1) – (3), (5) and (8) above, increase alkalinity and/or DIC in the pore fluids and under favorable circumstances may allow the tracing of carbon back to its source. An additional constraint on the source of carbon is provided by the $\delta^{13}C$ of DIC because of distinct isotope differences between organic and inorganic sources (Aharon et al. 1992). It is therefore feasible, using the coupling between dissolved carbonate parameters, their $\delta^{13}C$ compositions and the amount of residual sulfate, to distinguish between the carbon sources and specific pathways of bacterial CO_2 generation and migration within the seep sediments.

Equations (1) – (3) exhibit stoichiometric characteristics of sufficient difference to allow us to make a distinction between carbon substrates on the basis of Alk_c-DIC-SO_4 relationships. For example, a methane substrate can be inferred if the seep, pore fluid assays converge along the 1 : 1 line in coordinates of DIC and SO_4 (Fig. 7A) and along the 2 : 1 line in coordinates of Alk_c and DIC (Fig. 7B). This can be seen in Eq. (3), where a mole of CO_3^{2-} is released into the pore fluid for each mole of SO_4^{2-} consumed, which in turn affects the carbonate alkalinity by two units and DIC by one unit.

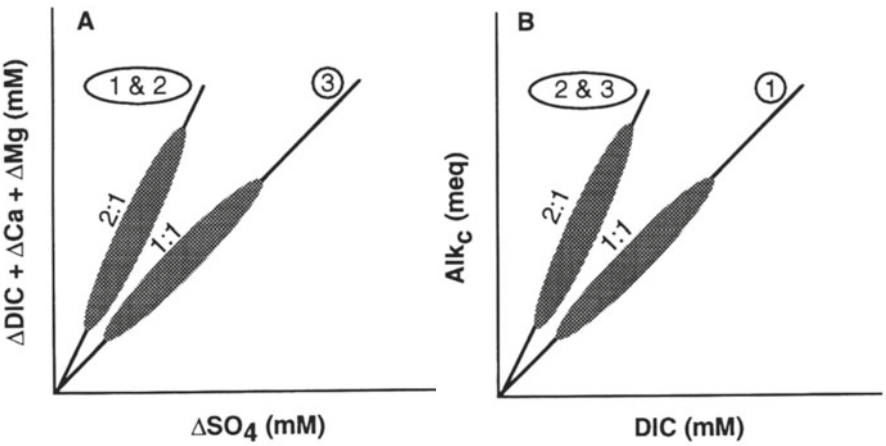

Fig. 7A,B. Geochemical criteria based on alkalinity/DIC/SO_4 relationships in pore fluids allowing distinction between specific microbial pathways and identification of the carbon substrate common in seeps. **A** Departure of pore fluid SO_4 and DIC values (corrected for carbonate deposition through Ca and Mg deficiencies) relative to a seawater source converge along lines with slopes of 1 and 2 when sulfate reducing bacteria use methane-derived carbon (Eq. 3 in text) and POM-derived carbon sources, respectively (Eqs. 1, 2). **B** Pore fluid data transporting anaerobic sulfate reduction products form lines with slopes of 1 and 2 in Alk_c and DIC coordinates when the carbon is derived from a nitrogen-poor POM source (Eq. 1) and nitrogen-rich POM and/or methane-derived carbon sources, respectively (Eqs. 2, 3). Northern Gulf of Mexico seep pore fluids yield two sets of data forming lines with slopes of 1 and 2 suggesting that methane and crude oil are concurrently used by bacteria as carbon substrates during anaerobic sulfate reduction

Conversely, a nitrogen-poor POM or crude oil substrate would be recognized by the pore fluids clustering along the 1 : 1 line in coordinates of Alk_c and DIC and along the 2 : 1 line in the DIC/SO_4 diagram. Nitrogen-rich POM substrates can be identified by the presence of high levels of ammonia and by the convergence of the pore fluid assays along the 2:1 lines in both Alk_c/DIC and DIC/SO_4 coordinates (Fig. 7).

Reports of complete pore fluid chemistry assays, allowing recognition of the carbon substrates utilized in seeps, are still rare. On the basis of considerations similar to the ones in the preceding paragraphs, Masuzawa et al. (1992) have concluded that sulfate reduction using methane as the energy source is active within the seep sediments of the Sagami Trough, whereas Suess and Whiticar (1989) and Paull et al. (1992) have concluded that pore fluid chemistries in sediments from the Oregon subduction zone and Florida Escarpment are compatible with microbially mediated oxidation of both nitrogen-rich POM and biogenic methane.

The nature of the carbon contributed to the pore fluids by microbial processes can also be evaluated on the basis of the relation between DIC values and their $\delta^{13}C$ compositions. For example, three sources of carbon and at least two microbial pathways can be distinguished in pore fluids from the northern Gulf of Mexico seeps (Fig. 8) on the basis of their DIC/$\delta^{13}C$ relationships, as follows: (1) precursor seawater DIC pool; (2) excess DIC values displaying highly ^{13}C-enriched compositions typical of methanogenesis; Eqs. (5) and (6), and (3) linear arrays of DIC/$\delta^{13}C$ values representing mixing lines between seawater and microbial sulfate reduction-derived carbon end members (lines 1, 2, Fig. 8). In the latter case, the $\delta^{13}C$ values ($\delta^{13}C_{sr}$) of the two distinct DIC sources added from sulfate reduction can be estimated from simple mass balance equations (see Paull et al. 1992) under the following assumptions: (a) the sample with the highest DIC and lowest $\delta^{13}C$ value is representative of the pore fluid marked by the most intense microbial overprint, (b) the observed DIC enrichments are added to the pre-existing seawater pool, and (c) carbon isotopic fractionations during the microbial sulfate reduction are small and insignificant compared with the isotope fractionations at the carbon source. These relationships can be described in the following equation:

$$\delta^{13}C_{sr} = (DIC_{pf}\delta^{13}C_{pf} - DIC_{sw}\delta^{13}C_{sw})/(DIC_{pf} - DIC_{sw}) \quad (11)$$

where, pf and sw stand for pore fluid and seawater carbon pools, respectively. Viewed this way, one obtains

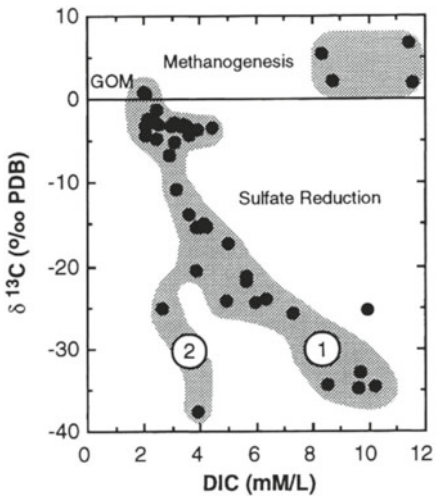

Fig. 8. Microbial sulfate reduction and methanogenesis leave distinct marks on the pore fluid DIC and their $\delta^{13}C$ compositions in seeps from the northern Gulf of Mexico. Microbial sulfate reduction data are compatible with two carbon sources having $\delta^{13}C$ values of −44‰ (*line 1*) and −78‰ (*line 2*), respectively (see text)

$\delta^{13}C$ values of −44.1‰ (line 1) and −77.9‰ (line 2) for two distinct types of carbon released into the pore fluids by sulfate reduction (likely crude oil and methane, respectively) using the following empirically derived values: DIC_{pf} = 10 mM; $\delta^{13}C_{pf}$ = -35‰ (line 1) and DIC_{pf} = 3.9 mM; $\delta^{13}C_{pf}$ = -37.6‰ (line 2); DIC_{sw} = 2.04 mM, $\delta^{13}C_{sw}$ = 0.63‰ (Gulf of Mexico bottom waters away from seeps, Aharon et al. 1992).

On the basis of $\delta^{13}C$ values derived here, it appears that pore fluid chemistries from the northern Gulf of Mexico seeps are compatible with concurrent microbially mediated oxidation of nitrogen-poor crude oils (−44.1‰) and methane of uncertain origin or residual methane recycled through the gas hydrates (−77.9‰). Strongly elevated baselines (UCM, unresolved complex mixtures) and weak or absent n-alkanes and isoprenoids, commonly observed in hydrocarbons underlying chemosynthetic communities consuming H_2S (primarily *Beggiatoa* sp.), led Sassen et al. (1994) to conclude that seeping oils are intensely altered by microbial oxidation processes. Recent studies (Rueter et al. 1994) have indicated that, contrary to general belief (e.g., Nazina et al. 1985), sulfate-reducing bacteria can directly biodegrade crude oil anaerobically by utilizing aliphatic and aromatic hydrocarbons as electron donors. Using a similar model, Paull et al. (1992) have obtained a $\delta^{13}C$ value of −73.5‰ for microbial-derived carbon from the Florida Escarpment seeps that is compatible with a pathway of anaerobic sulfate reduction using methane-derived carbon. It must be noted, however, that isotopic fractionation during anaerobic methane oxidation is on the order of 10–15‰, where the lighter isotope is oxidized preferentially (Barker and Fritz 1981; Alperin and Reeburgh 1988). Inclusion of this isotope fractionation effect adds uncertainties to the evaluation of the nature and pathway of microbially recycled carbon in seeps.

6 Permanent Records of Microbial Processes in Seeps

Many of the massive carbonate buildups consist of a framework of calcareous shells of dead chemosynthetic clams and mussels (Fig. 3D) that have been lithified by carbonate (Fig. 3H) and sulfide cements (Fig. 3I). These carbonate buildups are the most ubiquitous geological products of modern seeps and preserve detailed records of microbial processes long after seepage has ceased and the chemosynthetic communities have vanished (Clari and Martire, this Vol.). Seep carbonates are therefore of great value for identification and reconstruction of hydrocarbon seepage in the geologic record (Aharon 1994a; Aharon et al. 1997). The northern Gulf of Mexico seep province is exceptional in the sense that, in addition to massive carbonates, it also exhibits massive deposits of barite consisting of chimneys and crusts which are deposited from barium-rich formation waters advecting from depth (Fu et al. 1994, 1996). Because of the rarity of barite associated with seeps relative to the ubiquitous carbonate deposits, and the uncertainties concerning the links between microbial processes and barite deposition, the former are excluded from any further discussion.

Two questions need to be answered concerning the permanent records of microbial processes in seeps: (1) Why are carbonate deposits commonly associated with seeps? (2) How can the records of the microbial processes they contain be deciphered? The answer to the first question implies that pore fluids in seeps are supersaturated with respect to carbonate, the degree of saturation being a function of the relative [Ca] and [CO_3] ion concentrations:

$$Ca^{2+} + CO_3^{2-} \rightarrow CaCO_3 \qquad (12)$$

In the vast majority of seeps the pore fluids originating from the overlying seawater contain a fixed amount of Ca (and Mg), and so the only way to achieve supersaturation is to vary the amount and speciation of the dissolved carbonate produced during microbial processes. Under these circumstances there are two factors that exert an appreciable control on the precipitation of $CaCO_3$, namely (1) loss of CO_2 from pore fluids, and (2) establishment of high alkalinity conditions.

Removal of CO_2 from a pore fluid solution enriched in bicarbonate as a result of anaerobic sulfate reduction (Eq. 1) will cause an increase in carbonate ion concentration:

$$2HCO_3 \rightarrow CO_2 + H_2O + CO_3^{2-} \qquad (13)$$

The CO_2 removal could be caused by either release of excess pore pressure during fluid venting, as proposed by Han and Suess (1989), or by CO_2 fixation by chemolithotrophs using the Calvin-Benson cycle (this study). Either one of the two processes above will lead to carbonate precipitation in seeps.

Development of high alkalinity in the pore fluids, resulting from release of OH^- and HS^- during microbial sulfate reduction (Eqs. 1–3), would also enhance carbonate precipitation because of higher pH shifting the carbonate equilibria toward the carbonate ion. In addition, conversion of CO_2 to carbonate can be derived by hydrolysis of ammonia produced from organic nitrogen compounds (Eq. 3) by actively metabolizing cells. This process typically results in aragonite formation on the bacteria cells, which in turn may serve as nuclei for further $CaCO_3$ precipitation. Ehrlich (1990) proposed the hydrolysis of microbially derived ammonia as the mechanism for oolite formation and I suggest that such a model be extended to explain zoned botryoidal aragonite cements in seep carbonates (Fig. 3H). Microbial processes could not only lead to precipitation of carbonates but also to episodic dissolution. For example,

the CO_2 produced during methanogenesis (Eq. 5) and methane oxidation (Eq. 8) could lower the degree of saturation of pore fluids to carbonates by lowering the pH and consequently causing partial dissolution of carbonates.

Botryoidal aragonite splay cements (Fig. 3H) are among the most common textural features occurring in seep carbonates (Hovland et al. 1987; Ritger et al. 1987; Roberts and Aharon 1994) and have been interpreted as products of microbial processes on account of their: (1) anomalously negative $\delta^{13}C$ values, suggesting a methane-derived carbon source (Aharon and Sen Gupta 1994), and (2) the presence of dead bacterial bodies filling the dark centers of the botryoids, which are suspected of acting as seeding sites for carbonate deposition (Roberts et al. 1992). These observations support previous morphological and physiological studies showing that bacteria may cause precipitation of $CaCO_3$ mostly in the immediate environment around their cells (Krumbein 1974; Ehrlich 1990). Episodic phases of dissolution interrupting carbonate precipitation can be recognized on the basis of distinct dissolution lines imprinted on the isopachous botryoids (Fig. 3H). Botryoid aragonite cements coexisting with opaque sulfides are also common in seep carbonates, suggesting that anaerobic sulfate reduction accompanied by carbonate ion enrichment occurred in the pore fluids (Fig. 3I). Removal of H_2S from pore fluids into solid sulfides and/or H_2S consumption by sulfur-oxidizing chemolithotrophs is documented by the observed shift of the H_2S/SO_4 ratio from a predicted slope of 1 (Eqs. 1–3) to a slope substantially lower than 1 (Fig. 5). Viewed this way, it can be estimated that about 28% of sulfide has been removed from the pore fluids as sulfide (Fig. 3I) and/or native sulfur (Fig. 3G) in the northern Gulf of Mexico seeps.

7 What We Still Do Not Know About Processes in Seeps

While the past decade has witnessed a proliferation in the number of discoveries of new seeps from active and passive continental margin settings, inquiries on processes and products in general, and microbial aspects in particular, have lagged behind significantly. The time is ripe to move from a descriptive to a quantitative mode. Hydrocarbon fluxes, frequency of seepage, rates of anaerobic and aerobic bacterial respiration, transport rates of metabolites, are but a few of the parameters needed to be unveiled in order to assess the impact of seeps on marine habitats and to establish their role in the cycling of carbon, sulfur and nitrogen. Presently there are only few complete assays of pore fluid chemistries in seeps reported in the literature, and many more are needed in order to appraise the interaction between the various microbial processes and establish the nature of their substrates.

Another important issue that needs improvement is our present impairment in deciphering the permanent records of microbial processes imprinted in geological products of seeps. For this purpose, a link must be established between pore fluid chemistry alterations attributed to specific bacteria and unique textures containing bacterial imprints. Such an association can be best documented by investigating prolific extant seeps exhibiting multiple hydrocarbon sources, luxuriant symbiont-bearing benthic fauna, and varied massive carbonates. Quantifying the effect of bacteria on the partition of major and trace elements between pore fluids and carbonates can be of exceptional benefit in the quest to establish the influence of microbial processes on the precipitation and sequestering of metals in seeps. In addition, laboratory simulations of bacterial effects on crystal habits of carbonates (e.g., Buczynski and Chafetz 1991) and barites, their mineralogies and textures could prove helpful in establishing the links between microbial processes and products and enhance our ability to decipher microbial imprints on geologic materials.

Acknowledgements. Discussions with Michael Lang, Baoshun Fu, Paul LaRock, John Larkin and Paul Dando on microbial processes in seeps helped clarify some of the ideas presented in this study. Paul LaRock and an anonymous reviewer are thanked for their constructive criticisms. Funding from the Mineral Management Service (MMS) provides the support to seek answers to some of the questions posed in the chapter.

References

Aharon P, Graber ER, Roberts HH (1992) Dissolved carbon and $\delta^{13}C$ anomalies in the water column caused by hydrocarbon seeps on the northwestern Gulf of Mexico slope. Geo-Marine Lett 12:33–40

Aharon P, Sen Gupta BK (1994) Bathymetric reconstructions of the Miocene-age "calcari a Lucina" (northern Apennines, Italy) from oxygen isotopes and benthic Foraminifera. Geo-Marine Lett 14:219–230

Aharon P (1994a) Geology and biology of modern and ancient submarine hydrocarbon seeps and vents: An introduction. Geo-Marine Lett 14:69–73

Aharon P (1994b) Carbon and oxygen isotope tracers of submarine hydrocarbon emissions: Northern Gulf of Mexico. Isr J Earth Sci 43:157–164

Aharon P, Schwarcz HP, Roberts HH (1997) Radiometric dating of submarine hydrocarbon seeps in the Gulf of Mexico. Geol Soc Am Bull 109 (5):568–579

Alperin MJ, Reeburgh WS (1988) Carbon and hydrogen fractionation resulting from anaerobic methane oxidation. Global Biochem Cycles 2:279–288

Amann R, Ludwig W, Schleifer KH (1995) Phylogenetic identification and in-situ detection of individual microbial cells without cultivation. Microbiol Rev 59:143–169

Anderson RK, Scalan RS, Parker PL (1983) Seep oil and gas in Gulf of Mexico slope sediment. Science 222:619–622

Barker JF, Fritz P (1981) Carbon isotope fractionation during microbial methane oxidation. Nature 293:289–291

Brooks JM, Kennicutt MC, Fisher CR, Macko SA, Cole K, Childress JJ, Bidigare RR, Vetter RD (1987) Deep-sea hydrocarbon seep

communities: Evidence for energy and nutritional carbon sources. Science 238:1138–1142
Buczynski C, Chafetz HS (1991) Habitat of bacterially induced precipitates of calcium carbonate and the influence of medium viscosity on mineralogy. J Sediment Petrol 61:226–233
Carney RS (1994) Consideration of the oasis analogy for chemosynthetic communities at Gulf of Mexico hydrocarbon vents. Geo-Marine Lett 14:149–159
Cavanaugh CM (1983) Symbiotic chemoautotrophic bacteria in marine invertebrates from sulfide-rich habitats. Nature 302: 58–61
Cavanaugh CM, Levering RR, Maki JS, Mitchell R, Lidstrom ME (1987) Symbiosis of methylotrophic bacteria and deep-sea mussels. Nature 325:346–348
Chanton JP, Martens CS, Paull CK (1991) Control of pore water at the base of the Florida Escarpment by processes within the platform. Nature 349:229–231
Childress JJ, Fisher CR, Brooks JM, Kennicutt MC, Bidigare R, Anderson AE (1986) A methanotrophic marine molluscan (Bivalvia, Mytilidae) symbiosis: Mussels fueled by gas. Science 233:1306–1308
Craig H (1957) Isotopic standards for carbon and oxygen and correction factors for mass spectrometric analysis of carbon dioxide. Geochim Cosmochim Acta 12:133–149
Dando PR, Jensen P, O'Hara SCM, Niven SJ, Schmaljohann R, Schuster U ,Taylor LJ (1994a) The effects of methane seepage at an intertidal/shallow subtidal site on the shore of the Kattegat, Vendsyssel. Denmark. Bull Geol Soc Denmark 41:65–79
Dando PR, O'Hara SCM, Schuster U, Taylor LJ, Clayton CJ, Baylis S, Laier T (1994b) Gas seepage from a carbonate-cemented sandstone reef on the Kattegat coast of Denmark. Mar Petrol Geol 11 (2):182–189
Ehrlich HL (1990) Geomicrobiology. Marcel Dekker, New York
Felbeck H, Childress JJ, Somero GN (1981) Calvin-Benson cycle and sulfide-oxidation enzymes in animals from sulfide-rich habitats. Nature 293:291–293
Fisher CR, Hand SC (1984) Chemoautotrophic symbionts in the bivalve Lucina floridana from seagrass beds. Biol Bull Mar Biol Lab Woods Hole 167:445–459
Fisher CR, Childress JJ, Oremland RS, Bidigare RR (1987) The importance of methane and thiosulfate in the metabolism of the bacterial symbionts of two deep-sea mussels. Mar Biol 96:59–71
Fu B, Aharon P, Byerly GR, Roberts HH (1994) Barite chimneys on the Gulf of Mexico slope: Initial report on their petrography and geochemistry. Geo-Marine Lett 14:81–87
Fu B, Aharon P, Van Gent DL, Scott LM (1996) Anomalously high ^{226}Ra in fluids advecting to the sea floor: a new radioactive source in the Gulf of Mexico. Trans Gulf Coast Assoc Geol Soc 46:125–131
Fu B, Aharon P (1997) Pore-fluid chemistry reveal processes occurring in hydrocarbon seeps from deepwater Gulf of Mexico. Trans Gulf Coast Assoc Geol Soc 47:653
Gamo T, Sakai H, Ishibashi J, Shitashima K, Boulègue J (1992) Methane, ethane and total inorganic carbon in fluid samples taken during the 1989 Kaiko-Nankai project. Earth Planet Sci Lett 109:383–390
Graber ER, Aharon P (1991) An improved microextraction technique for measuring dissolved inorganic carbon (DIC), $\delta^{13}C$ (DIC), and $\delta^{18}O$ (H_2O) from milliliter-size water samples. Chem Geol (Isotope Geosci Sect) 94:137–144
Han MW, Suess E (1989) Subduction-induced pore fluid venting and the formation of authigenic carbonates along the Cascadia continental margin: implications for the global Ca-cycle. Palaeogeogr Palaeoclimatol Palaeoecol 71:97–118
Hovland M, Talbot MR, Qvale H, Olaussen S, Aasberg L (1987) Methane-related carbonate cements in pockmarks of the North Sea. J Sediment Petrol 57:881–892
Hyun JH, Bennison BW, LaRock PA (1997) The formation of large bacterial aggregates at depth within the Louisiana hydrocarbon seep zone. Microb Ecol 33:216–222
Irwin I, Coleman ML, Curtis CD (1977) Isotopic evidence for the source of diagenetic carbonate during burial of organic-rich sediments. Nature 269:209–213
Jahnke BA (1988) A simple, reliable, and inexpensive pore-water sampler. Limnol Oceanogr 33 (3):483–487
Jasper JP, Gagosian RB (1989) Glacial-interglacial climatically forced δ^{13} C variations in sedimentary organic matter. Nature 342:60–62
Jones ML (1981) Riftia pachyptila Jones: observations on the vestimentiferan worm from the Galapagos rift. Science 213:333–336
Jørgensen NO (1976) Recent high magnesian calcite/aragonite cementation of beach and submarine sediments from Denmark. J Sediment Petrol 46 (4):940–951
Kaplan IR (1994) Identification of formation processes and source of biogenic gas seeps. Isr J Earth Sci 43:297–308
Kennicutt MC, Brooks JM, Bidigare RR, Fay RR, Wade TL, McDonald TJ (1985) Vent-type taxa in a hydrocarbon seep region on the Louisiana slope. Nature 317:351–353
Kennicutt MC, McDonald TJ, Comet PA, Denoux GJ, Brooks JM (1992) The origins of petroleum in the northern Gulf of Mexico. Geochim Cosmochim Acta 56:1259–1280
Krumbein WE (1974) Precipitation of aragonite on the surface of marine bacteria. Naturwissenschaften 61:167
Kulm LD et al. (1986) Oregon subduction zone: venting, fauna and carbonates. Science 231:561–566
Larkin J, Aharon P, Henk MC (1994) Beggiatoa in microbial mats at hydrocarbon vents in the Gulf of Mexico and Warm Mineral Springs, Florida. Geo-Marine Lett 14:97–103
LaRock PA, Hyun JH, Bennison BW (1994) Bacterioplankton growth and production at the Louisiana hydrocarbon seeps. Geo-Marine Lett 14:104–109
Levorsen AI (1967) Geology of petroleum. WH Freeman, San Francisco
Masuzawa T, Handa N, Kitagawa H, Kusakabe M (1992) Sulfate reduction using methane in sediments beneath a bathyal "cold seep" giant clam community off Hatsushima Island, Sagami Bay, Japan. Earth Planet Sci Lett 110:39–50
Nazina TN, Rozanova EP, Kuznetsov SI (1985) Microbial oil transformation processes accompanied by methane and hydrogen sulfide formation. Geomicrobiol J 4 (2):103–130
Paull CK, Hecker B, Commeau R, Freeman-Lynde RP, Neumann C, Corso WP, Golubic S, Hook JE, Sikes E , Curray J (1984) Biological communities at the Florida Escarpment resemble hydrocarbon vent taxa. Science 226:965–967
Paull CK, Chanton JP, Neumann AC, Coston JA, Martens CS, Showers W (1992) Indicators of methane-derived carbonates and chemosynthetic organic carbon deposits: examples from the Florida Escarpment. Palaios 7:361–375
Rice DD (1980) Chemical and isotopic evidence of the origins of natural gases in offshore Gulf of Mexico. Trans Gulf Coast Assoc Geol Soc 30:202–213
Ritger S, Carson B, Suess E (1987) Methane-derived authigenic carbonates formed by subduction-induced pore-water expulsion along the Oregon/Washington margin. Geol Soc Am Bull 98:147–156
Roberts HH, Aharon P, Walsh MM (1992) Cold-seep carbonates of the Louisiana continental slope to basin floor. In: Rezak R, Lavoie D (eds) Carbonate microfabrics. Springer, Berlin Heidelberg New York, pp 95–104
Roberts HH, Aharon P (1994) Hydrocarbon-derived carbonate buildups of the northern Gulf of Mexico continental slope: a review of submersible investigations. Geo-Marine Lett 14:135–148
Rueter P, Rabus R, Wilkes H, Aeckersberg F, Rainey FA, Jannasch HW, Widdel F (1994) Anaerobic oxidation of hydrocarbons in crude oil by new types of sulphate-reducing bacteria. Nature 372:455–458
Sand MD, LaRock PA, Hodson RE (1975) Radioisotope assay for the quantification of sulfate reducing bacteria in sediment and water. Appl Microbiol 29:626–634
Sassen R, Roberts H, Aharon P, Larkin J, Chinn E, Carney R (1993) Chemosynthetic bacterial mats at cold hydrocarbon seeps, Gulf of Mexico continental slope. Organic Geochem 20:77–89
Sassen R, MacDonald IR, Requejo AG, Guinasso NL, Kennicutt MC, Sweet ST, Brooks JM (1994) Organic geochemistry of sediments from chemosynthetic communities, Gulf of Mexico slope. Geo-Marine Lett 14:110–119
Sassen R, MacDonald IR (1997) Hydrocarbons of experimental and natural gas hydrates, Gulf of Mexico continental slope. Organic Geochem 26 (3/4):289–293

Schamljohann R, Flügel HJ (1987) Methane-oxidising bacteria in Pogonophora. Sarsia 72:91–98

Schamljohann R, Faber E, Whiticar MJ, Dando PR (1990) Co-existence of methane and sulphur-based endosymbioses between bacteria and invertebrates at a site in the Skagerrak. Mar Ecol Progr Ser 61:119–124

Southward AJ, Southward EC, Dando PR, Rau GH, Felbeck H, Flügel H (1981) Bacterial symbionts and low $^{13}C/^{12}C$ ratios in tissues of *Pogonophora* indicate unusual nutrition and metabolism. Nature 293:616–620

Suess E, Whiticar MJ (1989) Methane-derived CO_2 in pore fluids expelled from the Oregon subduction zone. Palaeogeogr Palaeoclimatol Palaeoecol 71:119–136

Microbial Contribution to Reefal Mud-Mounds in Ancient Deep-Water Settings: Evidence from the Cambrian

Brian R. Pratt

Department of Geological Sciences, University of Saskatchewan, 114 Science Place, Saskatoon, Saskatchewan, S7N 5E2, Canada

Abstract. Deep-water mud-mounds are reefs whose micrite-dominated frameworks have resulted from the activities of microbes. Clotted micrite thromboids and crusts of micritic filaments and other microfossils arise through calcification of near-pristine to degraded organic material. By contrast, biomicrite sheltering stromatactis cavities derives from sediment held in place by mats until stabilized by synsedimentary cementation. It is likely, too, that microbes have played a role in the precipitation of much of this lime mud. The relative importance of each of these mechanisms will have depended in large part upon the associated sediment-producing benthic community which, in turn, will have been governed by its evolutionary history and specific environmental factors. Proterozoic stromatolitic mud-mounds were succeeded in the Cambrian by thromboids. Biomicrite mud-mounds existed in the Early Cambrian but mass extinction caused this reef style to vanish until the Middle Ordovician when diversity was restored. Shelf margin frameworks in the depauperate Middle Cambrian to Early Ordovician interval are composed of calcified filaments.

1 Introduction

Mud-mounds are carbonate buildups composed dominantly of microcrystalline calcium carbonate. A rather wide variety of deposits has been collected under this term, ranging from prominent reefs to low-relief, detrital mud banks (see Monty et al. 1995). Reefal mud-mounds deposited in relatively deep water have been identified in strata as old as Paleoproterozoic (Beukes 1987). The youngest are Miocene (Braga et al. 1995), although analogous frameworks do occur in Holocene forereefs (James and Ginsburg 1979; Brachert and Dullo 1991). Here, using Cambrian examples, I summarize the constructional role of microbial components. I build upon the microbial evidence I perceived 15 years ago (Pratt 1982b), which has since been documented extensively (see Camoin 1995; Lees and Miller 1995; Monty 1995; Pratt 1995; Reitner and Neuweiler 1995; Pickard 1996). Essentially the full spectrum of Phanerozoic style mud-mound frameworks appeared in the Early Cambrian. However, extinctions then stripped the reefal benthos of its diversity (Pratt et al. 1998), such that Middle Cambrian to Lower Ordovician mud-mounds provide an instructive perspective on the microbial community in the absence of significant reef-derived detritus.

In this context, "deep" refers to the environment at and beyond the lower limits of storm wave base and light penetration. While these conditions are variable and difficult to gauge from independent lithologic evidence, depths of 50–150 m are commonly contemplated (e.g. Lees and Miller 1995). Isolated metre- to hectometre-, and even kilometre-size mud-mounds from these settings are encased abruptly in thin-bedded argillaceous limestones, sometimes with proximal flanking grainstones. They lack the windward-leeward facies zonation typical of shallow-water fringing and barrier reefs because lateral changes in turbulence were less pronounced. They may, however, exhibit vertical change in composition that reflects growth into shallower water. These mud-mounds often exhibit primary, centimetre- to decimetre-size cavities lined with fibrous marine calcite cement, forming structures generally called "stromatactis". Proterozoic mud-mounds are purely stromatolitic, whereas Phanerozoic ones contain bioclasts and sporadic sessile metazoans such as siliceous sponges and branching corals. Reefs in shallower settings tend to show an increasing proportion and diversity of these metazoans or, commonly in the case of stromatolites, enhanced lamination.

Buildups that grew in shallow water have been regarded traditionally as true "reefs" because they exhibit an easily identified "framework" composed of the in situ skeletons of sessile metazoan "framebuilders". Some recent reviews have thus differentiated such reefs from those buildups – variously microbial mounds, skeletal mounds, mud-mounds and biodetrital mounds – composed of dominantly microbial framework elements or bioclastic sediment moulded into piles. I have stressed (Pratt 1995), and so has Webb (1996), that such distinctions are unsatisfactory because microbial mud-mounds, with or without accompanying sessile metazoans, are reefs too, because they also developed a relatively rigid framework, even if deep-water versions were never tested by strong turbulence. Ancient shallow-water reefs with conspicuous metazoans usually exhibit encrusting elements, part or most of which is also microbial. Purely biodetrital mounds stand apart as allochthonous, unbound material: these are not reefs. Size is relevant ecologically, not to distinguish

R. E. Riding and S. M. Awramik (Eds.)
Microbial Sediments

reefs from mounds, but because changing topographic relief and water depth affected the reef-dwelling biota. The wide variety of biohermal facies probably defies a simple classification that does not obscure ecological relationships. Terms like "framestone", "bafflestone" and "bindstone" involve hazardous ecological interpretation (see Precht 1994) or are essentially synonymous with "boundstone" or "biolithite".

2 Taphonomy of Microbes in Reefs

Of the prokaryotes, the cyanobacteria may have achieved a fairly modern level of diversity during the Proterozoic (Knoll and Bauld 1989; Schopf 1994). However, it could be taken as axiomatic that the "Cambrian Explosion" brought about a radiation of other bacterial forms in tandem with what happened to multicellular life, as a broad range of new organic substrates were introduced (see also Pratt 1998a,b). In modern reefs bacteria occur as free-floating cells and cell aggregates or colonies, as cells and biofilms (including mats) on living organisms, bioclasts and sediments, as decomposers within tissues, fecal matter and soft sediments, and as bioeroders. Eubacteria include photoautotrophs, chemoautotrophs and heterotrophs. All cyanobacteria are photoautotrophs although some are facultative heterotrophs.

No prokaryotes are known to be obligate calcifiers, although calcification of cyanobacteria in freshwater and under experimental conditions points to some taxonomic control on mineralogy and crystallography (e.g. Merz 1992). Calcification of living eubacterial and cyanobacterial cells and secreted exopolymers has not been reported from modern marine reefs, suggesting that they neither form simply convenient substrates for precipitation nor induce it with metabolic byproducts in sea water. Cyanobacterial calcification seems, rather, to occur during decay and bacterial degradation of sheaths and cell contents, but the chemical and taxonomic controls and timing are only beginning to be understood (Reitner 1993). The same sort of biofilm or cell aggregate might calcify in one place on (or in) a reef but not in another because of complex biogeochemical factors operating in individual microhabitats. Given the volume, rapid growth rate and variability of microbial matter on a normal-marine reef, most of it was probably never prone to calcification. This may not have been the case, however, in some lacustrine reefs and those that developed in response to venting of methane-rich or hydrothermal fluids (Kauffman et al. 1996).

3 Microbial Activity in Cambrian Mud-Mounds

The foregoing discussion indicates that microbes operated on the finest of ecological, biogeochemical, temporal and spatial scales, such that most of the microbial biota has virtually no chance of preservation in limestones, especially after any recrystallization (Pratt 1994). Thus, the geologic record of the microbial contribution to framebuilding in deep-water reefal mud-mounds is inferred from: (1) problematic microfossils, (2) laminated structures, i.e. stromatoids, (3) clotted and fenestral micrite, i.e. thromboids, and (4) biomicrite with unoriented bioclasts (see also Pratt 1995).

3.1 Microbial Microfossils

Some mud-mounds are constructed by micritic microfossils which are accepted as having a microbial origin – structures that have been referred to as microbial "skeletons", "skeletal stromatolites", "dendrolites", and "calcimicrobes" (see Riding 1991), because relatively undegraded microbial material has been faithfully replicated by calcification. Middle Cambrian to Lower Ordovician frameworks along platform margins are composed of hemispheroids or cones of discontinuous, millimetre-thick crusts formed of prostrate tangles, meshes or rows of micritic tubes and filaments referable to *Girvanella* (Fig. 1A,B; James 1981; Pratt 1989). They are 10 – 30 mm in diameter, the large size supporting a cyanobacterial affinity. Individual domains of tubes grade laterally to those with ill-defined filaments and clotted micrite with fenestral porosity. Because these crusts typically lack much geopetal micrite, the observed gradation in the fidelity of filament preservation must reflect variation in the state of the organic substrate, not patchy sediment binding. Assuming environmental conditions were constant (although this may not be valid), the fact that the entire mat grew before the calcification event argues that permineralization affected cell walls or sheaths after death. Preserved tubes suggest prompt calcification, a matter of days after death (see Bartley 1996), whereas gradation to thinner micrite threads suggests some collapse of the filaments first or calcification just of trichomes. The clotted micrite is likely due to ragged and decayed substrates and patchy infestation by degrading eubacteria. Micron-wide organic filaments in these biolithites (Fig. 1C), and similar ones 3 – 10 μm wide in the Upper Silurian of Michigan (Coron and Textoris 1974), must be different taxa than those that calcified to form *Girvanella* because they are not pock-marked from crystal impregnation or encrustation. After the Early Ordovician, *Girvanella* is mainly seen as a bioclast in mud-mounds (Fig. 1G; Monty 1995, Fig. 4A – C); it has been

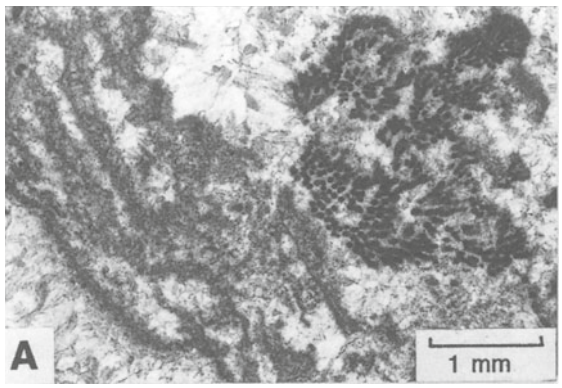
A
1 mm

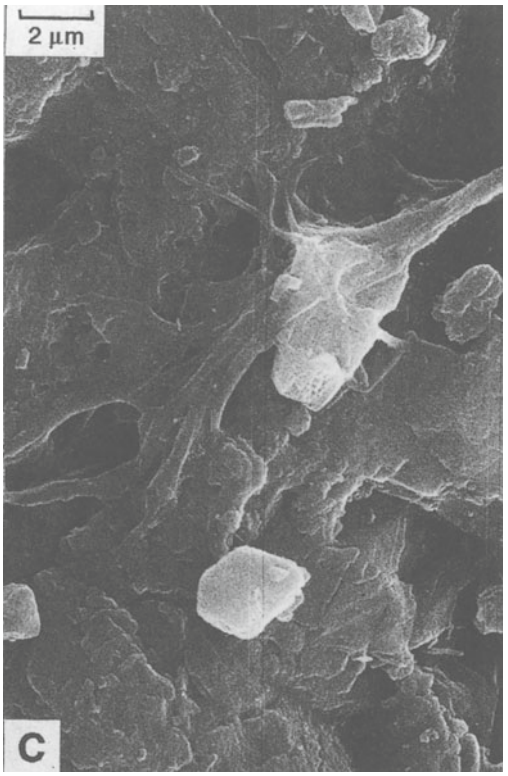
2 µm
C

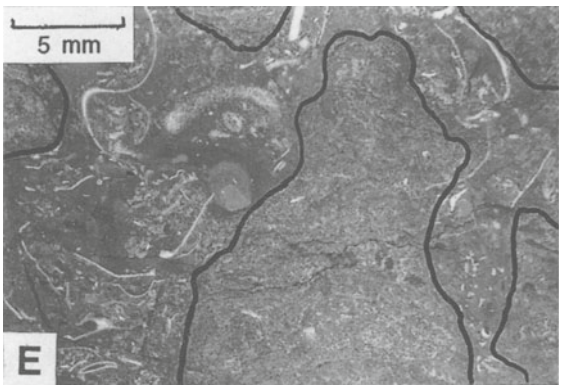
5 mm
E

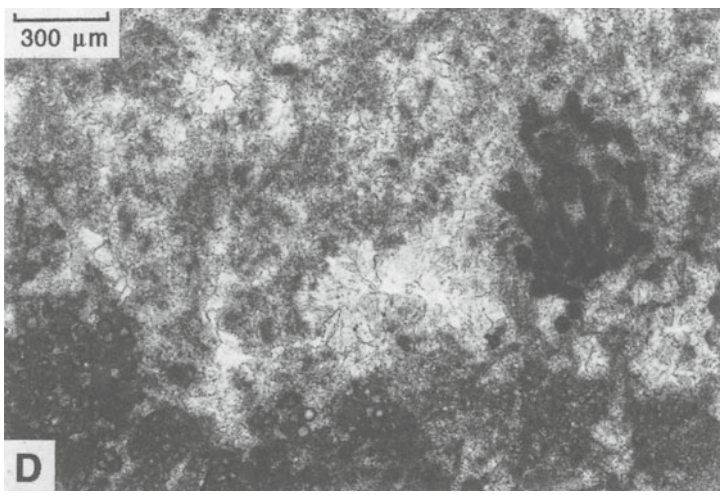
300 µm
D

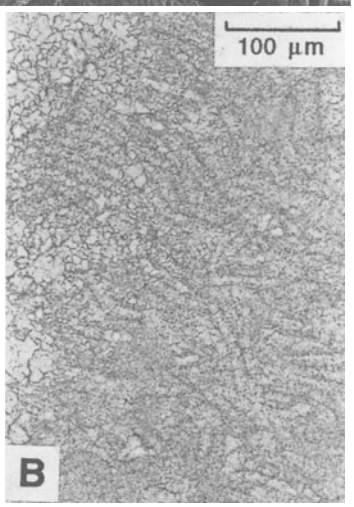
100 µm
B

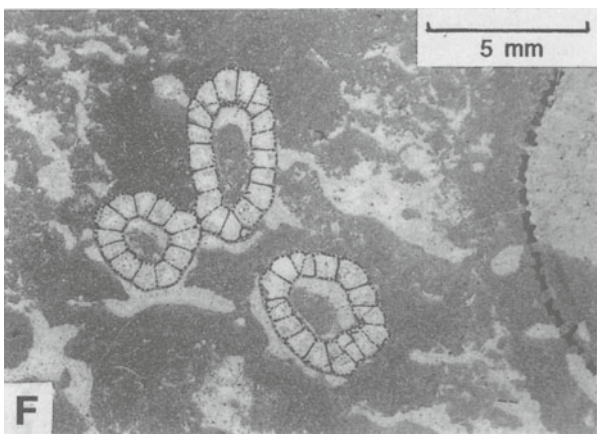
5 mm
F

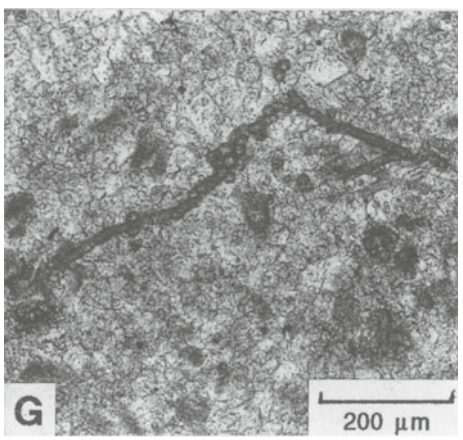
G
200 µm

observed in shallow-water reefs as young as Miocene (C. Perrin, pers. comm. 1996). Iron-oxidizing filamentous and coccoidal eubacteria observed in some mud-mounds did not participate in framebuilding (Bourque and Boulvain 1993).

Dendritic *Epiphyton* locally forms deep-water frameworks in the Middle Cambrian, but mainly it and its grape-like "sister" taxon, *Renalcis*, encrust cavities within Cambrian and Lower Ordovician *Girvanella*-dominated mud-mounds; similar but less well-defined examples have been observed in the Neoproterozoic and Upper Triassic (Pratt 1995). Uninterrupted cell growth, small shrinkage cracks, and presence of dense, micron-sized micrite clots suggest that they formed by the calcification of aggregates of small coccoidal cells that were dead but only barely starting to decay (Pratt 1984); this may not be strictly true if there were fluctuations in whatever environmental conditions that promoted calcification of living material. *Renalcis* and *Epiphyton* are absent in stromatactis after the Early Ordovician, and *Renalcis* occurs as a bioclast in Upper Devonian mud-mounds (Mamet and Boulvain 1992). These observations argue either that the microbial substrate responsible for these microfossils may have been mainly phototrophic and did not live in these cavities, or that it was simply not calcified before it degraded. However, *Renalcis* in neptunian fissures (Mamet and Boulvain 1988) points to chemotrophy in such cases. While success has been reported (Camoin et al. 1989), I have not yet been able to isolate coccoids ("nanobacteria") from *Epiphyton* and *Renalcis*.

A variety of other microbial elements may encrust mud-mound surfaces. Layers of hollow spheroidal cells 30–50 μm in diameter belonging to *Gemma* (Fig. 1D), which grade into clotted micrite, occur rarely in the Upper Cambrian (Pratt 1995). Millimetre-sized hemispheroids of radiating tubules referable to *Ortonella* and similar form-taxa occur commonly in Middle and Upper Triassic deep-water reefs (e.g. Wendt 1982; Pratt 1995). More widespread in the Permian, Triassic and Jurassic are the various forms of *Shamovella* (= *Tubiphytes*; Riding 1993). *Shamovella* has been interpreted to consist of filamentous, clotted or fairly uniform micrite from calcification of microbial mats that enveloped projecting tubular foraminifera (Senowbari-Daryan and Flügel 1993; Pratt 1995). Alveolar masses of *Bacinella*, important especially in middle Cretaceous mud-mounds, are probably microbial (Neuweiler and Reitner 1992; Camoin 1995).

3.2 Microbial Micrite

The most common structures of presumed microbial origin in both deep- and shallow-water reefs of all ages are crusts, knobs and crudely anastomosing columns composed of dense micrite that is typically clotted, peloidal and "lacy" with fenestral porosity (Fig. 1E); intercalated micrite laminae and dispersed small bioclasts may be present. The resulting structures are called "stromatoids" when laminated, and "thromboids" when not. ("Stromatolite" and "thrombolite" refer to the mound-shaped reef, or reefal subunit of a larger buildup; Pratt 1995.) Thromboidal frameworks are characteristic of Cambrian mud-mounds in deeper shelves and intrashelf basins. Intergradation with biomicrite is common, and siliceous sponges are frequently intergrown in late Cambrian and younger mud-mounds.

Stromatoids and thromboids are accepted as microbial because they exhibit the criteria of uneven, domical or conical lamination that is locally gravity-defying, together with fenestral pores, clotted texture, and grain size finer than that of adjacent sediment. Thin micritic laminae in crusts are explained as calcification within laterally continuous biofilms (Macintyre et al. 1996). Clotted microstructure does not reflect micritization of bioclasts or ooids (see Reid et al. 1995), or disruption by burrowing (Walter and Heys 1985). Rather, it is taken as having been influenced by organically mediated calcification, either forming clots or cementing peloids together, or both. Chafetz (1986) detected bacterial-type fatty acids in Recent examples of related peloidal high-Mg calcite cement. Kennard and James (1986) believed that laminated microstructure represents trapping and binding by filamentous cyanobacterial mats and that clotted microstructure resulted from calcification of coccoids. This has proved to be an oversimplification of the microbial and biochemical processes involved. For example, Défarge et al. (1996) noted calcification only in degraded cyanobacterial sheath material; Chafetz and Buczynski's (1992) experiments suggest that eu-

◁

Fig. 1A–G. Microbial structures in deep-water reefal mud-mounds of Cambro-Ordovician age; thin sections (**A, D-G**), acetate peel (**B**), and SEM (**C**). **A** Crusts of *Girvanella* and clotted micrite (*left*) with *Epiphyton* (*right*); Upper Cambrian, Maly Karatau, Kazakhstan. **B** Tangential section of *Girvanella* crust showing subparallel, micrite-walled filaments; Upper Cambrian, Shallow Bay Formation (Cow Head Group), western Newfoundland, Canada. **C** Organic filaments etched by dilute EDTA from *Girvanella-Epiphyton* biolithite; Upper Cambrian, Maly Karatau. **D** Spheroidal *Gemma* cells overlain by poorly defined *Girvanella* and *Epiphyton* (*right*); Upper Cambrian, Maly Karatau. **E** Clotted micrite thromboids (outlined with *black lines*) flanked by burrowed biomicrite; Upper Cambrian, Bison Creek Formation, Alberta, Canada. **F** Fenestral sparse biomicrite with archaeocyaths; Lower Cambrian, Wilkawillina Limestone, South Australia. **G** Peloidal biomicrite with *Girvanella* fragments. Middle Ordovician, Lower Head Formation (Cow Head Group), western Newfoundland. Samples sectioned for (**F**) and (**G**) courtesy of N.P. James and R. Ludvigsen respectively

bacterial infestation is the key factor that promotes calcification of dead cyanobactera. Reitner (1993) observed nucleation on eubacteria in biofilms, and perhaps bacterial nanofossils await discovery (see Folk 1993).

3.3 Biomicrite

Except for Middle Cambrian to Lower Ordovician *Girvanella* frameworks, most Paleozoic mud-mounds contain large proportions of crudely bedded, poorly sorted biomicrite which on flanks dips up to 60° (e.g. Brachert et al. 1992). The "classical" stromatactis is developed within this biomicrite, an association that first appeared in the Early Cambrian (Fig. 1F; James and Gravestock 1990). Discontinuous layers of crinoidal grainstone, lenses of brachiopods, and meshes of fenestrate bryozoans may be intercalated, suggesting exposure to persistent currents and consequent winnowing (see Pratt 1995). The biomicrite exhibits laminoid fenestral porosity, and bioclasts are commonly poorly sorted and unoriented – in attitudes inconsistent with normal hydraulic processes. The biomicrite is frequently closely associated with, and grades into, clotted and lacy micrite thromboids of direct microbial origin via calcification. Bioturbation is essentially absent within biomicrite mud-mounds, even though it typically exists in surrounding strata.

It is now widely accepted that the sediment of mud-mounds was generated on their surface (see Monty et al. 1995); the lime mud precipitation was perhaps organically mediated through some sort of microbial activitity. (In mud-mounds related to hydrothermal vents, precipitation may have been chemically controlled; Mounji et al. 1996.) To account for the topographic relief and fenestral porosity, the sediment is presumed to have been trapped by a microbial mat. Unoriented bioclasts in biomicrite suggest that some mats were thick and quite flocculent rather than thin and smooth or leathery; possibly analogous, loose organic coverings have been observed in Recent forereef areas (James and Ginsburg 1979). While the presence of pyrite suggests that there would have been organic matter available to infaunal deposit feeders, and the commonly abundant epibenthos indicates food resources for infaunal suspension feeders, burrowing was inhibited. This was probably due to the mat cover rather than sediment consistency, since populations of burrowing organisms would have theoretically been able to get established before the onset of cementation. Stromatactis cavity formation appears to be related mainly to centimetre-scale patchiness and vertical variation in degree of microbial binding and cementation, such that domains and layers of unbound sediment were prone to removal by winnowing (Pratt 1982b, 1995; Matyszkiewicz 1993). Seismic shock was important in some mud-mounds by causing dilation, rupturing and crumbling of layers, which then became exposed to winnowing (Pratt 1998c). Decay of microbial mats and siliceous sponges probably accounted for some small stromatactis, but I believe this process fails for large cavity networks (contra Bourque and Boulvain 1993).

4 Summary and Evolution of Microbial Contribution to Mud-Mounds

The various, intergrading microbial structures resulted from calcification of cell material ranging from more or less pristine, in which the shape of the precursor microbes is preserved, as in *Girvanella*, to degraded, in which masses of clotted or laminated micrite – thromboids and stromatoids – were produced (Pratt 1995, Fig. 62). In parts of many biomicritic mud-mounds, such as "Waulsortian" ones from the upper Paleozoic, the microbial contribution appears to have been more in a sediment-stabilizing capacity than as a template for synsedimentary calcification, although a microbial origin of the lime mud is suspected. The result was a cavernous framework and topographically irregular reef surface on which dwelt – after the Proterozoic – a filter-feeding, browsing and grazing fauna (see Pratt 1995). The significant height of many reefal mud-mounds suggests that they accreted relatively quickly, far outpacing background sedimentation, which accords with the rapid growth rate of eubacteria and cyanobacteria.

The relative contribution of the three types of microbial structures identified in reefal mud-mounds is a function of the: (1) evolution and extinction of specific microbial taxa, (2) diversification and extinction of benthic organisms and therefore the sediment-generating capacity of the surface, (3) position with respect to the photic zone, (4) degree and persistence of current activity, and (5) composition and temperature of sea water. Proterozoic examples are made of stromatoids with variably well-defined lamination configured as steep-sided cones (*Conophyton*), branching hemispheroids (commonly *Baicalia*), and domes (e.g. Narbonne and James 1996). Thromboids which succeed them in the Phanerozoic are only weakly laminated at most (e.g. Leinfelder et al. 1993), but a few examples exhibit lamination in areas presumed to have been deposited under slightly shallower conditions (e.g. Bridges and Chapman 1988; Braga et al. 1995). But during the post-Early Cambrian, pre-Middle Ordovician interval when faunal diversity was low, ocean-facing slopes were characterized by *Girvanella* frameworks from rapid calcification of filamentous mats, while thromboidal mud-mounds accreted in shelf interiors. An important change in the late Paleozoic was the appearance of sessile tubular Foraminifera that became substrates for microbial encrustation, forming *Shamovella*. The role

played by calcifying microbial mats and biofilms in constructing reefs in deeper water seems to have declined in the Cenozoic with the expansion of crustose coralline red algae. Finally, it is necessary to reiterate that the presence of gastropods in many mud-mounds indicates that grazing organisms did not appreciably limit biolithite construction by microbes (Pratt 1982a). Other, physicochemical factors must have been important (Riding 1994).

Acknowledgements. I am grateful to the Natural Sciences and Engineering Research Council of Canada for funding my reef studies, B. A. Abernethy for SEM, and R. Baron-Szabo, R. Riding and the referees for commenting on the manuscript.

References

Bartley JK (1996) Actualistic taphonomy of cyanobacteria: implications for the Precambrian fossil record. Palaios 11:571–586

Beukes NJ (1987) Facies relations, depositional environments and diagenesis in a major early Proterozoic stromatolitic carbonate platform to basinal sequence, Campbellrand Subgroup, Transvaal Supergroup, southern Africa. Sediment Geol 54:1–46

Bourque P-A, Boulvain F (1993) A model for the origin and petrogenesis of the red stromatactis limestone of Paleozoic carbonate mounds. J Sediment Petrol 63:607–619

Brachert TC, Dullo W-C (1991) Laminar micrite crusts and associated foreslope processes, Red Sea. J Sediment Petrol 61:354–363

Brachert TC, Buggisch W, Flügel E, Hüssner HM, Joachimski MM, Tourneur F, Walliser OH (1992) Controls of mud mound formation: the Early Devonian Kess-Kess carbonates of the Hamar Laghdad, Antiatlas, Morocco. Geol Rundsch 81:15–44

Braga JC, Martín JM, Riding R (1995) Controls on microbial dome fabric development along a carbonate-siliciclastic shelf-basin transect, Miocene, SE Spain. Palaios 10:347–361

Bridges PH, Chapman AJ (1988) The anatomy of a deep water mud-mound complex to the southwest of the Dinantian platform in Derbyshire, UK. Sedimentol 35:139–162

Camoin GF (1995) Nature and origin of Late Cretaceous mud-mounds, north Africa. In: Monty CLV, Bosence DWJ, Bridges PD, Pratt BR (eds) Carbonate mud-mounds: their origin and evolution. Int Assoc Sedimentol, Spec Publ 23:385–400

Camoin G, Debrenne F, Gandin A (1989) Premières images des communautés microbiennes dans les écosystèmes cambriens. C R Acad Sci Paris 308 (s II):1451–1458

Chafetz HS (1986) Marine peloids: a product of bacterially induced precipitation of calcite. J Sediment Petrol 56:812–817

Chafetz HS, Buczynski C (1992) Bacterially induced lithification of microbial mats. Palaios 7:277–293

Coron CR, Textoris DA (1974) Non-calcareous algae in Silurian carbonate mud mound, Indiana. J Sediment Petrol 44:1248–1250

Défarge C, Trichet J, Jaunet A-M, Robert M, Tribble, J, Sansone, FJ (1994) Texture of microbial sediments revealed by cryo-scanning electron microscopy. J Sediment Petrol 66:935–947

Folk RL (1993) SEM imaging of bacteria and nannobacteria in carbonate sediments and rocks. J Sediment Petrol 63:990–999

James NP (1981) Megablocks of calcified algae in the Cow Head Breccia, western Newfoundland: vestiges of a Cambro-Ordovician platform margin. Geol Soc Am Bull 92:799–811

James NP, Ginsburg RN (1979) The seaward margin of Belize barrier and atoll reefs. Int Assoc Sedimentol, Spec Publ 3

James NP, Gravestock DI (1990) Lower Cambrian shelf and shelf margin buildups, Flinders Ranges, South Australia. Sedimentol 37:455–480

Kauffman EG, Arthur MA, Howe B, Scholle PA (1996) Widespread venting of methane-rich fluids in Late Cretaceous (Campanian) submarine springs (Tepee Buttes), Western Interior Seaway, U.S.A. Geology 24:977–802

Kennard JM, James NP (1986) Thrombolites and stromatolites: two distinct types of microbial structures. Palaios 1:492–503

Knoll AH, Bauld J (1989) The evolution of ecological tolerance in prokaryotes. Trans R Soc Edinb, Earth Sci 80:209–223

Lees A, Miller J (1995) Waulsortian banks. In: Monty CLV, Bosence DWJ, Bridges PD, Pratt BR (eds) Carbonate mud-mounds: their origin and evolution. Int Assoc Sedimentol, Spec Publ 23:191–271

Leinfelder RR, Nose M, Schmid DU, Werner W (1993) Microbial crusts of the Late Jurassic: composition, palaeoecological significance and importance in reef construction. Facies 29:195–230

Macintyre IG, Reid RP, Steneck RS (1996) Growth history of stromatolites in a Holocene fringing reef, Stocking Island, Bahamas. J Sediment Res 66:231–242

Mamet B, Boulvain F (1988) Remplissages bacteriens de cavités biohermales frasniennes. Bull Soc Belge Géol 97:63–76

Mamet B, Boulvain F (1992) Microflore des monticules micritiques frasniens «F2j» de Belgique. Rev Micropaléont 35:283–302

Matieszkiewicz J (1993) Genesis of stromatactis in an Upper Jurassic carbonate buildup (Mlynka, Cracow region, southern Poland): internal reworking and erosion of organic growth cavities. Facies 28:87–96

Merz MUE (1992) The biology of carbonate precipitation by cyanobacteria. Facies 26:81–102

Monty CLV (1995) The rise and nature of carbonate mud-mounds: an introductory actualistic approach. In: Monty CLV, Bosence DWJ, Bridges PD, Pratt BR (eds) Carbonate mud-mounds: their origin and evolution. Int Assoc Sedimentol, Spec Publ 23:11–48

Monty CLV, Bosence DWJ, Bridges PH, Pratt BR (eds) (1995) Carbonate mud-mounds: their origin and evolution. Int Assoc Sedimentol, Spec Publ 23

Mounji D, Bourque P-A, Savard M (1996) Architecture and isotopic constraints on origin of Lower Devonian conical mounds (Kess Kess) of Tafilalt, Anti-Atlas, Morocco (Abstr). Int Assoc Sedimentol, 17th Regtional Meet, Sfax, Abstr, pp 192–193

Narbonne GM, James NP (1996) Mesoproterozoic deep-water reefs from Borden Peninsula, Arctic Canada. Sedimentol 43:827–848

Neuweiler F, Reitner J (1992) Karbonatbänke mit *Lithocodium aggregatum* Elliot/*Bacinella irregularis* Radoicic. Paläobathymetrie, Palökologie und stratigraphisches Äquivalent zu thrombolitischen Mud Mounds. Berlin Geowiss Abh (E) 3:273–293

Pickard NAH (1996) Evidence for microbial influence on the development of Lower Carboniferous buildups. In: Strogen P, Somerville ID, Jones GLl (eds) Recent advances in Lower Carboniferous geology. Geol Soc Spec Publ 107:65–82

Pratt BR (1982a) Stromatolite decline – a reconsideration. Geology 10:512–515

Pratt BR (1982b) Stromatolitic framework of carbonate mud-mounds. J Sediment Petrol 52:1203–1257

Pratt BR (1984) *Epiphyton* and *Renalcis* – diagenetic microfossils from calcification of coccoid blue-green algae. J Sediment Petrol 54:948–971

Pratt BR (1989) Deep-water *Girvanella-Epiphyton* reef on a mid-Cambrian continental slope, Rockslide Formation, Mackenzie Mountains, Northwest Territories. In: Geldsetzer HHJ, James NP, Tebbutt GE (eds) Reefs, Canada and adjacent areas. Can Soc Petrol Geol Mem 13:161–164

Pratt BR (1994) Synsedimentary fibrous neomorphism of high-Mg calcite and aragonite retaining metastable mineralogy: new process with implications for stromatolite, ooid and skeletal microstructure (Abstr). Geol Soc Am, Abstr Prog 26 (7):66

Pratt BR (1995) The origin, biota and evolution of deep-water mud-mounds. In: Monty CLV, Bosence DWJ, Bridges PD, Pratt BR (eds) Carbonate mud-mounds: their origin and evolution. Int Assoc Sedimentol, Spec Publ 23:49–123

Pratt BR (1998a) Molar-tooth structure in Proterozoic carbonate rocks: origin from synsedimentary earthquakes, and implications for the nature and evolution of basins and marine sediment. Geol Soc Am Bull 110:1028–1045

Pratt BR (1998b) Syneresis cracks: subaqueous shrinkage in argillaceous sediments caused by earthquake-induced dewatering. Sediment Geol 117:1–10

Pratt BR (1998c) Effects of synsedimentary earthquakes on cavity development in deep-water reefal mud-mounds (Abstr). Geol Assoc Can Annu Meet, Québec, Abstr 23, p 149

Pratt BR, Spincer BR, Wood RA, Zhuravlev AYu (1998) Ecology and evolution of Cambrian reefs. In: Zhuravlev AYu, Riding R (eds) Ecology of the Cambrian radiation. Columbia Univ Press, New York (in press)

Precht WF (1994) The use of the term guild in coral reef ecology and paleoecology: a critical evaluation. Coral Reefs 13:135–136

Reid RP, Macintyre IG, Browne KM, Steneck RS, Miller T (1995) Modern marine stromatolites in the Exuma Cays, Bahamas. Facies 33:1–18

Reitner J (1993) Modern cryptic microbialite/metazoan facies from Lizard Island (Great Barrier Reef, Australia): formation and concepts. Facies 29:3–40

Reitner J, Neuweiler F (compilers) (1995) Mud mounds: a polygenetic spectrum of fine-grained carbonate buildups. Facies 32:1–70

Riding R (1990) Classification of microbial carbonates. In: Riding R (ed) Calcareous algae and stromatolites. Springer, Berlin Heidelberg New York, pp 21–51

Riding R (1993) *Shamovella obscura:* the correct name for *Tubiphytes obscurus* (Fossil). Taxon 42:71–73

Riding R (1994) Evolution of algal and cyanobacterial calcification. In: Bengtson S (ed) Early life on earth. Nobel Symp 84. Columbia Univ Press, New York, pp 426–438

Schopf JW (1994) Disparate rates, differing fates: tempo and mode of evolution changed from the Precambrian to the Phanerozoic. Proc Natl Acad Sci USA 91:6735–6742

Senowbari-Daryan B, Flügel E (1993) *Tubiphytes* Maslov, an enigmatic fossil: classification, fossil record and significance through time. Part I: discussion of late Paleozoic material. In: Barattolo F, De Castro P, Parente M (eds) Studies on fossil benthic algae. Boll Soc Paleont Ital Spec 1:353–382

Walter MR, Heys GR (1985) Links between the rise of the metazoa and the decline of stromatolites. Precambrian Res 29:149–174

Webb GE (1996) Was Phanerozoic reef history controlled by the distribution of non-enzymatically secreted reef carbonates (microbial carbonate and biologically induced cement)? Sedimentol 43:947–971

Wendt J (1982) The Cassian patch reefs (lower Carnian, southern Alps). Facies 6:185–202

Mesozoic Reefal Thrombolites and Other Microbolites

Reinhold R. Leinfelder, Dieter U. Schmid

Institut für Paläontologie und historische Geologie, Ludwig-Maximilians-Universität München, Richard-Wagner-Strasse 10, D-80333 München, Germany

Abstract. Calcareous microbolites are widespread in the Mesozoic. They play a paramount role in reef-building and often contribute to the reef framework. In the Early Triassic, stromatolites took over the vacant reef habitats. During the Middle Triassic and Late Jurassic, microbolites reached their peak development in the Mesozoic, often forming reefs together with different groups of metazoans. No major break in microbolite development appeared from the Late Jurassic to the Early Cretaceous. In the course of the Cretaceous, microbolites in shallow water reefs were for the most part replaced by encrusting corallinaceans.

1 Introduction and General Trends

Microbolites ("microbialites" sensu Burne and Moore 1987; see Riding 1991) are widespread throughout the Mesozoic, occurring in a great variety of environments ranging from freshwater settings (Leinfelder 1985; Bignot 1981) to the deep shelf (e.g. Pratt 1995). Reefal microbolites were especially frequent during the Triassic and Jurassic (Fig. 1). In particular, they were powerful reef-builders, often contributing greatly to the reef framework, although they were also of importance for baffling with digitate crusts in microbolite reefs and for binding in many mud-mounds. Reefal microbolites are clearly dominated by thrombolites, although stromatolites and leiolites (sensu Braga et al. 1995) developed as well. Non-reefal stromatolites and oncoids occur throughout the Mesozoic.

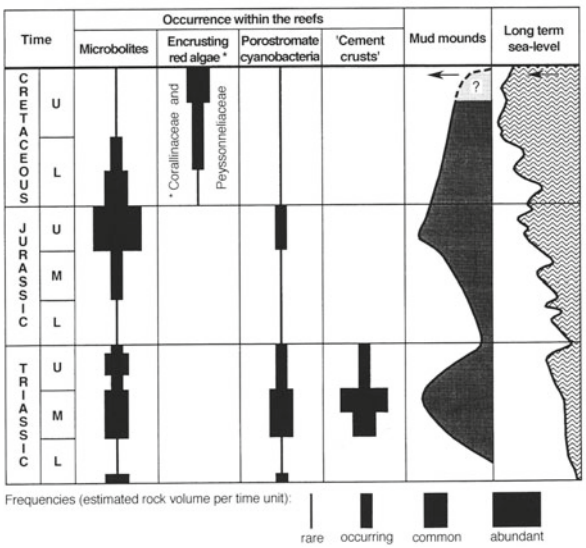

Fig. 1. General trends in Mesozoic microbolites. (Based mainly on data from Baud et al. 1997; Flügel 1981; Haq et al. 1987; Harris 1993; Moussavian 1992; Neuweiler 1995; Senowbari-Daryan et al. 1993; Wendt 1982)

Jurassic pseudobioherms, which formed at cold seeps, are generally marked by extremely low ^{13}C values of −10 to −30‰ PDB (Gaillard et al. 1992). However, in some pseudobioherms, Gaillard et al. found exceptional ^{13}C values of up to +15‰ PDB, probably due to CO_2 produced during bacterial methanogenic fermentation. The microbolites described here exhibit normal isotope values and are in no way related to those of cold seeps or hydrothermal vents.

2 Triassic Microbolites

2.1 Early Triassic

Early Triassic stromatolites are reported from several localities in North America, Europe and Asia (Baud et al. 1997). They appear to be more frequent than during the Permian and during the later epochs of the Triassic, so that Schubert and Bottjer (1992) interpreted them as "disaster forms," taking over vacant reef habitats after the major extinction event at the Permian-Triassic boundary. The first metazoan reefs known from the Triassic are middle Anisian, calcisponge-rich reefs apparently avoid of microbolite crusts (Flügel and Senowbari-Daryan 1996).

2.2 Mid-Triassic

The widespread mid-Triassic sphinctozoan reefs are characterized by a large amount of what is known as "cement crusts," consisting of radiaxial-fibrous calcite. These crusts (including the so-called Grossoolithe from the Ladinian Wetterstein Kalk of the Northern Calcareous Alps, see Brandner and Resch 1981) are especially abundant in Middle Triassic reefs (Figs. 1, 4),

R.E. Riding and S.M. Awramik (Eds.)
Microbial Sediments

but also still occur in younger Triassic deposits. The cement crusts formed syndepositionally (see Harris 1993). Their precipitation was possibly triggered by microbes (Flügel 1989), as indicated by a brownish color, inclusion of minute microbial peloids, and the occasional repetitive intercalation of micritic crusts. Harris (1993) provided a detailed description of microbial crusts from the Dolomites of Southern Italy, where the crusts together with syndepositional cements create the boundstone fabric. Brachert and Dullo (1994) identified micritic crusts in allochthonous reef blocks ("Cipit" boulders) from the Ladinian of the Dolomites and compared them with Recent crusts from the Red Sea which formed below the euphotic zone.

2.3 Late Triassic

Late Triassic, reefal microbolites are generally less frequent than in Middle Triassic reefs (e.g. Flügel 1981), although for the first time well-developed scleractinian coral reefs appeared. Wendt (1982) described thrombolitic patch reefs from the Carnian of the Southern Alps. Reid (1987) concluded that peloidal sediments and crusts, probably of microbial origin, form up to 75% of Upper Triassic reefs from Canada. As to non-reefal microbolites, cyclic, peritidal fenestral limestones developed extensively in platform carbonates of the Northern and Southern Calcareous Alps. Wright and Mayall (1981) reported stromatolites and thrombolites from the Upper Triassic of England; these also form cyclic successions which are mainly controlled by sedimentation, early lithification and salinity changes.

3 Jurassic Microbolites

3.1 Lower and Middle Jurassic Carbonate Microbolites

Whereas non-reefal microbolites, such as oncoids and peritidal fenestral carbonates, were common during the Early Jurassic (e.g. Calcare Massiccio-platform, Cozza and Gandin 1990), reefs were actually rather rare and restricted to certain regions (Leinfelder 1994). Milhi (1992) describes siliceous sponge-microbolite bioherms from the Sinemurian of the High Atlas (Morocco). In the Atlantic realm, deep water microbolites were reported by Jansa et al. (1989).

During the Mid-Jurassic, microbolites developed widely in siliceous sponge reefs (e.g. Rehfeld-Kiefer in Leinfelder et al. 1994), but were still mostly absent in shallow-water coral reef facies. This may be at least deduced from the Bajocian-Bathonian coral reef facies of the Paris Basin (see Geister and Lathuilière 1991). Peritidal fenestral limestones and oncoids are again a common feature of Mid-Jurassic carbonate platforms, but stromatolitic structures and oncoids were widespread even in the pelagic Rosso Ammonitico facies from the Southern Alps (Massari 1983).

3.2 The Extensive Development of Carbonate Microbolites During the Late Jurassic

The Late Jurassic represents a time of extensive microbolite development (Fig. 1), with many different environments being conquered by calcifying microbes. This section mainly focuses on examples from the northern Tethys margin (see Leinfelder 1994; Leinfelder et al. 1994; Nose 1995).

3.3 Classification

Schmid (1996) suggested a new classification of Jurassic microbolites based on the classification of Kennard and James (1986). This system (Fig. 2) may also be applied to the entire Mesozoic, but it is apparently not applicable to Precambrian and Early Palaeozoic microbolites due to the larger variability of the latter. In this new classification, both macro- and microstructure are taken into account, but we would like to emphasize the importance of clearly distinguishing between both categories. It is also crucial to separate structure from growth form (e.g. "oncoids"). A special growth form frequently found in Upper Jurassic coral-thrombolite reefs is represented by "downward-facing hemispheroids" (Fig. 3; Leinfelder et al. 1993).

3.4 Environmental Interpretation

Upper Jurassic microbolites are often associated with reef-building fauna such as corals, stromatoporoids and siliceous sponges, but pure microbolite reefs, up to 30 m in height, can also be found. Non-reefal microbolites, such as oncoids or peritidal, fenestral laminated limestones (loferites), existed as well (e.g. Leinfelder 1992).

Combining microbolite fabrics, growth forms and abundance allows the interpretation of several environmental parameters. However, thrombolites in particular were widespread, occurring in very different settings. Therefore, some additional characteristics are needed for the precise reconstruction of the environmental setting, especially when reef metazoans are lacking or their bathymetric distribution is discussed controversially (e.g. siliceous sponges). These characteristics are represented by micro-encruster associations which allow deduction of a much more detailed, palaeoecological interpretation (Schmid 1996; Leinfelder et al. 1993). New results on the enigmatic micro-encrusters "*Tubiphytes*"

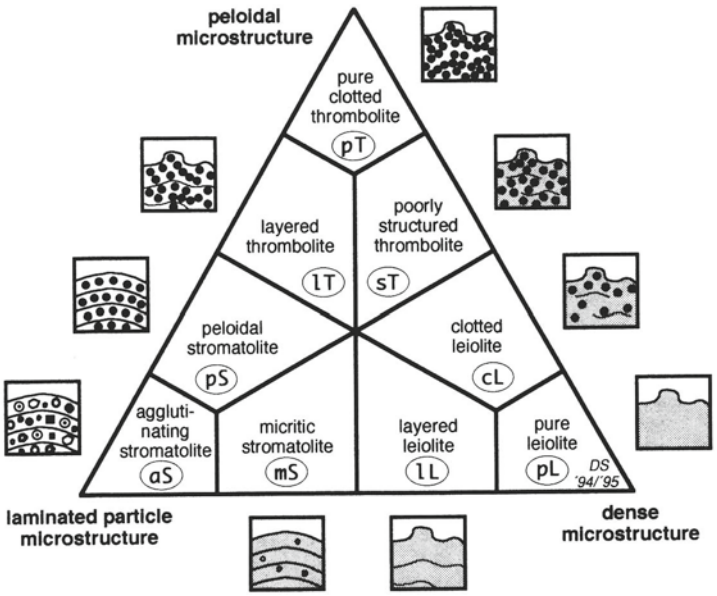

Fig. 2. Classification of Upper Jurassic microbolites according to their fabric, which may also be applied to Mesozoic microbolites in general. Partly based on the classification of Kennard and James 1986.(Schmid 1996)

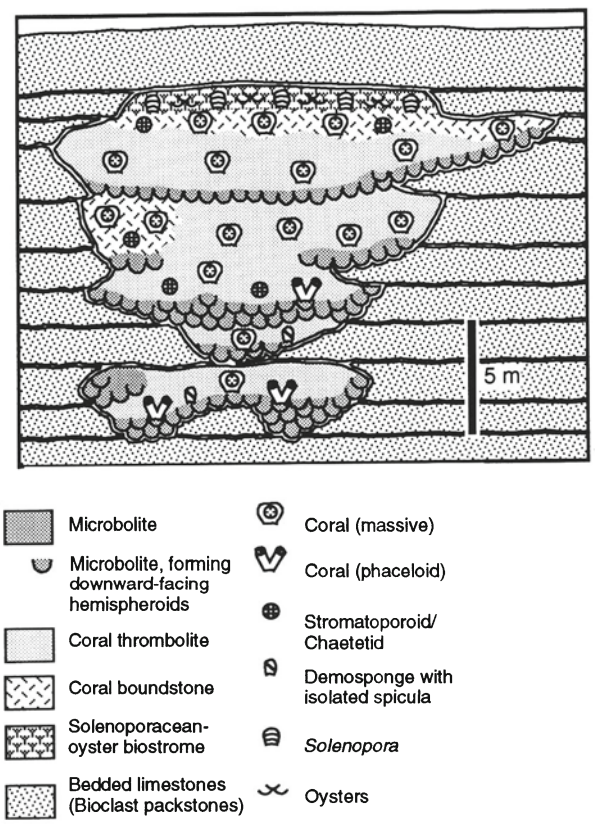

Fig. 3. Schematic diagram of a Late Jurassic coral-thrombolite reef, including downward-facing hemispheroids. Several reef growth stages are indicated, each with a relief of 2 m. (Schmid 1996)

morronensis Crescenti and *Lithocodium aggregatum* Elliott show that both should be interpreted as foraminifers (Schmid 1995, 1996; Schmid and Leinfelder 1996).

Pure microbolite reefs which contain hardly any macroorganisms occur in deep-ramp settings and tolerate dysaerobic conditions. Only clusters of the dysaerobic, epibenthic pectinid bivalve *Aulacomyella* probably living in symbiosis with sulfur bacteria and *Chondrites* burrows can be found in distinct horizons between the reef bodies. Additionally, framboidal pyrite and authigenic glauconite may be abundant in such dysaerobic levels (Leinfelder et al. 1993).

A cryptic micro-encruster association dominated by thecideid brachiopods has been found in the aphotic part of reef caves which developed within and between the coral thrombolite reefs of La Rochelle, France (Leinfelder et al. 1996). This demonstrates that the thrombolite-forming microbes were at least partly light-independent. This is also demonstrated by microbolite reefs that grew in aphotic settings in water depths of approximately 400 m (Dromart et al. 1994).

Another interesting feature of Upper Jurassic microbolites is that they are normally restricted to poorly agitated environments. High energy reefs of the Late Jurassic are normally represented by debris-rich coral reefs with microbolites largely lacking. This indicates that high accumulation of bioclastic particles and, possibly, high abrasion could not be tolerated. If steep, tectonically induced reef margins allowed the export of most of the debris produced by the high wave energy, microbolites suddenly appeared and were able to stabilize the remaining reef debris (Leinfelder 1992, 1994).

Interestingly, very well-developed coral-thrombolite reefs are largely restricted to settings close to siliciclastic coastlines. Although during the time of growth of these reefs direct siliciclastic influx was minimal, it may be concluded that nutrient values were mesotrophic rather than oligotrophic, supporting the flourish-

ing of microbes. Such an interpretation is corroborated by the ecological analysis of coral faunas, which indicates that many Upper Jurassic reef corals, though having already developed symbiosis with zooxanthellae, benefited from slightly elevated nutrient levels (Nose and Leinfelder 1997). This may partially explain the less frequent occurrence of reefal microbolite crusts and the apparently lower diversities of coral faunas in large carbonate platform settings such as the Paris Basin.

3.5 Microbially Induced Calcification

Microbolites both from Upper Jurassic reefs and from oncoids normally exhibit distinct microbial fabrics. However, in peritidal limestones as well as in mud-mounds, microbial activity is obvious but did not necessarily lead to distinct calcification products: Laminated fenestral fabrics developed frequently in intertidal and supratidal environments from the Late Jurassic (e.g. Leinfelder 1992). Although the fabric of the carbonates is often very dense, microbial trapping, binding and, probably, calcification are obvious by the laminoid character of the fenestrae, owing to repetitive desiccation and decay of organic matter in combination with the existence of horizontal microbial mats and rapid cementation. The lack of diagnostic microbolite calcification fabrics is thought to be due to a higher sedimentation rate than in the reef examples described above.

Siliceous sponge-bearing mud-mounds from the Late Jurassic may show great variations in the content of distinct microbolite participation (also known as automicrites). The steepness of mud-mound walls and the relatively large amount of firm-bottom dependent fauna suggest that microbial activity helped to stabilize, and possibly to cement, such mounds. Leinfelder and Keupp (1995) developed a generalized model for the formation of Upper Jurassic mud-mounds, implying that mounds with a high participation of distinct microbolites may indicate episodes of very reduced background sedimentation, whereas mounds with less well-developed microbolite crusts may represent episodes of higher background sedimentation. In the latter case, distinct microbial calcification fabrics could not develop owing to "dilution" with allochthonous material.

Some Upper Jurassic mud-mounds from southern Germany show large amounts of peloids and coated grains being stabilized by thin layers of leiolitic microbolites. Poor sorting, partial clotting and domed structures suggest that all these grains are products of microbial activity, representing incompletely calcified or partially reworked remnants of microbial mats. Koch et al. (1994) interpreted these peloids and coated grains as allochthonous particles of shallow-water origin. Whereas we agree that parts of these grains are of allochthonous, partly even shallow-water, origin, we relate the origin of the majority of the grains to in-place microbial activity.

4 Cretaceous Microbolites

From the Late Jurassic up to the end of the Early Cretaceous, no major break existed in microbolite development. Peritidal fenestral microbolites were widespread (Strasser 1988). Masse (1979) reported pure Lower Cretaceous microbolite reefs from Urgonian limestones of France and Algeria. Neuweiler (1995) described microbial reefs and mounds from the Albian of Spain, with a siliceous, sponge-dominated aphotic community and a coral-calcisponge dominated photic community. Scott (1990) found a reef core rich in stromatolites in one Albian coral reef from the Gulf of Mexico.

Although solenoporaceans and *Marinella lugeoni* Pfender, a precursor of the corallines (Leinfelder and Werner 1993), existed already prior to the Cretaceous, it was only in the late Early Cretaceous that red algae, both corallines and the newly arisen peyssonneliacean algae, started playing a major role in shallow-water reef formation, initially competing with the microbial crusts. Especially during the Late Cretaceous, microbolites were gradually substituted by encrusting red algae (Corallinaceae and Peyssonneliaceae) in shallow-water coral reefs (see Leinfelder 1992; Moussavian 1992). Interestingly, neither microbolites nor coralline algae play a major role in most rudist reefs, which might be related to higher background sedimentation rates (Fig. 4).

In deeper settings, microbes appear to be of continued importance, to some extent. Camoin (1995) describes deeper water mud-mounds from the Turonian and Coniacian of North Africa with abundant microbial fabrics in the core matrix. Cretaceous, siliceous sponge facies from northern Spain also includes microbolite development (Rehfeld and Otto 1995), although the importance seems to be less than for many Jurassic examples. Also, deeper shelf biogenic mound structures became rare during the Late Cretaceous. This could possibly be an effect of elevated sedimentation rates of calcareous nannoplankton remains, so that habitats for calcifying microbial activity were less common. Alternatively, the longevity of the high sea-level might have caused a global reduction of microbially induced and inorganic carbonate precipitation as a consequence of high rates of skeletal precipitation (Riding 1993).

Coralline algae probably grew faster, could stabilize better, were better adapted to abrasive settings and could conquer oligotrophic environments. Therefore, extant microbolites are only found in restricted settings unsuitable for corallines such as reef cavities, hypersaline or brackish ponds, or freshwater deposits (see Reitner 1993; Burne and Moore 1987). However, microbolites have one great advantage over coralline

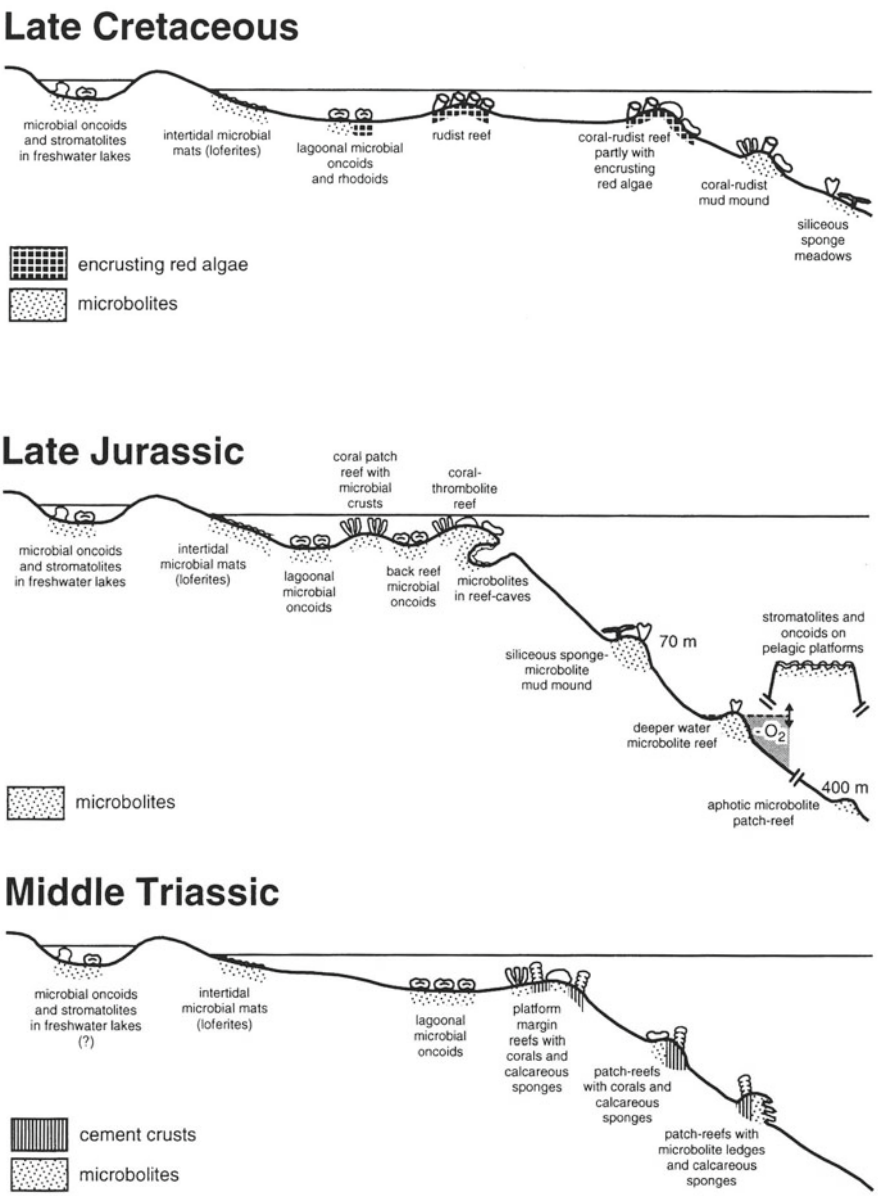

Fig. 4. The occurrence of microbolites, encrusting red algae and cement crusts within mesozoic shelf-slope carbonate systems. Large reef caves have to date only been reported from the Late Jurassic and middle Cretaceous. Based mainly on data from: Triassic: Brachert and Dullo (1994); Brandner and Resch (1981); Flügel (1989); Harris (1993); Jurassic: Leinfelder (1985); Leinfelder et al. (1993); Dromart et al. (1994); Massari (1983); Cretaceous: Bignot (1981); Camoin (1995); Moussavian (1992); Rehfeld and Otto (1995); Reitner et al. (1995); Scott (1990)

algae: they are facultatively independent of light. This is why, even today, calcifying microbes greatly contribute to reef formation by fixing and binding reef material from voids, cavities and reef caves.

Acknowledgements. This is a contribution to the Priority Program "Biogenic Sedimentation – Evolution of Reefs." Financial support by the German Research Foundation (DFG-Project Le 580/4) is gratefully acknowledged.

References

Baud A, Cirilli S, Marcoux J (1997) Biotic response to mass extinction: The lowermost Triassic stromatolites. In: Neuweiler F, Reitner J, Monty C (eds) Biosedimentology of microbial buildups. Facies 36:238 – 242

Bignot G (1981) Illustration and paleoecological significance of Cretaceous and Eocene *Girvanella* limestones from Istria (Yugoslavia, Italy). In: Monty C (ed) Phanerozoic stromatolites. Springer, Berlin Heidelberg New York, pp 134 – 139

Brachert TC, Dullo WC (1994) Micrite crusts on Ladinian foreslopes of the Dolomites seen in the light of a modern scenario from the Red Sea. Abh Geol B-A 50:57 – 68

Braga JC, Martin JM, Riding R (1995) Controls on microbial dome fabric development along a carbonate-siliciclastic shelf-basin transect, Miocene, SE Spain. Palaios 10:347 – 361

Brandner R, Resch W (1981) Reef development in the Middle Triassic (Ladinian and Cordevolian) of the Northern Limestone Alps near Innsbruck, Austria. In: Toomey DF (ed) European fossil reef models. Spec Publ Soc Econ Paleontol Mineral 30:203 – 231

Burne RV, Moore LS (1987) Microbialites: Organosedimentary deposits of benthic microbial communities. Palaios 2:241 – 254

Camoin GF (1995) Nature and origin of Late Cretaceous mud-mounds, north Africa. In: Monty CLV, Bosence DWJ, Bridges PH,

Pratt BR (eds) Carbonate mud-mounds: their origin and evolution. Spec Publ Int Assoc Sediment 23:385–400
Cocozza T, Gandin A (1990) Carbonate deposition during early rifting: The Cambrian of Sardinia and the Triassic-Jurassic of Tuscany, Italy. Spec Publ Int Assoc Sediment 9:9–37
Dromart G, Gaillard C, Jansa LF (1994) Deep-marine microbial structures in the Upper Jurassic of western Tethys. In: Bertrand-Sarfati J, Monty C (eds) Phanerozoic stromatolites II. Kluwer, Dordrecht, pp 295–318
Flügel E (1981) Paleoecology and facies of Upper Triassic reefs in the Northern Calcareous Alps. In: Toomey DF (ed) European fossil reef models. Spec Publ Soc Econ Paleontol Mineral 30:291–359
Flügel E (1989) "Algen/Zement"-Riffe. Arch Lagerst Forsch Geol B-A 10:125–131
Flügel E, Senowbari-Daryan B (1996) Evolution of Triassic reef biota: State of the art. In: Reitner J, Neuweiler F, Gunkel F (eds) Global and regional controls on biogenic sedimentation. I. Reef evolution. Research Reports. Göttinger Arb Geol Paläont Sb 2:285–294
Gaillard C, Rio M, Rolin Y, Roux M (1992) Fossil chemosynthetic communities related to vents or seeps in sedimentary basins: the pseudobioherms of southeastern France compared to other world examples. Palaios 7:451–465
Geister J, Lathuilière B (1991) Jurassic coral reefs of the northeastern Paris Basin (Luxembourg and Lorraine). VI. Int Symp Fossil Cnidaria, Münster, 1991, Excursion-Guidebook, Excursion A3. Münster, pp 1–112
Haq BU, Hardenbohl J, Vail PR (1987) Chronology of fluctuating sea levels since the Triassic. Science 235:1156–1167
Harris MT (1993) Reef fabrics, biotic crusts and syndepositional cements of the Latemar reef margin (Middle Triassic), northern Italy. Sedimentology 40:383–401
Jansa LF, Pratt BR, Dromart G (1989) Deep water thrombolite mounds from the Upper Jurassic of offshore Nova Scotia. In: Geldsetzer HHJ, James NP, Tebbutt GE (eds) Reefs, Canada and adjacent areas. Mem Can Soc Petrol Geol 13:725–735
Kennard JM, James NP (1986) Thrombolites and stromatolites: two distinct types of microbial structures. Palaios 1:492–503
Koch R, Senowbari-Daryan B, Strauss H (1994) The Late Jurassic "Massenkalk Fazies" of Southern Germany: calcareous sand piles rather than organic reefs. Facies 31:179–208
Leinfelder RR (1985) Cyanophyte calcification morphotypes and depositional environments (Alenquer Oncolite, Upper Kimmeridgian?, Portugal). Facies 12:253–274
Leinfelder RR (1992) A modern-type Kimmeridgian reef (Ota Limestone, Portugal): Implications for Jurassic reef models. Facies 26:11–34
Leinfelder RR (1994) Distribution of Jurassic reef types: a mirror of structural and environmental changes during breakup of Pangea. In: Embry AF, Beauchamp B, Glass DJ (eds) Pangea: global environments and resources. Mem Can Soc Petrol Geol 17: 677–700
Leinfelder RR, Keupp H (1995) Upper Jurassic mud mounds: Allochthonous sedimentation versus autochthonous carbonate production. In: Reitner J, Neuweiler F (coord) Mud mounds: a polygenetic spectrum of fine-grained carbonate buildups. Facies 32:17–26
Leinfelder RR, Werner W (1993) Systematic position and palaeoecology of the Upper Jurassic to Tertiary alga *Marinella lugeoni* Pfender. Zitteliana 20:105–122
Leinfelder RR, Nose M, Schmid DU, Werner W (1993) Microbial crusts of the Late Jurassic: Composition, palaeoecological significance and importance in reef construction. Facies 29:195–230
Leinfelder RR, Krautter M, Laternser R, Nose M, Schmid DU, Schweigert G, Werner W, Keupp H, Brugger H, Herrmann R, Rehfeld-Kiefer U, Schroeder JH, Reinhold C, Koch R, Zeiss A, Schweizer V, Christmann H, Menges G, Luterbacher H (ed. and coord. by Leinfelder RR) (1994) The origin of Jurassic reefs: Current research developments and results. Facies 31:1–56
Leinfelder RR, Werner W, Nose M, Schmid DU, Krautter M, Laternser R, Takacs M, Hartmann D (1996) Paleoecology, growth parameters and dynamics of coral, sponge and microbolite reefs from the Late Jurassic. In: Reitner J, Neuweiler F, Gunkel F (eds) Global and regional controls on biogenic sedimentation. I. Reef evolution. Research Reports. Göttinger Arb Geol Paläont Sb 2:227–248
Massari F (1983) Oncoids and stromatolites in the Rosso Ammonitico sequences (Middle-Upper Jurassic) of the Venetian Alps, Italy. In: Peryt T (ed) Coated grains. Springer, Berlin Heidelberg New York, pp 358–366
Masse JP (1979) Schizophytoïdes du Crétacé inférieur. Caractéristiques et signification écologique. Bull Cent Rech Explor-Prod Elf-Aquitaine 3:685–703
Milhi A (1992) Stratigraphie, Fazies und Paläogeographie des Jura am Südrand des zentralen Hohen Atlas (Marokko). Berliner Geowiss Abh A144:1–100
Moussavian E (1992) On Cretaceous bioconstructions: composition and evolutionary trends of crust-building associations. Facies 26:117–144
Neuweiler F (1995) Dynamische Sedimentationsvorgänge, Diagenese und Biofazies unterkretazischer Plattformränder (Apt/Alb; Soba-Region, Prov. Cantabria, N-Spanien). Berliner Geowiss Abh E17:1–235
Nose M (1995) Vergleichende Faziesanalyse und Palökologie korallenreicher Verflachungsabfolgen des iberischen Oberjura. Profil 8:1–237
Nose M, Leinfelder RR (1997) Upper Jurassic coral communities within siliciclastic settings (Lusitanian Basin, Portugal): implications for symbiotic and nutrient strategies. Proc 8th Int Coral Reef Symp, Panama City, pp 1755–1760
Pratt BR (1995) The origin, biota and evolution of deep-water mud-mounds. In: Monty CLV, Bosence DWJ, Bridges PH, Pratt BR (eds) Carbonate mud-mounds: their origin and evolution. Spec Publ Int Assoc Sediment 23:49–123
Rehfeld U, Otto A (1995) Distribution and preservation of siliceous sponges of the rhythmically bedded spongiolitic rocks in the Lower Campanian of N-Spain (Cantabria, Santander area): response to autecology and sea level development. Berl Geowiss Abh E16:109–127
Reid RP (1987) Nonskeletal peloidal precipitates in Upper Triassic reefs, Yukon territory (Canada). J Sediment Petrol 57:893–900
Reitner J (1993) Modern cryptic microbialite/metazoan facies from Lizard Island (Great Barrier Reef, Australia) – formation and concepts. Facies 29:3–40
Reitner J, Wilmsen M, Neuweiler F (1995) Cenomanian/Turonian sponge microbialite deep-water hardground community (Liencres, northern Spain). Facies 32:203–212
Riding R (1991) Classification of microbial carbonates. In: Riding R (ed) Calcareous algae and stromatolites. Springer, Berlin Heidelberg New York, pp 21–51
Riding R (1993) Phanerozoic patterns of marine $CaCO_3$ precipitation. Naturwissenschaften 80:513–516
Schmid DU (1995) "*Tubiphytes*" *morronensis* – eine fakultativ inkrustierende Foraminifere mit endosymbiontischen Algen. Profil 8:305–317
Schmid DU (1996) Marine Mikrobolithe und Mikroinkrustierer aus dem Oberjura. Profil 9:101–251
Schmid DU, Leinfelder RR (1996) The Jurassic *Lithocodium aggregatum–Troglotella incrustans* foraminiferal consortium. Palaeontology 39:21–52
Schubert JK, Bottjer DJ (1992) Early Triassic stromatolites as post-mass extinction disaster forms. Geology 20:883–886
Scott RW (1990) Models and stratigraphy of Mid-Cretaceous reef communities, Gulf of Mexico. SEPM Concepts Sedimentol Paleontol 2:1–102
Senowbari-Daryan B, Zühlke R, Bechstädt T, Flügel E (1993) Anisian (Middle Triassic) buildups of the northern Dolomites (Italy): the recovery of reef communities after the Permian/Triassic crisis. Facies 28:181–256
Strasser A (1988) Shallowing-upward sequences in Purbeckian peritidal carbonates (lowermost Cretaceous, Swiss and French Jura Mountains). Sedimentology 35:369–383
Wendt J (1982) The Cassian patch reefs (Lower Carnian, Southern Alps). Facies 6:185–202
Wright VP, Mayall M (1981) Organism-sediment interactions in stromatolites: an example from the Upper Triassic of south western Britain. In: Monty C (ed) Phanerozoic stromatolites. Springer, Berlin Heidelberg New York, pp 74–84

Proterozoic Stromatolite Taxonomy and Biostratigraphy

Mikail A. Semikhatov, Maria E. Raaben

Geological Institute, Russian Academy of Sciences, Pyzhevsky 7, Moscow 109017, Russia

Abstract. Precambrian stromatolites are unique objects in Earth history. The predominance of microbes in ecosystems that they document, their specific global environments, and the scale of their evolution have no counterparts in the Phanerozoic. Among several, basically different stromatolite classifications known in the literature, the current version of the traditional system is most extensively employed in the study of Precambrian buildups. It is artificial in nature but follows conventional rules of paleontological classification and requires definition of a hierarchy of taxa: forms (form-species), groups (form-genera), and types. At present, there is a common understanding of stromatolite characteristics, providing the most efficient basis for definition and identification of the traditional system taxa. The types are based on the most general features of the buildup's morphology. Groups are based on particular combinations of morphological characteristics defined by the mode of accretion and shape of stromatolite laminae (plus some general features of the microstructure in several cases). Forms are predominantly or exclusively based on microstructure. The stratigraphic potential of Precambrian stromatolites, revealed by empirical time-and-space distribution data of the distinctive assemblages, is evident. Stromatolites are not suitable for the subdivision of the Proterozoic, but provide paleontological characterization of units which have been defined by other methods and significantly contribute to their correlation especially within the limits of particular stromatolite provinces. Interprovincial stromatolite-based correlations are of lower reliability and time-resolution due to strong variations in the taxonomic composition of coeval stromatolite assemblages across provincial boundaries. Precambrian stromatolites demonstrate distinctive directional secular changes in taxonomic composition and diversity which were defined by the evolution of both global environmental and biological factors relevant to the construction and habitat restrictions of these biolites.

1 Introduction

The Proterozoic was the "golden age" of stromatolites. During this extended period of time they reached a maximum in abundance, diversity, and lateral environmental expansion. By the very end of the Precambrian, stromatolites had declined in response to important ecosystem changes (Walter and Heys 1985; Awramik 1991; Grotzinger 1990, 1994; Sochava and Podkovyrov 1992; Semikhatov and Raaben 1994, 1996; Fedonkin 1996, and references therein). The stromatolite buildups were (and are) often regarded as representing a self-sufficient model for resolving general problems of their morphogenesis, classification, stratigraphic significance and environmental setting. At the same time, impressive results in the study of Holocene, predominantly intertidal, stromatolites (e.g. Logan et al. 1964; Walter 1976) brought a group of influential workers to the conclusion that all the above problems regarding Precambrian forms can and should be resolved by means of comparative actualistic analysis. As a result, two schools of stromatolite workers – biostratigraphic and environmental ones – arose in the 1960s. Mechanisms of stromatolite formation, the range of settings inhabited by Proterozoic forms, the degree of environmental impact on morphology, as well as the very necessity and required resolution of stromatolite classification were all treated differently by the two schools in the 1960s and 1970s. Subsequently, contradictions were partly smoothed-out, but progress in understanding the morphogenesis, environmental setting and stratigraphic potential of Proterozoic stromatolites was ultimately based on empirical data concerning their distribution in long-ranging successions, whereas the direct actualistic interpretation of Precambrian forms gave rise to several, at one time widely accepted, but misleading dogmas (see Serebryakov 1975; Monty 1977 for discussion).

Pioneer attempts to understand the stratigraphic potential of Precambrian stromatolites were made by Walcott, the Fentons, Maslov and others as far back as the 1910s-1940s (see Maslov 1960, for review), but it was not until the 1960s-1970s that the first straightforward relevant results were obtained by a number of Russian, Australian, American and French workers (see Raaben 1969; Semikhatov 1976, 1991; Preiss 1977; Bertrand-Sarfati and Walter 1981 for review). Progress in this field was related to the development of an improved classification and taxonomy of Precambrian stromatolites and the recognition of directional secular changes among their lower taxa, firstly in northern Eurasia and, later on, elsewhere.

2 Taxonomy

Disagreements on principles of classification and taxonomy have always been an impediment to the understanding of the biostratigraphic potential of Protero-

R.E. Riding and S.M. Awramik (Eds.)
Microbial Sediments

zoic stromatolites. The very nature of stromatolitic constructions even gave rise to the opinion that their morphology was under complete environmental control and that they did not need to be classified. However, most workers admitted the necessity of stromatolite classification for the sake of rapid and adequate identification leading to their employment as biostratigraphic or environmental indicators. It is evident that biostratigraphic and environmental disciplines require classifications of differing resolution. Nevertheless, it was generally accepted that classifications are artificial and should be based primarily upon gross morphology. The largest taxonomic categories of stromatolites, however one names them (e.g. Korolyuk 1960; Krylov 1963, 1975; Logan et al. 1964), are based on the principal characteristics of morphology. This level of classification is adequate for the purposes of environmental interpretation. However, Precambrian biostratigraphy requires a classification of higher resolution.

2.1 Traditional System

The literature contains descriptions of about 1500 stromatolite taxa of various ranks. About 90% of them have been designated within the framework of the traditional system. This is artificial in nature, but follows conventional rules of paleontological classification: recognition of a number of hierarchic taxa, usage of binomial Linnean nomenclature, formal definition of the type form and type species (holotype), and acceptance of the priority principle.

Such an approach originated when stromatolites were considered as blue-green algae or primitive animals. The first step in elaborating a separate stromatolite system was made by Pia (1927), who subordinated previously described genera to the new higher-rank taxon Stromatolithi Pia and treated these genera as conventional taxa, representing growth-types of a subfamily of blue-green algae. Understanding of the real nature of stromatolites gave rise to debate concerning the appropriateness and rationale of applying biological nomenclature to what are in fact organo-sedimentary structures (e.g. Cloud 1942; Maslov 1960; Hofmann 1969). As a result, several stromatolite systems have been suggested as alternatives to the traditional one (see Hofmann 1969; Walter 1972, for review), but an improved version of the latter, based on newly recognized morphological features of buildups (Korolyuk 1960; Krylov 1963) has won wide recognition. It is this system that meets the requirements of Proterozoic stromatolite biostratigraphy. Its basic categories are the form (= form-species) and the group (= form-genus). In addition, several suprageneric categories are in use and certain workers have distinguished subspecies or varieties.

2.2 Form-Genera and Form-Species

In the infancy of the system, when genera were considered to be the main stromatolite taxa, some authors distinguished them according to both the "mode of growth" of the laminae and the configuration of the structures (e.g. Pia 1927), whereas others concentrated on the lamina shape alone (e.g. Fenton and Fenton 1937; Maslov 1939). Such a concentration of emphasis resulted in a swelling of the genus *Collenia*, so that it engulfed almost all other genera. More recently, the employment of a number of stromatolite characteristics has led to a more restricted notion of what constitutes a genus.

Bertrand-Sarfati and Walter (1981) considered the current state of stromatolite systematics to be confused and referred to Krylov's (1975, 1976) opinion that there were 12 separate classifications exploring different diagnostic features and overlapping to varying extents. However, these classifications (or more precisely, as recognized by Krylov, different approaches to stromatolite classification) are by no means competing, concurrently used systems. The differences between them are not related to dissimilar principles of classification, but mainly concern either integral properties of buildups of different types (e.g. stratiform and columnar), transfer from an original to an amended definition of a taxon, or, to a lesser extent, dissimilar estimations of taxonomic importance of a diagnostic feature.

Although several workers have advocated the use of any outstanding morphological and/or microstructural characteristic of buildups for the definition of stromatolite genera (e.g. Walter 1972; Bertrand-Sarfati 1972; Preiss 1972; Bertrand-Sarfati and Walter 1981; Grey 1984), most of the valid taxa of generic rank are based on morphological characteristics (see Krylov 1963, 1975, 1976; Raaben 1969; Semikhatov 1976, 1991, for review) that are defined by the mode of accretion and shape of stromatolitic laminae (Hofmann 1969; Raaben 1969). A suggestion to consider peculiarities of microstructure as an obligatory attribute of form-genera (e.g. Komar 1966) has not gained widespread acceptance.

At present, there is a fairly uniform understanding of characteristics providing the most useful basis for definition and identification of stromatolite form-genera. For stratiform and nodular buildups these are the shape of the laminae (plus microstructure in some cases), and, for columnar forms, the presence or absence of branching, its pattern, the general shape of the columns, and the type of their margins (plus microstructure and/or lamina shape in some cases). The method of serial sectioning and graphic reconstruction proposed by Krylov (1963) provided the common basis for revealing these characteristics of columnar build-

ups (see Walter 1976). In an attempt to express the differences between taxa quantitatively, a morphometric approach to stromatolite systematics was proposed (Hofmann 1977, 1994) but has not gained wide recognition.

Different combinations of the above characteristics have been employed to specify all the valid stromatolite genera known in the current literature and to verify the diagnoses and contents of some popular groups previously established by using alternative criteria (e.g. *Gymnosolen, Boxonia*). The employment of the above characteristics provides a higher level of taxonomic resolution for columnar stromatolites compared to stratiform and nodular ones. At the same time, overestimation of the diagnostic significance of minor morphological variations of buildups of any kind has resulted in discrimination of form-genera that are in fact environmentally dependent "ephemeral" modifications which should be regarded as junior synonyms of pre-existing taxa. Such practice has locally been commonplace (e.g. Liang et al. 1984; Xing et al. 1985; Liang 1992) but is not widespread elsewhere because most specialists have reached a general understanding of the extent of the morphological attributes of buildups that are required for the identification of a valid stromatolite genus.

It should be emphasized that any form-genus in the current stromatolite classification is defined by a *combination* of diagnostic features. Any single feature, no matter how spectacular and pronounced it may be, is not sufficient for identification of a genus, although attempts to use incomplete sets of features for identifications of columnar stromatolites are known in the literature. Related misidentification of taxa at one time provoked unsuccessful criticism of Proterozoic stromatolite stratigraphy (see Semikhatov 1978, 1991; Bertrand-Sarfati and Walter 1981; Raaben 1981, for details).

A particular problem in the designation of stromatolite form-genera is related to the current conception of an abiogenic precipitated origin of some Precambrian stromatolites, and especially of microstromatites (Asperiform or small digitate stromatolites, etc.; Grotzinger and Read 1983; Hofmann and Jackson 1987; Grotzinger 1990, 1994; Lowie 1994; Grotzinger and Rothmans 1996; Kah and Knoll 1996; Knoll and Semikhatov 1998, and references therein). However, microstromatites are stromatolites in a field sense, are shown to be distinctive members of many regional stromatolite assemblages (Semikhatov 1978; Raaben 1980, 1991; Makarikhin and Kononova 1983; Grey 1984, 1994a,b; Liang et al. 1984), and demonstrate a particular time range which is supposed to reflect directional secular change in global environments. In addition, some of the small digitate forms appear to be biophoric as well as biogenic (Hofmann and Jackson 1987; Raaben 1998). Therefore, it would be of no purpose to exclude them from the traditional stromatolite system.

The discrimination and identification of form-species (forms) in modern stromatolite classification is based either on: (1) a complex of three characteristics, minor variations in stromatolite lamination, morphological details of the buildups, and the pattern of their microstructure (texture), or (2) a combination of any two of these characteristics, or (3) any one of them. In practice, the leading or single criterion for species identification is usually the microstructure, i.e. the distinctive features of the shape, construction, size, and mutual arrangement of micritic or microsparitic components of stromatolite laminae (Komar 1966). Accordingly, many species originally defined by morphological features alone have been revised according to the details of their microstructure (e.g. *Conophyton ressoti* Menchikoff, *Boxonia gracilis* Korolyuk, *Linella ukka* Krylov).

The microstructural concept for the definition of formal stromatolite species initiated by Maslov (1960) and Semikhatov (1962) gained wide acceptance. Objections raised against this concept have been based on the obvious fact that the microstructure of any fossil stromatolite has been subjected to diagenetic alteration. To date, however, the impact of these processes on stromatolite microstructure has been considered explicitly in only a few publications (Krylov 1963; Walter et al. 1988; Fairchild et al. 1990). Nevertheless, stromatolite microstructures are usually considered to reflect aspects of the stromatolite-forming microbial communities (Semikhatov et al. 1979; Walter 1983; Awramik 1991, 1992; Walter et al. 1992, and references therein) and/or secular change in global environments (Grotzinger 1990, 1994; Sochava and Podkovyrov 1992; Semikhatov and Raaben 1994, 1996; Knoll and Semikhatov 1998). Unfortunately, there is only one specific example of correlation between microbiota composition, microstructure and stromatolite morphology: three vertically intergrading varieties of Early Proterozoic silicified stromatolites differing in both microstructure and gross morphology that yield three statistically different sets of microfossils (Awramik and Semikhatov 1979). It is interesting to note that associated silicified microphytolites (*Osagia* spp.) contain a particular set of microfossils other than any reported in stromatolites (Sergeev et al. 1998).

In practice, discrimination between the overwhelming majority (up to 80–85%) of Proterozoic stromatolite form-species is based, entirely or predominantly, on microstructure and these are precisely the species which are most useful in stratigraphy. Species defined by minor morphological features are usually, but not necessarily (e.g. *Linella ukka* Krylov and *L. simica* Krylov), confined to metamorphosed Proterozoic successions (e.g. Krylov and Perttunen 1978; Makarikhin and Kononova 1983). However, a portion of microstructurally defined species is based on poorly preserved or re-

crystallized material (e.g. Bertrand-Sarfati and Awramik 1992). The occurrence of undiscerned synonyms among them is very likely.

Variations in the evaluation of the relative importance of characteristics employed in the definition of stromatolite taxa of any rank are another source of synonyms. Incomplete and polyglot descriptions of taxa also contribute to this problem. However, our experience in the study of Proterozoic stromatolites indicates that no more than a fifth of the species and genera of stromatolites described within the framework of the current classification should be considered as synonyms.

Stromatolite taxonomy is complicated by lack of correlation between morphological and microstructural characteristics – identical microstructures are known in buildups of different morphology, and morphologically similar structures assigned to a particular genus can yield various microstructures that offer a means of species definition. Such relationships have been cited as a reason for considering morphological and microstructural characters as non-hierarchical but parallel (Hofmann 1977). In practice, however, microstructural criteria dominate the definition of species, comprise a part of some generic diagnoses based primarily on morphological features, but are not considered in regard to suprageneric taxa.

2.3 Suprageneric Categories

The increasing number of described stromatolites of lower taxonomic rank demanded the recognition of suprageneric categories to embrace large groupings united by the most common features of morphology. The largest groupings (e.g. stratiform, columnar, columnar branching) have been in use for more than three decades and represent integral components of modern stromatolite systematics. Hierarchic ranking of all groupings suggests that they can be regarded as suprageneric taxonomic categories of four ranks. Authors of recent classifications of stromatolites have arbitrarily denominated them families, orders, classes, and subtypes (conferring the type rank to Stromatolithi Pia; Konyushkov 1978; Raaben 1986; Raaben and Sinha 1989), or families, subtypes, types, and supertypes with no references to the formal status of the main entity (Liang et al. 1984, 1985; Xing et al. 1985; Liang 1992). Although the application of biological nomenclature to the suprageneric classification of stromatolites was specifically advocated by Konyushkov (1978), such practice has met objections related to the origin of the buildups. Consequently, it was suggested that informal categories – the morphotypes – should be used (Semikhatov and Raaben 1994, 1996) which correspond to the most distinctive entities among the two superior formal taxa of Raaben and Sinha (Fig. 1).

Development of an integrated stromatolite classification attracted the attention of many researchers. Maslov (1960), returning to a restricted notion of generic-level stromatolite taxa, suggested uniting certain morphological groups into morphological types within his non-traditional classification. Korolyuk (1960) was the first to formally distinguish, within the framework of the traditional system, three types of stromatolites – columnar, stratiform and nodular. This subdivision gained wide acceptance and later was supplemented by columnar-stratiform and columnar-nodular types (Krylov 1963, 1975) and microstromatites (Raaben 1980). More detailed schemes for Proterozoic stromatolite classification (Table 1) that initially concentrated on columnar forms were subsequently expanded to include all morphologies (Konyushkov 1978; Liang et al. 1984, 1985; Raaben 1986; Raaben and Sinha 1989; Liang 1992). The classifications by Liang et al. and Raaben and Sinha are similar as far as family-level is concerned, but differ in the interpretation of the diagnostic features and content of higher taxa. But the fact that informal categories equivalent to formal suprageneric taxa are often explored in stromatolites research, and furthermore that they show distinctive secular trends in diversity (Semikhatov and Raaben 1996), suggests that suprageneric classification has a good chance of being appreciated in the near future. At present, the grouping of stromatolites into a hierarchy of types, groups (form-genera), and forms (form-species) is generally accepted.

2.4 Alternative Classifications

Two draft schemes for alternative classifications of Precambrian stromatolites were published in the last decades by Vlasov (1977) and Komar (1989, and references therein). Vlasov strove to present a natural system and as a starting point established the Family Tyssageatacea, containing subordinate genera and species. However, all of Vlasov's taxa were defined on the basis of the very characteristics used for the definition in the taxa of the traditional system and were incorporated in it (Raaben and Komar 1982). Komar (1989) proposed that stromatolite classification should be based consistently on microstructure, and in particular on the morphology and spatial arrangement of its major elements. He suggested the recognition of four hierarchic formal taxa based on these criteria: supertype, type, genus and species. Komar described two supertypes, based on major features of the above elements, and five types defined by the element's shape, distribution and mode of arrangement. He also suggested that the two lowest-rank taxa should be based on the configuration, spacing and size of the elements. Unfortunately, details of the classification have not been elaborated and the rele-

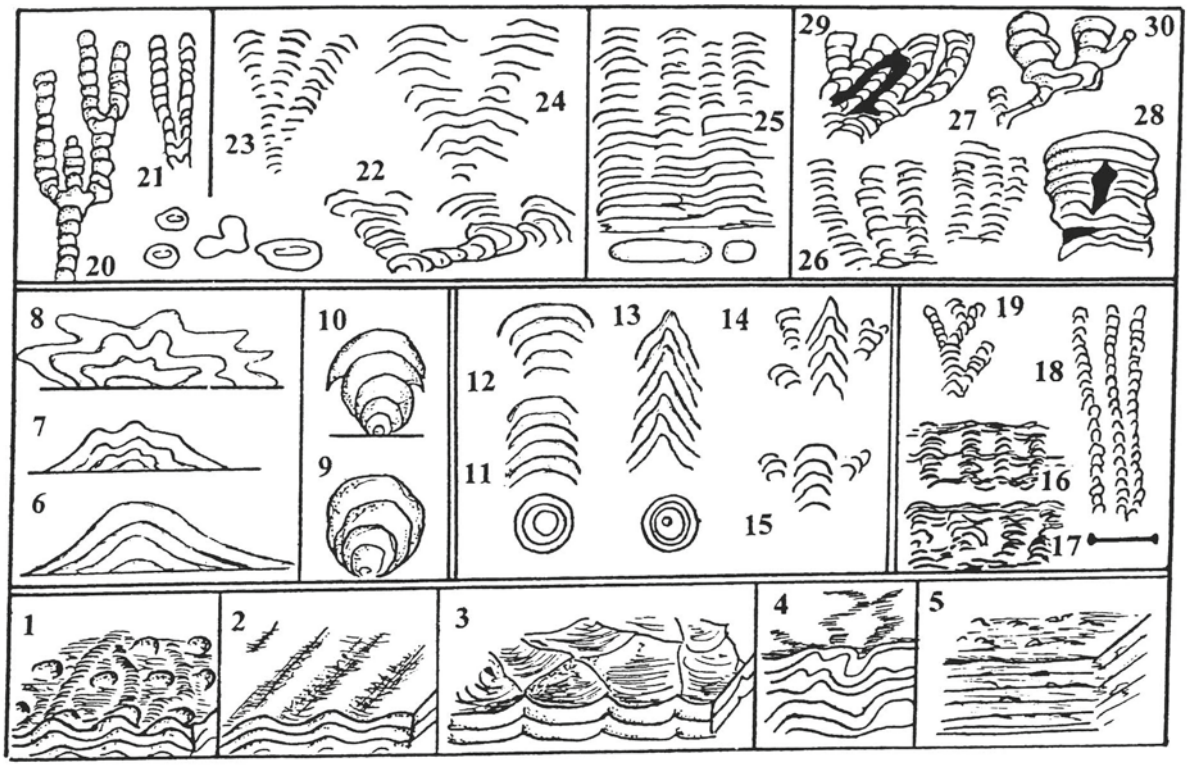

Fig. 1. Sketches of some representative Precambrian stromatolites morphotypes. *1-5* Stratiform stromatolites: *1,2 Stratifera* Koroliuk, *3 Tyssagaetes* Vlasov, *4 Irregularia* Koroliuk, *5 Malginella* Komar and Semikhatov; *6-10* Nodular stromatolites: *6-8* Domical: *6 Paniscollenia* Koroliuk, *7 Colleniella* Koroliuk, *8 Plicatina* Raaben, *9,10* "Cabbage-like": *9 Cryptozoon* (sensu Pia), *10 Cryptophyton* Raaben and Komar; *11-13* Columnar non-branching stromatolites: *11 Colonnella* Komar, *12 Conusella* Golovanov, *13 Conophyton* Maslov; *14 Yakutophyton* Schapovalova; *15 Songjiella* Cao et al.; *16-19* Microstromatites: (*scale bar* 1 cm) *16 Asperia* Semikhatov, *17 Lochmecolumella* Liang and Zhang, *18 Minicolumella* Raaben, *19 Vetella* Krylov; *20-30* Columnar branching stromatolites: *20 Gymnosolen* Steinmann, *21 Boxonia* Koroliuk, *22-24* Tungussida: *22 Tungussia* Semikhatov, *23 Anabaria* Komar, *24 Baicalia* Krylov, *25 Kussiella* Krylov, *26-30* Intricatida: *26 Kussoidella* Semikhatov, *27 Sundia* Butin, *28 Pilbaria* Walter, *29 Confunda* Semikhatov, *30 Kanpuria* Raaben

vant publications should be regarded as a "declaration of intent", rather than the presentation of a substantial classification.

Among a number of earlier alternative stromatolite classifications (see Maslov 1960; Hofmann 1969, for review and bibliography) only the following two are of broad interest.

Maslov (1960) disapproved of the use of binomial nomenclature for stromatolites and proposed a new polynomial scheme for their classification and naming to be used in stratigraphic and environmental analysis. Each important morphological and microstructural feature was given a Latin name, and the title of a taxon was formed by listing several of these names. This led to unwieldy terminology that was not a substitute for the description of a taxon.

An environmentally oriented scheme (Logan et al. 1964) was developed on the basis of modern buildups, but occasionally was applied to Precambrian forms as well. Logan et al. emphasized variations and intergradations in stromatolite morphology and proposed a system of symbolic Latin letter designations and formulae derived from English descriptive morphological terms. The "taxa" of this well-known scheme correspond to the largest suprageneric entities of the traditional classification.

None of the alternative classifications of Precambrian stromatolites has been particularly successful. For the moment, in its present state, the traditional system, exploring both morphological and microstructural features, provides a means for communication among workers.

3 Stratigraphic Significance

Attempts to use Precambrian stromatolites as a biostratigraphic tool initially proved very promising, and they are still a significant means of correlation for Proterozoic, especially Meso- and Neoproterozoic, successions. However, the available data demonstrate that some important limitations need to be taken into account.

The first empirical data underlying the current inference about the stratigraphic importance of Protero-

Table 1. Successive stages in the development of the traditional stromatolite classification system

Pia 1923	Genus	Archeozoon	Gymnosolen				Weedia		Collenia		Cryptozoon	
Maslov 1960	Morphotype	Conophyton	Collenia									
	Supergr.		C. columnaris						C. undosa			
Koroluk 1960	Type Subtype		Columnar				Stratiform		Nodular			
Krylov 1963	Type		Columnar			Strati co-lumn.	Stratiform		(Columnar)			
	Subtype		Branching						Nodular			
Raaben 1964 1969	Type		Columnar				Stratiform		Nodular			
		Non-branching		Actively branch.	Passively branching							
	Categorgy	Conophytonida		Gymnosole-nida Tungussida	Kussiellida							
Komar 1966	Type	Columnar					Non-columnar					
	Subtype	Non-branching	Branching				Stratiform		Nodular			
				Actively branching	Passively branch.							
Krylov 1975	Type	Columnar				Stratico-lumn.	Stratiform		Column nodul.	Nodular		
	(unnamed)		Branching (1) (2) (3)									
Koniushkov 1978	Subtype	Columnar (Colonnelithi)					Stratiform (Stratiferithi)		Nodular			
	Class	Non-branching (Colonnelitha)	Branching (Gymnosolenitha)			Strati co-lumn.	Stratiferitha					
	Order	Colonnelida	Gymnosolenida		Kussi-ellida	Omach-tenida	Stratiferida					
	Family	Alveolidae Colonnelidae Conophytonidae	Gymnosolenidae Tungussida		Kussiel-lidae	Omach-tenidae	Irregularidae Stratiferidae					
Raaben et Sinha 1989	Subtype	Columnar (Columnithi)					Non-columnar (Compactithi)					Microstroma-tithi
	Class	Non-branching	Branching (Ramificantha)				Tabulitha (Stratiform)		Pienostroma (Nodular)			
	Order	Conophytonida	Intricatida (Irregularly branching)	Acrescentida (Actively branching)	Kussiellida (Passively branching)		Anaglip-honida	Decumbenta	Cupolida (Domelike)	Cryptiida		Minicolumel-lida
	Family	Euconophy-tonidae Ephyaltidae	Prokussielli-dae Discorsiidae Kanpiridae Illietidae	Gymnosole-nidae Tungussidae Alterniidae	Kussiellidae Omachtenidae		Stratiferidae Tyssagaet-idae	Malginelli-dae	Tinnidae Confluentidae	Cryptophy-tonidae Bulboidea		Minicolumel-lidae Pseudogym-nosolenidae

zoic stromatolites were obtained in the 1960s in the course of the study of the Riphean and Vendian build-ups in northern Eurasia (see Raaben 1969; Semikhatov 1976, for review and bibliography). During these years an advanced version of stromatolite classification was presented (see above), and reliable data on the time-and-space distribution of the Late Proterozoic taxa were obtained for the first time. It was revealed that the Riphean and Vendian sections from several widely separated regions of Siberia and the Urals yield directional successions of taxa of columnar stromatolites, and that these successions, in the most complete sections, fall into four, time-specific, taxonomically distinct complexes laterally linked by a number of common genera and some common species. In addition, K-Ar glauconite ages of the comparable complexes in different regions were shown to be similar (Keller et al. 1960; Semikhatov 1962; Krylov 1963; Raaben 1964; Komar 1966). Before long, these results were supported by data from other continents (e.g. Bertrand-Sarfati 1972; Walter 1972, 1976; Preiss 1972, 1973, 1977; Bertrand-Sarfati and Walter 1981, and references therein), and by the record of non-columnar morphotypes (e.g. Komar 1966).

The accumulated data suggested that stromatolites are an effective tool for both general four-fold subdivision and interregional correlation of the Late Proterozoic (e.g. Keller et al. 1960; Semikhatov 1962, 1974; Krylov 1963, 1975, 1985; Cloud and Semikhatov 1969; Raaben 1969, 1975; Bertrand-Sarfati 1972; Walter 1972, 1976; Preiss 1977). Occurrence of specific stromatolite complexes within the type section of each previously recognized Riphean erathem (the Lower, Middle and Upper Riphean) provided, for the first time, paleontological characteristics of these widely used units and created the impression that they were paleontologically defined subdivisions with distinct boundaries. This view was facilitated by the fact that stromatolite workers in the 1960s–1970s failed to discriminate between two chronostratigraphic procedures – subdivision and correlation.

Although initial results looked promising, subsequent studies revealed a number of problems in Proterozoic stromatolite biostratigraphy related to taxonomy, discrete distribution of assemblages in the successions, provincialism of time-dependent taxonomically distinct complexes, and variability in the time ranges of taxa at the interregional scale. An appreciation of these problems and of the requirements of chronostratigraphy are the basis for the current evaluation of the stratigraphic potential of Precambrian stromatolites (Semikhatov 1991, 1995; Raaben 1997).

In evaluating the applicability of stromatolites for general subdivision of the Proterozoic, i.e., for defining the boundaries of chronostratigraphic units, several factors have to be taken into account. The confinement of the bulk of Proterozoic stromatolites to carbonate platforms, together with the environmental specialization of some distinctive morphotypes (e.g. Serebryakov 1975; Grey and Thorne 1985; Grotzinger 1990; Zhu and Chen 1992), predetermines the discrete distribution of these biolites and of their assemblages in the sedimentary successions. In this respect, the Uralian stratotype of the Riphean is no exception, since stromatolites are present here only in the middle and/or upper parts of the unconformity-bounded type units of the Lower, Middle, and Upper Riphean erathems (Krylov 1975; Raaben and Komar 1982). Their lower boundaries are traditionally located at unconformities at the bases of siliciclastic stromatolite-free formations that constitute the lower parts of these type units. Attempts to substitute Siberian sections, containing more prolific stromatolites, for the Uralian ones in stromatolite definition of the boundaries (e.g. Semikhatov 1974) cannot be regarded as a correct approach for two reasons. Firstly, the Siberian sections also show discrete time distribution of stromatolite assemblages. Secondly, such substitution, quite trivial in the Phanerozoic, is fraught with serious misleading consequences if applied to the Proterozoic. This is due to the limited possibility for precise long-distance correlation in this part of the geological record and to strong lateral variations in the taxonomic composition of stromatolite assemblages.

In other words, researchers in the 1960s–1980s overlooked the obvious fact that Riphean (as well as any other) stromatolites are unsuitable for defining *chronostratigraphic boundaries*, and, hence they cannot serve as a tool for subdivision of the Proterozoic. This became clear later, when attention was focused on the application of chronostratigraphic requirements to Proterozoic stratigraphy (Semikhatov 1991, 1993, 1995).

However, stromatolites provide unique, essentially paleontological, characterization of units which have been defined by other methods. They contribute to both the establishment of the paleontological characterization of the units, and their correlation in separated sections. The time-and-space distribution of such units is defined by the time range and lateral persistence of successive stromatolite complexes.

The available data demonstrate that the most distinct change in the Proterozoic stromatolite succession occurred across the Paleo-Mesoproterozoic transition. Although at one time believed to be similar to the Late Riphean complex (Hofmann 1977, and references therein), the Paleoproterozoic stromatolite complex was shown to be dominated by genera and species unknown in the Riphean and Vendian. Most Paleoproterozoic forms "of Upper Riphean aspect", which suggested the taxonomic similarity of Paleo- and Neoproterozoic stromatolites, were assigned to peculiar taxa at both specific and generic levels (Semikhatov 1978; Raaben 1980, 1991, 1997; Makarikhin and Kononova 1983;

Grey 1984, 1994a,b; Liang et al. 1984; Xing et al. 1985; Semikhatov and Raaben 1994, 1996). But despite its distinctive taxonomic composition and very large time range, the Paleoproterozoic stromatolite complex can only be subdivided into subordinate, stratigraphically useful taxonomic entities on a regional scale (e.g. Grey 1984; Liang et al. 1984). As for the Meso- and Neoproterozoic (Riphean and Vendian) stromatolite succession, it falls into four intercontinentally recognizable assemblages of taxa which provide the paleontological characteristics for the Lower, Middle, and Upper Riphean and Vendian (e.g. Krylov 1975; Semikhatov 1976, 1991; Bertrand-Sarfati and Walter 1981, and references therein). The datings of the lower boundaries of these units are considered to be 1650 ± 50, 1350 ± 20, 1000 ± 50[1], and 650 ± 20 Ma (Semikhatov 1993 and references therein). A survey of available data on the distribution of stromatolite genera and species demonstrates that in certain vast regions (e.g. northern Eurasia, China) some informal subdivisions that are subordinate to the three Riphean erathems also have specific stromatolite characteristics (Krylov 1975, 1985; Raaben 1969, 1975; Liang et al. 1984, 1985; Semikhatov and Raaben 1994, 1996).

It is significant that time-dependent successions of Proterozoic stromatolites are governed by the secular change of time-restricted taxa defined by different combinations of selected attributes. The notion that at one time was popular, of directional development ("evolution") of their real attributes (e.g. Krylov 1963, 1975), lacks support from recent data. Consequently, Proterozoic stromatolite stratigraphy remains strictly empirical.

Important constraints on the stratigraphic value of Proterozoic stromatolites in long-distance correlation are imposed by distinct provincialism in time-dependent complexes (Semikhatov 1980, 1985, 1991; Golovenok 1984). The degree of provincialism is evident from the fact that among all the taxa present in five, Middle-Late Riphean, northern Eurasian and African stromatolite provinces, only 12% of species and 52% of genera are known to extend beyond the boundaries of at least one province. A survey of the global data shows that a high degree of endemism of Proterozoic (and especially pre-Riphean) stromatolites is the rule rather than the exception – only about 8.5% of species and 31% of genera occur in common in two or more super-regions such as northern Eurasia, China, India, Africa, North America, and Australia (Semikhatov and Raaben 1996). Consideration of the so-far-unrecognized synonyms will somewhat change the above figures, but is unlikely to affect the general situation with regards to the high endemism of Proterozoic stromatolites.

1 New isotope-geochronological data obtained in Siberia demonstrate that the Middle-Upper Riphean boundery should be dated at 1050 ± 20 Ma

Variability of the time range of taxa at interregional and, especially, interprovincial scale presents additional problems in the stratigraphic employment of Proterozoic stromatolites. For instance, *Conophyton cylindricus* Maslov is confined only to the lower Upper Riphean in Eastern Siberia, but in the integrated north Eurasian scale it is distributed from Lower Riphean to lower Upper Riphean. Similarly, *Kussiella kussiensis* Krylov is confined to the lower Lower Riphean in the Urals, northern Siberia, northern Australia, and India but is reported from the Lower and lower Middle Riphean in SE Siberia (Uchur-Maya Region), and *Linella simica* Krylov occurs in the lower upper Riphean in eastern China, in the uppermost part of the Upper Riphean in the Urals, and in the Vendian-Cambrian boundary beds in the Uchur-Maya Region.

Judging by independent correlation criteria, not only particular taxa but also some associations of taxa can change their time range when passing from one province to another.

This is not to say that all stromatolite taxa are wide-ranging and time-transgressive at the interprovincial scale. Some characteristic members of regional assemblages possess relatively short (by Proterozoic standards) time ranges, both at regional and interregional scales, and can be used for long-distance correlation. To take the most convincing examples, *Baicalia lacera* Semikhatov, which stands out because of its very distinctive microstructure (Knoll and Semikhatov 1998), is restricted to lower Upper Riphean sections in Siberia, northern Africa, north-western Canada, and south-western Alaska, while *Jurusania nizvensis* Raaben was reported from the lower or middle part of the Upper Riphean in the Urals, eastern China and South Australia (see Semikhatov and Raaben 1994, 1996 for bibliography). Unfortunately, the number of such relatively short-ranging but laterally widespread (interprovincial) taxa is very limited.

Taken together, these considerations indicate that stromatolite-based interprovincial correlations should be based on similarities in the secular successions of particular stromatolite assemblages, rather than on occurrence of individual common taxa, and wherever possible must be supported by radiometric and/or chemostratigraphic data. Such correlations allow the tracing, at the interprovincial scale, of Paleoproterozoic, Lower, Middle, and Upper Riphean and Vendian deposits, and, between some provinces, of particular parts of Riphean erathems.

The effectiveness of stromatolites in the intrabasinal correlation of Proterozoic successions is much higher. It is convincingly demonstrated by many Late Proterozoic (e.g. Semikhatov 1962; Raaben 1964, 1975; Komar 1966; Bertrand-Sarfati 1972; Semikhatov and Serebryakov 1983; Liang et al. 1984; Raaben et al. 1995) and Early Proterozoic examples (e.g. Makarikhin and Kononova

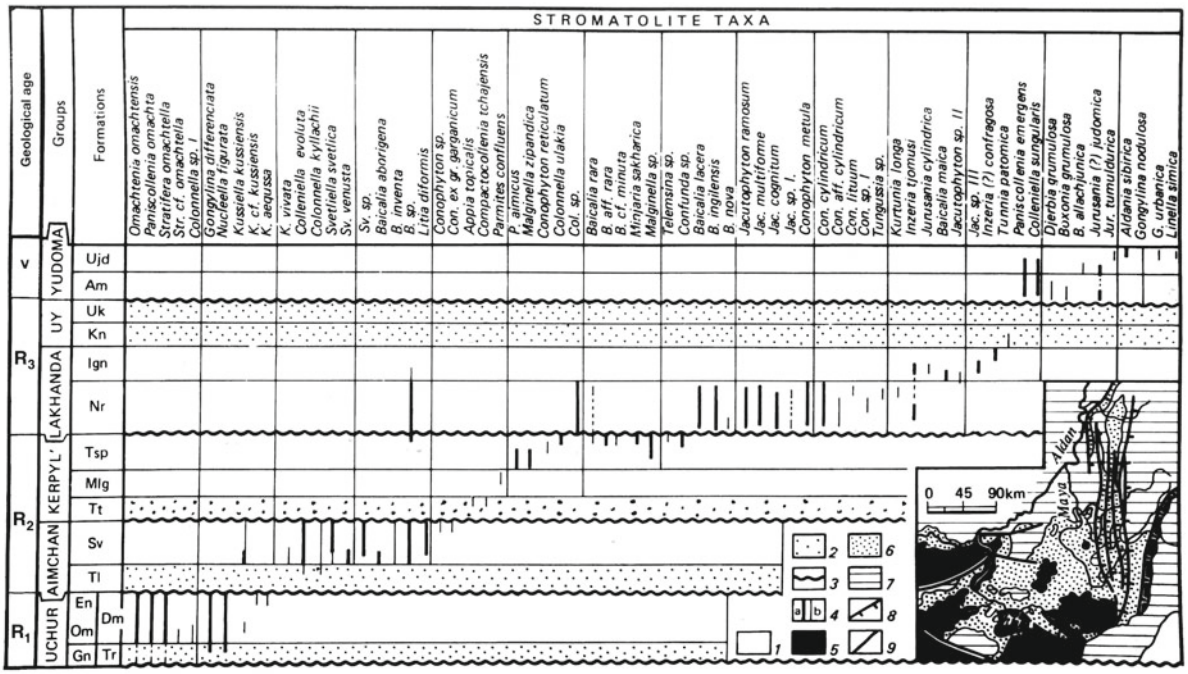

Fig. 2. Vertical distribution of stromatolite taxa in the Riphean and Vendian of the Uchur-Maya Region and its geological setting (*inset map*; modified from Semikhatov and Serebryakov 1983). *1,2* Dominant rock composition: *1* carbonate and siliciclastic-carbonate, *2* siliciclastic, *3* principal unconformities, *4* vertical distribution of dominant (*a*) and subordinate (*b*) taxa in assemblages; *5-9* on the *inset map: 5* pre-Riphean rocks, *6* Riphean and Vendian: *7* Phanerozoic, *8* principal thrusts and upthrusts, *9* other faults. Formations: *Gn* Gonam; *Om* Omakhta; *En* Ennin; *Tr*, Trekhgorka; *Dm* Dim; *Tl* Talyn; *Sv* Svetly; *Tt* Totta; *Mlg* Malgina; *Tsp* Tsipanda, *Nr* Neryuen; *Ign* Ignikan; *Kn* Kandyk; *Uk* Ust'kirba; *Am* Aim; *Ujd* Ust'-Yudoma

1983; Liang et al. 1984 1985; Grey 1984, 1985), amongst which the Riphean and Vendian stratigraphically complete and stromatolite-rich succession of the Uchur-Maya Region can be considered a model (Fig. 2). It demonstrates the occurrence of a unique vertical change in stromatolite taxa and their grouping into definite assemblages of various diversity which differ from one another at both the generic and, especially, at the specific levels. Each assemblage characterizes a certain interval of the section equal to, or smaller than, the regional lithostratigraphic units. Assemblages are usually delimited by siliciclastic horizons and/or unconformities; only two assemblages intergrade in the section. As to lateral distribution, some assemblages maintain their taxonomic composition throughout the whole region while others show rapid changes over short distances that are not necessarily in concert with lithological variations in the enclosing rocks (see Semikhatov and Serebryakov 1983).

The Uchur-Maya section, together with other examples, shows that although the distribution of a regional stromatolite assemblage in time and space was clearly affected by environment, environmental pressure is not the main, and even less the only, factor governing the taxonomic composition and time range of a particular assemblage, since an overwhelming majority of Proterozoic stromatolite lower-rank taxa (almost all species and most genera) have definite, though in part very large, time ranges at the interregional scale.

Secular change in taxa defined the dynamics of the global taxonomic diversity of Proterozoic stromatolites. Analysis of theses dynamics at specific and generic levels in an environmental context, and with a relatively high time-resolution (Semikhatov and Raaben 1994, 1996), clarified the previously established patterns (Walter and Heys 1985; Awramik 1992) and revealed that the main variations in stromatolite diversity have been linked by direct relationships and feed-back mechanisms to abiotic, biologically induced, and biotic events. The most important among these were global tectonics (partly reflected in the variations in mantle fluxes and continental run-off into the World ocean, as recorded in the Sr-isotopic composition of sea water), significant climatic variations and related glacioeustatic sea-level fluctuations, directional changes in pCO_2, the degree of carbonate oversaturation in surface sea water and related evolution of carbonate sedimentation, secular variations in the production and burial of organic and carbonate carbon, and, last but not least, evolutionary changes in the Riphean and Vendian biota. The last link is evident from the chronological coincidence between important variations in Neoproterozoic stromatolite diversity and principal biological events (see Knoll and Sergeev 1995; Fedonkin 1996, and

references therein). It may, therefore, be deduced that the very existence of time-restricted stromatolite taxa and their assemblages was defined by the evolution of global environments and, partly, of microbial communities, on the early Earth. The documented relationships explain an obvious contradiction between evolutionary conservatism of stromatolite-forming microorganisms and the empirically established secular change of Proterozoic stromatolite taxa. In the present state of the art, these relationships confirm Maslov's (1959) surmise that the stratigraphic potential of Precambrian stromatolites was defined by the evolution of both environmental and biological factors relevant to the construction and facies restrictions of these bialites.

4 Conclusions

1. The traditional stromatolite system has proved to be the most useful in the study of Proterozoic buildups. A number of stromatolite classifications published during the past decades represent successive stages in the development of that system. It is artificial in nature but follows conventional rules of paleontological classification and requires definition of hierarchy of taxa. The ranking of taxa into forms (form-species), groups (form-genera), and types is accepted in the system and a more detailed hierarchy of suprageneric categories is also frequently used in stromatolite research.
2. At the present time, there is a fairly uniform understanding of the stromatolite characteristics that provide the most useful basis for reproducible definition and identification of taxa within the framework of the traditional system. Analysis of the distribution of taxa in the Proterozoic time-and-space matrix offers a sound empirical method for evaluating the stratigraphic potential of Precambrian stromatolites.
3. Stromatolites cannot be used for definition and long-distance correlation of the boundaries of Proterozoic chronostratigraphic units, and hence they are not suitable for subdivision of the geological record. However, they provide paleontological characterization of units which have been defined by other methods and thus contribute to their correlation.
4. Stratigraphic correlations based on stromatolites can be constructed with confidence within the limits of particular stromatolite provinces. In such cases, almost all the recorded taxa contribute to the substantiation of the correlations by defining a succession of unique, time-dependent taxonomic assemblages of variable lateral extent. The time ranges of particular assemblages were governed mainly by abiotic factors, whereas the taxonomic composition of any assemblage was determined by its time-and-space position with regard to the time range of relevant stromatolite taxa and their preferred environmental settings.
5. Interprovincial correlations by means of stromatolites are of lower reliability and time-resolution than intraprovincial ones and should be constrained by independent methods of long-distance correlation.
6. Precambrian stromatolites are unique objects in Earth history, since the predominance of microbes in ecosystems, as well as the global environments themselves and the scale of their evolution recorded in the Archean and Proterozoic, had no counterparts in the Phanerozoic.

Acknowledgements. We sincerely thank S.M. Awramik, K. Grey, and the late V. Komar for fruitful discussions of the problems considered in this paper, and gratefully acknowledge the constructive comments of the reviewers of the manuscript. This work was supported by the Russian Foundation for Basic Research, Project 96-05-64329.

References

Awramik SM (1991) Archean and Proterozoic stromatolites. In: Riding R (ed) Fossil algae and stromatolites. Springer, Berlin Heidelberg New York, pp 289-304

Awramik SM (1992) The history and significance of stromatolites. In: Schidlowski M (ed) Early organic evolution: implications for mineral and energy resources. Springer, Berlin Heidelberg New York, pp 435-449

Awramik SM, Semikhatov MA (1979) The relationship between morphology, microstructure and microbiota in three vertically intergrading stromatolites from the Gunflint Iron Formation. Can J Earth Sci 16:484-495

Bertrand-Sarfati J (1972) Stromatolites columnies du Precambrian Superieur du Sahara Nord-Occidental. CRNS Ser Geol 14, Paris

Bertrand-Sarfati J, Walter MR (1981) Stromatolite biostratigraphy. Precambrian Res 15:353-371

Bertrand-Sarfati J, Awramik SM (1992) Stromatolites from the Mescal Limestone (Apache Group, middle Proterozoic, central Arizona): taxonomy, biostratigraphy, and paleoenvironments. Geol Soc Am Bull 104:1138-1155

Cloud PE (1942) Notes on stromatolites. Am J Sci 250:363-379

Cloud PE, Semikhatov MA (1969) Proterozoic stromatolite zonation. Am J Sci 267:1017-1061

Fenton CL, Fenton MA (1937) Belt Series of the North: stratigraphy, sedimentation, paleontology. Geol Soc Am Bull 48:1873-1970

Fedonkin MA (1996) The Precambrian fossil record: new insight of life. Mem Soc Ital Sci Nat Mus Livico Storia Nat Milane XXVII:41-48

Fairchild IJ, Marshall JD, Bertrand-Sarfati J (1990) Stratigraphic shifts in carbon isotopes from Proterozoic stromatolitic carbonates (Mauritania): influence of primary mineralogy and diagenesis. Am J Sci 290A:46-79

Golovenok VK (1984) Stromatolites and microphytolites in the Precambrian stratigraphy: a hope and reality. Soviet Geol 8:43-54

Grey K (1984) Biostratigraphic studies of stromatolites from the Proterozoic Earaheedy Group, Nabbera Basin, Western Australia. Bull Geol Surv W Austzal 130

Grey K (1985) Stromatolites and other organic remains in the Bangemall Basin. Bull Geol Surv W Austzal 128:221-241

Grey K (1994a) Stromatolites from the Paleoproterozoic Earaheedy Group, Earaheedy Basin, Western Australia. Alcheringa 18: 187-218

Grey K (1994b) Stromatolites from the Paleoproterozoic (Orosirian) Glengarry Group, Glengarry Basin, Western Australia. Alcheringa 18:275–300
Grey K, Thorn AM (1985) Biostratigraphic significance of stromatolites in upward shallowing sequences of the Early Proterozoic Duck Creek Dolomite, Western Australia. Precambrian Res 29:183–206
Grotzinger JP (1990) Geochemical model for Proterozoic stromatolite decline. Am J Sci 290 A:80–103
Grotzinger JP (1994) Trends in Precambrian carbonate sediments and their implication for understanding evolution. In: Bengston S (ed) Early life on Earth. Columbia Univ Press, New York, pp 245–258
Grotzinger JP, Read JF (1983) Evidence for primary aragonite precipitation, Lower Proterozoic (1,9 Ga) dolomite, Wopmay orogen, NW Canada. Geology 11:710–713
Grotzinger JP, Rothmans DH (1996) An abiotic model for stromatolite morphogenesis. Nature 383:423–425
Hofmann HJ (1969) Attributes of stromatolites. Geol Surv Can Pap 39:58–69
Hofmann HJ (1977) On Aphebian stromatolites and Riphean stromatolite stratigraphy. Precambrian Res 5:175–205
Hofmann HJ (1987) Precambrian biostratigraphy. Geosci Can 14:135–154
Hofmann HJ (1994) Quantitative stromatolitology. J Paleontol 68:704–709
Hofmann HJ, Jackson GD (1987) Proterozoic ministromatolites with radial-fibrous fabric. Sedimentology 34:963–971
Kah LC, Knoll AH (1996) Microbenthic distribution on Proterozoic tidal flats: environmental and taphonomic considerations. Geology 24:79–82
Keller BM, Kazakov GA, Krylov IN, Nuzhnov SV, Semikhatov MA (1960) New data on stratigraphy of the Riphean Group (Upper Proterozoic). Izv Akad Nauk SSSR Ser Geol 12:26–41
Knoll AH, Sergeev VN (1995) Taphonomic and evolutionary changes across the Mesoproterozoic-Neoproterozoic transition. N Jahrb Geol Paleont Abh 195:289–302
Knoll AH, Semikhatov MA (1998) The genesis, diagenesis and time-distribution of two distinctive Proterozoic stromatolite microstructures. Palaios 13:407–421
Komar VA (1966) Upper Precambrian stromatolites of the northern part of the Siberian Platform and their stratigraphic significance. Nauka, Moscow (Tr Geol Inst Acad Nauk SSSR, vol 154)
Komar VA (1989) Classification of microstructures of the USSR Precambrian stromatolites. Himalayan Geol 13:229–238
Konyushkov KN (1978) On diagnostic features and systematics of Precambrian stromatolites. In: Paleontology and stratigraphy of Paleozoic of the USSR. VSEGEI, Leningrad, pp 74–86
Korolyuk IK (1960) Stromatolites of the Lower Cambrian and Proterozoic of the Irkutsk Amphitheatre. In: Tr Inst Geol Razrab Goryuchikh Iskop Akad Nauk SSSR, vol 1, Akad Nauk SSSR publ, Moscow, pp 112–167
Krylov IN (1963) Columnar branching stromatolites of the Riphean deposits of the South Urals and their significance in stratigraphy of the Upper Precambrian. Akad Nauk SSSR publ, Moscow (Tr Geol Inst Akad Nauk SSSR, vol 69)
Krylov IN (1975) Riphean and Phanerozoic stromatolites in the USSR. Nauka, Moscow (Tr Geol Inst Akad Nauk SSSR, vol 274)
Krylov IN (1976) Approaches to the classification of stromatolites. In: Walter MR (ed) Stromatolites. Developments in sedimentology 20. Elsevier, Amsterdam, pp 31–43
Krylov IN (1985) Stromatolites in the Upper Precambrian stratigraphy – problems'85. Izv Akad Nauk SSSR Ser Geol 11:44–55
Krylov IN, Perttunen V (1978) Aphebian stromatolites from the Trevola Region, Northern Finland. In: Lower boundary of the Riphean and stromatolites of the Aphebian. Tr Geol Inst Akad Nauk SSSR Nauka, Moscow, 312:87–105
Liang Yu (1992) On the biostratigraphic significance of Precambrian stromatolites. In: Late Precambrian stromatolites and its relative ore deposits. Geol Publ, Beijing, pp 19–60
Liang Yu, Cao R, Zhang L et al. (1984) Pseudogymnosolenacea of Late Precambrian in China. Geol Publ House, Beijing
Liang Yu, Zhu S, Zhang L, Cao R, Gao Z, Bu D (1985) Stromatolite assemblages of Late Precambrian in China. Precambrian Res 29:15–32
Logan BW, Rezak R, Ginsburg RN (1964) Classification and environmental significance of algal stromatolites. J Geol 72:314–325
Lowie DR (1994) Abiogenic origin of described stromatolites older than 3.2 Ga. Geology 22:387–390
Makarikhin VV, Kononova GM (1983) Lower Proterozoic phytolites of Karelia. Nauka Leningrad
Maslov VP (1939) The genus *Collenia*. In: Gartmann-Veinberg AP (Editor), Problems of Paleontology 5, The Laboratory of Paleontology, Moscow University, Moscow: 285–310
Maslov VP (1959) Stromatolites and facies. Dokl Akad Nauk SSSR 125:1085–1088
Maslov VP (1960) Stromatolites (genesis, study methods, facies relation and geological significance). (Tr Geol Inst Akad Nauk SSSR, vol 41.) Akad Nauk SSSR, Moscow
Monty CLV (1977) Evolving concepts on the nature and the geological significance of stromatolites: a review. In: Flugel E (ed) Fossil algae. Springer, Berlin, Heidelberg New York, pp 15–35
Pia J (1927) Thallophyta. In: Hirmer M (Editor), Handbuch der Paleobotanik, vol 1. R. Oldenburg, Munich, Berlin, pp 31–136
Preiss WV (1972) The systematics of South Australian Precambrian and Cambrian stromatolites. Part I. Aust R Soc Trans 90:67–100
Preiss WV (1973) The systematics of South Australian Precambrian and Cambrian stromatolites. Part II. Aust R Soc Trans 97:91–125
Preiss WV (1977) The biostratigraphic potential of Precambrian stromatolites. Precambrian Res 5:207–219
Raaben ME (1964) Upper Riphean stromatolites of the Polyudov Ridge and their time range. Bull MOIP Otd Geol 69:86–101
Raaben ME (1969) Columnar stromatolites and Late Precambrian stratigraphy. Am J Sci 267:1–18
Raaben ME (1975) Upper Riphean as a unit of the general stratigraphic scale. (Tr Geol Inst Akad Nauk SSSR, vol 271) Nauka, Moscow
Raaben ME (1980) Microstromatites – a characteristic element of the Lower Proterozoic stromatolite assemblage. Dokl Akad Nauk SSSR 250:734–737
Raaben ME (1981) "Riphean" stromatolites in the Lower Proterozoic. Izv Akad Nauk SSSR Ser Geol 6:51–64
Raaben ME (1986) Topical problems of stromatolite systematics. In: Topical problems of the recent Paleoalgology. Naukova Dumka, Kiev, pp 137–143
Raaben ME (1991) Columnar microstromatites in the Early Riphean. Izv Akad Nauk SSSR Ser Geol 9:87–96
Raaben ME (1997) Stromatolites in the Riphean stratigraphy of North Eurasia. In: Riphean of North Eurasia. Geology, general problems of stratigraphy. Uralian Branch Russ Akad Nauk, Ekaterinburg, pp 13–20
Raaben ME (1998) Microstromatites and their genesis. Lithol Min Resour 2:153–161
Raaben ME, Komar VA (1982) Stromatolites of the Riphean of southern Urals. In: Stratotype of the Riphean. Paleontology. Paleomagnetism (Tr Geol Inst Akad Nauk SSSR, vol 368) Nauka, Moscow, pp 6–62
Raaben ME, Sinha AK (1989) Classification of stromatolites. Himalayan Geol 13:215–227
Raaben ME, Lyubtsov VV, Predovsky AA (1995) Correlation of stromatolitic formations of northern Norway (Finnmark) and northwestern Russia (Kildin Island and Kanin Peninsula). Nor Geol Unders Spec Publ 7:233–246
Semikhatov MA (1962). Riphean and Lower Cambrian of the Enisey Ridge. Akad Nauk SSSR Publ, Moscow (Tr Geol Inst Akad Nauk SSSR, vol 68)
Semikhatov MA (1974) Stratigraphy and geochronology of the Proterozoic. (Tr Geol Inst Akad Nauk SSSR, vol 256) Nauka, Moscow
Semikhatov MA (1976) Experience in stromatolite studies in the USSR. In Walter MR (ed) Stromatolites. Developments in sedimentology 20. Elsevier, Amsterdam, pp 337–358
Semikhatov MA (1978) Aphebian assemblage of stromatolites: general characteristics and comparision with the Riphean ones. In: Lower boundary of the Riphean and stromatolites of the Aphebian. (Tr Geol Inst Akad Nauk SSSR) Nauka, Moscow, 312:148–158
Semikhatov MA (1980) On the Upper Precambrian stromatolite standard of North Eurasia. Earth Sci Rev 16:235–247
Semikhatov MA (1985) Stromatolites in the Precambrian stratigraphy: Analysis'84. Izv Akad Nauk SSSR Ser Geol 8:3–13

Semikhatov MA (1991) General problems of Proterozoic stratigraphy in the USSR. Soviet Sci Rev Sec G Geol Rev, vol 1. Harwood Acad, New York

Semikhatov MA (1993) General subdivision of the Precambrian: comparision of the latest scales. Stratigr Geol Corr 1:4–16

Semikhatov MA (1995) Methodical principles of the Riphean stratigraphy. Stratigr Geol Corr 3:559–574

Semikhatov MA, Raaben ME (1994) Dynamics of the global diversity of Proterozoic stromatolites. Article 1: northern Eurasia, China and India. Stratigr Geol Corr 2:492–513

Semikhatov MA, Raaben ME (1996) Dynamics of the global diversity of Proterozoic stromatolites. Article 2: Africa, Australia, North America, and general syntesis. Stratigr Geol Corr 4:24–50

Semikhatov MA, Serebryakov SN (1983) Siberian hypostratotype of the Riphean. (Tr Geol Inst Akad Nauk SSSR, vol 367) Nauka, Moscow

Semikhatov MA, Gebelein CD, Cloud PE, Awramik SM, Benmore WC (1979) Stromatolite morphogenesis – progress and problems. Can J Earth Sci 16:992–1015

Serebryakov SN (1975) Peculiarities of formation and location of Riphean Siberian stromatolites. (Tr Geol Akad Nauk SSSR, vol 200) Nauka, Moscow

Sergeev VN, Semikhatov MA, Mudrenko LM (1998) Microfossils in Paleoproterozoic microphytolites, Gunflint Formation, South Canada. Stratigr Geol Corr 6:457–468

Sochava AV, Podkovyrov VN (1992) Changes in carbonate composition and taxonomic diversity of stromatolites. Lithol Min Resour 6:576–680

Vlasov FYa (1977) Precambrian stromatolites from the Satka Formation, South Urals. In: Materials on the Middle Paleozoic paleontology of the Urals and Siberia. Ural Sci Centre Akad Nauk SSSR, Sverdlovsk, pp 101–124

Walter MR (1972) Stromatolites and the biostratigraphy of the Australian Precambrian and Cambrian. Palaeontol Assoc Spec Pap, vol 11

Walter MR (ed) (1976) Stromatolites. Developments in sedimentology, vol 20. Elsevier, Amsterdam

Walter MR (1983) Archean stromatolites: evidence of the Earth's earliest benthos. In: Schopf WJ(ed) Earth's earliest biosphere. Princeton Univ Press, Princeton, pp 187–213

Walter MR, Heys GR (1985) Links between the rise of the Metazoa and the decline of stromatolites. Precambrian Res 29:149–174

Walter MR, Krylov IN, Muir MD (1988) Stromatolites from Middle and Late Proterozoic sequences in the McArthur and Georgina basins and the Mount Isa Province, Australia. Alcheringa 12:79–106

Walter MR, Grotzinger JP, Schopf JW (1992) Proterozoic stromatolites. In: Schopf JW, Klein C (eds) The Proterozoic biosphere. A multidisciplinary study. Cambridge Univ Press, Cambridge, pp 253–260

Xing Yu, Duan C, Liang Yu, Cao R et al. (1985) Late Precambrian paleontology of China. Geol Publ House, Beijing

Zhu S, Chen H (1992) Characteristics of Paleoproterozoic stromatolites in China. Precambrian Res 57:135–163

Microbial vs Environmental Influences on the Morphology of Late Archean Fenestrate Microbialites

Dawn Y. Sumner

Geology Department, University of California, Davis, CA 95616, USA

Abstract. Stromatolite morphology is the most abundant record of Archean life, but interpretations of the role of microbial communities in stromatolite growth are difficult because stromatolites are the result of complex interactions among abiotic and biotic processes. Archean fenestrate microbialites are a group of structures in which the roles of biotic and abiotic processes can be constrained more than in most stromatolites. Fenestrate microbialites from the 2.52 Ga Gamohaan and Fairfield formations, South Africa, the 2.6 Ga Bulawayo greenstone belt, Zimbabwe, and the ~2.8 Ga Steeprock greenstone belt, Ontario, each contain two morphologically distinct microbial communities that grew contemporaneously. One community grew as very fine, filmy laminae, and the other grew as wider, often vertically oriented "supports". The distinction of filmy laminae and supports persists with various microbialite structures over hundreds of millions of years and with two carbonate precipitation styles. Comparisons of these microbialites imply that the growth structure was determined by the microbial communities, and the timing and location of carbonate precipitation influenced preserved morphology.

1 Introduction

Recent discoveries of well preserved microfossils as old as 3.5 Ga (e.g. Buick 1990; Walsh 1992; Schopf 1993) as well as refinements in Archean carbonate and organic carbon isotope analyses (e.g. Schidlowski 1988; Des Marais 1994; Eiler et al. 1997; Mojzsis et al. 1997) leave little doubt that life existed on Earth by the time the oldest preserved sediments and metasediments were deposited. Thus, most, possibly all, sedimentary rocks were influenced to a greater or lesser degree by microbial activity. These influences can be observed as morphological features such as stromatolites or microbialites in addition to geochemical signatures and cellular remains. The morphology of stromatolites and microbialites, however, is a complex function of both environmental physiochemical processes and microbial behavior. To use stromatolites and microbialites to constrain the early evolution of life, it is necessary to identify specific microbial characteristics.

Several productive approaches have been used to identify various influences on stromatolite morphology. For example, Walter et al. (1976) studied the behavior of microbes in their description of and experimentation with the dominant cyanobacteria in conophyton stromatolites in a Yellowstone hot spring. Their data demonstrate that *Phormidium tenue*, a gliding, filamentous cyanobacterium with a strong phototactic response, formed peaked mats, whereas *Chloroflexus aurantiacus*, another gliding, filamentous cyanobacterium, did not. Other microbes also form peaked mats (i.e. Horodyski 1977; Farmer and DesMarais 1994), so a peaked morphology cannot be attributed solely to *P. tenue*, but the study documents a behavioral characteristic that creates specific morphological characteristics that can be preserved in the geological record.

A second approach to morphological interpretations of stromatolites is the statistical analysis of stromatolite form. Morphometrics have been used to quantitatively characterize morphological variations in stromatolites (e.g. Hofmann 1976, 1994; Zhang and Hofmann 1982; Banerjee and Chopra 1986). This method aids in the identification of statistically important variations in stromatolite morphology that can be contrasted to more subjective classification of stromatolites into groups and forms (analogous to genera and species). Another approach is to compare the statistical properties of laminae within stromatolites (or other sediments) with surfaces synthetically generated by specific growth rules (Grotzinger and Rothman 1996). This method uses specific theoretical modes of surface growth, whether driven by physiochemical or biological processes, to produce characteristic surfaces that are compared to observed stromatolite surfaces. For example, dendritic surfaces occur when growth is limited by diffusion and can be produced by metal oxidation (Chopard et al. 1991) and bacterial colony growth (Ben-Jacob et al. 1994) among other processes. Other examples of growth processes relevant to sediments include lateral sediment diffusion, surface normal accretion (mineral precipitation), and random noise. By characterizing the surfaces of stromatolites in terms of the modes of accretion, specific surface characteristics can be identified and compared to predicted characteristics of known biological and physiochemical processes. Although this technique may not specifically distinguish between biological and physiochemical influences on morphology, it can help identify the modes of surface growth that are consistent with the surface

R. E. Riding and S. M. Awramik (Eds.)
Microbial Sediments

characteristics (Grotzinger and Rothman 1996). This approach has great potential to provide new insights into the accretion of stromatolites.

A third approach to the characterization of stromatolite and microbialite morphology is the comparison of features within and across environments (many studies including: Raaben 1969; Awramik 1971; Hoffman 1974; Eriksson et al. 1976; Walter et al. 1976; Semikhatov et al. 1979; Bertrand-Sarfati and Moussine-Pouchkine 1985; Grotzinger 1990; Buick 1992). This is the most common approach; it has produced tremendous insights into the behavior of microbial communities, and it will continue to provide valuable information for decades to come. As work progresses, the extent of interpretation can increase, given appropriate rocks. Here, I provide a brief example of this approach applied to Late Archean fenestrate microbialites from four different deposits.

2 Fenestrate Microbialites

Fenestrate microbialites are a newly characterized group of microbial structures that consist of three components (Fig. 1; Sumner 1997b): draping, mat-like laminae; vertically oriented structures called supports or axial planes; and voids filled with carbonate cements. Mat-like laminae are 1–10 μm thick, very smooth, and defined by organic inclusions. These laminae were flexible and laterally cohesive during growth as demonstrated by recumbent synsedimentary folding of laminae (Fig. 2), implying that the laminae are the remnants of microbial mats composed of filamentous microbes with diameters of only a few microns (Sumner 1997b). Supports are 100–>300 μm wide and commonly are oriented vertically. They are interlocking surfaces in three dimensions and branch in some microbialites (Fig. 3; Sumner 1997b). They are defined by organic inclusions and are interpreted as microbial in origin due to their three-dimensional geometry and their soft, folded character in some microbialites (see Sumner 1997b, for further discussion). The supports are similar to axial planes in ribbed conophyton stromatolites (Komar et al. 1965) and may have a similar but as yet unknown origin. Dish-shaped to equant primary voids were created by the draping of filmy laminae over the supports (Fig. 1). These voids commonly contain marine cements that precipitated contemporaneously

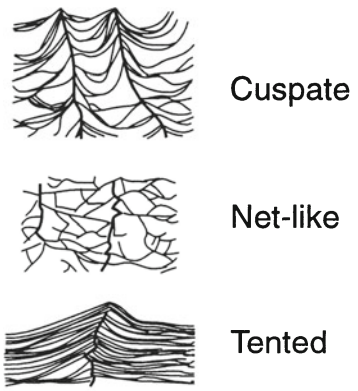

Fig. 1. Sketch of three fenestrate microbialite textures. *Thicker, mostly vertically oriented lines* represent supports. The *thinner, draping lines* represent laminated mat. *White area* is void space filled with calcite. Note that the laminated mat in the net-like microbialites is less regular and commonly ends in voids. The laminated mat in cuspate and tented microbialites is more continuous

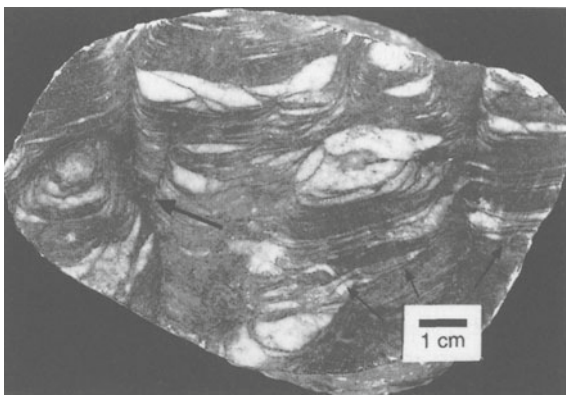

Fig. 3. Polished slab of a cuspate microbialite from the Bulawayo greenstone belt. Voids are *white*, and supports and laminated mat are *gray to black*. Supports branch at one point (*large arrow*) with the *upper right* branch showing evidence of compactional folding. Rare fibrous pseudomorphs project through the microbialites (*small arrows*)

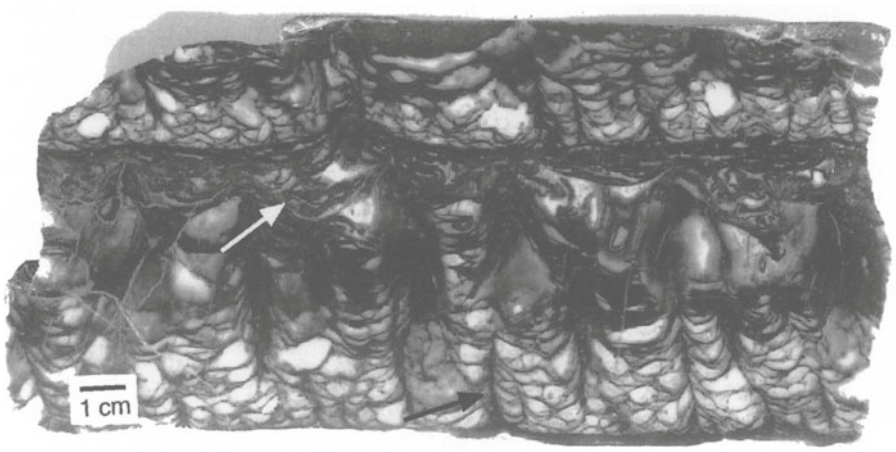

Fig. 2. Polished slab of a cuspate microbialite from the Gamohaan Formation. Void filling calcite is *white and gray*, whereas supports and laminated mat are *black*. The supports (*black arrow*) are spaced by 1–2 cm and are draped by laminated mat. The lower bed of microbialites is overlain by a thin layer of recumbently folded, reworked laminated mat (*white arrow*)

with microbialite growth (Sumner 1997b). The abundant and universally present voids give rise the name fenestrate microbialites.

The fenestrate microbialites show diverse morphologies due to varying proportions and relationships among the laminated mat, supports/axial planes, and cement-filled voids, in addition to physiochemical processes. However, the filmy laminae and supports are morphologically distinct in all of the fenestrate microbialites. This distinction remains even as the relationships among the supports, laminated mat, and carbonate cements change. The following four examples demonstrate some of the variations in these relationships where both laminated mat and supports are present.

2.1 Gamohaan Microbialites

Remnants of microbial communities are abundant in the 2521±3 Ma (Sumner and Bowring 1996) Gamohaan Formation, which was deposited during a transgression that resulted in drowning of the Campbellrand-Malmani carbonate platform, Transvaal Supergroup, South Africa (Beukes 1987; Sumner 1995, 1997a). Fenestrate microbialites were deposited in subwave base depositional environments that were highly supersaturated with respect to calcite (Sumner 1997a,b). The microbialites are well preserved as organic inclusions in unmetamorphosed and unstrained calcite and minor secondary dolomite.

Cuspate microbialites are common in the Gamohaan Formation (Fig. 2) and are characterized by Sumner (1997b). Supports are typically spaced a few centimeters apart, and layers of laminated mat range from 4-μm to decimeters thick. Voids are typically concave up and are isopachously filled with fibrous herringbone, bladed, and blocky calcite cements (Sumner and Grozinger 1996a; Sumner 1997b). The first generation of void-filling cement, the herringbone calcite, precipitated contemporaneously with microbialite growth. It also preferentially precipitated on the supports over the laminated mats, as demonstrated by the concentration of herringbone calcite near supports, growth banding in herringbone calcite, which indicates that calcite nucleated on and grew away from supports but not the laminated mat, and the abutment of herringbone calcite coatings against laminated mat attached to supports (Sumner 1997b). These relationships suggest that the microbial communities in the supports and the laminated mats affected the nucleation and/or precipitation of calcite differently.

2.2 Bulawayo Microbialites

The 2.6 Ga Bulawayo greenstone belt, Zimbabwe, consists of volcanics with lesser arkose to greywacke, shale, banded iron-formation, and limestone (Macgregor 1941). In Huntsman Quarry, 55 km north-northeast of Bulawayo, limestones contain abundant stromatolites that were long considered the oldest evidence of life on earth (Macgregor 1941; Schopf et al. 1971; Walter 1983). Macgregor (1941) originally described the stromatolites as giant, domal, conical to dentated, and columnar structures. Recent field work, including stratigraphic sections through two of the three pits at Huntsman quarry (Sumner and Grotzinger, in press), demonstrates that later workers described cuspate stromatolites in hand samples from the Huntsman quarry upside down as "columnar" stromatolites (Schopf et al. 1971; Walter 1983), due to the lack of opportunity to observe in situ stromatolites in the water-filled quarry (Kvenvolden, personal communication, 1997). The depositional environment for the Huntsman carbonates is poorly constrained. The cuspate microbialites described here are associated with giant stromatolites mounds (see Fig. 1 in Macgregor 1941) and probably grew in a subtidal depositional environment.

Cuspate microbialites (Fig. 3), similar to those described from the Gamohaan Formation, are found throughout thick beds of calcite. They did not initiate on and grow off of specific surfaces; rather, individual centimeter- to decimeter- tall cuspate microbialites begin and end within decimeter- to meter-thick beds. The microbialites contain abundant filmy, very fine laminae defined by organic inclusions that draped over similarly defined supports. Supports are spaced a few centimeters apart and show minor synsedimentary compactional folding. Layers of laminated mat range from millimeter to centimeters thick. Voids between laminae are dish-shaped and commonly centimeter-scale. Laminae and void characteristics, extensively described by Schopf et al. (1971), are consistent with the cuspate microbialites documented here when the hand samples are viewed as cuspate rather than domal-columnar stromatolites. The carbonaceous fill between "columns" of Schopf et al. (1971) corresponds to supports in the centers of cuspate microbialites.

Extensive recrystallization destroyed most of the primary carbonate fabrics. Thus, the style of precipitation in most of the voids and on the various microbial communities is poorly constrained. However, rare fibrous mineral pseudomorphs (probably after aragonite) project linearly through the microbialites irrespective of the orientation of microbial components (Fig. 3). The presence of the pseudomorphs does not correlate with changes in microbial texture (Sumner and Grotzinger, in press).

2.3 Fairfield Microbialites

The net-like microbialites (Fig. 4) of the < 2521 Ma Fairfield Formation, Transvaal Supergroup, were deposited on the Campbellrand-Malmani carbonate platform in a transgressive systems tract prior to deposition of the Gamohaan Formation (Beukes 1987; Sumner 1995). They are interbedded with giant, elongate stromatolite mounds that were deposited in a deep subtidal depositional environment above wave base. The lack of scouring and the delicate nature of the microbialites suggest that the net-like microbialites were deposited in a low-energy environment, probably below wave base. The net-like microbialites are found in centimeter to decimeter-thick beds (Fig. 4). Microbial growth initiated on sharp surfaces, and the net-like texture grades upward into very small tented microbialites and then planar laminated mat with irregular laminae. Most beds are capped by coarsely laminated dolomite that occasionally contains either poorly preserved, ripple cross-stratification or centimeter-scale domal stromatolites.

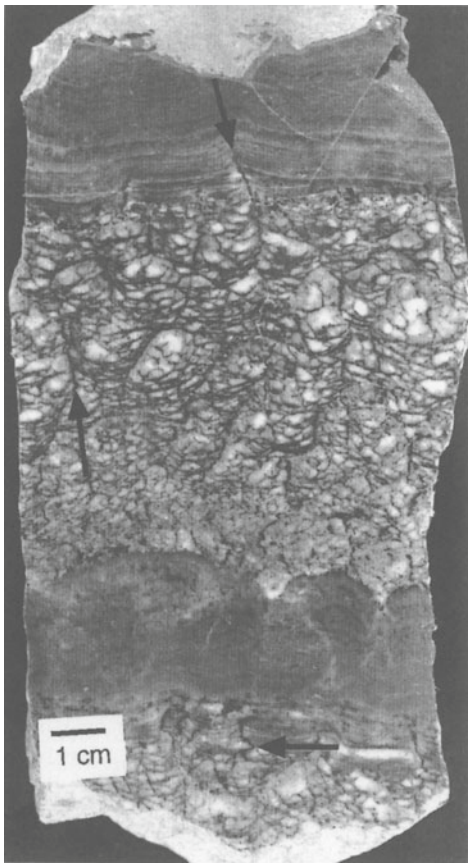

Fig. 4. Polished slab of a net-like microbialite from the Frisco Formation. Supports (*arrows*) are more closely spaced and show abundant evidence of compaction (*lowest arrow*). Layers of laminated dolomite separate beds of microbialites. Supports project up into the bases of some of these layers (upper arrow)

The coarsely laminated dolomite is capped by a sharp surface on which the next microbialites grew.

The net-like microbialites consist of filmy laminae and supports. Both are defined by organic inclusions in coarsely crystalline dolomite. Supports are typically spaced about 2 mm apart and are usually folded, suggesting synsedimentary compaction (Fig. 4). Layers of laminated mat are typically several hundred microns thick and are vertically separated by about 1 mm along the supports. Layers of laminae are commonly discontinuous, sometimes ending within a void. Voids are equant rather than dish-shaped and are consistently small, averaging 2 mm in diameter. Carbonate cement textures are not preserved, but faint color zonation from the edge to the middle of voids suggests the former presence of isopachous, void-filling cements. Upward in each bed, supports project into the overlying laminated, fenestrae-poor layers forming the supports for tented microbialites (Fig. 4).

2.4 Steeprock Microbialites

Carbonates in the ~2.8 Ga Steeprock greenstone belt are underlain by a basal conglomerate that grades upward into 500 m of limestone and dolostone (Jolliffe 1955 1966; Wilks and Nisbet 1985). The carbonates are truncated by an extensive karst surface that cuts out large parts of the section and is overlain by banded iron formation. The carbonates are typically banded to massive with extensive brecciation near fold noses (Jolliffe 1955, 1966; Wilks and Nisbet 1985). Stromatolites were found in the carbonates as early as 1891 (Smyth 1891) and have been studied repeatedly. Most recently, they have been described by Wilks and Nisbet (1985), who reported a variety of columnar, domal, and linked conical stromatolite forms. Field work by John Grotzinger, who provided the samples described here, documented the presence of microbialites similar to the net-like microbialites of the Fairfield Formation.

The Steeprock net-like microbialites are preserved in finely crystalline limestone with minor dolomite and are cut by secondary calcite veins (Fig. 5). The microbialites commonly are found in wavy layers with alternating void-rich and void-poor microbialites, which produce the bedding. Microbialites commonly are crosscut by fibrous mineral pseudomorphs. These pseudomorphs are replaced by calcite, but preserved their primary fibrous character with blunt crystal bundle terminations which suggests an aragonite primary mineralogy (e.g. Sandberg 1985). The pseudomorphs form fanning bundles of crystals that grew upward. Laterally, neighboring fans of crystals interfered with each others growth (Fig. 5B). Wavy bedding in the microbialites is due to doming of microbialites over areas with abundant fibrous pseudomorphs. This geometry suggests

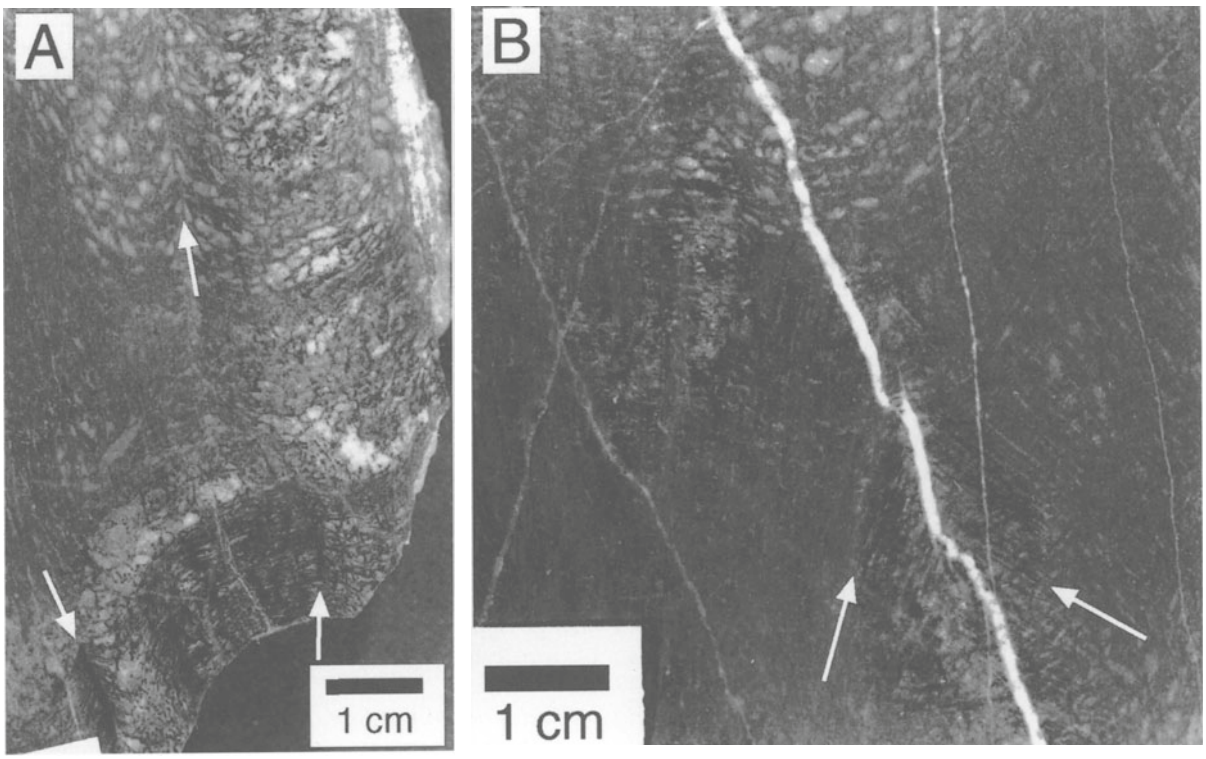

Fig. 5A,B. Polished slabs of a cuspate microbialite from the Steeprock greenstone belt. **A** Alternating layers of void-poor (*bottom*) and void-rich (*top*) microbialites. Laminated mat and supports at the base of the sample are preserved better than those above and thus appear blacker. Supports (*arrows*) are visible in this layer. A support (*arrow*) is also apparent in the upper, void-rich microbialite layer. **B** Fibrous pseudomorphs projecting through void-poor microbialites. The pseudomorphs from neighboring botryoids converge (*arrows* indicate growth direction of fibers). The sample is cross-cut with calcite-filled veins (*white*)

that fibrous mineral precipitation and microbialite growth were contemporaneous (Sumner and Grotzinger, in press).

Void-rich, net-like microbialites contain abundant supports draped by thin laminae. The supports are spaced 2–10 mm and commonly show compactional folding. Layers of laminated mat are typically several hundred microns thick. Voids are equant to flattened ovals and 0.5–2 mm in diameter (Fig. 5). Isopachous void-filling carbonate cements are not apparent, and only rare aragonite(?) pseudomorphs project through the void-rich microbialites. Thus, the origin of void-filling carbonate is unclear. Void-poor microbialites contain abundant compacted supports draped by filmy laminae, similar to very closely spaced tented microbialites (Fig. 5). Voids are rare and are flattened parallel to the filmy laminae where present. Both the laminae and voids follow the wavy nature of bedding. Aragonite(?) pseudomorphs are common in void-poor areas.

3 Interpretation

The presence of morphologically distinct filmy laminae and supports in fenestrate microbialites from diverse deposits suggests that the processes promoting and preserving their growth were long-lived. Sumner (1997b) suggested that the supports and filmy laminae represent two distinct microbial communities that grew contemporaneously within the same structure. This interpretation is based on the distinct morphological expression of the supports and laminated mat without gradations between them and on their different influences on the location of calcite cement precipitation in the Gamohaan fenestrate microbialites (Sumner 1997b). The consistent expression of filmy laminae and supports in the diverse occurrences described here supports this interpretation. Morphological similarities among the various types of fenestrate microbialites suggest that the aggregate behavior of the two microbial communities composing the laminated mat and the supports was similar. Differences in morphology may be due to variations in the proportion of microbes composing the supports and filmy laminae or to variations in depositional environment.

The precipitation style of encasing carbonate cements probably played a passive role in the preserved morphology of the microbialites. Aragonite vs calcite precipitation did not control microbialite morphology: The Gamohaan cuspate microbialites were coated with

isopachous calcite cements, whereas the Bulawayo cuspate microbialites contain elongate aragonite(?) pseudomorphs that project through the microbial structures. These two styles of carbonate precipitation would have provided very different structural support for the laminated mat and supports, but the overall morphology of the microbialites is similar. The same is true of net-like microbialites from the Fairfield Formation and Steeprock greenstone belt: The morphology of the microbial structures is similar, but the Steeprock microbialites contain elongate aragonite(?) pseudomorphs whereas the Fairfield microbialites do not. Thus, it appears that the mineralogy and style of carbonate precipitation in-filling the voids did not substantially influence their morphology.

In contrast, the timing of carbonate precipitation appears to have had a substantial influence on preserved microbialite morphology. Comparisons of void-rich and void-poor net-like microbialites from Steeprock suggest that the differences in texture can be attributed to the extent of synsedimentary compaction. The flattening of voids and common compaction of supports in the void-poor microbialites may be due to a lack of carbonate precipitation on the supports which would have increased the structural rigidity of supports in other microbialites, possibly including the associated void-rich microbialites. The abundance of aragonite(?) pseudomorphs projecting through the compacted microbial structures is consistent with aragonite precipitation below the mat-water interface after microbialite growth. Void-rich microbialites may have formed when conditions were favorable (either environmentally or biologically) for carbonate precipitation on the supports contemporaneously with microbialite growth.

3.1 Temporal Distribution

Variations in fenestrate microbialite morphology are not due to the evolution and extinction of individual microbial strains. The morphological similarity of the Bulawayo and Gamohaan-Frisco cuspate microbialites is striking considering their 100 Ma age difference. The same is true of the Steeprock and Fairfield net-like microbialites. These similarities over millions of years imply that the differences in morphology between net-like and cuspate microbialites are not due to the evolution or extinction of individual organisms. However, similar microbialites have not been reported in Proterozoic rocks. Three interpretations for their apparent absence are possible.

First, they may be present, but have not been reported. This is unlikely given the extensive description of Proterozoic stromatolites. They do have some similarities to conophyton stromatolites, however, particularly the axial planes of ribbed conophyton (Komar et al. 1965). It is unclear how the ribs formed, and more extensive comparisons between fenestrate microbialites and ribbed conophyton stromatolites may prove insightful.

Second, biological evolution may have produced organisms that inhibited the production of fenestrate microbialites or caused the extinction of essential microbes for their construction. Modern microbial communities are capable of producing structures similar to the cuspate microbialites described here. Modern mats in Yellowstone hot and cold springs (Walter et al. 1976; Farmer and DesMarais 1994) and in sub-ice lakes in Antarctica (Wharton 1994) produce complex, three-dimensional structures with abundant voids. The dominant organisms in these environments vary, implying that many different organisms are capable of constructing complex, void-filled mats. Thus, microbes still exist that can produce similar mats to those preserved in fenestrate microbialites, suggesting that evolutionary change is unlikely to be the sole reason for the absence of cuspate and net-like microbialites in younger marine carbonates.

Third, sedimentary environments may have changed to the extent that appropriate depositional environments were no longer widespread or did not favor preservation of void-rich microbial structures. Archean depositional environments have several similarities to those from Yellowstone springs and Antarctic sub-ice lakes. All of these environments contain still water with low influx of sediment (Walter et al. 1976; Farmer and DesMarais 1994; Wharton 1994; Sumner 1997a,b). These two conditions, in addition to very early lithification, may be essential for the growth and preservation of such complex microbial structures. Clearly, low energy environments persisted into Proterozoic time. However, the modes of carbonate precipitation may have changed. Sumner and Grotzinger (1996b) propose that Fe^{2+} in Archean sea water promoted the precipitation of carbonate crystals on the sea floor rather than of micrite in suspension. A rise in oxygen at about 2 Ga may have shifted carbonate precipitation from in situ encrustations to micrite in the water column. This may have dramatically changed the preservation of microbial structures by increasing the influx of particulates in low energy environments and reducing the abundance of isopachous cement and aragonite fan precipitation (Sumner and Grotzinger 1996b; Sumner 1997a).

An example of the morphological effects of micrite vs in situ carbonate precipitation may be preserved in the morphological variation in net-like microbialites from the Fairfield Formation. The upward transition in each bed from net-like microbialites to tented microbialites to planar laminated mat (Fig. 4) may be due to an influx of micrite or silt-sized carbonate. Through this

transition, the microbialites lose the void-rich structure and become more compacted. The rare presence of cross-stratification in the carbonate above the tented microbialites suggests an influx of carbonate grains. A gradual increase in sediment supply could aid in the compaction of the underlying microbialites affecting their preserved morphology. Thus, long-term changes in the style of carbonate precipitation may have influenced the preservation and texture of microbial structures.

4 Conclusions

Fenestrate microbialites are a widespread class of microbial structures in Archean carbonates. Their morphological variations appear to be mostly attributable to microbial processes, including the segregation of individuals into two morphologically distinct communities. Contemporaneous to early diagenetic carbonate precipitation on and within the structures appears to have been essential for their preservation. However, the style of this carbonate precipitation does not appear to have affected the structure of the microbial communities.

Acknowledgements. I would like to thank John P. Grotzinger for extensive discussions and support during analysis of the various microbial structures and for sharing his field observations from the Steeprock greenstone belt and the Huntsman Quarry. Thanks also go to Nicolas Beukes for field support in South Africa and his observations at Huntsman Quarry. This manuscript greatly benefited from reviews by Janine Sarfati and Roger Buick, which led to substantial improvements in both content and presentation. Financial support was provided by the Gretchen L. Blechschmidt Fund of GSA and the O.K. Earl Postdoctoral Scholarship, California Institute of Technology, to me, and NASA grant NAGW-2795 to John P. Grotzinger at Massachusetts Institute of Technology.

References

Awramik SM (1971) Precambrian columnar stromatolite diversity: reflection of metazoan appearance. Science 174:825–827

Banerjee DM, Chopra J (1986) Morphometric analysis of Proterozoic stromatolites from India – preliminary report on testing of a new technique. Precambrian Res 33:265–282

Ben-Jacob E, Schochet O, Tenenbaum A, Cohen I, Czirok A, Vicsek T (1994) Generic modeling of cooperative growth patterns in bacterial colonies. Nature 368:46–49

Bertrand-Sarfati J, Moussine-Pouchkine A (1985) Evolution and environmental conditions of *Conophyton-Jacutophyton* associations in the Atar Dolomite (Upper Proterozoic, Mauritania). Precambrian Res 29:207–234

Beukes NJ (1987) Facies relations, depositional environments and diagenesis in a major early Proterozoic stromatolitic carbonate platform to basinal sequence, Campbellrand Subgroup, Transvaal Supergroup, southern Africa. Sediment Geol 54:1–46

Buick R (1990) Microfossil recognition in Archean rocks; and appraisal of spheroids and filaments from a 3500 m.y. old chert-barite unit at North Pole, Western Australia. Palaios 5:441–459

Buick R (1992) The antiquity of oxygenic photosynthesis: evidence from stromatolites in sulphate-deficient Archean lakes. Science 255:74–77

Chopard B, Herrmann HJ, Vicsek T (1991) Structure and growth mechanism of mineral dendrites. Nature 353:409–412

DesMarais DJ (1994) Tectonic control of the crustal organic carbon reservoir during the Precambrian. Chem Geol 114:303–314

Eiler JM, Mojzsis SJ, Arrhenius G (1997) Carbon isotope evidence for early life [discussion]. Nature 386:665

Eriksson KA, Truswell, JF, Button A (1976) Palaeoenvironmental and geochemical models from an early Proterozoic carbonate succession in South Africa. In: Walter MR (ed) Stromatolites. Elsevier, New York, pp 635–643

Farmer JD, DesMarais DJ (1994) Biological versus inorganic processes in stromatolite morphogenesis: observations from mineralizing sedimentary systems In: Stal LJ, Caumette P (eds) Microbial mats; structure, development and environmental significance. Springer, Berlin Heidelberg New York, pp 61–68

Grotzinger JP (1990) Geochemical model for Proterozoic stromatolite decline. Am J Sci 290-A:80–103

Grotzinger JP, Rothman DH (1996) An abiotic model for stromatolite morphogenesis. Nature 383:423–425

Hoffman F (1974) Shallow and deep-water stromatolites in lower Proterozoic platform-to-basin facies change, Great Slave Lake, Canada. Am Assoc Pet Geol Bull 58:856–867

Hofmann HJ (1976) Stromatoid morphometrics. In: Walter MR (ed) Stromatolites. Elsevier, New York, pp 45–54

Hofmann HJ (1994) Quantitative stromatolitology. J Paleontol 68:704–709

Horodyski RJ (1977) *Lyngbya* mats at Laguna Mormona, Baja California, Mexico: Comparison with Proterozoic stromatolites. J Sediment Petrol 47:1305–1320

Jolliffe AW (1955) Geology and iron ores of Steep Rock Lake. Econ Geol 50:373–398

Jolliffe AW (1966) Stratigraphy of the Steep Rock Group, Steep Rock Lake, Ontario. In: Goodwin AM (ed) Precambrian symposium. Geol Assoc of Can, Spec Pap 3:75–98

Komar A, Raaben ME, MA (1965) Konofitony rifeya SSSR i ikh stratigraficheskoe znachenie (Conophytons of the Riphean of the USSR and their stratigraphic significance), vol 131. Akademii Nauk SSSR, Geologicheskii Institut Trudy

Macgregor AM (1941). A pre-Cambrian algal limestone in southern Rhodesia. Trans Geol Soc S Afr 43:9–16

Mojzsis SJ, Arrhenius G, McKeegan KD, HarrisonTM, Nutman AP, Friend CRL (1997) Evidence for life on Earth before 3,800 million years ago. Nature 384:55–59

Raaben (1969) Columnar stromatolites and late Precambrian stratigraphy. Am J Sci 267:1–18

Sandberg P (1985) Aragonite cements and their occurrence in ancient limestone. In: N Schneidermann, PM Harris (ed) Carbonate cements. SEPM Spec Publ 36:33–57

Schidlowski M (1988) A 3,800-million-year isotopic record of life from carbon in sedimentary rocks. Nature 333:313–318

Schopf JW (1993) Microfossils of the early Archean Apex Chert; new evidence of the antiquity of life. Science 260:640–64

Schopf JW, Oehler DZ, Horodyski RJ, Kvenvolden KA (1971) Biogenicity and significance of the oldest known stromatolites. J Paleontol 45:477–485

Semikhatov MA., Gebelein CD, Cloud S, Awramik SM, Benmore WC (1979) Stromatolite morphogenesis–progress and problems. Can J Earth Sci 16:992–1015

Smyth HL (1891) Structural geology of Steep Rock Lake, Ontario. Am J Sci 43:317–331

Sumner DY (1995) Facies, paleogeography, and carbonate precipitation on the Archean (2520 Ma) Campbellrand-Malmani Carbonate Platform, Transvaal Supergroup, South Africa. Doctoral Thesis, Massachusetts Institute of Technology

Sumner DY (1997a) Carbonate precipitation and oxygen stratification in late Archean seawater as deduced from facies and stratigraphy of the Gamohaan and Frisco formations, Transvaal Supergroup, South Africa. Am J Sci 297:455–487

Sumner DY (1997b) Late Archean calcite-microbe interactions: Two morphologically distinct microbial communities that affected calcite nucleation differently. Palaios 12:300–316

Sumner DY, Bowring SA (1996) U-Pb geochronologic constraints on deposition of the Campbellrand Subgroup, Transvaal Supergroup, South Africa. Precambrian Res 78:25–35

Sumner DY, Grotzinger JP (1996a) Herringbone calcite: petrography and environmental significance. J Sediment Res 66:419–429
Sumner DY, Grotzinger JP (1996b) Were kinetics of Archean calcium carbonate precipitation related to oxygen concentration? Geology 24:119–122
Sumner DY, Grotzinger JP (in press) Late Archean aragonite precipitation. In: JP Grotzinger, NP James (ed) Carbonate Sedimentation and diagenesis in the evolving Precambrian world. SEPM Spec Publ 65
Walsh MM (1992) Microfossils and possible microfossils from the early Archean Onverwacht Group, Barberton Mountain Land, South Africa. Precambrian Res 54:271–293
Walter MR (1983) Archean stromatolites: evidence of the Earth's earliest benthos. In: Schopf JW ed) Earth's earliest biosphere. Princeton University Press, Princeton. pp 187–213
Walter MR, Bauld J, Brock TD (1976) Microbiology and morphogenesis of columnar stromatolites (*Conophyton, Vacerrilla*) from hot springs in Yellowstone National Park. In: Walter MR (ed) Stromatolites. Elsevier, New York, pp 273–310
Wharton RA (1994) Stromatolitic mats in Antarctic lakes. In: Bertrand-Sarfati J, Monty C (eds) Phanerozoic stromatolites II. Kluwer Academic, Dordrecht, pp 53–70
Wilks MW, Nisbet EG (1985) Archean stromatolites from the Steep Rock Group, northwestern Ontario, Canada. Can J Earth Sci 22: 792–799
Zhang Y, Hofmann HJ (1982) Precambrian stromatolites: image analysis of lamina shape. J Geol 90:253–268

Archean Stromatolites as Microbial Archives

H. J. Hofmann

Department of Geology, University of Montreal, P.O. Box 6128, Sta. A, Montreal, Quebec H3C 3J7, Canada
Present address: H.J. Hofmann, Redpath Museum, and Department of Earth and Planetary Sciences, McGill University, 3450 University St., Montreal, QC. H3A 2A7, Canada

Abstract. Stromatolites are morphologically circumscribed accretionary growth structures with a primary lamination that is, or may be, biologically influenced (biogenic). They are found in Archean sedimentary carbonate rocks, almost always associated with extensive volcanic sequences. Thirty-two occurrences have been reported from 11 small regional clusters representing the world's principal preserved Archean cratons: North America 16, Africa 7, Australia 5, Asia 3, and Europe 1; none are presently known from Archean rocks of South America and Antarctica; less than two dozen of the occurrences are viewed as definitely Archean and stromatolitic. The earliest stromatolite records date back to nearly 3.5 Ga, and their worldwide distribution and abundance increase as time progresses.

Morphological types include structures with flat, convex-up, concave-up, and globoidal laminae; stacking patterns producing nodular, columnar (unbranched as well as branched), and oncoidal forms are represented. The observed diameters of the structures show a gradual increase in size as the stratigraphic column is ascended, spread over two orders of magnitude in geon 34 (centimetric to decimetric), but ranging over six orders of magnitude by geon 25 (sub-millimetric to dekametric). Unlike Proterozoic stromatolites, most are developed in limestones rather than dolostones, with sideritic/ankeritic and cherty types also present. Microfossils are only very rarely preserved. Ministromatolites with radial-fibrous microstructure, probably almost exclusively the result of chemical precipitation, developed after 3.0 Ga, as did mesoscopic aragonite/calcite crystal fans, indicating carbonate supersaturation of ambient Meso- and Neoarchean ocean waters.

1 Introduction

The search for the oldest fossils is intimately tied to one of the fundamental philosophical questions that humankind has posed, the enigma of the origin of life itself. Diverse scientific disciplines have provided a degree of understanding of the processes, conditions, and time-frame involved. Nature is reluctant to give up its secrets, and continues to provide surprises that challenge the prevailing, sometimes long-established, views of our planet's past, such as the existence of exotic biotas associated with submarine hydrothermal vents. Humans are curious about how life began and how it evolved, and thus Precambrian paleontology has come to play a central role in assembling relevant data that can assist in tracing the pathways subsequent to the rise of the first organisms.

Direct evidence for the existence of an early, Archean biosphere (>2500 Ma) presents itself at three levels of observation: (1) amongst the group of megascopic remains called stromatolites and the related oncoids, (2) microscopic fossils, and (3) chemical evidence at the atomic, elemental, and molecular levels, such as isotopically light signatures of metabolized stable isotopes, carbon in the form of kerogen or graphite, and organic biomarker compounds. The focus in this chapter is on the stromatolite evidence. Previous reviews of Archean stromatolites are those of Walter (1983, 1994), Nisbet (1987), Awramik (1991, 1992), and Schopf (1994).

I begin with a brief historical perspective of the study of Archean stromatolites, followed by discussion of what they are or may be, and how the known record is distributed in space and time.

2 Historical Review

Progress in the study of Archean stromatolites is closely tied to the growth of Precambrian paleontology in general, and can be considered in the context of a succession of three main phases (Fig. 1A), each defined by a different tempo of significant contributions to our knowledge of the most ancient fossil record. The initial period extends from the uncertain beginnings of Precambrian paleontology in the mid-nineteenth century (description of laminated structures, later called "*Eozoon canadense*") to the discovery and description of the first real stromatolites in real Archean rocks at Steep Rock Lake, Ontario, in 1911 (Lawson 1912; Walcott 1912).

The second period, between 1912 and the early 1960s, is characterized not only by some classic studies on Proterozoic and modern stromatolites, but also the discovery of three notable occurrences of bona fide Archean stromatolites, whose biologic nature, however, was initially met with much scepticism. The first of the new discoveries was made in South Africa in 1927 in what is now the Transvaal Supergroup – originally regarded as Proterozoic (Young 1928, 1933–1935, 1940a,b, 1942, 1944; Young and Mendelsohn 1949). Young (1928) at first favoured a mechanical origin, then argued

R.E. Riding and S.M. Awramik (Eds.)
Microbial Sediments

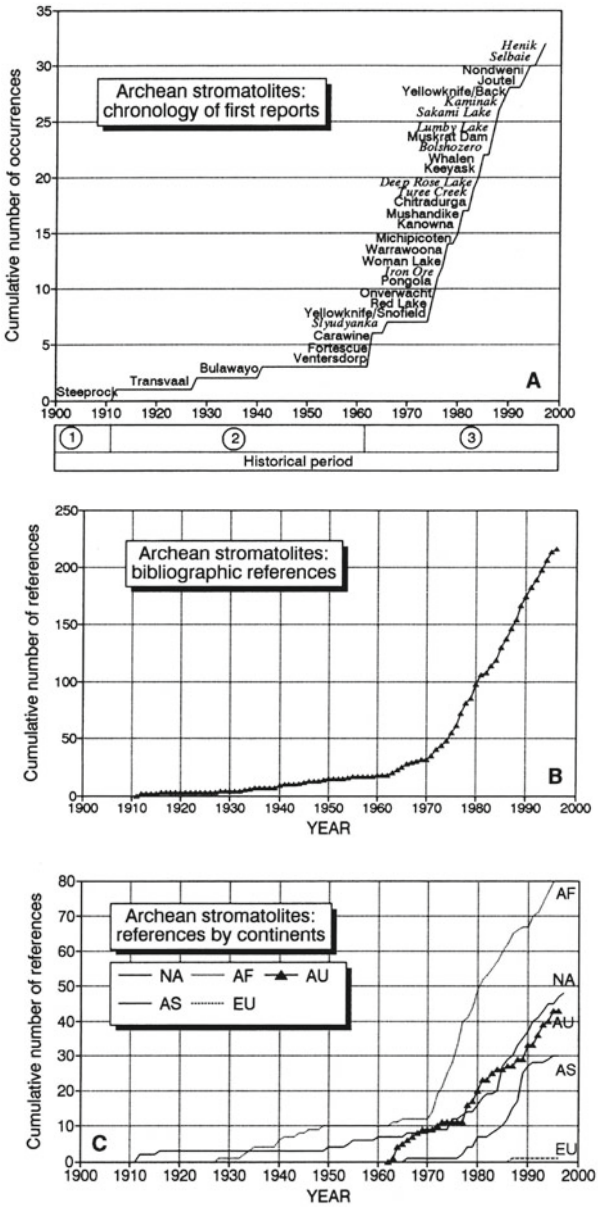

Fig. 1A–C. Chronology of bibliographic references to Archean stromatolites. **A** Discoveries and first reports; items in *italics* are questionable occurrences. The cumulative curve is divided into three historical periods: *1* initial period of Precambrian paleontology largely overlapping with the Eozoon controversy, *2* period of pioneering work with true Archean stromatolites and slow growth of field, and *3* modern period of surging interest in Precambrian fossils. **B** Growth of bibliographic references on all Archean stromatolites. **C** Growth of bibliographic references on Archean stromatolites categorized by continents

strongly for their biogenicity (Young 1933–1935, 1940a), but later partially reversed himself again in favour of a deformational explanation for some (Young 1944). Young (1933, Plate 4, Fig. 2) also provided the first illustration of what has recently been referred to as "herringbone cement", a sea floor precipitate that indicates waters supersaturated with respect to calcite, and is a useful criterion in assessing the saturation states of the Precambrian oceans (Sumner and Grotzinger 1996a,b).

Finds initially or eventually attributed to the Archean ensued in 1935 in the Bulawayo Group in Southern Rhodesia, now Zimbabwe (Macgregor 1941), followed by one in the Ventersdorp Supergroup in South Africa (Winter 1963), and others in the Fortescue and Hamersley Groups in Western Australia (de la Hunty 1963, 1964).

The third period is one of substantially more widespread interest in Precambrian paleontology, and in stromatolites in general, generated most likely as a result of a series of seminal papers on Precambrian metazoa, microfossils and stromatolites in the 1960s, as well as English-language reviews that made the results of pioneering Russian literature on Proterozoic stromatolites more accessible (e.g., Hofmann 1969, 1973; Cloud and Semikhatov 1969; Raaben 1969; Walter 1972). Also, the discovery of modern, marine columnar stromatolites in Western Australia provided a modern model for Precambrian structures. During the following decade one can also see the application of the experience gained earlier with the Proterozoic and Phanerozoic stromatolites to ever older rocks. Geologists mapping in Archean terrains, now more broadly trained in sedimentary geology, were probably sensitized to look for and recognize similar structures, and new occurrences came to be described with increased tempo in North America, Africa, India, and Australia (Fig. 1B,C), and more can be expected. Various types of accompanying geochemical and geochronologic studies of Archean sediments yielded better quantitative information on the ancient rocks and thereby elucidated processes and histories. The early and mid-1970s also experienced a renaissance in studies of stromatolitic units investigated earlier this century, interest that continues today.

3 Stromatolites as Evidence for Archean Life

So, what are stromatolites, and why are they important? A long-standing controversy has existed over the definition and meaning of the term stromatolite and its synonyms. This matter is of particular relevance to the Archean, inasmuch as it is the stromatolites that have in the past been used to demonstrate the existence of a biosphere and benthic ecosystems on the early Earth. Furthermore, stromatolites are now also primary targets in the search for past extraterrestrial life, specifically on Mars, because they are potentially recognizable by remote imaging by a camera mounted on a planetary rover; this new field has been baptized exopaleontology (Farmer and Des Marais 1994). Thus stromatolites, as proxies for microbial ecosystems, can have far-reaching implications in the exploration for life in

the universe in general. Accordingly, it is imperative to discuss here the question of how such laminated structures in Archean sequences can be formed, and the criteria that might help establish the involvement of biologic activity. It has been said that the evidence for recognizing the oldest fossils must be judged with the most exacting standards of critical evaluation with respect to both age and biogenicity. This challenge is more easily stated than resolved in practice, particularly with regard to the latter, as discussions in the literature demonstrate (e.g. Lowe 1994, 1995; Buick et al. 1995).

For the purpose of the present chapter I follow the reasoning given in an earlier paper (Hofmann 1973, pp. 348–350), and include under stromatolites all *morphologically circumscribed accretionary growth structures with primary lamination that is, or may be, biogenic.* The more recent term microbialite (Burne and Moore 1987, p. 10) also exists, but it refers to both laminated and unlaminated benthic accumulations of undisputed microbial origin.

On a theoretical level, three primary processes – physical, chemical, and biologic – can be envisaged as contributing to the formation of laminated constructs with particular morphologic characteristics. The resulting products represent the complex interactions between them; each process will forge its own morphologic and material contribution to the final stromatolite attributes. The relative effects of each mechanism can be represented by a ternary diagram, with soft microbial mats (B), chemically precipitated laminates (C), and mechanical/detrital deposits (M) as end members. One can add biological skeletal lamination (S), such as produced by crustose coralline algae, as a fourth end member, and thus represent the phase space of laminated (stromatolitic) structures by a tetrahedron (Fig. 2). However, the skeletal laminates are of no relevance to the Archean biosphere and are not discussed further inasmuch as this phenomenon is confined to Neoproterozoic and younger deposits; Archean structures are restricted to the B-C-M face.

Also following earlier practice (Hofmann 1973), I distinguish between the concepts of biophoric (microfossil-bearing) and biogenic (microbially influenced). A stromatolite can be biogenic without being biophoric (having no microfossils preserved), or biophoric without being biogenic (having accidentally trapped allogenic inclusions of microbes in otherwise purely chemical or mechanically formed accretionary structures, or secondarily introduced younger microbes). Ideally, of course, a stromatolite is both biogenic and biophoric, as modern laminated mats are, but for most Precambrian occurrences such clear-cut evidence is rarely preserved. This makes it difficult in practice to identify the extent of the biologic contribution to a particular structure. The shape of a Precambrian sample may further be the result of secondary modification. For instance, deformation of flat crenulated layers into a domed structure is inferred by Lowe (1994, Fig. 3) to explain a specimen from the Paleoarchean Warrawoona Group (Fig. 3A). But even here, while the larger structure is arguably interpreted as mechanical, the possibility is admitted that the small-scale crenulation may be biogenic. Inasmuch as there is a possible biologic contribution to the primary lamination, one can consider that particular structure to be a stromatolite. On the other hand, secondary modification may involve introduction of younger microbes into an older sediment, as postulated for another Warrawoona stromatolite (Buick 1984). In this case the biophoric nature is secondary and has little to do with the production of the primary lamination.

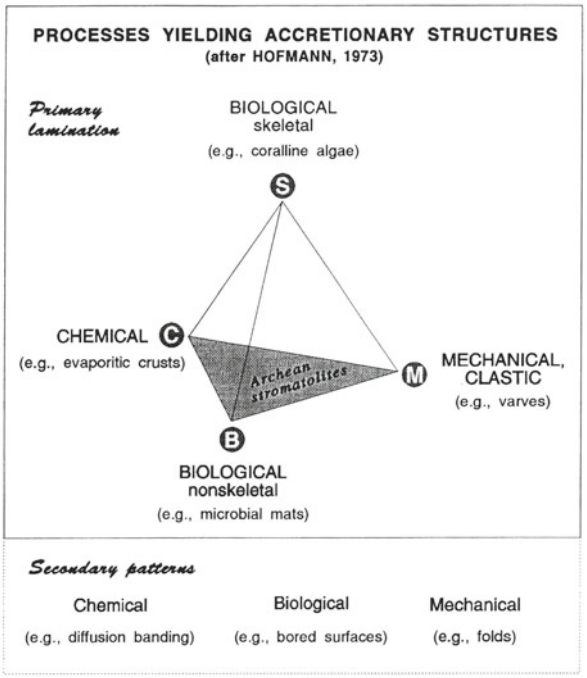

Fig. 2. Graphic representation of the three primary processes contributing to the formation of Archean stromatolites: *B* biological; *C* chemical; *M* physical (mechanical). (After Hofmann 1973, Fig. 5)

Discussions of the biogenic vs abiogenic nature of certain Archean stromatolites, and the reversal of earlier interpretations (e.g., Lowe 1980, 1994, 1995; Walter et al. 1980; Buick et al. 1981, 1995), serve to underline the difficulties not only with the terminology, but also with the interpretation of the origin of ancient laminated structures. Such difficulties of interpretation are not new, as shown by the nineteenth century *Eozoon* controversy, or the alternating explanations provided by Young in his series of papers earlier this century on the Transvaal stromatolites. Criteria for assessing the biogenicity of problematic remains, including stromato-

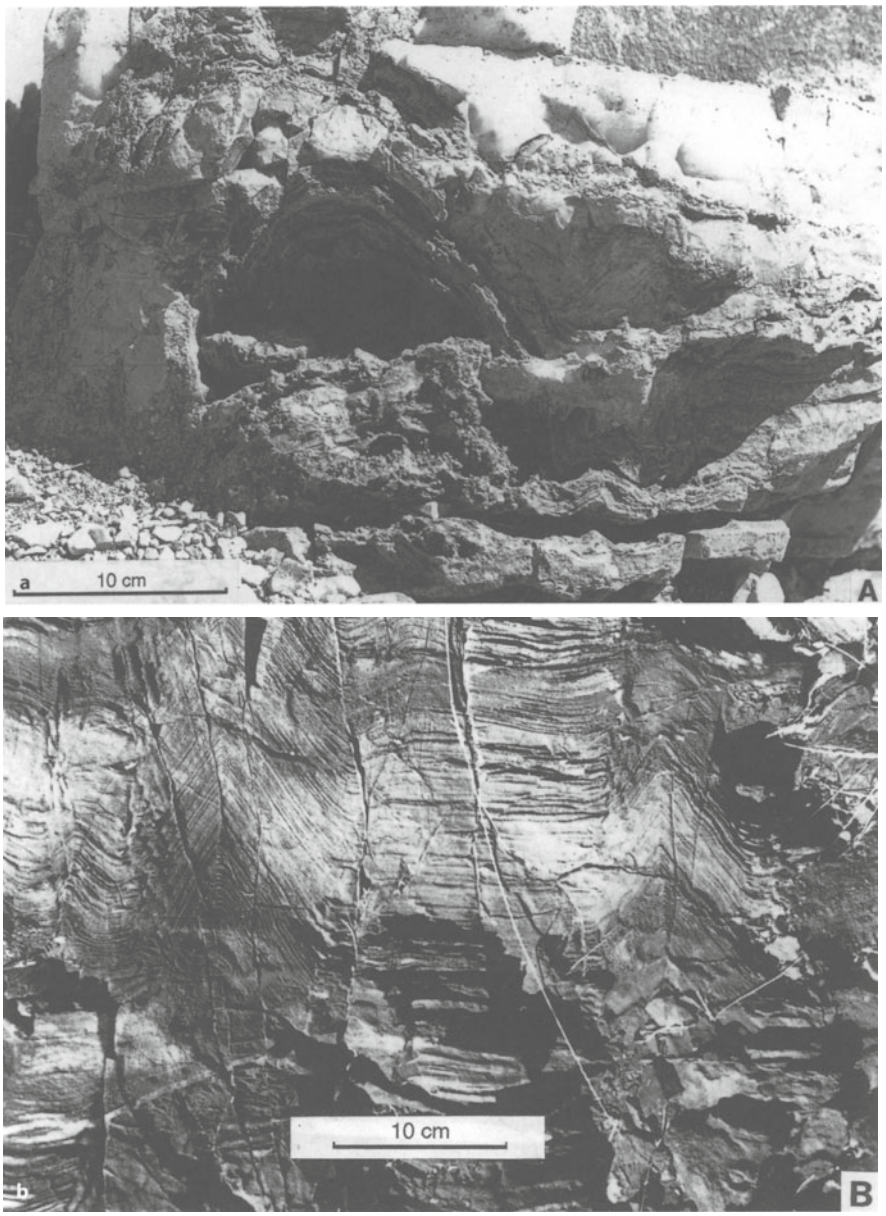

Fig. 3. Paleoarchean stromatolites. **A** Outcrop of domal and stratiform stromatolites in the Towers Formation (Warrawoona Group), North Pole, Western Australia. The arguments for and against biogenicity of these widely illustrated structures has been much discussed (see Lowe 1994, 1995; Buick et al. 1995; photo by H.J. Hofmann). **B** Outcrop of conically laminated stromatolites in the Panorama Formation (Warrawoona Group), Shaw River area, Western Australia. These pseudocolumnar conically laminated forms with erect axial zones, broad fields of intervening horizontal and gently domed laminae, steep slopes with modulated second order curvature, and high degrees of inheritance, are indicative of microbial influence on their growth. (Photo courtesy of R. Thorpe, GSC photo 205428)

lites, have been discussed in the previously cited papers by Lowe and Buick et al., and also by Hofmann (1972), Cloud (1976), Walter (1978, 1983, 1994); and Buick et al. (1981). To the criteria mentioned by these authors (for list and discussion, see Sumner, this Vol.), I would add as supporting items: (1) brecciated mat chips accumulated in depressions between convexly laminated mounds, (2) thin, rolled-up fragments as indications of the existence of coherent flexible laminae that are reasonably interpretable as microbial mats, and (3) distinct compositional differences between the laminated growth structures and their surrounding matrix, such as carbonate stromatolites set within terrigenous detritus. But even a combination of all the criteria may not be sufficient for some researchers to allow for the biogenicity of particular structures. On the other hand, many complex, Proterozoic, columnar branching forms seem to offer no problems in this respect for those same researchers. Morphologic complexity, and the presence of microfossils resembling modern microbes arranged in patterns like those in modern microbial mats appear to be the most reliable criteria to gauge biogenicity.

Lowe (1994) has reinterpreted "all" Archean stromatolite occurrences older than 3.2 Ga as probably abiogenic, citing inorganic precipitation and soft-sediment deformation as the probable principal processes leading to their formation. The main conclusion of that

paper was challenged by Buick et al. (1995), who presented arguments why some of the structures in the Warrawoona Group at North Pole are neither deformational nor precipitational, but are likely to have had a biological origin. Among several reasons cited are three orders of lamina curvature, microlaminae with 5–10 μm kerogenous clots that define semidiscrete columnar microstructures, and lamina thickening over crests. In his reply to Buick et al. (1995), Lowe (1995) suggested that their diagnostic criteria for biogenicity could arguably apply as well to abiogenic geyserite and speleothems. However, neither of these two appear to be reasonable analogue settings for the stromatolite occurrences discussed, judging from published accounts of the geology of the particular regions involved. Moreover, columnar geyserites previously regarded as abiogenic have now been found to contain biofilms (e.g., Cady et al. 1995). Lowe (1995) also retreated somewhat from the rather strong statement about the abiological nature in the title of the original paper (Lowe 1994) by acknowledging that a biological contribution to the formation of Paleoarchean stromatolites cannot be ruled out; in other words, these stromatolites cannot be placed into one of the corners of the B-C-M triangle (Fig. 2), but lie at some undetermined intermediate position. He concluded that our present criteria for biogenicity are inadequate, and one may tend to agree. These discussions do not refer to some other, recently reported, Paleoarchean stromatolite occurrences with very convincing biogenic aspect: (1) large, well defined domes in the Nondweni Group (Wilson and Versfeld 1994), and (2) new material in the Towers Formation (Walter 1994, Fig. 1). Both have strong morphologic resemblance to certain Proterozoic stromatolites whose biogenicity is not in question. Inasmuch as these discussions no more disprove the biogenicity of "all" reported Paleoarchean stromatolites than they prove it, we should continue to keep our interpretation options open and regard them as legitimate objects for study to illuminate aspects of the Archean biosphere until such time when definitive criteria become available. In this connection one may note that Neoarchean ministromatolites with radial-fibrous microfabric, which constitute excellent evidence for primarily or exclusively precipitational structures, continue to be seen as having a potential bacterially influenced contribution (Grotzinger 1989), and are treated as a distinct type of stromatolite with binominal epithets. If these can be dealt with as stromatolites, why not also others that may be largely chemical? The conically laminated structures in the Panorama Formation of the Warrawoona sequence in the Shaw River area (Fig. 3B) do not appear to have axial zones like those found in true *Conophyton*, whose biogenicity is accepted. Conical structures from this area were studied by Grey (1984) and interpreted as abiogenic, probably the result of enterolithic folding of evaporitic laminations. Enterolithic folding involves change in sediment volume and intestine-like convolutions, neither of which apply to the structures in Fig. 3B. Accretion of microbial films on the substrate better explain the combination of erect axial zones of inflexed lamina profiles, the steep slopes and high degrees of inheritance, the uniformly broad intervening zones of horizontal laminae, in places with convex-up sections, and the presence of modulated second-order curvature on the angulate laminae in these pre-3.2 Ga stromatolites (Hofmann et al. 1999).

Disagreements in interpretation, and the consequent usage of the term stromatolite, can lead to the exclusion of particular structures from the paleontologic realm by some (those for whom a stromatolite should only be an unquestionable biogenic structure), whereas others would leave them included. While some exceptional occurrences in the Proterozoic can be demonstrated to be fossilized structured mats of microbes (e.g., Hofmann 1976; Knoll and Golubic 1979), many, if not most, Archean and Proterozoic stromatolites can only be pinpointed roughly within the ternary compilation. For these, the region of uncertainty extends from the B, C and M poles onto the triangle (Fig. 2), therefore implying probable biological contributions (e.g., biofilms), and thus making them suitable objects for study that may elucidate life on the early Earth. Consequently, I prefer to use the all-inclusive ternary concept of stromatolites given in italics in Sect. 3; adjectival terms can be employed to refer to the known or inferred genesis (probable position on the B-C-M ternary or tetrahedral plot) of a particular structure, e.g., cyanobacterial stromatolite, eubacterial stromatolite, predominantly chemical stromatolite. Until all specialists can be firmly convinced to accept a particular laminated structure as entirely abiologic, structures that are possibly partly biogenic should continue to receive appropriate scrutiny deserving of laminated dubiofossils, because they may have relevance for elucidating the Archean biosphere.

The assumption, then, is that a biologic contribution played a role, however minor, in the formation of the laminated constructs under consideration; the phenomenon includes all the Archean laminated structures with distinct morphology that were originally described as stromatolites or oncolites (oncoids), and for which a biologic contribution has been postulated (Table 1). Excluded are unlaminated microbialites, such as the plumose structures illustrated by Beukes (1987, Figs. 6A, 10C), structures which are discussed in more detail by Sumner (this Vol.).

Table 1. Summary of selected data on Archean stromatolites

Stratigraphic unit[a]	Occurrence[b] (No.)	No of geon	No of taxa	Environment[c]	Size range	Morphological attributes[d]	Fabrics[e*]	Microfossils[f]
Deep Rose Lake, Archean or Aphebian, Unit 3 of basement	*NA16*	26–21	1	v	cm, dm	p, d		
Whalen Gp. Unit D, Wildcat Hills Fm.	*NA15b*	25–22	3	v	mm, cm, dm	s, p, b		
Whalen Gp. Unit A, Rawhide Canyon Fm.	*NA15a*	25–22	1	v	mm, cm, dm, m	p, d, m		
Yellowknife Supgp., Snofield Lake	NA14	26	7	v	mm, cm, dm	s, p, d, co, b, o, m	xlf	
Yellowknife Spgp., Back River volcanic complex	NA13	26	3	v	cm, dm	s, p, d		
Henik Gp., Angikuni Lake	*NA12*	26	2	v	dm	s, d		
Kaminak Gp.	*NA11*	26	1	v		s		
Archean, Sakami Lake	*NA10*	27	1	v	cm	s?		
Selbaie volcanics	*NA 9*	27	1	v		s?		
Joutel Volcanic Complex	NA 8	27	3	v	cm, dm	s, p, c	fen	
Michipicoten Gp., Helen Fm.	NA 7	27	1	v	cm	s?, c		
Muskrat Dam greenstone belt	NA 6	27	1	v	cm	p		
Woman Lake marble, Unit 5d	NA 5	28	2	v	cm	s, d	fen	
Keeyask metasediments, Eyapamikama Lake	NA 4	28	3	v	cm	s, d, c		
Steeprock Gp.	NA 3	29–27	8	v	mm, cm, dm, m, dm	s, p, d, c, co, b, w, o, m	xlf	
Archean, Red Lake (Ball Assemblage)	NA 2	29	3	v	cm, dm, m	s, p, d	her, xlf	
Lumby Lake carbonate	*NA 1*	29	1	v		s?		
Turee Creek Gp.	*AU 5*	24	1		cm	p, c		
Hamersley Gp., Carawine Dol.	AU 4	26	7	v	cm, dm, m	s, p, d, c, co, o	her, xlf	
Kanowna	AU 3	27–26	1	v	mm, cm	c		M, F, G
Fortescue Gp., Tumbiana Fm., (Pillingini Tuff)	AU 2	27	9	v, L	mm, cm, dm	s, p, d, c, co, b	fen	M, F
Warrawoona Gp., Panorama Fm.	AU 1d	34	1	v	dm	s, c		
Warrawoona Gp., Strelley Pool Chert	AU 1c	34–32	3	v	cm, dm	s, c, o	xlf	
Warrawoona Gp., Apex Basalt	AU 1b	34	1	v		s		
Warrawoona Gp., Talga Talga Sbgp., Towers Fm.	AU 1a	34	4	v	cm, dm	s, p, d, o		M, F, G
Slyudyanka Gp.	*AS 3*	?	1			o?		
Dharwar Spgp., Chitradurga Gp., Vanivilas Fm.	AS 2d	29–27	4	v	cm, dm	s, p, d, co, b		M, F
Dharwar Spgp., Deogiri Fm., Sandur belt	AS 2c	27–26	2	v	cm, dm	d, c?		
Dharwar Spgp., Chidradurga Gp., Joldhal Fm., Shimoga belt	AS 2b	28–26	4	v	cm, dm	s, p, d, c, co, w		
Dharwar Spgp., Kalche area	AS 2a	28–26	4	v	cm, dm	s, p, d, c, co, w		M, G
Iron Ore Gp., Koira Gp.	*AS 1b*	32–31	4	v	cm, dm	s, p, d, o?		
Iron Ore Gp., Bonai-Keonjhar area	*AS 1a*	32–31	4	v	cm	s, p, d, o?		
Bolshozero area	*EU 1*	25–24	1		co			
Transvaal Spgp., Campbellrand Sbgp., Ghaap Plateau Dol.	AF 7b	25	14	v	mm, cm, dm, m, dam	s, p, d, c, co, b, w, r, m	fen	M, F, G
Transvaal Spgp., Chuniespoort Gp., Malmani Dol.	AF 7a	25	10	v	µm, mm, cm, dm, m, dam	s, p, d, c, co, b, o	her, xlf	
Bulawayo Spgp., Kwekwe (Que Que) area, Lannes Ls.	AF 6e	27–26	1	v		s?		

Table 1. (Contin.)

Stratigraphic unit[a]	Occurrence[b] (No.)	No of geon	No of taxa	Environment[c]	Size range	Morphological attributes[d]	Fabrics[e*]	Microfossils[f]
Bulawayo Spgp., Mount Hampdon area (Ascot Vale)	AF 6d	27–26	1	v	cm	p, co		
Bulawayo Spgp., Ngesi Gp., Cheshire Fm.	AF 6c	26	4	v	mm, cm, dm	s, p, d, c, b, m?	fen, xlf	
Bulawayo Spgp., Ngesi Gp., Manjeri Fm.	AF 6b	27–26	2	v	cm	s, p	fen	
Bulawayo Spgp., Zwankendaba Gp.	AF 6a	27–26	4	v	cm, dm, m	p, d, c, o, m	her	
Ventersdorp Spgp., Bothaville Fm.	AF 5d	26	2	v, FL	mm, cm	s, c		
Ventersdorp Spgp., Platberg Gp., Rietgat Fm.	AF 5c	26	3	v, L	mm, cm, dm	p, d, b, o, m	fen	
Ventersdorp Spgp., Platberg Gp., Klippan Fm.	AF 5b	26	1	v, L	cm	s, p		
Ventersdorp Spgp., Contact Reef	*AF 5a*	27	1	v	mm	o?		
Mushandike Fm.	AF 4	28	2	v	mm, cm	s, p, d, b		
Pongola Spgp., Insuzi Gp.	AF 3	29	6	v	mm, cm, dm, m	s, p, d, c, co, b, m		
Nondweni Gp., Witkop Fm.	AF 2	34	2	v	cm, dm	p, d	xlf	
Swaziland Spgp., Onverwacht Gp., Kromberg Fm.	AF 1b	34	4	v	cm, dm	sp, c, o		M, F, G
Swaziland Spgp., Onverwacht Gp., Hooggenoeg Fm.	AF 1a	34	1	v		s?		M, F

[a] Occurrences in italics are questionably Archean and/or questionably stromatolitic.
[b] Abbreviations: NA; North America; AU, Australia; AS, Asia; EU, Europe; AF, Africa.
[c] Environment: v, volcanic association; F, fluvial; L, lacustrine.
[d] Stromatolite type: s, stratiform; p, pseudocolumnar; d, domal; c, conical; co, columnar; b, branching; w, walled; o, oncoids; r, rolled-up; m, ministromatolite.
[e] Fabrics: fen, fenestral; her, herringbone cement; xlf, radial-fibrous crystalline fabrics.
[f] Microfossils (M): F, filamentous; G, globoidal (coccoid).

4 Stromatolite Types

Despite diverse attempts during the past 30 years or so to put some order and stability into stromatolite classification and taxonomy, many aspects remain largely unresolved; problems related to them are not trivial, and are beyond the scope of the present chapter; no treatise-like synthesis has been published. Archean stromatolites are mostly stratiform and pseudocolumnar types, and, with only a few exceptions (e.g., Rothpletz 1916; Cloud and Semikhatov 1969; Hofmann 1971; Walter 1972; Bertrand-Sarfati and Eriksson 1977), they have not been given the systematic paleontologic treatment accorded the columnar types from the Proterozoic. Most reports are descriptive, supported by photographic illustrations of outcrop surfaces, or thin or polished sections, so a standard taxonomic review is not applicable. Only specimens of manageable size have received laboratory study. The Archean stromatolites are here categorized according to features considered to be their main distinguishing characteristics, following the terminology of attributes given in Hofmann (1969, Fig. 13, reproduced in Walter 1976, Appendix Fig. 1, pp. 688–689, and largely incorporated in Fig. 6.2.1 in Walter et al. 1992), and by Hofmann (1989). The main morphologic features are summarized in Fig. 4 and comprise: size (dimensions such as column and bioherm widths and heights); shape of synoptic surface (snapshot representation of configuration of the laminae in plan view and section at an instant in time, providing information on relief, lateral relations such as linkage, spacing, orientation): four basic lamina shapes are recognized: flat, convex, concave (inflexed), and globoidal (oncoidal); stacking pattern of laminae (inheritance, accretion patterns, duration, branching; analysis may require deconvolution of shape to eliminate effects of secondary deformation); petrology (lithology, mineralogy, microstructure, fabric; grain size; secondary effects?); and fossil content (if any).

With regard to size, Archean stromatolites range over six orders of magnitude in horizontal dimensions of the morphologic elements such as column width or span of lamina convexities, from microstromatolites less than 100 μm across (e.g., Lanier 1986, 1988), through ministromatolites, to giant dekametric domes (megastromatolites; Jolliffe 1955; Truswell and Eriksson 1973, 1975; Simonson et al. 1993). Most occurrences are,

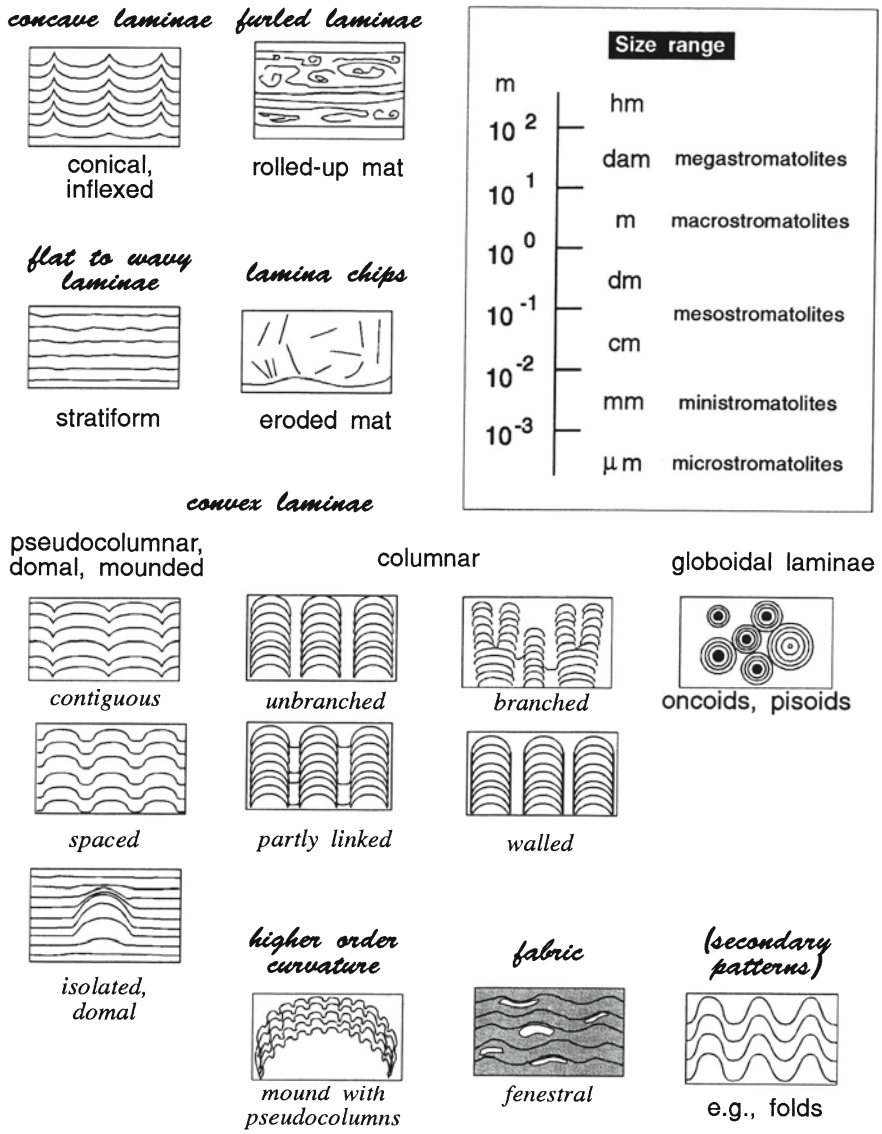

Fig. 4. Graphic summary of main attributes of Archean stromatolites

however, in the centimeteres and decimeters size range (mesostromatolites; Table 1). The extremes of the size range have so far been observed only in the Neoarchean.

With respect to shape, Archean stromatolites are less complex than younger ones, mostly lacking the well developed, branching columnar forms with distinct walls, except for some in the latest Archean. Based on lamina shape and stacking pattern, they can be grouped into the following morphologic categories: stratiform, pseudocolumnar, domal, coniform-layered, and columnar types, with further distinctions as to the presence or absence of walls and branching, and oncoids. Additional categorizations are structure- or texture-based (rolled-up laminae; fenestral fabric).

5 Geographic Distribution

Figure 5 gives an overview of the geographic distribution of all reported occurrences, numbered in general chronological order from oldest to youngest for each continent. The localities plot as 11 small clusters on five continents, representing the world's principal Archean cratons or provinces (Goodwin 1991, Fig. 2.1); other areas with preserved ancient stratigraphic records in Europe, Asia, South America, and Antarctica have not yet yielded any stromatolites. Given factors such as their great antiquity, unstable tectonic regimes of the time, and the cannibalistic nature of the exogenic and endogenic geologic processes, it is not surprising that the stromatolite record from the Archean is scarce. Al-

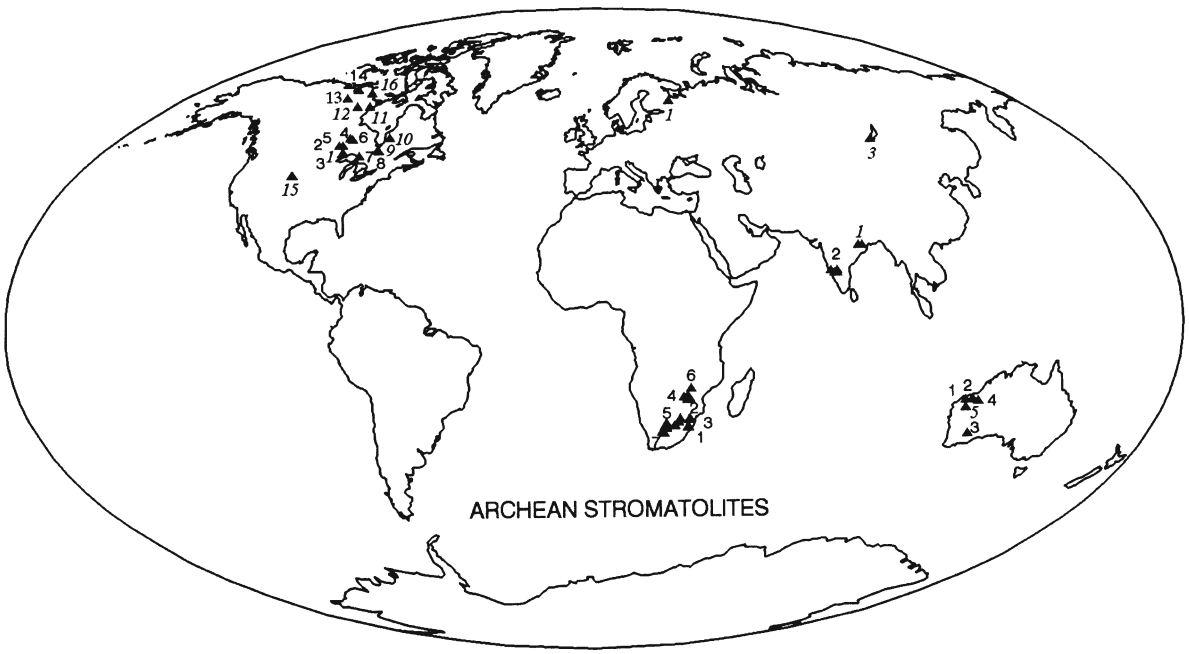

Fig. 5. Geographic distribution of Archean stromatolites. Occurrences are numbered from oldest to youngest for each continent; *numbers in italics* are questionable occurrences. Note the clustering on 11 small remnants of Archean cratons: the Slave, Superior, and Wyoming provinces in North America, the Kaapvaal and Zimbabwe cratons in Africa, the Baltic Shield in Europe, the Dharwar, Singhbum and Aldan shields in Asia, and the Pilbara and Yilgarn blocks in Australia. For key to numbers, see Fig. 6 and Table 1

though temporally shorter, and volumetrically inferior to that of the Proterozoic (e.g., Goodwin 1991, Figs. 3.1, 4.1, 5.1, Table 1-2), this record is, nevertheless, crucial because in it reside the most important clues to the Earth's early biosphere.

6 Stratigraphic Distribution

What is included in the Archean? The earliest and longest part of the geologic record is commonly referred to as pre-Cambrian, Precambrian, or Cryptozoic. This interval, encompassing approximately the first 85% of our planet's history, has traditionally been split into Archean and Proterozoic divisions, although the nature of the definition and placement of the actual boundary (some call it a transition) between the two units had been a long-standing dilemma. The problem was only "solved" in 1977 by a decision of the IUGS to place it geochronologically at 2500 Ma, rather than define it at some boundary stratotype section (James 1978). This approach, nevertheless, took into consideration the traditional usage that reflected the major secular changes in the geospheres and attendant differences in the geologies representing these two eons. The arbitrary decision to place it at 2500 Ma has also had the effect of making it necessary to reassign to the Archean certain stromatolitic rocks that had long been considered to have Early Proterozoic characteristics, namely the Transvaal, Ventersdorp, Fortescue, and Hamersley sequences. The most important example is the prolifically stromatolitic platform carbonate assemblage in the Transvaal Supergroup of South Africa; it has recently yielded a precise U/Pb zircon age of 2517 ± 3 Ma (Sumner and Bowring 1996). With the transfer to the Archean, the superbly preserved Transvaal stromatolites have now become the best studied and most diversely fossiliferous of all Archean occurrences. Evaluation of the newer radiometric data also indicates that the Turee Creek stromatolites of Western Australia, one of the 11 cited by Walter (1983) as Archean, may now be better regarded as early Paleoproterozoic.

The base of the Archean is undefined. In some schemes it is preceded by a Hadean interval without a terrestrial geological record (Cloud 1972), whereas in others this interval is included in the Archean. Whichever scheme one adopts, the relevant substantiating fossil evidence can only come from the surviving rock record, which is Archean by either scheme. At present, the oldest dated terrestrial materials (excluding meteorites) are 4.276 Ga recycled zircons in the Yilgarn Province of Australia (Froude et al. 1983; Compston and Pidgeon 1986), and 4.0 Ga gneisses in the Slave Province of northwest Canada (Bowring et al. 1989).

The Archean itself has further provisional subdivisions, also based on arbitrary geochronometric boundaries (Lumbers and Card 1991): Eoarchean (>3600 Ma), Paleoarchean (3600–3200 Ma), Mesoarchean (3200–

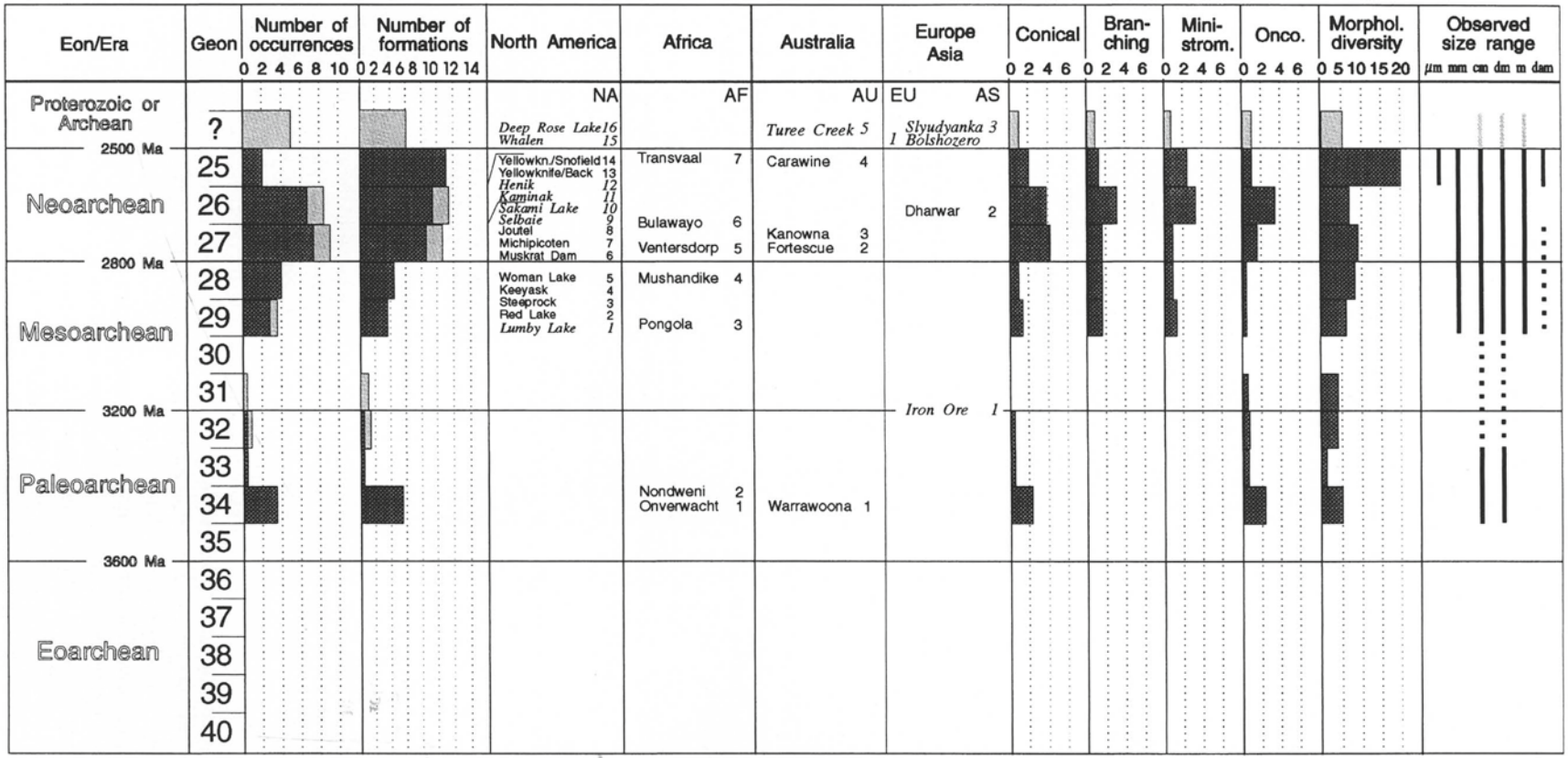

Fig. 6. Time-distribution of Archean stromatolites and selected attributes. Fractional occurrences result from apportioning imprecisely dated units; items in *italics* are questionable Archean occurrences

2800 Ma), and Neoarchean (2800–2500 Ma). This is the classification followed here (Fig. 6), with 100-million-year bins (geons of Hofmann 1990) as further subdivisions for purposes of compiling the normalized age distributions of the occurrences; some intrinsic imprecision is unavoidable, given the poorly constrained ages for certain of the stromatolitic units. The occurrences here examined (chiefly lithostratigraphic units of the highest rank – groups or supergroups) are numbered as in Fig. 5 and are compiled using apportioned fractions of units according to the extent of the range for the time interval of the unit: an occurrence known to be within a particular geon is counted as 1, a unit known to lie within a range of 2 geons is counted as a half for each of the two contiguous geons in which it could lie, as a third of a unit for each of three contiguous geons possible, etc. The resulting histogram for groups/supergroups (leftmost histogram in Fig. 6) thus contains fractional units; it reveals two distinct groupings: a small Paleoarchean peak, representing sequences on Archean cratons in the former Gondwana in Australia and southern Africa, and a much larger mode for the remaining occurrences younger than 3000 Ma on cratons in the former Laurasia in addition to Gondwana. An adjoining, separate histogram in the same figure summarizing formation-level units shows increasing abundances with decreasing age. Like the geographic clustering, this stratigraphic assortment is likely a reflection of accidents of preservation, and factors such as thicker and more extensive development of stromatolitic sediments, the state of geologic mapping, and the more refined lithostratigraphic characterization for the younger Archean intervals. An additional complication in the compilation is that a few Neoarchean stratigraphic units in South Africa are not yet unequivocally defined (e.g., see Altermann and Wotherspoon 1995, p. 129, Fig. 2), and some may have been counted collectively when they should have been counted separately or vice versa. The inventory must be considered approximate for that interval, though the abundance peak would not be affected greatly if the few units involved were correlated differently. Figure 6 also shows how some other selected variables change with time.

7 Discussion and Summary

Archean stromatolites constitute the dominant record of early life on Earth, but the messages in these archives still remain largely undeciphered. Inasmuch as stromatolites are the result of interactions of biological, physical, and chemical processes, and microfossils are rarely preserved, it is generally difficult to sort out the contribution each makes individually to the edification of a particular structure. What is reasonable is to assume that (neglecting secondary, postdepositional effects) the shape, size, and makeup of each stromatolite represents the cumulative net contributions of each of these three processes over the time period recorded between the initial and last lamina. Each constituent lamina represents a particular surface of equilibrium between the interacting mechanisms involving water, under a particular set of environmental constraints. Although it is commonly not possible to determine the magnitude of each individual contributory process from the stromatolite attributes alone, associated primary structures, affiliated sediments, geochemistry, and, all too rarely, contained microbiota contribute clues to deciphering their morphogenesis.

Except for the extensive latest Archean Transvaal and Carawine sequences, practically all Archean stromatolites occur in thin, often discontinuous, localized carbonate units that are associated with volcanic rocks (Table 1). They appear to have formed at times of brief, transient stability in areas of tectonic instability and extensive volcanism in what are now the preserved greenstone belts of Archean cratons.

The main lithologies harbouring Archean stromatolites are limestone and dolostone, often silicified or ferruginous; several occurrences are affiliated with evaporitic sediments; one occurrence is in siderite of sufficient quantity to have been exploited as an iron ore (Michipicoten).

The interpretation of Archean stromatolites clearly involves making judgments at different levels, and in evaluating the attributes of each set of structures in terms of one's experience with similar but better preserved Proterozoic and Phanerozoic examples. One can ask questions such as: Is the laminated construct biogenic? How large is the biologic contribution? What major group makes that contribution? What can we deduce from this? How does this interpretation fit with what is known? An affirmative answer to the first question is made simpler if specific evidence can be adduced in answering one or more of the others. While progress continues to be made in understanding and evaluating the ancient structures, sporadic setbacks can occur, as recent discussions in the literature show.

What, then, can be said with some degree of confidence about Archean stromatolites? As far as the contributing organisms are concerned, the direct evidence of preserved microfossils is extremely meagre and confined to a few localities, mostly in early diagenetic chert; different interpretations of their affinities are possible. The preserved remains, their geologic setting, and organic and isotope geochemistry suggest that the Archean mats were produced by coccoid and filamentous prokaryotes, probably mostly photoautotrophs.

Archean stromatolites are important archives of biological, chemical, and mechanical processes on the primitive Earth, recording their interactions under var-

ious environmental conditions. While the messages from the past have become better understood over the years, we need to expand an interdisciplinary approach, apply new and more rigorous quantitative and analytical techniques, and try out new ideas to explain the phenomena the record render. As more precise geochronometric data become available, the age uncertainties attached to many stromatolitic units will disappear, revealing a better calibrated picture of the succession of events on the primitive Earth. The importance of microbial processes on, above, and below the water-sediment interface during the Archean, as in the Proterozoic and Phanerozoic, is recorded in the stromatolites and the all too rarely contained microbiotas. The script is there, expressed in a language we have not quite mastered yet.

Acknowledgements. I am indebted to Kath Grey for providing an open-file compilation of Australian occurrences, as well as for discussions of material familiar to her, and for critical review of an earlier version of the manuscript. Dawn Sumner made available a copy of her thesis on the Transvaal carbonates. Victor Melezhik contributed information and references on the probable Archean stromatolite occurrence at Bolshozero (EU-1) on the Baltic Shield. Ralph Thorpe very kindly furnished the photograph of the Shaw River stromatolite occurrence in the Warrawoona Group of Western Australia (Fig. 3B). I greatly appreciate the technical assistance of Mona Kachaami. Financial support from the Natural Sciences and Engineering Research Council of Canada (Grant No. A7484) is gratefully acknowledged.

References

Altermann W, Wotherspoon JMcD (1995) The carbonates of the Transvaal and Griqualand West sequences of the Kaapvaal craton, with special reference to the Lime Acres limestone deposit. Miner Deposita 30:124–134

Awramik SM (1991) Archaean and Proterozoic stromatolites. In: Riding R (ed), Calcareous algae and stromatolites. Springer, Berlin Heidelberg New York, pp 289–304

Awramik SM (1992) The history and significance of stromatolites. In: Schidlowski M et al. (eds) Early Organic Evolution: implications for mineral and energy resources. Springer, Berlin Heidelberg New York, pp 435–449

Bertrand-Sarfati J, Eriksson KA (1977) Columnar stromatolites from the Early Proterozoic Schmidtsdrift Formation, northern Cape Province, South Africa. Part 1. Systematic and diagnostic features. Palaeontol Afr 20:1–26

Beukes NJ (1987) Facies relationships, depositional environments and diagenesis in a major Early Proterozoic stromatolitic carbonate platform to basinal sequence, Campbellrand Subgroup, Transvaal Supergroup, southern Africa. Sediment Geol 54:1–46

Bowring SA, Williams IS, Compston W (1989) 3.986 Ga gneisses from the Slave province, Northwest Territories, Canada. Geology 17:971–975

Buick R (1984) Carbonaceous filaments from North Pole, western Australia: are they fossil bacteria in Archaean stromatolites? Precambrian Res 24:157–172

Buick R, Groves DI, Dunlop JSR (1995) Abiological origin of described stromatolites older than 3.2 Ga: comment and reply. Comment. Geology 23:191

Buick R, Dunlop JSR, Groves DI (1981) Stromatolite recognition in ancient rocks: an appraisal of irregularly laminated structures in an Early Archaean chert-barite unit from North Pole, Western Australia. Alcheringa 5:161–181

Burne RV, Moore LS (1987) Benthic microbial communities and microbialites. Baas Becking Geobiological Laboratory, Annu Rep 1985, pp 10–12

Cady SL, Farmer J, Des Marais DJ, Blake DF (1995) Columnar and spicular geyserites from Yellowstone National Park, WY; scanning and transmission electron microscopy evidence for biogenicity. Geol Soc Am, Abstr Progr 27 (6):305

Cloud PE Jr, Semikhatov MA (1969) Proterozoic stromatolite zonation. Am J Sci 267:1017–1061

Cloud P (1972) A working model of the primitive Earth. Am J Sci 272:537–548

Cloud PE Jr (1976) Beginnings of biospheric evolution and their biogeochemical consequences. Paleobiol 2:351–387

Compston W, Pidgeon RT (1986) Jack Hills, evidence of more very old detrital zircons in Western Australia. Nature 321:766–769

de la Hunty L.E (1963) The geology of the manganese deposits of Western Australia. Geol Surv Western Aus Bull 116

de la Hunty LE (1964) Balfour-Downs, Western Australia. Geol Surv Western Australia. 1:250,000 Geological Series, Sheet SF/51–9, Explanatary Notes

Farmer JD, Des Marais DJ (1994) Exopaleontology and the search for a fossil record on Mars. Lunar Planet Sci Conf 25:367–368

Froude DO, Ireland TR, Kinny PD, Williams IS, Compston W, Williams IR, Myers JS (1983) Ion microprobe identification of 4100–4200 Myr-old terrestrial zircons. Nature 304:616–618

Goodwin AM (1991) Precambrian geology – the dynamic evolution of the continental crust. Academic Press, London

Grey K (1984) Abiogenic stromatoloids from the Warrawoona Group (Early Archaean), Shaw River, Marble Bar, 1:250 000 Sheet area. Geol Surv Western Aust, Palaeontology Report 74/84

Grotzinger JP (1989) Facies and evolution of Precambrian carbonate depositional systems: emergence of the modern platform archetype. In: Crevello PD, Wilson JL, Sarg JF, Reed JF (eds) Controls on carbonate platform and basin development. Soc Econ Paleont Mineral, Spec Publ 44:79–106

Hofmann HJ (1969) Attributes of stromatolites. Geol Surv Can Pap 69–39

Hofmann HJ (1971) Precambrian fossils, pseudofossils, and problematica in Canada. Geol Surv Can Bull 189

Hofmann HJ (1972) Precambrian remains in Canada: fossils, dubiofossils, and pseudofossils. Int Geol Cong 24th Sess, Montreal, Proc Sect 1:20–30

Hofmann HJ (1973) Stromatolites: characteristics and utility. Earth-Sci Rev 9:339–373

Hofmann HJ (1976) Precambrian microflora, Belcher Islands, Canada: significance and systematics. J Paleontol 50:1040–1073

Hofmann HJ (1989) Size classification of stromatolites. Stromatolite Newslett 14:36

Hofmann HJ (1990) Precambrian time units and nomenclature – the geon concept. Geology 18:340–341

Hofmann HJ, Grey K, Hickman AH, Thorpe RI (1999) Origin of 3.45 Ga coniform stromatolites in Warrawoona Group, Western Australia. Geol Soc Amer Bull 111:1256–1262

James HL (1978) Subdivision of the Precambrian – a brief review and a report on recent decisions by the Subcommission on Precambrian Stratigraphy. Precambrian Res 7:193–204

Jolliffe AW (1955) Geology and iron ores of Steep Rock Lake. Econ Geol 50:373–398

Knoll AH, Golubic S (1979) Anatomy and taphonomy of a Precambrian algal stromatolite. Precambrian Res 10:115–151

Lanier WP (1986) Approximate growth rates of Early Proterozoic microstromatolites as deduced by biomass productivity. Palaios 6:525–542

Lanier WP (1988) Structure and morphogenesis of microstromatolites from the Transvaal Supergroup, South Africa. J Sediment Petrol 58:89–99

Lawson AC (1912) The geology of Steeprock Lake, Ontario. Geol Surv Can Mem 28:7–15

Lowe DR (1980) Stromatolites 3,400-Myr old from the Archaean of Western Australia. Nature 284:441–443

Lowe DR (1994) Abiological origin of described stromatolites older than 3.2 Ga. Geology 22:387–390

Lowe DR (1995) Abiological origin of described stromatolites older than 3.2 Ga: comment and reply. Reply. Geology 23: 191–192

Lumbers SB, Card KD (1991) Chronometric subdivision of the Archean. Geol Assoc. Canada, Geology 20(3):56–57
Macgregor AM (1941) A pre-Cambrian limestone in Southern Rhodesia. Geol Soc S Afr Trans 43:9–15
Nisbet EG (1987) The Beginning of life, Chapter 4. In: Nisbet EG (ed) The young earth – an introduction to Archaean geology, Allen and Unwin, Boston, pp 101–145
Raaben ME (1969) Columnar stromatolites and Late Precambrian stratigraphy. Am J Sci 267:1–18
Rothpletz A (1916) Über die systematische Deutung und die stratigraphische Stellung der ältesten Versteinerungen Europas und Nordamerikas mit bedonderer Berücksichtigung der Cryptozoen und Oolithe. Über Cryptozoon, Eozoon, und Atikokania. Bayerische Akad Wissenschaften, Abh Math-Physik Kl 28 (4): 92
Schopf JW (1994) The oldest known records of life: Early Archean stromatolites, microfossils, and organic matter. In: Bengtson S (ed) Early life on Earth. Nobel Symposium 84. Columbia Univ Press, New York, pp 193–206
Simonson BM, Schubel KA, Hassler SW (1993) Carbonate sedimentology of the early Precambrian Hamersley Group of Western Australia. Precambrian Res 60:287–335
Sumner DY, Bowring SA (1996) U-Pb geochronologic constraints on deposition of the Campbellrand Subgroup, Transvaal Supergroup, South Africa. Precambrian Res 79:25–35
Sumner DY, Grotzinger JP (1996a) Were kinetics of Archean calcium carbonate precipitation related to oxygen concentration? Geology 24:119–122
Sumner DY, Grotzinger JP (1996b) Herringbone calcite – petrography and environmental significance. J Sedimentary Res, Sect A A66:419–429
Truswell JF, Eriksson KA (1973) Stromatolite associations and their palaeoenvironmental significance: a re-appraisal of a Lower Proterozoic locality from the Northern Cape Province, South Africa. Sediment Geol 10:1–23
Truswell JF, Eriksson KA (1975) A palaeoenvironmental interpretation of the Early Proterozoic Malmani Dolomite from Zwartkops, South Africa. Precambrian Res 2:277–303
Walcott CD (1912) Notes on fossils from limestone of Steeprock series, Ontario, Canada. Geol Surv Can, Mem 28:16–23 (Abstr in Bull Geol Soc Am 23: 723)
Walter MR (1972) Stromatolites and the biostratigraphy of the Australian Precambrian and Cambrian. Palaeontol Assoc Spec Pap Palaeontol, no 11
Walter MR (ed) (1976) Stromatolites. Developments in Sedimentology 20. Elsevier, Amsterdam
Walter MR (1978) Recognition and significance of Archaean stromatolites. In: Archaean cherty metasediments:their sedimentology, micropalaeontology, biogeochemistry, and significance to mineralization. Univ Western Aust, Spec Publ 2:1–10
Walter MR (1983) Archean stromatolites: evidence of the Earth's earliest benthos. In: Schopf JW (ed) Earth's earliest biosphere – its origin and evolution. Princeton Univ Press, Princeton, pp 187–213
Walter MR (1994) Stromatolites: the main geological source of information on the evolution of the early benthos. In: Bengtson S (ed) Early life on Earth. Nobel Symposium 84. Columbia Univ Press, New York, pp 270–286
Walter MR, Buick R, Dunlop JSR (1980) Stromatolites 3,400–3,500 Myr old from the North Pole area, Western Australia. Nature 248:443–445
Walter MR, Grotzinger JP, Schopf JW (1992) Proterozoic stromatolites. In: Schopf JW, Klein C (eds) The Proterozoic biosphere – a multidisciplinary study. Cambridge Univ Press, Cambridge, pp 253–260
Wilson AH, Versfeld JA (1994) The early Archean Nondweni greenstone belt, southern Kaapvaal Craton, South Africa, Part I. Stratigraphy, sedimentology, mineralization and depositional environment. Precambrian Res 67:243–276
Winter H de la R (1963) Algal stromatolites in the sediments of the Ventersdorp System. Geol Soc S Afr Trans 65:115–121
Young RB (1928) Pressure phenomena in the dolomitic limestones of the Campbell Rand Series in Griqualand West. Geol Soc S Afr Trans 31:157–165
Young RB (1933) The occurrence of stromatolitic or algal limestone in the Campbell Rand Series of Griqualand West. Geol Soc S Afr Trans 35:29–36
Young RB (1934) Conditions of deposition of the Dolomite Series. Geol Soc S Afr Trans 36:121–135
Young RB (1935) A comparison of certain stromatolitic rocks in the Dolomite Series of South Africa with modern algal sediments in the Bahamas. Geol Soc S Afr Trans 37:153–162
Young RB (1940) Note on an unusual type of concretionary structure in limestones of the Dolomite Series. Geol Soc S Afr Trans 43:23–25
Young RB (1940) Further notes on algal structures in the Dolomite Series. Geol Soc S Afr Trans 43:17–21
Young RB (1944) The domical-columnar structure and other minor deformations in the Dolomite Series. Geol Soc S Afr Trans 46:91–105
Young RB, Mendelssohn E (1949) Domed algal growths in the Dolomite Series of South Africa, with associated fossil remains. Geol Soc S Afr Trans 51:53–62

Subject Index